The late Silurian – Early Devonian adaptive radiation of vascular land plants: palynological evidence from the Anglo-Welsh Basin, U.K.

ALEXANDER CAMPBELL BALL[†*]

A thesis submitted in partial fulfilment of the requirements for the degree of
Doctor of Philosophy

[†]*School of Biosciences, University of Sheffield, Alfred Denny Building, Western Bank, Sheffield. S10 2TN, UK (Host institution to ACB)*

[*]*Dept. of Earth Sciences, The Natural History Museum, Cromwell Road, London. SW7 5BD, UK (CASE partner to ACB)*

October 2022

Declaration

I, the author, confirm that this thesis is my own work. I am aware of the University of Sheffield's guidance on the Use of Unfair Means (www.sheffield.ac.uk/ssid/unfair-means). This work has not been previously been presented for an award at this, or any other, University.

The following chapters are intended for publication or have already been published at the time of thesis submission:

Chapter III: Ball, A.C. (in prep.) Taxonomy and biostratigraphy of late Silurian – Early Devonian cryptospores and trilete spores from the Lower 'Old Red Sandstone' of the Anglo-Welsh Basin, U.K. *Monograph for the Palaeontographical Society.*

Chapter IV: Ball, A.C. (in prep.) Floral diversity, disparity and community turnover at the Silurian - Devonian boundary: palynological evidence from the Anglo-Welsh Basin, UK.

Chapter V: Ball, A.C. (in prep.) Early Lochkovian (Early Devonian) mesofossil assemblages from the Anglo-Welsh Basin, UK.

Chapter VI: Ball, A.C. and Taylor, W.A., 2022. Reconstructing the Lower Devonian (Lochkovian) vegetation from the Anglo-Welsh Basin: Two spore masses containing Emphanisporites McGregor spores. Review of Palaeobotany and Palynology, 301, p.104647.

Chapter VII: Wellman, C.H. and Ball, A.C., 2021. Early land plant phytodebris. Geological Society, London, Special Publications, 511(1), pp.309-320.

"Sometimes the best way of starting out to understand something better is simply to ask: what's out there? And then you collect data and try and make sense of it… there's not an experiment as such, just lots of good *looking."*

Alice Roberts: Tamed: ten species that changed our world.

"By Endurance, we conquer"

Shackleton family & HMS Endurance *ship's motto*

Acknowledgments

Thanks must first go to Charles Wellman for, *inter alia*, his excellent supervision, support and insights throughout the project, for always having his door open and giving me the freedom to pitch (on hindsight) some rather left-field ideas, and for making my PhD experience so fulfilling. Steve Stukins for being so accommodating on my museum visits, offering fresh insights and methods with which to explore my data, and allowing me extended access to his office, kettle and tea bags. Paul Kenrick, thanks again for being so accommodating at the museum, your keen interest and insights into the work, especially the mesofossils. And John Richardson, who collected and processed many of the samples investigated here, laid the foundations of Siluro-Devonian palynology, and offered advice and direction in the early parts of the project; it is to John that this thesis is dedicated. Together, my supervisors have provided a steady stream of encouragement, vision and sage counsel which greatly enriched the project, and for which I will be forever grateful.

A special thanks is owed to Dave Bodman, for his expertise, patience and advice in the lab, and especially for carrying on processing and ultimately keeping the project from stagnating when I was unable to get in because of restrictions. Thanks must also go to Martha Gibson, for being the best coffee drinking, mountain climbing and lab 'meat'-ing paly-pal and mentor I could have asked for, your support and friendship has, and continues to be, invaluable: *Let there be meat!* I must also thank the 'Sheffield Cartel' and the countless other palynologists and palaeontologists at Christmas dinners, conferences and post conference pubs who proffered their advice, encouragement and more than a few laughs which helped in so many ways. Paul Shepherd and Scott Renshaw at the British Geological Survey, for providing samples in the depths of lockdown, and allowing me access to the BGS core store as soon as restrictions lifted, providing valuable material *in lieu* of field samples. Thanks to Margaret Collinson for her excellent lecturing and cultivation of my early interests in palynology and palaeobotany, and her continued interest and collaboration as the project developed, and together with Neil Holloway and Sharon Gibbons at the Earth Sciences department at Royal Holloway, University of London, used their expertise to give insights into the wildfires that produced the mesofossils described herein. Thanks also to Chris and Svet at the University of Sheffield Electron Microscopy facility, for all their support and help and for managing to keep the SEM open through lockdowns for research to continue, and Ria Mitchell for her interest in the mesofossils and excellent CT work which opened up more than a few interesting lines of enquiry.

On a personal note, I must first thank Mum and Dad for everything: for encouraging me in my books and for all the opportunities you afforded me to cultivate an interest in the natural world, for giving me alternative, useful views on many aspects of my work ("*Son, modelling is like…*" and I'll leave it there) and for only raising your eyebrows a little when I mentioned that I might like to study obscure microfossils for four years. Much of the logging and early taxonomic work was carried out during lockdown(s), so thank-you again for allowing me to dominate the dining room and routinely empty the fridge. Thanks also to James and Catherine for your constant support throughout – a debt is owed for all the pasties and bacon sandwiches. Thanks also to Hazelle, Lottie and Willow for their patience, support and soggy-tennis-balls-on-my-lap. To the Cornish Contingency, cheers for always being ready with a pint and/ or a rusty, broken car to tinker with - you lot have always been *proper*. Thanks also to 26 Albert and the Monday-nighters, for all the love and encouragement, no matter what corner of the world we find ourselves in. L and Vince at Truro College, who (largely by accident) introduced me to Geology and to whom I owe my love of the geosciences to. Finally, I am indebted to Steve, Colter, Sturgill, Charles, Hans, Klaus, Chopin, Howard, Hannah, Adam, Stephen and many, many others for keeping me company and largely(?) sane during those long, lonely, hours (years) on the microscope with your music, thoughts and curios.

Abstract

The classic Anglo-Welsh Basin sequence yields a rich assemblage of plant macrofossils, mesofossils and spores. The terrestrial basin straddles the Silurian – Devonian boundary and is well placed to investigate vegetation change during a transformative episode of plant evolution. Between the late Silurian and Early Devonian, tracheophytes (vascular plants) (± represented by trilete spores) were beginning to radiate and dominate variously less derived, ancestral embryophytes (cryptospores), having wide ranging ramifications for biogeochemical cycles, geomorphology and the atmosphere. Here, the palynological record of Ludlow to mid Lochkovian (late Silurian – Early Devonian) aged rocks from the Welsh borderlands and south Wales, encompassing the uppermost Palaeozoic Marine Welsh Basin and the Lower 'Old Red Sandstone' of the Anglo-Welsh Basin is examined. Temporal changes in the abundance of spore species and ornament types is documented, and species ranges are assessed. 183 species in 42 genera of trilete spores and cryptospores are catalogued. A gradual proliferation of trilete spore and cryptospore species through the sequence is observed, and a major radiation is seen for both between the earliest and early Lochkovian. Morphological diversity (disparity) shows a similar pattern and is driven by several key trilete spore and cryptospore genera. The spatial diversity and disparity of coeval assemblages are assessed, and 'pockets' of specialised vegetation seem to occur by the early Lochkovian. The drivers of this radiation are uncertain, but it may have been facilitated by a shift in climate and change of environment, with facies change also playing a role in the final observed patterns. The radiation of spore species allows the preliminary construction of spore assemblage biozones around, and defining, the Silurian – Devonian boundary in the Anglo-Welsh Basin. The source plants of several dispersed spores are investigated, giving insights into their morphology and affinities, and glimpses of cryptogamic communities and plant-animal interaction are also recorded.

Contents

Chapter I Introduction, literature review and key questions

1. Introduction

The colonisation of land by plants was one of the most important episodes in Earth history, driving changes in biogeochemical cycles, land morphology and river systems, and having far reaching consequences for the atmosphere, long-term carbon cycle and marine and terrestrial biospheres (Algeo and Scheckler, 1998; Berner, 2006; Davies and Gibling, 2010a; Gibling et al., 2014), even amongst the earliest land plants (Boucot and Gray, 2001). A major driver of these changes, and perhaps the most important phase in land plant evolution, was the emergence of tracheophytes (vascular plants), which saw a plethora of biological innovation facilitating continual exploration of new morphospace and ecospace (e.g. Algeo and Scheckler, 1998) with a marked 'explosion' in diversity occurring in the Early Devonian (Kenrick et al., 2012). Such success and diversification quickly led to the ecological dominance of tracheophytes and underpinned the onward development of terrestrial and marine environments. Indeed, such was the influence of land plants, and particularly tracheophytes, on the Earth system that 'coevolutionary' hypotheses have been fielded for rivers (Gibling et al., 2014) and climate (Morris et al., 2018a).

The phylogenetic relationships amongst embryophytes and the nature of the earliest land plant remain problematic, however. While embryophyta and tracheophyta are accepted to be monophyletic, the bryophytes are more enigmatic. Recently, Puttick et al. (2018) found support for bryophyte monophyly, and also shed new light on the nature of the earliest embryophyte, which for a considerable amount of time has seen liverworts, especially Marchantopsida, fielded as a model for the ancestral land plant because of their simplicity (Gray, 1985; Fletcher et al., 2006; Shimamura, 2016; Bowman et al., 2017). However, the findings of Puttick et al. (2018) suggests that the ancestral land plant was probably more complex than liverworts, with the latter's absence of characters due to trait loss rather than ancestral simplicity.

The understanding of early land plant phylogenetic relationships are complicated by the paucity of the fossil record, and the timing of lineage emergence is similarly affected by this problem. The first unequivocal plant body fossil is *Cooksonia* cf. *pertoni*, recovered from Wenlock sediments (426 Ma) (Edwards and Freehan, 1980; Edwards *et al*., 1983), with the earliest bona fide tracheophyte body fossil recovered from slightly younger Ludlovian sediments (420.7 Ma) (Kotyk et al., 2002). However, it is well documented that the macrofossil record is too sparse and biased towards plants with recalcitrant tissues and the rock record too nonuniform, to directly inform the timing of land plant terrestrialisation (e.g. Kenrick et al., 2012; Morris et al., 2018a). The less biased palynological record which documents the dispersed propagules of these earliest embryophytes extends the timing of terrestrialisation to at least the mid Ordovician (Rubinstein et al., 2010), although more equivocal spore evidence, some of which may be derived from algal – embryophyte transitional forms (Strother and Foster, 2021), may extend their emergence further back into the earlier Ordovician or Cambrian (Strother and Beck, 2000; Strother et al., 2004; Strother, 2016). Because of the paucity of the fossil record, molecular clock techniques are typically utilised to estimate the timing of terrestrialisation. While earlier molecular clock studies place the invasion of land by plants as far back as 1061±106ma (Heckman *et al*., 2001), more recent studies by Morris et al. (2018a) estimate that the living clade of land plants emerged between the mid Cambrian and Early Ordovician, with the living clade of tracheophytes emerging between the Late Ordovician and Silurian, with an 'explosive' radiation occurring in the Early Devonian (Kenrick et al., 2012).

The Ludlovian – Early Devonian rocks of southern Wales and the Welsh Borderlands, including the classic late Silurian – Early Devonian terrestrial Anglo-Welsh Basin sequence in Southern Britain has been instrumental in advancing the understanding of terrestrial ecosystems since the seminal

palaeobotanical work of Lang in 1937 (e.g. Lang, 1937; Jeram et al., 1990; Burgess and Edwards, 1991; Edwards et al., 1992, 1994; Honegger et al., 2013; Edwards and Kenrick, 2015). In particular, since Lang's (1937) description of *Cooksonia* and other 'plant' remains from the Anglo-Welsh Basin, a raft of palaeobotanical and palynological work documenting floral diversity, affinities and evolution has been presented from the basin (e.g. Richardson and Lister, 1969; Edwards, 1970; Edwards and Rogerson, 1979; Wellman et al., 1998b, 2000; Edwards and Richardson, 2004; Morris et al., 2011a, b, 2012a, 2018b). Moreover, the ± continuous terrestrial sequence straddles the Silurian – Devonian boundary, making it ideally placed to study of the nature of the adaptive radiation of vascular plants discussed by Kenrick et al. (2012). Indeed, important aspects of the evolution of plants have long been shown in exquisite detail (Edwards *et al*., 2014) from the basin, including vascular tissue and *in situ* spores (e.g., Edwards et al., 1992, 2014; Morris et al., 2011b, 2012a, 2018b).

As with the wider global fossil record, the macrofossil record of the Anglo-Welsh Basin is affected by taphonomic and facies biases (e.g. Edwards and Richardson, 2004), but has nonetheless demonstrated a wide diversity of land plants including diminutive rhyniophytoids such as *Cooksonia* (e.g. Edwards, 1970; Fanning et al., 1992; Morris et al., 2011a, 2012a), and larger zosterophylls. Moreover, the macrofossils hint at a floral turnover between these two groups in the Early Devonian (Morris and Edwards, 2014). The more widespread and taxonomically richer palynological record elucidates the pattern of floral development through the basin, with a radiation amongst one of the two major groups of spores (the trilete spores) being noted in early palynological work in the basin (Richardson and Lister, 1969). Further palynological work has further shown the taxonomic richness and morphological diversity of trilete spores, and has demonstrated the diversity amongst the other major group of spores (cryptospores), also (e.g. Richardson, 1996a, b, 2007; Burgess and Richardson, 1991, 1995; Wellman et al., 2000). The rapid diversification of spores through the sequence has facilitated the construction of detailed spore biostratigraphic schemes in the late Silurian and Early Devonian (e.g. Richardson et al., 1981, 1984, 2001; Richardson and McGregor, 1986; Richardson and Edwards, 1989; Burgess and Richardson, 1995), but the mid Přídolí remains problematic due to a dearth of suitable sampling horizons. Furthermore, the spore biostratigraphy around the Silurian – Devonian boundary remains unclear, owing in part to the difficulties associated with correlating terrestrial spore sequences with the pelagic type section at Klonk (e.g. Richardson et al., 1984; Edwards and Richardson, 2004).

A principal caveat of the dispersed spore record in that their parent plants and more nuanced affinities remain largely uncertain. The recovery of several sites of exceptionally preserved charcoalified mesofossils have been instrumental in beginning to harmonise this problem (e.g. Edwards et al., 1992, 2012, 2014; Morris et al., 2011b, 2012a, 2018b). In particular, the recovery of *in situ* spores from variously complete spore masses and sporangia have elucidated the sporangial morphology of several source plants (e.g. Wellman, 1999; Edwards and Richardson, 2000; Morris et al., 2011b, 2012a), revealed cryptic diversity (Wellman et al., 1998b) and evolution (Fanning et al., 1988) amongst morphologically simple spores and plants, and has shed new light on source plant affinities (e.g. Edwards et al., 2014) and hitherto unknown lineages of plants (Edwards et al., 2022a, b, c).

Key questions remain with respects to the nature of the diversification of trilete spores and cryptospores in the palynological record, in addition to the nature of their source plants and affinities with contemporary and modern flora. Furthermore, the regional spore biostratigraphy of the mid Přídolí (late Silurian) and earliest Lochkovian (Early Devonian) remains unclear, and correlation with the global Silurian – Devonian type section in Klonk remains untested. These themes are explored further in the proceeding literature review and underpin the research into the dispersed and *in situ* palynological record of the late Silurian – Early Devonian Anglo-Welsh Basin and immediately preceding strata presented in this research.

2. Introduction to the Late Silurian – Early Devonian World

2.1. Palaeocontinental Reconstructions and Palaeogeography

Interpretations of palaeocontinental reconstructions vary slightly for late Silurian – Early Devonian reconstructions (compare Torsvik and Cocks, 2016 and Boucott *et al*., 2013), but there is general agreement that two major landmasses, Gondwana and Euramerica, existed in the southern hemisphere (fig. 1), separated by the Rheic Ocean.

Gondwana, the larger of the two continents, lay in the higher latitudes of the southern hemisphere and comprised southern and northern Africa, south America and Antarctica, amongst other continental blocks (Torsvik and Cocks, 2016). Gondwana was the largest and oldest landmass on Earth at the time, having amalgamated in the Ediacaran and Cambrian (e.g. Pisarevsky *et al*., 2008). In contrast, the smaller continent of Euramerica, which lay to the north of Gondwana in the lower latitudes of the southern hemisphere, had only recently amalgamated during the mid Silurian (Torsvik and Cocks, 2016). The amalgamation involved the palaeocontinents of Laurentia, Baltica and Avalonia, and involved the closure of the Iapetus Ocean. The exact mechanisms and sequence of unification are uncertain, with some workers (e.g. Cocks and Torsvik, 2002) suggesting an initial collision between Avalonia and Baltica (*ca*.440ma), followed by a parallel collision with Laurentia *ca*.425-420ma. Others (e.g. Dewey and Strachan, 2003), postulate that Laurentia and Baltica collided first, *ca*.435-425ma, with Avalonia colliding via oblique sinistral transtension *ca*.425ma.

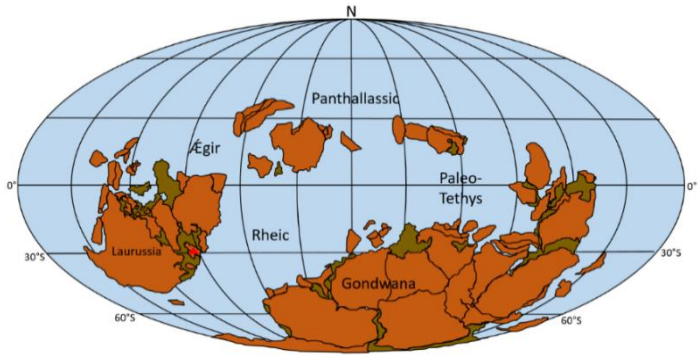

Figure I-1 Palaeocontinental reconstruction of the late Silurian – early Devonian world. Two major continental landmasses, Gondwana and Euramerica, existed at this time, both largely in the southern hemisphere. Gondwana, to the south, is separated from Euramerica by the Rheic Ocean. Red triangle indicates the approximate location of Britain, on the southern edge of Euramerica. Map modified from Torsvik and Cocks (2016).

Irrespective, the closure of the Iapetus Ocean in the mid Silurian was driven by the Caledonian orogeny, an extensive mountain building episode that developed along the Iapetus suture within Laurussia during the continental amalgamation. Caledonian uplift and mountain building resulted in extensive terrestrial sedimentation across Laurussia, commencing in the late Llandovery of Scotland (Friend *et al*, 2000), and continuing into the Early Devonian across the continent. The Anglo-Welsh Basin developed from Caledonian and later Acadian inversion of the lower Palaeozoic Marine Welsh Basin (Kendall, 2017), which lay along the southern margin of Euramerica, between the Caledonian mountain chain and the Rheic ocean. Marine sedimentation was gradually replaced by quasi-marine and then fully terrestrial sedimentation, which initiated in the south west of the Anglo – Welsh Basin in the Ludlow in south Pembrokeshire and Carmarthenshire (Barclay *et al*., 2015). Basin wide sedimentation had commenced by the Přídolí, as sea levels continued to fall and the shoreline retreated southwards (Cope *et al*., 1992; Barclay *et al*., 2015), with littoral and alluvial environments following the retreat (Bassett *et al*., 1982; Bluck *et al*., 1992).

2.3. Palaeoenvironment

Atmosphere

The proportions of atmospheric CO_2 and O_2 through geological time can be estimated from geochemical models (based on certain geochemical cycles) and from proxies, or elements within the earth system,

whose development has a covariant relationship with atmospheric CO_2 and O_2 fluctuations through Earth history (Royer, 2014).

Three principal box models are available to predict atmospheric oxygen concentration (pO_2) in the Palaeozoic; the GEOCARBSULF model (Berner et al., 2009), the COPSE-reloaded model (Lenton et al., 2018), and the GEOCARBSULFOR model (Krause et al., 2018). These models all support a steep rise in pO_2 in the mid Ordovician, and a subsequent decline initiating in the early Devonian (Lenton et al., 2018). The pO_2 estimations derived from the GEOCARBSULF and GEOCARBSULFOR models between the Ordovician and Devonian are roughly comparable, with some difference in the estimations from the COPSE-reloaded model (Glasspool and Gastaldo, 2022). Charcoal is an effective proxy for indicating pO_2 at the time of burning (Belcher et al., 2010; Glasspool, 2015), providing a minimum threshold required for sustained burning (Belcher and McElwain, 2008), which is 16% pO_2, or 0.75 of present atmospheric oxygen level (PAL) (Cope and Chaloner, 1980; Chaloner, 1989), and constraining pO_2 in the range of 0.7 – 1.4 PAL (Belcher et al., 2010). As such, the occurrence of charcoal can be used to test the efficacy of the above models, although fire data across long intervals are preferred for testing the model estimations, given the coarse resolutions of the models (Glasspool and Gastaldo, 2022).

Charcoal deposits are known from Silurian – Early Devonian alluvial and marine deposits (e.g. Glasspool *et* al., 2004, 2006; Glasspool and Scott, 2010; Glasspool and Gastaldo, 2022) , with the fire window recently being pushed back to 430 Ma by Glasspool and Gastaldo (2022). The recovery of charcoal from the mid Silurian indicates that the minimum burn pO_2 had been attained (16%) by this time, which is at odds with the GEOCARBSULFOR and COPSE-reloaded models, the former placing pO_2 at <15%. Furthermore, the minimum burn threshold was not considered by Glasspool and Gastaldo to be sufficient to ignite and self-sustain burning of the homiohydric, diminutive rhyniophytic and nematophytic vegetation, which necessarily grew in moist settings. Indeed, Belcher et al. (2010) suggested that a pO_2 of >18% would be required to burn the vegetation, unless the area was seasonally very dry, the fuel was dry and/ or there was very low rainfall. As such, the estimates for the GEOCARBSULFOR and COPSE-reloaded models do not accurately estimate the pO_2 of the atmosphere at the time of burning (fig. 2a, b), with the best estimates being predicted by the Berner (2009) model.

The GEOCARBSULFvolc model (which models CO_2 and O_2 based on Carbon and Sulphur cycles), demonstrates that atmospheric oxygen levels typically varied between 15% and 23% in the early Palaeozoic, with a dramatic increase from *ca.*15% to *ca*.26% between the Ordovician and Devonian, with a near-peak atmospheric Oxygen concentration of *ca.*25% occurring around the Silurian – Devonian boundary (fig. 2a, b).

Theoretical models (e.g. Berner, 1994, 2006a) and proxies indicate that Palaeozoic atmospheric CO_2 concentration was significantly higher than at present, and intense fluctuations of atmospheric CO_2 were common during the earlier Palaeozoic. Atmospheric CO_2 proxies including calcretes (e.g. Mora *et* al., 1991; Driese *et al*., 2000) indicate that there was a significant atmospheric CO_2 high across the Silurian – Devonian boundary. This is concordant with the GEOCARBSULFvolc model which similarly implies a zenith in the rise of atmospheric CO_2 in the Late Silurian – Early Devonian from *ca.*1500ppm in the Late Ordovician to some 3000ppm at the Silurian - Devonian boundary, the largest peak in atmospheric CO_2 since the mid Cambrian. This peak represents the last point in earth history (thus far) where atmospheric CO_2 exceeded 3000ppm and precedes an interrupted decline to present day atmospheric CO_2 levels.

Continued research has successfully linked atmospheric CO_2 and global temperatures through much of the Phanerozoic (e.g. Berner, 1991; Came *et al*., 2007; Crowley and Berner, 2001), with high proportions of atmospheric CO_2 typically leading to hot house conditions, and low atmospheric CO_2 leading ice house conditions. Following this, the Silurian – Devonian boundary is postulated to have been associated with a hot house climate, with temperatures increasing through the latter half of the Silurian and reaching a peak average temperature of *ca.*25°C. During the Late Silurian – Early

Devonian, a relatively high and well-defined global climate gradient was established (Boucott, 1988). A tropical belt existed along the paleoequator, with wide arid belts extending beyond 30°S. Cool temperate and cold belts existed at increasing latitudes southwards (Boucott *et al*., 2013).

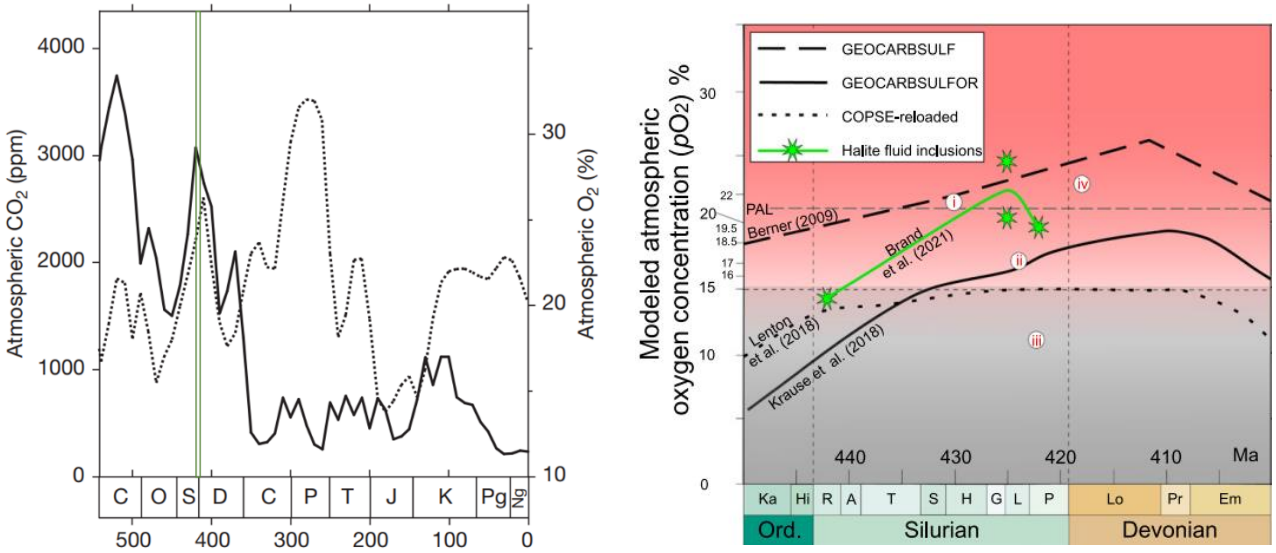

*Figure I-2: (**left**) Atmospheric Carbon Dioxide (solid line) and Oxygen fluctuations (dashed line) through the Phanerozoic, based on the results given by the GEOCARBSULFvolc model. Atmospheric CO_2 was high and fluctuating during the former half of the Palaeozoic and was experiencing a peak of 3000ppm at the Silurian - Devonian boundary (indicated by the green box). Similarly, atmospheric O_2 was experiencing a high at this boundary of* ca.*26%, and continued to rise through to the mid Devonian, prior to falling once more towards the end of the period. Both atmospheric CO_2 and O_2 were present in significantly higher proportions than in the present atmosphere. Figure modified from Royer (2014) - CO_2 history is from Berner (2008), O_2 history is from Berner (2009). **(right)** GEOCARBSULF, GEOCARBSULFOR and COPSE-reloaded models indicating estimations for* pO_2 *between the Ordovician and Devonian. Numbered circles indicate temperatures attained by fires producing certain localities; **i:**Rumney (UK), **ii:** Winnica (Poland),; **iii:** Ludford Lane (UK); **iv:** North Brown Clee Hill (UK). All indicate that* pO_2 *should be a minimum of 16%. Modified from Glasspool and Gastaldo (2022)*

Climate

During the late Silurian and early Devonian, much of Laurussia lay in an arid belt (Scotese 2009; Torsvik and Cocks, 2016), with the Anglo-Welsh basin residing 17˚S±5˚of the paleoequator (Channel *et al*. 1992) (fig. 3), close to the southern margin of the arid belt (Boucott *et al*., 2013). While southern Euramerica lay within an arid belt, local climate in the Anglo-Welsh Basin appears to have been chiefly semi-arid, with well-developed wet and dry seasons (Allen, 1974; Marriott and White, 2004) through the late Silurian – Early Devonian, which were possibly related to orogenic relief rainfall or monsoonal cyclicity (Hillier et al., 2007; Morris et al., 2012b).

3. Geology of the Anglo – Welsh Basin

3.1. The Late Silurian – Early Devonian of the Anglo–Welsh Basin

Tectonic Setting

The Lower Old Red Sandstone of the Anglo – Welsh basin was deposited in an extramontane, tectonically active depocentre. The development of the Lower Old Red Sandstone is bracketed by the Caledonian orogeny and the Variscan Orogeny (Friend *et al*., 2000), which occurred in the Silurian and Mid-Devonian respectively, and is influenced by the mid Devonian Acadian Orogeny (Torsvik and Cocks, 2004).

The Silurian closure of the Iapetus Ocean and the resulting Caledonian orogeny is postulated to have initiated Anglo Welsh Basin Formation through load induced flexural subsidence of the Avalonian

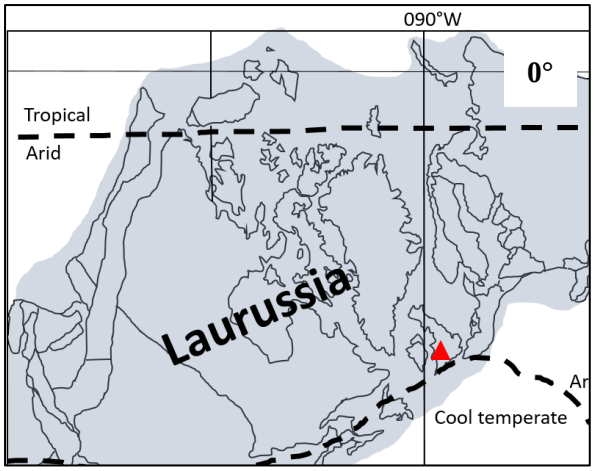

Figure I-3: Line map illustrating the distribution of climate bands across Euramerica in the early Devonian. A tropical band covers the paleoequator and some of northern Euramerica, but much of Euramerica down to the southern coast is contained within an arid belt. A small proportion of Euramerica is covered by a cool temperate belt. Dashed lines indicate limits of climatic bands; grey mass indicates paleo-landmasses, white areas indicate paleo-oceans; red triangle indicates position of Anglo-Welsh Basin at 17°S±5°; solid outlines indicate extents of modern countries. Map modified from Boucott et al. (2013).

foreland (James, 1987; King, 1994; Friend *et al*., 2000), although other workers (e.g. Dewey and Strachan, 2003; Soper and Woodcock, 2003) prefer basin wide, sinistral mega-shearing as a basin forming mechanism.

Initial local sedimentation began in the Ludlow of South Pembrokeshire and Carmarthenshire, with basin wide sedimentation commencing by the Přídolí (Barclay *et al*., 2015). Subsidence was not continuous from the Ludlow to Late Emsian and an extended, basin wide quiescent period occurred in the Early Devonian, allowing thick palaeosols to develop (Allen, 1974; 1985). Shifts in sediment provenance appear to indicate a basin wide tectonic transition from flexural subsidence to sinistral transtensional regimes and the development of half grabens (Crowley *et al*., 2009), an event that is likely to have significantly influenced drainage patterns across the alluvial plain. Synsedimentary extensional and transpressional faulting is postulated to have occurred across the basin and is thought to have been especially active in Pembrokeshire during the Late Silurian – Early Devonian (Barclay *et al*., 2015). The minor faulting events occurring across the basin may have periodically developed isolated subbasins throughout Lower Old Red Sandstone deposition (Crowley *et al*., 2009). Seismic events are posited to have occurred during the deposition of the Lower Old Red Sandstone, with soft sediment deformation indicating seismically induced liquefaction in some Early Devonian sediments (Owen, 2016). Deposition of alluvial material continued until uplift from the proto-Variscan Acadian Orogeny terminated Lower Old Red Sandstone deposition and the subsequent development of the Acadian unconformity in the Late Emsian (Barclay *et al*., 2015).

There was no proximal volcanic activity during Lower Old Red Sandstone deposition, however, layers of distal air fall tuffs derived from plinian style volcanic ejecta are found within the basin, the primary outcrop being the Townsend Tuff Bed (Allen and Williams, 1981).

Structure of the Anglo Welsh Basin

Much of the surface outcrop of the Anglo Welsh Basin is confined to the south-east of Wales, but proven boreholes indicate the basin extends in the subsurface across south-east England (Chaloner and Richardson, 1977) reaching a maximum spatial extent of *c*.20 000km^2 (Allen and Williams 1981, 1982), but outliers such as those in Anglesey and the Lake District may indicate that the basin had a greater spatial extent than is now exhibited. Alternatively, these outliers may also have been small, isolated internal basins which formed within the orogen during the Early Devonian (Friend *et al*., 2000).

The main body of the Lower ORS outcrop is largely constrained by the Welsh Borderland Fault System (constituting three main elements – the Tywi, Pontesford and Church Stretton lineaments - Woodcock and Gibbons, 1988) in the north, by the Malvern Lineament in the south-east, and in the south by the Variscan front (fig. 4). In the South-west, the Benton Fault represents an important northern border for the Lower ORS.

The Welsh Borderland Fault System is an important regional feature, trending in a similar manner to other major fault systems across the United Kingdom. All three of the major constituent elements of the Welsh Borderland Fault System were reactivated during the Early Devonian (Woodcock and Gibbons, 1988), and there are tentative spatial relationships between these and seismically derived soft sediment deformation (Owen, 2017). The faulting is also postulated to have strongly influenced sedimentation patterns and deposition, and this is demonstrated clearly in the south-west, where the ESE-WNW trending Benton and Ritec faults clearly affect the Lower ORS (Powell, 1987, 1989; Woodcock and Gibbons, 1988).

The Lower ORS has been variously folded and cleaved by contemporaneous and later orogenic events, including the Acadian Orogeny which developed a regional cleavage and unconformity, and later Variscan folding that developed during the Carboniferous.

The thickness of the Anglo-Welsh Basin is variable. The thickest regions are found in the south west, where they range between 3.4km to over 4km in the hanging wall of the Benton fault (King *et al*., 2000) and are thickest north of the Ritec Fault near Pembrokeshire, reaching 4.3km (Friend *et al*., 2000). Elsewhere in the central and eastern regions, the Old Red Sandstone has a mean thickness of 1.7km and a maximum thickness of 2.3km (Friend *et al*., 2000).

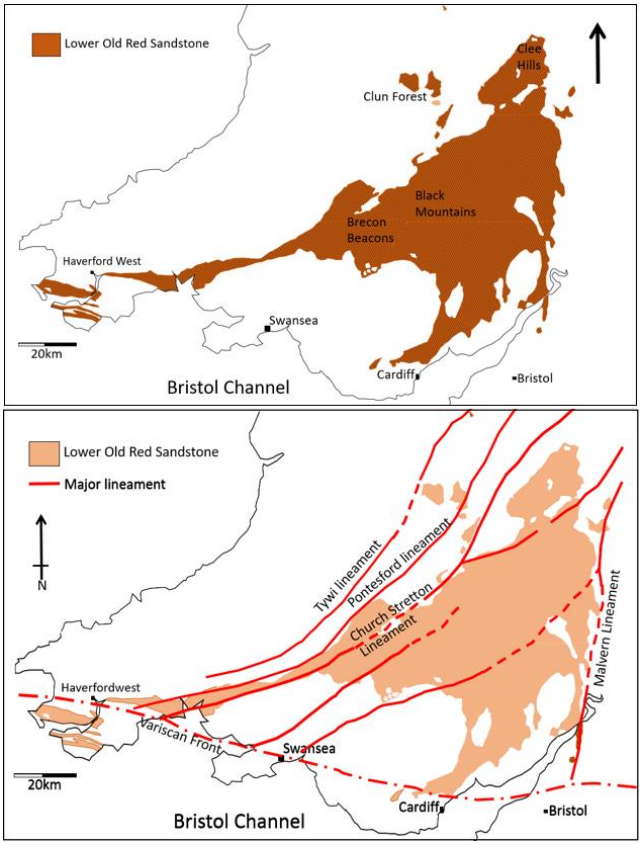

Figure I-4 The spatial extent of the Lower ORS (Přídolí to Lochkovian) of the Anglo-Welsh Basin. Much of the basin outcrops in the central and eastern regions of Wales, and extends towards Pembrokeshire in the south west, Cardiff in the south and Clee Hills in the north. Outliers exist in Clun Forest, North Devon and the Lake District, and these may either indicate a once wider spatial extent to the basin, or may represent isolated subbasins. The Welsh Borderland Fault system largely constrains on the basin. Modified from Wellman et al. (*2000*).

Stratigraphy

Despite, or perhaps partly because of, the classic nature of the Anglo-Welsh Basin, the stratigraphic nomenclature of the area has until recently been complicated. The large body of work carried out prior to the introduction of formal stratigraphical procedures resulted in an unsystematic naming system and additional further work, whilst greatly improving local stratigraphic resolution, has resulted in a plethora of local names that impedes simple lithostratigraphic correlation across the basin. Following this, Barclay *et al*. (2015) erected a new naming scheme for the various groups, subgroups and some formations in the Anglo-Welsh Basin in an attempt to formalise the nomenclature across the basin (figs. 5, 6). Subsequently, Barclay *et al*. (2015) have divided the overall ORS succession into two main

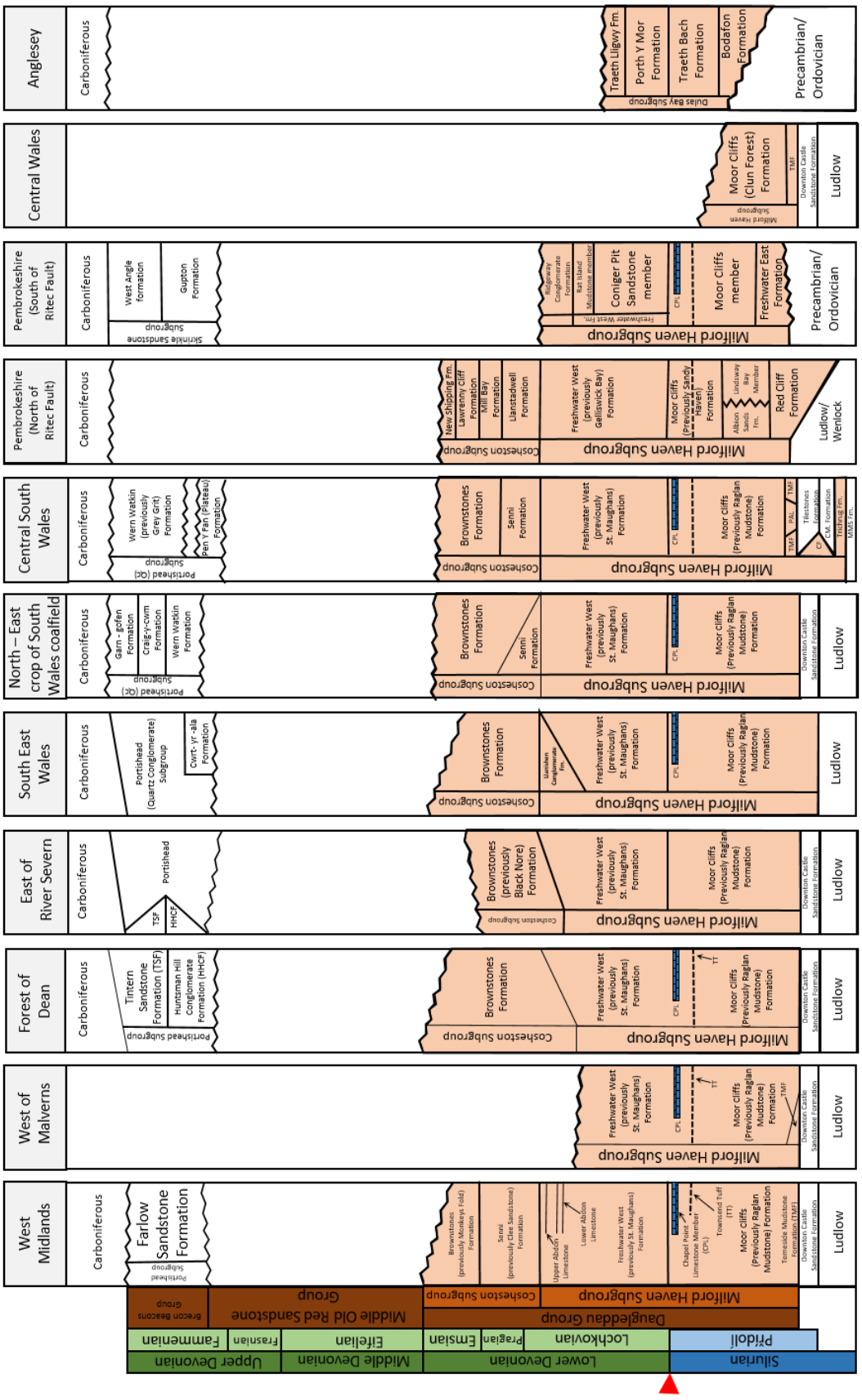

Figure I-5: The stratigraphy of the Old Red Sandstone in the Anglo-Welsh Basin. The Lower Old Red Sandstone is shaded pale brown and extends from the Přídolí to the Emsian. The basin conformably overlies the Palaeozoic welsh marine basin and is capped by the Acadian unconformity. The Lower ORS is encompassed by the Daugleddau Group, which is further subdivided into the Milford Haven and Cosheston subgroups. The older divisions of Downtonian, Dittonian and Breconian have been removed in this version. Modified from Barclay et al.*, 2015*

groups: the Brecon Beacons Group, which encompasses successions of Late Devonian material (informally the Upper ORS), and the Daugleddau Group, which includes successions of late Silurian – Latest Early Devonian material (informally the Lower ORS) (Barclay *et al*., 2015). There is no mid

Devonian succession in the Anglo-Welsh Basin, with the Brecon Beacons Group laying unconformably on the Daugleddau group, separated by basin-wide Acadian unconformity.

Following a general consensus that the Lower ORS should commence at the onset of the first major red or green terrestrial facies, Barclay *et al*. (2015) redefined the base of the Lower ORS in the Anglo-Welsh Basin. Traditionally (Stamp, 1920, 1923; Allen and Tarlo, 1963) the Downton Castle Formation and regionally correlative Tilestones Formation, were regarded as the basal formations of the Lower ORS of the Anglo-Welsh Basin, however they have been reconsidered on the basis of their shallow marine associations. Given, *inter alia*, that they do not represent continental material (Allen and Tarlo, 1963) and additionally represent marine transgressions, it seems unsuitable to use them as the base of the Lower ORS and following this, the Temeside Mudstone, Red Cliff and Freshwater East Formations have been designated as the basal formations of Lower ORS in the Anglo-Welsh Basin (Barclay *et al*., 2015). Some workers (e.g. Turner *et al*., 2017) have raised concerns regarding the exact nature of boundary definition and also regarding the addition of more nomenclature to an already confused system. The BGS has since adopted the revised stratigraphy outlined in Barclay *et al*., (2015), and it is the one used here.

The Přídolí – Lochkovian Anglo-Welsh Basin succession principally comprises the Moor Cliffs, Freshwater West and Brownstones formations. These develop upwards through a variety of dryland alluvial settings, and a number of important marker beds exist in the earlier parts of the succession, and these are recognisable across much of the basin. The Townsend Tuff is a significant, basin wide marker bed in the Moor Cliffs Formation which is laterally extensive in the Přídolí of Pembrokeshire (north and south of Ritec Fault), the Black Mountains, Forest of Dean and Clee Hills (Allen and Williams, 1981); the horizon appears to be absent from some successions however, including those east of the River Severn and the north-east crop of South Wales (Barclay *et al*., 2015). Composed of three closely related distal air fall tuffs with characteristic internal stratigraphy (Allen and Williams, 1981), it was produced by distal, plinian eruptions from volcanic centres 100 – 200km away, east or west of the basin (Allen and Williams, 1981), produced by eruptions broadly similar to Santorini (Bond and Sparks, 1976).

Lying above the Townsend Tuff Bed in the earliest Lochkovian is the Chapel Point Limestone (previously the Bishop's Frome Limestone, Chapel Point Calcrete in Pembrokeshire and *Psammosteus* limestone in the Welsh Borderlands), a well-developed, pedogenically formed regional marker horizon. Terminating the Moor Cliffs Formation (Raglan mudstone) the Chapel Point Limestone is a thick sequence of calcrete horizons (Love and Williams, 2000) characterised by high maturity (contrasting with most other calcrete horizons in the basin – e.g. Allen, 1986) and erosional top surfaces, and is postulated to represent a long period of tectonic quiescence and landscape stability (Love and Williams, 2000). The calcrete horizon extends laterally across much of the Lower ORS, south and east of the Ritec Fault, however, it is absent from the successions north of the Ritec Fault (Allen and Williams, 1978) in Pembrokeshire.

The Lower ORS continues upwards without any major unconformities through the rest of the Silurian and Early Devonian, into the Emsian, where the Lower ORS is unconformably juxtaposed against the Upper ORS at the Acadian unconformity (Barclay *et al*., 2015).

The terrestrial nature of the Lower ORS in the Anglo-Welsh Basin presents profound difficulties for biostratigraphic correlation and analysis. Namely, the low preservation potential for organisms, a typical problem for terrestrial strata, is a major factor in reducing the number of stratigraphically useful remains (Barclay *et al*., 2015). Furthermore, the near-complete terrestrial nature of the succession precludes the use of other widely used zone fossils, namely those confined to the marine realm, when correlating strata and determining ages. Because of this, well established Late Silurian – Early Devonian marine fossil zones including graptolites, ammonoids, brachiopods, conodonts and some fish and microvertebrates cannot be used (Barclay *et al*., 2005a), and the basin cannot be easily correlated with the Silurian – Devonian type section at Klonk. Furthermore, within the terrestrial material comprising

the lower part of the Lower ORS there is a dearth of well-preserved, stratigraphically useful flora and fauna (Love and Williams, 2000).

Despite these limitations, extensive and largely successful biostratigraphic work has been carried out on the Anglo-Welsh Basin and presently the biostratigraphy of the basin is based on spore and fish biozones (White, 1961; Richardson and McGregor, 1986) (fig. 6).

Vertebrate fossils provide excellent biostratigraphic tools and following the classic work on Silurian and heterostracan pteraspidomorph biozonation by White (1935, 1950 a, b, 1961) and Ball and Dineley (1961) in the Anglo-Welsh Basin, an initial vertebrate biozonation scheme for the Late Silurian – Early Devonian was devised. Important modifications were made by Turner (1973, 1978) with the addition of the Devonian agnathan thelodont *Turinia pagei*. Further revision of the vertebrate biozones was made by Blieck and Janvier (1979) in which the range biozones of *Traquairaspid pococki* and *T. symondsi* and the assemblage biozones of *Protopteraspis leathensis, Rhinopteraspis crouchi, Althaspis leachi and R. dunensis* were modified into interval biozones. Currently, the *Traquairaspid* biozones is considered as one, the *P. leathensis* zone was changed to the *Protopteraspis zone* following the work of Blieck and Tarrant (2001), and an additional *Pteraspis rostrata* zone was added; *crouchi* and *leachi* remain the same. The *R. dunensis* zone is considered by Blieck and Elliot (2017) to be in need of redefinition, but currently remains as before. The ORS of the Anglo-Welsh Basin primarily uses pteraspidids and thelodonts for vertebrate biozonation and correlation. Thelodonts are important biostratigraphic

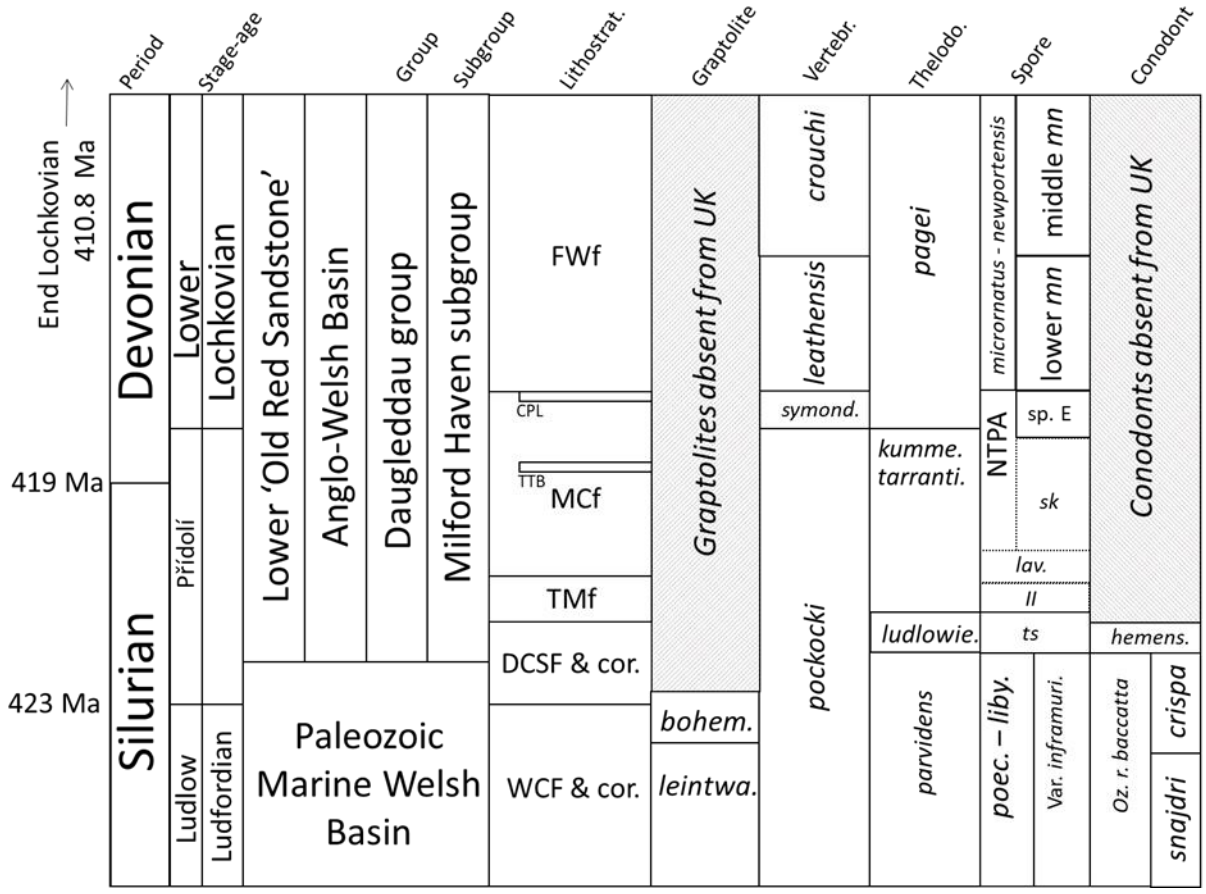

Figure I-6: Generalised lithostratigraphy and biostratigraphy of the portion of the Anglo-Welsh Basin succession studied in this work. Modified from Barclay et al. (2015). ***Ludl.*** *= Ludlow;* ***Ludf.*** *= Ludfordian. Ludlow – Přídolí date from Catlos et al. (2020) zircons in the Ludlow Bone Bed. Other dates from Gradstein et al. (2012).* ***WCF & cor:*** *Whitcliffe formation and correlatives;* ***DCSF & cor:*** *Downton Castle Sandstone formation and correlatives;* ***TMf:*** *Temeside mudstone formation;* ***MCF*** *Moor Cliffs formation;* ***TTB:*** *Townsend Tuff Bed;* ***CPL:*** *Chapel Point Limestone member;* ***FWf:*** *Freshwater West formation. Chart modified from Barclay et al., 2015 (lithostratigraphy), Edwards and Richardson, 2004)spore biozones), Burgess and Richardson, 1995 (Graptolites) and Marrs and Miller, 2004 (Conodonts).*

controls through the Silurian and into the early Devonian, with *Tu. pagei* dominating assemblages from what may be the base of the Lochkovian through to the Pragian, where thelodonts disappear from British assemblages (Turner *et al*., 2017). Pteraspidomorph biozones outlined above are also important, and together the biozonation scheme has been successful in correlating Early Devonian successions across the Laurussian continent in Spitsbergen, the U.S.A., Arctic Canada and the Baltic States, amongst others (references in Blieck *et* al., 2002). There is a dearth of fish fossils in the south and south-west of the Anglo-Welsh Basin, and even in areas with vertebrate fossils, spore biozones form an important part of biostratigraphy in the area.

Work began on determining spore zones in the Anglo-Welsh Basin quite sometime after the establishment of vertebrate biozonation schemes. Initial descriptions into Silurian and Devonian spores in basins across England, Scotland and Wales by Richardson (1967) led to initial spore assemblage construction in these areas. Richardson and Lister (1969) carried out spore sequence descriptions and recognised time-controlled changes in spore assemblages in the Anglo-Welsh Basin and by the 1980s Silurian and Devonian spore biozones were synthesised and erected for much of the northern hemisphere (Laurussia) (Richardson, 1974; Richardson *et al*., 1984). Adjacent regions were integrated into this synthesis shortly after (Richardson and McGregor, 1986), and the biozones erected by Richardson and McGregor (1986) for the British ORS, and European ORS (Streel et al., 1987) largely hold today, but uncertainty surrounding the mid Přídolí – earliest Lochkovian spore assemblages persists.

The IUGS subcommission defined the Devonian GSSP in the pelagic realm which, while a standard practice, introduces profound difficulties when correlating between marine, continental and intergradational sequences (Becker and Kirchgasser, 2007). Because the correlation of Devonian sequences relies heavily on, *inter alia*, the available fossil record, correlation between the continental facies of the Anglo-Welsh basin and the wider, often marine sequences, of the Old Red Sandstone continent has traditionally been fraught with difficulties derived mostly from the substantial variability in facies and concomitant fossil record. This variability gives rise to the preservation of very different suites of potential zone fossils, with very few recognisable across multiple facies belts (Becker and Kirchgasser, 2007). Since the 1960s, increasing interest in terrestrial marine sections began to reconcile some of the correlative difficulties between marine and non-marine environments, as the ability of spores to be washed into the marine settings from terrestrial environments gives a level of facies independence (Richardson and Lister, 1969). This goes some way towards reconciling the problems associated with correlating environmentally variable sequences. Work by Richardson and McGregor (1986) on sporomorph sequences in the Anglo-Welsh Basin, and contemporary work by others (Streel, 1986; Streel *et al*., 1987; Steemans, 1982) in the Lower ORS of the Ardennes – Rhenish and Rhineland regions show that the separate biozonal schemes are relatively harmonious between continental and shallow marine settings. Problems do still exist however, and the correlation between more proximal and deeper marine settings remain due to ever increasing palaeoecological contrasts and taphonomic biases between these settings. Whilst the issues with correlating Devonian continental sequences with the overall IUGS timescale remain, more recent work has identified similarities between fish taxa found in the Anglo-Welsh Basin and marine sequences in similarly aged areas such as Russia and Spain. Following the identification of these relationships, terrestrial spore and fish biozones can be equated with Devonian conodont zonation schemes used in the standard IUGS timescale (Turner *et al*., 2017), an important step towards reducing correlative ambiguities between palaeoenvironments.

The position of Silurian - Devonian boundary in the Anglo-Welsh Basin has long been contentious, largely because of the correlative difficulties between marine and non-marine strata outlined above. Allen and Williams (1981) postulated that the Townsend Tuff Bed may lay close to the Silurian - Devonian boundary i, close to the top of the Moor Cliffs (previously Raglan Mudstone) Formation, but the tuffs cannot be currently related to either palynomorph or vertebrate schemes (Edwards and Richardson, 2004). Turner (1973) correlated the first appearance datum (FAD) of *T. pagei* with the FAD of key graptolite species (*Monograptus uniformis uniformis*) in Podolia and postulated that the

FAD *T. pagei* in the Anglo-Welsh Basin may indicate the onset of the Devonian there, which occurs 33m below the Chapel Point Limestone. The Townsend Tuff bed resides some 133m below the Chapel Point Limestone, suggesting that it is well below the FAD of *T. pagei* and the postulated onset of the Devonian. A spore biozone, the so called Biozone B/ *Apiculiretusispora* sp. E zone, corresponding to the FAD of *T. pagei* and therefore indicating the onset of the Devonian has been variously alluded to (Richardson et al. 1981, 1984; Richardson and Edwards, 1989; Edwards and Richardson, 2004), but this has not been fully described or tested. As such, a remaining challenge for the spore biozonation schemes in the area has been to circumscribe this zone.

3.2. The Přídolí – Lochkovian of the Anglo – Welsh Basin

Přídolí – Lochkovian strata are widely distributed between Haverfordwest, Clee Hills and Newport (fig. 4) and represent a large proportion of the exposed lower Old Red Sandstone of the Anglo-Welsh Basin. Stratigraphically, the Přídolí – Lochkovian is equivalent to Barclay *et al*. (2015)'s Milford Haven Subgroup, forming a significant proportion of the Daugleddau group and covers a time span of *ca*.20 myr. The sequence is continuous in most areas from the Ludlow termination of the Palaeozoic Welsh Marine Basin (?Downton Castle Sandstone Formation), where earlier marine sediments give way to the red bed sequences of terrestrial Lower ORS. In some other areas, such as in Pembrokeshire (south of the Ritec Fault) a distinct unconformity is developed, with the Milford Haven Subgroup resting unconformably on Ordovician sediments and Precambrian basement (fig. 5). The Milford Haven Subgroup is principally composed of two major formations (figs. 5, 6): the Moor Cliffs Formation (previously the Raglan Marl), and the Freshwater West (previously St. Maughans) Formation, with several other more minor, laterally discontinuous and locally prevalent formations and members. Conformably below the Moor Cliffs Formation are, *inter alia*, the Downton Castle Sandstone Formation and Whitcliffe Formation and their lateral correlatives. These do not form part of the Anglo-Welsh Basin *sensu* Barclay et al. (2015).

The Milford Haven subgroup is mostly well correlated across the basin with the prevalent Townsend Tuff Bed and Chapel Point Limestone extending across large areas of the Upper Moor Cliffs Formation.

The Milford Haven Subgroup comprises several biostratigraphic zones of both vertebrates (heterostracan pteraspidomorphs and thelodonts) and spores. The subgroup corresponds to the *Pococki* zone in the Přídolí and evolves into the *symondsi*, *leathensis*, *crouchi* and *leachi* vertebrate zones through the Lochkovian. The Spore zonation is less clear in the Přídolí. The *tripapillatus-spicula* zone comprises the lowermost Přídolí, but much of the middle of the stage is yet to be adequately divided into distinct spore biozones. Similarly, the earliest Lochkovian is somewhat unclear, with the enigmatic *Apiculiretusispora* Species E zone being the initial biozone, the base of which remains poorly defined. This zone is then succeeded by the well-established *micrornatus-newportensis* biozone and associated subzones (lower, middle and upper *micrornatus-newportensis*) and the *breconensis-zavallatus* zone, which terminates the Lochkovian stage.

The sedimentology of the Anglo-Welsh Basin varies through time, and a brief summary of each Formation is given here, pending future fieldwork. The Lower ORS of the Anglo-Welsh Basin represents a near continuous succession of terrestrial strata, with no major unconformities within the Lower ORS itself.

Whitcliffe Formation and correlatives

The Whitcliffe Formation occurs in the Welsh Borderlands, with regional correlatives occurring in South Wales. The sediments are broadly similar, comprising dark grey siltstones with terrestrial and marine derived fossils, including brachiopods (e.g. Basset, 1974), palynomorphs (Burgess and Richardson, 1995) and charcoalified nematophytes (Glasspool and Gastaldo, 2022). These sediments are interpreted to have been deposited in nearshore, shallow marine shelfal settings in the Ludlow, and the palynological assemblages are comparable to the *poecilomorphus – libycus* zone.

Downton Castle Sandstone Formation

The sediments of the Downton Castle Sandstone Formation have been interpreted as being deposited in a near shore marine environment as part of a wave dominated deltaic system during a brief period of marine transgression. The sequence is an argillaceous to arenaceous 'cleaning up' sequence, coarsening upwards from grey mudstones to yellow sandstones. The palynological assemblage is indicative of the *tripapillatus – spicula* biozone (early Přídolí).

Temeside Mudstone Formation

Chiefly green mudstones with subordinate lenses of micaceous sandstones. Calcrete glaebules are prevalent throughout the Formation and scattered vertebrate bone fragments and lingulid brachiopods are found in the sandstones (Barclay *et al*., 2015). Fuller descriptions are given by White and Lawson (1989).

Moor Cliffs Formation

The Moor Cliffs Formation, which until Barclay *et al*. (2015)'s stratigraphic revision was widely referred to as the Raglan Mudstone Formation, is principally composed of chiefly red, but also some green, mudstones and siltstones. Subordinate fine sandstone horizons and occasional exotic conglomerates are also found. The Formation is rich in variously well-developed calcrete associations, ranging from poorly developed calcrete glaebules to thick, well-developed calcrete horizons, especially near the top of the Formation (Chapel Point Limestone Member). Throughout the sequence laterally continuous distal air fall tuffs are found, including amongst others the Townsend Tuff Bed (Allen and Williams, 1981). The Formation is approximately equivalent to the early Přídolí and earliest Lochkovian.

Freshwater West Formation

The Freshwater West Formation (previously widely referred to as the St. Maughans Formation) lies conformably above the Moor Cliffs Formation. It is broadly composed of red, fine to medium sandstones with calcrete-bearing mudstones and intraformational conglomerates dispersed throughout. The sedimentary associations vary across the basin, with alluvial cycles of sandstones, siltstones and mudstones dominating the area around Pembrokeshire, and fluvial cycles in the Welsh Borders. Variously developed calcrete associations are common across this Formation, but well-developed calcretes are patchier and less laterally extensive than in the Moor Cliffs Formation. The Formation is approximately equivalent to the early (not: earliest) Lochkovian to late Lochkovian.

3.3. Anglo-Welsh Basin Přídolí-Lochkovian palaeontology

As previously mentioned, the poor preservation potential of terrestrial strata leaves little likelihood for well-preserved fossils, and the same taphonomic biases have also had an effect on the fossil record of the Anglo-Welsh Basin. Whilst much of the record here is made up of fragmentary, disarticulated remains with far rarer articulated remains resulting from unfavourable taphonomic conditions, a rich diversity of vertebrates, invertebrates, ichnofossils and plants have nonetheless been recovered from the Anglo-Welsh Basin, and a brief review of the most common taxa found in the Přídolí – Lochkovian is given here.

Fragmentary remains of fish, including scales, armour plates and spines are abundant throughout the Přídolí and Lochkovian of the basin. The first fossil fish species from the succession were described by Agassiz in the early 19th century. These Heterostracans, *Pteraspis rostratus* (Agassiz, 1835) were the first of many to be described over the next few centuries, showing a high diversity through the Přídolí and Lochkovian (e.g. Miles, 1973; Dineley and Metcalf, 1999). Additionally, an abundance of osteostracan fish has also been described from the area (e.g. Tarrant, 1991; Keating *et* al., 2012) with their inception in Britain from the late Silurian (Dineley and Metcalf, 1999). The combined

heterostracan and osteostracan abundances of the Anglo-Welsh Basin are significantly greater than in contemporaneous Lower ORS basins in Scotland (Newman *et al*., 2017). Other Agnathan fish, including abundant Thelodont assemblages have also been extensively studied (e.g. Allen *et al*., 1968; Turner, 1978), with thelodonts such as *T. pagei* dominating the Anglo-Welsh Lower ORS. In line with heterostracan and osteostracan assemblages, Thelodonts show a greater diversity relative to contemporaneous basins in Scotland (Newman *et al*., 2013). Gnathostomes (jawed fish) have received less attention than Agnathans (Newman *et al*., 2017) and the Gnathostome fossil record is largely composed of fragmentary remains. Placoderms are known from the Anglo-Welsh Basin and a number of species have been described based on their fragmentary remains (e.g. White, 1961). This is also true for acanthodians which are largely known from their fin spines and isolated jaws (e.g. White, 1961) but rarer, articulated acanthodians have also been described (Miles, 1973). Body fossils are not the only indication of fish in the Anglo-Welsh Basin, and several *Undichna* trails from the Freshwater West Formation illustrate the swimming activities of Lochkovian fish (Morrissey *et al*., 2004).

A diverse suite of other ichnofossils is found throughout the Milford Haven Subgroup with diverse ichnofossil assemblages occurring throughout the Přídolí – Lochkovian successions (Morrissey *et al*., 2012). These include arthropod trackways (e.g. *Diplichnites*), dwelling burrows (e.g. *Arenicolites*), deposit feeding burrows (*Beaconites antarcticus*) and resting traces (e.g. *Rusophycus* type B), amongst many others, which occur across a variety of palaeoenvironmental settings (Morrissey *et al*., 2012). In addition to traces produced by invertebrate behaviours, some invertebrate body fossils are also known, including lingulids (White and Lawson, 1989) and fragmentary aquatic eurypterids and scorpions (Jeram *et al*., 1990). Highly fragmentary and rarer, more complete terrestrial arthropod remains such as the relatively complete malacostracan or hexapod example described by Fayers *et al*. (2010) are also found in the Přídolí and Lochkovian.

Another abundant fossil group in the Milford Haven Subgroup (and indeed the rest of the Anglo-Welsh Basin succession) is plants and their associated microfossils. Apparent rooting structures, occurring across a number of Přídolí – Lochkovian settings with the basin, were described by Hillier *et al*. (2008) and tentatively linked with the giant, enigmatic fungus-like *Prototaxites*. Body fossils of *Prototaxites* are yet to be described from the Anglo-Welsh Basin but *ex situ* specimens of *Nematasketum,* which is closely similar to *Prototaxites* (Burgess and Edwards, 1988), have been found here (Morris, 2009).

A kaleidoscope of plants and spores have been described from the Anglo-Welsh Basin over the past century, beginning with Heard's (1927) descriptions of pyritised *Gosslingia breconensis*. The plant body fossils are universally allochtonous, with no *in situ* specimens known from the basin. A wide variety of preservation states from poor to exceptional are encountered and whilst the principal mode of preservation is that of compressed, charcoalified films (Edwards and Richardson, 2004) of fragmented land plants, but exceptionally preserved pyritised macrofossils (e.g. Heard, 1927) and charcoalified mesofossils also occur (e.g. Edwards et al., 1992), albeit less often.

3.4. Přídolí- Lochkovian Palaeoenvironment

In light of the large body of sedimentary evidence, it is widely accepted that the Milford Haven Subgroup was largely deposited under terrestrial conditions (e.g. Allen and Tarlo, 1963; Allen, 1974a,b; Allen and Williams, 1978) and this is complimented by a wealth of palaeontological data which similarly indicates terrestrial deposition (e.g. Wellman *et al*., 2000; Morrissey and Braddy, 2004; Fayers *et al*., 2010). Broadly, the environment during the Přídolí and Lochkovian was that of a wide alluvial plain that lay on the Caledonian foreland, across which perennial and ephemeral rivers and streams traversed, draining the Caledonian mountains to the north as well as more localised areas within the basin itself.

Detailed examination of palaeosols and other sedimentary features indicates a semi-arid climate, with seasonal wet and dry seasons (Allen, 1974; Marriott and White, 2004). Vertisols are common throughout the succession and exhibit a range of features that are indicative of climate, including: (i) well-developed desiccation cracks, (ii) conspicuous slickenslides and wedge shaped peds in the soils,

and (iii) variously well-developed calcite and dolomite concretions (Wright, 1992, 2007). Whilst well developed calcrete horizons do exist in the basin, they are rare (Allen, 1986; Hillier and Williams, 2007), instead being typically nodular and discrete. In addition to sub-soil evidence, fluvial deposits strongly indicate 'event nature' deposition, with ephemeral discharge indicators commonly found within inclined and non-inclined heterolithic associations (Hillier and Williams, 2007). Whilst the environment was clearly semi-arid, with dryland deposition across the basin, temperatures are not thought to have been extreme. A lack of advanced evaporites such as halite and potassium (K) - salts preclude extreme temperatures and exceptionally high evaporation rates such as those seen in the present Middle East, with mean annual temperatures instead being postulated to have ranged between 16°C to 20°C (Goudie, 1983).

Evidence exists that suggests that the climate shifts may have been occurring in the Anglo-Welsh Basin through the Přídolí and Lochkovian, shifting towards a relatively wetter climate into the Lochkovian. Sandstone dominated perennial paleo-river channels commence in the Lochkovian, corresponding with an upward decrease in the maturity and frequency of vertisols, indicating a transition towards less defined seasonality and perhaps an increase in the length and intensity of wet seasons (Morris *et al*., 2012b) into the Lochkovian. Regardless of shifting climates, seasonality was still well defined in the Anglo-Welsh Basin during the Přídolí and Lochkovian.

Estimates for annual rainfall vary in the Anglo-Welsh Basin is variously, possibly ranging between 100 – 500mm (Goudie, 1983), or exceeding 760mm (Royer, 1999). Much of this precipitation would have been concentrated in wet seasons and caused a significant shift in the dynamics of the environment compared with dry seasons. The Přídolí landscape was largely low-gradient muddy floodplains which during wet seasons were periodically inundated with flash-flood waters which incised ephemeral channels into the landscape (Love and Williams, 2000; Morris *et al*., 2012b; Morrissey *et al*., 2012). Later Lochkovian landscapes saw the inception of sandier, perennial river channels which during wet seasons would have experienced increased discharge on floodplains (Morris *et al*., 2012b), but flow would have persisted at a low rate in dry seasons.

Both Přídolí and Lochkovian ephemeral channels, as well as Lochkovian perennial channels, would have periodically inundated proximal settings and interfluves with high energy ephemeral flood waters during periods of high discharge, depositing fresh sediments and detritus (Hillier *et al*., 2007; Williams and Hillier, 2004). This is postulated to have led to opportunistic colonisation of fresh sediments by communities in search of nutrition and may have led to population explosions among these soft-sediment communities (Morrissey *et al*., 2012). During lower discharge periods, biomats are suggested to have colonised periodically wet, muddy substrates (Marriot *et al*., 2013). Ephemeral and semi-permanent lakes developed on flood out zones and in topographic depressions (Marriott and Wright, 2004; Hillier *et al*., 2007), with the ichcoenosis indicating that aquatic organisms may have become trapped in these lakes once flood waters had receded and may also have acted as refugia for organisms during low discharge periods (Carrol, 1991).

Once wet seasons had abated, ephemeral Přídolí and Lochkovian river channels would have dried up and Lochkovian Perennial river discharge will have been much reduced as the environment returned to a largely dryland setting. The exposure of muddy bars and adjacent flood out zones led to the desiccation of these muddy deposits, as well as those of ephemeral and semi-permanent lakes (e.g. Wright and Tucker, 1991), and terrestrial arthropods and land plants are postulated to have exploited these areas one flood waters had receded (Hillier *et* al., 2008; Morrissey *et al*., 2012). The Přídolí landscapes are postulated to have been water deficient overall, whilst Lochkovian environments may have been wetter and benefited from higher water tables than the previous landscapes (Morris *et al*., 2012b), a change possibly driven by a shift towards a wetter climate. In more distal environments, away from flood waters, calcrete soils developed. During dry seasons, wildfires may have proliferated in vegetated areas (Glasspool *et al*., 2006), burning living and dead vegetation.

Aside from the environmental perturbations derived from seasonality there is evidence for rarer and more destructive events occurring through the Přídolí – Lochkovian. Air fall tuffs from distal, plinian

eruptions are common in the Moor Cliffs Formation (e.g. Allen and Williams, 1981) and there has been some suggestion that tsunamis, associated with the eruption and collapse of volcanic calderas, may have temporarily inundated the Anglo-Welsh Basin (Marriot *et al*., 2009). The effects on the early ecosystems from these events is unclear, but there appears to be no great faunal turnover (indicated by the ichcoenosis) after these events, although disaster taxa may be demonstrated (Marriot *et al*., 2009).

4. Palynological record of the Přídolí – Lochkovian

4.1. Overview: The Late Silurian – Early Devonian Record of the Anglo – Welsh Basin

A distinctive increase in the disparity and diversity of spores was identified in early studies of the basin palynoflora (e.g. Richardson and Lister, 1969). The significant difference between Přídolí and Lochkovian spore assemblages in the Lower ORS of the Anglo-Welsh Basin was explored by Richardson and Lister (1969) and was attributed to evolution amongst the parent plants. The trend was clear and a range of evidence suggested that evolution underpinned the change. The possibility that the trends were a factor of facies bias is largely negated by the overall trend seen in the basin from the Llandovery to the Lochkovian (table 1), where a significant increase in species, genera and to a lesser extent, sculpture is demonstrated; although there is some level of facies bias (Richardson and Lister, 1969; Richardson, 2007). Comparisons with other assemblages (e.g. the Silurian of Usk) conformed to the trend, also. Work by Muller (1959) and Hopping (1967) also demonstrated that to a reasonable extent, the dispersed spore record in modern sediments was relatable to the adjacent flora, suggesting that the changes in spore taxa were reflecting evolutionary changes in the parent plants.

Stage	Genera	Species	Sculptures
Lochkovian	11	29	21
Přídolí	8	24	13
Ludlow	6	15	24
Llandovery	1	2	0

Table I-1: Trends in spore taxa through the Llandovery and early Devonian. Genera and species show a clear increase towards the Devonian, although sculptural changes are less clear. Table modified from Richardson and Lister, 1969.

Work over the preceding years on the dispersed spore record in both the Anglo-Welsh Basin and elsewhere, coupled with the growing body of macrofossil data, indicated considerable diversification amongst trilete spore producing plants following a prolonged period of apparent evolutionary stasis amongst cryptospore producing plants at the Silurian - Devonian boundary. Wellman *et* al. (2013) made taxon counts of spore assemblages from the mid Ordovician to the Lochkovian which demonstrate this adaptive radiation as trilete spore diversity increases considerably (fig. 7a). The clear increase in trilete spore diversity is seen through the latter half of the Silurian here, but also a variety of patterns are seen in monads, non obligate dyads and obligate cryptospores. Diversification begins in the latter two groups after the Llandovery, with trilete spore diversity remaining relatively static until the Sheinwoodian, where exponential diversification begins. The Přídolí and Lochkovian see a continued increase in the diversity of trilete spores, in addition to a renewed diversification of monads and non-obligate dyads. Obligate cryptospores continue to fall from a previous peak in diversity which occurred in the Ludlow. Diversity and disparity amongst dispersed spore taxa were also plotted in Wellman *et al*. (2013), and these plots considered, amongst others, trends in the Anglo-Welsh Basin. Both plots indicate a significant increase in diversity and disparity amongst trilete spores, with a significant increase in diversity during the Přídolí. The decreases in diversity and disparity seen amongst the Anglo-Welsh Basin taxa were attributed to a dearth of strata and dispersed spore assemblages of this age at these time intervals (Wellman *et al*., 2013).

While the broad patterns of this diversification amongst trilete spores have been well defined (Wellman et al., 2000), the nuances around the diversification remain clouded. The key driving genera of the

diversification amongst the trilete spores have not been defined, and the cryptospore story is far from fully explored.

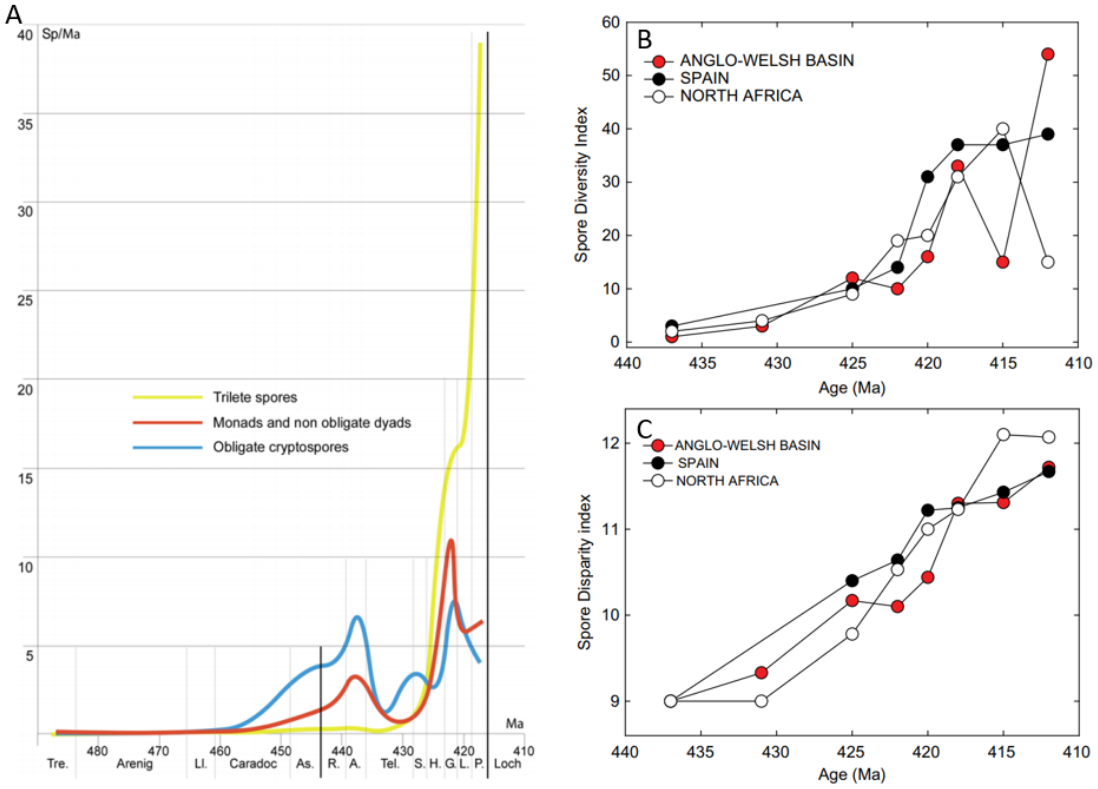

Figure I-7: Dispersed spore diversity curves. ***A*** *– Dispersed spore diversity curve from for mid Ordovician – Early Devonian taxa, showing the exponential increase of trilete spores during the latter half of the Silurian, which strongly contrasts with the low diversity of cryptospores seen until the Ludlow, where initial diversification begins.* ***B*** *– Spore diversity index: spore diversity shows a gradual increase, which appears rapid in the Přídolí and Lochkovian, although this may be skewed by a lack of strata and dispersed spore assemblages.* ***C*** *- Spore disparity curve, also showing significant increase through the Přídolí-Lochkovian. The dip seen in this periods may also be a result of strata and assemblage paucity. Modified from Wellman* et al., *2013.*

4.2. The Přídolí – Lochkovian Record of the Anglo – Welsh Basin

The dispersed spore record

The dispersed spore record experiences significantly less bias than the megafossil record. Spores are much more readily preserved and occur in far higher abundances over a wide area. Therefore, whilst estimations regarding diversity using macrofossils may underestimate or miss episodes of diversity and disparity changes amongst early land plants, it is much more likely that the dispersed spore record will preserve these changes (Edwards and Wellman, 2001).

In view of this, the dispersed spore record offers a powerful and high resolution tool for understanding the nature and extent of the Přídolí-Lochkovian vascular plant radiations in the Anglo-Welsh Basin, in terms of diversity, disparity and evolutionary tempo. In addition, the dispersed spore record is also a powerful tool for biostratigraphy (4.2) and also adds an alternative, quantitative method for interpreting vegetation variation, both spatially and temporally (4.3). Whilst the dispersed spore record is much less fragmentary and less biased than the macrofossil record, biases do still occur. These are largely related to facies and taphonomic influences, but it is also difficult to biologically contextualise the dispersed spore species.

Biostratigraphy: spore zones

Spores are useful stratigraphic tools for a variety of reasons, including high abundance, resistant composure and facies independence as a function of their dispersal methods (e.g. Richardson and McGregor, 1986).

Spore zones in the Anglo-Welsh Basin have been constructed according to the zonal concept, after Richardson and McGregor (1986), whereby a zone is defined by the widespread, first appearance of certain spore species and features. The selected first appearances are typically geographically widespread and happen instantaneously relative to geological time. These changes are assumed to reflect the evolution of taxa, and some lineages are noticeable. The last appearance of taxa or species receives less focus here, as this may be variously affected by the persistence of relict floras (Richardson and McGregor, 1986). Richardson and McGregor (1986) combine the co-occurrence of entire assemblages, defined by a number of characteristic taxa alongside the first appearance of selected species and form features, in addition to the earliest records of some selected species, to define an assemblage biozone, which occur in a set order. These are typically observed in a range of facies and are not affected by species abundance.

Spore zones for the Přídolí-Lochkovian of the Anglo-Welsh Basin were initially erected by Richardson and McGregor (1986) in an attempt to correlate the British ORS with other basins across Euramerica. These comprised three main biozones (fig. 6) covering the Přídolí and Lochkovian: (i) *tripapillatus-spicula*, (ii) *micrornatus-newportensis* and (iii) *breconensis-zavallatus*. Further work by Richardson and colleagues later resulted in the reassessment of the spore zones, with the *tripapillatus-spicula* biozone being reduced to the lower Přídolí, with Biozone A (later *II* zone, based on Spanish sporomorphs (Richardson et al., 2001)), was erected just above the *tripapillatus-newportensis* zone. Further reassessments were made with the *Apiculiretusispora* species E zone being placed just below the *micrornatus-newportensis* biozone, representing the earliest spore zone of the Lochkovian. Between the *II* zone and the *Apiculiretusispora* species E zone, much of the Přídolí remains uncertain in its zonation scheme due to a major sampling gap. Similarly, the *Apiculiretusispora* sp. E zone is yet to be properly defined.

Synorisporites tripapillatus – Apiculiretusispora spicula biozone

The *Synorisporites tripapillatus – Apiculiretusispora spicula* assemblage biozone in Richardson and McGregor (1986) was initially approximate to the early Přídolí to earliest Lochkovian. The type section for the base of the zone is located at the base of the Downton Castle Sandstone Formation (now excluded from the Anglo-Welsh Basin *sensu* Barclay *et al*., 2015) and terminated at the base of the Freshwater West Formation. It was noted in Richardson and McGregor (1986) that further study of spores in the Přídolí of the Anglo-Welsh Basin may result in further subdivision of this zone. Following further study the *tripapillatus-spicula* biozone was subdivided, and the *II* zone erected (Richardson and Edwards, 1989; Richardson et al., 2001). Currently, the *tripapillatus-spicula* zone represents the lowermost Přídolí (Edwards and Richardson, 2004), having been differentiated in Edwards and Richardson (1989) into Biozones A and B (below).

Characteristic species of the *tripapillatus-spicula* biozone are given in table 2. The biozone begins with the first appearance of interadial proximal papillae (e.g. in *Synorisporites tripapillatus*), distally sculptured patinate spores (e.g. *Cymbosporites*) and reticulate sculpture (e.g. *Chelinospora*). The biozone does not mark the last appearance of any taxa, with nearly all species from the previous zone (*Synorisporites libycus - ?Lophonzonotriletes poecilomorphus* zone) persisting.

Biozone ‘A’ (*II)*

This zone is alluded to in Edwards and Richardson (1989) as ‘biozone A’ but no published description of characteristic species exists. The zone is clear in southern Britain (Wellman and Richardson, 1996) and contains *Perotrilites,* common patinate miospores and *Synorisporites* sp. and lacks *Aneurospora*

species (Wellman and Richardson, 1996). Additional description from Wellman and Richardson (1996) indicates the presence of crassitate miospores with rugulate-murornate sculpture and hilate cryptospores with distal regulate sculpture. The biozone has thus far only been described from southern Britain (Wellman and Richardson, 1996). The extent of this biozone is uncertain but is suggested in Edwards and Richardson (2004, their fig. 2) to occupy the late early Přídolí.

Lavidensis biozone

The *Lavidensis* biozone has recently been described by Higgs (2022) from freshwater East in Pembrokeshire. The zone is marked by the incoming of *Chelinospora lavidensis*, in addition to *C.* cf. *hemisphaerica* and *C. hemisphaerica*. The zone is associated with a diversification amongst *Cymbohilates* and is suggested to occur closely after Biozone A in the mid Přídolí. This biozone has not yet been proven outside of Pembrokeshire.

Apiculiretusispora sp. E zone

This biozone was first mentioned as a distinctive biozone in Richardson *et al*. (1984) but was precluded from the biostratigraphy of Richardson and McGregor (1986), after which it has been variously alluded to (e.g. Edwards and Richardson, 1989; Richardson, 1996; Wellman and Richardson, 1996; Richardson *et al*., 2000; Richardson *et al*., 2001; Richardson, 2007) in the literature, but no characteristic species lists have been published to date. The zone is described in Wellman and Richardson (1996) to contain *Aneurospora* with prominent spines, and *Perotrilites*. Patinate miospores and *Synorisporites* are common, whilst *Aneurospora* is rare (Wellman and Richardson, 1996 their text fig. 8). Tripapillate *Aneurospora* are not recorded.

The range is constrained above by the *microrнatus-newportensis* zone (below), with a possible *Aneurospora* zone closely associated below or as part of the *Ap.* sp. E zone (Richardson, 2007). The *Ap.* sp. E biozone is thought to initiate at the Silurian - Devonian boundary (e.g. Richardson *et al*., 2001), close to the FAD of *T. pagei* and persisting to the MN zone (Richardson *et al*., 2000) although the lower bound is not yet secure. It is separated from 'biozone A' (Edwards and Richardson, 1989) by an uncertain zone, which occupies much of the Přídolí and to date has been difficult to define given the poorly preserved palynomorphs preserved there (Wellman and Richardson, 1996). The biozone is suggested to correlate internationally, with the sequence in Podolia exhibiting a distinctive biozone possibly relatable to the *Ap.* sp. E biozone between the first appearance of *Monograptus uniformis uniformis* (Silurian - Devonian Boundary) and the MN zone (Richardson *et al*., 1981, 1984, 2001). No detailed comparisons have been made since, however.

Emphanisporites microrнatus – *Streelispora newportensis* assemblage zone

The *microrнatus-newportensis* assemblage zone is more firmly established than the earlier biozones. The zone represents much of the Lochkovian, excluding the earliest and latest, and is well correlated with the *Crouchi* and *Leathensis* vertebrate biozones. The base of the zone is postulated to lie near to, but not on, the Silurian - Devonian boundary at the base of the Freshwater West Formation (Richardson and McGregor, 1986), just above the Chapel Point Limestone.

Characteristic species for the *microrнatus-newportnensis* biozone are given in table 2. The biozone is defined by multiple novel structural and sculptural features. The zone represents the first appearance of prominent, flimsy zona in spores, however, this feature is rare until the succeeding *breconensis-zavallatus* zone. Sloughing, sculptured exoexine is seen for the first time and the variety of proximally radially ribbed spores increases (e.g. *Emphanisporites*), which is coupled with the first appearance and subsequently common conate and granular distal sculpture on specimens (e.g. *E. microrнatus*). Finally, the proliferation of reticulate sculpture is seen variously in species throughout the zone. Spores with proximal interadial papillae, which first appears in the *tripapillatus-spicula* zone, persists through the *microrнatus-newportensis* zone (Richardson and McGregor, 1986).

Since its initial establishment, the *micrornatus newportensis* biozone has been subdivided into the lower, middle and upper biozones, and correlated well with the MN oppel zone developed in Belgian sequences by Streel et al. (1987).

Assemblage Spore Zone and Age	**Characteristic Species**
Poecelomorphus – libycus (late Ludlow)	- *Stellatispora inframurinatus* var. *inframurinatus* - *Lophonzotriletes poecilomorphus* - *Apiculiretusispora asperata* - *Hispanaediscus major*
Synorisporites tripapillatus -Apiculiretusispora spicula (earliest Přídolí)	- *Synorisporites tripapillatus* Richardson and Lister, 1969 - *Apiculiretusispora spicula* Richardson and Lister, 1969 - *Ambitisporites* sp. B of Richardson and Ioannides, 1973 - *Amicosporites splendidus* Cramer, 1967 - *Apiculiretusispora synorea* Richardson and Lister, 1969 - *Cymbosporites echinatus* Richardson and Lister, 1969 - *C. verrucosus* Richardson and Lister, 1969 - *Emphanisporites neglectus* Vigran, 1964 - *E. splendens* Richardson and Ioannides, 1973 - *Synorsporites downtonensis* Richardson and Lister, 1969 - *S. verrucatus* Richardson and Lister, 1969
II zone / Biozone A (mid-early Přídolí)	Not Published, Wellman and Richardson (1996) indicate: - irregular granulated *Apiculiretusispora* - *Retusotriletes* spp., - Characterised by the incoming of alete cryptospores with a thin proximal surface and distal rugulate sculpture.
Lavidensis	- *Chelinospora lavidensis* - *C.* cf. *hemisphaerica* - *C. hemisphaerica* - Diversification of *Chelinospora* species.
? Zone (Late-early Přídolí – Silurian - Devonian Boundary)	Uncertain
Apiculiretusispora species E (?Silurian - Devonian boundary to early Lochkovian)	'Distinct', but unpublished; at least two distinct non-tripapillate *Aneurospora* spp. and one *Apiculiretusispora* spp. **This work.**
Aneurospora spp.	non-papillate *Aneurospora*? **This work.**
Emphanisporites micrornatus – Streelispora newportensis (early to late Lochkovian)	- *Emphanisporites micrornatus* Richardson and Lister, 1969 - *Streelispora newportensis* (Chaloner and Streel) Richardson and Lister, 1969 - *Acinosporites salopiensis* Richardson and Lister, 1969 - *Apiculiretusispora plicata* (Allen) Streel, 1967; Allen, 1965 - *Chelinospora cassicula* Richardson and Lister, 1969 - *Cymbosporites proteus* McGregor and Camfield, 1976 - *Emphanisporites epicautus* Richardson and Lister, 1969 - *Perotrilites microbaculatus* Richardson and Lister, 1969 - *Retusotriletes maculatus* McGregor and Camfield, 1976

Table I-2 Characteristic sporomorph species comprising the assemblage spore biozones of the Přídolí-Lochkovian of the Anglo-Welsh Basin. Tripapillatus-spicula, micrornatus-newportensis *and* breconensis zavallatus *zones are after Richardson and McGregor (1986).*

Biozones: Further work

It is clear that the spore biozones in the Přídolí and Lochkovian of the Anglo-Welsh Basin require further work, building on that of Richardson and McGregor (1986) and later work. Most specifically, the spore biozones around the Silurian – Devonian boundary need to be investigated and defined, following the methods developed in Richardson and McGregor (1986). Once the spore zones are established in the Anglo-Welsh Basin, they need to be correlated with other sequences of similar age, e.g. the Cantabrian Mountains, Northern Spain and the deep marine sequences in Podolia. Ultimately, they must show a level of correlation with the Silurian - Devonian type marine sequences of the IUGS, which may be complicated by the disparities between terrestrial and marine strata.

4.3. Palynological interpretation of vegetation

Spore dispersal and taphonomy

Plants rely on spore dispersal for gene mixing and invasion of new habitats. The abundance of spores in the palynological fossil record is influenced by the fecundity (reproductive output) of the source plants, with extant free sporing plants, including bryophytes such as *Sphagnum*, producing vast numbers of spores (e.g. Sundberg, 2012). Studies of *in situ* spores in charcoalified spore masses and sporangia from late Silurian and Early Devonian mesofossil assemblages similarly suggest that early land plants also produced high quantities of spores (e.g. Wellman, 1999; Edwards and Wellman, 2001; Wellman et al., 2003; Ball and Taylor, 2022; Chapters V and VI).

Work by Muller (1957) found that a clear relationship existed between spore assemblages in modern sediments and vegetation, in that the spore rain was largely representative of local vegetation. Whilst obvious differences exist in the nature of the vegetation between present and Silurian - Devonian floras, the same is likely to be also true of palynofloras of this age.

Tauber (1965) summarises transportation pathways available to spores and pollen, however it must be again borne in mind that the dispersal and transportation interpretations of these early land plant spores differs somewhat to more modern interpretations (e.g. Steemans et al., 2007). Foremost, the structure of the vegetation in the late Silurian and Early Devonian contrasts strongly with extant floras. Indeed, the early Devonian vegetation is considerably different even from mid Devonian floras, where the first arborescent tracheophytes and forests appear (e.g. Stein et al., 2012, 2020). Arborescence had not yet been attained amongst plant groups with dispersal of spores from the diminutive plants, the tallest of which were tens of centimetres tall, limited by their height (Steemans et al., 2007). This likely resulted in the majority of spores settling close to the source plant, but Steemans et al. (2007) point out that the absence of tall plants would have led to less obstruction by air currents, perhaps facilitating more distal dispersal of spores. In addition, it is unlikely that animals, such as insects, will have played a major role in spore dispersal at this time.

Nonetheless, accepting this modification, the mechanisms outlined by Tauber (1965) remain applicable. Following dehiscence of the sporangium and spore liberation, initial spore dispersal is driven by air currents. The process of spore liberation and dehiscence may be facilitated by sporangial mechanisms such as elaters or explosive dehiscence, or by external factors such as rain drops. Such mechanisms have not been recognised in late Silurian or Early Devonian spores, but there is some evidence that spores of *Cooksonia* were liberated by the disintegration of part of the sporangia and structures, such as dehiscence lines, are also known (Gonez and Gerrienne, 2010). These simple dehiscence mechanisms, and the restricted size of these early land plants, likely resulted in most of the liberated spores settling rapidly via gravity close to the source plant (>95% Steemans et al., 2007). The small size of the plants may have largely prevented spores being entrained by air currents and hence from being dispersed much further. Those entrained by air currents will also eventually settle via gravity, with the distance travelled controlled by, *inter alia*, atmospheric turbulence, wind speed and the terminal velocity of the spore, the latter of which is controlled by spore morphology (Tauber, 1965).

Following spore settling, there is the possibility of further transportation by overland water flow, or by reworking of sediments within which palynomorphs have been contained. This onward transportation may lead to spores being delivered into rivers and other water bodies, including marine settings. Those entrained in fluvial systems may be further transported to lacustrine or marine environments, and in some cases the palynomorphs may be transported thousands of kilometres by wind and/ or water (Traverse, 1988, 2009). Spores transported such distances may remain viable and have the potential to colonise new environments (Steemans et al., 2007). The initial dispersal and onward transportation of spores facilitate the mixing of palynomorphs from across the catchment area, and depending on the size of this area, and the depositional setting, it is possible to distinguish local and regional spores. In small basins and certain facies, the local vegetation is likely to be well represented. Meanwhile, in deltaic or fluvial systems, amongst others, the addition of more distal vegetation is likely to be observed, thereby offering a more regional view of the palynoflora. In the context of late Silurian and Early Devonian plants, especially, Sugita's (1994) assumption that distal plants contribute less to a palynoflora holds, but it must be borne in mind that spore assemblages and species proportions are also influenced by a species' reproductive capacity, spore dispersal mechanisms and facies.

The representation of spores in the palynological record also depends on their preservation, which is influenced by several factors. Spores are resistant to decay and are found abundantly in the sedimentary record because their spore walls are impregnated with sporopollenin (e.g. Wellman, 2004), but the amount of sporopollenin, and hence thickness of the exine, controls the resistance of the spore to decay. The sporopollenin content of the exine varies within and between broad taxonomic groupings of plants. In addition to sporopollenin content, the nature of the substrates within which spores are eventually captured also control their preservation potential, as with other fossil groups. Oxidising environments are particularly unfavourable for the preservation of spores (fig. 8), which includes the large proportions of terrestrial environments and red bed sequences. In addition, acidic alkaline environments may facilitate the loss of palynomorphs, alongside high energy environments. Sorting and winnowing of spores, particularly in fluvial settings, may also influence the palynoflora. In these cases, spores below or above a certain size may be removed or concentrated in a sequence

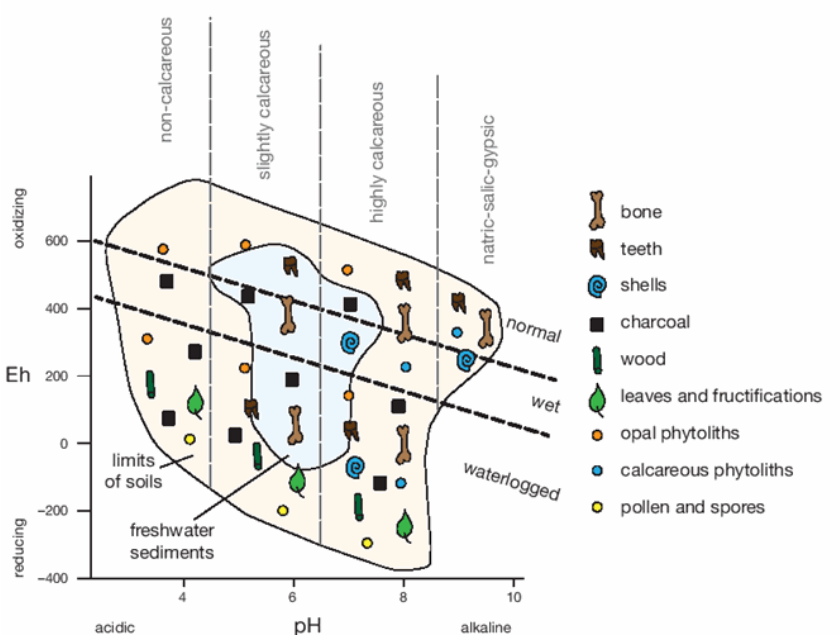

Figure I-8: Eh and pH effects on the fossilisation potential of various fossil groups. Spores and pollen indicated by yellow circles. Modified from Holland and Loughlin (2021).

Interpretation of vegetation

Quantitative reconstructions of Silurian - Devonian vegetation using dispersed spores has been carried out for areas across Laurussia (e.g. Richardson, 1996a, 2002) and in the Anglo-Welsh Basin (Richardson, 2007). The analysis assumes that within a given area the wind derived spore rain will chiefly reflect the local vegetation (after Muller, 1957), although a number of biases, whilst less disruptive than the megafossil record, do exist, including facies bias (e.g. winnowing and water transport) and variation amongst local vegetation (Edwards and Richardson, 2004; Richardson, 2007). The quantitative analysis involves exploring the proportions of certain spore types in order to identify dominant sporomorphs in a given assemblage, thereby indicating the type of plant that dominated that area. This may then be used to infer the palaeoecology of an area when coupled with sedimentary evidence and established ideas regarding the physiologies of parent/producer plants (Richardson, 2007).

Richardson (2007) analysed the dispersed spore assemblages from three Přídolí-Lochkovian sequences in order to investigate temporal and paleoenvironmental changes amongst early land plants (fig. 9), and found three distinct palynological zones which corresponded with the palaeoenvironment. Distal alluvial plains are exhibited in the lower parts of the sequences, and in some there was an abundance of laevigate cryptospores

The base of the sequence has been interpreted to represent the distal margins of an alluvial plain, which shows evidence for marine influence (e.g. Allen and Tarlo, 1963; Barclay *et al*., 1994). The highest proportion of laevigate cryptospores is found at the base of the succession, with a gradual decrease higher up. This was suggested to indicate that the plants producing the laevigate cryptospores were largely restricted to areas of marine influence and were perhaps halophytic based on the associations with acritarchs in some areas; a clear relationship is found between increasing acritarch proportions (indicating marine incursion) and increasing laevigate cryptospore proportions. The possibility of wind or water transport concentrating the spores into near shore marine environments is negated by the likelihood that these processes would not have separated the spores into distinct groups.

Medial alluvial plains were dominated by high sinuosity streams and rivers (Allen, 1974) with a variety of interfluvial areas (Marriot and Wright, 2004). These areas initially see an increase in sculptured cryptospores which may have then dominated interfluvial areas (Edwards and Richardson, 2004).

The top of the successions represent a proximal alluvial plain. There is a peak in alete cryptospores, with a decrease in laevigate and sculptured miospores. Sculptured cryptospores remain relatively

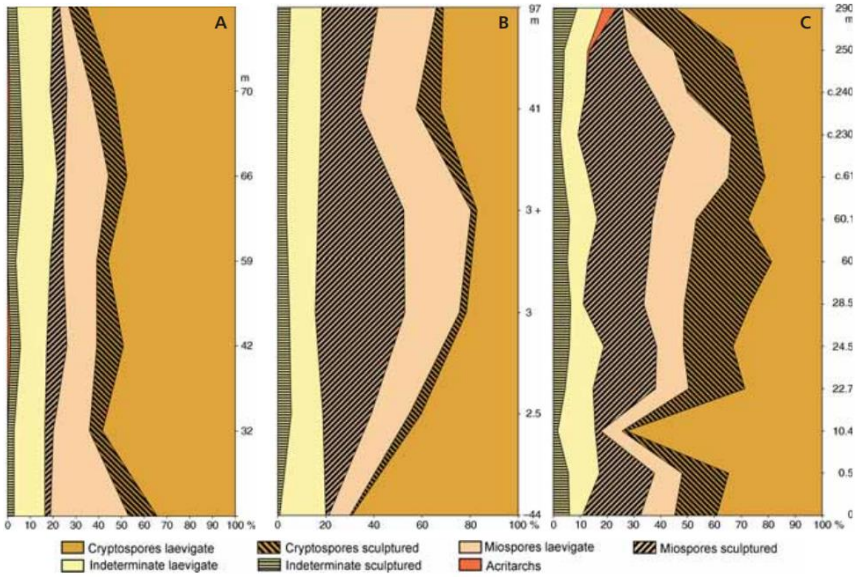

Figure I-9: Proportions of sporomorphs from three Přídolí-Lochkovian sequences of the Anglo-Welsh Basin. ***A****: Ammons Hill;* ***B****: M50 motorway;* ***C****: Clee Hills. Numbers on y-axis correspond to distance above (+) and below (-) Chapel Point Limestone. After Richardson (2007).*

constant through the top of the succession, suggesting a continuous presence in this environment. Richardson (2007) hypothesises that the lack of *in situ Emphanisporites* spores may be a result of the parent plant preferentially growing in upland areas and thus away from the immediate catchment area of rivers, as *Emphanisporites* becomes common in these environments.

However, the presence of the parent plants of the spores, identified by *in situ* spores, in a variety of environments (Morris et al., 2011b, 2012a, b), amongst other lines of evidence (e.g. Richardson and Lister, 1969) strongly suggest that facies change is not the principal underlying factor to floral change in the Anglo-Welsh Basin.

The proportions of spores between basins may indicate regional variation, and this is particularly enlightening when *in situ* spores enable the comparison of the dispersed spore record with the macrofossil record.

Subtle differences exist between the spore assemblages of the Anglo-Welsh basin and those of the coeval Midland Valley in Scotland. A larger maximum spore size exists in Scotland, in addition to a lower relative abundance of *Aneurospora-Streelispora* spore complexes compared with southern Britain, amongst others (e.g. Richardson *et al*., 1984; Wellman and Richardson, 1996). The variation in spore assemblages are thought to reflect variations in vegetation between alluvial plains (Anglo-Welsh Basin) and intramontane basins (Midland Valley). Potential facies biases are negated, as coeval sequences representing a variety of palaeoenvironments show similar patterns (Wellman *et al*., 1999).

Larger spores, particularly those of azonate retusoid forms are linked to Zosterophylls and other lycophytes (e.g. Allen, 1980; Edwards and Richardson, 1986), whilst those of the *Aneurospora-Streelispora* complex are linked to rhyniophytoids such as *Cooksonia* (e.g. Fanning *et al*., 1988). It has therefore been postulated that intramontane basins were dominated by zosterophylls and alluvial plains by rhyniophytoids (Wellman *et al*., 2000), with zosterophylls encroaching into alluvial plains through the Lochkovian, perhaps as environments became more suitable due to renewed Acadian uplift. Some support is found in the megafossil record, with zosterophylls appearing in Scotland in the lower MN spore zone, and in the Anglo-Welsh basin by the middle MN spore zone (Wellman *et al*., 2000).

5. Palaeobotanical record of the Přídolí – Lochkovian

5.1. Přídolí-Lochkovian palaeobotany

Preservation of plant material

Global Přídolí-Lochkovian fossil assemblages are thus far allocthonous, with many of the assemblages being preserved in marine strata (thesis appendix 1.1, figs. 12, 13). Other assemblages have been described from terrestrial strata (thesis appendix 1.1, 1.2, e.g. Welsh Borderlands), but still show evidence for transportation and reworking. It is typically unclear to what extent the material has been transported and fragmented, with transport histories affecting both the extent of fragmentation and the affinities of the plants (Gerrienne and Streel, 1974). Typically, plants are preserved as either mega- or mesofossils as coalified compressions in which, for the most part, only gross morphological information can be derived (Edwards and Richardson, 2004; Morris et al, 2011a). Exceptional preservation of allochtonous plants does occur, however, through pyritisation (e.g. Heard, 1927) or charcoalification of the plant (e.g. Edwards *et al*., 1996; Glasspool et al., 2006). *In situ* palaeobotanical assemblages are exceptionally rare, with the slightly younger Pragian Rhynie Chert being the closest in age here. Valuable information on anatomies of early land plants are obtained from this assemblage, however some workers (e.g. Shopf *et al*., 1966) suggest that the plants represent an ecologically specialised flora and therefore caution is warranted when relating these plants to other early land plants.

The plant megafossil record is affected by preservational biases. Typically, only plants with recalcitrant tissues such as lignin are preserved, resulting in a bias towards the preservation of vascular plants (Gensel, 2008). According to the dispersed spore record, this results in a significant proportion of the ecosystem being excluded from the fossil record - Bryophyte grade plants and those plants without

recalcitrant tissues, are typically not preserved as body fossils, despite being well represented by dispersed cryptospores (e.g. Wellman *et al*., 2000). A second source of bias is the preferential inclusion in the fossil record of plants that grow near to depositional areas. Plants that grow away from rivers or lakes are unlikely to be transported into depositional environments and are therefore lost (e.g. Wellman, 2004). Moreover, the effects of sedimentation may also influence the macrofossil record, through processes such as sorting as might the proportion of marine and terrestrial strata in the rock record (e.g. Wellman, 2004).

Přídolí-Lochkovian floral phylogeny

The first unequivocal evidence of land plants are envelope enclosed cryptospores from the lower-mid Ordovician (473-471ma) (Rubinstein *et al*., 2010; Wellman, 2010), but the first plant body fossils are not known until the Katian (453-445ma) (Wellman *et al*., 2003). The first vascular land plants are known from the Ludlow (427-423) (Edwards *et al*., 1983), and assemblages see a marked increase in preserved flora from the Llandovery (Wellman *et al*., 2013). Flora through the Silurian and Devonian was herbaceous, with a mixture of diminutive vegetation and shrub like plants distributed both regionally (e.g. Wellman *et* al., 2000) and globally (e.g. Wellman *et al*., 2013). The axes were typically naked, and rooting structures were negligible, with horizontal axes or shallow subterranean rhizoids thought to connect the plants to the ground (Taylor *et al*., 2009).

Despite extensive research, the phylogenetic relationships of land plants are still somewhat unclear, having undergone numerous revisions since the first pioneering attempts to integrate fossil and extant taxa into inclusive evolutionary schemes (e.g. Bower, 1935; Smith, 1938; Zimmermann, 1930; 1938). A major re-evaluation using numerical cladistic techniques by Kenrick and Crane (1997) revised older categorizations of fossil land plants (e.g. those of Banks, 1968) and set them in context with extant examples. Further work building on the scheme of Kenrick and Crane (1997) has revised and updated the phylogenies whilst retaining the gross structure of that given in Kenrick and Crane (1997) (fig. 10). Amongst others, ever more modern techniques (e.g. molecular and genomic analysis, Qui *et al*., 2006; Puttick et al., 2018) have gone some way towards clarifying the relationships amongst land plants, but many remain unresolved and controversial, hindering crucial evolutionary interpretations (Edwards and Kenrick, 2015).

Charophyceae, a group of chiefly freshwater algae are widely considered the closest sister group to land plants (Graham, 1993; Mishler *et al*., 1994; Kranz *et al*., 1995; Melkonian and Surek, 1995; McCourt *et al*., 1996). Various workers (e.g. Graham, 1993; Kenrick and Crane, 1997) have attempted to determine which of the three groups of Charophyceae (Coleochaetales, Charales or Zygnematales) represents the closest extant land plant sister group, but presently this remains uncertain. Kenrick and Crane (1997) postulated that either the Coleochaetales, Charales or a group containing both represented this. Later work by Karol *et al*. (2003) used genome analyses that indicated that the sister group was represented by Charales and Qiu *et al*. (2006), using three complimentary data sets found consistency with Karol *et al* (2003)'s findings. More recent work by Timmes *et al*. (2012), however, using extensive phylogenomic analysis has given weight to the hypothesis that the species rich group Zygnematales, rather than the previously hypothesized Charales, represent the extant sister group of land plants; this hypothesis has found wide support (Edwards and Kenrick, 2015), indicating that the species rich Zygnematales ('pond scum' – Timmes *et al*., 2012) was a pioneering group in early terrestrialisation, moving onto land perhaps as early as the Cambrian (e.g. Taylor and Strother, 2008, 2009) and certainly by the mid Ordovician.

Embryophytes (land plants) are a monophyletic group, nestled within the Charophyceaen algae. This is supported by a wealth of comparative morphological (Bremer *et* al., 1987; Graham, 1993; Mishler *et* al., 1994; Kenrick and Crane, 1997) and gene sequencing evidence (Heisel *et al*., 1994; Kranz *et al*., 1995), alongside more recent phylogenetic analyses which have found continuity with earlier studies (Qui *et al*., 2006; Karol *et al*., 2010; Wickett *et al*., 2014; Puttick et al., 2017).

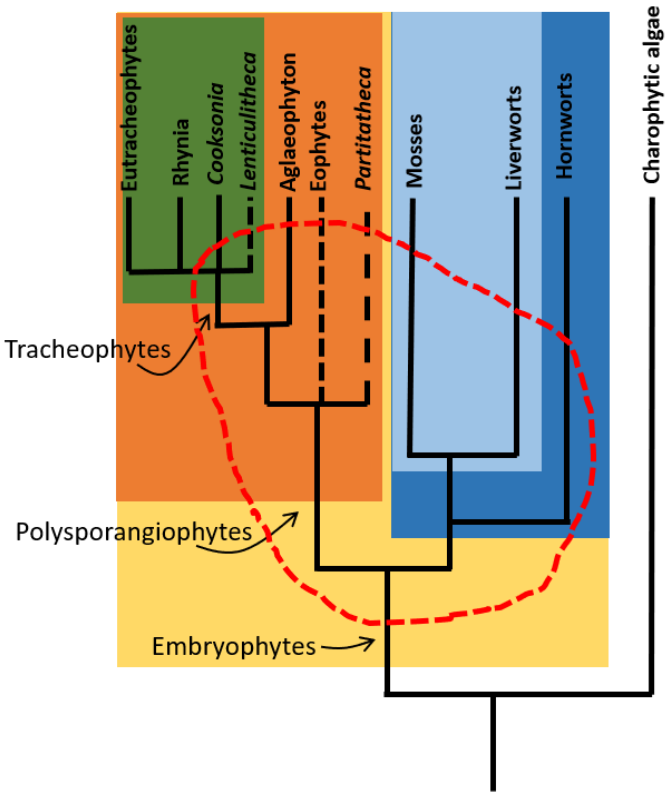

Figure I-10: Phylogenetic relationships of land plants and possible positions which cryptospore producing plants may occupy (red dashed oval), following Edwards et al. (2014, 2021a) and Puttick et al (2018). Green: tracheophytes; Orange: Polysporangiophytes; pale blue: Setaphytes; dark blue: bryophytes; yellow: embryophytes. ***A.*** *modified from Kenrick and Crane (1997);* ***B.*** *modified from Edwards et al., 2022a.*

Consistently more problematic is the phylogenetic relationships amongst the bryophytes and the nature of the earliest land plants. An indication of the suite of features of these earliest land plants is necessary for understanding their onward evolution, however, basal topology remains contentious with a variety of possibilities being explored by various authors (e.g. Wickett *et al*., 2014; Cox *et al*., 2014). Until recently, the most widely accepted hypothesis fielded by Kenrick and Crane (1997) was that the liverworts (Marchantopsida) occupied a basal position within embryophytes, with either hornworts (Anthcerotopsida) or mosses (Bryopsids) forming the closest sister group to tracheophytes. More recently, analyses by Puttick et al. (2018) point towards liverwort simplicity resulting from a loss of features, rather than primitive absence, with these authors instead suggesting that the earliest land plants were probably more complex than the liverworts. Irrespective of the nature of the earliest land plant, the question of bryophyte monophyly or paraphyly has been debated for over three decades. Kenrick and Crane (1997) found bryophyte monophyly to be unparsimoneous and this view is widely held, with a large body of evidence indicating a paraphyletic relationship between bryophytes and tracheophytes (e.g. Mishler *et* al., 1994, Qui *et al*., 2006). Alternatively, *inter alia*, analysis of chloroplast phylogenies by Nishiyama *et al*. (2004) and Karol *et al*. (2010) lends support to a monophyletic bryophyte lineage. Furthermore Cox *et al*. (2014), upon review of Karol *et al*. (2010)'s amino acid data, attribute the conclusions of Qui *et al*. (2006) to a failure to correct for mutation-driven compositional biases in data and therefore find a monophyletic relationship as the best supported hypothesis. Both monophyletic and paraphyletic hypotheses for bryophyte phylogenies have their merits, and the topic remains debated, with understanding of this phylogenetic relationship crucial for understanding the evolution of the embryophytic lifecycle and for appreciating the evolutionary implications presented by early land plant fossils (Edwards and Kenrick, 2015). Most recently, Puttick et al. (2018) resolved the bryophytes as a monophyletic group, the Bryophyta, although this finding was not considered equivocal. Within the

Bryophyta, Puttick et al. (2018) resolved the setaphyta clade, or setaphytes, comprising liverworts and mosses, and a separate hornwort clade. The position of hornworts within Bryophyta was unresolved and remains problematic, but previous hypotheses suggesting that hornworts represented the sister group to all other embryophytes (Renzeglia *et al*., 2000; Nickent *et* al., 2000) or occupied the sister group to tracheophytes (Lewis *et al*., 1997; Samigullen *et al*., 2002; Kelch *et al*., 2004; Groth-Malonek *et al*., 2005; Turmel *et al*., 2006; Qui *et al*., 2006) found little support in their analyses.

The polysporangiophytes comprise both tracheophytes and protracheophytes, the latter of which contains the Rhyniopsida, a group that cannot be discriminated using extant taxa. These groups include some of those plants that were previously grouped into Rhyniophytina *sensu* Banks 1975b and the Rhyniophytina of later revisions (e.g. Edwards and Edwards, 1986). These were characterised as unnatural by Kenrick and Crane (1997) on the basis that the group was paraphyletic by definition and likely polyphyletic, with research indicating a variety of conditions amongst these basal land plants, with some being tracheophytic (e.g. *C. pertoni*) and variously related to major tracheophytic grades. Other *Cooksonia* species and similar fossils (e.g. *Salopella*) appear to occupy indeterminate topologies and possibly represent a protracheophyte grade. Indeed, some early land plants such as *Horneophyton* have been grouped as intermediate between bryophytes and tracheophytes, based on the mixture of derived tracheophytic features (e.g. branched, nutritionally independent sporophyte) and retention of primitive, bryophytic features (e.g. absence of annular or helically thickened tracheids). Recently however, vascular tissue has been recovered in *Horneophyton* (Cascales-Miñana et al., 2019). Uncertainty surrounds these basal tracheophytes because of the typically poor quality of the fossil record (below) and the realization of their true affinities relies on more detailed knowledge of, *inter alia*, stem anatomy, which is rarely afforded by the typically inadequate megafossil record. Because of the gaps in knowledge here, the non-cladistic rhyniophyte/rhyniophytoid groupings are used to differentiate between those plants of a rhyniophyte character with definite tracheids, and those of rhyniophyte character but with uncertain vascular affinity, respectively.

Tracheophytes (vascular plants) are characterised as having developed annular or helical thickenings in xylem (water conducting cells) and comprise two major clades: the Eutracheophytes and Rhyniopsida. The Rhyniopsida (not to be confused with the rhyniophytina) comprise distinctive, diminutive and somewhat enigmatic vascular plants that, similar to the protracheophytes, require a greater depth of anatomical and morphological understanding than is currently afforded by the fossil record for further clarification of phylogenetic relationships (Kenrick and Crane, 1997). The Rhyniopsida represent the sister group to the Eutracheophytes, the latter of which represents the tracheophyte crown group (Kenrick and crane, 1997) and comprise all other vascular plants.

Within Eutracheophytes, the Lycophytes form a sister group to all other vascular plants (euphyllophytes) with divergence between the groups being postulated to have occurred early on in the Silurian (Kenrick and Crane, 1997). The lycophytes comprise the Zosterophylls and the lycopods (club mosses), which, based the early appearance of both in the fossil record and, amongst others, sporangial morphologies, have long been postulated to have a close phylogenetic relationship (Banks, 1968; 1975b; Kenrick and Crane, 1997). The lycophytes are a monophyletic group, with lycopods emerging from the largely monophyletic zosterophylls, although the zosterophyll-like group from which this occurred is poorly resolved (Kenrick and Crane, 1997). Herbaceous, leafy taxa such as *Baragwanathia* are postulated to be basal amongst the lycopods (Batemen *et al*., 1992; Kenrick and Crane, 1997). Interestingly, Kenrick and Crane (1997) also identified some *Cooksonia* species to be allied to the lycopod lineage. The Lycophytes form the sister group to all other vascular plants, which are encompassed under the euphyllophytes. This group includes the pteridophytes, equisetopsids and many others aside (Kenrick and Crane, 1997).

The affinities of dispersed spores

The relationship between the above phylogenies and the early land plant palynological record of cryptospores and trilete spores are not clear cut. Historically, trilete spores have been associated

exclusively with the tracheophytes (Gray, 1985), and have been used to indicate their presence in the fossil record. Whilst some trilete spores have been recovered *in situ* in plants with definite vascular tissue (e.g. *Cooksonia pertoni* – Edwards et al., 1992), most have not. Such an absence of unequivocal vascular tissue associated with trilete spores may be attributable to the low quality of the macrofossil record, but more recent work has suggested that trilete spores are produced by some extant bryophytes (e.g. Kenrick et al., 2012; Salamon et al, 2018) such as *Sphagnidae*. Consequently, the position that trilete spores are always produced by tracheophytes is problematic, and therefore some trilete spore producing rhyniophytoids may not be tracheophytic. Such a hypothesis has been fielded for certain *Emphanisporites* species (Taylor et al., 2011).

Meanwhile, the cryptospores also have problematic affinities. Generally considered to represent the most primitive land plant spores, they have historically been considered to represent bryophytes. However, as the most recent phylogenetic analyses suggest, bryophytes are not likely to be true representatives of the earliest land plants. Whilst the first spore evidence of early land plants are envelope enclosed cryptospores from the lower-mid Ordovician (473-471ma) (Rubinstein *et al*., 2010; Wellman, 2010) indeed indicating an ancient lineage for some, other cryptospores have been suggested to be more derived. The relationships of certain apiculate hilate cryptospores and their spore masses to *Paracooksonia* and *Cooksonia* (Morris et al., 2011b), led Edwards et al. (2014) to suggest that the apiculate hilate cryptospores were more closely related to the tracheophytes than other cryptospore groups. Meanwhile, other cryptospores including certain dyads have been linked to liverworts on the basis of a lamellate spore wall ultrastructure (Taylor, 1996). The lamellar wall is considered the plesiomorphic condition of early aero terrestrial algae and embryophyte exospores (Taylor et al., 2017), and in light of Puttick's et al. (2018) findings, the lamellar wall is likely better interpreted in liverworts as a retention of primitive features from the basal embryophyte. Nonetheless, Edwards et al. (2014) do suggest that whilst little is known of their morphology and biology, some cryptospores may have been products of 'proto-bryophytes' and some may have been 'bryophyte-like' in size and in certain aspects of their organisation, but cryptospores were by no means all related to stem-bryophytes. Complicating the bryophyte-tracheophyte association of cryptospores further is the recent description of the eophytes which exhibit a mixture of bryophytic and tracheophytic features such as a branching sporophyte, stomata and permanent tetrads and dyads (cryptospores) (Edwards et al., 2014, 2021a, b, 2022). Edwards et al. (2021a) considered the possible phylogenetic position of the eophytes and placed them as probably an early branching group of the polysporangiophytes, which diverged prior to the loss of matrotrophy and gain of water conducting cells. Ultimately, then, the current consensus based on the growing evidence is that cryptospores are derived from a pool of variously derived embryophytes, which may have been variously related to the tracheophytes, bryophytes and more ancient lineages.

Early land plant life cycles and reproduction

All extant plants exhibit an alternation of generations (fig. 11) between distinct haploid gametophyte and diploid sporophyte stages. Land plant terrestrialisation, occurring by at least the mid Ordovician (Rubinstein et al., 2010) required a suite of adaptive innovations (Wellman, 2004; Kenrick, 2017). The division of generations facilitated this terrestrialisation by allowing different generations to occupy different niches, and hence ease terrestrialisation through sequential adaptation. While land plants share their biochemistry with ancestral green algae, the fundamental tissues of these organisms evolved after terrestrialisation. A haplontic life cycle is typical of the closest algal relatives of land plants, which exhibit a multicellular sexual phase (gametophyte) a unicellular diploid zygote. The ancestral land plant is also considered to have had a similar haplontic life cycle (Kenrick, 2017). Following terrestrialisation, the unicellular zygote became multicellular, and the evolution of key tissues and organs followed with the multicellular diploid zygote phase evolving into a specialised spore dispersal mechanism (the sporophyte).

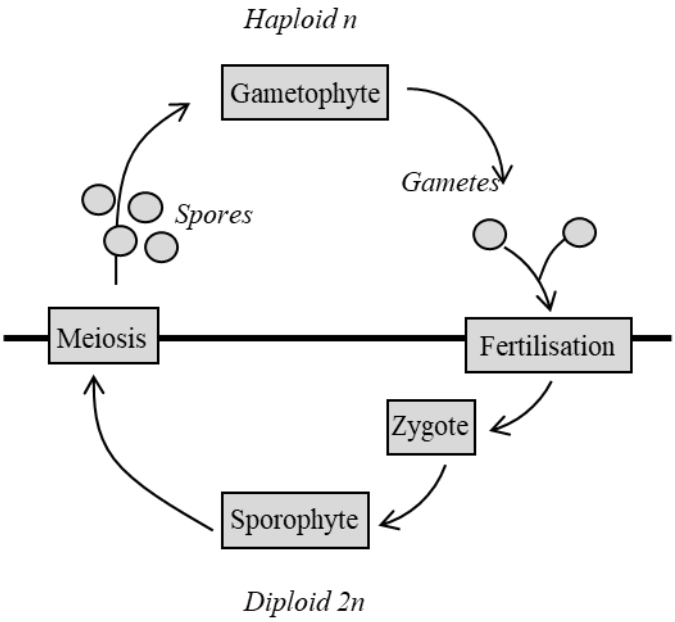

Figure I-11: alternation of generations in bryophytes and vascular lycopods and ferns.

These changes in lifecycle were foundational to the diversification of early land plants, but the mechanism of change remains largely enigmatic. Indeed, there is a dearth of fossil evidence for life cycles in early land plants. It is clear, however, that sporic meiosis, a key indicator of the alternation of generations, was present in the Ordovician (Kenrick et al., 1997; Raven et al., 1999; Graham and Wilcox, 2000). The relationship between the sporophyte and gametophyte varies between plant groups, with Bryophytes exhibiting a small diploid sporophyte, which is nutritionally dependent on its cosexual or female gametophyte (Kenrick, 2017) and vascular ferns and lycopods having independent gametophytes and sporophytes. The sporophytes of these plants exhibit a high degree of complexity, while the gametophyte has limited tissue development.

Phylogenetically, bryophytes have been suggested to form an intermediary between the green algal ancestor and vascular plants (Puttick et al., 2018), although they are no longer thought to be representative of the early land plant body plan, with the ancestral land plant likely being more complex (Puttick et al., 2018). Nonetheless, the bryophytic alternation of generations is likely to be representative of the life cycles of the earliest land plants, including some smaller species of *Cooksonia*. Indeed, following physiological consideration Boyce (2008) concluded that there would have been very little space in the smallest *Cooksonia* species for photosynthetic tissues, and these were likely to instead be nutritionally dependent on a gametophyte. In addition, Gerrienne et al. (2006) reported a cluster of *Cooksonia paranensis* axes which were basally attached to what they interpreted as a female or bisexual gametophyte. From this, they suggested that Rhyniopsida were fundamentally different from Eutracheophytes in that they exhibited isomorphic, rather than heteromorphic, alternation of generations. However, further fossil evidence is yet to be found (Edwards and Kenrick, 2015). The Rhynie Chert plants may proffer some insights into the move towards sporophyte independence, with changes to sporophyte form and function likely to involve the co-opting of tissue systems and ancient genes which facilitated gametophyte independence into the sporophyte (Kenrick, 2017). Irrespective of the independence of the sporophyte and gametophyte phases, the spores facilitating the reproduction of these early land plants would have required moisture.

Phytogeography

Global Přídolí-Lochkovian palaeobotanical assemblages have been collated from the literature and tabulated (thesis appendix 1.1). Assemblage components are presented here alongside the locality and

where possible, palaeoenvironmental, paleolatitudinal and palaeoclimatic data has also been collected. Each assemblage has been plotted in approximate chronological order. Taxa such as *Parka* and *Prototaxites* have been excluded because of their enigmatic affinities. Similarly, species diversity of the assemblage has not been alluded to as this is easily distorted by, amongst others, facies differences and preservational effects (Edwards and Richardson, 2004)

The assemblage localities were then plotted on palaeogeographic reconstructions from Torsvik and Cocks (2016). Reconstructions are separated into late Silurian and Early Devonian palaeogeographic reconstructions, with Přídolí and Lochkovian assemblages being plotted onto each reconstruction respectively.

There are some 41 known palaeobotanical assemblages known globally from the Přídolí and Lochkovian. Tabulated localities from the Přídolí indicate that rhyniophytoids and rhyniophytes are a common component of all known assemblages and are sometimes the only plant represented. Zosterophylls are also a common component of assemblages, being represented in *ca.*36% of assemblages. Rarer Lycophytes (*ca.*10%) are found in some assemblages. No Trimerophytes are demonstrated in Přídolí assemblages, and a number of taxa with uncertain affinities are also found.

Lochkovian assemblages show an increase in more complex tracheophytes. Zosterophylls become a common aspect of the preserved flora, being represented in *ca.*76% of assemblages and in some assemblages zosterophylls are the only component. Rhyniophytes and rhyniophytoids remain a common component of Lochkovian assemblages, being represented in most cases. Similar to the Přídolí, lycophytes are not widely represented in Lochkovian assemblages. Trimerophytes begin to appear towards the end of the Lochkovian.

Palaeogeographically, Přídolí assemblages (fig. 12) show some phytogeographic tendencies. Rhyniophytoids appear to be cosmopolitan across the major landmasses, with assemblages distributed between the poles and equator. Rhyniophytes appear restricted to Laurussia. Zosterophylls and Lycopods appear to be restricted to lower latitudes on landmasses either side of the palaeoequator.

Lochkovian assemblages show a similar distribution of assemblages, with rhyniophytoids remaining cosmopolitan. Zosterophylls and lycopods remain apparently confined to latitudes ≤30°S/N. newly emerging Trimerophytes are also apparently confined to tropical latitudes.

5.2. Přídolí and Lochkovian phytogeographic distribution

Descriptions of palaeobotanical assemblages have been commonplace since the 1930s (e.g. Lang *et al*., 1937) and qualitative attempts to relate the assemblages to a palaeogeographical context have become widespread (e.g. Edwards, 1990). As data sets have improved, quantitative attempts using a variety of statistical methods including cluster analysis and multidimensional scaling have been used in attempts to better understand phytogeographic distributions, with varying results (e.g. Raymond *et al*., 2006; Wellman *et al*., 2013). Despite the ever-increasing number of described assemblages and somewhat increased quality of the data set, any attempts to reconstruct the phytogeographic distribution of early land plants must consider the significant pit-falls that are inherent within the fragmentary and largely inadequate palaeobotanical data set. Originally outlined by Edwards (1990) in her initial analysis of palaeophytographic distributions of Silurian land plants, inherent problems that arise from using such a fragmentary database, which include issues with stratigraphic accuracy, facies bias and the accuracy of identification and affinity of fossils, persist in recent palaeophytogeographic reconstructions and have the potential to skew results (Wellman *et al*., 2013). Whilst any reconstruction must pay close attention to these shortcomings, investigating the positions of assemblages regarding phytogeographic distribution is both an interesting and useful exercise, giving richer insights into floral changes in the early stages of terrestrialisation.

As previously discussed, a significant disparity exists in the fossil record between megafossils and palynomorphs. Because of the paucity of land plant megafossils in pre-Silurian rocks, the less fragmentary and data rich dispersed spore record has been used to analyse the phytogeographic

distributions of Ordovician and early Silurian embryophytes. Wellman *et al*. (2013) used multidimensional scaling to investigate palaeophytogeographic variation amongst the cryptospore assemblages of the earliest embryophytes, which are widely believed to be physiologically relatable to liverworts (Gray, 1985, 1991), although to what extent they were physically similar remains unknown (Wellman *et al*., 2013). Cryptospore assemblages remained largely uniform through the mid Ordovician, but there is some indication of phytogeographic differentiation even in these early assemblages, with, *inter alia*, infrapunctuate ornamentation on cryptospores being confined to south-east Gondwana (Wellman *et* al., 2013). Following the multidimensional scaling analysis of Silurian assemblages, Wellman et al. (2013) found that phytogeographic differentiation remained largely unpronounced through much of the Silurian also. This tendency to retain phytogeographic uniformity points towards evolutionary stasis amongst the earliest cryptophytes for at least 40 myr.

Wellman *et al*. (2013) did find some indication of early phytogeographic differentiation in the latter half of the Silurian, developing from the Llandovery to the Přídolí between Gondwanan and North American-Baltic regions. Whilst this trend in phytogeographic differentiation is expected, the results are certainly not final; the data indicates initial trends derived from an incomplete but improving database alongside which patterns derived from the data will change (Wellman *et al*., 2013). This trend is coupled with a marked increase in the abundance, diversity and disparity of trilete spores and a reduction in cryptospores, presumably as early tracheophytes and their immediate ancestors began to diversify. Indeed, it is during the Llandovery that the first significant megafossil assemblages begin to appear (table 29.1 Wellman *et al*., 2013), with the emergence of larger, more readily preserved plants. Figs. 12 and 13 outlines Silurian megafossil assemblages (thesis appendix 1.1) and, accepting the short-comings of the megafossil record, the first order observations made there are in line with other conclusions regarding the state of the flora (e.g. Edwards, 1996).

Fig. 12 shows the Přídolí megafossil assemblages plotted on Přídolí palaeogeography. Přídolí assemblages (table 1) are largely dominated by rhyniophytoids and rhyniophytes, with Zosterophylls becoming more common towards the end Přídolí, but are excluded from the Anglo-Welsh Basin. Fig. 12 indicates that rhyniophytoids were cosmopolitan across landmasses at this time, forming often significant components of assemblages across landmasses. Postulations regarding the likely life-styles of rhyniophytoids and rhyniophytes by Wellman *et al*. (2000) and Edwards and Richardson (2004) suggested that a dependence on constant humidity was likely. Additionally, a ruderal life cycle was suggested for these plants, growing in settings where rapid colonisation, growth and reproduction would have been adventitious, such as in frequently flooded settings. In periods of seasonably arid or unequable conditions, it was postulated that rhyniophytoids and rhyniophytes persisted as dormant spores until suitable conditions returned (Edwards and Richardson, 2004), or perhaps persisted as horizontal rhizomatous growths (Raymond *et al*., 2006). This ruderal hypothesis and ephemeral life-cycle was suggested by Raymond *et al*. (2006) to possibly explain the phytogeographically cosmopolitan appearance of rhyniophytoids and rhyniophytes in the Late Silurian and Early Devonian.

Zosterophylls and lycopods, too, are relatively common in late Silurian assemblages although these plants appear to be confined to equatorial assemblages, in line with Raymond *et al*. (2006) and it is possible that these plants preferentially occupied these palaeoequatorial regions, whilst rhyniophytoids and rhyniophytes preferentially inhabited subequatorial and temperate regions (Cascales-Miñana in Meyer-Berthaud *et al*., 2015). It has also been suggested that zosterophylls and lycopods were initially endemic to north-east Gondwana, emerging there in the Silurian before gradually migrating west into the Lochkovian (Wellman *et al*., 2013) finding indicated a lack of phytogeographic differentiation, even in the late Silurian. Some phytogeographic variation was noticeable, however, between the Llandovery and Přídolí, especially between the north American and Baltic regions.

Some very early assemblages have necessitated a revaluation of the floral complexity that was emerging by the Přídolí. The Ludlow-Přídolí assemblage in Victoria, Australia (Douglas and Holmes, 2006), is in stark contrast to coeval assemblages. The assemblage has yielded both rhyniophytoids and

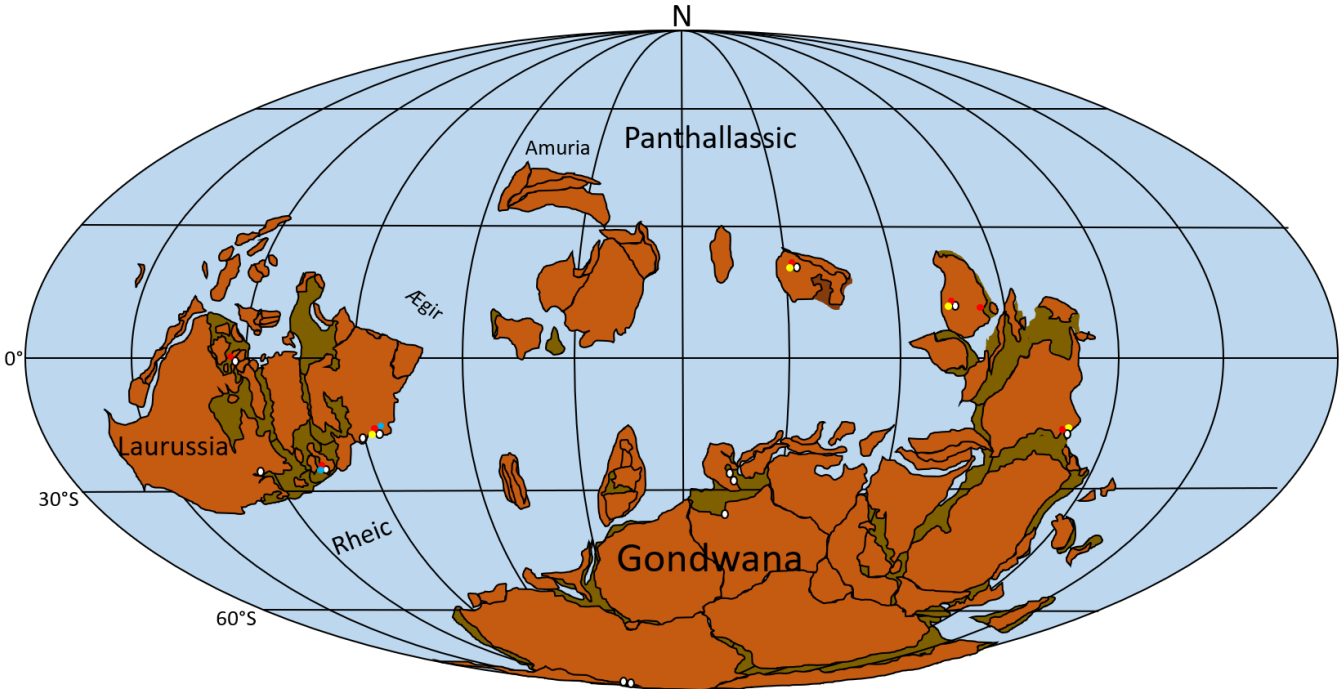

Figure I-12 Palaeophytogeography of Přídolí palaeobotanical assemblages. Rhyniophytoids (white circles) appear to be cosmopolitan across landmasses with assemblages located in a range of latitudes from pole to equator. Rhyniophytes, whilst possibly partially relatable to rhyniophytoids, appear confined to lower tropical latitudes. Similarly, zosterophylls and lycopods appear confined to tropical and equatorial latitudes. Map after Torsvik and Cocks, 2016. Sites in thesis appendix 1.1.

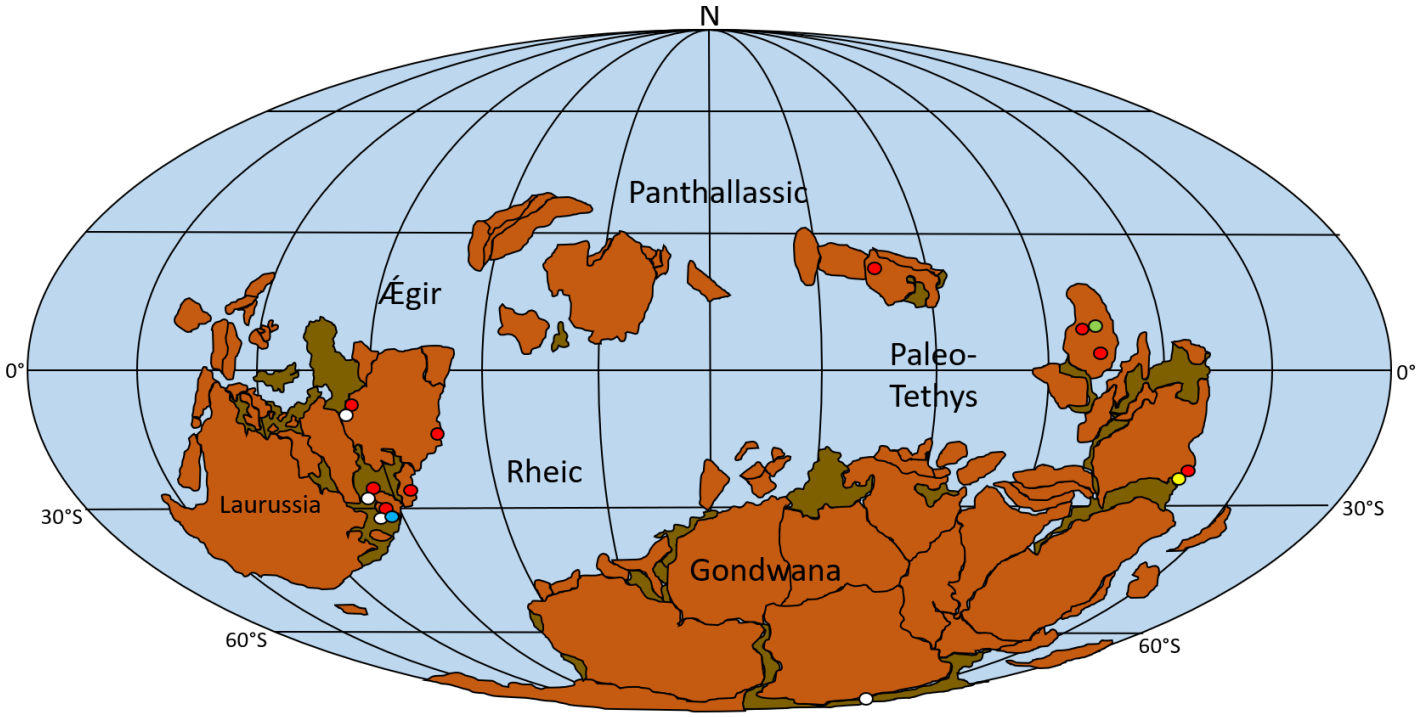

Figure I-13: Palaeophytogeography of Lochkovian megafossil assemblages. Reminiscent of the Přídolí, rhyniophytoids remain cosmopolitan across landmasses from pole to equator. Zosterophylls remain largely confined to latitudes ≤30° either side of the palaeoequator, as do lycopods and newly emergent Trimerophytes. Palaeogeographic map after Torsvik and Cocks, 2016. Sites in thesis appendix 1.1.

zosterophylls, but also the more complex basal, leafy lycopod *Baragwanathia* (Tims and Chambers, 1984). The initial dating of this horizon was considered suspect as the occurrence of a basal lycopod in the Ludlow was considered unrealistic (Cleal and Thomas, 1999), as a Ludlovian age for these lycophytes would place their existence *ca*.5 million years after the first appearance of Cooksonia in the Wenlock (e.g. Edwards *et* al., 1992; Gonez and Gerrienne, 2010). The Ludlovian affinity, however, of the Australian fossils is now strongly supported (e.g. Rickards, 2000) and thus a suitable explanation for these plants must be found elsewhere. Wellman *et al*. (2013) postulated that the Ludlow *Baragwanathia* may represent an extreme form of endemism or that they may have a divergent morphology owing to a specialised ecology, perhaps relating to subaqueous existence. Alternatively, it was also postulated that the surprising appearance of Lycophytes in the Ludlow may be a product of the fragmentary and incomplete megafossil record, which may not fully represent all Silurian plant life (Wellman *et al*., 2013) due to the plethora of biases related to the record.

Lochkovian assemblages appear to show a similar distribution to the Silurian, although zosterophylls appear to increase in their distribution, but remain within the subequatorial zones. Conversely, undefined stems of lycopods have been described from Argentina (Southernmost Gondwana) by Edwards *et al*. (2009), indicating a shift towards greater phytogeographic distribution in lycopods.

5.3. Palaeobotany of the Přídolí-Lochkovian of the Anglo-Welsh Basin

Several sites yielding standard and exceptionally preserved macrofossils are known from the Anglo-Welsh Basin, and these are illustrated in fig. 14.

Sites of Standard Preservation

Several important sites yielding plant macrofossils exist in the Přídolí and Lochkovian of the Anglo-Welsh Basin (fig. 14, thesis appendix 1.2).

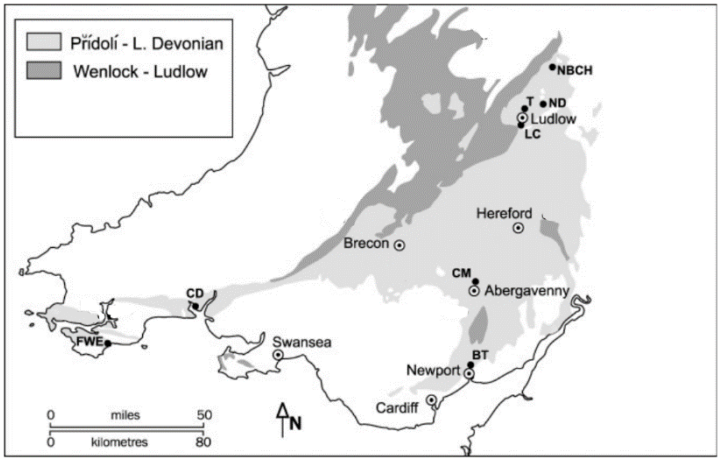

Figure I-14: Line map illustrating the Přídolí-Lochkovian localities in the Anglo-Welsh Basin, modified from Edwards and Richardson, 2004. ***BT:*** *Brynglas tunnels;* ***CD:*** *Cwm Graig Ddu;* ***FEW:*** *Freshwater East;* ***LC:*** *Ludford Corner/Lane* ***NBCH:*** *North Brown Clee Hill – Hudwick Dingle;* ***ND****: Newton Dingle;* ***T****: Targrove Quarry. Assemblages and further information is given in thesis appendix 1.2.*

Insights from Standard preservation

MACROFOSSILS

The preservation of macro- and mesofossils in the Anglo-Welsh Basin is relatively poor. The record mainly consists of heavily compressed, coalified films which are variously found as tangled mats of isolated sporangia and fragmented axes, some of which may exhibit terminal sporangia (e.g. Edwards,

1970). Due to the poor level of preservation exhibited by these fossils, only gross morphological and very limited (cuticular) anatomical information can be obtained from them (Edwards and Richardson, 2004). These fossils are all allochtonous, with some specimens clearly demonstrating sorting and current alignment (e.g. *Gosslingia*). Transportation is largely postulated to have occurred during high energy flash flooding where plants were washed downstream or out to sea. Dry seasons also saw living and dead of plants burned by wildfires (Glasspool et al., 2006). These remains may have been later transported and deposited in desiccated depressions by wind (Edwards and Richardson, 2004). Because of the highly fragmented nature of the plants and the lack of a 'complete', *in situ* plant (*cf*. Rhynie Chert) the degree of fragmentation is uncertain, and it is possible that smaller fragmentations are distal axes of a larger plant – the diminutive nature of the vegetation, however, is variously supported by similarly sized axes between multiple localities (Edwards and Richardson, 2004).

'Standard' preservation, that is, compressed coalified fossils, are relatively common in the Anglo-Welsh Basin, being typically represented as tangled mats on the surfaces of bedding plains (e.g. Edwards, 1970; Edwards and Rogerson, 1979). Initial investigations on the fragmented 'tea-leaf' assemblages of Silurian - Devonian vascular plant remains were made by Lang (1937), who defined the genus *Cooksonia* and described two associated species, *C. pertoni* and *C. hemisphaerica*, differentiated by the gross morphologies of their sporangia. Despite the poor preservation of these plants, Lang (1937) was able to describe tracheids from *Cooksonia specimens*. Later, more rhyniophytoids were described from Přídolí and Lochkovian strata, including *C. cambriensis*, (Edwards, 1979) and *Caia langii* (Fanning *et al*., 1990) in localities such as Targrove Quarry and Perton Lane. Enigmatic, possibly bryophytic taxa *Steganotheca striata* (Edwards, 1970) were also described. Despite new discoveries of rhyniophytoids, the ability to assign the new taxa to the vascular rhyniophytes was frustrated by the paucity of anatomical information available in the coalified specimens, a problem that persists at present. Additionally, the lack of fossils attributable to the cryptophytes, known to be present because of the persistence of their cryptospores, greatly hindered the understanding of the ecosystems. It was not until discoveries of exceptionally preserved specimens in the Ludlovian locality of Capel Horeb that tracheids were again demonstrated in *C. pertoni*, allowing their placement within the vascular plants.

TUBULES

Fragmentary, enigmatic tubules are regularly recovered from the Přídolí-Lochkovian of the Anglo-Welsh Basin (e.g. Edwards, 1981). These are typically very small and, especially towards the Devonian, show a high level of disparity (Burgess and Edwards, 1991) relative to earlier tubes, which are variously known since the Cambrian (Gensel, 2008).

For the most part, the tubules remain enigmatic (e.g. Edwards. 1996), and this is due to a number of reasons, including their diminutive, fragmentary nature and a lack of modern analogues and homologues (Wellman, 1995). Various workers have postulated the affinities of the plants however, with some similarities being found between fossil and extant plants and fungi (Wellman, 1995). They have been variously collected from terrestrial strata and the tubules themselves indicate a terrestrial habit for the parent plants (Edwards, 1982).

Some workers have postulated an affinity with bryophytic plants, in that they may represent the acid hydrolysis or decay resistant remains of basal embryophytes (e.g. Graham and Gray, 2001; Graham *et al*., 2004). This hypothesis followed the treatment of extant bryophytes to simulated fossilisation processes, and decay resistant elements of these bryophytes somewhat resembled the tubular microfossils (e.g. Graham and Gray, 2001), although this was not definitive. Edwards *et al*.(2013) suggested an affinity between the tubules and lichenised fungi, based on reconstructions of the stratified thalli from Nematophytes (Wellman and Ball, 2021).

Sites of Exceptional Preservation

LUDFORD LANE

The Ludford Lane locality is represented by productive siltstone horizons in a small cliff exposure Shropshire (Jeram *et al*., 1990). Sediments of the Platyschisma Shale member (within the Downton Castle Sandstone Formation) and are interpreted to have been deposited in shallow marine environments above the wave base (Richardson and Rasul, 1990). Sediments are correlated with the *tripapillatus-spicula* spore biozone (Richardson and McGregor, 1986; Richardson and Edwards, 1989; fig. 6) and are therefore of earliest Přídolí age. The exposure may initially have been alluded to by Lang (1937), but it was not until the 1990s that the locality was properly investigated. Bulk maceration of material yielded, amongst others, terrestrial arthropod remains and charcoalified plant mesofossils (Jeram *et al*., 1990; Edwards *et al*., 1996, 1999; Wellman *et al*., 1998).

HUDWICK DINGLE

The Hudwick Dingle lagerstatte is located in a stream section north of Brown Clee Hill (Edwards *et al*., 1994), Shropshire. The sediments are related to the Freshwater West Formation (Lower Ditton Group) (Ball and Dineley, 1961) and were laid down during fluvial sedimentation. The locality is of early-mid Lochkovian age (Edwards *et al*., 1994), having been correlated with the middle subzone of the *micrornatus-newportensis* spore biozone (Richardson and McGregor, 1986). Hudwick Dingle has yielded more taxa than any other (Edwards and Richardson, 2004) and has offered exceptionally rich insights into Lochkovian terrestrial ecosystems, regarding early embryophytes and animal-plant interactions. Quantitative studies of the mesofossils found at this locality have determined that the fossils are charcoalified and were formed by means of wildfires (Glasspool *et al*., 2006), with the chemically inert fossils being readily preserved and demonstrating exceptional anatomical detail.

Insights from Exceptional Preservation

Cellular Detail

Three-dimensional information on cellular detail in early embryophytes is found in charcoalified specimens in both Ludford Lane and Hudwick Dingle, but much of the exquisite anatomical detail is derived from the latter.

Sterile and fertile axes of rhyniophytoids bearing stomata have been described from the Ludlow Lane locality (e.g. Jeram *et al*., 1990), and these Přídolí specimens represent the earliest examples of stomata (Edwards, 1996). It is clear, however, that a number of stomatal types were present by this time, with specimens exhibiting distinctive dimensional variation in guard cells and poral characters (Edwards *et al*., 1996). Currently, no earlier plants well enough preserved to demonstrate unambiguous stomata have been described despite the macrofossil record extending back to the Wenlock (Edwards *et* al., 1992), leaving stomatal development enigmatic. Despite stomata being present in these late Silurian plants, they are rare and exhibit low stomatal densities, a theme that persists into the Lochkovian (Edwards *et* al., 1986; Edwards *et al*., 1992) on specimens of *C. pertoni* (Edwards *et al*., 1986). There is some indication of stomatal densities increasing around the sporangia and sporangial walls, however, in some Silurian - Devonian taxa (Edwards *et al*., 1992; Li *et al*., 1992). The presence of stomata (and associated cuticle) clearly demonstrates the embryophytic affinities of these fossils. Additionally, phylogenetic relationships, including the monophyletic relationships of embryophytes and their derivation from a single algal group is also indicated, given the presence of stomata on these fossils in addition to bryophytes and tracheophytes (Edwards *et al*., 1986; Kenrick and Crane, 1997).

Three specimens of *C. pertoni* subsp. *pertoni* from the Hudwick Dingle Locality were demonstrated by Edwards *et al*. (1992) to contain *in situ* tracheids. Whilst this finding clarified the affinity of *C. pertoni* subsp. *pertoni* amongst the tracheophytes (rhyniophytes), other morphologically similar specimens, including other species of *Cooksonia*, remain as rhyniophytoids, until such a time as tracheids can be demonstrated in their axes. This caution is warranted, given the amount of 'cryptic' diversity that has been found within these morphologically simplistic rhyniophytoids (see *in situ* spores). In addition to confirmation of vascular status, the tracheids in *C. pertoni* subsp. *pertoni* allowed the comparisons of

conducting elements with a closely related hepatic specimen with similar gross morphology but varying cellular detail (Edwards *et al*., 1995). The latter specimen exhibits slightly thicker wall thickenings than *C. pertoni*, and thus xylem evolution may have been derived from structural material, as the latter was reduced to accommodate for extensional growth and water exchange (Edwards *et al*., 1995), instead accumulating in the vascular strand. Stereome has also been described from specimens of *Cooksonia* in Hudwick Dingle (Edwards *et al*., 1986), and this allowed speculation regarding the physiology of the plant. It was postulated by Edwards *et al*. (1986) that the stereome played a supporting function in *Cooksonia in lieu* of well developed, lignified vascular tissue, perhaps allowing *Cooksonia* to tolerate inequable conditions.

In Situ Spores

As previously discussed, rhyniophytes and rhyniophytoids have been historically defined by the morphology of their terminal sporangia (e.g. Lang, 1937; Edwards, 1974; Fanning *et al*., 1990), and many show a high degree of morphological similarity with perhaps minor differences in shape. Both Ludford Lane and Hudwick Dingle yield sporangia from rhyniophytes and rhyniophytoids, and their exceptional preservation has allowed the scrutiny of *in situ* spores and their ultrastructure. *In situ* spores are not exclusively known from exceptional preservation sites, and *in situ* examples from other sites in the have been included in the discussion here for completeness.

Analysis of the *in situ* spores liberated from rhyniophytoid sporangia has revealed cryptic evolution and diversity amongst these taxa and hinted at the biological affinities of some dispersed spore species.

In situ spores shed light on apparently cryptic rhyniophyte diversity, which would otherwise go unnoticed given the morphological similarities of sporangia, by which species of *Cooksonia* are distinguished (e.g. Fanning *et* al., 1991). Fanning *et al*. (1988) found that identical sporangia of *C. pertoni* yielded four different types of *in situ* spore, which were related to the dispersed miospores *Ambitisporites (C. pertoni* subsp. *pertoni), Synorisporites* (*C. pertoni* subsp. *synorispora*) and *Streelispora/Aneurospora (C. pertoni* subsp. *aneurospora*) Habgood *et al*. (2002) described a further subspecies, *C. pertoni* subsp. *retusispora* from the Hudwick Dingle locality, after finding that some *C. pertoni* sporangia yielded reticulate spores relatable to *Synorisporites* species. Cryptic Interspecific variation between rhyniophytoid genera is also seen through *in situ* spore analysis. *In situ* spores from morphologically similar sporangia of *Pertonella* sp. and *C. pertoni* exhibit retusoid *Apiculiretusispora arcidecus* (Richardson *et al*., 2001) and crassitate *Ambitisporites* respectively, (Fanning *et al*., 1991), enabling a definite distinction to be made between these taxa, despite apparent morphological consistency (Edwards *et al*., 1996). Similarly, other rhyniophytoids with similarly shaped sporangia such as *Caia langii* and *Cooksonia cambrensis* are able to be confidently differentiated, yielding laevigate retusoid spores and *Ambitisporites* sp. Respectively (Fanning *et al*., 1991). Morris *et al*. (2012b) used spore wall ultrastructure to analyse the similarities between *Cooksonia banksii* and *C. pertoni*. Significant differences were found between the two, and *C. banksii* was reassigned to the genus *Concavatheca*, further highlighting the cryptic diversity amongst rhyniophytoid taxa.

In situ spores have also been found to give some insight into the cryptic evolution of rhyniophytes and rhyniophytoids. Where variously aged *in situ* spores are obtained from the sporangia of the same species, 'cryptic' evolution may be observed, whereby, amongst others, spore ornament changes despite apparent stasis in the gross morphology of the plant. The rhyniophyte *Cooksonia pertoni* is an excellent example of this, where *in situ* spores exhibit a gradual change in ornament between the Přídolí and Lochkovian whilst retaining an equatorially crassitate structure (Fanning *et al*., 1988) (table 5).

Feature	Llandovery	Upper Wenlock	Lower Přídolí	Lower Lochkovian
Spore taxa	*Ambitisporites*	*Synorisporites*	*Synorisporites*	*Aneurospora*
Ornament	Distally laevigate	Distally murinate - verrucate	Distally verrucate – murinate with proximal inter-radial papillae	Distally apiculate, proximally tripapillate

Table I-3: The evolution of spore ornament (exine sculptural pattern) associated with in situ *spores of* C. pertoni *through the Llandovery – Lochkovian. Overall spore structure remains as equatorially crassitate throughout, and the gross morphology of the plant remains attributable to that of* C. pertoni. *Content from Fanning* et al.*, 1988.*

From the observations of the trends in spore sculpture, Fanning *et al*. (1988) were able to define three subspecies of *C. pertoni* based on *in situ* spores, thereby demonstrating a previously unseen level of diversity amongst the same species of plants through geological time. Similar trends in spore ornament have also been identified amongst other dispersed, proximally thin trilete miospores including retusoid forms as well as cryptospores (Richardson and Burgess, 1988; Richardson, 1996a), with ornament evolving through smooth, verrucate, apiculate and retusoid forms over similar periods of time (Edwards and Richardson, 2004). The inception of new ornament in other taxa is not synchronous with those of *C. pertoni* (Fanning *et al*., 1988), with miospores typically lagging behind cryptospores (Richardson, 1995). Whilst the development of new ornament is clearly observed, the evolutionary advantages of such changes remains an enigma. Kevan *et al*. (1975) suggested that the increasing complexity of exine ornamentation may have been less palatable for arthropods. Indeed, arthropod coprolites from Hudwick Dingle and the North Brown Clee Hill localities may indicate some level of spore-centred feeding in early terrestrial organisms (see animal-plant interactions). This hypothesis does not explain the lack of synchronicity seen in spore ornament evolution between taxa, however (Fanning *et al*., 1988). Other workers have postulated that ornament evolution may have been a response to inequable environments, perhaps offering some level of drought resistance or more precise control on germination amongst spores, thereby allowing the invasion of more water stressed, distal settings as competition amongst early plants for equable environments increased (Mogenson, 1981; Richardson and Burgess, 1988).

The discovery of *in situ* spores allows biological affinities between the dispersed spore record and parent/ producer plants to be established, offering richer insights into the palaeoecology of the Anglo-Welsh basin and *in situ* spores enable a biological affinity between a fossil plant and a dispersed spore to be ascertained, allowing interpretation of the dispersed spore record in terms of parent plants (e.g. Richardson, 2007). A large proportion of the dispersed spore record has not been found *in situ* and therefore lack any biological affinity with parent/producing plants (Richardson, 2007), which may be due to the parent plants living outside of the immediate catchment area of rivers, or due to low preservation potential of parent plants (Richardson, 2007). However, a number of dispersed spore taxa have been connected to important megafossil taxa (e.g. Fanning *et* al., 1988; Fanning *et al*., 1991; Edwards *et al*., 1995). This includes various rhyniophytoids and rhyniophytes, including *Cooksonia* (e.g. Fanning *et al*., 1988), various zosterophylls (e.g. Edwards and Wellman, 2001) and cryptospore producing plants (e.g. Fanning *et al*., 1991; Wellman, 1998a; Morris *et al*., 2011b), adding a further dynamic when interpreting dispersed spore assemblages.

The taxonomic affinities of parent plants may also be elucidated through the analysis of spore wall ultrastructure, from exceptionally preserved *in situ* spores in Ludlow Lane and Hudwick Dingle. Morris *et al*., (2011b) compared the ultrastructures of hilate and trilete spores that had been extracted from morphologically coherent spore masses of *lenticulatheca* and *paracooksonia*, which were then related to the genus *Cooksonia*. Whilst the spores showed broad differences (hilate cryptospores and trilete spores), broad similarities in ornament and spore ultrastructure, and nature of the spore mass, facilitated postulations that the two genera represent closely related lineages, and that at least some hilate cryptospores were closely related to the tracheophytes (Edwards et al. 2014). Wellman *et* al. (1998)

used spore wall ultrastructure to postulate the affinities of *Pertonella* and *Cooksonia* and despite similar sporangia, they were found to have very different spore ultrastructures (reinforcing the findings of Edwards *et* al., 1996). Furthermore, the absence of extrasporal layers in *Pertonella* (*cf.* Cooksonia) points towards affinities with certain basal lycopods (Tryon and Lugardon, 1991) and this finding may add some weight to Hueber's (1992) hypothesis that lycophytes emerged from a plexus of rhyniophytoid plants - although a lack of coeval spores from homosporous lycopods hinders further investigation of this. Most recently, the combination of *in situ* spores and axial anatomy from exceptionally preserved mesofossils has allowed the description of a new lineage of plants, the eophytes, which share a mixture of bryophytic and tracheophytic features (Edwards et al., 2022a,b, 2022).

In situ spores may also shed light on possible specialised flora, giving novel insights into the ecology of an area. The discovery of a section of bifurcating axis containing *in situ* spores relatable to *Emphanisporites* in the Welsh Borderlands reminiscent to that of the Rhynie Chert plant *Horneophyton lignieri* by Edwards and Richardson (2000), and later confirmation that Scottish specimens contained *Emphanisporites* also (Edwards and Richardson, 2004) may give some insight into more specialised flora in the Lochkovian. Discussion based around likely high water use efficiency of Rhynie Chert plants (Edwards *et al*., 1998) and long standing debate that the Rhynie Chert plants may be specialised to certain niches (Scott, 1920; Schopf *et al*., 1966) may point towards the Welsh *Horneophyton* sp. also being adapted to specialist niches, which may have included water and chemically stressed environments. This specialisation may explain why this plant has not been found elsewhere (situated away from depocentres) and is represented sporadically in the dispersed spore record across the basin (widespread but uncommon constituent of vegetation, possibly situated away from rivers) (Edwards and Richardson, 2000, 2004).

In situ spores therefore provide a powerful tool for the investigation of early land plant floras. However, the proportion of dispersed spore taxa that remain to be assigned a parent plant far outweighs those that have, and the biological affinities of many currently remain uncertain beyond broad groupings. Analyses of spore wall ultrastructures, despite considerable advances, remain susceptible to a number of problems, including problems with ascertaining ontogenetic variation in spores (Wellman *et al*., 1998).

Spore dehiscence mechanisms

Exceptional preservation has also yielded information regarding the liberation of spores from sporangia, shedding light on an important phase of the land-plant life cycle. The ability to shed spores when conditions were optimal for spore dispersal would have been vital for early embryophytes. Some rhyniophytes such as *Cooksonia* show no clear mechanism for spore release, with some specimens indicating that the distal portion of the sporangia disintegrated to release spores (Edwards, 1996). Other Přídolí specimens exhibit two types of dehiscence mechanisms: (i) dissociation of a distal 'lid' from the main sporangia, thereby exposing spores, and (ii) predetermined dehiscence into two 'valves' via a sporangia-encircling convex margin (Edwards, 1996). The latter is present in the Devonian (e.g. on zosterophylls), and may represent a more efficient mechanism for spore dispersal.

Přídolí-Lochkovian Plant-Animal Interactions

Whilst the Lochkovian Hudwick Dingle locality far surpasses the contributions of Ludford Lane in terms of the understanding of Silurian - Devonian plants, the latter gives unparalleled insights into animal-plant interactions at this pivotal point in time. Jeram *et al*. (1990) described a diverse terrestrial arthropod assemblage from Ludford Lane, comprising fragmented arachnids, eurypterids and myriapods, deposited alongside plant remains in the shallow marine Platyschisma Shales. This Přídolí assemblage represents the earliest (known) assemblage of terrestrial animals, and Jeram *et al*. (1990) postulated that it may suggest a closer relationship between the separate invasions of land by plants and animals than had postulated before (e.g. Gray and Boucot, 1985). In this assemblage, predators were

exclusively represented, indicating that herbivorous aspects of the biota remained enigmatic. Regardless, the biota at Ludford Lane gives a valuable insight into an important component of the terrestrial biosphere.

The Hudwick Dingle locality has shed light on Lochkovian animal-plant interactions through coprolites, in addition to body fossils of eurypterids and myriapods (Edwards *et al*., 1995). The coprolites were initially mistaken for sporangia, as they are essentially concretions of spores, however, *inter alia*, the lack of a sporangial wall, irregular shape and variety of spore taxa within each specimen precluded this. The affinities and feeding behaviours of the animals remains largely elusive. Feeding on sporangia and spores would presumably have provided a relatively nutrient rich diet compared to feeding on the axes of the plants, but to what extent nutrients could be extracted from the spores is unclear, especially as the spores appear largely undigested. It is also possible that the animals were detritovores, which may explain the dearth of fungal material in the coprolites, as this is more readily digested (Edwards *et al*., 1995). Indeed, Edwards *et al*., (2012) reported coprolites containing *Nematosketum* and *Nematothallus* tissues, suggesting that these animals (probably millipedes) were mycophagus and selectively fed on fungi. These coprolites fill an important trophic gap in the fossil record, representing the first direct evidence for herbivory in terrestrial settings (Edwards *et al*., 2012).

6. Conclusions

The Anglo-Welsh Basin represents an exceptionally important site for studying the nature and tempo of the adaptive radiation of vascular plants, having a rich dispersed spore record and useful, if fragmentary, fossil record (Edwards *et al*., 2004). Much remains to be investigated regarding the cryptic evolution and diversity amongst the rhyniophytes and rhyniophytoids, which has important ramifications for phylogenetic relationships and the tempo of evolution amongst these morphologically similar plants (e.g. Wellman *et al*., 1998).

The patterns seen in the dispersed spore record of the Anglo-Welsh Basin are reflected in multiple sites around the world in a variety of facies, indicating that facies bias is not a significant factor in the increasing quantity, diversity and disparity of dispersed spores, and supporting the hypothesis that the trend is related to evolution of parent/producer plants (after Richardson and Lister, 1969). Further sampling may help to reduce the problems associated with data paucity in some aspects of the diversity and disparity trends of Wellman *et al*. (2013).

The dispersed spore record has a significant potential to be a powerful tool in international correlation and biostratigraphy, with some spore zones already being well defined (e.g. *micrornatus-newportensis*) and well correlated, both regionally and globally (e.g. Richardson and McGregor, 1986). Others, especially in the Přídolí, are in need of clarifying and defining (compare spore zones in Richardson and McGregor, 1986 and Edwards and Richardson, 2004). Dispersed spores are also useful for quantitatively analysing proportions of sporomorphs in assemblages and relating them to facies changes over time, giving insights into the habitats of early land plants *in lieu* of *in situ* land plants (Richardson, 2007), reconciling some of the bias in the macrofossil record. Dispersed spores are also useful for identifying regional variance in vegetation, such as that seen between intramontane basins in the Midland Valley and alluvial plains of the Anglo-Welsh Basin (e.g. Wellman *et al*., 1999)

Whilst the macrofossil record is inherently fragmentary, it still offers unparalleled insights into the morphologies and diversity of early land plants. The trends seen in macrofossils in the Anglo-Welsh Basin differ significantly from coeval assemblages from elsewhere - Rhyniophytoid dominated floras exist in the former, whilst in others, such as Victoria (Australia) complex, leafy vegetation exists. The reasons for this disparity are unclear, with speculations regarding extreme endemism and the bias of the fossil record (Wellman *et al*., 2013).

Exceptional preservation offers insights into the physiology and affinities of early plants (e.g. Edwards, 1996) and reveal cryptic diversity and evolution that would be lost in standard preservation. Information

regarding the earliest terrestrial ecosystems are further enriched by animal remains and coprolites (e.g. Jeram *et al*., 1990).

7. Key questions

The sediments of the Anglo-Welsh Basin and those of the latter parts of the Palaeozoic Marine Welsh Basin have greatly contributed to the current understanding of early land plant biology, dynamics and evolution, in addition to contributing greatly to major spore biostratigraphic schemes. Nonetheless, key questions remain to be answered, and these are explored in the proceeding thesis.

(1) What is the nature of the pre-*micrornatus – newportensis Apiculiretusispora* sp. E zone? What spore species define this zone, and can these be integrated into current biostratigraphic schemes and utilised for regional and global biostratigraphic correlation?

(2) The mid – late Přídolí sampling gap presents a major challenge for advancing the regional spore biostratigraphy of the area. What is the nature of the spore assemblages in this zone? Moreover, given the recovery of *Aneurospora* species in the mid Přídolí of Saudi Arabia (Breuer et al., 2017), is this genus still suitable for indicating the base of the Devonian in Euramerica? (*sensu lato* Richardson et al., 1981, 1984, 2001).

(3) A major diversification event has been posited to occur amongst the basin's vegetation between the Přídolí and Lochkovian by the palynological record, and to a lesser extent, the mesofossil and macrofossil record. The nature of this diversification remains unclear, including the tempo of change, the degree of turnover in the community, its timing and how distinguishable it is in the fossil record. The diversification event has been broadly attributed to the trilete spores, but the key spore genera contributing to the diversification have not been defined. Furthermore, the was a similar pattern of diversification seen amongst the cryptospores? Finally, the causes underpinning the diversification require more targeted discussion.

(4) In spite of over thirty years of study on *in situ* spores and mesofossils, which has greatly advanced the understanding of early land plants, many dispersed spore species are yet to be associated with their parent plants. Can more dispersed spore species be linked to their source plants, and are there more charcoal horizons yet to be recovered which can contribute to further contextualisation of the dispersed spore record with reference to the source plant morphology and affinities?

(5) From the diversity of dispersed spores, range of embryophytic and non-embryophytic and animal remains, it is clear that the Anglo-Welsh Basin exhibited a rich biota. How was the flora distributed in space and time, and is there any indication for floral specialisation? An important component of the landscape is indicated by dispersed tubes, cuticles, and mesofossils; what were the affinities of these fossils? What can be gleaned of the biotic interactions between organisms, in terms of feeding strategies and decay?

8. Bibliography

ALGEO, T.J., SCHECKLER, S.E., 1998. Terrestrial-marine teleconnections in the Devonian: links between the evolution of land plants, weathering processes, and marine anoxic events. Philosophical Transactions of the Royal Society of London B 353, 113–130

ALLEN, J.R.L., 1974. Studies in fluviatile sedimentation: Implications of pedogenic carbonate units. Lower Old Red Sandstone, Anglo-Welsh outcrop. *Geological Journal*, *9*(2), pp.181-208.

ALLEN, J.R.L. AND TARLO, L.B., 1963. The Downtonian and Dittonian facies of the Welsh borderland. *Geological Magazine*, *100*(2), pp.129-155.

ALLEN, J.R.L. AND WILLIAMS, B. P. J. 1978. The sequence of the earlier Lower Old Red Sandstone (SiluroDevonian), north of Milford Haven, southwest Dyfed (Wales). Geological Journal, 13, 113-136.

ALLEN, J.R.L. AND WILLIAMS, B.P.J., 1981. Sedimentology and stratigraphy of the Townsend Tuff Bed (Lower Old Red Sandstone) in South Wales and the Welsh Borders. *Journal of the Geological Society*, *138*(1), pp.15-29.

ALLEN, J.R.L., 1986. Pedogenic calcretes in the Old Red Sandstone facies (late Silurian–early Carboniferous) of the Anglo-Welsh area, southern Britain. In: Wright, V.P. (Ed.), Palaeosols: their Recognition and Interpretation. Blackwell, Oxford, pp. 56–86.

BALL, H.W., DINELEY, D.L. AND WHITE, E.I., 1961. *The Old Red Sandstone of Brown Clee Hill and the adjacent area.* British Museum (Natural History)

BARCLAY, W.J., 2005. Introduction to the Old Red Sandstone of Great Britain. *The Old Red Sandstone of Great Britain Geol. Cons. Rev. Series. Joint Nature Conservation Committee, Peterborough (393 pp.)*.

BARCLAY, W.J., RATHBONE, P.A., WHITE, D.E. AND RICHARDSON, J.B., 1994. Brackish water faunas from the St Maughans Formation: The Old Red Sandstone section at Ammons Hill, Hereford and Worcester, UK, re-examined. *Geological Journal*, *29*(4), pp.369-379.

BARCLAY, W J, DAVIES, J R, HILLIER, R D, AND WATERS, R A. 2015. Lithostratigraphy of the Old Red Sandstone successions of the Anglo-Welsh Basin. British Geological Survey Research Report, RR/14/02. 96pp.

BASSETT, M.G., 1974. The articulate brachiopods from the Wenlock Series of the Welsh Borderland and South Wales. *Monographs of the Palaeontographical Society*, *128*(541), pp.79-123.

BASSETT, M G, LAWSON, J D, AND WHITE, D E. 1982. The Downton Series as the fourth Series of the Silurian System. Lethaia, Vol. 15, 1–24.

BERNER, R.A., 2001. Modelling atmospheric O2 over Phanerozoic time. *Geochimica et Cosmochimica Acta*, *65*(5), pp.685-694.

BERNER RA, 1994. GEOCARB II: A revised model of atmospheric CO2 over Phanerozoic time. American Journal of Science 294: 56–91

BERNER RA, 2006A. GEOCARBSULF: A combined model for Phanerozoic atmospheric O2 and CO2. Geochimica et Cosmochimica Acta 70: 5653–5664.

BERNER RA, 2009. Phanerozoic atmospheric oxygen: New results using the GEOCARBSULF model. American Journal of Science 309: 603–606.

BLUCK, B J, COPE,J C W, AND SCRUTTON, C T. 1992. Devonian. 57–66 in Atlas of Palaeogeography and Lithofacies. COPE, J C W, INGHAM, J K, and RAWSON, P F (editors). Memoir of the Geological Society of London, No. 13.

BLIECK, A. AND ELLIOTT, D.K., 2017. Pteraspidomorphs (Vertebrata), the Old Red Sandstone, and the special case of the Brecon Beacons National Park, Wales, UK. *Proceedings of the Geologists' Association*, *128*(3), pp.438-446.

BLIECK, A. AND TARRANT, P.R., 2001. Protopteraspis gosseleti (Vertebrata: Pteraspidomorphi: Heterostraci) from the Lower Devonian of Shropshire, England. *Palaeontology*, *44*(1), pp.95-112.

BOND, A. AND SPARKS, R.S.J., 1976. The Minoan eruption of Santorini, Greece. *Journal of the Geological Society*, *132*(1), pp.1-16.

BOUCOT, A.J. 1988. Devonian biogeography: an update. *Devonian of the World: Proceedings of the 2nd International Symposium on the Devonian System — Memoir 14, Volume III: Paleontology, Paleoecology and Biostratigraphy, 1988*
Pages 211-227

BOUCOT, A. J. & GRAY, J. 2001. A critique of Phanerozoic climatic models involving changes in the CO2 content of the atmosphere. Earth Science Reviews, 56, 1–159.

BOUCOT, A.J., XU, C., SCOTESE, C.R. AND MORLEY, R.J., 2013. *Phanerozoic paleoclimate: an atlas of lithologic indicators of climate*. SEPM (Society for Sedimentary Geology).

BOWMAN, J.L., KOHCHI, T., YAMATO, K.T., JENKINS, J., SHU, S., ISHIZAKI, K., YAMAOKA, S., NISHIHAMA, R., NAKAMURA, Y., BERGER, F. AND ADAM, C., 2017. Insights into land plant evolution garnered from the Marchantia polymorpha genome. *Cell*, *171*(2), pp.287-304.

BURGESS, N.D. AND EDWARDS, D., 1991. Classification of uppermost Ordovician to Lower Devonian tubular and filamentous macerals from the Anglo-Welsh Basin. *Botanical Journal of the Linnean Society*, *106*(1), pp.41-66.

BURGESS N.D. & RICHARDSON, J.B. 1991. Silurian cryptospores and miospores from the type Wenlock area, Shropshire, England. *Palaeontology*, **34** (3), 601 – 628. Pls.

BURGESS N.D. & RICHARDSON, J.B. 1995. Wenlock to early Prídolí cryptospores and miospores from south and southwest Wales, Great Britain. Palaeontographica Abteilung B, **236**, 1 – 44. Pls.

CAME RE, EILER JM, VEIZER J, AZMY K, BRAND U, AND WEIDMAN CR, 2007. Coupling of surface temperatures and atmospheric CO2 concentrations during the Palaeozoic era. Nature 449: 198–201.

CASCALES-MIÑANA, B., STEEMANS, P., SERVAIS, T., LEPOT, K. AND GERRIENNE, P., 2019. An alternative model for the earliest evolution of vascular plants. *Lethaia*, *52*(4), pp.445-453.

CATLOS, E.J., MARK, D.F., SUAREZ, S., BROOKFIELD, M.E., MILLER, C.G., SCHMITT, A.K., GALLAGHER, V. AND KELLY, A., 2021. Late Silurian zircon U–Pb ages from the Ludlow and Downton bone beds, Welsh Basin, UK. *Journal of the Geological Society*, *178*(1).

CHALONER, W.G., 1989. Fossil charcoal as an indicator of palaeoatmospheric oxygen level. *Journal of the Geological Society*, *146*(1), pp.171-174.

CHANNELL, J.E.T., MCCABE, C. AND WOODCOCK, N.H., 1992. Early Devonian (pre-Acadian) magnetization directions in Lower Old Red Sandstone of south Wales (UK). *Geophysical Journal International*, *108*(3), pp.883-894.

COCKS, L.R.M. AND TORSVIK, T.H., 2002. Earth geography from 500 to 400 million years ago: a faunal and palaeomagnetic review. *Journal of the Geological Society*, *159*(6), pp.631-644.

COPE, J.C.W., INGHAM, J.K., RAWSON, P.F. (EDS.), 1992. Atlas of Palaeogeography and Lithofacies. Geol. Soc. London Mem.. Geological Society of London, London, pp. 57–66.

COPE, M.J. AND CHALONER, W.G., 1980. Fossil charcoal as evidence of past atmospheric composition. *Nature*, *283*(5748), p.647.

COX, C.J., GOFFINET, B., WICKETT, N.J., BOLES, S.B. AND SHAW, J., 2010. Moss diversity: a molecular phylogenetic analysis of genera. Phytotaxa 9: 175–195.

CROWLEY TJ AND BERNER RA (2001) CO2 and climate change. Science 292: 870–872.

DAVIES, N.S., GIBLING, M.R., 2010A. Cambrian to Devonian evolution of alluvial systems: the sedimentological impact of the earliest land plants. Earth-Science Reviews 98, 171–200

GIBLING, M.R., DAVIES, N.S., FALCON-LANG, H.J., BASHFORTH, A.R., DIMICHELE, W.A., RYGEL, M.C. AND IELPI, A., 2014. Palaeozoic co-evolution of rivers and vegetation: a synthesis of current knowledge. *Proceedings of the Geologists' Association*, *125*(5-6), pp.524-533.

DEWEY, J.F. AND STRACHAN, R.A., 2003. Changing Silurian–Devonian relative plate motion in the Caledonides: sinistral transpression to sinistral transtension. *Journal of the Geological Society*, *160*(2), pp.219-229.

DRIESE SG, MORA CI, AND ELICK JM (2000) The paleosol record of increasing plant diversity and depth of rooting and changes in atmospheric pCO2 in the Silurian - Devonian. In: Gastaldo RA and DiMichele WA (eds.) Phanerozoic Terrestrial Ecosystems, pp. 47–61. Paleontological Society Special Papers 6.

EDWARDS, D., 1970. Fertile Rhyniophytina from the lower Devonian of Britain. *Palaeontology*, *13*(3), pp.451-461.

EDWARDS, D., 1981. Studies on Lower Devonian petrifactions from Britain. 2. Sennicaulis, a new form genus for sterile axes based on pyrite and limonite petrifactions from the Senni Beds. *Review of Palaeobotany and Palynology*, *32*(2-3), pp.207-226.

EDWARDS, D., 1996. New insights into early land ecosystems: a glimpse of a Lilliputian world. *Review of Palaeobotany and Palynology*, *90*(3-4), pp.159-174.

EDWARDS, D. AND FEEHAN, J., 1980. Records of Cooksonia-type sporangia from late Wenlock strata in Ireland. *Nature*, *287*(5777), pp.41-42.

EDWARDS, D. AND KENRICK, P., 2015. The early evolution of land plants, from fossils to genomics: a commentary on Lang (1937)'On the plant-remains from the Downtonian of England and Wales'. *Phil. Trans. R. Soc. B*, *370*(1666), p.20140343.

EDWARDS, D. AND RICHARDSON, J.B., 2000. Progress in reconstructing vegetation on the Old Red Sandstone Continent: two Emphanisporites producers from the Lochkovian sequence of the Welsh Borderland. *Geological Society, London, Special Publications*, *180*(1), pp.355-370.

EDWARDS, D. AND RICHARDSON, J.B., 2004. Silurian and Lower Devonian plant assemblages from the Anglo-Welsh Basin: a palaeobotanical and palynological synthesis. *Geological Journal*, *39*(3-4), pp.375-402.

EDWARDS, D. AND ROGERSON, E.C.W., 1979. New records of fertile Rhyniophytina from the late Silurian of Wales. *Geological Magazine*, *116*(2), pp.93-98.

EDWARDS, D. AND WELLMAN, CH. Embryophytes on Land: The Ordovician to Lochkovian (Lower Devonian) Record. *In* GENSEL, P.G. AND EDWARDS, D. EDS., 2001. *Plants invade the land: evolutionary and environmental perspectives*. Columbia University Press.

EDWARDS, D., FEEHAN, J. & SMITH, D. G. 1983. A late Wenlock flora from Co. Tipperary, Ireland. Botanical Journal of the Linnean Society, 86, 19–36.

EDWARDS, D., FANNING, U. AND RICHARDSON, J.B., 1994. Lower Devonian coalified sporangia from Shropshire: Salopella Edwards & Richardson and Tortilicaulis Edwards. *Botanical Journal of the Linnean Society*, *116*(2), pp.89-110.

EDWARDS, D., DUCKETT, J. G. & RICHARDSON, J. B. 1995B. Hepatic characters in the earliest land plants. Nature, 374, 635–636.

EDWARDS, D., MORRIS, J.L., RICHARDSON, J.B. AND KENRICK, P., 2014. Cryptospores and cryptophytes reveal hidden diversity in early land floras. *New Phytologist*, *202*(1), pp.50-78.

EDWARDS, D., MORRIS, J.L., AXE, L., DUCKETT, J.G., PRESSEL, S. AND KENRICK, P., 2022A. Piecing together the eophytes–a new group of ancient plants containing cryptospores. *New Phytologist*, *233*(3), pp.1440-1455.

EDWARDS, D., MORRIS, J.L., AXE, L., TAYLOR, W.A., DUCKETT, J.G., KENRICK, P. AND PRESSEL, S., 2022B. Earliest record of transfer cells in Lower Devonian plants. *New Phytologist*, *233*(3), pp.1456-1465.

EDWARDS, D., MORRIS, J.L., AXE, L. AND DUCKETT, J.G., 2022C. Picking up the pieces: New charcoalified plant mesofossils (eophytes) from a Lower Devonian Lagerstätte in the Welsh Borderland, UK. *Review of Palaeobotany and Palynology*, *297*, p.104567.

FANNING, U., RICHARDSON, J.B. AND EDWARDS, D., 1988. Cryptic evolution in an early land plant. *Evolutionary Trends in Plants (ETP)*, *2*(1), pp.13-24.

FANNING, U., EDWARDS, D. & RICHARDSON, J. B. 1990. Further evidence for diversity in late Silurian land vegetation. Journal of the Geological Society London, 147, 725–728

FANNING, U., EDWARDS, D. & RICHARDSON, J. B. 1991A. A new rhyniophytoid from the late Silurian of the Welsh Borderland. Neues Jahrbuch fu¨r Geologie und Pala¨ontologie. Abh., 183, 37–47

FANNING, U., RICHARDSON, J. B. & EDWARDS, D. 1991B. A review of in situ spores in Silurian land plants. In: Blackmore, S. & Barnes, S. H. (eds) Systematics Association Special Volume. Pollen and Spores, 44, 25–47.

FAYERS, S.R., TREWIN, N.H. AND MORRISSEY, L., 2010. A large arthropod from the Lower Old Red Sandstone (Early Devonian) of Tredomen Quarry, south Wales. *Palaeontology*, *53*(3), pp.627-643.

FLETCHER, B.J., BRENTNALL, S.J., QUICK, W.P. AND BEERLING, D.J., 2006. BRYOCARB: a process-based model of thallose liverwort carbon isotope fractionation in response to CO2, O2, light and temperature. *Geochimica et Cosmochimica Acta*, *70*(23), pp.5676-5691.

FRIEND, P.F., WILLIAMS, B.P.J., FORD, M. AND WILLIAMS, E.A., 2000. Kinematics and dynamics of Old Red Sandstone basins. *Geological Society, London, Special Publications*, *180*(1), pp.29-60.

GENSEL, P.G., 2008. The earliest land plants. *Annual Review of Ecology, Evolution, and Systematics*, *39*, pp.459-477.

GERRIENNE, P., DILCHER, D.L., BERGAMASCHI, S., MILAGRES, I., PEREIRA, E. AND RODRIGUES, M.A.C., 2006. An exceptional specimen of the early land plant Cooksonia paranensis, and a hypothesis on the life cycle of the earliest eutracheophytes. *Review of Palaeobotany and Palynology*, *142*(3-4), pp.123-130.

GLASSPOOL, I.J., EDWARDS, D. AND AXE, L., 2004. Charcoal in the Silurian as evidence for the earliest wildfire. *Geology*, *32*(5), pp.381-383.

GLASSPOOL, I.J., EDWARDS, D. AND AXE, L., 2006. Charcoal in the Early Devonian: a wildfire-derived Konservat–Lagerstätte. *Review of Palaeobotany and Palynology*, *142*(3-4), pp.131-136.

GLASSPOOL, I.J. AND SCOTT, A.C., 2010. Phanerozoic concentrations of atmospheric oxygen reconstructed from sedimentary charcoal. *Nature Geoscience*, *3*(9), p.627.

GONEZ, P. AND GERRIENNE, P., 2010. A new definition and a lectotypification of the genus Cooksonia Lang 1937. *International Journal of Plant Sciences*, *171*(2), pp.199-215.

GOUDIE, A. S. 1983 Calcrete. In Chemical sediments and geomorphology (ed. A. S. Goudie & K. Pye), pp. 91—131. London: Academic Press

GRAHAM LE, GRAY J. 2001. The origin, morphology and ecophysiology of early embryophytes. See Gensel & Edwards 2001, pp. 140–58

GRAY, J. 1985. The microfossil record of early land plants; advances in understanding of early terrestrialization, 1970–1984. Philosophical Transactions of the Royal Society, London, B309, 167–195.

HASSAN, A.M., 1982. *Palynology, stratigraphy and provenance of the lower old red sandstone of the Brecon Beacons (Powys) and Black Mountains (Gwent and Powys), South Wales*(Doctoral dissertation, King's College London (University of London)).

HEARD, A., 1927. On Old Red Sandstone Plants showing Structure, from Brecon, South Wales. *Quarterly Journal of the Geological Society*, *83*(1-5), pp.195-209.

HECKMAN, D.S., GEISER, D.M., EIDELL, B.R., STAUFFER, R.L., KARDOS, N.L. AND HEDGES, S.B., 2001. Molecular evidence for the early colonization of land by fungi and plants. *Science*, *293*(5532), pp.1129-1133.

HILLIER, R.D., MARRIOTT, S.B., WILLIAMS, B.P. AND WRIGHT, V.P., 2007. Possible climate variability in the Lower Old Red Sandstone Conigar Pit Sandstone Member (early Devonian), South Wales, UK. *Sedimentary Geology*, *202*(1-2), pp.35-57.

HILLIER, R.D. AND WILLIAMS, B.P., 2007. The Ridgeway Conglomerate Formation of SW Wales, and its implications. The end of the Lower Old Red Sandstone?. *Geological Journal*, *42*(1), pp.55-83.

HILLIER, R.D., WATERS, R.A., MARRIOTT, S.B. AND DAVIES, J.R., 2011. Alluvial fan and wetland interactions: evidence of seasonal slope wetlands from the Silurian of south central Wales, UK. *Sedimentology*, *58*(4), pp.831-853.

HONEGGER, R., EDWARDS, D., AXE, L. AND STRULLU-DERRIEN, C., 2018. Fertile Prototaxites taiti: a basal ascomycete with inoperculate, polysporous asci lacking croziers. *Philosophical Transactions of the Royal Society B: Biological Sciences*, *373*(1739), p.20170146.

JERAM, A.J., SELDEN, P.A. AND EDWARDS, D., 1990. Land animals in the Silurian: arachnids and myriapods from Shropshire, England. *Science*, *250*(4981), pp.658-661.

KEATING, J.N., SANSOM, R.S. AND PURNELL, M.A., 2012. A new osteostracan fauna from the Devonian of the Welsh Borderlands and observations on the taxonomy and growth of Osteostraci. *Journal of Vertebrate Paleontology*, *32*(5), pp.1002-1017.

KENDALL, R.S., 2017. The Old Red Sandstone of Britain and Ireland—a review. *Proceedings of the Geologists' Association*, *128*(3), pp.409-421.

KENRICK, P., 2017. How land plant life cycles first evolved. *Science*, *358*(6370), pp.1538-1539.

KENRICK, P. & CRANE, P. R. 1997. The Origin and Early Diversification of Land Plants: A Cladistic Study. Smithsonian Institution Press, Washington, DC

KENRICK, P., WELLMAN, C.H., SCHNEIDER, H. AND EDGECOMBE, G.D., 2012. A timeline for terrestrialization: consequences for the carbon cycle in the Palaeozoic. *Philosophical Transactions of the Royal Society B: Biological Sciences*, *367*(1588), pp.519-536.

KOTYK, M. E., BASINGER, J. F., GENSEL, P. G. & DE FREITAS, T. 2002. Morphologically complex plant macrofossils from the Late Silurian of Arctic Canada. American Journal of Botany, 89, 1004–1013

LANG, W.H., 1937. IV-On the plant-remains from the Downtonian of England and Wales. *Phil. Trans. R. Soc. Lond. B*, *227*(544), pp.245-291.

LARSEN, P.-H., EDWARDS, D. & ESCHER, J. C. 1987. Late Silurian plant megafossils from the Peary Land Group, North Greenland. Rapp. Gronlands Geologiske Undersogeise, 133, 17–112

LERBERKMO, J. F. & CAMPBELL, F. A. 1969. Distribution, composition and source of the White River Ash, Yukon Territory. Can. J. Earth Sci. 6, 109-16.

LOVE, S.E. AND WILLIAMS, B.P., 2000. Sedimentology, cyclicity and floodplain architecture in the Lower Old Red Sandstone of SW Wales. *Geological Society, London, Special Publications*, *180*(1), pp.371-388.

MARRIOTT, S.B. AND WRIGHT, V.P., 2004. Mudrock deposition in an ancient dryland system: Moor Cliffs Formation, Lower Old Red Sandstone, southwest Wales, UK. *Geological Journal*, *39*(3-4), pp.277-298.

MARRIOTT, S.B., MORRISSEY, L.B. AND HILLIER, R.D., 2009. Trace fossil assemblages in Upper Silurian tuff beds: evidence of biodiversity in the Old Red Sandstone of southwest Wales, UK. *Palaeogeography, Palaeoclimatology, Palaeoecology*, *274*(3-4), pp.160-172.

MARRIOTT, S.B., HILLIER, R.D. AND MORRISSEY, L.B., 2013. Enigmatic sedimentary structures in the Lower Old Red Sandstone, south Wales, UK: possible microbial influence on surface processes and early terrestrial food webs. *Geological Magazine*, *150*(3), pp.396-411.

MORA, C.I., DRIESE, S.G. AND SEAGER, P.G., 1991. Carbon dioxide in the Paleozoic atmosphere: Evidence

from carbon-isotope compositions of pedogenic carbonate. *Geology*, *19*(10), pp.1017-1020.

MORRISSEY, L.B., BRADDY, S.J., BENNETT, J.P., MARRIOTT, S.B. AND TARRANT, P.R., 2004. Fish trails from the lower old red sandstone of Tredomen Quarry, Powys, southeast Wales. *Geological Journal*, *39*(3-4), pp.337-358.

MORRISSEY, L.B., HILLIER, R.D. AND MARRIOTT, S.B., 2012. Late Silurian and Early Devonian terrestrialisation: ichnological insights from the Lower Old Red Sandstone of the Anglo-Welsh Basin, UK. *Palaeogeography, Palaeoclimatology, Palaeoecology*, *337*, pp.194-215.

MORRIS, J.L., WRIGHT, V.P. AND EDWARDS, D., 2012B. Silurian - Devonian landscapes of southern Britain: the stability and nature of early vascular plant habitats. *Journal of the Geological Society*, *169*, p.173.

MORRIS, J.L., PUTTICK, M.N., CLARK, J.W., EDWARDS, D., KENRICK, P., PRESSEL, S., WELLMAN, C.H., YANG, Z., SCHNEIDER, H. AND DONOGHUE, P.C., 2018A. The timescale of early land plant evolution. *Proceedings of the National Academy of Sciences*, *115*(10), pp.E2274-E2283.

MORRIS, J.L., EDWARDS, D. AND RICHARDSON, J.B., 2018B. The advantages and frustrations of a plant Lagerstätte as illustrated by a new taxon from the Lower Devonian of the Welsh Borderland, UK. In *Transformative Paleobotany* (pp. 49-67). Academic Press.

MULLER, J., 1959. Palynology of Recent Orinoco delta and shelf sediments; reports of the Orinoco shelf expedition, volume 5. *Micropaleontology*, *5*(1), pp.1-32.

NEWMAN, M.J., BURROW, C.J., DAVIDSON, R.G., DEN BLAAUWEN, J.L. & JONES, R., 2017. Comparison of the vertebrate faunas of the Lower Old Red Sandstone of the Anglo-Welsh Basin with contemporary faunas in Scotland. *Proceedings of the Geologists' Association*, *128*(3), pp.447-459.

OWEN, G., 2017. Origin and significance of soft-sediment deformation in the Old Red Sandstone of central South Wales, UK. *Proceedings of the Geologists' Association*, *128*(3), pp.422-430.

PISAREVSKY, S.A., MURPHY, J.B., CAWOOD, P.A. AND COLLINS, A.S., 2008. Late Neoproterozoic and Early Cambrian palaeogeography: models and problems. *Geological Society, London, Special Publications*, *294*(1), pp.9-31.

PUTTICK, M.N., MORRIS, J.L., WILLIAMS, T.A., COX, C.J., EDWARDS, D., KENRICK, P., PRESSEL, S., WELLMAN, C.H., SCHNEIDER, H., PISANI, D. AND DONOGHUE, P.C., 2018. The interrelationships of land plants and the nature of the ancestral embryophyte. *Current Biology*, *28*(5), pp.733-745.

RICHARDSON, J.B., 1967. Some British Lower Devonian spore assemblages and their stratigraphic significance. *Review of Palaeobotany and Palynology*, *1*(1-4), pp.111-129.

RICHARDSON, J.B. AND EDWARDS, D., 1989. Sporomorphs and plant megafossils.

RICHARDSON, J.B. 1996A. Taxonomy and classification of some new Early Devonian cryptospores from England. *Special papers in palaeontology*, **55**, 7 – 40. 10 pls.

RICHARDSON, J.B., 1996B. Abnormal spores and possible interspecific hybridization as a factor in the evolution of Early Devonian land plants. *Review of Palaeobotany and Palynology*, *93*(1-4), pp.333-340.

RICHARDSON, J.B., 2002. English Lower Devonian cryptospores and the habit and habitat of their parent plants. In *IPC*.

RICHARDSON, J.B., 2007. Cryptospores and miospores, their distribution patterns in the Lower Old Red Sandstone of the Anglo-Welsh Basin, and the habitat of their parent plants. *Bulletin of Geosciences*, *82*(4), pp.355-364.

RICHARDSON, J.B. AND LISTER, T.R., 1969. Upper Silurian and lower Devonian spore assemblages from the Welsh borderland and south Wales. *Palaeontology*, *12*(2), pp.201-245.

RICHARDSON, J.B., MCGREGOR, D.C. 1986. Silurian and Devonian spore zones of the Old Red Sandstone continent and adjacent regions. *Geol. Surv. Canada, Bulletin*, *354*, pp.pl-1.

ROYER, D.L., 2001. Stomatal density and stomatal index as indicators of paleoatmospheric CO2 concentration. *Review of Palaeobotany and Palynology*, *114*(1-2), pp.1-28.

ROYER, D.L., 1999. Depth to pedogenic carbonate horizon as a paleoprecipitation indicator?. *Geology*, *27*(12), pp.1123-1126.

ROYER, D.L. 2014. Atmospheric CO2 and O2 during the Phanerozoic: Tools, patterns and impacts. In *Treatise on Geochemistry, 2nd ed.*; Holland, H., Turekian, K., Eds.; Elselvier: Amsterdam, The Netherlands,; pp. 251–267.

RUBINSTEIN, C. V., GERRIENNE, P., DE LA PUENTE, G. S., ASTINI, R. A. & STEEMANS, P. 2010. Early Mid Ordovician evidence for land plants in Argentina (eastern Gondwana). New Phytologist, 188, 365–369.

SHIMAMURA, M., 2016. Marchantia polymorpha: taxonomy, phylogeny and morphology of a model system. *Plant and Cell Physiology*, *57*(2), pp.230-256.

STEEMANS, P., 1982. Gedinnian and Siegenian spores stratigraphy in Belgium.

STEEMANS, P., LE HERISSE, A., MELVIN, J., MILLER, M. A., PARIS, F., VERNIERS, J. & WELLMAN, C. H. 2009. Origin and radiation of the earliest vascular land plants. Science, 324, 353.

STEIN, W.E., BERRY, C.M., HERNICK, L.V. AND MANNOLINI, F., 2012. Surprisingly complex community discovered in the mid-Devonian fossil forest at Gilboa. *Nature*, *483*(7387), pp.78-81.

STEIN, W.E., BERRY, C.M., MORRIS, J.L., HERNICK, L.V., MANNOLINI, F., VER STRAETEN, C., LANDING, E., MARSHALL, J.E., WELLMAN, C.H., BEERLING, D.J. AND LEAKE, J.R., 2020. Mid-Devonian Archaeopteris roots signal revolutionary change in earliest fossil forests. *Current biology*, *30*(3), pp.421-431.

STROTHER, P.K., 2016. Systematics and evolutionary significance of some new cryptospores from the Cambrian of eastern Tennessee, USA. *Review of Palaeobotany and Palynology*, *227*, pp.28-41.

STROTHER, P.K., BECK, J.H., HARLEY, M.M., MORTON, C.M. AND BLACKMORE, S., 2000. Spore-like microfossils from Middle Cambrian strata: expanding the meaning of the term cryptospore. *Pollen and spores: morphology and biology. Royal Botanic Gardens, Kew*, pp.413-424.

STROTHER, P.K., WOOD, G.D., TAYLOR, W.A. AND BECK, J.H., 2004. Middle Cambrian cryptospores and the origin of land plants. *Memoir-Associations of Australasian Palaeontologists*, *29*, pp.99-114.

SUNDBERG, S., 2013. Spore rain in relation to regional sources and beyond. *Ecography*, *36*(3), pp.364-373.

TARRANT, P.R., 1991. The ostracoderm Phialaspis from the Lower Devonian of the Welsh Borderland and South Wales. *Palaeontology*, *34*(2), pp.399-438.

TAYLOR, W.A., GENSEL, P.G., WELLMAN, C.H., 2011. Wall ultrastructure in three species of the dispersed spore Emphanisporites from the Early Devonian. Rev. Palaeobot. Palynol. 163 (3–4), 264–280.

TIMME, R.E., BACHVAROFF, T.R. AND DELWICHE, C.F., 2012. Broad phylogenomic sampling and the sister lineage of land plants. *PLoS one*, *7*(1), p.e29696.

THOMAS, C.W. AND KENDALL, R., 2017. Welsh Borderland Geological Framework Project: the geology and applied geological issues of the region around Knighton, Powys: a scoping study.

TORSVIK, T.H. AND COCKS, L.R.M., 2004. Earth geography from 400 to 250 Ma: a palaeomagnetic, faunal and facies review. *Journal of the Geological Society*, *161*(4), pp.555-572.

TORSVIK, T.H. AND COCKS, L.R.M., 2016. *Earth history and palaeogeography*. Cambridge University Press.

TURNER, S., BURROW, C.J., WILLIAMS, R.B. AND TARRANT, P., 2017. Welsh Borderland bouillabaisse: Lower Old Red Sandstone fish microfossils and their significance. *Proceedings of the Geologists' Association*, *128*(3), pp.460-479.

WATERS, C.N., AMBROSE, K., BARCLAY, W.J., BARRON, A.J.M., BRIDGE, D.M., CARNEY, J.N., COOPER, A.H., CROFTS, R.G., ELLISON, R.A., HOPSON, P.M. AND MATHERS, S.J., 2008. *Stratigraphical Chart of the United Kingdom: Southern Britain [wallchart]*. British Geological Survey.

WELLMAN, C.H., 1995. "Phytodebris" from Scottish Silurian and Lower Devonian continental deposits. *Review of Palaeobotany and Palynology*, *84*(3-4), pp.255-279.

WELLMAN, C.H., 1999. Sporangia containing Scylaspora from the lower Devonian of the Welsh Borderland. *Palaeontology*, *42*(1), pp.67-81.

WELLMAN, C. H. 2003. Dating the origin of land plants. In: Donoghue, P. C. J. & Smith, M. P. (eds) Telling the Evolutionary Time: Molecular Clocks and the Fossil Record. CRC Press, Boca Raton, FL, 119–141

WELLMAN, C.H., 2004. Origin, function and development of the spore wall in early land plants. In: Hemsley, A.R., Poole, I. (Eds.), The Evolution of Plant Physiology. Royal Botanic Gardens, Kew, pp. 43–63.

WELLMAN, C. H., EDWARDS, D. & AXE, L. 1998A. Ultrastructure of laevigate hilate cryptospores in sporangia and spore masses from the Upper Silurian and Lower Devonian of the Welsh Borderland. Philosophical Transactions of the Royal Society, London, 353, 1983–2004

WELLMAN, C. H. & GRAY, J. 2000. The microfossil record of early land plants. Philosophical Transactions of the Royal Society, London, B355, 717–732.

WELLMAN, C.H. AND RICHARDSON, J.B., 1996. Sporomorph assemblages from the Lower Old Red Sandstone' of Lorne, Scotland. *Special Papers in Palaeontology*, *55*, pp.41-102.

WELLMAN, C.H., HABGOOD, K., JENKINS, G. AND RICHARDSON, J.B., 2000. A new plant assemblage (microfossil and megafossil) from the Lower Old Red Sandstone of the Anglo–Welsh Basin: its implications for the palaeoecology of early terrestrial ecosystems. *Review of Palaeobotany and Palynology*, *109*(3-4), pp.161-196.

WELLMAN, C.H., STEEMANS, P. AND VECOLI, M., 2013. Palaeophytogeography of Ordovician–Silurian land plants. *Geological Society, London, Memoirs*, *38*(1), pp.461-476.

WILDING, L. P., AND D. TESSIER. 1988 "Genesis of Vertisol shrink–well phenomena. p. 55–81. LP Wilding and R. Puentes (ed.) Vertisols: Their distribution, properties, classification and management. Texas A&M Univ., College Station

WRIGHT, V.P., 1992. Paleosol recognition: a guide to early diagenesis in terrestrial settings. In *Developments in Sedimentology* (Vol. 47, pp. 591-619). Elsevier.

WRIGHT, W.P., 2007. Calcrete. *Geochemical Sediments and Landscapes*, p.10.

YAALON, D.H. AND KALMAR, D., 1978. Dynamics of cracking and swelling clay soils: Displacement of skeletal grains, optimum depth of slickensides, and rate of intra-pedonic turbation. *Earth Surface Processes*, *3*(1), pp.31-4

Thesis appendix 1

Thesis appendix 1.1: Global macrofossil assemblages

Assem. Number	Age	Locality	Assemblage	Paleolatitude, Continent	Palaeoclimate	Palaeoenvironment	Reference
	?Ludlow-Přídolí						
1	**Ludlow – Přídolí**	Australia, Victoria	**Rhyniophytoid** *Salopella australis* **Lycopods** *Baragwanathia longfolia* **Zosterophylls** *Zosterophyll* spp.	10˚ - 30˚S Eastern Gondwana	Uncertain, ?tropical	Uncertain Palaeoenvironment, preserved in marine strata.	Douglas and Holmes, 2006
2	**?Ludlow-Přídolí**	Tarija, Bolivia	**Rhyniophytoid** *Cooksonia* cf. *caledonica*	50°- 60°S, Gondwana	Uncertain. High precipitation possible.	Uncertain Palaeoenvironment, preserved in marine strata.	Morel *et al*., 1995
3	**Ludlow – Přídolí?**	Arctic Canada (Bathurst Island)	**Zosterophylls** *Zosterophyllum* spp. *Disticophytum* sp. *Macivera gracilis* **Rhyniophytoids**	Low latitudes, ~0˚-15˚N Laurussia	Uncertain. ?equatorial climate	Uncertain Palaeoenvironment, preserved in marine strata	Kotyk *et al*., 2002
4	**Ludlow – Přídolí**	Poland (Holy Cross Mountains)	**Rhyniophytoid** *Cooksonia* spp. *Hostinella*	10˚- 20˚S Laurussia	Uncertain, ?tropical	Uncertain Palaeoenvironment, preserved in marine strata	Bodzioch *et al*., 2003
	Přídolí						
5	**(Basal) Přídolí (TS zone)**	Welsh Borderland (Ludford Lane)	**Rhyniophytina** *Cooksonia Pertoni* **Rhyniophytoid** *Hollandophyton collicullum*	17±5°S Laurussia	Semi-arid, seasonal	Fluvio-marine	Edwards 1979
6	**Přídolí**	Bohemia	**Rhyniophytoid** *Cooksonia* sp.			Uncertain Palaeoenvironment, preserved in marine strata	Obrhel, 1962
7	**Přídolí**	Czech Republic	**Rhyniophytoid** *Cooksonia bohemica*			Uncertain Palaeoenvironment, preserved in marine strata	Scweitzer, 1983; Libertin *et al*., 2002
8	**Přídolí (ultimus?) (TS Zone)**	England (Hereford)	**Rhyniophytina** *Cooksonia Pertoni* **Rhyniophytoid**	17±5°S Laurussia	Semi-arid, seasonal	Fluvio-marine	Lang (1937); Fanning, Edwards, and Richardson (1990, 1991); Fanning, Richardson and Edwards (1991), Edwards (1979)

			C. cambriensis *Salopella* *Pertonella dactylethra* *Caia langelli*				
9	**Přídolí (Early)** **(TS Zone)**	Wales (Dyfed)	**Rhyniophytina** *Cooksonia pertoni* **Rhyniophytoid** *C. caledonica* *C. cambrensis* *C. hemisphaerica* *Tortillicaulis Transwalliensis* (*uncertae sedis*) ***incertae sedis*** *Psilophytites* sp.	17±5°S Laurussia	Semi-arid, seasonal	Fluvio-marine	Edwards 1979
10	**Přídolí (Early)** **(TS Zone)**	Wales (Dyfed)	**Rhyniophytoid** *Cooksonia sp.* *Steganotheca striata*	17±5°S Laurussia	Semi-arid, seasonal	Fluvio-marine	Edwards and Rogerson (1979)
11	**Přídolí (?Early)** **(TS Zone)**	England (Shropshire)	**Rhyniophytoid** *Cooksonia pertoni*	17±5°S Laurussia	Semi-arid, seasonal	Fluvio-marine	Rogerson *et al*., 1993
12	**Přídolí**	Kazakhstan	**Rhyniophytoid** *Cooksonia sp.* **Zosterophylls** *Zosterophyllum sp.*				Petrosyan (In Edwards and Wellman, 2001)
13	**Přídolí**	China (Yunnan, Yulongsi fmn.)	**Zosterophylls** *Zosterophyllum qujingense*			Marine	Hao *et al*., 2007
14	**Přídolí (late)**	Kazakhstan (Balkhash area)	**Lycopod** *Baragwanathia* sp. ? **Rhyniophytoid** *Cooksonella* sp. **?Zosterophylls** *Jugumella burubaensis* ***Incertae sedis*** *Taeniocrada* sp.?				Senkevitch (1975)
15	**Přídolí (late)**	China (Xinjiang, Junggar Basin)	**Rhyniophytoid** *Cooksonella* sp. *Junggaria spinosa* *Salopella xinjianjensis* **Lycophytina** *Lycopodolica* **Zosterophyllophytina**				Cai *et al*., 1993

			Zosterophyllum sp.				
16	**Přídolí (late)**	Podolia, Ukraine	**Rhyniophytina** *Cooksonia pertoni* **Rhyniophytoid** *C. hemisphaerica* *Eorhynia (Salopella)* **Zosterophylls** *Zosterophyllum* sp. **Lycopod** *lycopodolica*				Ishchenko, 1975
17	**Přídolí (late)**	USA (New York State)	**Rhyniophytoid** *Cooksonia* sp. *Cooksonia* spp. *Histonella*	Laurussia		Marine	Banks, 1973; Edwards *et al*., 2004
18	**Přídolí**	Libya	**Rhyniophytoid** *Cooksonia* sp.				Daber, 1971
19	**Uppermost Silurian – Lochkovian**	Brazil (Parana Basin)	**Rhyniophytoid** *Cooksonia* cf. *pertoni* *Sporogonites* sp. Nov. cf. *C. cambrenensis* *C. paranensis* *Pertonella* sp. *Psilophytites* sp. *Salopella* sp. *Tarrantia* sp. ***Incertae sedis*** ?leafy axes				Mussa *et al*., 1996; Gerrienne, 1999; Gerrienne *et al*., 2001, 2006
	Lochkovian						
20	**(Basal) Lochkovian**	Argentina	**Rhyniophytoids,** *Hostinella* sp. ***Incertae sedis*** *Bowerphyloides mendozaensis* *Isidrophyton iniguezii* **Lycopod** Unidentified lycopod stems			Marine	Edwards *et al*., 2001; Edwards *et al*., 2009
21	**Early Lochkovian**	China (Yunnan, Xiaxishancun fmn.)	**Zosterophylls** *Zosterophyllum xishanense*				Hao *et al*., 2007
22	**Lochkovian (*l*–*m*MN zone)**	Scotland (Forfar)	**Rhyniophytoid** *Cooksonia caledonica* **Zosterophylls**				Lang, 1927; Edwards, 1975

			Zosterophyllum myretonianum				
23	**Lochkovian (*l-m*MN zone)**	Scotland (Arbilot)	**Zosterophyllophytina** *Zosterophyllum* fertile				Edwards, 1972
24	**Lochkovian (*l*MN zone)**	England (Shropshire)	**Rhyniophytina** *C. pertoni* **Rhyniophytoid** *Tortilicaulis transwalliensis,* *Resilitheca,* *Uskiella reticulata* *Tarrantia salopensis* *Cooksonia hemisphaerica* *C. cambriensis* *C. caledonica* *Salopella marcensis*				Edwards and Fanning, 1985
25	**Lochkovian (mMN)**	England (Shropshire, North Brown Clee Hill)	**Rhyniophytina** *Cooksonia pertoni* **Rhyniophytoid** *Salopella* cf. *marcensis* *Tortilicaulis offaeus* *Resilitheca salopensis* *Cooksonia hemisphaerica* *Griselatheca salopensis* *Pertonella* sp. *Fusitheca fanningiae* *Culullitheca richardsonii* Spherical and reniform sporangia *Tarrantia Salopensis* Other unnamed rhyniophytoids.			Distal fluviatile	Fanning, 1987; Fanning *et* al., 1988; Edwards *et al*., 1994; Edwards *et al*., 1995b, d; Edwards, 1996; Wellman *et al*., 1998b; Edwards *et al*., 1999; Habgood, 2000a; Edwards and Richardson, 2000; Edwards *et al*., 2001; Habgood *et al*., 2002
26	**Lochkovian (*m*MN)**	Wales (Newport, Brynglas tunnels)	**Rhyniophytoid** *Cooksonia hemisphearica* *Tarrantia salopensis* *Tortilicaulis transwalliensis* **Zosterophylls** *Zosterophyllum* cf. *fertile*				Wellman *et al*., 2000
27	**Lochkovian (*m*MN)**	Wales (Cwm Mill)	**Rhyniophytoid** *Salopella* cf. *marcensis* *Cooksonia* sp. *Cf. renalia* sp. **Zosterophylls** *Zosterophyllum fertile*			Fluviatile (distal)	Fanning, 1987; Kenrick, 1988

28	**Lochkovian *u*MN**	Belgium (Nonceveux)	**Zosterophylls** *Zosterophyllum fertile*			Marine (Rhenish)	Leqlercq, 1942
29	**Lochkovian (upper Ditton)**	England (Shropshire, Newton Dingle)	**Rhyniophytoid** *Salopella allenii* **Zosterophylls** *Zosterophyllum* sp.			Fluvial, medial	Edwards and Richardson, 1974; Fanning , 1987
30	**Lochkovian (BZ zone)**	Wales (Brecon Beacons)	**Rhyniophytoid** *Salopella allenii* *C.* cf. *caldenonica* *Uskiella* **Zosterophylls** *Deheubarthia splendens* *Gosslingia breconensis* *Zosterophyllum fertile* *Zosterophyllum* sp.			Fluviatile (medial)	Edwards and Kenrick, unpublished; Kenrick, 1988; Edwards *et al*., 1989
31	**Lochkovian (BZ Zone)**	Wales (Pembrokeshire, Mascle Bridge Quarry)	**Rhyniophytoid** *Dawsonites* **Zosterophylls** *Deheubarthia splendens* *Zosterophyllum llanoveranum*			ORS fluviatile (medial)	Kenrick, 1988; Edwards *et al*., 1989; Wellman *et al*., 1998c
32	**Lochkovian (BZ Zone)**	Belgium (Gileppe, la Vesdre)	**Zosterophylls** *Gosslingia breconensis* Abundant remains, work in progress			Marine (Rhenish)	Steemans and Gerrienne (1984)
33	**Lochkovian (Upper Geddenian)**	Germany (Rhineland)	**Zosterophylls** *Drepanophycus spinaeformis* *Zosterophyllum rhenanum* ***Incertae sedis*** *Taeniocrada* sp.			Marine littoral	Shweitzer, 1983
34	**Lochkovian (?lower Geddenian)**	Kazakhstan	**Rhyniophytoid** *Cooksonella sphaerica* **Zosterophylls** *Jugumella burubaensis* ***Incertae sedis*** *Taeniocrada pilosa*			Marine	Senkevitch, 1978
35	**Lochkovian (?Upper Geddenian)**	Kazakhstan	*Tastaephyton bulakus* *Taeniocrada pilosa* *Mointina quadripartite* *Balchaschella tenera* **Zosterophylls**			Marine	Senkevitch, 1978

			Jugumella jugata *J. burubaensis*				
36	**Lochkovian (Geddenian)**	South-west China (E. Yunnan)	**Zosterophylls** *Zosterophyllum* sp.				Li and Cai, 1978
37	**Lochkovian**	Australia (Tyers, Victoria)	**Lycophytina** *Baragwanathia longifolia* *Baragwanathia* n. sp. **Zosterophylls** *Zosterophyllum* n. sp.				J. Tims (pers. comm. In Edwards and Wellman, 1999)
38	**Lochkovian (Geddenian)**	Spitsbergen	Sterile remains only: **Rhyniophytoid** *Hostinella* **Zosterophylls** *Zosterophyllum* ***Incertae sedis*** *Taeniocrada* sp.				Høeg, 1942
39	**Pragian – pre Pragian ?geddenian**	Vietnam	Undetermined terminal sporangia				Janvier *et al*., 1987
40	**?Lochkovian (BZ Zone)**	Wales (Rhiw Wen, Black Mountains)	**Rhyniophytoid** *Cooksonia ?cambriensis* *Salopella allenii* *Tortilicaulis* sp.				Habgood, 2000a
41	**Upper Lochkovian**	China (Yunnan province, Xiton fmn.)	**Trimerophytina** *Huia* sp. **Zosterophylls** *Xituria spinitheca* *Zosterophyllum minorstachyum* *Z. shengfengense* *Z.* sp.				Xue, 2009; Hao *et al*., 2010; Xue, 2011

Thesis appendix 1.2: Přídolí – Lochkovian macrofossil assemblages in the Anglo-Welsh Basin

Age/ Strata	Geographic Area	Assemblage composition	Facies	Author
Přídolí				
Přídolí (*tripapillatus-spicula* spore zone) Platyschisma shale member	Ludford Corner, Ludlow, England	*Cooksonia pertoni* *Hollandophyton colliculum*	Coastal marine (?fluvio)	Edwards *et al*., 1995b Rogerson *et al*., 2002
Přídolí (lower *tripapillatus-spicula* spore zone) Rushall Beds	Perton Lane, Hereford, England	*Caia langii* *Cooksonia cambrensis* *Cooksonia pertoni* *Petronella dactylethra* *Salopella* sp.	?Fluvio-marine	Lang, 1937 Fanning, 1987 Fanning *et al*., 1988, 1990, 1991a,b
Early Přídolí (*tripapillatus-spicula* spore zone) Freshwater East Fmn.	Freshwater East, Pembrokeshire, South Wales	*Cooksonia cambrensis* *Cooksonia hemisphaerica* *Cooksonia pertoni* *Cooksonia* sp. *Psilophytites* sp. *Tortilicaulis transwalliensis*	Fluvio-marine	Lang, 1937 Edwards, 1979
Early Přídolí (*tripapillatus-spicula* spore zone) Tilestones Fmn (Long Quarry Fmn.)	Capel Horeb, Powys, Wales	*Cooksonia* sp. *Steganotheca striata*	Fluvio-marine	Heard, 1939 Edwards, 1970a Edwards and Rogerson, 1979
Early Přídolí (*tripapillatus-spicula* spore zone) Temeside Mudstone Fmn.	Little Wallop Hall, Long Mountain, Shropshire, England	*Cooksonia pertoni*	Restricted marginal marine	Rogerson *et al*., 1993
Lochkovian				
Lochkovian (lower *micrornatus-newportnesis* spore zone)	Targrove, Shropshire, England	cf. *Cooksonia caledonica/ Renalia* *Cooksonia cambrensis* *Cooksonia hemisphaerica* *Cooksonia pertoni*	Distal fluviatile	Lang, 1937 Edwards and Fanning, 1985 Fanning, 1987 Fanning *et al*., 1988, 1992

		Salopella marcensis *Tarrantia salopensis* *Tortilicaulis Transwalliensis* *Uskiella reticulata*		
Lochkovian **(middle *micrornatus-newportnesis* spore zone)**	Stream section, north of Brown Clee Hill, Shropshire, England	*Cooksonia banksia* *Cooksonia pertoni* *Culullitheca richardsonii* *Fusitheca fanningiaea* *Ficoiditheca aenigma* *Grisellatheca salopensis* Cf. *Horneophyton* sp. *lenticulotheca* *Resilitheca salopensis* *Salopella* cf. *marcensis* *Sporathylacium salopense* Cf. *sporogonites* *Tortilicaulis offaeus* *Paracooksonia* *Petronella* sp. *Partitatheca* *Tarrantia salopensis*	Distal fluviatile	Fanning, 1987 Fanning *et al*., 1988 Edwards *et al*., 1994 Edwards *et al*., 1995b,d Edwards, 1996 Wellman *et al*., 1998b Edwards *et al*., 1999 Habgood, 2000a Edwards and Richardson, 2000 Edwards *et al*., 2001 Habgood *et al*., 2002 Morris *et al*., 2011 Morris *et al*., 2012 Edwards *et al*., 2012
Lochkovian **(middle *micrornatus-newportnesis* spore zone)**	Brynglas Tunnels, M4 motorway, Newport, Wales	*Cooksonia hemisphaerica* *Tarrantia salopensis* *Tortilicaulis transwalliensis* *Zosterophyllum* cf. *fertile*	Distal fluviatile	Wellman *et al*., 2000
Lochkovian **(*micrornatus-newportnesis* spore zone; *Crouchi* fish zone)**	Cwm Hill, Monmouthshire, Wales	*Cooksonia* sp. cf. *Renalia* sp. Salopella cf. *marcensis* *Zosterophyllum* cf. *fertile*	Distal fluviatile	
Lochkovian **Upper Gedinnian (?*breconensis-zavallatus* spore zone)**	Newton Dingle, Shropshire, England	*Salopella allenii* *Zosterophyllum* sp.	Medial fluviatile	Edwards and Richardson, 1974 Fanning, 1987
Lochkovian **(*breconensis-zavallatus* spore zone)** **Senni Fmn.**	Allt Ddu, Brecon Beacons, Powys, Wales	Cf. *Cooksonia* *Deheubarthia splendens* *Gosslingia breconensis* cf. *Salopella* sp.	Medial fluviatile	Kenrick, 1988 Edwards *et al*., 1989

		Uskiella spargens cf. *Zosterophyllum. fertile*		
Lochkovian **(*breconensis-zavallatus* spore zone)** **Cosheston Group**	Mascle Bridge Quarry, Pembrokeshire, Wales	*Deheubarthia splendens* *Dawsonites* sp. *Zosterophyllum llanoveranum*	Medial fluviatile	Kenrick, 1988 Edwards *et al*., 1989 Wellman *et al*., 1998c
Lochkovian **(*breconensis-zavallatus* spore zone**	Rhiw wen Black Mountains, Powys, Wales	*Cooksonia ?cambrensis* *Salopella allenii* *Tortilicaulis* sp.	Medial fluviatile	Habgood, 2000a

Chapter II Methods and materials

1. Methods

1.1. Palynological preparation

Samples were prepared by Alexander C. Ball. or David J. Bodman at the University of Sheffield (UoS) between 2019 and 2021, or by John B. Richardson between 1970 and 1990 (NHM). The latter were not spiked with *Lycopodium* (below) and some additional processing was used in the production of palynological preparations. JBR's processing methods were obtained from lab books at the Natural History Museum and from microscope slides. In some cases, data such as lithology, rock colour and dilutions are not known – such gaps in the data are indicated. Slides processed at the University of Sheffield were spiked with *Lycopodium* in all cases. Spiking and processing details are given below and in thesis appendix 1.

Raw sample maceration

UoS: 20g ± 1g of each sample was ground into <5mm gravel-sized fragments using a pestle and mortar. 50ml of 35% concentrated hydrochloric acid (HCl) was added to the samples in order to digest any carbonate present in the rock. The samples were left to fully react for 24 hours. Two dilutions then followed, whereby water was added to the sample and HCl mixture and then poured off. Prior to each dilution, samples were left to settle for 24 hours in order to minimise the potential loss of suspended palynomorphs. Following initial dilutions, a further 10ml of 35% HCl and 12ml of 40% concentrated hydrofluoric acid (HF) was added to the samples. HF was added in order to digest any silicates that were present in the rock. The samples were then agitated over several days, to fully react before a further eight dilutions per sample were carried out to neutralise the acids, with 24 hours left between each dilution to allow settling of palynomorphs.

NHM: General maceration methods as above (HF + HCl) maceration. Sieving details are uncertain.

Heavy mineral separation

UoS: Sieving of the macerated material was carried out using a nylon sieve mesh and plastic sieves in order to remove minute fragmentary, indeterminate organic material and mineral residue that may obscure palynomorphs. Sieve size was selected based on the smallest palynomorph present in the assemblage. Initially, a 7µm mesh was used for 19M50-01, but this was later deemed too fine and the remaining samples (19M50-02 through 19M50-29) were sieved using a 10µm mesh. Diluted mixtures were poured onto the mesh and washed through with running water whilst being gently agitated over a suction flask. >10µm fraction was then collected. The >10µm residue was then checked under light microscope to assess effectiveness of sieving; samples typically needed two to three sieves to sufficiently remove fine particulates <10µm. Samples that were barren of organic material were disposed of.

Once the samples had been sieved, they were transferred to 45ml centrifuge tubes and centrifuged in an Eppendorf centrifuge 5702 for ten minutes at 3000 RPM in order to separate excess water, organics and mineral residue. Water was then poured off as far as possible from the tube, and a Zinc Chloride ($ZnCl_2$) and Hydrochloric acid (HCl) mixture was added to the organic and mineral residue. Because of its high density, $ZnCl_2$ + HCl facilitates the separation of the less dense organic material and higher density mineral residue. The samples were then centrifuged at 2000 RPM for ten minutes. Following centrifugation, organic material was separated and collected. The mineral residue fraction was then checked for organic material and, if separation was successful, disposed of. Organic material was diluted with water and 10% HCl, then sieved again using a 10µm sieve to remove $ZnCl_2$ + HCl and any remnant material <10µm.

Oxidation (NHM only)
Some samples were processed with additional HNO_3 for two minutes, while others were unoxidized (thesis appendix 1.1).

Lycopodium spiking (UoS only)
In this study, the exotic marker method whereby a known amount of distinctive spores from the Stag's Horn Clubmoss *Lycopodium clavatus* Linneaus (herein *Lycopodium*) are added to the sample to enable quantitative analysis of palynomorph abundances (Benninghoff, 1962; Stockmarr, 1971). *Lycopodium* tablets containing a known amount of (3666) *L. clavatus* spores were added to 10% HCl, liberating the *Lycopodium* spores into solution (1 *Lycopodium* tablet was added per 1ml of organic residue in the sample). The number of *Lycopodium* tablets in each sample varied according to the amount of organic residue, and this is detailed in appendix 2.1. *Lycopodium* spores were then added to the organic residue and mixed using a pipette. Spiked samples were then transferred to a vial and 2-3 drops of HCl were added to prevent fungal growth.

Light microscope slides
UoS: Once the samples had been spiked, light microscope slides were made via strew mounting. Samples were initially agitated using a pipette to ensure an even distribution of palynomorphs, before 5ml of each sample was pipetted into a separate vial. 1 – 2 drops of mounting fluid (water + 1% PVA glue) was added in order to improve adhesion and promote an even distribution of palynomorphs across the slide cover. 5ml of sample was mixed and strew mounted onto 22x32 rectangular glass microscope cover slips and allowed to dry on a hot plate. Once dry, the cover slips were mounted onto standard glass microscope slides using petropoxy 154, cured on a hotplate and labelled.
NHM: Palynological preparations were mounted using H_2O + Elvacite.

SEM stubs
UoS: 5 ml of sample was mixed and strew mounted with organic residue from key samples M50-85-2C, M50-3, 19M50-26 and M50-7, which were selected due to (1) their stratigraphic position (each sample represents examples of palynofloras from current *Ap.* sp. E –to middle MN spore biozones), and (2) their excellent preservation and high diversity (recognised during logging under LM) which gives the greatest chance of identifying suitable specimens for taxonomic plates and morphometric analyses. Two stubs for each sample were made. If mounting fluid had previously been added to the palynological preparation, the preparations were diluted and sieved in water to remove the glue. These samples were gold coated in an Edwards S105B gold sputter coater for three minutes.

1.2. Mesofossil preparation

Bulk maceration
100g of samples 19M50-26 and 19M50-27 were selected based on the size of fragment, here, fragments between 15 and 50mm were selected. The samples were not ground down or altered in anyway before acid treatment. 200ml of concentrated HCl were added to the samples, which were then left for five days, allowing the reaction to reach completion. The HCl-sample mixture was then diluted with water seven times, waiting twenty-four hours between individual dilutions to allow settling and minimise sediment loss. 300ml of 40% concentrated HF was added in order to digest silicates that were adhering to the mesofossils and left for two days to react. The HF solution was then diluted eight times with water, leaving twenty-four hours between each dilution to allow for settling. The diluted solution was then sieved through an 80μm nylon mesh with organic matter >80μm being collected for picking and SEM analysis (4.9).

Stub preparation

UoS: SEM stubs were prepared by SEM either affixing a graphite disc or using Araldite® brand epoxy resin to attach a glass disc to a stub. a small amount of agitated sample was strewn over the slip using a pipette.

Picking

Mesofossils were prepared for SEM analysis using either picking or strew mounting. Mesofossils were picked from macerated material using a single-bristled size 1 paintbrush under a Vickers dissection microscope and individually mounted on SEM stubs with graphite discs mounted to the surface. Samples were then covered and left to dry. Samples were then gold coated using an Edwards S105B sputter coater, prior to imaging with a Philips XL-20 Scanning Electron Microscope at 15 - 20Kv.

Strew mounting

In order to investigate the very fine fraction of the mesofossil assemblage (<400µm), a small amount of fine material was collected with a plastic pipette from the mesofossil suspension and strewed onto an SEM slide with a carbon tab attached and left to dry. Samples were then gold coated using an Edwards S105B sputter coater, prior to imaging with a Philips XL-20 Scanning Electron Microscope at 15 - 20Kv.

Reflectance

Preparation for reflectance

Ammons Hill MPA25242 and M50 section sample DE98 samples were gently sieved using a 1mm brass mesh in order to separate a coarse (>1mm) and fine (<1mm) fraction, before being sent to the Earth Sciences Dept. at Royal Holloway, University of London for vitrinite reflectance. Blocks for Vitrinite reflectance were prepared by Neil Holloway of the Earth Sciences dept. at Royal Holloway, University of London, and vitrinite reflectance measurements were made by Margaret Collinson and Sharon Gibbons at the Earth Sciences Dept. at Royal Holloway, University of London.

The samples were embedded in a polyester resin block, cut and then polished. Two blocks each from Ammons Hill and the M50 were made as replicates.

Measurement of reflectance

Medium reflectance standards used for calibration were [Spinel [0.393] YAG [0.929] GGG [1.749)]. The r^2 value for the calibration line was 0.999994. These were considered the most appropriate set of standards to use because most of the measured values are between 0.393 and 1.749, with 48 of 200 measurements (24%) of samples falling below 0.393, and 4 of 200 measurements (2%) falling above 1.749.

Reflectance measurements were carried out on transects across the middle of the blocks of the fine fraction. Every particle that was useable was measured. 'Usable particles' were defined as having a 2µm-by-2µm area that was free of scratches at 50x magnification. Measurements were taken under a x50 objective on a Nikon Microphot microscope using J&M analytics software. Particles measured were not discriminated by particle morphology, with 100 'useable' particles measured in a transect. The Ammons Hill sample required two transects of the block to obtain 100 measured particles. The M50 sample required ¾ of the length of one transect to obtain 100 measured particles.

1.3. Imaging and micrographs

Light microscopy

Samples were viewed using an Olympus CH-2 light microscope. Micrographs were taken using either: a), a Meiji Techno infinity 1-5C microscope camera, mounted on a Meiji Techno MT5300H transmitted light microscope, or b) a GXCAM-U3-5 5.1-megapixel camera which is interchangeable with one of the eyepieces on the Olympus CH-2 light microscope. The camera is used in conjunction with GXCapture-T software. Unless otherwise stated, all micrographs are taken at x100 magnification, with microil immersion oil used when viewing and taking micrographs of palynomorphs at 100x magnification to improve image clarity. The locations of palynomorphs are recorded using a Pyser–SGI Ltd. S7 England Finder and coordinates on the Olympus CH-2 light microscope. Slides were always loaded onto the stage with the label on the left-hand side. Images were prepared for plates using GIMP version 2.8.

Scanning Electron Microscopy:

UoS: Mesofossils and palynomorph stubs were imaged with a Philips XL-20 Scanning Electron Microscope at 15 - 20Kv at the University of Sheffield Electron Microscopy Unit.

NHM: SEM micrographs were collected by JB Richardson at the Natural History Museum, London. The date, exact methods and SEM used are not known, but folders of SEM 'proofs' are housed in the Micropaleontological collections of the Natural History Museum, London. These proofs are extensive, covering many taxa from the M50 series. These proofs have been scanned and integrated into this taxonomy.

Transmission electron microscopy:

Once examined under SEM, a fragment (approximately half) of each spore mass was prised from the carbon tab using a steel razor blade and placed in a solution of pure ethanol. Samples were then sent to the University of Wisconsin Eau-Claire for TEM analysis by Wilson Taylor. The spore masses were not oxidised or stained prior to imaging. The specimens were set in Agar jelly and sectioned using a diamond knife prior to imaging with a JEOL 2010 Transmission Electron Microscope.

1.4. Quantitative and semi-quantitative palynology

Terminology and measurements

Spore taxa have been identified using the relevant holotype descriptions (see Chapter III, and references therein). New taxa have been described using the terminology of Grebe (1971). Trilete spore taxa have been classified according to Potonié and Kremp (1954). Cryptospore taxa have been classified according to the schema laid out by Richardson (1996a). Steemans' (2000) cryptospore definition, which states that cryptospores are the explicit product of embryophytes, is favoured here (Steemans and Wellman, 2018). Terminology is outlined in schematics below (figs. 1 and 2).

Amb measurements were made using the eyepiece graticule on an Olympus CH-3 light microscope following calibration at 1000x magnification, with an error of <0.5μm. Measurements of ornament, particularly of those on a sub-micrometre scale, were measured using a GXCAM-U3-5 microscope camera which was calibrated at 1000x magnification. The Software interface used was GXCapture-T. Calculated error for the GXCAM-U3-5 camera is <0.05μm. measurements are given as minimum (mean) maximum (μm). Explanations of measurements included in terminology schematics (figs. 1 and 2)

Figs. 1 and 2 illustrate the measurement techniques for palynomorphs and their features encountered in this research. Trilete miospores are the simplest to measure, with amb measurement taken along a consistent line through the Y mark (fig. 1). Amb measurement ignored sculpture such as spines or muri, and only specimens with very little compression were measured, although it is accepted that no 'perfect', uncompressed and perfectly presented spore is possible. Hilate cryptospore monads were

measured in much the same way as trilete spores. Cryptospore tetrads were measured consistently across the crassitudes (fig. 2) and permanent dyads were measured laterally from distal hemisphere to distal hemisphere. Non obligate, or 'true', dyads, were measured with caution, as the degree of separation often varies between specimens which may cause a false sense of spore-size variation. In all cases, however, the maximum size-amplification due to separation is < 5µm. In permanent and true dyads, the diameter of individual spore 'units' was also measured. Various features of the spores were included in the measurements (figs. 1 and 2).

Spore counts

Because many of JB Richardson's slides are not spiked with *Lycopodium* but could not be excluded from the study due to their importance and abundance, two count methods were employed here to fully utilise the available materials.

In semi-quantitative and quantitative counts, palynomorphs were counted to 250 grains and then logged for 'rare' species. Several slides from each assemblage were logged in addition to the counted slides. The decision was made to count to 250 grains based on Traverse (2009) and previous work by Morris (2009). Morris (2009) developed rarefaction curves from spore count charts from palynological assemblages in the Anglo-Welsh Basin (Tredomen Quarry). The cumulative number of species shown by the graphs increases to *c.*200 counted grains, after which it begins to flatten out (fig. 3). This indicates that most of the species present in the assemblage have been counted 200 grains are exceeded. In richer assemblages, Morris (2009) found that the cumulative counts begin to plateau nearer to 250 grains. Following Morris (2009) all assemblages in this work were counted to 250 grains where possible.

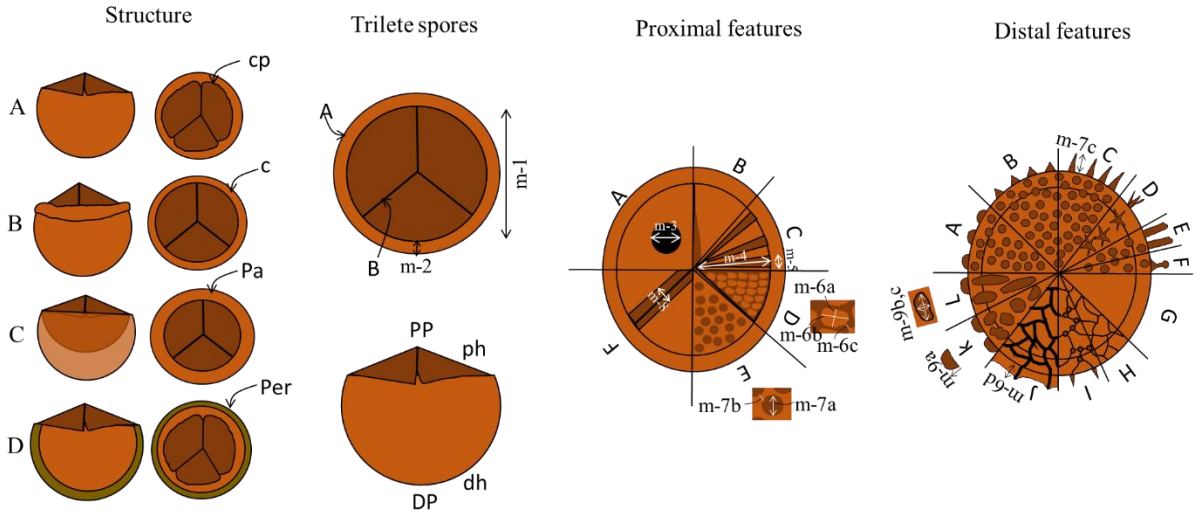

Figure II-1: ***Structure: A:*** *retusoid;* ***cp:*** *curvaturae perfectae;* ***B:*** *crassitate;* ***c:*** *crassitude;* ***C:*** *Patinate;* ***Pa:*** *patina;* ***D:*** *Perispore;* ***Per:*** *perine;* ***Trilete spores: A:*** *crassitude;* ***B:*** *trilete 'y' mark; m-1: Amb measurement, taken along longest axis; m-2: Crassitude width;* ***PP:*** *proximal pole;* ***ph:*** *proximal hemisphere;* ***Dp:*** *Distal pole;* ***dh:*** *distal hemisphere;* ***Proximal features: A:*** *interadial papillae:* ***m-3****: diameter of interadial papillae;* ***m-4****: length of interadial muri;* ***B****: Proximal thickening;* ***C****: interadial muri:* ***m-5****: width of interadial muri;* ***D****: muri:* ***m-6****: muri:* ***a****: width,* ***b****: length;* ***c****: lumen width;* ***E****: apiculate ornament:* ***m-7****: apiculate ornament;* ***a****: diameter;* ***b****: distance between elements;* ***F****: lips accompanying Y-mark****; m-8****: lip width;* ***Distal features: A:*** *Grana;* ***B:*** *Coni;* ***C:*** *Spinae;* ***D:*** *Clustered spinae;* ***E:*** *Baculae;* ***F:*** *Biform elements;* ***A- F*** *measurements as for* ***m-7a-b;*** ***G:*** *Laevigate;* ***H:*** *Reticulum;* ***I:*** *Apiculiretusoid;* ***J:*** *Murornate reticulum;* ***I – J*** *measurements as for* ***m6 a – c, m-6d*** *(height) and* ***m7a – b, m-7c*** *(height);* ***K:*** *Verrucae****; L:*** *Elongate verrucae****; K-L****: measurements* ***m-9a:*** *height;* ***m-9b, c:*** *width and length.*

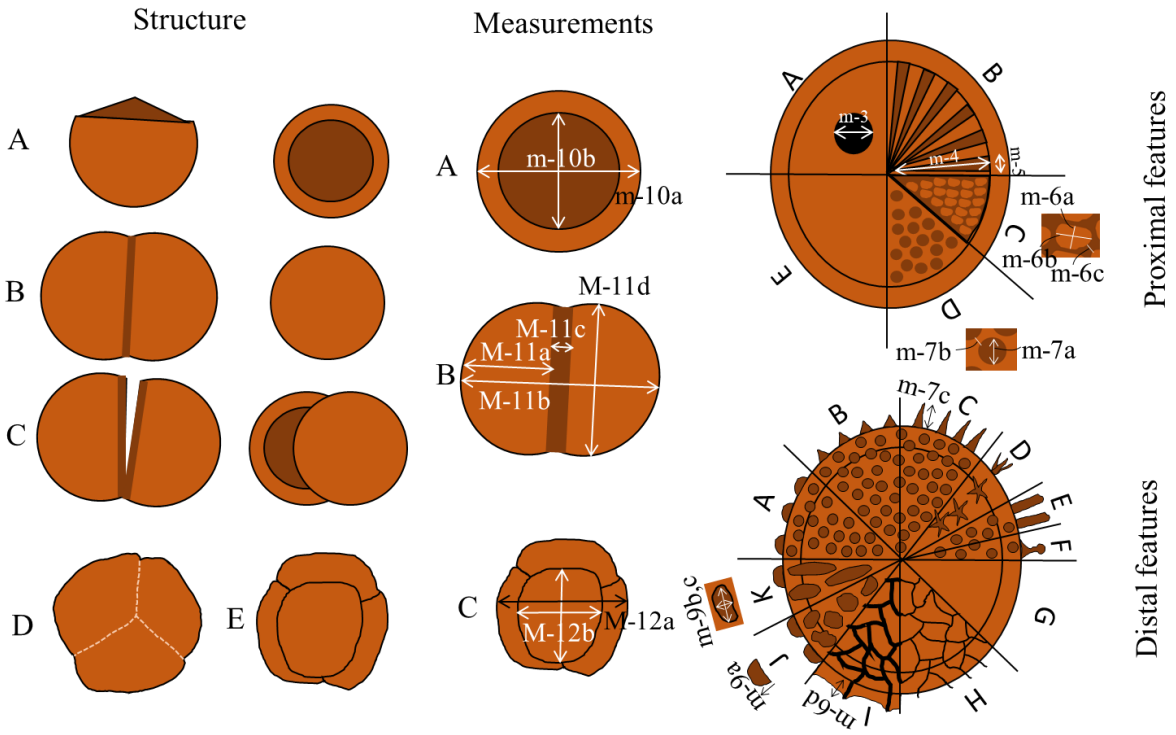

Figure II-2: ***Structure: A:*** *Hilate monad;* ***B:*** *Fused dyad;* ***C:*** *Unfused dyad:* ***D:*** *fused cryptospore tetrad;* ***E:*** *Unfused tetrads; Loose and fused dyads and tetrads may be incorporated in a variously adherent envelope.* ***Measurements: A: m-10b*** *hilum width;* ***m-10a:*** *amb diameter;* ***B: m-11a****: dyad unit width;* ***m-11b:*** *Dyad width;* ***m-11c:*** *collar width;* ***m-11d:*** *Dyad unit/ dyad length;* ***D: m-12a:*** *tetrad width;* ***m-12b:*** *tetrad unit width;* ***Proximal features: A:*** *papillae;* ***B:*** *radial muri; measurements as for fig. 1;* ***C:*** *proximal muri; measurements as for fig. 1;* ***D:*** *apiculate ornaments;* ***E:*** *Laevigate;* ***Distal ornament: A:*** *Grana;* ***B:*** *Coni;* ***C:*** *Spinae;* ***D:*** *Clustered spinae;* ***E:*** *Baculae;* ***F:*** *Biform elements;* ***A- F*** *measurements as for* ***m-7a-b; G:*** *Laevigate;* ***H:*** *Reticulum;* ***I:*** *Murornate reticulum;* ***H – I*** *measurements as for fig. 1;* ***K:*** *Verrucae****; L:*** *Elongate verrucae****; K-L****: as for fig 1.*

Relative abundance counts (UoS & NHM3

All slides (spiked slides and non-spiked slides) were subjected to a standard, 'semi-quantitative' palynomorph count, where native sporomorph species were counted to 250 specimens, excluding *Lycopodium* spores in spiked samples. Sporomorphs in spiked samples were counted to 250 including *Lycopodium* spores.

Quantitative counts (UoS only)

Quantitative palynomorph counts are calculated here as the total number of a given indigenous palynomorph species per unit of processed rock. This calculation enables the abundance of any given taxon to be expressed as a proportion of the total palynomorph concentration in a sample. The equation used here (equation 1) is that of Benninghoff's (1962) method for absolute pollen determination:

$$C = \frac{m_c \cdot L_t \cdot t}{L_c \cdot w} \quad \textbf{(1)}$$

Where C is the number of indigenous palynomorphs per gram of dry rock processed (the concentration), M_c is the number of indigenous palynomorphs counted, L_t is the number of *Lycopodium* spores in each tablet, with t being the number of *Lycopodium* tablets added to the sample; L_c is the number of *Lycopodium* spores counted in the sample, and w is the weight of dried sediment processed for palynomorphs, in grams.

Because not all of the samples were able to be spiked with *Lycopodium* (especially those from the mid Lochkovian) these quantitative counts were used to confirm, where possible, the trends shown by relative abundance counts.

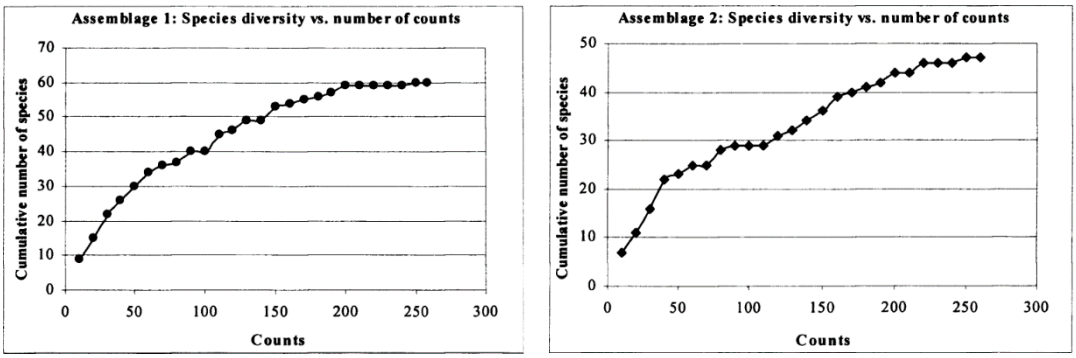

Figure II-3: cumulative plots of assemblages from Tredomen Quarry from Morris (2009).

1.5. Computational analyses

Software versions:

R: Version 4.1.3 (2022-03-10) - "One Push-Up" (R core team, 2022).

PAST: Version 1.3 (Hammer et al., 2006).

EXCEL: Microsoft 365 2016, version 2208.

STRATABUGS: Biostratigraphic computing system version 3.0.

Spore charts

Semi-quantitative and quantitative counts were consolidated into data sheets on Microsoft Excel (thesis appendix 3.1). Abundance charts illustrating the proportional stratigraphic changes in species and gross ornament percentages were produced using the R studio package `library("rioja")` (Juggins, 2020).

Due to the inefficiency of Rioja for palynological use, specifically the inability to account for uneven sampling depths, range charts were drafted in Stratabugs.

Final counts for this study are presented in thesis inserts 1 and 2, and thesis appendices 3.1 – 3.3.

Dendrograms

One dimensional dendrograms were calculated from the results of the spore charts (binary and count data) and were produced in R and StrataBugs. For charts produced in `library("rioja")`, the function `vegdist()` in the package `library("vegan")` (Okasanen et al., 2020) was used with argument `method="raup"`. Raup-Crick coefficients (Raup and Crick, 1979) were selected due to their relative insensitivity to rare taxa and to uneven sampling sizes (e.g. Pardoe et al., 2021). Raup-Crick coefficients use Monte-Carlo simulations to find how often a comparable level of similarity occurs between randomly replicated samples of the same size. Subsequent one-dimensional dendrograms were then visually inspected and compared with the established biostratigraphic schemes (Burgess and Richardson, 1995; Richardson and Edwards, 1989; Richardson and McGregor, 1986; Chapter III).

Statistical analysis

Descriptive statistical analyses, those which summarize and describe the features of the resultant datasets, were carried out in R studio, PAST and Microsoft Excel, with graphical outputs produced in PAST and R.

Total species counts, and counts of other features of the palynoflora, (e.g. ornament change) were summarised in Microsoft Excel using the `quick analysis` tool, which sum the number of counts in a row. The percentages of spore species in an assemblage were calculated using the `=sum()` function in Microsoft Excel. Features of the palynoflora, including genera, trilete spore/ cryptospore/ marine affinity and ornament type were colour coded and sorted by colour using the `Sort` tool in separate spreadsheets.

R Studio

Box plots, line plots and bar plots were produced for diversity and disparity variance to identify possible patterns and trends in the data set using `library("ggplot2")` (Wickham, 2020) (Chapter IV).

Two sample t-tests and Welch's t-tests were used in some analytics to test for statistical significance of temporal diversity and disparity changes through the sequence (Chapter IV). A null hypothesis and alternate hypothesis for each test was defined prior to testing from the graphical outputs developed prior to testing. The t-test compares the means between two independent groups to test these hypotheses, that is, whether there is a significant difference between the means. The two sample t-test assumes that data sets are normally distributed and have equal variance. These assumptions were tested for through the *ad hoc* Shapiro-Wilke test (equation 2) and F-test (equation 3), respectively (e.g. Box, 1953; Markowski and Markowski, 1990; McDonald, 2014).

The Shapiro-Wilke test (equation 2) is calculated as:

$$W = \frac{\left(\sum_{i=1}^{n} a_i x_{(i)}\right)^2}{\sum_{i=1}^{n}(x_i - \bar{x})^2} \quad \textbf{(2)}$$

Where $x_{(i)}$ is the i^{th} order statistic (the i^{th} smallest number in the sample), $\bar{X}$ is the sample mean, a_i is the coefficient given by dividing the vector for expected values by the vector norm (Shapiro and Wilke, 1965).

The second *ad hoc* test, the F-test (Equation 3), is calculated as:

$$F = \frac{s_1^2}{s_2^2} \quad \textbf{(3)}$$

Where F is the ratio of variances and S_1 and S_2 are the variances of the samples, respectively.

Where both *ad hoc* tests were passed, the two paired t-test was used (equation 4). Where the F-test failed (variance was not equal) the Welch t-test was used (equation 5). Where both *ad hoc* tests failed, or the Shapiro-Wilke test failed and F-test passed, no testing was carried out.

$$t = \frac{(\bar{x}, -\bar{x}_2) - (\mu_1 - \mu_2)}{Sp\ \sqrt{\frac{1}{n_1} + \frac{1}{n_2}}} \quad \textbf{(4)}$$

$$t = \frac{(\bar{x}_1 - \bar{x}_2) - (\mu_1 - \mu_2)}{\sqrt{\frac{S_1^2}{n_1} + \frac{S_2^2}{n_2}}} \quad \textbf{(5)}$$

Where $\bar{X}_1$ and $\bar{X}_2$ are the means of the first and second sample, respectively, $\mu 1$ and $\mu 2$ are the means of second population, respectively, *Sp* is the pooled standard deviation, n_1 and n_2 are the sizes of the first and second samples, respectively, and S_1 and S_2 are the standard deviation of first sample second samples, respectively.

The *ad hoc* tests for normal distribution and equal variance tests, and t-tests, were carried out on R studio using Base R functions `with()`, `var.test()` and `t.test()` respectively. The Shapiro-Wilke test was used to test for normal distribution using the function `with()` and the argument `shapiro.test()` in base R (equations 6 and 7). The Shapiro-Wilke test was carried out independently for each biozone according to equation 4, where x_n is the data set, *y* is the diversity/ disparity measurements in that data set, *z* selects the biozone z_n. Where p = > 0.05, the distribution of the data are not be significantly different from normal distribution.

```
with(x1, shapiro.test(y1[z == "z1"]))
```
(6)

```
with(x2, shapiro.test(y2[z == "z2"]))
```
(7)

The F-test was used to test for normal variance using the function `var.test()` in base R (equation 8), where *x* is the diversity/ disparity, *y* is the biozone, and *z* is the data set. Normal variance is shown (no significant difference between variances) where p = > 0.05, such that there is no significant deviation from normal variance.

```
var.test(x ~ y, data = z)
```
(8)

The two sample t-test (equation 9) and Welch t-test (equation 10) were distinguished in the `t.test()` function through the argument `var.equal =`, which was defined as `"TRUE"` (two paired t-test) or `"FALSE"` (Welch's t-test). P-values for these tests are given in table 1.

```
t_test <- t.test(x ~ Biozone, data = z, var.equal = TRUE)
```
(9)

```
welch.test <- t.test(x ~ Biozone, data = z, var.equal = FALSE)
```
(10)

Where `t.test()` is the function for executing a two sample and a welch t-test in base R, *x* is the means to be compared, in this case the mean diversity/ disparity of samples in a biozone, *y*, in the data frame *z*. The argument `var.equal` refers to whether the data set has equal variance. If `=TRUE` the variance is equal, and if `=FALSE` variance is not equal. This argument differentiates the `t.test()` function into a two sample t-test or a Welch's t-test, respectively.

Test	When	Significant P value when
Two paired t-test	When Shapiro-Wilke and F-test are not significant.	$P < 0.05$
Welch's t-test	When Shapiro-Wilke is not significant but F-test is significant.	$P < 0.05$
Shapiro-Wilke	*Ad hoc*	$P > 0.05$
F-test	*Ad hoc*	$P > 0.05$

Table II-1: Statistical tests and ad hoc tests for test assumptions used in this work.

Further descriptive statistics exploring the frequency of variables, including features in mesofossils, and the distribution of measurements such as amb diameter in samples (Chapters V and IV, respectively). Means were calculated using the `summary()` function in R and graphical outputs including line graphs, bar charts and box plots were produced using `library("ggplot2")`.

PAST

PAST was used to summarise measurements from spores (e.g. amb diameter), with particular focus on minimum, maximum and mean scores. Bar plots were produced from this data showing the frequency of scores in suitable bins. Normal distribution curves were fitted to the bar plots using the option in PAST.

Dissimilarity indices

The Jaccards dissimilarity coefficient was used to quantify the dissimilarity between coeval, spatially variable samples and temporally variable samples. The Jaccards dissimilarity coefficient is similar to the Jaccards similarity coefficient, but compares the pairwise dissimilarity between two assemblages. The Jaccards dissimilarity index is calculated as for the Jaccards similarity index, except 1 is subtracted from the final Jaccards similarity index score (equation 11).

$$D7(A,B) = \left(\frac{|A \cap B|}{|A \cup B|}\right) - 1 \quad \textbf{(11)}$$

Where *D7(A,B)* is the Jaccards dissimilarity and *A* and *B* are the observations in both sets. The dissimilarity index is still measured on a scale of 0 – 1, with D7 = 0 indicating that the assemblages share 100% of taxa, with no unique taxa occurring in either of compared assemblages. Meanwhile, D7 = 1 indicates the assemblages are 100% distinct from one another and share no taxa.

The Jaccards dissimilarity index was calculated in R studio using the `vegdist()` function in `library("vegan")`. To avoid calculating extended Jaccard, the argument `binary = TRUE` was included in the `vegdist()` function (Equation 12 and Chapter IV).

```
vegdist(x, method = "jaccard", binary = TRUE)
```
(12)

where *x* is the data set, comprising count data for species in coeval localities. Species count data in the data set, *x*, is converted to presence/ absence data by the argument `binary = TRUE`.

2. Materials

2.1. Localities

Material is drawn from outcrop and boreholes from the late Silurian – Early Devonian Lower 'Old Red Sandstone' of the Welsh Borderlands and South-East Wales (fig. 4, table 2). Outcrop material was collected either during fieldwork by the author between 2019 – 2021, or by J.B. Richardson, D. Edwards

or C.H. Wellman between 1970 and 1998. Core material was drilled by a series of companies between 1960 and 1990. Ten localities in total were explored, with nine yielding spores. One locality, in Anglesey, was investigated but did not yield any spores and is not discussed further here. Further details on sample sites can be found below. In all, nine field sites across the Welsh borderlands and south Wales were collected from. These range from short sections (*c.* 1m thick) to over 300m long.

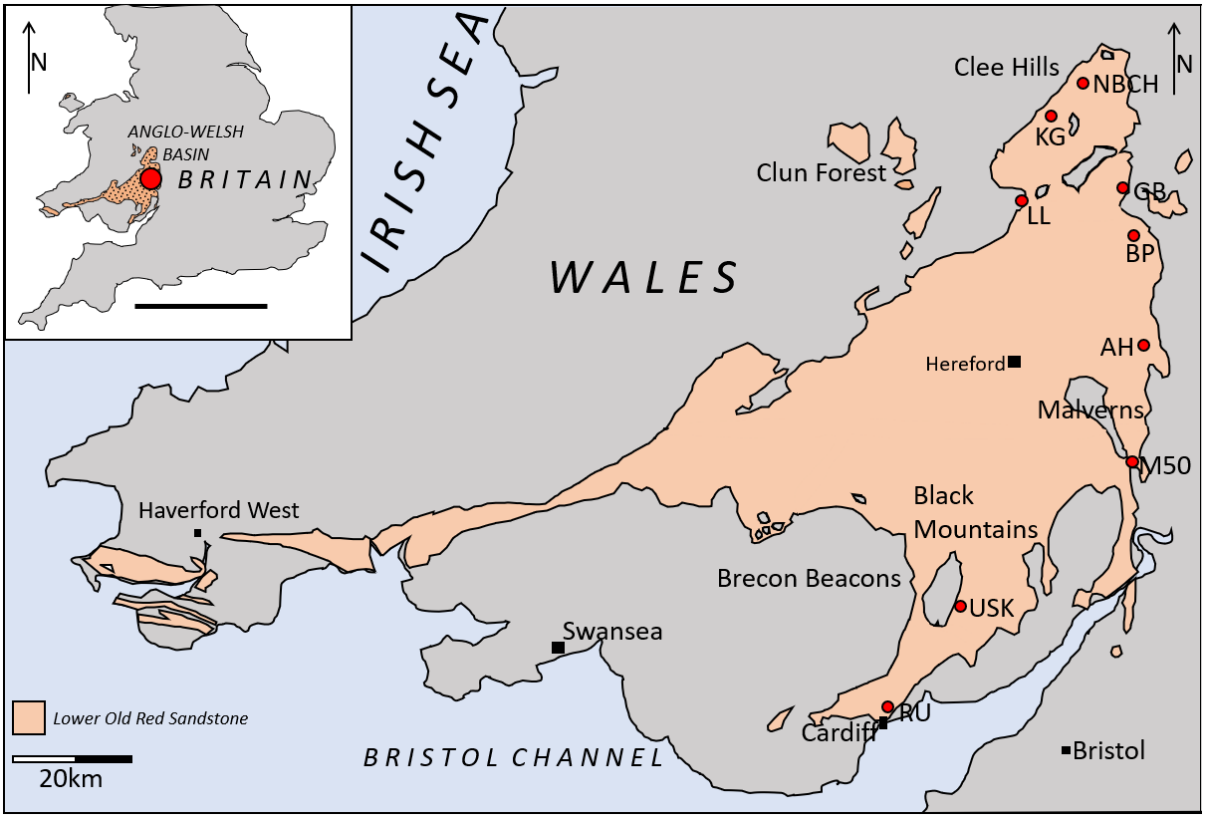

Figure II-4: ***top left)*** *map of southern Britain showing position of the Anglo-Welsh Basin in Western England (the Welsh Borderlands), and its central, south and west extents in Wales, scale bar 200km;* ***(main):*** *The Přídolí and Lochkovian (late Silurian – Early Devonian) outcrop of the Anglo-Welsh Basin, showing the positions of the field localities investigated here, curving along the eastern edge of the basin to southern Wales, scale bar 20km. Sites detailed in section 5. Maps modified from Digimap*

Studied localities do not all have detailed sedimentary logs associated with them. Where possible, schematic logs using published sources have been drafted with sample positions indicated. Where one or two closely spaced samples were collected from a section, no log was made. The details of the surrounding lithologies, where known, are given in the text.

Locality	Period	Collector(s)	Collected	Sampled by & yield	Publications	Housed
Ammons Hill	Lochkovian	John B. Richardson	1994	(JBR & ACB) Spores, mesofossils	Barclay et al., 1994; Richardson, 2007	British Geological Survey
Anglesey	Lochkovian	Alexander C. Ball	2021	(ACB) Barren	n/a	University of Sheffield
Bromyard Plateau	Přídolí – Lochkovian	Alexander C. Ball	2020 - 2021	(ACB) Rare spores	n/a	University of Sheffield
Gardeners Bank	Lochkovian	Charles H. Wellman	1995	(ACB) Spores	n/a	University of Sheffield
Kidnall Gutter	Lochkovian	John B. Richardson	1980*	(ACB) Spores	n/a	Natural History Museum, London

Ludlow Lane	Přídolí	John B. Richardson	1990*	(JBR) Spores	Richardson and Rasul, 1990	University of Sheffield
North Brown Clee Hill	Lochkovian	John B. Richardson (SD) Charles H. Wellman (HD) Alexander C. Ball (HD)	(JBR) 1988* (CHW) 1995 (ACB) 2021	(JBR + CHW) Spores; (ACB) Barren	e.g. Edwards et al., 2012. Richardson, 2007	University of Sheffield (HD); Natural History Museum, London (SD)
M50 motorway	Přídolí – Lochkovian	John B. Richardson Dianne Edwards Alexander C. Ball	(JBR) 1974 (JBR + DE) 1979 (ACB) 2019	(JBR + DE) Spores, Mesofossils; (ACB) Barren	Edwards et al., 1994; Wellman, 1999; Richardson, 2007	Natural History Museum, London (palynopreps); Cardiff University (mesofossils)
Rumney	Ludlow – Přídolí	R.A. Waters D.E. White A.C.Ball	(RAW, DEW) 1960 (ACB) 2021	(ACB) Spores, mesofossils	Burgess and Richardson, 1995 Glasspool and Gastaldo, 2022	British Geological Survey
Usk	Ludlow – Přídolí	*Core shared by*: Sovereign Oil, Union Texas, Amerada Hess Ltd., Superior Oil (UK) Ltd., Coalite Group Plc., Industrial Scotland Energy Ltd.	(Core) 1988 (ACB) 2021	(ACB) Spores, mesofossils	n/a	British Geological Survey

Table II-2: Sample provenance, yield and curation data for the material used in this study.

2.1.1. Ammons Hill section (AH), Shropshire, SO 6850 5290 – 7020 5300

Material was collected from outcrop by the BGS during a re-excavation of the section (Barclay *et al.*, 1994), where a 170m trench was dug between SO 6850 5290 – 7020 5300 in an abandoned railway cutting (fig. 5). The exposure was covered up following BGS investigation and the area is now heavily overgrown. The section comprises steeply dipping beds (50°SW) of the Freshwater West and Moor Cliffs formations, which are juxtaposed against one another by the NW-SE tending Brockhampton Fault. Minor extensional faults, related to the Brockhampton Fault, complicate the section further. The Chapel Point Limestone member has been faulted out of the sequence by the Brockhampton fault (Barclay et al., 1994), precluding the assessment of relative stratigraphic height from this lithostratigraphic marker. The lithologies of the Freshwater West and Moor Cliffs formations are typical (section 4.3) at Ammons Hill.

Ten samples from Ammons Hill were studied, all of which were collected by J.B. Richardson. Nine samples were studied from the Freshwater West Formation, and one from the Moor Cliffs Formation. The Freshwater West Formation samples were processed at the University of Sheffield and quantitative and semi-quantitative analyses were made. The Moor Cliffs Formation sample was processed by John B. Richardson and was not spiked with *Lycopodium* (thesis appendix 2.1). All of the samples had a good spore yield with >200 spores reported from each studied slide.

Sediments of the Moor Cliffs Formation are interpreted to have been deposited by muddy, sheet flood ephemeral streams and rivers, whilst those of the overlying Freshwater West Formation deposited by sandy perennial and ephemeral channelised rivers (Allen and Tarlo, 1965; Allen and Williams, 1976; Morris et al., 2012b). *In situ* ostracods and acritarchs recovered from the Freshwater west Formation are indicative of repeated brackish water incursions (Barclay et al., 1994) (Palynofacies) into the otherwise terrestrial fluvial system. Palynomorphs were isolated from horizons across 150m of the trench section, and indicate that the section spans between the *Apiculiretusispora* sp. E biozone and middle MN subzone. Charcoalified mesofossils of embryophytic and non-embryophytic affinities (e.g. Nematophytes) were isolated from one sample in the lower MN subzone (Chapter V).

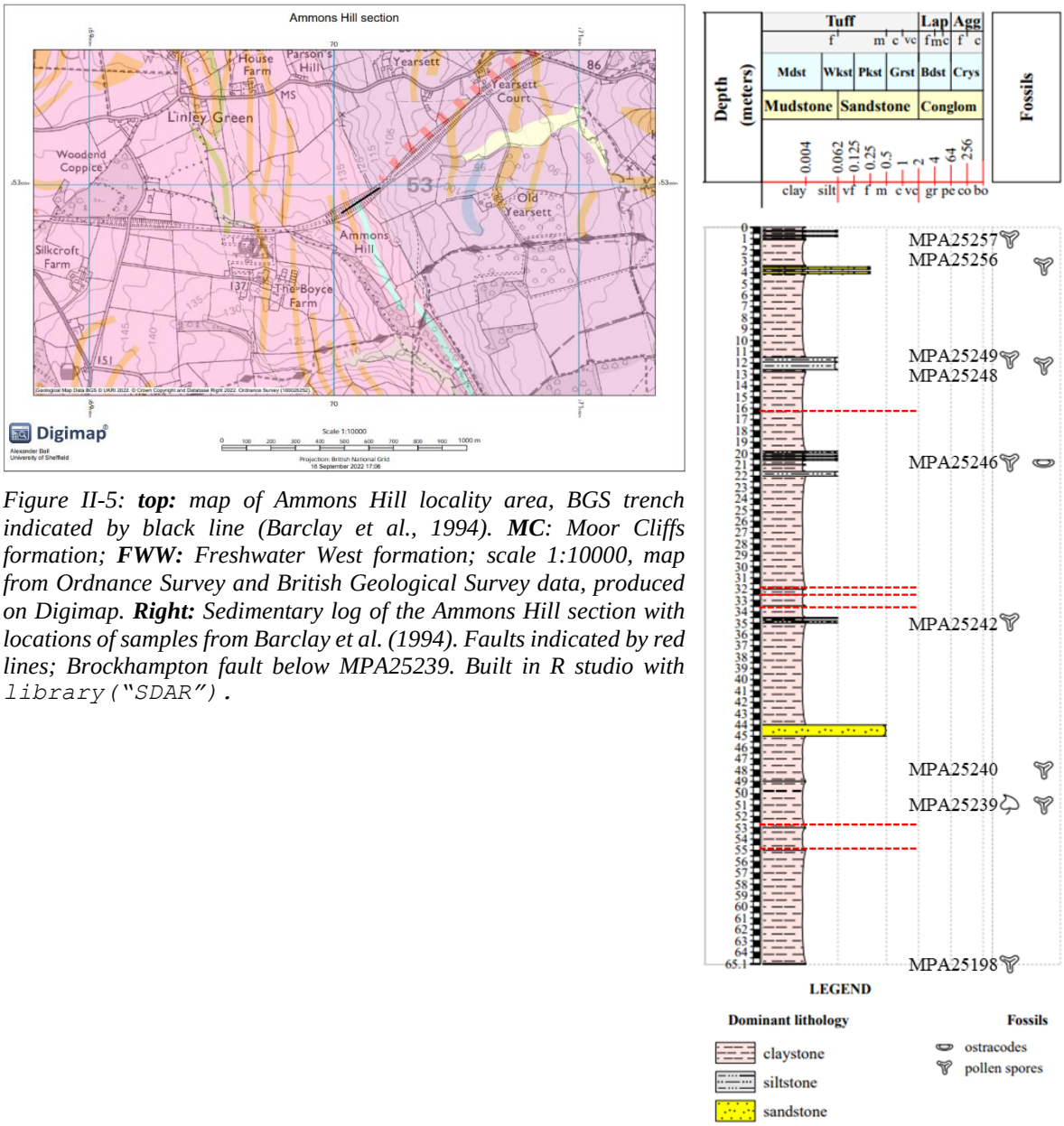

Figure II-5: ***top:*** *map of Ammons Hill locality area, BGS trench indicated by black line (Barclay et al., 1994).* ***MC****: Moor Cliffs formation;* ***FWW:*** *Freshwater West formation; scale 1:10000, map from Ordnance Survey and British Geological Survey data, produced on Digimap.* ***Right:*** *Sedimentary log of the Ammons Hill section with locations of samples from Barclay et al. (1994). Faults indicated by red lines; Brockhampton fault below MPA25239. Built in R studio with* `library("SDAR").`

2.1.2. Bromyard plateau (BP), Shropshire. SO 6856 6615

This site comprises multiple stream sections which dissect the Freshwater West and Moor Cliffs Formation (fig. 6). Samples were collected from +1m (Witchery Hole) and +3m (Temple Dingle) relative to the Chapel Point Limestone. The short sections from Temple dingle (near Stanford-on-Teme) and Witchery Hole (near Shelsey Beauchamp) comprise ± horizontally dipping beds with a <5° maximum dip. Lithologies are typical of the Freshwater West and Moor Cliffs formations, with principally red, mottled mudstones and siltstones being replaced by red sandstones and siltstone. Subordinate conglomerates and variously mature calcretes occur throughout. The Chapel Point Limestone is present in the sections allowing lithostratigraphic correlation. Minor faulting occurs in the sequence but it typically perpendicular to strike and do not interrupt the sequence considerably.

Three samples from Bromyard plateau were studied, all of which were collected by A.C. Ball. All three samples are from separate dingles and all are from the Freshwater West Formation. Samples were processed at the University of Sheffield and quantitative and semi-quantitative analyses were made

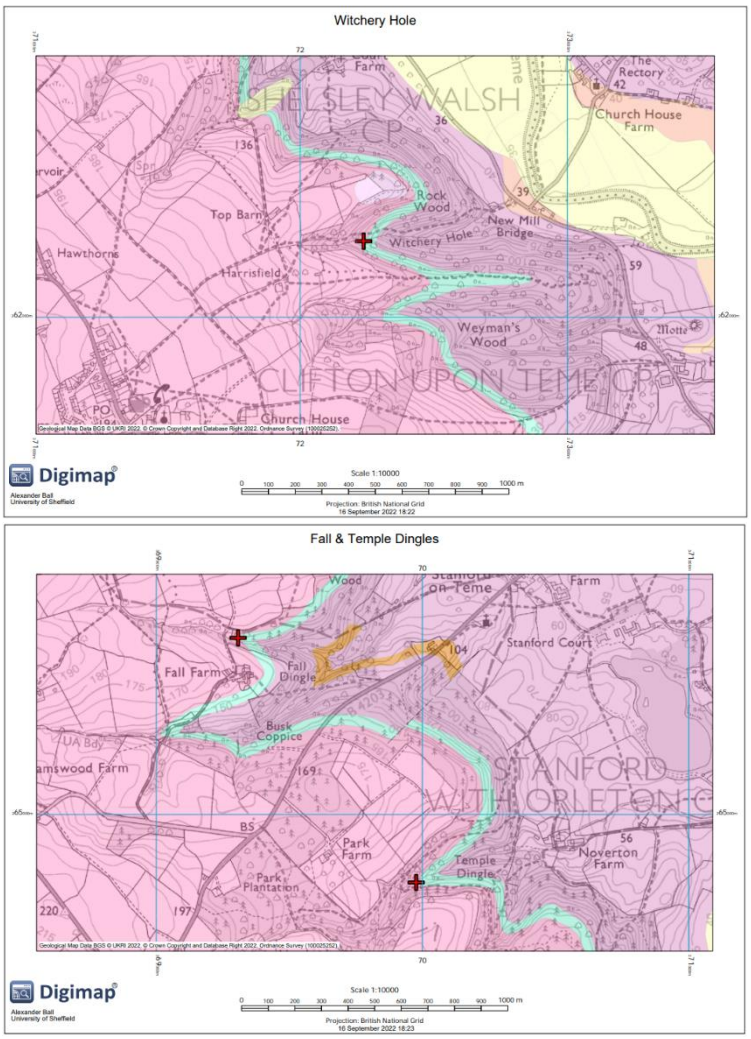

Figure II-6: Map of Bromyard plateau localities, with sample sites indicated by red crosses. Localities are all dingle sections. ***MC****: Moor Cliffs formation;* ***CPL:*** *Chapel Point Limestone member;* ***FWW:*** *Freshwater West formation;* ***top:*** *Witchery Hole locality;* ***bottom:*** *Fall and Temple dingle localities. scale 1:10000, map from Ordnance Survey and British Geological Survey data, produced on Digimap.*

(thesis appendix 2.1). Two samples had a low spore yield (<30), whilst one had a good yield of >200 spores.

Depositional setting of the sediments is interpreted to be typical of the formations, with muddy ephemeral rivers of the Moor Cliffs Formation giving way to sandier, perennial rivers of the Freshwater West Formation following a period of depositional hiatus represented by the Chapel Point Limestone. Palynomorph productivity was poor from Temple Dingle, but reasonable from Witchery Hole. Both samples yield assemblages indicative of the MN zone.

2.1.3. Gardener's Bank (GB), Shropshire. SO 6809 7450

This short outcrop section in the Freshwater West Formation was collected from by CH Wellman in 1995 (fig. 7). Originally described in Turner (1970) and later in Märss and Miller (2004), the outcrop is +8m above the Chapel Point Limestone. The material outcrops in a motocross track *c.* 1.5km south of Cleobury Mortimer near The Rookery. The small section comprises shallow dipping beds (<5°) and is not thought to be affected by faulting. Four samples were collected from a 1m thick green siltstone, which overlies a red palaeosol with immature calcrete glaebules, and is overlain by a well sorted, fine red sandstone. Quantitative and semi-quantitative analyses were made for these samples (thesis

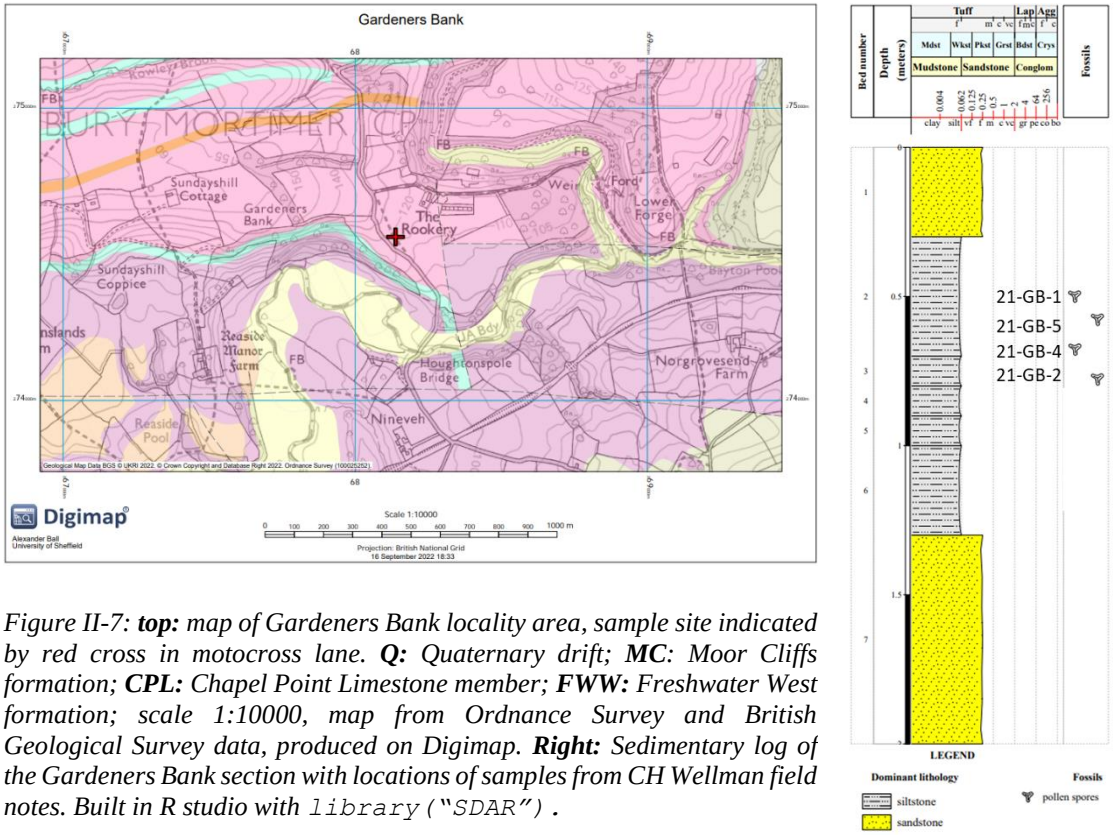

Figure II-7: ***top:*** *map of Gardeners Bank locality area, sample site indicated by red cross in motocross lane.* ***Q:*** *Quaternary drift;* ***MC:*** *Moor Cliffs formation;* ***CPL:*** *Chapel Point Limestone member;* ***FWW:*** *Freshwater West formation; scale 1:10000, map from Ordnance Survey and British Geological Survey data, produced on Digimap.* ***Right:*** *Sedimentary log of the Gardeners Bank section with locations of samples from CH Wellman field notes. Built in R studio with* `library("SDAR")`.

appendix 2.1). All of the samples had a good spore yield with >200 spores reported from each studied slide.

The sedimentology of the site is typical of the Freshwater West Formation, comprising red mudstones, sandstones and variously developed calcrete palaeosols with rare grey to green siltstones and mudstones. These sediments have been interpreted as the deposits of variously meandering sandy streams and rivers., a depositional environment typical of the Freshwater West Formation. The palynomorph assemblage indicates the assemblage belongs in the ?lower *micrornatus-newportensis* spore assemblage biozone.

2.1.4. Kidnall Gutter (KG), Shropshire. SO 5620 8703

This short section in the Freshwater West Formation was collected from outcrop by JB Richardson in the 1970s (fig. 8). The material outcrops in a steep dingle just south of Tugford on the western slope of North Brown Clee Hill, *ca.* 9km south-east of Hudwick and Sudford Dingles (NBCH, 2.1.5). Both samples were processed at the Natural History Museum and were not spiked with *Lycopodium*. These samples were collected from the Freshwater West Formation and had good spore yields of >200 spores per slide (thesis appendix 2.1.).

The sedimentology of the site is much the same as that found around North Brown Clee Hill (2.1.6), comprising red mudstones, sandstones and variously developed calcrete palaeosols. These sediments have been interpreted as the deposits of variously meandering sandy streams and rivers. The palynomorph assemblage is indicative of the lower *micrornatus-newportensis* spore assemblage biozone.

2.1.5. Ludlow Lane (LL), Shropshire SO 5123 7413

One sample was collected from the Downton Castle Sandstone Formation near the junction between Ludford Lane and Leominster Road, near Ludlow, by JB Richardson (fig. 9). This sample was not spiked. The sample yielded >200 spore per slide (thesis appendix 2.1).

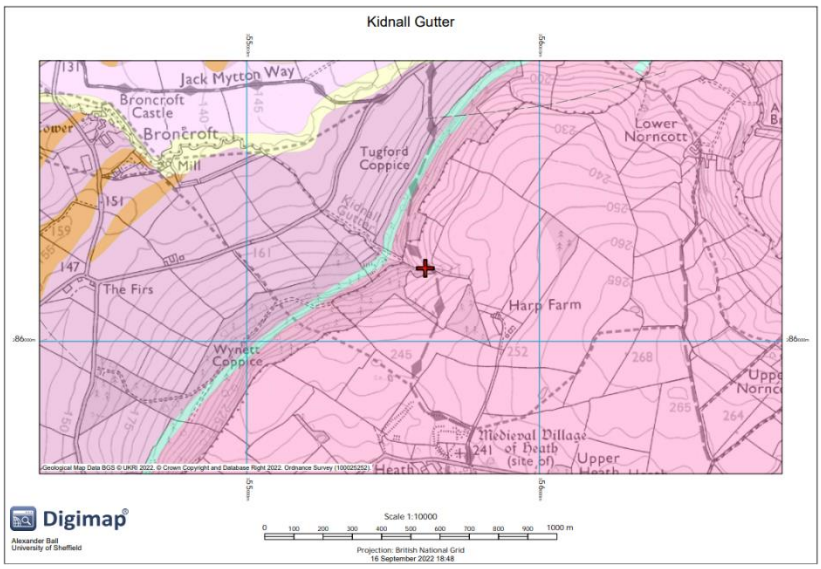

Figure II-9: map of Kidnall Gutter area with sample site indicated by red cross. ***MC****: Moor Cliffs formation;* ***CPL:*** *Chapel Point Limestone member;* ***FWW:*** *Freshwater West formation; Scale 1:10000, map from Ordnance Survey and British Geological Survey data, produced on Digimap.*

The sediments of the Downton Castle Sandstone Formation are typical of that Formation and have been interpreted as being deposited in a near shore marine environment as part of a wave dominated deltaic system during a brief period of marine transgression. The palynological assemblage is indicative of the *tripapillatus – spicula* biozone (early Přídolí) (Richardson and Rasul, 1990).

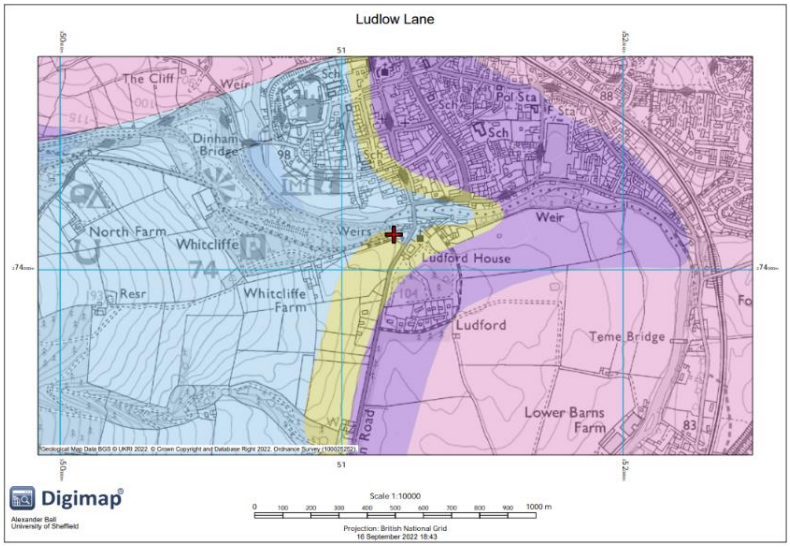

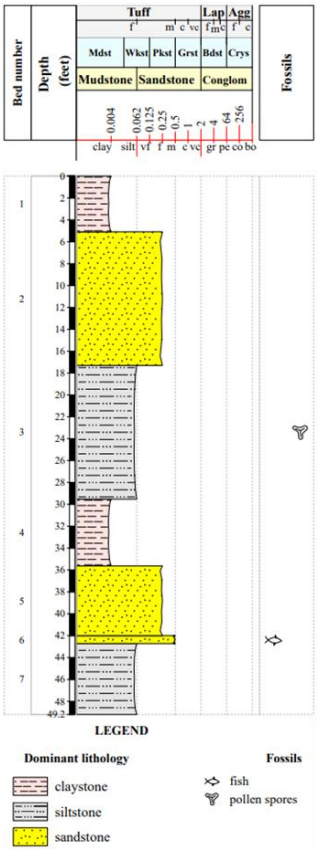

Figure II-8: ***top:*** *map of Ludlow Lane locality, indicated by red cross.* ***W:*** *Whitcliffe formation, Ludlow;* ***D****: Downton Castle Sandstone formation;* ***T:*** *Temeside mudstone formation. Scale 1:10000, map from Ordnance Survey and British Geological Survey data, produced on Digimap.* ***Right:*** *Schematic sedimentary log of part of the Ludlow Succession, showing the approximate position of sample LL3.* ***LBB:*** *Ludlow bone bed. Log modified from Basset et al., 1982 and built in R studio with* `library("SDAR").`

2.1.6. North Brown Clee Hill (NBCH), Shropshire. SO 6317 9272

This outcrop section (fig. 10) was identified during routine logging by JB Richardson in the 1980s and has since been extensively published on following the recovery of exceptionally preserved, fragmentary

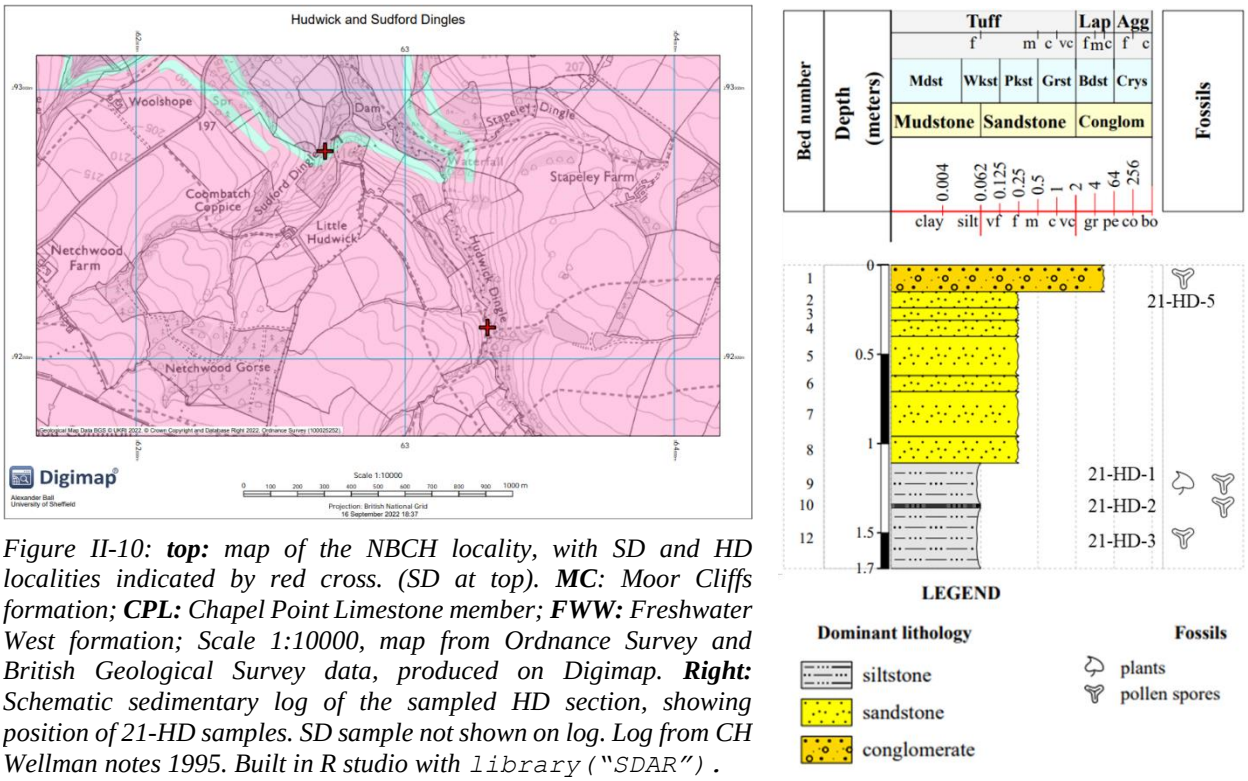

Figure II-10: ***top:*** *map of the NBCH locality, with SD and HD localities indicated by red cross. (SD at top).* ***MC****: Moor Cliffs formation;* ***CPL:*** *Chapel Point Limestone member;* ***FWW:*** *Freshwater West formation; Scale 1:10000, map from Ordnance Survey and British Geological Survey data, produced on Digimap.* ***Right:*** *Schematic sedimentary log of the sampled HD section, showing position of 21-HD samples. SD sample not shown on log. Log from CH Wellman notes 1995. Built in R studio with* `library("SDAR")`.

mesofossils of early land plants (e.g., Edwards *et al*., 1994; Morris *et al*., 2011a, 2012a; Edwards *et al*., 2014; Morris *et al*., 2018b). Six samples were collected from Hudwick Dingle by CH Wellman in 1995 from the Freshwater West Formation (thesis appendix 2.1). The short section lies between 59.8m and 61.6m above the Chapel Point Limestone, outcropping beneath a small waterfall. These slides were processed at the University of Sheffield and were spiked with *Lycopodium* (Thesis appendix 2.1.).

One sample was collected from the adjacent Sudford Dingle by JB Richardson in the 1980s from -7m below the Chapel Point Limestone in the Moor Cliffs Formation. This slide was processed at the Natural History Museum and was not spiked with *Lycopodium* (Thesis appendix 2.1.).

In both cases, the formations comprise shallow to horizontally dipping beds (<5° dip), and no faults interrupt the sequence. The sediments around NBCH of the Freshwater West and Moor Cliffs formations are typical of those formations. Depositional environments are also considered to be typical, with muddy ephemeral rivers of the Moor Cliffs Formation giving way to sandier, perennial rivers of the Freshwater West Formation following a period of depositional hiatus represented by the Chapel Point Limestone (Edwards *et al*., 1994). The palynomorph assemblages indicate that the NBCH section spans the *A.* sp. E and MN biozones.

Ross – Tewkesbury Spur (M50) motorway section, Hereford and Worcester. SO 6605 2584 – 6663 2612

Outcrop samples were collected by JBR and JRA when the section was exposed in the 1970s. The section extends 207 metres through the Moor Cliffs Formation and Freshwater West Formation, between the 29.4 and 29.8 marker posts (Allen and Dineley, 1976) (fig. 11). Twenty-six samples were collected by JB Richardson from the Moor Cliffs (10 samples) and Freshwater West Formation (sixteen samples). The Chapel Point Limestone is exposed in the sequence. The section comprises steeply dipping beds (45°) and some sections are affected by faulting, although the section collected from is not faulted (Allen and Dineley, 1976). The section is no longer exposed. Four samples were processed

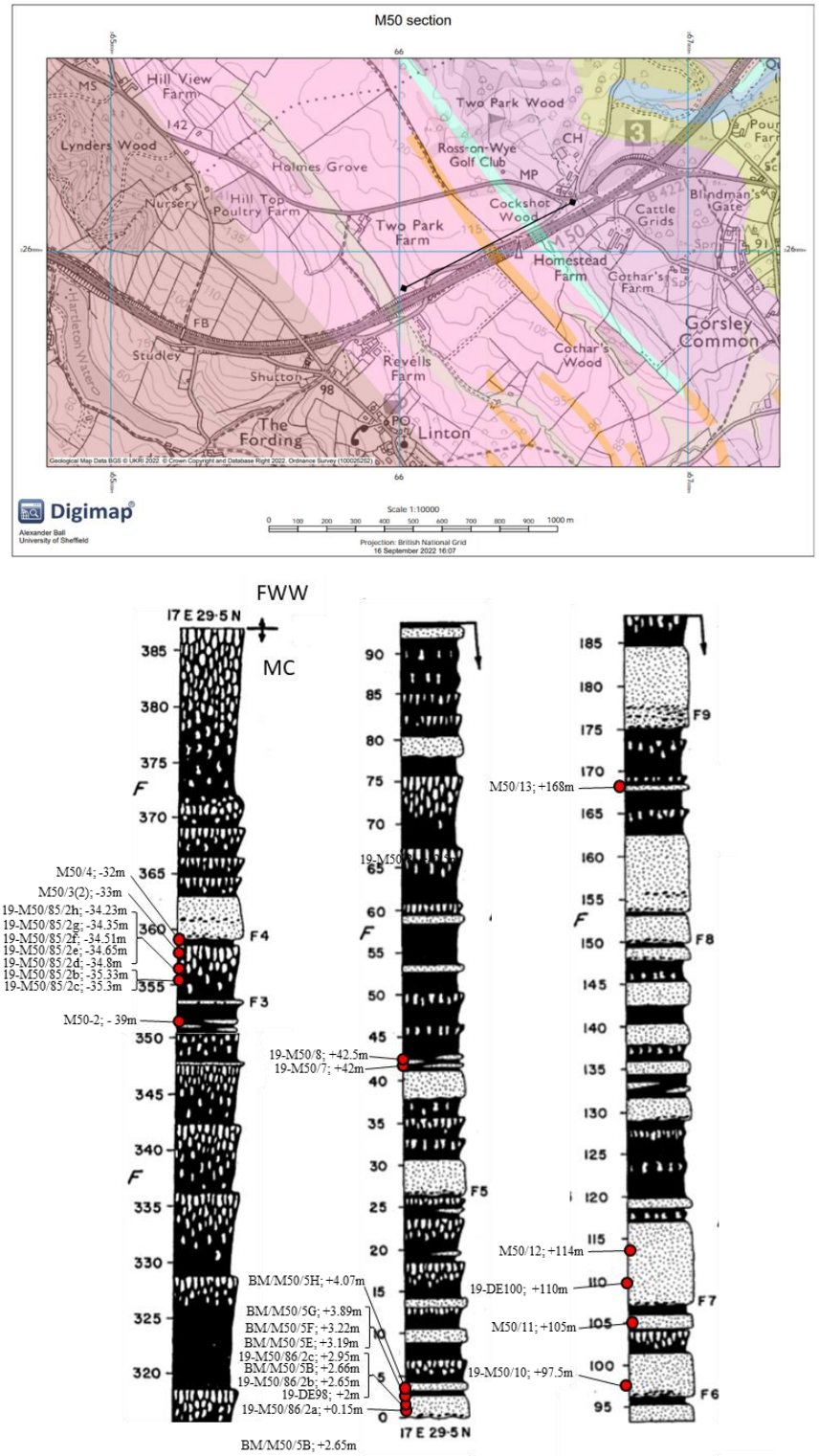

Figure II-11: ***top:*** *map of the M50 motorway section, with studied section indicated by black line.* ***MC****: Moor Cliffs formation;* ***CPL:*** *Chapel Point Limestone member;* ***FWW:*** *Freshwater West formation;* ***BS:*** *Brownstones formation. Red line indicates fault. Scale 1:10000, map from Ordnance Survey and British Geological Survey data, produced on Digimap.* ***Bottom:*** *log section of the M50 section modified from Allen and Dineley (1976), with M50 samples indicated. Scale in metres.*

at the University of Sheffield and spiked with *Lycopodium*. The others were processed by JB Richardson at the Natural History Museum and were not spiked. All of the samples yielded >200 spores per slide.

The sediments are typical of the Moor Cliffs and Freshwater West Formation. The depositional environments are also considered typical with muddy, ephemeral rivers of the Moor Cliffs Formation giving way to sandier, perennial and ephemeral rivers of the Freshwater West Formation. Analysis of dispersed spore assemblages from the same material indicates that this section extends between the pre-*Apiculiretusispora* sp. E zone and middle MN zone. Mesofossils have been recovered from this locality from sample DE98 (Chapter V and VI).

2.1.8. Rumney-1 borehole (RU), Cardiff, South Wales. ST 2108 7925

First described by Sollas (1879) the Rumney inlier, near Cardiff, comprises an anticline with a core of Wenlock sediments, which pass conformably into Ludlow and Přídolí aged sediments (Basset, 1974) towards the outside of the inlier. The Rumney-1 Borehole (BGS reference: ST27NW307) was drilled by the BGS to establish the nature of the Downton and Ludlow series boundary in the Rumney Silurian inlier (fig. 12). The borehole covers Recent, Pleistocene, Silurian and Wenlock materials. The Moor Cliffs Formation extends from a depth of 5m to 57.43m where it transitions into the Ludlow Llanedeyrn Formation. One sample was retrieved from the Moor Cliffs Formation and three from the preceding

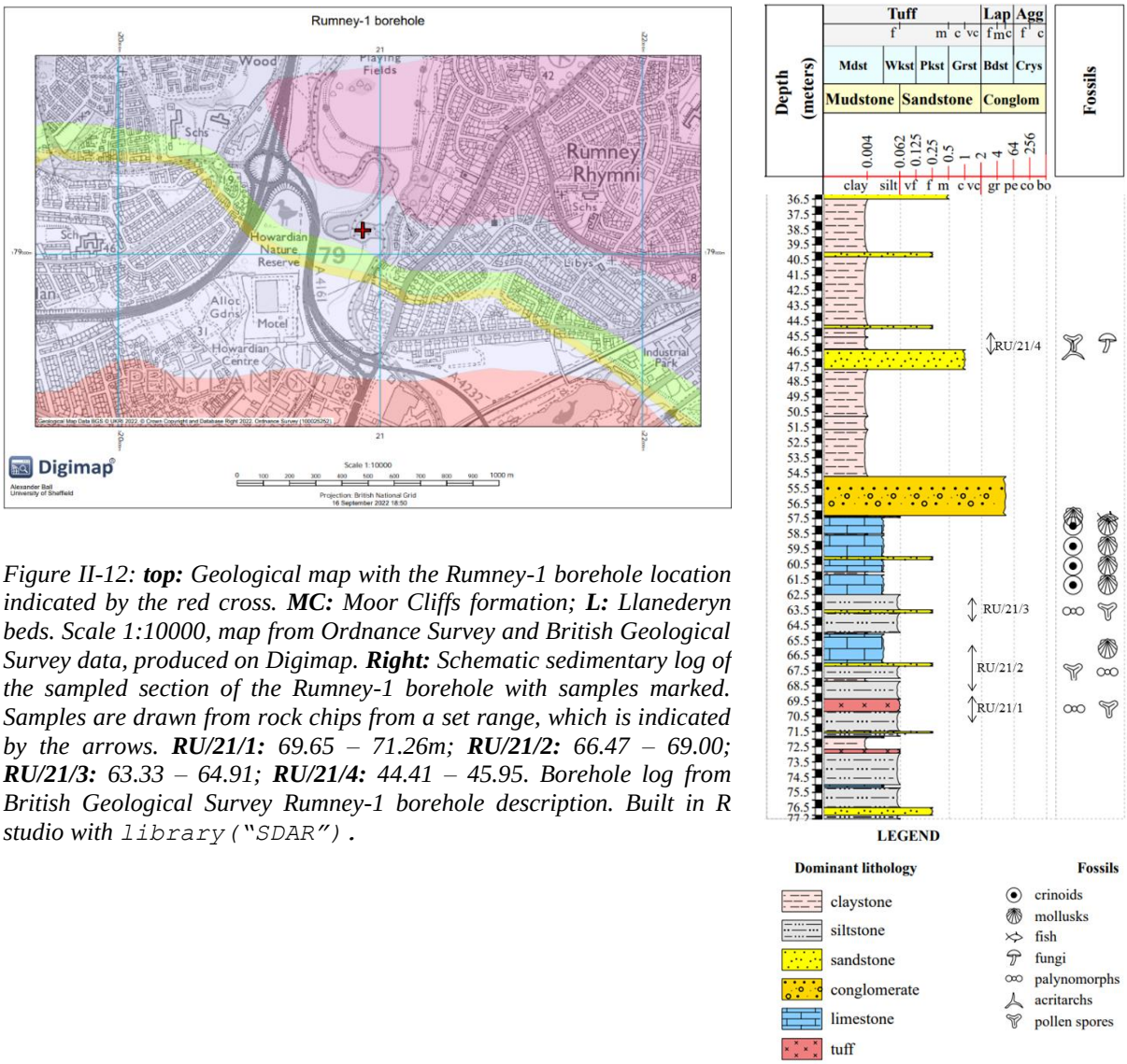

Figure II-12: ***top:*** *Geological map with the Rumney-1 borehole location indicated by the red cross.* ***MC:*** *Moor Cliffs formation;* ***L:*** *Llanederyn beds. Scale 1:10000, map from Ordnance Survey and British Geological Survey data, produced on Digimap.* ***Right:*** *Schematic sedimentary log of the sampled section of the Rumney-1 borehole with samples marked. Samples are drawn from rock chips from a set range, which is indicated by the arrows.* ***RU/21/1:*** *69.65 – 71.26m;* ***RU/21/2:*** *66.47 – 69.00;* ***RU/21/3:*** *63.33 – 64.91;* ***RU/21/4:*** *44.41 – 45.95. Borehole log from British Geological Survey Rumney-1 borehole description. Built in R studio with* `library("SDAR")`.

Llanedeyrn Formation. Spore yields in these samples were comparatively poor, with between 84 – 176 spores per slide (thesis appendix 2.1.).

The Moor Cliffs Formation comprises chiefly red, red-brown and red-purple mudstones, siltstones and sandstones with rare green mudstones and intraclastic breccias. The sediments often exhibit, *inter alia*, crossbedding, laminations and cross laminations, and are therefore typical of the Moor Cliffs Formation. The green mudstone is of particular interest here as it was noted to contain plant fragments. The depositional setting is interpreted to have been essentially typical of the Moor Cliffs Formation with variously braided, muddy ephemeral rivers deposited under a semi-arid, seasonal climate. Green mudstones with marine palynomorphs indicate marine influence in the Moor Cliffs Formation at this time. Rocks from the Ludlovian Llanedeyrn Formation comprise dark grey siltstones with terrestrial and marine derived fossils, including brachiopods (e.g. Bassett, 1974), palynomorphs (Burgess and Richardson, 1995) and charcoalified nematophytes (Glasspool and Gastaldo, 2022). These sediments are interpreted to have been deposited in nearshore, shallow marine environments.

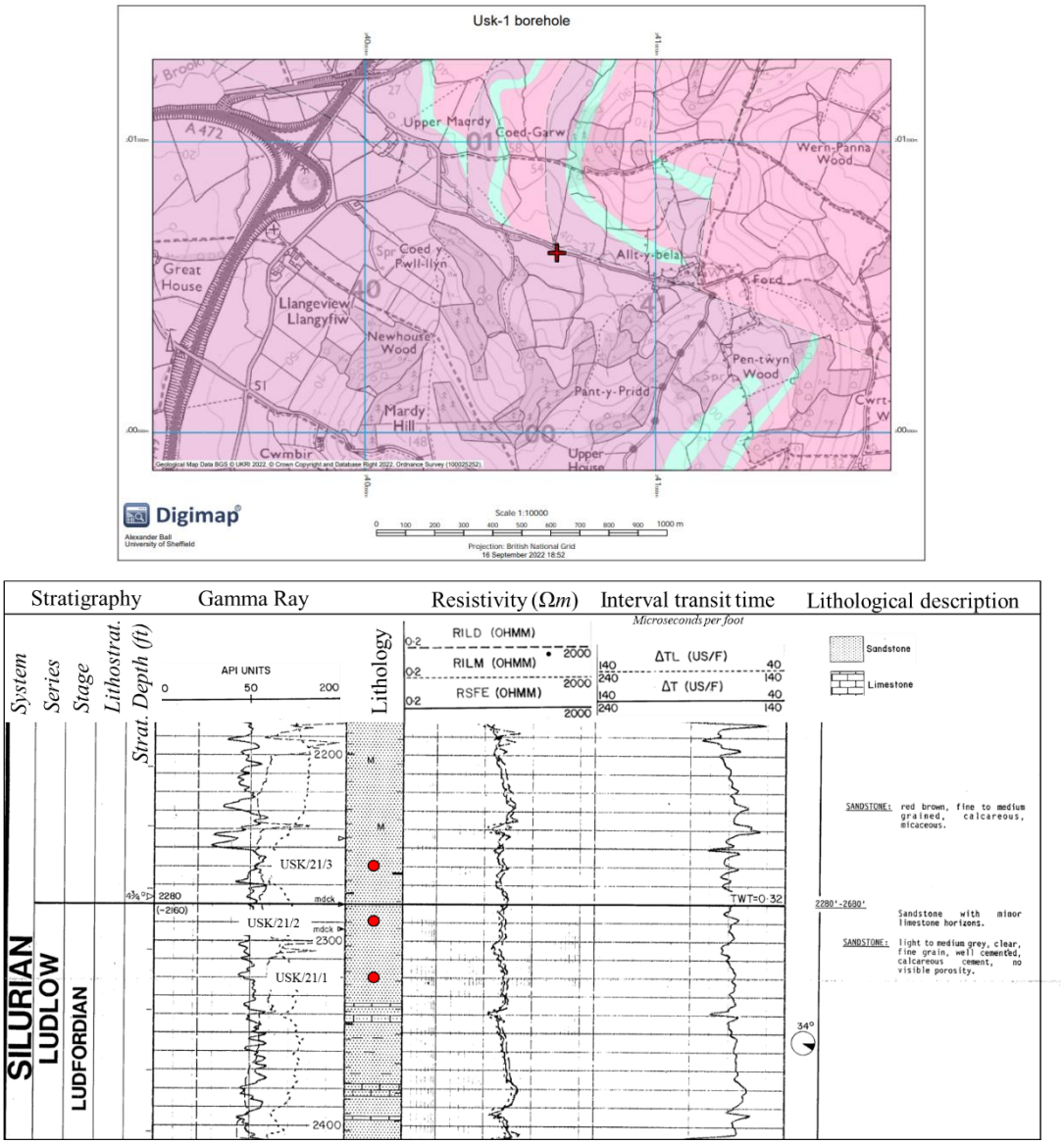

Figure II-13: ***Top:*** *geological map of the locality of the Usk-1 borehole, position indicated by the red cross.* ***FWW:*** *Freshwater West formation;* ***CPL:*** *Chapel Point Limestone member;* ***MC:*** *Moor Cliffs formation. Scale 1:10000, map from Ordnance Survey and British Geological Survey data, produced on Digimap.* ***Bottom:*** *log section of the studied section of the Usk-1 borehole, with sample positions indicated. Stratigraphic depth in feet.*

2.1.9. Usk – 1 borehole (USK), Monmouthshire, South Wales. SO 4020 0085

The Usk inlier is a periclinal structure exhibiting Wenlock – Přídolí sediments (Walmsley, 1958), with gently folding beds with dips <10°. The Usk-1 borehole was drilled adjacent to an extensional fault (fig. 13), but this is not though to cut the borehole. The Usk-1 borehole penetrates 700m of stratigraphy with a considerable proportion of the Moor Cliffs Formation collected and preceding Ludlow series. This borehole was drilled by Sovereign Oil and Gas PLC and is housed in the BGS core store. Despite the promising extent of the borehole, very few samples were retrieved. No samples were obtained from the Moor Cliffs Formation, with samples instead retrieved from the early Přídolí 'Speckled Grit Beds' and Ludlow upper Langibby beds (*sensu* Walmsley, 1958).

Much of the borehole comprises rocks that typical of the Moor Cliffs Formation, being principally red mudstones, fine siltstones and sandstones interpreted as having been deposited by muddy, ephemeral rivers in a semi-arid climate. These terrestrial sediments conformably overlie the Walmsley's (1958) 'Speckled Grit Beds', which are laterally and lithologically comparable with the Downton Castle Sandstone Formation. These sediments were deposited in a near shore, shallow marine environment as part of a wave-dominated deltaic system (Basset et al., 1982). The preceding Ludlow series comprises the upper Langibby beds (*sensu* Walmsley, 1958) and comprises dark green-grey shales with alternating ripple marked siltstones to have been deposited in a shallow marine environment, with deposition occurring further offshore than the sediments of the overlying 'Speckled Grit Beds' (Walmsley, 1958).

2.3. Material curation

Raw sample, light microscope slides, SEM stubs and palynological preparations for HD, GB, BP, DE98,99,100 are stored at the Centre for Palynology at The University of Sheffield, U.K. Raw sample, Light microscope slides, SEM stubs and proofs, and palynological preparations for the M50 are housed in the Micropalaeontological unit at the Natural History Museum, London. Raw sample, Light microscope slides, SEM stubs and palynological preparations for Ammons Hill, Rumney and USK are housed at the British Geological Survey, Keyworth, U.K. TEM blocks housed at the University of Wisconsin Eau-Claire, Eau-Claire, WI, U.S.A.

3. Bibliography

ALLEN, J.R.L. AND TARLO, L.B., 1963. The Downtonian and Dittonian facies of the Welsh borderland. *Geological Magazine, 100*(2), pp.129-155.

ALLEN, J.R.L. & DINELEY, D.L. 1976. The succession of the Lower Old Red Sandstone (Siluro-Devonian) along the Ross-Tewkesbury Spur Motorway (M. 50), Hereford and Worcester. *Geological Journal*, **11** (1), 1 – 14.

BARCLAY, W.J., RATHBONE, P.A., WHITE, D.E. & RICHARDSON, J.B., 1994. Brackish water faunas from the St Maughans Formation: The Old Red Sandstone section at Ammons Hill, Hereford and Worcester, UK, re-examined. *Geological Journal*, **29** (4), 369 – 379

BASSETT, M. G. 1974. Review of the stratigraphy of the Weulock Series in the Welsh Borderland and South Wales. *Palaeontology*, Vol. 17, 745–777.

BENNINGHOFF, W.S., 1962. Calculation of pollen and spores density in sediments by addition of exotic pollen in known quantities. *Pollen et Spores* 4, 332–333

BOX, G.E., 1953. Non-normality and tests on variances. *Biometrika*, *40*(3/4), pp.318-335.

BURGESS, N.D. & RICHARDSON, J.B. 1995. Late Wenlock to early Prídolí cryptospores and miospores from south and southwest Wales, Great Britain. Palaeontographica Abteilung B, **236**, 1 – 44. Pls.

EDWARDS, D., FANNING U., & RICHARDSON, J.B. 1994. Lower Devonian coalified sporangia from Shropshire: Salopella Edwards & Richardson and Tortilicaulis Edwards. Botanical Journal of the Linnean Society **116**, *89–110*.

EDWARDS, D., RICHARDSON, J.B., AXE, L., DAVIES, K.L., 2012A. A new group of Early Devonian plants with

valvate sporangia containing sculptured permanent dyads. Bot. J. Linn. Soc. 168 (3), 229–257.

EDWARDS, D., MORRIS, J.L., RICHARDSON, J.B. & KENRICK, P. 2014.Cryptospores and cryptophytes reveal hidden diversity in early land floras. New Phytologist **202** (1), 50-78.

GREBE H. 1971. a recommended terminology and descriptive method for spores. Comm.
Intern. Micro/lore Paleoz., 4: Les Spores. 1: 7-34.

GLASSPOOL, I.J. & GASTALDO, R.A., 2022. Silurian wildfire proxies and atmospheric oxygen. *Geology*, *50*(9), pp.1048-1052.

HAMMER, Ø., HARPER, D.A.T. AND RYAN, P.D., 2006. Past-Palaeontological Statistics, ver. 1.32. *Universidad de Oslo (http://folk. uio. no/ohammer/past/)*.

JUGGINS, S., 2020. rioja: Analysis of Quaternary Science Data, R package version (0.9-26). (https://cran.r-project.org/package=rioja).

MARKOWSKI, C. A., & MARKOWSKI, E. P. 1990. Conditions for the Effectiveness of a Preliminary Test of Variance. *The American Statistician*, *44*(4), 322–326.

MÄRSS, T. & MILLER, C.G., 2004. Thelodonts and distribution of associated conodonts from the Llandovery–lowermost Lochkovian of the Welsh Borderland. *Palaeontology*, *47*(5), pp.1211-1265.

MCDONALD, J. H., 2014. Handbook of Biological Statistics, 3rd Edn. Baltimore: Sparky House Publishing, 157–164

MORRIS, J.L., 2009. Integrated approaches to the reconstruction of early land plant vegetation and environments from Lower Devonian strata, central-south Wales. PhD thesis, Cardiff University.

MORRIS, J.L., EDWARDS, D., RICHARDSON, J.B., AXE, L. & DAVIES, K.L. 2012. Further insights into trilete spore producers from the Early Devonian (Lochkovian) of the Welsh Borderland, U.K. *Review of Palaeobotany and Palynology* **185**, 35– 63.

MORRIS, J.L., EDWARDS, D. & RICHARDSON, J.B. 2018. The advantages and frustrations of a plant Lagerstätte as illustrated by a new taxon from the Lower Devonian of the Welsh Borderland, U.K. *In* KRINGS, M., HARPER, C.J., RUBÉN CÚNEO, N. AND ROTHWELL, G.W. (Eds). Transformative Paleobotany. Academic Press, 49-67.

OKSANEN, J., BLANCHET, F.G., FRIENDLY, M., KINDT, R., LEGENDRE, P., MCGLINN, D., MINCHIN, P.R., O'HARA, R. B., SIMPSON, G.L., SOLYMOS, P., STEVENS, M.H.H., SZOECS, E. AND WAGNER, H. 2020. vegan: Community Ecology Package. R package version 2.5-7. https://CRAN.R-project.org/package=vegan.

ORTIZ, J., AND JARAMILLO, C., 2020. SDAR: a Toolkit for Stratigraphic Data Analysis. R package version 0.9-55.

PARDOE, H.S., CLEAL, C.J., BERRY, C.M., CASCALES-MIÑANA, B., DAVIS, B.A., DIEZ, J.B., FILIPOVA-MARINOVA, M.V., GIESECKE, T., HILTON, J., IVANOV, D. AND KUSTATSCHER, E., 2021. Palaeobotanical experiences of plant diversity in deep time. 2: How to measure and analyse past plant biodiversity. *Palaeogeography, Palaeoclimatology, Palaeoecology*, *580*, p.110618.

POTONIE., R. & KREMP, G. 1954. [the genera of the Palaozoic sporae dispersae and their stratigraphy], *Geol. Jb*. **69**, 111 – 194. Pl. 4 – 20. [In German].

RAUP, D.M. AND CRICK, R.E., 1979. Measurement of faunal similarity in paleontology. *Journal of Paleontology*, pp.1213-1227.

R CORE TEAM, 2022. R: A language and environment for statistical computing. R Foundation for Statistical Computing, Vienna, Austria.

RICHARDSON, J.B. 1996. Taxonomy and classification of some new Early Devonian cryptospores from England. *Special papers in palaeontology*, **55**, 7 – 40. 10 pls.

RICHARDSON, J.B. 2007. Cryptospores and miospores, their distribution patterns in the Lower Old Red Sandstone of the Anglo-Welsh Basin, and the habitat of their parent plants. *Bulletin of Geosciences*, **82** (4), 355-364.

RICHARDSON, J.B. & EDWARDS, D. 1989. Sporomorphs and plant megafossils. *In*: Holland, C.H. and Bassett, M.G. (editors). A global standard for the Silurian System. *Natural Museum of Wales, Cardiff, Geological Series*, 9: 216–226.

RICHARDSON, J.B. & MCGREGOR, D.K. 1986. Silurian and Devonian spore zones of the Old Red Sandstone Continent and adjacent regions. *Geological Survey of Canada, Bulletin* **364**, 1– 79.

RICHARDSON J.B., RASUL, S.M. 1990. Palynofacies in a Late Silurian regressive sequence in the Welsh Borderland and Wales.. Journal of the Geological Society147: 675–686.

SHAPIRO, S. S. & WILKE, M. B., 1965. An Analysis of Variance Test for Normality (Complete Samples). *Biometrika*, *52*(3/4), 591–611.

SOLLAS, W. J. 1879. On the Silurian district of Rhymney and Pen-y-Lan, Cardiff. Q. *J. Geol. Soc. London*, Vol. 35, 475–507.

STEEMANS P. 2000. Miospore evolution from the Ordovician to the Silurian. Review of Palaeobotany and Palynology 113:189–196.

STEEMANS, P. & WELLMAN, C.H., 2018. A key for the identification of cryptospores. *Palynology*, *42*(4), pp.492-503.

STOCKMARR, J.A., 1971. Tablets with spores used in absolute pollen analysis. *Pollen et spores*, *13*, pp.615-621.

TRAVERSE, A. 2009. *Paleopalynology*. Second Edition. Springer Dordrecht.

TURNER, S. 1970. Timing of the Appalachian/Caledonian orogen contraction. *Nature*, *227*(5253), pp.90-90.

WALMSLEY, V.G., 1958. The geology of the Usk inlier (Monmouthshire). *Quarterly Journal of the Geological Society*, *114*(1-4), pp.483-521.

WELLMAN, C.H., 1999. Sporangia containing Scylaspora from the lower Devonian of the Welsh Borderland. *Palaeontology*, *42*(1), pp.67-81.

WICKHAM, H. 2016. ggplot2. Elegant Graphics for Data Analysis. Springer-Verlag New York.

Thesis appendix 2

Thesis appendix 2.1. Sample details.

See thesis appendix 2.3 for brief fieldwork outlines.

Ammons Hill

Sample	Depth (m)*	Quantitative (*l*) †	Non-quantitative**	Spore assemblage biozone	Lithology	Colour	Spore yield	Housed
MPA 25198	-150	n/a (n/a)	✓	Sp. E	vf. siltstone	?	>200	BGS
MPA 25239	-48.65	✓ (1)	✓	Lower MN	vf. siltstone	Pale grey green	>200	BGS
MPA 25240	-46.65	✓(1)	✓	Lower MN	vf. siltstone	Pale grey	>200	BGS
MPA 25242	-35.65	✓(1)	✓	Middle MN	vf. siltstone	Pale grey green	>200	BGS
MPA 25246	-20.65	✓(1)	✓	Middle MN	vf. siltstone	Grey	>200	BGS
MPA 25248	-12.65	✓(1)	✓	Middle MN	vf. siltstone	Pale grey	>200	BGS
MPA 25249	-11.95	✓(1)	✓	Middle MN	vf. siltstone	Grey	>200	BGS
MPA 25252	-5.5	✓(1)	✓	Middle MN	vf. siltstone	Pale grey green	>200	BGS
MPA 25256	-2.5	✓(1)	✓	Middle MN	vf. siltstone	Green	>200	BGS
MPA 25257	-1	✓(1)	✓	Middle MN	vf. siltstone	Grey	>200	BGS

* Depth relative to the top of the trench dug by the BGS (Barclay et al. 1994). Chapel Point Limestone not present in section.

† Slides spiked with *Lycopodium*; (*l*) number of lycopodium tablets used in sample.

** non-quantitative count

Bromyard plateau

Sample	Depth (m)*	Quantitative (*l*) †	Non-quantitative**	Spore assemblage biozone	Lithology	Colour	Spore yield	Housed
SO/07/321	+1	✓(1)	✓	Lower MN	siltstone	Pale grey	27	UoS
SO/08/321	+5	✓(1)	✓	Lower MN	siltstone	Pale grey	25	UoS
SO/16/321	+1	✓(1)	✓	Lower MN	Fine sandstone	Grey	>200	UoS

* Depth relative to the Chapel Point Limestone.

† Slides spiked with *Lycopodium;* (*l*) number of lycopodium tablets used in sample.

** non-quantitative count

Gardeners Bank

Sample	Depth (m)*	Quantitative (*l*) †	Non-quantitative**	Spore assemblage biozone	Lithology	Colour	Spore yield	Housed
21-GB-1	+8.7	✓(1)	✓	Middle MN biozone	Siltstone	Pale green	>200	UoS
21-GB-5+6	+8.6	✓(1)	✓	Middle MN biozone	Siltstone	Pale green	>200	UoS
21-GB-4	+8.5	✓(1)	✓	Middle MN biozone	Siltstone	Pale green	>200	UoS
21-GB-2	+8.4	✓(1)	✓	Middle MN biozone	Siltstone	Pale green	>200	UoS
21-GB-3	+8.3	✓(1)	✓	Middle MN biozone	Siltstone	Pale green	>200	UoS

* Depth relative to the Chapel Point Limestone.

† Slides spiked with *Lycopodium;* (*l*) number of lycopodium tablets used in sample.

** non-quantitative count

Clee Hill (Kidnall Gutter)

Sample	Depth (m)*	Quantitative (*l*) †	Non-quantitative	Spore assemblage biozone	Lithology	Colour	Spore yield	Housed
TG1B	+22.69	n/a (n/a)	✓	Lower MN biozone	Siltstone	?	>200	NHM
TG1A	+22.6	n/a (n/a)	✓	Lower MN biozone	Siltstone	?	>200	NHM

* Depth relative to the Chapel Point Limestone.

† Slides not spiked with *Lycopodium;* (*l*) number of lycopodium tablets used in sample.

** non-quantitative count

Clee Hill (Hudwick and Sudford dingles)

Sample	Depth (m)*	Quantitative (*l*) †	Non-quantitative**	Spore assemblage biozone	Lithology	Colour	Spore yield	Housed
CH/SD/88/2C	-7.13	n/a (n/a)	✓	?Pre - MN	Siltstone	?	>200	NHM
21-HD-005	+61.6	✓(1)	✓	Middle MN	Siltstone	Pale green	>200	UoS
21-HD-001	+60.22	✓(1)	✓	Middle MN	Siltstone	Dark blue	>200	UoS
21-HD-002, 004	+60.21	✓(1)	✓	Middle MN	Siltstone	Dark, iron stained	>200	UoS
21-HD-003	+59.86	✓(1)	✓	Middle MN	Siltstone	Pale green grey	>200	UoS

* Depth relative to the Chapel Point Limestone.

† Slides not spiked with *Lycopodium;* (*l*) number of lycopodium tablets used in sample.

** non-quantitative count

Ross – Tewkesbury Spur (M50) motorway section, Hereford and Worcester

Sample	Depth (m)*	Quantitative (*l*) †	Non-quantitative**	Spore assemblage biozone	Lithology	Colour	Spore yield	Housed
M50-2	-39	n/a (n/a)	✓	Sp. E	?	?	>200	NHM

19-M50/85/2b	-35.33	✓ (2)	✓	Sp. E	Siltstone	Grey	>200	NHM
19-M50/85/2c	-35.3	✓ (2)	✓	Sp. E	Siltstone	Grey	>200	NHM
19-M50/85/2d	-34.8	✓ (5)	✓	Sp. E	Siltstone	Grey	>200	NHM
19-M50/85/2e	-34.65	✓ (3)	✓	Sp. E	Siltstone	Grey	>200	NHM
19-M50/85/2f	-34.51	✓ (2)	✓	Sp. E	Siltstone	Grey	>200	NHM
19-M50/85/2g	-34.35	✓ (2)	✓	Sp. E	Siltstone	Grey	>200	NHM
19-M50/85/2h	-34.23	✓ (3)	✓	Sp. E	Siltstone	Grey	>200	NHM
M50-3(2)	-33	n/a (n/a)	✓	Sp. E	?	?	>200	NHM
M50-4	-32	n/a (n/a)	✓	Sp. E	?	?	>200	NHM
19-M50/86/2a	+0.15	✓ (2)	✓	Lower MN	?	?	>200	NHM
19-DE98	+2	✓ (2)	✓	Lower MN	Siltstone	Beige	>200	NHM
BM/M50/5B	+2.65	n/a (n/a)	✓	Lower MN	?	?	>200	NHM
19-M50/86/2b	+2.66	✓(2)	✓	Lower MN	Siltstone	Grey	>200	NHM
19-M50/86/2c	+2.95	✓ (2)	✓	Lower MN	Siltstone	Grey	>200	NHM
BM/M50/5E	+3.19	n/a (n/a)	✓	Lower MN	?	?	>200	NHM
BM/M50/5F	+3.22	n/a (n/a)	✓	Lower MN	?	?	>200	NHM
BM/M50/5G	+3.89	n/a (n/a)	✓	Lower MN	?	?	>200	NHM
BM/M50/5H	+4.07	n/a (n/a)	✓	Lower MN	?	?	>200	NHM
19-M50-7	+42	✓(5)	✓	Middle MN	Siltstone	Green - buff	>200	NHM
M50-8	+42.5	n/a (n/a)	✓	Middle MN	?	?	>200	NHM
M50-10	+97.5	n/a (n/a)	✓	Middle MN	?	?	>200	NHM
M50-11	+105	n/a (n/a)	✓	Middle MN	?	?	>200	NHM
M50-12	+114	n/a (n/a)	✓	Middle MN	?	?	>200	NHM
M50-13	+168	n/a (n/a)	✓	Middle MN	?	?	>200	NHM

* Depth relative to the Chapel Point Limestone.

† Slides not spiked with *Lycopodium;* (*l*) number of lycopodium tablets used in sample.

** non-quantitative count

Rumney-1 borehole

Sample	**Depth (m)* (*x*)*y***	**Quantitative (*l*) †**	**Non-quantitative****	**Spore assemblage biozone**	**Lithology**	**Colour**	**Spore yield**	**Housed**
RU/21/4	(44.41 - 45.95) - 937.75	✓(1)	✓	*Tripapillatus – spicula*	siltstone	Green	84	BGS
RU/21/3	(63.33 - 64.91) - 956.74	✓(1)	✓	*Poecelomorphus - libycus*	siltstone.	Grey-green purple stained	176	BGS
RU/21/2	(66.47 - 69.00) -960.3	✓(1)	✓	*Poecelomorphus - libycus*	siltstone.	Purple	151	BGS
RU/21/1	(69.65 - 71.26) - 963.02	✓(1)	✓	*Poecelomorphus - libycus*	siltstone	Grey green	152	BGS

* (x) depth range from which rock chips are derived; y estimated depth relative to CPL.

† Slides not spiked with *Lycopodium;* (*l*) number of lycopodium tablets used in sample.

** non-quantitative count

Usk-1 borehole

Sample	Depth (m)* (x)y	Quantitative (*l*) †	Non-quantitative**	Spore assemblage biozone	Lithology	Colour	Spore yield	Housed
USK/21/3	(689) - 930	✓(1)	✓	*Tripapillatus – spicula*	siltstone	Gray	>200	BGS
USK/21/2	(698) - 960	✓(1)	✓	*Poecelomorphus - libycus*	siltstone	Gray	>200	BGS
USK/21/1	(707) - 990	✓(1)	✓	*Poecelomorphus - libycus*	siltstone	Gray	>200	BGS

* (x) depth range from which rock chips are derived; y estimated depth relative to CPL.

† Slides not spiked with *Lycopodium;* (*l*) number of lycopodium tablets used in sample.

** non-quantitative count

Thesis appendix 2.2. SDAR code scripts

```
# these are scripts for the
graphic logs made using SDAR
(Ortiz and #Jaramillo, 2020)

install.packages("SDAR",
dependencies = TRUE)
library("SDAR")
install.packages("base64enc")

SDAR_data_model

setwd("C:/Users/AlexB/Documents/AB
PhD/Research/Localities,
fieldwork/logs")
######################

LL <- read.csv("LL3.csv")
LL <- LL[-1]
head(LL)
fossils <-
read.csv("LL_fossils.csv")

fossils <- fossils[-1]

head(fossils)

validated_beds <- strata(LL, datum
= "top")

head(validated_beds)

class(validated_beds)

plot(validated_beds, fossils =
fossils, symbols.size = 0.8)

##################################

gb <- read.csv("GB.csv")
gb <- gb[-1]
head(gb)
fossils <-
read.csv("gb_fossils.csv")

fossils <- fossils[-1]

head(fossils)

validated_beds <- strata(gb, datum
= "top")

head(validated_beds)

class(validated_beds)

plot(validated_beds, fossils =
fossils, symbols.size = 0.8, scale
= 10, data.units = "meters",
barscale = 0.5)

##########################
```

```
hd <- read.csv("hd.csv")
hd <- hd[-1]
head(hd)
fossils <-
read.csv("hd_fossils.csv")

fossils <- fossils[-1]

head(fossils)

validated_beds <- strata(hd, datum
= "top")

head(validated_beds)

class(validated_beds)

plot(validated_beds, fossils =
fossils, symbols.size = 0.8, scale
= 30, data.units = "meters",
barscale = 0.5)

########################

rum <- read.csv("rumney_lith.csv")
rum <- rum[-1]
head(rum)
fossils <-
read.csv("rum_foss.csv")

fossils <- fossils[-1]

head(fossils)

validated_beds <- strata(rum,
datum = "top")

head(validated_beds)

class(validated_beds)

plot(validated_beds, fossils =
fossils, symbols.size = 0.8, scale
= 300, data.units = "meters",
barscale = 0.5)

#########################

ah <- read.csv("ammons_lith.csv")
ah <- ah[-1]
head(ah)
fossils <-
read.csv("ammons_foss.csv")

fossils <- fossils[-1]

head(fossils)

validated_beds <- strata(ah, datum
= "top")

head(validated_beds)

class(validated_beds)

plot(validated_beds,   fossils   =
fossils, symbols.size = 0.8, scale
=  400,  data.units  =  "meters",
barscale = 0.5)
```

Chapter III Chapter III: Taxonomy and biostratigraphy of late Silurian – Early Devonian cryptospores and trilete spores from the Lower 'Old Red Sandstone' of the Anglo-Welsh Basin, U.K.

This Chapter has been accepted for review as a Paleontographical Society monograph by the Paleontographical Society Committee (2022) and is submitted as a manuscript according to the Society's specifications.

A.C. Ball and J.B. Richardson conceived this study. A.C. Ball carried out the research and wrote the manuscript.

Abstract

Systematic analysis of late Silurian – Early Devonian (Ludlow – mid Lochkovian) terrestrial palynomorphs from the classic Anglo-Welsh Basin sequence, U.K., has clarified the major early land-plant diversification event which occurred at this time amongst miospores and cryptospores. Over 100 known and novel trilete spore and cryptospore species occur in over 30 genera through the sequence, with a significant increase in species richness near the Silurian - Devonian boundary. New spore data from the latest Přídolí and earliest Lochkovian allows the definition of a new 'non-tripapillate *Aneurospora* spp.' spore biozone. This is further subdivided into the latest Přídolí *Aneurospora sheafensis* and earliest Devonian *Apiculiretusispora sceacga* subzones. The latter subzone initiates within two metres of the Silurian - Devonian boundary and facilitates local and international corelation.

Résumé

L'analyse systématique des palynomorphes terrestres du Silurien tardif - Dévonien précoce (Ludlow - Lochkovien moyen) de la séquence classique du bassin anglo-gallois, Royaume-Uni, a clarifié le principal événement de diversification précoce des plantes terrestres qui s'est produit à cette époque parmi les miospores et les cryptospores. Plus de 100 espèces connues et nouvelles de spores triletes et de cryptospores sont présentes dans plus de 30 genres tout au long de la séquence, avec une augmentation significative de la richesse spécifique près de la limite Silurien - Dévonien. De nouvelles données sur les spores du dernier Přídolí et du premier Lochkovien permettent de définir une nouvelle biozone de spores «non tripapillées Aneurospora spp.». Ceci est en outre subdivisé en sous-zones les plus récentes de Přídolí Aneurospora sheafensis et les premières sous-zones du Dévonien Apiculiretusispora sceacga. Cette dernière sous-zone commence à moins de deux mètres de la limite Silurien - Dévonien et facilite la corrélation locale et internationale.

Zusammenfassung

Die systematische Analyse von terrestrischen Palynomorphen aus dem späten Silur – frühen Devon (Ludlow – mittleres Lochkovium) aus der klassischen Anglo-Welsh Basin-Sequenz, Großbritannien, hat das große frühe Diversifizierungsereignis von Landpflanzen geklärt, das zu dieser Zeit unter Miosporen und Kryptosporen stattfand. Über 100 bekannte und neue trilete Sporen- und Kryptosporenarten treten in über 30 Gattungen in der gesamten Sequenz auf, mit einer signifikanten Zunahme des Artenreichtums nahe der Grenze zwischen Silur und Devon. Neue Sporendaten aus dem jüngsten Přídolí und dem frühesten Lochkovium ermöglichen die Definition einer neuen „nicht-tripapillären Aneurospora spp."-Sporenbiozone. Diese ist weiter unterteilt in die späteste Subzone Přídolí Aneurospora sheafensis und die früheste devonische Subzone Apiculiretusispora sceacga. Die letztgenannte Subzone beginnt innerhalb von zwei Metern von der Silur-Devon-Grenze und erleichtert die lokale und internationale Korrelation.

Реферат

Систематический анализ позднесилурийско-раннедевонских (лудлоу-среднелочковских) наземных палиноморф из классической последовательности англо-валлийского бассейна, Великобритания, прояснил главное событие ранней диверсификации наземных растений, которое произошло в это время среди миоспор и криптоспор. Более 100 известных и новых видов трилетных спор и криптоспор встречаются в более чем 30 родах в последовательности, со значительным увеличением видового богатства вблизи границы силура и девона. Новые данные о спорах из позднего пржидоли и самого раннего лохковского века позволяют определить новую споровую биозону «нетрехпапиллярных Aneurospora spp.». Далее она подразделяется на позднейшую подзону Přídolí Aneurospora sheafensis и самую раннюю девонскую подзону Apiculiretusispora sceacga. Последняя подзона начинается в пределах двух метров от границы силура и девона и способствует локальной и международной корреляции.

1. Introduction

Research in the Anglo-Welsh Basin, a continuous 'Old Red Sandstone' sedimentary sequence of principally terrestrial sediments in Southern Britain, has contributed extensively to Silurian and Devonian palaeobotanical and palynological understanding. Indeed, research over the last 300 years in the basin has included numerous significant contributions in palaeontology (e.g. Lang, 1937; Edwards, 1996, 2009), stratigraphy (Murchison, 1839; King, 1925; Richardson and McGregor, 1986) and sedimentology (Allen and Tarlo, 1963).

While correct that no economically viable coal seams were present in the area, Murchison's proposition that no plants were present in the red rocks of the basin has not aged well. Lang's (1937) recovery of a diverse suite of diminutive land plants in the Přídolí of the Anglo-Welsh Basin has triggered nearly a century of ground-breaking palaeobotanical research, revealing an incredible diversity of compressed plant macrofossils (e.g. Edwards, 1970, Morris et al., 2011a; Morris and Edwards, 2014) and exceptionally preserved charcoalified mesofossils (e.g. Edwards, 1996; Edwards et al., 2014; Morris et al., 2011b, 2018b; Wellman, 1999). These remains have shed light on the diversity, floral dynamics, affinities and evolution amongst Silurian and Devonian land plants (e.g. Edwards, 1996; Edwards et al., 1994; Fanning et al., 1988; Edwards et al., 2022a, b, c; Morris et al., 2011b), and have indicated the comparative level of complexity and composition of Anglo-Welsh plant communities (e.g. Kotyk et al., 2002; Edwards and Richardson, 2004).

The well-documented preservational bias in the macrofossil record was highlighted by early palynological studies in the Anglo-Welsh Basin (Chaloner and Streel, 1966; Richardson, 1967; Richardson and Lister, 1969), which demonstrated a high level of species and morphological diversity amongst the recovered spore species. The database of spore species in the late Silurian and Early Devonian of the Basin (e.g. Burgess and Richardson, 1991, 1995; Burgess, 1991; Richardson, 1996a, b; Wellman et al., 2000) and coeval localities across the world (Arkhangelskaya, 1980; Breuer et al., 2017; Breuer and Steemans, 2015; Lavender and Wellman, 2002; Richardson and Ioannides, 1973; Rubinstein and Steemans, 2002; Steemans et al., 2007) continues to grow. Meanwhile, the recovery of *in situ* spores from two localities in the Anglo-Welsh Basin from exceptionally preserved mesofossils (e.g. Jeram et al., 1996; Edwards et al., 1995, 1996; Edwards and Richardson, 2000; Edwards et al., 1994; Wellman et al., 1998) has gone someway towards harmonising the megafossil and palynological record in the basin. Ultimately, the study of the macro-, mesofossil and palynological record indicated that a sustained increase in species diversity and morphological diversity occurred between the late Silurian and Early Devonian, particularly amongst trilete spores and their associated parent plants (e.g. Richardson and Lister, 1969). Based on the common attribution of these trilete spores to the vascular plants (e.g. Gray, 1985), this striking change was suggested to represent the first major proliferation of vascular plants on land. While later workers demonstrated that trilete spores are also produced by some bryophytes (e.g. Kenrick et al. 2012; Edwards et al., 2014; Salamon et al., 2018), such a proliferation

amongst these spores still reflects a considerable diversity increase amongst several groups of derived embryophytes. The causes behind this event are uncertain, but workers have suggested that the floral assemblages in the Anglo-Welsh Basin may have been influenced by climate change (e.g. Morris et al., 2012b) and punctuated invasions by plants such as zosterophylls, from extrabasinal sources (e.g. Morris and Edwards, 2014).

Part of the value in studying spore assemblages from the Anglo-Welsh Basin is their use in regional and global biostratigraphy, and the assemblages featured heavily in Richardson and McGregor's (1986) seminal international spore biozonation scheme. The continuity of the sedimentary sequence through the late Silurian – Early Devonian, in combination with the rapid increase in species diversity and their often-short ranges, are ideal for constraining such spore-based biozonation schemes (e.g. Richardson and McGregor, 1986; Streel et al., 1987). As such, a high-resolution suite of spore assemblage biozones in the Basin exists for much of the late Silurian and Early Devonian (Edwards and Richardson, 1974; House et al., 1977; Richardson et al., 1981, 1984). However, a major sampling gap in the Přídolí and earliest Devonian exists, leaving the spore species from this time undescribed. Importantly, this gap brackets the Silurian – Devonian boundary, which based on the presence of *Turiana pagei*, has been suggested to lay *c.* 35m below the key regional lithostratigraphic marker horizon, the Chapel Point Limestone (Turner, 1973; Edwards and Richardson, 2004). With the identification of *T. pagei* in the Anglo-Welsh Basin, the challenge became to align a spore species or assemblage with its appearance and the Silurian – Devonian boundary. Such a spore assemblage, indicative of the onset of the Devonian, would facilitate regional and international Silurian and Devonian spore-based correlation and provide key biostratigraphic information where little or no vertebrates, graptolites or other zonal fossils occur (e.g., terrestrial strata). With this in mind, Richardson and colleagues (e.g., Richardson et al. (1981, 1984, 2001) studied and correlated spore assemblages from around the world, fielding several hypotheses for promising zonal spore species. While more recent research in Gondwana has indicated that some of these key species, notably *Aneurospora*, occur long before the Silurian – Devonian boundary (Rubinstein and Steemans, 2002; Breuer et al., 2017, Richardson's work in the Anglo-Welsh Basin (unpublished) importantly suggested the promising occurrence of "…one *Apiculiretusispora* sp. with at least two *Aneurospora* species" (Edwards and Richardson, 2004, p. 382) near the FAD of *T. pagei*. These findings hinted that a spore assemblage biozone closely corresponding to the Silurian – Devonian boundary was present in the Anglo-Welsh Basin.

Here, palynological data has been gathered from nine localities from the south and east of the Anglo-Welsh Basin. The studied section extends through a ± uninterrupted regressive offlap sequence of Ludlow to mid Lochkovian shallow marine and terrestrial fluvial sediments. Through semi-quantitative and quantitative assessment of the dispersed spore record, the ranges of an abundant suite of spore species have been studied, and the temporal abundance changes in species, ornament and structure are also reported. This study sheds light on the spore assemblages around the Silurian – Devonian boundary in the Anglo-Welsh Basin, hinted at by Richardson (in Edwards and Richardson, 2004), and clarifies the trilete spore and cryptospore species radiations, which was never fully explored by pioneering researchers (e.g. Richardson and Lister, 1969). The processes underpinning this radiation are explored elsewhere (Chapter IV).

2. Acknowledgments

This work has been carried out as part of A.C.B.'s Ph.D. and is supported by a NERC funded ACCE (Adapting to Challenges of a Changing Environment) Doctoral Training Partnership Ph.D. studentship [grant number NE/L002450/1] that is a CASE partnership with the Natural History Museum, London. DTP funding and Covid-19 extension grants from NERC and the Natural History Museum are gratefully acknowledged. ACB would like to thank Stephen Stukins for access to samples and materials from the Micropaleontology Unit at the Natural History Museum, and Charles Wellman, the British Geological Survey and Cardiff University for additional samples. A.C.B. thanks his Ph.D. supervisors Paul Kenrick, John Richardson, Stephen Stukins and Charles Wellman for reviewing early copies of the

manuscript and their helpful comments. Dave Bodman is thanked for his assistance with sample processing at the University of Sheffield. The University of Sheffield Electron Microscopy Unit is thanked for use of the Scanning Electron Microscope.

3. A brief history of research in the Welsh Borderlands

The sedimentology and palaeontology of the Anglo-Welsh Basin has been studied for over three-hundred years, with some of the earliest descriptions of fossilised land plants coming from the overlying Carboniferous coal measures in 1699 by Lluyd (Edwards, 2017). The 1800s saw an increasing interest in the Earth sciences, in part for its economic value for the burgeoning industrial revolution, and so it was that in the early 1830's, while seeking to revise George Greenough's general map, that Roderick I. Murchison visited the Welsh Borderlands. He was attempting to resolve the problematic Old Red Sandstone – underlying greywacke (now Silurian rocks) boundary, which William Buckland had previously found to be conformable in that area. Following field seasons in 1831 and 1832, Murchison delivered papers on the character and stratigraphy of the Old Red Sandstone and preceding 'transitional' (now Silurian) greywackes in the Welsh Borderlands in 1834. Later in the same year, he and Sedgewick circumscribed the transitional rocks in the Welsh Borderlands and Wales, with Murchison proposing the sequence in the Welsh borderlands to be the 'type' (the first of its kind) for the transitional rocks in 1834. In the same year, Murchison's work in the Welsh borders led to heated debate around Henry de Le Beche's reports of plants in the 'transitional' series of north Devon, which "…turned [the discussion in the Geological Society] topsy turvy without scruples" (Turner to De la Beche, 1834, in Rudwick, 1985 p. 99) as Murchison fervently rejected claims that plants or coals existed in the Old Red Sandstone or underlying 'transitional strata'. Later that decade, the rocks and faunal fossils of the Anglo-Welsh Basin were used for the circumscription of the Silurian Period by Murchison (1839).

Palaeontological research, particularly that of plants, in the Silurian and Devonian of the Welsh Borderlands has continued to challenge and delight researchers in equal amounts since this breakdown of Victorian sensibilities in 1834 (e.g. Morris et al., 2018b). The first formal paleontological studies of the Old Red Sandstone began with jawed and jawless fish by Louis Agassiz from a newly exposed section of the Ludlow Bone Bed in the1830s (e.g. Murchison, 1839; Turner, 1973; Turner et al., 2017). These findings were used by Murchison (1839) in his definition of the Silurian period (1839, 1854), and vertebrate remains have continued to play a prominent role in research in the basin, especially when integrated with the continued study of the sedimentology and lithostratigraphy (e.g. Allen and Tarlo, 1963; Allen and Dineley, 1976). Fish and plants represent the key biostratigraphic fossils in the sequence, and with respects to vertebrates, biostratigraphic studies have built on initial work by King (1925, 1934), Ball et al. (1961) and Gross (1967). The first major biostratigraphic survey of vertebrates from the Anglo-Welsh Basin was made by Turner (1973a, b, 1984), and this aligned the fossils with the international Silurian – Devonian standard. Microvertebrates in particular played a prominent role in defining the biostratigraphy of the basin and aligned it with international sequences (e.g. Turner, 1973; Anita, 1979), and studies of the taxonomy and biostratigraphy of macro and microvertebrates continue (e.g. Turner et al., 1995; 2017; Miller and Marss, 1999, 2004, but see Turner et al., 2017). These microvertebrate and vertebrate zones are now well defined and have been used, *inter alia*, to correlate the terrestrial sediments of the Anglo-Welsh Basin with the pelagic type section at Klonk (Turner, 1973; Edwards and Richardson, 2004).

The study of plant fossils in the Old Red Sandstone of the Anglo-Welsh Basin came much later, with Lang's seminal work of 1937 where he reported crowded plant fragments from the 'grey and red Downtonian' (Přídolí and Lochkovian, respectively) of the Welsh Borderlands. Since Lang's (1937) work, a diverse suite of diminutive '*Cooksonoids*' and rhyniophytoids; diminutive, leafless plants with branching axes and terminal sporangia with a variety of morphologies (e.g., Edwards, 1969, 1970, 1979; Edwards and Rogerson, 1979; Edwards et al., 1979, 1994; Fanning et al., 1990, 1991a, 1992; Morris et al., 2011a; Morris and Edwards, 2014) from the late Silurian and Early Devonian of the basin have been recovered. Compression fossils have also shed light on larger, more complex plants which occur in the

basin from the mid Lochkovian including zosterophylls (e.g. Edwards, 1969a, b; Edwards and Kenrick, 1986; Wellman et al., 2000; Morris and Edwards, 2014), giving insights into the array of vegetation which inhabited the Anglo-Welsh Basin during this time and demonstrating a succession of punctuated floral invasions (e.g. Morris and Edwards, 2014). The recovery of zosterophylls and complex vascular plants in older strata outside of the Anglo-Welsh Basin, however (e.g. Kotyk et al., 2002; Rickards, 2000) has indicated that the vegetation exhibited in the Přídolí and Lochkovian of the Anglo-Welsh Basin was not representative of the state of global vegetation, and may have been relatively restricted.

Lang's (1937) initial findings had wide ranging implications for palaeobotany. Firstly, his formal description of the diminutive, leafless *Cooksonia* genus and two associated species, *C. pertoni* and *C. hemisphaerica* revealed the morphology of some of the earliest land plants and gave tentative evidence of the earliest vascular tissue. He also demonstrated the terrestrial nature of the plants by recovering trilete spores from the coalified sporangia (Lang, 1937; Edwards, 2017; Edwards and Kenrick, 2015). Continued work (e.g. Edwards 1970; Fanning et al., 1990; Morris et al., 2011a) has revealed a striking diversity amongst the sporangial morphologies in compressed plant remains, and exceptionally preserved fossils have shed further light on their affinities, including vascular tissue in pyritised zosterophylls (Kenrick and Edwards, 1988). The recovery of several horizons yielding charcoalified, exceptionally preserved (although fragmentary) early land plant 'mesofossils' in the Přídolí and Lochkovian of the basin has been of great importance for improving the understanding of morphology and affinities of early land plants. Such fossils have allowed the demonstration of vascular tissue in a rhyniophytoid (Edwards et al., 1992), hepatic features in another (Edwards et al., 1994), in addition to a suite of anatomical features which would not have been identified of compressed fossils, such as stomata (Edwards, 1996). The sporangia of these plants are often recovered from the charcoalified mesofossil assemblages (e.g. Edwards, 1979, 1996; Edwards and Richardson, 1979, 2004; Edwards et al., 1994, 2014; 2021a; Morris et al., 2011b, 2012a; Morris et al., 2018b; Chapter V) and the study of associated *in situ* spores has been valuable for identifying cryptic evolution amongst plants with similar sporangial morphologies (Fanning et al., 1988) and identifying the parent plants of many dispersed spore species. Cryptic diversity amongst morphologically simple *in situ* spore groups has been elucidated through transmission electron microscopy (e.g. Wellman et al., 1998b), with spores belonging to the same morphospecies exhibiting strikingly different spore wall ultrastructures. Such ultrastructural analysis in combination with morphological analysis has also revealed relationships between tracheophytes and certain cryptospores (Morris et al., 2011b; Edwards et al., 2014). Most recently, the integration of *in situ* spores and anatomical features amongst mesofossils has shed light on a new group of plants, the eophytes, which exhibit a mixture of tracheophytic and bryophytic features (Edwards et al. 2021a, b, 2022).

The study of *in situ* spores has been influential for contextualising the dispersed spore record, which is both more diverse and widespread than the macrofossil record, not being subject to the same preservational biases (e.g. Edwards et al., 2004). The studies of the palynology of the Anglo-Welsh Basin, with which this monograph/Chapter is concerned, could be considered to have begun as early as the 1930s, with the recovery of *in situ* spores collected by acetate pulls by Lang (1937). Studies of the dispersed spores from the Anglo-Welsh Basin began with Chaloner and Streel (1966), who described a diverse selection of dispersed spores from near Newport in south Wales from what is now the lower *micrornatus – newportensis* subzone in the Freshwater West Formation. Shortly afterwards, John B. Richardson turned his attention to the Anglo-Welsh Basin (Richardson, 1967; Wellman and Riding, 2022), co-producing the first detailed analysis of trilete spore species and their ranges from the late Silurian and Early Devonian of the Anglo-Welsh Basin (Richardson and Lister, 1969). This seminal work demonstrated that dispersed spore species in the basin were diverse, readily accessible and showed a gradual increase in species richness between the Silurian and Devonian. Much of the early work on the dispersed spore species from the Anglo-Welsh Basin which involved Richardson focussed on the biostratigraphic value of these spore species (e.g. Chaloner and Richardson, 1977; House et al., 1977; Owens and Richardson,1972; Richardson, 1974, 1985; Richardson and Ioannides, 1973; Richardson

and Rasul, 1979; Richardson et al., 1981, 1984) and led to the development of the still internationally important spore and pollen biostratigraphic scheme of Richardson and McGregor (1986). His meeting with Dianne Edwards in the late 1960s (Wellman and Riding, 2022) led to a long and fruitful collaboration, particularly concerning *in situ* spores (above), and in this manner Richardson contributed significantly to the current understanding terrestrial vegetation (e.g. Edwards et al., 1986, 1994, 1995a, b, c, 1996, 2014; Edwards and Richardson, 2000; Fanning et al., 1988, 1990, 1991, 1992; Morris et al., 2011a, b, 2012a, b, 2018b; Rogerson et al., 1993), and the collaboration between Edwards and Richardson highlights the importance of integrating the palynological, mesofossil and macrofossil records. Richardson (2007) also began to consider the control of the ecology of parent plants on the distribution of their dispersed spores in the Anglo-Welsh Basin.

Early palynological work focussed exclusively on trilete spores, not recognising the importance of the enigmatic cryptospores until much later (Burgess and Richardson, 1991; Richardson, 1996). Cramer (1966) described a now-cryptospore genus *Hispanaediscus* from northern Spain, and from the late 1970s this additional facet of dispersed terrestrial spore assemblages began to be more fully appreciated following focussed studies in Silurian and Devonian strata in north America (Johnson, 1985; Miller and Eames, 1982; Strother and Traverse, 1979), north Africa (Hill et al., 1985; Richardson, 1988) and Scotland (Richardson et l., 1984). These spores began to be incorporated into dispersed spore studies in the Anglo-Welsh Basin from the 1990s, with Burgess and Richardson (1991, 1995) and Burgess (1991) describing varied assemblages of cryptospores from Silurian sections. Richardson (1996) described a varied suite of cryptospores from the upper Přídolí and Lochkovian of the basin in a landmark monograph, and revised Strother and Traverse's (1979) initial cryptospore classification. Later studies from across the Anglo-Welsh basin revealed further diversity amongst cryptospores (e.g. Wellman et al., 2000) which were expanded through ultrastructural studies of *in situ* spores (Wellman et al., 1998b).

Together, then, palaeobotanical and palynological research in the Anglo-Welsh Basin has contributed greatly to the current understanding of early land plants. Studies, particularly of exceptionally preserved mesofossils and *in situ* spores, have been invaluable for elucidating the affinities of plants and harmonising the plant macrofossil and palynological records, and are testament to the power of interdisciplinary collaboration. Despite the long history of research in the basin, however, much remains to be uncovered. Emerging techniques and continued sampling of the sequence promises to shed further light on the challenges presented by the Anglo-Welsh Basin sequence, particularly with respects to the Přídolí section.

4. Setting, Formation and stratigraphy of the Anglo-Welsh Basin

4.1. Setting

The name 'Old Red Sandstone' has been used widely by a variety of workers, either as a long standing informal or formal lithostratigraphic name, as a formal facies name, or as a 'pseudochronostratigraphical' name for red beds of Devonian age (see Barclay et al., 2015). Barclay et al. (2015) favours the use of the term as an informal descriptive term for late Silurian to Carboniferous aged red bed sequences. The Anglo-Welsh Basin in southern Britain (southern Wales and western England) is one of several major basins in the UK comprising such red bed sequences. Others include the Orcadian and Midland Valley basins of Scotland (e.g. Browne et al., 2002), in addition to other minor basins including the Mell Fell trough in the Lake District (e.g. Capewell, 1955), and the Peel Sandstone Group on the Isle of Man (e.g. Crowley et al., 2009) (fig. 1a).

The Old Red Sandstone of the Anglo-Welsh Basin is subdivided into two megasequences in Barclay et al. (2015), which are traditionally referred to as the Upper and Lower Old Red Sandstone. These cycles were formed in the terminal stages of the Caledonian Orogeny and the initial stages of the Variscan Orogeny, respectively, separated by the Acadian Orogeny. They are also divisible by age. The 'Lower' Old Red Sandstone conformably succeeds the marine sediments of the Palaeozoic Marine Welsh Basin (section 4.2.2.) in the early Přídolí (late Silurian) and terminates in the Emsian (late – Early Devonian).

The 'Upper' Old Red Sandstone was deposited unconformably on the Lower Old Red Sandstone between the late Frasnian to the Fammenian (Late Devonian). It is conformably overlain by Carboniferous sediments. The mid Devonian is not represented in the Anglo-Welsh Basin.

The Lower Old Red Sandstone section is the focus of this study, and extends some 20,000km^2 across southern Wales and the Welsh Borderlands. The greatest surface outcrop is in south-east Wales, but significant outcrop extends as far as Pembrokeshire and straddles the Welsh– English border as far as Telford in the Welsh Borderlands (fig. 1b). Outliers in Anglesey, the Lake District and south-west England may hint at a once greater spatial extent of the basin and subsurface exploration indicates that the basin extends as far as south-eastern England (Chaloner and Richardson, 1977), but it is possible that some or all of these now isolated outcrops were formed in smaller basins independently of the main Anglo-Welsh Basin. The main Anglo-Welsh Basin outcrop is constrained by the Welsh Borderland Fault System (Woodcock and Gibbons, 1988) (fig. 1b), and the constituent strata have been variously folded and cleaved by contemporaneous and later orogenic events, including the Acadian and Variscan orogenies).

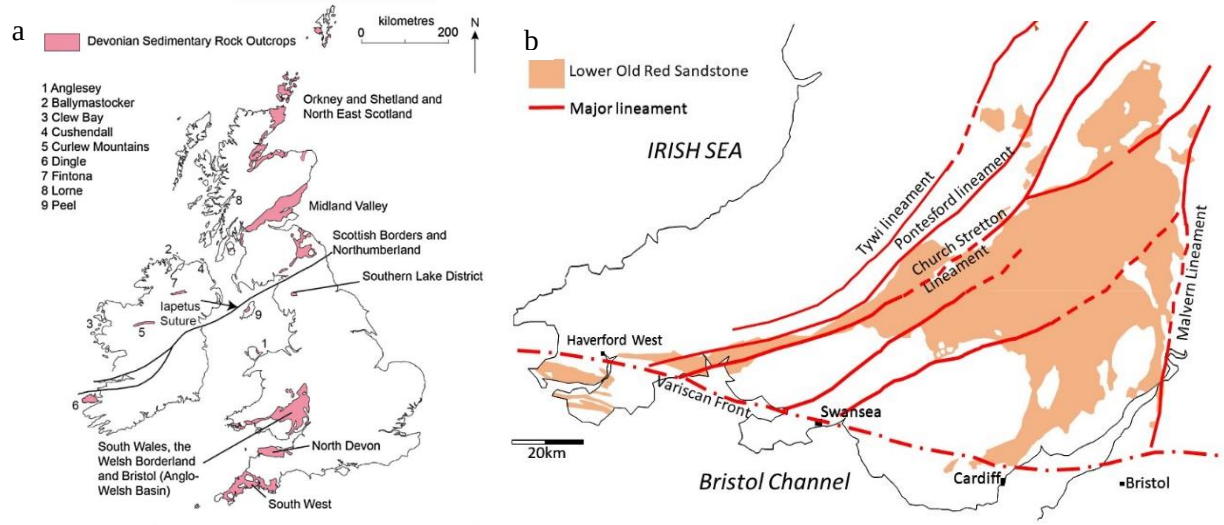

Figure III-1: ***A:*** *Lower Old Red Sandstone outcrops in the British Isles, from Kendall (2017).* ***B:*** *Extent of the Lower 'Old Red Sandstone' in the Anglo-Welsh Basin, and major lineaments in the Anglo-Welsh Basin. Modified from Barclay et al. (2015).*

4.2. Basin Formation

4.2.1. Tectonics

The Lower Old Red Sandstone of the Anglo – Welsh basin was deposited in an extra-montane, tectonically active foreland basin, and its development is bracketed by the Caledonian and Variscan Orogenies (Friend *et al*., 2000) which occurred in the mid-Silurian and mid-Devonian respectively. Basin Formation is attributed to the Caledonian orogeny, with some workers positing load induced flexural subsidence of the Avalonian foreland (James, 1987; King, 1994; Friend *et al*., 2000), while others prefer basin wide, sinistral mega-shearing (e.g. Dewey and Strachan, 2003; Soper and Woodcock, 2003) as a method of Formation.

Local terrestrial sedimentation in Pembrokeshire and Carmarthenshire initiated as early as the Ludlow, with basin wide sedimentation initiating by the Přídolí (Barclay et al., 2015). Subsidence was not continuous between the Ludlow and Late Emsian and an extended, basin wide quiescent period occurred in the early Devonian, allowing thick palaeosols to develop (Allen, 1974; 1985). Shifts in sediment provenance appear to indicate a basin wide tectonic transition from flexural subsidence to sinistral transtensional regimes and the development of half grabens (Crowley *et al*., 2009), an event that is likely to have significantly influenced drainage patterns across the alluvial plain. Synsedimentary extensional and transpressional faulting is posited to have occurred across the basin and is thought to

have been especially active in Pembrokeshire during the Late Silurian – Early Devonian (Barclay *et al*., 2015), and these minor faulting events may have periodically developed isolated subbasins across the Anglo-Welsh Basin (Crowley *et al*., 2009). Seismic events associated with faulting also occurred, with soft sediment deformation indicating seismically induced liquefaction in some Early Devonian sediments (Owen, 2016). Deposition of alluvial material continued until uplift from the proto-Variscan Acadian Orogeny resulted in the eventual termination of Lower Old Red Sandstone deposition and the subsequent development of the Acadian unconformity in the Late Emsian (Barclay *et al*., 2015). There was no proximal volcanic activity during Lower Old Red Sandstone deposition, however, layers of distal air fall tuffs derived from Plinian style volcanic ejecta are found within the basin, a prominent example being the Townsend Tuff Bed (Allen and Williams, 1981).

4.2.2. Sedimentary deposition and climate

A detailed understanding of the sedimentary sequence of the Anglo Welsh basin has developed from intensive sedimentary research in the area (e.g. Allen and Tarlo, 1963; Hillier et al., 2007, 2019; Morris et al., 2012b). Section 4.2.1. detailed the complex tectonic evolution of the basin, which was driven by late Caledonian tectonics and led to the shrinkage of the Palaeozoic Marine Welsh Basin and onset of terrestrial sedimentation. Much of this sedimentation was confined by the Welsh Borderlands Fault System (Woodcock and Gibbons, 1988), which was active in the Early Devonian and influenced depositional patterns (Powell, 1987, 1989; Woodcock and Gibbons, 1988).

The regression of the Palaeozoic Marine Welsh Basin towards the end of the Ludlow initiated local terrestrial sedimentation in Pembrokeshire and Carmarthenshire (Barclay et al., 2015). Terrestrial basin-wide sedimentation followed in the Přídolí with the ± south-eastward retreat of the sea (Bassett et al., 1992; Bluck et al., 1992, but see Barclay et al., 2015) (fig. 2). Whilst terrestrial sedimentation dominated the depositional environment of the Anglo-Welsh Basin through the Přídolí and Lochkovian, occasional marine incursions, perhaps via large estuaries, occurred in the east of the basin (Barclay et al., 1994).

Terrestrial sedimentation was principally alluvial (e.g. Allen and Tarlo, 1963; Allen and Dineley, 1976; Hillier and Williams, 2006; Hillier et al., 2007, 2019; Morris et al., 2012b) including fluvial deposition, palaeosol development in interfluvial areas (Allen, 1974; Wright and Marriot, 1996) and ephemeral wetlands (Hillier et al., 2011a). These major river systems, extending some 500 km in length, linked multiple Lower 'Old Red Sandstone' basins (Morris et al., 2012b) in a principally south/ south easterly flow direction (Simon and Bluck, 1982; Allen and Crowley, 1983). Through the Přídolí, distal Plinian volcanism deposited air fall tuffs (e.g. Allen and Williams, 1978) which may have been reworked or influenced by tsunamis (Marriot et al., 2009) (section 4.3.3) The character of the rivers evolved throughout the Ludlow – Lochkovian of the Anglo-Welsh Basin, from ephemeral, muddy sheet flood rivers to sandier perennial channelised rivers with accompanying ephemeral channels (section 4.3.2 and 4.3.5). This change has been attributed to climate change (Morris et al., 2012b) and tectonic regime transition (Soper and Woodcock, 2003), and occurred following a basin wide depositional hiatus, which may have been due to a period of prolonged aridity or basin-wide fluvial shutdown (Morris et al., 2012b) (section 4.3.4)

Whilst principally south to south easterly flowing (e.g. Allen and Crowley, 1983), the local palaeoflow direction of the river systems changed through the Ludlow – Lochkovian. In the Ludlow and earliest Přídolí, southerly and north westerly highs were eroded and delivered sediment into the shrinking Palaeozoic Marine Welsh Basin (Bassett et al., 1992; Hillier et al., 2019) and early alluvial systems in the south west Anglo-Welsh Basin. Northerly flowing rivers persisted in the south of the basin (around Pembrokeshire) in the Mid-Přídolí, with southerly flow occurring to the north. The rivers adopted a principally southerly flow direction by the Lochkovian (Barclay et al., 2015). Provenance of sediment changed also, with the initial sediment sources being derived from high grade metamorphic complexes in the north west of Britain (Caledonian mountains) and possibly beyond (Allen and Crowley, 1983). Into the early Devonian (Lochkovian) granitic intrusion derived uplift separated the Anglo-Welsh Basin from these northerly metamorphic sediment sources via a wide belt of lower Palaeozoic sedimentary

and igneous rocks (Allen and Crowley, 1983). Sediment source consequently switched to more local supplies, which Crowley et al. (2009) posited were likely the result of the development of half grabens forming intrabasinal highs. The reworking of older Silurian sediments is demonstrated in the palynological record with the occurrence of Early Silurian palynomorphs and marine phytoplankton in wholly terrestrial sediments (e.g. Richardson and Rasul, 1978; Morris et al., 2011a; this work).

The seasonal, semi-arid climate of the Anglo-Welsh basin is inferred from the palaeolatitudinal position and concomitant sedimentary evidence. The fluvial systems described above and in section 4.3 operated under semi-arid, strongly seasonal conditions (Allen and Tarlo, 1963; Allen, 1974; Allen and Williams, 1978; Marriot and White, 2004; Morris et al., 2012b). Desiccation cracks (e.g. Allen and Tarlo, 1963; Morris et al., 2012b) indicate seasonal wetting and drying of mud surfaces, whilst conspicuous slickensides and pseudoanticlinal features and wedge shaped peds (e.g. Morris et al., 2012b; Hillier et al., 2019) indicate seasonal swelling and shrinkage of the clay rich soil profile. Typically weakly

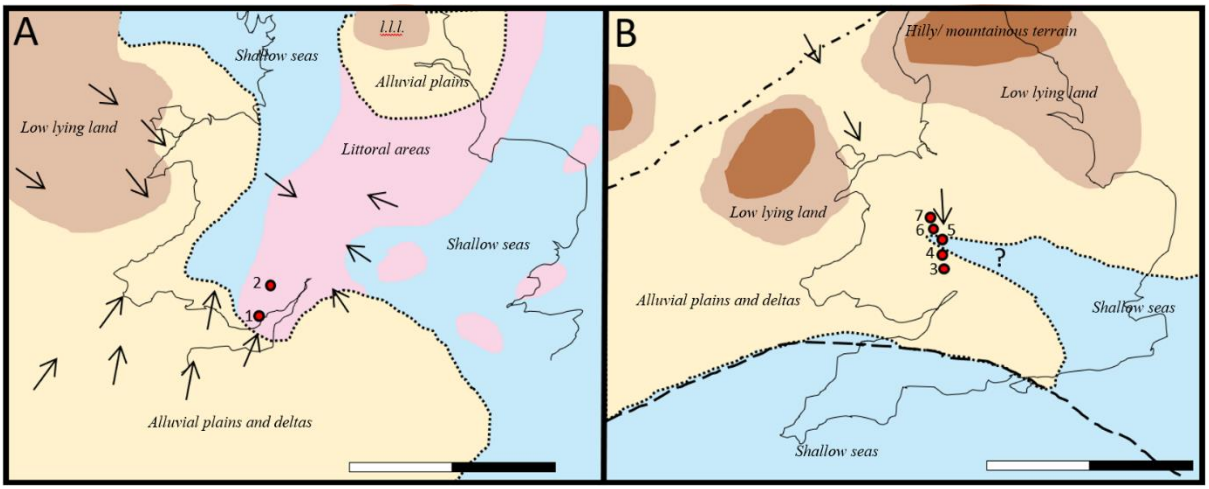

*Figure III-2: Paleoenvironmental reconstruction of the depositional environments in the Ludlow (**A**) and Lochkovian (**B**). **Arrows** indicate paleocurrent directions. Red circles represent localities studied in this work. 1: Rumney; 2: Usk; 3: M50; 4: Bromyard Plateau; 5: Ammons Hill; 6: Gardeners Bank; 7: Clee Hill. Modified from Barclay et al. (2015).*

developed, calcic vertisols (e.g. Allen, 1974; Marriot and White, 2009; Morris et al., 2012b) generally comprising calcrete nodules and colour mottling suggest pedogenic redoximorphic processes, pointing towards seasonal groundwater saturation (e.g. Hillier et al., 2011a, b). Some well-developed calcretes do occur across the basin, however, and suggesting prolonged periods of aridity (Morris et al., 2012b, section 4.3.4). Cyclic seasonality is also evidenced by the 'event deposition' nature of many fluvial deposits (e.g. Hiller and Williams, 2008; Morris et al., 2012b), including sheetflood conglomerates and mudstone interbeds representing bar top drapes (e.g. Hillier et al., 2019), suggesting ephemeral, flashy rivers (section 4.3.2 and 4.3.5). It is not thought that the basin represents a desert climate. The absence of advanced evaporites such as halite and gypsum salts preclude high temperatures and exceptionally high evaporation rates, with mean annual temperatures not thought to exceed 20°C (Goudie, 1983). Estimates for annual rainfall across the Anglo-Welsh Basin, which would have been mostly confined to wet seasons, has been estimated to have been between 100mm to over 760mm (Goudie, 1983; Royer, 1999). Hillier et al. (2007) posited that the seasonality in the Anglo-Welsh basin may have been controlled by monsoonal cyclicity and increasing monsoonal strength through the Přídolí and Lochkovian may have contributed to the shift towards a relatively wetter climate and the development of perennial river systems in the Lochkovian (Morris et al., 2012b).

The role of vegetation in the Anglo-Welsh basin is likely to have been varied. In the Ludlow, the unstable muddy environments hosted a diminutive flora of rhyniophytes/ rhyniophytoids, eophytes and cryptospore producing plants. Deep rooting structures were not present on these early land plants, but some may have exhibited a thallus (Edwards et al., 2022b) similar to modern bryophytes, whilst others

may have had shallowly subsurface or surface rhizomatous systems (e.g. Edwards, 1986). Regardless, the shallow or surface 'rooting' structures would have had limited effects on weathering and soil stabilisation. Similarly, biomats colonising muddy areas during periods of low discharge (Marriot et al., 2013) and cryptogamic soil crusts (Edwards and Kenrick, 2015) would have had limited influence on weathering and stabilisation. Larger vertical and horizontal rooting structures, interpreted as possible anchoring and/ or foraging structures from the giant fungus *Prototaxites* by Hillier et al. (2008) may have gone some way towards stabilising a range of environments. The appearance of more complex, taller and presumably perennial Zosterophylls in the Anglo-Welsh Basin in the Lochkovian (e.g. Edwards and Davies, 1990; Wellman et al., 2000) may have contributed to the increased stability of Lochkovian fluvial systems and soil development, although to what degree is equivocal and probably minor (e.g. Gibling et al., 2014).

4.3. Sedimentology

4.3.1. Termination of the Marine Welsh Basin: Ludlow and earliest Přídolí

The inception of the Anglo-Welsh Basin is defined as the incoming of major terrestrial deposition in the early Přídolí (red and green beds) following the shrinking of the Rheic ocean in the Ludlow *sensu* Barclay et al., 2015. This terrestrial sedimentation conformably overlies shallow marine and near shore sediments which represent the terminal phases of the Palaeozoic marine Welsh Basin, where sedimentation had been active since the Early Ordovician (Cherns et al., 2006; Schofield, 2009). Whilst not strictly part of the Anglo-Welsh Basin *sensu* Barclay et al. (2015) (section 4), samples from the terminal marine Welsh Basin have been historically important in discerning the palynology of the region (e.g. Richardson and Lister, 1969; Burgess, 1991; Burgess and Richardson, 1991, 1995), and have been studied in this work, also. These final stages are represented by marine strata recovered from the Rumney-1 and Usk-1 boreholes, and the Ludford Lane outcrop (section 5).

By the late Ludlow, calcareous, shelly silts were spread across the receding Welsh Basin (Holland and Lawson, 1963) as the sea gradually shrank, and frequent shell lags and tempestites alongside hummocky cross laminations and current ripples, *inter alia*, testify to the shallow marine conditions prevailing at this time. Allen and Tarlo (1963) posited that the Ludlow series exhibited depositional setting similar to those forming presently in the Gulf of Mexico (e.g. Parker, 1956), and Nigeria (Allen and Wells, 1962) at less than 100 metres depth. Whilst a general pattern of marine regression was seen throughout the Ludlow, several phases of transgression punctuated this. These events resulted in the Formation of several bone beds throughout the Ludlow section, which formed following initial scouring of existing sediments and concomitant sediment and debris accumulation as the sea retreated, followed by the infill of erosional scours with the concentrated debris (Allen and Tarlo, 1963).

The earliest samples investigated here are recovered from the Ludlow of Rumney and Usk and reflect this shallow marine depositional system. Rumney yields material from the Ludlow Llanedeyrn Formation in the upper Cardiff Group and comprises mudstones, siltstones, sandstones and limestones deposited in a shallow marine, muddy shelf environment (Waters and Lawrence, 1987; Kendall and Humpage, 2012). The siltstone beds are typically wavy and lenticular, with laminated and cross bedded sandstones, and shelly fauna such as brachiopods and gastropods, and disarticulated crinoids, occur alongside abundant burrows. The Ludlow series of the Usk inlier comprises calcareous silts and impure limestones which were also deposited under shallow marine conditions and yield shelly faunas. Walmsley (1958) divided the Ludlow series of Usk into seven parts, all of which he considered to be of a shelf facies. Of interest here are the Llangibby beds which form the upper part of the Ludlow serries *sensu* Walmsley (1958). The lower Llangibby beds are comprised of thin silts and sandstones with thin seams of fossiliferous, shelly limestones. The upper Llnagibby beds transition into unfossiliferous, olive grey shales which alternate with similarly barren siltstones, the latter of which exhibit ripple marks. Interbedded with these lithologies are coarse, calcareous siltstones and limestones which crowded with broken shells and disarticulated crinoids. Throughout the Ludlow, cephalopods, graptolites and ostracods are sparse (Allen and Tarlo, 1963).

Following the Ludlow series, further regressive – transgressive events occurred, forming the Ludlow Bone Bed in the Welsh borderlands which represents a distinct disconformity (Allen and Tarlo, 1963). Allen and Tarlo (1963) noted that this feature was lithologically similar to preceding Ludlovian bone beds, with a similar fauna of brachiopods, ostracods and vertebrates. Microvertebrates were first recognised in the Ludlow Bone Bed by Antia (1979), and later workers identified microvertebrate remains of thelodonts and acanthodians resulting in an assemblage which contrasted with the preceding Ludlovian (Turner et al., 2017). Later workers have recorded conodont assemblages similar to preceding Ludlow assemblages (Märss and Miller, 2004).

Allen and Tarlo (1963) posited that the Ludlow Bone Bed signifies a second period of retreat of the Silurian sea from the Welsh Borderlands and south Wales, followed by another transgression, represented by the proceeding Downton Castle Sandstone Formation. This regressive phase is not exhibited ubiquitously across the Anglo-Welsh Basin, with the Ludlow Bone Bed being absent west of the Brecon anticline towards Pembrokeshire (Barclay et al., 2015). The Ludlow Bone Bed, however, has been recognised as a complex series of stacked beds with geographical variation (e.g. Antia, 1979; Jeram et al., 1990; Veevers and Thomas, 2011), and given the variation in fossil colouration, may be diachronous (Turner et al., 2017). The stacked bone beds are separated variously by rippled, muddy siltstones. These arenaceous lithologies compliment the fossiliferous bone beds with a crowded, mixed assemblage of eurypterids, aquatic scorpions, myriapods and land plants alongside marine brachiopods and ostracods, *inter alia* (Jeram et al.,1990). Together, the terrestrial arthropods and land plant remains testify to the influx of terrestrial sediments being delivered into the shallow marine setting by nearby river systems. The Ludlow bone bed is observed in both the Rumney and Usk boreholes examined here, and at Ludford Corner.

The subsequent transgression of the Rheic Ocean is indicated by the Downton Castle Sandstone Formation in the Welsh borderlands, which progresses from lower argillaceous rocks to distinctly arenaceous material comprising thick, well sorted yellow sandstones in the upper reaches of the Formation. The sandstones commonly exhibit current bedding, graded bedding, hummocky cross stratification and ripple marks, alongside scoured erosional surfaces capped by thin, pebbly conglomerates with vertebrates and shells (Allen and Tarlo, 1963; Smith and Ainsworth, 1989). Towards the top of the Formation, the deepened seas formed during the brief transgression leading to Ludlow Bone Bed deposition was rapidly terminated, with beaches and sandy shoals forming along the coast in this area. Hillier et al (in progress, see 2019) surmised that a wave dominated delta, supplied by sediments from the north-east, formed the Downton Castle Sandstone Formation, while a river dominated delta, with sediments deriving from the north west, supplied the regionally correlative Tilestones Formation. Allen and Tarlo (1963) posited that that near the mouths of rivers and along beaches, brackish waters would have been developed. Indeed, wider changes in salinity are posited to have occurred at this time relative to the preceding Ludlow, as uplift isolated the already shrinking sea (Woodcock et al., 1988), leading to a restriction in the diversity of fossil faunas relative to the preceding Ludlow assemblages. Nonetheless, abundant invertebrates are found throughout the Formation, often forming concentrated bands of fossiliferous limestones. Other beds are crowded with lingulids and ostracods, alongside terrestrially derived plants and invertebrates (e.g. Lang, 1937; Fanning et al., 1990) which again point towards the influx of terrestrial material from nearby river systems. Indeed, Allen and Tarlo (1963) compared the depositional environment of the Downton Castle Sandstone Formation with present day depositional systems in the Mississippi (e.g. Fisk et al., 1954) and Niger (Allen and Wells, 1963) river delta systems.

The Downton Castle Sandstone Formation is present in the Usk borehole and represents the highest Formation that was able to be sampled from that locality in this work. Walmsley (1958) named the Downton Castle Sandstone Formation at Usk the ‘speckled grit beds’, which were largely devoid of fossils and comprised pale yellow to orange gritty sandstones with subordinate, thin beds of quartz siltstones. In the absence of fossils reported by Walmsley (1958) the Downton Castle Formation correlative at Usk is somewhat peculiar, but he did report crinoidal and shelly remains from the

Formation. The Ludford Corner sample is taken from a classic example of the Downton castle Formation as described, for example, by Basset et al. (1982) and Smith and Ainsworth (1989), which shows a gradation from dark argillaceous silty mudstones and silts with wave rippled sands, to cleaner arenaceous sands exhibiting, *inter alia*, hummocky cross stratification. The restricted, although abundant, flora from this outcrop of the Downton Castle Sandstone Formation comprises thelodont denticles, ostracods, lingulids and plant debris (Basset et al., 1982), although contrasts with the preceding Ludlow materials in that it lacks articulated brachiopods.

The shallowing up succession with punctuated regressions and transgressions seen in the Welsh Borderlands is broadly correspondent to the succession observed in South Wales in the Rumney Inlier, although the sedimentology of coeval lithologies represented there are quite different. In the Rumney borehole, a thin bone bed rich in vertebrate and shelly remains, attributed to the Ludlow Bone Bed by Waters and Lawrence (1987) precedes a thin, purplish sandstone body of *c.* 2m thickness. The sandstone is characterised by a coarse, pebbly base which fines into sands and silts at the top, where an immature calcrete profile is developed. Some laminations in the mudstone occur. The strong contrast between this sandstone and the Downton Castle Sandstone in the Welsh Borderlands, led Waters and Lawrence (1987) to avoid labelling the sandstone as the latter, due to the obvious sedimentological and lithological differences. The shallow marine beaches and sandy shoals that developed as part of the wave dominated delta to form the Downton Castle Sandstone Formation in the Welsh Borderlands in the early Přídolí were not present in the Cardiff area, with coaeval, muddy tidal flats being developed instead with subaerial exposure and palaeosol development.

4.3.2. Initial terrestrial sedimentation: Earliest Přídolí to Earliest Lochkovian

The first major terrestrial sediments in the Welsh borders following continued marine regression is the Temeside mudstone Formation, which represents the new base of parts of the eastern Anglo-Welsh Basin *sensu* Barclay et al. (2015). Allen and Tarlo (1963) outline the main features of the Formation, which is principally comprised of green siltstones and mudstones interbedded with numerous subsidiary thin sandstone beds. In the mudstones and siltstones, calcrete nodules are often developed. The subsidiary sandstones are typically well sorted and range from very fine to coarse in grade. Common sedimentary features in the siltstones include current ripples, which are also seen in the sandstones, alongside cross stratification and parallel laminations. Burrows are common throughout the mudstones and siltstones, and the latter also commonly yield lingulids. In the mudstones, isolated occurrences of freshwater stromatolites have been reported (Antia, 1981). In certain areas, richer assemblages comprising modiolopsis, fragmented eurypterids and plant remains are reported. Vertebrates, including thelodonts and acanthodians, have also been reported. The contact between the sandstones and siltstones is typically erosional, and 'pseudo-bone beds' are developed at the contact, comprising *lingula* valves, fragmented eurypterids and vertebrates, alongside plant debris. The Temeside Mudstone Formation was interpreted by Allen and Tarlo (1963) as a broad, intertidal mudflats and shoals which were marginal to large rivers. The Formation was deposited in advance of the better drained alluvial materials of the fully terrestrial Old Red Sandstone (Hillier et al., 2016). The Formation is present in the northern Welsh borders and thins southwards. In some cases, including at Usk, the preceding Moor Cliffs Formation directly contacts the Downton Castle Sandstone Formation where the Temeside Mudstone Formation is absent. This Formation was not sampled in this work, but JB Richardson recovered spore assemblages from it previously.

Following the deposition of the Temeside Mudstone Formation across broad intertidal flats, continued sedimentation led to the Formation of the terrestrial Moor Cliffs Formation across the low lying landscape. Allen and Tarlo (1963) divided the sediments bracketed by the Temeside Shales Formation/ Downton Castle Sandstone Formation, and the thick, well-developed calcrete of the Chapel Point Limestone member, into three distinct groups based on slightly variable cyclothems. However, in general the Moor Cliffs Formation principally comprises red and rare green mudstones and siltstones, the former of which are typically pedogenically altered. Interbedded with these are subordinate, very

fine to fine grained sandstones, extra- and intraformational exotic conglomerates and air fall tuffs (4.3.3). The sandstone and siltstone beds throughout the sequence are variously structured with cross stratification and current ripples or may be parallel laminated or massive (e.g. Allen and Tarlo, 1963; Morris et al., 2012b; Barclay et al., 2015). In the mudstones, desiccation cracks are common, as are drab haloes. Allen and Tarlo (1963) noted that scoured bases typified the start of new cyclothems, and these were typically initiated by conglomerates, which yield water sorted vertebrate remains such as acanthodians and thelodonts. Plant macrofossil remains are extremely rare in the Formation,and are absent from the top. A variety of ichnofaunas, including burrows such as *Beaconites barretti*, occur at the tops of the cyclothems also (Allen and Tarlo, 1963; Morris et al., 2012b; Morrissey et al., 2012). Towards the top of the Formation, stacked, well developed pedogenic limestones of the Chapel Point Limestone member occur (4.3.4).

Allen and Tarlo (1963) posited that, especially in the lower parts of the Moor Cliffs Formation, there was some marine influence and Barclay et al. (2015) concurs, interpreting the Formation as dryland alluvial and coastal plain environments. Morris et al. (2012b) surmised that the Moor Cliffs Formation represented a mud dominated, ephemeral river system. Indeed, Allen and Tarlo (1963) note that the river channels observed though the Formation were short lived. Morris et al. (2012b) envisage a wet – dry season cyclicity across the basin, with wet seasons typified by high discharge, flashy ephemeral rivers, either confined to shallow channels or as non-channelised flows. Those flows confined to channels were separated by interfluvial bars, and in some cases, terraces may have developed resulting in a pronounced topography (Morris et al., 2012b). Vertisols developed as floodplains and interfluves proximal to the activated channels were waterlogged, whilst non-vertic palaeosols developed in those areas in distal and raised areas away from flooding. During dry seasons, discharge in the channels and crevasse splays was much reduced or stopped altogether, but topographically lower splays and deep channel scours retained stagnant pools of water (Morris et al., 2012b). Until the mid-Přídolí, Hiller et al. (2019) envisage a pediment alluvial plain developing before a basin wide incision event in the mid Přídolí cut several valleys into the Southern Anglo-Welsh Basin. In the Welsh Borderlands and south Wales, one such valley formed the Rushall Formation valley system (Hillier et al., 2019). The termination of the Moor Cliffs Formation by the Chapel Point Limestone Member, a series of stacked, well developed calcrete horizons up to *c.* 12 m thickness (Barclay et al. 2015) is interpreted to represent a significant period of minimal to absent deposition across the muddy dryland facies. Whilst the Chapel Point Limestone is widespread across the basin, it is also diachronous indicating that depositional hiatus occurred at different times across the basin (Morris et al., 2011a, 2012b).

The lower and middle part of the Moor Cliffs Formation are not represented in this work due to (1) difficulties in access due to a paucity of outcrop, and (2) the dearth of sediments suitable for the preservation of palynological materials. Towards the top of the sequence, samples were collected from the Welsh Borderlands from within 40 metres of the Chapel Point Limestone member. The sediments from these localities are typical of the upper moor cliffs Formation, being dominated by pedogenic mudstones with occasional conglomerates and sandstones. Whilst represented at Usk, the Moor Cliffs Formation there failed to yield palyniferous samples. The longest sequence of the Formation was collected from the M50 section, which is now poorly exposed but represents the example section for the Formation in the Welsh borderlands (Allen and Dineley, 1976; Barclay et al., 2015).

4.3.3. Distal ash falls in the Moor Cliffs Formation

As mentioned, fine grained distal air fall tuffs occur throughout the Moor Cliffs Formation across the Anglo-Welsh Basin. Three principal, laterally extensive tuffs are developed; the Rook's Cave (e.g. Morrisey, 2006), Townsend Tuff Bed (e.g. Allen and Williams, 1978) and Pickard's Bay Tuff (Barclay et al.,2015). In addition to these laterally extensive tuffs, minor, subordinate and more aerially restricted tuffs are also observed, typically decimetre thick or arranged in minor complexes with interbedded mudstones (Allen and Williams, 1978). For example, Allen and Williams (1982) note that the 15 – 30

m gap between the Townsend Tuff Bed and Pickard's Bay Tuff is populated by six minor airfall tuffs. The tuffs are all distinctive in their fine grained, mottled green to purple appearance.

The best-known tuff bed with the widest lateral extent in the Welsh Borderlands is the Townsend Tuff Bed, which lies *c.* 100 m below the Chapel Point Limestone member (4.3.4) at the top of the Moor Cliffs Formation (4.3.2). Allen and Williams (1981) formally described this volcaniclastic feature, although it had been known lithologically since Strahan (1914), with Cantrill (1916) first positing that the feature was derived from distal volcanic activity. The Townsend Tuff Bed is a tightly stacked suite of three individual beds, separated by narrow red mudstone horizons. The three stacked beds differ slightly from each other in subtle sedimentary features, but the nature of each bed is laterally continuous and is borne out across the basin (Allen and Williams, 1981). All three beds are normally graded, comprising fine grained lithic tuffs and intervening dust tuffs, or so-called 'porcellanite'. The entire unit is <4 metres thick, with sharp lower and upper bounds where it overlies, and is overlain by, red mudstones. Throughout the unit, ichnofossils are common with Allen and Williams (1981) identifying five typical organic features, including burrows, faecal pellets and locomotion traces. The top of each of the individual ash falls varies, with the lowermost horizon exhibiting abundant bioturbation and faecal pellets, the next an erosional surface, and the final bed a sharp contact with overlying red mudstones (Allen and Williams, 1983). Parker et al. (1983) posited that the bed could be traced laterally through the clay mineralogy of the tuffs, but found that there were distinct variations, from smectite to illite, towards the west. These changes were attributed to diagenetic influences and the proximity to basement.

The tuff beds recorded from the Anglo-Welsh Basin have been interpreted as being derived from distal volcanic eruptions. Allen and Williams (1981) posited that the tuffs were laid down by temporally closely spaced Plinian eruptions, which delivered ash by wind from a (present day) west – east orientation from 100 – 200 km away. Those authors posited that, regarding the eruptions that produced the stacked Townsend Tuff Beds, the eruptions were separated by quiescent periods of up to tens of years. The airfall deposits were in wet settings which were occasionally affected at times by waves and currents. Later workers (e.g. Marriot et al., 2009) postulated that the scoured surfaces present between the ash falls, distinct fining up of materials and incorporation of red mudstones were evidence that the tuff beds had been deposited as part of tsunami events, specifically in the stillstand phase prior to backwash which allowed the gradational settling of minerals. They also noted certain eurypterid ichnofossils, which were more typically associated with brackish waters, in the tuffs and perhaps suggested short lived marine incursions. Marriot et al. (2009) suggested that tsunamis would likely have been caused by slope collapse or caldera Formation during particularly violent eruptions, which may have occurred as part of ongoing volcanism resulting from the recent amalgamation of Euramerica (Friend et al., 2000). As part of their tsunami hypothesis, they posited that the intense bioturbation seen in the tuffs was probably derived from opportunistic fauna colonising the deposits following deposition.

The Townsend Tuff Beds provide an important regional marker horizon across the Anglo-Welsh Basin (4.4). In this manner, it can be used to give a stratigraphic height of samples or localities relative to its ± standard stratigraphic level in the Moor Cliffs Formation, much like the Chapel Point Limestone member has been (e.g. Edwards and Richardson, 2004). U-Pb dating of the tuffs is under investigation by the BGS (Barclay et al. 2015), but the results of this work have not yet been published. Because of its use as a lithostratigraphic marker, sample collection from near the tuffs would be particularly informative, but this was unsuccessful in this work. A tuff bed outcrops near the Clee Hill section, but upon examination this is not thought to be the Townsend Tuff Bed, as it (1) is not comprised of stacked beds, (2) is *c.* 1m thick, and (3) occurs stratigraphically closer to the Chapel Point Limestone than

Figure III-3: Schematic stratigraphy and sedimentology of the studied Anglo-Welsh Basin sequence. Summaries of formations given on right, see text for details. ***TMF:*** *Temeside mudstone formation;* ***DCSF:*** *Downton Castle Sandstone formation;* ***LBB:*** *Ludlow Bone Bed;* ***WCf:*** *Whitcliffe formation (Welsh borderlands);* ***Ll:*** *Llanedeyrn beds (Rumney);* ***Lan****: Langibby beds (Usk).Stratigraphy sensu Barclay et al (2015) (section 4.4). Figure modified from Allen and Tarlo (1963), Allen and Dineley (1976), Morris et al. (2012b) and personal observations.*

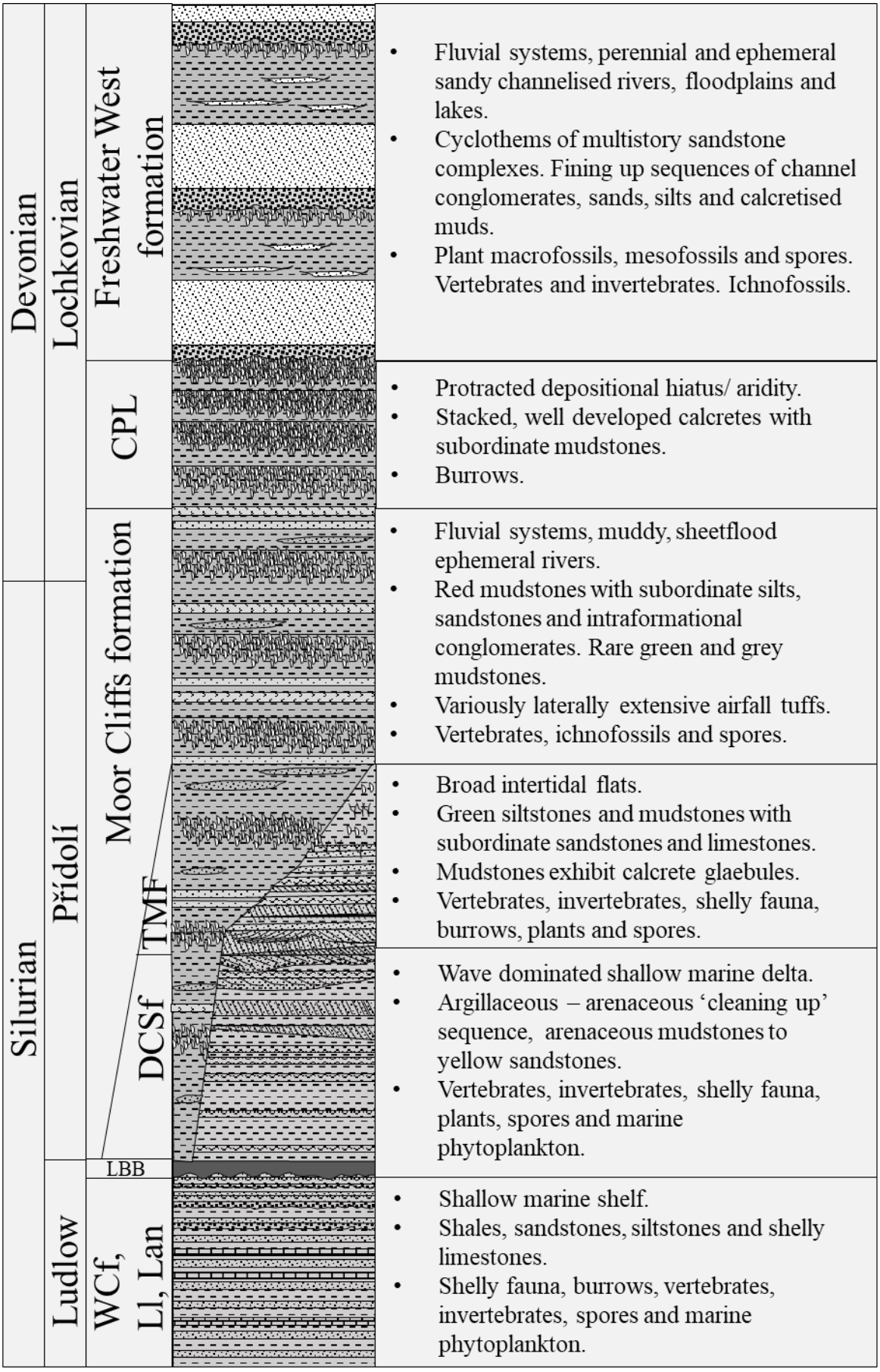
Devonian
Lochkovian
Silurian
Přídolí
Ludlow
Freshwater West formation
CPL
Moor Cliffs formation
TMF
DCSf
LBB
WCf, Ll, Lan
• Fluvial systems, perennial and ephemeral sandy channelised rivers, floodplains and lakes.
• Cyclothems of multistory sandstone complexes. Fining up sequences of channel conglomerates, sands, silts and calcretised muds.
• Plant macrofossils, mesofossils and spores. Vertebrates and invertebrates. Ichnofossils.
• Protracted depositional hiatus/ aridity.
• Stacked, well developed calcretes with subordinate mudstones.
• Burrows.
• Fluvial systems, muddy, sheetflood ephemeral rivers.
• Red mudstones with subordinate silts, sandstones and intraformational conglomerates. Rare green and grey mudstones.
• Variously laterally extensive airfall tuffs.
• Vertebrates, ichnofossils and spores.
• Broad intertidal flats.
• Green siltstones and mudstones with subordinate sandstones and limestones.
• Mudstones exhibit calcrete glaebules.
• Vertebrates, invertebrates, shelly fauna, burrows, plants and spores.
• Wave dominated shallow marine delta.
• Argillaceous – arenaceous 'cleaning up' sequence, arenaceous mudstones to yellow sandstones.
• Vertebrates, invertebrates, shelly fauna, plants, spores and marine phytoplankton.
• Shallow marine shelf.
• Shales, sandstones, siltstones and shelly limestones.
• Shelly fauna, burrows, vertebrates, invertebrates, spores and marine phytoplankton.

bonafide examples of the Townsend Tuff Beds. Allen and Dineley (1976) did not report the Townsend Tuff Bed from the M50 section, probably because of a 240m stratigraphic gap occurring after *c.* 100m below the top of the Moor Cliffs Formation.

4.3.4. Depositional hiatus: the Chapel Point Limestone, early Lochkovian

The Chapel Point Limestone (*sensu* Barclay et al., 2015), as mentioned in 4.3.3., occurs at the top of the Moor Cliffs Formation (4.3.2) as a conspicuous, well developed calcrete profile. The Chapel Point Limestone member comprises red mudstone with very well developed calcrete profiles. The member initiates with a gradational boundary of calcretisation of mudstones of the Moor Cliffs Formation. The calcretisation develops upwards into stacked groups or single horizons of thick, massive rubbly limestones at the top of the Moor Cliffs Formation. The member is terminated with a sharp, scoured contact with the basal conglomerates of the overlying Freshwater West Formation. At the type section in Pembrokeshire, the thickness of the member can be up to 30 metres in thickness, but in the Welsh Borderlands it is typically < 12 m thick. The member is laterally extensive across the Anglo-Welsh Basin, across the Welsh borderlands and in Pembrokeshire, south of the Ritec Fault. The member is not developed north of that fault. Whilst the member is used extensively as a lithostratigraphic marker horizon, the member is diachronous (e.g. Morris et al., 2011a, 2012b)

The Chapel Point Limestone was interpreted (e.g. Allen, 1974) as a pedogenic palaeosol formed under semi-arid conditions for an extended period of time. The thickness and maturity of the Chapel Point Limestone member relative to the subordinate calcretes which are developed further down in the Moor Cliffs Formation is debated, although it is clear a prolonged period of depositional hiatus may have persisted for up to 100,000 years (Allen, 1974). This basin wide shutdown of sediments is posited to have resulted from the transition of tectonic regime in the earliest Lochkovian (Early Devonian) from a foreland flexural to a sinistral transtensional regime (Soper and Woodcock, 2003), with the proceeding sandier facies being developed due to a change in sediment provenance from the metamorphic Caledonides to intrabasinal topographic highs (Allen and Crowley, 1983; Crowley et al., 2009). Alternatively, or perhaps in addition to the tectonic regime change, climate change to a wetter regime in the Devonian has been posited (Hillier et al., 2007; Morris et al., 2012b). Hillier et al. (2007) suggested that tropical monsoonal cyclicity accounted for the variability in the Coniger Sandstone member, and later Morris et al. (2012b) hypothesised that this wetter climate resulted in the facies change shift between the Moor Cliffs Formation (4.3.3) and Freshwater West Formation (4.3.5). In this climate change scenario the Chapel Point Limestone member may have developed from monsoonal weakening and a subsequent period of prolonged aridity, with minimal deposition from much reduced discharge.

Both possibilities for the development of the Chapel Point Limestone involve a prolonged hiatus in deposition. It is important to note that the member is diachronous across the basin, occurring at slightly different times in certain places (Morris et al., 2011a, 2012b; Turner et al., 2017). This indicates that deposition was still active in some areas, although was much reduced. Regarding the tectonic model, this switching tectonic regime perhaps concentrated discharge elsewhere for longer periods of time, with occasional switching, resulting in the diachronous Formation of the Chapel Point Limestone. Alternatively, reduced discharge due to weakening monsoons may have reduced flow across large areas of the basin at different times, resulting in prolonged pedogenesis. It is plausible that, given the suite of evidence for climate and tectonic regime change, that both factored into the prolonged depositional hiatus.

The Chapel Point Limestone member is observed in many of the localities studied in this work and is a useful lithostratigraphic marker horizon (despite its diachroneity) to gauge relative distances of samples. Easily identifiable in the field, it typically develops steep-sided waterfalls and small cliffs, providing a useful marker in the field and on topographic maps. All of the localities either directly exhibit the member in the sequence, or have it developed nearby, except at Ammons Hill. Here, the Brockhampton fault which bisects the section has obscured the member (Barclay et al., 1994).

4.3.5. Renewed terrestrial sedimentation: the Freshwater West Formation

Following the thick, well developed Chapel Point Limestone, a sharp change in the sedimentary facies is observed (e.g. Allen and Tarlo, 1963; Allen and Dineley, 1976; Morris et al., 2012b). Principally, the Formation comprises multistorey sandstone complexes, separated into distinct cyclothems metres to tens of metres thick. These cyclothems are initiated by an erosional scour and associated intraformational conglomerate, which fines upwards into sandstones, siltstones and mudstones, before being terminated by well-developed calcrete vertisols. The sandstones are a brick red to red-brown, with local green or grey horizons developed also. The conglomerates, capping the erosional scours initiating new cyclothems, are typically comprised of sandstone and mudstone clasts, which are imbricated and current bedded. Overlying sandstones normally grade from medium to fine sands with a variety of sedimentary structures observed throughout. The sandstones immediately preceding the intraformational conglomerates can be massive, or exhibit parallel laminations. Further up, planar and trough-cross bedded structures are developed, alongside ripple cross lamination. Into the siltstones, argillaceous laminae alternate with arenaceous laminae, and wavy lamination is developed. Grey reduction spots, pseudo anticlinal features and calcrete nodules are developed in silts and mudstones at the tops of cyclothems (Allen and Tarlo, 1963; Allen and Dineley, 1976; Morris et al., 2012b). Allen and Dineley (1976) report that calcrete horizons can be well developed towards the top of cyclothems. Distal ash falls, such as those observed in the Moor Cliffs Formation, are not observed in the Freshwater West Formation.

Typically, the green conglomerates forming the bases of the cyclothems are the most fossiliferous, yielding the remains of vertebrates such as thelodonts and acanthodians, as well as fragmentary eurypterids and plant remains. The subordinate green sandstones and siltstones also yield vertebrate, invertebrate and plant remains (King, 1934; Allen and Tarlo, 1963; Morris et al., 2012b). Carbonised plant macrofossils and mesofossils are common in grey and green sandstone beds (Lang, 1937; Fanning et al., 1988; Wellman et al., 2000; Morris et al., 2011a; 2012b). Exceptionally preserved, albeit fragmentary, charcoalified plant mesofossil remains including *in situ* spores have been recovered from Clee Hill (e.g. Edwards et al., 1994, 2014. 2022a, b, c; Edwards, 1996; Edwards and Richardson, 2000; Morris et al., 2018b), and similar, although less well preserved mesofossils including *in situ* spores have been recovered from the M50 section (e.g. Wellman, 1996; Ball and Taylor, 2022; Chapter V). In addition to plant mesofossils, remains of nematophytes *sensu* Lang (1937) have been recovered, with some probably representing the remains of lichenised fungi (Wellman and Ball, 2021). Coprolites from detritovores have also been observed (e.g. Edwards, 1996; Chapter V), and body fossils of terrestrial arthropods have also been recovered (e.g. Fayers et al., 2010). A diverse range of ichnofossils are also known, including burrows, trackways and resting traces (e.g. Morrissey et al., 2004, 2012).

The distinct change in sedimentary associations between the Freshwater West Formation and underlying Moor Cliffs Formation from mud dominated to sand dominated regimes is posited to relate to either a change in climate, although the semi-arid character of the basin persisted, or a result of tectonic change from foreland flexure to a sinistral transtensional regime (Morris et al., 2012b). A distinct change in fluvial character occurred, with major sand dominated perennial river channels, accompanied by minor mud dominated ephemeral river channels which drained interfluvial areas (Allen and Williams, 1979; Morris et al., 2012b), developing across the basin. The cyclic wet – dry phases posited for the Přídolí Moor Cliffs Formation remained active in the Lochkovian. During wet phases, channelised perennial rivers overtopped with subsequent unconfined sheet flows depositing conglomerates and waterlogging floodplains, leading to the development of vertisols. Meanwhile, more minor ephemeral river channels would have been activated, with high discharge observed in both major perennial channels and the minor ephemeral rivers.

As the seasonal dry phase took hold, the network of ephemeral channels draining interfluves dried up, and flow in perennial river channels fell and became channelised. Deep scours in ephemeral river channels, and presumably topographic lows across floodplains, developed as stagnant pools which may

have persisted for some time, although wavy laminations in silts may suggest some aeolian influence on the sediments. Similarly, flow would be much reduced in perennial channels, perhaps with minor, single channel flow persisting though the dry phases, or cessation of drainage and the development of water holes in deeply scoured sections. Floodplains were desiccated at this time, with calcic vertisol development persisting (e.g. Morris et al., 2012b).

The lower part of the Freshwater West Formation is observed and sampled in this work from the Welsh Borderlands. There is a distinct bias developed in sampling between this Formation and the underlying Moor Cliffs Formation, which occurs as a result of the former comprising more resistant lithologies which produce better outcrop. Furthermore, a distinct increase in sample availability is seen in the Freshwater West Formation with the occurrence of sporadic green and grey palyniferous siltstones. Morris et al. (2012b) attributed the increase in macrofossil plant remains in the Freshwater West Formation to the elevated water table which was present at this time. Nonetheless, samples are still occasionally sporadic, with long sequences rare. The M50 section comprises the longest section, exhibiting nearly 170 m of stratigraphy, but a range of sections are also seen at Clee Hill and Ammons Hill. Single localities occur also. The presence of the Chapel Point Limestone member immediately below the base of the Formation means that stratigraphic positioning of samples relative to the member is possible for most of the samples collected from the Freshwater West Formation.

4.4. Lithostratigraphy and biostratigraphy

Lithostratigraphy

The varied depositional environments detailed in section 4.3 culminate in a complex sequence of semiterrestrial and terrestrial sediments which develop into variously laterally extensive formations and members. Despite, or perhaps because of, the classic status of the Anglo-Welsh Basin in the history of geology (section 3), the stratigraphy of these deposits has until recently been somewhat confused, with local, non-systematic nomenclature making regional lithostratigraphic correlation across the basin difficult. A reappraisal by Barclay et al. (2015) formalised the nomenclature of the basin into a more systematic and logical stratigraphic framework which can be applied across much of the Přídolí and Lochkovian of the Anglo-Welsh Basin. Barclay's et al. (2015) new system discards many names which were either assigned prior to formalised stratigraphical nomenclature, and local names which were assigned later but which complicate the stratigraphy of the basin. In this work, the stratigraphy of Barclay et al. (2015) is used.

Barclay et al. (2015) placed the Lower 'Old Red Sandstone' of the Anglo-Welsh Basin into the Daugleddau group, which is in turn divided into the Cosheston subgroup and Milford Haven subgroup, of which the latter of interest here (fig. 3, 4). This subgroup extends between the Přídolí (late Silurian) and upper Lochkovian (Early Devonian) and with respects to the older nomenclature of the Anglo-Welsh Basin, encompasses the Ditton and Dittonian subgroups which have been extensively utilised in studies of the sediments, tectonics and palaeontology of the basin (e.g. Allen, 1965; Edwards and Richardson, 2004; Waters et al., 2007). The Milford Haven subgroup is divided into several formations and members by Barclay et al. (2015) (fig. 3, 4).

Traditionally, the base of the Anglo-Welsh Basin has been defined by the shallow marine Downton Castle Sandstone Formation. The Ludlow Bone Bed, recently dated to 424±<1 Ma by Catlos et al. (2022), is close to the base of this Formation. However, because the Downton Castle Sandstone Formation represents a marine transgression, Barclay et al. (2015) considered it unsuitable for defining the onset of a terrestrial basin, despite later comment by Turner et al. (2017) that the Formation exhibits significant proportions of red sediments. Nonetheless, the Lower Old Red Sandstone of the Anglo Welsh Basin is not considered to initiate with the incoming of red and green terrestrial sediments in the early Přídolí (*sensu* Barclay et al., 2015). In the Welsh Borderlands, this is largely represented by the Temeside Mudstone Formation, and is represented by its correlatives in Pembrokeshire (Red Cliffs Formation). Where this green mudstone unit is not found, including in South Wales, the Anglo-Welsh

Basin is initiated by the Moor Cliffs Formation. The Lowermost Moor Cliffs Formation is either contemporaneous with, or conformably overlies, the Temeside mudstone Formation and is composed of chiefly bright red, calcretised mudstones and siltstones with subordinate fine sandstone horizons and occasional exotic conglomerates, which were deposited by muddy ephemeral rivers (e.g. Morris et al., 2012b) The Formation is laterally extensive across the Anglo-Welsh Basin and is up to 1400 metres thick. Variously laterally extensive tuff beds are found in the Moor Cliffs Formation, most notably the Townsend Tuff Bed which extends between Pembrokeshire (north and south of Ritec Fault), the Black Mountains, Forest of Dean and Clee Hills (Allen and Williams, 1981), but is absent from some areas including sites east of the River Severn and the north-east outcrop in South Wales (Barclay *et al*., 2015). U-Pb dating of this bed by the BGS has yielded an approximate age of 420 Ma (pers. comm. BGS, 2022).

The Moor cliffs Formation is terminated by the laterally extensive complex of well-developed calcrete horizons of the Chapel Point Limestone member (previously the Bishop's Frome Limestone, Chapel Point Calcrete in Pembrokeshire and *Psammosteus* limestone in the Welsh Borderlands). This member is postulated to represent a long period of tectonic quiescence and landscape stability (Love and Williams, 2000). The calcrete horizon extends laterally across much of the Lower ORS, south and east of the Ritec Fault, however, it is absent from the successions north of the Ritec Fault (Allen and Williams, 1978).

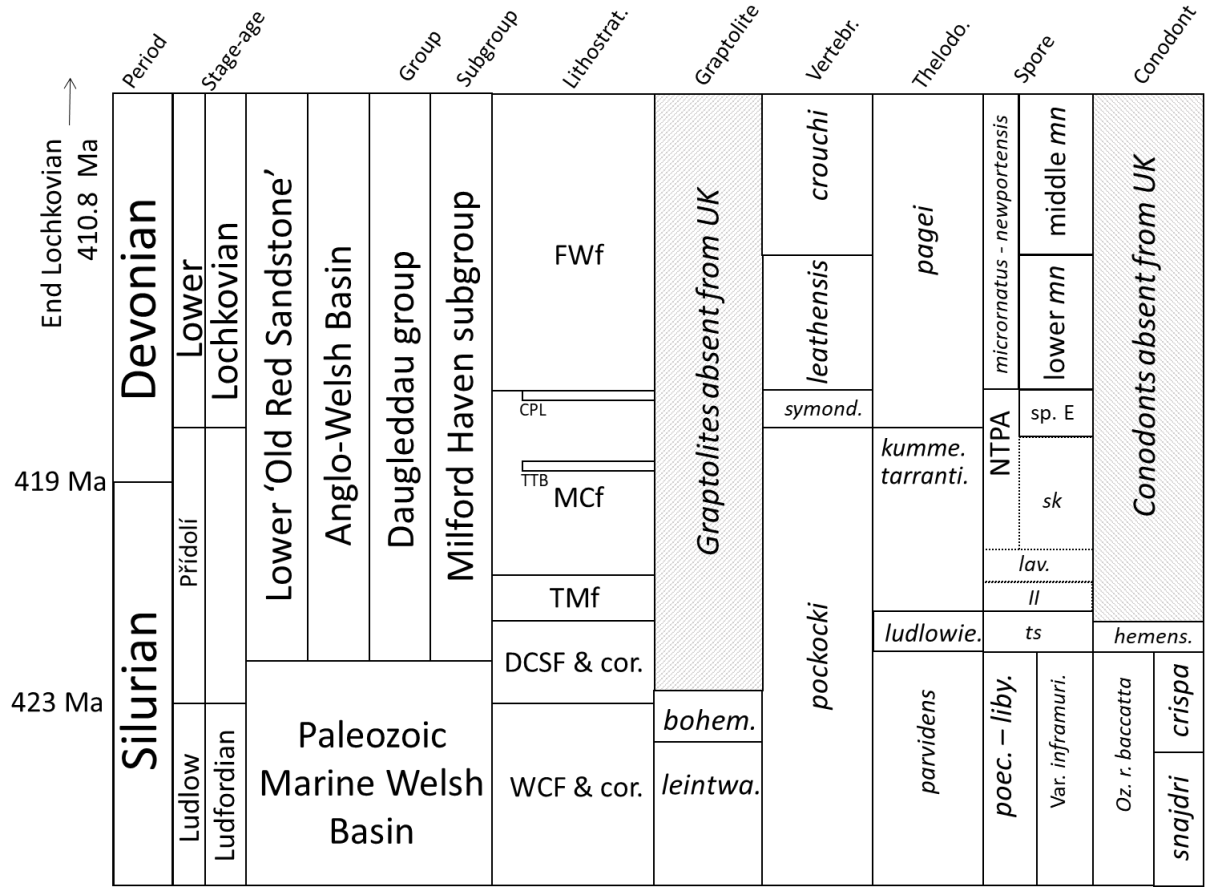

Figure III-4: Generalised lithostratigraphy and biostratigraphy of the portion of the Anglo-Welsh Basin succession studied in this work. Modified from Barclay et al. (2015). ***Ludl.*** *= Ludlow;* ***Ludf.*** *= Ludfordian. Ludlow – Přídolí date from Catlos et al. (2020) zircons in the Ludlow Bone Bed. Other dates from Gradstein et al. (2012).* ***WCF & cor:*** *Whitcliffe formation and correlatives;* ***DCSF & cor:*** *Downton Castle Sandstone formation and correlatives;* ***TMf:*** *Temeside mudstone formation;* ***MCF*** *Moor Cliffs formation;* ***TTB:*** *Townsend Tuff Bed;* ***CPL:*** *Chapel Point Limestone member;* ***FWf:*** *Freshwater West formation. Chart modified from Barclay et al., 2015 (lithostratigraphy), Edwards and Richardson, 2004)spore biozones), Burgess and Richardson, 1995 (Graptolites) and Marrs and Miller, 2004 (Conodonts).*

The Chapel Point Limestone is terminated by the incoming of the Freshwater West Formation, which comprises typically brick red cyclothems of very fine to medium sandstones, with subordinate mudstones and intraformational conglomerates. Mudstones commonly exhibit calcrete glaebules and may also exhibit well-developed calcrete horizons, although these are laterally restricted in the lower part of the Formation. These sediments were deposited in a semi-arid, seasonal climate by perennial and ephemeral rivers and streams (e.g. Morris et al., 2012b). The Freshwater West Formation is up to 1500m thick in Pembrokeshire but in the Welsh borderlands is *c.* 630m thick (Barclay et al., 2015).

Biostratigraphy

The terrestrial nature of the Anglo-Welsh Basin precludes marine fossils, which are widely used for biostratigraphy in the Silurian and Devonian. Such is the case for the Silurian – Devonian boundary type section in pelagic facies at Klonk, Czech Republic, which is defined by the incoming of graptolites. Such fossils are absent in the Anglo-Welsh Basin, with graptolites, conodonts, chitinozoans and acritarchs principally being lost by the early Přídolí (e.g. Marrs and Miller, 2004). Nonetheless, the biostratigraphy of the Anglo-Welsh Basin is well defined, principally with macro- and microfaunal remains of fish (White, 1955a, b, 1961; Ball and Dineley, 1961) and plant spores (e.g. Richardson and Lister, 1969; Richardson et al., 1981, 1984; this Chapter) (fig. 4).

Indeed, some of the earliest workers in the Anglo-Welsh Basin were attracted to the area by the abundant fish remains (Turner et al., 2017), which has culminated in a well-defined biostratigraphic understanding with several key species of thelodonts and pteraspids lending high resolution correlation throughout the sequence. Modifications to the classic works of White (1950) and Ball et al. (1961) were made by Turner (1973) with the description of the key Devonian thelodont *Turina pagei*. Soon after, Blieck and Janvier (1999) revised vertebrate range and assemblage biozones into interval biozones. Later modifications and additions by Blieck and Tarrant (2001) produced the current vertebrate biostratigraphy of the basin (fig. 4), although Blieck and Elliot (2017) have suggested that the *dunensis* zone may need revision. These thelodont and pteraspidomorph zones have facilitated correlation across Euramerica (e.g. Blieck et al., 2000).

The other major biostratigraphic tool in the Anglo-Welsh Basin are dispersed spores. These are abundant and widespread throughout the sequence, although have not yet been reported from the mid – late Přídolí. Initial descriptions of Silurian and Devonian spores in the British Isles were made by Richardson (1965, 1967). An analysis of spores and their biostratigraphy across the Anglo-Welsh Basin was made by Richardson and Lister (1969) which was later modified and expanded by Richardson et al. (1981, 1984) and adapted into a global correlative tool by Richardson and McGregor (1986), which along with the closely comparable system developed by Streel et al. (1986) remains in use today (fig. 4). These spore biozones have a higher resolution than vertebrate biozones, and biostratigraphically useful spore species are more readily recovered from sediments. Nonetheless, correlation with marine sections, particularly with type sections, have remained problematic (e.g. Edwards and Richardson, 2004). Continued work has begun to shed light on these problems (Richardson et al., 1981, 1984, 2001; Edwards and Richardson, 2004; this paper), particularly with respects to defining the hitherto equivocal position of the Silurian – Devonian boundary in the Anglo-Welsh Basin with spores (e.g. Edwards and Richardson, 2004).

5. Localities

2.1. Field sites and samples

Material is drawn from outcrop and boreholes from the late Silurian – Early Devonian Lower 'Old Red Sandstone' of the Welsh Borderlands and South-East Wales (figs. 5 and 6). Outcrop material was collected either during fieldwork by the author between 2019 – 2021, or by J.B. Richardson, D. Edwards or C.H. Wellman between 1970 and 1998. Core material was extracted by a series of companies between 1960 and 1990. Further details on sample sites can be found below. In all, nine field sites across the

Welsh borderlands and south Wales were collected from. These range from short sections (*c.* 1m thick) to over 300m long (fig. 6).

The nine localities give an insight into much of the Ludlow and Lochkovian of the Lower Old Red Sandstone, from the *poecilomorphus – libycus* to middle *micrornatus-newportensis* spore assemblage biozones (fig. 6). While much of the latter half of the sequence is represented in the sampling, much of the former half, represented by the Moor Cliffs Formation, remains un-investigated due to a dearth of suitable sampling horizons. However, whilst the middle of the former half of the sequence has been unproductive, the lower and upper Moor Cliffs Formation yields some spore assemblages. This problem, and the juxtaposition of the relatively fossil rich Freshwater West Formation and essentially barren Moor Cliffs Formation derives largely from the sedimentology of the formations.

2.1.1. Ammons Hill section (AH), Shropshire, SO 6850 5290 – 7020 5300

Material was collected from outcrop by the BGS during a re-excavation of the section (Barclay *et al.*, 1994), where a 170m trench was dug between SO 6850 5290 – 7020 5300 in an abandoned railway cutting. The exposure was covered up following BGS investigation and the area is now heavily overgrown. The section comprises steeply dipping beds (50°SW) of the Freshwater West and Moor Cliffs formations, which are juxtaposed against one another by the NW-SE tending Brockhampton Fault. Minor extensional faults, related to the Brockhampton Fault, complicate the section further. The Chapel Point Limestone member has been faulted out of the sequence by the Brockhampton fault (Barclay et al., 1994), precluding the assessment of relative stratigraphic height from this lithostratigraphic marker. The lithologies of the Freshwater West and Moor Cliffs formations are typical (section 4.3) at Ammons Hill.

Sediments of the Moor Cliffs Formation are interpreted to have been deposited by muddy, sheet flood ephemeral streams and rivers, whilst those of the overlying Freshwater West Formation deposited by sandy perennial and ephemeral channelised rivers (Allen and Tarlo, 1963; Allen and Williams, 1976; Morris et al., 2012b). *In situ* ostracods and acritarchs recovered from the Freshwater west Formation are indicative of repeated brackish water incursions (Barclay et al., 1994) (section 8.1: Palynofacies) into the otherwise terrestrial fluvial system. Palynomorphs were isolated from horizons across 150m of the trench section and indicate that the section spans between the *Apiculiretusispora* sp. E biozone and middle MN subzone. Charcoalified mesofossils of embryophytic and non-embryophytic affinities (e.g. Nematophytes) were isolated from one sample in the lower MN subzone (Chapter V).

2.1.2. Bromyard plateau (BP), Shropshire. SO 6856 6615

This site comprises multiple stream sections which dissect the Freshwater West and Moor Cliffs Formation. Samples were collected from +1m (Witchery Hole) and +3m (Temple Dingle) relative to the Chapel Point Limestone. The short sections from Temple dingle (near Stanford-on-Teme) and Witchery Hole (near Shelsey Beauchamp) comprise ± horizontally dipping beds with a <5° maximum dip. Lithologies are typical of the Freshwater West and Moor Cliffs formations, with principally red, mottled mudstones and siltstones being replaced by red sandstones and siltstone. Subordinate conglomerates and variously mature calcretes occur throughout. The Chapel Point Limestone is present in the sections allowing lithostratigraphic correlation. Minor faulting occurs in the sequence but it typically perpendicular to strike and do not interrupt the sequence considerably.

Depositional setting of the sediments is interpreted to be typical of the formations, with muddy ephemeral rivers of the Moor Cliffs Formation giving way to sandier, perennial rivers of the Freshwater West Formation following a period of depositional hiatus represented by the Chapel Point Limestone. Palynomorph productivity was poor from Temple Dingle, but reasonable from Witchery Hole. Both samples yield assemblages indicative of the MN zone.

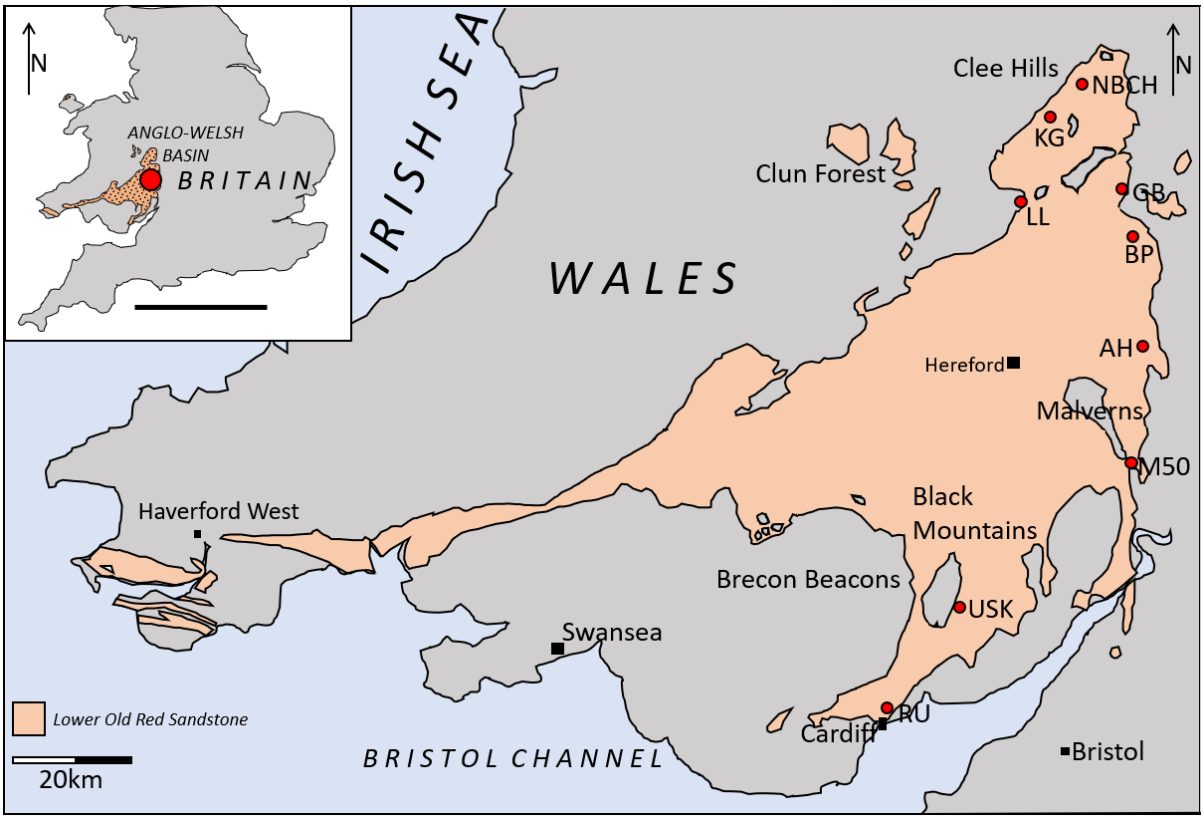

Figure III-5: ***top left)*** *map of southern Britain showing position of the Anglo-Welsh Basin in Western England (the Welsh Borderlands), and its central, south and west extents in Wales, scale bar 200km;* ***(main):*** *The Přídolí and Lochkovian (late Silurian – Early Devonian) outcrop of the Anglo-Welsh Basin, showing the positions of the field localities investigated here, curving along the eastern edge of the basin to southern Wales, scale bar 20km. Sites detailed in section 5. Maps modified from Digimap*

2.1.3. Gardener's Bank (GB), Shropshire. SO 6809 7450

This short outcrop section in the Freshwater West Formation was collected from by CH Wellman in 1995. Originally described in Turner (1970) and later in Märss and Miller (2004), the outcrop is +8m above the Chapel Point Limestone. The material outcrops in a motocross track *c.* 1.5km south of Cleobury Mortimer near The Rookery. The small section comprises shallow dipping beds (<5°) and is not thought to be affected by faulting.

The sedimentology of the site is generally concordant with the rest of the Freshwater West Formation, comprising red mudstones, sandstones and variously developed calcrete palaeosols. However, the samples from which the samples studies here were collected are derived from an unusually thick (1m) pale green siltstone. Nonetheless, sediments have been interpreted as fluvial and lacustrine deposits, a depositional environment typical of the Freshwater West Formation. The palynomorph assemblage indicates the assemblage belongs in the (?) lower *micrornatus-newportensis* spore assemblage biozone.

2.1.4. Kidnall Gutter (KG), Shropshire. SO 5620 8703

This short section in the Freshwater West Formation was collected from outcrop by JB Richardson in the 1970s. The material outcrops in a steep dingle just south of Tugford on the western slope of North Brown Clee Hill, *ca.* 9km south-east of Hudwick and Sudford Dingles (NBCH, 2.1.5).

The sedimentology of the site is much the same as that found around North Brown Clee Hill (2.1.6), comprising red mudstones, sandstones and variously developed calcrete palaeosols. These sediments have been interpreted as the deposits of variously meandering sandy streams and rivers. The palynomorph assemblage is indicative of the lower *micrornatus-newportensis* spore assemblage biozone.

2.1.5. Ludlow Lane (LL), Shropshire SO 5123 7413

This sample was collected from the Downton Castle Sandstone Formation near the junction between Ludford Lane and Leominster Road, near Ludlow, by JB Richardson. The sediments of the Downton Castle Sandstone Formation are typical of that Formation and have been interpreted as being deposited in a near shore marine environment as part of a wave dominated deltaic system during a brief period of marine transgression. The palynological assemblage is indicative of the *tripapillatus* – *spicula* biozone (early Přídolí).

2.1.6. North Brown Clee Hill (NBCH), Shropshire. SO 6317 9272

This outcrop section was identified during routine logging by JBR in the 1980s and has since been extensively published on following the recovery of exceptionally preserved, fragmentary mesofossils of early land plants (e.g., Edwards *et al*., 1994; Morris *et al*., 2012a; Edwards *et al*., 2014; Morris *et al*., 2018b). Samples 21HD 1 – 6 were collected from Hudwick Dingle by CH Wellman in 1995 from the Freshwater West Formation. The short section lies between 59.8m and 61.6m above the Chapel Point Limestone, outcropping beneath a small waterfall. Sample CH/SD/882C was collected from the adjacent Sudford Dingle by JB Richardson in the 1980s from -7m below the Chapel Point Limestone in the Moor Cliffs Formation. In both cases, the formations comprise shallow to horizontally dipping beds (<5° dip), and no faults interrupt the sequence.

The sediments around NBCH of the Freshwater West and Moor Cliffs formations are typical of those formations. Depositional environments are also considered to be typical, with muddy ephemeral rivers of the Moor Cliffs Formation giving way to sandier, perennial rivers of the Freshwater West Formation following a period of depositional hiatus represented by the Chapel Point Limestone (Edwards *et al*., 1994). The palynomorph assemblages indicate that the NBCH section spans the *A.* sp. E and MN biozones.

2.1.7. Ross – Tewkesbury Spur (M50) motorway section, Hereford and Worcester. SO 6605 2584 – 6663 2612

Outcrop samples were collected by JBR when the section was exposed in the 1970s. The section extends 207 metres through the Moor Cliffs Formation and Freshwater West Formation, between the 29.4 and 29.8 marker posts (Allen and Dineley, 1976). 26 samples were collected by JB Richardson from the Moor Cliffs and Freshwater West Formation. The Chapel Point Limestone is exhibited in the sequence. The section comprises steeply dipping beds (45°) and some sections are affected by faulting, although the section collected from is not (Allen and Dineley, 1976). The section is no longer exposed.

The sediments are typical of the Moor Cliffs and Freshwater West Formation. The depositional environments are also considered typical with muddy, ephemeral rivers of the Moor Cliffs Formation giving way to sandier, perennial and ephemeral rivers of the Freshwater West Formation. Analysis of dispersed spore assemblages from the same material indicates that this section extends between the pre-*Apiculiretusispora* sp. E zone and middle MN zone. Mesofossils have been recovered from this locality from sample DE98.

2.1.8. Rumney-1 borehole (RU), Cardiff, South Wales. ST 2108 7925

First described by Sollas (1879) the Rumney inlier, near Cardiff, comprises an anticline with core of Wenlock sediments, which pass conformably into Ludlow and Přídolí aged sediments (Bassett, 1974) towards the outside of the inlier. The Rumney-1 Borehole (BGS reference: ST27NW307) was drilled by the BGS to establish the nature of the Downton and Ludlow series boundary in the Rumney Silurian inlier. The borehole covers Recent, Pleistocene, Silurian and Wenlock materials. The Moor Cliffs Formation extends from a depth of 5m to 57.43m where it transitions into the Ludlow Llanedeyrn

Formation. Samples were retrieved from the Moor Cliffs Formation and the preceding Llanedeyrn Formation.

The Moor Cliffs Formation comprises chiefly red, red-brown and red-purple mudstones, siltstones and sandstones with rare green mudstones and intraclastic breccias. The sediments often exhibit, *inter alia*, crossbedding, laminations and cross laminations, and are therefore typical of the Moor Cliffs Formation. The green mudstone is of particular interest here as it was noted to contain plant fragments. The depositional setting is interpreted to have been essentially typical of the Moor Cliffs Formation with variously braided, muddy ephemeral rivers deposited under a semi-arid, seasonal climate. Green mudstones yielding marine palynomorphs indicate marine influence in the Moor Cliffs Formation at this time. Rocks from the Ludlovian Llanedeyrn Formation comprise dark grey siltstones with terrestrial and marine derived fossils, including brachiopods (e.g. Bassett, 1974), palynomorphs (Burgess and Richardson, 1995) and charcoalified nematophytes (Glasspool and Gastaldo, 2022). These sediments are interpreted to have been deposited in nearshore, shallow marine environments.

2.1.9. Usk – 1 borehole (USK), Monmouthshire, South Wales. SO 4020 0085

The Usk inlier is a periclinal structure exhibiting Wenlock – Přídolí sediments (Walmsley, 1958), with gently folding beds with dips <10°. The Usk-1 borehole was drilled adjacent to an extensional fault, but this is not though to cut the borehole. The Usk-1 borehole penetrates 700m of stratigraphy with a considerable proportion of the Moor Cliffs Formation collected and preceding Ludlow series. This borehole was drilled by Sovereign Oil and Gas PLC and is housed in the BGS core store. Despite the promising extent of the borehole, very few samples were retrieved. No samples were obtained from the Moor Cliffs Formation, with samples instead retrieved from the early Přídolí 'Speckled Grit Beds' and Ludlow upper Langibby beds (*sensu* Walmsley, 1958).

Much of the borehole comprises rocks that typical of the Moor Cliffs Formation, being principally red mudstones, fine siltstones and sandstones interpreted as having been deposited by muddy, ephemeral

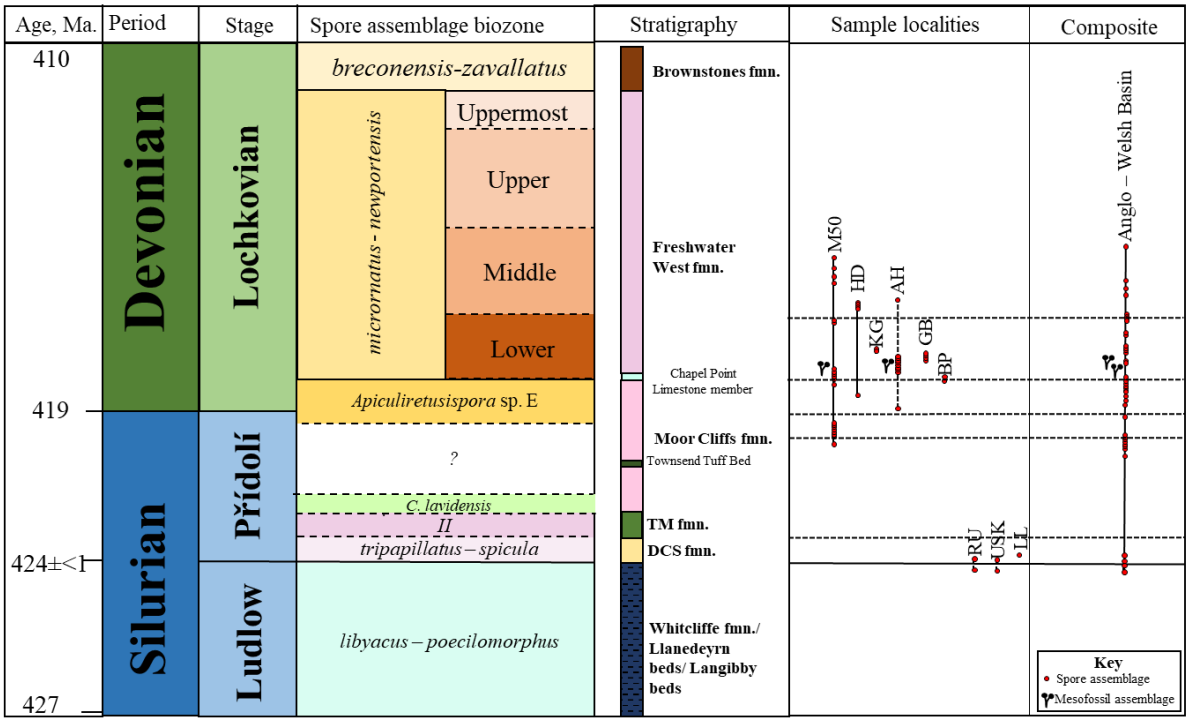

Figure III-6: Composite stratigraphy and biostratigraphy of the studied sequence, showing the stratigraphic location and range of localities and sections. Biostratigraphy is shown as present understanding. For an emended biostratigraphy developed from the findings of this work, see figure 18, section 9. Modified from Edwards and Richardson (2004) and Barclay et al. (2015). Mesofossil localities shown are the M50 and Ammons Hill horizons; see Chapter V.

rivers in a semi-arid climate. These terrestrial sediments conformably overlie the Walmsley's (1958) 'Speckled Grit Beds', which are laterally and lithologically comparable with the Downton Castle Sandstone Formation. These sediments were deposited in a near shore, shallow marine environment as part of a wave-dominated deltaic system (Bassett et al., 1982). The preceding Ludlow series comprises the upper Langibby beds (*sensu* Walmsley, 1958) and comprises dark green-grey shales with alternating ripple marked siltstones to have been deposited in a shallow marine environment, with deposition occurring further offshore than the sediments of the overlying 'Speckled Grit Beds' (Walmsley, 1958).

6. Methods

6.1. Palynological processing

Non-quantitative slides for light microscopy*:* Standard (non-quantitative) slides were processed by JB Richardson at the Natural History Museum (London) between 1977 and 1985. Some methodological information is garnered from JB Richardson's unpublished notes alongside information recorded on the microscope slide labels. Hydrofluoric and hydrochloric acid maceration was employed to collect organic residue. In some cases, samples were oxidised using HNO_3 for two minutes, whilst others were left unoxidised. Preparations were then mounted using H_2O + Elvacite. Slides were examined using an Olympus CH-2 light microscope.

Quantitative slides for light microscopy*:* Hydrofluoric and hydrochloric acid maceration was employed as above. Centrifugation and heavy mineral separation using $ZnCl_2$ + HCl followed sieving with a 10µm mesh. Following centrifugation lycopodium tablets ($CaCO_3$ + a known number of *Lycopodium clavatus* Linnaeus spores) are added to the sample along with a small amount of HCl and allowed to dissolve. *Lycopodium* tablets from batch 3869 are added according to the approximate amount of organic material in the sample (1 tablet:1ml of organic material) (thesis appendix 2.1). Samples are then diluted and sieved again using a 10µm mesh, before being mounted on glass microscope slides using Araldite® and covered with a glass slip for light microscopy with an Olympus CH-2 light microscope.

Semi – quantitative and quantitative counts*:* Because many of JB Richardson's slides are not spiked with *Lycopodium* but could not be excluded from the study due to their importance, two count methods were employed here to fully utilise the available materials. All slides (spiked slides and non-spiked slides) were subjected to a standard, 'semi-quantitative' palynomorph count, where native sporomorph species were counted to 250 specimens, excluding *Lycopodium* spores in spiked samples. Sporomorphs in spiked samples were counted to 250 including *Lycopodium* spores, and once this 250-count limit was reached, the native sporomorph count (250 – no. of *Lycopodium* spores) was continued to 250 native sporomorphs. Thus, spiked slides yield two counts: a quantitative count (native sporomorphs + *Lycopodium*) and a semi-quantitative count (native sporomorphs only), whilst non-spiked slides yield the latter only. Raw species count ornament data sets are collated in thesis appendices 3.1 – 3.4.

Quantitative palynomorph counts are calculated here as the total number of a given indigenous palynomorph species per unit of processed rock. This calculation enables the abundance of any given taxon to be expressed as a proportion of the total palynomorph concentration in a sample. The equation used here (equation 1) is that of Benninghoff's (1962) method for absolute pollen determination:

$$C = \frac{m_c \cdot L_t \cdot t}{L_c \cdot w} \quad \textbf{(1)}$$

Where C is the number of indigenous palynomorphs per gram of dry rock processed (the concentration), M_c is the number of indigenous palynomorphs counted, L_t is the number of *Lycopodium* spores in each

tablet, with *t* being the number of *Lycopodium* tablets added to the sample; L_c is the number of *Lycopodium* spores counted in the sample, and *w* is the weight of dried sediment processed for palynomorphs, in grams.

These preliminary quantitative counts were then consolidated into data sheets on Microsoft Excel 2016 and distribution charts illustrating the proportional stratigraphic changes in species and gross ornament were produced using the Rstudio v. 3.5.1 package `Library("rioja")` (Juggins, 2020). Due to the general inefficiency of this software for palynological use, specifically for uneven sampling depths, primary, large scale counts and range charts are executed and illustrated using Stratabugs, but `Library("rioja")` was used in smaller scale graphical outputs where stratigraphic distance between samples was of less importance (i.e. for general successions and patterns).

Because not all of the samples were able to be spiked with *Lycopodium* (especially those from the mid Lochkovian) these quantitative counts were used to confirm, where possible, the trends shown by relative abundance counts.

***Computational analyses**:* R version 4.1.3 (2022-03-10) - "One Push-Up" (R core team, 2022) was the principal software used for data analysis and graphical output, via RStudio, using a variety of packages including `library("rioja"), library("vegan")` (Oksanen et al., 2020) and `library("ggplot2")` (Wickham, 2020). Data was illustrated with `library("ggplot2")` and `Base R`, which together offer most graphical outputs together with manipulations and personalisation. Where R and/ or an R package has been used in a statistical analysis or graphical output, the details are given in-text and a full code script is reproduced in the appendices (appendix 3.5). Where a statistical analysis has been used, the methodology is outlined below, and further details may be found in the respective Chapter.

6.2. Imaging

Light micrographs: Preliminary micrographs are taken using a GXCAM-U3-5 5.1-megapixel camera which is interchangeable with one of the eyepieces on the Olympus CH-2 light microscope. The camera is used in conjunction with GXCapture-T software. Unless otherwise stated, all micrographs are taken at x100 magnification with the aid of Microil immersion oil which facilitates better resolution at higher magnifications. The position of the palynomorph on the slide is recorded using a Pyser SG1 New England Finder.

***Scanning Electron Microscopy**:* SEM micrographs were collected by JB Richardson at the Natural History Museum, London. The date, exact methods and SEM used are not known, but folders of SEM 'proofs' are housed in the Micropaleontological collections of the Natural History Museum, London. These proofs are extensive, covering many taxa from the M50 series. These proofs have been scanned and integrated into this taxonomy.

SEM stubs were also strew mounted with organic residue from key samples M50-85-2C, M50-3, 19M50-26 and M50-7, which were selected due to (1) their stratigraphic position (each sample represents examples of palynofloras from current *Ap.* sp. E –to middle MN spore biozones), and (2) their excellent preservation and high diversity (recognised during logging under LM) which gives the greatest chance of identifying suitable specimens for taxonomic plates and morphometric analyses. Two stubs for each sample were made. These samples were gold coated in an Edwards gold sputter coater for three minutes and analysed using a Tescan-Vega 3 Scanning Electron Microscope at 15 – 20Kv at the University of Sheffield Electron Microscopy facility.

6.3. Data storage and material curation

Data storage

Data sets were transferred from physical count and logging sheets to Microsoft Office 365 package Excel 2021 v. 2208 and stored as sheets in query specific (e.g. species count or ornament data) workbooks and saved as .xlsx and .csv files. These files are saved on a CD-ROM disc which is provided with the physical thesis copy.

Material curation

Raw sample, Light microscope slides, SEM stubs and palynological preparations for HD, GB, BP, DE98,99,100 are stored at the Centre for Palynology at The University of Sheffield, Sheffield, U.K. Raw sample, Light microscope slides, SEM stubs and palynological preparations for the M50 are housed in the Micropalaeontological unit at the Natural History Museum, London, U.K. Raw sample, Light microscope slides, SEM stubs and palynological preparations for Ammons Hill, Rumney and USK are housed at the British Geological Survey, Keyworth, U.K.

7. Systematic palaeontology

7.1. Taxa

Trilete spores

94 species in 25 genera are described here, with 73 apparently novel species.

Genus	Species	Reference	Plate, fig.
Acinosporites	*salopiensis*	Richardson and Lister 1969	Plate III, m – o
Ambitisporites	*avitus – dilutus*	Hoffmeister, 1959	Plate IV, d – e
Ambitisporites	*eslae*	(Cramer and Diez) Richardson et al. 2001	Plate IV, f
Ambitisporites	*tripapillatus*	Moreau-Benoit 1976	Plate IV, g
Ambitisporites	*warringtoni*	(Richardson and Lister) Richardson *et al.* 2001	Plate IV, h – i
Ambitisporites	sp. A	Wellman and Richardson 1996a	Plate IV, j
Amicosporites	*miserabilis*	(Cramer) Cramer and Diez 1975	Plate V, b
cf. *Amicosporites*	sp.		Plate V, c – d
Aneurospora	cf. *geikiei*	Wellman and Richardson 1996	Plate V, f
Aneurospora	*gerreinnei*	Steemans 1989	Plate V, g
Aneurospora	*goensis*	Streel 1964	Plate V, h
Aneurospora	*isidori*	(Cramer and Diez) Richardson *et al* 1984	Plate V, i
Aneurospora	*kensingtonii*	sp. nov.	Plate V, j
Aneurospora	cf. *richardsonii*	(Rodriguez) Richardson *et al* 2001	Plate V, k
Aneurospora	*sheafensis*	sp. nov.	Plate V, l
Aneurospora	*trilabiata*	Richardson 2011	Plate V, m – n
Aneurospora	cf. sp. A	Wellman *et al.*, 2000	Plate V, o
Apiculiretusispora	*asperata*	Burgess and Richardson 1995	Plate II, a
Apiculiretusispora	*microconus*	Richardson and Lister 1969	Plate II, b
Apiculiretusispora	*sceacga*	sp. nov.	Plate II, i – k
Apiculiretusispora	*spicula*	Richardson and Lister 1969	Plate II, c
Apiculiretusispora	cf. *spicula*	Richardson and Lister 1969	Plate II, d
Apiculiretusispora	*synorea*	Richardson and Lister 1969	Plate II, e
Apiculiretusispora	Sp. A	Burgess and Richardson 1995	Plate II, f
Apiculiretusispora	Sp. B	Burgess and Richardson 1995	Plate II, g
Apiculiretusispora	Sp. C	Richardson and Lister 1969	Plate II, h
Archaeozonotriletes	*chulus* var. *chulus*	(Cramer) Richardson and Lister 1969	Plate VII, h – i

Archaeozonotriletes	*chulus* var. *nanus*	Richardson and Lister 1969	Plate VII, j - k
Archaeozonotriletes	cf. *chulus*		Plate VII, l
Brochotriletes	sp. 1		Plate III, p
Chelinospora	*cassicula*	Richardson and Lister 1969	Plate VIII, a – d
Chelinospora	cf. *cantabrica*	Richardson and Ioannides 1973	Plate VIII, c – f
Chelinospora	*obscura*	Burgess and Richardson 1995	Plate VIII, g
Chelinospora	*retorrida*	Turnau 1986	Plate VIII, h
Chelinospora	*vermiculata*	Chaloner and Streel 1966	Plate VIII, i – j
Concentricosporites	*saggitarius*	Rodriguez 1983	Plate V, a
Cymbosporites	*dittonensis*	Richardson and Lister 1969	Plate VII, m
Cymbosporites	*echinautus*	Richardson and Lister 1969	
Cymbosporites	cf. *verrucosus*	Richardson and Lister 1969	Plate VII, n
Dibolisporites	sp. 1		Plate II, l – m
Dibolisporites	sp. 2		Plate II, n
Dictyotriletes	*williamsii*	Higgs, 2004	Plate III, q
Dictyotriletes	Sp. A	Richardson and Lister 1969	Plate III, r
Emphanisporites	*epicautus*	Richardson and Lister 1969	Plate III, a
Emphanisporites	cf. *epicautus*	Richardson and Lister 1969	Plate III, b
Emphanisporites	*corralinus*	Richardson and Lister 1969	Plate III, c – d
Emphanisporites	*micrornatus*	Richardson and Lister 1969	Plate III, e – f
Emphanisporites	cf. *micrornatus*	Richardson and Lister 1969	Plate III, g – h
Emphanisporites	*neglectus*	Vigran 1964	Plate III, i – j
Emphanisporites	cf. *rotatus*	(McGregor) McGregor and Camfield 1973	Plate III, k – l
Ibereospora	*glabella*	Cramer and Diez 1975	Plate VI, b – c
Insolisporites	*bassetti*	Burgess and Richardson	Plate VII, d
Insolisporites	*anchistinus*		Plate VII, e
Leonispora	*argovejo*	Cramer and Diez 1975	Plate V, e
Lophonzotriletes	*poecilomorphus*	Richardson and Ioannides 1973	Plate VII, f
Lophonzotriletes	cf. sp. A		Plate VII, g
Perotrilites	*microbaculatus* var. *microbaculatus*	Richardson and Lister 1969	Plate IV, a
Perotrilites	*microbaculatus* var. *attenuatus*	Richardson and Lister 1969	Plate IV, b
Perotrilites	sp. A	Wellman *et al*. 2000	Plate IV, c
Retusotriletes	*dittonensis*	Richardson and Lister 1969	Plate I a – b
Retusotriletes	cf. *dittonensis*	Richardson and Lister 1969	Plate I, c
Retusotriletes	*fraudator*	sp. nov.	Plate I, d
Retusotriletes	cf. *goensis*	Lele and Streel 1969	Plate I, e
Retusotriletes	*maculatus*	McGregor and Camfield 1976	Plate I, f
Retusotriletes	cf. *maculatus*	McGregor and Camfield 1976	Plate I, g – h
Retusotriletes	*minor*	Kedo 1963	Plate I, i - j
Retusotriletes	cf. *minor*	(Kedo) Richardson and Lister 1969	Plate I, k
Retusotriletes	*triangulatus*	(Streel) Streel 1967	Plate I, l
Retusotriletes	cf. *triangulatus*	(Streel) Streel 1967	Plate I, m
Retusotriletes	Sp. A	Wellman *et al*. 2000	Plate I, n
Retusotriletes	Sp. A	Burgess and Richardson 1995	Plate I, o
Scylaspora	*downiei*	Burgess and Richardson 1995	Plate VI, d
Scylaspora	Sp. 1		Plate VI, e
Scylaspora	Sp. 2		Plate VI, f – g
Streelispora	*newportensis*	(Chaloner and Streel) Richardson and Lister 1969	Plate VI, h – i
Streelispora	*granulata*	Richardson and Lister 1969	Plate VI, j
Stellatispora	*Inframurinatus* var. *inframurinatus*	Burgess and Richardson 1995	Plate IX, a

Stellatispora	*Inframurinatus* cf. var. *inframurinatus*	Burgess and Richardson 1995	Plate IX, b
Stellatispora	*Inframurinatus* cf. var. *cambrensis*	Burgess and Richardson 1995	Plate IX, c
Synorisporites	*downtonensis*	Richardson and Lister 1969	Plate VI, k – l
Synorisporites	cf. *labeonis*	Burgess and Richardson 1995	Plate VI, m
Synorisporites	cf. *libycus*		Plate VI, n
Synorisporites	*tripapillatus*	Richardson and Lister 1969	Plate VI, o – p
Synorisporites	*verrucatus*	Richardson and Lister 1969	Plate VII, a – b
Synorisporites	? Sp. B	Burgess and Richardson 1995	Plate VII, c
Zonate spores			Plate XIV, g – h

Table III-1: trilete spore genera and species reported in this work.

Cryptospores

38 species in 15 genera are described here, with 17 apparently novel species.

Genus	**species**	**Reference**	**Plate, fig.**
Abditudyadus	*laevigatus*	Wellman and Richardson, 1996	Plate IX, e - f
Acontotetras	*inconspicuis*	Richardson 1996a	Plate X, j – k
Artemopyra	*brevicosta*	Burgess and Richardson 1991	Plate XI, f – h
Artemopyra	cf. *radiata*	Breuer *et al*., 2007	Plate XI, i
Artemopyra	*recticosta*	Burgess and Richardson 1991	Plate XI, j – k
Artemopyra	cf. *inconspicuis*	Breuer *et al*., 2007	Plate XI, l
Chelinohilates	*erraticus*	Richardson 1996a	Plate XII, i – k
Chelinohilates	*sinuosus* var. *sinuosus*	Wellman and Richardson 1996	Plate XIV, a
Cheliotetras	*caledonica*	Wellman and Richardson 1993	Plate X, b
Cymbohilates	*allenii* var. *allenii*	Richardson 1996a	Plate XI, m
Cymbohilates	*allenii* var. *magnus*	Richardson 1996a	Plate XII, a
Cymbohilates	*cymosus*	Richardson 1996a	Plate XII,, b – c
Cymbohilates	*disponerus*	Richardson 1996a	Plate XII, d
Cymbohilates	*horridus* var. *splendidus*	(Richardson) Richardson 2012	Plate XII, e
Cymbohilates	*horridus* var. *horridus*	(Richardson) Richardson 2012	Plate XII, f
Cymbohilates	*mesodecus*	Richardson 2011	Plate XII, g – h
Cymbohilates	cf. *mesodecus*	Richardson 2011	Plate XIII, a
Cymbohilates	*rhabdionus*	Richardson 2011	
Cymbohilates	*variabilis* var. *variabilis*	Richardson 1996a	Plate XIII, b – c
Cymbohilates	*variabilis* var. *parvidecus*	Richardson 1996a	Plate XIII, d – e
Cymbohilates	*variabilis* var. *tenuis*	Richardson 1996a	Plate XIII, f
Cymbohilates	*variabilis* var. A	Richardson 1996a	Plate XIII, g – h
Dyadospora	*murusattenuata* - *murusdensa*	(Strother and Traverse) emend Burgess and Richardson 1991.	Plate X, l – n
Hispanaediscus	cf. *major*	Burgess and Richardson 1995	Plate XIV, b
Hispanaediscus	*verrucatus*	(Cramer) Burgess and Richardson 1995	Plate XIV, c – d
Laevolancis	*divellomedium-plicata*	Burgess and Richardson 1991	Plate XI, b – d
Laevolancis	sp. 1		Plate XI, e
Pseudodyadospora	*laevigata*	Johnson 1985	Plate X, c
Pseudodyadospora	*petasus*	Wellman and Richardson 1996a	Plate X, d – f
Qualisaspora	*fragilis*	Richardson *et al* 1984	Plate XIV, e – f
Rimosotetras	*problematica*	Burgess 1991	Plate XI, a

Segestrespora	sp. 1		Plate IX, d
Tetrahedraletes	*medinensis*	Strother and Traverse 1979	Plate X, g – i
Velatitetras	*anatoliensis*	Burgess and Richardson 1991	Plate IX, j
Velatitetras	*laevigata*	Burgess and Richardson 1991	Plate IX, g
Velatitetras	*reticulata*	Burgess and Richardson 1991	Plate IX, h – i

Table III-2: cryptospore genera and species reported in this work.

7.2. Trilete spores

RETUSOID TRILETE SPORES

Anteturma SPORITES Potonié 1893
Turma TRILETES Reinsch 1891
Subturma AZONOTRILETES Luber 1935
Infraturma LAEVIGATI (Bennie and Kidston) Potonié and Kemp 1954

Genus RETUSOTRILETES (Naumova) Richardson 1965 non. Streel 1964

TYPE SPECIES: *Retusotriletes pychovii* Naumova 1953 (lectotype species of Richardson, 1965).

TYPE LOCALITY: Moscow Basin, Russia (Russian Platform).

DIAGNOSIS: Proximally and distally laevigate trilete spores with subequatorial curvaturae perfectae which clearly delimit contact areas on the proximal face.

BOTANICAL AFFINITIES: *Retusotriletes* sp. have been found *in situ* in a number of higher plant taxa, including *Renalia hueberi* (*Retusotriletes* sp.) (Gensel, 1976), *Zosterophyllum* cf. fertile (*R.* cf. *R. dubius*) (Edwards, 1969b), *Psilophyton dawsonii* (*R.* cf. *R. triangulatus*) (Streel, 1967; Banks *et al*., 1975) and *P. princeps* (*Retusotriletes* sp.) (Hueber, 1968).

Retusotriletes dittonensis Richardson and Lister 1969
Plate I figures a - b

STRATIGRAPHIC RANGE: Lower micrornatus – newportensis subzone.

DIAGNOSIS: Curvaturae perfectae well developed, contact areas slightly depressed; exine of variable thickness, with the greatest thickness distally.

DESCRIPTION: 33 - 47µm, mean 39µm (three specimens measured). Amb is circular in polar compression. Exine thickness varies between proximal and distal surfaces, being thickest distally. Curvaturae perfectae produce narrow ridges <1µm wide delimiting a distinct contact area $\frac{2}{3}$ to $\frac{3}{4}$ of the radius of the spore. The contact area itself is flattened or slightly concave, and one interadial area may be larger than the other two. A subtle apical thickening is sometimes observed. The contact areas may be shagrinate, faintly striate or infragranular, with the exine outside the contact areas being laevigate and raised. The triradiate mark extends $\frac{3}{5}$ to $\frac{3}{4}$ of the spore radius and in some specimens exhibits low lips.

COMPARISONS AND REMARKS: These specimens compare well with the original specimens described in Richardson and Lister (1969).

Retusotriletes* cf. *dittonensis Richardson and Lister 1969
Plate I figure c

STRATIGRAPHIC RANGE: Non-tripapillate *Aneurospora* spp. zone; *Apiculiretusispora* sp. E zone

DESCRIPTION: 21 - 23μm (two specimens measured). Amb is circular in polar compression. Exine is thickest distally. Curvaturae perfectae produce narrow ridges <1μm wide which delimit the occasionally concave contact area, $\frac{2}{3}$ to $\frac{3}{4}$ of the radius of the spore. Occasionally one interadial area may be larger than the other two; apical thickening is sometimes observed. The contact areas may be shagrinate, faintly striate or infragranular, with exine outside the contact areas being laevigate and raised. The triradiate mark extends $\frac{3}{5}$ to $\frac{3}{4}$ of the spore radius and in some specimens exhibits low lips.

COMPARISONS AND REMARKS: Amb diameters in the original specimen descriptions for *R. dittonensis* in Richardson and Lister (1969) range between 35 – 57μm. These specimens fall distinctly below that range (21 - 23μm) despite being otherwise similar in morphology.

Retusotriletes fraudator sp. nov.
Plate II figure d

HOLOTYPE: Plate II, figure d. Slide 19M5001.3, E.F. no. N21-3, Freshwater West Formation, Ross – Tewkesbury Spur Motorway (M50), Hereford and Worcester.

SYNONYMS:
Barclay et al., 1994; *Retusotriletes* cf. *Emphanisporites epicautus*

DERIVATION OF NAME: From the Latin for deceit. So named because of the distinct similarity to *Emphanisporites epicautus*, particularly the thickenings associated with the proximal apex and y-rays, although *R. fraudator* lacks interadial muri.

STRATIGRAPHIC RANGE: Lower to middle *micrornatus* – *newportensis* subzone.

DIAGNOSIS: Circular to subcircular laevigate spores, with a well-defined proximal face marked by clear curvaturae perfectae. The Y-rays are distinctive in that they exhibit triangular thickenings where the Y-rays diverge into curvaturae perfectae and are also often accompanied by a circular to triangular thickening at the proximal pole.

DESCRIPTION: 21 – 44μm, mean 31μm (fifteen specimens measured). Circular to subcircular ambs. Laevigate proximally and distally. Contact areas clearly defined by distinct curvaturae perfectae, with the contact face comprising $\frac{3}{4}$ to $\frac{4}{5}$ of the spore diameter. The triradiate mark is distinct with laesurae

extending between $\frac{2}{3}$ – $\frac{4}{5}$ of the amb radius. Rarely, the triradiate mark is accompanied by lips 0.7µm wide. Laesurae and lips extend to the near equatorial curvaturae perfectae, where they diverge. There is distinct invagination at the junction. In some specimens (*c.* 60%) a circular to triangular apical thickening is developed, which extends $\frac{1}{3}$ - $\frac{1}{2}$ of the length of the laesurae. In all specimens, a triangular shaped thickening, between 1.2 – 3.5µm, mean 2.2µm, is developed where the Y-rays diverge into the curvaturae perfectae. The apex of the triangle in directed towards the proximal pole, and the thickening is approximately equivalent to the invagination of the curvaturae perfectae.

COMPARISONS AND REMARKS: The Y-ray thickenings at the Y-ray – curvaturae perfectae juncture distinguish this species of *Retusotriletes*. The Y-ray thickenings, amb shape and size are reminiscent of *E. epicautus*, but *R. fraudator* lacks the well-defined interadial muri. *R. minor* is similar but the curvaturae are confluent with the equator in interadial areas. Could be comparable to *R. actinomorphus* Chibrikova 1962 which has curvaturae perfectae, well developed contact areas and lacks an apical thickening, but may also lack the Y-ray thickening. There is little cause to differentiate the species further to account for the presence/ absence of lips and apical thickenings with the current data set, given similar morphometrics and stratigraphic range.

Retusotriletes* cf. *goensis (Streel) Lele and Streel 1969

Plate I figure e

STRATIGRAPHIC RANGE: Non-tripapillate *Aneurospora* spp. zone; *Aneurospora sheafensis* subzone.

DESCRIPTION: 23 (34.6) 50µm (five specimens measured), circular amb. Proximally and distally laevigate. Curvaturae perfectae distinct, interadial curvaturae perfectae are confluent with equator; with gentle but distinct invagination where the lipless triradiate mark diverges. Variously subtle circular apical thickening.

COMPARISONS AND REMARKS: Amb diameter in Lele and Streel (1969) for *R. goensis* ranges between 38 – 80µm, whilst some of these specimens correspond with those measurements, the mean amb diameter (34.6µm) falls just below. Richardson and Ioannides (1973) described spores somewhat comparable to these *R.* cf. *goensis* from North Africa, especially in terms of size, where they correspond well (North Africa: 27 (37.5) 50µm, Anglo-Welsh Basin: 23 (34.6) 50µm). Both the North African specimens and those described here are slightly smaller than those specimens detailed in Lele and Streel (1969), however, the specimens detailed in Richardson and Ioannides (1973) are somewhat more triangular than those described here and in Lele and Streel (1969).

Retusotriletes maculatus McGregor and Camfield 1976

Plate I figure f

STRATIGRAPHIC RANGE: Lower – middle *micrornatus* – *newportensis* subzones.

DIAGNOSIS: Subcircular to subtriangular amb, trilete mark $\frac{1}{2}$ to near equatorial in extent, occasionally accompanied by narrow folds. Near equatorial divergence of curvaturae perfectae delimit the contact areas; proximal face laevigate except for large interadial papillae. Exine laevigate, may show concentric folds near the equator.

DESCRIPTION: 32μm (One specimen measured). Subcircular to circular amb. Proximally laevigate apart from three interadial papillae, one in each contact area. Papillae are oval to rounded, 6.9μm in diameter. The triradiate mark is distinct with laesurae extending close to the equator. The triradiate rays extend $\frac{2}{3}$ to near equatorial limits, where they diverge into curvaturae perfectae, with prominent invaginations. Distally, the exine is entirely laevigate.

COMPARISONS AND REMARKS: The amb diameters of *R. maculatus* McGregor and Camfield are 35 (49) 58μm, which while larger than specimens described here, is not distinctly so. The interadial papillae in McGregor and Camfield's (1976) specimens have a diameter between 8 - 12μm, while those described here exhibit smaller interadial papillae, 7μm which is not considered significant enough to separate these specimens. The specimens described from Lorne by Wellman and Richardson (1996) are much larger (40 – 67μm).

R. maculatus, and these *R.* cf. *maculatus*, are comparable to *Ambitisporites tripapillatus* in their proximally and distally laevigate sculpture, in addition to the prominent inter radial papillae in each contact area - *A. tripapillatus* exhibits a prominent equatorial crassitude, however, and has more distinct inter radial papillae. Wellman and Richardson (1996) postulate that there is a degree of intergradation between *R. maculatus* and *A. tripapillatus*, based on the considerable coincidence of the spore equator by the curvaturae perfectae in an appreciable number of specimens, thereby forming an equatorial crassitude. However, *R. maculatus* is retained here, as in Wellman and Richardson (1996), within the azonate genus *Retusotriletes* as the majority of specimens have curvaturae perfectae which fall entirely within the proximal face (i.e. not contacting the equator). In those specimens where the curvaturae perfectae do intersect the equator, the crassitude formed is incomplete due to invaginations occurring where laesurae diverge into curvaturae perfectae.

Retusotriletes* cf. *maculatus McGregor and Camfield 1976

Plate I figures g – h

STRATIGRAPHIC RANGE: Lower – middle *micrornatus* – *newportensis* subzones.

DESCRIPTION: Small spores, 11.9 – 19.7μm (two specimens measured), subcircular to subtriangular ambs. Proximally laevigate except for three distinct interadial papillae, one in each area, 2.3 – 4.4μm in diameter. Papillae are arranged relatively closely to the proximal pole. The triradiate mark is distinct but lacks lips, with laesurae extending $\frac{2}{3}$ to $\frac{4}{5}$ of the amb radius before diverging into distinct curvaturae perfectae; a slight invagination is present at the radial juncture. Distally laevigate.

COMPARISONS AND REMARKS. These spores are broadly comparable to *R. maculatus* in that the spore is retusoid with interadial papillae, however these species are distinguished by (1) smaller amb size, (2) curvaturae perfectae which are not confluent with the equator, as in *R. maculatus*, (3) small papillae arranged very close to the proximal pole, and (4) lack of lips accompanying the triradiate mark.

Retusotriletes minor Kedo 1963

Plate I figures i – j

STRATIGRAPHIC RANGE: Non-tripapillate *Aneurospora* spp. zone (*Apiculiretusispora* sp. E subzone) – middle *micrornatus* – *newportensis* subzone.

DIAGNOSIS: Circular to subtriangular amb, with a thin, proximally and distally laevigate. Contact areas are often concave with some specimens having a thinned apical region on the contact area. These spores lack lips.

DESCRIPTION: 13 – 46μm, mean 27μm (twenty-five specimens measured). Amb is circular to sub triangular with rounded angles and convex sides. The exine is thin and proximally and distally laevigate. Contact areas are typically concave and some specimens show thinning in the exine towards the proximal pole. The triradiate mark is simple and lacks lips, extending to near equatorial limits and diverging to form curvaturae perfectae which delimit the contact area.

COMPARISONS AND REMARKS: These spores compare well with the original descriptions in Kedo (1963), although the amb size exceeds those given there (26 - 30μm) in some cases.

R. minor is comparable to *Retusotriletes* cf. *minor* Richardson and Lister 1969, although the latter exhibits low lips. *R. minor* is differentiated from. *R. simplex* Naumova 1959 by the presence of lips and curvaturae imperfectae in the latter.

***Retusotriletes* cf. *minor* (**Kedo) Richardson and Lister 1969

Plate I figure k

STRATIGRAPHIC RANGE: Non-tripapillate *Aneurospora* spp. zone (*Apiculiretusispora* sp. E subzone) – middle *micrornatus* – *newportensis* subzone.

DESCRIPTION: 20 - 45μm, mean 30μm (nine specimens measured). Circular amb with a thin, laevigate exine proximally and distally. The triradiate mark is accompanied by distinct lips up to 1μm wide, which extend to the curvaturae perfectae. Curvaturae perfectae are confluent with the equator in interadial areas.

COMPARISONS AND REMARKS: Comparable to *Retusotriletes* cf. *minor* Richardson and Lister 1969, although in some cases the amb size of these specimens exceeds the measurements given in the original descriptions (14 - 36μm). *R. minor* is differentiated from. *R. simplex* Naumova 1959 by the presence of lips and curvaturae imperfectae in the latter. These spores are similar to *Ambitisporites warringtoni* (Richardson and Lister) Richardson. *R.* cf. *minor* is distinguishable in that it has a circular amb, whilst *A. warringtoni* is distinctly triangular.

Retusotriletes triangulatus (Streel) Streel 1967

Plate I figure l

STRATIGRAPHIC RANGE: Non-tripapillate *Aneurospora* spp. zone (*Apiculiretusispora* sp. E subzone) – middle *micrornatus* – *newportensis* subzone.

SYNONYMS:

Streel, 1964; *Phyllothecotriletes triangulatus*

DIAGNOSIS: Amb is circular to sub circular with a laevigate exine. Contact areas are delimited by distinct curvaturae perfectae which are equatorial except in radial areas. Sutures are distinct with a pronounced triangular thickening encompassing the apical part of the triradiate mark.

DESCRIPTION: 41 - 60μm (seven specimens measured), spores have a circular to sub-circular amb with a thin, laevigate exine and are typically preserved in polar or slightly oblique compression. The triradiate mark is distinct and extends $\frac{2}{3}$ to $\frac{3}{5}$ of the spore radius before diverging into well-defined curvaturae which follow the equatorial margin in interadial areas, delimiting the proximal face. A conspicuous triangular thickening in the apical region of the contact area is exhibited in these spores. The triangular thickening may be variably dense, and may show concave, straight or slightly convex sides. The triradiate mark within the triangular thickening remains pronounced and extends *ca.* $\frac{1}{2}$ of the spore radius. May show some folding.

COMPARISONS AND REMARKS: *'Calamospora' witneyana* Chaloner 1963, *Phyllothecotriletes triangulatus* and *P. rotundus* are all comparable to *R. triangulatus*. *C. witneyana* however is much larger. *P. rotundus* is comparable in size to *R. triangulatus* but the apical thickening is most reminiscent of *P. triangulatus*. Distinguishable from *R.* sp. A in that the exine is generally robust and lacks extra-exosporal material.

Retusotriletes* cf. *triangulatus (Streel) Streel 1967

Plate I figure m

STRATIGRAPHIC RANGE: Non-tripapillate *Aneurospora* spp. zone (*Apiculiretusispora* sp. E subzone) – middle *micrornatus – newportensis* subzone.

DESCRIPTION: 26 - 38μm, mean 33μm (five specimens measured) circular ambs. Robust exine, proximally and distally laevigate. Well-defined curvaturae perfectae do not intersect the equator. Triradiate ark distinct, accompanied by a robust, triangular apical thickening which extends $\frac{1}{2}$ of the length of the Y-rays.

COMPARISONS AND REMARKS: Whilst essentially identical to *R. triangulatus* (Streel) Lele and Streel 1967, these specimens are distinctly smaller. Wellman *et al*. (2000) also described a population of *R.* cf. *triangulatus* from the middle *micrornatus – newportensis* zone of the Anglo-Welsh Basin. These spores measured 38 (45) 54μm, however, and are as such larger than the specimens described here, although there is some overlap in amb size.

***Retusotriletes* sp. A** Wellman *et al* 2000

Plate I figure n

STRATIGRAPHIC RANGE: Non-tripapillate *Aneurospora* spp. zone (*Apiculiretusispora* sp. E subzone) – middle *micrornatus – newportensis* subzone.

DESCRIPTION: 24 – 57μm, mean 40μm (twenty-five specimens measured). Circular amb, exine thin and often folded. Proximally, contact face distinct, bounded by distinct curvaturae perfectae 0. 5 - 1μm wide. The triradiate mark is distinct, accompanied by a triangular apical thickening which may extend half-way to the entirety of the extent of the Y-rays. Proximally and distally affected by variously distributed extra-exosporal material, possibly tapetal in origin. Typically globular, the material does not exceed 1.3μm in size.

COMPARISONS AND REMARKS: Differs from *R.* cf. *triangulatus* in its thin and frequently folded exine, and in the abundant extraexosporal material. Wellman *et al*. (2000) described essentially identical spores, although the specimens described here are smaller with a distinctly different mean amb diameter.

***Retusotriletes* sp. A** Burgess and Richardson 1995
Plate I figure o

STRATIGRAPHIC RANGE: *Tripapillatus* – *spicula* biozone

DESCRIPTION: 29 – 31μm (two specimens measured). Subtriangular to subcircular amb, triradiate mark indistinct or accompanied by narrow lips <1μm. Sutures merge into subequatorial – equatorial curvaturae perfectae. Narrow rugulae and scabrae ornament the interadial areas, and about the proximal pole a triangular thinning is developed, which is delimited by a laevigate ridge. The thinning extends 2/3 of the length of the sutures. Distally laevigate.

COMPARISON AND REMARKS: These spores are comparable to the specimens figured in Burgess and Richardson (1995). These spores differ from *R. triangulatus* in that the triangular region about the proximal pole is thinned rather than thickened and is accompanied by ridges. Furthermore, the rugulae and scabrae and smaller amb size differentiate *R.* sp. A further from *R. triangulatus.*

Infraturma APICULATI (Bennie and Kidston) Potonié and Kremp 1954
Genus APICULIRETUSISPORA Streel 1964

TYPE SPECIES: *Apiculiretusispora brandtii* Streel 1964

TYPE LOCALITY: Goé, Belgium.

DIAGNOSIS: Retusoid apiculate spores with a distally ornamented exoexine of spinae or coni. The proximal face may be laevigate, ornamented or murornate.

BOTANICAL AFFINITIES: *In situ* spores comparable to dispersed species of *Apiculiretusispora* have been identified in a variety of Late Silurian - Early Devonian Rhyniophyte and Trimerophyte taxa: *Apiculiretusispora* cf. *plicata* in *Cooksonia crassiparietalis* (McGregor, 1973), *Ap. brandtii* in *Psilophyton forbesii* and *P. charientos* (Gensel, 1978), *Ap. brandtii*/*arenorugosa* in *Pertica varia* (Granoff *et al*., 1976) and *Ap. brandtii*/*plicata* in *Pertica dalhousii* (Doran *et al*. 1978).

Apiculiretusispora? asperata Burgess and Richardson
Plate II figure a

STRATIGRAPHIC RANGE: *poecilomorphus* – *libycus* biozone.

DIAGNOSIS: A retusoid azonate miospore with unevenly distributed and irregularly shaped distal microconate and scabrate sculpture outside the rugulate contact areas.

DESCRIPTION: 31 – 45μm, mean 37μm (six specimens measured). Amb subcircular to circular. The triradiate mark is distinct and extend 4/5 of the radius of the spore. The sutures are accompanied by lips

1μm wide. The suturae merge into subequatorial to equatorial curvaturae perfectae. The interadial areas are rugulate. Distally the spores are ornamented with irregular microconi and micrograna <1μm tall and wide, and 0.2 – 1.3μm apart.

COMPARISONS AND REMARKS: These species compare well with *Apiculiretusispora asperata* in terms of morphology and amb size.

Apiculiretusispora microconus Richardson and Lister 1969
Plate II figure b

STRATIGRAPHIC RANGE: Non-tripapillate *Aneurospora* spp. zone (*Apiculiretusispora* sp. E subzone) – middle *micrornatus* – *newportensis* subzone.

DIAGNOSIS: Small spores with minute distal sculpture of barely discernible coni or grana to distinct coni.

DESCRIPTION: 11 – 29μm, mean 20μm (six specimens measured). Subtriangular amb with rounded apices and convex sides. Proximally smooth. The triradiate mark is distinct, with laesurae extending 9/10 of the amb radius, where they diverge to form curvaturae perfectae; these are confluent with the equator in the equatorial areas. Outside of the proximal face, the exine is ornamented with dense microconi, 0.3 – 0.5μm wide, mean 0.3μm approximately isodiametric. Elements are densely arranged, 0.2 – 0.4μm apart, mean 0.2μm.

COMPARISONS AND REMARKS: These specimens correspond well with descriptions given for *A. microconus* in Richardson and Lister (1969). The amb diameter falls within the size description given there (19 - 24μm), and the microconi are comparable in diameter to those given in Richardson and Lister (1969) (0.5 x 0.5μm). While very similar to other *Apiculiretusispora* spp. with dense micrograna, Richardson and Lister (1969) differentiated this species based on the amb size, and this seems to hold here. Other similar species are *A.* sp. B Burgess and Richardson (1995) with an amb diameter between 21.5 - 36μm, and *A.* sp. C Richardson and Lister (1969) with an amb diameter between 40 - 50μm, although their otherwise close similarities hints at a close relationship, further specimens are required to clarify the size relationship between these species as the features of the elements are similar across the three species.

Apiculiretusispora sceacga sp. nov.
Plate II i – k

LOCALITY: Moor Cliffs Formation, Ross – Tewkesbury Spur Motorway (M50), Hereford and Worcester.

HOLOTYPE: Plate II, figure i, Slide M50-85-2C(1) E.F. no. N30-4. Ross – Tewkesbury Spur (M50) Motorway, Herefordshire, UK.

DERIVATION OF NAME: *Sceacga*, from the Latin for rough hair, wool.

STRATIGRAPHIC RANGE: Non-tripapillate *Aneurospora* spp. zone (*Apiculiretusispora* sp. E subzone) – ?lower *micrornatus* – *newportensis* subzone.

DIAGNOSIS: Circular to roundly triangular amb. Distally ornamented with dense, irregular spinae. Triradiate mark distinct, accompanied by lips and extending to the curvaturae perfectae. The proximal contact areas exhibit circular to oblong interadial papillae and a much-reduced ornament of microspinae. Curvaturae perfectae mark the contact areas and are accompanied by radial to tangential spinose ridges.

DESCRIPTION: Circular to subtriangular amb, 25 - 42µm, mean: 35µm, (twenty-one specimens measured) in diameter. The proximal face is delimited by a region of chiefly radial, but also tangential, often anastomosing spinose ridges 0.66 - 4.27µm (mean 2.45µm) long and 0.36 – 1.55µm wide (mean 0.65µm) associated with the curvaturae perfectae. A reduced ornament of dense, blunt tipped spines and cones up to 0.5µm tall are exhibited across the proximal face, and these are often developed into short, anastomosing ridges. The triradiate mark is distinct, extending to the curvaturae perfectae with rays 9 – 15.9µm long (mean 12.3µm), accompanied by lips 1.19 – 1.88µm wide (mean 1.49µm). In each interadial area, circular to oblong inter-radial papillae are developed, one in each area, 5.52 – 8.54µm in diameter (mean 6.65µm). Equatorially and distally the spore is ornamented with extremely dense, irregular spinose ornament. Spines have rounded to pointed tips and are sometimes biform, being 0.22 – 2.14µm tall (mean 0.97µm) and 0.18 – 1.5µm wide (mean 0.54µm), 0.09 – 1.16µm apart (mean 0.45µm). Ornament density 63 – 172 elements/100µm^2, mean 98 elements/100µm^2.

COMPARISONS AND REMARKS: There may be a case for designating an *Ap.* cf. *sceacga*. These spores may have noticeably shorter spines, verging on cones, which are different to *Ap. sceacga* proper, as they are not tall or 'hair like'. This may be a question of taphonomy; i.e. the spines have been destroyed, but even on poor specimens of *Ap. sceacga* hair like spines are preserved, being folded onto the exine rather than broken off. Histograms of spines from *Ap. sceacga* and suspected *Ap.* cf. *sceacga* show normal gaussian distribution for, although are slightly skewed left. For amb diameter, a weakly gaussian distribution is observed when suspected *Ap.* cf. *sceacga* specimens are removed, which is bipolar when they are included. This may point towards a genuine differentiation between the two, but the distinction is not considered strong enough to separate the species at this time.

The proximal face is often lost or partially disrupted in specimens. Exine thickness varies, and the spore is often slightly torn.

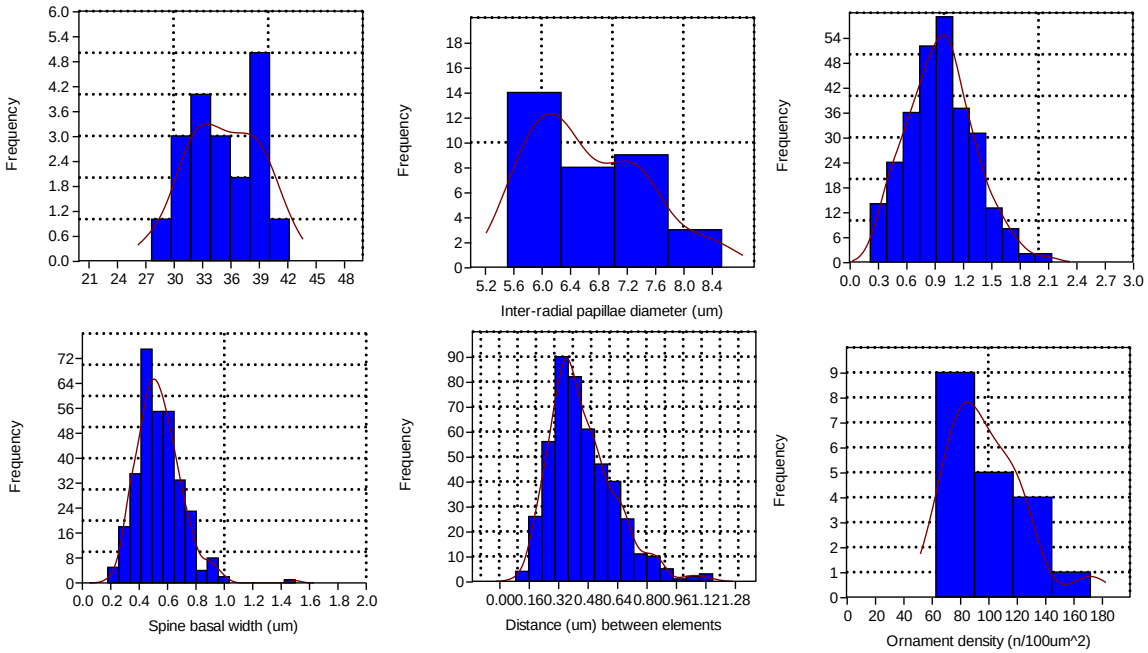

Figure III-7: Morphometrics of Apiculiretusispora *sp. E. top left: amb diameter, top right: spine height.*

It is noted here that two spores have been recorded as *Apiculiretusispora sceacga* (‘*Apiculiretusispora* sp. E’) in the literature. *Apiculiretusispora sceacga* is not correspondent to the *A.* sp. E figured in Richardson et al. (2001), which Rubinstein and Steemans (2002) suggested may be similar to *A. perfecta* Steemans 1989.

Apiculiretusispora spicula Richardson and Lister 1969
Plate II figure c

STRATIGRAPHIC RANGE: *tripapillatus* – *spicula* zone – lower *micrornatus* – *newportensis* subzone.

DIAGNOSIS: Contact areas distinct, sculpture consists of sparse, sharply pointed, slender cones or small spines.

DESCRIPTION: 34 – 37µm (two specimens measured). Relatively large spores with a circular to subcircular ambs. The contact areas are delimited by fine curvaturae perfectae. The triradiate mark is distinct, accompanied by narrow lips 0.6 – 0.9µm wide. The lips and laesurae extend ¾ - 4/5 of the spore radius to the inner edge of the curvaturae perfectae. There is some invagination of the curvaturae perfectae where the laesurae diverge. The proximal face may be laevigate or exhibit faint granules or interadial muri. Equatorially and distally ornamented with spines or cones 0.3 – 0.7µm, wide, mean 0.5µm and 0.3 – 1.5µm, tall, mean 0.9µm. Elements are densely arranged 0.2 – 1.1µm apart, mean 0.6µm with a density of 82 – 86 elements/100µm^2.

COMPARISONS AND REMARKS: These specimens compare favourably with those described in Richardson and Lister (1969). The specimens described here fall into the lower end of the amb size range given there (30 – 46µm). Ornament size differs very subtly, with elements being 0.5 - 1µm wide and 1 – 2µm tall in Richardson and Lister (1969), compared to 0.3 – 0.7µm and 0.3 – 1.5µm respectively in these specimens. Richardson and Lister (1969) also note that the element size is two to four times the basal diameter, and this is fulfilled in these specimens. The distance between elements differs slightly, also, being 1 - 3µm apart in Richardson and Lister (1969) and 0.2 – 1.1µm apart here, and hence slightly denser; this is the most significant difference between these specimens and those of Richardson and Lister (1969). At present, these specimens are kept amongst *A. spicula*.

Apiculiretusispora* cf. *spicula Richardson and Lister 1969
Plate II figure d

.

STRATIGRAPHIC RANGE: *tripapillatus* – *spicula* zone - middle *micrornatus* – *newportensis* subzone.

DESCRIPTION: 21.3 – 23.2µm (two specimens measured), subtriangular to subtriangular ambs. Proximally, the laesurae extend 4/5 to 9/10 of the spore radius, with interadial curvaturae perfectae confluent with the equator. There is a slight invagination where laesurae diverge into the curvaturae perfectae. Equatorially and distally ornamented with cones and spines. Elements range in basal width from 0.4 – 1.1µm, mean 0.6µm, and between 0.6 – 1.2µm tall, mean 0.9µm. The elements are 0.2 – 1.7µm apart, mean 0.6µm with a density of 61 – 87 elements/100µm^2.

COMPARISONS AND REMARKS: These spores fall well below the size range given for *A. spicula* in Richardson and Lister (1969) (30 - 46µm), and considerably below the *A. spicula* described here (34 – 37). These spores also differ from those described in Richardson and Lister in terms of ornament. the

basal width of these spores is slightly greater than that given there (0.5 - 1μm (Richardson and Lister, 1969) vs 0.4 – 1.1μm) also differ slightly (1 - 2μm (Richardson and Lister, 1969) vs 0.6 – 1.2μm). The elements in these spores are spaced slightly closer together than those figured in Richardson and Lister (1969). The most significant difference between these spores and *A. spicula* proper is the amb size, and hence they are not differentiated further. Interestingly, there appears to be some continuation between the elements measured in *A. spicula* and *A.* cf. *spicula* from these assemblages. It may be that this is a population of *A.* cf. *spicula* with some overlap in amb size with *A. spicula* proper, but more specimens are required to test this. Height: width ratio is 1.3, so the elements appear to be verging towards to isodiametric.

Apiculiretusispora synorea Richardson and Lister 1969
Plate II figure e

STRATIGRAPHIC RANGE: *tripapillatus* – *spicula* zone – middle *micrornatus* – *newportensis* subzone.

DESCRIPTION: *c.*26.2μm (one specimen measured). Subcircular amb with a relatively thick, dark exine. Proximally smooth with some minor folds on the proximal exine. Triradiate mark distinct, accompanied by lips 2.4μm wide. Lips extend to inner edge of curvaturae perfectae. Outside of the proximal area the exine is sculptured by approximately isodiametric cones with a height: width ratio of 1:1. The cones are 0.7 – 1.5μm tall, mean 1.1μm, and 0.8 – 1.2μm in width, mean 1.1μm. Elements are densely packed, being 0.2 – 0.9μm apart, mean 0.51μm. In plan, they either taper smoothly from base to tip, or exhibit rapidly tapered bases topped with slender, pointed tips.

COMPARISONS AND REMARKS: These spores correspond well with the original descriptions given in Richardson and Lister (1969). The amb size, whilst difficult to measure due to tipping is *c.* 26μm, which is at the lower end of the size range given in the original descriptions (26 - 43μm). Element height, width and distribution also compares well to the original descriptions of Richardson and Lister (1969): 0.5 – 1.5μm tall and wide, 0.5 - 1μm apart. Crucially, the description of the elements is very similar. In the original descriptions, elements are "… rounded in plan, in profile may be uniformly tapered, or have rapidly tapered bases surmounted by slender pointed stems…" (Richardson and Lister, 1969; pp. 221). The elements here are identical to that description.

***Apiculiretusispora* sp. A** Burgess and Richardson 1995
Plate II figure f

STRATIGRAPHIC RANGE: *poecilomorphus* – *libycus* zone - *tripapillatus* – *spicula* zone.

DESCRIPTION: 21 – 42μm, mean 28μm (seven specimens measured). Subcircular to subtriangular ambs with laevigate contact areas. Trilete mark is distinct, accompanied by narrow lips, <1μm wide. The triradiate mark extends up to $\frac{7}{8}$ of the spore radius before merging into subequatorial curvaturae perfectae. Distally, the spores are ornamented with dense spinae and rare coni, <0.5μm apart, 0.5μm wide and up to 1.5μm tall, but generally <1μm.

COMPARISONS AND REMARKS: These correspond well with the original descriptions for the species in Burgess and Richardson (1995) in terms of amb diameter and ornament size, although in some cases the amb diametr is larger than in the original specimens. These spores differ from *A.* sp. B Burgess and Richardson in that *A.* sp. A exhibits spinose ornament, whilst *A.* sp. B exhibits coni.

***Apiculiretusispora* sp. B** Burgess and Richardson 1995
Plate II figure g

STRATIGRAPHIC RANGE: *tripapillatus* – *spicula* zone - lower *micrornatus* – *newportensis* subzone.

DESCRIPTION: 25 – 43µm, mean 33µm (seventeen specimens measured). Subcircular to subtriangular ambs with laevigate contact areas. Distinct trilete mark accompanied by low lips 1.5µm wide, extending ¾ to $^{9}/_{10}$ of the amb radius. Laesurae then diverge to form sub-equatorial to equatorial curvaturae perfectae. Distally ornamented with densely packed microconi/ rare grana typically 0.07 – 0.8µm apart, mean 0.4µm. Elements ± isodiametric, 0.2 – 0.7µm wide, mean 0.3µm.

COMPARISONS AND REMARKS: These spores correspond well with the descriptions given in Burgess and Richardson (1995) in terms of amb size (21 - 36µm) and element diameter, although element height is slightly smaller in these specimens than those in Burgess and Richardson (1995) (height up to 1µm), but this difference is negligible. Additionally, amb size is larger in some specimens.

***Apiculiretusispora* sp. C** Richardson and Lister 1969
Plate II figure h

STRATIGRAPHIC RANGE: Non-tripapillate *Aneurospora* spp. zone (*Apiculiretusispora* sp. E subzone) – middle *micrornatus* – *newportensis* subzone.

DESCRIPTION: 40.4 – 43µm, mean 41.8µm (three specimens measured). Subcircular to subtriangular ambs. Proximally laevigate with a distinct triradiate mark. The laesurae extend ¾ to 4/5 of the amb radius before they diverge into well defined curvaturae perfectae, which are confluent with the equator in interadial areas. Outside of the proximal face, the exine is densely ornamented with microconi and grana, 0.2 – 0.8µm wide, mean 0.4µm, approximately equidimensional, elements are spaced 0.2 – 1.4µm apart, mean 0.4µm.

COMPARISONS AND REMARKS: These spores correspond well with descriptions given for *A.* sp. C in Richardson and Lister (1969), although some elements are further apart than given in the original descriptions, most fall within the measurements.

Genus DIBOLISPORITES Richardson 1965

TYPE SPECIES: *Dibolisporites echinaceus* (Eisenack) Richardson 1965

TYPE LOCALITY: Baltic

DIAGNOSIS: Radial, trilete, azonate miospores. Amb subcircular to subtriangular. Dominantly biform sculptural elements but otherwise highly variable, including cones, rod-like processes, pila, verrucae and spines. These spores lack anastomosing ridges such as those seen in *Acinosporites. Dibolus* – two pointed; refers to chiefly biform elements on the distal and equatorial regions of the spores.

BOTANICAL AFFINITIES: *Wattiezia*

***? Dibolisporites* sp. 1**

Plate II figures l – m

STRATIGRAPHIC RANGE: Non-tripapillate *Aneurospora* spp. zone (*Apiculiretusispora* sp. E subzone) – middle *micrornatus* – *newportensis* subzone.

DESCRIPTION: 29 – 36µm, mean 33µm (four specimens measured). Circular amb, proximal face missing. Equatorially and distally ornamented with very sparse, slender spines, 2.2 – 3.4µm tall, mean 2.8µm, with a basal width of 0.4 - 1µm, mean 0.6µm and 2.2 – 4.3µm apart, mean 3.2µm.

COMPARISONS AND REMARKS: These spores differ from those *D.* sp. 2. The spines are long and slender, with subtle bifurcation, and are much taller and thinner than those of *D.* sp. 2. Some *D. eifeliensis* figured in the literature (e.g. Breuer *et al*., 2007, their Plate 6, figures 9.) have long, slender, sparsely distributed spines, but they are denser than in this specimen.

***? Dibolisporites* sp. 2**

Plate III figures n

STRATIGRAPHIC RANGE: Non-tripapillate *Aneurospora* spp. zone (*Apiculiretusispora* sp. E subzone) – middle *micrornatus* – *newportensis* subzone.

DESCRIPTION: 20.2 – 37.8µm, mean 31.6µm (eight specimens measured). Circular amb, proximally laevigate. The proximal face is often lost, but where present exhibit an indistinct trilete mark and sub equatorial curvaturae perfectae. Equatorially and distally ornamented with predominantly biform elements. These are variable, with most being wide based before narrowing tightly and then expanding back into a bulbous tip. Some elements are stout. While others are tall. Other elements may be sharply tipped spines and cones, pilae, or may even bifurcate at the tip. Elements are 0.6 – 3.1µm tall, mean 1.7µm, and 0.5 – 1.4µm wide at the base, mean 0.9µm. They are variously densely arranged, with elements 0.3 – 2.7µm apart, mean 0.9µm.

DESCRIPTION: These spores conform to the description of *Dibolisporites* given their predominantly biform elements, but do not appear to conform to any published examples. The spinae of these spores are more robust that those of ?*D.* sp. 1.

Infraturma MURORNATI Potonié and Kremp 1954

Genus EMPHANISPORITES McGregor 1961

TYPE SPECIES: *Emphanisporites rotatus* McGregor 1961

TYPE LOCALITY: Battery Point Formation, Gaspé Pensinsula, Canada.

DIAGNOSIS: Radial, trilete spores exhibiting a distinctive ornament of variously sized and well-defined inter-radial muri on the proximal contact areas. The distal exoexine may be laevigate or ornamented.

BOTANICAL AFFINITIES: Mesofossils yielding *in situ Emphanisporites* have been recovered from Scotland (Rhynie Chert) and the Anglo-Welsh Basin (NBCH and M.50), chiefly the latter. Diverse sporangial morphologies are found, ranging from bifurcating to cylindrical to discoid. The sporangia are derived from at least two lineages, and most have unknown affinities. *In situ* and ultrastructural work suggests tracheophytic and possibly bryophytic (hornwort) affinities. While most are categorised amongst the rhyniophytoids, their affinities are unknown.

Emphanisporites corralinus sp. nov.
Plate III figures c - d

STRATIGRAPHIC RANGE: Non-tripapillate *Aneurospora* spp. zone (*Apiculiretusispora* sp. E subzone).

DERIVATION OF NAME: from the Latin for the radial septa in coral.

HOLOTYPE: Plate III, figure c. Slide 19M50-24.3, E.F. no. K18-1, Freshwater West Formation, Ross – Tewkesbury Spur Motorway (M50), Hereford and Worcester.

Diagnosis: Circular to subtriangular spores, Distally laevigate with distinct interadial muri. The radial muri taper sharply towards the proximal pole and appear 'ragged' under light microscope.

DESCRIPTION: 19.4 – 24.5µm, mean 21.4µm (six specimens measured). Amb circular to subtriangular. Proximal face bounded by equatorial curvaturae perfectae. The trilete mark is indistinct, extending to the equator. interadial areas exhibit 5 – 8 low, robust interadial muri, which extend at least ½ to all of the amb radius, generally the latter. Muri are strongly tapered towards the apex, between 0.6 – 2.6µm wide, mean 1.4µm, and sinuous. Distally laevigate.

COMPARISONS AND REMARKS: These spores are distinguished by their distinctively wide tapering, sinuous, 'ragged' muri. Other species of *Emphanisporites* such as *E. rotatus* exhibit straight to slightly tapering muri, which are solid and robust. Other species with finer interadial muri, such as *E. neglectus*, do not appear 'ragged'.

Emphanisporites epicautus Richardson and Lister 1969
Plate III figure a

STRATIGRAPHIC RANGE: Non-tripapillate *Aneurospora* spp. zone (*Apiculiretusispora* sp. E subzone) – middle *micrornatus* – *newportensis* subzone.

DIAGNOSIS: Small, distally laevigate spores with well-defined curvaturae perfectae delimiting the contact areas; fine inter-radial muri are found in these areas, alongside a thickened apical area and Y-ray thickenings.

DESCRIPTION: 23 – 37µm, mean 29µm (seventeen specimens measured). Sub-circular to subtriangular amb with a homogenously thin, distally laevigate exine. Proximally, the contact face is well defined by distinct curvaturae perfectae which diverge from well-defined triradiate rays; sutures are 2/3 to near equatorial in length. Sometimes, the contact face is wrinkled with folds associated with the triradiate mark. 7 to 12 fine inter-radial muri between 0.5 to 1.5µm in width are found in each contact area.

Interadial muri taper towards the proximal apex where the muri sometimes fuse. A distinctive apical triangular thickening and y-ray thickenings, where the laesurae diverge into the curvaturae perfectae, are present on these spores. Distally laevigate.

COMPARISONS AND REMARKS: These spores compare well with the original descriptions of *E. epicautus* (Richardson and Lister, 1969), although some specimens are slightly smaller. *E. epicautus* differs from *Retusotriletes* sp. 4 as the latter does not exhibit radial muri.

Emphanisporites* cf. *epicautus Richardson and Lister 1969
Plate III figure b

STRATIGRAPHIC RANGE: Non-tripapillate *Aneurospora* spp. zone (*Apiculiretusispora* sp. E subzone) – middle *micrornatus* – *newportensis* subzone.

DESCRIPTION: 20 - 31µm, mean 27µm (five specimens measured). Circular amb. Fine subequatorial curvaturae perfectae. Triradiate mark distinct and is accompanied by narrow lips. The proximal face is ornamented with distinct, robust muri, extend from the curvaturae perfectae towards the proximal pole; terminating approx. ½ to 2/3 towards the pole, leaving a distinctive 'bald patch' about the apical pole. No apical thickening is observed in these spores. Distally laevigate.

COMPARISONS AND REMARKS: Reminiscent of *E. rotatus* in terms of robust radial muri, although this specimen differentiated by the 'bald spot' and >8 muri per contact face. Reminiscent of *E. protophanus* although muri are more robust and extend further in this specimen. Proximal thickening and well developed curvaturae perfectae make aligns this spore with *E. epicautus*. Previously referred to here as *E.* sp. 9.

Emphanisporites micrornatus Richardson and Lister 1969
Plate III figures e – f

STRATIGRAPHIC RANGE: middle *micrornatus* – *newportensis* subzone.

DIAGNOSIS: Small, circular spores with distinct curvaturae, well defined inter-radial muri in the contact areas and distally sculptured with diminutive micro-coni or micro-grana.

EXTENDED DIAGNOSIS: 13.5 – 31.2µm, mean 20.26µm (twenty-two specimens measured). Sub-circular to circular amb with a homogenous, thin exine which is distally ornamented with minute coni or grana. Distal ornament of micro-grana to micro-coni is sparsely distributed across the distal surface and individual elements are always <1µm in height. Proximally, well defined curvaturae perfectae delimit the contact areas which are slightly subequatorial to equatorial in extent. Each contact area is ornamented with 5-7 radially arranged muri which show negligible tapering and are relatively well defined, typically between 1-2.5µm wide. The triradiate rays are accompanied by well-developed folds.

COMPARISONS AND REMARKS: These spores compare well in terms of ornament and ornament dimensions given for the original descriptions for this species in Richardson and Lister (1969), although some have smaller ambs that those given there. *Emphanisporites micrornatus* is distinguished by the diminutive distal sculpture of coni or grana. *E. decoratus* Allen 1965 has much more robust distal sculpture of cones and spines, and *E. neglectus* Vigran 1964 has a triangular amb.

Emphanisporites* cf. *micrornatus Richardson and Lister 1969

Plate III figures g – h

STRATIGRAPHIC RANGE: Lower – middle *micrornatus* – *newportensis* subzones.

DIAGNOSIS: Small, radial trilete spores with a thin, often crumpled exine and densely packed micro-grana or micro-coni on the distal surface. Radial muri populate the contact areas.

EXTENDED DIAGNOSIS: 15 – 24μm, mean 18μm (twenty-one specimens measured). Subcircular to subtriangular amb, with thickened equatorial curvaturae perfectae delimiting a well-defined contact area. Contact areas are populated by 7 – 10 relatively indistinct radial muri 1 – 1.5μm wide which gradually taper towards the proximal pole. Distally, the spore is ornamented with densely packed micro-grana or micro-coni less than 1μm in height. The triradiate mark extends to the equator and is accompanied by folds.

COMPARISONS AND REMARKS: These spores compare well with original descriptions of *E.* cf. *epicautus* given in Richardson and Lister (1969), although some fall below the size range given there. *Emphanisporites* cf. *micrornatus* is distinguished from other *Emphanisporites* species by the densely packed micro-grana or micro-coni on the distal surface, alongside the thin, often crumpled exine.

Emphanisporites* cf. *neglectus Vigran 1964

Plate III figures i – j

STRATIGRAPHIC RANGE: Non-tripapillate *Aneurospora* spp. zone (*Apiculiretusispora* sp. E subzone) – middle *micrornatus* – *newportensis* subzone.

DESCRIPTION: 15 – 33μm, mean 21μm (forty-six specimens measured). Subcircular to subtriangular ambs. The triradiate mark is distinct, accompanied by lips 1μm wide. Lips extend to near equatorial extent, diverging to form equatorial curvature perfectae. The equator is thickened. Each interadial area is ornamented by 7 – 14 radial muri 0.5 – 1μm wide, with a slight taper in some examples. Distally laevigate.

COMPARISONS AND REMARKS: Many of these spores have a greater amb diameter than those in the original descriptions of Vigran (1964) (9.5 - 19μm), but they are otherwise identical. Upon measuring, there is little cause to separate the species by size.

Emphanisporites* cf. *rotatus (McGregor) McGregor 1973

Plate III figures k – l

STRATIGRAPHIC RANGE: Non-tripapillate *Aneurospora* spp. zone (*Aneurospora sheafensis* subzone) – middle *micrornatus* – *newportensis* subzone.

DESCRIPTION: 14 & 22μm, (two specimens measured). Circular to subtriangular spores. Proximally ornamented with coarse, straight inter-radial muri, which extend from the proximal pole to the equator. The number of interadial muri ranges from 4 – 8, and they are 1-2μm wide. The trilete mark is distinct,

with lips extending near to the equator, before diverging into distinct curvaturae perfectae which do not intersect the equator. Distally, the exine is laevigate.

COMPARISONS AND REMARKS: These spores differ from those described in McGregor (1961) chiefly in terms of amb size. In the original descriptions, amb size ranges between 33 – 60μm whereas the specimens here range between 14 - 32μm. The spores are otherwise very similar to the original descriptions. These spores differ from *E. neglectus* and *E.* cf. *neglectus* in terms of interadial muri number (4 – 8 in *E.* cf. *rotatus* vs. 7 – 14 in *E. neglectus*) and they are also more robust in *E. rotatus*.

Genus ACINOSPORITES Richardson 1965

TYPE SPECIES: *Acinosporites acanthomammillatus* Richardson 1965

TYPE LOCALITY: Orcadian Basin, Cromoty Nodule Bed, north-east Scotland.

DIAGNOSIS: Radial, trilete spores. Ornamented with a series of convoluted and anastomosing ridges which bear verrucae with microspinae, spinose projections or microconi. Ridges are fairly wide and 'globular', tightly packed across distal exine. Spinae extend from the rounded edge of verrucae, verrucae do not taper into spinae.

BOTANICAL AFFINITIES: Wellman (2022) found that dispersed species of *A. macrospinosus* exhibited a spore ultrastructure comparable to extant and fossil lycopods. The possibility of such an affinity for other species of the genus is currently untested.

Acinosporites salopiensis Richardson and Lister 1969

Plate III figures m – o

STRATIGRAPHIC RANGE: lower - middle *micrornatus* – *newportensis* subzone.

DIAGNOSIS: Spores with well-defined contact areas, distally ornamented with a reticulum formed by low muri, which distinctively bear small coni or spinae at their intersections.

DESCRIPTION: Size 19 - 44μm, mean 31μm (fifty specimens measured). Amb subtriangular, with a smooth proximal face. Triradiate mark accompanied by lips, 1 – 1.5μm which extend to the equator. Laesurae diverge there to form equatorial curvaturae perfectae. The distal hemisphere is ornamented with a fine reticulum, generally completely developed with muri 0.2 – 0.8μm wide, mean 0.5 μm and lumen between 0.3 - 2.9μm wide, mean 1μm. At the junctures between muri, stout cones or spines are developed, between 0.4 – 3.4μm tall, mean 1μm.

COMPARISONS AND REMARKS: These spores generally compare well with the original descriptions in Richardson and Lister (1969), although some slight size differences are present in these populations. Richardson and Lister (1969) gave a size range of 21-39μm and hence the specimens here compare well in terms of amb diameter but are in some cases slightly larger in general than those originally described. Muri widths are slightly smaller than the original descriptions, which were between 0.5 - 1μm compared with 0.2 – 0.8μm here. Similarly, there is a slightly wider range of lumen sizes in this population compared with the original descriptions. None of these variations is particularly significant and so these spores are retained in *A. salopiensis*.

There is a high degree of intraspecific variation amongst specimens of *A. salopiensis* and there may be cause to divide the species into variants pending further study.

Genus BROCHOTRILETES Naumova ex. Naumova 1953

TYPE SPECIES: *Brochotriletes foveolatus* Naumova 1933

TYPE LOCALITY: Upper Devonian of the Russian Platform.

DIAGNOSIS: Radial, trilete miospores with curvature perfectae. Exhibit a distal foveolate sculpture comprising variably formed fovea.

BOTANICAL AFFINITIES: Uncertain.

?*Brochotriletes* sp. 1 sp. nov.

Plate III figure p

STRATIGRAPHIC RANGE: Non-tripapillate *Aneurospora* spp. zone (*Apiculiretusispora* sp. E subzone) – lower *micrornatus* – *newportensis* subzone.

DESCRIPTION: 16 – 37µm, mean 27µm (nine specimens measured). Subcircular ambs. Proximal face thin, typically lost but where present is laevigate. Distally foveolate sculpture, comprising circular to slightly oblong fovea, 0.49 – 1.35µm wide, mean 0.86µm. Irregularly arranged, 0.35 – 1.3µm apart, mean 0.67µm.

COMPARISONS AND REMARKS: These spores are larger than those figured in Naumova (1953) and the fovea are more circular. Richardson and Ioannides (1973) describe a cf. *Brochotriletes* sp. A from North Africa, and this form is somewhat comparable except in *B.* sp. 1 lacks the more elongate fovea seen in that species, have slightly smaller fovea (0.49 – 1.35µm in *B.* sp. 1 vs 0.5 - 3µm in *B.* sp. A).

Genus DICTYOTRILETES (Naumova) emend Smith and Butterworth 1967

TYPE SPECIES: *Dictyotriletes bireticulatus* (Ibrahim) Potonié and Kremp 1955

TYPE LOCALITY: Freshwater West, south of Little Furzenip Headland, sample FW3, 165 m above the base of the Conigar Pit Sandstone Member, Freshwater West Formation

DIAGNOSIS: Azonate, retusoid trilete spores with a distal reticulate sculpture.

BOTANICAL AFFINITIES: Uncertain.

Dictyotriletes williamsii Higgs 2004

Plate III figure q

STRATIGRAPHIC RANGE: Non-tripapillate *Aneurospora* spp. zone (*Apiculiretusispora* sp. E subzone) – lower *micrornatus* – *newportensis* subzone.

DIAGNOSIS: Spores with well-defined contact areas, distally ornamented with a continuous reticulum formed by low, narrow muri and describing large lumen.

DESCRIPTION: 18 - 37μm, mean 29μm (five specimens measured). Subcircular amb. Distally, narrow muri 0.5 - 1μm wide, mean 0.7μm delimit 11 relatively large lumina, 3 - 11μm wide that define a broad, web-like reticulum.

COMPARISONS AND REMARKS: These spores are comparable to original descriptions of *D. williamsii* in Higgs (2004). However, some of the lumen are smaller in these specimens than in Higgs's (2004) descriptions, where they are 5 - 12μm in width.

***Dictyotriletes* sp. A** Richardson and Lister 1969

Plate III figure r

STRATIGRAPHIC RANGE: Non-tripapillate *Aneurospora* spp. zone (*Aneurospora sheafensis* subzone) – lower *micrornatus* – *newportensis* subzone.

DESCRIPTION: 20 - 29μm, mean 25μm (three specimens measured). Subtriangular amb. Proximally laevigate, with a distinct triradiate mark accompanied by robust lips up to 3μm wide. Distally, a reticulum is developed by muri 0.7 – 1μm wide, mean 0.9μm, forming lumen 1.8 - 4μm wide, mean 2.8μm.

COMPARISONS AND REMARKS: These spores are generally comparable to descriptions of *D.* sp. A in terms of amb diameter and lumen size, although here some of the lumen on the specimen are slightly smaller than those in Richardson and Lister's (1969) specimens (1.8 - 4μm vs 3 - 7μm, respectively). These spores may also be comparable to *Dictyotriletes* sp. B Richardson and Lister (1969), except the muri are thicker in these specimens.

Subturma PERINOTRILETES Erdtman 1947

Genus PEROTRILITES (Erdtman) Couper 1953

TYPE SPECIES: ?*Perotrilites pseudoreticulatus* Couper 1953 pl.3 figures 30, slide Ll2/2 30'2xl07'9 C30(2)

TYPE LOCALITY: New Zealand

DIAGNOSIS: Large retusoid trilete spores with an outer 'perine' which may be laevigate or variously ornamented.

BOTANICAL AFFINITIES: Uncertain.

Perotrilites microbaculatus Richardson and Lister 1969

STRATIGRAPHIC RANGE: lower – middle *micrornatus* – *newportensis* subzones.

DESCRIPTION Thin, diaphanous perine which is closely attached to the spore exine, except across the proximal face. Excluding the contact area, the perine is sculptured by densely packed, small rods, grana or cones.

COMPARISONS AND REMARKS: The close attachment of the perine across the spore except across the proximal face distinguishes this species from other spores assigned to this genus.

Perotrilites microbaculatus* var. *microbaculatus Richardson and Lister 1969
Plate IV figure a

STRATIGRAPHIC RANGE: Lower middle *micrornatus* – *newportensis* subzones.

DIAGNOSIS: 'perine' forms prominent folds around the margins of the contact areas, frequently wrinkled or folded over the contact areas, distally sculptured by microbaculae; exine relatively thick, thickness at the equator 2 – 3.5µm, distally 3 - 6µm.

DESCRIPTION: Size 62-95µm, mean 71.8µm. (seven specimens measured). Amb subcircular to subtriangular. Perine and exine closely attached over distal and equatorial areas, and loosely attached over proximal face. The perine is thin, diaphanous and ornamented except over the contact areas. Sculptured with diminutive, barely discernible microbaculae less than 1µm high and less than 0.5µm wide. Exine of the internal spore is thick, robust and laevigate. About the triradiate mark, prominent folds are developed in the perine and a distinct, triangular apical thickening is developed.

COMPARISONS AND REMARKS: Large size, thick exine, diminutive sculpture and loosely adherent perine distinguish this variant. These spores compare well with the original descriptions in Richardson and Lister (1969), although is some cases exceed the size ranges given there (28 - 61µm).

Perotrilites microbaculatus* var. *attenuatus Richardson and Lister 1969
Plate IV figure b

STRATIGRAPHIC RANGE: Lower MN – middle MN subzone.

DIAGNOSIS: Perine is closely adherent to the exine, with small folds forming around the contact areas. The perine is distally sculptured with microbaculae, coni or grana, which is relatively coarse. The exine is relatively thin.

DESCRIPTION: 28 - 56µm, mean 42µm (twelve specimens measured). Circular amb. Internal spore is laevigate, with a well-defined contact area. The triradiate mark is distinct, with suturae extending to near equatorial limits before diverging into curvaturae perfectae. Perine and exine closely attached except over contact areas. Sculpture may be microbaculae, coni or grana 0.3 – 0.7µm wide, mean 0.5µm, 0.2 – 0.8µm tall.

COMPARISONS AND REMARKS: Ornament coarser and more variable than var. *microbaculatus* and the amb is smaller, with a more tightly adherent perine. These spores compare well with descriptions in Richardson and Lister (1969), with similar element sizes and a tightly adherent perine. In some cases, the amb diameter slightly exceeds that given in Richardson and Lister (1969) (27 – 48µm).

***Perotrilites* sp. A** Wellman *et al*., 2000
Plate IV figures c

STRATIGRAPHIC RANGE: Lower middle *micrornatus* – *newportensis* subzones.

DESCRIPTION: 38 – 68µm, mean 49µm (eleven specimens measured). Circular amb, laevigate spore and perine. Triradiate mark distinct, curvaturae perfectae coincide with equator. The laesurae are associated with a distinct triangular apical thickening. The perine is tightly adherent but occasionally detached distally, except on the contact face, where folds in the perine mimic the triradiate mark.

COMPARISONS AND REMARKS: These spores compare well with those figured in Wellman *et al*. (2000), except some specimens are smaller than those given in the original descriptions (50 - 73µm).

CRASSITATE TRILETE SPORES

Subturma ZONOTRILETES Waltz 1935
Infraturma CRASSITI Bharadwaj and Venkatachala 1961
Genus AMBITISPORITES Hoffmeister 1959

TYPE SPECIES: *Ambitisporites avitus* Hoffmeister 1959

TYPE LOCALITY: Atshan Well no. 1-1, state of Atshan, Libya. 'Early Silurian'.

DIAGNOSIS: Proximally and distally laevigate exoexine with a narrow equatorial crassitude. The crassitude delimits the extent of the contact area, diverging from the trilete mark (curvaturate). In polar compression the trilete mark reaches, or nearly reaches, the equator to form an equatorial structure.

STRATIGRAPHIC RANGE: *poecilomorphus* – *libycus* zone – middle *micrornatus* – *newportensis* subzone.

BOTANICAL AFFINITIES: *In situ* spores of *Ambitisporites* have been found in the rhyniophyte *Cooksonia pertoni* subsp. *pertoni* (Fanning *et al*., 1991b), a bonafide tracheophyte. *Ambitisporites* have also been identified *in situ* from probable rhyniophytoid sporangia.

Ambitisporites avitus – dilutus Hoffmeister 1959
Plate IV, figures d – e

STRATIGRAPHIC RANGE: *poecilomorphus* – *libycus* zone – middle *micrornatus* – *newportensis* subzone.

DIAGNOSIS: Trilete, radial miospore, subcircular to roundly triangular in equatorial outline, and possessing a well defined, simple trilete and an equatorial situdo.

DESCRIPTION: Size range 11 - 53µm, mean 28µm (one hundred and ten specimens measured). Amb is sub-circular to roundly subtriangular with rounded angles and convex sides. The exine is proximally and distally laevigate. A narrow, well-defined to subtle equatorial crassitude delimits the contact area. The triradiate mark may have lips up to 1.5µm or lack them entirely. Lips extend to the inner edge of

the equatorial crassitude for an equatorial or near-equatorial termination; curvaturae perfectae are only seen in obliquely compressed specimens.

COMPARISONS AND REMARKS: These spores compare well with the original descriptions given for *A. avitus* in Hoffmeister (1959) and *A. dilutus* in Richardson and Lister (1969). Steemans *et al*. (1996) are grouped these two species into a single morphon based on the clear intergradation of the two species and difficulties in differentiating intermediate members. Only end members can be reliably differentiated, with *A. avitus* being larger and having a distinct, well-defined crassitude while *A. dilutus* is smaller and has a 'diluted' crassitude.

The size range amongst *Ambitisporites avitus-dilutus* specimens differs from those given in Hoffmeister (1959) and Ricardson and Lister (1969) (figure 8). The former indicates that size ranges from 35-65µm, whilst the latter are (for *A.* cf. *dilutus*) are listed as 28 - 40µm. The upper measurements of these M50 specimens correspond reasonably well with those in the above two publications, however some specimens here are considerably smaller. Burgess and Richardson (1995) outlined *Ambitisporites parvus* as an *Ambitisporites* species with an amb diameter <18µm. A population of such spores is distinguishable in the histogram of amb diameters (figure 8), but because this does not affect the gaussian distribution of the spores, such a distinction is suggested to be unnatural here.

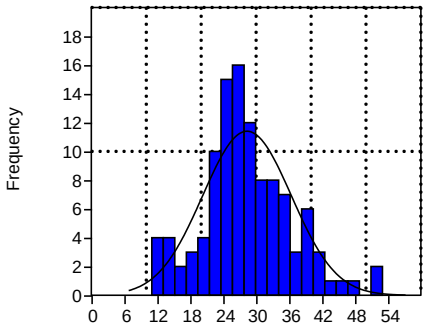

Figure III-8: Amb diameter distribution of the Ambitisporites avitus – dilutus *complex with normal distribution curve fitted.*

Ambitisporites eslae (Cramer and Diez) Richardson *et al*. 2001
Plate IV figure f

STRATIGRAPHIC RANGE: *poecilomorphus* – *libycus* zone – middle *micrornatus* – *newportensis* subzone.

DIAGNOSIS: Trilete, radial miospore, with circular interadial papillae in the interadial areas. A thickening is present at the apical pole.

DESCRIPTION: 21.5 - 41.7µm, mean 30.6µm (three specimens measured). Subcircular to subtriangular amb. narrow crassitude, triradiate mark is sometimes accompanied by lips up to 2µm wide. Circular papillae, 3 – 6.4, mean 4.9µm, inhabit the interadial areas. At the apical pole there is a slight circular to triangular thickening which extends up to 20% of the triradiate mark. May be microgranulate on the proximal face. The distal hemisphere is laevigate.

COMPARISONS AND REMARKS: These spores compare well with those specimens described in Cramer and Diez (1975). *A. eslae* differs from *Amb. tripapillatus* due to presence of the apical thickening.

Ambitisporites tripapillatus Moreau-Benoit 1976
Plate IV figure g

STRATIGRAPHIC RANGE: *poecilomorphus* – *libycus* zone – middle *micrornatus* – *newportensis* subzone.

DIAGNOSIS: An *Ambitisporites* spore with circular interadial papillae developed in the interadial areas.

DESCRIPTION: 13 – 24µm, mean 17µm (three specimens measured). The amb is subcircular to triangular with rounded angles and straight to convex sides. Triradiate laesurae extend to near equatorial limits where they diverge into curvaturae perfectae, forming a prominent equatorial crassitude which delimits the contact area. The trilete rays are sometimes accompanied by folds or lips 1-2µm wide that terminate at the crassitude. Interadial areas exhibit distinctive circular or phaseolate interadial papillae, 1.5 – 3.7µm in diameter. The spores are proximally and distally laevigate, with prominent peripheral folds developed in some specimens.

COMPARISONS AND REMARKS: Circular to phaseolate interadial papillae discriminate *A. tripapillatus* from other species of *Ambitisporites*. These specimens compare well with the original descriptions of the species given in Moreau-Benoit (1976). In terms of Amb size, they also compare well with *A.* sp. (tripapillate sp.) in Richardson and Ioannides (1973), which are considered the same species here.

Ambitisporites eslae has an apical thickening. The distal ornament differentiates *Aneurospora* species from *A. tripapillatus*. *Leiotriletes* sp. Mortimer, 1967 (plate 1, figures B) and Spore type 4 Jardiné and Yapaudijian 1968 (pl. 1, figures 16) are similar. May be confused for *R. maculatus*, although *A. tripapillatus* exhibits a crassitude and the interadial papillae are smaller in the latter.

Ambitisporites warringtonii (Richardson and Lister, 1969) emend Richardson *et al.*, 2001
Plate IV, figures h – i

STRATIGRAPHIC RANGE: *poecilomorphus* – *libycus* zone – middle *micrornatus* – *newportensis* subzone.

SYNONYMS:
Richardson and Lister, 1969; *Retusotriletes warringtonii*

DIAGNOSIS: A small *Ambitisporites* with a thin exine and narrow crassitude.

DESCRIPTION: 11 – 31µm, mean 19µm (thirteen specimens measured). Spores with a subtriangular to triangular amb, showing rounded edges and convex sides. The exine is proximally and distally laevigate. Proximally, the triradiate mark is distinct, reaching near equatorial limits before diverging into equatorial, curvaturae perfectae. The triradiate mark is sometimes accompanied by well-defined lips, 1-2µm high, which taper distinctly inwards from the pole to the equatorial crassitude, where they terminate.

COMPARISONS AND REMARKS: These specimens compare well to the original species descriptions. Of *A. warringtoni* is closely comparable to *A. avitus-dilutus*, except for the size and thickness of the equatorial crassitude, which is darker and more pronounced in the latter. In addition, *A. warringtoni* has radial curvaturate invaginations on the proximal face, with interadial curvaturae perfectae congruent with equator. The species differs from *R. minor* in this respect alongside *A. warringtoni* exhibiting a triangular amb.

***Ambitisporites* sp. A** Wellman and Richardson 1996
Plate IV, figure j

STRATIGRAPHIC RANGE: *poecilomorphus* – *libycus* zone – middle *micrornatus* – *newportensis* subzone.

DESCRIPTION: 18 - 42μm, mean 32μm (thirty specimens measured). Subcircular to roundly subtriangular amb. Proximally and distally laevigate. Proximally, the triradiate mark is distinct with tall, well-defined lips, 1.5 - 2μm wide. Rays extend to the equator, diverging to form equatorial curvaturae perfectae. with a distinct crassitude.

COMPARISONS AND REMARKS: The specimens here compare well with the original descriptions of the species in Wellman and Richardson (1996), although some of these specimens are smaller than those described from Lorne.

This *Ambitisporites* species is distinguished by the wide lips. Lips that accompany the triradiate mark are noticeably thicker than those in *A. avitus-dilutus*, being a minimum of 1.5μm wide and up to 3μm wide. The equatorial crassitude retains the distinct to dilute nature of *Ambitisporites avitus-dilutus* and is of a similar width. The distal exine is laevigate.

Genus CONCENTRICOSPORITES Rodriguez 1983

TYPE SPECIES: *Concentricosporites saggitarius* Rodriguez 1983

TYPE LOCALITY: La Cordillera basin, Cantabria, Spain

DIAGNOSIS: Laevigate, crassitate, trilete spores with a robust distal thickening about the distal pole.

BOTANICAL AFFINITIES: Uncertain.

Concentricosporites saggitarius Rodriguez 1983

Plate V figure a

STRATIGRAPHIC RANGE: *poecilomorphus* – *libycus* zone – *tripapillatus* – *spicula* zone.

DIAGNOSIS: Radial, trilete spores with a conspicuous, circular thickening developed on the distal hemisphere.

DESCRIPTION: 26 – 41μm, mean 36μm (six specimens measured). Triangular to subtriangular amb, with convex sides and rounded apices. Proximally laevigate, with the contact areas bounded by a well defined equatorial crassitude which is up to 3.5μm wide. The trilete mark is simple but distinct. Sutures extend to the equator. Distally, the spore is laevigate except for a robust, circular thickening about the distal pole. This thickening is $< \frac{1}{2}$ - the spore radius to nearly all of it.

COMPARISONS AND REMARKS: These spores compare well with the original descriptions in Rodriguez (1983) and with descriptions in Burgess and Richardson (1995) in terms of amb size and characteristics. These spores are distinguished by the robust distal thickening.

Burgess and Richardson (1995) note that the spores described there differ from Rodriguez's (1983) specimens in that the thickening is developed on the distal hemisphere, while in the former they appear to be developed on the proximal face. The *C. saggitarius* specimens described here align with Burgess and Richardson's (1995) specimens, and thus reinvestigation of the type material may be required to

ascertain whether the spores described in Burgess and Richardson (1995) and here are the same as Rodriguez's (1983) specimens.

Genus AMICOSPORITES Cramer 1966

TYPE SPECIES: *Amicosporites miserabilis* Cramer 1966.

TYPE LOCALITY: Basal Lower Gedinnian sediments in Northern Leon, Spain

DIAGNOSIS: Radial, trilete miospores with a distinctive annulus developed on the distal hemisphere.

BOTANICAL AFFINITIES: Uncertain.

Amicosporites miserabilis **(**Cramer) Cramer and Diez 1975

Plate V, figure b

STRATIGRAPHIC RANGE: Non-tripapillate *Aneurospora* spp. zone (*Aneurospora sheafensis* subzone)

DIAGNOSIS: Trilete, radial, laevigate miospores with a distinctive annulus developed on the distal hemisphere.

DESCRIPTION: 27µm (one specimen measured). Subtriangular amb. Proximally and distally laevigate. Triradiate mark accompanied by distinctive lips 1µm wide which extend to the equator. Crassitude narrow and dilute, up to 1.5µm. Distally, the exine is laevigate except for an annulus 1µm wide which lies approximately half-way between the equator and distal pole.

COMPARISONS AND REMARKS: The distal annulus distinguishes this genus. This specimen compares well with the original specimens described by Cramer and Diez (1975).

cf. *Amicosporites* sp.

Plate V, figures c – d

STRATIGRAPHIC RANGE: Middle *micrornatus* – *newportensis* subzone.

DESCRIPTION: Size 21.2 – 29.8µm (two specimens measured). Circular amb. Proximal face not observed. Distally sculptured with a distinct 'annulus' 2.6 – 2.8µm wide, separated from the equator by a thinned region 1µm wide. The 'annulus' describes a circular, thinned region 10 - 14µm across. Otherwise laevigate.

COMPARISONS AND REMARKS: This species is comparable to *Amicosporites* species figured in Cramer (1966), although the amb is much more circular than those specimens.

Genus LEONISPORA Cramer and Diez 1975

TYPE SPECIES: *Leonispora argovejo* Cramer and Diez 1975

TYPE LOCALITY: San Pedro Formation, León, Spain.

DIAGNOSIS: Radial, trilete miospores. Laevigate with proximal inpissitations (nb: *not* papillae) developed on the inner edge of the crassitude on the proximal face. Folding developed on the proximal exine.

BOTANICAL AFFINITIES: Uncertain.

Leonispora argovejo Cramer and Diez 1975
Plate V, figure e

STRATIGRAPHIC RANGE: Non-tripapillate *Aneurospora* spp. zone (*Aneurospora sheafensis* subzone) – middle *micrornatus* – *newportensis* subzone.

DIAGNOSIS: subcircular trilete miospores. Triradiate mark is distinct with lips, these extend to the equator. The crassitude is distinctly wide. Inspissitions (circular thickenings beneath the proximal exine) are developed at the edge of the crassitude in the interadial areas and these are accompanied by folds in the proximal face.

DESCRIPTION: 27µm (one specimen measured). Proximally laevigate. The triradiate mark is distinct, accompanied by lips 1µm wide, extending to the equator. The contact areas are defined by a relatively wide crassitude. In each interadial area, inspissitions (note: not papillae) are developed towards the inner edge of the crassitude, accompanied by folds. Distally laevigate.

COMPARISONS AND REMARKS: Similar to *Streelispora* in terms of interadial features and folding, except *L. argovejo* lacks apiculate structural features and has a wider crassitude. In some cases, *Streelispora* appears to have been sloughed of its ornament and may resemble *Leonispora argovejo*. In these cases, *L. argovejo* is discernible by the inpissitations that are developed adjacent to the crassitude.

Genus ANEUROSPORA (Streel) Richardson *et al*. 1982

TYPE SPECIES: *Aneurospora goensis* Streel, 1964

TYPE LOCALITY: Goé, Carrière Brandt, Vesdre Syncline, Basal Givetian.

DIAGNOSIS: Radial, trilete miospores with a rigid, thickened subequatorial proximal region of variable width, even in the same specimen; inner limits often ill defined. Distally sculptured with grana, coni, spinae or biform element. Proximal contact areas may be laevigate, variously sculptured or exhibit interadial papillae and are not multi layered.

BOTANICAL AFFINITIES: Certain species are associated with *Cooksonia pertoni* subsp. *apiculispora* (Fanning et al., 1988) and *Paracooksonia* (Morris et al., 2011b).

Aneurospora* cf. *geikiei Wellman and Richardson 1996a
Plate V, figure f

STRATIGRAPHIC RANGE: Lower - middle *micrornatus* – *newportensis* subzone.

DIAGNOSIS: Trilete, radial miospores with a laevigate proximal face, distally and equatorially ornamented with a mixture of distinct spines and biform elements.

DESCRIPTION: Size 18 - 37μm, mean 29μm (five specimens measured). Amb subcircular. Indistinct trilete mark. Laesurae straight and simple, extend to equatorial crassitude. Proximal face laevigate or with faint microgranulate sculpture sometimes a thickened triangular apical region. Distally and equatorially ornamented with spines and biform elements. Elements 1.5-3.0μm high, 0.7-1μm wide at the base and 1 – 4μm apart.

COMPARISONS AND REMARKS: cf. as ambs in these specimens are significantly smaller than the 50 - 70μm size range given in Wellman and Richardson (1996a). The spinae have finer points and are less dense.

Aneurospora gerriennei Steemans, 1989
Plate V, figure g

STRATIGRAPHIC RANGE: Lower – middle *micrornatus* – *newportensis* subzone.

DIAGNOSIS: Trilete, radial spores. Proximally laevigate, except for small papillae in the interadial regions. Distally and equatorially ornamented with spines.

DESCRIPTION: 25 - 31μm (two specimens measured). Subtriangular amb. Distal exine of spinae 0.5 – 1.5μm at the base, 0.5 - 2μm tall and 0.5 - 2μm apart. Proximally, the triradiate mark is accompanied by 1μm wide lips. In interadial areas, small papillae are developed.

COMPARISONS AND REMARKS: The spinose elements in *A. gerriennei*, which are tall and spinose, and small interadial papillae distinguish this species. The specimens in these samples compare well with the original descriptions in Steemans (1989).

Aneurospora goensis Streel, 1964
Plate V, figure h

STRATIGRAPHIC RANGE: Non-tripapillate *Aneurospora* spp. zone (*Apiculiretusispora* sp. E subzone) – lower *micrornatus* – *newportensis* subzone.

DIAGNOSIS: Radial, trilete spores with a subequatorial proximal region which is especially rigid and probably thickened so as to appear like a dark band (equatorial crassitude); the inner limits of it are often ill-defined and its width is also +/- variable even in the same specimen. Spores distally sculptured with grana, coni, spinae and biform elements. Proximally smooth, or with interadial papillae, or variously sculptured.

DESCRIPTION: 39 - 60μm (three specimens measured). Circular amb. Proximally laevigate or ornamented with sparse micro-coni. Triradiate mark accompanied by narrow lips, which extend to the equator. Distally ornamented with densely packed micro-coni <1μm in height and width.

COMPARISONS AND REMARKS: These spores compare well with original descriptions for this species in Streel (1964).

Aneurospora isidori (Cramer and Diez) Richardson *et al*., 1982
Plate V, figure i

STRATIGRAPHIC RANGE: Lower - middle *micrornatus* – *newportensis* subzone.

DIAGNOSIS: Trilete, radial miospores with circular, interadial papillae developed in the proximal interadial regions. Equidimensional coni are unevenly distributed across the distal exine.

DESCRIPTION: 13 – 28µm, mean 21µm (thirteen specimens measured). Relatively thick exine, subtriangular amb with convex sides and rounded apices. Proximally laevigate apart from circular interadial papillae in each contact area. The trilete mark is distinct with well-defined lips. Distally ornamented with unevenly distributed equidimensional coni, 1µm in width and height.

COMPARISONS AND REMARKS: Triradiate mark is very distinct compared with *An. trilabiata*. Distinguished from other species of *Aneurospora* by the equidimensional coni. *An.*cf. *tojoides* lacks interadial papillae and has slightly finer coni (0.5 – 1µm x 0.5 - 1µm).

Aneurospora kensingtonii sp. nov.
Plate V, figure j

HOLOTYPE: Plate VII, figures c. slide M50-85-2B-2, E.F. no. T37. Moor Cliffs Formation, Ross – Tewkesbury Spur Motorway (M50), Hereford and Worcester

DERIVATION OF NAME: Named for the Royal Borough of Kensington where the Natural History Museum, London, is situated. In recognition of the long history of palynological and palaeobotanical research which continues there.

STRATIGRAPHIC RANGE: Non-tripapillate *Aneurospora* spp. zone (*Aneurospora sheafensis* subzone) - lower *micrornatus* – *newportensis* subzone.

DIAGNOSIS: subcircular to subtriangular spores with laevigate, gently wrinkled or lightly ornamented proximal faces. Narrow lips accompany the well defined triradiate mark. Equatorially and distally ornamented with irregularly distributed microconi and rare microspinae.

DESCRIPTION: 19 – 53µm, mean 39µm (fifteen specimens measured). Subcircular to subtriangular amb. Proximally laevigate, which may be wrinkled or have sparse reduced ornament; lacks inter radial papillae. The triradiate mark is distinct, accompanied by narrow lips 1-2µm which extend to inner edge of the crassitude. The crassitude is distinct, 1. 5 – 3µm wide. The spore is equatorially and distally ornamented with sharply pointed microconi and sometimes rare spines. Microconi are 1µm wide and <1µm tall, while spines are up to 1µm in length and 0.2µm wide; they taper rapidly from the base of the spine into a sharp tip. Elements are irregularly distributed, with 2 – 3µm between them.

COMPARISONS AND REMARKS: These spores may be comparable to *A. goensis* in terms of amb diameter and nature of the elements. However, the lips do not appear to extend to the crassitude in the line

drawings of Streel (1964). These spores differ from *A. sheafensis* as that species exhibits a triangular apical thickening. Specimen with spines: M50/85/2C (19M50-18) 1, E.F. no. F25-2

Aneurospora* cf. *richardsonii (Rodriguez) Richardson *et al*. 2001
Plate V, figure k

STRATIGRAPHIC RANGE: Lower - middle *micrornatus* – *newportensis* subzone.

DESCRIPTION: 32 – 53µm, mean 34µm (four specimens measured). Subcircular amb. The proximal face is missing in these specimens. The spores have a distal sculpture of spaced, slender spines ('fimbriae') with blunt apices, 0.5 – 2.3µm tall, mean 1.6µm and 0.3 – 0.7µm wide, mean 0.5µm. The elements are 0.3 – 4.5µm apart, mean 1.5µm.

COMPARISONS AND REMARKS: These spores compare well with spores described in Rodriguez (1983) and Richardson *et al*. (2001), although these spores straddle the measurements given by those workers, being slightly smaller than the former, where they are between 38 – 50µm (Rodriguez, 1983), but fall just above those in the latter, where they measure between 32 – 47µm (Richardson *et al*., 2001).

Aneurospora sheafensis sp. nov.
Plate V, figure l

HOLOTYPE: Plate VII, figures e. slide M50-85-2C-1, E.F. no. V32-4, Moor Cliffs Formation, Ross – Tewkesbury Spur Motorway (M50), Hereford and Worcester.

DERIVATION OF NAME: Named after the River Sheaf, the river for which the city of Sheffield is named. In recognition of 75 years of palynological research carried out at the Centre for Palynology at The University of Sheffield.

STRATIGRAPHIC RANGE: Non-tripapillate *Aneurospora* spp. zone (*Aneurospora sheafensis* subzone – *Apiculiretusispora* sp. E subzone).

DIAGNOSIS: Subcircular to subtriangular spores with an equatorial and distal ornament of irregularly arranged microconi. Proximally, these spores have a distinctive triangular thinning which is centred around the proximal face and Y-rays of the spore. The proximal face is otherwise laevigate.

DESCRIPTION: 32 – 51µm, mean 40.9µm (thirty-four specimens measured). Subcircular to subtriangular ambs. Proximally laevigate. The triradiate mark is distinct and may be accompanied by lips up to 2µm wide, which extend to inner edge of the crassitude. The proximal face shows a thinning of the exine about the triradiate mark, which is generally triangular in shape and extends $\frac{1}{2}$ to $\frac{3}{4}$ of the length of the triradiate mark. The crassitude is distinct, 1-4µm wide. The spore is equatorially and distally ornamented with sharply pointed microconi, 0.5 - 1µm wide and 0.5 - 1µm tall, irregularly distributed across the exine with 0.5 – 5µm, mean 2.4µm between elements.

COMPARISONS AND REMARKS: These spores are distinguished by the triangular apical thickening on the proximal face. While generally similar to *A. kensingtonii* sp. nov., those spores do not exhibit the apical triangular thinning.

Aneurospora trilabiata Richardson 2011

Plate V, figures m – n

STRATIGRAPHIC RANGE: Lower - middle *micrornatus* – *newportensis* subzone.

DIAGNOSIS: An *Aneurospora* with a narrow curvatural crassitude, trilete ridges, flanked on each side by paired, prominent parallel ridges which is continuous across the spore apex. The proximal face is partially invaginated, distal surface inflated with sculpture on the sub-equatorial and distal surfaces, ornament of spaced isodiametric microconi – micrograna and microbaculae.

DESCRIPTION: 20 – 24μm, mean 22μm (four specimens measured). Subcircular to subtriangular amb. Proximally, trilete ridges flanked by prominent parallel ridges. A fold may be exhibited along the inner edge of the crassitude. Sometimes inter-radial papillae are developed in the otherwise laevigate contact areas. Distal sculpture of isodiametric microconi – micrograna and microbaculae, 0.5 – 1.5μm wide, 0.5 – 1.5μm tall, and up to 1μm apart.

COMPARISONS AND REMARKS: Distinguished from *An. isidori* by the parallel folds in this species: these appear as thickenings about the triradiate mark, the non-isodiametric elements and the 'fold' which occasionally develops along the inner edge of the crassitude.

These spores compare well with the descriptions given in Richardson (2011).

***Aneurospora* cf. sp. A** Wellman *et al*., 2000

Plate V, figure o

STRATIGRAPHIC RANGE: Lower - middle *micrornatus* – *newportensis* subzone.

DESCRIPTION: 27 - 40μm (two specimens measured). Roundly subtriangular amb. Proximally laevigate, with a distinct triradiate mark which is accompanied by lips 1.8μm wide. Equatorially and distally ornamented by slender spines with slightly bulbous tips. Spines up to 3μm tall and 0.4μm wide, elements are densely packed, 0.4 – 0.9μm apart.

COMPARISONS AND REMARKS: These spores compare reasonably well with *Aneurospora* sp. A in Wellman *et al*. (2000), except in some cases the amb diameter is considerably smaller than in those descriptions, where they measure between 33 - 41μm. *A.* sp. A here also lacks the distinctively wide crassitude seen in the original specimens. Spores of *Aneurospora* sp. A *sensu* Wellman et al. (2000) were assigned by Breuer and Steemans (2015) to *Cymbosporites wellmanii*, but those spores are described as having slender pointed spines, which these specimens lack.

Genus IBEREOSPORA Cramer and Diez 1975

TYPE SPECIES: *Ibereospora cantabrica* Cramer and Diez 1975

TYPE LOCALITY: Cantabria, Spain.

DIAGNOSIS: Equatorially cingulate, radial trilete spores. The triradiate mark is straight and simple and terminates at the edge of the cingulum; rays are typically accompanied by low lips which terminate equatorially. At least three inpissations (cf. interadial papillae) populate the edges of the contact areas, often symmetrically.

BOTANICAL AFFINITIES: An 'emphanoid' ?*Ibereospora* sp. has been reported *in situ* from a probable rhyniophytoid with a discoidal sporangium from NBCH (Morris *et al*., 2011b).

Ibereospora glabella Cramer and Diez 1975

Plate VI, figures b – c

STRATIGRAPHIC RANGE: Lower – middle *micrornatus* – *newportensis* zones

DIAGNOSIS: Trilete, radial miospores with inpissations developed in the proximal radial areas, close to the edge of the cingulum. Distally ornamented with a fine reticulum.

DESCRIPTION: 25 – 25.3µm (two specimens measured). Circular to subtriangular amb. The triradiate mark is accompanied by low lips which extend to the inner edge of the crassitude. The proximal and distal exine is smooth. Inspissations are developed distally, close to the edge of the cingulum.

Genus SCYLASPORA Burgess and Richardson 1995

TYPE SPECIES: *Scylaspora scripta* Burgess and Richardson 1995

TYPE LOCALITY: Rumney Borehole, Cae Castell Formation, Homerian.

DIAGNOSIS: Radial, trilete monads with a bi-layered exine. The proximal face is ornamented with irregular muri, whilst the distal exine may be laevigate or ornamented with coni, grana or spinae, which may occasionally be biform.

BOTANICAL AFFINITIES: Found *in situ* in elongate sporangia by Wellman (1999) and the author (sample ABM5021-001), associated with rhyniophytoids.

Scylaspora ?downiei Burgess and Richardson 1995

Plate VI, figure d

STRATIGRAPHIC RANGE: Non-tripapillate *Aneurospora* spp. zone (*Apiculiretusispora* sp. E subzone).

DIAGNOSIS: A *Synorisporites* with a distinctive proximal ornament of verrucae arranged close to the inner edge of the crassitude. Distally ornamented with microconi.

DESCRIPTION: 33µm (one specimen measured). Circular amb, exine quite dark. Triradiate mark well defined, lips 1.5µm wide, extend near to the equator. The crassitude is 2µm wide. Proximally, Dark

circles – verrucae, papillae or fungi? circular, 3 - 5μm in diameter, are arranged around edge of crassitude and towards centre. The spore is distally ornamented with microconi, 1μm wide and <1μm tall. They are randomly distributed and densely packed, typically <1μm apart.

COMPARISONS AND REMARKS: These specimens are slightly larger than the size range given in Burgess and Richardson 1995 (25 - 31μm), but not significantly so. Verrucae in this specimen are much more defined than in those specimens figured in Burgess and Richardson (1995) but correspond to the size variations given in the original description (0.3 - 6μm long x 0.3 - 2μm wide). Hence, these spores are grouped into this species.

***Scylaspora* sp. 1**

Plate VI, figure e

STRATIGRAPHIC RANGE: Lower - Middle *micrornatus* – *newportensis* subzone.

DESCRIPTION: 21.2 - 30μm, mean 24.3μm (five specimens measured). Triangular amb with rounded apices and convex sides. Proximally sculptured with a very fine reticulum, comprising continuous muri 0.3μm wide forming lumina up to 0.5 – 0.6μm wide. The triradiate mark is distinct, may lack lips or be accompanied by distinct, wide lips which taper towards the narrow crassitude. Distally laevigate.

COMPARISONS AND REMARKS: Differs from *S. scripta* because *S.* sp. 1 lacks the scattered grana on the distal hemisphere and the muri are finer. The presence/ absence of lips does not seem to necessitate the distinction into separate species at present. The *Scylaspora* species found *in situ* by Wellman (1999) and in Chapter V is closely similar to this species.

***Scylaspora* sp. 2**

Plate VI, figures f – g

STRATIGRAPHIC RANGE: Non-tripapillate *Aneurospora* spp. zone (*Apiculiretusispora* sp. E subzone) – middle *micrornatus* – *newportensis* subzone.

DESCRIPTION: 21 – 26.4μm, mean 24.3μm (four specimens measured). Subtriangular amb with rounded apices and convex sides. Proximally ornamented with micrograna 0.3 – 0.47μm in diameter, 0.3 – 0.5μm apart. The triradiate mark is distinct, accompanied by lips 1μm wide which taper towards the equatorial crassitude. The spores are distally laevigate.

COMPARISONS AND REMARKS: These spores are differentiated from *S.* sp. 1 by the granate proximal ornament and tapering lips. This species could be comparable to *Synorisporites* sp. D in Richardson *et al*. (1984) (their Pl. 3, figures 7), although no description is given there so direct comparison is difficult.

Genus STREELISPORA (Chaloner and Streel) Richardson *et al*. 1982

HOLOTYPE: *Streelispora newportensis*

TYPE LOCALITY: Freshwater west Formation, Newport, South Wales.

DIAGNOSIS: Radial, trilete spores. Contact areas delimited by a near equatorial-to-equatorial crassitude. Spores exhibit a distal ornament of grana, coni, spinae or biform elements; proximal contact areas may be laevigate or have inter radial papillae or may be variously sculptured. The contact areas may be bi-layered and show distinctive folding.

BOTANICAL AFFINITIES: Identified *in situ* in rhyniophytoids, forms part of the *Lenticulitheca-Paracooksonia-Cooksonia* complex.

Streelispora newportensis (Chaloner and Streel) Richardson and Lister 1969
Plate VI, figures h – i

STRATIGRAPHIC RANGE: Lower to middle *micrornatus* – *newportensis* subzone.

SYNONYMS:
Chaloner and Streel, 1968; *Granulatisporites newportensis*

DIAGNOSIS: Distinctive contact face exhibiting three well developed interadial papillae which are associated with consistent radial and tangential folds; proximal exine is thin. Distally sculptured with coni or biform coni. Equatorial crassitude is narrow and variably distinct.

EXTENDED DIAGNOSIS: Size 15 - 36μm, mean 26μm (ninety specimens measured). Triangular amb with rounded angles and convex sides. Homogenous, thin distal exine. The distinctive contact areas bare three interadial papillae, one in each interadial area. The papillae are sub-circular in plan and are accompanied by folds in the bi-layered proximal exine. Folds are distinctive and the most prominent are found running parallel to the equator, but other folds are often seen at high angles to the equator. The equatorial crassitude varies in distinctiveness but is typically 1-2μm wide. Sculpture is restricted to the equatorial margin and distal portion of the spore. Sculptural elements comprise occasionally biform coni which taper sharply upwards from the base with rounded or pointed apices. Elements do not generally exceed 0.2 – 3.4μm in height, mean 0.55μm and 0.2 - 3μm in width, mean 0.7μm. Sculpture is variably distributed with elements being between 0.1 – 2.9μm apart, mean 0.6μm.

COMPARISONS AND REMARKS: These spores compare well with the original descriptions of *S. newportensis* in Richardson and Lister (1969) in terms of amb diameter variation and element dimension, although in some cases ornament may be taller and wider than in those descriptions, where they do not exceed 2μm wide and 1μm tall (fig. 9). *S. newportensis* has a thinner exine than *S. granulata*, with the latter also having a sculpture of small cones and grana rather than coni and biform coni. There may be cause to differentiate members of this species based on amb diameter as the histogram is distinctly bipolar, however, the other features of the spores remain similar across irrespective of amb diameter.

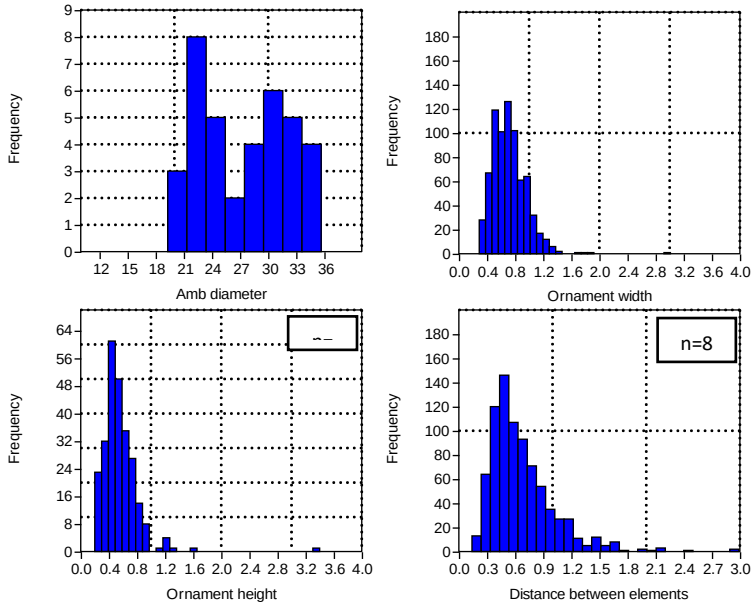

Figure III-9: morphometrics of Streelispora newportensis

Streelispora granulata Richardson and Lister

Plate VI, figure j

STRATIGRAPHIC RANGE: Lower – middle *micrornatus* – *newportensis* subzone.

DIAGNOSIS: The spore has a relatively thick exine with a distinctive equatorial crassitude which thickens in interadial areas. Distally sculptured with small, tightly packed grana or coni.

DESCRIPTION: 22 - 31µm (two specimens measured). Subtriangular amb with convex sides and rounded angles. Proximal exine is generally laevigate, but the contact faces may bare three interadial papillae in some specimens. Equatorial and distal exine is ornamented with densely packed grana or coni, no greater than 1µm in height and width. The triradiate mark is well-developed and extends to near equatorial limits and may be accompanied by low lips.

COMPARISONS AND REMARKS: *S. granulata* is distinguished by its thickened exine and variably thick equatorial crassitude. *S. granulata* does not exhibit biform elements as in *S. newportensis*.

Genus SYNORISPORITES Richardson and Lister 1969

TYPE SPECIES: *Synorisporites downtonensis* Richardson and Lister, 1969.

TYPE LOCALITY: Linton Quarry, lower Moor Cliffs Formation.

DIAGNOSIS: Crassitate, trilete spores with laevigate proximal contact areas and a distal exine which is ornamented with verrucae and/ or muri.

BOTANICAL AFFINITIES: Species of *Synorisporites* have been found associated with the vascular rhyniophyte *Cooksonia pertoni* (Fanning *et al*., 1988).

Synorisporites downtonensis Richardson and Lister 1969.
Plate VI, figures k – l

STRATIGRAPHIC RANGE: Middle *micrornatus* – *newportensis* subzone.

DIAGNOSIS: Trilete, radial miospores with robust accompanying the triradiate mark. Distally ornamented with verrucae, which may coalesce to form ridges and lumen. The verrucae transition into radial muri onto the proximal face, which tend towards, and diminish near, the proximal pole.

DESCRIPTION: 30 – 54µm, mean 45µm (seven specimens measured). Subtriangular amb. The proximal face has a distinct triradiate mark accompanied by robust lips up to 5µm wide. The contact faces are delimited by a thick, crassitude 4.16µm. Equatorially and distally the exine is sculptured with dense verrucae, 0.4 – 0.7µm wide, mean 0.5µm and 1.6 – 2µm tall, mean 1.8µm. The verrucae may coalesce to form ridge and produce lumen 2.4 – 4µm wide, mean 3µm. Verrucae on the equator extend over onto the proximal face and become radial, tending towards the proximal pole. The muri diminish towards the proximal pole.

COMPARISONS AND REMARKS: These spores compare well with the original descriptions of the species in Richardson and Lister (1969), although the amb diameter of some species fall below the lower values for the range given there by up to 15µm.

Synorisporites* cf. *labeonis Burgess and Richardson 1995
Plate VI, figure m

STRATIGRAPHIC RANGE: Lower – middle *micrornatus* – *newportensis* subzone.

DESCRIPTION: 14 – 15.8µm (two specimens measured). Subtriangular amb. Distally sculptured with muri forming an irregular reticulum. Muri are broad and distinctive, 1.3 – 1.9µm wide, mean 1.5µm, which appear as elongate verrucae.

COMPARISONS AND REMARKS: The irregular reticulum distinguishes this species. The specimens examined here have lost their proximal faces and as such cannot be fully compared to those specimens described in Burgess and Richardson (1995). The specimens here are also considerably smaller than the smallest amb diameter given in Burgess and Richardson (1995), where they range between 27 - 32µm.

Synorisporites* cf. *libycus Richardson and Ioannides 1973
Plate VI figure n

STRATIGRAPHIC RANGE: *poecilomorphus* – *libycus* zone – middle *micrornatus* – *newportensis* subzone.

DESCRIPTION: 14.8 – 26.7µm, mean 21.3µm (seventeen specimens measured). Subtriangular ambs. Proximal face delimited by a crassitude up to 2.5µm wide. The triradiate mark is variously distinct, sometimes accompanied by narrow lips up to 1.5µm wide. Distally ornamented with verrucae which

are strictly contained within crassitude. The verrucae are 1.4 – 7.4μm in length, mean 3.5μm and 1.2 - 3μm wide, mean 1.9μm.

COMPARISONS AND REMARKS: *S. libycus* contrasts with *S. verrucatus* in having more robust verrucae which are often arranged as ridges. These specimens compare well with the original descriptions in Richardson and Ioannides (1973) in terms of element measurements and amb diameters, except in some cases these spores are slightly smaller than in the original descriptions.

Synorisporites tripapillatus Richardson and Lister 1969
Plate VI, figures o – p

STRATIGRAPHIC RANGE: *tripapillatus* – *spicula* zone – middle *micrornatus* – *newportensis* subzone.

DIAGNOSIS: Trilete, radial miospores with circular, interadial papillae developed on the proximal face, distally ornamented with circular to convoluted, tightly packed muri and verrucae.

DESCRIPTION: 11.5 – 23μm, mean 16.4μm (six specimens measured). These small spores are proximally laevigate except for phaseolate interadial papillae, on each area, 2 – 4μm long. The triradiate mark is distinct and is sometimes accompanied by low lips. The spores are distally sculptured with tightly packed, low (<1μm) circular to convoluted muri or verrucae 1.4 – 3.9μm wide.

COMPARISONS AND REMARKS: *S. verrucatus* is distinguished by the consistent presence of interadial papillae. These spores compare well with the original descriptions of the species in Richardson and Lister (1969).

Synorisporites verrucatus Richardson and Lister 1969
Plate VII, figures a – b

STRATIGRAPHIC RANGE: *tripapillatus* – *spicula* zone – middle *micrornatus* – *newportensis* subzone.

DIAGNOSIS: Trilete, radial miospores, with a smooth proximal face. The distal hemisphere is ornamented with distinct, discrete circular verrucae, which may occasionally fuse into small groups.

DESCRIPTION: 16.1 – 29.2μm, mean 21μm (nineteen specimens measured). Subtriangular amb. The proximal face is smooth and lacks sculpture. The triradiate mark is distinct and equatorial in extent; rays are often accompanied by tall lips. The contact areas are well defined by curvaturae perfectae which diverge at the equator, forming a slightly thickened crassitude *ca*.3μm wide. The crassitude is proximally and distally smooth. The distal exine is ornamented with distinct, variously wide and tightly packed verrucae <5μm wide and up to 1.5μm high. Verrucae may occasionally fuse into small groups to simulate muri but verrucae are always dominant.

COMPARISONS AND REMARKS: *S. verrucatus* is distinguished by the presence of verrucae elements, even where some may have coalesced to form muri; verrucate elements are not present on *S. downtonensis* and additionally the proximal face of the latter is ornamented with diminutive, radially arranged muri. These spores compare well with the species descriptions in Richardson and Lister (1969)

***Synorisporites* ?sp. B** Burgess and Richardson 1995
Plate VII, figure c

STRATIGRAPHIC RANGE: Middle *micrornatus* – *newportensis* biozone.

DESCRIPTION: 27.9 – 35.7μm (two specimens measured). Roundly subtriangular amb. Proximally, the contact faces are ornamented with fine, tightly spaced folds. The trilete mark is distinct and is straight to sinuous, accompanied by narrow lips. Distally, the exine is ornamented with tightly spaced, low muri which are anastomosing and convoluted; occasionally, verrucae are also exhibited.

COMPARISONS AND REMARKS: These spores are generally similar to the specimens figured in Burgess and Richardson (1995), although they fall just below the size range given there.

Genus INSOLISPORITES Burgess and Richardson

TYPE SPECIES: *Insolisporites bassettii* Burgess and Richardson, 1995

TYPE LOCALITY: Rumney borehole, South Wales.

DIAGNOSIS: Radial, trilete spores with an equatorial crassitude. Distally ornamented with irregular grana and apiculate elements. Proximally smooth.

BOTANICAL AFFINITIES: Uncertain.

Insolisporites bassettii Burgess and Richardson 1995
Plate VII figure d

STRATIGRAPHIC RANGE: *poecilomorphus* – *libycus* zone.

DIAGNOSIS: An *Insolisporites* with distal grana and microconi.

DESCRIPTION: 20 – 31μm (two specimens measured). Subtriangular amb. distinct equatorial crassitude circumscribes the laevigate proximal face. The triradiate mark is distinct, with suturae extending to the equator. The triradiate mark is occasionally accompanied by narrow lips. Distally ornamented with irregularly distributed and sized microconi and micrograna, 0.5 – 1.5μm tall and apart.

COMPARISONS AND REMARKS: *I. anchistinus* is thicker walled with more variable sculpture. These spores differ from species of *Aneurospora* in that they have a mixture of distal elements. These spores compare well in terms of ornament and dimensions to the specimens descried in Burgess and Richardson (1995), although in some cases the amb diameter is smaller than the lower limits given in those descriptions (27 - 37μm).

Insolisporites anchistinus Burgess and Richardson 1995
Plate VII figure e

STRATIGRAPHIC RANGE: *poecilomorphus* – *libycus* zone.

DIAGNOSIS: A thick walled *Insolisporites* with a distal sculpture of small baculae, coni, grana and spinae fused into irregular groups.

DESCRIPTION: 25 – 46μm, mean 37μm (four specimens measured). Subtriangular amb. distinct equatorial crassitude circumscribes the laevigate proximal face. The triradiate mark is simple and often indistinct, with suturae extending to the equator. Distally ornamented with irregularly distributed and sized coni, microconi, grana, baculae and rare spinae up to 2μm tall but typically <1μm and apart. Elements are up to 1μm wide and are often coalesced into groups.

COMPARISONS AND REMARKS: *I. bassettii* has much thinner walls and does not exhibit grouped elements. These spores compare well with the original descriptions of the species in Burgess and Richardson (1995).

Genus LOPHONZOTRILETES Naumova 1953

TYPE SPECIES: *Lophonzotriletes lebedianensis* (Naumova) Potonie 1958.

TYPE LOCALITY: Moscow Basin, Russia.

DIAGNOSIS: A spore with a well-developed cingulum, distally and equatorially sculptured with verrucae and muri. Verrucae occur at different levels of focus. Uncertainty regarding the type species (See Richardson and Ioannides 1973).

BOTANICAL AFFINITIES: Uncertain.

Lophonzotriletes poecilomorphus Richardson and Ioannides 1973

Plate VII, figure f

STRATIGRAPHIC RANGE: *poecilomorphus* – *libycus* zone – *tripapillatus* – *spicula* zone.

DIAGNOSIS: A *Lophonzotriletes* with a well developed equatorial thickening; proximal surface thin, distal surface sculptured with discrete to coalescent verrucae and muri.

DESCRIPTION: 26.9μm (one specimen measured). Circular amb. Well-developed equatorial thickening. Proximal face is thin, with a subtle triradiate mark. Distally, the exine is sculptured with discrete to coalescent verrucae and verrucate ridges. These elements may be circular, being 1.9 – 4.6μm wide, mean 3μm and the elongate ridges are between 6.8 – 14.6μm long, mean 10.9μm. The distal sculpture is arranged on differing levels of focus.

COMPARISONS AND REMARKS: This spore compares well with descriptions in Richardson and Ioannides (1973) in terms of the amb diameter and element dimensions.

***Lophonzotriletes* cf. sp. A** Richardson and Ioannides 1973

Plate VII, figure g

STRATIGRAPHIC RANGE: Non-tripapillate *Aneurospora* spp. zone (*Apiculiretusispora* sp. E subzone) – lower *micrornatus* – *newportensis* subzone

DESCRIPTION: 24.3µm (one specimen measured). Triangular amb with rounded apices and convex sides. Proximally laevigate with a distinct triradiate mark, accompanied by lips 2.3µm wide at equator, tapering suddenly at the proximal apex. The lips extend to the equator. A distinct, thick crassitude, 4µm wide, circumscribes the proximal face. A series of narrow folds are organised along the inner edge of the crassitude. Distally, the exine is ornamented with distinct variously sized and shaped verrucae. Generally organised as discrete (although tightly packed) verrucae, 1.9 – 6.2µm long, mean 3.3µm and 1.2 – 2.6µm wide, mean 1.9µm. Verrucae may also be organised into rarer anastomosing and elongate verrucate ridges, up to 10µm long and 4µm wide. They are densely packed.

COMPARISONS AND REMARKS: This species is comparable to *L. poecilomorphus*, except this specimen exhibits robust lips. The specimen compares favourably with those figured in Richardson and Ioannides (1973), although the lips in this specimen appear more robust than the specimen figured there, and no mention is made of the lips tapering out at the proximal pole.

PATINATE TRILETE SPORES

Infraturma PATINATI Butterworth and Williams 1958

Genus ARCHAEOZONOTRILETES (Naumova) Allen 1965

Type species: *Archaeozonotriletes variablis* (Naumova) Allen 1965.

TYPE LOCALITY: Upper San Pedro Formation, Leon, Spain.

DIAGNOSIS: Radial, trilete, patinate spores with thickened equatorial and distal exoexine and thin, diaphanous contact areas.

BOTANICAL AFFINITIES: Uncertain, possible tracheophyte affinity?

Archaeozonotriletes chulus (Cramer) emend Richardson and Lister 1969

STRATIGRAPHIC RANGE: *poecilomorphus* – *libycus* zone – middle *micrornatus* – *newportensis* subzone.

SYNONYMS:

Cramer, 1966; *Retusotriletes chulus*

DIAGNOSIS: Patinate trilete spores with a thin, laevigate and diaphanous contact area that is often folded, collapsed or lost, and a distinctly equatorially and distally thickened laevigate exoexine; although a distinctive infrastructure of radial or convoluted muri may be developed. A thick, equatorial crassitude delimits the contact area and its presence often results in the equatorial exine thickness being greater than that of the distal region. Typically, the contact area exhibits a concentric fold separating the equatorial crassitude and the contact face; these folds simulate curvaturae perfectae.

COMPARISONS AND REMARKS: Variants of *Archaeozonotriletes chulus* are comparable to *Ambitisporites avitus*, however the latter lacks the thin, diaphanous contact areas, concentric fold, thickened equatorial and distal exine, and wider equatorial crassitude of the former. Furthermore, the triradiate mark does not equal the spore radius (terminating equatorially) in *Ar. chulus*, as it does in *A. avitus*.

Subtle, but important, variations in size and structure amongst *Ar. chulus* led Richardson and Lister (1969) to differentiate three variants within the species.

Archaeozonotriletes chulus* var. *chulus Richardson and Lister 1969

Plate VII, figures h – i

STRATIGRAPHIC RANGE: *poecilomorphus* – *libycus* zone – middle *micrornatus* – *newportensis* subzone.

DIAGNOSIS: An *Archaeozonotriletes chulus* with an amb size greater than 36µm.

DESCRIPTION: Size 36 - 65µm, mean 44µm (twenty-nine specimens measured). Triangular amb with rounded angles and convex sides in proximal view; hemisphaerical in equatorial aspect. The proximal contact area is thin and diaphanous and is frequently folded, collapsed or lost altogether. The triradiate mark is well developed with high, narrow lips which extend to the inner edge of the equatorial crassitude, where a thin, concentric fold simulating curvaturae perfectae is often developed. The crassitude itself is wide and the exine is thickened here, as well as on the distal surface; the exine of the distal surface is typically thinner than that of the equatorial region. The proximal and distal exoexine is entirely laevigate. Downtonian specimens may show a poorly developed apical thickening on the proximal face.

COMPARISONS AND REMARKS: *Ar. chulus* var. *chulus* is comparable to *Ambitisporites avitus*, although the latter lacks the diaphanous contact areas, thickened equatorial and distal exoexine and triradiate lips found on *Ar. chulus* var. *chulus*. *Ar. chulus* var. *chulus* can be differentiated from other variants in *Ar. chulus* as it is larger than *Ar. chulus* var. *nanus*, which does not exceed 36µm.

Archaeozonotriletes chulus* var. *nanus Richardson and Lister 1969

Plate VII, figures j – k

STRATIGRAPHIC RANGE: *poecilomorphus* – *libycus* zone – middle *micrornatus* – *newportensis* subzone.

DIAGNOSIS: An *Archaeozonotriletes chulus* with an amb size less than 36µm.

DESCRIPTION: Size: 17 - 35µm, mean 23µm (twenty-nine specimens measured). Not greater than 36µm. Proximally and distally laevigate exine. Contact face is thin and diaphanous, often folded, damaged or lost entirely. Distally and equatorially thick exine, typically thickest in the former.

COMPARISONS AND REMARKS: Comparable to *Archaeozonotriletes chulus* var. *chulus*, but is distinguished by its smaller size, not exceeding 36µm.

Archaeozonotriletes* cf. *chulus

Plate VII, figure l

STRATIGRAPHIC RANGE: *poecilomorphus* – *libycus* zone – middle *micrornatus* – *newportensis* subzone.

DESCRIPTION: 34 – 46µm, mean 38.6µm (four specimens measured). These spores are essentially identical to spores belonging to *A. chulus*, except for the very wide lips, which are 3 - 5µm wide, mean 3.7µm and they tend to lack the fold along the inner edge of the crassitude which is seen in *A. chulus* spores.

COMPARISONS AND REMARKS: Comparable to *Archaeozonotriletes chulus* var. *chulus* and var. *nanus*,but is distinguished by the very wide lips. Differ from *Ambitisporites* sp. A in that these spores are patinate, whilst *A.* sp. A is crassitate.

Genus CYMBOSPORITES Allen 1965

TYPE SPECIES: *Cymbosporites cyathus* Allen 1965

TYPE LOCALITY: Estheriahaugen, Central Dicksonland, Spitsbergen, Estheriahaugen Formation, Givetian.

DIAGNOSIS: Radial, trilete, patinate miospores with circular to roundly triangular ambs. Typically laevigate proximally, with a distal ornament of coni, spinae and granules.

BOTANICAL AFFINITIES: Uncertain.

Cymbosporites* cf. *dittonensis Richardson and Lister 1969

Plate VII, figure m

STRATIGRAPHIC RANGE: Lower - middle *micrornatus* – *newportensis* subzones.

DESCRIPTION: 24 – 29µm, mean 26 µm (six specimens measured). Triangular amb, with rounded apices and convex sides. Proximally laevigate, with a subtle triradiate mark, accompanied by narrow lips. Equatorially and distally the spores are ornamented with verrucate or rugulate elements and small cones, 0.7 – 1.8µm tall, mean 1µm and 0.7 – 1.7µm wide, mean 1.1µm.

COMPARISONS AND REMARKS: These spores compare well with those described in Richardson and Lister (1969).

Cymbosporites echinautus Richardson and Lister 1969

Not figured

STRATIGRAPHIC RANGE: *tripapillatus* – *spicula* zone.

DIAGNOSIS: Sculpture consists of individually biform spinose elements; elements basally broad, conical, terminated by cones, or parallel-sided to spatulate spines, discrete or fused into groups, commonly of 2 – 3 elements. Patina thickest in the equatorial region.

DESCRIPTION: 43 - 65µm, mean 49.4µm (ten specimens measured). Subtriangular amb, with convex sides and rounded apices. Proximally laevigate, with a diaphanous proximal face. The triradiate mark is distinct when present, accompanied by lips up to 3µm wide. Equatorially and distally, the spore is ornamented with predominantly biform, robust spinae. Broadly based elements, 1 - 5µm in width, sharply taper into sharply tipped cones or spines, or spines with spatulate tips. The height of elements is typically between 1 – 4µm. In plan, elements may be discrete or coalesced into groups of up to three. The density, height and width of elements vary considerably between specimens.

COMPARISONS AND REMARKS: These spores compare well with those described in Richardson and Lister (1969).

Cymbosporites* cf. *verrucosus Richardson and Lister 1969
Plate VII, figure n

STRATIGRAPHIC RANGE: Non-tripapillate *Aneurospora* spp. zone (*Apiculiretusispora* sp. E subzone) – middle *micrornatus* – *newportensis* subzone.

DESCRIPTION: 22 – 37µm, mean 28µm (fourteen specimens measured). Subcircular to subtriangular amb. Proximally laevigate with distinct triradiate mark, sometimes accompanied by wide lips. Equatorially and distally ornamented with round-topped, densely packed verrucae. Verrucae are 0.6 – 1.2µm tall, mean 1µm and 1.3 – 2.8µm wide, mean 1.8µm.

COMPARISONS AND REMARKS: These spores compare reasonably well with the descriptions in Richardson and Lister (1969), except the proximal radial wrinkles are not well exhibited here and the amb diameters are somewhat less than those given in Richardson and Lister (1969), where they measure between 29 – 52µm, although there is some overlap.

Genus CHELINOSPORA (Allen) McGregor and Camfield, 1976

TYPE SPECIES: *Chelinospora concinna* Allen 1965

TYPE LOCALITY: North ridge of Kinanderfjellet, Central Dicksonland, Spitsbergen; Upper Mimer Valley series, Givetian.

DIAGNOSIS: Trilete spores with distinct laesurae which are usually long, simple or accompanied by narrow folds. Proximal exine is thin, whilst being distally thickened. Distal patina is reticulate or foveoreticulate, with contact areas being laevigate or ornamented with reduced muri, grana and cones.

BOTANICAL AFFINITIES: Uncertain.

Chelinospora cassicula Richardson and Lister 1969
Plate VIII, figures a – d

STRATIGRAPHIC RANGE: Non-tripapillate *Aneurospora* spp. zone (*Apiculiretusispora* sp. E subzone) – middle *micrornatus* – *newportensis* subzone.

DIAGNOSIS: Patina relatively thin, sculptured equatorially and distally with muri which form an irregular reticulum; proximal face smooth.

DESCRIPTION: 23 – 60µm, mean 36µm (twenty specimens measured). Subtriangular to subcircular amb with a variably thickened exine. Typically, the equatorial exine is thickest, with the distal exine being slightly thinner. The proximal face is distinctly thinner than the rest of the exine. Equatorially and distally the exine is sculptured with prominent, membranous muri which commonly form an irregular reticulum, 2 – 5.5µm tall. Contact areas are delimited by distinct curvaturae perfectae which diverge from the triradiate mark which is accompanied by low lips which extend to near-equatorial limits.

COMPARISONS AND REMARKS: Tall muri are comparable to the cryptospore *Chelinohilates erraticus* Richardson, except *C. cassicula* Richardson and Lister is trilete. This may be difficult to ascertain in specimens which have lost their proximal faces, as any invaginations evidencing the lost triradiate mark may be obscured by the distal muri. These spores generally compare well those specimens described in Richardson and Lister (1969) in terms of amb size and sculptural dimensions. Some specimens fall below the measurements given in the original descriptions, where they measure between 35 - 52µm, but these smaller specimens are included in this species as they are otherwise identical.

Chelinospora* cf. *cantabrica Richardson and Ioannides 1973

Plate VIII, figures c – f

STRATIGRAPHIC RANGE: Non-tripapillate *Aneurospora* spp. zone (*Apiculiretusispora* sp. E subzone) – lower *micrornatus* – *newportensis* subzone.

DESCRIPTION: 32 – 44µm (four specimens measured). Circular ambs. Proximal face not seen. Equatorially and distally ornamented with a robust reticulum comprising wide muri and circular to polygonal lumina. Muri are robust and continuous, 1.8 – 3.8µm wide, mean 2.5µm, describing lumina 2 – 3.4µm wide, mean 2.7µm.

COMPARISONS AND REMARKS: These spores are comparable to the original descriptions in Richardson and Ioannides (1973) in terms of amb size and muri dimensions, but the lumina here are slightly smaller than those in Richardson and Ioannides' (1973), where they measure between 2.5 – 10µm, but are otherwise comparable. In addition, the specimens figured in Richardson and Ioannides (1973) appear to have fewer lumen exhibited on the distal hemisphere than the ones identified here, although lumen number is not defined in the original descriptions.

Interestingly, the specimens identified under SEM are associated with one another as a pair, which is similar to the specimens figured in Richardson and Ioannides (1973). The latter authors determined these specimens as part of a partially dissociated tetrad, but it is interesting that neither exhibited a triradiate mark. Similarly, the SEM and LM specimens identified here did not exhibit a triradiate mark. It may be possible, then, that these spores are in fact alete cryptospores, rather than patinate trilete spores.

Chelinospora obscura Burgess and Richardson 1995

Plate VIII, figure g

STRATIGRAPHIC RANGE: *poecilomorphus* – *libycus* zone.

DIAGNOSIS: low and broad muri form an irregular reticulum on the distal hemisphere, which is confined within the crassitude.

DESCRIPTION: 32 - 42µm, mean 36µm (seven specimens measured). Subcircular to subtriangular amb. Proximally laevigate with a distinct trilete mark, which extends to the inner edge of the crassitude. Distally, the spores are ornamented with low, rounded which are generally confined within the crassitude. Muri are 1 – 3.5µm wide, <1µm tall and set 1 – 6µm apart. The muri anastomose and joint to form an irregular reticulum where some muri are left unconnected.

COMPARISONS AND REMARKS: These specimens compare well with the original descriptions given in Burgess and Richardson (1995). A single specimen very similar to *C. obscura* but measuring 67µm was found and referred to as *C.* cf. *obscura* given the much greater amb size.

Chelinospora retorrida Turnau 1986
Plate VIII, figure h

STRATIGRAPHIC RANGE: Lower - Middle *micrornatus* – *newportensis* subzone.

DIAGNOSIS: A *Chelinospora* with a smooth proximal face and a distal hemisphere ornamented with elongate, straight verrucate ridges.

DESCRIPTION: 23.6 – 35.7µm, mean 30.5µm (seven specimens measured). Subcircular to subtriangular amb. Proximally laevigate with a distinct triradiate mark, accompanied by narrow lips, 1µm wide, extending to the inner edge of the crassitude. Equatorially and distally ornamented with elongate, straight verrucate ridges, 0.7 – 5.6µm long, mean 2.1µm and 0.4 – 1.4µm, mean 0.8µm and are 0.3 – 1.6µm apart, mean 0.7µm.

COMPARISONS AND REMARKS: These spores compare favourably with the original descriptions in Turnau (1986), however, some minor differences exist: firstly, whilst there is an overlap in amb diameter between this population and those described in Turnau (1986), the latter of which measure between 26 – 37µm, some specimens here fall slightly below that range. Furthermore, the grooves which separate the vermiculate ridges are distinctly wider in some cases here than in Turnau's (1986) descriptions, where they are 0.5µm wide.

Chelinospora vermiculata has finer, angular vermiculate ridges. *Cymbohilates glabrimarginatus* Turnau and Jakubowska is a hilate cryptospore with finer, although otherwise similar, ornament.

Chelinospora vermiculata Chaloner and Streel 1966
Plate VIII, figures i – j

STRATIGRAPHIC RANGE: Lower *micrornatus* – *newportensis* subzone.

DIAGNOSIS: A *Chelinospora* with a laevigate proximal face, and a distal hemisphere of fine vermiculae.

DESCRIPTION: 30.4 – 40µm, mean 34.6µm (five specimens measured). Subtriangular amb with rounded apices and convex sides. Proximally laevigate, sometimes with distinct lips accompanying the triradiate mark, up to 2µm wide. Equatorially and distally sculptured with fine vermiculae, 0.5 – 3.5µm long, mean 1.3µm and 0.3 – 0.9µm apart, mean 0.5µm.

COMPARISONS AND REMARKS: These spores compare reasonably well to those described in Chaloner and Streel (1966), but the vermiculae are closer together (compared to 2μm in Chaloner and Streel, 1966) and the vermiculae are slightly larger that those in the original descriptions, where they are <1μm.

Genus STELLATISPORA Burgess and Richardson 1995

BASIONYMS: *Archaeozonotriletes chulus* var. *inframurinatus* Richardson and Lister 1969

TYPE SPECIES: *Stellatispora inframurinatus* (Richardson) Burgess and Richardson 1995

TYPE LOCALITY: Upper Ludlovian, Linton Quarry, Welsh Borderland.

DIAGNOSIS: Radial, trilete miospores with a thin, laevigate proximal face and distally ornamented with radially arranged, distinct muri.

BOTANICAL AFFINITIES: Uncertain.

Stellatispora inframurinatus Burgess and Richardson 1995

STRATIGRAPHIC RANGE: *poecilomorphus* – *libycus* zone – lower *micrornatus* – *newportensis* subzone.

DIAGNOSIS: A *Stellatispora* where the distal, radial muri are anastomose towards the proximal pole.

Stellatispora inframurinatus* var. *inframurinatus Burgess and Richardson 1995
Plate IX, figure a

STRATIGRAPHIC RANGE: *poecilomorphus* – *libycus* zone.

SYNONYMS:
Richardson and Lister, 1969; *Archaeozonotriletes chulus* var. *inframurinatus*

DIAGNOSIS: A *S. inframurinatus* with narrow and straight radial muri on the distal hemisphere.

DESCRIPTION: 29 – 53 μm, mean 42μm (twenty-one specimens measured). Subtriangular amb with rounded apices and convex sides. Proximally, the contact face is often missing, and when present is often torn or folded. The triradiate mark is distinct, often accompanies by narrow lips <1μm wide. Distally, the spore is ornamented with typically straight, radial muri 1 – 3.5μm wide and extend up to 18μm; these radial muri never reach the equator and are generally absent over the distal pole. The muri are set 0.5 – 1.5μm apart.

COMPARISONS AND REMARKS: These spores compare well with the original species descriptions in Burgess and Richardson (1995). They are larger with a significantly larger mean than *S.* cf. *inframurinatus*. The distal muri are narrower, more straight and more closely packed than *S. inframurinatus* var. *cambrensis*.

Stellatispora inframurinatus* cf. var. *inframurinatus
Plate IX, figure b

STRATIGRAPHIC RANGE: Non-tripapillate *Aneurospora* spp. zone (*Aneurospora sheafensis* subzone) – lower *micrornatus* – *newportensis* subzone.

DESCRIPTION: Size 20 - 36μm, mean 26μm (28 specimens measured). Subtriangular amb with a generally robust, although often ?thin, exine. The proximal face is laevigate, and the distinct triradiate mark is accompanied by narrow lips which extend to inner edge of crassitude. The lips are often accompanied by small folds which run parallel to them. The crassitude is wide and robust. Distally ornamented with generally straight, although sometimes tapering radial muri 0.5 – 1.4μm wide, mean 0.8μm, which extend from the equator towards the proximal pole, which they often reach.

COMPARISONS AND REMARKS: *S. inframurinatus* cf. var. *inframurinatus* is differentiated from other variants of *S. inframurinatus* by its smaller size and mean size, and more robust proximal face, which is almost always present. Additionally, the exine is thinner and the distal radial muri appear to extend to the equator, a feature that does not occur in *S. inframurinatus* var. *inframurinatus* proper.

Stellatispora inframurinatus* var. *cambrensis Burgess and Richardson 1995
Plate IX, figure c

STRATIGRAPHIC RANGE: *poecilomorphus* – *libycus* zone.

DIAGNOSIS: A *Stellatispora* with broad, sinuous distal radial muri which anastomose towards the distal pole.

DESCRIPTION: 30 – 53μm, mean 37μm (forty-four specimens measured). Amb subtriangular with convex sides. Proximally, the contact face is laevigate but is often missing, torn or folded. The triradiate mark is accompanied by narrow lips <1μm wide, which extend to the inner edge of the crassitude. Distally, the spore is ornamented with broad, sinuous distal radial muri which anastomose towards the distal pole, up to 18μm long, 1.5 – 4.5μm wide and set 1 – 3μm apart. The muri may be straight to sinuous, often bifurcating, as they extend from the equator towards the proximal pole which they do not intersect. There is sometimes discrete muri present.

COMPARISONS AND REMARKS: These spores are distinguished from *S. inframurinatus* var. *inframurinatus* by the broad, sinuous distal radial muri which anastomose towards the distal pole. These specimens compare well with the original descriptions in Burgess and Richardson, although the amb diameter is larger in some specimens they have a similar mean.

7.3. Cryptospores

ENVELOPED CRYPTOSPORES

Anteturma CRYPTOSPORITES Richardson, Ford and Parker 1984
Turma INVOLUCRALETES Richardson 1996a

Suprasubturma PSEUDOPOLYADI Richardson 1996a
Infraturma LAEVIGATI Richardson 1996a

Genus SEGESTRESPORA Burgess and Richardson 1991

TYPE SPECIES: *Segestrespora (Dyadospora) membranifera* (Johnson) Burgess 1991

TYPE LOCALITY: *c*. 75m from base of Mill Hall section, Tuscarora Formation. US route 220, 1km SE of Mill Hall, Clinton County, Pennsylvania, USA.

DIAGNOSIS: Laevigate and permanently fused pseudodyads, separated by a single central thickening. The pseudodyads are completely enclosed within a variously adherent envelope which may be laevigate or variously ornamented with apiculi, rugulae, muri or verrucae.

BOTANICAL AFFINITIES: Cryptosporophytes.

***Segestrespora* sp. 1** sp. nov.
Plate IX, figure d

STRATIGRAPHIC RANGE: Middle *micrornatus* – *newportensis* subzone.

DESCRIPTION: 39 - 47µm (two specimens measured). Spores with a tightly adherent envelope ornamented with irregularly sized, closely spaced verrucae 0.9 – 2.8µm long, mean 1.6µm. Internal spore units are laevigate and permanently adherent, with a dense, wide encircling band 6.8µm wide with no discernible suture.

COMPARISONS AND REMARKS: Verrucate ornament on the envelope differentiates this species from other species of *Segestrespora.* The tightly adherent spore units with a fused encircling band suggests that this spore is a pseudopolyad and does not belong in the genus *Abditudyadus*.

Infraturma APICULATI Richardson 1996a
Infraturma SYNORATI Richardson 1996a
Suprasubturma EUPOLYADI Richardson 1996a
Infraturma LAEVIGATI Richardson 1996a

Genus ABDITUSDYADUS Wellman and Richardson 1996a

TYPE SPECIES: *Abditusdyadus histosus* Wellman and Richardson 1996*a.*

TYPE LOCALITY: Basal strata of the 'Lower Old Red Sandstone', near Eilean Orasaig, Kerrera, Scotland, UK.

DIAGNOSIS: True (unfused) dyads which are enclosed within a variously adherent membranous envelope which may be variously ornamented or laevigate.

BOTANICAL AFFINITIES: Uncertain.

Abditusdyadus laevigata Wellman and Richardson 1993
Plate IX, figures e – f

STRATIGRAPHIC RANGE: Lower *micrornatus* - *newportensis* subzone.

DIAGNOSIS: A distally laevigate *Artemopyra.* Hilum sculptured with 25 – 40 radially disposed, narrow muri of variable character. The length of the muri is variable within specimens, extending from the crassitude for one-third to all the way to the proximal pole.

DESCRIPTION: 42.9 – 66.8µm, mean 58µm (three specimens measured). Enveloped dyads. Internal 'spore' units are 16.2 – 27.5µm, mean 22.3µm wide and entirely laevigate. They are separated from one another. The envelope is crumpled and folded and variously adherent to the internal spore units.

COMPARISONS AND REMARKS: These specimens have a much more folded envelope than those figured in Wellman and Richardson (1996a). Nonetheless, they are grouped with this species as 'extreme' examples of folding. Additionally, the folds have little regularity or structure to them, indicating that the ornament is a result or folding and is not a mururonate reticulum, hence they are grouped into *A. laevigatus*.

Genus VELATITETRAS Burgess and Richardson 1991

TYPE SPECIES: *Velatitetras laevigata* Burgess and Richardson 1991

TYPE LOCALITY: Rhuddanian/ Aeronian type boundary section, Trefawr Formation.

DIAGNOSIS: Tightly adherent, obligate cryptospore tetrads that are entirely enclosed within a laevigate or ornamented envelope. The 'spores' in the tetrad are subtriangular to sub-circular in outline with smooth, low equatorial crassitudes. Envelope may be variously adpressed about the tetrad.

BOTANICAL AFFINITIES: Uncertain.

Velatitetras laevigata Burgess 1991
Plate IX, figure g

STRATIGRAPHIC RANGE: *tripapillatus* – *spicula* zone – lower *micrornatus* – *newportensis* subzone.

DIAGNOSIS: A *Velatitetras* with a laevigate envelope, which is diaphanous and often folded.

DESCRIPTION: 44µm. Obligate, tightly adherent tetrads with a sub-circular to circular outline which are completely enclosed within an envelope. The envelope is laevigate, diaphanous and often folded. The envelope is variously adherent to the tetrad within. The tetrad itself comprises laevigate, subtriangular spores with unfused, 18µm is diameter, with low and rounded equatorial crassitudes; the distal exine is thinned.

COMPARISONS AND REMARKS: Similar to *Tetrahedraletes medinensis*, although those spore lack an envelope. *V. laevigata* have been recovered from the middle *micrornatus* – *newportensis* subzone but these specimens are thought to be reworked.

Velatitetras reticulata Burgess and Richardson 1991

Plate IX, figures h – i

STRATIGRAPHIC RANGE: *tripapillatus* – *spicula* zone – lower *micrornatus* – *newportensis* subzone.

DIAGNOSIS: A *Velatitetras* with an envelope ornamented with low muri, which form a fine, continuous reticulum.

DESCRIPTION: Size 30 – 43, mean 36µm (ten specimens measured). Obligate tetrads which are sub-circular to circular in outline and completely enclosed within an envelope. The envelope may be tightly adherent to loosely attached to the tetrad within and is ornamented with low muri which form a fine, regular reticulum with small lumen across the envelope. muri are 0.5 – 0.8µm wide, mean 0.6µm. The muri describe lumen 1.9 – 4.6µm wide. The 'spores' in the tetrad are subtriangular to sub-circular in shape with laevigate exines and unfused equatorial crassitudes. The distal exine is thinned.

COMPARISONS AND REMARKS: The regular reticulum ornamenting the envelope distinguishes *Velatitetras reticulata* from other species in *Velatitetras*. *Velatitetras rugulata* has sinuous to convoluted, anastomosing rugulae across its envelope, whilst *Velatitetras laevigata* has a laevigate envelope. The spores here compare well with the original descriptions in Burgess (1991) in terms of amb diameter and sculptural dimensions. *V. reticulata* have been recovered from the middle *micrornatus* – *newportensis* subzone but these specimens are thought to be reworked.

Velatitetras anatoliensis Steemans et al., 1996

Plate IX, figure j

STRATIGRAPHIC RANGE: *tripapillatus* – *spicula* zone – lower *micrornatus* – *newportensis* subzone.

DIAGNOSIS: A *Velatitetras* with an envelope ornamented with coni and grana.

DESCRIPTION: Size 34µm (one specimen measured). An obligate, sub-circular tetrad enclosed within a loosely adherent envelope which is densely ornamented with coni, grana. Grana are 0.6 – 1µm tall, mean 0.8µm and 0.5 – 1.2µm wide, mean 0.7µm. The elements are set 0.3 – 0.7µm apart, mean 0.5µm. The obligate tetrad within comprises laevigate subtriangular spores with low, rounded crassitudes and thinned distal exines.

COMPARISONS AND REMARKS: *Velatitetras anatoliensis*is distinguished from other species within *Velatitetras* by its distinctive grana-ornamented envelope; the pseudodyad *Segestrespora* sp. A has a similarly ornamented envelope. These spores compare reasonably well with the description of this species in Steemans *et al*. (1996) and Burgess (1991), except these spores appear to exhibit cones and, in some cases, spines, rather than solely grana.

NAKED CRYPTOSPORES

Turma NUDIALETES Richardson 1996a
Suprasubturma PSEUDOPOLYADI Richardson 1996a
Infraturma LAEVIGATI Richardson 1996a

Genus CHELIOTETRAS Wellman and Richardson, 1993

TYPE SPECIES: *Cheliotetras caledonica* Wellman and Richardson 1996a

TYPE LOCALITY: Logan Formation at Logan Water, Lesmahagow inlier, Scotland, UK.

DIAGNOSIS: Cryptospore tetrads which are with entirely fused crassitudes (i.e. lack a line of attachment). These crassitudes have distinctive flanges between adjacent spore units.

BOTANICAL AFFINITIES: Uncertain.

Cheliotetras caledonica Wellman and Richardson 1993
Plate X, figure b

STRATIGRAPHIC RANGE: *poecilomorphus* – *libycus* zone – middle *micrornatus* – *newportensis* subzone.

DIAGNOSIS: A laevigate *Cheliotetras* where the exine of each spore unit is drawn out beyond the fused crassitude to form a distinct flange-like extension between adjacent spore units.

DESCRIPTION: 23 – 47μm, mean 31μm (forty specimens measured). Permanent tetrahedral tetrad with circular to subtriangular spore units. Spore units permanently fused with a crassitude drawn out into distinct flanges 2-8μm wide. No line of attachment is seen along the crassitude. Distal hemispheres of spore units are laevigate and rigid.

COMPARISONS AND REMARKS: *Tetrahedraletes medinensis* exhibits a clear line of attachment along the crassitudes. Wellman and Richardson (1993) indicate that the lower limit of amb size is 29μm. Here, the smallest examples are 23μm, but these spores otherwise compare favourably with the original descriptions.

Genus PSEUDODYADOSPORA Johnson 1985

TYPE SPECIES: *Pseudodyadospora laevigata* Johnson 1985

TYPE LOCALITY: Tuscarora Formation, Central Pennsylvania.

DIAGNOSIS: Pseudodyads comprising two permanently fused spores joined by a thick, encircling band which shows no plane of attachment.

BOTANICAL AFFINITIES: Uncertain.

Pseudodyadospora laevigata Johnson 1985

Plate X, figure c

STRATIGRAPHIC RANGE: *tripapillatus* – *spicula* zone – lower *micrornatus* – *newportensis* zone.

DIAGNOSIS: A distally laevigate *Pseudodyadospora,* with a distinct, fused central band connecting the 'spore' units.

DESCRIPTION: 21µm (one specimen measured), a naked, obligate dyad, approximately oval in outline and entirely laevigate. The two 'spore' components have a thin distal exine, and the distal surface is inflated; the dyad is isomorphic. Smooth, slightly thicker crassitudes are fused together to produce a central thickening between the two 'spore' components. This central band shows no line of attachment and is entirely fused.

COMPARISONS AND REMARKS: *P. laevigata* is comparable to *P. petasus* in gross structure, however the distally inflated distal surface distinguishes *P. laevigata* from the distally invaginated surfaces of *P. petasus*.

Pseudodyadospora petasus Wellman and Richardson 1993

Plate X, figures d – f

STRATIGRAPHIC RANGE: *poecilomorphus* – *libycus* zone – middle *micrornatus* – *newportensis* subzone.

DIAGNOSIS: A *Pseudodyadospora* with distally invaginated 'spore' units. The units are fused together by a thickened band.

DESCRIPTION: Unit size 15 - 45µm, mean 28µm (thirty-five species measured). Circular to sub-circular outline in proximal view and distally invaginated. In equatorial view the pseudodyad exhibits a constricting band with two distally invaginated, isomorphic spores on either side. The central band where the crassitudes of the spores are fused shows no plane of attachment and is thickened relative to the exine on the distal surface of the spores, which is relatively thin and rigid, but is occasionally folded.

COMPARISONS AND REMARKS: *P. petasus* is comparable to *P. laevigata*, however the distinctive invaginated distal surface on the former clearly distinguishes it from the latter, which exhibits inflated distal surfaces on the fused spores.

Genus TETRAHEDRALETES Strother and Traverse 1979

TYPE SPECIES: *Tetrahedraletes medinensis* Strother and Traverse 1979

TYPE LOCALITY: Tuscarora Formation, Section – Mann Narrows along route 322, NW of Burnham, Mifflin County, Pennsylvania, USA.

DIAGNOSIS: Laevigate, obligate tetrahedral tetrads.

BOTANICAL AFFINITIES: Cryptophytes.

Tetrahedraletes medinensis (Strother and Traverse) Burgess and Richardson 1995
Plate X, figures g - i

STRATIGRAPHIC RANGE: *poecilomorphus* – *libycus* zone – middle *micrornatus* – *newportensis* subzone.

SYNONYMS:
Wellman and Richardson, 1993; *Tetrahedraletes medinensis* Strother and Traverse; Burgess and Richardson 1991.
For full list see Wellman and Richardson, 1993.

DIAGNOSIS: Laevigate, obligate tetrahedral tetrads. Component units are sub-triangular and unfused, with the thickened crassitudes showing a clear line of attachment.

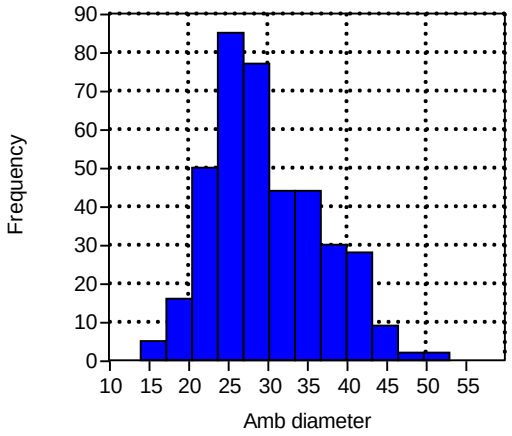

Figure III-10: Distribution of amb diameter of T. medinensis, *n = 392.*

DESCRIPTION: Size 14 - 53µm, mean 29.7µm (three hundred and ninety-two specimens measured). In outline, these tetrahedral spores are typically circular to roundly subtriangular, depending on the angle of compression. Individual units in the tetrad are sub-circular to subtriangular and are bounded by an unfused equatorial crassitude, 2 – 6µm, mean 4µm, which delimits the usually invaginated, thinned distal exine.

COMPARISONS AND REMARKS: This species has been divided into variants based on amb size by previous workers (Burgess, 1991). However, upon extensive measuring (figure 10) these spores show gaussian distribution amongst Silurian - Devonian *Tetrahedraletes medinensis,* and as such the differentiation based on amb size has not been made here. It is likely that the variously sized species are from different, although possibly quite similar plants, but it does not seem practical to divide the species up based solely on size. As such, this species is referred to simply as *T. medinensis*. Some specimens of *T. medinensis* may exhibit a flange like extension similar to that seen in *C. caledonica*, but specimens of the former always exhibit a clear line of attachment.

Infraturma APICULATI Richardson 1996a

Genus ACONTOTETRAS Richardson 1996a

TYPE SPECIES: *Acontotetras inconspicuis* Richardson 1996a, plate 10, figures6 -7, E.F. no. G38, FM746, sample CH/SD/88/2C. Upper Moor Cliffs Formation, Brown Clee Hill.

TYPE LOCALITY: Upper Moor Cliffs Formation, Brown Clee Hill.

DIAGNOSIS: Permanent tetrads comprising subtriangular to subcircular spore like units which are closely adherent but separated from each other by distinct lines of attachment. The exines of each eucryptospore unit may be ornamented with grana, coni or microconi.

BOTANICAL AFFINITIES: Uncertain.

Acontotetras inconspicuis Richardson 1996a
Plate X, figures j – k

STRATIGRAPHIC RANGE: *tripapillatus* – *spicula* zone – middle *micrornatus* – *newportensis* subzone.

DIAGNOSIS: An *Acontotetras* with small, wide low grana (microconi).

DESCRIPTION: 20.7 – 35μm, mean 27μm (twelve specimens measured). Subtriangular eucryptospore units. Distal hemispheres of spore units are ornamented with dense, low and wide micrograna and microconi, 0.2 – 0.7μm tall, mean 0.4μm and 0.3 – 0.8μm wide, mean 0.5μm. Elements are set 0.2 – 1μm apart, mean 0.5μm.

COMPARISONS AND REMARKS: Distinguished from *T. medinensis* by the apiculate ornament on the distal exine of spore units. Differs from *Cheliotetras* sp. 1 as *A. inconspicuis* does not exhibit flanges.

Infraturma SYNORATI Richardson 1996a
Suprasubturma EUPOLYADI Richardson 1996a
Infraturma LAEVIGATI Richardson 1996a

Genus DYADOSPORA Strother and Traverse

TYPE SPECIES: *Dyadospora murusattenuata* (Strother and Traverse) emend Burgess and Richardson 1991.

DIAGNOSIS: Naked, true dyads comprising two laevigate, hilate cryptospores which are loosely attached and show a distinct line of attachment between the two cryptospore units.

BOTANICAL AFFINITIES: Spores of the *D. murusattenuata* morphon have been found *in situ* by Wellman *et al*., 1998*a* (in *Lenticulitheca* Edwards), which shares similarities with the trilete-bearing genus *Paracooksonia*. One terminal sporangium was associated with a bifurcating sporophytic axis, suggesting that the affinity of these plants is not purely 'bryophytic'.

Dyadospora murusattenuata morphon Steemans *et al*. 1996

This morphon includes the two species *Dyadospora murusattenuata* and *D. murusdensa* Strother and Traverse, 1979. These two species have very similar morphologies. *D. murusattenuata* is distinguished by a thin, typically folded exine, compared with the thick, robust exine of *D. murusdensa* (Burgess and Richardson, 1991). However, between the two end members all intermediate forms exist, and differentiation is difficult. Furthermore, the folding of the spore exine may depend on the nature of preservation and compression alongside the wall rigidity. Additionally, the two species appear to have a similar stratigraphic range. Hence, this morphon is applied to the two species here.

Dyadospora murusattenuata - murusdensa (Strother and Traverse) emend Burgess and Richardson 1991.

Plate X, figures l – n

STRATIGRAPHIC RANGE: *poecilomorphus* – *libycus* zone – middle *micrornatus* – *newportensis* subzone.

DIAGNOSIS: Naked, true dyads comprising two laevigate, hilate cryptospores which are loosely attached and show a distinct line of attachment between the two cryptospore units. The exine may be rigid or show varying amounts of folding.

DESCRIPTION: Size 11 - 37μm, mean 25μm (thirty-three specimens measured). loosely attached naked dyads comprising two laevigate cryptospores which exhibit either thin and folded with narrow crassitudes, or robust and thick with wide crassitudes, describing hilums 11.3 – 35.9μm wide. The attachment point between the crassitudes is narrow and exhibits a distinct line of attachment between the two cryptospores. Often, the cryptospores become partially separated along this line of attachment.

COMPARISONS AND REMARKS: *P. laevigata* may be comparable to *D. murusattenuata - murusdensa*, but the latter exhibits a clear line of attachment between the two cryptospore units and is often partially dissociated along this line.

These dyads may be related to the *Laevolancis divellomedium-plicata* complex, with individual spore units being indistinguishable from them.

Genus RIMOSOTETRAS Burgess 1991

TYPE SPECIES: *Rimosotetras problematica* Burgess 1991

TYPE LOCALITY: Forestry track F.33, Bronydd Formation, *acinaces* Graptolite biozone, Rhuddanian.

DIAGNOSIS: Adherent, but often partially separated tetrahedral tetrads comprising laevigate spore like units with subtriangular to subcircular ambs.

Rimosotetras problematica Burgess 1991

Plate XI, figure a

STRATIGRAPHIC RANGE: *poecilomorphus* – *libycus* zone – middle *micrornatus* – *newportensis* subzone.

DIAGNOSIS: A *Rimosotetras* with subtriangular 'spores' possessing rounded, non-projecting equatorial crassitudes.

DESCRIPTION: 28.3µm (one specimen measured). Subcircular to circular cryptospore tetrads. Composed of loosely attached, laevigate spore units. The distal exine is usually inflated. The proximal faces typically lack features attributable to trilete miospores, but the triradiate mark may be simulated by cracks in the proximal exine; generally alete, however.

COMPARISONS AND REMARKS: Distal exine of spore units in inflated rather than invaginated, as in *T. medinensis*. Furthermore, in *T. medinensis*, the spore units are much more tightly adherent. In *C. caledonica* the crassitudes show a distinctive, extended flange.

Infraturma APICULATI Richardson 1996a
Infraturma SYNORATI Richardson 1996a
Suprasubturma HILATES Richardson 1996a
Infraturma LAEVIGATI Richardson 1996a

Genus LAEVOLANCIS Richardson 1996a

TYPE SPECIES: *Laevolancis divellomedium* (Chibrikova) Richardson 1996a

DIAGNOSIS: Alete spores exhibiting a laevigate proximal and distal exine, with an equatorial to subequatorial crassitude which delimits a proximal hilum.

BOTANICAL AFFINITIES: Found *in situ* by Wellman *et al*. (1998*b*) in a rhyniophytoid, possibly with bryophytic affinities.

MORPHONS: *Laevolancis divellomedium* and *L. plicata* are grouped into the *L. divellomedium* morphon here, after Steemans *et al*. (1996). The above end members with thick, robust distal exines and wide crassitudes or thin, folded exines with thin crassitudes (respectively) exist on a continuum and intermediates are indistinguishable from one another.

Laevolancis divellomedium – plicata (Chibrikova) Richardson 1996a
Plate XI, figures b – d

STRATIGRAPHIC RANGE: *poecilomorphus* – *libycus* zone – middle *micrornatus* – *newportensis* subzone.

SYNONYMS:
Richardson and Lister, 1969; ?*Archaeozonotriletes* cf. *divellomedium* Chibrikova

DIAGNOSIS: Alete spores exhibiting a laevigate proximal and distal exine, with an equatorial to subequatorial crassitude which delimits a proximal hilum.

DESCRIPTION: Size 15 – 73µm, mean 30.8µm (three hundred and twenty-five specimens measured). Amb is sub-circular to circular in outline with a narrow to wide subequatorial crassitude which delimits a

circular proximal hilum. The amb: hilum ratio is typically between 1.1 – 1.82. The exine over the hilum is laevigate and very thin to very thick and robust. The former is often found folded.

COMPARISONS AND REMARKS: *L. divellomedium* is distinguished from *L. plicata* Richardson and Burgess and Richardson 1991 by its thicker, rigid and rarely folded distal exine and more pronounced crassitude; *L. plicata* has a thinner, frequently folded distal and proximal exoexine and a much less pronounced equatorial crassitude. Some specimens identified in the assemblages exhibit circular 'stepped' pores. These have been identified *in situ* by various authors (e.g. Wellman *et al*., 1998a) and were identified as a possible *Laevolancis* variant. Strother (1991) described *Confossuspora reniforma* Strother, which these spores correspond to in terms of size (figure 11) and general characteristics. However, Strother (1991) indicates that there is approximately 60 pores per spore, and none of the specimens described here exhibit that number of spores.

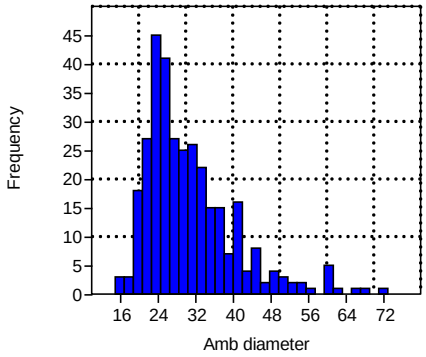

Figure III-11: Distribution of L. divellomedium – plicata *amb diameter. N = 325.*

***Laevolancis* sp. 1**

Plate XI, figure e

STRATIGRAPHIC RANGE: Lower - middle *micrornatus* – *newportensis* subzone.

DESCRIPTION: Size 24 - 39µm, mean 32µm (three specimens measured). Circular amb. The proximal face is laevigate except for two to three inter radial papillae 4.4 – 7.6µm, mean 5.6µm in diameter are exhibited in the hilum. Distally laevigate, proximal face and distal exine sometimes folded and variously robust.

COMPARISONS AND REMARKS: These spores are distinguished by the presence of inter radial papillae. They are similar in some respects to *Ambitisporites tripapillatus* except they lack a triradiate mark; these specimens are hilate.

Genus ARTEMOPYRA (Burgess and Richardson) Richardson 1996a

TYPE SPECIES: *Artemopyra brevicosta* Burgess and Richardson, 1991.

TYPE LOCALITY: Farley member, late Wenlock *nassa* graptolite zone. Eaton track, upper coalbrookdale Formation, UK.

DIAGNOSIS: Alete proximally hilate cryptospores. Proximally, the hilum is sculptured with chiefly radial muri, whilst the distal exine is laevigate or variously ornamented with grana, coni, biform elements or spinae.

BOTANICAL AFFINITIES: Uncertain.

Artemopyra* cf. *brevicosta Burgess and Richardson 1991
Plate XI, figures f – h

STRATIGRAPHIC RANGE: Lower – middle *micrornatus* – *newportensis* subzone.

DESCRIPTION: 29 - 48μm, mean 37.5μm (three specimens measured). Circular amb and circular hilum, the latter of which is 2/3 to 5/6 of the amb diameter. A narrow ring along the edge of the hilum comprises radial muri 1.3 – 3.8μm long, mean 2.4μm and 0.4 – 1μm wide, mean 0.6μm. They are always less than half of the spore radius in length. The spores are distally laevigate.

COMPARISONS AND REMARKS: *A. brevicosta* differs from *A. recticosta* as the former has muri less than half of the equatorial radius and are less robust. These spores compare reasonably well with the original descriptions in Burgess and Richardson (1991) in terms of amb size and general characteristics, although the muri are slightly narrower than those measurements given in Burgess and Richardson (1991), where they measure between 1 – 2μm. Furthermore, the muri do not appear to taper as distinctly in these specimens as they do in those specimens figured in the original descriptions.

Artemopyra* cf. *radiata (Strother) Burgess and Richardson 1995
Plate XI, figure i

STRATIGRAPHIC RANGE: *tripapillatus* – *spicula* zone – non-tripapillate *Aneurospora* spp. zone (*Apiculiretusispora* sp. E subzone).

DESCRIPTION: Size 42μm (one specimen measured). Sub circular to circular amb. Proximally, the hilum is concave, restricted to subequatorial regions of the proximal hemisphere, ornamented with convolute, essentially radial muri. These muri are 5 – 6μm, mean 6 μm long and 0.8 – 1.7μm, mean 1.2μm wide and set <2μm apart. In this specimen, the muri become anastomosing and convolute over the proximal pole. Distally laevigate.

COMPARISONS AND REMARKS: This specimen compares well with descriptions for the species in Burgess and Richardson 1995, although the amb diameter exceeds the maximum diameter given there (35μm), and in some cases the thickness of the radial muri exceeds the widths given there also.

There is some variation in the character of the radial muri, which are either radial, radial into convolute (as here) or radial into concentric. With further study, there may be cause to differentiate the species into variants.

Artemopyra recticosta (Strother) Burgess and Richardson 1995
Plate XI, figure j – k

STRATIGRAPHIC RANGE: Non-tripapillate *Aneurospora* spp. zone (*Apiculiretusispora* sp. E subzone) - lower *micrornatus* – *newportensis* subzone.

DIAGNOSIS: An *Artemopyra* with radial muri ornamenting the proximal hilum, but not extending fully the proximal pole. Distally laevigate.

DESCRIPTION: Size 37µm (one specimen measured). Circular amb and hilum. Hilum ornamented with 21 robust radial muri, extending 6.9 – 12.2µm long, mean 10.3µm and 0.9 – 1.7µm wide, mean 1.4µm. Muri are 0.6 – 1.3µm apart at the hilum edge. Muri extend half of the spore radius to the apical pole. Muri may be anastomosing but are generally straight. The distal hemisphere is laevigate.

COMPARISONS AND REMARKS: These spores differ from *A. brevicosta* as they have more robust radial muri which extend beyond halfway towards the proximal pole. They differ from *A. inconspicuis* as species of *A. recticosta* have fewer and more robust radial muri. These spores compare favourably with original descriptions in Breuer *et al*. (2007) in terms of amb diameter, which are between 34 – 70µm in Breuer *et al*. (2007), and sculptural dimensions. The number of muri also correspond well with the original descriptions, where radial muri number between 18 – 46.

Artemopyra* cf. *inconspicuis Breuer *et al* 2007
Plate XI, figure l

STRATIGRAPHIC RANGE: Lower – middle *micrornatus* – *newportensis* subzone.

DESCRIPTION: 33 – 36.9µm, mean 34.9µm (three specimens measured). Circular amb and hilum. The hilum is ornamented with radial muri which extend more than half to all the way to the proximal pole. The radial muri are fine and barely discernible, 0.3 – 1µm wide and 0.4 – 0.6µm apart at the edge of the hilum. There are 45 – 60 radial muri on the proximal face.

COMPARISONS AND REMARKS: These spores are distinguished by their fine, numerous muri on the proximal face. These spores compare reasonably well with specimens described in Breuer *et al*. (2007) in terms of amb size and general characteristics, although there are slightly fewer muri sculpturing the hilum than in the original descriptions, where Breuer *et al*. (2007) indicate there are between 60 - 90 muri.

Infraturma APICULATI Richardson 1996a

Genus CYMBOHILATES Richardson 1996a

TYPE SPECIES: *Cymbohilates horridus* Richardson 1996a

TYPE LOCALITY: Freshwater West Formation, 65m above the Chapel Point Limestone, North Brown Clee Hill, Shropshire.

DIAGNOSIS: Proximally hilate monad cryptospores. Subequatorial and distal exine is sculptured with apiculate elements of grana, coni or spinae, sometimes elements are biform or fused into groups; baculae are occasionally developed also. Proximally, the hilum is smooth or may be ornamented with random or concentric folding which may be accompanied by radial muri.

BOTANICAL AFFINITIES: Cryptosporophytes. A number of *Cymbohilates* species have been found *in situ* in spore masses from the Welsh Borderlands, associated with cryptosporophytes *Lenticulitheca* Morris *et al*., *Cymbohilates allenii* var. *allenii* is found in *Lenticulitheca allenii* Morris *et al.* (2011b). *Cymbohilates allenii* var. *magnus* is found in *Lenticulitheca magna* Morris *et al.* (2011b). *Cymbohilates variabilis* is found in *Lenticulitheca variabilis* Morris *et al.* (2011b).

Cymbohilates allenii Richardson 1996a

DIAGNOSIS: A *Cymbohilates* with a double wall, possibly excluding the hilum. Hilum has an irregular, frequently folded margin and whilst laevigate, is characterised by folds. Sub equatorially and distally sculptured with very densely packed micrograna

COMPARISONS AND REMARKS: This species has been divided into two variants based on size by Richardson (1996). *C. allenii* var. *allenii* has a size <30µm, whilst *C. allenii* var. *magnus* has a size greater than 30µm.

Cymbohilates allenii* var. *allenii Richardson 1996a

Plate XI, figure m

STRATIGRAPHIC RANGE: Lower middle *micrornatus* – *newportensis* subzone.

DIAGNOSIS: A *Cymbohilates allenii* with a size <30µm.

DESCRIPTION: 22 – 29.4µm, mean 26.7µm (ten specimens measured). Amb circular to subcircular. Proximally, the hilum is laevigate and sometimes lost. Equatorially and distally the spores are ornamented with densely packed, ± equidimensional micrograna, 0.2 – 0.5µm wide, mean 0.4µm and are set 0.1 – 0.9µm apart, mean 0.4µm.

COMPARISONS AND REMARKS: The smaller size and thinner exine distinguishes *C. allenii* var. *allenii* from *C. allenii* var. *magnus*. Spores of a similar character, except with radial muri/ folds on the proximal hilum, are referred to as *C.* allenii var. A in Richardson (1996). These spores compare well with the original descriptions on the species variant in Richardson (1996) in terms of amb size and element dimensions.

Cymbohilates allenii* var. *magnus Richardson 1996a

Plate XII, figure a

STRATIGRAPHIC RANGE: Lower middle *micrornatus* – *newportensis* subzone.

DIAGNOSIS: A *Cymbohilates allenii* with a amb diameter >30µm.

DESCRIPTION: 38.7– 54µm, mean 41.4µm (four specimens measured). Circular amb. The proximal hilum is laevigate, folded and is sometimes lost. Equatorially and distally the spores are ornamented with dense micrograna, ± equidimensional, 0.2 – 0.5µm wide, mean 0.3µm and are set 0.2 – 0.6µm apart, mean 0.4µm.

COMPARISONS AND REMARKS: The spores are essentially identical to *C. allenii* var. *allenii* except for the amb size, which exceeds 30µm. These spores compare well with the original descriptions of the species variants in Richardson (1996) in terms of amb diameter and element dimensions. They also differ from *C. allenii* var. *allenii* in having greater distal inflation.

Cymbohilates cymosus Richardson 1996a

Plate XII, figures b – c

STRATIGRAPHIC RANGE: Lower middle *micrornatus* – *newportensis* subzone.

DIAGNOSIS: A *Cymbohilates* ornamented with short spines arranged in star-shaped clusters.

DESCRIPTION: 38 - 44µm, mean 41µm (three specimens measured). Circular to subcircular amb. Proximally laevigate except for occasional fine radial folds. Equatorially and distally ornamented with short, sharp spines arranged in closely packed clusters, each exhibiting 3 – 7 spines. Clusters are 1.2 – 2.3µm wide, mean 1.8µm.

COMPARISONS AND REMARKS: The star-shaped clusters are diagnostic. These specimens compare well to the original descriptions of the species in Richardson (1996) in terms of amb diameter and element dimensions.

Thee spores occasionally appear as dyads, and tetrads were described in Richardson (1996a). In terms of the latter, these may be undissociated examples of *Cymbosporites* sp. 15. The dyads are probably undissociated examples of *C. cymosus*.

Cymbohilates disponerus Richardson 1996a

Plate XII, figures d

STRATIGRAPHIC RANGE: Non-tripapillate *Aneurospora* spp. zone (*Apiculiretusispora* sp. E subzone) – middle *micrornatus* – *newportensis* subzone.

DIAGNOSIS: A *Cymbohilates* sculptured with evenly spaced microconi to coni; sculptural elements isodiametric to broader than high.

DESCRIPTION: 20 - 37µm, mean 28µm (six specimens measured). Circular to subcircular amb. Proximal hilum is laevigate. Equatorially and distally ornamented with closely spaced, ± isodiametric to broader than high microconi, 0.3 – 0.8µm wide, mean 0.5µm, 0.2 – 0.5µm tall, mean 0.3µm and set 0.3 – 1.3µm apart, mean 0.7µm.

COMPARISONS AND REMARKS: These spores differ from *C. variabilis* by having small and regularly spaced coni, and from *C. allenii,* which exhibits very densely packed, minute grana. The former has a mixture of elements on the distal surface and a thicker exine. These specimens compare well with the original descriptions of the spores in Richardson (1996) in terms of amb diameter (although some specimens exceed the upper 30µm amb diameter limit given there) and element dimensions.

Cymbohilates horridus **(**Richardson) Richardson 2012

DIAGNOSIS: A *Cymbohilates* with a double wall and circular hilum. May occur as individual hilate monads or as partially or fully associated dyads. In individual monads, the hilum is often lost or torn. Acinoform (spinosereticulate) and scabrate spinose forms are differentiated into two variants.

Cymbohilates horridus **var. *horridus*** **(**Richardson) Richardson 2012

Plate XII, figure f

STRATIGRAPHIC RANGE: Lower - middle *micrornatus* – *newportensis* subzone.

DIAGNOSIS: A *Cymbohilates horridus* with broad based spines ornamented on a reticulum (spinosereticulate).

DESCRIPTION: 60 - 77µm, mean 69µm (nine specimen measured). Circular amb. Proximally, the hilum is thin and diaphanous. Distally ornamented with large, prominent, pointed spines which uniformly taper and may become biform on some specimens, and are fused into ridges. Spines are 3.7 – 4.9µm tall, mean 4.4µm and 3.3 – 4.8µm, mean 4µm wide at the base.

COMPARISONS AND REMARKS: These spores compare well with the original species descriptions in Richardson (1996a) and with emended descriptions in Richardson 2012 (Edwards et al., 2012) in terms of amb diameter and element dimensions. This variant is differentiated from *C. horridus* var. *splendidus* by the broad based spines and spinosereticulate habit.

***Cymbohilates horridus* var. *splendidus* (**Richardson) Richardson 2012
Plate XII, figure e

STRATIGRAPHIC RANGE: Lower - middle *micrornatus* – *newportensis* subzone.

DIAGNOSIS: A *Cymbohilates horridus* with narrow spines, which are not linked by a reticulum.

DESCRIPTION: 45µm, (one specimen measured). Circular amb. Proximally, the hilum is thin and diaphanous. Distally ornamented with long, prominent, pointed spines which uniformly taper and may become biform on some specimens. Spines are 3 – 7µm tall, mean 4.35µm and 1 – 3µm, mean 2µm wide at the base, narrowing to 0.5µm towards the top. Spines can bend and become hairlike and are not linked by a reticulum.

COMPARISONS AND REMARKS: These spores compare well with the original species descriptions in Richardson (1996a) and with emended descriptions in Richardson 2012 (Edwards et al., 2012) in terms of amb diameter and element dimensions. This variant is distinguished from var. *horridus* in that the spines are narrower and these spores are not acinoform.

Cymbohilates mesodecus Richardson 2011
Plate XII, figures g – h

STRATIGRAPHIC RANGE: Lower - middle *micrornatus* – *newportensis* subzone.

DIAGNOSIS: A *Cymbohilates* with a distal ornament of micrograna or microconi. About the proximal hilum, a distinctive, thickened collar is developed.

DESCRIPTION: 23 - 33µm, mean 27µm (four specimens measured). Circular amb. Proximally laevigate, although the hilum is sometimes folded. The hilum is entirely described by a narrow (<1µm), distinctly thickened collar, outside of the hilum and across the distal hemisphere, the exine is ornamented with ± equidimensional micrograna and microconi, 0.4 – 0.9µm wide, mean 0.6µm and 0.4 – 0.5µm tall. The elements are set 0.2 – 1.5µm apart, mean 0.7µm. Sometimes, elements are developed on the curvatural collar, too.

COMPARISONS AND REMARKS: The broad, curvatural crassitude is diagnostic of this cryptospore and distinguishes the species from *C. disponerus*, alongside the presence of micrograna. These specimens compare well with the original descriptions of the species in Richardson (2011) in terms of amb size and element distribution.

Cymbohilates* cf. *mesodecus Richardson 2011

Plate XIII, figure a

STRATIGRAPHIC RANGE: Lower - middle *micrornatus* – *newportensis* subzone.

DESCRIPTION: 29.3 – 30µm (two specimens measured). Roundly triangular amb. Proximally, a narrow, distinct curvaturate collar 0.8 – 1.6µm wide describes the laevigate hilum. The collar is associated with broad based spinae, which occur regularly along the feature, up to 2µm tall and 1.5µm wide with sharp or blunt apices. Outside of the hilum, sparse robust spinae 0.8 – 2.2µm tall, mean 1.6µm and 0.9 – 1.6µm wide, mean 1.2µm. The elements are set 0.5 – 4.6µm apart, mean 2.3µm. Interspersed amongst these, is a dense, irregular micro-ornament.

COMPARISONS AND REMARKS: Distinguished by the small hilum accompanied by a narrow curvaturate collar, with associated spines, which together appears as a 'crown of thorns', and the sharp or blunt robust spaced spinae. The collar is redolent of *C. mesodecus*, but the ornament is notably different.

Cymbohilates rhabdionus Richardson 2011

Not figured

STRATIGRAPHIC RANGE: Middle *micrornatus* – *newportensis* subzone.

DIAGNOSIS: A *Cymbohilates* with a distal ornament of spaced microbaculae with flat apices.

DESCRIPTION: 32µm (one specimen measured). Circular amb with a smooth hilum. Equatorially and distally ornamented with spaced microbaculae with flat apices, up to 1µm tall and <1µm wide. Elements are set up to 2µm apart.

COMPARISONS AND REMARKS: This specimen compares well with specimens described in Richardson (2011).

Cymbohilates variabilis Richardson 1996a

DIAGNOSIS: A *Cymbohilates* with a hilum that may be laevigate or exhibit proximal radial ribs. Distally, variously sized and shaped biform, verrucose, aciculate and spatulate tipped spinose sculptural elements are exhibited on the same specimen. Thick equatorial and distal exine. Elements may be crowded to well dispersed across the distal exine.

COMPARISONS AND REMARKS: This *Cymbohilates* species is divided into four variants, based on element size, amb size and proximal hilum sculpture.

Cymbohilates variabilis* var. *variabilis Richardson 1996a
Plate XIII, figures b – c

STRATIGRAPHIC RANGE: Middle *micrornatus* – *newportensis* subzone.

DIAGNOSIS: A *Cymbohilates variabilis* with a distal sculpture of coalesced, broad based to biform coni, and a proximal face ornamented with radial muri and a papillae; the latter of which is developed at the proximal pole.

DESCRIPTION: 36 – 49µm, mean 43µm (thirteen specimens measured). Circular amb. Proximally, the hilum exhibits radial muri which extend towards the proximal face, tapering from the outer edge of the hilum, but they do not reach the proximal pole, where instead a circular thickening (? apical papilla) is exhibited. Distally the spores are sculptured with a mixture of coalesced, broad based to biform coni, 2.3 – 7.9µm wide, mean 4.7µm and 0.9 – 2µm tall, mean 1.6µm.

COMPARISONS AND REMARKS: These spores differ from other variants of *C. variabilis* in their coalesced distal sculpture and short radial muri. These specimens compare well with the original descriptions of the variant in Richardson (1996) in terms of amb diameter and sculptural dimensions.

Cymbohilates variabilis* var. *parvidecus Richardson 1996a
Plate XIII, figures d – e

STRATIGRAPHIC RANGE: Lower - middle *micrornatus* – *newportensis* subzone

DIAGNOSIS: A *Cymbohilates variabilis* coni, grana or microbaculae; width of elements at the base less than 2µm, typically less than 1µm.

DESCRIPTION: 24 - 43µm, mean 29µm (five specimens measured). Proximally ornamented with radial muri, extending from the inner edge of the hilum. Outside of the hilum, the distal exine is sculptured with a mixture of coni and flat-topped elements, 0.4 – 0.7µm tall, mean 0.5µm and 0.4 – 0.8µm wide, mean 0.6µm.

COMPARISONS AND REMARKS: These spores compare favourably with the original descriptions in Richardson (1996).

Cymbohilates variabilis* var. *tenuis Richardson 1996a
Plate XIII, figure f

STRATIGRAPHIC RANGE: Lower - middle *micrornatus* – *newportensis* subzone.

DIAGNOSIS: A *Cymbohilates variabilis* with a relatively thin exine and a sculpture of spaced, broad based coni and microbaculae.

DESCRIPTION: 22 - 36µm, mean 27µm (nine specimens measured). Circular amb, exine thinned and often folded. Proximally, the hilum is laevigate. Outside of the hilum, the exine is ornamented with fine coni, 0.5 – 0.8µm wide, mean 0.6µm and 0.4 – 0.5µm tall, mean 0.4µm.

COMPARISONS AND REMARKS: Small microconi similar to var. *parvidecus* but distinguished by thinner, frequently folded exine. These specimens compare well with the original descriptions in Richardson (1996).

***Cymbohilates variabilis* var. A** Richardson 1996a
Plate XIII, figures g – h

STRATIGRAPHIC RANGE: Lower - middle *micrornatus* – *newportensis* subzone

DESCRIPTION: 25 – 41μm, mean 33μm (eight specimens measured). Circular amb. Proximally ornamented with radial muri, extending from the inner edge of the hilum to the proximal pole. Sometimes, interadial papillae are developed, also which are up to 2μm long. Outside of the hilum, the spores are sculptured with coni, 0.5 – 1.9μm wide, mean 1μm and 0.4 – 1μm high, mean 0.8μm.

COMPARISONS AND REMARKS: Similar distal sculpture to var. *variabilis*, except the basal width is generally smaller, fewer elements are coalesced and proximal radial muri extend almost to the apex. These specimens compare well to the original descriptions of the variant in Richardson (1996).

Infraturma SYNORATI Richardson 1996a

Genus CHELINOHILATES Richardson 1996a

TYPE SPECIES: *Chelinohilates erraticus* Richardson 1996a

TYPE LOCALITY: Lower Ditton (Freshwater West) Formation, Brown Clee Hill, Shropshire.

DIAGNOSIS: Eucryptospores or paracryptospores where the exine has been differentiated into at least two layers. The outer layer does not extend over the proximal hilum and is sculptured, thin and variably adpressed to the inner exine, which may be folded over the hilum or collapsed.

BOTANICAL AFFINITIES: Cryptosporophytes.

Chelinohilates erraticus Richardson 1996a
Plate XIII, figures i – k

STRATIGRAPHIC RANGE: Non-tripapillate *Aneurospora* spp. zone (*Aneurospora sheafensis* subzone) – middle *micrornatus* – *newportensis* subzone.

DIAGNOSIS: A *Chelinohilates* with a distinct proximal hilum surrounded by a narrow subequatorial zone of more or less radial muri; outer exoexine loosely to firmly appressed, distally and equatorially sculptured by flexuous muri forming an irregular, reticulate pattern.

DESCRIPTION: 26.4 – 61μm, mean 41.9μm (thirteen specimens measured). Circular to subcircular amb. Proximally, a distinct hilum is surrounded by a narrow subequatorial zone of chiefly radial muri. The

outer exine is variously adpressed to the inner and is equatorially and distally ornamented with by continuous, flexuous muri which form an irregular reticulum. Muri are 0.7 – 1.8μm wide, mean 1.2μm and are 3 – 8.9μm in height, mean 4.9μm. The muri describe polygonal, triangular or rectangular lumen 2.8 – 10.8μm wide, mean 6.1μm.

DESCRIPTION: These spores compare well with the original descriptions of the species in Richardson (1996a) in terms of amb diameter and general characteristics. However, in some cases the muri are greater in height than the upper limits given in Richardson (1996a). These spores are closely similar to *Chelinospora cassicula* except those spores are trilete.

Chelinohilates sinuosus Wellman and Richardson 1996a

STRATIGRAPHIC RANGE: Lower *micrornatus* – *newportensis* subzone.

DESCRIPTION: A *Chelinohilates* which is ornamented outside of the hilum by tightly packed sinuous and bifurcating muri; the hilum typically exhibits radial folds. 'Brain-like' appearance.

COMPARISONS AND REMARKS: Differs from *C. lornensis* in having a highly irregular reticulum. Differs from *C. erraticus* in having lower, less membranous muri. Wellman and Richardson (1996a) divide this species into two variants: var. *sinuous* (having muri >1μm wide) and var. *angustus* (having muri <1μm wide).

Chelinohilates sinuosus* var. *sinuosus Wellman and Richardson 1996a
Plate XIV, figure a

STRATIGRAPHIC RANGE: Lower *micrornatus* – *newportensis* subzone.

DIAGNOSIS: A *Chelinohilates sinuosus* with distal muri 1.0 – 1.5μm wide, up to 0.75 μm high and up to 1.5 μm apart.

DESCRIPTION: 38μm (one specimen measured). Circular to subcircular amb. Proximally ornamented with a narrow crassitude, which exhibits tightly packed sinuous and bifurcating muri. On the distal hemisphere, elongate, bifurcating and tightly packed muri 0.7 – 1.2μm wide, mean 0.9μm and <1μm tall sculpture the spore. Muri are 0.2 – 0.6μm apart, mean 0.4μm and produce an irregular reticulum. Together, gives a 'brain-like' appearance across the distal hemisphere of the spore

COMPARISONS AND REMARKS: *Chelinohilates* var. *sinuosus* differs from var. *augustus* in that the muri are <1μm in this variant.

Genus HISPANAEDISCUS (Cramer) emend Burgess and Richardson 1991

TYPE SPECIES: *Hispanaediscus verrucatus* Cramer, 1966.

TYPE LOCALITY: San Pedro Formation, Valporquero, Léon, Northwest Spain.

DIAGNOSIS: Alete, proximally hilate cryptospores. Amb is circular to sub-circular in proximal view, elliptical to hemisphaerical in equatorial view. An equatorial to near equatorial crassitude surrounds the hilum which may be ornamented with muri and/ or folds or may be laevigate. Distally, the exine is ornamented with verrucae or muri.

BOTANICAL AFFINITIES: A species of *Hispanaediscus* has been found *in situ* in circular sporangia from a plant with apparent rhyniophyte aspect (ACB current research). The vascular, or indeed bryophytic, status of the plant is uncertain given the lack of anatomical detail afforded by the specimen. This plant is likely to belong to the enigmatic cryptophytes.

Hispanaediscus* cf. *major Burgess and Richardson 1995
Plate XIV, figure b

STRATIGRAPHIC RANGE: *poecilomorphus* – *libycus* zone.

DESCRIPTION: 30µm (one specimen measured). Sub circular amb, hilum absent in this specimen. Distally ornamented with small, low verrucae 1µm wide, set 0.5 - 1µm apart.

COMPARISONS AND REMARKS: This specimen compares well in terms of morphological characteristics to original descriptions of the species in Burgess and Richardson (1995), but the amb diameter falls below the diameters given there (37 – 57µm).

Hispanaediscus verrucatus (Cramer) Burgess and Richardson 1991
Plate XIV, figures c – d

STRATIGRAPHIC RANGE: *poecilomorphus* – *libycus* – middle *micrornatus* – *newportensis* subzone.

DIAGNOSIS: A *Hispanaediscus* with a laevigate proximal hilum and distal ornament of verrucae and/ or muri.

DESCRIPTION: 15.4 – 28.7µm, mean 21.5µm (six specimens measured). Circular to subcircular amb. Proximally, the hilum is laevigate and diaphanous. Distally, the exine is variably convex and is sculptured with thin, low verrucae, which are sometimes coalesced, which are <1µm in height, 0.4 – 3.7µm wide, mean 1.6µm and 0.3 – 2.6µm apart, mean 0.7µm. Where elements fuse together, they may form longer and occasionally anastomosing muri.

COMPARISONS AND REMARKS: These spores compare favourably with the original descriptions of the species in Burgess and Richardson (1991), although the amb diameter is in some cases slightly smaller than those original descriptions (where they measure between 23 - 32µm) and the elements are slightly smaller in some cases, too, falling below the 1µm lower limit given by Burgess and Richardson (1991). *H. verrucatus* is comparable to *Artemopyra* Richardson 1996a as they are structurally similar, however, the latter has a laevigate, apiculate or spinose distal exine and the proximal hilum is ornamented with radial muri ± folds. *H. verrucatus* is smaller than *H. wenlockensis* and has closely packed radial muri on the proximal face. *H. verrucatus* may also be confused with *Synorisporites verrucatus*, although the latter species has a distinctive triradiate mark on the proximal face and has a triangular thickening.

7.4 Incertae sedis

Genus QUALISASPORA Richardson, Ford and Parker 1984

TYPE SPECIES: *Qualisaspora fragilis* Richardson, Ford and Parker

TYPE LOCALITY: Lower Arbuthnott Group, Wormit, Fife and Angus, Scotland, UK.

DIAGNOSIS: monad, bilayered cryptospores. Outer exine is sculptured over the entire spore by radial muri which converge at two foci on opposite surfaces.

BOTANICAL AFFINITIES: ?algal or fungal (Richardson *et al*., 1984).

Qualisaspora fragilis Richardson, Ford and Parker 1984
Plate XIV, figures e – f

STRATIGRAPHIC RANGE: Middle *micrornatus* – *newportensis* subzone.

DIAGNOSIS: 21 – 34μm, mean 28μm (nine specimens measured). Circular amb. Thin outer layer, ornamented with radial muri 0.3 – 0.7μm wide, mean 0.5μm and 0.4 – 0.7μm, mean 0.5μm, mean 0.5μm. The muri are arranged 0.4 – 1.7μm apart, mean 1μm. The muri extend from the equator to the poles, bifurcating once or twice towards a small ring on one surface and a thickened area on the other.

Zonate trilete spores
Plate XIV, figures g – h

STRATIGRAPHIC RANGE: Lower – middle *micrornatus* – *newportensis* subzone.

DIAGNOSIS: 25.2 – 61μm, mean 39μm (four specimens measured). Subcircular to subtriangular ambs. These spores comprise a large central body (?intexine) which is extremely dark. The central body is circular to subtriangular in habit, with convex sides. No ornament can be discerned on this body. Outside of this body is a slightly thinner zona which extends 5.3 – 10.5μm, mean 7.9μm, from the central body. Often, this zona is folded and is sometimes torn, given the impression membranous muri, but not reticulum is identified.

COMPARISONS AND REMARKS: These spores compare well with the zonate specimens figured in Lavender and Wellman (2002) (their Pl. V, figures 13) from the Midland Valley of Scotland, except the zona on these specimens appears to extend further from the central body. They also compare well with the zonate spores identified from Glencoe by Wellman (1994) (their Figures 2, a) in terms of overall size and the extension of the zona, in addition to the folded, 'membranous' appearance of that feature. These spores differ from species of *Samarisporites* Richardson in that they lack ornament on the proximal and distal surfaces (Richardson, 1965). They also differ from *Cristatisporites* Potonie and Kremp (1955) in that they lack a distal ornament of coni or spines. These spores may be confused with *C. cassicula* or *C. erraticus*, but those spores show a well-developed reticulum of membranous muri which is identifiable on the distal hemisphere, and which is, in addition, generally lesser in height than the zona seen in these

specimens. *C. cassicula* and *C. erraticus* also show distinct proximal features; a triradiate mark in the former, and a hilum surrounded by radial muri in the latter. Neither of those features are identified on these zonate specimens.

7.5. Other palynomorphs

Other non-pollen palynomorphs, marine palynomorphs and phytodebris are abundant throughout the sequence in all of the assorted assemblages.

Putative endobiontic fungal bodies have been identified in some spores throughout the sequence (plate XV, figs. a – c). These occur as small, circular bodies, irregularly distributed throughout the palynomorphs and can be mistaken as sculpture. The fungal bodies sometimes disrupt the original structure of the spores which they occur in. The fungal bodies occur in varying densities throughout the spores. The occurrence of these fungal bodies is rare, with twelve specimens identified in the entire sequence. With so few specimens, it is difficult to ascertain whether the putative fungal bodies preferentially inhabit a particular spore-type or species, but many of the specimens here can be attributed to laevigate patinate trilete spores such as *Archaeozonotriletes*. Spores attributable to *Ambitisporites*, *Retusotriletes* and ?*Streelispora* have also been found to exhibit these fungal bodies. There does not appear to be any change in the incidence of the fungal bodies through the sequence. There is a dearth of reports of Palaeozoic fungi in the literature, with similar fungal bodies to these specimens described from the Permian (Gibson, 2022). Otherwise, none have been reported from the late Silurian – Early Devonian. It is not clear if the presence of these fungal bodies suggests anything beyond normal background fungal presence in this basin during late Silurian – Early Devonian times, however, the near-constant occurrence of them in low proportions throughout the sequence suggests this. They may be associated with the putative saprotrophic organisms which are found associated with some mesofossils in the M50, Ammons Hill and Hudwick Dingle mesofossil horizons, but this is equivocal.

Marine palynomorphs also occur to varying degrees in some of the assemblages, notably in the Lochkovian of Ammons Hill, where in some horizons they are reasonably abundant (plate XVI, figs. d – j) and in the Přídolí Rumney and Usk sections. In the M50, too, these palynomorphs occur, but are extremely rare and probably reworked. In the Ammons Hill section, Barclay *et al.* (1994) concluded that these acritarchs were probably concomitant with the terrestrial palynomorphs, having been deposited in brackish waters which are thought to have persisted into the *micrornatus-newportensis* spore assemblage biozone. Laevigate chitinozoans are also found rarely in the M50 assemblage but may be reworked also. Interestingly, they have not been identified from Ammons Hill. Thus far, no other assemblages have consigned these marine palynomorphs. The implications of the presence/ absence of these palynomorphs in the various assemblages for reworking and palaeoenvironment are discussed elsewhere. Where marine palynomorphs are purportedly *in situ*, they are included in count, identified to genus level. As the principal focus of this work is to explore the terrestrial palynomorphs through the sequence, the marine palynomorphs are of little interest to this work beyond paleoenvironmental indication and biostratigraphy.

Phytodebris are particularly common throughout the assemblages, comprising various tubes, cuticular sheets and small clusters of spores (plate XV, figures d – j). Many of the tubes and cuticles are thought to derive from the nematophytes, some of which have fungal or fungal-lichen associations. These fragmentary specimens are revealing, as they hint that the organisms from which they are derived comprised an important component of the terrestrial ecosystem. Many may have exploited a saprotrophic niche, as often the tubes are found associated with mesofossils (Edwards and Richardson, 2000). Some of the cuticles are derived from putative fungi, *Prototaxites*, while others are probably derived from a variety of land plants and lichens. Small spore masses are derived from the sporangia of various plants. While a coprolite association is possible, only a single type of spore is exhibited in each mass. These spores have a range of associations, including cryptospores and trilete miospores. These specimens are interesting, because they may either be fragmented pieces of sporangia, similar to those

larger examples identified in the M50 and Hudwick Dingle, which have been broken apart by decay and/ or transport or may be part of the natural lifecycle of the plants. While it is equivocal, Edwards (?) suggested that some plants may have shed spore clusters or masses as part of their reproductive cycles, and it remains possible that the some of the plants from which these spore clusters were shed may have followed this dispersal technique.

8. Results

8.1. Palynofacies

The palynomorph data illustrated in fig. 12 (spore count charts) is based on either semi-quantitative counts of up to 250 palynomorphs and/or non-quantitative logging of strewn slides. All terrestrial palynomorphs were characterised as either miospores or cryptospores, which were further subdivided into groups and identified to species and species variant level. Marine palynomorphs were subdivided into acritarchs, chitinozoans and scolecodonts, but were not identified to genus/ species level. Combined counts were carried out for terrestrial and marine palynomorphs in addition to wholly terrestrial palynomorph counts. The latter was important as the principal focus of this study was of the changing dynamics of terrestrial vegetation. For a more detailed analysis and discussion of the changes in marine

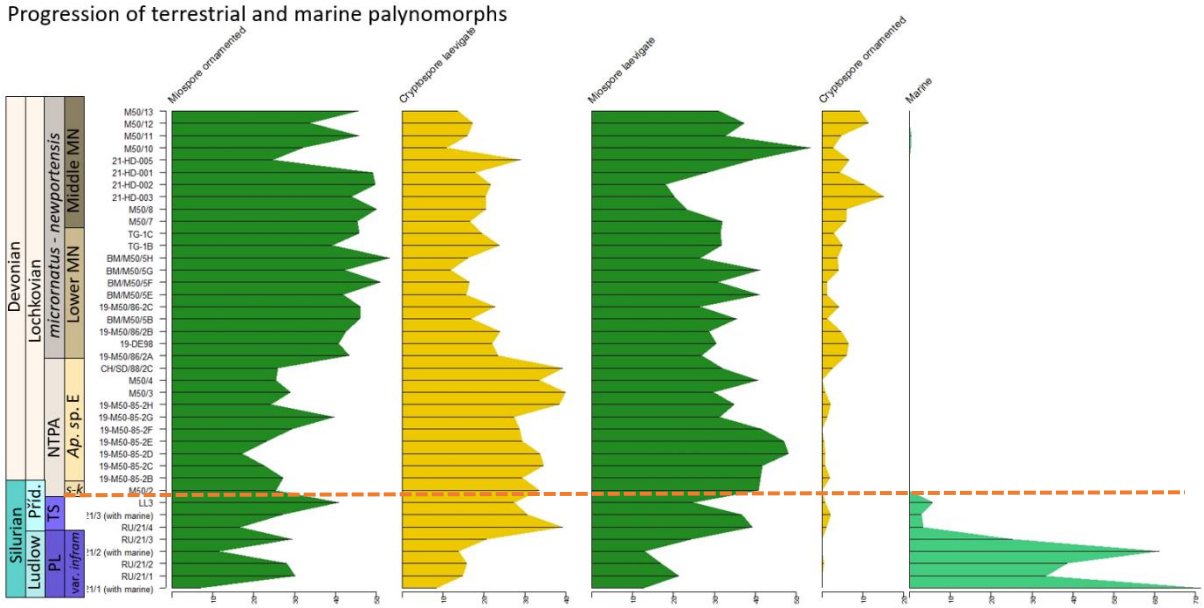

Figure III-12: the progression of marine and terrestrial palynomorphs through a composite section. Terrestrial palynomorphs are divided into ornamented and laevigate cryptospores and miospores. `library("rioja")`. *Chart not corrected for stratigraphic height. Orange line denotes position of mid – late Přídolí stratigraphic gap between the mid and late Přídolí.*

phytoplankton in the Ludlow and early Přídolí, the reader is referred to Richardson and Lister (1969), Lister (1970) and discussions in Gray and Boucot (1970) and Richardson and Ioannides (1973).

Fig. 12 shows a composite succession of miospores, cryptospores and marine palynomorphs (acritarchs, chitinozoans and scolecodonts) from the late Ludlow – mid Lochkovian of the Lower Old Red Sandstone, where the transition from marine influenced assemblages in the lowermost part of the section to wholly terrestrial assemblages in the upper-lower, middle and upper parts of the section is clearly visible. The terrestrial components are subdivided into their gross ornament types, after Richardson (2007). The composite section comprises temporally arranged, representative samples from most of the localities studied here (fig. 12). As such, certain features may be a peculiarity of the locality rather than representative of the overall succession, but these are noted and locality nuances are discussed later. For this reason, the early Lochkovian Gardeners Bank locality is excluded from the

composite section due to its unique palynofloral and sedimentological character. Likewise, Ammons Hill is excluded from the section as a confident stratigraphic height relative to the Chapel Point Limestone member cannot be ascertained.

The Anglo-Welsh Basin sequence shows continual marine regression (4.3., fig. 12). The lower portions of the studied section all show marine influences in the palynoflora. Here, marine palynomorphs including chitinozoans and acritarchs are an important component of the palynoflora, comprising up to 40% of assemblages in the Ludlow *poecilomorphus – libycus* biozone. In the proceeding lower Přídolí *tripapillatus – spicula* zone the proportion of marine palynomorphs is much reduced (<5%), while the proportions of cryptospores and miospores increase, presumably as littoral and then terrestrial settings are attained. The major stratigraphic sampling gap in the middle – late Přídolí precludes the assessment of further marine regression in the middle to late Přídolí.

By the upper Přídolí and Lochkovian of the Anglo-Welsh Basin, there is no sedimentological or palynological evidence for marine influence in most of the localities (cf. Allen and Dineley, 1976). Ammons Hill is the exception, with rare acritarchs occurring in in the non-tripapillate *Aneurospora* spp. and *micrornatus-newportensis* zones. These acritarchs are associated with ostracods, and their combined presence was interpreted by Barclay et al. (1994) as indicative of brackish water incursions. Acritarchs and rare chitinozoans occur in very low abundances at certain points in the lower Lochkovian of the M50, but these specimens are reworked.

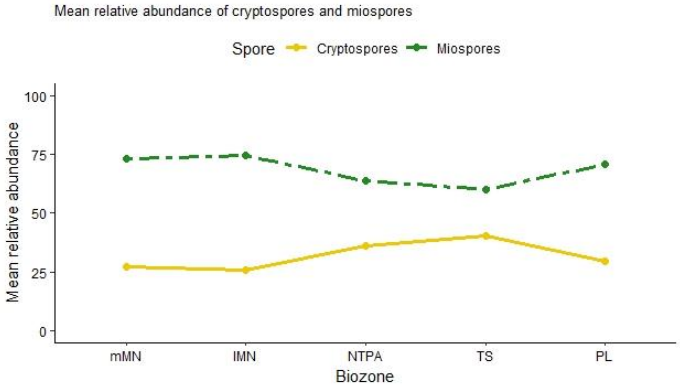

Figure III-13: *Mean relative abundance of cryptospores and miospores from the Anglo-Welsh Basin sequence, organised by biozone.* ***mMN*** *= middle micrornatus – newportensis zone;* ***lMN*** *= lower micrornatus – newportensis zone (Lochkovian);* ***NTPA*** *= non tripapillate Aneurospora spp. zone (Lochkovian – Přídolí);* ***TS*** *= tripapillatus – spicula zone (Přídolí);* ***PL*** *= poecilomorphus – libycus*

Throughout the sequence in marine influenced and wholly terrestrial settings there is an approximately consistent proportion of cryptospores and miospores with little change in overall mean relative abundance (fig. 13). Miospores generally comprise *c.* ⅔ - ¾ of assemblages, while cryptospores comprise between *c.* ¼ - ⅓. Whilst cryptospores are secondary in dominance to miospores throughout the sequence, at times proportional differences are reduced. This is most clearly demonstrated in the Přídolí *tripapillatus – spicula* and non-tripapillate *Aneurospora* zone, where the mean relative

abundance of miospores decreases, which is paralleled by a proportional increase in cryptospore abundance. Here, the mean abundance cryptospores in some assemblages can be up to 40% of the palynoflora, especially towards the end of the *Aneurospora* spp. zone (earliest Lochkovian). This increase in cryptospore abundance is not restricted to any single locality, and is instead observed across the Welsh borderlands, most notably at the Clee Hills and M50 localities. Following this intermittent increase in cryptospore abundance, miospore abundance returns to *c.* ¾ of the assemblage in the lower and middle *micrornatus – newportensis* subzone.

The broad relationships between the relative abundances of cryptospores and miospores is shown in fig. 13, and whenever cryptospore abundance increases, miospore abundance falls. The miospore –

cryptospore – marine palynomorph relationship is more complex and is best observed in the Ludlow and lower Přídolí sections of Rumney and Usk (*poecilomorphus – libycus* and *tripapillatus – spicula*

zones) and the earliest to mid Lochkovian Ammons Hill section (*Aneurospora* spp. and *micrornatus – newportensis* zones). In the stratigraphically lowermost Rumney and Usk assemblages (fig. 13, 14), cryptospores show a gradual increase through the *poecilomorphus-libycus* and *tripapillatus-spicula* biozones, from 8% in the lowest sample to 34% at the top of the sample in the *tripapillatus-spicula* zone. There is a negligible fluctuation in cryptospore proportions with changing miospore and marine phytoplankton proportions. The marine phytoplankton – miospore relationship appears to be more coupled. In the lowermost sample (USK/21/1) marine phytoplankton dominate the palynoflora at 71%. Meanwhile, whilst remaining the dominant terrestrial palynomorphs, miospores comprise 19% of the palynoflora. In the succeeding sample a reduction in marine phytoplankton is paralleled by a proportionate increase in miospores, and this is seen in reverse where, through the remaining samples of the *poecilomorphus – libycus* zone a reduction in miospores is paralleled by a proportionate increase in marine phytoplankton. The incoming of the *tripapillatus – spicula* zone (earliest Přídolí) exhibits a major reduction of marine palynomorphs (61% to 3%). Again, this is accompanied by an increase in miospores (13 to 62%). Here, cryptospores become more important than marine phytoplankton.

In the marine influenced Lochkovian Ammons Hill section the abundance of miospores and cryptospores is influenced by the low proportions of acritarchs in the assemblages (0.2 – 0.4%). Where marine phytoplankton are observed there appears to be some associated subtle changes in the palynoflora. This is clearest between samples MPA25246 and MPA25249, where acritarchs are continuously observed and an apparent increase in laevigate trilete spores (e.g., *A. avitus – dilutus*, *R.* sp. A) and laevigate cryptospores (*D. murusdensa – murusattenuata*) occurs. The loss of acritarchs in the subsequent assemblage is accompanied by a decrease in the laevigate forms. Meanwhile, coeval assemblages remain entirely terrestrial. Lavender and Wellman (2002) recorded acritarchs in Early Devonian assemblages from Scotland, and considered them to be freshwater, rather than marine, organisms. Such an interpretation is possible for Ammons Hill, also, but the association with ostracods supports the brackish water hypothesis fielded by Barclay et al. (1994). Indeed, McGairy et al. (2021) recorded upper Silurian Ostracods in estuarine environments in Vietnam, which may be analogous to Ammons Hill.

8.2. Sequence of spore assemblages

The stratigraphic distribution and abundances of miospores and cryptospores from the studied localities are given in figs. 14 and 18. From these sections, four principal biozones can be identified with an additional five sub-biozones by further dividing three of them (section 8.3). The stratigraphically lowest Rumney-1 and Usk-1 boreholes each exhibit the earliest *poecilomorphus-libycus* and *tripapillatus-spicula* spore assemblage biozones, while the Ludlow Lane outcrop only exhibits the latter. The uppermost M50, Clee Hill and Ammons Hill localities each contain the Non-tripapillate *Aneurospora* spp. and *micrornatus-newportensis* spore assemblage biozones, whilst Gardeners Bank only exhibits the *micrornatus newportensis* biozone. All of the assemblages contain well-preserved spores and non-pollen palynomorphs, with varying incidences of marine palynomorphs (fig. 12). Four major phases occur in the sequence, which generally correlate to the spore assemblage biozones (PL, TS, NTPA, lower and middle MN zones) and broadly represent (1) increases in species richness (including major species proliferations) and the mean relative abundances of genera, and (2) the ascension/ waning of dominant species. Concomitant with species changes occur in addition to gains and losses of proximal and distal sculptural features in miospores (fig. 15) and cryptospores (fig. 16).

1. Lower assemblages, Rumney-1 and Usk-1 boreholes

Lophonzotriletes poecilomorphus - Synorisporites libycus biozone

The low [illegible]s, tal mean

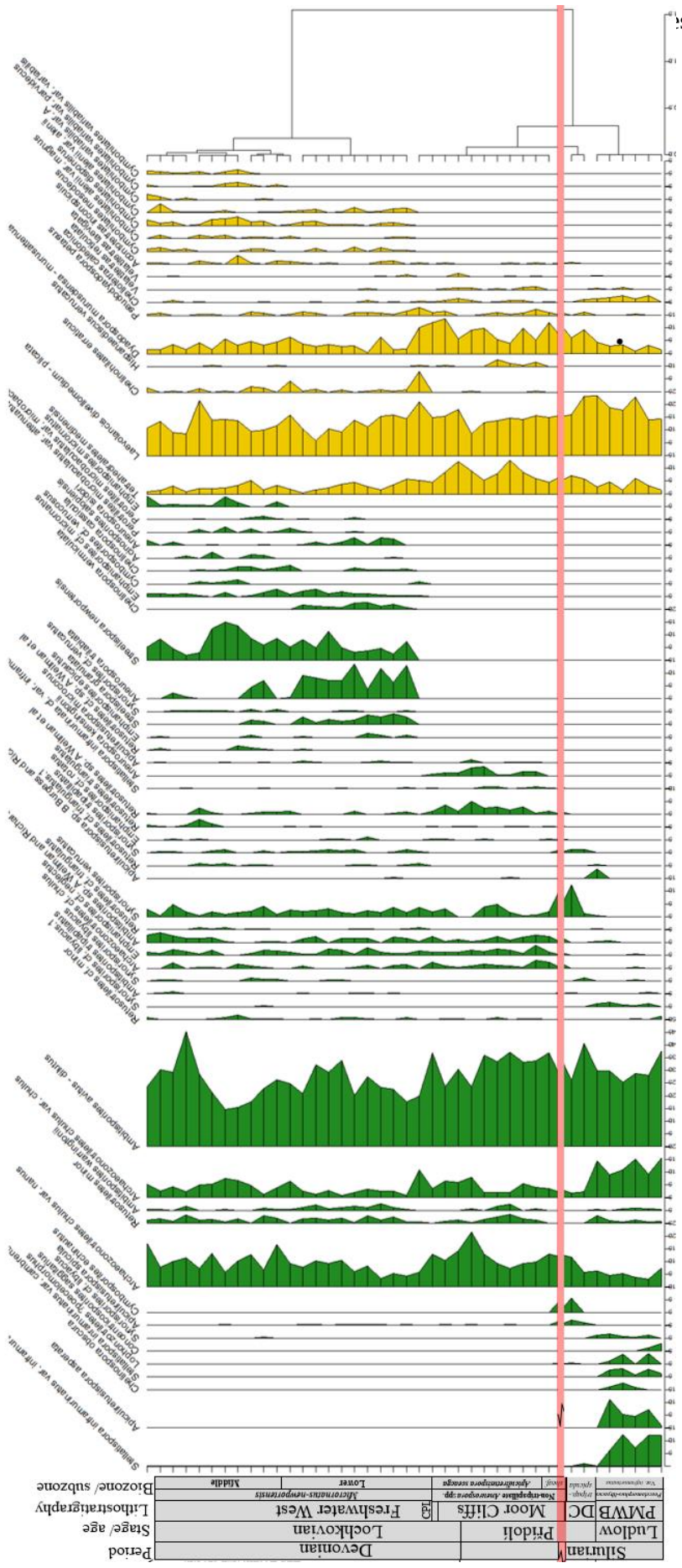

Figure III-14: relative abundances of trilete spore (green) and cryptospore (gold) species comprising >4% of the assemblages through a composite Ludlow – Lochkovian Anglo-Welsh Basin section. Chronostratigraphic, lithostratigraphic and biostratigraphic data is included on the left. ***PMWB:*** *Palaeozoic Marine Welsh Basin ;* ***DC:*** *Downton Castle Sandstone formation;* ***CPL:*** *Chapel Point Limestone member ;* ***sheaf:*** *Apiculiretusispora sheafensis preliminary subzone;* ***red region:*** *Middle – late Pridoli stratigraphic sampling gap.* ***Dendrogram****: calculated with Raup-Crick indices, illustrating biozones. Note that concordance is not directly correspondent with qualitative biozones.* ***423:*** *U-Pb age for the Ludlow Bone Bed, Catlos et al., 2020;* ***419:***

species richness (for terrestrial palynomorphs) of 22.4. Whilst the species richness between the two sites is essentially comparable, Usk has a slightly higher mean species richness (24.5) than Rumney (21). The former also exhibits a slightly higher mean richness of miospore species (18) compared with the latter (16.33), although they are again essentially comparable. Cryptospore diversity is also relatively low and comparable between both sites, at 4.6 in Rumney and 6.5 in Usk.

All samples from the *poecelomorphus – libycus* zone exhibit a significant proportion of marine palynomorphs, contrasting with stratigraphically higher localities. Marine palynomorphs principally comprise acritarchs and chitinozoans, but rare scolecodonts also occur. At Usk, marine palynomorphs make up between 61 – 72% of the total palynoflora, whilst miospores and cryptospores comprise between 19 – 24% and 8 – 13% respectively. Meanwhile at Rumney the proportions of marine palynomorphs are appreciably lower (33 – 39%). Miospore and cryptospore proportions are greater (44 – 51% and 15 – 16% respectively). Of the marine palynomorphs, acritarchs comprise 98 – 100% of the marine palynomorph component, with chitinozoans typically comprising <2% in Usk. At Rumney, acritarchs make up 72 – 100% of the total marine palynoflora, with Chitinozoans comprising between 7 – 33% of the total marine palynoflora. Chitinozoans may also be absenThere is limited diversity of proximal and distal ornament in the *poecilomorphus – libycus* zone when compared with later assemblages. Proximally laevigate spores dominate the assemblage, with a total mean relative abundance (combined miospore and cryptospore) of 89%, associated with spores belonging to the *Ambitisporites avitus – dilutus* and *Laevolancis divellomedium – plicata* complexes. After proximally laevigate taxa, miospores exhibiting rugulae on their proximal face (*Apiculiretusispora asperata*) are the other key proximal ornament, comprising 3% (fig. 15). Other ornaments, such as interadial papillae (e.g. on *Ambitisporites tripapillatus,* fig. 15) and interadial/ radial muri (e.g. species of *Emphanisporites* and *Artemopyra,* figs. 15 and 16) are largely unimportant at this time, comprising <1% of the overall palynoflora. There is little variation in the proportion of proximally laevigate spores between Rumney and Usk (88% compared with 91% respectively). However, there is a disproportionate distribution of minor proximal ornaments between the localities. Most importantly, spores with proximal rugulae comprise a greater proportion of the Rumney palynoflora (4%) than at Usk (1%). In addition, spores with interadial papillae are only observed in Rumney at this time, whereas spores with proximal thickenings are only observed at Usk. There is a ± even distribution of miospores with interadial muri, but cryptospores with radial muri have only been reported from Usk.

A limited diversity of distal ornament is also observed. Laevigate forms dominate, comprising 77.7% of the total palynoflora (figs 15 and 16). There is some contrast in the proportions of laevigate taxa between the Usk (82%) and Rumney (72%). Distal Radial muri are common on the patinate spores *Stellatispora inframurinatus*, with 12% of spores from Rumney and Usk exhibiting this ornament. Coni are also important, comprising 4% of the overall palynoflora. Again, there is a disproportionate distribution of this ornament between Usk (2%) and Rumney (6%). Distally verrucate taxa comprise an overall mean abundance of 2.29% across both localities. The proportions of these distally verrucate forms, however, is heavily skewed towards Rumney, where they make up a mean abundance of 4%, compared with <1% at Usk. Other proximal ornaments, including muri, well-developed reticula and spinae, *inter alia*, comprise <1% of the overall palynoflora. As with proximal ornament, there is some proportional differences between the localities. Distally murornate taxa comprise a 1% of distal ornament at Rumney, compared with Usk (0.6%); meanwhile, taxa which are distally thickened are slightly more prevalent at Usk (1.48%) than at Rumney (0.4%).

2. Lower – middle assemblages, Rumney-1 and Usk-1 boreholes and Ludlow Lane outcrop ***tripapillatus – spicula*** **biozone**

There is no considerable difference in mean species richness of miospores and cryptospores between the *tripapillatus* – *spicula* biozone and the preceding *poecilomorphus* – *libycus* zone (22.4 to 22.66 in

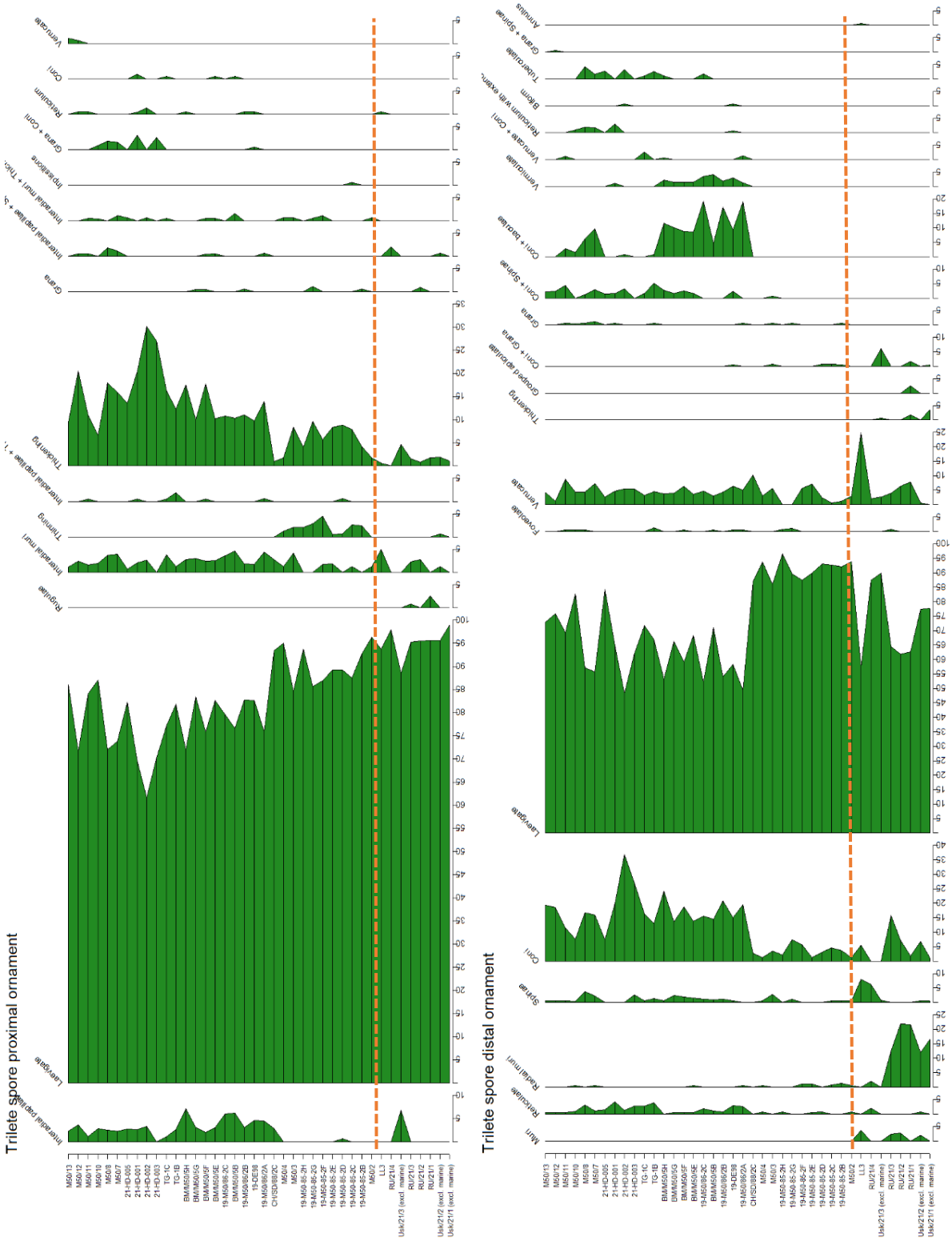

Figure III-15: Proximal (top) and distal (bottom) sculptural changes in miospores through a composite section of the Anglo Welsh Basin. Orange line denotes major stratigraphic gap.

the latter). Species richness varies between the localities, ranging from 15 at Rumney, 23 at Ludlow Lane and 30 at Usk. The low value at Rumney may be a result of the paucity of palynomorphs in the sample rather than a genuine reflection of diversity. Miospore species richness is also disproportionate,

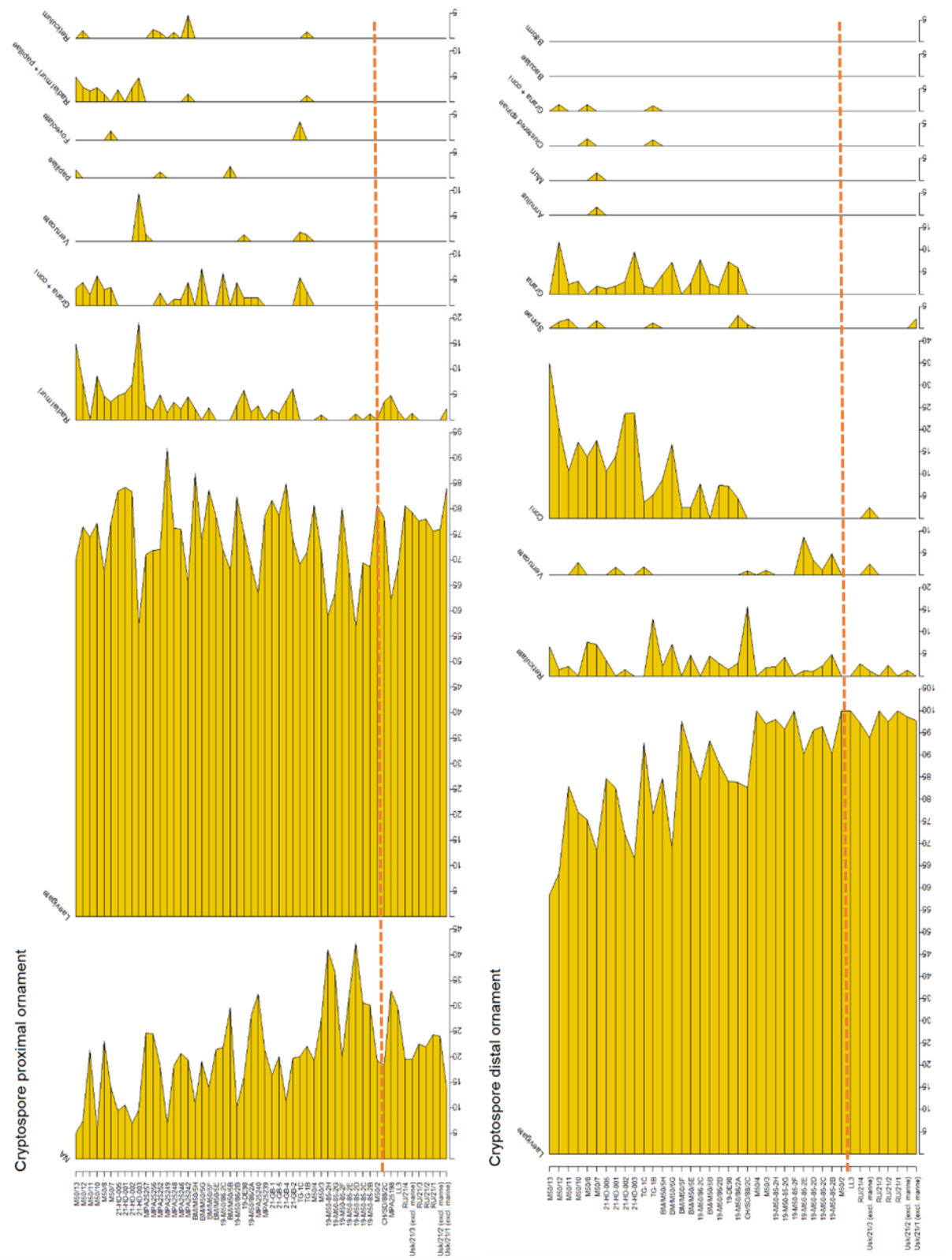

Figure III-16 Proximal (top) and distal (bottom) sculptural changes in cryptospores through a composite section of the Anglo Welsh Basin. Orange line denotes major stratigraphic gap.

with Rumney again exhibiting the lowest (9) compared with Usk (19). The latter is not considerably greater than the miospore species richness at Ludlow Lane (16). Cryptospore species richness is more equal, with Rumney and Ludlow Lane having a comparable mean species richness (9 and 7 respectively), and Usk having a slightly richer cryptospore species richness (11). A slight decrease in

overall mean species richness occurs between the *poecilomorphus – libycus* and *tripapillatus – spicula* zones at Rumney falling from 21 to 15 with a significant loss of miospore species. At the Usk locality, overall mean species richness increases to 30 from 24.5, with cryptospores experiencing a notable increase in species richness.

As with the preceding *poecilomorphus – libycus* zone, all of the localities in the *tripapillatus – spicula* zone exhibit varying proportions of marine and terrestrial palynomorphs (fig. 12), although the marine phytoplankton contribution is considerably lower than in the preceding zone (3.%), with terrestrial palynomorphs dominating the assemblage (95%). These proportions are ± consistent across the three localities, with the greatest terrestrial component observed at Usk (97%) compared with lowest at Ludlow Lane (94%). At all localities, acritarchs are the principal, often exclusive, contributors of the marine phytoplankton component, with rare Chitinozoans only occurring at Rumney.

As with the preceding biozone, miospores and cryptospores with laevigate proximal faces dominate the *tripapillatus – spicula* zone, with a mean relative abundance of 86%, with a variation of <1% between Usk and Rumney, but a considerably lower proportion observed at Ludlow Lane (76%). The proportional change between the PL and TS zone is greatest at Rumney with an increase of *c.* 3%, while Usk remains ± concordant. The most striking change from the preceding zone is the total loss in all localities of proximally rugulate miospores (*Apiculiretusispora asperata*). There is also a loss of proximally thinned miospore taxa and miospores exhibiting interadial muri, although the latter have been reported in this zone by other workers (e.g. Richardson and Lister, 1969; Burgess and Richardson, 1995). There is a slight increase in emphanoid cryptospores (+*c.* 0.2%) at Usk, which also occur at Ludlow Lane but remain unreported from Rumney.

Distally laevigate miospore and cryptospore taxa dominate *tripapillatus – spicula* zone assemblages (91%). Whilst Usk and Rumney have similar proportions (91 and 91% respectively), Ludlow Lane exhibits considerably less (66%). Distally verrucate miospores such as *Synorisporites verrucatus* become much more prevalent in this zone with a mean overall abundance of 9%. At Rumney, however, there is a small decrease in this distal sculpture. A significant proportion of the Ludlow Lane assemblage comprises distally verrucate spores (24%), and a small increase in this morphology is observed at Usk, also. Alternatively, miospores with distal coni are much reduced in this zone relative to the preceding zone, with a mean relative abundance of 2%. These forms are drastically reduced in Rumney and Usk but comprise 5% of the Ludlow Lane assemblage. Meanwhile, miospores with a mixture of cones and spines are increased at Usk (3%). Miospores with a distal annulus also appear in this zone but remain a minor component of the overall palynoflora (0.1%). Most strikingly, loss of distally radial murornate sculptures (*Stellatispora inframurinatus*) occurs in the TS zone, despite having been a principal component of *poecilomorphus – libycus* assemblages. These taxa are absent from Usk and Ludlow Lane and are rare at Rumney. Miospores with a distally thickened hemisphere (*Concentricosporites saggitarius*) are also lost in this zone.

The first noteworthy changes in the palynoflora occur at the PL/TS transition (thesis inserts 1 and 2). Here, *S. inframurinatus* becomes a minor aspect of the palynoflora. Numerous reductions and losses occur amongst species of *Apiculiretusispora* and *Retusotriletes*. Meanwhile, numerous species become relatively more important, including spores of the *Ambitisporites avitus – dilutus* complex and *Archaeozonotriletes chulus* var. *nanus*. Amongst the cryptospores, too, *T. medinensis*, monads of the *L. divellomedium – plicata* complex and dyads of the *D. murusdensa – murusattenuata* complex become increasingly important. There are several first occurrences in the *tripapillatus – spicula* zone, including the nominal species *Synorisporites tripapillatus* and *Apiculiretusispora spicula*, which are extremely rare in the early stages of the section at Rumney and Usk, but are more common in stratigraphically higher samples at Ludlow Lane. In addition, apiculate patinate spores become common at Ludlow Lane, including *C. echinautus*, but are not observed at Rumney or Usk. The appearance of taxa with a distal annulus occurs in Ludlow Lane (*Amicosporites miserabilis*).

There is a considerable difference in the proportion of proximally and distally laevigate taxa in Rumney and Usk when compared with Ludlow Lane, which is probably a function of the latter's higher stratigraphic position (Section 8). The considerable differences in these proportions, alongside the addition of new taxa such as *Cymbosporites echinautus* at Ludlow Lane, points towards considerable species addition between these times, alongside the proliferation of species such as *Synorisporites verrucatus*, between the lowermost and higher levels of the *tripapillatus – spicula* zone. Indeed, Ludford Lane may represent an acme for *S. verrucatus* in the studied Anglo-Welsh Basin sequence.

3. Middle assemblages: Ammons Hill, Clee Hill and the M50 section
Non-tripapillate *Aneurospora* spp. zone

The overall mean species richness of assemblages in the non-tripapillate *Aneurospora* spp. zone is 43.25, which is considerably greater than in the preceding *tripapillatus – spicula* zone. The highest overall species diversity is observed at Clee Hill, where a mean species richness of 46 is observed. This is comparable to the mean species richness observed in the M50 section (44). Clee Hill and the M50 have a considerably greater mean species richness than Ammons Hill (33). Regarding mean miospore species richness, Clee Hill and the M50 section are comparable (32 and 32.6 respectively), and these are greater than the mean miospore species richness at Ammons Hill (24). Cryptospores show less diversity than miospores, which is more evenly spread across the localities. Clee Hill shows the greatest mean cryptospore diversity (14), followed by the M50 section (11) and finally Ammons Hill (9). In contrast to the preceding biozone, a total loss of marine palynomorphs is observed.

There is a greater diversity of spores in the non-tripapillate *Aneurospora* spp. zone than in preceding zones. Nonetheless, the palynoflora is dominated by proximally laevigate miospores and cryptospores (81.2%) (figs. 15 and 16). The mean proportions of proximally laevigate taxa varies slightly between localities, with Clee Hill having the greatest proportion (84%) and Ammons Hill having the lowest proportion (75%). Proportions of proximally thickened trilete spores increase in this biozone compared with preceding zones (2%). There is a disproportionate distribution of such taxa between Ammons Hill (4%), the M50 section (2%) and Clee Hill (0.9%). Interadial muri in miospore species and radial muri in cryptospore species also become more important (1% and 1% respectively), with some proportional disparity between localities. Emphanoid miospores are absent at Ammons Hill but have comparable proportions at Clee Hill (2%) and the M50 section (2%). Interestingly, emphanoid cryptospores show a similar, but opposite pattern. These spores comprise a minor proportion of the palynoflora at the M50 section (0.1%) and have similar proportions at Clee Hill (1%) and Ammons Hill (2%). Other proximal morphologies, including muri in *Scylaspora* species, become more prevalent in certain localities; in the non-tripapillate *Aneurospora* spp. zone, proximally murornate forms are only observed at Ammons Hill (2%).

Proportions of distal ornament also change relative to the preceding *tripapillatus spicula* zone (figs. 15 and 16). Distally laevigate forms are again dominant in this biozone (88%). Laevigate forms are most prevalent in the M50 section (93%), with Clee Hill (84%) and Ammons Hill (87.5%) having comparable proportions. The proportion of laevigate taxa at the M50 section slightly exceeds the proportions of laevigate taxa at Rumney and Usk in the preceding biozone, but both Ammons Hill and Clee Hill exhibit slightly lower proportions. Trilete spores with a well-developed distal reticulum have a considerable increase in total mean abundance from the preceding biozone (1% to 3%). The increase in this distal ornament occurs disproportionately at Clee Hill, where these distally reticulate spores comprise a mean proportion of 8%. Ammons Hill exhibits a considerably smaller proportion of these spores (1%), whilst at the M50 a negligible abundance of these spores is observed (0.7%). Distally verrucate trilete spores become more important in this biozone (3%), with a more even distribution across the localities. Finally, trilete spores with distal coni increase in mean abundance in this biozone to 2%.

There are several first occurrences of species in this biozone, although it is stressed that in most cases a well-defined stratigraphic point for their inception has not been resolved (section 8) given the middle

– late Přídolí stratigraphic gap (Figs 5, 18). Most importantly, at least two species of non tripapillate *Aneurospora* occur, *A. sheafensis* sp. nov. and *A. kensingtonii* sp. nov. in this biozone, alongside *Emphanisporites corralinus*. All of these species are present in the lowermost sample (M50/2) of the non-tripapillate *Aneurospora* spp. zone (‘*A. sheafensis* subzone, section 8) immediately above the stratigraphic gap, but are absent in the *tripapillatus* – *spicula* zone, Biozone ‘A’ and *Chelinohilates lavidensis* biozone (Richardson and Edwards, 1989; Higgs, 2022). As such, their FAD is hypothesized to occur in the mid Přídolí, but it is not currently possible to resolve a precise stratigraphic height. *E. epicautus* and *E.* cf. *epicautus* also occur in the lowermost sample of this zone, albeit in very low proportions. Nonetheless, they may also appear earlier in the mid Přídolí. Numerous other species are also posited to appear in/ around mid Přídolí and range into this biozone, including *E.* sp. 4 and *E.* cf. *rotatus*. Further up the biozone, *Apiculiretusispora* sp. E occurs within 2.33 metres of the Silurian - Devonian boundary and indicates the start of the *Apiculiretusispora sceacga* subzone and the Lochkovian (section 8.3). In this earliest Devonian (earliest Lochkovian) biozone, several more non-tripapillate *Aneurospora* spp. appear (thesis inserts 1 and 2).

4. Upper middle assemblages, Ammons Hill, Clee Hill, Gardeners Bank and the M50
lower *micrornatus-newportensis* subzone

The total mean species richness of all localities in the lower middle *micrornatus-newportensis* subzone is 71.82, a marked increase from the preceding non-tripapillate *Aneurospora* spp. zone. The M50 section exhibits the highest mean species richness (91.7) here, which is considerably higher than Ammons Hill (62.5), Clee Hill (59.5) and Gardeners Bank (37.75). The species richness amongst miospore species is considerably increased in all cases relative to the preceding biozone. The M50 section exhibits the highest mean miospore species richness (72.4) which is markedly more than Ammons Hill (48), Clee Hill section (42) and Gardeners Bank (26.5). The mean species richness for cryptospores between localities is markedly lower than that of miospores and is also, in most cases, not considerably greater than the mean species richness for cryptospores in the preceding biozone. Furthermore, the mean cryptospore species richness between sites is relatively more even than that of the miospores. Nonetheless, the M50 exhibits the greatest cryptospore species richness (19), but this is not considerably greater than Clee Hill (17) or Ammons Hill (14.5). The lowest diversity of cryptospores is observed at Gardeners Bank (mean species richness 11.25).

The M50, Clee Hill and Gardeners Bank exhibit a wholly terrestrial palynoflora, which combined with the sedimentology of the sites indicates exclusively terrestrial deposition. In contrast, the Ammons Hill palynoflora varies between wholly terrestrial or exhibiting a small (*c.* 0.8%) proportion of marine palynomorphs. The palynoflora is therefore principally interpreted as terrestrial in character but, when combined with the macrofossil record, appears to have been influenced by probably brackish waters (Barclay et al., 1994), perhaps in an estuarine setting (McGairy et al., 2021), which will have fully mixed the palynoflora.

A diverse range of proximal and distal ornaments are observed amongst spores in the lower *micrornatus-newportensis* subzone, contrasting with the preceding biozone. Proximally laevigate miospores and cryptospore are most common (78%). The M50 section and Clee Hill show the lowest proportions of proximally laevigate spores (70 and 75% respectively), whilst Ammons Hill (82%) and Gardeners Bank (86%) show the highest proportions. The dominance of proximally laevigate spores is attributed to the sustained importance of spores belonging *Ambitisporites* and *Laevolancis.* Interadial papillae, while remaining a minor component of the palynoflora, appear for the first time amongst *Aneurospora* and *Streelispora* species, with a notable turnover in dominance from *Ambitisporites tripapillatus* and *Synorisporites tripapillatus*. The M50 section exhibits the highest mean abundance of tripapillate spores (15%), which is followed by the Clee Hill section (10%). These latter sites have strikingly higher proportions of tripapillate species than Ammons Hill (3%) or Gardeners Bank (3%).

Emphanoid miospores also become more prevalent in the lower *micrornatus-newportensis* subzone palynofloras, with a mean abundance of 2%, although there is no considerable change from the

preceding biozone. The M50 and Clee Hill localities exhibit similar proportions, which, redolent of tripapillate forms, contrasts sharply with Gardeners Bank (0.8%) and Ammons Hill (0.4%). Emphanoid cryptospores, principally belonging to species of *Artemopyra*, comprise 0.9% of the palynoflora, which is not a significant change from the preceding biozone.

Distally laevigate cryptospores and miospores remain the primary component of the palynoflora (72%), with a 16% reduction from the preceding biozone. Ammons Hill has the greatest proportion of distally laevigate forms (78%), exceeding the M50 section (59%), Clee Hill (69%) and Gardeners Bank (61%). This dominance in these forms is again attributable to long ranging species of *Ambitisporites*, *Laevolancis* and *Retusotriletes*. The abundance of spores with distal coni (and mixed ornament including coni) are increased by *c.* 10% overall in this subzone. The proportions of conate spores is greatest at the Clee Hill locality (20%) and M50 section (15%), with Ammons Hill (6%) and Gardeners Bank (3%) having lower incidences of this sculpture. Spores with a mixed ornament of coni and baculae (principally *Aneurospora trilabiata*) become more prevalent in some places. This is principally observed in the M50 section, where spores with this ornament comprise 6% of the palynoflora there. In contrast, these spores comprise <1% of the palynoflora in the other localities. Distally verrucate spores remain relatively important (3%), with Ammons Hill having the greatest proportion (4%), which is not considerably greater than the M50 or Clee Hill localities (3% in both), but Gardeners Bank shows a considerably lower proportion of these spores (0.9%). Miospores with a reticulate distal hemisphere are a further notable component of the palynoflora from this time slice. The relative proportions are not distributed evenly however, with Gardeners Bank exhibiting the greatest proportion of reticulate miospores (7%), principally *Dictyotriletes williamsii*. This contrasts with the other coeval localities, which are all <3%. Interestingly, the proportion of reticulate spores at Clee Hill (2%) is much reduced from the 8% seen in the non-papillate *Aneurospora* spp. zone, while there is little change in proportion in the M50 and Ammons Hill (<1%). Similarly, spores with a distal ornament comprising a well-developed reticulum with extended intersections (*Acinosporites salopiensis*) also become more common (4%). The abundance of these spores is disproportionately greatest at the Gardeners Bank section, where they comprise 14% of the palynoflora, compared with <1% elsewhere. It is also of interest to note that undissociated tetrads of these spores also occur in very high abundances at Gardeners Bank. The proportions of less abundant ornament types between the non-tripapillate *Aneurospora* spp. and lower *micrornatus-newportensis* subzone vary little, with distally murornate species (e.g. *Chelinospora cassicula* and *Chelinohilates erraticus*) and certain distal ornaments such as tuberculae, clustered spinae and spinae all remaining approximately the same.

A major turnover of palynomorphs occurs at the late Přídolí/earliest Lochkovian NTPA – early Lochkovian lower MN transition, which occurs over a relatively continuously sampled section (thesis inserts 1 and 2). Here there is a major proliferation of miospore species, chiefly amongst *Aneurospora*, *Streelispora* and *Emphanisporites*, amongst others, with a contemporaneous, initial proliferation amongst the cryptospore genera *Cymbohilates* and *Acontotetras*. Variants of *Archaeozonotriletes chulus* become less important at this time, with var. *chulus* finally becoming a ± minor component of the palynoflora. Several species show a considerable increase in proportion, including *Aneurospora trilabiata* and *Streelispora newportensis*, and to a lesser extent, *S. granulata* (figs. 14, 18). The proliferation of miospore species continues throughout the lower MN subzone towards the middle MN subzone. The proportions of *T. medinensis* tetrads, and dyads of the *D. murusdensa – attenuatus* complex spores are much reduced through the lower MN, and proliferation of the newly emergent cryptospores is not as continuous as the miospores, with few additional species added before the onset of the middle MN subzone. Several key zone taxa appear on or near the onset of this subzone, including the nominal lower *micrornatus-newportensis* subzone species *Streelispora newportensis*, *Emphanisporites* cf. *micrornatus*, alongside *Chelinospora vermiculata*, tripapillate *Aneurospora* species including *A. isidori* and *A. trilabiata* and *Ibereospora glabella*. Several cryptospore species also have their first occurrence at or near the onset of the lower *micrornatus-newportensis* subzone, including a major proliferation of *Cymbohilates* species, including *Cymbohilates cymosus*, *C.*

mesodecus, *C. disponerus* and *C. allenii* variants (var. *allenii* and var. *magnus*). Towards the latter-half of the subzone at Clee Hill, *Cymbohilates variabilis* begins to proliferate with several variants occurring; this is not observed in the other sections until the middle *micrornatus-newportensis* subzone. The onset of the lower *micrornatus-newportensis* subzone coincides with the inception of spores with a well-developed distal reticulum with extended intersections (i.e. *Acinosporites salopiensis*), alongside those with proximal inpissitations (*Ibereospora glabella*) and bilayered proximal faces (*Streelispora* spp.). Tuberculate and vermiculate distal ornament also appear. Several spores with mixed ornament, such as *Synorisporites dittonensis* (verrucae + coni) also appear at this time, and a combination of different ornaments is observed in several species, such as *Streelispora newportensis*, which often exhibits coni with biform elements.

5. Uppermost assemblages, Ammons Hill, Clee Hill and the M50 section

Middle *micrornatus-newportensis* subzone.

The total mean species richness of sites in the middle *micrornatus-newportensis* subzone is 62.6, which is a slight reduction from the preceding lower *micrornatus-newportensis* zone. The M50 section exhibits the mean highest species richness (73), compared with Ammons Hill (57.6) and Clee Hill (55.8). Miospores maintain the highest species richness of 44.5 across the localities, compared with a mean species richness of 17.6 amongst cryptospores. Across all of the localities, miospore species richness is reduced relative to the proceeding lower *micrornatus-newportensis* zone, most distinctly in the M50 section. Alternatively, cryptospore species richness increases in the M50 with negligible change in mean species richness at Ammons Hill and Clee Hills respectively. Apart from at Ammons Hill, no marine palynomorphs are observed in this portion of the sequence. Ammons Hill shows a very small proportion of acritarchs in the marine palynoflora, again suggesting intermittent influx of brackish waters alongside ostracod occurrences (Barclay et al., 1994).

Proximally laevigate spores remain the principal component of the palynoflora in the middle *micrornatus-newportensis* subzone, with a mean proportion of 77%. As with former biozones, the appreciable proportion of laevigate proximal faces in the palynoflora is attributable chiefly to the sustained abundance of spores belonging to the *Ambitisporites avitus – dilutus* complex and *Laevolancis divellomedium – plicata* complex, amongst others. The highest proportion of laevigate proximal faces in the middle *micrornatus - newportensis* is observed at Ammons Hill (83%), with fewer observed at Clee Hill (73%) and the M50 section (75%). Interadial papillae become more important in the middle *micrornatus-newportensis* zone, although the increase in mean proportion is negligible (8.36% compared with 8% respectively). The Clee Hills section exhibits the highest proportion of these spores (11%) which is closely followed by the M50 section (10%), compared with 3% at Ammons Hill. As with the preceding lower *micrornatus-newportensis* subzone, the continued importance of tripapillate spores is sustained by species of *Aneurospora* and *Streelispora*, although in comparison with the preceding zone, *S. newportensis* becomes the most important tripapillate species, which is paralleled with a decrease in *Aneurospora* species, including *A. isidori*. An increase in the proportion of cryptospore species exhibiting papillae also occurs. This change is mostly attributable to the proliferation of variants of *Cymbohilates variabilis* and is most clearly observed in the M50 and Ammons Hill sections. The overall increase in the proportion of proximal thickenings (chiefly in species of *Retusotriletes* and *Perotrilites*) continues in the middle *micrornatus-newportensis* subzone, with a minor increase in mean abundance relative to the lower *micrornatus-newportensis* subzone, from 3–4%. The prevalence of proximal thickenings is similar between Ammons Hill and Clee Hills (5 and 4% respectively), with Ammons Hill exhibiting the highest proportion by a small margin. By contrast, proximal thickenings only occur on 2% of the spores in the M50 section.

There is an increase in emphanoid miospores (principally belonging to miospore species of *Emphanisporites*) in the middle *micrornatus-newportensis* subzone. The M50 and Clee Hill (4% and 3.8% respectively) show similar proportions, contrasting with Ammons Hill (0.4%). Emphanoid cryptospore species are also observed (principally species of *Cymbohilates* and *Artemopyra*), with a

slight increase in mean abundance to 1.5%. This increase is principally due to the proliferation of *C. variabilis* variants. The greatest proportion of emphanoid cryptospores is observed in Clee Hills (2.1%), which is shortly followed by the M50 section (1.5%). Similarly, with emphanoid miospores, emphanoid cryptospores are lowest in abundance in the Ammons Hill section. Other proximal ornaments observed on <1% of miospores and cryptospores in the middle *micrornatus-newportensis* palynoflora also change relative to the preceding lower *micrornatus-newportensis* subzone. Proximal grana, verrucae and muri become more prevalent into the middle *micrornatus-newportensis* subzone, as do more complex combinations of ornament, including grana + coni. Some proximal ornaments see a slight decrease, including proximal fovea (figs. 15 and 16).

Distally laevigate remain dominant with a mean abundance of 74% (*c.* 2% increase from the preceding lower *micrornatus-newportensis* subzone), maintained by the persistence of spores belonging to the *Ambitisporites avitus – dilutus* and *Laevolancis divellomedium – plicata* complexes, in addition to species of *Retusotriletes*, amongst others (figs. 15 and 16; fig. 14). Ammons Hill exhibits the highest proportion (83%) of distally laevigate spores, contrasting with Clee Hill and the M50 section (69 and 69% respectively). Coni are the principal distal sculpture of spores in the middle *micrornatus-newportensis* subzone (mean abundance of 14%). Coni also appear in variously important proportions when mixed with other ornament types such as spinae, verrucae and tuberculae. Spores with ornament exclusively comprising coni (i.e., not mixed), the Clee hills section shows the highest proportion (20%), followed by the M50 section (15%), with Ammons Hill exhibiting fewer (6%). Coni in combination with spinae occur ±evenly across the localities, but coni in combination with verrucae and tuberculae are disproportionately found in higher abundances in the M50 section. Distally verrucate spores also remain important components of the middle *micrornatus-newportensis* palynoflora, with a similar distribution across the localities. There is a slight reduction in spores exhibiting a well-developed distal reticulum between the lower and middle *micrornatus-newportensis* subzones (mean abundance 3 – 2% respectively), and this is likely due in large part to the loss of Gardeners Bank in the middle subzone. The proportions of distally reticulate spores is similar across the localities (1 – 2%) with the M50 exhibiting the lowest incidence and Ammons Hill the highest. These proportions are not particularly different from those observed in the preceding biozone.

There is a fluctuation of less abundant distal ornaments between the lower and middle *micrornatus-newportensis* zones also. Of note is the distinct reduction, and often loss, of spores with a well-developed distal 'acinospinose' reticulum with spines (i.e. *Acinosporites salopiensis*) relative to the preceding biozones. This is largely attributable to the removal of the Gardeners Bank locality. Interestingly, the proportions of spores exhibiting a reticulum with extended intersections is otherwise ± continuous within localities between the lower and middle *micrornatus-newportensis* subzones, with Clee Hills exhibiting the next highest incidence.

The final major turnover of palynomorphs which occurs between the early Lochkovian lower MN subzone and mid Lochkovian middle MN zone is also recorded across a ± continuous section of stratigraphy. A secondary proliferation of miospores is observed, with new species of *Emphanisporites*, *Aneurospora* and *Perotrilites* emerging, coupled with increases in the relative importance of species such as *S. newportensis*. Associated with this is a reduction and/ or loss of certain species, most prominently of *S. granulata, A. trilabiata* and *Ambitisporites warringtonii*. Many of the species which emerged in the lower MN persist, also. There is also a further proliferation of cryptospores, especially amongst *Cymbohilates*. This occurs alongside a reduction of previously important *T. medinensis* tetrads and *D. murusdensa – murusattenuata* dyads (thesis inserts 1 and 2).

Several key species appear at the onset of the middle *micrornatus-newportensis* subzone. Of particular importance is *Emphanisporites micrornatus* var. *micrornatus*. The previously occurring *E.* cf. *micrornatus* persists for a short time alongside *E. micrornatus* var. *micrornatus* before being lost. The proliferation of *Cymbohilates variabilis* variants becomes widespread in this zone, with the appearance of *C. variabilis* var. *variabilis, C. variabilis* var. *tenuis* and *C. variabilis* var. *parvidecus* in the M50 and elsewhere. The proximal and distal reticulum peculiar to *Q. fragilis* is first seen at the onset of the

middle *micrornatus-newportensis* subzone in the Welsh borderlands. Meanwhile, spores with a proximal thinning (e.g. *Aneurospora sheafensis*) are lost entirely by the middle *micrornatus-newportensis* subzone, after a dramatic reduction in the preceding subzone.

9. Discussion

9.1. Biostratigraphy

Most of the biozones in the Silurian - Devonian of the Anglo-Welsh Basin are well known (Richardson *et al*., 1982; Richardson and McGregor, 1986; Streel *et al*., 1987; Richardson, 2007) and are standardised in Richardson and McGregor (1986). The respective subzones were outlined in later publications (Burgess and Richardson, 1995). Nonetheless, distinct gaps between the *tripapillatus – spicula* and Lower *micrornatus – newportensis* zones (late Přídolí – earliest Lochkovian) require clarification, and this problem, *inter alia*, is investigated here.

The stratigraphic occurrence of palynomorphs is given in thesis inserts 1 and 2, with a statistical analysis included in fig. 14 as a dendrogram constructed using Raup-Crick indices. All of the previously described biozones and subzones are resolved by this dendrogram. However, the *tripapillatus – spicula* zone is somewhat problematic as the dendrogram analysis places the uppermost Usk sample into the *poecilomorphus – libycus* zone, despite qualitative attribution to the *tripapillatus – spicula* zone (as defined by Burgess and Richardson, 1995; this work) by the incidence of biozone nominal species. This problem is discussed below.

Five biozones have been qualitatively and quantitatively clarified in this succession: the Ludlow *poecilomorphus – libycus* zone, lower Přídolí *tripapillatus - spicula* zone, latest Přídolí/ earliest Lochkovian non-tripapillate *Aneurospora* spp. zone and the early – mid Lochkovian *micrornatus – newportensis* zone. Within these zones, the *Stellatispora inframurinatus* var. *inframurinatus* (Burgess and Richardson, 1995) subzone is recognised in the *poecilomorphus – libycus* zone, the *Aneurospora sheafensis* subzone and proceeding *Apiculiretusispora sceacga* subzone is recognised in the upper non-tripapillate *Aneurospora* spp. biozone alongside the lower and middle *micrornatus – newportensis* subzones in the *micrornatus – newportensis* biozone. Palynomorphs from 'Biozone A', of Edwards and Richardson (1989; 2004), from the Temeside Shales, have not been sampled or studied in this work but should be a focus for future research.

***Lophonzotriletes poecilomorphus – Synorisporites libycus* assemblage spore biozone**

Sensu Richardson and McGregor 1986

This biozone is defined by the presence of the two nominal species *Lophonzotriletes poecilomorphus* (Plate VII, fig. f) and *Synorisporites libycus* (Plate VI fig. n) *sensu* Richardson and McGregor (1986). Burgess and Richardson (1995) later subdivided this biozone into four distinct divisions in the Anglo-Welsh basin, of which the upper subzone of their scheme, the *Stellatispora inframurinatus* var. *inframurinatus* subzone, is identified here with the incidence of *Stellatispora inframurinatus* var. *inframurinatus* (Plate IX, fig. a).

***Stellatispora inframurinatus* var. *inframurinatus* assemblage sub-biozone**

Sensu Burgess and Richardson 1995

Description: Defined by the appearance of the trilete miospores *Stellatispora inframurinatus* var. *inframurinatus, Apiculiretusispora asperata* and the cryptospore *Hispanaediscus major*.

Age and range: This subzone is present in the lowermost Rumney-1 borehole samples (RU/21/1 – RU/21/ 3) in the upper Llanederyn Formation (Cardiff group) and the lowermost Usk-1 borehole

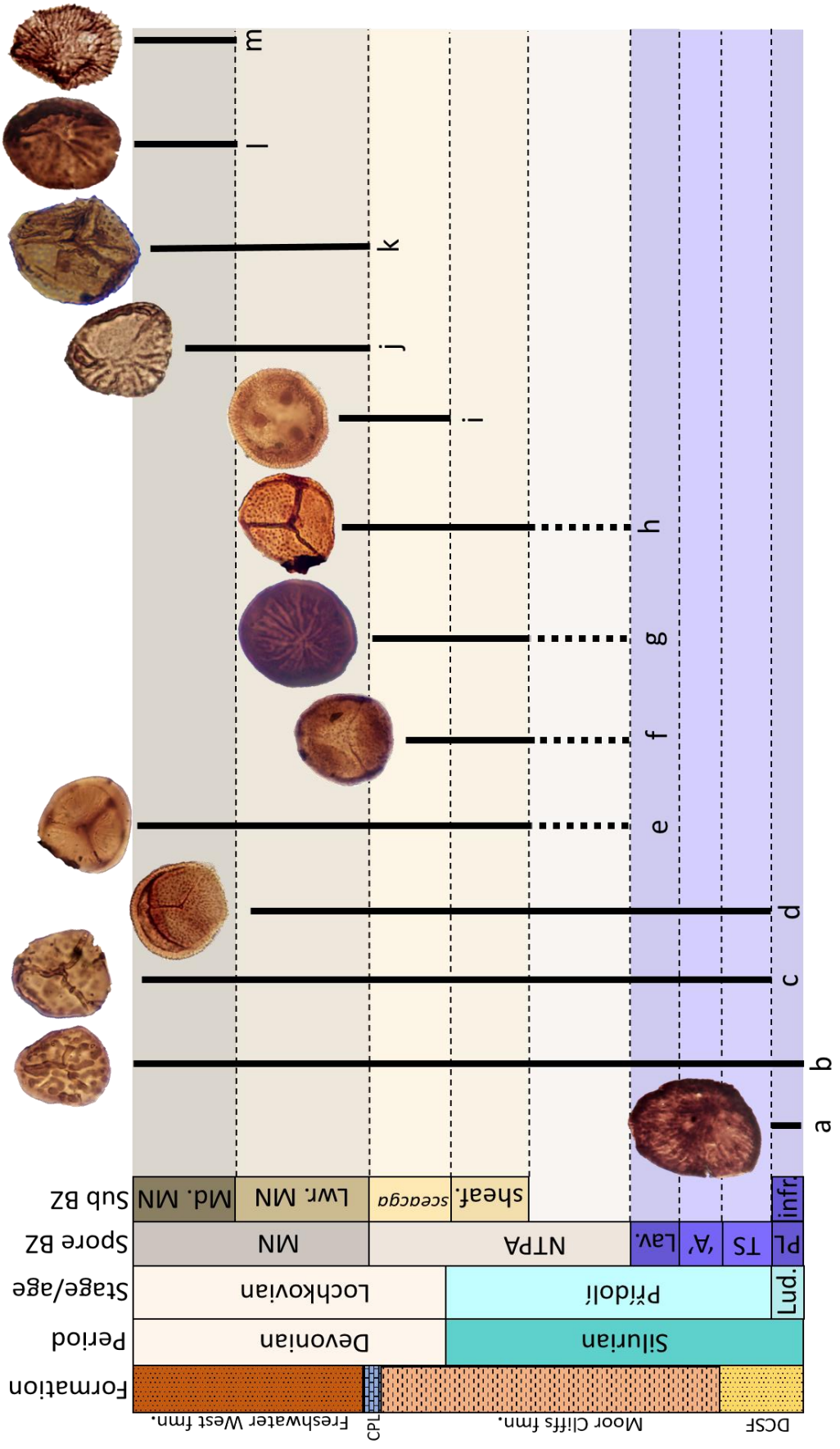

Figure III-17: Schematic showing key species ranges around the NTPA zone, highlighting the problems presented by the mid Přídoli stratigraphic gap and its implications for the NTPA zone. ***BZ: biozone; PL:*** *poeciomorphus – libycus;* ***TS:*** *tripapillatus – spicula;* ***'A' :*** *biozone A;* ***Lav:*** *lavidensis;* ***NTPA:*** *non-tripapillate Aneurospora zone;* ***MN:*** *micrornatus – newportensis.* ***Subzones: infr:*** *Stellatispora inframurinatus* var. *inframurinatus:* ***sheaf:*** *Aneurospora sheafensis;* ***Lwr/ Md. MN:*** *lower and middle MN subzones. Spore species:* ***a:*** *Stellatispora inframurinatus* var. *inframurinatus;* ***b:*** *Synorisporites libycus;* ***c:*** *Synorisporites tripapillatus;* ***d:*** *Apiculiretusispora spicula;* ***e:*** *Aneurospora kensingtonii;* ***f:*** *Aneurospora sheafensis;* ***g:*** *Emphanisporites corallinus;* ***h:*** *Apiculiretusispora sceacga;* ***i:*** *Emphanisporites epicautus;* ***j:*** *Emphanisporites cf. micrornatus;* ***k:*** *Streelispora newportensis;* ***l:*** *Emphanisporites micrornatus;* ***m:*** *Qualisaspora fragilis. Not plotted according to stratigraphic thickness or time. Solid lines indicate known stratigraphic range; dashed lines indicate maximum stratigraphic range. See also .*

samples (Usk/21/1, Usk/21/2) in the ?upper Llangibby beds in the Ludlow (late Silurian). Burgess and

Richardson (1995) posited that these samples correspond to part of the *leintwardensis* – *bohemicus* Graptolite biozones of White and Lawson (1973), placing these spores in the upper Ludlow (late Silurian).

Discussion: The palynoflora from this zone is generally consistent with that reported from Burgess and Richardson (1995). However, those workers reported that *Chelinospora obscura* was only present in the lowermost 15m of the biozone at Rumney, but here it is reported from the upper levels of the Llanederyn Formation, extending the range of the species at Rumney. This species also appears in the upper Llangibby beds at Usk. In addition, this work has indicated that *S. inframurinatus* var. *inframurinatus* does not disappear at the end of the *poecilomorphus* – *libycus* zone *sensu* Burgess and Richardson (1995), and instead ranges someway into the Přídolí *tripapillatus* – *spicula* zone, but only at Rumney. This variant is also reported from the stratigraphically higher *lavidensis* biozone by Higgs (2022) from Pembrokeshire, which may indicate its persistence much later than originally posited by Burgess and Richardson (1995) although this is yet to be qualified elsewhere in the basin. A possible variant of the species, *Stellatispora inframurinatus* cf. var. *inframurinatus* is present in the latter stages of the non-tripapillate *Aneurospora* spp. biozone.

This subzone is quantitatively well resolved by the dendrogram using Raup-Crick indices (fig. 14) to include the lower three Rumney-1 and all of the Usk-1 samples. For the uppermost samples from Usk (USK/21/3), this is problematic as the nominal species of the proceeding *tripapillatus* – *spicula* biozone have been identified in these samples, indicating that they should qualitatively be placed in that zone, rather than the *poecilomorphus* – *libycus* zone. The disparity between observed and quantitatively resolved biozones here is a result of the close similarity of the palynofloras between the uppermost samples of the *poecilomorphus* – *libycus* zone and the lowermost samples of the *tripapillatus* – *spicula* zone. This is compounded by the very rare occurrence of the latter zone's nominal species which are at the very early stages of their range and hence remain rare. This disparity of results stresses the importance of an equal appreciation of both qualitative and quantitative assessment when considering the establishment of biozones, and it is not put forward here to alter the base of the *tripapillatus* – *spicula* biozone based on the quantitative dendrogram, as the presence/ absence of the nominal species is still a significant 'first appearance' moment with strong biochronological significance for the basin and globally (e.g. Richardson and McGregor, 1986).

Burgess and Richardson (1995) reported only rare spores from the upper *poecelomorphus* - *libycus* zone. While this is to some extent agreed with here as slides were generally sparse, most of the Rumney and Usk samples were able to be counted to 250 terrestrial palynomorphs in this zone. As such, it is with some confidence that these samples are suggested to be a reasonable indicator of the spore diversity at this time, but some caution is retained because of the depositional setting and small number of samples.

***Synorisporites tripapillatus – Apiculiretusispora spicula* assemblage biozone**

Sensu Richardson and McGregor 1986

Description: This biozone is defined by the appearance and persistence of the two nominal species *Synorisporites tripapillatus* (Plate VI, figs. p – q) and *Apiculiretusispora spicula* (Plate II, fig. g) and other key taxa, as defined by Richardson and McGregor (1986). This zone was further subdivided by Richardson and Edwards into three parts: the early Přídolí *tripapillatus* – *spicula* zone, the immediately proceeding Biozone A in the Temeside Shales (not investigated here), and the earliest Devonian Biozone B, which was later renamed the *Apiculiretusispora* sp. E zone (below) and is defined formally here. Based on the qualitative contrast of the palynoflora between the lowermost *tripapillatus* – *spicula* samples (RU/21/4 and USK/21/3) and stratigraphically higher samples (LL3) (thesis inserts 1 and 2), including the appearance of distinctive taxa such as *Cymbosporites echinautus* in the latter, and (2) the additional distinction of the uppermost Usk sample from the Ludlow Lane sample by quantitative

assessment by Raup-Crick controlled dendrograms, the *tripapillatus* – *spicula* zone may be further subdivisible. Nonetheless, because of the lack of samples investigated from this zone this distinction is not made here and no subzones are used or defined.

Age and range: This zone is recorded in the uppermost Rumney-1 borehole in the lowermost ?Moor Cliffs Formation/ uppermost Cardiff Group (RU/21/4) and Usk-1 borehole in the ?Downton Castle Sandstone Formation/uppermost Llangibby beds (USK/21/1) and Ludlow Lane (LL3) in the Downton Castle Sandstone Formation (late Silurian). No graptolite zones exist in the British Isles after the *bohemicus* graptolite zone in the Ludlow (fig. 4) (White and Lawson, 1989; Burgess and Richardson, 1995, their text-fig. 8), but for Ludford Lane the stratigraphically adjacent Ludlow Bone bed provides a rich assemblage of fish remains and conodonts (e.g. Turner et al., 2017). The onset of the Přídolí is marked by a distinct change in thelodont species composition, most notably the incoming of *Paralogania ludlowiensis, Thelodus parvidens* and *T. trilobatus* and the conodont *Ozarkodina hemensis*, which are all recovered from the Ludlow Bone Bed (Miller and Marrs, 2004) at the base of the Downton Castle Sandstone Formation. The latter are the youngest recorded conodonts from the Welsh Borderlands. More recently, Catlos et al. (2021) used detrital zircon grains ($ZrSiO_4$) and ^{238}U – ^{206}Pb geochronology to give a maximum depositional age of the bone bed of 424.85 Ma ± <1 Ma, which corresponds well to the type section of the base of the Přídolí (423 ± 2.3 Ma) in the Czech republic and the lower Přídolí. The Rumney and Usk Samples are more problematic in their age constraint as no diagnostic macrofossils were obtained by Burgess and Richardson (1995) or other workers, with subsequent reliance on lithostratigraphy for regional correlation (Barclay et al., 2015). In Rumney, the upper samples retrieved from red beds are problematic as the marine phytoplankton are not diagnostic and no macrofossils have been reported, although the sample is +10m above the putative Ludlow Bone Bed. Burgess and Richardson (1995) attributed the red beds to the local Raglan Mudstone Formation (now referred to as the Moor Cliffs fmn., *sensu* Barclay et al., 2015) and assigned them an earliest Přídolí age based on the presence of nominal species of the *tripapillatus* – *spicula* biozone, which is concurred with here. Similarly, Usk does not yield diagnostic marine palynomorphs or vertebrates. However, the lithology of the upper Llangibby beds is comparable with the Downton Castle Sandstone Formation and the palynoflora is indicative of the *tripapillatus* – *spicula* biozone, suggesting an early Přídolí age. The contrast between the Rumney and Usk *tripapillatus* – *spicula* biozone assemblages, and the Ludlow Lane *tripapillatus* – *spicula* biozone assemblage, the latter may be slightly younger than Rumney and Usk.

Discussion: As mentioned above, the zone is not subdivided here into separate sub-biozones, despite previous workers hypothesising that the zone may be further subdivisible. The clear differences in palynoflora observed in this work, and the quantitative Raup-Crick analysis indicating that the Ludford Lane and Rumney samples are appreciably different from Usk. While a target for future work, this subdivision has not been made here simply due to a lack of ranging samples, which would allow the identification of key taxa and construction of biozones. The extent of the *tripapillatus* – *spicula* biozone as defined by Richardson and Edwards (1989) is maintained.Non-tripapillate *Aneurospora* spp. assemblage biozone

Novel assemblage biozone

Description: This biozone is defined by the incoming of non-tripapillate *Aneurospora* spp. including *Aneurospora sheafensis, A. kensingtonii* and *A. goensis*, although it is not possible to determine if these are the first examples of non-tripapillate *Aneurospora* to appear. In addition, new species of *Emphanisporites* and tripapillate *Aneurospora* appear (fig. 14, 18). Systematic logging of the available material from the M50 section, Ammons Hill and Clee Hill suggest that two distinct zones may be identifiable based on the qualitative assessment of presence/ absence of *Apiculiretusispora sceacga*.

Quantitative dendrogram analysis with Raup-Crick indices do not resolve two separate subzones (fig. 14), although this may be due to a paucity of sample from lower in the sequence. Here, these zones are described separately but caution is stressed until more material from this section is examined, despite attempts within and outside of the Anglo-Welsh Basin to define the zone (Richardson *et al*. 2001; Rubinstein and Steemans, 2002; Spina and Vecoli, 2009; Morris *et* al., 2011a; Breuer *et al*., 2017, section 5).

Streel et al (1987) suggested that zonal construction should be a 'step by step' process, and Loboziak and Streel (1981) used the phase concept of Van der Zwan (1980) to indicate that the zones were not yet controlled by application in other localities, and as such may only have local significance. Roman ciphers (Streel et al., 1980, 1981, 1987; Loboziak et al. 1983) and Greek letters (Steemans et al., 1987) have been utilised to confer the implication that the zone is not yet fully qualified. The same method was not used by JB Richardson and colleagues (Richardson et al., 1984, 2001; Edwards and Richardson, 1989) who instead did not assign definite nominal species to the zones. For continuity with the previous work in the Welsh Borderlands, and to prevent further confusing terminology entering the discussion, Richardson's preferred method is followed, with zones simply referred to with one nominal species.

Aneurospora sheafensis assemblage sub-biozone

Novel assemblage subzone

Description: Defined by the appearance of one or both *Aneurospora sheafensis* (Plate V, fig. l) and/ or *Aneurospora kensingtonii* (Plate V, fig. j), and *Emphanisporites corralinus* (Plate III, fig. i). In addition, the appearance of *Emphanisporites epicautus* (Plate III, fig. c – d) *and E.* cf. *epicautus* (Plate III, fig. a), although these taxa are rare. First recorded appearance of non-tripapillate *Aneurospora* species in the Anglo-Welsh Basin.

Age and range: The subzone has been identified from the lowermost M50 section (M50/2) in the upper Moor Cliffs Formation in the late Přídolí. The timing of subzone inception is not certain but may be as early as the mid Přídolí (fig. 17, see discussion). Aside from spores, variously fragmentary fish, ostracods, acanthodians and thelodonts are found nearby the sample, which is situated -39 metres below the Chapel Point Limestone member and enables some faunal biostratigraphic control. Allen and Dineley (1976) report several vertebrates, most importantly *Turinia pagei* in two faunal horizons within 13 and 20 metres of this sample in the M50 section. Only unidentifiable ostracoderm remains were reported from the fossiliferous horizons below this sample and it is significant that *T. pagei* has not been reported from more than -33 metres below the Chapel Point Limestone member (Edwards and Richardson, 2004). The inception of *T. pagei* is concomitant with the onset of the Devonian, and hence its absence probably indicates that the *sheafensis* sub-biozone is of latest Silurian (late Přídolí) age (Turner, 1973; Edwards and Richardson, 2004).

Discussion: It is imperative to note that at present, the FAD of the nominal species for this preliminary sub-biozone are not yet known due to the long stratigraphic gap between the lower-middle and latest Přídolí. However, the earliest timing of the subzone inception can be posited, with some caution based on the presence/ absence of key spore species (see description) which (1) are not present in the biozones immediately preceding the gap, and (2) are present in the samples immediately after the gap (fig. 17). The former biozones include the *tripapillatus – spicula* (Richardson and McGregor, 1986; Burgess and Richardson, 1995), biozone 'A' (White and Lawson, 1989; Edwards and Richardson, 1989, 2004) and the *lavidensis* zone (Higgs, 2022). None of these zones exhibit or report species of non-tripapillate *Aneurospora* sp., including *Aneurospora sheafensis* or *A. kensigntonii*, or *Emphanisporites epicautus*/cf. *epicautus* and *E.* sp. 3 which are reported from the first sample following the stratigraphic

gap. It follows that those species occur at some point in the middle to late Přídolí, prior to the M50/2 sample (latest Přídolí), but after the *lavidensis* biozone (early-mid Přídolí, Higgs, 2022) which immediately precedes the gap.

Whilst this gives some indication of the timing and range of the zone, *A. sheafensis* and *A. kensingtonii* have not yet been reported from coeval assemblages outside of the M50 section in the non-tripapillate *Aneurospora* spp. zones of Ammons Hill and Clee Hill, which might cast doubt on their spatial distribution and hence reduce the efficacy of these taxa as a nominal species. This absence may be attributed to taphonomy, or because the spore parent plants did not inhabit these areas, or because *A. kensingtonii* is lost between -32m (The last appearance of the species, and final pre-MN sample, of the M50) and -7m relative to the CPL (the latter being the proximity of the only non-tripapillate *Aneurospora* spp. zone Clee Hills sample relative to the CPL). However, amongst others, *A. sheafensis*, which persists into the lower MN in the M50, is not present and this may suggest that the absence could be taphonomic. Further samples are necessary to qualify the possibilities outlined above and as the distance relative to the CPL of the Ammons Hill non-tripapillate *Aneurospora* spp. zone sample is uncertain, the zone cannot be tested further at present, although this 'pre-MN' Ammons Hill sample most probably belongs to the *Apiculiretusispora sceacga* zone.

***Apiculiretusispora sceacga* assemblage sub-biozone**

Novel assemblage subzone

Description: characterised by the appearance of *Apiculiretusispora sceacga* (Plate II, figures i – k) and the persistence of *Aneurospora sheafensis, A. kensingtonii* and *Emphanisporites corrallinus*.

Age and range: This zone is present in the M50 samples above -35.3 metres relative to the Chapel Point Limestone to the Chapel Point Limestone (fig. 17). The pre-*micrornatus-newportensis* sample from Ammons Hill belongs in this zone following the identification of *Apiculiretusispora sceacga* there, but the relative stratigraphic distance from the Chapel Point Limestone member is not known. It is plausible that the pre- *micrornatus-newportensis* sample from Clee Hill also belongs to this zone given its proximity to the Chapel Point Limestone member (-7m below), but the nominal *Apiculiretusispora sceacga* species has not been observed from that assemblage. The samples from the M50 section occur 2 metres below the first incidence of *T. pagei* at -33 metres below the Chapel Point Limestone member, indicating that the earliest part of subzone is of latest Silurian (latest Přídolí) age (Edwards and Richardson, 2004; fig. 17). The rest of the zone in the M50 is associated with *T. pagei* and is therefore largely Devonian (Turner, 1973). At Clee Hill, the pre-*micrornatus-newportensis* sample is drawn from the *Symondsii* zone, but the earliest record of *T. pagei* from Clee hill is from just above the Chapel Point Limestone (Turner *et al*., 2017). *T. pagei* has been recorded from nearby sites at a similar and greater depth below the Chapel Point Limestone to the Clee Hill sample, however, including from the nearby Gardeners Bank (e.g. Miller and Marrs, 2004). It is therefore suggested that the presence of *symondsi*, and despite no direct association with *T. pagei*, CH/SD/88/2C is probably of earliest Devonian age, although caution must be exercised as *Ap. sceacga* has not been recorded there yet. In the Ammons Hill section, *Apiculiretusispora sceacga* has been identified in the pre-*micrornatus-newportensis* sample (MPA25198), but no faunal remains were recorded by Barclay et al. (1994). Those workers did report *pteraspis leathensis* and a palynoflora typical of the *micrornatus-newportensis* zone from samples stratigraphically above MPA25198, but *T. pagei* was not observed. Considering the general association of *Apiculiretusispora sceacga* with *symondsii* and *T. pagei* in the M50 section, in addition to the absence of tripapillate *Aneurospora* species and lithological association, it is probable that the pre-MN Ammons Hill sample is also of earliest Devonian age.

Discussion: While the lack of associated faunal remains is problematic for clarifying a precise temporal range for the *Apiculiretusispora sceacga* zone, the M50 section indicates that it occurs within 2 metres of the Silurian - Devonian boundary as indicated by the occurrence of *T. pagei* at -33m below the Chapel

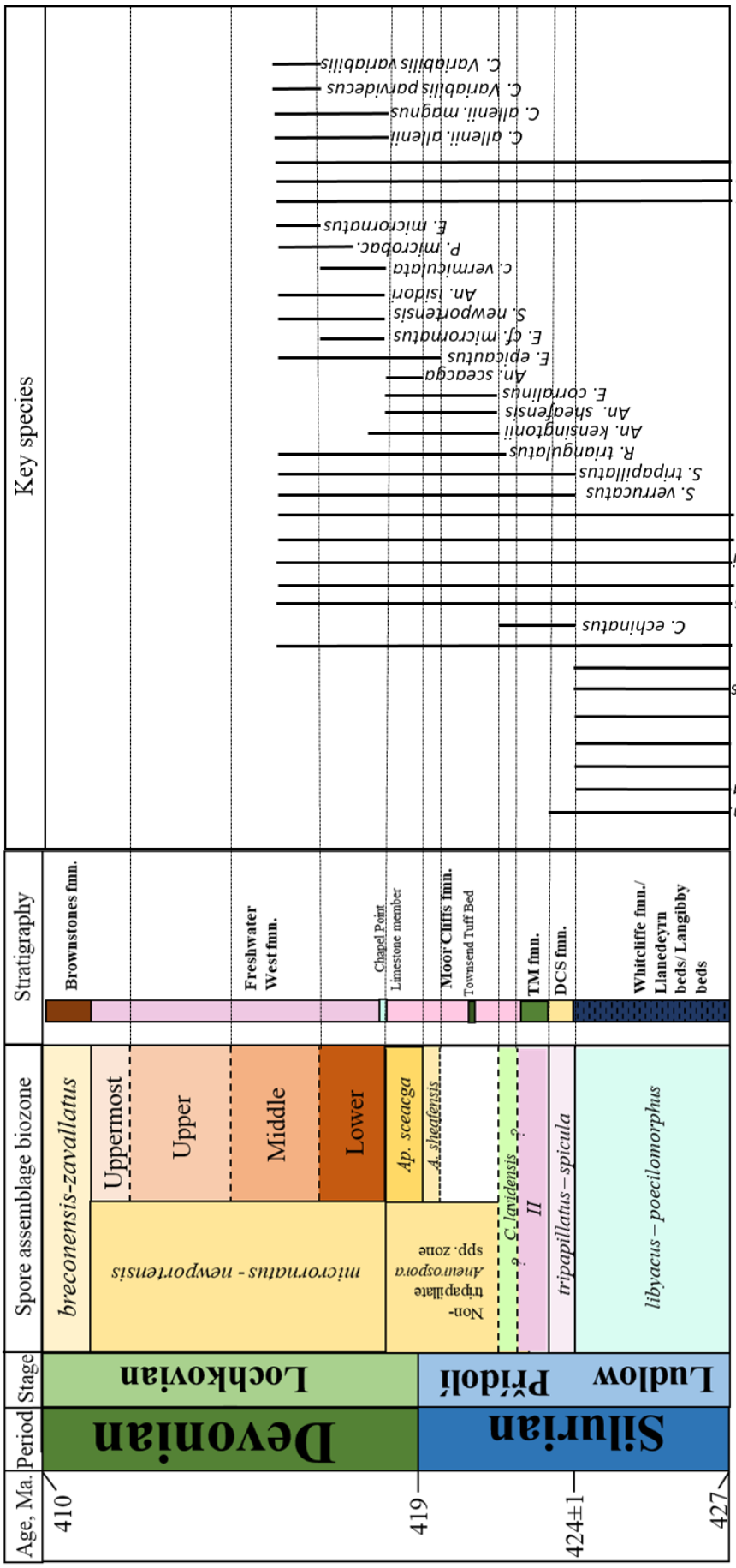

Figure III-18: updated biostratigraphy for the Welsh Borderlands of the Anglo-Welsh Basin developed from the findings of this work. The MN zone and subzones remain unchanged sensu *Richardson and McGregor (1986). The preliminary Non-tripapillate* Aneurospora *spp. zone is hypothesised to extend from the end of Higgs' (2022) C. lavidensis biozone to the inception of the lower MN subzone (Richardson and McGregor, 1986). The inception of the first preliminary division, the* Aneurospora sheafensis *subzone, is uncertain, but it is suggested to terminate with the incoming of* Apiculiretusispora sceacga *and the* Ap. sceacga *zone, previously the* Apiculiretusispora *sp. E zone (e.g. Edwards and Richardson, 2004).*

Point Limestone. *T. pagei* has been determined as an indicator of the onset of the Devonian by Turner

(1973), given its association with key graptolite species in Ukraine (see section 5; Turner, 1973). As such, if this association is true of the wider *Apiculiretusispora sceacga* occurrences, then the spore itself is a useful indicator of the earliest Devonian, as it does not occur above 3 metres or before -35 metres relative to the Chapel Point Limestone. Furthermore, the range of the subzone correlates well with the *P. symondsi* vertebrate subzone, which initiates *c.* 30 metres below the Chapel Point Limestone (e.g. Turner et al., 2017). While the earliest stages of the *Apiculiretusispora sceacga* sub-biozone occur slightly prior to the first appearance of *T. pagei* it is reasoned that, given their exceptionally close proximity, the inception of the former is also indicative of the inception of the Devonian period. This conclusion is tenuous, but *Ap. sceacga* may be a more promising candidate for the inception of the Devonian than *Aneurospora*, which was suggested by Richardson et al. (1984, 2001) to initiate in the earliest Devonian (see section 8.5).

The diachronous nature of the Chapel Point Limestone across the Anglo-Welsh Basin does lead to further uncertainty to the spatial range of the *Apiculiretusispora sceacga* zone as a pre-MN zone of earliest Devonian age. This is particularly clear at Tredomen Quarry, where palynological analysis indicated a pre-MN spore assemblage, while containing spores typical of the early Lochkovian, lacked

Streelispora newportensis and tripapillate *Aneurospora* spp., occurred +35m above the Chapel Point Limestone (Morris et al., 2011a), with a lower *microrнatus* – *newportensis* assemblage identified at CPL +42m. This 'spore zone' was also peculiar because of the dominance of cryptospores, many of which are generally associated with earlier Wenlockian and Llandoverian strata, which was interpreted as largely reworked (Morris et al. 2011a). Reworking does not explain the absence of *S. newportensis* and tripapillate *Aneurospora* spp. Winnowing or sorting may be an alternative cause (Wellman et al., 2000), although judging by the range of amb diameters presented by Morris et al. (2011a), this explanation does not seem to fit. Similarly, no key taxa reported from the *Apiculiretusispora sceacga* or *sheafensis* – *kensingtonii* subzones from the M50 section are recorded from Targrove Quarry. No independent biostratigraphic control was identified in Morris et al. (2011a), but Ball and Dineley (1961) and Turner (1973b) (but see Turner et al. 2017) report *T. pagei* and *P. crouchi* from *c.* +33m relative to the Chapel Point Limestone at Targrove. The occurrence of the latter is interesting, as it is generally associated with the middle *microrнatus* – *newportensis* sub-biozone (below), and hence mid Lochkovian, (Edwards and Richardson, 2004) in the Welsh Borderlands but it has been reported from 'just above' the Chapel Point Limestone elsewhere (Ball and Dineley, 1961; Turner, 1973b). Its occurrence at this level, associated with this peculiar spore assemblage, is not conclusive. The question still remains, then, of whether this 'pre-MN' Tredomen Quarry assemblage is a genuine pre-MN assemblage which can be correlated with the *Ap. sceacga* zone, or is a taphonomically influenced assemblage where key taxa are either very rare or have been 'lost'. The problem is compounded by a dearth of samples, with only one ?pre-MN sample retrieved from Tredomen, and none from below the Chapel Point Limestone. To fully correlate Tredomen with the *Apiculiretusispora sceacga* and lower *microrнatus* – *newportensis* subzones, and gauge how the former zone interacts with the diachronous Chapel Point Limestone, further work is required.

***Emphanisporites microrнatus* – *Streelispora newportensis* assemblage biozone**

Sensu Richardson and McGregor (1986)

Description: defined by the appearance of one of the nominal species, *Streelispora newportensis* (Plate VI, h – i), and *Emphanisporites microrнatus* (Plate III, figures e – f), *E.* cf. *microrнatus* (Plate III, figures e – f) as defined by Richardson and McGregor (1986). This is in addition to the appearance of tripapillate *Aneurospora* species such as *A. isidori* (Plate V, fig. i) and *A. trilabiata* (Plate V, figures m – n), and numerous cryptospore species including *Cymbohilates allenii* var. *allenii* (Plate XI, fig. m) and *Cymbohilates disponerus* (Plate XII, figure d) (e.g. Richardson et al, 1981; Richardson, 1996b). *E. microrнatus* proper occurs +30 to +60 metres above the Chapel Point Limestone in the Welsh

borderlands, which partly prompted later subdivision of the biozone into four parts (lower, middle, upper and uppermost *micrornatus – newportensis sub*-biozones), of which the lower and middle subzones are observed here.

Lower *Emphanisporites micrornatus – Streelispora newportensis* assemblage subzone

Description: characterised by the appearance of *Streelispora newportensis* and *Emphanisporites* cf. *micrornatus*, in addition to a variety of tripapillate *Aneurospora* species and apiculate cryptospore species. Triradiate zonal spores also appear in this subzone.

Age and range: this subzone includes samples from the M50 section between +0.15 and +3.87 metres (19-M50/86/2A – BM/M50/5H) above the Chapel Point Limestone member, Clee Hill (TG-1B, 1C +22.6 and +24 metres above the Chapel Point Limestone), Gardeners Bank (21/GB/1 – 5, +8.4 – 8.7 metres above the Chapel Point Limestone) and Ammons Hill (MPA25239, MPA25240); all samples occur in the lower Freshwater West Formation. All of these samples, except Ammons Hill, have a well constrained distance from the key Chapel Point Limestone and independent faunal age constraint for the localities is good. The lower Freshwater West Formation is typically associated with the key Devonian thelodont *T. pagei*, in addition to the *Protopteraspis (Simopteraspis) leathensis* zone (Ball et al., 1961), and this latter zone correlates well with typical lower *micrornatus – newportensis* spore assemblages. As such, the zone is considered here as early (but not earliest) Lochkovian age.

Discussion: The diachroneity of the Chapel Point Limestone, discussed above, also has relevance for the inception of the base of the lower *micrornatus – newportensis* zone. In the M50, a ± continuous suite of samples indicates that the zone initiates immediately after the onset of the zone, with *Streelispora newportensis* identified +0.15m above the horizon. At Brown Clee Hill, the lower *micrornatus – newportensis* zone also initiates just above the Chapel Point Limestone (Edwards and Richardson, 2004). Similarly, by +8m above the Chapel Point Limestone at Gardeners Bank the lower *micrornatus* is well established. Tredomen Quarry, again, offers a complication: does the lower *micrornatus – newportensis* zone initiate after 35 metres above the Chapel Point Limestone in this area, or is the assemblage simply heavily affected by taphonomy and reworking? Further sampling is required to resolve this issue.

Middle *Emphanisporites micrornatus – Streelispora newportensis* assemblage subzone

Description: characterised by the incoming of *Emphanisporites micrornatus* proper and the continuation of *Streelispora newportensis*. This is in addition to the appearance of cryptospores including variants of *Cymbohilates variabilis* (Plate XIII).

Age and range: this sub-biozone is present in the M50 section (M50/7 – M50/13), Clee Hill (HD/21/1 – 5) and Ammons Hill (MPA25242 – MPA25257). The former two localities are well constrained relative to the Chapel Point Limestone (+42 – 168 and +59.8 – 61.6 metres respectively), but the Ammons Hill samples are again lacking. The upper Freshwater West Formation is associated with *T. pagei* and *Pteraspis crouchi* faunal zones (Barclay et al., 2015), and all of the assemblages investigated here belonging to the middle *micrornatus – newportensis* sub-biozone are directly or lithostratigraphically associated with these remains.

Discussion: concerning the base of the subzone, a suite of samples documenting the actual turnover between the lower and middle *micrornatus – newportensis* assemblages have not been recovered, and the event probably occurs at slightly different heights relative to the Chapel Point Limestone as a result

of varying sedimentation. At Clee Hill (Kidnall Gutter samples) *E. micrornatus* is not observed until +59.8m, although a sampling gap exists between this sample as those of Kidnall gutter at CPL + 22m. Raup-Crick indices group the Kidnall Gutter samples into the lower *micrornatus – newportensis* zone. In the M50 section, spores typical of the middle *micrornatus – newportensis* do not appear until +42m relative to the Chapel Point Limestone, although it is noted that a stratigraphic gap of *c*. 38m exists between this middle *micrornatus - newportensis* sample and the highest lower *micrornatus – newportensis* sample (+3.89m). Furthermore, the earliest middle *micrornatus – newportensis* sample in the M50 exhibits a well-developed middle assemblage typical of the later biozone, although *E.* cf. *micrornatus* is still present. In addition to being qualitatively distinct, the spore assemblage of the middle *micrornatus – newportensis* sub-biozone is also well defined by quantitative Raup – Crick analysis (fig. 14).

9.2. Correlation across the Anglo-Welsh Basin

In the Anglo-Welsh Basin, most of the established and novel biozones outlined above and in figs. 17, 18 are identified in at least one of the studied sections, excepting the significant stratigraphic gap between the *sheafensis* subzone and the *tripapillatus – spicula* zone in the Welsh Borderlands and central south Wales (this work; fig. 18, thesis inserts 1 and 2), and between the middle *micrornatus – newportensis* subzone and the *lavidensis* zone in Pembrokeshire (Higgs, 2004, 2022). There are considerably more samples in the middle *micrornatus newportensis* zone across the basin, with ± decreasing incidence with increasing age. Furthermore, few long or continuous sequences are known, with the M50 section representing the largest ± unbroken sequence of spore zones in the basin. This work did not cover all of the Ludlow – Lochkovian outcrop and borehole sites yielding spore assemblages from the Anglo-Welsh Basin and other key localities are correlated with the studied section here. Fig. 19 illustrates the correlation of known sites across the Anglo-Welsh Basin. Despite numerous palyniferous localities

being known (e.g. Richardson and Lister, 1969; Burgess and Richardson, 1995; Wellman et al., 2000; Edwards and Richardson, 2004; Higgs, 2022; Richardson unpub.), significant stratigraphic gaps exist across the basin's 'regions', and certain areas of the basin, such as Clun Forest (fig. 5), are yet to yield palynomorphs, either because of previous unproductive sampling or lack of exploration. Future studies of the area should focus on these stratigraphic intervals and unexploited/hitherto barren sites to shed further light on correlations and vegetation dynamics from the basin.

The lowermost portions of Rumney and Usk correlate well with one another in the *Stellatispora inframurinatus* var. *inframurinatus* subzone of the *poecilomorphus – libycus* biozone (fig. 19) and are the only representatives of this biozone studied here. Richardson and Lister (1969) reported the basionym of *S. inframurinatus*, *'Archaeozonotriletes chulus* var. *inframurinatus*', from various sites across the Anglo-Welsh Basin, which may be indicative of the *S. inframurinatus* var. *inframurinatus* subzone also, and hence correlate with Rumney and Usk. The most promising correlations occur in samples collected from the upper Whitcliffe beds in the Ludlow and Millichope areas (around Ludford Bridge and Milford Lodge) detailed by Richardson and Lister (1969). These palynofloras all yield *Stellatispora inframurinatus*, although given that this work was published some time before Burgess and Richardson (1995) recategorised and sub-divided the species, it is not possible to confidently ascertain which variant is present in the Upper Whitcliffe Beds from the figured specimens at Ludford Bridge and Milford Lodge. Nonetheless, a specimen showing 'breakdown' muri figured in Richardson and Lister (1969; their Plate 43, fig.8) does appear to exhibit the fine muri typical of var. *inframurinatus*. In addition to the stratigraphic position of the Whitcliffe beds, it is reasonable to suggest that at least part of the Upper Whitcliffe Beds belong in the var. *inframurinatus* subzone. All of the Usk samples investigated in this work yielded var. *inframurinatus*, but whether this encompasses the Usk material investigated in Richardson and Lister (1969) is equivocal, although *S. inframurinatus* (*A. inframurinatus* in Richardson and Lister, 1969) is reported from there. As such, at present only the Usk

and Rumney material investigated in this work can be confidently correlated with one another through the var. *inframurinatus* subzone.

The listed species in Richardson and Lister (1969) from Usk, Ludford Bridge and Milford Lodge probably correlate with the localities investigated here via the *poecilomorphus – libycus* zone. This again is tentative given the absence of the key nominal species recorded by those workers, but this is likely a function of the early taxonomic understanding rather than whether the species are present. Burgess and Richardson (1995) note that the first incidence of *S. inframurinatus* (var. *cambrensis*) occurs in the lower *poecilomorphus – libycus* zone and coupled with the absence of the key nominal species from the proceeding *tripapillatus – spicula* zone, it is probable that these sites belong to the *poecilomorphus – libycus* zone and hence at least coarsely correlate with the Usk and Rumney samples investigated here. A reappraisal of the material would be useful to clarify and improve the resolution of correlation between the above localities. Based on this tentative spore evidence, the Llandeberyn beds present in the Rumney inlier can be correlated with the Upper Whitcliffe beds at Usk through the var. *inframurinatus* subzone, and to elsewhere in the northern Welsh Borderlands through the *poecilomorphus – libycus* zone.

S. inframurinatus was recorded by Richardson and Lister (1969) in Downton Gorge, Gorsley and Perton Lane, alongside *Apiculiretusispora spicula* and *Synorisporites tripapillatus*. The presence of the latter two species indicates that those localities belong to the *tripapillatus – spicula* zone, and therefore correlate with the upper portions of the Rumney-1 borehole (Burgess and Richardson, 1995; this work), Usk-1 borehole (this work) and Ludlow Lane (this work; Richardson and Lister, 1969). Whilst the *tripapillatus – spicula* zone is probably subdivisible (Richardson and McGregor, 1986; this work) formal divisions are yet to be erected and hence higher-resolution correlation is not possible at this time except for tentative assessment. Integration of details of the relative distance from the Ludlow Bone Bed of samples with the assemblage composition may enable higher resolution correlation here. The uppermost Rumney sample (RU/21/4) lies around 10 m above the horizon posited to be the Ludlow Bone Bed, and while the bone bed is not reported in Usk, the similarities in palynoflora may suggest that these samples are able to be correlated. The Ludford Corner, Ludlow Lane, Gorsley, Downton Gorge and Perton Lane all yield *Cymbohilates echinautus*, which, amongst others, was a palynomorph conspicuously absent in the Rumney and Usk *tripapillatus – spicula* assemblages. Bearing in mind the earlier caveats (temporal ± facies ± palaeoecology), this may indicate closer correlations between the Ludford Corner, Ludlow Lane, Perton Lane, Gorsley and Downton Gorge localities than with the upper Usk and Rumney samples; certainly, the Raup-Crick analysis again supports this. It is stressed here that such a correlation is tentative at best, and independent biostratigraphic and lithostratigraphic relationships must be resolved, in addition to further analysis of *tripapillatus – spicula* zone spore assemblages, to facilitate a more nuanced understanding of the biozone.

Edwards and Richardson (2004) reported that the Temeside Shales yielded a spore assemblage that was sufficiently different from the preceding *tripapillatus – spicula* assemblage to warrant differentiation into a separate biozone, 'Biozone A'. This spore assemblage is reported in Richardson and Lister (1969) but given that (1) the current work has not investigated material from this Formation, and (2) no specific zonal species are identified, nor identifiable, in Richardson and Lister (1969) or elsewhere, correlation with this zone is not attempted at present. Similarly, more recently Higgs (2022) erected a new *lavidensis* biozone from material collected from Freshwater East (Pembrokeshire) which precedes the *tripapillatus – spicula* and 'Biozone A'. Because material of a similar age in the Welsh Borderlands lies within the Přídolí Moor Cliffs Formation sampling gap, correlation is not currently possible.

Following the major stratigraphic gap that obscures much of the Přídolían palynofloras in the Welsh Borderlands and South-Central Wales, the earliest palyniferous horizons occur at the M50 section, Ammons Hill, Clee Hill and ?Tredomen quarry. These sections typically form part of a longer sequences which are followed through to the middle *micrornatus – newportensis* subzone. A single sample is known from the uppermost Přídolí across the Basin, from -39 m below the Chapel Point Limestone in the M50 section. This sample yields a palynoflora sufficiently different from those preceding the

stratigraphic gap in the *tripapillatus* – *spicula* zone, 'Biozone A' (in the Welsh Borderlands) and the *lavidensis* zone (Pembrokeshire) to warrant a clear distinction of biozones. Considering , it is probable that the hiatus in sedimentation represented by the Chapel Point Limestone and the stratigraphic gap obscure a more gradual addition of novel species and innovations between the middle and latest Přídolí. As outlined in section 3, this earliest M50 section sample occurs 6 m below the first occurrence of the first incidence of *T. pagei* and the onset of the Devonian, and contains several novel species and genera, including non-tripapillate *Aneurospora* species and *Emphanisporites corralinus* which together indicate the *sheafensis* subzone of the non-tripapillate *Aneurospora* spp. zone. Unfortunately, given that no other palyniferous samples have been studied from this preliminary zone, basin-wide correlation cannot be discussed further for this subzone at present.

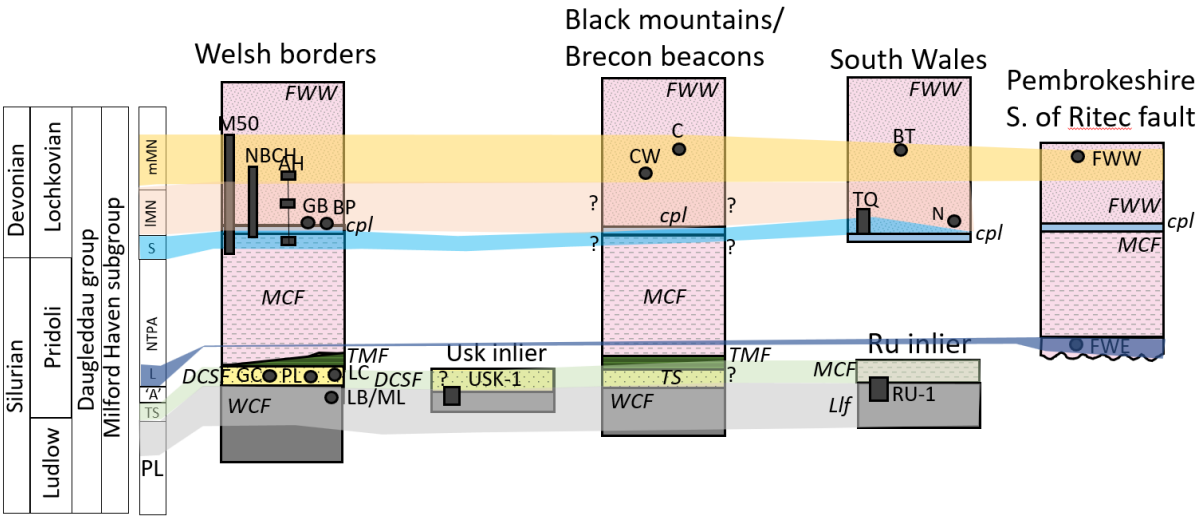

Figure III-19: Schematic correlation across the Anglo-Welsh Basin, showing selected localities described in the text. ***M50:*** *M50 motorway section;* ***NBCH:*** *North Brown Clee Hill;* ***AH:*** *Ammons Hill;* ***GB:*** *Gardeners Bank;* ***BP:*** *Bromyard plateau;* ***GC:*** *Gorsley Common;* ***PL:*** *Perton Lane;* ***LC:*** *Ludford Corner;* ***LB/ML:*** *Ludford bridge/ Milton Lodge;* ***USK-1:*** *Usk borehole;* ***C:*** *Creswall;* ***CW:*** *Cwm mill;* ***BT:*** *Bryn Glas tunnels;* ***TQ:*** *Tredomen Quarry;* ***N:*** *Newport;* ***RU-1:*** *Rumney borehole;* ***FWW:*** *Freshwater west;* ***FWE:*** *freshwater east. Rectangles denote long sections, circles denote single horizons.* ***?****correlation not demonstrated. Formations indicated by italics;* ***FWW:*** *Freshwater West formation;* ***MCF:*** *Moor Cliffs formation;* ***cpl:*** *Chapel Point Limestone member;* ***TMF:*** *Temeside Shales formation;* ***DCSF:*** *Downton Castle Sandstone formation;* ***TS:*** *Tilestones formation;* ***Llf:*** *Llanederyn formation;* ***LB:*** *Llangibby beds;* ***WCF:*** *Whitcliffe formation. Stratigraphic and biozone thickness approximate. References in text. Stratigraphy after Barclay et al. (2015).*

The succeeding *Apiculiretusispora sceacga* subzone provides a greater opportunity for basin-wide correlation as it is present in the Welsh Borderlands and Central - South Wales, in at least the M50 section and Ammons Hill and is probably present at Clee Hill. Its presence at Tredomen Quarry is questionable, but plausible. The zone has not been reported from Pembrokeshire. The inception of the tripapillate *Apiculiretusispora sceacga c.* 2m below the first incidence of *T. pagei* in the M50 section (at -35 m below the Chapel Point Limestone) means the former has the potential to be an important biostratigraphic marker for the onset of the Devonian. The rarity of *A. sceacga* is a problem for its utility as a marker, but it has been recognised in the lowest Ammons Hill sample. The Ammons Hill section is tectonically disrupted, with the major Brockhampton fault juxtaposes the lower *micrornatus* – *newportensis* spore assemblages to the west, and 'pre- *micrornatus* – *newportensis* assemblages to the east, resulting in the loss of the Chapel Point Limestone in that area. Barclay et al. (1994), who originally studied the section, posited that the assemblage from the eastern side of the Brockhampton fault was pre- *micrornatus* – *newportensis* but *A. sceacga* was not formally recognised. This species has now been recorded following extensive logging here, and if the range of *Apiculiretusispora sceacga* in the M50 section is representative of the overall range of the species, then the sediments on the eastern side of the Brockhampton fault encompassed by the *Apiculiretusispora sceacga* zone are thus between latest

Přídolí and earliest Lochkovian in age. This conclusion is posited with the acceptance that other 'long sections' demonstrating the range of the *A. sceacga* zone need to be recorded and associated with faunal control. The absence of non-tripapillate *Aneurospora* species, such as *Aneurospora sheafensis*, is problematic in the Ammons Hill section, and precludes more confident correlation with the M50.

Unlike Ammons Hill, the pre- *micrornatus – newportensis* sample from Clee Hill can be correlated relative to the Chapel Point Limestone (-7m below), which may suggests by lithostratigraphic correlation that the sample is included in the *Apiculiretusispora sceacga* zone, accepting the possible diachronous nature of the Chapel Point Limestone, indicating an earliest Devonian age (although faunal control is lacking in this area). The principal issue with correlating this depauperate Clee Hill assemblage with the M50 and Ammons Hill is the absence of *A. sceacga*, non-tripapillate *Aneurospora* species and key *Emphanisporites* species, with only long-ranging, biostratigraphically irrelevant taxa identified. The strongest indicators of this samples' age and correlation, then, is the absence of key *micrornatus – newportensis* taxa, and the proximity/ position of the assemblage to the Chapel Point Limestone. As such, whilst a pre- *micrornatus – newportensis Apiculiretusispora sceacga* zone earliest Lochkovian age is posited here, further testing is necessary.

Tredomen Quarry yields an apparently pre-*micrornatus – newportensis* biozone which occurs above the Chapel Point Limestone, in contrast to all of the other *Apiculiretusispora* sp. E localities (Morris et al., 2011a). This zone, while probably being influenced by reworking, can be tentatively correlated with the *Apiculiretusispora* sp. E zone by the absence of tripapillate *Aneurospora* species and *Streelispora*. The correlation based on this absence can be made with some confidence because, even in the most depauperate *micrornatus – newportensis* spore assemblages tripapillate *Aneurospora* species occur. As such, it is posited here that the absence is probably indicative that the parent plants of those key spores were not present in the area around Tredomen Quarry at that time. Whether this is a function of temporal, spatial, or facies factors cannot be ascertained for certain. However, given the widespread occurrence of tripapillate *Aneurospora* and *Streelispora* species on a global scale in the *micrornatus – newportensis* zone (e.g. Richardson and Ioannides, 1973; Richardson et al., 1981, 1984), spatial variance seems unlikely. Furthermore, whilst facies factors, including taphonomic reworking, are present there (Morris et al., 2011a), there does not seem to be cause for tripapillate *Aneurospora* and *Streelispora* species to be excluded from the assemblage based on winnowing or sorting, nor removal of other taxa which appear elsewhere in the lower *micrornatus – newportensis* such as *Perotrilites microbaculatus*. As such, a temporal cause for their absence remains the most likely reason and hence a pre-*micrornatus- newportensis* age is probable for the lowermost Tredomen Quarry assemblage, although without the nominal species from the *Apiculiretusispora sceacga* zone from the M50 and/ or faunal evidence this cannot be unequivocally confirmed.

Considering the M50 section, which exhibits the entire subzone range, the thickness of the *Apiculiretusispora sceacga* zone is probably *c.* 35 m in that area, given that the first sample occurs at -35m below the Chapel Point Limestone, and the *micrornatus – newportensis* biozone initiates at +0.15 m. The extent of the zone elsewhere is not currently attainable.

Many of the localities exhibiting pre- *micrornatus – newportensis* assemblages that have been studied here continue into the lower *micrornatus – newportensis* subzone. In addition, there are several other localities, which have not been studied here, which also yield spore assemblages from this subzone (Chaloner and Streel, 1966; Richardson and Lister, 1969; Barclay et al., 1994; Morris et al., 2011a; Richardson, unpub.) which leads to excellent correlation across the Anglo-Welsh Basin. In the localities studied here, strong correlation is found with the key nominal species (*S. newportensis* and *E.* cf. *micrornatus*) identified in all cases, and given the early circumscription of these key taxa, most previous work is immediately able to be correlated across the Welsh Borderlands and Central – South Wales (fig. 19). Nonetheless, the subzone has not yet been reported from Pembrokeshire. The earliest reported assemblage corresponding to this zone was published by Chaloner and Streel (1966) from Newport, South Wales, where *S. newportensis* ('*Granulatisporites newportensis'*) was first described alongside *Chelinospora vermiculata*. Whilst *E.* cf. *micrornatus* was not recognised by these earliest

workers, again likely a function of the early taxonomic work, the locality can still be confidently assigned to the lower *micrornatus – newportensis* zone. Firstly, the proximity to the Chapel Point Limestone is strongly indicative, as across this region of the basin the lower *micrornatus – newportensis* zone initiates immediately above the Chapel Point Limestone (e.g., the M50 section). In addition, the presence of *C. vermiculata* indicates a lower *micrornatus – newportensis* subzone age, as this species is not reported outside of the subzone in any other localities, although *C.* cf. *vermiculata* is reported rarely in the middle *micrornatus – newportensis* subzone. In general, the base of the zone is corresponds more or less to the Chapel Point Limestone. Tredomen Quarry, however, again presents an interesting contrast to the rest of the basin, with *S. newportensis* not appearing until +42 m above the Chapel Point Limestone. This lower *micrornatus – newportensis* subzone assessment is interesting regarding the upper limits of the zone as well, given that by +42 m above the Chapel Point Limestone in the M50, the middle *micrornatus – newportensis* zone is initiated with the incoming of *E. micrornatus*. The uppermost sample from Tredomen Quarry (+60m) also yields a lower *micrornatus – newportensis* assemblage, whereas samples from *c*. 60m above the Chapel Point Limestone at Brown Clee Hill yield a characteristically middle *micrornatus – newportensis* assemblage. This may point to the sedimentary hiatus which eventually affected the entire Anglo-Welsh Basin which may have initiated much earlier in the area around Tredomen Quarry than elsewhere, and further study of the area around the quarry offers a fascinating line of enquiry.

The total thickness of the lower *micrornatus – newportensis* subzone across the Anglo-Welsh Basin is still equivocal, given the lack of long, continuous sequences which clearly demonstrate the lower to middle subzone transition. Nonetheless, by assessing the relative thickness of sections encompassing lower *micrornatus – newportensis* samples, it is suggested here that the zone is no thicker than 50 metres. This is based principally on the thickness pf the M50 section, where lower *micrornatus – newportensis* palynofloras initiate at +0.15m above the Chapel Point Limestone, and are terminated at the latest at +42m, where middle *micrornatus – newportensis* assemblages appear. Relative to the Chapel Point Limestone, the highest sample in the lower *micrornatus – newportensis* zone is at +22 m, and is drawn from Clee Hill, where the subzone initiates just above the Chapel Point Limestone (Edwards and Richardson, 2004).

Much like the preceding lower *micrornatus – newportensis* subzone, there are a relatively large number of palyniferous localities yielding middle *micrornatus – newportensis* subzone assemblages and hence the subzone benefits from a good level of basin-wide correlation (fig. 19). The Clee Hill and M50 section correlate well here, and give an insight into the initiation of the subzone relative to the Chapel Point Limestone in the Welsh Borderlands. The earliest sample yielding *Emphanisporites micrornatus* occurs in the M50 section, at +42 m relative to the Chapel Point Limestone. As previously mentioned, the lower to middle *micrornatus – newportensis* transition has not yet been observed and therefore a point of initiation relative to the Chapel Point Limestone for the middle *micrornatus – newportensis* zone is not currently known.

Confident correlation can be made between the middle *micrornatus – newportensis* Clee Hill and M50 section assemblages at Ammons Hill, despite the latter being tectonically complex and lacking a relative position to the Chapel Point Limestone. Interestingly, the key middle *micrornatus – newportensis* subzone indicator, *E. micrornatus*, is largely absent at Ammons Hill, and hence a reliance on other key species is required to ascertain the biostratigraphic position of many of the Ammons Hill samples, the sequence of which is complicated by faulting. The appearance of certain cryptospores including variants of *Cymbohilates variabilis* var. *variabilis* and *C. horridus* are indicative of the middle *micrornatus – newportensis* subzone. Coupled with faunal control (Barclay et al., 1994), it is with some confidence that the Ammons Hill samples in question can be correlated to the middle *micrornatus – newportensis* subzone.

Several other sites in the Welsh Borderlands and Central - South Wales have been studied by previous workers and can be correlated with the localities studied here (fig. 19). A diverse spore assemblage from the Bryn-Glas tunnels in South Wales was reported by Wellman et al. (2000), and contained

contain *E. micrornatus*, indicative of the middle *micrornatus – newportensis* sub zone. The latter was only present in associated tetrads, which is probably a result of winnowing of smaller spores. Nonetheless, the spore assemblage reported by Wellman et al. (2000) is similar to the middle *micrornatus – newportensis* assemblages reported here, and as such is correlated with the upper M50 section, upper Brown Clee Hill and upper Ammons Hill sections. As expected, there is some subtle variation in spore assemblages, which may be palaeoecological (Chapter IV).

Cwm Mill (Fanning et al., 1987; Kenrick, 1988) and Craswell (Morris and Edwards, 2014) can be coarsely correlated (i.e. *micrornatus – newportensis* zone) based on the fish remains recovered there, but a lack of spores precludes higher resolution correlation. The presence of *P. crouchi*, indicative of the middle and upper *micrornatus – newportensis* zone, does however preclude the lower *micrornatus – newportensis* zone and the preceeding *breconensis – zavallatus* zone. Cwm Mill is placed stratigraphically lower than Craswell (Morris and Edwards, 2014), but a strong lithostratigraphic and spore control relative to the Chapel Point Limestone for both sites is lacking.

The stratigraphic gap from the *lavidensis* zone (Higgs, 2022) in Pembrokeshire is terminated by samples from the middle *micrornatus – newportensis* subzone, recorded from freshwater West (Higgs, 2004). Higgs (2004) describes assemblages which are essentially comparable to the *micrornatus -newportensis* assemblages from the Welsh Borderlands described here and elsewhere (e.g. Richardson and Lister, 1969). There is some variation in spore assemblages, especially amongst the trilete spores where species such as *Calamospora atava* are reported which are absent in the Welsh Borderlands. Key species, including *Streelispora newportensis* and *Emphanisporites micrornatus* var. *micrornatus* are present in Pembrokeshire, the latter indicating a middle *micrornatus – newportensis* age. The variation between the Welsh Borderlands and Pembrokeshire may be due to the factors listed earlier, including subtle variations in depositional timing and palaeoecology. The absence of *C. paulus* in the Welsh Borderlands may be indicative of temporal variation, as it initiates in the early middle MN zone (Richardson and McGregor, 1986), with the Pembrokeshire material possibly being slightly younger than the Welsh Borderlands material.

8.5. Global spore correlations: Euramerica, Gondwana and elsewhere

There is a global distribution of marine and terrestrial deposits yielding early land plant spores between the late Silurian and Early Devonian across both major palaeocontinents (Eurasia and Gondwana) and other land masses (fig. 20). This wide distribution has historically allowed the construction of globally relevant spore assemblage biozones (Richardson and McGregor, 1986; Streel et al., 1987; Steemans, 1989) and subsequent international correlation has been generally possible, although there is a distinct sampling bias concentrated around western Gondwana and southern Euramerica, but recent work is beginning to shed light on the global record (e.g. Shen et al., 2020; Legrand et al., 2021; Wellman et al., 2022).

Comparisons and correlations between global assemblages across large geographic distances are difficult. Firstly, by the Přídolí -Lochkovian well-developed floral provinces were established across the planet (e.g. Steemans et al., 2007, 2010; Wellman et al., 2013). Indeed, the presence of the phylogenetic lineage of *Emphanisporites micrornatus* (Steemans and Gerrienne, 1984; Breuer et al., 2005b) in the Anglo-Welsh Basin and palaoegeographically adjacent regions (e.g. Belgium, Scotland, Bulgaria), and absence of these species elsewhere (e.g. Canada, South America) led Steemans and Lakova (2004) to circumscribe the *sinuosus - zavallatus* phytogeographic province, which included much of southern Euramerica and, interestingly, the Moesian Platform in northern Gondwana (Steemans and Lakova, 2004). Steemans and Lakova (2004) postulated that based on the current, although incomplete, global record at least two global phytogeographic provinces existed in eastern Euramerica and western Gondwana, with the former further subdivisible into two, separated by the Caledonian mountains.

Secondly, as a function of this provincialisation, stratigraphically useful ‘bridge-taxa’ (taxa that are shared between provinces) are rare (e.g. *Streelispora newportensis*, *Zonotriletes* spp., *Iberoespora* spp.).

Nonetheless, spore assemblages between some phytogeographic provinces may be more similar than others. For example, western Gondwanan assemblages yield rare *Streelispora newportensis* spores (e.g. Richardson et al., 2001) in common with Euramerica (e.g. Richardson and Lister, 1969; Richardson et al., 1984; Streel et al., 1987). Meanwhile, *S. newportensis* has not been described from assemblages further south in Gondwana, such as those from South America (e.g. Rubinstein et al., 2005).

A final problem with correlating Přídolí and Lochkovian spore assemblages is the lack of independent biostratigraphic age control in many of the studied sections. Such independent age control may be drawn from other fossils including fish and chitinozoans, although concomitant problems exist with these groups also, such as reworking. This problem is compounded by the relatively small sample size of miospore assemblages which are used to date and correlate assemblages and define phytogeographic provinces. As such, caution must be used when attempting to correlate across large geographic distances where independent biostratigraphy is limited for one or more of the spore assemblages in question. Absolute dating also plays a role in constraining the ages of spore assemblages, although in the Devonian such a combination of techniques is rare, often due a lack of horizons suitable for absolute dating. Barclay et al. (2015) reports that U-Pb dating on the Townsend Tuff Bed is currently ongoing. Provisional findings suggest an age of *c.* 420 Ma (K. Higgs pers. omm. 2022), giving a maximum age limit for the late Přídolí NTPA spore zone. Whilst such dating is useful, a more concentrated investigation of possible avenues for absolute dating in Silurian – Devonian sediments, and a relation of the results to spore assemblages, would go someway towards an independent age control between geographically distant spore assemblages. The Anglo-Welsh Basin is one basin of several sedimentary basins across the Euramerica, or the 'Old Red Sandstone continent', which are derived from a variety

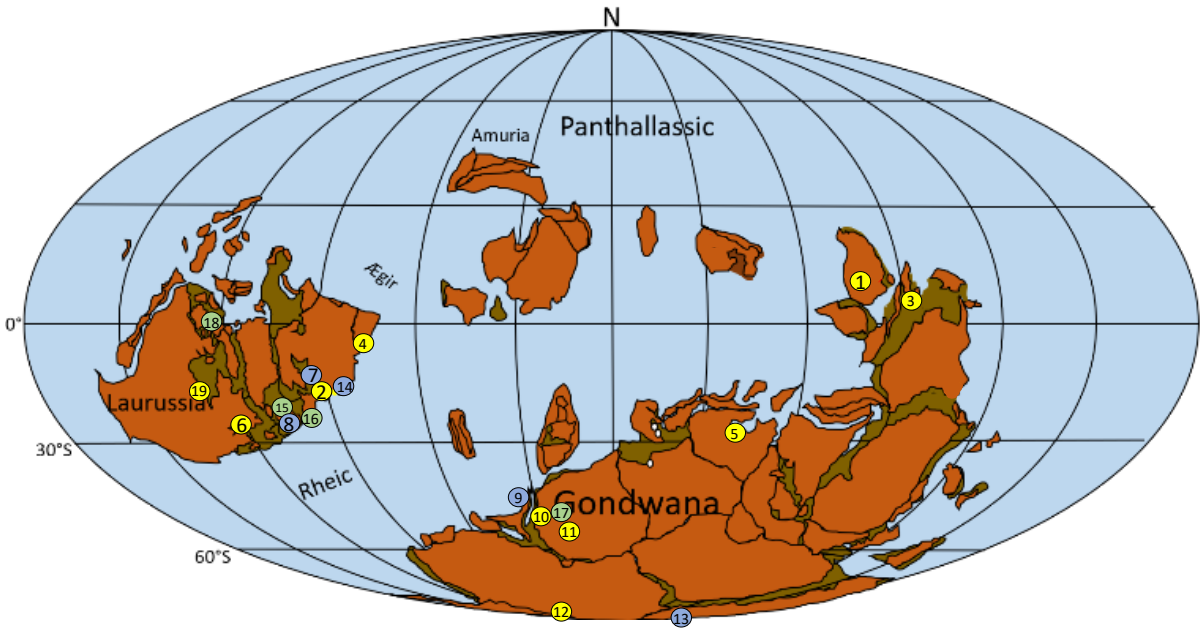

Figure III-20: Localities of Přídolí and Lochkovian spore assemblages. ***1****: China (Wang et al., 2006, 2007; Xue et al., 2015);* ***2****: Estonia (Aristova and Arkangelskaya, 1976; Richardson et al., 1981);* ***3****: Indochina (Tian et al., 2011);* ***4****: Turkey (Steemans et al., 1996);* ***5****: Saudi Arabia (Steemans et al. 2007; Breuer et al., 2017);* ***6****: Nova Scotia (McGregor and Camfield, 1976; Beck and Strother, 2001);* ***7****: Sweden (Mehlqvist et al., 2012; 2015);* ***8:*** *England & Wales (e.g. Richardson and Lister, 1969; Higgs, 2004, 2022; this work);* ***9****: Spain (Richardson et al., 2001);* ***10****: Algeria (Kermandji, 2007);* ***11****: Libya (Al-Ameri, 1980; Rubinstein and Steemans, 2002);* ***12****: Brazil (Steemans et al., 2008);* ***13****: Argentina (Rubenstein et al, 1992; Rubinstein, 1995);* ***14****: Balkans (Aristova and Arkangelskaya, 1976; Kirjanov, 1978; Richardson et al., 1981);* ***15****: Scotland (Richardson et al., 1984; Wellman, 1994; Wellman and Richardson, 1996; Lavender and Wellman, 2002);* ***16****: Belgium (Streel et al., 1987);* ***17****: Tunisia (Spina and Vecoli, 2009);* ***18****: Svalbard (Wellman et al., 2022);* ***19****: Ontario (McGregor et al., 1970; McGregor and Camfield, 1976).* ***Yellow:*** *Přídolí assemblages;* ***Blue:*** *Přídolí – Lochkovian;* ***Green:*** *Lochkovian. Map modified from Torsvik and Cocks, 2013.*

of depositional settings. Here, a qualitative assessment gauging the degree of correlation between the Anglo-Welsh Basin, Euramerica and wider late Silurian – Early Devonian spore assemblages is made, integrating previously established work (e.g. Ricardson and McGregor, 1986) and the findings of this study.

Přídolí

Euramerica

Přídolían spore assemblages are comparatively rare relative to palyniferous Lochkovian assemblages in Euramerica. They are principally marine influenced with poor miospore assemblages, and in addition to the Anglo-Welsh Basin, occur in Estonia (Aristova and Arkangelskaya, 1976; Richardson et al., 1981), Ukraine (Kirjanov, 1978; Richardson et al., 1981), Bohemia (Richardson et al., 1981), Canada (Beck and Strother, 2001) and Sweden (Mehlqvist et al., 2012, 2015). Wellman et al. (2013) utilised cluster analysis and multidimensional scaling to assess Ordovician – Silurian palaophytogeography using megafossil and palynological data. A distinct cluster comprising North Africa + Peri-Gondwana + South America + Avalonia was clearly separated from a Laurentia + South China cluster and a Baltica cluster. These results conflicted somewhat with Raymond's et al. (2006) macrofossil-based paleophytogeographical findings, but Wellman et al. (2013) noted that the results of the study were likely to evolve with the application of future data sets and more harmonious reporting.

Aristova and Arkangelskaya (1976) and Richardson et al. (1981) examined spore assemblages from marine sequences in Estonia (figs. 20 and 21). Simple miospores formed a minor component of the assemblage which was dominated by marine phytoplankton, and Richardson et al., (1981) could make few specific miospore comparisons between their work and Aristova and Arkangelskaya's (1976) findings. A review of the published figured in the latter work similarly drew few confident comparisons. Nonetheless, Richardson et al. (1981) were able to identify *Emphanisporites protophanus, Amicosporites splendidus*, and *E.* sp. D in Aristova and Arkangelskaya's (1976) work. Whilst the former two have been recovered widely from Silurian material (Richardson and Ioannides, 1973; Richardson et al., 1981; Steemans et al., 1996), *E.* sp. D has only been reported from the Early Devonian of the Welsh Borderlands. Richardson et al. (1981) relied chiefly on acritarchs to determine that the Estonian section was of 'high-Silurian (Downtonian)' age, and together with the occurrence of *E. protophanus* and *A. splendidus*, posited that the Kaugotoma Formation in Estonia was Přídolían. Indeed, the recovery of *A. splendidus* in the Přídolí of Turkey (Steemans et al., 1996), Argentina (Rubenstein, 1992; Rubinstein et al., 1995) and the UK (Richardson et al., 1981) supports this late Silurian assessment, however, the species has also been reported from the Ludlow of Turkey, Argentina and Germany (Walter et al., 1998). A reinvestigation of the Estonian material, both of Aristova and Arkangelskaya's (1976) and Richardson's et al. (1981) material may consign further spore species and proffer better correlation with the wider Old Red Sandstone continent, particularly with the terrestrial Anglo-Welsh Basin.

Polish material from the Radom-Lublin area of central Poland (fig. 21) have produced spore assemblages comparable to the lower *micrornatus – newportensis* subzone and R interval zone (Turnau, 1986; Turnau and Jakubowska, 1986) from the upper part of the Scycna Formation (below). The lower parts of this Formation however have not been investigated for spores on account that boreholes only penetrated the upper part of the Formation (Turnau, 1986), but the early Devonian age assigned to the upper part of the Formation may indicate that these shallowing marine deposits would yield latest Silurian – Earliest Devonian spore assemblages.

Beck and Strother (2001) reported Silurian palynomorph assemblages from the Arisaig Group of Nova Scotia, Canada (fig. 20, 21**)** which range from the early Llandovery to Přídolí and are independently dated with conodonts, fish and marine phytoplankton (e.g. Dineley, 1963). The uppermost formations from the section, the upper McAdam Brook Member and Moydart Formation (Ludlow) and Stonehouse

Formation (Přídolí) reported from this work are of particular interest here. From the Ludlow formations, the nominal species of the terminal subzone of the *poecilomorphus – libycus* zone *sensu* Burgess and Richardson (1995), the *Stellatispora inframurinatus* var. *inframurinatus* subzone, were identified from the upper McAdam Brook Formation. The presence of *S. inframurinatus* var. *inframurinatus* and other key species including *Lophonzotriletes poecilomorphus* allows a strong correlation between the McAdam Brook member + Moydart Formation of Nova Scotia, and the Upper Whitcliffe beds of the Welsh Borderlands in the Anglo Welsh Basin via the *S. inframurinatus* var. *inframurinatus* subzone, supported by Graptolites. It is also interesting to note that a broad similarity in spore assemblages exists between these two localities, although Nova Scotia appears to lack *Apiculiretusispora asperata* and *Insolisporites bassetti,* amongst others. Spore assemblages comparable to the *S. inframurinatus* var. *inframurinatus* zone in the Nova Scotia and Anglo-Welsh Basin are derived from shallow marine facies. Stratigraphically higher-up in the Nova Scotian Arisaig Group, the Stonehouse Formation was attributed by Beck and Strother (2001) to the *tripapillatus – spicula* biozone. Whilst the nominal species of this zone (*Synorisporites tripapillatus* and *Apiculiretusispora spicula*) were not reported from the Stonehouse Formation, the inception of *Ambitisporites parvus,* coupled with the loss of key *poecilomorphus – libycus* nominal species including *S. inframurinatus* var. *inframurinatus* was used to posit the inception. Whilst this does suggest that the Stonehouse Formation belongs to the *tripapillatus – spicula* zone, the assignation is more tenuous based solely on spores compared to the preceding evidence for the *S. inframurinatus* var. *inframurinatus* subzone. Nonetheless, a tentative correlation between the Stonehouse Formation of Nova Scotia and the Downton Castle Sandstone Formation and Tilestones Formation of the Southern Britain can be made. Indeed, it is reiterated that in both the upper Rumney-1 and Usk-1 boreholes from the Anglo-Welsh Basin attributed to the *tripapillatus – spicula* zone, *A. spicula* and *S. tripapillatus* are extremely rare; this may also be the case in Nova Scotia.

Mehlqvist et al. (2012, 2015) reported spore assemblages from the late Silurian of Skåne, Sweden (fig. 20, 7). The boreholes described by Mehlqvist et al. (2012) are of Ludfordian age, and exhibit spore assemblages suggesting a pre *S. inframurinatus* var. *inframurinatus* subzone age, thereby exceeding the oldest assemblages discussed here, and are not considered further. Mehlqvist et al. (2015) reported assemblages which correlate with the latest Silurian – Earliest Devonian spore assemblages described from the Anglo-Welsh Basin from the Övedskloster 2 borehole, also from Skåne. These workers identified three 'assemblages' from this borehole, comprising the latest Silurian (Přídolí) assemblage, a Přídolí-Lochkovian 'transitional' assemblage, and a Devonian (Lochkovian) assemblage. The Silurian assemblage was firmly attributed to the Přídolí, based on the presence of spores including *S. tripapillatus* and *A. spicula,* and tentaculids (Mehlqvist et al., 2015). Whilst the spore assemblage was not especially diagnostic it was compared with late Wenlock – early Přídolí assemblages from Euramerica and Gondwana (Mehlqvist et al., 2015). The absence of key *poecilomorphus – libycus* zone species (i.e., *inter alia, S. inframurinatus* var. *inframurinatus*) and the presence of key *tripapillatus – spicula* species favours an early Přídolí age in Mehlqvist et al. (2015), allowing tentative correlation with other Euramerican localities via this zone.

The close stratigraphic proximity of the Silurian assemblages and Devonian assemblages in Skåne is of interest here, as in the Anglo-Welsh Basin a marked stratigraphic separation between the *tripapillatus – spicula* zone and earliest Devonian spore assemblages (the NTPA zones) exists. Furthermore, no key species from the *lavidensis / hemisphaerica* zones, or from the NTPA/ *Apiculiretusispora sceacga* zones (section 8.3), are reported from the Silurian or Devonian Skåne boreholes. The general assemblage is probably best correlated with the *elegans – cantabrica* zone, reported from Cantabrica (Richardson et al., 2001; Mehlqvist et al., 2015), and as such the lowermost samples from Skåne may correlate with the 'upper' portion of the stratigraphic gap in the Anglo-Welsh Basin, although this is problematic. The absence of diverse *Chelinospora* species does indicate that the assemblage may be of *tripapillatus – spicula* age, but this would suggest that the progression of spore assemblages between the latest Silurian and Early Devonian of Skåne and the Anglo-Welsh Basin are quite different, perhaps due to phytogeographic differences.

Steemans et al. (1996) investigated palynological assemblages from the Dadas Formation in Turkey (fig. 20, 4) and found that part of the assemblage corresponds with the *libycus – poecilomorphus* biozone. However, because *Stellatispora inframurinatus* var. *cambrensis* or *S. inframurinatus* var. *inframurinatus* were not reported from the Dadas section, correlation between Turkey and the studied sections in the Anglo-Welsh Basin (Rumney and Usk) is tenuous, and the material reported from the former may precede the earliest Anglo-Welsh Basin assemblages studied here. The absence of these key nominal species may again be a function of phytogeographic differences.

Gondwana and other islands

In Gondwana several localities are comparable with Přídolían assemblages of the Anglo-Welsh Basin, bearing in mind previously outlined caveats. Principally, sampled sites from Gondwana are concentrated around peri- and northern Gondwana with scattered reports from the south-west of the paleocontinent. Other sparse reports of spore assemblages come from island forming microplates such as China. Much of central Gondwana remains unexplored or unproductive, and alongside sites in Euramerica, many of the Gondwanan sites are marine influenced.

Peri-Gondwana

Spanish material (fig. 20, 9) from the Cantabrian mountains was assessed by Richardson et al. (2001), who found that the continual marine sequence extended through much of the Přídolí and Lochkovian. The analysis of this sequence elucidated Přídolían spore successions and several palynological correlations are possible with the Anglo-Welsh Basin. Whilst many key biostratigraphic taxa from the Anglo-Welsh Basin are absent or sporadic in the lower sections from Cantabria, the lower *reticulata – sanpetrensis* zone may be correlated with the *poecilomorphus – libycus* zone, specifically the upper *Stellatispora inframurinatus* zones *sensu* Burgess and Richardson (1995) in the Anglo-Welsh Basin. This assessment is based on the co-occurrence of *Stellatispora inframurinatus* var. *cambrensis* and spores similar to *Synorisporites libycus* in Spain. Co-occurring chitinozoans, whilst long ranging, indicate a minimum lower Přídolí age (Richardson et al., 2001). The proceeding *hemisphaerica* zone was recently posited by Higgs (2022) to correlate with the *lavidensis* zone described by him from Freshwater East in Pembrokeshire, based on the common occurrence of *Chelinospora* species, including *C. hemisphaerica*, and chitinozoan species *Margachitina elegans* and *Pseudoclathrochitina carmenchui*, which together indicate a mid Přídolí age. In the Welsh borderlands, the mid Přídolí sampling gap precludes correlation with Cantabrian spore assemblages.

Northern Gondwana

Richardson and Ioannides (1973) reported Silurian palynomorphs from Tripolitania in Libya (fig. 20, 11**)** from the Tanezzuft and Acacus formations. Limited comparison is possible between the former and the Anglo-Welsh Basin given the absence of key zonal species, but the upper portion (Acacus) may be tentatively correlatable with the *tripapillatus – spicula* biozone. This is drawn from the co-occurrence of *Apiculiretusipora spicula*, *A. synorea* and *Synorisporites verrucatus* in the assemblages. However, *S. tripapillatus* is not reported in Libya, and as such the correlation remains tentative. Richardson and Ioannides (1973) noted that the presence of *Emphanisporites* and cf. *Brochotriletes* in Libya was the principal difference with possibly coeval Anglo-Welsh Basin assemblages, where these genera are limited or do not occur.

Boreholes from the Ghadamis basin, also in Libya, yielded Ludlow to earliest Devonian assemblages (Rubinstein and Steemans, 2002). The Late Silurian assemblages, from the Alternaces Argilo – Greseuses Formation, were independently dated with acritarchs and chitinozoans and yield palynomorph assemblages comparable to the Ludlow '*Apiculiretusispora* zone' (not: *A. sceacga* subzone) of Edwards and Richardson (1989) and the proceeding *tripapillatus – spicula* zone (Richardson and McGregor, 1986). These lower assemblages may therefore be comparable with the

lowermost assemblages investigated from the Anglo-Welsh Basin in this work. The *Apiculiretusispora* zone (Edwards and Richardson, 1989) corresponds approximately to the upper *poecilomorphus – libycus* zone (Richardson and McGregor, 1986). This upper portion of the zone was later divided into the *Apiculiretusispora asperata* and *Stellatispora inframurinatus* var. *inframurinatus* biozones by Burgess and Richardson (1995). Because *S. inframurinatus* var. *inframurinatus* was not reported from the Ghadamis Basin, it is possible that these Ludlovian samples correlate with the *A. asperata* zone and may therefore be slightly older than the *poecilomorphus – libycus* assemblages in this work, although it is also possible that *S. inframurinatus* is not present due to phytogeographic variation. *Apiculiretusipora spicula, A. synorea* and *S. verrucatus* are all reported from Ghadamis Basin, which led Rubinstein and Steemans (2002) to correlate these levels with the *tripapillatus – spicula* zone. Following this, the samples correlate with the Ludford Lane and upper Rumney and Usk samples reported from the Anglo-Welsh Basin here, but *Synorisporites tripapillatus* and *E. echinautus* are not reported from the Ghadamis basin, which again may be a function of phytogeography.

Several boreholes from Algeria (fig. 20, 10) yield late Silurian spore assemblages (Kermandji, 2007). Key species, including *Streelispora newportensis* were absent from these sections, although Kermandji (2007) posited a late Silurian – Earliest Devonian age based on the presence of *Chelinospora cassicula*, *Synorisporites tripapillatus, S. verrucatus* and *Apiculiretusispora synorea*. Furter correlation with the late Silurian – Early Devonian of Southern Britain is difficult given the absence of *inter alia*, key *Aneurospora* species and independent dating.

North eastern - eastern Gondwana and other regions

Saudi Arabian assemblages (fig. 20, 5) have been investigated by Steemans et al. (2007), and more recently by Breuer et al. (2017). Steemans et al. (2007) reported spore assemblages from the Tawil Formation, and despite the assemblages being diverse, confident assignation to a spore biozone was difficult given the absence of *Streelispora newportensis* and a single, very poor example of *Emphanisporites* cf. *micrornatus*. Nonetheless, based on spores that were present (e.g. *Cymbosporites proteus, Aneurospora isidori* and *Cymbosporites dittonensis*) and the absence of spores indicating a later Silurian age, Steemans *et al*. (2007) tentatively posited an earliest Lochkovian age, possibly corresponding to the *Aneurospora* spp. subzone of the *elegans – cantabrica* zone of Richardson et al. (2001) based on the presence of species of *Aneurospora isidori*, but they noted that in Gondwana, at least, species of *Aneurospora* seem to appear prior to the Devonian (e.g. Rubinstein and Steemans, 2002) and therefore the assemblages may be older. Based on the absence of key species reported by Steemans et al. (2007), correlations with the Anglo-Welsh Basin are difficult. If the Saudi Arabian assemblages are indeed earliest Devonian, it is not expected that *E.* cf. *micrornatus* or *Streelispora* would be identified, as they do not appear until the early Devonian *micrornatus – newportensis* zone, and the former may be excluded from assemblages altogether due to the phytogeographic range of the species (Rubinstein and Steemans, 2002). If the site does correlate with the '*Aneurospora* spp.' subzone of Richardson et al. (2001), then it may correlate tentatively with the pre-*micrornatus-newportensis Apiculiretusispora sceacga* zone, although *Aneurospora isidori* does not appear until the early Devonian in the Anglo-Welsh Basin and the absence of key species precludes a more confident correlation.

Later, Breuer et al. (2017) reported a diverse assemblage, also from Saudi Arabia, which was assigned a (predominantly) late Silurian (mid Přídolí) age, based on spores and chitinozoans. Specifically, the *elegans* global chitinozoan zone of Verniers et al. (1995) was identified, suggesting a basal *elegans – cantabrica* spore zone of Richardson et al. (2001) which was based on the presence of the key nominal species *Synorisporites elegans* and *Ibereospora glabella*. Breuer's et al. (2017) assemblage precedes the assemblages reported by Steemans et al. (2007) in age. The *elegans – cantabrica* zone occurs immediately after the *hemisphaerica* zone (Richardson et al., 2001), the latter of which may correlate with the recently circumscribed *lavidensis* zone (Higgs, 2022) in the Anglo-Welsh Basin. Because the *lavidensis* zone is at present the final biozone reported prior to the major stratigraphic gap present in

the Anglo-Welsh Basin, the assemblage of Breuer et al., (2017) cannot currently be correlated with southern Britain.

Several reports of Late Silurian palynomorph assemblages are known from North and South China and Indochina (e.g. Wang et al., 2005; Tian et al., 2011; Xue et al., 2015) (fig. 20, 1, 3) which during this time were separate microcontinents (Torsvik and Cocks, 2013). North China was essentially isolated in the lower Panthallasic Ocean, whilst Southern China terminated a string of large islands extending out from north-eastern Gondwana. A biozonation scheme for China and Indochina was presented by Tian et al. (2011) comprising four biozones based on the FAD of certain spores. These broadly correlate with the scheme of Richardson and Lister (1986), although key differences, particularly in terms of the nominal species selected, are present. The ~ Přídolí assemblages of China and Indochina correspond approximately to the *Ambitisporites dilutus – Apiculiretusispora spicula* biozone (Tian et al., 2011). Several assemblages have been assigned Ludlow – Přídolí ages corresponding to the *dilutus - spicula* zone, and whilst these assemblages are problematic to correlate fully with the Anglo-Welsh Basin biozones and elsewhere, the common observations of *Cymbosporites echinautus* and *Apiculiretusispora spicula* may suggest a tentative correlation with the *tripapillatus – spicula* zone, although the absence of *Synorisporites tripapillatus* precludes a more confident assignment. A recently reported assemblage from the Si Ka Formation of Northern Vietnam has also been assigned to the *dilutus – spicula* assemblage (Tian et al., 2011) and may therefore tentatively correlate with the *tripapillatus – spicula* zone, although again the absence of key nominal species and independent dating precludes more confident correlation. Whilst considering comparisons between Pragian/Emsian spore assemblages from China and Euramerica, Wellman et al. (2013) noted that such comparisons were particularly problematic given the isolated position of China in the lower Devonian, the distinct spore assemblages which probably derive from the extreme distance between Euramerica and the lower Devonian of China, in addition to the paucity of co-occurring biostratigraphically useful fossils between the two regions. Indeed, the MDS analyses carried out by Wellman et al. (2013) indicate clearly distinguished clusters, separating south China from Baltica and Avalonia, although it is interesting that Laurentia closely clusters with South China.

Southern Gondwana

Steemans et al. (2008) reported spore assemblages from the Urubu basin in Brazil (fig. 20, 12). Three assemblages were reported, two of which were assigned a latest Silurian age. The oldest assemblages were assigned a late Ludlow age based in the presence of *Lophonzotriletes poecilomorphus*, *Cymbosporites downeii* and *Synorisporites verrucatus*, alongside long ranging taxa such as *Ambitisporites avitus*. It was noted that cryptospores were rare in this assemblage. Whilst unsurprising given the geographical distance and likely climatic variance between southern Gondwana and southern Euramerica, the absence of species such as *Stellatispora* preclude a firm correlation with the subzones of the assemblages assigned to the *poecilomorphus – libycus* zone in the Anglo-Welsh Basin. The second assemblage was problematic to assign an age to, given the conflicting occurrences of Lochkovian spore species such as *Chelinohilates sinususosus* var. *sinuosus* amongst a sparse cryptospore assemblages which was otherwise redolent of Přídolí assemblages in the Anglo-Welsh Basin, alongside *Brochotriletes foveolatus* which occurred alongside Ludlow – Přídolí spores such as *Lophonzotriletes poecilomorphus.* This was in addition to the occurrence of Přídolí aged chitinozoans. The presence of *Aneurospora richardsonii* in the assemblages did little to improve the confidence of assemblage biozonation, as the oldest *Aneurospora* spp. in Gondwana are known from the early mid Přídolí (Breuer et al., 2017) *elegans – Cantabria* zone. The presence of *Aneurospora* does, however, give an oldest likely age of lower *elegans – cantabrica* zone (mid Přídolí), although further correlation with southern Britain is not currently possible.

Garcia-Muro et al. (2014) and Garcia-Muro and Rubinstein (2018) investigated miospore assemblages from the Los Espejos Formation, amongst others, of the central precordillera basin of Argentina (fig. 20, 13). While difficult to correlate, they tentatively posited that the base of the Formation was not older

than the *poecilomorphus – libycus* zone based on the presence of *Clivisispora verrucatus*. In addition, they reported *Stellatispora inframurinatus* var. *inframurinatus*, *Synorisporites verrucatus* and *S. tripapillatus*, alongside species of *Brochotriletes*, the latter of which was reported from Brazil, also. Indeed, cluster analyses in Garcia-Muro et al. (2014) indicates a close similarity between these Argentinian spore assemblages and Brazilian ones. Garcia-Muro et al. (2014) do not assign a confident biozone to the spore assemblages but suggest that a late Silurian age is probable. Later, Garcia-Muro and Rubinstein (2018) surmised that, based on new and previously obtained evidence (e.g. Garcia-Muro et al., 2014), the Los Espejos Formation ranged from the Ludlow, through the Přídolí and into the Lochkovian. Some broad correlations can be made between Argentina and the Anglo-Welsh Basin in terms of age, and indeed the occurrences of *S. inframurinatus* var. *inframurinatus* and *S. tripapillatus* together in Los Espejos may allow some tentative correlation between Argentina and the *poecilomorphus – libycus* and *tripapillatus – spicula* Anglo-Welsh localities studied here (e.g. Rumney, Usk and Ludford Lane). Likewise, the Lochkovian section from the upper Los Espejos may be correlated with the upper Anglo-Welsh Basin localities studied here, but a more definite recording of *S. newportensis* in the former, and other diagnostic species, is necessary to improve confidence, and it was noted by the Muro and Rubinstein (2018) that the often poor preservation of the spore assemblages precluded firm correlations. It would not be surprising, given the extreme geographic distance, that direct correlation using zonal species from the Anglo-Welsh Basin is not possible with South America.

Lochkovian

Relative to the Přídolí, there is a greater number of palyniferous localities across Euramerica, and these generally yield spore assemblages which are relatable to established (Richardson and McGregor, 1986; Streel et al., 1987) and (this work) spore biozonation schemes. Alongside the Anglo-Welsh Basin, Lochkovian localities across Euramerica include Scotland (Richardson et al., 1984; Wellman, 1994; Wellman and Richardson, 1996, Lavender and Wellman, 2002), the Ardennes – Rhenish region (e.g. Streel et al., 1987; Steemans, 1989), Poland (e.g. Turnau et al., 2005), Ukraine (Arkangelskaya, 1980; Richardson et al., 1984), Bohemia (Richardson et al., 1984), Sweden (Mehlqvist et al., 2015), Spitsbergen (Wellman et al., 2022), Bulgaria (Steemans and Lakova, 2004), Romania (Steemans, 1989) and Canada (McGregor and Camfield, 1976).

The Old Red Sandstone crops out across the Midland Valley and Grampian highlands of Scotland (fig. 20, 15), yielding palyniferous assemblages of interest to this work from the earliest to mid Lochkovian (*Apiculiretusispora sceacga* to middle *micrornatus – newportensis* subzones) (Richardson et al., 1984; Wellman 1993; 1994; Wellman and Richardson, 1993, 1996; Lavender and Wellman, 2002). The oldest spore assemblages are recovered from the Lorne lava plateau in the Grampian Highlands and were determined by Wellman and Richardson (1996) to be of pre-*micrornatus – newportensis Apiculiretusispora sceacga* subzone. Although Wellman and Richardson (1996) encountered difficulties with precisely aging the sediments as a result of a dearth of taxa with well documented stratigraphic ranges, they determined an earliest Lochkovian 'bracket' based on: (1) the absence of key *micrornatus – newportensis* zonal species, including *Streelispora newportensis*, indicating an upper limit, and (2) the presence of crassitate miospores with large apiculate elements, including *Aneurospora geikie*; these features have not been reported from below the Silurian – Devonian boundary, and hence gave a lower age limit. As such, there is an indication that these Lorne sediments correlate with the earliest Devonian sediments of the Anglo-Welsh Basin, although some distinct differences in the palynological assemblage occur between these areas. Most notably, the absence of nominal species, including *Aneurospora sheafensis*, defining the spore zone in Southern Britain are absent in the Lorne assemblages, although it is interesting to note that a diverse suite of non-tripapillate *Aneurospora* species were reported from the latter by Wellman and Richardson (1996), while tripapillate *Aneurospora* species are not reported.

Elsewhere in the Grampian Highlands, an assemblage from Glencoe (Wellman, 1994) yielded poorly preserved spores which were attributed to the *micrornatus – newportensis* biozone, although higher-

resolution determination was not possible due to the high thermal maturity of the specimens. Most of the spores were not identified to species level given their poor preservation, and hence comparisons with only generic comparison with localities from Southern Britain are possible. Nonetheless, the Glencoe assemblage can be coarsely correlated with the *micrornatus-newportensis* biozone and the Freshwater West Formation, although it must be borne in mind that this assemblage may be of upper *micrornatus-newportensis* age, and hence may be younger than the assemblages studied from the Anglo-Welsh Basin in this work.

The Midland Valley of Scotland yields several early Devonian sites which can be confidently correlated to the *micrornatus-newportensis* zone in the Anglo-Welsh Basin. Richardson et al. (1984) described several assemblages from the eastern Midland Valley around the Firth of Tay (Arbruthnott Group) which ranged between the lower and middle *micrornatus-newportensis* zones, yielding key nominal species including *Streelispora newportensis* and *Emphanisporites micrornatus*. As such, the Arbuthnot group correlates well with similarly aged sediments (Freshwater West Formation) in the Anglo-Welsh Basin. Likewise, a small section from the western Midland Valley from Sandys Creek beds (Wellman, 1993) yields a middle *micrornatus-newportensis* assemblage, and correlates well with the Arbuthnot group and middle *micrornatus-newportensis* sediments of the Anglo-Welsh Freshwater West Formation.

The differences in spore assemblages and characteristics between the Lochkovian of Scotland and southern Britain are well documented (e.g. Richardson et al. 1984; Wellman, 1993; Wellman and Richardson, 1996; Wellman et al., 2000; Lavender and Wellman, 2002; Edwards and Richardson, 2004). Despite the assemblages being broadly similar, such as the presence of key zonal species facilitating correlation between both areas, there are some interesting differences. Internally in Scotland, Wellman and Richardson (1993) noted that the Arbruthnott Group, whilst being rich in patinate spores such as *Archaeozonotriletes*, exhibited a paucity of *Aneurospora* species. The opposite was true in Lorne assemblages, and the richness of *Aneurospora* species in the latter is an interesting parallel with the Anglo-Welsh Basin. Later, Lavender and Wellman (2002) explored the variation between coeval Scottish assemblages, noting a minor variation in taxonomic composition and abundances, which were probably a function of temporal, facies and palaeoecological differences. More distinct differences have been noted between the Anglo-Welsh Basin and these are almost certainly derived at least in part by the differences by vegetational differences deriving from facies variation, with the Anglo-Welsh Basin representing a foreland alluvial plain, while Scotland represents a series of intramontane basins. Patinate spores (e.g. *Archaeozonotriletes*, *Chelinospora*) and species of *Synorisporites* are less prevalent in the Lorne assemblages than in coeval Anglo-Welsh assemblages, and conversely *Dibolisporites* appears much earlier in Lorne than in the Anglo-Welsh Basin (Wellman and Richardson, 1996). Furthermore, Scottish assemblages are dominated by laevigate retusoid spores including *Retusotriletes*, contrasting with southern Britain, and moreover Scottish spores are generally larger (Wellman et al., 2000; Edwards and Richardson, 2004).

Geographically close to the British assemblages are the Ardennes – Rhenish assemblages (fig. 20, 16), which yield diverse and stratigraphically well constrained spore assemblages (e.g. Streel et al., 1987; Steemans, 1989). The assemblages are remarkably similar to those of the Anglo-Welsh Basin, and the oppel/ interval zones of Streel et al (1987) correlate well with the assemblage biozones erected by Richardson and McGregor (1986). The lower *micrornatus – newportensis* subzone (lower Freshwater West Formation) correlates strongly with the Fepin and lower Haybes formations in the Ardenne – Rhenish region, which comprise the lower MN oppel zone and N and R interval zones of Streel et al. (1987). The middle MN zone of the Anglo-Welsh basin correlates with the M and Si zones (middle MN oppel zone) of the Ardennes – Rhenish, where the inception of *E. micrornatus* var. *micrornatus* occurs. The earliest Lochkovian, represented by the *Apiculiretusispora sceacga* zone in the Anglo-Welsh Basin, is not present in the Ardennes – Rhenish due to the onlapping of Lower ORS sediments onto basement and subsequent lack of Devonian rock in the latter, precluding correlation from the earliest Lochkovian upper Moor Cliffs Formation. Similarly, the base of the *micrornatus – newportensis* biozone is not

observed in the Ardennes – Rhenish region. No cryptospores have been reported from the Ardennes – Rhennish region, but this is likely a function of the early taxonomic work (e.g. Steemans, 1989) rather that their absence.

Elsewhere in Belgium, the La Gilleppe locality (Steemans and Gerrienne, 1984), also yields a comparable assemblage to the Ardennes – Rhenish and Anglo-Welsh Basin. The lowermost of these assemblages are comparable to the M interval zone/ middle *micrornatus – newportensis* oppel zone (Streel et al., 1987) and the middle *micrornatus – newportensis* zone of Richardson and McGregor (1986). The occurrence of key species and others, such as *Aneurospora isidori*, *Emphanisporites neglectus* and *Leonispora argovejo* all correlate well with the middle *micrornatus – newportensis* zone in the Freshwater West Formation of the Anglo-Welsh Basin. The Prescence of *Cymbosporites echinautus* in the La Gillepe section is interesting, as this species is recorded solely from the *tripapillatus – spicula* zone of the Anglo-Welsh Basin (Ludford Corner). This observation may, *inter alia*, indicate reworking of earlier Přídolí sediments in this region.

The Upper Sycna and lower to middle Czarnolas formations in Poland yield (fig. 20, 14), *inter alia, Streelispora newportensis,* but lack *Emphanisporites micrornatus,* which led Turnau et al. (2005) to associate this part of the sequence with the R interval zone of the *micrornatus – newportensis* Oppel zone/ the lower *micrornatus – newportensis* subzone. As such, the Upper Sycna and lower to middle Czarnolas correlates with the lower Freshwater West Formation in the Anglo-Welsh Basin. Meanwhile, the upper Czarnolas Formation consigned *E. micrornatus* and is equitable to the M interval zone of the MN oppel zone, and the middle *micrornatus – newportensis* subzone (middle Freshwater West Formation) of the Anglo Welsh Basin. In addition to the similarities observed between the Polish and Anglo-Welsh basin palynofloras, there are some interesting differences (Turnau et al., 2005). Redolent of Scottish material, *Dibolisporites* appears earlier in Poland than in the Anglo-Welsh Basin, occurring in the former from the middle *micrornatus – newportensis* subzone. Similarly, several species of *Retusotriletes* and *Aneurospora* appear to be peculiar to Poland, along with genera not reported from southern Britain, such as *Camptozonotriletes*. It is also interesting to note that the cryptospore diversity of Poland appears to be lower in the middle *micrornatus – newportensis* when compared with coeval sites (e.g. the M50 section) in the Anglo-Welsh Basin, specifically with regards to the diversity of *Cymbohilates* species, which may be a function of provincialism or facies variation (Steemans et al., 2007; Chapter IV). The boreholes used to retrieve this material did not penetrate further than the upper Scyna Formation. Providing that the sequence is continuous below this point, further correlations may be possible with the lower *micrornatus – newportensis* (lower Freshwater West Formation) and this represents an interesting line of enquiry for future workers to further qualify the earliest Lochkovian palynoflora of Poland and compare this to the terrestrial assemblages of the Anglo-Welsh Basin and elsewhere.

Correlatives with the Lochkovian sections in the Anglo-Welsh Basin also occur in Sweden (fig. 20, 7). Above Mehlqvist's et al. (2015) Přídolí 'assemblage A' is a 'transitional zone' of uncertain age, followed by bona fide Devonian spore assemblages. The transitional and Devonian assemblages here are peculiar as no nominal species from the *micrornatus – newportensis* biozone have been recorded from over 100m of Devonian strata. Mehlqvist et al. (2015) considered this section of stratigraphy as Devonian (Lochkovian) based on the inception of, *inter alia*, *Cymbohilates allenii* and *Cymbosporites microgranulatua,* but did not assign a spore assemblage zone to the unit. In British assemblages these species are very rare, but present, from the *Ap. sceacga* zone and become common in the lower MN zone (Richardson, 1996; this work), indicating an early Lochkovian age. The absence of *Streelispora newportensis* and *Emphanisporites* cf. *micrornatus*, may suggest that the Skåne Devonian assemblages are pre-*micrornatus – newportensis*, although possible taphonomic effects must be considered. Given the abundance of *Streelispora* in *micrornatus – newportensis* assemblages, even when they are sparse, it is posited here that the parent plant was not present at the time of deposition. Meanwhile, the presence of *C. allenii*, *C. microgranulatus* and especially *Aneurospora geikie* suggests that the 'transitional zone' and preceding assemblages are early Devonian. As such, it is possible that the 'transitional assemblage'

and at least part of the 'Devonian assemblage' can be tentatively correlated with the *Apiculiretusispora sceacga* zone, or lower *micrornatus – newportensis* subzone but this is far from certain as the absence of, *inter alia*, *E.* cf. *micrornatus* and *S. newportensis*, may be a function of phytogeography, amongst other things. The upper portion of the Övedskloster 2 borehole necessitates more caution, as these assemblages are particularly depauperate, sometimes only yielding a single long ranging species such as *Tetrahedraletes medinensis*. It may be, then, that the Devonian assemblages from Skane are simply poorly preserved. The lack of independent biostratigraphic control is particularly problematic for more confident biostratigraphic correlation with southern Britain.

Recently, Wellman et al. (2022) described novel Lochkovian spore assemblages from Red Bay group of Spitsbergen in Svalbard (fig. 20, 18). The Red Bay group has independent faunal control, being correlated by Blieck et al. (1987) to the upper *pocockii* through *symondsii* and *leathensis* to *crouchi* biozones. Higher resolution spore biozonation was not carried out by Wellman et al. (2013), but given the faunal biostratigraphy, it is probable that the Red Bay Group can be coarsely correlated with the *micrornatus – newportensis* spore biozone in the Anglo-Welsh Basin, although the key species *Streelispora newportensis* and *Emphanisporites micrornatus* and *E.* cf. *micrornatus* were not reported. In terms of the similarity between palynofloras, the most striking difference between the Anglo-Welsh Basin is the low diversity of miospores and near absence of cryptospores in Spitsbergen. Regarding the former, the Anglo-Welsh Basin consigns an incredible diversity of miospores. The Spitsbergen palynoflora is dominated by laevigate species of *Retusotriletes* and *Ambitisporites*, with a low incidence of simply ornamented spores, including *Aneurospora*. At least six species of *Aneurospora* are identified from the Red Bay Group, which may suggest that, like the Anglo-Welsh Basin and elsewhere, there was a salient diversification of this genus in the Lochkovian. On the other hand, species of *Emphanisporites* are rare and low diversity, contrasting especially with the Lochkovian of the Anglo-Welsh basin. The absence of cryptospores in this section is peculiar, even of long ranging, widespread forms such as *Laevolancis* spp. and *Tetrahedraletes* spp., and again contrasts with the Anglo-Welsh Basin where there is sustained cryptospore diversification in the early and mid Lochkovian. The absence of cryptospores is not likely to be facies derived, as the Red Bay Group is of 'typical old red sandstone fluvial' facies (Wellman et al., 2022). Thus, the absence may be due to the absence of parent plants in Spitsbergen, either because they have been lost in the area or were not present, either due to competition or unsuitable environments.

The Clam Bank Formation on the western coast of Newfoundland (fig. 20, 21) has a similar suite of paleoenvironments to the Anglo-Welsh Basin, with braided streams and rivers and shallow tidal zones. Burden et al. (2002) investigated conodont, marine palynomorphs and miospores from this Formation, and determined that the sediments were basal Devonian in age. From assessment of the spores recovered from the sediments, Burden et al. (2002) posited that the Clam Bank Formation is either of lower *micrornatus – newportensis* or *Apiculiretusispora sceacga* age. The absence of *Streelispora* is problematic for assigning the former biozone to the Formation, although Burden et al. (2002) did report a possible cf. *Emphanisporites micrornatus*, which whilst comparable did not have a clearly developed distal ornament of cones and spines. The cf. *E. micrornatus* differs from *E.* cf. *micrornatus sensu* Richardson and Lister (1969) as it has a circular amb and coarser muri. The absence of these key taxa precludes confident assignment to the *micrornatus newportensis* zone. The presence of *Aneurospora geikie*, as for the Lorne (Wellman and Richardson, 1996) and Skåne (Mehlqvist et al., 2015) does suggest a minimal age of earliest Devonian, although an earlier appearance of this species in Newfoundland is not discounted. Coupled with the appearance and presence of *Cymbohilates allenii* var. *allenii*, *C. allenii* var. *magnus* and *C. disponerus* which appear towards the latest *A. sceacga* and lower *micrornatus – newportensis* subzone in the Welsh Borderlands, Burden's et al. (2002) assignation of the Clam Bank Formation to the earliest to early Lochkovian is agreed with here, although caution is retained in the absence of key miospore species and a tentative correlation is made between the upper Moor Cliffs and lower Freshwater West formations of the Anglo-Welsh Basin. The Kenogami Formation in Northern Ontario (fig. 20, 19) is divided into three (lower, middle, upper) members

(Armstrong et al., 2018). Following palynological analysis, the uppermost member was found to yield Lochkovian to Emsian spores (McGregor et al., 1970; McGregor and Camfield, 1976), although similar problems with correlation between the Clam Bank and the Anglo Welsh Basin exist for this region, too.

Peri-Gondwana

Brittany, Normandy and the Cantabrian Mountains of Spain were located across Peri-Gondwana (fig. 20: 9 & 20). Spore assemblages from the former were described by Deunff and Chateuneuff (1976) and Steemans (1989). In Brittany, Steemans (1989) described spore assemblages from the Pont au Bouchers Formation in Saint-Germaine-Sur-Ay, and concluded that, alongside independent chitinozoan biostratigraphy (Paris, 1981), the section belonged to the *micrornatus – newportensis* oppel zone. Specifically, based on the continual succession of spores, Steemans (1989) assigned a 'lower' *micrornatus – newportensis* oppel zone age, with a successive sequence of N, M and R interval zones. This section therefore correlates well with the lower *micrornatus – newportensis* zone localities, such as the lower M50 section, in the Anglo-Welsh Basin and across Euramerica. However, the absence of *C. proteus* in the reported Anglo-Welsh Basin localities precludes more exact correlation. Considering the spore assemblage composition reported by Steemans (1989) some similarities can be made however, which include the incidence of key species (e.g. *S. newportensis*) and others such as *Amicosporites miserabilis* and *Ibereospora glabella*. These species are also known from Cantabrian sections, which were investigated by Rodriguez (1978a, b, c) and Richardson et al. (2001).

The uppermost sections of the localities studied by Richardson et al. (2001), which related the biostratigraphy laid out by Rodriguez (1978a, b, c) to wider biostratigraphic correlations, revealed that while dominated by late Silurian spores, the uppermost parts of some of the sections yielded spore assemblages equivalent to the lower *micrornatus – newportensis* zone. Given the continuity of the section, and the realization that the lower *micrornatus – newportensis* probably had a least one biozone beneath it before the Silurian - Devonian boundary (e.g. Richardson et al., 1984), a portion of sections below the lower *micrornatus – newportensis* sections were considered likely to be earliest Devonian in age. Richardson et al., (2011) took the occurrence of *Aneurospora* species to potentially indicate the onset of the Devonian. As such, the uppermost sections of the La Peral section in Cantabria correlate reasonably well with the lower *micrornatus – newportensis* zone in the Anglo-Welsh Basin, although the paucity of *Streelispora newportensis* was noted, in addition to other key taxa such as *Emphanisporites protophanus* which appears to have been absent in Euramerica. Similarly, the occurrence of non-tripapillate *Aneurospora* species, *inter alia*, in the pre- *micrornatus – newportensis* '*Aneurospora* spp.' subzone of the *elegans – cantabrica* zone, suggests some correlation with the *Apiculiretusispora* sp. E and preceding *Aneurospora sheafensis* biozone. However, the paucity of shared, key species between the Anglo-Welsh Basin and Cantabria which delimit the pre- *micrornatus – newportensis* 'zone' in both localities is problematic for more precise correlation.

Northern Gondwana (present-day Libya, Tunisia and Algeria – fig. 20: 10, 11, 17) yields late Silurian – Early Devonian spores which correlate with the rest of Gondwana and Euramerica. In his thesis, Al-Ameri (unpub. Thesis, 1980) correlates his DN zone in Libya with the lower *micrornatus – newportensis* zone in the Anglo-Welsh Basin, based on the incoming of *Streelispora newportensis*. Likewise in Libya, Rubinstein and Steemans (2002) reported spores comparable to the *micrornatus – newportensis* zone from the upper Alternances Argilo-greseuse Formation, including *Chelinospora rettorida*.

Bulgaria and Romania (fig. 20, 14) were positioned on the northern edge of Gondwana, forming part of the Moesian platform. Steemans and Lakova (2004) described miospores from marine assemblages of the Kalarashi Formation in Bulgaria. The lowermost samples were assigned to the Siα interval zone/ middle *micrornatus – newportensis* subzone based on the presence of *Streelispora newportensis*, *Emphanisporites micrornatus* var. *micrornatus* and *E. micrornatus* var. *sinuosus*. Thus, the lowermost assemblages of the Kalarashi Formation correlate well with the middle *micrornatus – newportensis* subzone assemblages of the Anglo-Welsh Basin, although the absence of *E. micrornatus* var. *sinuosus*

in the latter may suggest that the lowermost Kalarashi Formation is slightly younger than the middle *micrornatus – newportensis* material studied here. Likewise, in the Romanian Chilia borehole (Steemans, 1989) key zonal spores similar to those of Bulgaria were observed (indicating an Siα interval zone/ middle *micrornatus – newportensis* subzone) alongside, *inter alia*, *Aneurospora isidori, Leonispora argovejo* and *Apiculiretusispora spicula*. The former two are reported from the middle *micrornatus – newportensis* Anglo-Welsh Basin assemblages studies here, although *Apiculiretusispora spicula* is absent from the stratigraphically higher assemblages in the Welsh Borderlands.

Southern Gondwana

Several sites have been attributed to the Lower Devonian in South America (fig. 20: 12, 13), although many of these are slightly younger than the assemblages reported from the Anglo-Welsh Basin in this work, appearing in the upper middle *micrornatus – newportensis* zone (e.g. Melo and Loboziak, 2003). Rubenstein et al. (2005) reported spore assemblages from the Furnas Formation in the Parana basin of Southern Brazil (fig. 20: 12), which they related to the Early Lochkovian based on the occurrence of *Dictyotriletes emsiensis*, amongst others. Steemans et al. (2008) reported an earliest Devonian assemblage from the Urubu river in Brazil, yielding *Aneurospora isidori*, *Grandispora* sp. A, and related to assemblage to that described from the Furnas Formation in Brazil. In both cases, whilst the assemblages are assignable to the early Lochkovian, they are considered no older than the Si interval zone / middle MN oppel zone (Streel et al., 1987) and are hence younger than the Anglo-Welsh basin assemblages studied here. Garcia-Muro et al. (2014) report the Silurian - Devonian boundary from Argentine Precodillera (fig. 20: 13), based on the first occurrence of possible cf. *Streelispora newportensis*, amongst other species, from the upper Los Espejos Formation. Whilst the assemblage is not diagnostic of the *micrornatus – newportensis* zone, the occurrence of cf. *S. newportensis* may allow correlations between the *micrornatus – newportensis* assemblages of Gondwana and Euramerica, but the lack of other diagnostic species makes the correlations tentative. Likewise, below the first occurrence of cf. *S. newportensis*, no correlation can be made with earliest Devonian assemblages of

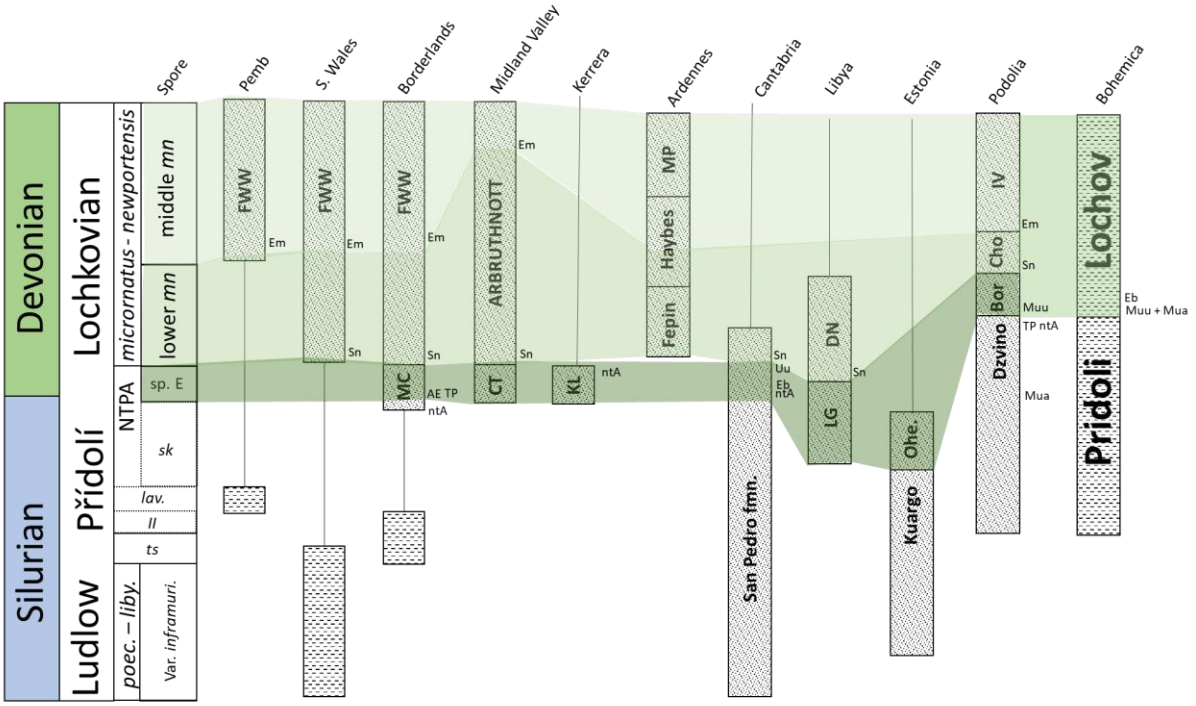

Figure III-21: Schematic diagram illustrating corellation of Lochkovian spore assemblages across selected localties in Euramerica and Northern Gondwana with the type section at Klonk. See text for details. Modified from Richardson et al. (1981).

the *Apiculiretusispora sceacga* zone. As with Přídolían assemblages, it is likely that the vast geographic distances between these South American sites and the Anglo-Welsh Basin limit the occurrence of 'bridge taxa' between the localities.

International correlation with the Silurian - Devonian boundary and the role of *Aneurospora*

Work assessing the phytogeography of spore assemblages from Silurian – Devonian assemblages has raised some caveats regarding international correlations in terms of assemblage composition and first appearances of species. As noted above, there is evidence that some key species, such as *Aneurospora* spp. and *Synorisporites tripapillatus* occur earlier in Gondwana than elsewhere before radiating globally (Breuer et al., 2017). While Richardson and McGregor (1986) posited that these diachronous appearances for many key taxa are essentially simultaneous in terms of geological time, for some taxa there is a more significant difference in appearance, especially between Gondwana and Laurussia. This may be due to the dispersal rate of parent plants, or due to sampling difficulties precluding direct assessment of fossil evidence. In the Anglo-Welsh Basin, this problem may be resolved with further sampling of the mid Přídolí gap.

The type section for the Silurian – Devonian boundary is located in Klonk, Czech Republic, in a deep marine succession. The onset of the Devonian is indicated by the FAD of two variants of the graptolite *Uncinatograptus uniformis*, var. *uniformis* and var. *augustidiens.* A key chitinozoans, *Eisenackitina bohemica*, occurs also, but the section is absent of fish, terrestrial spores and acritarchs. Meanwhile, graptolites and chitinozoans are absent in the terrestrial sequences straddling the Silurian – Devonian boundary in the Anglo-Welsh Basin, which causes major problems for correlations between southern Britain and Klonk. Previous workers have used a 'step-wise' correlation between the two areas in order to identify co-occurrences amongst key taxa in both basins, such as between graptolites and fish (e.g. Richardson et al., 1981, 1984; Edwards and Richardson, 2004). Most sections where the Silurian – Devonian boundary occurs do not exhibit a useful combination of these key taxa (e.g. Richardson and Lister, 1969; Richardson and Ioannides, 1973; Richardson et al. 1984; Al-Ameri, 1980; Arkangelskaya, 1980; Streel et al., 1980; Steemans, 1989; Edwards and Richardson, 2004), or indeed distinctive taxa useful for stratigraphic determination (e.g. Richardson et al, 1984). Nonetheless, by comparing spore + chitinozoan assemblages in Cantabria (Richardson et al., 2001) and then comparing Cantabrian assemblages with a Ukrainian section yielding spores + chitinozoans + fish + graptolites, correlatives were able to be made across global assemblages. Importantly, the Ukrainian section demonstrated that the appearance of *U. uniformis* var. *uniformis* is coincident with *T. pagei*, making the latter a useful indicator of the Devonian, especially as it occurs in the Anglo-Welsh Basin (Turner, 1973). Thus, the challenge is to align a spore assemblage and / or a key spore species with *T. pagei* in the Anglo-Welsh Basin in order to define the Silurian – Devonian boundary with spores.

Richardson et al. (2001) observed the key early Devonian chitinozoans *A. chlupaci* and *E. bohemica* below the *micrornatus – newportensis* zone, alongside what was then considered as the first appearance of *Aneurospora* in Cantabria. From this, Richardson et al. (2001) suggested that the '*Aneurospora* sp. Subzone' of the Cantabrian EC zone was Devonian, and that non-tripapillate *Aneurospora* were promising candidates for indicating the onset of the Devonian. The putative '*Aneurospora'* zone between the MN and Silurian – Devonian boundary was recorded widely, including in Ukraine (Richardson et al., 1984; 2000, Archangelskaya, 1980) and the Anglo-Welsh Basin (Edwards and Richardson, 2004). However, later work by Rubinstein and Steemans (2002) and Breuer et al. (2017) in Libya and Saudi Arabia recovered *Aneurospora* from pre-Devonian materials. In Libya, the non-tripapillate species *Aneurospora richardsonii* is reported from just above the base of the *elegans – cantabrica* zone in the mid Přídolí, just above the *Hemisphaerica* zone. The latter biozone is correlated to Higg's (2022) *lavidensis* zone from the Anglo-Welsh Basin (Pembrokeshire), from which no *Aneurospora* have been identified. In Libya, Rubenstein and Steemans (2002) reported two species of non-tripapillate *Aneurospora* species, *A.* sp. 1 and *A.* sp. 2, from the *tripapillatus spicula* and

'*Apiculiretusispora* sp. E' zones, respectively, reinforcing the early occurrence of the genus in Gondwana, and Steemans et al. (2008) posited that *Aneurospora* was not a suitable indicator of the Silurian-Devonian boundary. In light of the reports of *Aneurospora* species from well below the Silurian – Devonian boundary in Gondwana, while currently equivocal it is perhaps not too great a leap of the imagination to posit that *Aneurospora* species may have occurred earlier in Euramerica than currently observed. Indeed, the recovery of *Aneurospora* from 6 m below the Silurian – Devonian boundary in the M50 section indicates this. However, this remains tentative because of the narrow stratigraphic gap between the occurrence of *Aneurospora* and the Silurian – Devonian boundary, combined with the current inability to elucidate the FAD of the non-tripapillate *Aneurospora* species because of the major stratigraphic gap in the Anglo-Welsh Basin. Nonetheless, *Aneurospora* species are not considered indicative of the onset of the Devonian here, even if they occur closer to the Silurian – Devonian boundary in Euramerica than they do in Gondwana.

10. Conclusions

- Over 100 species of cryptospores and trilete spores in over 30 genera have been recovered from the late Silurian – Early Devonian (Ludlow – Lochkovian) Anglo-Welsh Basin sequence. Counts demonstrate that a considerable increase in species richness and morphological diversity occurs, principally amongst trilete spores but also amongst cryptospores at the onset of the Lochkovian. Trilete spores show the greatest increase in species and morphological diversity, but there are considerable changes amongst certain cryptospore genera. A gradual loss of marine palynomorphs occurs with the assemblages being entirely terrestrial by the late Přídolí, although sporadic brackish water incursions result in rare acritarchs in the Ammons Hill assemblage.

- Study of the spore assemblages around the Silurian – Devonian boundary (the *Apiculiretusispora* sp. E (Edwards and Richardson, 2004) zone) demonstrated a distinct assemblage of non-tripapillate *Aneurospora* and *Apiculiretusispora* species, which occurs before the lower *micrornatus* – *newportensis* subzone (Edwards and Richardson, 2004). *Aneurospora sheafensis* sp. nov., *Aneurospora kensingtonii* sp. nov., *Emphanisporites corralinus* sp. nov. and *Apiculiretusispora sceacga* sp. nov. define the non-tripapillate *Aneurospora* spp. assemblage biozone, which straddles the Silurian – Devonian boundary and terminates at the lower *micrornatus* – *newportensis* biozone. The inception of this zone is unclear because of the mid – late Přídolí sampling gap, but it is sufficiently different in species composition from the gap-preceding *lavidensis* biozone (mid Přídolí) (Higgs, 2022) to warrant distinction. The non-tripapillate *Aneurospora* spp. zone can be subdivided into the preliminary *Aneurospora sheafensis* assemblage subzone and the *Apiculiretusispora sceacga* assemblage subzone. The latter initiates with the FAD of *Ap. Sceacga*, which closely corresponds to the FAD of *Turina pagei*.

- Regional and global correlation is facilitated by the established and preliminary biostratigraphy of the basin (Richardson et al., 1981, 1985; Richardson and McGregor, 1986; Richardson and Edwards, 1989; Burgess and Richardson, 1995). Regional biostratigraphy is generally very good, although some problems are presented by the diachroneity of the Chapel Point Limestone (Morris et al., 2011a). International biostratigraphic correlation is hindered by palynological provincialization and the vast geographical distances, in addition to an occasional lack of independent dating of sequences

Plates

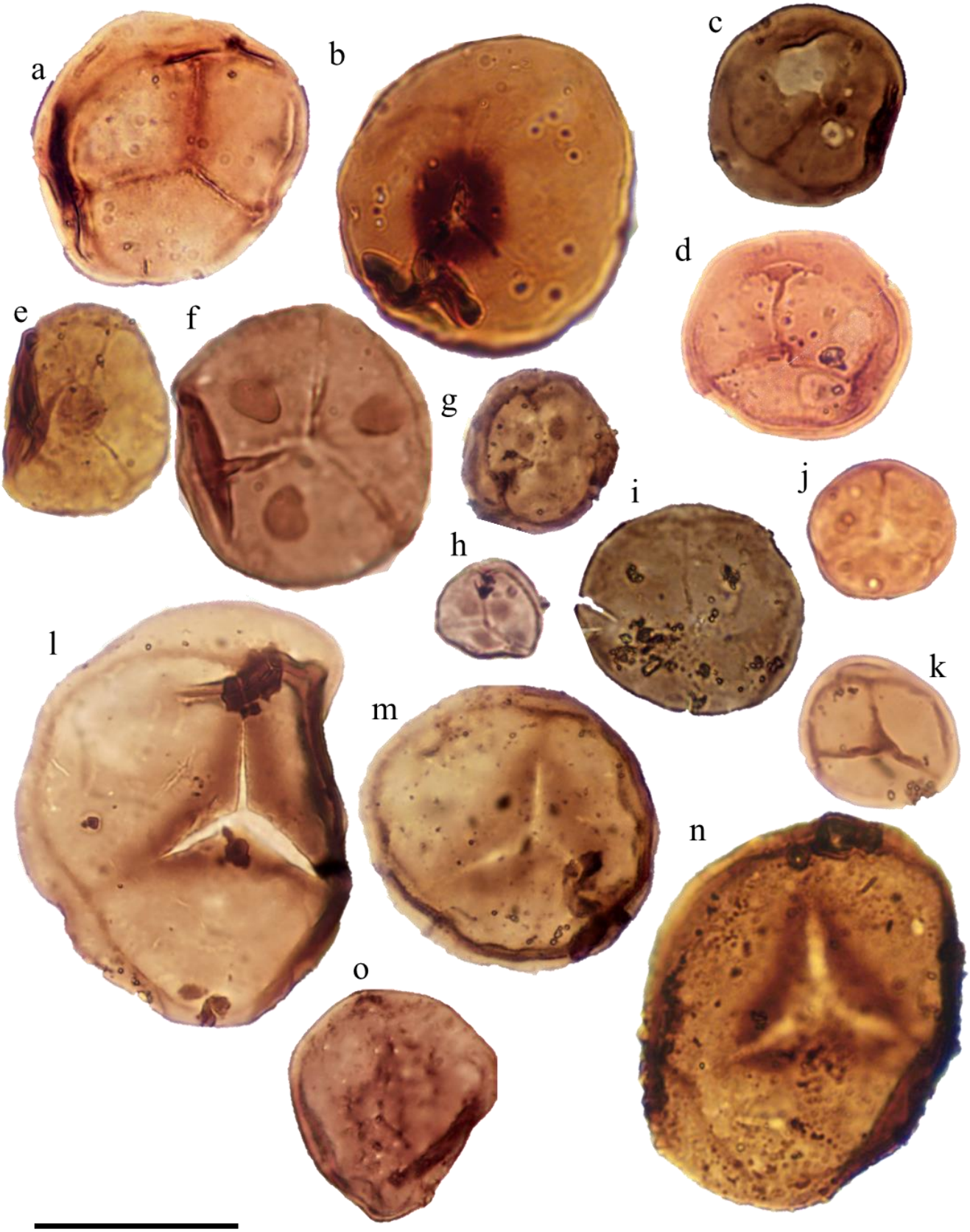
a
b
c
d
e
f
g
h
i
j
k
l
m
n
o

Plate I

a - b *Retusotriletes dittonensis;* **a**: *R. dittonensis,* slightly tipped. Slide: 19M5001.3, E.F. no. U21-1, Freshwater West Formation, Ross-Tewkesbury Spur (M50) motorway, Hereford and Worcester. **b:** *R. dittonensis*; note distinct apical thickening, slide 19M5001.3, E.F. no. T23, Freshwater West Formation, Ross – Tewkesbury Spur Motorway (M50), Hereford and Worcester

c: *R.* cf. *dittonensis;*

d: *R. fraudator* showing lips and y-ray thickenings. Slide 19M5001.3, E.F. no. N21-3, Freshwater West Formation, Ross – Tewkesbury Spur Motorway (M50), Hereford and Worcester.

e: *R.* cf. *goensis,* note circular apical thickening. M50-3(2)-1, E.F. no. H30. Moor Cliffs Formation, Ross – Tewkesbury Spur Motorway (M50), Hereford and Worcester;

f: *R. maculatus,* slide GB/21/5-1, E.F. no. C37-2, Freshwater West Formation, Gardeners Bank, Shropshire;

g – h: *R.* cf. *maculatus;* **g:** slide M50-12-1, E.F. no. T27-3, Freshwater West Formation, Ross – Tewkesbury Spur Motorway (M50), Hereford and Worcester. **h:** slide M50-5G-6, E.F. no. K26, Freshwater West Formation, Ross – Tewkesbury Spur Motorway (M50), Hereford and Worcester.

i – j: *R. minor;* **i:** *R. minor,* polar compression, note near equatorial divergence of curvaturae perfectae. Slide 19M50-16.1, E.F. no. T25-3, Freshwater West Formation, Ross-Tewkesbury Spur (M50) motorway, Hereford and Worcester; **j:** *R. minor,* slightly tipped. Note near equatorial curvaturae perfectae. Slide M50-10-1, E.F. no. C32-3, Freshwater West Formation, Ross-Tewkesbury Spur (M50) motorway, Hereford and Worcester;

k: *R.* cf. *minor,* note the lips, differentiating the specimen from k and l. Slide M50-5E-2, E.F. no. T31, Freshwater West Formation, Ross-Tewkesbury Spur (M50) motorway, Hereford and Worcester;

l: *R. triangulatus,* slightly folded specimen, showing well developed curvaturae perfectae and distinct triangular apical thickening. Slide M50-85-2F-5, E.F. no. D23-1, Moor Cliffs Formation, Ross – Tewkesbury Spur Motorway (M50), Hereford and Worcester.

m: *R.* cf. *triangulatus,* note smaller size, slide: M50-85-2C-6, E.F. no. G17-2, Moor Cliffs Formation, Ross – Tewkesbury Spur Motorway (M50), Hereford and Worcester.

n: *R.* sp. A Wellman et al., Slide M50-3(2)-1, E.F. no. C38-3, Moor Cliffs Formation, Ross – Tewkesbury Spur Motorway (M50), Hereford and Worcester.

o: *R.* sp. A Burgess and Richardson 1995. Slide USK/21/2, E.F. no. S25, Downton Castle Sandstone Formation, Usk-1 Borehole, South Wales.

Scale bar 30μm.

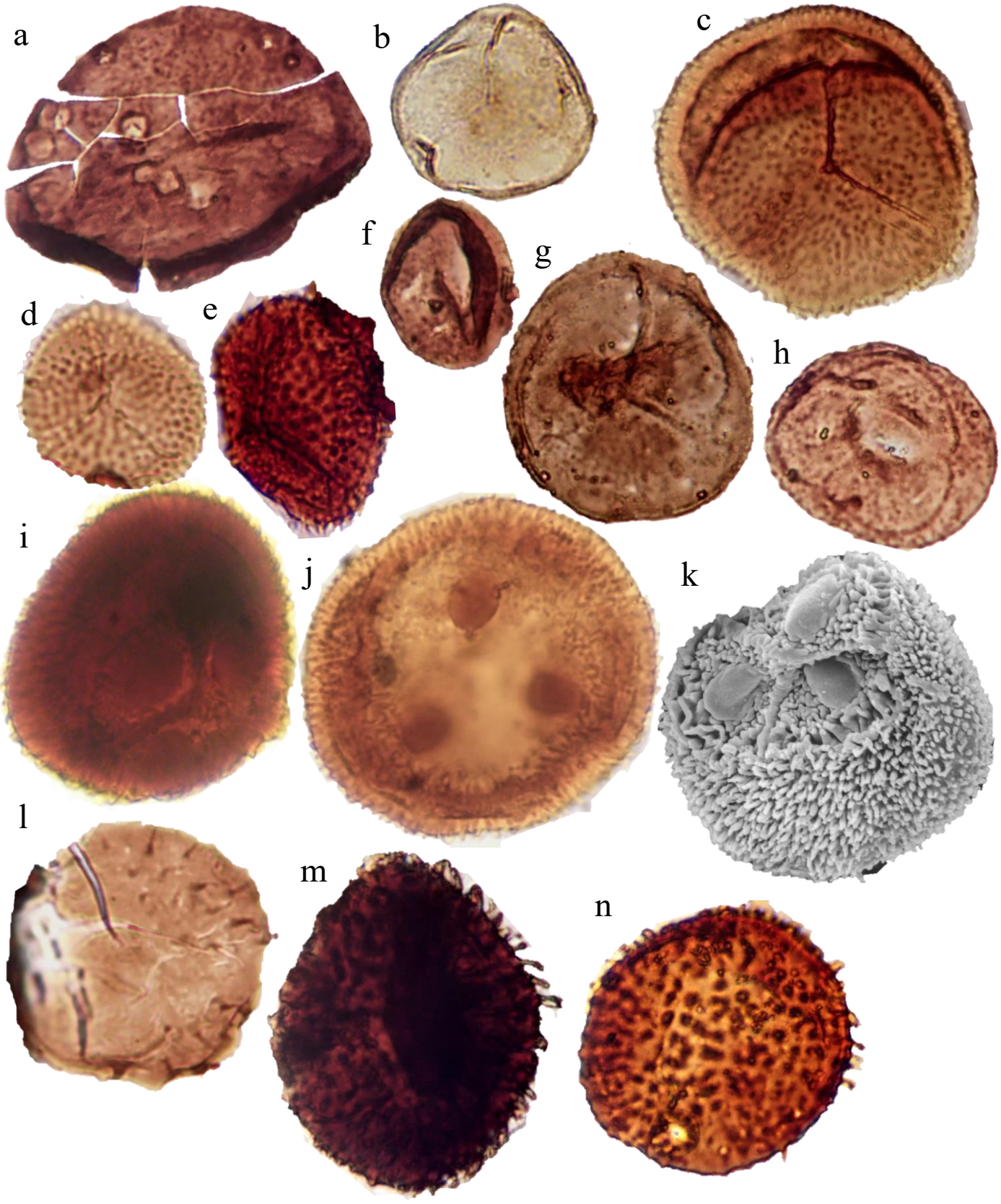
a
b
c
f
g
d
e
h
i
j
k
l
m
n

Plate II:

a: *Apiculiretusispora asperata*. Slide RU/21/3, E.F. no. E28. Downton Castle Sandstone formation. Rumney Borehole, Rumney, South Wales.

b: *Apiculiretusispora microconus*, slide 19M5026.1, E.F. no. V28-1, , Freshwater West Formation, Ross – Tewkesbury Spur Motorway (M50), Hereford and Worcester.

c: *A. spicula*, showing curvaturae perfectae and distinct triradiate mark, slide 19HD5-1, E.F. no. B36, Freshwater West Formation, North Brown Clee Hill, Shropshire.

d: *A.* cf. *spicula*, Showing dense, relatively regular spines, slide 19GB-5-1, E.F. no. S32, Freshwater West Formation, Cleobury Mortimer, Shropshire.

e: *A. synorea*, slide 19M5028.1, E.F. no. O25, Freshwater West Formation, Ross – Tewkesbury Spur Motorway (M50), Hereford and Worcester.

f: *A.* sp. A Burgess and Richardson 1995, slide RU/21/1, E.F. no. H25-1, Downton Castle Sandstone formation. Rumney Borehole, Rumney, South Wales.

g: *A.* sp. B Burgess and Richardson 1995, slide USK/21/1, E.F. no. O27-2, Downton Castle Sandstone formation, Usk-1 borehole, Usk, South Wales.

h: *A.* sp. C Richardson and Lister 1969, slide 19DE98-1, E.F. no. H49, Freshwater West Formation, Ross – Tewkesbury Spur Motorway (M50), Hereford and Worcester.

i - k: i: *A. sceacga* showing a triangular amb, slide M50/85/2C-1, E.F. no. N30-4, Moor Cliffs Formation, Ross – Tewkesbury Spur Motorway (M50), Hereford and Worcester; **j:** Showing a circular amb, slide M50/85/2D-3, E.F., no. M13-2, Moor Cliffs Formation, Ross – Tewkesbury Spur Motorway (M50), Hereford and Worcester; **k :** *Apiculiretusispora sceacga*; SEM image, x2K. Sample M50/85/2C, Moor Cliffs Formation, Ross – Tewkesbury Spur Motorway (M50), Hereford and Worcester.

l – m: *Dibolisporites* sp. 1*;* **l:** showing a circular amb with a mixture of stout, bulbous spines, slide 19M5027.2, E.F. no. K48-3, Freshwater West Formation, Ross – Tewkesbury Spur Motorway (M50), Hereford and Worcester; **m:** showing elongate, bulbous elements, slide M505C-3, E.F. no. W21-1, Freshwater West Formation, Ross – Tewkesbury Spur Motorway (M50), Hereford and Worcester.

n*: D.* sp. 2, note the sparse, slender spinae, slide 19HD5-1, E.F. no. N32-3, Freshwater West Formation, North Brown Clee Hill, Shropshire.

Scale bar 30µm.

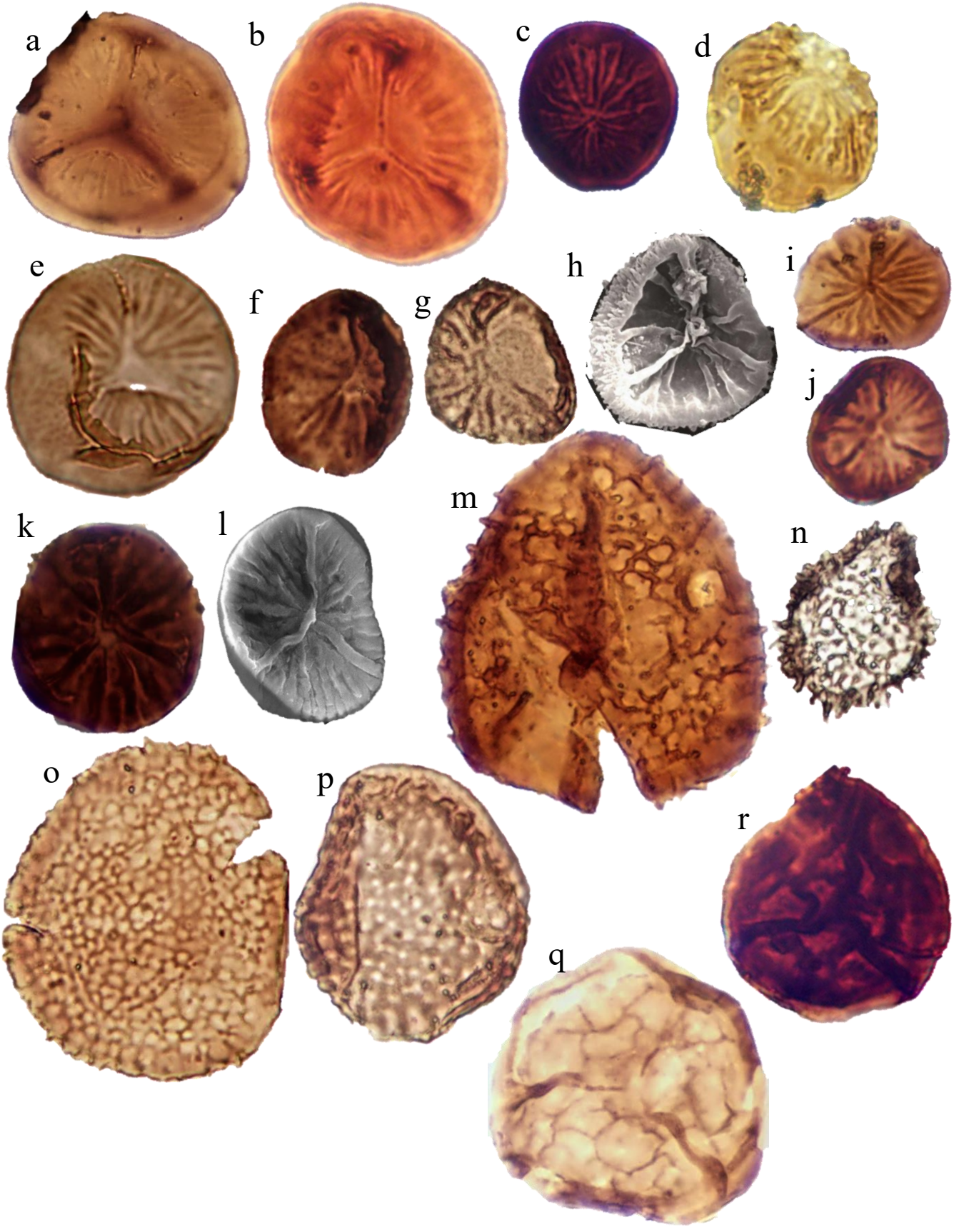
a
b
c
d
e
f
g
h
i
j
k
l
m
n
o
p
q
r

Plate III:

a: *Emphanisporites epicautus*, showing wrinkled proximal face, slide M50-7-1, E.F. no. F47-4, Freshwater West Formation, Ross – Tewkesbury Spur Motorway (M50), Hereford and Worcester.

b: *E.* cf. *epicautus*, showing apical 'bald patch', slide M50-85-2D-1, E.F. no. F38, Moor Cliffs Formation, Ross – Tewkesbury Spur Motorway (M50), Hereford and Worcester.

c– d: *E. corralinus*; **c:** showing circular amb, slide 19M50-24.3, E.F. no. K18-1, Freshwater West Formation, Ross – Tewkesbury Spur Motorway (M50), Hereford and Worcester. **d**: slide M50-4-1, E.F. no. M15-1, Moor Cliffs Formation, Ross – Tewkesbury Spur Motorway (M50), Hereford and Worcester.

e – f: *Emphanisporites micrornatus*; **e:** large specimen, showing interadial muri, slide 19HD2-1, E.F. no. L27-4, Freshwater West Formation, Ross – Tewkesbury Spur Motorway (M50), Hereford and Worcester; **f**: showing robust inter radial muri, slide M50-13-2, E.F. no. T27-4, Freshwater West Formation, Ross – Tewkesbury Spur Motorway (M50), Hereford and Worcester.

g – h: *E.* cf. *micrornatus;* **g:** showing triangular amb, slide M505H-4, E.F. no. W25-3, Freshwater West Formation, Ross – Tewkesbury Spur Motorway (M50), Hereford and Worcester; **h:** SEM micrograph, M50-5G, Freshwater West Formation, Ross – Tewkesbury Spur Motorway (M50), Hereford and Worcester.

i – j: *Emphanisporites neglectus*; **i:** Slide M50-2-6, E.F. no. J50-3, Moor Cliffs Formation, Ross – Tewkesbury Spur Motorway (M50), Hereford and Worcester; **j:** M50-4-1, E.F. no. N25-1, Moor Cliffs Formation, Ross – Tewkesbury Spur Motorway (M50), Hereford and Worcester.

k – l: *Emphanisporites* cf. *rotatus* **k:** larger specimen showing a dark exine with robust lips and interadial muri, slide M50-5H-1, E.F. no. F27-1, Freshwater West Formation, Ross – Tewkesbury Spur Motorway (M50), Hereford and Worcester; **l:** SEM micrograph, 19M5026, Freshwater West Formation, Ross – Tewkesbury Spur Motorway (M50), Hereford and Worcester.

m – o: *Acinosporites salopiensis;* **m:** large specimen, slide M50-7-1, E.F.no. W13, Freshwater West Formation, Ross – Tewkesbury Spur Motorway (M50), Hereford and Worcester; **n:** small specimen showing long spines, slide M50-11-3, E.F. no. D28-3, Freshwater West Formation, Ross – Tewkesbury Spur Motorway (M50), Hereford and Worcester; **o:** showing small lumen, slide GB4-1, E.F. no. V27, Freshwater West Formation, Gardener's Bank, Cleobury Mortimer.

p: *Brochotriletes* sp. 1, slide M50-7-6, E.F. no. O8, Freshwater West Formation, Ross – Tewkesbury Spur Motorway (M50), Hereford and Worcester.

q: *Dictyotriletes williamsii*, showing triradiate mark and wide lumina, slide M50-85-2E-4, E.F. no. R27, Moor Cliffs Formation, Ross – Tewkesbury Spur Motorway (M50), Hereford and Worcester.

r: *D.* sp. A , slide M50-5B-5, E.F. no. T24, Freshwater West Formation, Ross – Tewkesbury Spur Motorway (M50), Hereford and Worcester.

Scale bar 30µm.

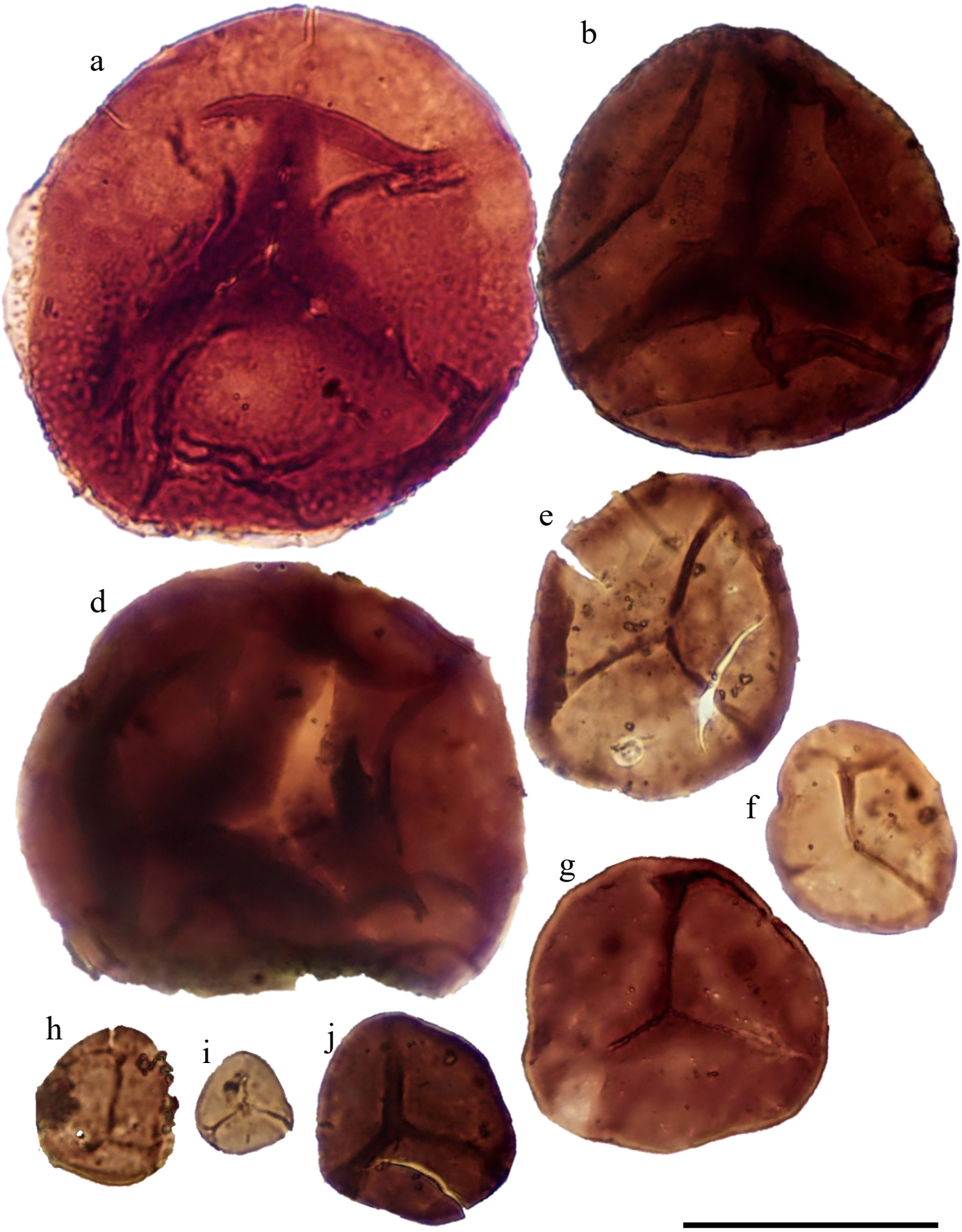
a
b
e
d
f
g
h
i
j

Plate IV:

a: *Perotrilites microbaculatus* var. *microbaculatus* showing fine ornament and loosely adherent perine, slide 19M5025-1, E.F. no. Q26, Freshwater West Formation, Ross – Tewkesbury Spur Motorway (M50), Hereford and Worcester.

b: *Perotrilites microbaculatus* var. *attenuatus*, note tightly adherent perine, slide M50-7-2, E.F. no. O9, Freshwater West Formation, Ross – Tewkesbury Spur Motorway (M50), Hereford and Worcester.

c: *Perotrilites* sp. A M50-5B-2, E.F. no. V23, Freshwater West Formation, Ross – Tewkesbury Spur Motorway (M50), Hereford and Worcester.

d – e*: Ambitisporites avitus – dilutus* complex; **d:** slightly tipped specimen showing equatorial curvaturae perfectae, slide M50-4-6, E.F. no. J28, Moor Cliffs Formation, Ross – Tewkesbury Spur Motorway (M50), Hereford and Worcester **e:** slightly tipped specimen showing equatorial curvaturae perfectae, slide M50-4-6, E.F. no. J28, Moor Cliffs Formation, Ross – Tewkesbury Spur Motorway (M50), Hereford and Worcester.

f: *Ambitisporites eslae,* slide USK/21/3, E.F. no. X26-2, Downton Castle Sandstone formation, Usk-1 borehole, Usk, South Wales.

g: *Ambitisporites tripapillatus*, showing crassitude, slide M50-12-2, E.F. no. G26, Freshwater West Formation, Ross – Tewkesbury Spur Motorway (M50), Hereford and Worcester.

h – i: *Ambitisporites warringtoni;* **h**: showing a triangular amb, slide M50-5G-3, E.F. no. U23-1, Freshwater West Formation, Ross – Tewkesbury Spur Motorway (M50), Hereford and Worcester**; i:** showing curvaturae and narrow lips, slide M50-13-2, E.F. no. R23, Freshwater West Formation, Ross – Tewkesbury Spur Motorway (M50), Hereford and Worcester.

j: *Ambitisporites* sp. A Wellman and Richardson 1996, showing wide lips and dark exine, M50-10-1, E.F. no. T21-1, Freshwater West Formation, Ross – Tewkesbury Spur Motorway (M50), Hereford and Worcester.

Scale bar 30μm.

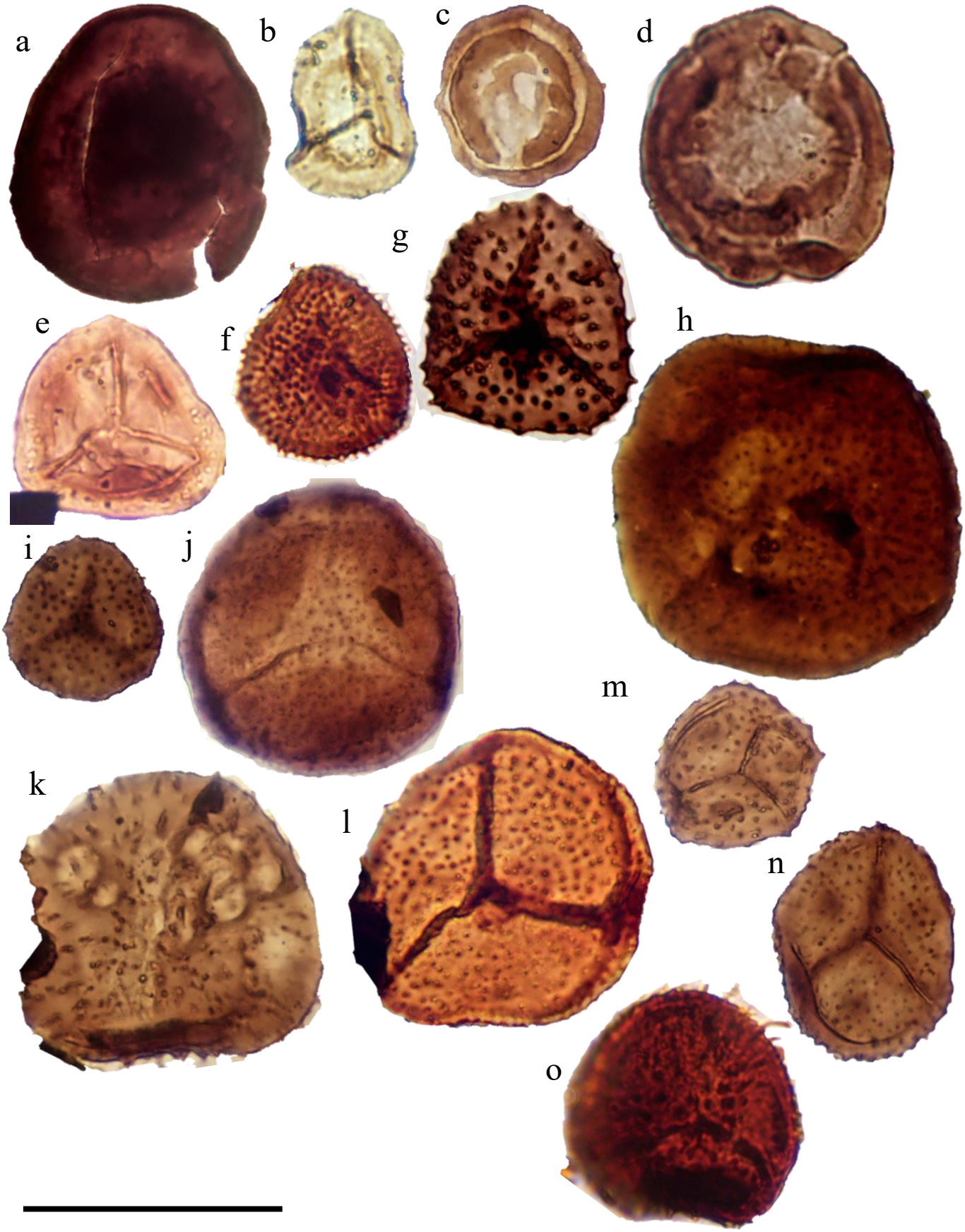
a
b
c
d
e
f
g
h
i
j
k
l
m
n
o

Plate V

a: *Concentricosporites saggitarius*, slide RU/21/1, E.F. no. F30-1, Downton Castle Sandstone formation, Rumney-1 borehole,Rumney, South Wales.

b: *Amicosporites miserabilis*, slide M50-2-2, E.F. no. U38-1, Moor Cliffs Formation, Ross – Tewkesbury Spur Motorway (M50), Hereford and Worcester.

c – d: cf. *Amicosporites* sp.; **c:** small specimen, slide M50-7-1, E.F. no. U4-3, Freshwater West Formation, Ross – Tewkesbury Spur Motorway (M50), Hereford and Worcester; **d:** large specimen, slide M50-7-6, E.F. no. K29, Freshwater West Formation, Ross – Tewkesbury Spur Motorway (M50), Hereford and Worcester.

e: *Leonispora argovejo*, slide 19M5001.3, E.F. no. L20-2, Freshwater West Formation, Ross – Tewkesbury Spur Motorway (M50), Hereford and Worcester

f: *Aneurospora* cf. *geikie*, slide M50-5B-5, E.F. no. F30, Freshwater West Formation, Ross – Tewkesbury Spur Motorway (M50), Hereford and Worcester;

g: *Aneurospora gerreinnei*, slide MPA25252-1, E.F. no. X28, Freshwater West Formation, Ammons Hill section, Shropshire.

h: *Aneurospora goensis*, slide M50-3(2)-1, E.F. no. J25, Moor Cliffs formation, Ross – Tewkesbury Spur Motorway (M50), Hereford and Worcester**.**

i: *Aneurospora isidori* slide M50-12-2, E.F. no. J26-1, Freshwater West Formation, Ross – Tewkesbury Spur Motorway (M50), Hereford and Worcester

j: *Aneurospora kensingtonii*; showing triangular thinning, slide M50-85-2B-2, E.F. no. T37. Moor Cliffs formation, Ross – Tewkesbury Spur Motorway (M50), Hereford and Worcester

k: *Aneurospora richardsonii*, slide M50-7-1, E.F. no. G6-1, Freshwater West Formation, Ross – Tewkesbury Spur Motorway (M50), Hereford and Worcester.

l: *Aneurospora sheafensis***:** slide M50-85-2C-1, E.F. no. V32-4, Moor Cliffs Formation, Ross – Tewkesbury Spur Motorway (M50), Hereford and Worcester.

m – n: *Aneurospora trilabiata*, **m:** showing the parallel folds about the triradiate mark, slide M50-5G-2, E.F. no. W22, Freshwater West Formation, Ross – Tewkesbury Spur Motorway (M50), Hereford and Worcester; **n:** small specimen, slide M50-5F-1, E.F. no. O22-4, Freshwater West Formation, Ross – Tewkesbury Spur Motorway (M50), Hereford and Worcester.

o: *Aneurospora* cf. sp. A, slide 19M5026.3, E.F. no. M29, slide Freshwater West Formation, Ross – Tewkesbury Spur Motorway (M50), Hereford and Worcester.

Scale bar 30μm.

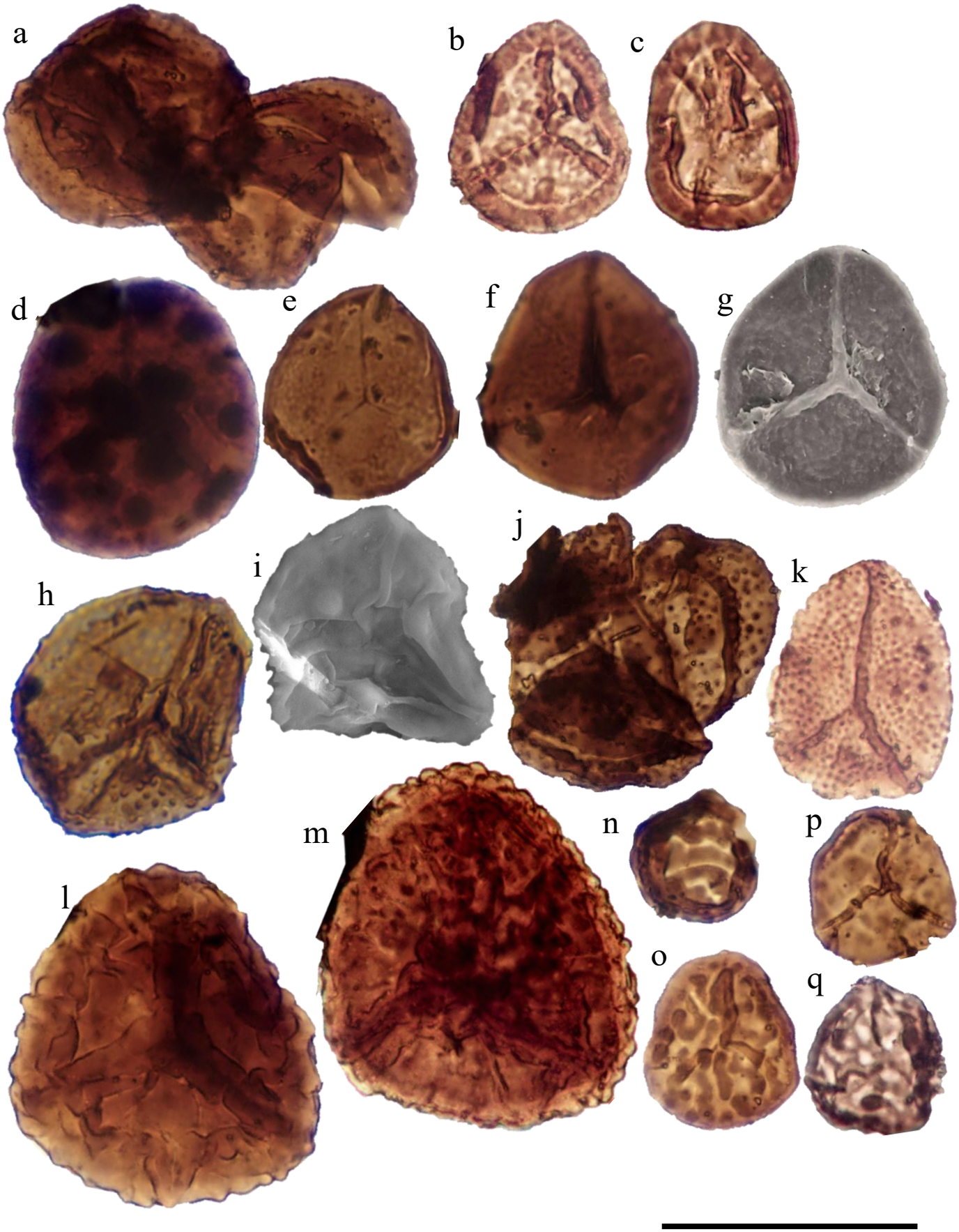
a
b
c
d
e
f
g
h
i
j
k
l
m
n
o
p
q

Plate VI

a: partially dissociated tetrad, showing low coni and interadial papillae and folds, possibly attributable to *Aneurospora trilabiata*, slide M50-5H-1, E.F. no. V20-4, Freshwater West Formation, Ross – Tewkesbury Spur Motorway (M50), Hereford and Worcester.

b – c: *Ibereospora glabella;* **b:** slide M50-5G-6, E.F. no. E29-2, Freshwater West Formation, Ross – Tewkesbury Spur Motorway (M50), Hereford and Worcester; **c:** slide M50-5B-5, E.F. no. P34-4, Freshwater West Formation, Ross – Tewkesbury Spur Motorway (M50), Hereford and Worcester.

d: *Scylaspora downiei*, slide M50-85-2B-2, E.F. no. M5, Freshwater West Formation, Ross – Tewkesbury Spur Motorway (M50), Hereford and Worcester.

e: *Scylaspora* sp. 1, slide M50-5F-3, E.F. no. K27-1, Freshwater West Formation, Ross – Tewkesbury Spur Motorway (M50), Hereford and Worcester;

f – g: *Scylaspora* sp. 2, **f:** slide M50-11-2, E.F. no. Q11, Freshwater West Formation, Ross – Tewkesbury Spur Motorway (M50), Hereford and Worcester; **g:** 084612 SEM micrograph, M50-5D, Freshwater West Formation, Ross – Tewkesbury Spur Motorway (M50), Hereford and Worcester.

h – i: *Streelispora newportensis:* **h:** with dense ornament, 19M5001.1, E.F. no. X23-1, Freshwater West Formation, Ross – Tewkesbury Spur Motorway (M50), Hereford and Worcester; **i:** SEM of proximal face, note folds about the interadial papillae, AB19M5026; **j:** partially dissociated tetrad of *S. newportensis*, M50-12-2, E.F. no. U19-3, Freshwater West Formation, Ross – Tewkesbury Spur Motorway (M50), Hereford and Worcester.

j: *S. granulata* slide M50-5H-6, E.F. no. W22, Freshwater West Formation, Ross – Tewkesbury Spur Motorway (M50), Hereford and Worcester.

k – l: *Synorisporites downtonensis*; **k:** slide M50-12-2, E.F. no. G39-1, Freshwater West Formation, Ross – Tewkesbury Spur Motorway (M50), Hereford and Worcester; **l:** slide MPA25248-1, E.F. no. D47-4, Ammons Hill Section, Shropshire.

m: *Synorisporites* cf. *labeonis*, slide M50-5E-1, E.F. no. V47-2, Freshwater West Formation, Ross – Tewkesbury Spur Motorway (M50), Hereford and Worcester;

n: *Synorisporites* cf. *libyacus*, slide M50-8-1, E.F. no. K26-1, Freshwater West Formation, Ross – Tewkesbury Spur Motorway (M50), Hereford and Worcester.

o - p*: Synorisporites tripapillatus*; **o:** slide M50-5E-1, E.F. no. J29-2, Freshwater West Formation, Ross – Tewkesbury Spur Motorway (M50), Hereford and Worcester; **p:** showing well developed distal ornament, slide M50-12-3, E.F. no. D39-4, Freshwater West Formation, Ross – Tewkesbury Spur Motorway (M50), Hereford and Worcester

Scale bar 30μm.


a
b
c
d
e
f
g
i
j
h
k
l
m
n

Plate VII:

a – b: *Synorisporites verrucatus*; **a:** slide M50-7-1, E.F. no. J18, Freshwater West Formation, Ross – Tewkesbury Spur Motorway (M50), Hereford and Worcester; **b:** slide m50-7-1, E.F. no. K19-3, Freshwater West Formation, Ross – Tewkesbury Spur Motorway (M50), Hereford and Worcester.

c: *Synorisporites* sp. B, slide M50-12-3, E.F. no. W27, Freshwater West Formation, Ross – Tewkesbury Spur Motorway (M50), Hereford and Worcester.

d: *Insolisporites bassettii*, slide RU/21/2, E.F. no. J27-4, Downton Castle Sandstone formation, Rumney – 1 borehole, Rumney, South Wales.

e: *I. anchistinus*, slide RU/21/1, E.F. no. S33, Downton Castle Sandstone formation, Rumney – 1 borehole, Rumney, South Wales.

f: *Lophonzotriletes poecilomorphus*, slide M50-7-1, E.F. no. N26, Freshwater West Formation, Ross – Tewkesbury Spur Motorway (M50), Hereford and Worcester.

g: *Lophonzotriletes* cf. sp. A, slide M50-7-6, E.F. no. P8, Freshwater West Formation, Ross – Tewkesbury Spur Motorway (M50), Hereford and Worcester.

h – i: *Archaeozonotriletes chulus* var. *chulus*, **h:** slide M50-85-2C-7, E.F. no. R27, Freshwater West Formation, Ross – Tewkesbury Spur Motorway (M50), Hereford and Worcester. **i:** showing discrete triradiate mark, slide 19M5016.1, E.F. no. W25, Freshwater West Formation, Ross – Tewkesbury Spur Motorway (M50), Hereford and Worcester.

j – k: *Archaeozonotriletes chulus* var. *nanus**; j*:** slide M50-11-1, E.F. no. O33, Freshwater West Formation, Ross – Tewkesbury Spur Motorway (M50), Hereford and Worcester; **k:** SEM micrograph, 19M5026, Freshwater West Formation, Ross – Tewkesbury Spur Motorway (M50), Hereford and Worcester.

l: *Archaeozonotriletes* cf. *chulus* var. *chulus*, showing wide lips and patinate structure, slide 19M5016.1, E.F. no. H18-1, Freshwater West Formation, Ross – Tewkesbury Spur Motorway (M50), Hereford and Worcester.

m: *Cymbosporites dittonensis*, slide MPA25249-1, E.F. no. P27-1, Freshwater West Formation, Ammons Hill Section, Shropshire.

n: *Cymbosporites verrucosus*, showing lips, note the lack of radial 'muri' but rounded distal verrucae. Slide M50-12-2, E.F.no. R30-3, Freshwater West Formation, Ross – Tewkesbury Spur Motorway (M50), Hereford and Worcester.

Scale bar 30µm.

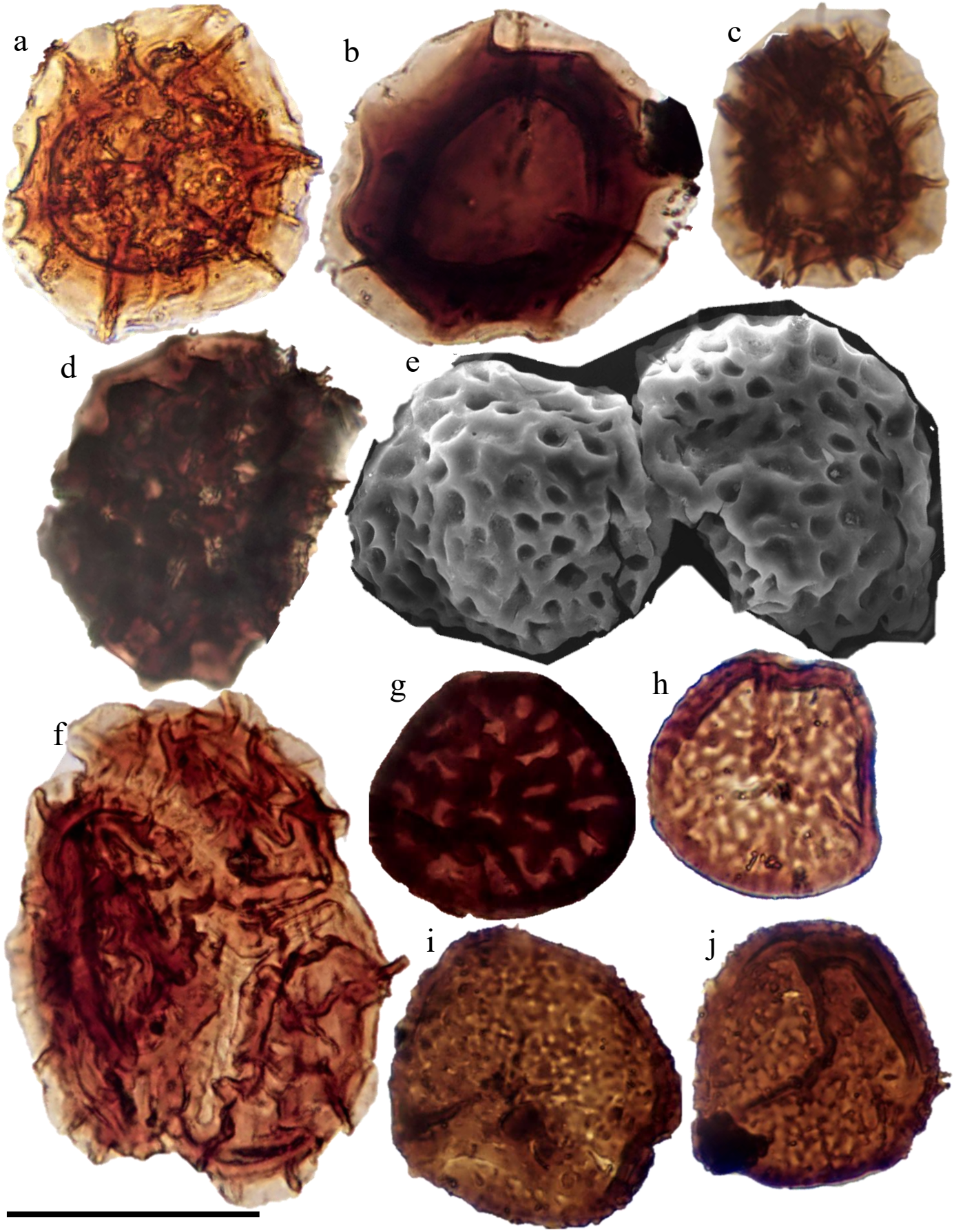
a
b
c
d
e
f
g
h
i
j

Plate VIII

a - c: *Chelinospora cassicula*; **a:** slide 19M5001.3, E.F. no. R23, Freshwater West Formation, Ross – Tewkesbury Spur Motorway (M50), Hereford and Worcester; **b:** slide M50-5C-5, E.F. no. X3, Freshwater West Formation, Ross – Tewkesbury Spur Motorway (M50), Hereford and Worcester; **c:** slide M50-5H-3, E.F. no. G23-3, Freshwater West Formation, Ross – Tewkesbury Spur Motorway (M50), Hereford and Worcester;

d: Dispersed *C. cassicula* tetrad, slide HD4-1, E.F. no. V25-2, Hudwick Dingle, North Brown Clee Hill, Shropshire.

e – f: *Chelinospora* cf. *cantabrica* **e:** dispersed specimen, M50-5H-4, E.F. no. V25-3, Freshwater West Formation, Ross – Tewkesbury Spur Motorway (M50), Hereford and Worcester; **f:** SEM of ?partially dissociated tetrad, 19M5026, Freshwater West Formation, Ross – Tewkesbury Spur Motorway (M50), Hereford and Worcester.

g: *Chelinospora obscura*, slide RU/21/3, E.F. no. G28, Downton Castle Sandstone formation, Rumney-1 borehole, Rumney, South Wales.

h: *Chelinospora retorrida*, slide M50-8-4, E.F. no. L29-2, slide M50-5G-5, E.F. no. O32-4, Freshwater West Formation, Ross – Tewkesbury Spur Motorway (M50), Hereford and Worcester;

i – j: *Chelinospora vermiculata;* **i:** slide M50-5H-1, E.F. no. Q27-1, Freshwater West Formation, Ross – Tewkesbury Spur Motorway (M50), Hereford and Worcester; **j:** slide M50-5B-1, E.F. no. H26-2, Freshwater West Formation, Ross – Tewkesbury Spur Motorway (M50), Hereford and Worcester.

Scale bar 30μm.

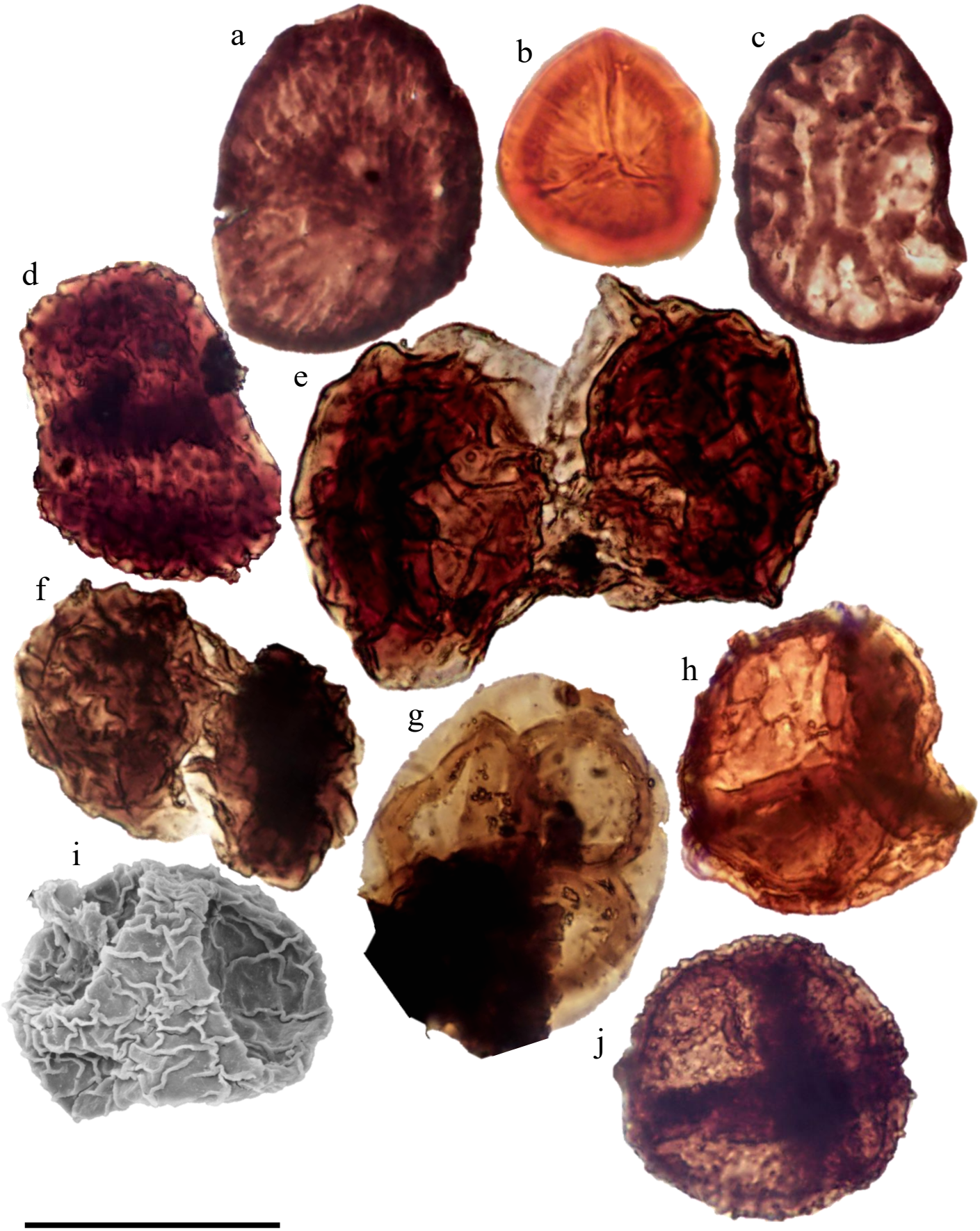
a
b
c
d
e
f
g
h
i
j

Plate IX:

a: *Stellatispora inframurinata* var. *inframurinata*, slide RU/21/3, E.F. no. Q34, Downton Castle Sandstone formation, Rumney-1 borehole, Rumney, South Wales.

b: *Stellatispora inframurinata cf.* var. *inframurinata***,** slide M50-85-2D-1, E.F. no. F25-3, Moor Cliffs Formation, Ross – Tewkesbury Spur Motorway (M50), Hereford and Worcester.

c: *Stellatispora inframurinata* var. *cambrensis* slide RU/21/3, E.F. no. P24-4, Downton Castle Sandstone formation, Rumney-1 borehole, Rumney, South Wales.

d: *Segestrespora* sp. 1, slide M50-11-3, E.F. no. V29-2, Freshwater West Formation, Ross – Tewkesbury Spur Motorway (M50), Hereford and Worcester.

e - f: *Abditusdyadus laevigata;* **e:** slide 19M5002.1, E.F. no. G24, Freshwater West Formation, Ross – Tewkesbury Spur Motorway (M50), Hereford and Worcester; **f:** slide M50-5H-4, E.F. no. H23-3, Freshwater West Formation, Ross – Tewkesbury Spur Motorway (M50), Hereford and Worcester.

g: *Velatitetras laevigata*, slide M50-5-1, E.F. no. F26.-2, Freshwater West Formation, Ross – Tewkesbury Spur Motorway (M50), Hereford and Worcester.

h – i: *Velatitetras reticulata;* **h:** slide M50-85-2C-1, E.F. no. R19, Moor Cliffs Formation, Ross – Tewkesbury Spur Motorway (M50), Hereford and Worcester; **i:** SEM micrograph, 107539, M50/85/2C, Moor Cliffs Formation, Ross – Tewkesbury Spur Motorway (M50), Hereford and Worcester.

j: *Velatitetras anatoliensis*; showing cones and grana, slide M50-5E-3, E.F. no. H22-4, Freshwater West Formation, Ross – Tewkesbury Spur Motorway (M50), Hereford and Worcester.

Scale bar 30μm.

.

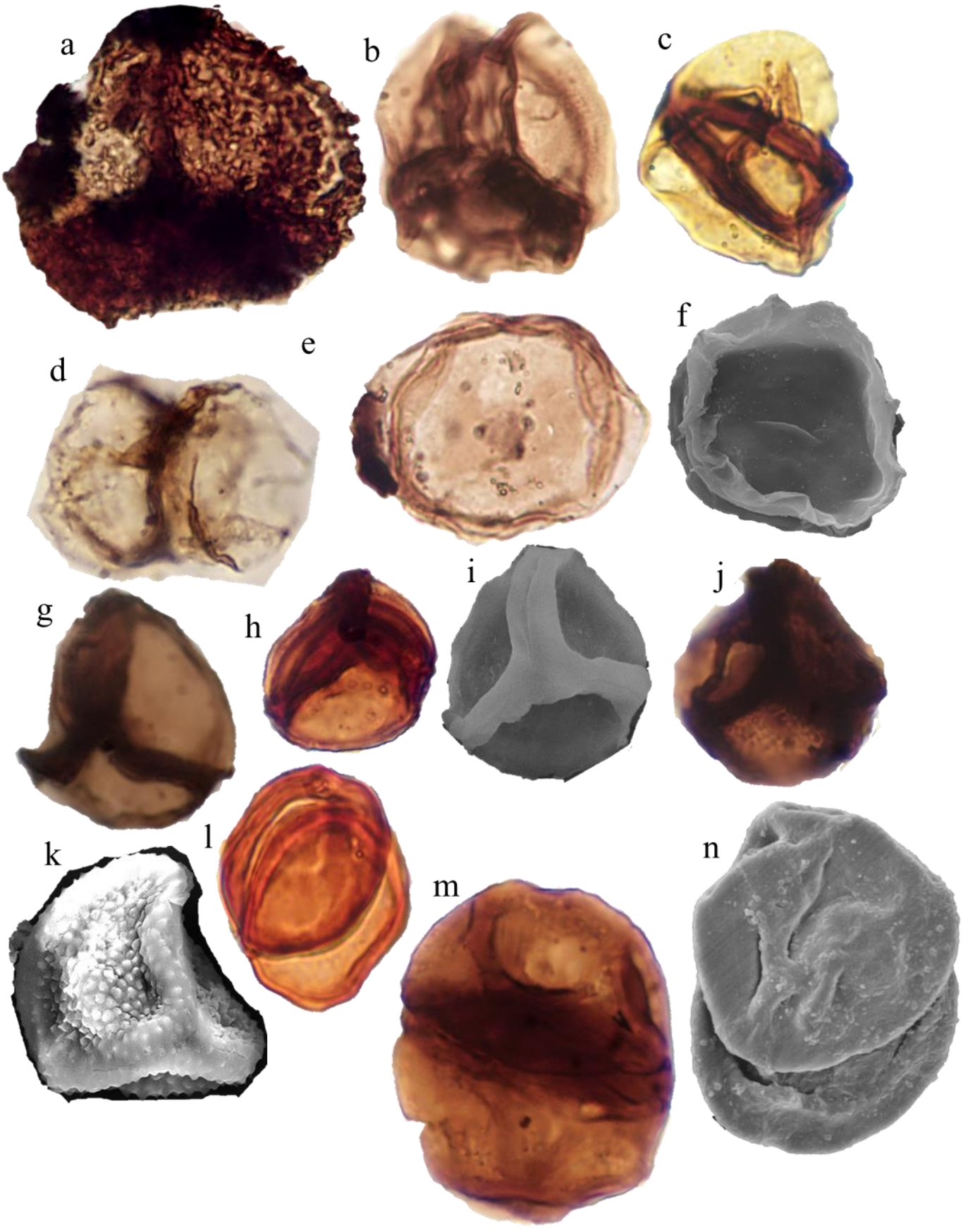
a
b
c
d
e
f
g
h
i
j
k
l
m
n

Plate X:

a: *Velatitetras anatoliensis*; showing spines, slide M50-5G-5, E.F. no. B34, Freshwater West Formation, Ross – Tewkesbury Spur Motorway (M50), Hereford and Worcester.

b: *Cheliotetras caledonica;* slide 19M5026.1, E.F. no. U26-3, Freshwater West Formation, Ross – Tewkesbury Spur Motorway (M50), Hereford and Worcester;

c: *Pseudodyadospora laevigata*, slide M50-3(2)-1, Moor Cliffs Formation, Ross – Tewkesbury Spur Motorway (M50), Hereford and Worcester.

d – f: *Pseudodyadospora petasus;* **d:** lateral compression, slide M50-5C-5, E.F. no. T14, Freshwater West Formation, Ross – Tewkesbury Spur Motorway (M50), Hereford and Worcester; **e:** proximal view, M50-5C-5, E.F. no. S25, Freshwater West Formation, Ross – Tewkesbury Spur Motorway (M50), Hereford and Worcester; **f:** SEM micrograph, polar compression, 19M5019, Moor Cliffs Formation, Ross – Tewkesbury Spur Motorway (M50), Hereford and Worcester.

g – i: *Tetrahedraletes medinensis*, **g:** slide M50-85-2D-5, E.F. no. S47-2, Moor Cliffs Formation, Ross – Tewkesbury Spur Motorway (M50), Hereford and Worcester; **h:** small specimen, slide 19M5016.1, E.F. no. N19, Moor Cliffs Formation, Ross – Tewkesbury Spur Motorway (M50), Hereford and Worcester; **i:** showing suture along crassitude, SEM micrograph, 19M5019, Moor Cliffs Formation, Ross – Tewkesbury Spur Motorway (M50), Hereford and Worcester.

j – k*:* *Acontotetras inconspicuis*: **j:** slide M50-85-2D-5, E.F. no. U19, Moor Cliffs Formation, Ross – Tewkesbury Spur Motorway (M50), Hereford and Worcester; **k:** SEM micrograph, 19M5026, Freshwater West Formation, Ross – Tewkesbury Spur Motorway (M50), Hereford and Worcester.

l – n: *Dyadospora murusdensa – murusattenuata* complex; **l:** M50-85-2C-4, E.F. no. O6-4, Moor Cliffs Formation, Ross – Tewkesbury Spur Motorway (M50), Hereford and Worcester; **m:** associated specimen, note suture on crassitude, slide M50-7-1, E.F. no. G19-3, Freshwater West Formation, Ross – Tewkesbury Spur Motorway (M50), Hereford and Worcester; **n:** SEM micrograph, 108496 showing some extra-exosporal material, M50-85-2C, Moor Cliffs Formation, Ross – Tewkesbury Spur Motorway (M50), Hereford and Worcester.

Scale bar 30μm.

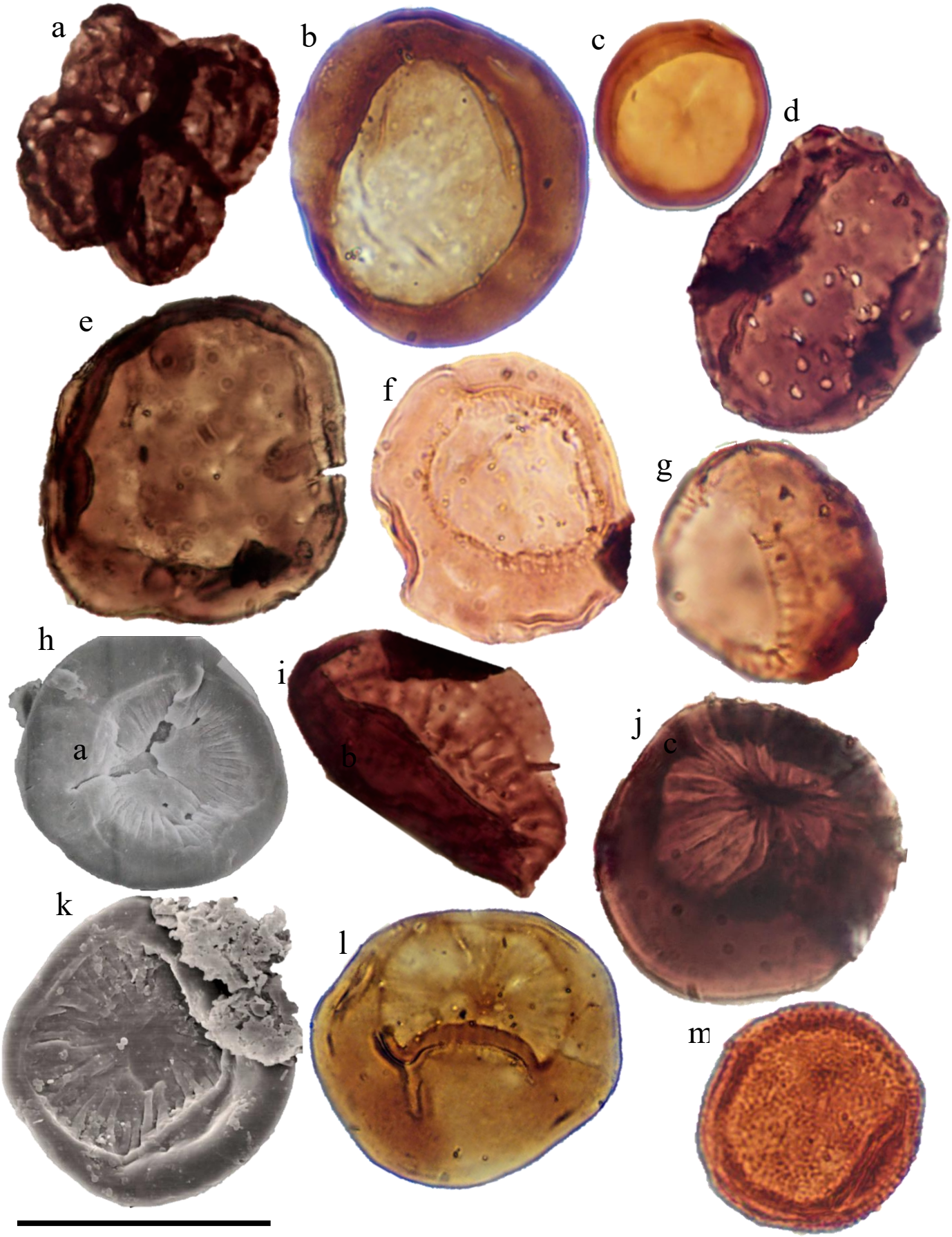

11

Plate XI

a: *Rimosotetras problematica*, slide RU/21/2, E.F. no. R26, Downton Castle Sandstone formation, Rumney-1 borehole, Rumney, South Wales.

b – d: *Laevolancis divellomedium – plicata;* **b:** large specimen, slide 19M5001.3, E.F. no. F51, Freshwater West Formation, Ross – Tewkesbury Spur Motorway (M50), Hereford and Worcester; **c:** small specimen, M50-4-1, E.F. no. E20-3, Moor Cliffs Formation, Ross – Tewkesbury Spur Motorway (M50), Hereford and Worcester; **d:** specimen with bevelled pits. Slide M50-5G-5, E.F. no. L31-1, Freshwater West Formation, Ross – Tewkesbury Spur Motorway (M50), Hereford and Worcester;

e: *Laevolancis* sp.1, showing three interadial papillae, slide M50-7-4, E.F. no. D26, Freshwater West Formation, Ross – Tewkesbury Spur Motorway (M50), Hereford and Worcester.

f – h: *Artemopyra brevicosta*, **f:** slide 19M5001.3, E.F. no. Q21-1, Freshwater West Formation, Ross – Tewkesbury Spur Motorway (M50), Hereford and Worcester; **g:** small specimen with inflated proximal face, slide M50-85-2E-1, E.F. no. T11, Moor Cliffs Formation, Ross – Tewkesbury Spur Motorway (M50), Hereford and Worcester; **h:** 088158 SEM micrograph, M50-5G, Freshwater West Formation, Ross – Tewkesbury Spur Motorway (M50), Hereford and Worcester.

i: *Artemopyra* cf. *radiata*, slide USK/21/3, E.F. no. P25-2, Moor Cliffs formation, Formation, Ross – Tewkesbury Spur Motorway (M50), Hereford and Worcester.

j: *Artemopyra recticosta***:** showing robust radial muri, slide M50-8-4, E.F. no. H38, Freshwater West Formation, Ross – Tewkesbury Spur Motorway (M50), Hereford and Worcester.

k: *Artemopyra recticosta***:** 086075 SEM micrograph, M50-5F, Freshwater West Formation, Ross – Tewkesbury Spur Motorway (M50), Hereford and Worcester.

l: *Artemopyra* cf. *inconspicuis*, slide 19M5001.3, E.F. no. S24-3, Freshwater West Formation, Ross – Tewkesbury Spur Motorway (M50), Hereford and Worcester.

m: *Cymbohilates allenii* var. *allenii*; slide 19M5001.3, E.F. no. Q22-3, Freshwater West Formation, Ross – Tewkesbury Spur Motorway (M50), Hereford and Worcester.

Scale bar 30µm.

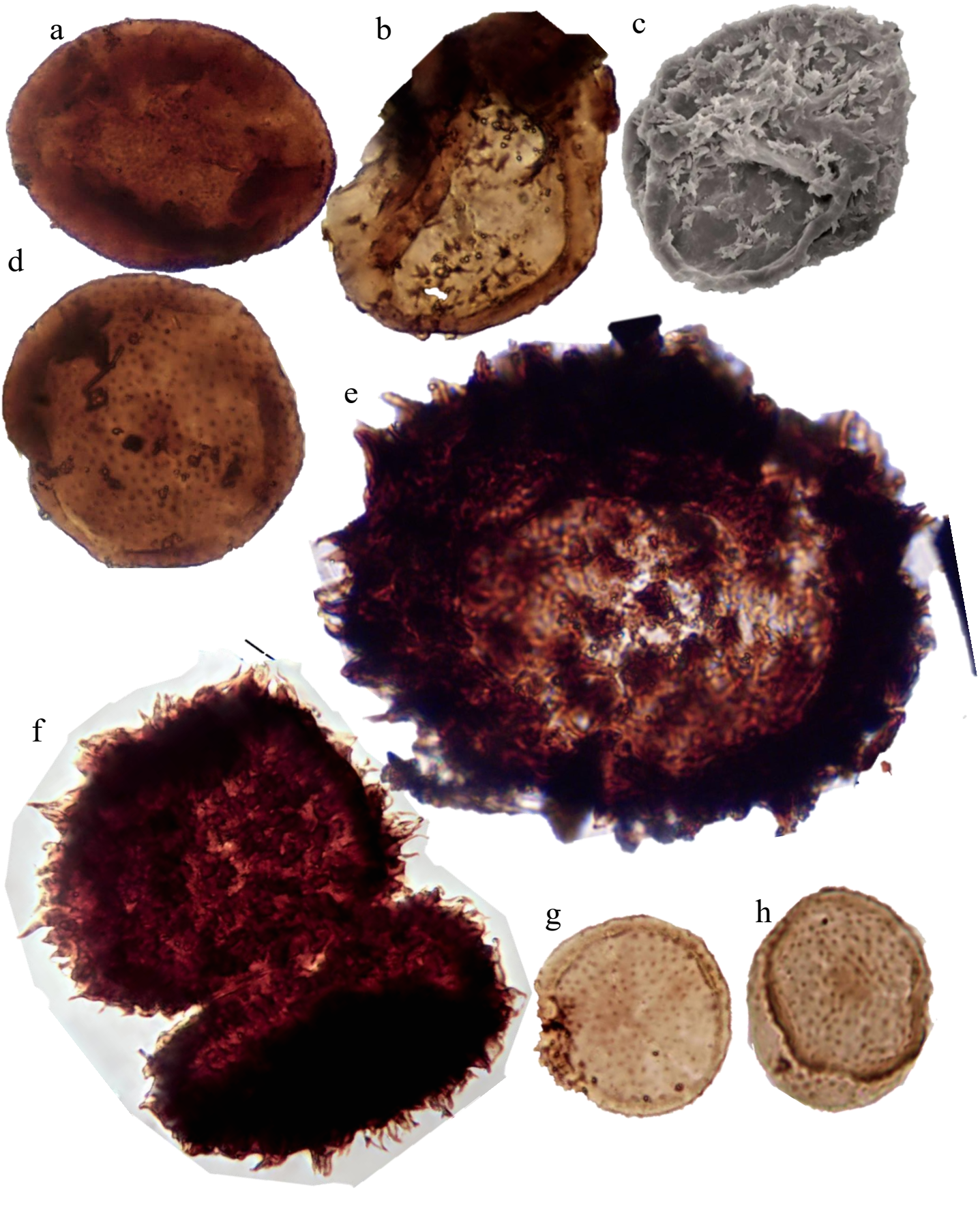
a
b
c
d
e
f
g
h

Plate XII:

a: *Cymbohilates allenii* var. *magnus*, slide M50-11-1, E.F. no. J19-4, Freshwater West Formation, Ross – Tewkesbury Spur Motorway (M50), Hereford and Worcester.

b - c: *Cymbohilates cymosus;* **b:** Slide M50-8-1, E.F. no. R18-2, Freshwater West Formation, Ross – Tewkesbury Spur Motorway (M50), Hereford and Worcester; **c:** SEM micrograph, M505G, Freshwater West Formation, Ross – Tewkesbury Spur Motorway (M50), Hereford and Worcester;

d: *Cymbohilates disponerus;* slide M50-5B-3, E.F. no. K29-4, Freshwater West Formation, Ross – Tewkesbury Spur Motorway (M50), Hereford and Worcester

e: *Cymbohilates horridus* var. *splendidus*: slide 19M50862b-1, E.F. no. M22-3. Freshwater West Formation, Ross – Tewkesbury Spur Motorway (M50), Hereford and Worcester.

f: *Cymbohilates horridus* var. *horridus*, slide M50-12-1, E.F. no. X27, Freshwater West Formation, Ross – Tewkesbury Spur Motorway (M50), Hereford and Worcester.

g – h: *Cymbohilates mesodecus;* **g:** slide GB5-1, E.F. no. G46-2, Gardeners Bank, Cleobury Mortimer, Shropshire; **h:** slide HD1-1, E.F. no. S39, Freshwater West Formation, Hudwick Dingle, North Brown Clee Hill, Shropshire.

Scale bar 30μm.

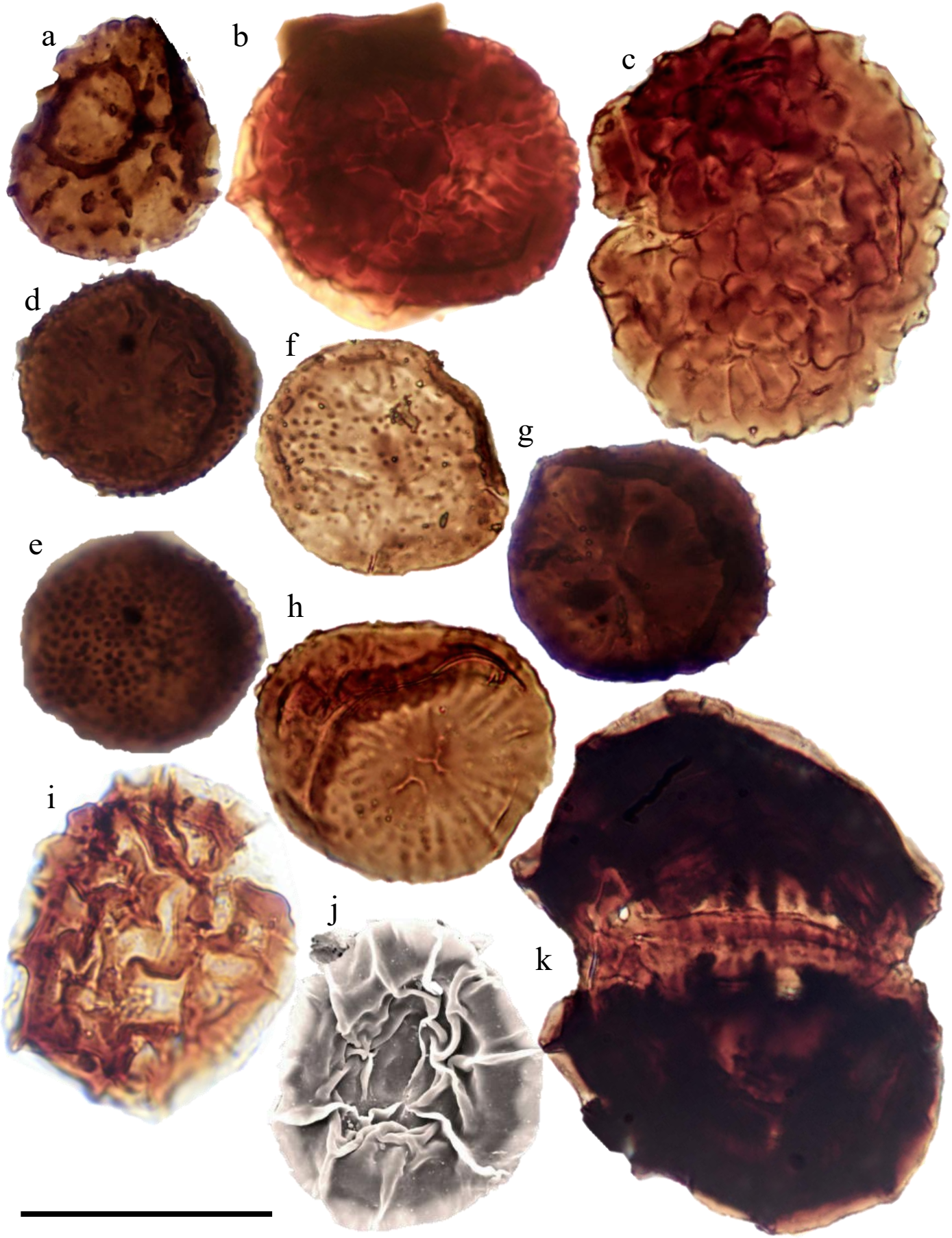
a
b
c
d
f
g
e
h
i
j
k

Plate XIII

a: *Cymbohilates* cf. *mesodecus,* slide M50-7-1, E.F. no. F13-3, Freshwater West Formation, Ross – Tewkesbury Spur Motorway (M50), Hereford and Worcester.

b – c: *Cymbohilates variabilis* var. *variabilis*; **b:** proximal face, showing apical papilla, slide M50-7-1, E.F. no. C15-1, Freshwater West Formation, Ross – Tewkesbury Spur Motorway (M50), Hereford and Worcester; **c:** distal view, showing coalesced elements, slide HD2-1, E.F. no. K30-3, Freshwater West Formation, Hudwick Dingle, North Brown Clee Hill, Shropshire.

d – e: *Cymbohilates variabilis* var. *parvidecus; **d***: proximal view, showing radial muri, slide M50-12-2, E.F. no. J22, Freshwater West Formation, Ross – Tewkesbury Spur Motorway (M50), Hereford and Worcester; **e:** distal view, M50-12-2, E.F. no. J22, Freshwater West Formation, Ross – Tewkesbury Spur Motorway (M50), Hereford and Worcester.

f: *Cymbohilates variabilis* var. tenuis, slide M50-13-2, E.F. no. S32-1, Freshwater West Formation, Ross – Tewkesbury Spur Motorway (M50), Hereford and Worcester;

g - h: *Cymbohilates variabilis* var. A; **g:** showing hilate papillae, slide M50-12-1, E.F. no. U21-1, Freshwater West Formation, Ross – Tewkesbury Spur Motorway (M50), Hereford and Worcester; **h:** Showing interadial muri, slide HD5-1, E.F. no. X42-1, Hudwick Dingle, North Brown Clee Hill, Shropshire.

i – k: *Chelinohilates erraticus*; **i:** slide 19M5026.1, E.F. no. N49-1, Freshwater West formation, Ross-Tewkesbury Spur (M50) motorway, Herefordshire and Worcester; **j:** SEM micrograph, proximal hemisphere, Freshwater West formation, Ross-Tewkesbury Spur (M50) motorway, Herefordshire and Worcester. **k:** as dyad, slide M50-7-6, E.F. no. S35-3, Freshwater West formation, Ross-Tewkesbury Spur (M50) motorway, Herefordshire and Worcester.

Scale bar 30μm.

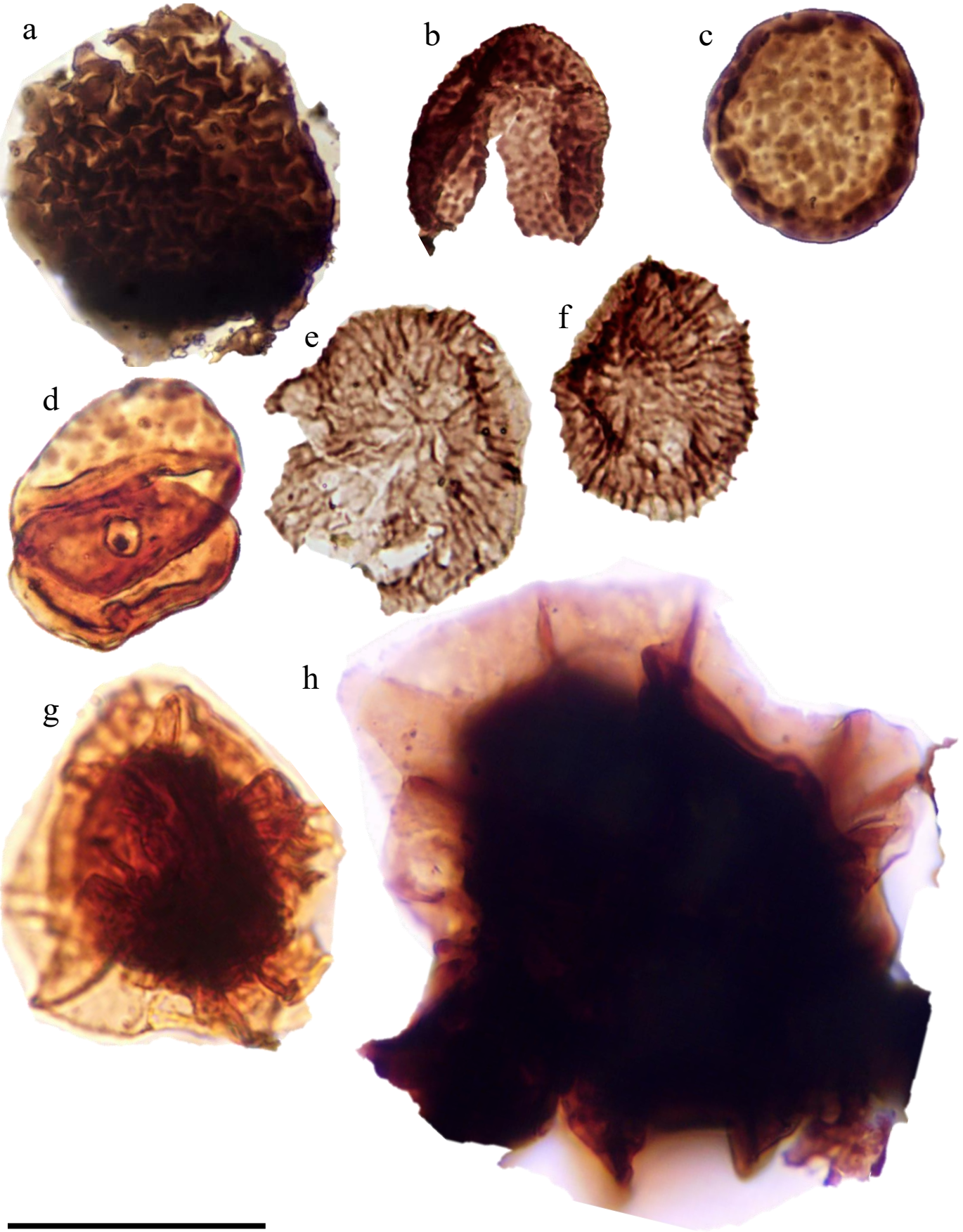
a
b
c
d
e
f
g
h

Plate XIV

a: *Chelinohilates sinuosus* var. *sinuosus*, slide M50-5E-1, E.F. no. J26-1, Freshwater West formation, Ross-Tewkesbury Spur (M50) motorway, Herefordshire and Worcester.

b: *Hispanaediscus* cf. *major*, slide USK/21/3, E.F. no. O27-3, Moor Cliffs Formation, Rumney – 1 borehole, Rumney, south Wales.

c – d: *Hispanaediscus verrucatus;* **c:** slide M50-85-2F-5, E.F. no. N32-3, Moor Cliffs Formation, Ross-Tewkesbury Spur (M50) motorway, Herefordshire and Worcester**; d:** as a dyad, slide M50-85-2D-1, E.F. no. T22-3, Moor Cliffs Formation, Ross-Tewkesbury Spur (M50) motorway, Herefordshire and Worcester.

e – f: *Qualisaspora fragilis;* **e:** slide MPA25249-1, E.F. no. G35, Freshwater West Formation, Ammons Hill section, Shropshire; **f:** slide MPA25249-1, E.F. no. V36, Freshwater West Formation, Ammons Hill section, Shropshire.

g: zonate ?trilete spores, M50-85-2C-4, E.F. no. G8-3, Moor Cliffs Formation, Ross-Tewkesbury Spur (M50) motorway, Herefordshire and Worcester.

h: zonate ?trilete spore, large specimen, slide 19M5026.1, E.F. no. O37-1, Freshwater West Formation, Ross-Tewkesbury Spur (M50) motorway, Herefordshire and Worcester.

Scale Bar 30μm.

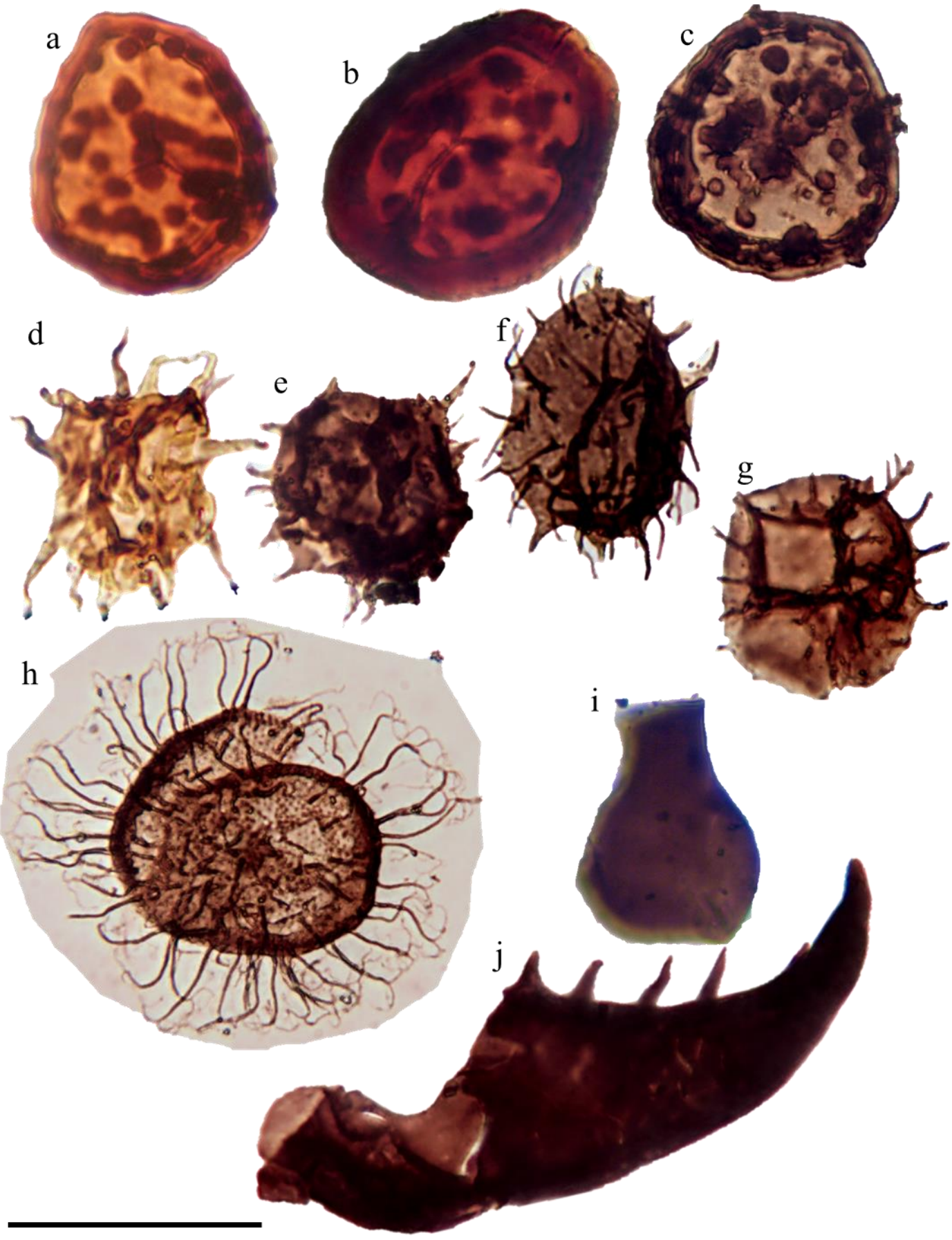
a
b
c
d
e
f
g
h
i
j

Plate XV

a – c: spores with circular, ?endobiontic fungal bodies; **a:** slide M50-85-2D-1, E.F. no. M14-2, Moor Cliffs Formation, Ross-Tewkesbury Spur (M50) motorway, Hereford and Worcester; **b:** M50-85-2d-1, E.F. no. S29-3, Moor Cliffs Formation, Ross-Tewkesbury Spur (M50) motorway, Hereford and Worcester; **c:** slide M50-8-2, E.F. no. M41-4, Freshwater West Formation, Ross-Tewkesbury Spur (M50) motorway, Hereford and Worcester.

d – g: Acritarchs; **d:** slide MPA25257-2, E.F. no. K38-4, Freshwater West Formation, Ammons Hill section, Shropshire; **e:** slide M50-11-5, E.F. no. J38-2, Freshwater West Formation, Ross-Tewkesbury Spur (M50) motorway, Hereford and Worcester; **f:** slide MPA25248-1, E.F. no. X27-4, Freshwater West Formation, Ammons Hill section, Shropshire; **g:** slide MPA25257-1, E.F. no. Q47, Freshwater West Formation, Ammons Hill section, Shropshire;

h: slide RU/21/2, E.F. no. G29-3, Downton Castle Sandstone Formation, Rumney-1 Acritarch spp., slide RU/21/2, E.F. no. N30, Downton Castle Sandstone Formation, Rumney-1 borehole, Rumney, South Wales.

i: Chitinozoan, probably reworked, slide M50-10-1, E.F. no. Q51-4, Freshwater West Formation, Ross-Tewkesbury Spur (M50) motorway, Hereford and Worcester.

j: Scolecodont spp., borehole, Rumney, South Wales.

Scale Bar 30μm.

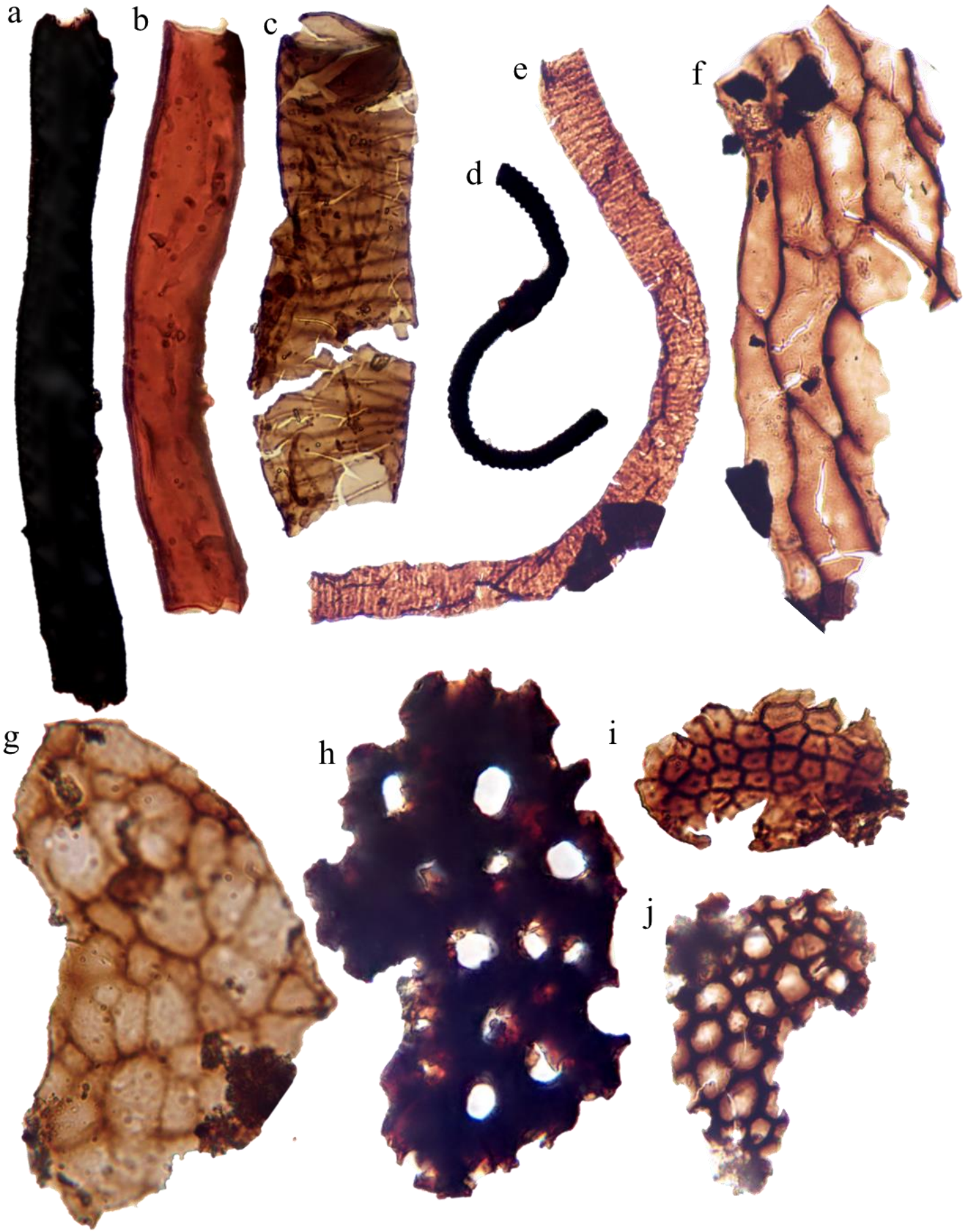
a
b
c
d
e
f
g
h
i
j

Plate XVI

a: *Laevitubulis tenuis*, slide M50-2-2, E.F. no. Q30-3, Moor Cliffs Formation, Ross-Tewkesbury Spur (M50) motorway, Hereford and Worcester.

b: *Laevitubulis plicatus*, slide M50-85-2C-7, E.F. no. J21, Moor Cliffs Formation, Ross-Tewkesbury Spur (M50) motorway, Hereford and Worcester.

c: *Porcatitubulus spiralis*, slide M50-85-2C-7, E.F. no. J20, Moor Cliffs Formation, Ross-Tewkesbury Spur (M50) motorway, Hereford and Worcester.

d: *Constrictitubulus cristatus*, slide M50-85-2C-1, E.F. no. O29, Moor Cliffs Formation, Ross-Tewkesbury Spur (M50) motorway, Hereford and Worcester.

e: *Porcatitubulis annulatus*, slide MPA25256-1, Freshwater West Formation, Ammons Hill section, Shropshire.

f – j: cuticular sheets; **f**: slide M50-3-3, E.F. no. L52, Moor Cliffs Formation, Ross-Tewkesbury Spur (M50) motorway, Hereford and Worcester; **g**: slide M50-2-2, E.F. no. P42, Moor Cliffs Formation, Ross-Tewkesbury Spur (M50) motorway, Hereford and Worcester; **h**: slide M50-2G-2, E.F. no. S13-1, Moor Cliffs Formation, Ross-Tewkesbury Spur (M50) motorway, Hereford and Worcester; **i:** slide SO06-2, E.F. no. J41-3, Bromyard Plateau, Shropshire; **j**: slide M50-2-3, E.F. no. S26-2, Moor Cliffs Formation, Ross-Tewkesbury Spur (M50) motorway, Hereford and Worcester.

Scale bar 30μm.

Bibliography

AL-AMERI, T.K., 1980. Palynology, biostratigraphy and palaeoecology of subsurface Mid-Palaeozoic strata from the Ghadames Basin, Libya. University of London, King's College (United Kingdom).

ALLEN, K.C. 1965. Lower and mid Devonian spores of north and central vestspitzbergen. Palaeontology, **8** (4), 687 – 748, pls. 94 – 108.

ALLEN, J R L. 1974A. The Devonian rocks of Wales and the Welsh Borderland. 47–84 in The Upper Palaeozoic and post-Palaeozoic rocks of Wales. OWEN, T R (editor). (Cardiff: University of Wales Press.)

_____ 1975. Source rocks of the Lower Old Red Sandstone: Llanishen Conglomerate of the Cardiff area, South Wales. Proceedings of the Geologists' Association, Vol. 86, 63–76.

_____ & CROWLEY, S.F., 1983. Lower Old Red Sandstone fluvial dispersal systems in the British Isles. Earth and Environmental Science Transactions of The Royal Society of Edinburgh, 74(2), pp.61-68.

_____ & DINELEY, D.L. 1976. The succession of the Lower Old Red Sandstone (Siluro-Devonian) along the Ross-Tewkesbury Spur Motorway (M50), Hereford and Worcester. Geological Journal, **11** (1), 1 – 14.

_____ & WILLIAMS, B. P. J. 1978. The sequence of the earlier Lower Old Red Sandstone (SiluroDevonian), north of Milford Haven, southwest Dyfed (Wales). Geological Journal, 13, 113-136.

_____ & TARLO, L.B., 1963. The Downtonian and Dittonian facies of the Welsh borderland. Geological Magazine, 100(2), pp.129-155.

_____ & WELLS, J.W., 1962. Holocene coral banks and subsidence in the Niger Delta. The Journal of Geology, 70(4), pp.381-397.

_____ HALSTEAD, L B, & TURNER, S. 1968. Dittonian ostracoderm fauna from the Brownstones of Wilderness Quarry, Mitcheldean, Gloucestershire. Proceedings of the Geological Society, No. 1649, 141–153.

_____ & WILLIAMS, B.P.J., 1981. Sedimentology and stratigraphy of the Townsend Tuff Bed (Lower Old Red Sandstone) in South Wales and the Welsh Borders. Journal of the Geological Society, 138(1), pp.15-29.

_____ & WILLIAMS, B.P.J., 1982. The architecture of an alluvial suite: rocks between the Townsend Tuff and Pickard Bay Tuff Beds (early Devonian), southwest Wales. Philosophical Transactions of the Royal Society of London. B, Biological Sciences, 297(1085), pp.51-89.

ANTIA, D.D.J., 1979. Bone-beds: A review of their classification, occurrence, genesis, diagenesis, geochemistry, palaeoecology, weathering, and microbiotas.

ARKHANGELSKAYA, A. D. 1980. Plant spores from some Lower Devonian sections of the western regions of the Russian Platform (in Russian). TRUDY VNIGNI (Moscow): Palynological research in the Proterozoic and Phanerozoic of oil- and gas-bearing regions of the USSR, 217, 26-46, 140-143, pls. 5-1 1.

ARISTOVA, K. E. & ARKHANGELSKAYA, A. D. 1976. Microfossils from stratotype sections of Upper Silurian horizons of Estonia. In: Byvsheva, T. V. (ed) Results of palynological research on Precambrian, Paleozoic and Mesozoic of the USSR. Trudy Vsesoiuznogo Nauchno-Issledovatel'skogo Geologorazvedochnogo Neftianogo Instituta, Kama Branch, 192, 28-38.

BALL, A.C. AND TAYLOR, W.A., 2022. Reconstructing the Lower Devonian (Lochkovian) vegetation from the Anglo-Welsh Basin: Two spore masses containing Emphanisporites McGregor spores. Review of Palaeobotany and Palynology, 301, p.104647.

BALL, H.W., DINELEY, D.L. & WHITE, E.I., 1961. The Old Red Sandstone of Brown Clee Hill and the adjacent area. British Museum (Natural History).

BANKS, H. P., LECLERQ, S. & HUEBER, F. M. 1975. Anatomy and morphology of *Psilophyton dawsonii*, sp. n. from the late Lower Devonian of Quebec (Gaspé) and Ontario, Canada. Paleontographica Americana, **8**, 75 – 127.

BARCLAY, W.J., RATHBONE, P.A., WHITE, D.E. & RICHARDSON, J.B., 1994. Brackish water faunas from the St Maughans Formation: The Old Red Sandstone section at Ammons Hill, Hereford and Worcester, UK, re-examined. Geological Journal, **29** (4), 369 – 379.

_____, DAVIES, J.R., HILLIER, R.D. AND WATERS, R.A., 2015. Lithostratigraphy of the Old Red Sandstone successions of the Anglo-Welsh Basin.

BASSETT, M.G., 1974. The articulate brachiopods from the Wenlock Series of the Welsh Borderland and South

Wales. Monographs of the Palaeontographical Society, 128(541), pp.79-123.

_____, LAWSON, J.D. AND WHITE, D.E., 1982. The Downton Series as the fourth series of the Silurian System. Lethaia, 15(1), pp.1-24.

BECK, J.H. AND STROTHER, P.K., 2001. Silurian spores and cryptospores from the Arisaig group, Nova Scotia, Canada. Palynology, 25(1), pp.127-177.

BENNIE, J. & KIDSTON, R., 1886. On the occurrence of spores in the carboniferous Formation of Scotland, Royal Physical Society.

BENNINGHOFF, W.S., 1962. Calculation of pollen and spores density in sediments by addition of exotic pollen in known quantities. Pollen et Spores 4, 332–333

BHARADWAJ, D.C. & VENKATACHALA, B.S. 1961. Spore assemblage out of a Lower Carboniferous shale from Spitzbergen. The Palaeobotanist, **10**, 18 – 47. 10 pls.

BLIECK, A. AND ELLIOTT, D.K., 2017. Pteraspidomorphs (Vertebrata), the Old Red Sandstone, and the special case of the Brecon Beacons National Park, Wales, UK. Proceedings of the Geologists' Association, 128(3), pp.438-446.

_____ & JANVIER, P., 1999. Silurian-Devonian vertebrate dominated communities, with particular references to agnathans. WORLD AND REGIONAL GEOLOGY, pp.79-105.

_____ & TARRANT, P.R., 2001. Protopteraspis gosseleti (Vertebrata: Pteraspidomorphi: Heterostraci) from the Lower Devonian of Shropshire, England. Palaeontology, 44(1), pp.95-112.

_____, TURNER, S., YOUNG, G.C., LUKSEVICS, E., MARK-KURIK, E., TALIMAA, V.N. AND VALIUKEVICIUS, J.J., 2000. Devonian vertebrate biochronology and global marine/non-marine correlation. Courier-Forschungsinstitut Senckenberg, pp.161-194.

BREUER, P. 2007. "Devonian miospore palynology in Western Gondwana: an application to oil exploration." Unpublished PhD thesis, University of Liège, Liège, Belgium 590.

_____, STRICANNE, L. AND STEEMANS, P., 2005. Morphometric analysis of proposed evolutionary lineages of Early Devonian land plant spores. Geological Magazine, 142(3), pp.241-253.

_____, AL-GHAZI, A., AL-RUWAILI, M., HIGGS, K.T., STEEMANS, P. & WELLMAN, C.H. 2007. Early to mid Devonian miospores from northern Saudi Arabia. Revue de micropaléontologie, **50** (1), 27 – 57. 12 pls.

_____, MILLER, M.A., LESZCZYŃSKI, S. AND STEEMANS, P., 2015. Climate-controlled palynofacies and miospore stratigraphy of the Jauf Formation, Lower Devonian, northern Saudi Arabia. Review of Palaeobotany and Palynology, 212, pp.187-213.

_____, LE HÉRISSÉ, A., PARIS, F., STEEMANS, P., VERNIERS, J. AND WELLMAN, C.H., 2017. A distinctive marginal marine palynological assemblage from the Přídolí of northwestern Saudi Arabia. Revue de Micropaléontologie, 60(3), pp.371-402.

BROWNE, M., SMITH, R. AND AITKEN, A.M., 2002. Stratigraphical framework for the Devonian (Old Red Sandstone) rocks of Scotland south of a line from Fort William to Aberdeen. British Geological Survey.

BURGESS, N.D. 1991. Silurian cryptospores and miospores from the type Llandovery area, south-west Wales. Palaeontology, **34** (3), 575 – 599. Pls.

_____ & RICHARDSON, J.B. 1991. Silurian cryptospores and miospores from the type Wenlock area, Shropshire, England. Palaeontology, **34** (3), 601 – 628. Pls.

_____ & RICHARDSON, J.B. 1995. Late Wenlock to early Prídolí cryptospores and miospores from south and southwest Wales, Great Britain. Palaeontographica Abteilung B, **236**, 1 – 44. Pls.

BURDEN, E.T., QUINN, L., NOWLAN, G.S. AND BAILEY-NILL, L.A., 2002. Palynology and micropaleontology of the clam bank Formation (Lower Devonian) of Western Newfoundland, Canada. Palynology, 26(1), pp.185-215.

BUTTERWORTH, M.A. & WILLIAMS, R.W. 1958. XVII.—The Small Spore Floras of Coals in the Limestone Coal Group and Upper Limestone Group of the Lower Carboniferous of Scotland. Earth and Environmental Science Transactions of The Royal Society of Edinburgh, **63** (2), 353 – 392. Pls.

CATLOS, E.J., MARK, D.F., SUAREZ, S., BROOKFIELD, M.E., MILLER, C.G., SCHMITT, A.K., GALLAGHER, V. AND KELLY, A., 2021. Late Silurian zircon U–Pb ages from the Ludlow and Downton bone beds, Welsh Basin, UK. Journal of the Geological Society, 178(1).

CHALONER, W.G. 1963. Early Devonian spores from a borehole in southern England. Grana, **4** (1), 100 – 110. Pls.

_____ & STREEL, M. 1968. Lower Devonian spores from South Wales. Argumenta Palaeobotanica, **1**, 87 – 101. Pls.

_____, & RICHARDSON, J.B. 1977. South-east England. In: House, M.R., Richardson, J.B., Chaloner, W.G., Allen, J.R.L., Holland, C.H. and Westoll, T.S. A correlation of Devonian rocks of the British Isles. Geological Society of London, Special Report, 8: 26–40.

CHERNS, L., COCKS, L.R.M., DAVIES, J.R., HILLIER, R.D., WATERS, R.A. & WILLIAMS, M., 2006. Silurian: the influence of extensional tectonics and sea-level changes on sedimentation in the Welsh Basin and on the Midland Platform. The geology of England and Wales, pp.75-102.

COUPER, R.A., 1953. Upper Mesozoic and Cainozoic spores and pollen grains from New Zealand. Palaeontological Bulletin, **22**, 1 – 97. 9 pls.

CRAMER, F.H. 1966. Palynology of Silurian and Devonian rocks in northwest Spain. Boletín del Instituto Geológico y Minero de España, **77**, 223-286.

_____ & DIEZ, M.D.C.R.1975. Earliest Devonian miospores from the Province of Leon, Spain. Pollen et Spores, **17**, 331 – 344. Pls.

CROWLEY, S.F., HIGGS, K.T., PIPER, J.D. & MORRISSEY, L.B., 2009. Age of the Peel Sandstone Group, Isle of Man. Geological Journal, 44(1), pp.57-78.

DEUNFF, J. AND CHATEAUNEUF, JJ, 1976. On the presence of a rich Siluro-Devonian microplankton with Acritarchs, spores and Chitinozoans at the top of the schists and quartzites of Plougastel (Rade de Brest-Finistere); its stratigraphic interest. Geobios , 9 (3), pp.337-343.

DEWEY, J F, & STRACHAN, R A. 2003. Changing Silurian–Devonian relative plate motion in the Caledonides: sinistral transpression to sinistral transtension. Journal of the Geological Society of London, Vol. 160, 219–229.

DINELEY, D.L., 1963. The" Red Stratum" of the Silurian Arisaig Series, Nova Scotia, Canada. The Journal of Geology, 71(4), pp.523-524.

EDWARDS, D. 1969. Zosterophyllum from the Lower Old Red Sandstone of South Wales. New Phytologist **68** (4), 923-931. Pls.

_____ 1970. Fertile Rhyniophytina from the Lower Devonian of Britain.Palaeontology13: 451–461.

_____ 1979. A late Silurian flora from the Lower Old Red Sandstone of south-west Dyfed.Palaeontology22: 23–52.

_____ 1996. New insights into early land ecosystems: a glimpse of a Lilliputian world. Review of Palaeobotany and Palynology, **90** (3-4),159-174.

_____ 2017. Glimpses of the botanical history of Wales. The Transactions of the Honourable Society of Cymmrodorion, 23, pp.8-18.

_____ & KENRICK, P., 2015. The early evolution of land plants, from fossils to genomics: a commentary on Lang (1937)'On the plant-remains from the Downtonian of England and Wales'. Philosophical Transactions of the Royal Society B: Biological Sciences, 370(1666), p.20140343.

_____ & RICHARDSON, J.B. 1974. Lower Devonian (Dittonian) plants from the Welsh borderland. Palaeontology, 17(2): 311–324.

_____ & RICHARDSON, J.B. 2000. Progress in reconstructing vegetation on the Old Red Sandstone Continent: two Emphanisporites producers from the Lochkovian sequence of the Welsh Borderland. Geological Society, London, Special Publications **180** (1), 355-370.

_____ & RICHARDSON, J.B., 2004. Silurian and Lower Devonian plant assemblages from the Anglo-Welsh Basin: a palaeobotanical and palynological synthesis. Geol. J. 39 (3–4), 375–402

_____ & ROGERSON ECW. 1979. New records of fertile Rhyniophytina from the late Silurian of Wales.Geological Magazine116: 93–98.

_____, KENRICK, P. & CARLUCCIO, L.M., 1989. A reconsideration of cf. Psilophyton princeps (Croft & Lang, 1942), a zosterophyll widespread in the Lower Old Red Sandstone of South Wales. Botanical Journal of the Linnean Society, 100(4), pp.293-318.

_____, FANNING U., & RICHARDSON, J.B. 1994. Lower Devonian coalified sporangia from Shropshire: Salopella Edwards & Richardson and Tortilicaulis Edwards. Botanical Journal of the Linnean Society 116, 89–110.

_____, DUCKETT JG, RICHARDSON JB. 1995A. Hepatic characters in the earliest land plants.Nature374: 635–636.

_____, DAVIES KL, RICHARDSON JB, AXE L. 1995B. The ultrastructure of spores ofCooksonia pertoni. Palaeontology38: 153–168.

_____, SELDEN PA, RICHARDSON JB, AXE L. 1995C. Coprolites as evidence for plant-animal interaction in Siluro-Devonian terrestrialecosystems.Nature377: 329–331.

_____, AXE L, DUCKETT JG. 2003. Diversity in conducting cells in early land plants and comparisons with extant bryophytes.BotanicalJournal of the Linnean Society141: 297–347

_____, RICHARDSON, J.B., AXE, L., DAVIES, K.L., 2012A. A new group of Early Devonian plants with valvate sporangia containing sculptured permanent dyads. Bot. J. Linn. Soc. 168 (3), 229–257.

_____ MORRIS, J.L., RICHARDSON, J.B. & KENRICK, P. 2014. Cryptospores and cryptophytes reveal hidden diversity in early land floras. New Phytologist **202** (1), 50-78.

_____, MORRIS, J.L., AXE, L., DUCKETT, J.G., PRESSEL, S. AND KENRICK, P., 2022A. Piecing together the eophytes–a new group of ancient plants containing cryptospores. New Phytologist, 233(3), pp.1440-1455.

_____, MORRIS, J.L., AXE, L., TAYLOR, W.A., DUCKETT, J.G., KENRICK, P. AND PRESSEL, S., 2022B. Earliest record of transfer cells in Lower Devonian plants. New Phytologist, 233(3), pp.1456-1465.

_____, MORRIS, J.L., AXE, L. AND DUCKETT, J.G., 2022C. Picking up the pieces: New charcoalified plant mesofossils (eophytes) from a Lower Devonian Lagerstätte in the Welsh Borderland, UK. Review of Palaeobotany and Palynology, 297, p.104567.

EISENACK, A. 1944. [On some plant finds in Geshoeeben, together with remarks on the Hystrichosphaeridean problem]. Z. Geschiebeforsch, **19**, 103 – 124. [In German].

ERDTMAN, G., 1947. Suggestions for the classification of fossil and recent pollen grains and spores. Svensk Botan. Tidskr., **41** (1), 104-114

FANNING U, RICHARDSON JB, EDWARDS D. 1988. Cryptic evolution in an early land plant. Evolutionary Trends in Plants 2: 13–24.

_____, EDWARDS D, RICHARDSON JB. 1990. Further evidence for diversity in late Silurian land vegetation.Journal of the Geological Society147: 725–728

_____, RICHARDSON, J.B. & EDWARDS, D. 1991. A review of in situ spores in Silurian land plants. In BLACKMORE, S. AND BARNES, S. H. (Eds). Systematics Association Special Volume, Pollen and Spores, **44**, 25–47.

_____, EDWARDS D, RICHARDSON JB. 1992. A diverse assemblage of early land plants from the Lower Devonian of the Welsh Borderland. Journal of the Linnean Society109: 161–188.

FAYERS, S.R., TREWIN, N.H. AND MORRISSEY, L., 2010. A large arthropod from the Lower Old Red Sandstone (Early Devonian) of Tredomen Quarry, south Wales. Palaeontology, 53(3), pp.627-643.

FRIEND, P F, WILLIAMS, B P J, FORD, M, AND WILLIAMS, E A. 2000. Kinematics and dynamics of Old Red Sandstone basins. 29–60 in FRIEND, P F, AND WILLIAMS, B P J (editors). New perspectives on the Old Red Sandstone. Geological Society of London Special Publication, No. 180.

FISK, H.W., MCFARLAN, E., KOLB, C. R., & WILBERT, L.R., 1954. Sedimentary framework of the modern Mississippi Delta. /. sediment. Petrol., 24, 76-99.

GENSEL, P.G., 1976. Renalia hueberi, a new plant from the Lower Devonian of Gaspé. Review of Palaeobotany and Palynology, **22** (1), 19 – 37.

GLASSPOOL, I.J. AND GASTALDO, R.A., 2022. Silurian wildfire proxies and atmospheric oxygen. Geology, 50(9), pp.1048-1052.

GRADSTEIN, F.M., OGG, J.G., SCHMITZ, M. AND OGG, G. eds., 2012. The geologic time scale 2012. elsevier.

GIBLING, M.R., DAVIES, N.S., FALCON-LANG, H.J., BASHFORTH, A.R., DIMICHELE, W.A., RYGEL, M.C. AND IELPI, A., 2014. Palaeozoic co-evolution of rivers and vegetation: a synthesis of current knowledge. Proceedings of the Geologists' Association, 125(5-6), pp.524-533.

GIBSON, M.E., 2022. First report of fungal palynomorphs from the Zechstein Group (Lopingian): implications for the stratigraphic completeness of the Earth's Paleozoic fungal record. Palaios, 37(6), pp.318-329.

GOUDIE, A. S. 1983 Calcrete. In Chemical sediments and geomorphology (ed. A. S. Goudie & K. Pye), pp. 91—131. London: Academic Press.

GRAY, J. 1985. The microfossil record of early land plants; advances in understanding of early terrestrialization, 1970–1984. Philosophical Transactions of the Royal Society, London, B309, 167–195.

GROSS, W., 1967. Über Thelodontier-Schuppen. Palaeontographica Abteilung A, pp.1-67.

HIGGS, K.T., 2004. An Early Devonian (Lochkovian) microflora from the Freshwater West Formation, Lower Old Red Sandstone, southwest Wales. Geological Journal, **39** (3-4), 359-374.

_____, 2022. Palynology of the Freshwater East Formation (Upper Silurian, Přídolí), Pembrokeshire, South Wales, UK. Palynology, (just-accepted), p.2070785.

HILL, P.J., PARIS, F. AND RICHARDSON, J.B. 1985. Silurian palynomorphs. Journal of Micropalaeontology, 4(1): 27–48

HILLIER, R.D. AND WILLIAMS, B.P.J., 2006. The alluvial old red sandstone: fluvial basins.

_____, MARRIOTT, S B, WILLIAMS, B P J, AND WRIGHT, V P. 2007. Possible climate variability in the Lower Old Red Sandstone Conigar Pit Sandstone Member (early Devonian), South Wales, UK. Sedimentary Geology, Vol. 202, 35–57.

_____, EDWARDS, D, AND MORRISSEY, L B. 2008. Sedimentological evidence for rooting structures in the Early Devonian Anglo-Welsh Basin (UK), with speculation on their producers. Paleogeography, Palaeoclimatology, Palaeoecology, Vol. 270, 360–380.

_____, WATERS, R.A., MARRIOTT, S.B. AND DAVIES, J.R., 2011A. Alluvial fan and wetland interactions: evidence of seasonal slope wetlands from the Silurian of south central Wales, UK. Sedimentology, 58(4), pp.831-853.

_____, MARRIOTT, S B, AND WILLIAMS, B P J. 2011b. Pedogenic and non-pedogenic calcretes in the Devonian Ridgeway Conglomerate Formation of SW Wales, UK: a cautionary tale. 311–325 in From river to rock record: the deposition of fluvial sediments and their subsequent preservation. NORTH, C P, LELEU, S, AND DAVIDSON, S. Society of Economic Palaeontologists and Mineralogists Special Publication No. 97.

_____, MARRIOTT, S.B., HIGGS, K.T. AND HOWELLS, S., 2019. Catchment inversion during the Silurian of SW Wales: Pediment plains, embryonic drainage networks and incised valley fills in a dryland range front alluvial system. Sedimentary Geology, 387, pp.126-151.

HOFFMEISTER, W.S., 1959. Lower Silurian plant spores from Libya. Micropaleontology, **5** (3), 331-334.

HOLLAND, C.H. AND LAWSON, J.D., 1963. Facies patterns in the Ludlovian of Wales and the Welsh Borderland. Geological Journal, 3(2), pp.269-288.

HOUSE, M.R., RICHARDSON, JB, CHALONER, WG, ALLEN, JRL, HOLLAND, CH, AND WESTOLL, TS. 1977. A correlation of the Devonian rocks in the British Isles. Geological Society of London Special Report, No. 7.

HUEBER, F.M. 1968. Psilophyton: the genus and the concept. In OSWALD, D.H. (Ed.), international Symposium on the Devonian System, Volume 1. Alberta Society of Petroleum Geologists, Calgary, Alta., 815 – 822.

JAMES, D M D. 1987. Tectonics and sedimentation in the Lower Palaeozoic back-arc basin of South Wales, UK. Some quantitative aspects of basin development. Norsk Geologisk Tidsskrift, Vol. 67, 419–426.

JARDINE S. & YAPAUDJIAN L. 1968. [Lithostratigraphy and palynology of the Sandstone Devonian-Gothlandian of the Polignac Basin (Sahara)]. Revue de l'Institut Français du Pétrole, **23**, 439 – 468. [In French].

JOHNSON, N.G., 1985. Early Silurian palynomorphs from the Tuscarora Formation in central Pennsylvania and their paleobotanical and geological significance. Review of Palaeobotany and Palynology, **45** (3-4), 307-359.

JUGGINS, S. (2020) rioja: Analysis of Quaternary Science Data, R package version (0.9-26). (https://cran.r-project.org/package=rioja).

KEDO, G.I., 1963. Spores of the Tournaisian Stage of the Pripyat Depression and their stratigraphical significance. Rep Palaeontologiskii I Stratigrafiskii Byelorussian SSR, **4**, 3-121.

KENDALL R , HUMPAGE, A. 2012. All fields on the title and cover should be amended by using File/Properties/Custom. British Geological Survey Commercial Report, CR/12/033. 84pp.

KENRICK, P., WELLMAN, C.H., SCHNEIDER, H. AND EDGECOMBE, G.D., 2012. A timeline for terrestrialization: consequences for the carbon cycle in the Palaeozoic. Philosophical Transactions of the Royal Society B: Biological Sciences, 367(1588), pp.519-536.

KERMANDJI, A.M.H., 2007. Silurian–Devonian miospores from the western and central Algeria. Revue de micropaléontologie, 50(1), pp.109-128.

KING, W W. 1925. Notes on the 'Old Red Sandstone' of Shropshire. Proceedings of the Geologists' Association, Vol. 36, 383–389.

_____, 1934. The Downtonian and Dittonian strata of Great Britain and north-western Europe. Quarterly

Journal of the Geological Society of London, Vol. 90, 526–570.

KING, L M. 1994. Subsidence analysis of Eastern Avalonian sequences: implications for Iapetus closure. Journal of the Geological Society of London, Vol. 151, 647–657.

KIRJANOV, V.V., 1978. The Acritarchs of Silurian of Volyno-Podolia. Kiev.

KOTYK, M. E., BASINGER, J. F., GENSEL, P. G. & DE FREITAS, T. 2002. Morphologically complex plant macrofossils from the Late Silurian of Arctic Canada. American Journal of Botany, 89, 1004–1013

LANNINGER, E. 1968. [Spore associations from the Ems der SW-Eifel]. Palaeontographica B, **122**, 95 – 170. Pls. 20 – 26. [In German].

LANG, W.H., 1937. IV-On the plant-remains from the Downtonian of England and Wales. Philosophical Transactions of the Royal Society of London. Series B, Biological Sciences, 227(544), pp.245-291.

LAVENDER, K. & WELLMAN, C.H. 2002. Lower Devonian spore assemblages from the Arbuthnott Group at Canterland Den in the Midland Valley of Scotland. Review of Palaeobotany and Palynology, **118** (1-4), 157 – 180.

LEGRAND, J., YAMADA, T., KOMATSU, T., WILLIAMS, M., HARVEY, T., DE BACKER, T., VANDENBROUCKE, T.R., NGUYEN, P.D., DOAN, H.D. AND NGUYEN, H.B., 2021, July. Implications of an early land plant spore assemblage for the late Silurian age of the Si Ka Formation, northern Vietnam. In Annales de Paléontologie (Vol. 107, No. 3, p. 102486). Elsevier Masson.

LELE, KM & STREEL, M. 1969. MID DEVONIAN (Givetian) plant microfossils from Goé (Belgium). Annals of the Geological Society of Belgium , **92** (1), 89-121.

LOBOZIAK, S. AND STREEL, M., 1981. Miospores in middle-upper Frasnian to Famennian sediments partly dated by conodonts (Boulonnais, France). Review of Palaeobotany and Palynology, 34(1), pp.49-66.

_____, STREEL, M. AND VANGUESTAINE, M., 1983. Miospores et acritarches de la Formation d'Hydrequent (Frasnien Supérieur à Famennien Inférieur, Boulonnais, France). Annales de la Société géologique de Belgique, 106.

LOVE, S.E. AND WILLIAMS, B.P., 2000. Sedimentology, cyclicity and floodplain architecture in the Lower Old Red Sandstone of SW Wales. Geological Society, London, Special Publications, 180(1), pp.371-388.

LUBER, A. A. 1935. Atlas of the spore and pollen of the palaeozoic deposits of Kazakhstan. Izd. Akad. Nauk Kazakh S.S.R. , Alma-Ata, 1 – 125. 10 pls. [In Russian].

MÄRSS, T. AND MILLER, C.G., 2004. Thelodonts and distribution of associated conodonts from the Llandovery–lowermost Lochkovian of the Welsh Borderland. Palaeontology, 47(5), pp.1211-1265.

MARRIOTT, S.B., MORRISSEY, L.B. AND HILLIER, R.D., 2009. Trace fossil assemblages in Upper Silurian tuff beds: evidence of biodiversity in the Old Red Sandstone of southwest Wales, UK. Palaeogeography, Palaeoclimatology, Palaeoecology, 274(3-4), pp.160-172.

MEHLQVIST, K., VAJDA, V. AND STEEMANS, P., 2012. Early land plant spore assemblages from the Late Silurian of Skåne, Sweden. GFF, 134(2), pp.133-144.

_____, STEEMANS, P. AND VAJDA, V., 2015. First evidence of Devonian strata in Sweden—A palynological investigation of Övedskloster drillcores 1 and 2, Skåne, Sweden. Review of Palaeobotany and Palynology, 221, pp.144-159.

MCGAIRY, A., KOMATSU, T., WILLIAMS, M., HARVEY, T.H., MILLER, C.G., NGUYEN, P.D., LEGRAND, J., YAMADA, T., SIVETER, D.J., BUSH, H. AND STOCKER, C.P., 2021. Ostracods had colonized estuaries by the late Silurian. Biology Letters, 17(12), p.20210403.

MCGREGOR, D.C. 1961. Spores with Proximal Radial Pattern from the Devonian of Canada. Geological Survey of Canada, Bulletin **76**, 1961. 1 – 11.

_____ 1973. Lower and mid Devonian spores of Eastern Gaspé, Canada. I. Systematics. Palaeontographica, Abteilung B, **142**, 1 – 77.

_____, & NARBONNE, G.M., 1978. Upper Silurian trilete spores and other microfossils from the Read Bay Formation, Cornwallis Island, Canadian Arctic. Canadian Journal of Earth Sciences, 15(8), pp.1292-1303.

_____ & CAMFIELD, M. 1982. mid Devonian miospore from the Cape de Bray, Weatherall, and Hecla Bay Formations of northeastern Melville Island, Canadian Artic. Geological Survey of Canada, Bulletin, 348, 1- 105.

MILLER, M.A. & EAMES, L.E. 1982. Palynomorphs from the Silurian Medina Group (Lower Llandovery) of the Niagara Gorge, Lewiston, New York, U.S.A.Pulynology, 6,221-254

_____ & MARRS, T .1999. A conodont, thelodont and acanthodian fauna from the Lower Přídolí an (Silurian) of the Much Wenlock Area, Shropshire.Palaeontology,42, 691±784

MOREAU – BENOIT, A. 1967. [First results of a palynological study of the Devonian of the Lime Kiln Quarry of Angers (Maine and Loure).] Ibid, **9**, 219 – 240. 4 pls. [In French].

MORRIS, J.L. AND EDWARDS, D., 2014. An analysis of vegetational change in the Lower Devonian: new data from the Lochkovian of the Welsh Borderland, UK. Review of Palaeobotany and Palynology, 211, pp.28-54.

_____, RICHARDSON, J.B., EDWARDS, D., 2011A. Lower Devonian plant and spore assemblages from Lower Old Red Sandstone strata of Tredomen Quarry, South Wales. Rev. Palaeobot. Palynol. 165 (3–4), 183–208.

_____, EDWARDS, D., RICHARDSON, J.B., AXE, L., DAVIES, K.L., 2011B. New plant taxa from the Lower Devonian (Lochkovian) of the Welsh Borderland, with a hypothesis on the relationship between hilate and trilete spore producers. Rev. Palaeobot. Palynol. 167, 51–81.

_____, EDWARDS, D., RICHARDSON, J.B., AXE, L. & DAVIES, K.L. 2012A. Further insights into trilete spore producers from the Early Devonian (Lochkovian) of the Welsh Borderland, U.K. Review of Palaeobotany and Palynology 185, 35– 63.

_____, WRIGHT, V.P. AND EDWARDS, D., 2012B. Siluro-Devonian landscapes of southern Britain: the stability and nature of early vascular plant habitats. Journal of the Geological Society, 169(2), pp.173-190.

_____, EDWARDS, D. & RICHARDSON, J.B. 2018B. The advantages and frustrations of a plant Lagerstätte as illustrated by a new taxon from the Lower Devonian of the Welsh Borderland, U.K. In KRINGS, M., HARPER, C.J., RUBÉN CÚNEO, N. AND ROTHWELL, G.W. (Eds). Transformative Paleobotany. Academic Press, 49-67.

MORRISSEY, L.B., BRADDY, S.J., BENNETT, J.P., MARRIOTT, S.B. AND TARRANT, P.R., 2004. Fish trails from the lower old red sandstone of Tredomen Quarry, Powys, southeast Wales. Geological Journal, 39(3-4), pp.337-358.

_____, HILLIER, R.D. AND MARRIOTT, S.B., 2012. Late Silurian and Early Devonian terrestrialisation: ichnological insights from the Lower Old Red Sandstone of the Anglo-Welsh Basin, UK. Palaeogeography, Palaeoclimatology, Palaeoecology, 337, pp.194-215.

MORTIMER, M.G. 1967. Some Lower Devonian microfloras from southern Britain. Review of palaeobotany and palynology, **1**, 95 – 109. 2 pls.

MURCHISON, R.I., 1839. The Silurian system, founded on geological researches in the counties of Salop, Hereford, Radnor, Montgomery, Caermarthen, Brecon, Pembroke, Monmouth, Gloucester, Worcester, and Stafford: with descriptions of the coalfields and overlying formations. J. Murray.

_____, 1854. Official Report of the Proceedings of the Exploring Party under Commander JC Prevost, of HMS Virago, Sent to Cross the Isthmus of Darien. The Journal of the Royal Geographical Society of London, 24, pp.249-256.

GARCIA-MURO, V.J., RUBINSTEIN, C.V., RUSTÁN, J.J. AND STEEMANS, P., 2018. Palynomorphs from the Devonian Talacasto and Punta Negra formations, Argentinean Precordillera: new biostratigraphic approach. Journal of South American Earth Sciences, 86, pp.110-126.

_____, RUBINSTEIN, C.V. AND STEEMANS, P., 2014. Palynological record of the Silurian/Devonian boundary in the Argentine Precordillera, western Gondwana. Neues Jahrbuch für Geologie und Paläontologie, Abhandlungen, 274(1), pp.25-42.

NUAMOVA. S.N. 1953. Spore-pollen assemblages of the Upper Devonian of the Russian Platform and their stratigraphic significance. Tr. Inst. geol. Nauk, Akad. Nauk S.S.S.R. **143** (60), 1 – 154, 6 + 22 pls. [In Russian].

_____ 1960. Spore-pollen complexes of upper devonian of the russian platform. International Geology Review, 2(8), 688–704.

OKSANEN, J., BLANCHET, F.G., FRIENDLY, M., KINDT, R., LEGENDRE, P., MCGLINN, D., MINCHIN, P.R., O'HARA, R. B., SIMPSON, G.L., SOLYMOS, P., STEVENS, M.H.H., SZOECS, E. AND WAGNER, H. 2020. vegan: Community Ecology Package. R package version 2.5-7. https://CRAN.R-project.org/package=vegan.

ORTIZ, J., AND JARAMILLO, C., 2020. SDAR: a Toolkit for Stratigraphic Data Analysis. R package version 0.9-55.

POTONIE., 1958. Idem; Teil 2, Sporites (Nachträge), Saccites, Aletes, Praecolpates, Polyplicates, Monocolpates. Ibid, **31**, 1 – 114. 11 pls.

_____ AND KREMP, G. 1954. [the genera of the Palaozoic sporae dispersae and their stratigraphy], Geol. Jb. **69**, 111 – 194. Pl. 4 – 20. [In German].

R CORE TEAM, 2022. R: A language and environment for statistical computing. R Foundation for Statistical Computing, Vienna, Austria.

RICHARDSON, J.B. 1965. Middle Old Red Sandstone spore assemblages from the Orcadian basin north-east Scotland. Palaeontology, **7**, 559-605

_____. 1967. Some British Lower Devonian spore assemblages and their stratigraphic significance. Review of Palaeobotany and Palynology, 1(1–4): 111–129

_____ 1985. Lower Palaeozoic sporomorphs: their stratigraphical distribution and possible affinities. Philosophical Transactions of the Royal Society B, 309(1138): 201–205.

_____1988. Late Ordovician and Early Silurian cryptospores and miospores from northeast Libya. In: El-Arnauti, A., Owens, B. and Thusu, B. (editors). Subsurface Palynostratigraphy of Northeast Libya. Garyounis University Publications, Benghazi, Libya, 89–110.

_____1996A. Taxonomy and classification of some new Early Devonian cryptospores from England. Special papers in palaeontology, **55**, 7 – 40. 10 pls.

_____1996B. Abnormal spores and possible interspecific hybridization as a factor in the evolution of Early Devonian land plants. Review of Palaeobotany and Palynology, 93(1–4): 333–340

_____ 2007. Cryptospores and miospores, their distribution patterns in the Lower Old Red Sandstone of the Anglo-Welsh Basin, and the habitat of their parent plants. Bulletin of Geosciences, **82** (4), 355-364.

_____ & EDWARDS, D. 1989. Sporomorphs and plant megafossils. In: Holland, C.H. and Bassett, M.G. (editors). A global standard for the Silurian System. Natural Museum of Wales, Cardiff, Geological Series, 9: 216–226.

_____ & IOANNIDES, N. 1973. Silurian palynomorphs from the Tannezuft and Acacus Formations, Tripolitania, North Africa. *Micropaleontology* **19**, 257–307.

_____ & LISTER, T.R. 1969. Upper Silurian and lower Devonian spore assemblages from the Welsh borderland and south Wales. Palaeontology, **12** (2), 201-245.

_____ & MCGREGOR, D.K. 1986. Silurian and Devonian spore zones of the Old Red Sandstone Continent and adjacent regions. Geological Survey of Canada, Bulletin **364**, 1– 79.

_____ & RASUL, S.M. 1978. Palynomorphs in Lower Devonian sediments from the Apley Barn Borehole, southern England. Pollen et Spores 20, 423–462.

_____ STREEL, M., HASSAN, A. & STEEMANS, P. 1982. A new spore assemblage to correlate between the Breconian (British Isles) and the Gedinnian (Belgium). Annales de la Société géologique de Belgique, **105**,135-143.

_____ FORD, J.H. & PARKER, F. 1984. Miospores, correlation and age of some Scottish Lower Old Red Sandstone sediments from the Strathmore region (Fife and Angus). Journal of Micropalaeontology, **3** (2), 109-124.

RICKARDS, R.B., 2000. The age of the earliest club mosses: the Silurian Baragwanathia flora in Victoria, Australia. Geological Magazine, 137(2), pp.207-209.

_____, RODRIGUEZ, R.M., SUTHERLAND, S.J.E. 2001. Palynological zonation of Mid-Palaeozoic sequences from the Cantabrian Mountains, NW Spain: implications for inter-regional and interfacies correlation of the Ludford/Přídolí and Silurian/Devonian boundaries, and plant dispersal patterns. Bulletin of the Natural History Museum London (Geology) **57**, 115–162.

RODRIGUEZ, 1983. [Palynology of the lower Devonian upper Silurian formations of the Cantabrian mountain range]. Servicio de Publicaciones, Universidad de Leon. 1 – 231. [In Spanish].

ROGERSON ECW, EDWARDS D, DAVIES KL, RICHARDSON JB. 1993. Identification of in situ spores in a Silurian Cooksonia from the Welsh Borderland. In Studies in Palaeobotany and Palynology in Honour of Professor W. G. Chaloner, F. R .S., COLLINSON ME, SCOTT AC (eds).Special Papers in Palaeontology49: 17–30

ROYER, D.L., 2001. Stomatal density and stomatal index as indicators of paleoatmospheric CO2 concentration. Review of Palaeobotany and Palynology, 114(1-2), pp.1-28.

RUBINSTEIN, C.V., 1995. Acritarchs from the upper Silurian of Argentina: their relationship with Gondwana. Journal of South American Earth Sciences, 8(1), pp.103-115.

_____ & STEEMANS, P., 2002. Miospore assemblages from the Silurian–Devonian boundary, in borehole A1-61, Ghadamis Basin, Libya. Review of Palaeobotany and Palynology, 118(1-4), pp.397-421.

_____, MELO, J.H.G. AND STEEMANS, P., 2005. Lochkovian (earliest Devonian) miospores from the Solimões Basin, northwestern Brazil. Review of Palaeobotany and Palynology, 133(1-2), pp.91-113.

_____, LE HÉRISSÉ, A. AND STEEMANS, P., 2008. Lochkovian (Early Devonian) acritarchs and prasinophytes from the Solimões Basin, nortwestern

Brazil. Neues Jahrbuch für Geologie und Palaontologie. Abhandlungen, 249(2).

RUDWICK, J.S. 1985. The Great Devonian Controversy: The Shaping of Scientific Knowledge among Gentlemanly Specialists. First edition. University of Chicago Press. Chicago, USA.

SALAMON, S.A., GERRIENNE, P., STEEMANS, P., GORZELAK, P., FILLIPIAK, P., HÉRISSÉ A, L.E., PARIS, F., CASCALES-MIÑANA, B., BRACHANIEC, T., MISZ-KENNAN, M., NIEDZWIEDZKI, R., 2018. Putative late Ordovician land plants. New Phytol. 218, 1305–1309.

SÄVE-SÖDERBERGH, G., 1941. Remarks on Downtonian and related Vertebrate Faunas. Geologiska Föreningen i Stockholm Förhandlingar, 63(3), pp.229-244.

SCHOFIELD, D., 2009. What's in the Welsh Basin? Insights into the evolution of Central Wales and the Welsh Borderlands during the Lower Palaeozoic. Proceedings of the Shropshire Geological Society, 14, pp.1-17.

SHEN, Z., MONNET, C., CASCALES-MINANA, B., GONG, Y., DONG, X., KROECK, D.M. AND SERVAIS, T., 2020. Diversity dynamics of Devonian terrestrial palynofloras from China: Regional and global significance. Earth-Science Reviews, 200, p.102967.

SMITH, C.A., AINSWORTH, D.M., HENDERSON, K.S. AND DEMPSEY, J.A., 1989. Differential responses of expiratory muscles to chemical stimuli in awake dogs. Journal of Applied Physiology, 66(1), pp.384-391.

SMITH, A.H.V. AND BUTTERWORTH, M.A. 1967. Miospores in the coal seams of the Carboniferous of Great Britain. Special papers in Palaeontology, **1**, 111 – 129. 4 pls.

SIMON, J.B. AND BLUCK, B.J., 1982. Palaeodrainage of the southern margin of the Caledonian mountain chain in the northern British Isles. Earth and Environmental Science Transactions of The Royal Society of Edinburgh, 73(1), pp.11-15.

SOLLAS, W. J. 1879. On the Silurian district of Rhymney and Pen-y-Lan, Cardiff. Q. *J. Geol. Soc. London*, Vol. 35, 475–507.

SOPER, N.J. AND WOODCOCK, N.H., 2003. The lost Lower Old Red Sandstone of England and Wales: a record of post-Iapetan flexure or Early Devonian transtension?. Geological Magazine, 140(6), pp.627-647.

SPINA, A. AND VECOLI, M., 2009. Palynostratigraphy and vegetational changes in the Siluro-Devonian of the Ghadamis Basin, North Africa. Palaeogeography, Palaeoclimatology, Palaeoecology, 282(1-4), pp.1-18.

STEEMANS 1989. [Palynostratigraphic study from the Lower Devonian in Western Europe]. Mém. Expl. Cartes Géologiques et Minières de la Belgique, **27**, 1 – 453. 47 pls. [In French].

_____ & GERRIENNE, P. 1984. La micro- et macroflore du Gedinnien de la Gileppe, Synclinorium de la Vesdre, Belgique. Annales de la Societ´ e g´ eologique de Belgique ´ 107, 51–71.

_____ & LAKOVA, I., 2004. The Moesian Terrane during the Lochkovian—a new palaeogeographic and phytogeographic hypothesis based on miospore assemblages. Palaeogeography, Palaeoclimatology, Palaeoecology, 208(3-4), pp.225-233.

_____, LE HÉRISSÉ, A. AND BOZDOGAN, N., 1996. Ordovician and Silurian cryptospores and miospores from southeastern Turkey. Review of Palaeobotany and Palynology, 93(1-4), pp.35-76.

_____, WELLMAN, C.H. AND FILATOFF, J., 2007. Palaeophytogeographical and palaeoecological implications of a miospore assemblage of earliest Devonian (Lochkovian) age from Saudi Arabia. Palaeogeography, Palaeoclimatology, Palaeoecology, 250(1-4), pp.237-254.

_____, RUBINSTEIN, C. AND DE MELO, J.H.G., 2008. Siluro-Devonian miospore biostratigraphy of the Urubu River area, western Amazon Basin, northern Brazil. Geobios, 41(2), pp.263-282.

STREEL, M. 1964. [A combination of spores of the lower Givetian of the vesdre, a goe (Belgium)]. Ann. Soc. Geol. de Belgique, **87**, 1 – 30. 2 pls. [In French].

_____1967. Spore associations of the Belgian Lower Devonian and their stratigraphic significance. Ibid. **90**, 11 – 54. 5 pls.

STREEL, M. AND BLESS, M.J.M., 1980. Occurrence and significance of reworked palynomorphs. Mededelingen-Rijks Geologische Dienst, 32(10).

_____, FAIRON-DEMARET, M., OTAZO-BOZO, N. AND STEEMANS, P., 1981. Etude stratigraphique des spores du Dévonien inférieur au bord sud du Synclinorium de Dinant (Belgique) et leurs applications. Annales de la Société Géologique de Belgique, 104.

_____ HIGGS, K., LOBOZIAK, S., RIEGEL, W. & STEEMANS, P. 1987. Spore stratigraphy and correlation with faunas and floras in the type marine Devonian of the Ardenne-Rhenish regions. Review of Palaeobotany and Palynology, **50** (3), 211-229.

STROTHER, P.K. 1991. A classification schema for the cryptospores. Palynology, **15** (1), 219-236.

_____ & TRAVERSE, A. 1979. Plant microfossils from Llandoverian and Wenlockian rocks of Pennsylvania. Palynology, **3** (1), 1-21.

TIAN, J., ZHU, H., HUANG, M. AND LIU, F., 2011. Late Silurian to Early Devonian palynomorphs from Qujing, Yunnan, southwest China. Acta Geologica Sinica-English Edition, 85(3), pp.559-568.

TORSVIK, T.H. AND COCKS, L.R.M., 2013. Gondwana from top to base in space and time. Gondwana Research, 24(3-4), pp.999-1030.

TURNAU, E., 1986. Lower to mid Devonian spores from the vicinity of Pionki (Central Poland). Review of Palaeobotany and Palynology, 46(3-4), pp.311-354.

_____ & JAKUBOWSKA, L., 1989. Early Devonian miospores and age of the Zwoleń Formation (Old Red Sandstone facies) from Ciepielów IG-1 borehole. In Annales Societatis Geologorum Poloniae (Vol. 59, No. 3-4, pp. 391-416).

_____, MIŁACZEWSKI, L. AND WOOD, G.D., 2005. Spore stratigraphy of Lower Devonian and Eifelian (?), alluvial and marginal marine deposits of the Radom-Lublin area (central Poland). In Annales Societatis Geologorum Poloniae (Vol. 75, No. 2, pp. 121-137).

TURNER, S., 1973A. Siluro-Devonian thelodonts from the Welsh borderland. Journal of the Geological Society, 129(6), pp.557-582.

_____, 1973. Appendix of locality data associated with 'Siluro-Devonian thelodonts from the Welsh Borderland'. Journal of the Geological Society of London, 129, pp. 557-584.

_____, 1984. Studies of Palaeozoic Thelodonti (Craniata: Agnatha). 2 vols. Unpublished Ph.D. Thesis. University of Newcastle-upon-Tyne.

_____., VERGOOSSEN, J.M.J. & WILLIAMS, R.B. 1995. Early Devonian from Pwll-Y-Wrach Talgarth, South Wales. Geobios Mémoire Spécial, 19. pp. 377-382

_____, BURROW, C.J., WILLIAMS, R.B. AND TARRANT, P., 2017. Welsh Borderland bouillabaisse: Lower Old Red Sandstone fish microfossils and their significance. Proceedings of the Geologists' Association, 128(3), pp.460-479.

Van der Zwan, C.J., 1980. Aspects of late devonian and early carboniferous palynology of southern Ireland. II. The Auroraspora macra morphon. Review of Palaeobotany and Palynology, 30, pp.133-155.

Veevers, S.J. & Thomas, A.T. 2011. The Ludlow Bone Bed and contiguous strata, Ludford CornerD.C. Ray (Ed.), Siluria Revisited: A Field Guide. International Subcommission on Silurian Stratigraphy, Field Meeting 2011, pp. 75-81.

VIGRAN, J. 1964. Spores from Devonian deposits: Mimerdalen, Spitzbergen. Skr. Norsk Polarinst. **132**, 1 – 30. 6 pls.

WALMSLEY, V.G., 1958. The geology of the Usk inlier (Monmouthshire). Quarterly Journal of the Geological Society, 114(1-4), pp.483-521.

WANG, Y., ZHU, H.C. AND LI, J., 2005. Late Silurian plant microfossil assemblage from Guangyuan, Sichuan, China.

WELLMAN, C.H., 1993. A Lower Devonian sporomorph assemblage from the Midland Valley of Scotland. Earth and Environmental Science Transactions of The Royal Society of Edinburgh, 84(2), pp.117-136.

_____., 1994. "Palynology of the 'Lower Old Red Sandstone'at Glen Coe, Scotland." Geological Magazine 131, 4. : 563-566.

_____., 1999. Sporangia containing Scylaspora from the lower Devonian of the Welsh Borderland. Palaeontology, 42(1), pp.67-81.

_____. 2009. Ultrastructure of dispersed and in situ specimens of the Devonian spore Rhabdosporites langii: Evidence for the evolutionary relationships of progymnosperms. Palaeontology, **52** (1), 139-167.

_____ & RICHARDSON, J.B. 1993. Terrestrial plant microfossils from Silurian inliers of the Midland Valley of Scotland. Palaeontology, **36** (1), 155-193.

_____ & RICHARDSON, J.B. 1996. Sporomorph assemblages from the Lower Old Red Sandstone of Lorne, Scotland. Special Papers in Palaeontology, **55**, 41-102.

_____. & RIDING, J.B., 2022. John Brian Richardson (1935–2021). Palynology, pp.1-5.

_____ EDWARDS, D, & AXE, L. 1998B. Ultrastructure of laevigate hilate spores in sporangia and spore masses from the Upper Silurian and Lower Devonian of the Welsh Borderland. Philosophical Transactions of the Royal Society London B, 353, 1983– 2004.

_____ HABGOOD, K., JENKINS, G. & RICHARDSON, J.B. 2000. A new plant assemblage (microfossil and megafossil) from the Lower Old Red Sandstone of the Anglo–Welsh Basin: its implications for the palaeoecology of early terrestrial ecosystems. Review of Palaeobotany and Palynology, **109** (3-4), 161 – 196.

_____, BERRY, C.M., DAVIES, N.S., LINDEMANN, F.J., MARSHALL, J.E. AND WYATT, A., 2022. Low tropical diversity during the adaptive radiation of early land plants. Nature Plants, 8(2), pp.104-109.

WHITE, D E, AND LAWSON,J D. 1989. The Přídolí Series in the Welsh Borderland and south-central Wales. 131–141 in A Global Standard for the Silurian System. HOLLAND, C H, AND BASSETT, M G (editors).

WHITE, E.I., 1950. The vertebrate faunas of the lower Old Red Sandstone of the Welsh borders. Bulletin of the British Museum, 1, pp.51-67. Geological Series, No. 9 (Cardiff: National Museum of Wales.)

WICKHAM, H. 2016. ggplot2. Elegant Graphics for Data Analysis. Springer-Verlag New York.

WRIGHT, V.P. AND MARRIOTT, S.B., 1996. A quantitative approach to soil occurrence in alluvial deposits and its application to the Old Red Sandstone of Britain. Journal of the Geological Society, 153(6), pp.907-913.

XUE, J., WANG, Q., WANG, D., WANG, Y. AND HAO, S., 2015. New observations of the early land plant Eocooksonia Doweld from the Přídolí (Upper Silurian) of Xinjiang, China. Journal of Asian Earth Sciences, 101, pp.30-38.

Thesis Appendix 3

For sample data, locality and methods data see chapter II and thesis appendix 2.1.

Thesis appendix 3.1, 3.2 & 3.3 Species counts and ornament

Raw counts of palynomorphs are given in workbook:

In sheets:

- **3.1_raw_counts:** raw counts and presence of rare spp. (+).
- **3.2_ornament_groups:** gross ornament after Richardson (2007).
- **3.3_ornament:** proximal and distal ornament after Grebe (1971).

Thesis appendix 3.4: Code scripts

Code scripts for graphical outputs on R version 4.1.3 (2022-03-10) - "One Push-Up" (R core team, 2022) are provided. In addition to `Base R`, `library ("rioja")`, `library("vegan")`, `library("ggplot2")` and `library("ggpubr")` are utilised. The scripts are intended to be user friendly and data can be found in associated appendices.

Mean relative abundance line graph on `Library("ggplot2")`

```
# this is a line plot for spp richness in
ggplot2 by Alexander C. Ball

install.packages("ggplot2")
library("ggplot2")

setwd("C:/Users/AlexB/Documents/AB
PhD/Research/Spores/Final counts/count
data/A1 Final data/.CSV")

AWBsp.raw <- read.csv("crypto_mio_MRA.csv")

AWBsp.raw <- AWBsp.raw[-1]

head(AWBsp.raw)

>    Spore     Biozone MRA
```

```
1    Miospores     mMN 72.97561
2    Miospores     lMN 74.37156
3    Miospores    NTPA 63.84427
4    Miospores      TS 61.26797
5    Miospores      PL 70.68012
6 Cryptospores     mMN 27.02439

ggplot(data = AWBsp.raw, aes(x=  Biozone,
y= MRA, group =  Spore)) +
  geom_line(aes(linetype=  Spore, colour =
Spore), size = 1.2) +
  geom_point(aes(color=Spore), size = 2) +
  scale_y_continuous(limits = c(0, 100)) +
  ggtitle("Mean relative abundance of
cryptospores and miospores")  +

scale_x_discrete(limits=c("mMN","lMN","NTPA
", "TS", "PL")) +
  ylab("Mean relative abundance") +
  scale_linetype_manual(values=c("solid",
"twodash"))+

scale_color_manual(values=c("gold2","forest
green")) +
  theme_bw() + theme(panel.border =
element_blank(), panel.grid.major =
element_blank(),
                     axis.text =
element_text(colour = "black"),
                     plot.title =
element_text(size = 10),
                     panel.grid.minor =
element_blank(), axis.line =
element_line(colour = "black"),
                     legend.position =
"top", text=element_text(color="black"))

++++++++++++++++++++++++++++++++++++++++++++++++++++++++++
```

Composite for biostratigraphy using library ("rioja") and library("vegan")

```
#this is a spore chart for composite
species ranges where spp. value > 2% and a
raup-crick dendrogram

setwd("C:/Users/AlexB/Documents/AB
PhD/Research/Biostratigraphy")

AWBsp.raw <-
read.csv("spore_counts_minor_coor.csv",
header = TRUE, row.names = 1, sep = ",",
check.names = FALSE)

#remove spores where % less than 2

AWB.sum <- colSums(AWBsp.raw) # calculate
column sums
AWB.spores1 <- AWBsp.raw[, which(AWB.sum >
4 )]
# subset data

# load rioja package

library("rioja")
library("vegan")


#define colour scheme

p.col <- c(rep("forestgreen", times =
47),rep("gold2", times = 33))
#define Y axis

y.scale <- 2:41

# plot bar plot

# create y names

fix(strat.plot) # line 157 for y.override,
add: my.xlabbt <- replace(xlabbt, grep("0",
xlabbt), NA)underneath line 249,
#and change labels = xlabbt to labels =
my.xlabbt on line 259

# edit x axis labels

fix(strat.plot)

y.override <- row.names(AWB.spores1)

# add curve to exagerrate low values

#ex <- c(rep(FALSE, times = 8), TRUE,
FALSE, TRUE, rep(FALSE, times = 5),
rep(TRUE, times = 10), FALSE, rep(TRUE,
times = 31),
       # rep(FALSE, times = 4), rep(TRUE,
times = 18), rep(FALSE, times = 2),
rep(TRUE, times = 2), FALSE, rep(TRUE,
times = 17))

# cluster analysis

ma.dist <- vegdist(AWB.spores1, method =
"raup", binary=FALSE, diag=FALSE,
upper=FALSE, na.rm = FALSE)

ma.chclust <- chclust(ma.dist, method =
"coniss")

#plot

pol.plot <- strat.plot(AWB.spores1, yvar =
y.scale, y.tks = y.scale, y.rev = TRUE,
                       plot.line = TRUE,
plot.poly = TRUE, plot.bar = TRUE, col.poly
= p.col, col.bar = "black", col.poly.line =
"black",
                       lwd.bar = 0.1,
scale.percent = TRUE, xSpace = 0.0001,
x.pc.lab = TRUE, x.pc.omit0 = TRUE,
```

```
                      las = 2, srt.xlabel
= 45, x.pc.inc = 5, cex.axis = 0.6,
cex.xlabel = 1, cex.ylabel = 0.05,
                     clust = ma.chclust)

# plot saved with dimensions 3000W x 1099

# As count_chart_dendrogram.tiff
# C:/Users/AlexB/Documents/AB
PhD/Research/Biostratigraphy
++++++++++++++++++++++++++++++++++++++++++++++++++++++++++
```

Composite miospore/ cryptospore ornaments using `library ("rioja")`

```
#this is a script for a composite
ornament chart

setwd("C:/Users/AlexB/Documents/AB
PhD/Research/Diversity -
disparity/Disparity new/orn_charts")
#tell R to read file, import data
cry.prox.raw <-
read.csv("cry_prox_orn.csv", header =
TRUE, row.names = 1, sep = ",",
check.names = FALSE)
cry.dist.raw <-
read.csv("cry_dist_orn.csv", header =
TRUE, row.names = 1, sep = ",",
check.names = FALSE)
mio.prox.raw <-
read.csv("mio_prox_orn.csv", header =
TRUE, row.names = 1, sep = ",",
check.names = FALSE)
mio.dist.raw <-
read.csv("mio_dist_orn.csv", header =
TRUE, row.names = 1, sep = ",",
check.names = FALSE)

mio.prox.raw <- mio.prox.raw[-16]

# load rioja package

library("rioja")

#define colour scheme

p.col.cry <- c("gold2")
p.col.mio <- c("forestgreen")
#define Y axis

y.scale <- 1:40

# plot bar plot

# create y names

fix(strat.plot) # line 157 for
y.override, add: my.xlabbt <-
replace(xlabbt, grep("0", xlabbt),
NA)underneath line 249,
#and change labels = xlabbt to labels
= my.xlabbt on line 259

# edit x axis labels

fix(strat.plot)

y.override <- row.names(cry.prox.raw)

#cry prox

prox.plot <- strat.plot(cry.prox.raw,
yvar = y.scale, y.tks = y.scale, y.rev
= TRUE,
                        plot.line =
TRUE, plot.poly = TRUE, plot.bar =
TRUE, col.poly = p.col.cry, col.bar =
"black", col.poly.line = "black",
                        lwd.bar = 0.1,
scale.percent = TRUE, xSpace = 0.01,
x.pc.lab = TRUE, x.pc.omit0 = TRUE,
las=2,
                        las = 2,
srt.xlabel = 45, x.pc.inc = 5,
cex.axis = 1, cex.xlabel = 1,
cex.ylabel = 0.05, title =
"Cryptospore proximal ornament")
# cry dist
prox.plot <- strat.plot(cry.dist.raw,
yvar = y.scale, y.tks = y.scale, y.rev
= TRUE,
                         plot.line =
TRUE, plot.poly = TRUE, plot.bar =
TRUE, col.poly = p.col.cry, col.bar =
"black", col.poly.line = "black",
                         lwd.bar = 0.1,
scale.percent = TRUE, xSpace = 0.01,
x.pc.lab = TRUE, x.pc.omit0 = TRUE,
las=2,
                         las = 2,
srt.xlabel = 45, x.pc.inc = 5,
cex.axis = 1, cex.xlabel = 1,
cex.ylabel = 0.05, title =
"Cryptospore distal ornament")


# mio prox
prox.plot <- strat.plot(mio.dist.raw, yvar = y.scale,
y.tks = y.scale, y.rev = TRUE,
                       plot.line = TRUE, plot.poly =
TRUE, plot.bar = TRUE, col.poly = p.col.mio, col.bar
= "black", col.poly.line = "black",
```

```
                        lwd.bar = 0.1, scale.percent
= TRUE, xSpace = 0.01, x.pc.lab = TRUE, x.pc.omit0 =
TRUE, las=2,
                        las = 2, srt.xlabel = 45,
x.pc.inc = 5, cex.axis = 1, cex.xlabel = 1,
cex.ylabel = 0.05, title = "Trilete spore distal
ornament")


# mio prox
prox.plot <- strat.plot(mio.prox.raw, yvar = y.scale,
y.tks = y.scale, y.rev = TRUE,
                        plot.line = TRUE, plot.poly =
TRUE, plot.bar = TRUE, col.poly = p.col.mio, col.bar
= "black", col.poly.line = "black",
                        lwd.bar = 0.1, scale.percent
= TRUE, xSpace = 0.01, x.pc.lab = TRUE, x.pc.omit0 =
TRUE, las=2,
                        las = 2, srt.xlabel = 45,
x.pc.inc = 5, cex.axis = 1, cex.xlabel = 1,
cex.ylabel = 0.05, title = "Trilete spore proximal
ornament")
```

Supplementary systematics section

Species outlined here are distinct enough to be initially described, but are not included in the main systematics section as they have not been recovered in sufficient numbers for formal description.

Anteturma SPORITES Potonié 1893
Turma TRILETES Reinsch 1891
Subturma AZONOTRILETES Luber 1935
Infraturma LAEVIGATI (Bennie and Kidston) Potonié and Kemp 1954

Genus RETUSOTRILETES (Naumova) Richardson 1965 non. Streel 1964

***Retusotriletes* sp. 1**

Plate i figure a

STRATIGRAPHIC RANGE: Non-tripapillate *Aneurospora* spp. zone; *Apiculiretusispora* sp. E subzone.

DESCRIPTION: 42µm (one specimen measured), large subtriangular trilete spore with rounded apices and convex sides. Proximally and distally laevigate. Subequatorial curvaturae, 1µm wide, small invagination where triradiate mark diverges. The laesurae extend 9/10 of the spore radius. The triradiate mark has distinct laesurae with tall membranous lips which extend 4/5 of the length of the laesurae. Exine thick.

COMPARISON AND REMARKS: The wide curvaturae perfectae and membranous lips differentiate this species.

***Retusotriletes* sp. 2**

Plate i figure b

STRATIGRAPHIC RANGE: Non-tripapillate *Aneurospora* spp. zone; *Apiculiretusispora* sp. E subzone.

DIAGNOSIS: 42µm (one specimen measured), subcircular amb. Proximally and distally laevigate with indistinct trilete mark, extending ¾ of spore radius and diverging into fine curvaturae perfectae. Inside of curvaturae are roughly semi-circular, discrete thickenings (?)verrucae which are confined to the inner edge of the curvaturae.

COMPARISONS AND REMARKS: The discrete thickenings on the proximal face distinguish this species.

***Retusotriletes* sp. 3**

Plate i figure c

STRATIGRAPHIC RANGE: Lower to middle *micrornatus – newportensis* subzone.

DESCRIPTION: 29 - 33µm (two specimens measured), roundly triangular amb. Circular contact face delimited by curvaturae perfectae. Triradiate mark is distinct, accompanied by lips 1µm wide, 17-19µm long, extending 9/10 of the spore radius. The well-developed curvaturae perfectae are nearly confluent with the equator. Where the Y-rays diverge into the curvaturae perfectae, there is no invagination of the latter. Proximally and distally laevigate.

COMPARISONS AND REMARKS: This species is reminiscent of *R.* cf. *minor* in terms of morphology and amb size, but is distinguished by sharp 'T' junctions where the Y-rays diverge into curvaturae perfectae. Reminiscent of *R.* cf. *minor* Kedo except that species exhibits invagination where the triradiate mark diverges into the curvaturae perfectae.

***Retusotriletes* sp. 4**

Plate i figure d

STRATIGRAPHIC RANGE: *Tripapillatus* - *spicula* biozone

Diagnosis: Subcircular amb and a distinct triradiate mark, accompanied by narrow lips. Subequatorial curvaturae perfectae delimit the contact area, which exhibits fine, randomly orientated rugulae or folds which form a well-developed reticulum. Distally, the spores are laevigate.

Description: 30 – 42μm, mean 35μm (five specimens measured). Amb subcircular to subtriangular. The contact face is delimited by fine, subequatorial curvaturae perfectae which diverge from straight sutures. The triradiate mark is accompanied by narrow lips <1μm wide. The interadial areas are ornamented with fine, randomly orientated rugulae or folds, <1μm wide, which form a well-developed 'reticulum', with lumen 1 - 4μm wide and 1 - 10μm long. Distally, the spores are laevigate.

Comparisons and remarks: These specimens are reminiscent of *Retusotriletes charulatus* McGregor and Narbonne (1978) in terms of compare well with the original specimen described in Burgess and Richardson (1995) in terms of amb size and general characteristics. However, in that species the contact face exhibits discontinuous folds/ rugulae which do not form a reticulum. Hence, the well-developed proximal reticulum distinguishes this species.

The muri/folds on the proximal face distinguish this species, but they are not known to be ornament or later formed folds in the exine. The former is tentatively favoured as they are (1) confined to the proximal face, and (2) continuous and somewhat regular. Despite having well defined curvaturae perfectae, the folds appear to extend beyond them, sometimes to an equatorial extent.

Infraturma APICULATI (Bennie and Kidston) Potonié and Kremp 1954

Genus APICULIRETUSISPORA Streel 1964

***Apiculiretusispora* sp. 1**

Plate i figures e – f

Stratigraphic range: Non-tripapillate *Aneurospora* spp. zone (*Apiculiretusispora* sp. E subzone) – lower *micrornatus – newportensis* subzone.

Diagnosis: 25 – 44μm, mean 36μm (four specimens measured). Circular to roundly subtriangular ambs. Proximally laevigate, with a distinct triradiate mark accompanied by wide lips, 2.1 - 3.8μm wide, mean 2.7μm. Lips extend ¾ to 9/10 of the radius of the amb, before diverging into curvaturae perfectae, which are often wide; these are sub-equatorial to equatorial in the interadial areas. There is no invagination at the juncture between the curvaturae and laesurae. Equatorially and distally ornamented by dense, stout cones and spines between 0.3 – 1.1μm tall, mean 0.6μm, and between 0.3 – 0.7μm wide, mean 0.5μm. elements are spaced 0.2 – 1.2μm apart, mean 0.5μm.

Comparisons and remarks: These spores are distinguished by the very wide lips accompanying the trilete mark. Elements are similar in dimension to *Apiculiretusispora spicula*, but it is distinguished by the wide lips and greater size range. Similarities are also found with *A. synorea*, but the elements lack the rapidly tapering spines and cones, and the lips are wider. There may be some cause to differentiate the species based on size, but this will require more data. Elements appear to correspond well across the specimens.

Infraturma MURORNATI Potonié and Kremp 1954

Genus EMPHANISPORITES McGregor 1961

***Emphanisporites* sp. 1**

Plate i figures g – h

Stratigraphic range: Non-tripapillate *Aneurospora* spp. zone (*Apiculiretusispora* sp. E subzone) – middle *micrornatus – newportensis* subzone.

Description: 15 – 21.5μm, mean 19.5μm (three specimens measured). Amb circular to subtriangular. Proximal face marked by 4 – 8

distinct, robust interadial muri which extend from proximal pole to equatorial margin. Muri taper distinctly towards the proximal pole. The triradiate mark is distinct, accompanied by lips. Distally laevigate.

Comparisons and remarks: Comparable to *E.* cf. rotatus in terms of size and general features, except the interadial muri in that species do not show a distinct taper. Differ from *E. rotatus* in terms of tapering muri and smaller size.

***Emphanisporites* sp. 2**

Plate i figure i

Stratigraphic range: Non-tripapillate *Aneurospora* spp. zone (*Apiculiretusispora* sp. E subzone) – lower *micrornatus* – *newportensis* subzone.

Description: 20 – 28µm, mean 25µm (nine specimens measured). Circular to roundly subtriangular amb. Proximally, the contact face is bounded by a thick crassitude, 2.3 – 3.8µm wide, mean 2.8µm. The interadial areas are ornamented by 8 – 16 variously distinct straight to slightly tapering muri which extend from the inner edge of the crassitude to the proximal apex, 0.4 – 0.9µm wide, mean 0.7µm. The triradiate mark is distinct, accompanied by lips 0.7 – 1.7µm wide, mean 1.2µm. Lips extend to near equatorial limits. Distally laevigate.

Comparisons and remarks: These spores differ from other species of *Emphanisporites* in terms of the wide crassitude. There may be cause to differentiate the species based on amb size but more specimens are required to confirm this, as apart from amb diameter there is little cause to differentiate the species (figures 9).

***Emphanisporites* sp. 3**

Plate i figures j – k

Stratigraphic range: Non-tripapillate *Aneurospora* spp. zone (*Aneurospora sheafensis* subzone) – lower *micrornatus* – *newportensis* subzone.

Diagnosis: 28.2 – 38.3µm, mean 31µm (five specimens measured). Circular to roundly triangular amb. proximally the contact areas are defined by distinct curvaturae perfectae, which bulge in the interadial areas. The triradiate mark is distinct but lack lips; they extend 2/3 to 4/5 of the amb radius before diverging into curvaturae perfectae with a distinctive invagination. Each interadial area exhibits 8 – 15 straight to slightly tapered interadial muri which extend from the curvaturae to the proximal pole. Muri are 0.4 – 1.4µm wide. Equatorially and distally laevigate.

Comparisons and remarks: These spores are distinctive by their bulging interadial areas. They differ from *E. epicautus* as they lack apical or y-ray thickenings and lips.

***Emphanisporites* sp. 4**

Plate i figures l – m

Stratigraphic range: Lower – middle *micrornatus* – *newportensis* subzones.

Diagnosis: 28.4 – 30.2µm (two specimens measured). Circular ambs. Proximal face exhibits distinct contact areas, marked by curvaturae perfectae. The triradiate mark is distinct but lacks lips. The laesurae extend 2/3 – 4/5 of the amb radius before diverging into curvaturae perfectae with no discernible invagination at the juncture. The interadial areas exhibit *c.* 13 interadial muri 0.5 - 1µm wide extending from the curvaturae to the apical pole. Outside of the contact areas the exine is laevigate.

Comparisons and remarks: Differs from *E.* sp. 4 as that species exhibits distinct invaginations at the laesurae – curvaturae perfectae juncture and the interadial areas bulge. The subtle interadial muri and circular amb may cause confusion with *Artemopyra inconspicuis*, however, that species is hilate and lacks a triradiate mark.

***Perotrilites* sp. 1**

Plate i figures n – o

Stratigraphic range: ?*tripapillatus* – *spicula* zone – middle *micrornatus* – *newportensis* subzone

Description: 31 - 38µm, mean 34.9µm (six specimens measured). Circular to subtriangular amb. The internal spore has a dark, laevigate exine and a distinct triradiate mark, which is sometimes accompanied by low lips, 2µm wide. The laesurae extend to the equator. The entire spore is enveloped by a very loosely adherent, crumpled laevigate

perine. About the triradiate mark, the perine is developed into accompanying folds.

COMPARISONS AND REMARKS: Distinguished by the small size and very loosely adherent perine.

***Perotrilites* sp. 2**

Plate i figure p

Stratigraphic range: Non-tripapillate *Aneurospora* spp. zone (*Apiculiretusispora* sp. E subzone) – lower *micrornatus* – *newportensis* subzone.

Description: Size 62-67µm (two specimens measured). These spores are essentially identical to *Perotrilites microbaculatus* var. *microbaculatus* except for the very coarse tuberculae, 1.1 – 4.3µm tall, mean 2.7µm and 0.9 – 3.5µm wide, mean 2µm. Some of the elements are distinctly gemmate.

Comparisons and remarks: The large size, loosely adherent perine and sculpture type associate these spores with var. *microbaculatus*, but the ornament is much coarser in these specimens. The ornament is much coarser, amb diameter larger and perine less adherent than in var. *attenuatus* despite the similarities with the former, these specimens are distanced from it by the very different perine sculpture.

Crassitate trilete spores

Subturma ZONOTRILETES Waltz 1935

Infraturma CRASSITI Bharadwaj and Venkatachala 1961

Genus AMBITISPORITES Hoffmeister 1959

***Ambitisporites* sp. 1**

Plate i, figure q

STRATIGRAPHIC RANGE: *tripapillatus* – *spicula* zone – lower *micrornatus* – *newportensis* subzone.

DESCRIPTION: Size 20.9 – 25.4µm, mean 23.5µm (five specimens measured). The contact areas are distinct, marked by a distinct crassitude 2.5 – 3.8µm wide, mean 3.35µm. The triradiate mark is distinct, accompanied by lips 0.7-2µm wide. These sometimes taper from the edge of the crassitude and dissipate out before reaching the apical pole; they extend to the equator. Proximally and distally laevigate.

COMPARISONS AND REMARKS: Somewhat comparable to *Ar. chulus* var. *nanus* Richardson and Lister in terms of the wide crassitude. However, in tipped specimens, it is clear that this thickening is confined to the equator. Additionally, the spore lacks a proximal concentric fold and diaphanous proximal exine, and is not patinate. Furthermore, lips extend across the crassitude to diverge equatorially. As such, this spore is grouped in *Ambitisporites*. Comparable to *Amb. Avitus – dilutus* Hoffmeister, except the crassitude is significantly wider than those spores (mean *A. avitus – dilutus:* 1.3µm, mean *A.* sp. 1: 3.35µm).

***Ambitisporites* sp. 2**

Plate i, figure r

STRATIGRAPHIC RANGE: *poecilomorphus – libycus* zone – middle *micrornatus – newportensis* subzone.

DESCRIPTION: Size 22 - 26µm (two specimens measured). triangular amb with rounded apices and convex sides. Distinct equatorial crassitude 1-2µm wide, exine thickest on equatorial crassitude. Proximal face laevigate, triradiate mark simple and lacking lips, rays extend to inner edge of the crassitude, laesurae extend to the equator. The spores have a notably thickened apical area, which is subcircular to subtriangular, extends approx. ¼ to ½ of the y-ray length. Distally laevigate.

COMPARISONS AND REMARKS: Comparable to *A. avitus – dilutus* except for the apical thickening; comparable to *R. triangulatus* except *A.* sp. 2 is significantly smaller, crassitate and has a triangular amb. These spores may be comparable to *Retusotriletes goensis* except these spores are crassitate.

Genus ANEUROSPORA (Streel) Richardson *et al.* 1982

***Aneurospora* sp. 1**

Plate i, figure s

STRATIGRAPHIC RANGE: Lower *micrornatus – newportensis* subzone.

DESCRIPTION: 26 – 33µm, mean 29.3µm (three specimens measured). Roundly triangular amb. Proximally ornamented with a reduced ornament of coni. The triradiate mark is simple, lacking lips. These extend 2/3 of the spore radius to the inner edge of the crassitude, which is up to 4µm wide,

marked by distinct inner edge. Distally ornamented with widely based spines up to 2um high, <1um wide at the base; densely and slightly irregularly ornamented across the distal exine (typically <1um between elements).

COMPARISONS AND REMARKS: Reminiscent of *Aneurospora sp.* A Wellman *et al* 2000, although the spines are much denser in these spores. The spines are also shorter than in *An.* cf. sp. A Wellman et al, which extend up to 3.0μm.

Aneurospora sp. 2

Plate i, figures t – u

STRATIGRAPHIC RANGE: Non-tripapillate *Aneurospora* spp. zone (*Apiculiretusispora* sp. E subzone) – middle *micrornatus* – *newportensis* subzone.

DESCRIPTION: 24 – 27μm, mean 25μm (three specimens measured). Roundly subtriangular amb. Proximally laevigate, with simple triradiate mark, laesurae extending to the equator. Distally ornamented with densely packed, sharply tipped microconi and microspinae, chiefly the former. Elements are 0.2 – 0.8μm tall, mean 0.4μm and 0.3 – 0.5μm wide, mean 0.4μm. Elements are 0.2 – 1μm apart, mean 0.4μm.

COMPARISONS AND REMARKS: Distinguished by the extremely dense microconi, reminiscent of *Cymbohilates allenii* var. *allenii*, although those spores are hilate cryptospores and do not show a triradiate mark.

?_Aneurospora_ 3

Plate ii, figures a – b

STRATIGRAPHIC RANGE: Non-tripapillate *Aneurospora* spp. zone (*Apiculiretusispora* sp. E subzone) – lower *micrornatus* – *newportensis* subzone.

DESCRIPTION: 37.9 – 42.4μm (two specimens measured). Roundly triangular amb, crassitude 3-4μm wide. The triradiate mark is distinct, accompanied by lips 1-2μm wide, extending to the inner edge of the crassitude. Proximally laevigate, equatorially and distally ornamented with sharply pointed coni, spinae and occasional baculae, which are unevenly distributed across the exine. Elements are 0.6 – 1.4μm tall, mean 0.8μm and 0.4 – 0.7μm wide, mean 0.5μm and 0.2 – 1.5μm apart, mean 0.8μm.

COMPARISONS AND REMARKS: Possibly verging on patinate given the robust equatorial thickening, but the structure appears to be crassitate. Differs from *Aneurospora sheafensis* in having a wider crassitude and spinose elements rather than cones but is similar in amb diameter and ornament distribution.

Aneurospora sp. 4

Plate ii, figures c – d

STRATIGRAPHIC RANGE: Lower – middle *micrornatus* – *newportensis* subzone.

DESCRIPTION: 16.8μm (one specimen measured). Proximal face lost but clear crassitude with invaginations where the triradiate mark intersects it. The crassitude is distinctive, 2μm wide. The spore is equatorially and distally ornamented by densely packed, rounded to pointed tipped spinae, some with a distinct tapering from the base to tip. Elements are 1 – 1.9μm tall, mean 1.5μm, and 0.4 – 0.9μm wide at the base, mean 0.67μm and 0.2 – 1.5μm apart, mean 0.64μm. In some cases, up to nine elements are arranged into discontinuous, meandering ridges up to 9.4μm long.

COMPARISONS AND REMARKS: It is difficult to fully resolve these spores without the proximal face, however the ornament of densely packed, wide based, slender spines differentiated this species. The character of the elements is somewhat similar to *A. gerreinnei*, except the elements are larger and spore amb diameter is smaller.

?_Aneurospora_ sp. 5

Plate ii, figure e

STRATIGRAPHIC RANGE: Lower *micrornatus* – *newportensis* subzone.

DESCRIPTION: 25.3μm (one specimen measured). Triangular amb with rounded apices and convex sides. Proximally ornamented with wide ± equally sized ?verrucae, rounded and up to 3μm wide. The triradiate mark is distinct, accompanied by robust lips 4μm wide which extend to the inner edge of the narrow crassitude. Equatorially and distally ornamented with round tipped grana-spinae, 1-2μm tall, 0.5 – 0.8μm wide, mean 0.6μm and 0.25 – 1.3μm apart, mean 0.66μm.

DESCRIPTION: The proximal ornament may be fungal in nature. The distal ornament is somewhat comparable to *A. trilabiata* however this spore differs as the lips are much more robust.

***Aneurospora* sp. 6**

Plate ii, figures f – g

STRATIGRAPHIC RANGE: Non-tripapillate *Aneurospora* spp. zone (*Apiculiretusispora* sp. E subzone) – middle *micrornatus* – *newportensis* subzone.

DESCRIPTION: 18 - 19µm (two specimens measured). Subtriangular to subcircular amb. Proximally laevigate, the triradiate mark is relatively indistinct but may be accompanied by narrow lips <1 wide. Equatorially and distally ornamented by round tipped ± isodiametric coni 0.4 – 0.6µm tall, 0.3 – 0.6µm wide, mean 0.4µm and 0.1 – 0.8µm apart, mean 0.45µm.

COMPARISONS AND REMARKS: Elements more rounded than in *A. isidori* or *A. trilabiata.*

***Aneurospora* sp. 7**

Plate ii, figures h – i

STRATIGRAPHIC RANGE: Non-tripapillate *Aneurospora* spp. zone (*Apiculiretusispora* sp. E subzone) – middle *micrornatus* – *newportensis* subzone.

DESCRIPTION: 17 - 24µm, mean 21µm (five specimens measured). Subcircular to subtriangular amb. Proximally laevigate. The triradiate mark is distinct, accompanied by narrow lips which extend to the inner edge of the crassitude. These spores are distally ornamented with variously sparse coni and spinae 0.4 – 0.7µm, tall mean 0.5µm, 0.2 – 1.3µm wide, mean 0.6µm and 0.2 – 1.1µm apart, mean 0.5µm.

COMPARISONS AND REMARKS: These spores are distinguished by their sparse cones and spines.

***Aneurospora* sp. 8**

Plate ii, figures j – k

STRATIGRAPHIC RANGE: Non-tripapillate *Aneurospora* spp. zone (*Apiculiretusispora* sp. E subzone) – middle *micrornatus* – *newportensis* subzone.

DESCRIPTION: 19 – 30µm, mean 23µm (five specimens measured). Triangular amb. Proximally laevigate with a distinct triradiate mark, accompanied by narrow lips which extend to the inner edge of the narrow crassitude. Equatorially and distally ornamented with small, dense microconi. Microconi are 0.4µm tall and 0.3 – 0.4µm wide, mean 0.37µm and 0.2 – 0.6µm apart, mean 0.32µm.

COMPARISONS AND REMARKS: Ornament denser than *A.* sp. 8 and does not exhibit spinae. The microconi are smaller than the coni exhibited on *A. isidori*, and these spores never exhibit interadial papillae. Some contemporaneous spores may be similar to *A.* sp. 8 but have circular ambs; these spores are referred to as *A.* cf. sp. 8.

***Aneurospora* sp. 9**

Plate ii, figures l – n

STRATIGRAPHIC RANGE: Lower - middle *micrornatus* – *newportensis* subzone.

DESCRIPTION: 29 – 31µm (two specimens measured). Proximally ornamented with reduced spinose ornament and distinct circular to oval interadial papillae 4 – 6µm long. The triradiate mark is indistinct and barely discernible, extending to the inner edge of the narrow crassitude. Equatorially and distally the exine is ornamented with robust, hooked spines 0.5 - 1.6µm tall and 0.3 - 0.7µm wide.

COMPARISONS AND REMARKS: Reminiscent of *Apiculiretusispora sceacga*, especially in terms of amb size and general character of ornament type and distribution. However, key differences exist in structure, with *Aneurospora* sp. 10 being crassitate, with equatorially diverging laesurae accompanied by subtle lips. Furthermore, subtle differences in the nature of the distal ornament exist, namely in the length and shape; *Ap. sceacga* generally exhibits sharply pointed spinae, whilst *An.* sp. 9 exhibits blunt tipped baculae and occasionally bulbous tipped spines. Perhaps most conclusively, *An.* sp. 9 does not exhibit the radial to tangential folds about the proximal face.

***Aneurospora* sp. 10**

Plate ii, figures o – p

STRATIGRAPHIC RANGE: Non-tripapillate *Aneurospora* spp. zone (*Apiculiretusispora* sp. E subzone) – middle *micrornatus* – *newportensis* subzone.

DESCRIPTION: 34 - 36µm (two specimens measured), subtriangular amb. Proximally laevigate. Distally ornamented with robust, hairlike spines with pointed tips and wide bases, which rapidly taper to pointed tips. Spines are 0.9 – 2.6µm tall, mean 1.8µm and 0.7 – 1.2µm wide, mean 1µm and 0.2 – 2.4µm apart, mean 0.9µm. Elements always remain discrete and do not form ridges. They often 'bend' and appear hair-like.

COMPARISONS AND REMARKS: The spines are larger and spaced farther apart than in *Aneurospora* sp. 10, and this species does not exhibit interadial papillae/ wedges.

***Aneurospora* sp. 11**

Plate ii, figure q

STRATIGRAPHIC RANGE: Lower *micrornatus* – *newportensis* subzone.

DESCRIPTION: 28.2 – 29.8µm (two specimens measured). Subcircular to subtriangular amb. Proximally laevigate except for ± subtriangular ('wedge shaped') proximal 'thickenings' in the interadial areas, 12.7 – 14.5µm in length. The triradiate mark is indistinct and often gaping, with laesurae extending to the equator. The spores are equatorially and distally ornamented by small, densely packed and irregularly arranged ± equidimensional cones, 0.4 – 0.7µm tall, mean 0.5µm, width 0.3 – 0.7µm, mean 0.5µm and 0.2 - 1.67µm apart, mean 0.5µm.

COMPARISONS AND REMARKS: Distinguished by the interadial, wedge like thickenings. Some spores may have their ornament sloughed off and appear to be laevigate but are distinguishable by their wedge-like interadial thickenings.

***Aneurospora* sp. 12**

Plate ii, figures r – s

STRATIGRAPHIC RANGE: Non-tripapillate *Aneurospora* spp. zone (*Apiculiretusispora* sp. E subzone) – lower *micrornatus* – *newportensis* subzone.

DESCRIPTION: 18.3 – 18.5µm (two specimens measured). Roundly subtriangular amb. Proximally laevigate with indistinct triradiate mark, with laesurae extending to the equator. Equatorially and distally ornamented with dense microconi, with are blunt to sharply tipped., 0.4 – 0.7µm tall, mean 0.5µm and 0.4 - 0.7µm wide at the base, mean 0.5µm and 0.2 – 0.9µm apart, mean 0.4µm. Evenly distributed.

COMPARISONS AND REMARKS: Denser ornament than *An. trilabiata*, *An. isidori* or other *Aneurospora* spp. Elements are coarser than *A.* sp. 8. *Aneurospora* sp. 7 does not exhibit a mixture of sharp and round tipped spines.

***Aneurospora* sp. 13**

Plate ii, figure t

STRATIGRAPHIC RANGE: Middle *micrornatus* – *newportensis* subzone.

DESCRIPTION: 28µm (one specimen measured). Circular amb. The crassitude is narrow and dark, 1µm wide. The spore is proximally laevigate, and slightly concave. The interadial areas exhibit distinct, circular inter radial papillae 5µm in diameter; they are arranged very close to the proximal pole. The spores are equatorially and distally ornamented by very fine, narrow micro-spinae, densely although irregularly arranged across exine. They are wide based, 0.4 – 0.6µm wide, mean 0.48µm, they taper rapidly into slender spines 0.4 – 0.7µm, mean 0.56µm. They are set 0.4 – 1.4µm apart, mean 0.9µm.

COMPARISONS AND REMARKS: This spore is distinguished by the closely spaced, circular interadial papillae and minute, irregular microspinae.

Genus SCYLASPORA Burgess and Richardson 1995

Genus SYNORISPORITES Richardson and Lister 1969

***?Synorisporites* sp. 1**

Plate iii, figure a

STRATIGRAPHIC RANGE: Lower MN biozone.

DESCRIPTION: 30µm (one specimen measured). Circular amb. The proximal face is laevigate aside from sparse, fine tangential ?folds or very narrow muri forming a wide reticulum. Possibly tripapillate although not certain. The triradiate mark is distinct and is accompanied by narrow lips <1 wide; extend to equator. Distally ornamented with low, rounded verrucae, sometimes coalesced to form ridges.

COMPARISONS AND REMARKS: The proximal muri may disassociate this species with *Synorisporites*. If these muri are confirmed, the spore should be moved to *Scylaspora*.

***Synorisporites* sp. 2**

Plate iii, figure b

STRATIGRAPHIC RANGE: Lower – middle *micrornatus* – *newportensis* subzone.

DESCRIPTION: 20 - 27µm (two specimens measured). Roundly triangular amb. Proximally, narrow lips accompany the triradiate mark which extends to the equator, slight tapering from the proximal pole to the narrow crassitude. One contact area appears smaller than the others, and subtle circular interadial papillae are developed in each. Distally, the spores are ornamented with short, narrow muri or folds which form discontinuous elongate ridges, but no reticulum.

COMPARISONS AND REMARKS: Comparable to *Ambitisporites tripapillatus* except for possible muri. The ornament could be folds in a diaphanous exine.

***Synorisporites* sp. 3**

Plate iii, figure c

STRATIGRAPHIC RANGE: Non-tripapillate *Aneurospora* spp. zone (*Apiculiretusispora* sp. E subzone) – middle *micrornatus* – *newportensis* subzone.

DESCRIPTION: 29.5 – 33.4µm, mean 31.4µm (five specimens measured). Subtriangular to triangular amb. Proximally, the spores are laevigate with a distinct triradiate mark, sometimes accompanied by narrow lips 0.9 – 1µm, which extend to the equator. Distally, the spores are ornamented with low, narrow and continuous muri 0.2 – 0.7µm wide, mean 0.4µm. These form a regular reticulum with lumen 0.3 – 3µm wide, mean 1.5µm.

COMPARISONS AND REMARKS: These spores are distinguished by the fine, distal reticulum.

***Synorisporites* sp. 4**

Plate iii, figure d

STRATIGRAPHIC RANGE: Lower *micrornatus* – *newportensis* subzone.

DESCRIPTION: 24µm (one specimen measured). Circular amb. The proximal face is concave and laevigate with a distinct triradiate mark accompanied by lips 2µm wide. The lips extend to the narrow crassitude at the equator. Distally, the spores are ornamented with distinctly radial, anastomosing verrucae and verrucate ridges, which are discontinuous and sometimes bifurcating. Verrucae are 1.9 – 6.3µm long, mean 0.9µm and 0.4 – 1.4µm wide, mean 0.6µm.

COMPARISONS AND REMARKS: These spores are defined by their distinctive, distally radial verrucae. The sculpture predominantly comprises discrete elements, distancing the species from *Stellatispora inframurinatus*; those spores are also patinate.

***Synorisporites* sp. 5**

Plate iii, figure e

STRATIGRAPHIC RANGE: Non-tripapillate *Aneurospora* spp. zone (*Apiculiretusispora* sp. E subzone) – lower *micrornatus* – *newportensis* subzone.

DESCRIPTION: 29.5µm (one specimen measured). Circular amb. Very narrow crassitude, proximally laevigate with a barely discernible, but lipless, triradiate mark. Distal exine markedly thin, ornamented by dense, thin and low muri <0.5µm which are radially arranged; these produce a radially arranged reticulum with long, narrow lumen up to 1µm wide and up to 7µm long.

COMPARISONS AND REMARKS: This spore is very similar to *Qualisaspora fragilis*, except that species does not exhibit a triradiate mark.

Genus CYMBOSPORITES Allen 1965

***Cymbosporites* sp. 1**

Plate iii, figure f

STRATIGRAPHIC RANGE: Non-tripapillate *Aneurospora* spp. zone (*Apiculiretusispora* sp. E subzone) – middle *micrornatus* – *newportensis* subzone

DESCRIPTION: 19 – 29µm, mean 25µm (four specimens measured). Circular amb. laevigate proximal face with simple triradiate mark extending to inner edge of wide crassitude. Distally and equatorially ornamented with sparse, low micro-

?grana. micrograna are 0.2 – 0.3µm tall, mean 0.23µm and 0.2 – 0.4µm wide, mean 0.3µm. The elements are irregular, and are spaced 0.3 – 1.6µm apart, mean 0.7µm.

COMPARISONS AND REMARKS: ? *C. catillus*; distinguished by sparse micrograna. Fold along the outer edge of the proximal face indicates that the spore is patinate.

***Cymbosporites* sp. 2**

Plate iii, figure g

STRATIGRAPHIC RANGE: Lower *micrornatus* – *newportensis* subzone.

DESCRIPTION: 24.4µm (one specimen measured). Circular amb. Proximally, the contact area is delimited by a thick crassitude, 2.8µm wide. The triradiate mark is distinct, accompanied by straight lips, 0.7 – 0.9µm wide. The lips extend to the inner edge of the crassitude. Proximally laevigate. Equatorially and distally ornamented by conspicuous verrucae. 0.6 – 1.3m tall, mean 0.8µm and 0.6 – 1.4µm wide, mean 1µm. Elements 0.3 – 1.3µm apart, mean 0.7µm.

COMPARISONS AND REMARKS: Spore distinguished by the robust equator and sculpture of rounded verrucae.

***Cymbosporites* sp. 3**

Plate iii, figures h – i

STRATIGRAPHIC RANGE: Non-tripapillate *Aneurospora* spp. zone (*Apiculiretusispora* sp. E subzone).

DESCRIPTION: 35µm (one specimen measured). Triangular amb. Patinate, wide crassitude 3 - 4µm wide. The triradiate mark is distinct, accompanied by lips which are 2.7 – 2.9µm, near equatorial in extent. Proximally, a reduced ornament of sparse grana and cones, 0.3µm wide and high. Distally and equatorially ornamented with blunt to sharply tipped spines 0.7 – 1.1µm tall, mean 0.95µm and 0.7 – 1.3µm wide, mean 1µm. The elements are taper rapidly from the base. Some elements are biform.

COMPARISONS AND REMARKS: Spore distinguished by the proximally reduced sculpture of spinae and distal ornament of distinct spinae.

***Cymbosporites* sp. 4**

Plate iii, figures j – k

STRATIGRAPHIC RANGE: Non-tripapillate *Aneurospora* spp. zone (*Apiculiretusispora* sp. E subzone) - Lower *micrornatus* – *newportensis* subzone.

DESCRIPTION: 28µm (one specimen measured). Triangular amb. Proximally laevigate with a wide crassitude and distinct triradiate mark, accompanied by narrow lips 1.5µm. The distal hemisphere is sculptured with coalesced, elongate, low verrucae, 2.8 – 7.4µm long, mean 4.3µm and 1.2 - 2µm wide, mean 1.6µm and <1µm apart, which bifurcate across the distal exine, and are ± radially arranged.

***Cymbosporites* sp. 5**

Plate iii, figures l – m

STRATIGRAPHIC RANGE: Lower *micrornatus* – *newportensis* subzone.

DESCRIPTION: 25µm (one specimen measured). Subtriangular amb with rounded apices and convex sides. Contact face bounded by a robust crassitude 2.4 – 2.6µm wide. The triradiate mark is distinct and is accompanied by lips 0.5 – 0.8µm, extending 9/10 of the spore radius, extending to the inner edge of crassitude. Equatorially and distally ornamented with a mixture of sharply- and rounded-tipped microconi typically 0.3 - 0.5µm tall and 0.4 – 0.9µm wide, mean 0.6µm. Elements irregularly arranged, 0.3 – 2µm apart, mean 0.6µm.

COMPARISONS AND REMARKS: Somewhat comparable to *Cymbosporites* sp. 1, although in this species the amb diameter and elements are larger.

***Cymbosporites* sp. 6**

Plate iii, figures n – q

STRATIGRAPHIC RANGE: Non-tripapillate *Aneurospora* spp. zone (*Apiculiretusispora* sp. E subzone) - Lower *micrornatus* – *newportensis* subzone.

DESCRIPTION: 22 - 33µm, mean 28µm (four specimens measured). Subcircular amb. Proximally laevigate with a robust crassitude, 2.9µm wide. The proximal face is distinctly concave. The triradiate mark is indistinct with narrow Y-rays. The rays extend to the inner edge of crassitude. Equatorially and distally, the spores are ornamented with very

dense, irregularly spaced microconi, 0.2µm tall and 0.2 - 0.5µm wide, mean 0.3µm and are set 0.1 – 0.8µm apart, mean 0.3µm.

COMPARISONS AND REMARKS: Distinguished by the very dense ornament, which is comparable to *Cymbohilates allenii*, except this species has a triradiate mark. *Aneurospora* sp. 2 is smaller and is crassitate, rather than patinate.

***Cymbosporites* sp. 7**

Plate iii, figures r

STRATIGRAPHIC RANGE: Middle *micrornatus* – *newportensis* subzone.

DESCRIPTION: 25 - 31µm (two specimens measured). Circular amb. Triradiate mark simple. Proximally laevigate. Distally and equatorially ornamented with dense, irregular microconi. Microconi are 0.4µm tall, 0.4 - 0.7µm wide, mean 0.5µm, and are set 0.3 – 1.4µm apart, mean 0.7µm.

COMPARISONS AND REMARKS: These ornament on these spores is less dense than on *Cymbohilates* sp. 6.

***Cymbosporites* sp. 8**

Plate iii, figure s

STRATIGRAPHIC RANGE: Middle *micrornatus* – *newportensis* subzone.

DESCRIPTION: 35.5µm (one specimen measured). Subtriangular amb. Proximally laevigate, with a distinct triradiate mark, accompanied by lips 2.3µm wide which extend to inner edge of the wide crassitude. Distally, the exine is ornamented with a mixture of grana and broad based tuberculae on equator and distal edge. These are scattered and irregular. Elements are 0.4 – 1.2µm tall, mean 0.8µm and 0.6 – 1.1µm wide, mean 0.8µm. The elements are between 0.4 – 1.3µm apart, mean 0.9µm.

***Cymbosporites* sp. 9**

Plate iii, figure t

STRATIGRAPHIC RANGE: Lower - middle *micrornatus* – *newportensis* subzone..

DESCRIPTION: 32µm (one specimen measured). Subtriangular amb. Proximal face thin, delicate, triradiate mark accompanied by lips, 1.8µm wide, which taper towards crassitude, which is 3µm wide. The spore is equatorially and distally ornamented with densely packed, small grana, often arranged into short ridges. Grana are <0.5µm tall, 0.3 – 0.7µm wide, mean 0.5µm and set 0.5 - 1µm apart, mean 0.8µm. Ridges are straight to curved, 1.6 – 2.4µm long, mean 0.9µm typically comprising three to six grana, joined by low ?muri.

***Cymbosporites* sp. 10**

Plate iii, figure u

STRATIGRAPHIC RANGE: Middle *micrornatus* – *newportensis* subzone.

DESCRIPTION: 23 – 29µm, mean 27µm (four specimens measured). Triangular amb with rounded apices and convex sides. Crassitude wide and robust, proximal face not seen but triradiate mark indications remain. Equatorially and distally ornamented with distinct, robust tuberculae with flat and rounded tips, 0.9 – 1.6µm tall, mean 1µm and 0.7 – 1.3µm wide, mean 1µm. Elements irregularly scattered, 0.3 – 1.8µm apart, mean 0.7µm.

COMPARISONS AND REMARKS: These spores may be comparable to *C. echinautus*, except the clusters of biform spinae and tuberculae are not present here. These spores are also smaller than those described in Richardson and Lister (1969).

***Cymbosporites* sp. 11**

Plate iv, figure a

STRATIGRAPHIC RANGE: Lower *micrornatus* – *newportensis* subzone.

DESCRIPTION: 24.4 – 34.3µm, mean 27.9µm (seven specimens measured). Subtriangular amb. Wide, robust crassitude. The proximal face is often lost, but where present is laevigate, often with a fold developed along the inner edge of the crassitude. The triradiate mark is distinct and is accompanied by lips 1 - 1.5µm wide, which extend to the inner edge of the crassitude. The spores are distally and equatorially ornamented with rounded to roundly-pointed equidimensional cones, densely and irregularly scattered. Elements are 0.4 – 1.3µm tall, mean 0.8µm and 0.4 – 1.7µm wide, mean 0.9µm and are set 0.2 – 1.5µm apart, mean 0.6µm.

***Cymbosporites* sp. 12**

Plate iv, figures b – c

STRATIGRAPHIC RANGE: Middle *micrornatus* – *newportensis* subzone.

DESCRIPTION: 33.2µm (one specimen measured). Triangular amb with rounded apices and convex sides. Proximally, these spores are laevigate, with the contact areas bounded by a robust crassitude 4µm wide. The triradiate mark is distinct, accompanied by narrow lips 1µm wide, extending to the inner edge of the crassitude. Equatorially and distally, the spore is ornamented with sparse, spinose elements arranged into star-like clusters. Clusters comprise of 3 – 4 spines, with individual spines being 1 – 1.8µm in length, mean 1.5µm. The spines are uniformly tapered, terminating with sharp tips. Elements are set 2.1 – 4.9µm apart, mean 3.5µm.

COMPARISONS AND REMARKS: The star-shaped ornament clusters are strongly reminiscent of *Cymbohilates cymosus*, except this specimen exhibits an unequivocal triradiate mark. In these specimens, it appears that, in some cases, the clusters are readily sloughed off or parted from the exine.

Genus CHELINOSPORA (Allen) McGregor and Camfield, 1976

***Chelinospora* sp. 1**

Plate iv, figure d

STRATIGRAPHIC RANGE: Lower *micrornatus* – *newportensis* subzone.

DESCRIPTION: 35µm (one specimen measured). Subtriangular amb with rounded apices and convex sides. Contact face bounded by a robust crassitude, 4µm wide. Proximally laevigate, the triradiate mark is distinct, accompanied by faint lips 1.5µm wide, which extend to inner edge of the crassitude. Equatorially and distally ornamented with a very fine, but well defined, irregular ?reticulum of tall, fine muri 0.6 – 1.4µm tall, mean 1µm and 0.4 – 0.6µm wide, mean 0.5µm, forming lumina *ca*.2.3 – 3.6µm wide, mean 2.9µm. In plan, the muri are flat topped and somewhat verrucate in appearance.

***Chelinospora* sp. 2**

Plate iv, figure e

STRATIGRAPHIC RANGE: Non-tripapillate *Aneurospora* spp. zone (*Apiculiretusispora* sp. E subzone).

DESCRIPTION: 42µm (one specimen measured). Subtriangular amb. Robust crassitude 5.8µm wide. Proximally laevigate, with a distinct triradiate mark, accompanied by robust lips, 2.7µm wide, tapering from the proximal pole to the inner edge of crassitude. Distally ornamented with low, continuous, and narrow muri 0.5 - 1µm wide, mean 0.7µm forming lumen up to 3 – 5.6µm wide, mean 4.3µm.

COMPARISONS AND REMARKS: These spores are reminiscent of *Dictyotriletes* spp., except this specimen is patinate.

***Chelinospora* sp. 3**

Plate iv, figures f – h

STRATIGRAPHIC RANGE: Lower - middle *micrornatus* – *newportensis* subzone.

DESCRIPTION: 34 - 39µm, mean 36.7µm (three specimens measured). Subcircular amb. Proximally laevigate, slightly concave. The triradiate mark is accompanied by lips 1µm wide which extend to inner edge of the crassitude. Equatorially and distally ornamented by low, narrow muri 0.3 – 0.6µm wide, mean 0.5µm which form a continuous reticulum. The muri delimit circular to oval lumina 0.6 – 3.6µm wide, mean 1.7µm.

COMPARISONS AND REMARKS: These spores are reminiscent of *Dictyotriletes* sp. A and *Synorisporites* sp. 3, except the latter is crassitate and the lumen in the former are much larger. The lumen width suggests that these spores may be further divisible (figures 12), and this is done so tentatively here. On the basis on lumen width, var. 1 has lumen <1.6µm and var. 2 has lumen >1.6µm. Muri widths are to be continuous between specimens.

***Chelinospora* sp. 4**

Plate iv, figure i

STRATIGRAPHIC RANGE: Middle *micrornatus* – *newportensis* subzone.

DESCRIPTION: 26.3µm (one specimen measured). Circular amb. The proximal face is laevigate, with the distinct triradiate mark accompanied by robust lips, 2.6µm wide. The lips extend to the inner edge of the wide crassitude. The spores are equatorially and distally ornamented with a regular reticulum, comprising wide muri 0.6 – 1.1µm wide, mean

0.9µm. These form a continuous reticulum which describe circular to elongate lumen, 0.8 – 2.6µm wide, mean 1.5µm.

COMPARISONS AND REMARKS: These spores have a wider crassitude and thicker muri than *C.* sp. 5.

***Chelinospora* sp. 5**

Plate iv, figure j

STRATIGRAPHIC RANGE: Lower *micrornatus* – *newportensis* subzone.

DESCRIPTION: 31µm (one specimen measured). Subcircular amb, wide crassitude 6µm wide. Proximal face appears to have been lost, some evidence of triradiate mark invagination. Equatorially and distally ornamented by low (0.5µm) globular verrucate-like muri 1 - 2µm wide and between 2-4µm long; these are coalesced, forming approximate ridges. The reticulum describes small, elongate to circular lumen, 0.3 – 0.8µm wide, mean 0.5µm and elongate examples are up to 1.6µm long.

COMPARISONS AND REMARKS: These spores are somewhat similar to *Chelinospora retorrida* except the muri are wider and lumen smaller and generally more circular. These spores also have a wider crassitude.

***Chelinospora* sp. 6**

Plate iv, figure k

STRATIGRAPHIC RANGE: Middle *micrornatus* – *newportensis* subzone.

DESCRIPTION: 31µm (one specimen measured), circular amb. Proximal face not seen but possible triradiate mark invaginations. Equatorially and distally ornamented with a mixture of discrete circular to polygonal verrucae and long, semi-continuous, sinuous and sometimes bifurcating verrucate ridges, which form a discontinuous reticulum. Elements are 1.4 – 5.7µm long, mean 3.2µm and 0.8 – 1.4µm wide, mean 1µm and up to 2.5µm tall. Where formed, lumen are narrow and long.

COMPARISONS AND REMARKS: These spores are differentiated by the mixture of elements (?verrucae and verrucate ridges) which form a discontinuous reticulum. This species is somewhat similar to *C. dittonensis*, except the elongate, muri-like verrucae are not seen in those spores.

***Chelinospora* sp. 7**

Plate iv, figure l

STRATIGRAPHIC RANGE: Middle *micrornatus* – *newportensis* subzone.

DESCRIPTION: 23.2µm (One specimen measured). Proximally laevigate, with an indistinct trilete mark, which extends to the inner edge of the crassitude, which is 2µm wide. There is a distinct fold along the inner edge of the crassitude. Equatorially, the spores are laevigate. Distally, a wide, continuous reticulum is developed. Muri are 1.5µm wide, with lumen up to 9.2µm wide.

COMPARISONS AND REMARKS: Chelinospora sp. 9 is defined by the very wide reticulum which is confined to the distal hemisphere. These spores are redolent of *Archaeozonotriletes chulus* var. *nanus* in terms of general structure and size, but are differentiated by the wide, well-developed reticulum on the distal hemisphere. These spores differ from species of *Dictyotriletes* as *Chelinospora* sp. 9 is patinate.

Cryptospores

ENVELOPED CRYPTOSPORES

Anteturma CRYPTOSPORITES Richardson, Ford and Parker 1984

Turma INVOLUCRALETES Richardson 1996a

Suprasubturma PSEUDOPOLYADI Richardson 1996a

Infraturma LAEVIGATI Richardson 1996a

Genus CHELIOTETRAS Wellman and Richardson, 1993

***?Cheliotetras* sp. 1**

Plate iv, figures m – n

STRATIGRAPHIC RANGE: Middle *micrornatus* – *newportensis* subzone.

DESCRIPTION: 43µm (one specimen measured). Large, permanent tetrads with a triangular outline, triangular comprising ‘spore’ units. Fused

crassitude, 4.6µm wide with flanges 6µm deep. The spore units have inflated distal surfaces, ornamented with dense micrograna, 0.4 – 1.2µm wide, mean 0.8µm and are set 0.4 – 1.6µm apart, mean 0.9µm.

COMPARISONS AND REMARKS: The micrograna distinguish this species from *C. caledonica*. The flanges distinguish this spore from *Acontotetras inconspicuis.*

Infraturma APICULATI Richardson 1996a

Genus CYMBOHILATES Richardson 1996a

***Cymbohilates* sp. 1**

Plate iv, figure o

STRATIGRAPHIC RANGE: *tripapillatus* – *spicula* zone – lower *micrornatus* – *newportensis* zone.

DESCRIPTION: 33.4µm (one specimen measured). Circular amb. Proximally, the hilum is laevigate and concave, 22.9µm across and marked by thickening 2µm wide. A narrow fold accompanies the inner edge of the hilum. Outside of the hilum, the spore is ornamented by cones and rare spines 0.6 - 2µm high, mean 1.1µm and 0.5 - 1µm wide, mean 0.8µm. The elements are set 0.2 – 1.5µm apart, mean 1.8µm. The cones are chiefly pointed, tapering evenly to a sharp point, but some are blunt.

***Cymbohilates* sp. 2**

Plate iv, figure p

STRATIGRAPHIC RANGE: Non-tripapillate *Aneurospora* spp. zone (*Apiculiretusispora* sp. E subzone).

DESCRIPTION: 50.2µm (one specimen measured). Very dark exine, proximal face not clear. Distally ornamented with very dense spinae (essentially side-by-side) blunt to sharp tipped, up to 2µm tall and 1µm wide.

COMPARISONS AND REMARKS: Ornament reminiscent of *Ap.* sp. E but proximal face appears hilate. These spores are also much larger.

***Cymbohilates* sp. 3**

Plate v, figure a

STRATIGRAPHIC RANGE: Lower - middle *micrornatus* – *newportensis* subzone.

DESCRIPTION: 45.8µm (one specimen measured). Subtriangular amb. Proximally laevigate, with a large hilum 37µm across. The spore appears to be double layered, with the outer layer partially separated from the inner exine outside of the hilum. The exine outside of the hilum is densely ornamented with a mixture of sharply pointed and blunt tipped cones and rare tuberculae. Elements are 0.9 – 1.8µm high, mean 1.1µm and 0.4 – 1µm wide, mean 0.7µm. The elements are set 0.3 – 1.2µm apart, mean 0.7µm.

COMPARISONS AND REMARKS: These spores are distinctive by their dense, mixed ornament and large size.

***Cymbohilates* sp. 4**

Plate v, figure b

STRATIGRAPHIC RANGE: Lower *micrornatus* – *newportensis* subzone

DESCRIPTION: 32.2µm (one specimen measured). Circular amb. Proximally laevigate with a wide hilum. Outside of the hilum, the exine is ornamented with closely arranged spinae, 1 – 2.3µm high, mean 1.6µm and 0.4 – 0.8µm wide, mean 0.6µm. The elements are set 0.7 – 2.6µm apart, mean 1.5µm. The elements are long and slender, sometimes sharply pointed and often biform with bulbous tips. Some elements occur as closely associated pairs.

COMPARISONS AND REMARKS: These spores are smaller than *C.* sp. 3 and have biform ornament, lacking the blunt tipped cones of that species. They may be comparable to *Cymbohilates* sp. A in Wellman *et al.* (2000) but those spores have a granular hilum.

***Cymbohilates* sp. 5**

Plate v, figure c

STRATIGRAPHIC RANGE: Non-tripapillate *Aneurospora* spp. zone (*Apiculiretusispora* sp. E subzone).

DESCRIPTION: 41.9µm (one specimen measured). Proximal hilum laevigate, extends close to the equator. Outside of the hilum, a mixture of broad-based elements comprising biform and sharply-pointed cones and spines, chiefly the latter, and rare baculae are exhibited on the equator and distal hemisphere. Elements are 0.8 – 2.8µm in height, mean 1.5µm and 0.9 – 2.2µm in basal width, mean

1.5µm. The elements are irregularly scattered across the distal hemisphere, being set 0.5 – 3.8µm apart, mean 1.9µm.

***Cymbohilates* sp. 6**

Plate v, figure d

STRATIGRAPHIC RANGE: Lower *micrornatus* – *newportensis* subzone

DESCRIPTION: 33.5µm (one specimen measured). Circular amb, thin exine. Proximally microgranular with faint papillae 4.5 – 5.4µm in diameter. The hilum is 28.9µm across and slightly concave. Outside of the hilum, the exine is sculptured with developed with very dense, sharply pointed microconi, 03 – 0.6µm in height, mean 0.4µm and 0.5 – 0.8µm wide, mean 0.6µm. The cones are set 0.2 – 0.7µm apart, mean 0.4µm.

COMPARISONS AND REMARKS: Differs from *C. allenii* var. *allenii* due to proximal papillae and dense coni. In *C. allenii* var. *allenii* grana are developed. In terms of distal ornament, these spores are also similar to *C. disponerus* but that species lacks interadial papillae.

***Cymbohilates* sp. 7**

Plate v, figures e – f

STRATIGRAPHIC RANGE: Lower - middle *micrornatus* – *newportensis* subzone.

DESCRIPTION: 25.9µm (one specimen measured). Circular amb. Proximally, the hilum is marked by a wide crassitude. Along inner edge of the crassitude there are pear shaped to circular verrucae which taper towards the proximal pole and are sometimes coalesced; these elements are 1.1 – 2.2µm wide, mean 1.8µm. The proximal pole is laevigate. Outside of the hilum, the exine is ornamented with scattered, irregular micrograna <0.5µm tall and 0.4 – 0.9µm wide, mean 0.7µm. The elements are set 0.3 – 1.7µm apart, mean 1µm.

COMPARISONS AND REMARKS: Comparable to *Laevolancis* sp. 2 except for less continuous proximal verrucae and distal elements.

Infraturma SYNORATI Richardson 1996a

Genus CHELINOHILATES Richardson 1996a

***Chelinohilates* sp. 1**

Plate v, figure g

STRATIGRAPHIC RANGE: Middle *micrornatus* – *newportensis* subzone.

DESCRIPTION: 31µm (one specimen measured). Subcircular amb. Proximal face populated by small, circular to elongate pits, 0.2 –9 0.9µm wide, mean 0.6µm. The triradiate mark is indistinct, accompanied by lips 1µm wide, which extend to the inner edge of the crassitude. The equator is ornamented with radial muri, 3 – 6.5µm long, mean 4.43µm and 0.5 – 1.5µm wide, mean 0.8µm. The radial muri are regular, spaced 0.4 – 1µm apart, mean 0.7µm. The muri may coalesce and form a reticulum distally, but this is not certain.

COMPARISONS AND REMARKS: These spores are somewhat comparable to *Artemopyra radiata* Strother in terms of the radial 'muri' about the equator, except that these spores to have a well-formed reticulum on the distal hemisphere. They may be comparable to *C. erraticus*, except the hilum differs. They differ from *Chelinohilates* sp. 1 as they have tighter radial muri and may have a reticulum developed distally.

***Chelinohilates* sp. 2**

Plate v, figure h

STRATIGRAPHIC RANGE: Non-tripapillate *Aneurospora* spp. zone (*Aneurospora sheafensis* – *Apiculiretusispora* sp. E subzone)

DIAGNOSIS: 41 - 44µm (two specimens measured). Circular amb, thick exine, thickest at equator. Distally ornamented by very fine interconnected muri forming a very fine reticulum. Muri <1µm tall, <0.5µm wide. Lumen 2-3µm wide. Hilum laevigate.

***?Chelinohilates* sp. 3**

Plate v, figure i

STRATIGRAPHIC RANGE: Lower *micrornatus* – *newportensis* subzone.

DESCRIPTION: 54 - 62µm, mean 58.9µm (three specimens measured). Subcircular to subtriangular amb. Crassitude 2µm wide, but the hilum is lost in all cases. The distal exine is sculptured with robust, continuous muri 0.8 – 2.2µm wide, mean 1.4µm, describing polygonal to rectangular lumen 1.1 – 6.9µm.

COMPARISONS AND REMARKS: These spores are distinguished by their large size and robust, continuous reticulum. They differ from *C. lornensis* Wellman and Richardson as the amb diameter in these spores is much larger (*C. lornensis* does not exceed 42μm) and the lumina in these spores exceed the sizes given in Wellman and Richardson (1996), which measure between 1.5 – 2.5μm.

***Chelinohilates* sp. 4**

Plate v, figures j

STRATIGRAPHIC RANGE: *poecilomorphus – libycus* zone – lower *micrornatus – newportensis* subzone.

DESCRIPTION: 35μm (two specimens measured). ?Circular amb. Proximally, the laevigate hilum is 16μm across, marked by a thickened collar. Between the collar and the equator, radial verrucate ridges are exhibited. These verrucate ridges are1-3μm wide and up to 10μm long. They are typically elongate and slightly sinuous but are sometimes more discrete; the ridges never bifurcate. There is a distinctly thick crassitude. The spores appear to be distally laevigate.

Plate i

a: *R.* sp. 1, slide 19M5026.1, E.F. no. L24, Freshwater West Formation, Ross – Tewkesbury Spur Motorway (M50), Hereford and Worcester

b*: R.* sp. 2. Note the radial ?verrucae along the inner edge of the curvaturae perfectae. Slide BM/M50/85/2D-8, E.F. no. V29-3. Moor Cliffs formation, Ross – Tewkesbury Spur Motorway (M50), Hereford and Worcester;

c: *R.* sp. 4, slide M50-2-2, E.F. no. L12, Moor Cliffs formation, Ross – Tewkesbury Spur Motorway (M50), Hereford and Worcester.

d: *R.* sp. 5, slide M50/85/2H-4, E.F. no. C30-1. Moor Cliffs formation, Ross – Tewkesbury Spur Motorway (M50), Hereford and Worcester.

e – f: *A.* sp. 1. e: small specimens showing triangular ambs, slide M50-11-1, E.F. no. X35, Freshwater West Formation, Ross – Tewkesbury Spur Motorway (M50), Hereford and Worcester; f: Large specimen, showing circular amb and robust lips, slide M50-85-2D-2, E.F. no. H13-4, Moor Cliffs Formation, Ross – Tewkesbury Spur Motorway (M50), Hereford and Worcester.

g - h: *E.* sp. 1; g: slightly compressed specimen showing robust, strongly tapering interadial muri and robust lips, slide M50-5E-4, E.F. no. X33, Freshwater West Formation, Ross – Tewkesbury Spur Motorway (M50), Hereford and Worcester; h: slide M50-3-3, E.F. no. O52-2, Moor Cliffs Formation, Ross – Tewkesbury Spur Motorway (M50), Hereford and Worcester.

i: *E.* sp. 2, showing robust muri and crassitude, slide M50/85/2F-4, E.F. no. E18, Moor Cliffs Formation, Ross – Tewkesbury Spur Motorway (M50), Hereford and Worcester.

j – k: *E.* sp. 4; j: showing circular amb and well defined curvaturae perfectae, slide MPA25242-1, E.F. no. P34-3, Freshwater West Formation, Ammons Hill section, Shropshire; k: SEM micrograph 105482, M50-5H, Freshwater West Formation, Ross – Tewkesbury Spur Motorway (M50), Hereford and Worcester.

l – m: *E.* sp. 5, l: slide MPA25246-1, E.F. no. O29-3, Freshwater West Formation, Ammons Hill section, Shropshire; m: showing subtle interadial muri, slide M50-4-2, E.F. no. F38, Freshwater West Formation, Ross – Tewkesbury Spur Motorway (M50), Hereford and Worcester.

n – o: *Perotrilites* sp. 1 n: showing simple triradiate mark, slide 19M5028-1, E.F. no. T25-4, Freshwater West Formation, Ross – Tewkesbury Spur Motorway (M50), Hereford and Worcester; o: showing triradiate mark accompanied by lips, slide M50-7-1, E.F. no. W32, Freshwater West Formation, Ross – Tewkesbury Spur Motorway (M50), Hereford and Worcester

p: *Perotrilites* sp. 2, showing gemmate elements, slide M50/8/2, E.F. no. S47-1, Freshwater West Formation, Ross – Tewkesbury Spur Motorway (M50), Hereford and Worcester.

q: *Ambitisporites* sp. 1 showing the thickened equator and thinner distal hemisphere, slide M50-3-2, E.F. no. M25-1, Moor Cliffs Formation, Ross – Tewkesbury Spur Motorway (M50), Hereford and Worcester.

r: *Ambitisporites* sp. 2, slide M50-3-2, E.F. no. M21-3, Moor Cliffs Formation, Ross – Tewkesbury Spur Motorway (M50), Hereford and Worcester.

s: *Aneurospora* sp. 1, slide 19M5001-3, E.F. no. D50-2, Freshwater West Formation, Ross – Tewkesbury Spur Motorway (M50), Hereford and Worcester.

t – u: *Aneurospora* sp. 2; t: proximal view, note the barely distinct triradiate mark, slide M50-5E-4, E.F. no. M52, Freshwater West Formation, Ross – Tewkesbury Spur Motorway (M50), Hereford and Worcester; u: distal, showing the fine, very dense ornament, slide M50-5E-4, E.F. no. M52, Freshwater West Formation, Ross – Tewkesbury Spur Motorway (M50), Hereford and Worcester.

Plate i

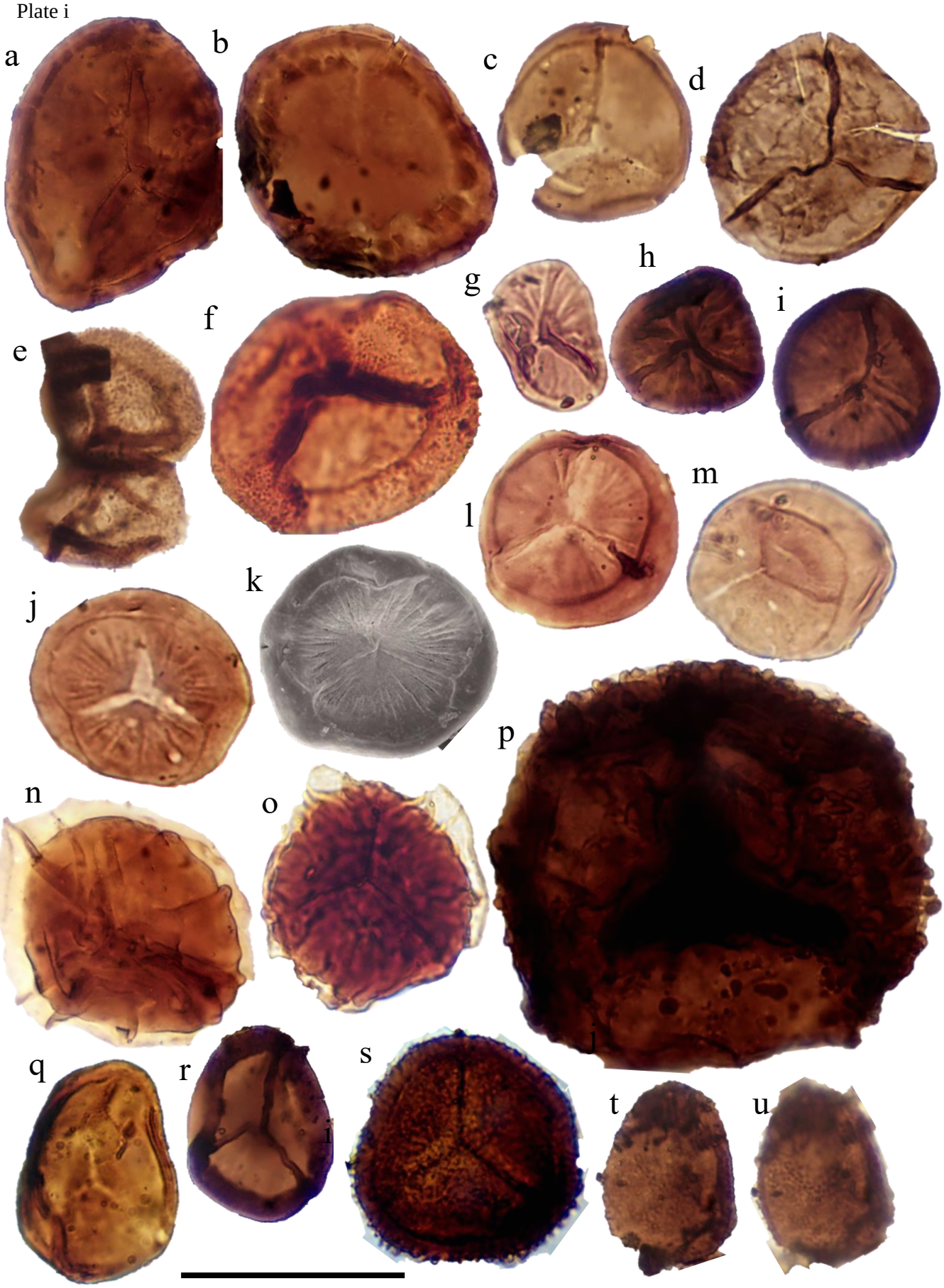

Plate ii

a – b: *Aneurospora* sp. 3; a: slide M50-3(2)-1, E.F. no. F21, Moor Cliffs Formation, Ross – Tewkesbury Spur Motorway (M50), Hereford and Worcester, b: slide M50-2-5, E.F. no. P52-4, Moor Cliffs Formation, Ross – Tewkesbury Spur Motorway (M50), Hereford and Worcester.

c – d: *Aneurospora* sp. 4; c: distal view, note densely packed elements and occasional ridges, slide 19M5027-1, E.F. no. P22, Freshwater West Formation, Ross – Tewkesbury Spur Motorway (M50), Hereford and Worcester; d: Proximal view, proximal face lost, note plan view of spines, slide 19M5027-1, E.F. no. P22, Freshwater West Formation, Ross – Tewkesbury Spur Motorway (M50), Hereford and Worcester;

e: *Aneurospora* sp. 5, 19M5026.2, E.F. no. G16-1, Freshwater West formation, Ross-Tewkesbury Spur (M50) motorway, Hereford and Worcester, UK.

f – g: *Aneurospora* sp. 6; f: showing indistinct triradiate mark, slide M50-5E-1, E.F. no. Q50-4, Freshwater West formation, Ross-Tewkesbury Spur (M50) motorway, Hereford and Worcester, UK; g: showing round-tipped, dense elements, slide M50-5F-2, E.F. no. D22-2, Freshwater West formation, Ross-Tewkesbury Spur (M50) motorway, Hereford and Worcester, UK.

h – i: *Aneurospora* sp. 7: h: slide MPA25252-1, E.F. no. U28, Freshwater West Formation, Ammons Hill section, Shropshire; i: slide M50-5E-1, E.F. no. H25, Freshwater West formation, Ross-Tewkesbury Spur (M50) motorway, Hereford and Worcester.

j – k: *Aneurospora* sp. 8; j: proximal view, showing distinct lips, slide M50-11-1, E.F. no. N9, Freshwater West formation, Ross-Tewkesbury Spur (M50) motorway, Hereford and Worcester; k: distal view, slide M50-11-1, E.F. no. N9, Freshwater West formation, Ross-Tewkesbury Spur (M50) motorway, Hereford and Worcester.

l – n: *Aneurospora* sp. 9; l: proximal view, showing interadial papillae, slide M50-12-1, E.F. no. E30-4, Freshwater West formation, Ross-Tewkesbury Spur (M50) motorway, Hereford and Worcester; m: distal view, showing dense elements, slide M50-12-1, E.F. no. E30-4, Freshwater West formation, Ross-Tewkesbury Spur (M50) motorway, Hereford and Worcester; n: SEM image, note the lack of the radial and tangential folds about the proximal face as there is in *Apiculiretusispora* sp. E, AB-M5026, Freshwater West formation, Ross-Tewkesbury Spur (M50) motorway, Hereford and Worcester.

o - p: *Aneurospora* sp. 10; o: slide M50-7-1, E.F. no. H5-4, Freshwater West formation, Ross-Tewkesbury Spur (M50) motorway, Hereford and Worcester; p: smaller specimen, slide M50-7-6, E.F. no. V19-4, Freshwater West formation, Ross-Tewkesbury Spur (M50) motorway, Hereford and Worcester.

q: *Aneurospora* sp. 11, showing apiculate ornament and wedge like interadial thickenings, slide M50-2-1, E.F. no. L13-5, Moor Cliffs Formation, Ross – Tewkesbury Spur Motorway (M50), Hereford and Worcester.

r – s: *Aneurospora* sp. 12, r: slide M50-5e-5, E.F. no. X33-2, Freshwater West Formation, Ross – Tewkesbury Spur Motorway (M50), Hereford and Worcester; s: proximal view, M50-5C-3, E.F. no. U21-1, Freshwater West Formation, Ross – Tewkesbury Spur Motorway (M50), Hereford and Worcester.

t: *Aneurospora* sp. 13, slide M50-11-4, E.F. no. M14-1, Freshwater West Formation, Ross – Tewkesbury Spur Motorway (M50), Hereford and Worcester.

Scale bar 30μm.

Plate ii

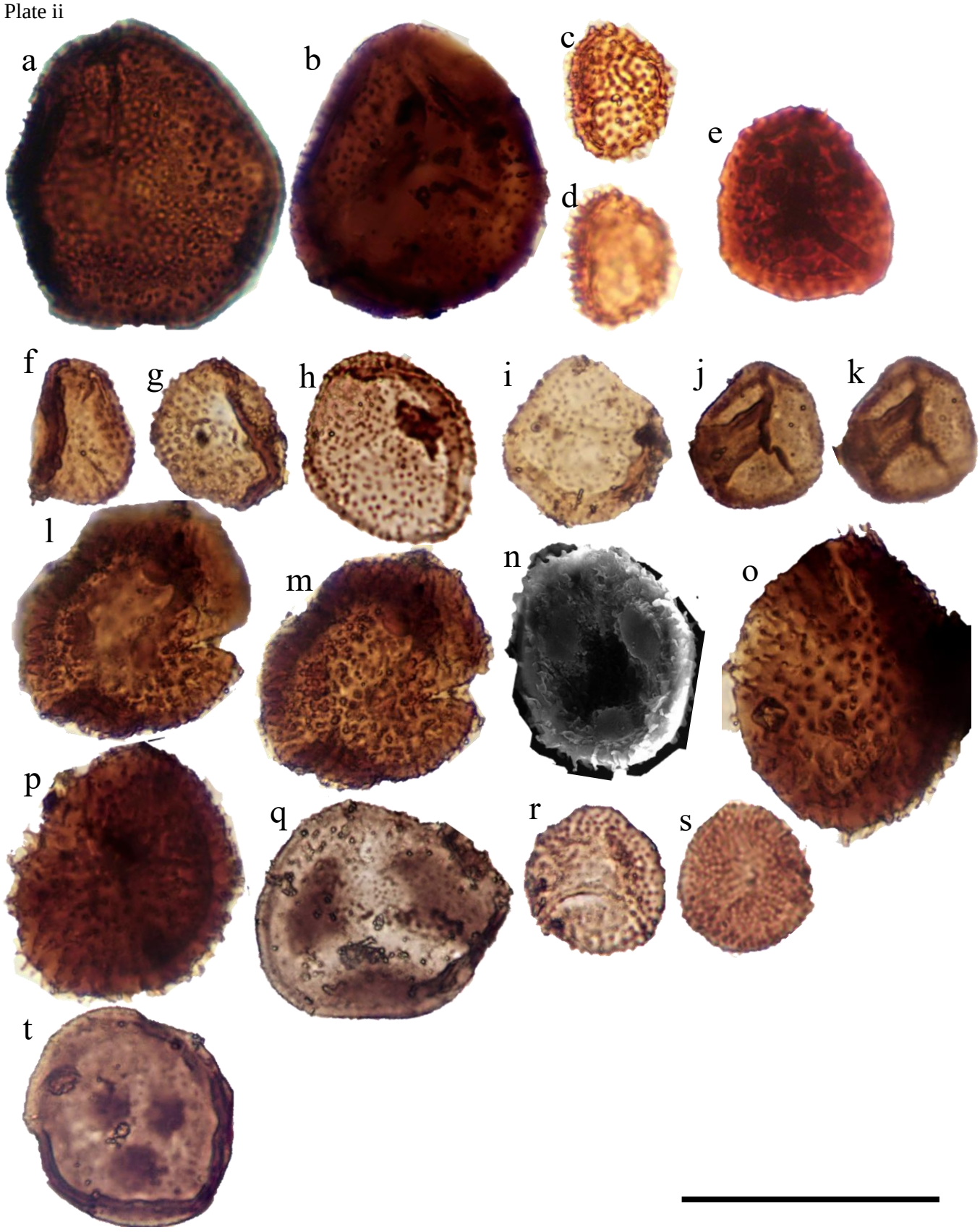

Plate iii

a – b: *Aneurospora* sp. 3; **a:** slide M50-3(2)-1, E.F. no. F21, Moor Cliffs Formation, Ross – Tewkesbury Spur Motorway (M50), Hereford and Worcester, **b:** slide M50-2-5, E.F. no. P52-4, Moor Cliffs Formation, Ross – Tewkesbury Spur Motorway (M50), Hereford and Worcester.

c – d: *Aneurospora* sp. 4; **c:** distal view, note densely packed elements and occasional ridges, slide 19M5027-1, E.F. no. P22, Freshwater West Formation, Ross – Tewkesbury Spur Motorway (M50), Hereford and Worcester; **d:** Proximal view, proximal face lost, note plan view of spines, slide 19M5027-1, E.F. no. P22, Freshwater West Formation, Ross – Tewkesbury Spur Motorway (M50), Hereford and Worcester;

e: *Aneurospora* sp. 5, 19M5026.2, E.F. no. G16-1, Freshwater West formation, Ross-Tewkesbury Spur (M50) motorway, Hereford and Worcester, UK.

f – g: *Aneurospora* sp. 6; **f: s**howing indistinct triradiate mark, slide M50-5E-1, E.F. no. Q50-4, Freshwater West formation, Ross-Tewkesbury Spur (M50) motorway, Hereford and Worcester, UK; **g:** showing round-tipped, dense elements, slide M50-5F-2, E.F. no. D22-2, Freshwater West formation, Ross-Tewkesbury Spur (M50) motorway, Hereford and Worcester, UK.

h – i: *Aneurospora* sp. 7: **h:** slide MPA25252-1, E.F. no. U28, Freshwater West Formation, Ammons Hill section, Shropshire; **i:** slide M50-5E-1, E.F. no. H25, Freshwater West formation, Ross-Tewkesbury Spur (M50) motorway, Hereford and Worcester.

j – k: *Aneurospora* sp. 8; **j:** proximal view, showing distinct lips, slide M50-11-1, E.F. no. N9, Freshwater West formation, Ross-Tewkesbury Spur (M50) motorway, Hereford and Worcester; **k**: distal view, slide M50-11-1, E.F. no. N9, Freshwater West formation, Ross-Tewkesbury Spur (M50) motorway, Hereford and Worcester.

l – n: *Aneurospora* sp. 9; **l:** proximal view, showing interadial papillae, slide M50-12-1, E.F. no. E30-4, Freshwater West formation, Ross-Tewkesbury Spur (M50) motorway, Hereford and Worcester; **m:** distal view, showing dense elements, slide M50-12-1, E.F. no. E30-4, Freshwater West formation, Ross-Tewkesbury Spur (M50) motorway, Hereford and Worcester; **n:** SEM image, note the lack of the radial and tangential folds about the proximal face as there is in *Apiculiretusispora* sp. E, AB-M5026, Freshwater West formation, Ross-Tewkesbury Spur (M50) motorway, Hereford and Worcester.

o - p: *Aneurospora* sp. 10; **o:** slide M50-7-1, E.F. no. H5-4, Freshwater West formation, Ross-Tewkesbury Spur (M50) motorway, Hereford and Worcester; **p:** smaller specimen, slide M50-7-6, E.F. no. V19-4, Freshwater West formation, Ross-Tewkesbury Spur (M50) motorway, Hereford and Worcester.

q: *Aneurospora* sp. 11, showing apiculate ornament and wedge like interadial thickenings, slide M50-2-1, E.F. no. L13-5, Moor Cliffs Formation, Ross – Tewkesbury Spur Motorway (M50), Hereford and Worcester.

r – s: *Aneurospora* sp. 12, **r:** slide M50-5e-5, E.F. no. X33-2, Freshwater West Formation, Ross – Tewkesbury Spur Motorway (M50), Hereford and Worcester; **s:** proximal view, M50-5C-3, E.F. no. U21-1, Freshwater West Formation, Ross – Tewkesbury Spur Motorway (M50), Hereford and Worcester.

t: *Aneurospora* sp. 13, slide M50-11-4, E.F. no. M14-1, Freshwater West Formation, Ross – Tewkesbury Spur Motorway (M50), Hereford and Worcester.

Scale bar 30μm.

Plate iii

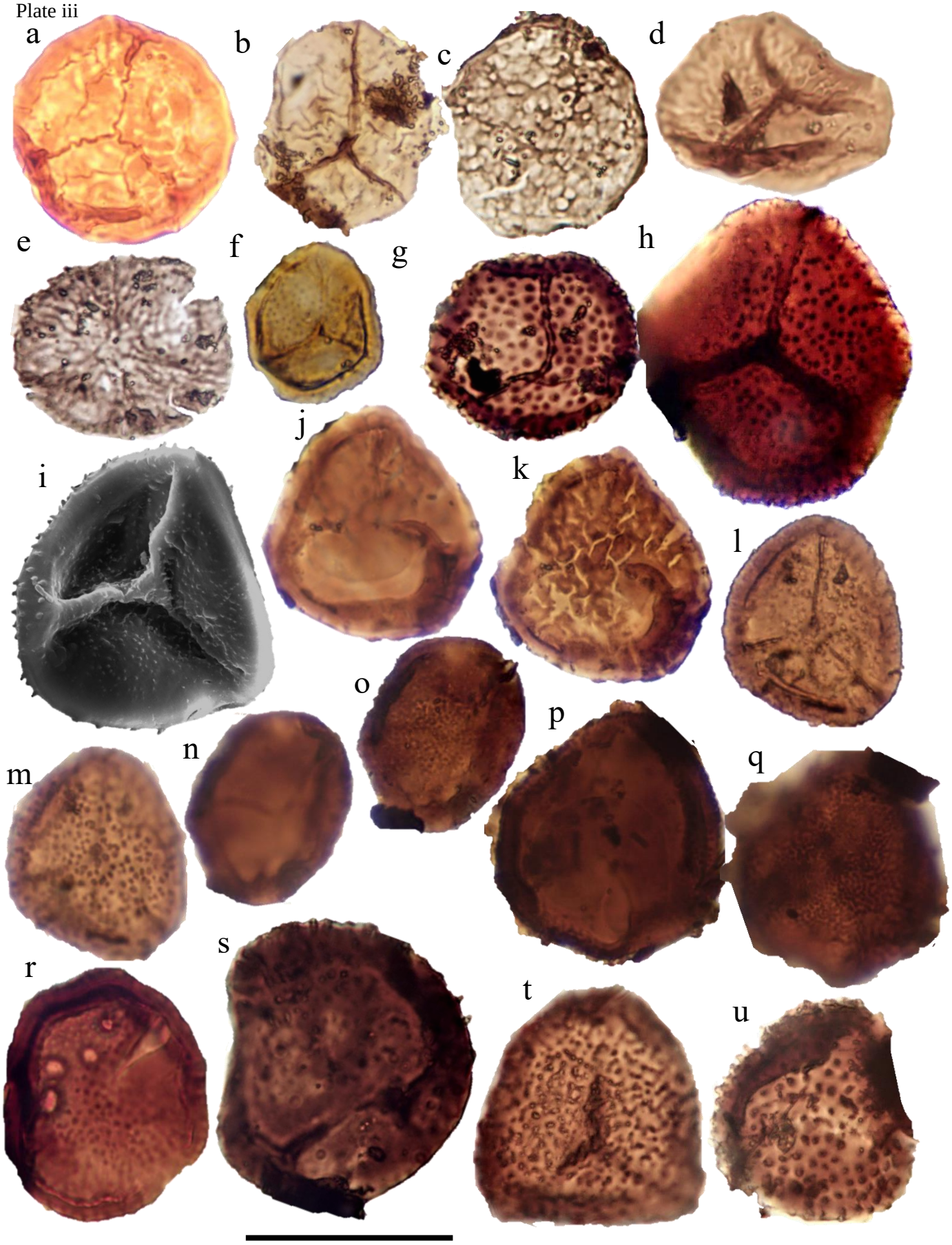

Plate iv

a: *Synorisporites* sp. 1, slide 19M5027.2, E.F. no. R43-1, Freshwater West Formation, Ross – Tewkesbury Spur Motorway (M50), Hereford and Worcester.

b: *Synorisporites* sp. 2, slide M50-5F-2, E.F. no. X20, Freshwater West Formation, Ross – Tewkesbury Spur Motorway (M50), Hereford and Worcester.

c: *Synorisporites* sp. 3, showing distinct reticulum, slide M50-5H-4, E.F. no. P46-1, Freshwater West Formation, Ross – Tewkesbury Spur Motorway (M50), Hereford and Worcester.

d: *Synorisporites* sp. 4, slide M50-5B-3, E.F. no. H27, Freshwater West Formation, Ross – Tewkesbury Spur Motorway (M50), Hereford and Worcester.

e: ?*Synorisporites* sp. 5, slide M50-12-3, E.F. no. P22-3, Freshwater West Formation, Ross – Tewkesbury Spur Motorway (M50), Hereford and Worcester.

f: *Cymbosporites* sp. 1, slide 19M5028.2, E.F. no. J18-2, Freshwater West Formation, Ross – Tewkesbury Spur Motorway (M50), Hereford and Worcester.

g. *Cymbosporites* sp. 2, slide M50-5B-1, E.F. no. W30-4, Freshwater West Formation, Ross – Tewkesbury Spur Motorway (M50), Hereford and Worcester.

h – i : *Cymbosporites* sp. 3; **h:** slide M50/85/2E-6, E.F.no. L28-1, Moor Cliffs Formation, Ross – Tewkesbury Spur Motorway (M50), Hereford and Worcester; **i:** SEM micrograph, 19M5019, Moor Cliffs Formation, Ross – Tewkesbury Spur Motorway (M50), Hereford and Worcester.

j – k: *Cymbohilates* sp. 4; **j:** proximal view, slide M50-5B-1, E.F. no. E28-1, Freshwater West Formation, Ross – Tewkesbury Spur Motorway (M50), Hereford and Worcester; **k:** distal view, slide M50-5B-1, E.F. no. E28-1, Freshwater West Formation, Ross – Tewkesbury Spur Motorway (M50), Hereford and Worcester;

l – m: *Cymbosporites* sp. 5; **l:** proximal view, M50-5E-1, E.F.no. R26, Freshwater West Formation, Ross – Tewkesbury Spur Motorway (M50), Hereford and Worcester; **m:** distal view, M50-5E-1, E.F.no. R26, Freshwater West Formation, Ross – Tewkesbury Spur Motorway (M50), Hereford and Worcester;

n – q: *Cymbosporites* sp. 6; **n:** proximal view, slide M50-5F-2, E.F. no. V21-3, Freshwater West Formation, Ross – Tewkesbury Spur Motorway (M50), Hereford and Worcester; **o:** distal view, slide M50-5F-2, E.F. no. V21-3, Freshwater West Formation, Ross – Tewkesbury Spur Motorway (M50), Hereford and Worcester; **p:** proximal view, slide M50-5F-3, E.F. no. R25-1, Freshwater West Formation, Ross – Tewkesbury Spur Motorway (M50), Hereford and Worcester; **q:** distal view, slide M50-5F-3, E.F. no. R25-1, Freshwater West Formation, Ross – Tewkesbury Spur Motorway (M50), Hereford and Worcester;

r: *Cymbosporites* sp. 7, slide HD3-1, E.F. no. H33, Freshwater West Formation, Ross – Tewkesbury Spur Motorway (M50), Hereford and Worcester; **j:** *Cymbosporites* sp. 9, slide M50-8-4, E.F. no. T18-3, Freshwater West Formation, Ross – Tewkesbury Spur Motorway (M50), Hereford and Worcester

s: *Cymbosporites* sp. 8, slide M50-7-4, E.F. no. U25, Freshwater West Formation, Ross – Tewkesbury Spur Motorway (M50), Hereford and Worcester;

t: *Cymbosporites* sp. 9, slide M50-5F-4, E.F. no. P23-3, Freshwater West Formation, Ross – Tewkesbury Spur Motorway (M50), Hereford and Worcester;

u *Cymbosporites* sp.10**,** slide M50-5H-5, E.F. no. T34-1, Freshwater West Formation, Ross – Tewkesbury Spur Motorway (M50), Hereford and Worcester.

Scale bar 30μm.

Plate iv

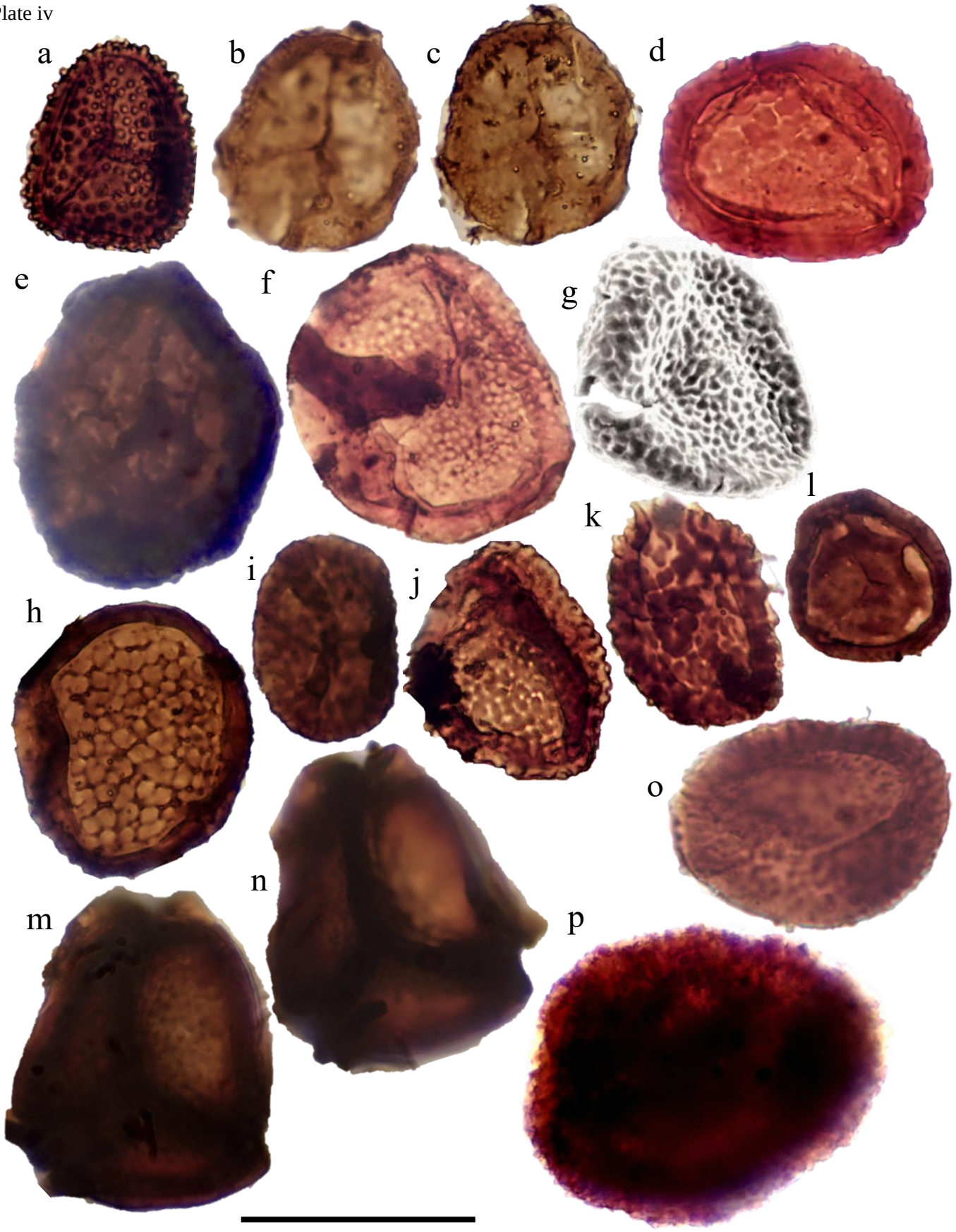

Plate v

a: *Cymbosporites* sp. 11, slide M50-5F-4, E.F. no. P23-3, Freshwater West Formation, Ross – Tewkesbury Spur Motorway (M50), Hereford and Worcester.

b – c: *Cymbosporites* sp. 12; **b:** proximal view, slide M50-7-2, E.F. no. N32-4, Freshwater West Formation, Ross – Tewkesbury Spur Motorway (M50), Hereford and Worcester; **c:** distal view, slide M50-7-2, E.F. no. N32-4, Freshwater West Formation, Ross – Tewkesbury Spur Motorway (M50), Hereford and Worcester

d: *Chelinospora* sp. 1, slide 19M5001.3, E.F. no. Q20, Freshwater West Formation, Ross – Tewkesbury Spur Motorway (M50), Hereford and Worcester.

e: *Chelinospora* sp. 2, slide M50-85-2E-3, E.F. no. C13, , Moor Cliffs Formation, Ross – Tewkesbury Spur Motorway (M50), Hereford and Worcester.

f – h: *Chelinospora* sp. 3; **f:** var. 1, showing fine reticulum, slide M50-5D-2, E.F. no. K47-2, Freshwater West Formation, Ross – Tewkesbury Spur Motorway (M50), Hereford and Worcester; **g:** SEM micrograph, 131534, GB1A, Freshwater West Formation, Gardeners Bank, Cleobury Mortimer; **h:** var 2, showing larger lumen, slide M50-7-1, E.F. no. J36-4, Freshwater West Formation, Ross – Tewkesbury Spur Motorway (M50), Hereford and Worcester.

i: *Chelinospora* sp. 4, M50-11-1, E.F. no. S17-3, Freshwater West Formation, Ross – Tewkesbury Spur Motorway (M50), Hereford and Worcester.

j: *Chelinospora* sp. 5, slide M50-5C-5, E.F. no. F28-1, Freshwater West Formation, Ross – Tewkesbury Spur Motorway (M50), Hereford and Worcester.

k: *Chelinospora* sp. 6, slide M50-12-4, E.F. no. C33-2, Freshwater West Formation, Ross – Tewkesbury Spur Motorway (M50), Hereford and Worcester.

l: *Chelinospora* sp. 7, slide MPA25256-1, E.F. no. Freshwater West Formation, Ammons Hill Section, Shropshire;

m – n: *Cheliotetras* sp. 1, ***m*:** showing flanges, slide M50-8-2, E.F. no. U18-1, Freshwater West Formation, Ross – Tewkesbury Spur Motorway (M50), Hereford and Worcester; **n:** showing micrograna, slide M50-8-2, E.F. no. U18-1, Freshwater West Formation, Ross – Tewkesbury Spur Motorway (M50), Hereford and Worcester.

o: *Cymbohilates* sp. 1. slide M50-7-6, E.F. no. H13-3, Freshwater West Formation, Ross – Tewkesbury Spur Motorway (M50), Hereford and Worcester.

p: *Cymbohilates* sp. 2, slide M50-2-5, E.F. no. P46-1, Moor Cliffs Formation, Ross – Tewkesbury Spur Motorway (M50), Hereford and Worcester.

Scale bar 30μm.

Plate v

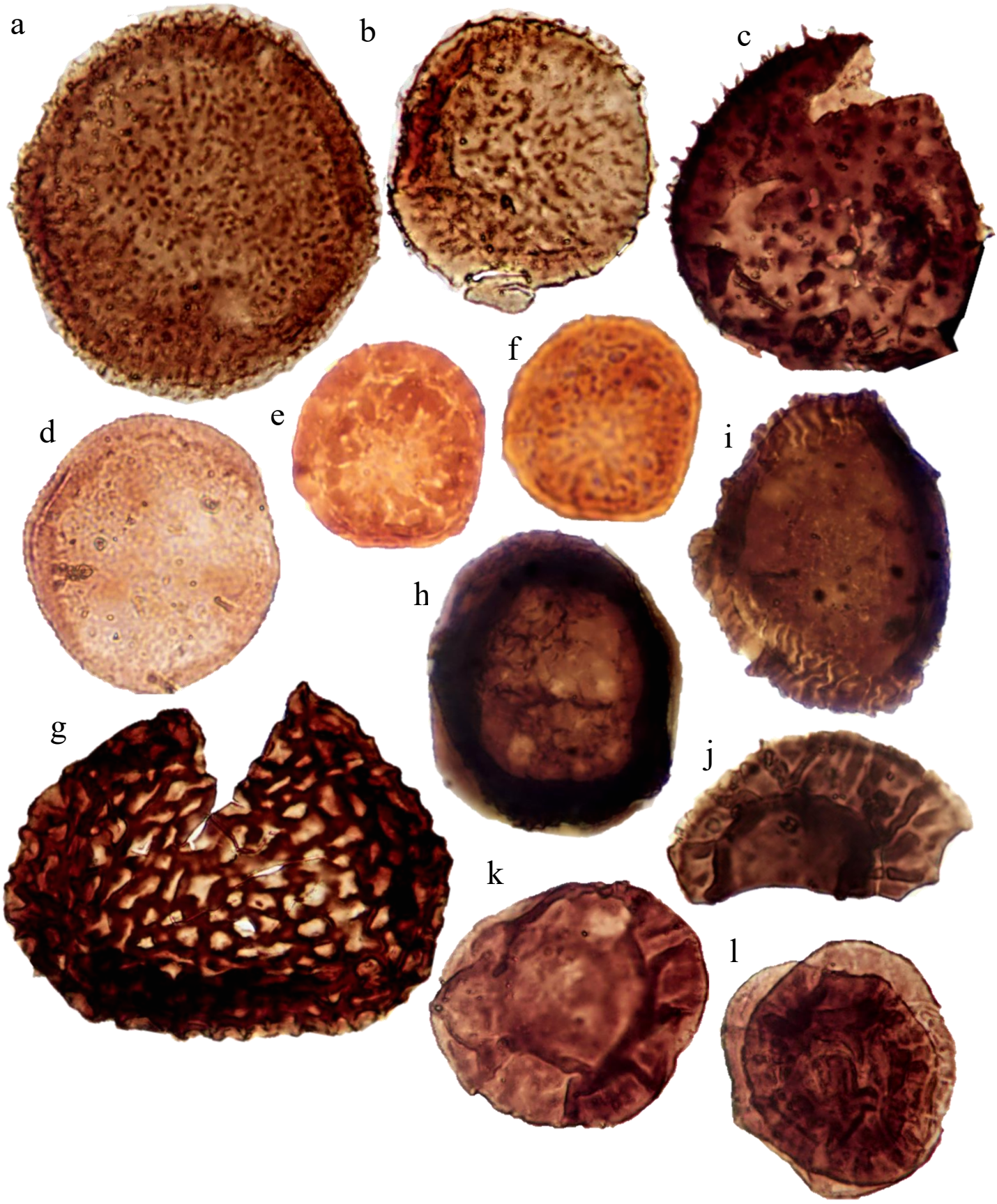

Plate vi

a: *Cymbohilates* sp. 3, slide M50-5f-2, E.F. no. O38. Freshwater West formation, Ross-Tewkesbury Spur (M50) motorway, Herefordshire and Worcester, UK.

b: *Cymbohilates* sp. 4, slide M50-7-2, E.F. no. J27-2, Freshwater West formation, Ross-Tewkesbury Spur (M50) motorway, Herefordshire and Worcester, UK.

c: *Cymbohilates* sp. 5.

d: *Cymbohilates* sp. 6, slide 19M5001.3, E.F. no. K21-1. Freshwater West formation, Ross-Tewkesbury Spur (M50) motorway, Herefordshire and Worcester, UK.

e – f: *Cymbohilates* sp. 7; **e:** proximal view, slide 19M5026.3, E.F. no. F22-4. Freshwater West formation, Ross-Tewkesbury Spur (M50) motorway, Herefordshire and Worcester, UK; **f:** distal view, slide 19M5026.3, E.F. no. F22-4. Freshwater West formation, Ross-Tewkesbury Spur (M50) motorway, Herefordshire and Worcester, UK.

g: *Chelinohilates* sp. 1, showing the pitted proximal face and radial, equatorial muri, slide M50-5E-1, E.F. no. E35, Freshwater West Formation, Ross – Tewkesbury Spur Motorway (M50), Hereford and Worcester.

h: *Chelinohilates* sp. 2, side M50-85-2D-4 E.F. no. C19-4. Moor Cliffs formation, Ross – Tewkesbury Spur motorway (M50).

i: *Chelinohilates* sp. 3; slide GB2-1, E.F. no. F31-3, Gardeners Bank, Cleobury Mortimer, Shropshire.

j – l: *Chelinohilates* sp. 4, **j:** slide M50-13-2, E.F. no. V50-2, Freshwater West Formation, Ross-Tewkesbury Spur (M50) motorway, Herefordshire and Worcester**; k:** complete monad, slide SO07-321-1, E.F. no. M34, Freshwater West formation, Bromyard Plateau, Shropshire; **l:** as dyad, slide 21/GB/4, E.F. no. H27-4, Gardeners Bank, Cleobury Mortimer, Shropshire.

Scale bar 30μm.

Chapter IV Floral diversity, disparity and community turnover at the Silurian - Devonian boundary: palynological evidence from the Anglo-Welsh Basin, UK.

A.C. Ball conceived the study, collected the data and wrote this manuscript.

Abstract

The late Silurian and Early Devonian was a key period in the evolutionary history of land plants. The emergence of the first tracheophytes (vascular plants) and their subsequent radiation had important ramifications for the biosphere, atmosphere and biogeochemical cycles. The continuous alluvial sequence of the Anglo-Welsh Basin in Southern Britain, which has a rich palynological and palaeobotanical record, is well suited for studying this episode. Earlier research has pointed towards a radiation amongst early land plant trilete spores and cryptospores in the basin at this time, and here palynological samples from the Welsh Borderlands and south Wales, recovered from the latest Ludlow (late Silurian) to the mid Lochkovian (Early Devonian), have been quantitatively investigated to further explore the radiation in spore species. Temporal and spatial spore species diversity and assemblage similarities are quantitatively investigated. Metrics for scoring the morphological diversity (disparity) of earlier Palaeozoic trilete spores, and a novel disparity scoring metric for cryptospores, are used to quantitatively explore temporal and spatial disparity changes. These investigations demonstrate considerable increases in spore diversity and disparity through the sequence, with a major species turnover and radiation occurring in the Early Lochkovian. Furthermore, the distribution of spores across the basin suggests that the vegetation distribution was heterogenous, with 'pockets' of specialised vegetation certainly occurring by the Early Lochkovian. The driving factors behind this observed change are unclear but may have been influenced by facies change. In addition, the shifting climate and changing tectonics in the basin are posited to be principal causal factors in establishing new and more equable microenvironments, facilitating the invasion and radiation of trilete spore and some cryptospore source plants.

1. Introduction

The Lower 'Old Red Sandstone' of the Anglo-Welsh Basin, U.K., has played a prominent role in improving the understanding of late Silurian – Early Devonian terrestrial vegetation through macrofossils, mesofossils and dispersed spores (e.g. Edwards and Richardson, 2004; Morris et al., 2018b). However, despite almost a century of study uncertainties remain around the degree of spatial and temporal floral variation through the sequence. The macrofossil record demonstrates that between the late Silurian and early Devonian (Přídolí – early Lochkovian) the vegetation was dominated by diminutive rhyniophytoids, including species of *Cooksonia* (Lang, 1937; Edwards, 1970; Edwards and Rogerson, 1979; Fanning et al., 1987) which is followed by a major turnover to zosterophyll dominated communities in the mid Lochkovian (Edwards and Richardson, 2004; Wellman et al., 2000), resulting from punctuated invasion (Morris and Edwards, 2014). Prior to the mid Lochkovian, there is little change amongst rhyniophytoid macrofossils and it is difficult to distinguish facies variation from genuine floral changes (e.g. invasion or evolution) (Edwards and Richardson, 2004). Indeed, a well-documented preservational bias exists in the macrofossil record which largely precludes plants lacking recalcitrant organic tissues (e.g. Edwards and Richardson, 2004), although continued study demonstrates an appreciable level of diversity amongst them (e.g. Morris and Edwards, 2014; Morris et al., 2011a).

The recovery of charcoalified mesofossils has, amongst other things, contributed to elucidating further diversity and disparity amongst these diminutive early land plants (e.g. Morris et al., 2018b), but the most reliable indicator of the true taxonomic diversity amongst the late Silurian and Early Devonian vegetation is the dispersed spore record, which is widespread and well-preserved throughout the sequence (e.g. Burgess and Richardson, 1991, 1995; Edwards and Richardson, 2004; Edwards et al., 2012; Higgs, 2004, 2022; Morris et al., 2011a, b, 2012a; Richardson and Lister, 1969; Richardson and Rasul, 1990; Wellman et al., 2000; Chapter III). A principal problem of the dispersed spore record is the uncertain affinities and characteristics of many of the source plants, but the recovery of *in situ* spores at least indicates that a single spore species, or complex of species, is peculiar to a single plant (e.g. Fanning et al., 1988; Edwards and Richardson, 2000; Morris et al., 2011b, 2018b; Wellman, 1999; Wellman et al., 1998b). Consequently, spore species can be used to indicate the presence of plants even where macrofossils are not recovered, although certain caveats, including the vast distances that spores may be transported from their source, do necessitate caution. The dispersed spore record in the Anglo-Welsh Basin comprises a diverse suite of cryptospores and trilete spores (Burgess and Richardson, 1991, 1995; Richardson and Lister, 1969; Wellman et al., 2000), with over 100 species reported in over 30 genera (Chapter III). The latter are generally attributed to basal tracheophytes, although some extant bryophytes also produce them (Kenrick et al., 2012; Salamon et al., 2018). The affinities of cryptospores are more enigmatic. These appear to be derived from a pool of variously derived embryophytes, some of which may be closely related to the tracheophytes (Edwards et al., 2014) while others may be more closely related to other extant plant groups, such as bryophytes. Others still may be associated with more ancient lineages.

Cryptospores had achieved a cosmopolitan distribution by the Early Devonian (Wellman et al., 2013), with very little change in diversity and disparity from their earliest firm records in the mid Ordovician (Rubinstein et al., 2010). This initial *c.*40myr evolutionary stasis amongst early land plants ended with initial radiations of trilete spores in the Silurian (Wellman et al., 2013, 2022) and Early Devonian, where tracheophytes became the dominant feature of terrestrial vegetation and show rapid increases in diversity and morphological innovations (e.g., Algeo and Sheckler, 1998; Gensel et al., 2020). The temporal placement and stratigraphic continuity of the Anglo-Welsh Basin makes it well-suited to tracking floral changes through this decisive moment in time, and a major increase in the taxonomic richness and species diversity of dispersed spores is observed in the early (not earliest) Devonian, principally amongst trilete spores (Richardson and Lister, 1969; Chapter III).

Here, the dispersed spore record from nine localities in the classic Anglo-Welsh Basin sequence, ranging between the Ludlow and mid Lochkovian (*Stellatispora inframurinatus* var. *inframurinatus* subzone to the middle *micrornatus – newportensis* subzone) has been examined. This chapter attempts to go beyond classical taxonomic and biostratigraphic analyses with a basic quantitative and statistical analysis of diversity, disparity and community turnover through the sequence. The temporal change in the diversity of trilete spores and cryptospores is quantified in terms of species richness, and community turnover between these assemblages. In addition, temporal disparity change amongst trilete spores is quantified after Wellman et al. (2013) and a novel disparity scoring method is used to quantify temporal change amongst cryptospores for the first time. The disparity amongst key trilete spore and cryptospore genera are also explored. Several of the studied localities are coeval, and the spatial diversity and disparity between coeval assemblages is quantified and assemblage similarities measured. The techniques used are subject to a critical evaluation before the spatial distribution of vegetation across the basin is examined and the underlying causes of the temporal changes recorded in Chapter III (fig. 14) are discussed.

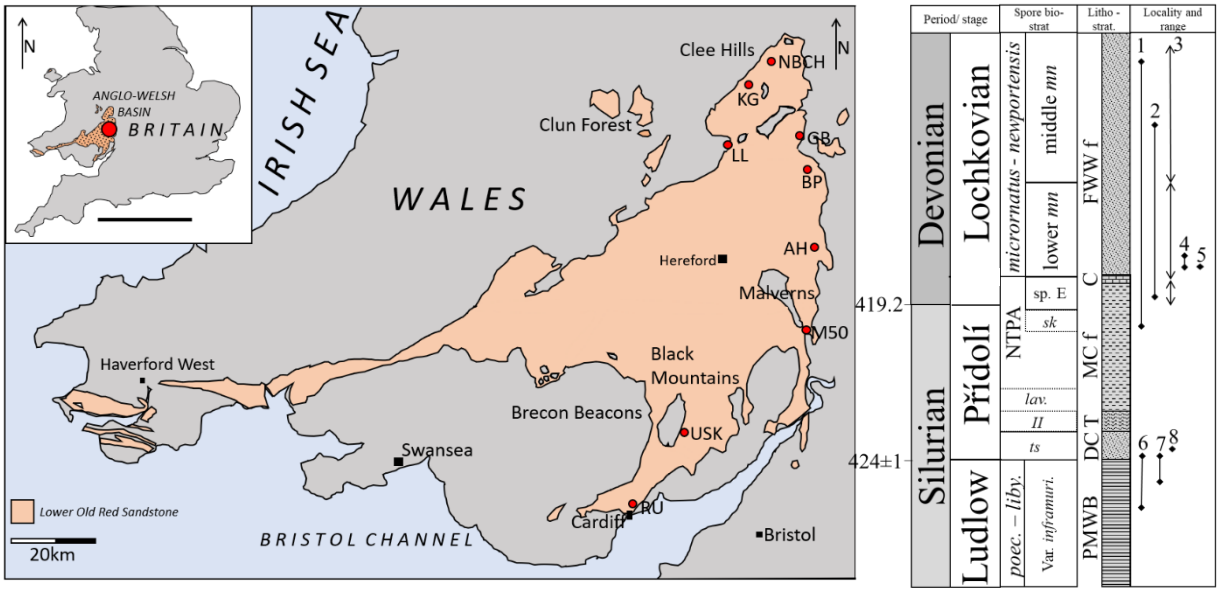

Figure IV-1: ***LEFT, inset:*** *Map of southern Britain showing position of the Anglo-Welsh Basin in Western England (the Welsh Borderlands), and its central, south and west extents in Wales, scale bar 200km;* ***(LEFT, main):*** *The Přídolí and Lochkovian (late Silurian – Early Devonian) outcrop of the Anglo-Welsh Basin, showing the positions of the field localities investigated here, curving along the eastern edge of the basin to southern Wales.* ***NBCH:*** *North Brown Clee Hill;* ***KG:*** *Kidnall Gutter;* ***GB:*** *Gardeners Bank;* ***LL:*** *Ludlow Lane;* ***BP:*** *Bromyard plateau;* ***AH:*** *Ammons Hill;* ***M50:*** *Ross Tewkesbury Spur (M50) motorway;* ***USK:*** *Usk-1 borehole;* ***RU:*** *Rumney-1 borehole.* ***RIGHT:*** *Lithostratigraphy and biostratigraphy of the studied Anglo-Welsh Basin sequence and the positions ± ranges of studied sections.* ***1:*** *M50 motorway;* ***2:*** *Brown Clee Hill area (NBCH + KG);* ***3:*** *Ammons Hill;* ***4:*** *Gardeners Bank;* ***5:*** *Bromyard Plateau;* ***6:*** *Usk-1 borehole;* ***7:*** *Rumney-1 Borehole;* ***8:*** *Ludlow Lane. Diamonds indicate known stratigraphic position of sample. Arrows indicate possible range based on spore assemblages.* ***PMWB:*** *Palaeozoic marine Welsh Basin****; DC:*** *Downton Castle Sandstone formation (also part of PMWB);* ***T – FWWf:*** *The lower Old Red Sandstone Anglo-Welsh Basin,* ***T:*** *Temeside shales formation****; MCf:*** *Moor Cliffs formation;* ***C:*** *Chapel Point Limestone member;* ***FWWf:*** *Freshwater West formation. Dates Ma,* ***424±1Ma*** *for the Ludlow Bone Bed sensu Catlos et al., 2021; 419Ma sensu Cohen et al., (2013). Lochkovian ends at 410Ma. Lithostratigraphy sensu Barclay et al., 2015, biostratigraphy after Richardson and McGregor (1986), Richardson and Edwards (1989), Burgess and Richardson (1995), Edwards and Richardson (2004), Higgs (2022) and chapter III.*

2. Materials and methods

2.2. localities and geological setting

The Anglo-Welsh Basin is a ± continuous, extra-montane foreland basin which developed as a result of either regressive load induced flexural subsidence of the Avalonian foreland (James, 1987; King, 1994; Friend *et al*., 2000) or basin wide, sinistral mega-shearing (e.g. Dewey and Strachan, 2003; Soper and Woodcock, 2003) associated with the Late Silurian – Early Devonian Caledonian Orogeny. The associated shrinkage of the Palaeozoic Marine Welsh Basin led to the Formation of a regressive offlap sequence whereby the basin was gradually infilled with shallow marine and then terrestrial sediments derived from the northern Caledonian Mountains. Deposition in the Přídolí and earliest Devonian (earliest Lochkovian) was dominated by muddy, ephemeral river channels. Intermittent ashfall from distant Plinian eruptions accompanied this fluvial deposition (Allen and Williams, 1981). Early Devonian (early to mid Lochkovian) deposition was dominated by more channelised, sandy perennial rivers (Allen and Tarlo, 1963; Hillier et al., 2008; Morris et al., 2012b) which deposited sediments derived from within the basin, following a shift from flexural subsidence to sinistral transtensional regimes in the earliest Devonian (Crowley et al., 2009). The shift in facies was accompanied by a basin-wide quiescent period in the Early Devonian which was associated with a depositional hiatus and the development of mature calcretes (Allen, 1974), the hiatus resulting from tectonics and/ or an extended period of aridity (Morris et al., 2012b). The Anglo-Welsh Basin lay 17±5° south of the paleoequator (Channel et al., 1992) and is suggested to have exhibited a strongly seasonal semi-arid climate with

well-developed wet and dry seasons (Allen, 1974; Marriot and White, 2004). The shift from ephemeral to dominantly perennial river systems between the late Silurian and Early Devonian has been attributed to a shift to a slightly wetter climate (Morris et al., 2012b).

Fig. 1 illustrates the lithostratigraphy of the studied section. The Anglo-Welsh Basin *sensu* Barclay et al. (2015) encompasses the early Přídolí Temeside Mudstone Formation, early mid Přídolí to earliest Lochkovian Moor Cliffs Formation, and the early to mid Lochkovian Freshwater West Formation. The preceding strata, including the early Přídolí Downton Castle Sandstone Formation and its correlatives, along with the underlying Ludlow Whitcliffe Formation and its correlatives, form the upper part of the Palaeozoic Marine Welsh Basin. Nine localities, seven from outcrops and two from boreholes, from the Welsh borderlands and South Wales were sampled between 1974 and 2022 by numerous workers (J.B. Richardson, D. Edwards, C.H. Wellman, and A.C. Ball) and extractive companies resulting in 58 palynologically productive samples from this sequence (fig. 1; Chapter II table 2; thesis appendix 2.1). This suite of samples ranges from the upper Ludlow to mid Lochkovian, although a significant gap in samples separates the early and late Přídolí (fig. 1), a function of outcrop paucity coupled with a dearth of suitable sampling horizons. The samples can be lithostratigraphically correlated relative to the basin-wide Chapel Point Limestone member (ex. *Psammosteus* limestone) which occurs in the early (not earliest) Lochkovian of the basin (Barclay et al., 2015). The excellent fossil record of the basin also means that materials can be correlated independently with vertebrates (e.g. Barclay et al., 2015; Turner et al., 2017)

2.3. Palynological processing

Following collection, 20±1 grams of raw sample were crushed into a fine powder before maceration with HF + HCl to digest silicates and carbonates. Following dilution, samples were sieved with a 10 µm mesh and then heavy mineral separation, including centrifugation, was used to separate organic matter and remaining mineral detritus. Samples were spiked with the exotic spore *Lycopodium clavatum* (herein: *Lycopodium*) from batch 3869 at a rate of 1 tablet per 1ml of organic matter (thesis appendix 2.1).

In some cases, raw sample was no longer available for materials collected by JB Richardson, in which case, his palynological slides were used. These were not spiked with *Lycopodium*. JB Richardson used similar methods to those used above, but in some cases used HNO_3 in addition. A list of spiked and unspiked samples are detailed in the thesis appendix 2. All slides were counted to 250 spores, followed by logging of the slide (thesis appendix 3.1. – 3.3.) Spores which occurred in the assemblage but did not feature in counts were labelled as 'rare'. Quantitative slides were counted with *Lycopodium* following Stockmar (1971), and equation (1) was utilised to find the number of indigenous palynomorphs per gram in the sample. Following counts, the results were rarified (1.2.1) and then assessed using the Rstudio package for palynology, `library("rioja")`, and the stratigraphic software StrataBugs, both as counts and as presence/absence ranges.

$$C = \frac{m_c \cdot L_t \cdot t}{L_c \cdot w} \quad \textbf{(1)}$$

Where C is the number of indigenous palynomorphs per gram of dry rock processed (the concentration), M_c is the number of indigenous palynomorphs counted, L_t is the number of *Lycopodium* spores in each tablet, with t being the number of *Lycopodium* tablets added to the sample; L_c is the number of *Lycopodium* spores counted in the sample, and w is the weight of dried sediment processed for palynomorphs, in grams.

Because not all of the samples were able to be spiked with *Lycopodium* (especially those from the mid Lochkovian) these quantitative counts were used to confirm, where possible, the trends shown by relative abundance counts.

2.4. Rarefaction

Spore counts vary between samples, and so the analysis of the taxonomic richness of these samples is only a useful measure of palynological richness if all the counts have been standardised to a fixed number of grains (Birks and Lines, 1992). Rarefaction analysis implements this standardisation, providing minimum variance unbiased estimates of the expected number of taxa *t* in a random sample of *n* individuals taken from a larger collection of *N* individuals containing *T* taxa. *T,* while a simple measure of taxonomic richness, is dependent on the number of palynomorphs counted in a sample, and thus cannot be used directly for taxonomic richness comparisons between samples as a myriad of problems will be encountered (Kempton, 1979). Rarefaction permits an estimation of palynomorph richness $(E(T_n))$ which would be expected if all the spore count across the samples had been the same size. The expected number of taxa $(E(T_n))$ must be based on a common value of *n*, and this is usually the smallest total count in the samples being compared, here, $n = 92$. Some loss of information (Williamson, 1973; Magurran, 1988) occurs when using rarefaction analysis, as prior to rarefaction, the number of taxa and relative abundances are known for each sample. Rarefaction analysis was undertaken using `rarefy()` with the R packages `library("vegan")` and `library("fossil")` (Oksanen et al., 2020).

2.5. Temporal and spatial diversity

Taxonomic diversity here refers to the taxonomic richness, or the number of species present in an assemblage. Other workers may use taxonomic evenness (whether there is an even spread or a few dominant taxa) instead of, or in addition to, taxonomic richness. However, inherent problems with relating the evenness of spore species to the evenness of the original vegetation (Birks and Line, 1992; Cleal *et al*., 2021; Pardoe et al., 2021) exist, especially for the palynological record and this metric is not used here. Taxonomic richness is assessed within localities, between localities and across the overall basin. Local scale diversity is approximate to Whittaker's (1960) α – diversity, and is the diversity from a single locality, reflecting, in the palynological context, *ca.*1km^2 (Cleal et al., 2021). Following this, β-diversity assess the diversity between individual localities, and acts as an intermediary between local and landscape diversity. Landscape scale diversity, approximate to Whittaker's (1960) ϒ – diversity, is the diversity in a typical depositional basin, up to *ca.* 10^5km^2, hence representing the entire depositional setting of the Anglo-Welsh Basin (Cleal *et al*., 2021; Pardoe et al., 2021). Such quantification of area should be treated only as a guide, however, because palynomorphs are capable of being transported vast distances by interconnected rivers, and may be derived from outside the 1km^2 area (local diversity) or basin (landscape diversity) (e.g. Traverse, 2009), and potentially mix between localities, affecting β-diversity also. Species richness was studied temporally and spatially on local to landscape scale.

Temporal species diversity was calculated from binary (presence / absence) data for: (1) overall species richness (miospores + cryptospores), (2) miospores only, and (3) cryptospores only. Binary data was calculated from each sample (counted and logged species) from each locality to give a biozone's mean species richness. The mean species richness of each biozone equated to landscape scale diversity. These were then compared with the other biozones. Descriptive statistics (mean, median, count, max and minimum values) were explored on PAST – paleontological statistics ver. 1.32 (Hammer et al., 2006).

Spatial species diversity from every coeval (same biozone) sample in a locality was used to calculate the mean locality species richness, which was used to assess α-diversity from observed and range through data. Barplots were made in R version 4.1.3 (2022-03-10) - "One Push-Up" (R core team, 2022) using the `ggplot()` function in `library("ggplot2")` (Wickham, 2016) and grouped using the `ggarrange()` function in `library("ggpubr")` (Kassambara, 2020) (thesis appendix 4.7.).

Spatial β-diversity was calculated from the Jaccards dissimilarity index (D7), which is a dissimilarity coefficient for pairwise comparison of groups. Using this index, observed binary species data between coeval localities was compared in a pairwise fashion. The Jaccards dissimilarity index is a metric difference calculated by subtracting 1 from the result of a Jaccards similarity test. The dissimilarity index is still measured on a scale of 0 – 1, with D7 = 0 indicating that the assemblages share 100% of taxa, with no unique taxa occurring in either of compared assemblages. Meanwhile, D7 = 1 indicates the assemblages are 100% distinct from one another and share no taxa. Jaccards dissimilarity was calculated in R studio with R version 4.1.3 (2022-03-10) - "One Push-Up" (R core team, 2022) using the `vegdist()` function in `library("vegan")` according to equation (2). To avoid calculating extended Jaccard, the argument `binary = TRUE` was included in the `vegdist()` function (thesis appendix 4.7). Landscape temporal dissimilarity was also calculated using D7. Dissimilarity indices were calculated from binary species data between biozones in a pairwise fashion, as for spatial β-diversity.

```
vegdist(x, method = "jaccard", binary = TRUE)
```
(2)

where *x* is the data set, comprising count data for species in coeval localities. Species count data in the data set, *x*, is converted to presence/ absence data by the argument `binary = TRUE`.

2.6. Temporal and spatial disparity

Disparity is the phenotypic, or morphological, diversity of spores. Disparity was quantified by trait scoring trilete spores and cryptospores. Trilete spore trait scores for disparity, based on the complexity of the development of the spore and its ornament during sporogenesis, were developed by Wellman *et al*. (2013), and the same system is used for the trilete spores reported here. Those workers did not config. a scoring chart for the cryptospores, due principally to the complexity of the group and the enigma of many of their relationships to one another (pers. comm. CH Wellman 2021) and the trilete spores (e.g. Edwards et al., 2014). However, given the importance of cryptospores in the Anglo-Welsh Basin dispersed spore record (up to 1/3 of the palynoflora, Chapter III), a preliminary step has been made here to develop a trait scoring metric to further illustrate the disparity of these Siluro-Devonian floras, and establish a better understanding of cryptospore evolution and development. Uncertainties exist around the specific process of sporogenesis amongst the cryptospores. Indeed, sporogenesis is a dynamic system which has facilitated a diverse suite of sculptures and organisations to evolve for a variety of environmental and ecological challenges (Wellman, 2004). Nonetheless, ultrastructural analysis of Silurian and Devonian spores has revealed some insights into the process (e.g., Morris et al., 2011b, 2012a; Edwards et al., 2012, 2014) (fig. 2).

The cryptospore scoring system presented here follows Wellman et al. (2013) in that it is developed around the complexity of sporogenesis for each cryptospore. Furthermore, as cryptospores show a range of organisations; tetrads, dyads and monads, the 'extent of meiosis' is taken into consideration as an extra facet of complexity during sporogenesis. The diversity of cryptospore organisation (monads, dyads and tetrads) is likely derived from variations in meiosis (Hemsley, 1994), and specifically in the timing and synthesis of sporopollenin (Blackmore and Barnes, 1987). Following monad Formation through cytokinesis in meiosis I, the timing and synthesis of sporopollenin during meiosis II might control whether permanent dyads or hilate monads result (Edwards et al., 2014). The development of permanent dyads, such as *Cymbohilates horridus*, was accompanied by plasmalemma activity forming an enclosing common outer perispore, which prevented further separation of the dyad. It is possible that enzymatic action, which in modern plants facilitates the separation of cells by the dissolution of the binding middle lamellar layer (Daher and Braybook, 2015) was inhibited preventing cytokinesis at the end of meiosis II. It is also possible that the biological pathway resulting in cytokinesis at the end of meiosis II was not in place in these permanent dyad producing plants. In 'loose' dyads and hilate spores developed from the full separation of loose dyads, especially those with a bilayered wall such as

Dyadospora murusdensa (Taylor, 1995a, 1996, 2000), plasmalemma activity would have been delayed until after the separation of the spore into monads, where the bilayered spore wall then developed (Edwards et al., 2014). Enzymatic action then likely facilitated further separation during cytokinesis towards the end of meiosis II (Daher and Braybook, 2015) as in meiosis I. For semi-permanent, 'loose' dyads, it is possible this enzymatic action, breaking down the middle lamellar wall binding the granddaughter cells together, is reduced or inhibited, preventing their full separation. Such timing and synthesis of sporopollenin and cytokinesis may have also controlled whether permanent tetrads or monads are developed following ± simultaneous meiosis I and II (fig. 2).

Envelopes observed amongst cryptospores would have presented another layer of complexity to sporogenesis. As for the exospore wall, the envelope would have formed immediately outside of the plasmalemma in early sporogenesis. This would have occurred prior to cytokinesis during meiosis I in permanent enveloped tetrads (Edwards et al., 2014), and probably following meiosis I and cytokinesis in permanent dyads, before the end of meiosis II.

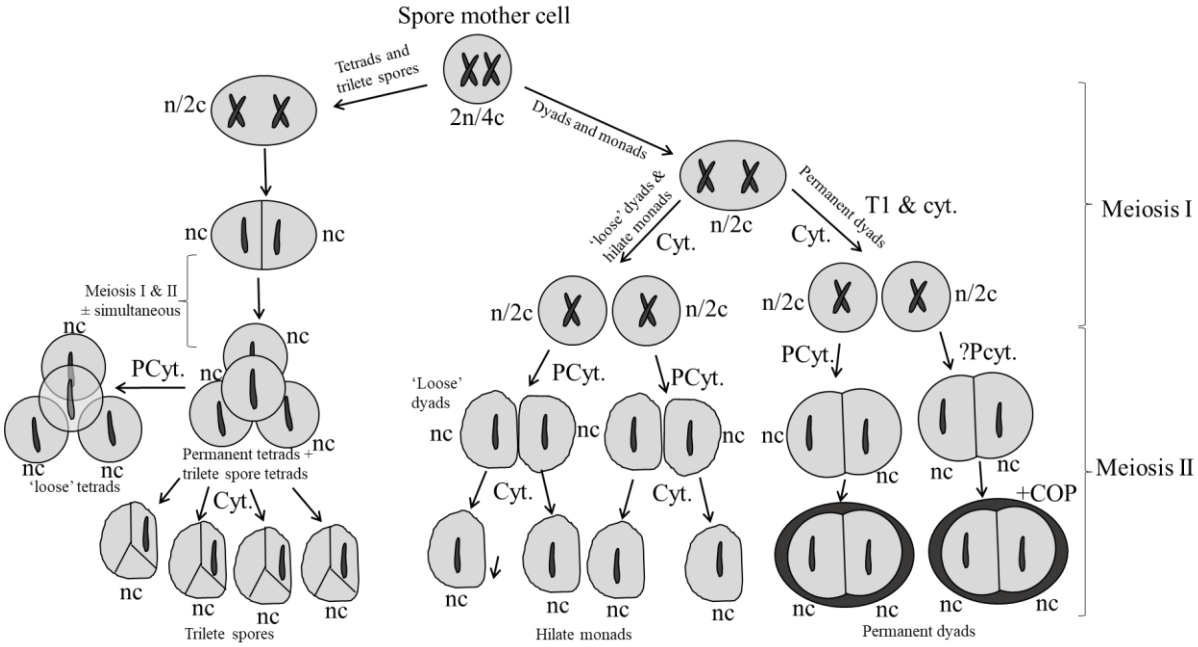

Figure IV-2: Sporogenesis schematic. ***n:*** *ploidy level;* ***c:*** *DNA content;* ***T1 & cyt:*** *Telophase 1 and cytokinesis;* ***Cyt.:*** *Cytokinesis;* ***PCyt:*** *Partial cytokinesis, ?incomplete removal of middle lamellar layer between gametes;* ***+COP:*** *Common outer exospore. Modified from Edwards et al. (2012, 2014).*

In terms of the scoring system, the 'degree of meiosis' is least advanced in permanent tetrads and dyads, followed closely by 'loose' tetrads and dyads, which have undergone a more advanced, although not complete, phase of cytokinesis relative to permanent forms. Control on this partial cytokinesis in meiosis II is posited to represent an additional layer of complexity, and hence this organisation is scored higher than permanent forms. The continued cytokinesis producing hilate monads is a further level of complexity, and hence scores higher again. The development of the common outer exospore in permanent dyads may be considered an additional layer of complexity, but this is comparable to the development of the exospore in bilayered spores, and is therefore not considered to increase the relative complexity. Enveloped cryptospores have an additional facet of complexity and therefore enveloped forms score higher than naked forms. Cryptospores show a wide variety of ornaments. Here, the scoring system for ornament follows that of Wellman et al. (2013) in that laevigate forms receive the lowest scores, and ornament with increasing complexity, from irregularly to regularly arranged elements (although no distinction is made in score between, e.g., regular murornate and apiculate), to biform to complex elements, which receive the highest complexity score. This model is naturally oversimplified, and it is again stressed that it is broached as a working hypothesis only to demonstrate, in some part,

the disparity changes amongst cryptospores. It is hoped that future workers will develop the scoring system further. Scores for species, and the determining metrics, are given in thesis appendix 4.

Locality and biozone disparity data was calculated for overall assemblage disparity (miospore + cryptospore), miospore disparity and cryptospore disparity and considered on a temporal and spatial basis. Presence absence scores were converted into disparity scores in MS Excel, with graphical outputs and statistical tests carried out in R version 4.1.3 (2022-03-10) - "One Push-Up" (R core team, 2022) using `Base R`, `Library("ggplot2")` and `Library("ggpubr")` (see appendix 4.6). Temporal disparity was calculated between coeval biozones. Spatial disparity was calculated between coeval localities.

2.7. Statistical analysis

Two sample and Welch t-tests

Statistical tests were carried out on R version 4.1.3 (2022-03-10) - "One Push-Up" (R core team, 2022) (R core team, 2021) (thesis appendix 4.7). The statistical significance of miospore, cryptospore and overall (miospore + cryptospore) mean taxonomic richness and mean disparity between groups of samples, organised by biozone, was tested for. Because the significance between two independent groups was being tested, the two-sample t-test or Welch t-test was selected as the best statistical test (assumption fulfillment dependent, below) to assess the similarities between species richness and disparity. A null hypothesis (H_o) and alternate hypothesis (H_1) for the t-tests were outlined as follows:

$\boldsymbol{H_o}$ = There is no significant difference in mean diversity/ disparity between biozones (null).

$\boldsymbol{H_1}$ = There is a significant difference in mean diversity/ disparity between biozones (alternate).

Where *ad hoc* tests were passed (below), the two-sample and Welch t-test rejects H_0 and accepts H_1 where p = <0.05. The two-sample t-test assumes that data is normally distributed and is of approximately equal variance. The Shapiro-Wilkes test and F-test were used to test these assumptions, respectively (below). Where these tests are passed (i.e. the data has normal variance and normal distribution), the two sample t-test is carried out using the function `t.test()` in base R (equation 3). The Welch t-test does not assume normal variance, and where the F-test failed, but the Shapiro-Wilkes test passed, this test was used to test significance (H_o and H_1 as above), also using the function `t.test()` in base R (equation 4) . Where the both tests failed, or the Shapiro-Wilkes test failed and F-test passed, no testing was carried out. Only observed data was used to test the significance between biozones.

```
t_test <- t.test(x ~ Biozone, data = z, var.equal = TRUE)          (3)
```

```
welch.test <- t.test(x ~ Biozone, data = z, var.equal = FALSE)     (4)
```

Where `t.test()` is the function for executing a two sample and a welch t-test in base R, *x* is the means to be compared, in this case the mean diversity/ disparity of samples in a biozone, *y*, in the data frame *z*. The argument `var.equal` refers to whether the data set has equal variance. If =`TRUE` the variance is equal, and if =`FALSE` variance is not equal. This argument differentiates the `t.test()` function into a two sample t-test or a Welch's t-test, respectively.

Ad hoc tests

Prior to the t-tests, *ad hoc* tests were carried out to test assumptions. The Shapiro-Wilkes test was used to test for normal distribution using the function `with()` and the argument `shapiro.test()` in

base R. The Shapiro Wilkes test was carried out independently for each biozone according to equation 5, where *x* is the data set, *y* is the diversity/ disparity measurements, *z* selects the biozone *z1*. Where p = > 0.05, the distribution of the data are not be significantly different from normal distribution.

```
with(x, shapiro.test(y[z == "z1"]))
```
(5)

The F-test was used to test for normal variance using the function `var.test()` in base R (equation 6), where *x* is the diversity/ disparity, *y* is the biozone, and *z* is the data set. Normal variance is shown (no significant difference between variances) where p = > 0.05, such that there is no significant deviation from normal variance.

```
var.test(x ~ y, data = z)
```
(6)

Sample size

Sample size is not equal between biozones (table 1), potentially reducing the power of the statistical tests if biozones with small sample sizes are compared. In order to ensure that statistical tests were as valid as possible the number of samples were maximized for each group for comparison. For example, pre- *micrornatus – newportensis* and *micrornatus – newportensis* samples were grouped and tested against one another, thereby comparing 20 and 33 samples. In general, comparisons between individual biozones are limited due to small sample sizes, particularly in the pre- *micrornatus – newportensis* bizones. Because of limited samples, significance testing of diversity and disparity variations were not tested for between coeval localities.

Biozone	Subzone	Biozone n	Subzone n	Coeval samples/ localities
micrornatus – newportensis	Middle MN	34	17	• M50/7 – M50-13 • 21/HD/001-005 • MPA25242 - 25256
	Lower MN		17	• BM/M50/5B – 5H • 19-M50/86-2C • 19-M50/86/2B • 19-DE98 • 19-M50/86/2A • MPA25239-25240 • 21/GB/1 – 5 • TG1B-1C
Non-tripapillate *Aneurospora* spp.	*Apiculiretusispora sceacga*	12	11	• M50/85/2B – 2H • M50/3 – 4 • CH/SD/88/2C • MPA25198
	Aneurospora sheafensis		1	• M50/2
tripapillatus – newportensis	n/a	3	3	• LL3 • RU/21/4 • USK/21/3
poecilomorphus - libycus	*Stellatispora inframurinatus* var. *inframurinatus*	5	5	• USK/21/1 – 2 • RU/21/1 – 3

Table IV-1: Sample details of studied palynological assemblages, n = number of samples; for biozone definitions see Chapter III.

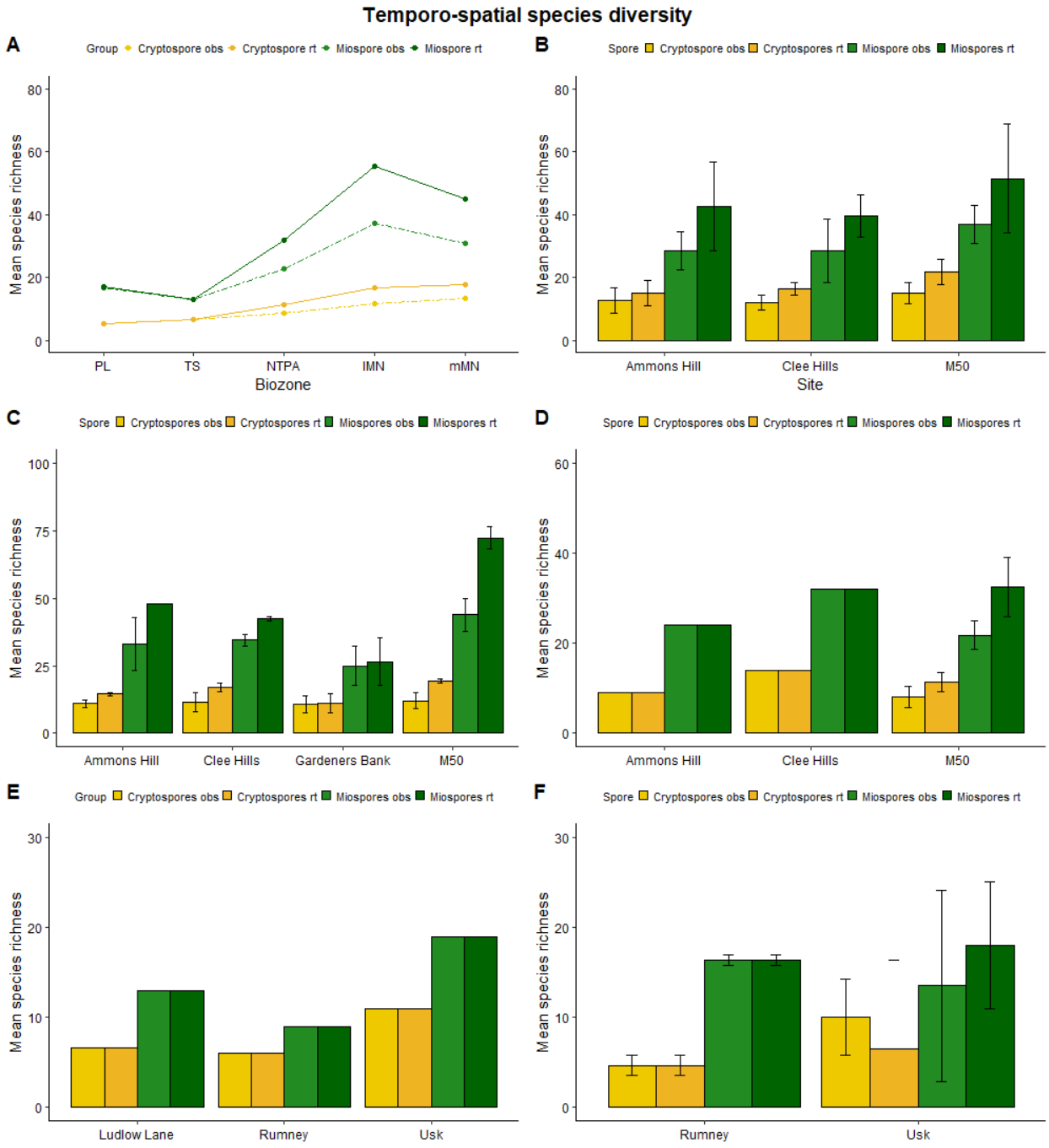

Figure IV-3: temporal and spatial species diversity by biozone in the Anglo-Welsh Basin. ***A:*** *line graph illustrating mean species richness (observed and range through data) through the biozones: mMN and lMN middle and lower micrornatus – newportensis biozone; NTPA: non tripapillate Aneurospora spp. Biozone; TS: tripapillatus – spicula biozone, and; PL poecilomorphus – libycus biozone.* ***B – F:*** *barplots illustrating mean spp. Richness between coeval (same biozone) sites (observed and range through data shown) and standard deviation.* ***B:*** *middle MN zone;* ***C:*** *lower MN zone;* ***D:*** *NTPA zone;* ***E:*** *TS zone;* ***F:*** *PL zone. Note Y axis scale change between some graphs. Plot made in R using* `library("ggplot2")` *and* `library("ggpubr")` *.*

3. Results

3.1. Temporal diversity and disparity change (landscape scale)

Fig. 3a shows that there is a considerable increase in overall species richness between the Ludlow and mid Lochkovian for both miospores and cryptospores across the Anglo-Welsh Basin, with miospores showing the greatest change. This is clear in both observed and range through data, with a similar pattern

for both datasets. T-tests on observed data demonstrate that in all groups (M_o, C_o and ALL_o) there is a significant increase in species richness between the pre-MN and MN spore biozones (fig. 3, a – c). Observed miospore diversity, M_o, was tested with the Welch t-test because the data did not show normal variance. Nonetheless, there a strongly significant result was obtained, where p = 4.362e-09 (t-test = 7.03). Observed cryptospore, C_o, and all observed data, ALL_O, ($M_o + C_o$) were tested with a two-sample t-test and there is a strongly significant change in both, with C_o p = 7.493e-07 (t-test = 5.62) and ALL_O p = 9.182e-09 (t-test = 6.83). There is a minor decrease in trilete spore species diversity in the *tripapillatus – spicula* zone before a renewed increase in the proceeding biozones. This decrease in species diversity is not observed amongst the cryptospores, which experience a sustained increase in species diversity through the sequence. Between the lower and middle MN subzones there is a fall in mean trilete spore diversity, which is coupled with a slight depression in the rate of increasing mean cryptospore species diversity for all spores in both observed and range through data. Two-sample t-tests assessing the change in mean species diversity between the lower MN and middle MN zones (fig. 3a – c) demonstrate that the overall fall in diversity is not significant (ALL_o p = 0.22). The change in diversity amongst cryptospores is similarly not significant between these subzones (C_o p = 0.09). However, the fall in miospore diversity is found to be weakly significant (p = 0.04).

Quantified disparity change through the Anglo-Welsh Basin sequence shows a similar pattern to species diversity (fig. 4a). A well-defined increase in disparity amongst both trilete spores and cryptospores occurs, with the largest increase in disparity occurring amongst trilete spores. Two-sample t-tests demonstrate that the change in disparity between the pre-MN and MN zones is significant overall (ALL_o p = 2.24E-09) (fig. 4, d – f), and individually amongst miospores (M_o p = 1.16E-07) and cryptospores (C_o p = 3.47E-09). Trilete spore species richness shows a fluctuating overall increase with a minor fall in disparity in the TS zone, between the PL and NTPA zones. Following this, species disparity increases considerably to the lower MN zone. Between the lower and middle MN zones, there is a fall in miospore disparity. This pattern is seen in both range through and observed data. T-tests assessing the significance of the disparity decrease amongst miospores between the lower and middle MN subzones indicate that the change is weakly significant (M_o p = 0.04; fig. 4, d – f). Two sample t-tests show that there is not a significant reduction in overall mean species disparity (ALL_o p = 0.29). Cryptospores show an uninterrupted increase in mean disparity between the PL and middle MN zones, although this is considerably less than the disparity changes seen amongst miospores. There is no fall in cryptospore disparity between the lower and middle MN subzones and while there is a slight reduction in the rate of disparity increase, the increase in mean cryptospore disparity between the lower and middle MN subzones is found to be significant (C_o p = 0.01).

3.2. Temporal β-diversity

Temporal β-diversity (turnover)

Table 2 shows the results of the pairwise Jaccards dissimilarity indices between biozones. For all species, assemblages are most similar between the lower and middle *micrornatus – newportensis* zones, with 35% of species being unique (D7 = 0.35). Assemblages have the highest dissimilarity when compared with the *poecilomorphus – libycus* zone, where there are >60% unique species (D7 = >0.6). Interestingly, the highest proportion of unique species is observed between the *poecilomorphus – libycus* and *tripapillatus – spicula* zone. Overall 68% of all species are unique between the pre-*micrornatus – newportensis* and *micrornatus – newportensis* biozones (D7 = 0.68). Cryptospore dissimilarities are typically low, indicating a high proportion of shared species. The greatest dissimilarity between cryptospore species occurs between the Non-tripapillate *Aneurospora* spp. zone and *poecilomorphus – libycus* zone (D7 = 0.57) and *tripapillatus – spicula* zone (D7 = 0.5), suggesting an earlier community turnover amongst this group than in trilete spores. There is a relatively low, but still considerable, degree of difference in cryptospores between the pre- *micrornatus – newportensis* and *micrornatus – newportensis* biozones, with 42% of species being unique (D7 = 0.42). Trilete spores

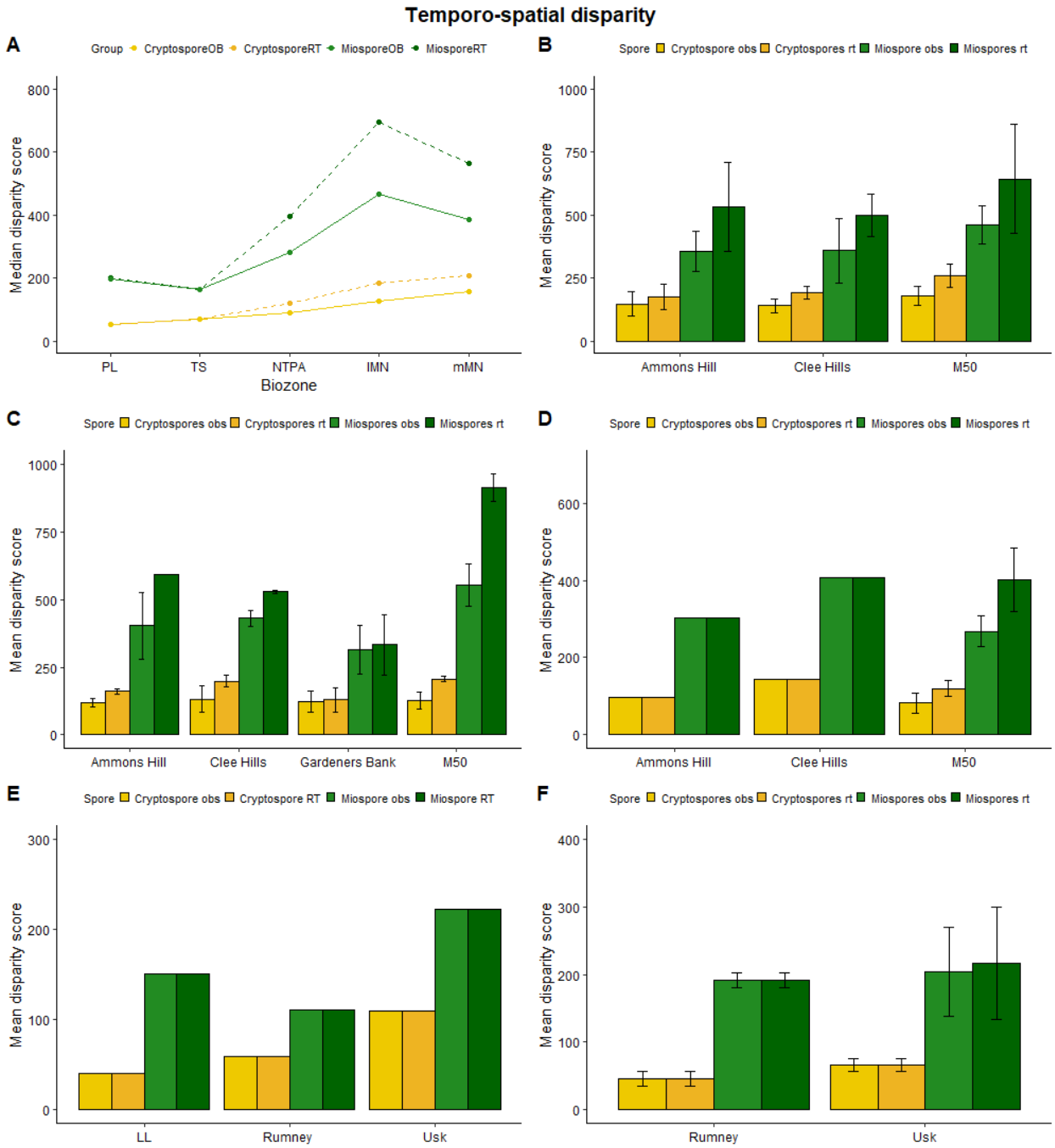

Figure IV-4: temporal and spatial species disparity by biozone in the Anglo-Welsh Basin. ***A:*** *line graph illustrating mean disparity (observed and range through data) through the biozones: mMN and lMN middle and lower micrornatus – newportensis biozone; NTPA: non tripapillate Aneurospora spp. Biozone; TS: tripapillatus – spicula biozone, and; PL poecilomorphus – libycus biozone.* ***B – F:*** *barplots illustrating mean spp. Richness between coeval (same biozone) sites (observed and range through data shown) and standard deviation.* ***B:*** *middle MN zone;* ***C:*** *lower MN zone;* ***D:*** *NTPA zone;* ***E:*** *TS zone;* ***F:*** *PL zone. Note Y axis scale change between some graphs. Plot made in R using* `library("ggplot2")` *and* `library("ggpubr")`*.*

show the greatest dissimilarity in all cases when biozones are compared with the *poecilomorphus – libycus* zone (D7 = >0.7). Between the lower *micrornatus – newportensis* subzone and Non-tripapillate *Aneurospora* spp. zone assemblages 66% of species are unique. There is a gradual decrease in dissimilarity through the sequence. 77% of trilete spore species are unique when pre- *micrornatus – newportensis* and *micrornatus – newportensis* biozone assemblages are compared.

3.3. Local (α) and spatial (β) palynological diversity and disparity

Fig. 3 b – f shows mean species richness for observed and range through cryptospores and miospores in coeval localities. For both observed and range through data, mean miospore diversity is always greater than mean cryptospore diversity, and coeval locality diversity is approximately even across coeval localities, with differences in species richness of typically <10. The overall increase in temporal species diversity (2.1) is observed in all long ranging localities and is most pronounced in the M50 section. Fig. 4, b – f compares the observed and range through disparity between coeval localities. In line with diversity patterns, disparity amongst trilete spores is always greater than the disparity of cryptospores. In coeval assemblages, there is some minor variation in disparity. Jaccards dissimilarity indices indicate that species composition varies between coeval localities (table 3**)**, with varying degrees of shared and unique taxa.

All species

	middle_mn	lower_mn	ntpa	ts
lower_mn	0.35			
ntpa	0.46	0.55		
ts	0.58	0.65	0.57	
pl	0.6	0.66	0.66	0.68
pre_mn	0.68			

Cryptospores

	middle_mn	lower_mn	ntpa	ts
lower_mn	0.25			
ntpa	0.5	0.33		
ts	0	0.25	0.5	
pl	0.25	0.4	0.57	0.25
pre_mn	0.42			

Trilete spores

	middle_mn	lower_mn	ntpa	ts
lower_mn	0.4			
ntpa	0.44	0.66		
ts	0.71	0.75	0.61	
pl	0.72	0.76	0.72	0.8
pre_mn	0.77			

Table IV-2: pairwise Jaccards dissimilarity indices comparing incidences of spore species between biozones for all species (miospores + cryptospores), cryptospores and trilete spores.

In the *poecilomorphus – libycus* biozone, diversity and disparity is ± comparable between the localities, although Usk exhibits a slightly higher diversity and disparity of miospores and cryptospores compared with Rumney (figures 3f, 4f). Jaccards dissimilarity testing indicates that species composition is similar, with 60% of species being shared between the localities ($D7_{all} = 0.4$). The proportion of cryptospores ($D7_c = 0.28$) and trilete spores ($D7_m = 0.33$) shared between the groups is relatively similar.

In the *tripapillatus – spicula* zone (figures 3e, 4e)., further differences between localities begin to appear (figs 3 and 4, table 3). Cryptospore and miospore diversity is greatest at Usk, followed by Ludlow Lane. The latter does not have a considerably greater diversity than Rumney. Despite having a higher diversity of cryptospores, the disparity of this group is lower in Ludlow Lane than it is at Rumney. The disparity of miospores, on the other hand, is greater at Ludlow Lane than at Rumney. Dissimilarity testing indicates that shared species composition is reduced relative to the *poecilomorphus – libycus* zone. Between Ludlow Lane and Rumney, 53% of species are unique ($D7_{all} = 0.53$), and between the former and Usk, 57% of species are unique ($D7_{all} = 0.57$). Between Rumney and Usk, however, 70% of species are shared ($D7_{all} = 0.3$). The greatest variation occurs amongst miospores, with 77% ($D7_m = 0.77$) and 80% ($D7_m = 0.8$) of miospores unique to Rumney and Usk respectively when compared with Ludlow Lane. Meanwhile, 50% of miospore species are unique between Rumney and Usk. Between all sites, cryptospore species are shared (D7 = 0).

	PL biozone		TS biozone			NTPA biozone			Lower MN biozone				Middle MN biozone		
All		**Rumney**		**Ludlow**	**Rumney**		**M50**	**CH**		**M50**	**CH**	**AH**		**M50**	**CH**
	Usk	0.33	**Rumney**	0.53		**CH**	0.36		**CH**	0.33			**CH**	0.2	
			Usk	0.57	0.3	**AH**	0.41	0.38	**AH**	0.18	0.2		**AH**	0.18	0.2
									GB	0.46	0.36	0.36			
Cryptospores		**Rumney**		**Ludlow**	**Rumney**		**M50**	**CH**		**M50**	**CH**	**AH**		**M50**	**CH**
	Usk	0.4	**Rumney**	0		**CH**	0.33		**CH**	0.2			**CH**	0	
			Usk	0	0	**AH**	0.2	0.42	**AH**	0	0.2		**AH**	0	0
									GB	0	0.2	0			
Miospores		**Rumney**		**Ludlow**	**Rumney**		**M50**	**CH**		**M50**	**CH**	**AH**		**M50**	**CH**
	Usk	0.286	**Rumney**	0.77		**CH**	0.4		**CH**	0.42			**CH**	0.33	
			Usk	0.8	0.5	**AH**	0.57	0.33	**AH**	0.28	0.2		**AH**	0.28	0.33
									GB	0.66	0.5	0.57			

Table IV-3: Jaccard dissimilarity metrics from pairwise comparisons of coeval localities. ***CH:*** *Clee Hill****; AH:*** *Ammons Hill****; GB:*** *Gardeners Bank****.*** *Calculated using* `vegdist()` *in* `library("vegan")` *.*

The non-tripapillate *Aneurospora* spp. zone is recorded here in three sites from terrestrial settings (figures 3d, 4d). Diversity and disparity of cryptospores and miospores is greatest in observed data at Clee Hill, which is considerably greater than Ammons Hill and the M50. The latter locality has the lowest mean diversity and disparity. Range through data suggests that the M50 has the highest miospore diversity and disparity. A relatively high degree of homogeneity exists between the localities, with the greatest proportion of unique taxa (40%) occurring between the M50 and Ammons Hill ($D7_{all} = 0.4$). The proportions of unique taxa are similar between Clee Hill and the other localities (36 – 38%). The largest variation is again found amongst miospore species, with 33 – 57% being unique to each locality, with the greatest difference ($D7_{mio} = 0.57$) occurring between the M50 and Ammons Hill. In contrast to the *tripapillatus* – *spicula* zone, species of cryptospore unique to localities begin to appear, with the proportion of shared species between 58 – 80%. The greatest proportion of unique cryptospore species at this time is found between Clee Hill and Ammons Hill ($D7_{cry} = 0.42$).

The lower MN localities show further variation in mean diversity and disparity (figures 3c, 4c)., with the M50 section exhibiting the highest mean diversity amongst the localities.in observed and range through data. Although the variation is not considerably great for observed data, range through data amplifies the variation. The lowest diversity is seen at Gardeners bank, although the observed cryptospore diversity is essentially comparable across all of the localities. A similar pattern is seen for mean miospore and cryptospore diversity, which is greatest amongst miospores in the M50 section. Disparity amongst cryptospores is again comparable across the localities. In terms of species composition, the proportion of unique taxa ranges between 18 – 46%, with the lowest proportion of shared taxa existing between the M50 and Gardeners Bank ($D7_{all} = 0.46$). Indeed, the proportion of unique taxa is greatest at Gardeners Bank in all cases when compared with the other coeval localities (36 – 46%). The highest proportion of shared taxa occurs between the M50 and Ammons Hill ($D7_{all} = 0.18$). Miospores account for much of the difference with unique taxa ranging between 20 – 66%, the highest proportion of unique taxa being found between the M50 and Gardeners Bank. Cryptospores, on the other hand, are typically comparable across localities, with the proportion of unique taxa ranging between 0 – 20%, with the Clee Hill assemblages appearing to show the highest degree of difference.

Diversity and disparity amongst middle MN localities is more even across localities than the preceding lower MN zone (figures 3b, 4b). Observed data indicates that miospore diversity and disparity is greatest in the M50 section, which does not greatly exceed the values for Clee Hill and Ammons Hill, which are in turn similar. Mean cryptospore diversity and disparity is slightly greater in the M50 relative to the other localities, but overall values are essentially comparable. The variation in species composition is reduced in this biozone. Jaccards dissimilarity indicates that the proportion of unique taxa varies between 10 – 20% overall, with the greatest proportion occurring in Clee Hill. The proportion of unique miospore taxa ranges between 20 – 33%, again with Clee Hill being the most unique. Cryptospore variation is negligible between all localities.

3.3. Disparity and diversity of selected miospore and cryptospore genera

Section 3.2. shows clear increases in the diversity and disparity amongst spores between the Ludlow and Lochkovian of the sequence. To explore this change further, some key trilete spore and cryptospore genera are explored in terms of the temporal diversity and disparity amongst their constituent species. This facilitates a better understanding of the key contributors of the cryptospore and miospore radiation through the sequence. Figs. 3 and 4 illustrate that trilete spores account for most of the temporal change in diversity and disparity through the Anglo-Welsh Basin sequence in both range through and observed data. Between the Ludlow and Přídolí, species of *Ambitisporites* (fig. 5a) show limited morphological change. Indeed, the morphology of the most common spores of the genus, *A. avitus* – *dilutus*, changes little from the Ordovician (e.g. Hoffmeister, 1959). However, subtle morphological changes do occur which deviate enough to necessitate differentiation into several morphospecies, and these are recorded in the Anglo-Welsh Basin and elsewhere, including Scotland (e.g. Wellman and Richardson, 1996).

Such morphological variations amongst *Ambitisporites* spores center around the thickness of lips, amb size and position of the crassitude, amongst others (e.g. Burgess and Richardson, 1995; Wellman and Richardson, 1996; Richardson et al., 2001). These subtle morphological changes, especially in isolation, do not considerably influence the complexity of ontogeny of these spores *sensu* Wellman et al., (2013). As such, the disparity of *Ambitisporites* remains relatively low and constant between the Ludlow and Lochkovian of the Anglo-Welsh Basin. Sporadically higher scores occur in the PL and lower MN zones with the combination of prominent lips and a proximal thickening accompanying the triradiate mark, such as in *Ambitisporites* sp. 2. Overall, however, there is little considerable change through the sequence amongst *Ambitisporites*.

Many of the other genera show similar minor changes in disparity though the system also, with occasionally complex forms increasing disparity in certain biozones, but with little effect on median score. This is the case for *Apiculiretusispora* (fig. 5c), which despite species addition in the MN zone, exhibits a ± consistent median disparity throughout the sequence. Indeed, many novel *Apiculiretusispora* species emerging in the NTPA and lower MN zones exhibit change in the character of spines, cones and grana, changes which are not valued in the trait scoring and are hence overlooked by the method. In other cases, novel species emerge with a relatively low disparity. This occurs amongst *Chelinospora* in the middle MN subzone, where several novel species with disparities less than the median are added (fig. 5d). Whilst this is a rare occurrence amongst genera, the occurrence may

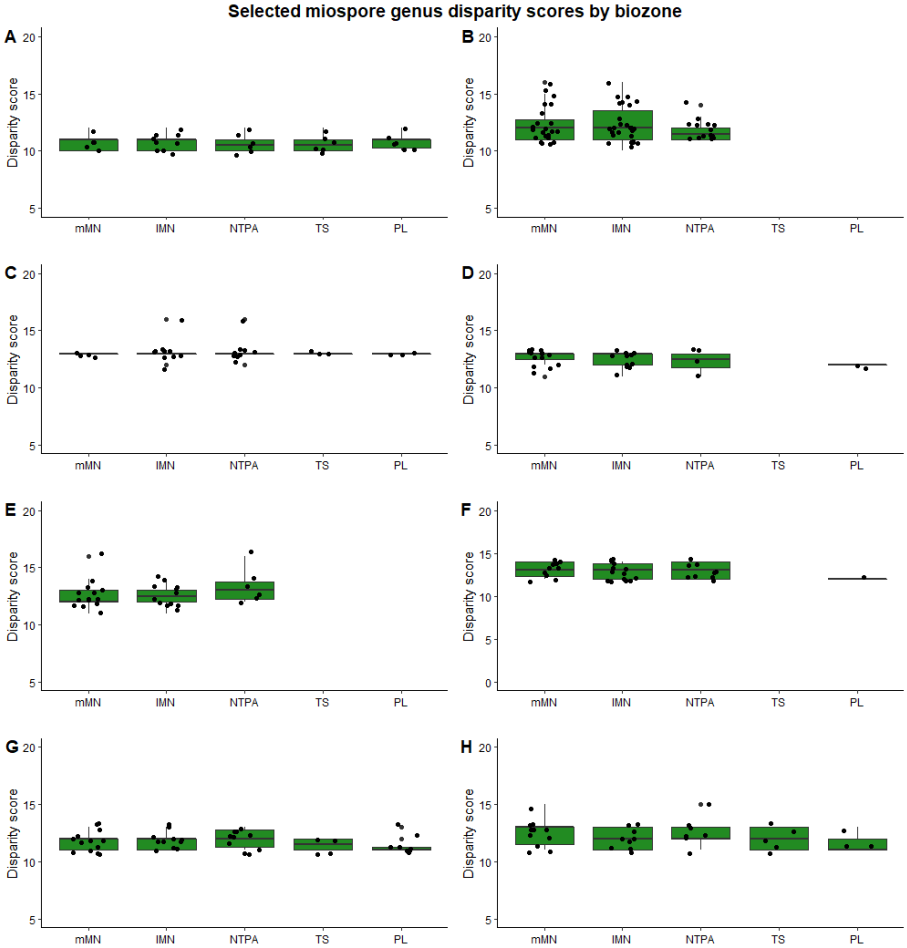

Figure IV-5: Temporal disparity of selected miospore genera, binned by biozone. ***A:*** *Ambitisporites;* ***B:*** *Aneurospora;* ***C:*** *Apiculiretusispora;* ***D:*** Chelinospora*;* ***E:*** *Cymbosporites;* ***F:*** *Emphanisporites;* ***G:*** *Retusotriletes;* ***H:*** *Synorisporites. Individual points indicate individual species within the selected genus. Species scored according to disparity matrices in thesis appendix 4.5. Charts produced in R with* `library("ggplot2")`*. Thesis appendix 4.5.*

contribute to the slight reduction in mean disparity between the lower and middle MN subzones. Species such as *Emphanisporites* (fig. 5f) show an increase in species richness between the Ludlow and Lochkovian, but species show a narrow disparity score distribution despite this proliferation.

Aneurospora (fig. 5b) shows a rapid increase in species diversity, with high disparity, in the biozone where it is first recorded (NTPA). Through the lower and middle MN subzones, there is a continued high rate of species addition with continued innovations contributing to increasingly greater disparity scores. The most distinct sculptural addition in *Aneurospora* is interadial papillae, which appear on several species in the lower MN zone (e.g. *A. isidori* and *A. trilabiata*). Interadial papillae often occur in combination with prominent lips and/ or triradiate thickenings leading to greater disparity scores. Continued innovation increases disparity further in the middle MN subzone with increasing complexity of sporogenesis. However, despite the high disparity of some *Aneurospora* species, the median disparity score does not increase considerably. The persistence and emergence of simpler *Aneurospora* spores, including non-papillate species, prevents the median disparity from increasing considerably. Nonetheless, species of *Aneurospora* achieve some of the highest disparity scores amongst the palynoflora, contributing significantly to increases in disparity between the NTPA and MN zones. Furthermore, despite the minor loss of disparity in the middle MN subzone, *Aneurospora* continues to proliferate.

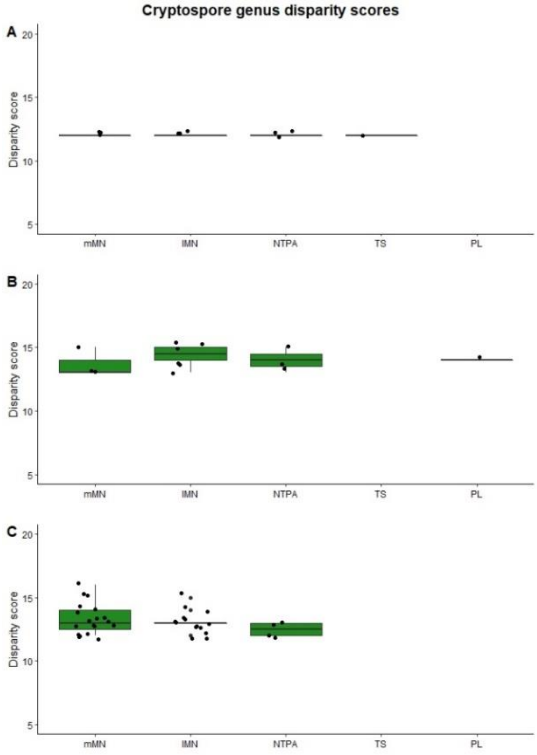

Figure IV-6: disparity scores of selected cryptospore species by biozone. ***A:*** *Artemopyra;* ***B:*** *Chelinohilates;* ***C:*** *Cymbohilates. Charts produced in R with* `library("ggplot2")`. *Thesis appendix 4.5.*

The sustained increase in cryptospore species diversity and disparity seen in section 2.2 is principally maintained by apiculate hilate cryptospores (fig. 6). Genera such as *Laevolancis* show little morphological innovation through the sequence. Emphanoid cryptospores such as *Artemopyra* (fig. 6a) show a small level of species addition, but disparity scores occur over a limited range. As with *Apiculiretusispora*, the morphological variations of *Artemopyra* which distinguish the species are not accounted for the trait scoring metric. Species of *Chelinospora* (fig. 6b) proliferate between the Ludlow and Lochkovian and appear to reach maximum diversity and disparity in the lower MN. Following this, Middle MN assemblages are reduced in diversity and disparity (figures 3b, 4b). *Cymbosporites* (fig. 6c)

proliferates in the lower MN, with persistence of high disparity spores into the middle MN. There are also several further additions of high disparity species and variants with complex innovations and combinations, including proximal papillae + radial muri. Such complexity contributes to the sustained increase in diversity and disparity observed amongst cryptospores between the lower and middle MN subzone.

3.4. Amb diameter measurements

In order to explore the possible effect of sorting on each sample, 150 amb measurements from each sample were collected and the results for the composite section are given in fig. 7. These measurements indicate that there is a slight decrease in amb diameter through the overall sequence, from a mean of mean 36µm (median 37µm) to a mean amb diameter of 30.5µm (median 26µm). The trendline reflects this decrease in amb diameter. There is a high degree of outliers throughout the sequence, especially for amb diameters which are greater than average. Particularly with the Lochkovian assemblages, this is attributable to the incoming of larger spore species such as *Perotrilites*. In general, there does not appear to be a clear exclusion of spores based on amb diameter from the assemblages such as that observed by Wellman et al. (2000), with wide interquartile ranges indicating a wide spread of amb diameters observed in each assemblage. Rarely, narrowing of interquartile ranges is observed, most notably in RU/21/4, and this may indicate a degree of sorting whereby the spores with a greater amb diameter have been lost.

Groups of samples drawn from different localities sometimes appear to have similar amb diameter ranges, which vary from other sites. Such differences may be partially responsible for the change in amb diameter observed through the composite section. Most notably, marine assemblages (Rumney, Usk) appear to have a mean and median amb diameter which is greater than the mean and median values of wholly terrestrial settings (compare Rumney and Usk with the M50, fig. 7). In addition, there is

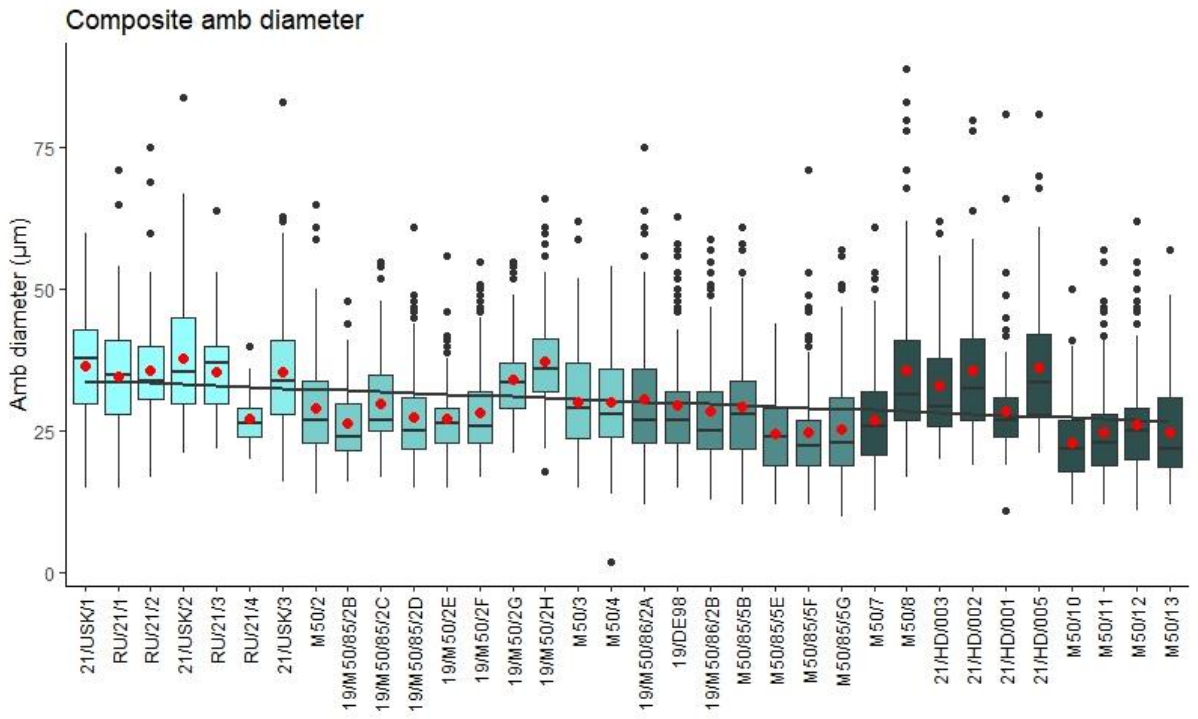

Figure IV-7: boxplot illustrating amb diameter change through the composite Anglo-Welsh Basin section, Ludlow to mid Lochkovian, arranged by stratigraphic height relative to the Chapel Point Limestone member. Colour change corresponds to spore assemblage biozones. Trendline uses formula y~x. `library("ggplot2")` *data in thesis appendix 4.6.*

sometimes a difference in median amb diameter between ±coeval localities, such as the middle *micrornatus – newportensis* of Clee Hill and the M50. These changes may be a result of the prevailing hydrodynamic properties present at the time of deposition, perhaps in addition to the prevalence of parent plants in individual areas. The median change of 11µm is considered the most reliable measurement here, as the mean is susceptible to outliers, and is considered negligible.

4. Discussion

4.1. Comparisons with the macrofossil and mesofossil record

There is a clear increase in overall palynological diversity and disparity in the Anglo-Welsh Basin, with a statistically significant increase in both miospore and cryptospore diversity and disparity between pre-MN and MN assemblages. While there is almost certainly some influence of facies change (**s**ection 4.5), the trend of increasing diversity observed in the palynological record in this and previous work (e.g. Richardson and Lister, 1969) may be reflected somewhat in the macrofossil record of the Anglo-Welsh Basin. Zosterophylls do not appear until the middle – upper MN of the Anglo-Welsh Basin (Wellman et al., 2000), with the major rhyniophytoid – zosterophyll turnover occurring between the upper Lochkovian *micrornatus – newportensis* and *breconesis – zavallatus* spore assemblage biozones (Edwards and Richardson, 2004). This turnover, which is likely to be observable in the dispersed record, is not observed here as the studied section terminates before its occurrence. Prior to this major turnover event, the macrofossil record may show an increase in the number of rhyniophytoid species between the lower and middle MN (Edwards and Richardson, 2004; Morris and Edwards, 2014). However, the well recorded preservational and facies biases, *inter alia*, which affect the macrofossil record may distort diversity studies and give false patterns (e.g. Edwards and Richardson, 2004; Kenrick et al., 2012). Such a radiation in rhyniophytoids might be expected given the radiation of crassitate miospores such as *Aneurospora*, which are typically associated with *Cooksonioid* sporangia (e.g. Fanning et al., 1992; Morris et al., 2012a). However, the low sporangial disparity amongst many rhyniophytoid compression fossils may obscure this pattern.

Whilst the mesofossil record shows a relatively higher sporangial diversity and disparity amongst rhyniophytoids than the macrofossil record, these changes have not been quantified or set into a continuous temporal context. However, the low morphological diversity of sporangia is well documented, with Fanning et al. (1988) demonstrating 'cryptic' evolution amongst the *in situ* spores of otherwise morphologically comparable *Cooksonia pertoni* sporangia. Indeed, the simplicity of *Paracooksonia* and *Lenticulitheca* (Morris et al., 2011b) which produce several of the proliferating *Aneurospora* and *Cymbohilates* genera, show little gross morphological variation and therefore do not reflect the disparity observed in the dispersed spore record. These simple, discoidal sporangia do not appear to vary considerably, even where *in situ* spores vary, and they show little morphological change between the lower and middle MN zones (Chapter V). Indeed, the simple discoidal sporangia of *Paracooksonia* and *Lenticulitheca* are reflected in the parent plants of other spore genera, including *Emphanisporites* (Morris et al., 2011a; Chapter V). In some cases certain genera do show a high sporangial disparity between species of *in situ* spores, most notably *Emphanisporites* where at least five variations occur, from bifurcating to discoidal (Ball and Taylor, 2022; Edwards and Richardson, 2000; Morris et al., 2011a; Chapter V), but the relative changes in disparity through time is difficult to gauge with the limited suite of samples.

While some workers have outlined an apparent global picture of plant diversification amongst macrofossils (Capel et al., 2022) of the 'Eotracheophytic' flora *sensu* Cleal and Cascalas-Minana (2014) between the Wenlock and Lochkovian, other workers urge caution, as these macrofossil patterns are likely driven by facies changes and the nature of the rock record (Kenrick et al., 2012). As such, no comparison between the diversification amongst the Anglo-Welsh Basin palynomorphs and global macrofossil record can yet be fielded.

4.2. Technique consideration

Cleal *et al*. (2021) and Pardoe *et al.* (2021) outline and discuss current methods for exploring the diversity and disparity of fossil plants and palynomorphs. They highlight the importance of considering what is being measured when carrying out various diversity tests. This is especially true for palynological samples, which while more accurately reflecting the taxonomic richness of vegetation than the macrofossil record in the late Silurian and Early Devonian, do have several caveats. In particular, the abundance of spores cannot be taken to directly affect the abundance of plants, as the individual fecundity and proximity of plants to the depocenter will influence its prevalence in the dispersed spore record. Nonetheless, it is reassuring that that currently all of the sporangia yielding *in situ* spores have yielded the same or closely comparable species (e.g. Fanning et al., 1992; Wellman et al., 1998b, 2004a; Wellman, 1999; Morris et al., 2011a, b, 2012a; Edwards and Richardson, 2000; Edwards et al., 2014, 2021a, b; Morris and Edwards, 2018; Ball and Taylor, 2022) indicating that (1) an individual spore species is a proxy for an individual parent plant, and (2) the presence/ absence of a spore species acts as a proxy for the presence/ absence of a parent plant. However, it is important to note that the dispersed spore record may not be exhaustive of the plants growing in a depositional basin, with some *in situ* spores not yet being recorded in the dispersed record (e.g. Edwards and Richardson, 2000; Ball and Taylor, 2022; Chapter V). Whilst this may be a function of the paucity of the plant near depocenters, it may also reflect immaturity of the *in situ* spores, *inter alia* (Chapter V). Similarly, diversity may be partly facies controlled; with wide ranging rivers collecting spores from a wider catchment area, and shallow marine sections reflecting spores from coastal vegetation and from the extent of the river catchment. Here, a brief critical overview of the techniques used to investigate the temporo-spatial diversity and disparity of the dispersed spores is given here, which should be considered in the proceeding discussion.

Diversity and disparity measures

Taxonomic richness has been used here to indicate the diversity amongst individual assemblages and through time. However, detecting the total richness of a community is complicated by the presence of rare taxa, which may be missed, or indeed for taxa which are so rare, or rare enough not to be properly categorised, that they were not included in a study or species list. As such, it must be borne in mind that diversity may be greater than observed. The degree to which the robustness of a given species survey, and hence taxonomic richness, can be gauged, can be judged according to sampling effort (Cleal et al., 2021b). In this case, each palynomorph assemblage was counted to 250 spores, and then logged for 'rare' species. 2 - 3 slides from each assemblage were logged in addition to the counted slides. As mentioned in methods, the decision was made to count to 250 based on Traverse (2009) and previous work by Morris (2009 unpublished thesis p. 5 – 3,), where cumulative counts from the same basin in coeval assemblages plateau between 200 – 250 counts, indicating that most of the species in the assemblage are represented in the count (Chapter II). Indeed, typically fewer than 5 additional species were recovered during further logging, and these were often singletons. However, it must be considered that an unknown number of rare forms may have been missed. As such, the taxonomic richness and disparity measurements of the assemblage may be an underestimate (Traverse, 2009), although this is likely to be negligible here.

A further problem, which is particularly problematic amongst morphologically similar forms such as *Laevolancis*, is the understanding that diversity can be 'cryptic'. Such hidden diversity is not observable under light microscope and is only revealed at present by ultrastructural analysis. Wellman et al. (1998b) demonstrated that the laevigate hilate cryptospore *Laevolancis* could be subdivided into five types based on ultrastructure. Such 'cryptic diversity' is also demonstrated amongst *Ambitisporites* (Taylor, 2003), *Tetrahedraletes* (Taylor, 2002) and *Emphanisporites* (Taylor et al., 2011). Such diversity, which cannot currently be accounted for in ordinary light microscopy, further underestimates diversity measurements,

although to what extent is unknown. Because disparity is a measurement of morphological diversity, these issues also result in an underestimate for this metric.

Comparisons of temporal and spatial diversity and disparity may also be affected by the number of samples collected between localities and biozones The diversity and disparity of localities has been binned by biozone (figs. 3, 4), and a mean calculated from all of the samples included within that biozone. As such, the mean diversity and disparity between localities is influenced by the number of samples taken from the locality, in addition to their temporal range and/ or stratigraphic position. demonstrates that, especially in the lower and middle *micrornatus – newportensis* subzones, there is a sustained addition of species through biozones. In this case this may lead to a higher mean diversity and disparity in longer/ stratigraphically higher sections compared with shorter/ stratigraphically lower sections, even in the same. 'coeval', biozone or subzone. To avoid this issue, an argument could be made to split long ranging biozones and compare localities of a similar stratigraphic height, perhaps relative to the Chapel Point Limestone member. This is problematic, however, because the comparative sedimentation rates between areas are unknown, and thus subtle temporal variation is still likely to occur. The possibility that greater sample number results in a higher mean diversity and disparity compared with other coeval localities is not always borne out, however, and it is maintained that there is a genuine signal suggesting that α-diversity is greater in some localities than in others. Despite a greater number of samples from the NTPA zone of the M50, the diversity and disparity of that locality is noticeably less than the diversity in Clee Hill, where there is only one sample known. However, the sample from Clee Hill is drawn from 7m below that Chapel Point Limestone member, whilst the closest M50 sample is drawn from -32 m below (25 metre gap). While the precise temporal difference and sedimentation rate between the samples is not known, it is possible that the time-gap was considerable enough to allow for the accumulation of more species between the last M50 sample and the Clee Hill sample.

Consequently, any interpretation of α-scale diversity should be treated as a broad pattern rather than a specific indication of a low or high diversity region, especially when the locality contains 'coeval' samples which extend across a wide stratigraphic continuum. Nonetheless, where a particularly strong signal is detected, it is possible to suggest that one area has a distinctly lower diversity and/ or disparity than other localities and betrays an ecological signal. Such a pattern is clear at Gardeners Bank, where *Acinosporites salopiensis* and associated tetrads of the same species occur in unusually large proportions, suggesting that the parent plants of these spores may have dominated this area at that time. Alternatively, this limited flora may represent subtle facies change, although against this is the observation that the sedimentary section from which the Gardeners Bank samples are drawn is typical of fluvial Old Red Sandstone sections (see 4.3 and 4.4).

Disparity scoring

Wellman *et al.* (2013) devised their disparity scoring chart exclusively for trilete spores, the principal components of assemblages especially by the late Silurian. Using this scoring system, they showed the great increase in disparity towards the Silurian and Devonian boundary. Wellman *et al*. (2013) did not devise a scoring system for cryptospores, however, which may constitute up to a third of any given late Silurian – Early Devonian assemblage in the Anglo-Welsh Basin (Chapter III). Here, a preliminary scoring system has been devised for the cryptospores in order to (a) provide a fuller indication of disparity changes occurring in the basin, and (b) to explore the diversification of cryptospores in more detail. Indeed, qualitative insights into morphological innovation amongst the cryptospores in the Ludlow, Přídolí and Lochkovian of the Anglo-Welsh Basin is already well documented, with the emergence of murornate hilate monads (e.g. *Chelinohilates erraticus*) and the high degree of variation in apiculate hilate monads, which prompted Richardson (1996a) to differentiate *Cymbohilates variabilis* into four distinct variants based on proximal structural features and the nature of the distal ornament.

Here, then, a preliminary suite of disparity scores is provided for cryptospores (thesis appendix 4.3). However, cryptospores are a highly diverse group, and as such are probably best approached at present as separate entities according to their gross morphology (e.g., permanent dyad, hilate monad, permanent tetrad, *inter alia*) (pers. comm. C.H. Wellman, 2021). In part, this is due to uncertainties in the complexity of their development. Wellman *et al*. (2013) devised the trilete scoring chart based on the degree of complexity in producing certain structures and ornaments during sporogenesis, rather than the stratigraphic occurrence of the spores. This logic is followed here, but uncertainties in the development of cryptospores, and concomitant uncertainties in comparing their complexities, means that cryptospore 'groups' cannot be scored against one another at present (e.g., permanent dyads such as *Pseudodyadospora petasus* cannot, at present, be compared to semi-permanent dyads, such as *Dyadospora murusdensa*, on a complexity-of-Formation basis). As such the scoring suites for each cryptospore group cannot be compared to one another, or to trilete spores. However, the relative increases and decreases in disparity may be comparable with caution when accounting for the change in diversity of the groups in question.

Comparing figures 3 and 4 illustrate the close relationship between species diversity and disparity in these assemblages; that is, the pattern observed for temporal species richness change is reflected in the temporal disparity change. This may be a function of using morphotaxa, rather than biological taxa, to describe the spore species. In essence, morphotaxa are a measurement of disparity; that is, with an increasing richness of morpho-species, there is increasing morphological diversity, or disparity. Nonetheless, the separate scoring system is retained to allow for the assessment of complexity of the cryptospores and miospores through time and spatially, which is not clearly demonstrated by morphospecies alone, and to gauge the changes in complexity amongst individual morphogenera. Moreover, the disparity scores seem to be capturing an aspect of ontogeny that is not completely reflected in how species of palynomorphs are recognised.

A note on range through vs observed data

The range through technique is commonly utilised in palynology (Cleal *et al*., 2021), filling stratigraphic gaps between species occurrences on the basis that the species' absence between these two occurrences is unlikely to represent the total loss of the plant from that system between the occurrences. Here, the range-through and observed data have been included in the analyses to explore the possible effects on interpretation that each may cause. It is shown that range – through data, while naturally, and sometimes significantly, inflating the species richness and disparity of the assemblages, does not change the overall sequence of events or key qualitative conclusions that can be drawn from the data. However, when considered statistically, range through data is problematic. In this work, the distribution and variance of the data becomes skewed, which in turn limits the reliability of the studies if the assumptions of statistical tests are not considered fully and/ or are not tested for with *ad hoc* tests. Especially in spatial analysis between ±coeval localities, mean diversity and disparity is inflated, which may exaggerate the differences between localities. Again, range through data does not appear to obscure or skew the overall trends in data, but the change is exaggerated relative to observed data. Similarly with temporal data, the distribution and variance of range-through data may be skewed, and statistical tests should account for this.

4.3. Floral heterogeneity in the Anglo-Welsh Basin

Assessing and interpreting local diversity (β-diversity) and disparity differences between spore assemblages in the same basin can be complicated by facies variances, taphonomic influences, subtle temporal variation and palaeoecological differences (e.g. Lavender and Wellman, 2002; Steemans et al., 2007). Nonetheless, some clear patterns emerge between ± coeval localities which elucidate floral heterogeneity patterns across the landscape. Such heterogeneity is likely to derive from specialisation amongst certain miospore and cryptospore producing parent plants, indicated by abundance and presence/ absence of spore species between localities in addition to disparity changes within genera.

Previous workers have deliberated the organisation of cryptospore and tracheophyte parent plants across the landscape. Wellman *et al*., (2000) suggested that cryptospore producing plants may have been confined to riparian, permanently damp environments, living out short life cycles in disturbed settings which would have been seasonally interrupted by flash flooding and other destructive environmental processes. Meanwhile, more complex tracheophytes such as zosterophylls were posited have grown further away from disturbed settings, living out longer life cycles in more stable settings. Later, Edwards and Richardson (2004) hypothesised that instead of growing in riparian settings, cryptospore producing plants were likely confined to less equable settings away from rivers, with survival in harsher settings facilitated by adaptations such as poikilohydry, allowing desiccation and subsequent rehydration of the plants, an adaptation observed amongst some modern bryophytes. Tracheophytes, meanwhile, were suggested to have dominated more equable riparian settings, having competitively displaced the cryptospore producing plants. Recently, Edwards *et al*. (2021) reinforced their earlier thoughts by demonstrating that many eophytes (producing cryptospore dyads and tetrads) exhibited conducting cells characteristic of poikilohydry, conferring resistance to desiccation. Steemans et al. (2007) supported Edwards and Richardson's (2004) interpretation and postulated, based partly on the abundance of trilete spores over cryptospores in marine assemblages, that miospore parent plants probably grew in more riparian settings, while cryptospores may have grown in ephemerally moist settings away from river catchment.

With the new dispersed spore record data presented in Chapter III, and results from diversity and disparity testing, it is possible to further explore this coeval spatial variation between the Ludlow and Lochkovian. Overall (table 2), there is a decline in mean locality heterogeneity through the studied sequence as measured by the Jaccard's dissimilarity index, despite the overall increasing diversity and disparity amongst spores. The decrease is observed amongst miospores and cryptospores, with the greatest dissimilarity between localities exhibited by miospore species. This finding indicates that there is a tendency towards similar species across the landscape, despite the increasing diversity and disparity of spores. Such a change in overall dissimilarity may correspond somewhat with facies variations, where the degree of mixing, *inter alia*, will affect the results of dissimilarity tests. The *poecilomorphus – libycus* and *tripapillatus – spicula* zones are all marine influenced localities. Subtle facies variations, and whether there was drainage into areas by rivers and hence mixing of coastal and relatively more inland riparian palynomorphs, will have influenced the proportions and presence of spore taxa there. Likewise, there is likely to be greater mixing of palynomorphs from a wider area amongst fluvial settings dominated by perennial rivers, such as those of the Freshwater West Formation, than by ephemeral rivers, such as those of the Moor Cliffs Formation. The latter may have impacted the earliest to mid Lochkovian assemblages, with the shift to wetter climates and perennial rivers supressing the dissimilarity scores through mixing, although the catchment differences between the rivers remain equivocal.

The lowest dissimilarity indices are encountered in the middle *micrornatus-newportensis* zone, which is perhaps a function of palynomorph mixing over a wider area by perennial rivers. The low dissimilarity scores may be indicative of the gradual domination of the landscape by an, albeit diverse, selection of plants which outcompeted less derived and some more recently emergent forms. Nonetheless, there are some indications of landscape heterogeneity which are not indicated by the Jaccard's dissimilarity indices, namely the preferential occurrence of *Q. fragilis* and the sustained dominance of laevigate forms at Ammons Hill (Richardson, 2007) relative to the other localities. Furthermore, the sporadic distribution and low proportions of certain spore species, such as *E.* cf. *micrornatus* and *E. epicautus*, indicate that some miospores may have been restricted to certain habitats (Edwards and Richardson, 2004; Ball and Taylor, 2022) further suggesting that there was at least some degree of floral heterogeneity in the mid Lochkovian of the basin.

Similar 'pockets' of vegetation are observed in the lower MN also and are most clearly demonstrated when comparing Gardeners Bank to other coeval localities. There, *Acinosporites salopiensis* and

abundant associated tetrads of that species are observed in significantly greater proportions in Gardeners Bank than in coeval sites. The abundance of the species here, coupled with its paucity in all other studied localities (table 5), suggests that the parent plant was not a common feature of the vegetation elsewhere and may have had specialised ecological requirements, which were fulfilled at Gardeners Bank (*sensu* Edwards and Richardson, 2000). The abundance of *A. salopiensis* most clearly demonstrates that certain areas exhibited a vegetation which was considerably different than other coeval localities. This may also be true of other species and genera, including *E.* cf. *micrornatus*, *E. epicautus* and *Scylaspora* sp. 1, when comparing the distribution and abundances of the species across the basin (Edwards and Richardson, 2004; Ball and Taylor, 2022; Chapter V respectively). Meanwhile, certain plants including the parents of *Laevolancis divellomedium* and *Ambitisporites avitus* spores were more cosmopolitan in their distribution, evidenced by the common incidence of those spores.

While less clear than Gardeners Bank, signals for landscape heterogeneity exist between earlier coeval biozones also. Rumney and Usk show a small variation in the *poecilomorphus – libycus* zone, although dissimilarity is low. It is difficult to gauge whether the differences are due to a degree of landscape heterogeneity or are the result of some subtle difference in facies. Regarding the latter, Usk may have had a greater terrigenous input from rivers than Rumney, with the former being associated with nearby wave dominated deltas (Walmsley, 1958; Basset et al., 1982). Nonetheless, some landscape heterogeneity may be indicated. As mentioned, marine areas adjacent to river input delivering terrigenous material will have gathered spores from along the river catchment. While tenuous, the presence of a greater diversity of species in Usk may be evidence of a disparity between coastal (Rumney) and inland riparian vegetation, with some of the spores found in Usk not being produced by coastal vegetation. This low, but present, degree of heterogeneity finds some support with the low Jaccard's dissimilarity score between the localities. Similarly, in the lower *tripapillatus – spicula* zone of Rumney and Usk, spore assemblages remained ± homogenous, with low dissimilarity scores. Between Rumney and Usk, which are probably more comparable than the putatively younger Ludlow Lane sample (which may account for the latter's low proportion of shared species; table 2), Rumney again has a lower diversity than coeval marine localities. As with the PL zone, this is likely to be a facies difference, with the deltaic system receiving terrigenous material accumulated over a wider catchment area than the assemblage recovered from the Rumney tidal flats. Again, the variation in diversity may suggest that elsewhere in the basin within river catchment there were plants growing which were not present in the coastal facies of Rumney, again pointing towards some degree of floral heterogeneity at this time.

4.4. Ecological inferences from the dispersed spore record

The variable locality heterogeneity combined with spore distribution and abundance between coeval sites, in addition to disparity changes amongst genera, may give some insights into the ecology and evolutionary trajectory of the parent-plants of some dispersed spores. Vegetation distribution in a landscape is controlled by the availability of key resources such as water and nutrients and the presence of biotic and abiotic stressors. Various plants or groups of plants in a landscape may be cosmopolitan as they are able to exploit a wide variety of habitats. Others may be more sensitive to environmental or biotic factors and may therefore be excluded from certain areas. Equally, others may have become specially adapted to exploit resources in stressed settings where other plants are unable to grow. All of the above leads to heterogeneity in the distribution of vegetation in a landscape, and the broad ecological implications of spore distribution can be explored through Edwards and Richardson's (2000) ecology – taphonomy rationale, which is explored further in chapter V.

As mentioned earlier, the Gardeners Bank locality (lower *micrornatus – newportensis* zone) may provide insights into 'pockets' of specialised vegetation, with the considerably greater abundance of *A. salopiensis* spores and associated tetrads relative to other ± coeval localities, thereby indicating local dominance of the parent plants at this time. Combined with the paucity of the spores elsewhere (table 4), the distribution of this spore species suggests that the population was restricted to certain, limited

habitats which were not widespread across the Anglo-Welsh Basin. Because of the high abundance of the species at Gardeners Bank, these habitats appear to have occurred within river catchment. As such, the preferred habitat of *A. salopiensis* may have been a restricted riparian niche. Wellman (2022) investigated the affinities of *Acinosporites macrospinosus* and found that the ultrastructure of the spore species was most comparable to fossil and extant lycopods. The ecology of the parent plant of *A. macrospinosus* is unclear (Wellman, 2022) given the wide range of possible ecological settings which fossil and extant lycopods exploit. Without ultrastructural analysis of *A. salopiensis* spores, it is not possible to determine whether the parents of these spores were also related to the lycopods but it is perhaps not too great a leap of the imagination to suggest that they were given the close similarities with *A. macrospinosus*. Equally, as with *A. macrospinosus*, it is not possible to determine the nature of the habitat which the parent plant was successfully exploiting at Gardeners Bank.

Gardeners Bank represents a typical suite of Lower 'Old Red Sandstone' lithologies, however, the outcrop is peculiar in that the samples are collected from an unusually thick (1m) bed of green siltstone. Such green siltstones are usually thin and subordinate in the Freshwater West Formation, and the implication from the green silts of a reducing, low energy setting may tentatively suggest a shallow lacustrine setting. This difference in facies, which may have had increased moisture availability or variations in soil or water chemistry, may have allowed the parent plant of *A. salopiensis* to exploit the area. Lavender and Wellman (2002) posited that early land plants may have been 'flexible' in their ability to produce tetrads if conditions became stressful; either producing single trilete spores with associated tetrads at the same or different times. This adaptation was suggested in line with hypotheses by Gray (1985) to be an adaptation to stressed environments, advantageous particularly for founder populations. The concomitant loss of genetic diversity was countered by the increased probability of reproduction in inequable settings. Spore masses and sporangia containing a mixture of *in situ* associated trilete tetrads and dissociated trilete miospores have been reported from the Přídolí and Lochkovian of the Anglo-Welsh Basin (Edwards et al., 1996, 1999), with those workers demonstrating, *inter alia*, that the parent plant of *Synorisporites downtonensis* dispersed spores as associated tetrads and fully dissociated miospores. It is possible, then, that the parent plants of *A. salopiensis*, too, were flexible in their ability to produce associated tetrads and fully dissociated miospores, perhaps as an adaptation to some enigmatic environmental stressor affecting the putative lacustrine environment present at Gardeners Bank.

Locality	**% *Acinosporites salopiensis***	**% *Acinosporites* tetrads**
Ammons Hill	Rare - 0.3%	Absent
Clee Hill	Rare	Absent
Gardeners Bank	9 - 21%, mean: 15.3%	2 - 17%, mean: 7.75%
M50 section	Rare - 0.4%	Absent

Table IV-4: abundances of Acinosporites salopiensis miospores and undissociated tetrads in lower MN assemblages of the Anglo-Welsh Basin.

Although less distinct, the ecology of other spore parent plants can be interpreted from the abundance and distribution of spores in ±coeval localities, combined with the occurrence of *in situ* spores (Chapter V**)**. Edwards and Richardson (2000) suggested that the parent plant of *E.* cf. *micrornatus* was probably restricted to a specialised, sporadically occurring ecological niche outside of general river catchment. Later, Ball and Taylor (2022) fielded a similarly sporadic, although perhaps less restricted, niche occurring outside of general river catchment for *E. epicautus*. The middle MN distribution of *Q. fragilis* may also indicate that the parent-plant was exploiting a specialised niche. The spore occurs most frequently at Ammons Hill, although remains rare. Such a paucity and sporadic distribution suggests, as for *E.* cf. *micrornatus*, a restriction to a specialised niche away from the catchment of rivers. It is of interest to note that the species also occurs in ±coeval localities in Scotland (Richardson et al., 1984),

perhaps suggesting that, despite the Scottish Old Red Sandstone being deposited in an intramontane basin, a similar suite of environmental pressures existed in certain areas which facilitated the growth of *Q. fragilis* in both basins. The distribution and abundance variations amongst cryptospores similarly point towards the exploitation of restricted ecological niches amongst some groups, such as *Artemopyra*. Meanwhile, other trilete spore producers appear to have been more cosmopolitan. The wide distribution and high incidence of spores of the *Ambitisporites avitus – dilutus* and *Laevolancis divellomedium – plicata* complex points towards their widespread occurrence in riparian habitats across the Anglo-Welsh Basin. Particularly for these complexes, however, caution must be exercised in deliberations of ecology. While morphologically similar, spores within each complex exhibit varying ultrastructures despite their morphological similarity and apparent simplicity (e.g. Wellman et al., 1998b; Taylor, 2002). This leaves the problem that until ultrastructural analysis can confirm a unilateral spatial distribution of species with similar ultrastructures, it is difficult to say whether the parent plants were more cosmopolitan or were more restricted to specific areas of the basin.

The proportions of laevigate and ornamented cryptospores and miospores may also indicate specialisation, and perhaps exclusion, to certain environments amongst the parent-plants of spores. Richardson (2007) demonstrated that there appeared to be substantially greater number of laevigate taxa at Ammons Hill when compared with coeval sites in the M50 section and Clee Hill and his findings are reflected here. Richardson (2007) attributed this variance to the laevigate spore producing parent plants preferentially inhabiting salt marshes and other sites adjacent to the brackish waters prevalent at times at Ammons Hill (Barclay et al., 1994; Richardson, 2007). This may be a function of these plants having a greater tolerance to the physiological drought and chemical stress imposed by brackish waters. However, the recovery of mesofossils bearing *in situ* cryptospores in a variety of environments (Wellman et al., 1998b; Morris et al., 2011b, 2012a; Chapter V) does go against Richardson's (2007) suggestion that the parent plants of such spores were solely restricted to these marine influenced settings. It remains possible that the parent plants of newly evolved/ invasive species such as *Aneurospora* could not exploit the physiologically difficult conditions presented by brackish water influenced environments, and thus they acted as something of a refugia for less derived plants. Ultrastructural analysis could further reveal whether the dispersed spores of *L. divellomedium – plicata* and *A. avitus – dilutus* spores had similar affinities between wholly terrestrial and marine influenced ±coeval localities, or whether certain 'types' *sensu* Wellman et al. (1998b) were restricted to certain environments.

The studies of disparity amongst key genera (3.3) may also give indications into the ecology of certain plants. Such deliberations require an acceptance that at least some of the sculptures observed on spores have a functional basis, which went some way towards facilitating the successful reproduction and exploitation of new environments by the parent plants. However, links between traits and a function are not always clear, with a single trait potentially having a variety of functions, or vice versa. Nonetheless, the putative presence of coeval evolution of certain features amongst spores, such as the proximal radial muri on *Emphanisporites* and *Artemopyra*, despite the differences in affinities between and amongst the genera, lends support to the suggestion that at least some of the sculptural features observed on spores are ecologically functional. Previous workers have hypothesised a functional morphology for certain features of these early land plant spores, including resistance to consumption by arthropods (e.g. Kevan et al., 1975) or as adaptations to various environmental stresses for the exploitation of specialised niches such as moisture sensing (Ball and Taylor, 2022; Taylor et al., 2011). Some features may not have had ecological functions however, and some, such as interadial papillae, may have instead optimised or facilitated tetrad differentiation during ontogeny (e.g. Taylor et al., 2011).

Despite the uncertainties, several workers have suggested that disparity can be used as a niche proxy, with a high disparity suggesting that organisms are functionally and ecologically diverse (e.g. Friedman, 2010, but see Minelli, 2019). This could be tentatively attributed to *Aneurospora* and *Cymbohilates*, which show a high disparity and high species addition rate through the latter parts of the sequence, perhaps adapting to a range of new microenvironments across the basin (4.5). Meanwhile, species with

lower disparity and species addition may be more marginalised in terms of their ecology, and this may be true of genera such as *Apiculiretusispora* and *Artemopyra*. However, such deliberations are tentative, as it is clear from the dispersed record that genera with low species addition rates and low disparity, such as *Ambitisporites* and *Laevolancis*, were cosmopolitan not only within the Anglo-Welsh Basin but globally (Steemans et al., 2007; Wellman et al., 2013) suggesting the ability to exploit a variety of habitats. However, the absence of features such as proximal radial muri may have equally presvented their invasion and exploitation of newly emergent niches, and this lack of specialisation may have led to their ultimate loss as they were outcompeted by more derived vegetation.

The variation in spore ornament distribution (e.g. Richardson, 2007) and species distributions across the basin (e.g. Edwards and Richardson, 2000; figs. 3 and 4) may suggest that the parent plants of many of the spores were exploiting a variety of environments and may have been excluded from others. The increasing diversity and disparity seen temporally though the sequence may suggest that newly emergent/ invasive plants were colonising the hitherto unexploited and/or newly emergent microenvironments which were developing across the Anglo-Welsh Basin with increased moisture and landscape stability (Morris et al., 2012b) and half-graben development (Crowley et al., 2009; Morris et al., 2012b). These more derived forms may have outcompeted conserved forms in established environments by competitive displacement. Indeed, indications of niche exploitation and patterns of ornament distribution point towards a degree of functionality amongst spore ornament, which may have variously facilitated the successful reproduction of their respective parent plants in particular environments.

4.5. Underlying causes of floral change

This chapter has shown that considerable changes in the disparity and diversity of cryptospores and miospores occurred throughout the sequence, with the greatest increase occurring between the pre-MN and MN assemblages. However, it is important to note that the organisation of vegetation in the Anglo-Welsh Basin is not representative of the global picture. Macrofossils indicate that more derived tracheophytes, including zosterophylls and lycophytes, appeared elsewhere in Euramerica and Gondwana in the Ludlow and Přídolí (Tims and Chambers, 1984; Kotyk et al., 2002; Steemans et al., 2010; Cascales-Minana et al., 2014), and Raymond et al. (2006) suggested a climatic explanation for their exclusion from areas such as the Anglo-Welsh Basin in the Přídolí and early Lochkovian. Broadly, causal factors which may have played a part in developing the temporal spore distribution through the sequence can be divided into abiotic and biotic factors, although a mixture of these factors are likely to have played a contributary role in the observed change in the palynological record.

Abiotic drivers

Transport, sorting and winnowing

Palynomorph preservation is generally good if not exceptional throughout the sequence, with a few exceptions. Palynomorphs are typically of low thermal maturity and show excellent detail of sub-micrometre ornament, but they may be variously affected by compression and/ or folding, tearing of the exine or proximal face loss. However, this generally has little effect on species level identification. Some palynomorphs in these well-preserved assemblages may be affected by contemporaneous fungal growth or mild to severe pyritisation, although again this is rare. In some cases, preservation of palynomorphs in an entire assemblage is poor, which hinders identification to species level as ornament may be damaged and/or barely visible. Often with these poorly preserved assemblages, palynomorph abundance is particularly low and taphonomic influences such as winnowing are identifiable (e.g. RU_4, fig. 7).

There does not seem to be a variation in preservation between samples collected from tectonically affected sections (such as those adjacent or affected by faults or affected by steeply dipping beds) such as the M50 or Ammons Hill, and sections which are only lightly affected, such as North Brown Clee

Hill or Bromyard Plateau, where few major faults are present and the bed dip is shallow (*ca.* 2 - 5˚). Preservation appears to be more variable within sections than between them, with some horizons being extremely well preserved with a high palynomorph abundance, whilst others are depauperate (e.g., cf. 19-DE98 with M50-10), and this may be due to a taphonomic or facies bias. PDI does not vary within sequences.

All of the samples were collected from alluvial or marine assemblages and are hence likely to have been subjected to some degree of transport and concomitant sorting of the spore assemblage. Wellman et al. (2000) described a spore assemblage from the middle *micrornatus – newportensis* zone and, upon finding that spores <33µm in diameter were excluded from the assemblage, surmised that smaller spores (those <33µm) had been winnowed out during transportation. Considering the effect of transport on the marine and fluvial assemblages described here is informative as it may have some responsibility for the spore sequence described above (figures 3a and 4a), especially given the clear facies change observed between the Moor Cliffs Formation and Freshwater West Formation.

The results of the amb measurements (3.4) through the sequence indicates that an exclusion of spores based on amb diameters, as observed by Wellman et al. (2000), is not replicated in the assemblages studied here. This not only suggests that the change in spore assemblage composition observed through the sequence is not a result of sorting (see also Richardson and Lister, 1969), but that the range of taxa observed in the assemblage is probably close to a representative sample.

The trend of decreasing median amb diameter does not follow the trend of increasing grain size through the Přídolí – Lochkovian strata, which gradually shifts from mud dominated systems to sand dominated systems. This suggests that the amb diameter size is not being controlled entirely by hydrodynamic processes, but it is difficult to attribute the change to any one process (e.g. sorting, evolution or facies change). Whether the overall decrease in amb diameter through the system is derived from evolutionary processes is questionable. Amb diameter gradually increases in size through the Devonian (e.g. Breuer, 2007), and so the pattern here contrasts with this. Whilst larger spores are added to the system (e.g. with the incoming of *Perotrilites* species), the median amb diameter is reduced. In part, this may be a result of the input of reworked spores (below), but unless a previously sorted palynoflora is reworked, there is little reason to exclude larger reworked spores, also.

It is prudent to consider the possible effects of reworking on individual assemblages and subsequently the overall pattern of miospore development. The switch in tectonic character between the Přídolí and Lochkovian led to a change in provenance and the activation of half grabens and the erosion of their hanging walls became a principal source of sediment (Crowley et al., 2009). Identifying the reworking of palynomorphs can be difficult, especially where smooth, long ranging taxa such as *Laevolancis* spp. exist throughout the sequence. However, more obviously reworked taxa, such as those that reappear following a clear LAD earlier in the sequence, in addition to the occurrence of marine palynomorphs in otherwise wholly terrestrial strata, can be used to infer reworking. The clearest recorded reworking event in the Anglo-Welsh Basin occurs in the ?*Apiculiretusispora sceacga* zone of Tredomen Quarry (Morris et al., 2011a; Chapter III), where an unexpected abundance of cryptospores such as *Segestrospora, Velatitetras* and *Tetrahedraletes* occurs. While long ranging genera, their inflated abundance was interpreted to have been derived from the reworking of Llandoverian and Wenlockian sediments from the nearby Swansea Valley Disturbance (Morris et al., 2011a). Rare acritarchs were also recovered, and the paucity of these marine palynomorphs suggests that the palynoflora recorded from this Tredomen quarry sample is a palimpsest of reworked and ambient spores. Possible reworking events have been recorded in this work, too, and is principally indicated by the occurrence of marine palynomorphs where no other evidence for marine influence exists. Such examples occur in the Lochkovian of the M50 (chapter III) with the identification of rare acritarchs and chitinozoans in the palynoflora, and correspond to the change in tectonic regime occurring at this time (e.g. Crowley et al., 2009). Marine palynomorphs notwithstanding, the addition of reworked taxa, such as *Velatitetras reticulata* in some middle MN assemblages, may artificially inflate the diversity of assemblages. However, such an inflation would be negligible, even if reworked taxa were not always identified.

Moreover, the low diversity of the assemblages being reworked is unlikely to contribute a considerable number of species to an assemblage. As such, reworking is not considered to be a factor in the sustained increase of spore diversity through the sequence.

Marine regression: facies change and elevation

The Anglo-Welsh Basin documents progressive marine regression leading to coastal and then terrestrial ephemeral to perennial fluvial settings (Barclay et al., 2015; Basset et al., 1992; Bluck et al., 1992; Morris et al., 2012b). This regression was accompanied by concomitant facies change, and some workers have posited that the progression in spore species and morphologies is a factor of this facies change, rather than of evolution. Richardson (2007) attributed the change in broad proportions of spore ornament through the Anglo-Welsh Basin sequence in laevigate cryptospores, and concomitant increase in ornamented cryptospores and trilete spores, may have been a function of facies change. He cited the high proportions of laevigate cryptospores recovered from putative coastal and marine influenced parts of the Moor Cliffs Formation from Clee Hill, Ammons Hill and the M50. He reported that the proportions of laevigate cryptospores decrease up the stratigraphic column as the coastline recedes in Clee Hill and the M50, while remaining ± constant in the perpetually marine influenced Ammons Hill section and suggested that this was evidence to "…preclude the possibility they [laevigate cryptospore producing plants] lived in proximal alluvial settings" (Richardson, 2007, p. 360). More recent evidence suggests otherwise. While there is a marine influence at Ammons Hill, evidenced by rare acritarchs, and the proportions of laevigate cryptospores show a relatively consistent abundance throughout the section (Chapter III), *in situ* laevigate cryptospores have been recovered from both marine settings (Ludford Corner, Přídolí Downton Castle Sandstone Formation, Edwards et al., 1990), and terrestrial settings (the M50 section (chapter V) and in the NBCH assemblage (e.g. Morris et al., 2011b), suggesting that the plants were growing in a variety of coastal and upland environments throughout the

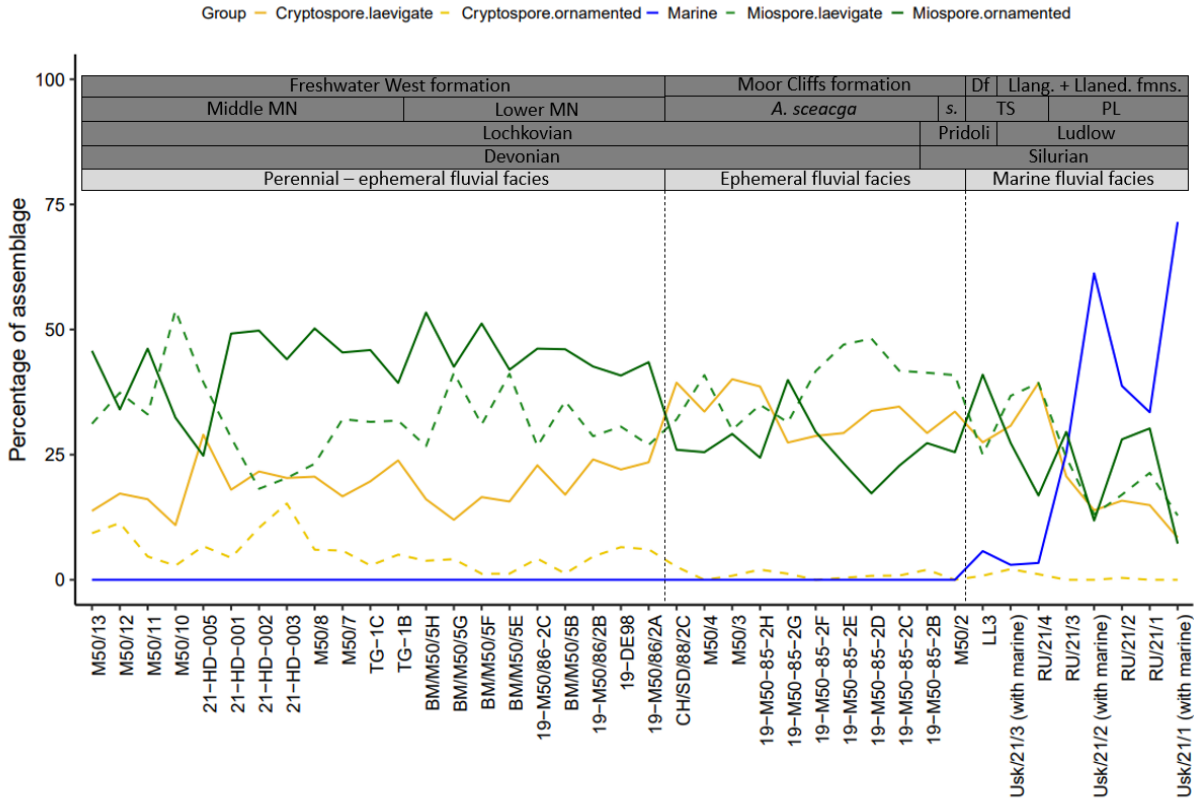

Figure IV-8: trilete and cryptospore ornament groups, and marine phytoplankton, through the Anglo-Welsh Basin sequence. Thesis appendix 3.2.

sequence. Indeed, Steemans et al. (2007) and later Wellman et al. (2013) suggested that cryptospores had an essentially cosmopolitan distribution across Euramerica and Gondwana and were tolerant to a wide variety of habitats.

It is possible that trilete spores were relatively limited in coastal environments, as the parent plants of these spores are posited to have been more sensitive to environmental stressors. However, in the Ludfordian *poecilomorphus – libycus* zone littoral and shallow marine localities, trilete spores dominate assemblages, with laevigate cryptospores secondary to these. If laevigate cryptospore producing plants were dominant in these settings, they might be expected to dominate assemblages washed out from coastal assemblages. Steemans et al. (2007) posited in his palaeoecological hypothesis that trilete spore producing plants inhabited equable, often riparian habitats, with cryptospore producing plants inhabiting less equable settings. As such, trilete spores dominate marine assemblages as these spores are more likely to be entrained by rivers and washed out to sea. This occurrence is borne out in the marine assemblages here (Rumney, Usk and Ludlow). Richardson's (2007) observations are recorded here, however, notably at the earliest terrestrial/ tidal mudflat facies at Rumney (RU/21/4). Here, a spike in laevigate cryptospores is observed where they comprise 39% of the assemblage which may suggest that this area was a preferable habitat for cryptospore producing plants. However, this is not a considerably greater proportion than in ±coeval assemblages at Usk and Ludford Corner, where laevigate cryptospores comprise 32% and 27% respectively of the assemblage. The minor differences may be due to differences in facies, with Ludford Corner and Usk involved in a wave dominated delta. Following this, the input from rivers in the latter two sites may contribute to the greater relative proportion of trilete spores in those sites, although this is tentative. Returning to Richardson's (2007) interpretation there is certainly a distinct difference in the observed spore succession between sites which are marine influenced (Ammons Hill) and those which are not (M50, Clee Hill, Gardeners Bank). Fig. 8 shows that the incidence of laevigate cryptospores is greatest in marine influenced settings and the disturbed, relatively dryer and more unstable settings of the Moor Cliffs Formation. In addition to their prevalence in Ammons Hill, and presence in the dispersed and *in situ* record in the relatively more proximal localities (M50, Clee Hill, Gardeners Bank), this suggests that (1) they were able to proliferate in a variety of habitats, and (2) these habitats included disturbed and stressed settings which may have limited, but did not exclude, trilete spore producing parent plants.

The change from marine to ephemeral and then perennial facies may also affect the diversity of the spore assemblage observed. Assemblages derived from ephemeral and perennial rivers will exhibit spores collected from the catchment of the rivers, and it is likely that the catchment of perennial rivers will be greater than that of ephemeral rivers, given that they generally operate over greater distances. As such, the diversity of spores in perennial river facies is likely to be greater than in ephemeral facies. Following this, the change in diversity between the Moor Cliffs to Freshwater West Formation is likely to be at least partially a result of facies change. Facies change from marine to ephemeral river systems between the PL + TS zones and NTPA zone may have contributed to the slight decrease in diversity observed between those zones in fig. 3a.

Recently, Holland and Loughlin (2021) posited that there may be cause to test whether putative evolutionary patterns observed through time in sedimentary basins may actually be partly or wholly a result of elevation change. Richardson (2007) noted that there was a difference in facies and elevation between the marine influenced settings and wholly terrestrial settings. Following this, there may be a possibility that the reported palynological succession (Chapter III) could simply be a result of elevation change and the transition from coastal vegetation to upland vegetation. Such a change in vegetation may be due to a host of abiotic changes, including moisture availability, altitude and soil pH (Holland and Loughlin, 2021). As has been discussed above and elsewhere (e.g. Wellman et al., 2000; Edwards and Richardson, 2004; Steemans et al., 2007) there was probably some variation in the distribution of parent plants across the Anglo-Welsh Basin, and this may have been attributable, in part, to altitude. However, the relative contribution is difficult to gauge. Indeed, because many of the assemblages are fluvial, they are allochtonous, and as such the spore assemblages and mesofossil assemblages towards

the terminus of the rivers (i.e. at the coast) might be expected to comprise a mixture of upland and lowland vegetation, that had been incorporated into the fluvial systems across the catchment (e.g. Lavender and Wellman, 2002). Without the contribution of other factors, such as punctuated invasion and perhaps evolution (see below), it would be expected to find many of the species observed in the dispersed record from the 'upland' vegetation in the assemblages drawn from the lowland and coastal vegetation, assuming that the rivers were interconnected. This is not observed to any great extent in the Anglo-Welsh Basin, and hence the relative contribution of elevation, whilst not rejected, is posited to be minor.

Climate change

Recent interpretations of the sedimentary succession in the Anglo-Welsh Basin have suggested a change in climate between the Moor Cliffs Formation and Freshwater West Formation (Hillier et al., 2008; Morris et al., 2012b). The changes were attributed by these workers to an increasingly wetter climate which in turn drove the development of perennial streams, an increase in the height of the water table and an increase in landscape stability.

It is of note that, with the change from unstable, relatively drier landscapes with ephemeral rivers to relatively wetter climates, perennial rivers and stabler landscapes, (1) the trilete spores radiate, (2) some cryptospores, particularly those which have been postulated to be close to the tracheophytes through mesofossil evidence, such as *Cymbohilates* (Morris et al., 2011b; Edwards et al., 2014), also radiate, and (3) many long ranging species persist. As has been mentioned, Steemans et al. (2007) and others have suggested that, based on the phytogeography and provincialisation of trilete spores, the parent plants of the trilete spores were sensitive to climate. Meanwhile, cryptospores appear to have been more tolerant of a range of climates and environmental stressors (Steemans et al., 2007; Wellman et al., 2013). The shift towards a relatively wetter climate in the Anglo-Welsh Basin was posited to by Morris et al. (2012b) to have been a factor in allowing the colonisation and ultimate domination of zosterophylls and later trimerophytes in the Anglo-Welsh Basin, the former from the middle *micrornatus – newportensis* zone. It may be possible that some of the rhyniophytic plants, especially those producing novel spore species from the latest Přídolí and hence contributing to the striking trilete spore radiation, were also more suited to the relatively wetter climates seen from the Early Lochkovian. Following the shift to a more suitable climate, the parent plants of these novel spore species were able to rapidly colonise the basin from elsewhere and proliferate in the basin. Similarly, cryptospores such as *Cymbohilates*, posited to be closely related to tracheophytes (e.g. Edwards et al., 2014) and may, tentatively, have had similar tolerances were also able to colonise and proliferate in the area with the incoming of wetter climates.

Biological drivers

Ecological

There may be some evidence for the sudden increase in spore diversity between the Moor Cliffs Formation and Freshwater West Formation being attributed to the ecology of the spore parent plants. As mentioned above, there is a clear change in facies which is likely driven by climate change (Hillier et al., 2007; Morris et al., 2012b), and this may have in turn established a more suitable habitat for trilete spore, and some cryptospore, producing plants. The semi-arid climate, low water table, ephemeral rivers and low stability environment present through the Přídolí and Earliest Devonian may have been an environment unsuitable for colonisation by many trilete spore producing plants, including many rhyniophytoids and higher tracheophytes such as zosterophylls later in the Lochkovian (Morris et al., 2012b). Instead, the parent plants of long ranging laevigate species such as *Laevolancis* sp. and *Ambitisporites* sp. colonised the landscape, facilitated by their wide ecological tolerances (e.g., Wellman et al., 2013) and hypothesised short life cycles (Wellman et al. 2000).

A mosaic of different environments developed across the basin (Morris et al., 2012b) as the environment became more equable in the lower *micrornatus – newportensis* zone, with the increasing water table height, landscape stability and changing tectonic regime initiating half graben development across the basin (e.g. Crowley et al., 2006; Morris et al., 2012b). The parent plants of many trilete spore producers appear to have become established and flourish in these new, equable microenvironments. Previously established plants, represented by long ranging spores, persist because of their wide ecological tolerances, but a distinct reduction in the relative abundances of some suggests a turnover in dominance, perhaps due to increased competition from newly emergent/ colonising species.

Punctuated invasions and evolution

The incoming of wetter climates and the development of a diverse array of environments may have facilitated the colonisation of more derived rhyniophytoids, and later zosterophylls, partly through competitive replacement (Edwards and Davies, 1990; Morris and Edwards, 2014), and may have allowed previously and/ or newly colonising plants to radiate and evolve into new niches.

Aneurospora shows a major radiation in diversity and disparity in the Anglo-Welsh Basin where they are first reported in the late Přídolí (NTPA zone), immediately following the middle – late Přídolí gap. Meanwhile, they are first reported from the mid Přídolí of Saudi Arabia (Breuer et al., 2017). It is plausible that the genera's arrival in Euramerica was delayed by the inequable climate and/ or unstable environment of the Anglo-Welsh Basin, however, there are some problems. Firstly, while the Lochkovian climate of Saudi Arabia is not particularly well constrained, it appears to have straddled a 45° south paleolatitude, which is the boundary between arid and warm-wet climates (Scotese, 2000; Breuer et al., 2015; Torsvik and Cocks, 2016). Furthermore, analysis of the sedimentary succession indicates that at times, aridity may have been great enough to restrict river flow, indicated by a loss of siliciclastic deposits and leading to the development of carbonates. Moreover, gypsum was identified in the sedimentary succession in Saudi Arabia (Breuer et al., 2015), perhaps suggesting greater aridity, extended periods of aridity or hotter climates when compared with the Anglo-Welsh Basin. As such, it is possible that the *Aneurospora* parent plants in Saudi Arabia (Breuer et al., 2017) were tolerant of relatively more arid conditions, and that the initial appearance of this genus in the Anglo-Welsh Basin has little to do with climate related delay. Another reason for the possible diachronous occurrence of *Aneurospora* between northern Gondwana and the Anglo-Welsh Basin is the geographical distance involved, which would have slowed the tempo of invasions by *Aneurospora* producing plants.

Given the sudden arrival of tripapillate species (chapter III), and the recognition of comparable species in the mid Přídolí of Saudi Arabia (Breuer et al., 2017) it is likely that at least some species appear in the Anglo-Welsh Basin as a result of invasion, rather than evolution. However, this does not preclude the possibility that certain species in the basin appear as a result of the latter. Given the time frame through which the Lower 'Old Red Sandstone' of the Anglo-Welsh Basin was deposited (*c.* 15ma) and the change in climate and abundance of new environments developing across the basin (Morris et al., 2012b), this is a distinct possibility. Indeed, the gradual addition of species in the sequence initiates in the Přídolí, with Higgs (2022) noting that the patinate trilete spore genus *Cymbosporites* begins to diversify in the ?mid Přídolí *Lavidensis* zone, indicating an initial diversification of some trilete spores at this time. In addition to the losses of some species such as *Stellatispora inframurinatus* var. *inframurinatus* there is an increase in the number of species and genera between the Ludlow and lower Přídolí (*poecilomorphus – libycus* and *tripapillatus – spicula* zones) and the latest Přídolí and early Lochkovian of the Moor Cliffs Formation, either side of the major stratigraphic gap. This indicates that some turnover has occurred between taxa, and that there has been additions of novel spore species in the same facies. Similarly, the gradual, sustained addition of novel species through the Freshwater West Formation may also be attributable partly to evolution. Future work may recover palynomorphs from the mid-late Přídolí gap in the Moor Cliffs Formation (fig. 1), and it is suggested that a gradual addition of taxa, including *Aneurospora* species, will be observed, either as a result of the invasion and colonisation from other basin, or from evolution. Such a change might be observed between *S.*

inframurinatus var. *inframurinatus* and *S. inframurinatus* cf. var. *inframurinatus*, although this is not quantified here. In the Anglo-Welsh Basin, the spore record has already elucidated some evidence for evolution amongst spore species. Fanning et al. (1988) described an evolutionary succession amongst crassitate trilete spores (laevigate – verrucate – apiculate), and Richardson (2007) posited that the sequence was likely adaptive, as it occurred in both trilete spores and cryptospores (4.3, 4.4).

The greatest increase in disparity occurs between the pre-MN and MN spore assemblages, which corresponds directly to the switch from unstable ephemeral river dominated facies to higher stability perennial river facies. As discussed, this facies change may correspond to a gradual transition to wetter climates (Morris et al., 2012b) and the opening up of new environments as a result of this facies change and intrabasinal structural changes (e.g. Crowley et al., 2009; Morris et al., 2012b). The increase in disparity and above changes in environment may be linked, with the plants adapting to and exploiting the new settings. Such a relationship is tentative and requires an acceptance that at least some of the changes in spore ornament seen throughout the sequence have a functional basis, as discussed earlier (ecology), but it is posited here that the major change in disparity between the pre-MN and MN was partially a result of plants radiating into, and adapting to, new microenvironments through sympatric speciation, with others colonising the basin from elsewhere. New species were added throughout the sequence in the same facies, pointing towards background evolution and speciation amongst certain lineages, and/ or the invasion of the region by plants from outside the Anglo-Welsh Basin. Finally, it is of interest to note that that competition can lead to morphological shifts amongst organisms, with the change in morphology typically occurring away from the competitor (Tyler and Leighton, 2011). The invasion and evolution of plants in the basin is likely to have resulted in high rates of competition, especially in equable settings and may have gone some way towards driving the changes in spore ornament observed in this and other work.

Tracking the evolution amongst spore species in the Anglo-Welsh Basin would be fascinating, but few workers have sought to track phylogenetic lineages of spores in the Palaeozoic, and fewer have made attempts to quantify such lineages (Streel, 1966, 1969; Marshall, 1996; Maziane et al., 2002; Breuer et al., 2005). Changing amb diameter, changing ornament characteristics and the successive replacement of older forms have been cited as possible indicators of evolutionary lineages between morphologically comparable species and variants (e.g. Marshall, 1996; Breuer et al., 2005). Following the identification of such indicators in the *Emphanisporites micrornatus* complex, Breuer et al. (2005) successfully utilised multivariate and cluster analyses, alongside temporal changes in amb diameter and variant abundance, to track evolution within the complex, from var. *micrornatus* to var. *nodosus*. This multifaceted study provides a framework by which other phylogenetic lineages may be explored, and while such a study is beyond the scope of the current work, the continuous, palynologically rich Anglo-Welsh Basin sequence may offer fertile ground for further work in this area.

Without such a study, it is difficult to unpick the relative contributions of facies change, invasion and evolution to the increase in spore diversity between the Přídolí and Lochkovian. Future work on the palynology of the Anglo-Welsh Basin may be able to explore the phylogenies of spore species through the identification of possible lineages, such as amongst species of *Stellatispora* and *Aneurospora*, using methods similar to those of Breuer et al. (2005). Marshall (1996) utilised recurring lacustrine deposits to quantify the evolutionary rate of spores from aneurophytalean progymnosperms to archaeopteridalean progymnosperms. The tempo of evolutionary lineages in the Anglo-Welsh Basin might be constrained by dating the tuff beds of the Moor Cliffs Formation (BGS ongoing, Barclay et al., 2015) in combination with previously dated lavas in Scotland (Thirlwall, 1988), and/ or with heavy mineral dating (e.g. Catlos et al., 2021), although the alteration of such materials must be considered carefully.

There are several lineages that may be interesting to explore. As mentioned, *S. inframurinatus* may show subtle morphological change between the PL and *Ap. sceacga* zone, demonstrating a slight decrease in amb diameter, in addition to changes in the character of the distal radial muri. The

Aneurospora lineage would be particularly interesting to investigate, given the proliferation of species into the Lochkovian. Whilst the Anglo-Welsh Basin provides a continuous sequence of spores it is probable that certain sculptures and ornaments did not emerge there. Interadial papillae apparently appear as early as the mid Přídolí in Gondwana (Breuer et al., 2017), and thus intermediary forms, between non-papillate and tripapillate forms, may not be expected to occur in Euramerica. In addition to trilete spores, cryptospores may also be promising candidates for phylogenetic analysis. Particularly amongst species of *Cymbohilates*, which proliferate rapidly between the lower and middle MN zones. The development of four variants of *C. variabilis*, with the addition of proximal muri and papillae, may offer opportunities to carry out similar morphometric analyses to those carried out by Breuer et al. (2005). The continuation of the lineages of *C. variabilis*, and whether they are successive, is currently unclear, but further work in the Lochkovian of the Anglo-Welsh Basin may elucidate this.

The interpretation of the change in palynomorphs may be assisted by examining extant moss genera, for which a good understanding of the phylogeny is present. Examining the development of spore wall morphology of these moss genera may facilitate the understanding of the various effects of evolution and ecological change.

5. Conclusions

- A quantitative assessment of spatial and temporal species and morphological change in the Anglo-Welsh Basin sequence shows a significant increase in species richness amongst trilete spores and cryptospores between the pre-MN and MN biozones (Ludlow – earliest Lochkovian and early – mid Lochkovian). A considerable turnover at this time amongst the cryptospore and trilete spore species occurs, with cryptospores having a lower degree of unique species and a lower species diversity between biozones and coeval localities than the trilete spores.

- A considerable increase in morphological diversity (disparity) is observed between the pre-MN and MN biozones. Miospores show the highest degree of disparity increase, with sharp changes between the pre-MN and MN spore assemblages. Similarly, a less pronounced but sustained disparity increase is observed amongst the cryptospores.

- Several underlying causes may have driven the radiation in species diversity and disparity between the Ludlow and Lochkovian of the Anglo-Welsh Basin. Previous workers attributed the change to evolution amongst the source plants, but facies change may also have contributed to the change, with a switch from ephemeral to perennial river systems. The shift towards a wetter climate which drove this facies change may have facilitated the invasion and establishment of a diverse suite of rhyniophytes, and later zosterophylls. Sorting and taphonomic influences are not considered to have considerably contributed to the changes observed in the spore assemblages though the Anglo-Welsh Basin.

- With the increasing diversity of vegetation, there is evidence for floral heterogeneity in the Anglo-Welsh Basin. Whilst such spatial differentiation is hinted at in the Ludlow, there is a clear development of ‘pockets’ of putatively specialised vegetation in the landscape by the lower MN (early Lochkovian). This is most clearly demonstrated in the lower MN Gardeners Bank locality, which is peculiarly dominated by the otherwise rare *Acinosporites salopiensis*. Subtler changes may also be observed in the abundance and distribution of other species, such as *Emphanisporites*, some of which appear to have been restricted to specialised, sporadically occurring ecological niches away from river catchment while others may have been more widespread.

6. Bibliography

ALGEO, T.J. & SCHECKLER, S.E. 1998. Terrestrial–marine telecommunications in the Devonian: links between the evolution of land plants, weathering processes, and marine anoxic events. Phil. Trans. R. Soc. London Series B, 353, pp. 113-130Allen, 1974.

ALLEN, J.R.L. AND LAWSON, J.D., 1985. Marine to fresh water: the sedimentology of the interrupted environmental transition (Ludlow-Siegenian) in the Anglo-Welsh region. *Philosophical Transactions of the Royal Society of London. B, Biological Sciences*, *309*(1138), pp.85-104.

ALLEN, J.R.L. AND TARLO, L.B., 1963. The Downtonian and Dittonian facies of the Welsh borderland. *Geological Magazine*, *100*(2), pp.129-155.

ALLEN, J.R.L. AND WILLIAMS, B.P.J., 1982. The architecture of an alluvial suite: rocks between the Townsend Tuff and Pickard Bay Tuff Beds (early Devonian), southwest Wales. *Philosophical Transactions of the Royal Society of London. B, Biological Sciences*, *297*(1085), pp.51-89.

BALL, A.C. AND TAYLOR, W.A., 2022. Reconstructing the Lower Devonian (Lochkovian) vegetation from the Anglo-Welsh Basin: Two spore masses containing Emphanisporites McGregor spores. *Review of Palaeobotany and Palynology*, *301*, p.104647.

BARCLAY, W.J., RATHBONE, P.A., WHITE, D.E. & RICHARDSON, J.B., 1994. Brackish water faunas from the St Maughans Formation: The Old Red Sandstone section at Ammons Hill, Hereford and Worcester, UK, re-examined. *Geological Journal*, **29** (4), 369 – 379.

BARCLAY, W.J., DAVIES, J.R., HILLIER, R.D. AND WATERS, R.A., 2015. Lithostratigraphy of the Old Red Sandstone successions of the Anglo-Welsh Basin.

BASSETT, M.G., LAWSON, J.D. AND WHITE, D.E., 1982. The Downton Series as the fourth series of the Silurian System. *Lethaia*, *15*(1), pp.1-24.

BECK, J.H. AND STROTHER, P.K., 2001. Silurian spores and cryptospores from the Arisaig group, Nova Scotia, Canada. *Palynology*, *25*(1), pp.127-177.

BIRKS, H.J.B. AND LINE, J.M., 1992. The use of rarefaction analysis for estimating palynological richness from Quaternary pollen-analytical data. *The Holocene*, *2*(1), pp.1-10.

BLUCK, B J, COPE,J C W, AND SCRUTTON, C T. 1992. Devonian. 57–66 in Atlas of Palaeogeography and Lithofacies. COPE, J C W, INGHAM, J K, AND RAWSON, P F (editors). Memoir of the Geological Society of London, No. 13.

BREUER, P. 2007. "Devonian miospore palynology in Western Gondwana: an application to oil exploration." *Unpublished PhD thesis, University of Liège, Liège, Belgium* 590.

BREUER, P., STRICANNE, L. AND STEEMANS, P., 2005. Morphometric analysis of proposed evolutionary lineages of Early Devonian land plant spores. *Geological Magazine*, *142*(3), pp.241-253.Breuer et al., 2015

BREUER, P., LE HÉRISSÉ, A., PARIS, F., STEEMANS, P., VERNIERS, J. AND WELLMAN, C.H., 2017. A distinctive marginal marine palynological assemblage from the Přídolí of northwestern Saudi Arabia. *Revue de Micropaléontologie*, *60*(3), pp.371-402.

BURGESS & RICHARDSON, J.B. 1991. Silurian cryptospores and miospores from the type Wenlock area, Shropshire, England. *Palaeontology*, **34** (3), 601 – 628. Pls.

BURGESS & RICHARDSON, J.B. 1995. Late Wenlock to early Prídolí cryptospores and miospores from south and southwest Wales, Great Britain. *Palaeontographica Abteilung B*, **236**, 1 – 44. Pls.

CAPEL, E., CLEAL, C.J., XUE, J., MONNET, C., SERVAIS, T. AND CASCALES-MIÑANA, B., 2022. The Silurian–Devonian terrestrial revolution: Diversity patterns and sampling bias of the vascular plant macrofossil record. *Earth-Science Reviews*, *231*, p.104085.

CASCALES-MIÑANA B, MEYER-BERTHAUD B. 2014. Diversity dynamics of Zosterophyllopsida. Lethaia. 47(2):205-215

CATLOS, E.J., MARK, D.F., SUAREZ, S., BROOKFIELD, M.E., MILLER, C.G., SCHMITT, A.K., GALLAGHER, V. AND KELLY, A., 2021. Late Silurian zircon U–Pb ages from the Ludlow and Downton bone beds, Welsh Basin, UK. *Journal of the Geological Society*, *178*(1).

CHANNELL, J.E.T., MCCABE, C. AND WOODCOCK, N.H., 1992. Early Devonian (pre-Acadian) magnetization directions in Lower Old Red Sandstone of south Wales (UK). *Geophysical Journal International*, *108*(3), pp.883-894.

CASCALAS-MIÑANA, B. & CLEAL, C.J. 2014. The plant fossil record reflects just two great extinction events. Terra Nova, 26, pp. 195-200

CLEAL, C., PARDOE, H.S., BERRY, C.M., CASCALES-MIÑANA, B., DAVIS, B.A., DIEZ, J.B., FILIPOVA-MARINOVA, M.V., GIESECKE, T., HILTON, J., IVANOV, D. AND KUSTATSCHER, E., 2021. Palaeobotanical experiences of plant diversity in deep time. 1: How well can we identify past plant diversity in the fossil record?. *Palaeogeography, Palaeoclimatology, Palaeoecology*, *576*, p.110481.

COHEN, K.M., FINNEY, S.C., GIBBARD, P.L. & FAN, J.-X. (2013; updated) The ICS International Chronostratigraphic Chart. Episodes 36: 199-204.

CROWLEY, S F, HIGGS, K T, PIPER, J D A, & MORRISEY, L B. 2009. The age of the Peel Sandstone Group. Geological Journal, Vol. 44, 57–78

DAHER, F.B. AND BRAYBROOK, S.A., 2015. How to let go: pectin and plant cell adhesion. *Frontiers in plant science*, *6*, p.523.

DEWEY, J F, AND STRACHAN, R A. 2003. Changing Silurian–Devonian relative plate motion in the Caledonides: sinistral transpression to sinistral transtension. Journal of the Geological Society of London, Vol. 160, 219–229.

EDWARDS D. & DAVIES M.S. 1990. Interpretations of early land plant radiations: ‘‘facile adaptationist guesswork’’ or reasoned speculation? *In* Major Evolutionary Radiations, Taylor PD, Larwood GP (eds). Clarendon Press: Oxford; The Systematics Association Special Volume42:351–376.

EDWARDS, D.E. & RICHARDSON, J.B. 2000. Progress in reconstructing vegetation on the Old Red Sandstone Continent: two Emphanisporites producers from the Lochkovian sequence of the Welsh Borderland. Geological Society, London, Special Publications 180 (1), 355-370.

EDWARDS, D. & RICHARDSON, J.B., 2004. Silurian and Lower Devonian plant assemblages from the Anglo-Welsh Basin: a palaeobotanical and palynological synthesis. *Geological Journal*, *39*(3-4), pp.375-402.Edwards et al 1996

EDWARDS D, WELLMAN CH, AXE LP. 1999. Tetrads in sporangia and spore masses from the Upper Silurian and Lower Devonian of the Welsh Borderland. Botanical Journal of the Linnean Society 130: 111–156.

EDWARDS, D., RICHARDSON, J.B., AXE, L., DAVIES, K.L., 2012A. A new group of Early Devonian plants with valvate sporangia containing sculptured permanent dyads. Bot. J. Linn. Soc. 168 (3), 229–257.

EDWARDS, D., MORRIS, J.L., RICHARDSON, J.B. & KENRICK, P. 2014. Cryptospores and cryptophytes reveal hidden diversity in early land floras. *New Phytologist* **202** (1), 50-78.

FANNING U, RICHARDSON JB, EDWARDS D. 1988. Cryptic evolution in an early land plant. Evolutionary Trends in Plants 2: 13–24.

FANNING U, EDWARDS D, RICHARDSON JB. 1992. A diverse assemblage of early land plants from the Lower Devonian of the Welsh Borderland. Botanical Journal of the Linnean Society 109: 161–188.

FRIEDMAN, M., 2010. Explosive morphological diversification of spiny-finned teleost fishes in the aftermath of the end-Cretaceous extinction. *Proceedings of the Royal Society B: Biological Sciences*, *277*(1688), pp.1675-1683.

FRIEND, P.F., WILLIAMS, B.P.J., FORD, M. AND WILLIAMS, E.A., 2000. Kinematics and dynamics of Old Red Sandstone basins. *Geological Society, London, Special Publications*, *180*(1), pp.29-60.

GENSEL, P.G., GLASSPOOL, I., GASTALDO, R.A., LIBERTIN, M. AND KVAČEK, J., 2020. Back to the beginnings: the Silurian-Devonian as a time of major innovation in plants and their communities. In *Nature through time* (pp. 367-398). Springer, Cham.

GRAY, J., 1985. The microfossil record of early land plants; advances in understanding of early terrestrialization, 1970–1984. Phil. Trans. R. Soc. Lond. B 309, 167–195

HAMMER, Ø., HARPER, D.A.T. AND RYAN, P.D., 2006. Past-Palaeontological Statistics, ver. 1.32. *Universidad de Oslo (http://folk. uio. no/ohammer/past/)*.

HIGGS, K.T., 2004. An Early Devonian (Lochkovian) microflora from the Freshwater West Formation, Lower Old Red Sandstone, southwest Wales. *Geological Journal*, **39** (3-4), 359-374.

HIGGS, K.T., 2022. Palynology of the Freshwater East Formation (Upper Silurian, Přídolí), Pembrokeshire, South Wales, UK. *Palynology*, (just-accepted), p.2070785.

HILLIER, R.D. & WILLIAMS, B.P.J., 2006. The alluvial old red sandstone: fluvial basins.

HOLLAND, S. & LOUGHNEY, K.M., 2021. *The stratigraphic paleobiology of nonmarine systems*. Cambridge University Press.

JAMES, D M D. 1987. Tectonics and sedimentation in the Lower Palaeozoic back-arc basin of South Wales, UK. Some quantitative aspects of basin development. Norsk Geologisk Tidsskrift, Vol. 67, 419–426.

KASSAMBARA, A. 2020. ggpubr: 'ggplot2' Based Publication Ready Plots. R package version 0.4.0. https://CRAN.R-project.org/package=ggpubr.

KEMPTON, R.A. 1979. The, structure of species abundance and measurement of diversity. Bionierrics 35. 307-21.

KING, L M. 1994. Subsidence analysis of Eastern Avalonian sequences: implications for Iapetus closure. Journal of the Geological Society of London, Vol. 151, 647–657.

KOTYK ME, BASINGER JF, GENSEL PG, DE FREITAS TA. 2002. Morphologically complex plant macrofossils from the Late Silurian of Arctic Canada. American Journal of Botany89: 1004–1013.

LANG, W.H., 1937. IV-On the plant-remains from the Downtonian of England and Wales. *Philosophical Transactions of the Royal Society of London. Series B, Biological Sciences*, *227*(544), pp.245-291.

LAVENDER, K. & WELLMAN, C.H. 2002. Lower Devonian spore assemblages from the Arbuthnott Group at Canterland Den in the Midland Valley of Scotland. *Review of Palaeobotany and Palynology*, **118** (1-4), 157 – 180.

MARRIOTT, S B, & WRIGHT, V P. 2004. Mudrock deposition in an ancient dryland system: Moor Cliffs Formation, Lower Old Red Sandstone, south-west Wales, UK. Geological Journal, Vol. 39, 277–298.

MARSHALL, J.E.A., 1996. Rhabdosporites langii, Geminospora lemurata and Contagisporites optivus: an origin for heterospory within the Progymnosperms. *Review of Palaeobotany and Palynology*, *93*(1-4), pp.159-189.

MAGURRAN, A.E., 1988. *Ecological diversity and its measurement*. Princeton university press.

MAZIANE, N., HIGGS, K.T. AND STREEL, M., 2002. Biometry and paleoenvironment of Retispora lepidophyta (Kedo) Playford 1976 and associated miospores in the latest Famennian nearshore marine facies, eastern Ardenne (Belgium). *Review of Palaeobotany and Palynology*, *118*(1-4), pp.211-226.

MINELLI, A., 2019. Biodiversity, Disparity and Evolvability. In *From Assessing to Conserving Biodiversity* (pp. 233-246). Springer, Cham.

MORRIS, J.L. 2009. Integrated approaches to the reconstruction of early land plant vegetation and environments from Lower Devonian strata, central-south Wales. PhD thesis, Cardiff University.

MORRIS, J.L. AND EDWARDS, D., 2014. An analysis of vegetational change in the Lower Devonian: new data from the Lochkovian of the Welsh Borderland, UK. *Review of Palaeobotany and Palynology*, *211*, pp.28-54.

MORRIS, J.L., EDWARDS, D., RICHARDSON, J.B., AXE, L. & DAVIES, K.L. 2012. Further insights into trilete spore producers from the Early Devonian (Lochkovian) of the Welsh Borderland, U.K. *Review of Palaeobotany and Palynology* **185**, 35– 63.

MORRIS, J.L., EDWARDS, D. & RICHARDSON, J.B. 2018. The advantages and frustrations of a plant Lagerstätte as illustrated by a new taxon from the Lower Devonian of the Welsh Borderland, U.K. *In* KRINGS, M., HARPER, C.J., RUBÉN CÚNEO, N. AND ROTHWELL, G.W. (Eds). Transformative Paleobotany. Academic Press, 49-67.

OKSANEN, J., BLANCHET, F.G., FRIENDLY, M., KINDT, R., LEGENDRE, P., MCGLINN, D., MINCHIN, P.R., O'HARA, R. B., SIMPSON, G.L., SOLYMOS, P., STEVENS, M.H.H., SZOECS, E. AND WAGNER, H. 2020. vegan: Community Ecology Package. R package version 2.5-7. https://CRAN.R-project.org/package=vegan.

PARDOE, H.S., CLEAL, C.J., BERRY, C.M., CASCALES-MIÑANA, B., DAVIS, B.A., DIEZ, J.B., FILIPOVA-MARINOVA, M.V., GIESECKE, T., HILTON, J., IVANOV, D. AND KUSTATSCHER, E., 2021. Palaeobotanical experiences of plant diversity in deep time. 2: How to measure and analyse past plant biodiversity. *Palaeogeography, Palaeoclimatology, Palaeoecology*, *580*, p.110618.

RAYMOND, A., GENSEL, P. AND STEIN, W.E., 2006. Phytogeography of late Silurian macrofloras. *Review of Palaeobotany and Palynology*, *142*(3-4), pp.165-192.

R CORE TEAM, 2022. R: A language and environment for statistical computing. R Foundation for Statistical Computing, Vienna, Austria.

RICHARDSON, J.B. 2007. Cryptospores and miospores, their distribution patterns in the Lower Old Red Sandstone of the Anglo-Welsh Basin, and the habitat of their parent plants. *Bulletin of Geosciences*, **82** (4), 355-364.

RICHARDSON, J.B. & EDWARDS, D. 1989. Sporomorphs and plant megafossils. *In*: Holland, C.H. and Bassett, M.G. (editors). A global standard for the Silurian System. *Natural Museum of Wales, Cardiff, Geological Series*, 9: 216–226.

RICHARDSON, J.B. & MCGREGOR, D.K. 1986. Silurian and Devonian spore zones of the Old Red Sandstone Continent and adjacent regions. *Geological Survey of Canada, Bulletin* **364**, 1– 79.

RICHARDSON, J.B. & LISTER, T.R. 1969. Upper Silurian and lower Devonian spore assemblages from the Welsh borderland and south Wales. *Palaeontology*, **12** (2), 201-245.

RICHARDSON J.B., RASUL, S.M. 1990. Palynofacies in a Late Silurian regressive sequence in the Welsh Borderland and Wales.Journal of theGeological Society147: 675–686.

RICHARDSON, J.B., FORD, J.H. & PARKER, F. 1984. Miospores, correlation and age of some Scottish Lower Old Red Sandstone sediments from the Strathmore region (Fife and Angus). *Journal of Micropalaeontology*, **3** (2), 109-124.

RICKARDS, R.B., 2000. The age of the earliest club mosses: the Silurian Baragwanathia flora in Victoria, Australia. *Geological Magazine*, *137*(2), pp.207-209.

RUBINSTEIN, C.V., GERRIENNE, P., DE LA PUENTE, G.S., ASTINI, R.A. AND STEEMANS, P., 2010. Early Mid Ordovician evidence for land plants in Argentina (eastern Gondwana). *New Phytologist*, *188*(2), pp.365-369.

SCOTESE, C.R. 2000. Atlas of Earth History PALEOMAP Project. 52 pp. Arlington. http://www.scotese.com/earth.html).

SOPER, N J, AND WOODCOCK, N H. 2003. The lost Lower Old Red Sandstone of England and Wales: a record of post-Iapetan flexure or Early Devonian transtension? Geological Magazine, Vol. 140, 627–647.

STEEMANS, P., WELLMAN, C.H. AND FILATOFF, J., 2007. Palaeophytogeographical and palaeoecological implications of a miospore assemblage of earliest Devonian (Lochkovian) age from Saudi Arabia. *Palaeogeography, Palaeoclimatology, Palaeoecology*, *250*(1-4), pp.237-254.

STREEL, M. 1966. Associations de spores de Dévonien inférieure belge et leur signification stratigraphique. Ann. Soc. Géol. Belg. Mém., 89.

TAYLOR, W.A., 2002. Studies in cryptospore ultrastructure: variability in the tetrad genus Tetrahedraletes and type material of the dyad Dyadospora murusattenuata. Rev. Palaeobot. Palynol. 119 (3–4), 325–334.

TAYLOR, W.A., GENSEL, P.G., WELLMAN, C.H., 2011. Wall ultrastructure in three species of the dispersed spore Emphanisporites from the Early Devonian. Rev. Palaeobot. Palynol. 163 (3–4), 264–280.

THIRLWALL, M.F., 1988. Geochronology of Late Caledonian magmatism in northern Britain. *Journal of the Geological Society*, *145*(6), pp.951-967.

TRAVERSE, A. 2009. *Paleopalynology*. Second Edition. Springer Dordrecht.

TIMS, J.D. AND CHAMBERS, T.C., 1984. Rhyniophytina and Trimerophytina from the early land flora of Victoria, Australia. *Palaeontology*, *27*(2), pp.265-279.

TORSVIK, T.H. AND COCKS, L.R.M., 2016. *Earth history and palaeogeography*. Cambridge University Press.

TURNER, S., BURROW, C.J., WILLIAMS, R.B. AND TARRANT, P., 2017. Welsh Borderland bouillabaisse: Lower Old Red Sandstone fish microfossils and their significance. *Proceedings of the Geologists' Association*, *128*(3), pp.460-479.

TYLER, C.L. AND LEIGHTON, L.R., 2011. Detecting competition in the fossil record: support for character displacement among Ordovician brachiopods. *Palaeogeography, Palaeoclimatology, Palaeoecology*, *307*(1-4), pp.205-217.

WELLMAN, C.H., 1999. Sporangia containing Scylaspora from the lower Devonian of the Welsh Borderland. *Palaeontology*, *42*(1), pp.67-81Wellman 2022

WELLMAN, C.H., EDWARDS, D. AND AXE, L., 1998. Permanent dyads in sporangia and spore masses from the Lower Devonian of the Welsh Borderland. *Botanical Journal of the Linnean Society*, *127*(2), pp.117-147.

WELLMAN, W.H., EDWARDS, D, & AXE, L. 1998B. Ultrastructure of laevigate hilate spores in sporangia and spore masses from the Upper Silurian and Lower Devonian of the Welsh Borderland. *Philosophical Transactions of the Royal Society London B*, 353, 1983– 2004.

WELLMAN, C.H., HABGOOD, K., JENKINS, G. AND RICHARDSON, J.B., 2000. A new plant assemblage (microfossil and megafossil) from the Lower Old Red

Sandstone of the Anglo–Welsh Basin: its implications for the palaeoecology of early terrestrial ecosystems. *Review of Palaeobotany and Palynology*, *109*(3-4), pp.161-196.

WELLMAN, C.H., STEEMANS, P. AND VECOLI, M., 2013. Palaeophytogeography of Ordovician–Silurian land plants. *Geological Society, London, Memoirs*, *38*(1), pp.461-476.

WELLMAN, C.H., BERRY, C.M., DAVIES, N.S., LINDEMANN, F.J., MARSHALL, J.E. AND WYATT, A., 2022. Low tropical diversity during the adaptive radiation of early land plants. *Nature Plants*, *8*(2), pp.104-109.

WHITTAKER, R.H., 1960. Vegetation of the Siskiyou mountains, Oregon and California. *Ecological monographs*, *30*(3), pp.279-338.

WICKHAM, H. 2016. ggplot2. Elegant Graphics for Data Analysis. Springer-Verlag New York.

WILLIAMSON, H.L. 1973. Species diversity in ecological communities. In Bartlett. h1.S. and Hiorns, R.W.. editors, The itiatliematical theory of die dyiianiics of biological popctlatiotis. London: Academic Press, 325-35.

Thesis appendix 4

Thesis appendix 4.1 & 4.2: miospore and cryptospore scoring metrics
Also in appendix 4.1 and 4.2(supplementary data)

Trilete spores	
Amb shape	**Score**
Circular - subcircular-subtriangular	1
Triangular	2
Triangular convex	3
Amb size µm	**Score**
0 - 50	1
50 -100	2
Structure	**Score**
Crassitate	1
Retusoid	2
Patinate	2
Cingulate	2
Zonate	3
Bilayered perine/ sloughing outer layer	3
Camerate	4
Tetrad configuration	**Score**
Trilete	1
Monolete	2
Laesurae	**Score**
Simple	1
Prominent lips	2
Proximal structural features	**Score**
None	1
Interadial papillae	2
Thickening associated with trilete mark	2
Thinning associated with trilete mark	2
Radial ribs	3
Radial ribs + thickening associated with trilete mark	4
Proximal Ornament	**Score**
Laevigate	1
Irregular murornate	2
Irregular apiculate	2
Irregular fovea	2
Regular murornate	3
Regular apiculate	3
Regular reticulate	3
Regular foveolate	3
Biform	4
Complex elements	4
Distal structural features	**Score**
None	1
Circular thickening	2
Infrastructure (proximal and/ or distal)	2
Annular thickening	3
Distal ornament	**Score**
Laevigate	1
Irregular murornate	2
Irregular apiculate	2
Irregular fovea	2
Regular murornate	3
Regular apiculate	3
Regular verrucate	3
Regular reticulate	3
Regular fovealate	3
Biform elements	4
Reticulate with extended intersections	4
Complex elements (e.g. grapnel tipped)	5
Irregular verrucate	2

Cryptospores	
Configuration	Score
Permanent pseudopolyad tetrad or dyad	1
Loose polyad tetrad or dyad	2
Hilate monad	3
Amb shape	Score
Circular - subcircular-subtriangular	1
Triangular	2
Amb size ?m	Score
0 - 50	1
50 -100	2
Structure	Score
Single walled	1
Enveloped or bilayered	2
Proximal structural features	Score
None	1
Papillae	2
Radial ribs	3
Radial ribs + papillae	4
Hilum collar	2
Proximal Ornament	Score
Laevigate	1
Irregular muromate	2
Irregular apiculate	2
Irregular fovea	2
Regular murornate	3
Regular apiculate	3
Regular reticulate	3
Regular foveolate	3
Biform	4
Complex elements	4
Distal or envelope ornament	Score
Laevigate	1
Irregular muromate	2
Irregular apiculate	2
Irregular fovea	2
Regular murornate	3
Regular apiculate	3
Regular verrucate	3
Regular reticulate	3
Regular fovealate	3
Biform elements	4
Reticulate with extended intersections	4
Complex elements (e.g. grapnel tipped)	5

Trilete spore scores

Genus	*Species*	*Score*	*Components*
Acinosporites	*salopiensis*	14	Circular - subcircular-subtriangular + 0 - 50 + Retusoid + Trilete + None + Laevigate + None + Reticulate with extended intersections
Ambitisporites	*avitus-dilutus*	10	Circular - subcircular-subtriangular + 0 - 50 + Crassiate + Trilete + None + None + Laevigate + None + Laevigate
Ambitisporites	*eslae*	11	Circular - subcircular-subtriangular + 0 - 50 + Crassitate + Trilete + Prominent lips + Interadial papillae + Laevigate + None + Laevigate
Ambitisporites	*tripapillatus*	11	Circular - subcircular-subtriangular + 0 - 50 + Crassitate + Trilete + Prominent lips + Interadial papillae + Laevigate + None + Laevigate
Ambitisporites	*warringtonii*	11	Circular - subcircular-subtriangular + 0 - 50 + Crassitate + Trilete + Prominent lips + None + Laevigate + None + Laevigate
Ambitisporites	sp. A	10	Circular - subcircular-subtriangular + 0 - 50 + Crassitate + Trilete + Prominent lips + None + Laevigate + None + Laevigate
Ambitisporites	sp. 1	10	Circular - subcircular-subtriangular + 0 - 50 + Crassitate + Trilete + Prominent lips + None + Laevigate + None + Laevigate
Ambitisporites	sp. 2	12	Circular - subcircular-subtriangular + 0 - 50 + Crassitate + Trilete + Prominent lips + Thickening associated with trilete mark + Laevigate + None + Laevigate
Amicosporites	*miserabilis*	11	Circular - subcircular-subtriangular + 0 - 50 + Crassitate + Trilete + Prominent lips + None + Laevigate + Annular thickening + Laevigate
Aneurospora	cf. *geikie*	14	Circular - subcircular-subtriangular + 0 - 50 + Crassitate + Trilete + Simple + None + Laevigate + None + Biform elements
Aneurospora	*gerriennei*	14	Circular - subcircular-subtriangular + 0 - 50 + Crassitate + Trilete + Simple + None +Interadial papillae + None + Regular apiculate
Aneurospora	*goensis*	14	Circular - subcircular-subtriangular + 0 - 50 + Crassitate + Trilete + Simple + None +Interadial papillae + None + Regular apiculate
Aneurospora	*isidori*	15	Circular - subcircular-subtriangular + 50 - 100 + Crassitate + Trilete + Prominent lips + Irregular apiculate +None + None + Regular apiculate
Aneurospora	*kensingtonii*	12	Circular - subcircular-subtriangular + 0 - 50 + Crassitate + Trilete + Prominent lips + None + None + None + Regular apiculate
Aneurospora	cf. *richardsonii*	11	Circular - subcircular-subtriangular + 0 - 50 + Crassitate + Trilete + Simple + None +None + None + Regular apiculate
Aneurospora	*sheafensis*	13	Circular - subcircular-subtriangular + 0 - 50 + Crassitate + Trilete + Prominent lips + Thinning associated with trilete mark + None + None + Regular apiculate
Aneurospora	*trilabiata*	12	Circular - subcircular-subtriangular + 0 - 50 + Crassitate + Trilete + Simple + Interadial papiillae +None + None + Regular apiculate
Aneurospora	cf. sp. A	12	Circular - subcircular-subtriangular + 0 - 50 + Crassitate + Trilete + Prominent lips + Interadial papiillae +None + None + Regular apiculate
Aneurospora	cf. hispidica	14	Circular - subcircular-subtriangular + 0 - 50 + Crassitate + Trilete + Prominent lips + None + Regular apiculate + None + Regular apiculate
Aneurospora	sp. 1	12	Circular - subcircular-subtriangular + 0 - 50 + Crassitate + Trilete + Simple + None + Irregular apiculate + None + Regular apiculate
Aneurospora	sp. 2	11	Circular - subcircular-subtriangular + 0 - 50 + Crassitate + Trilete + Simple + None + None + None + Regular apiculate
Aneurospora	sp. 3	11	Circular - subcircular-subtriangular + 0 - 50 + Crassitate + Trilete + Prominent lips + None + None + None + Irregular apiculate
Aneurospora	sp. 4	12	Circular - subcircular-subtriangular + 0 - 50 + Crassitate + Trilete + Simple + None + Laevigate + None + Biform elements
Aneurospora	sp. 5	16	Circular - subcircular-subtriangular + 0 - 50 + Crassitate + Trilete + Prominent lips + None + Regular murornate + None + Regular apiculate
Aneurospora	sp. 6	12	Circular - subcircular-subtriangular + 0 - 50 + Crassitate + Trilete + Prominent lips + None + Laevigate + None + Regular apiculate
Aneurospora	sp. 7	12	Circular - subcircular-subtriangular + 0 - 50 + Crassitate + Trilete + Prominent lips + None + Laevigate + None + Regular apiculate
Aneurospora	sp. 8	12	Circular - subcircular-subtriangular + 0 - 50 + Crassitate + Trilete + Prominent lips + None + Laevigate + None + Regular apiculate
Aneurospora	sp. 9	13	Circular - subcircular-subtriangular + 0 - 50 + Crassitate + Trilete + Prominent lips + None + irregular apiculate + None + Regular apiculate
Aneurospora	sp. 10	11	Circular - subcircular-subtriangular + 0 - 50 + Crassitate + Trilete + Simple lips + None + Laevigate + None + Regular apiculate
Aneurospora	sp. 11	11	Circular - subcircular-subtriangular + 0 - 50 + Crassitate + Trilete + Simple lips + Interadial papillae + Laevigate + None + Irregular apiculate
Aneurospora	sp. 12	11	Circular - subcircular-subtriangular + 0 - 50 + Crassitate + Trilete + Simple lips + None + Laevigate + None + Regular apiculate
Aneurospora	sp. 13	11	Circular - subcircular-subtriangular + 0 - 50 + Crassitate + Trilete + Simple lips + Interadial papillae + Laevigate + None + Irregular apiculate
Apiculiretusispora	*asperata*	14	Circular - subcircular-subtriangular + 0 - 50 + Retusoid + Trilete + Prominent lips + None + Regular murornate + None + Irregular apiculate
Apiculiretusispora	*microconus*	13	Circular - subcircular-subtriangular + 0 - 50 + Retusoid + Trilete + Prominent lips + None + Laevigate + None + Regular apiculate
Apiculiretusispora	*sceacga*	16	Circular - subcircular-subtriangular + 0 - 50 + Retusoid + Trilete + Prominent lips + interadial papillae + Regular apiculate + None + Regular apiculate
Apiculiretusispora	*spicula*	13	Circular - subcircular-subtriangular + 0 - 50 + Retusoid + Trilete + Prominent lips + None + Laevigate + None + Regular apiculate
Apiculiretusispora	cf. *spicula*	13	Circular - subcircular-subtriangular + 0 - 50 + Retusoid + Trilete + Prominent lips + None + Laevigate + None + Regular apiculate
Apiculiretusispora	*synorea*	13	Circular - subcircular-subtriangular + 0 - 50 + Retusoid + Trilete + Prominent lips + None + Laevigate + None + Regular apiculate

Apiculiretusispora	sp. A	13	Circular - subcircular-subtriangular + 0 - 50 + Retusoid + Trilete + Prominent lips + None + Laevigate + None + Regular apiculate
Apiculiretusispora	sp. B	13	Circular - subcircular-subtriangular + 0 - 50 + Retusoid + Trilete + Prominent lips + None + Laevigate + None + Regular apiculate
Apiculiretusispora	sp. C	12	Circular - subcircular-subtriangular + 0 - 50 + Retusoid + Trilete + Simple + None + Laevigate + None + Regular apiculate
Apiculiretusispora	sp. 1	13	Circular - subcircular-subtriangular + 0 - 50 + Retusoid + Trilete + Prominent lips + None + Laevigate + None + Regular apiculate
Archaeozonotriletes	*chulus* var. *chulus*	14	Circular - subcircular-subtriangular + 50 - 100 + Patinate + Trilete + Prominent lips + None + Laevigate+ None + Laevigate
Archaeozonotriletes	*chulus* var. *nanus*	13	Circular - subcircular-subtriangular + 0 - 50 + Patinate + Trilete + Prominent lips + None + Laevigate+ None + Laevigate
Archaeozonotriletes	cf. *chulus*	13	Circular - subcircular-subtriangular + 0 - 50 + Patinate + Trilete + Prominent lips + None + Laevigate+ None + Laevigate
Brochotriletes	sp. 1	12	Circular - subcircular-subtriangular + 0 - 50 + Retusoid + Trilete + Prominent lips + None + Laevigate+ None + Regular foveolate
Chelinospora	*cassicula*	13	Circular - subcircular-subtriangular + 0 - 50 + Patinate + Trilete + Prominent lips + None + Laevigate + None + Regular murornate
Chelinospora	cf. *cantabrica*	12	Circular - subcircular-subtriangular + 0 - 50 + Patinate + Trilete + Prominent lips + None + Laevigate +None + Regular reticulate
Chelinospora	*obscura*	12	Circular - subcircular-subtriangular + 0 - 50 + Patinate + Trilete + Prominent lips + None + Laevigate +None + Irregular murornate
Chelinospora	*retorrida*	13	Circular - subcircular-subtriangular + 0 - 50 + Patinate + Trilete + Prominent lips + None + Laevigate +None + Regular murornate
Chelinospora	*vermiculata*	12	Circular - subcircular-subtriangular + 0 - 50 + Patinate + Trilete + Prominent lips + None + Laevigate +None + Irregular murornate
Chelinospora	*verrucosus*	12	Circular - subcircular-subtriangular + 0 - 50 + Patinate + Trilete + Prominent lips + None + Laevigate +None + Regular verrucate
Chelinospora	sp. 1	13	Circular - subcircular-subtriangular + 0 - 50 + Patinate + Trilete + Prominent lips + None + Laevigate +None + Regular murornate
Chelinospora	sp. 2	13	Circular - subcircular-subtriangular + 0 - 50 + Patinate + Trilete + Prominent lips + None + Laevigate +None + Regular murornate
Chelinospora	sp. 3	13	Circular - subcircular-subtriangular + 0 - 50 + Patinate + Trilete + Prominent lips + None + Laevigate +None + Regular murornate
Chelinospora	sp. 4	13	Circular - subcircular-subtriangular + 0 - 50 + Patinate + Trilete + Prominent lips + None + Laevigate +None + Regular murornate
Chelinospora	sp. 5	12	Circular - subcircular-subtriangular + 0 - 50 + Patinate + Trilete + Simple + None + Laevigate +None + Regular reticulate
Chelinospora	sp. 6	12	Circular - subcircular-subtriangular + 0 - 50 + Patinate + Trilete + Simple + None + Laevigate +None + Regular murornate
Chelinospora	sp. 7	12	Circular - subcircular-subtriangular + 0 - 50 + Patinate + Trilete + Simple + None + Laevigate +None + Regular reticulate
Concentricosporites	*saggitarius*	11	Circular - subcircular-subtriangular + 0 - 50 + Crassitate + Trilete + Prominent lips + None + Laevigate + Circular thickening + Laevigate
Cymbosporites	*dittonensis*	14	Triangular + 0 - 50 + Patinate + Trilete + Prominent lips + None + Laevigate +None + Regular murornate
Cymbosporites	*echinautus*	15	Circular - subcircular-subtriangular + 50 - 100 + Patinate + Trilete + Prominent lips + None + Laevigate +None + Biform
Cymbosporites	cf. *verrucosus*	13	Circular - subcircular-subtriangular + 0 - 50 + Patinate + Trilete + Prominent lips + None + Laevigate +None + Regular murornate
Cymbosporites	sp. 1	12	Circular - subcircular-subtriangular + 0 - 50 + Patinate + Trilete + Simple + None + Laevigate +None + Regular apiculate
Cymbosporites	sp. 2	13	Circular - subcircular-subtriangular + 0 - 50 + Patinate + Trilete + Prominent lips + None + Laevigate +None + Regular murornate
Cymbosporites	sp. 3	16	Triangular + 0 - 50 + Patinate + Trilete + Prominent lips + None + irregular apiculate +None + Biform elements
Cymbosporites	sp. 4	14	Triangular + 0 - 50 + Patinate + Trilete + Prominent lips + None + laevigate +None + Regular murornate
Cymbosporites	sp. 5	12	Circular - subcircular-subtriangular + 0 - 50 + Patinate + Trilete + Prominent lips + None + Laevigate +None + Irregular apiculate
Cymbosporites	sp. 6	11	Circular - subcircular-subtriangular + 0 - 50 + Patinate + Trilete + Simple + None + Laevigate +None + Irregular apiculate
Cymbosporites	sp. 7	12	Circular - subcircular-subtriangular + 0 - 50 + Patinate + Trilete + Simple + None + Laevigate +None + Regular apiculate
Cymbosporites	sp. 8	12	Circular - subcircular-subtriangular + 0 - 50 + Patinate + Trilete + Prominent lips + None + Laevigate +None + Irregular apiculate
Cymbosporites	sp. 9	13	Circular - subcircular-subtriangular + 0 - 50 + Patinate + Trilete + Prominent lips + None + Laevigate +None + Regular apiculate
Cymbosporites	sp. 10	12	Circular - subcircular-subtriangular + 0 - 50 + Patinate + Trilete + Simple + None + Laevigate +None + Irregular apiculate
Cymbosporites	sp. 11	12	Circular - subcircular-subtriangular + 0 - 50 + Patinate + Trilete + Simple + None + Laevigate +None + Irregular apiculate
Cymbosporites	sp. 12	16	Triangular + 0 - 50 + Patinate + Trilete + Prominent lips + None + Laevigate +None + complex elements
Dibolisporites	sp. 1	13	Circular - subcircular-subtriangular + 0 - 50 + Retusoid + Trilete + Simple + None + Laevigate +None + Biform elements
Dibolisporites	sp. 2	13	Circular - subcircular-subtriangular + 0 - 50 + Retusoid + Trilete + Simple + None + Laevigate +None + Biform elements
Dictyotriletes	*williamsii*	13	Circular - subcircular-subtriangular + 0 - 50 + Retusoid + Trilete + Prominent lips + None + Laevigate +None + Regular reticulum
Dictyotriletes	sp. A	13	Circular - subcircular-subtriangular + 0 - 50 + Retusoid + Trilete + Prominent lips + None + Laevigate +None + Regular reticulum

Emphanisporites	*epicautus*	14	Circular - subcircular-subtriangular + 0 - 50 + Retusoid + Trilete + Prominent lips + Radial ribs and apical thickening + Laevigate +None + laevigate
Emphanisporites	cf. *epicautus*	14	Circular - subcircular-subtriangular + 0 - 50 + Retusoid + Trilete + Prominent lips + Radial ribs and apical thickening + Laevigate +None + laevigate
Emphanisporites	*corralinus*	12	Circular - subcircular-subtriangular + 0 - 50 + Retusoid + Trilete + Simple + Radial ribs + Laevigate +None + laevigate
Emphanisporites	*micrornatus*	14	Circular - subcircular-subtriangular + 0 - 50 + Retusoid + Trilete + Simple + Radial ribs + Laevigate +None + Regular apiculate
Emphanisporites	cf. *micrornatus*	14	Circular - subcircular-subtriangular + 0 - 50 + Retusoid + Trilete + Simple + Radial ribs + Laevigate +None + Regular apiculate
Emphanisporites	*neglectus*	12	Circular - subcircular-subtriangular + 0 - 50 + Retusoid + Trilete +Simple + Radial ribs + Laevigate +None + laevigate
Emphanisporites	cf. *rotatus*	12	Circular - subcircular-subtriangular + 0 - 50 + Retusoid + Trilete + Simple + Radial ribs + Laevigate +None + laevigate
Emphanisporites	sp. 1	13	Circular - subcircular-subtriangular + 0 - 50 + Retusoid + Trilete + Prominent lips + Radial ribs + Laevigate +None + laevigate
Emphanisporites	sp. 2	13	Circular - subcircular-subtriangular + 0 - 50 + Retusoid + Trilete + Prominent lips + Radial ribs + Laevigate +None + laevigate
Emphanisporites	sp. 3	12	Circular - subcircular-subtriangular + 0 - 50 + Retusoid + Trilete + Simple + Radial ribs + Laevigate +None + laevigate
Emphanisporites	sp. 4	12	Circular - subcircular-subtriangular + 0 - 50 + Retusoid + Trilete + Simple + Radial ribs + Laevigate +None + laevigate
Ibereospora	*glabella*	13	Triangular + 0 - 50 + Crassitate + Trilete + Prominent lips + interadial papillae + Laevigate +None + Regular murornate
Insolisporites	*bassettii*	11	Circular - subcircular-subtriangular + 0 - 50 + Crassitate + Trilete + Prominent lips + None + Laevigate +None + Irregular apiculate
Insolisporites	*anchistnus*	11	Circular - subcircular-subtriangular + 0 - 50 + Crassitate + Trilete + Prominent lips + None + Laevigate +None + Irregular apiculate
Leonispora	*argovejo*	11	Circular - subcircular-subtriangular + 0 - 50 + Crassitate + Trilete + Simple + Interadial papillae s + Laevigate + None + laevigate
Lophonzotriletes	*poecilomorphus*	12	Circular - subcircular-subtriangular + 0 - 50 + Crassitate + Trilete + Prominent lips + none + Laevigate +None + regular murornate
Lophonzotriletes	cf. sp. A	12	Circular - subcircular-subtriangular + 0 - 50 + Crassitate + Trilete + Prominent lips + none + Laevigate +None + regular murornate
Perotrilites	*microbaculatus* var. *microbaculatus*	15	Circular - subcircular-subtriangular + 50 - 100 + Perine + Trilete + Simple + Thickening associated with trilete mark + Laevigate + None + regular apiculate
Perotrilites	*microbaculatus* var. *attenuatus*	15	Circular - subcircular-subtriangular + 50 - 100 + Perine + Trilete + Simple + Thickening associated with trilete mark + Laevigate + None + regular apiculate
Perotrilites	sp. A Wellman et al	13	Circular - subcircular-subtriangular + 50 - 100 + Perine + Trilete + Simple + Thickening associated with trilete mark + Laevigate + None + Laevigate
Perotrilites	sp. 1	11	Circular - subcircular-subtriangular + 0 - 50 + Perine + Trilete + Simple + none + Laevigate + None + Laevigate
Perotrilites	sp. 2	14	Circular - subcircular-subtriangular + 50 - 100 + Perine + Trilete + Simple + None + Laevigate + None + Regular apiculate
Retusotriletes	*dittonensis*	12	Circular - subcircular-subtriangular + 0 - 50 + Retusoid + Trilete + Prominent lips + Thickening associated with trilete mark + Laevigate + None + Laevigate
Retusotriletes	cf. *dittonensis*	12	Circular - subcircular-subtriangular + 0 - 50 + Retusoid + Trilete + Prominent lips + Thickening associated with trilete mark + Laevigate + None + Laevigate
Retusotriletes	*fraudator*	12	Circular - subcircular-subtriangular + 0 - 50 + Retusoid + Trilete + Simple + Thickening associated with the trilete mark + Laevigate + None + Laevigate
Retusotriletes	cf. *goensis*	11	Circular - subcircular-subtriangular + 0 - 50 + Retusoid + Trilete + Simple + Thickening associated with trilete mark + Laevigate + None + Laevigate
Retusotriletes	*maculatus*	12	Circular - subcircular-subtriangular + 0 - 50 + Retusoid + Trilete + Prominent lips + Interadial papillae + Laevigate + None + Laevigate
Retusotriletes	cf. *maculatus*	12	Circular - subcircular-subtriangular + 0 - 50 + Retusoid + Trilete + Prominent lips + Interadial papillae + Laevigate + None + Laevigate
Retusotriletes	*minor*	11	Circular - subcircular-subtriangular + 0 - 50 + Retusoid + Trilete + Simple + None + Laevigate + None + Laevigate
Retusotriletes	cf. *minor*	11	Circular - subcircular-subtriangular + 0 - 50 + Retusoid + Trilete + Prominent lips + None + Laevigate + None + Laevigate
Retusotriletes	*triangulatus*	13	Circular - subcircular-subtriangular + 50 - 100 + Retusoid + Trilete + Simple + Thickening associated with trilete mark + Laevigate + None + Laevigate
Retusotriletes	cf. *triangulatus*	12	Circular - subcircular-subtriangular + 0 - 50 + Retusoid + Trilete + Simple + Thickening associated with trilete mark + Laevigate + None + Laevigate
Retusotriletes	sp. A Wellman et al	13	Circular - subcircular-subtriangular + 50 - 100 + Retusoid + Trilete + Simple + Thickening associated with trilete mark + Laevigate + None + Laevigate
Retusotriletes	sp. A Burgess and Richardson	11	Circular - subcircular-subtriangular + 50 - 100 + Retusoid + Trilete + Simple + Thinning associated with trilete mark + Laevigate + None + Laevigate
Retusotriletes	sp. 1	11	Circular - subcircular-subtriangular + 0 -50 + Retusoid + Trilete + Prominent lips + None + Laevigate + None + Laevigate
Retusotriletes	sp. 2	12	Circular - subcircular-subtriangular + 0 - 50 + Retusoid + Trilete + Simple + None + Regular murornate + None + Laevigate
Retusotriletes	sp. 3	11	Circular - subcircular-subtriangular + 0 - 50 + Retusoid + Trilete + Prominent lips + None + Laevigate + None + Laevigate
Retusotriletes	sp. 4	13	Circular - subcircular-subtriangular + 0 - 50 + Retusoid + Trilete + Prominent lips + None + Regular reticulate + None + Laevigate
Scylaspora	*downiei*	14	Circular - subcircular-subtriangular + 0 - 50 + Crassitate + Trilete + Prominent lips + None + Regular murornate + None + Regular apiculate
Scylaspora	sp. 1	13	Triangular amb + 0 - 50 + Crassitate + Trilete + Prominent lips + None + Regular reticulate + None + Laevigate

Scylaspora	sp. 2	13	Circular - subcircular-subtriangular + 0 - 50 + Crassitate + Trilete + Prominent lips + None + Regular apiculate + None + Laevigate
Scylaspora	sp. 3	13	Circular - subcircular-subtriangular + 0 - 50 + Crassitate + Trilete + Prominent lips + None + Regular murornate + None + Laevigate
Streelispora	*newportensis*	14	Circular - subcircular-subtriangular + 0 - 50 + Crassitate + Trilete + Prominent lips + Interadial papillae + Laevigate + None + Biform elements
Streelispora	*granulata*	13	Circular - subcircular-subtriangular + 0 - 50 + Crassitate + Trilete + Prominent lips + Interadial papillae + Laevigate + None + Regular apiculate
Stellatispora	*inframurinatus* var. *inframurinatus*	14	Circular - subcircular-subtriangular + 50 - 100 + Patinate + Trilete + Prominent lips + None + Laevigate+ None + Regular murornate
Stellatispora	*inframurinatus* var. *cambrensis*	14	Circular - subcircular-subtriangular + 50 - 100 + Patinate + Trilete + Prominent lips + None + Laevigate+ None + Regular murornate
Stellatispora	*inframurinatus* cf. var. *inframurinatus*	13	Circular - subcircular-subtriangular + 0 - 50 + Patinate + Trilete + Prominent lips + None + Laevigate+ None + Regular murornate
Synorisporites	*downtonensis*	15	Circular - subcircular-subtriangular + 50 - 100 + Crassitate + Trilete + Prominent lips + None + Regular murornate + None + Regular murornate
Synorisporites	cf. *labeonis*	11	Circular - subcircular-subtriangular + 0 - 50 + Crassitate + Trilete + Simple + None + Laevigate + None + Regular murornate
Synorisporites	cf. *libycus*	11	Circular - subcircular-subtriangular + 0 - 50 + Crassitate + Trilete + Simple + None + Laevigate + None + Regular murornate
Synorisporites	*tripapillatus*	13	Circular - subcircular-subtriangular + 0 - 50 + Crassitate + Trilete + Prominent lips + None + Laevigate + None + Regular murornate
Synorisporites	*verrucatus*	12	Circular - subcircular-subtriangular + 0 - 50 + Crassitate + Trilete + Prominent lips + None + Laevigate + None + Regular murornate
Synorisporites	?sp. B	13	Circular - subcircular-subtriangular + 0 - 50 + Crassitate + Trilete + Prominent lips + None + Irregular murornate + None + Regular murornate
Synorisporites	sp. 1	14	Circular - subcircular-subtriangular + 0 - 50 + Crassitate + Trilete + Prominent lips + Interadial papillae + Irregular murornate + None + Regular murornate
Synorisporites	sp. 2	13	Circular - subcircular-subtriangular + 0 - 50 + Crassitate + Trilete + Prominent lips + Interadial papillae + Laevigate + None + Regular murornate
Synorisporites	sp. 3	13	Circular - subcircular-subtriangular + 0 - 50 + Crassitate + Trilete + Prominent lips + None + Laevigate + None + Regular reticulum
Synorisporites	sp. 4	12	Circular - subcircular-subtriangular + 0 - 50 + Crassitate + Trilete + Prominent lips + None + Laevigate + None + Regular murornate
Synorisporites	sp. 5	11	Circular - subcircular-subtriangular + 0 - 50 + Crassitate + Trilete + Simple + None + Laevigate + None + Regular reticulate
Zonate		12	Circular - subcircular-subtriangular + 0 - 50 + Zonate + Trilete + Simple + None + Laevigate + None + Laevigate

Also in attached thesis appendix 4

Cryptospore scores

Genus	***Species***	***Score***	***Components***
Abditudyadus	*laevigatus*	10	Loose polyad tetrad or dyad + Circular - subcircular-subtriangular + 0 - 50 + Enveloped or bilayered + None + Laevigate + Laevigate
Acontotetras	*inconspicuis*	10	Loose polyad tetrad or dyad + Circular - subcircular-subtriangular + 0 - 50 + Single walled + None + Laevigate + Regular reticulate
Artemopyra	*brevicosta*	11	Hilate monad + Circular - subcircular-subtriangular + 0 - 50 + Single walled + Radial ribs + Laevigate + Laevigate
Artemopyra	cf. *radiata*	11	Hilate monad + Circular - subcircular-subtriangular + 0 - 50 + Single walled + Radial ribs + Laevigate + Laevigate
Artemopyra	*recticosta*	11	Hilate monad + Circular - subcircular-subtriangular + 0 - 50 + Single walled + Radial ribs + Laevigate + Laevigate
Artemopyra	cf. *inconspicuis*	11	Hilate monad + Circular - subcircular-subtriangular + 0 - 50 + Single walled + Radial ribs + Laevigate + Laevigate
Chelinohilates	*erraticus*	14	Hilate monad + Circular - subcircular-subtriangular + 50 - 100 + Enveloped or bilayered + Irregular murornate + Laevigate + Regular reticulate
Chelinohilates	*sinuosus* var. *sinuosus*	14	Hilate monad + Circular - subcircular-subtriangular + 0 - 50 + Enveloped or bilayered + None + Regular murornate + Regular murornate
Chelinohilates	Sp. 1	12	Hilate monad + Circular - subcircular-subtriangular + 0 - 50 + Enveloped or bilayered + None + Laevigate + Regular murornate
Chelinohilates	Sp. 2	12	Hilate monad + Circular - subcircular-subtriangular + 0 - 50 + Enveloped or bilayered + None + Laevigate + Regular reticulate
Chelinohilates	Sp. 3	13	Hilate monad + Circular - subcircular-subtriangular + 50 - 100 + Enveloped or bilayered + None + Laevigate + Regular reticulate
Chelinohilates	Sp. 4	13	Hilate monad + Circular - subcircular-subtriangular + 50 - 100 + Enveloped or bilayered + None + Laevigate + Regular reticulate
Cheliotetras	*caledonica*	9	Permanent pseudopolyad tetrad or dyad + Circular - subcircular-subtriangular + 0 - 50 + Single walled + None + Laevigate + Regular apiculate
Cheliotetras	sp. 1	9	Permanent pseudopolyad tetrad or dyad + Circular - subcircular-subtriangular + 0 - 50 + Single walled + None + Laevigate + Regular reticulate
Cymbohilates	*allenii* var. *allenii*	11	Hilate monad + Circular - subcircular-subtriangular + 0 - 50 + Single walled + None + Laevigate+ Regular apiculate
Cymbohilates	*allenii* var. *magnus*	12	Hilate monad + Circular - subcircular-subtriangular + 50 - 100 + Single walled + None + Laevigate + Regular apiculate

Cymbohilates	*cymosus*	13	Hilate monad + Circular - subcircular-subtriangular + 50 - 100 + Single walled + None + Laevigate + Complex elements
Cymbohilates	*disponerus*	11	Hilate monad + Circular - subcircular-subtriangular + 0 - 50 + Single walled + None + Laevigate+ Regular apiculate
Cymbohilates	*horridus*	12	Hilate monad + Circular - subcircular-subtriangular + 50 - 100 + Single walled + None + Laevigate + Regular apiculate
Cymbohilates	*mesodecus*	12	Hilate monad + Circular - subcircular-subtriangular + 0 - 50 + Single walled + Hilum collar + Laevigate+ Regular apiculate
Cymbohilates	cf. *mesodecus*	12	Hilate monad + Circular - subcircular-subtriangular + 0 - 50 + Single walled + Hilum collar + Laevigate+ Regular apiculate
Cymbohilates	*rhabdionus*	12	Hilate monad + Circular - subcircular-subtriangular + 0 - 50 + Single walled + Hilum collar + Laevigate+ Regular apiculate
Cymbohilates	*variabilis* var. *variabilis*	15	Hilate monad + Circular - subcircular-subtriangular + 0 - 50 + Single walled + Papillae and radial ribs + Laevigate+ Biform elements
Cymbohilates	*variabilis* var. *parvidecus*	13	Hilate monad + Circular - subcircular-subtriangular + 0 - 50 + Single walled + Radial ribs + Laevigate+ Regular apiculate
Cymbohilates	*variabilis* var. *tenuis*	11	Hilate monad + Circular - subcircular-subtriangular + 0 - 50 + Single walled + Laevigate + Laevigate+ Regular apiculate
Cymbohilates	*variabilis* var. A	14	Hilate monad + Circular - subcircular-subtriangular + 0 - 50 + Single walled + Papillae and radial ribs + Laevigate+ Regular apiculate
Cymbohilates	Sp. 1	11	Hilate monad + Circular - subcircular-subtriangular + 0 - 50 + Single walled + None + Laevigate+ Regular apiculate
Cymbohilates	Sp. 2	12	Hilate monad + Circular - subcircular-subtriangular + 50 - 100 + Single walled + None + Laevigate+ Regular apiculate
Cymbohilates	Sp. 3	12	Hilate monad + Circular - subcircular-subtriangular + 0 - 50 + Enveloped or double layered + None + Laevigate+ Regular apiculate
Cymbohilates	Sp. 4	12	Hilate monad + Circular - subcircular-subtriangular + 0 - 50 + Single walled + None + Laevigate + Biform
Cymbohilates	Sp. 5	12	Hilate monad + Circular - subcircular-subtriangular + 0 - 50 + Single walled + None + Laevigate + Biform
Cymbohilates	Sp. 6	13	Hilate monad + Circular - subcircular-subtriangular + 0 - 50 + Single walled + Papillae + Irregular apiculate + Regular apiculate
Cymbohilates	Sp. 7	12	Hilate monad + Circular - subcircular-subtriangular + 0 - 50 + Single walled + None + Regular murornate + Regular apiculate
Dyadospora	*murusattenuata - murusdensa*	8	Loose polyad tetrad or dyad + Circular - subcircular-subtriangular + 0 - 50 + Single walled + None + Laevigate + Laevigate
Hispanaediscus	cf. *major*	11	Hilate monad + Circular - subcircular-subtriangular + 0 - 50 + Single walled + None + Laevigate + Regular verrucate
Hispanaediscus	*verrucatus*	11	Hilate monad + Circular - subcircular-subtriangular + 0 - 50 + Single walled + None + Laevigate + Regular verrucate
Laevolancis	*divellomedium-plicata*	10	Hilate monad + Circular - subcircular-subtriangular + 50 - 100 + Single walled + None + Laevigate + Laevigate
Laevolancis	sp. 1	10	Hilate monad + Circular - subcircular-subtriangular + 0 - 50 + Single walled + Papillae + Laevigate + Laevigate
Pseudodyadospora	*laevigata*	7	Permanent pseudopolyad tetrad or dyad + Circular - subcircular-subtriangular + 0 - 50 + Single walled + None + Laevigate + Laevigate
Pseudodyadospora	*petasus*	7	Permanent pseudopolyad tetrad or dyad + Circular - subcircular-subtriangular + 0 - 50 + Single walled + None + Laevigate + Laevigate
Qualisaspora	*fragilis*	13	Hilate monad + Circular - subcircular-subtriangular + 0 - 50+ Single walled + None + Regular reticulum + Regular reticulum
Rimosotetras	*problematica*	8	Loose polyad tetrad or dyad + Circular - subcircular-subtriangular + 0 - 50 + Single walled + None + Laevigate + Laevigate
Segestrespora	sp. 1	10	Permanent pseudopolyad tetrad or dyad + Circular - subcircular-subtriangular + 0 - 50 + Enveloped or bilayered + None + Laevigate + Irregular apiculate
Tetrahedraletes	*medinensis*	8	Loose polyad tetrad or dyad + Circular - subcircular-subtriangular + 0 - 50 + Single walled + None + Laevigate + Laevigate
Velatitetras	*anatoliensis*	9	Permanent pseudopolyad tetrad or dyad + Circular - subcircular-subtriangular + 0 - 50 + Enveloped or bilayered + None + Laevigate + Irregular apiculate
Velatitetras	*laevigata*	8	Permanent pseudopolyad tetrad or dyad + Circular - subcircular-subtriangular + 0 - 50 + Enveloped or bilayered + None + Laevigate + Laevigate
Velatitetras	*reticulata*	10	Permanent pseudopolyad tetrad or dyad + Circular - subcircular-subtriangular + 0 - 50 + Enveloped or bilayered + None + Laevigate + Regular reticulate
Hilate cryptospore gen a sp 1		11	Hilate monad + Circular - subcircular-subtriangular + 0 - 50+ Single walled + None + Laevigate + Regular reticulum

Data in attached thesis appendix 4

Thesis appendix 4.3: Binary species data

Data manipulation

For tidied binary data (1) marine palynomorphs (Acritarchs, Chitinozoans, Scolecodonts) were removed, as were trilete tetrads and dyads of species which are normally dispersed as monads. In the latter case, where the species of monad (e.g. *C. allenii* var. *allenii*) was not represented in an assemblage, and hence the only representation of that species was the dyad, the monad occurrence was edited to show that the species was present. This was to prevent a false inflation or reduction of taxonomic richness.

Thesis appendix 4.4: Species and sequence disparity scores

Binary count sheet with incidence (1) converted into appropriate score for species.

Thesis appendix 4.5: Selected genera disparity

Genus disparity scores as .csv files, organised by biozone.

Thesis appendix 4.6: Amb diameter measurements

Amb diameter measurements for samples in composite sections (n = 150 per sample).

Thesis appendix 4.7: Code scripts

Rarefaction analysis

```
# Alexander C. Ball 15/02/2022
#this is a rarefaction analysis of assemblage data from the Ango-Welsh Basin.
# examples can be found in Gibson(unpub. Thesis, appendix E and at https://rdrr.io/cran/vegan/man/rarefy.html
# with a description in https://rdrr.io/cran/vegan/f/inst/doc/diversity-vegan.pdf.

library("vegan")

library("fossil")

# set working directory
setwd("E:/PhD/AB PhD/Research/Diversity - disparity/Diversity/sp richness")

#read data
 awb <- read.csv("rarifactiontestdata.csv")

 S <- specnumber(awb)# observed number of spp.

 (raremax <- min(rowSums(awb)))

 srare <- rarefy(awb, 200)

 plot(S, srare, xlab = "Observed number of species", ylab = "rarefied no. of species",
      title("Rarefaction analysis of Anglo-Welsh basin spores"))
 abline(0, 1)

 rarecurve(awb, step = 1, 200, col = "blue", label =TRUE)

#rareslope claculates top of rarecurve at given sample size

 S <- specnumber(awb) #obs number of spp

 (raremax <- min(rowSums(awb)))
 Srare <- srare <- rarefy(awb, raremax)
 plot(S, srare, xlab = "Observed number of species", ylab = "rarefied no. of species",
      title("Rarefaction analysis of Anglo-Welsh basin spores"))
 abline (0, 1)

 #write data into CSVs

 write.csv(awb, "AWBrrarefy200.csv")

++++++++++++++++++++++++++++++++++++++++
```

Diversity

For species richness per biozone plot (barplot)

```
#This is a barplot for species richness by spore biozone
```

```
#data imported is p/a, calculations in
species_richness_by_biozone.xlsx

library("tidyverse")
library("vegan")
library("ggplot2")

BSR <- read.csv("Biozonesprichness.csv",
header = TRUE, row.names = 1, sep = ",",
check.names = FALSE)
specnumber(BSR)

pal <- c("seagreen1",
"seagreen2","seagreen3", "seagreen4")



barplot(specnumber(BSR), beside=TRUE,
ylim = c(0, 200),
        col = pal, xlab = "Spore
assemblage biozones", ylab = "Species
richness",
        main = "Species richness by
spore biozone, Anglo - Welsh Basin")



        (axis(2, at = 0:100, labels =
c(0,50,100,150,200),
             rug(x = 0:200, ticksize = -
0.01, side = 2)))

++++++++++++++++++++++++++++++++++++
```

For species richness in coeval assemblages (barplot)

```
#This is a barplot for species richness
by spore biozone
#data imported is p/a, calculations in
species_richness_by_biozone.xlsx

library("tidyverse")
library("vegan")
library("ggplot2")

getwd()

setwd("E:/PhD/AB PhD/Research/Diversity
- disparity/Diversity new")

ABSR <- read.csv("MMNBSPR.csv", header =
TRUE, row.names = 1, sep = ",",
check.names = FALSE)
specnumber(ABSR)

pal <- c("Salmon","seagreen3",
"slategray2")



barplot(specnumber(ABSR), beside=TRUE,
ylim = c(0, 150),
        col = pal, xlab = "Sites", ylab
= "Species richness",
        main = "Middle MN zone species
richness in coeval sites")



        (axis(2, at = 0:100, labels =
c(0,50,100,150,200),
             rug(x = 0:140, ticksize = -
0.01, side = 2)))

++++++++++++++++++++++++++++++++++++
```

For the number of spp in genera, clustered barplot

```
#script for grouped bar chart for
species numbers in genera

getwd()

setwd("E:/PhD/AB PhD/Research/Diversity
- disparity/Diversity new/genus
richness")

ABSR <-
read.csv("cryptetradgenrichness.csv",
header = TRUE, sep = ",", row.names =
1,check.names = FALSE)

head(ABSR)

dat <- as.matrix(ABSR)

par(mar=c(5,4,3,2))

pal <- c("Salmon","seagreen3",
"slategray2", "thistle")

barplot(height = dat,
        beside = TRUE,
        col = pal,
        main = "Number of species in
cryptospore tetrad genera", xlab = "",
ylab = "Number of species", cex.axis =
1,
        cex.names = 1, las = 1,
```

```
        legend(x="topright", legend =
c("middle MN", "lower MN", "NTPA",
"TS"),cex = 1, fill = pal, title =
"Biozones"))

########################################
```

Disparity

For disparity scores between biozones, line chart

```
# this is a line plot for biozone
diversity in ggplot2
# following
http://www.sthda.com/english/wiki/ggplot
2-line-types-how-to-change-line-types-
of-a-graph-in-r-software
# https://felixfan.github.io/ggplot2-
remove-grid-background-margin/
#

install.packages("ggplot2")
library("ggplot2")
install.packages()

getwd()
setwd("C:/Users/AlexB/Documents/AB
PhD/Research/Diversity -
disparity/Disparity new")

AWBsp.raw <-
read.csv("mean_biozone_disparity.csv")

head(AWBsp.raw)

#plot graph

ggplot(data = AWBsp.raw, aes(x=
Biozone, y= Mean_score, group=
ï..Turma)) +
  geom_line(aes(linetype=ï..Turma,
colour = ï..Turma)) +
  geom_point(aes(color=ï..Turma)) +

scale_linetype_manual(values=c("solid",
"twodash", "solid", "twodash"))+

scale_color_manual(values=c("gold2","gol
d2","forestgreen","forestgreen")) +

scale_x_discrete(limits=c("mMN","lMN","N
TPA", "TS", "PL")) + ##manually arrange
the x axis order
  ggtitle("Mean biozone disparity") +
  scale_y_continuous(limits = c(0, 800))
+
  theme_bw() + theme(panel.border =
element_blank(), panel.grid.major =
element_blank(),
                     panel.grid.minor =
element_blank(), axis.line =
element_line(colour = "black"),
                     legend.position =
"top", text=element_text(color="black"))
## this removes grey background

########################################
```

For disparity scores between coeval localities, boxplot

```
# this is a boxplot for disparity
between coeval localities

# for boxplot, following boxplot section
of:
#http://www.randigriffin.com/2017/05/23/
mosquito-community-ecology-in-vegan.html

# boxplot made in base R

#tell R where to look

setwd("E:/PhD/AB PhD/Research/Diversity
- disparity/Disparity new")

#input the CSV

data <- read.csv("TSlocdisparity.csv",
row.names=1, sep = ",", header = TRUE)

head(data)
>head(data)
          Locality   Sample
          Miospore.RT Cryptospore.RT
          Miospore.obs Cryptospore.obs
AWB1.43   Rumney  RU/21/4         111
59          111              59
AWB1.44   Rumney  RU/21/3         228
51          228              51
AWB1.45   Rumney  RU/21/2         206
59          193              59
AWB1.46   Rumney  RU/21/1         230
39          218              39
AWB1.47     Usk Usk/21/3         211
109         211              109
AWB1.48     Usk Usk/21/2         264
59          251              59
```

```
pcol <- cc("burlywood", "antiquewhite",
"beige", "cornsilk")

#miospore locality c("thistle1",
"mediumorchid1", "purple4",
"darkorchid3")
#cyrptospore c("burlywood",
"antiquewhite", "beige", "cornsilk")

boxplot(data$Cryptospore.RT~data$Localit
y, main = "Locality cryptospore
disparity scores, TS zone (range
through)",
        xlab = "Locality", ylab =
"Disparity score", col = pcol)

########################################
```

Disparity scores for selected genera

```
# script for genus disparity/ biozone
fig.

#tell R where to look
setwd("C:/Users/AlexB/Documents/AB
PhD/Research/Diversity -
disparity/Disparity
new/Genus_disparity")

# load packages
library("ggplot2")
library("ggpubr")
library("tidyr")

# load genus disparity data for boxplots

ambiti <- read.csv("ambiti_disp.csv") #
load raw data
ambiti <- ambiti[-1] # remove
sacrificial column
head(ambiti) # check
ambiti_long <- pivot_longer(ambiti, cols
= "mMN":"PL", names_to = "Biozone",
                            values_to =
"Disparity", values_drop_na = TRUE) #
pivot data
head(ambiti_long)

ambiti_long$Disparity <-
as.numeric(ambiti_long$Disparity) # make
disparity data numeric

aneuro <- read.csv("aneuro_disp.csv") #
load raw data
aneuro <- aneuro[-1] # remove
sacrificial column
aneuro_long <- pivot_longer(aneuro, cols
= "mMN":"PL", names_to = "Biozone",
                            values_to =
"Disparity", values_drop_na = TRUE)
aneuro_long$Disparity <-
as.numeric(aneuro_long$Disparity) # make
disparity data numeric

apiculi <- read.csv("apiculi_disp.csv")
# load raw data
apiculi <- apiculi[-1] # remove
sacrificial column
apiculi_long <- pivot_longer(apiculi,
cols = "mMN":"PL", names_to = "Biozone",
                             values_to =
"Disparity", values_drop_na = TRUE)
apiculi_long$Disparity <-
as.numeric(apiculi_long$Disparity) #
make disparity data numeric

chelinosp <-
read.csv("chelinosp_disp.csv") # load
raw data
chelinosp <- chelinosp[-1] # remove
sacrificial column
chelinosp_long <-
pivot_longer(chelinosp, cols =
"mMN":"PL", names_to = "Biozone",
                               values_to
= "Disparity", values_drop_na = TRUE)
chelinosp_long$Disparity <-
as.numeric(chelinosp_long$Disparity) #
make disparity data numeric

cymbosp <- read.csv("cymbosp_disp.csv")
# load raw data
cymbosp <- cymbosp[-1] # remove
sacrificial column
cymbosp_long <- pivot_longer(cymbosp,
cols = "mMN":"PL", names_to = "Biozone",
                             values_to =
"Disparity", values_drop_na = TRUE)
cymbosp_long$Disparity <-
as.numeric(cymbosp_long$Disparity) #
make disparity data numeric

emphani <- read.csv("emphani_disp.csv")
# load raw data
emphani <- emphani[-1] # remove
sacrificial column
```

```
emphani_long <- pivot_longer(emphani,
cols = "mMN":"PL", names_to = "Biozone",
                             values_to =
"Disparity", values_drop_na = TRUE)
emphani_long$Disparity <-
as.numeric(emphani_long$Disparity) #
make disparity data numeric


retuso <- read.csv("retuso_disp.csv") #
load raw data
retuso <- retuso[-1] # remove
sacrificial column
retuso_long <- pivot_longer(retuso, cols
= "mMN":"PL", names_to = "Biozone",
                            values_to =
"Disparity", values_drop_na = TRUE)
retuso_long$Disparity <-
as.numeric(retuso_long$Disparity) # make
disparity data numeric


synorisp <-
read.csv("synorisp_disp.csv") # load raw
data
synorisp <- synorisp[-1] # remove
sacrificial column
synorisp_long <- pivot_longer(synorisp,
cols = "mMN":"PL", names_to = "Biozone",
                              values_to
= "Disparity", values_drop_na = TRUE)
synorisp_long$Disparity <-
as.numeric(synorisp_long$Disparity) #
make disparity data numeric


#box plots
# ambitisporites
ambiti_plot <- ggplot(ambiti_long,
aes(x= Biozone, y = Disparity, fill =
Genus)) +
  geom_boxplot() +
  geom_jitter(shape = 16, position =
position_jitter(0.2)) +
  theme_minimal() + # get rid of grey
background
  scale_y_continuous(limits = c(5,20)) +
# change y axis scale
  ylab("Disparity score") + # label y
axis
  xlab("") +

scale_x_discrete(limits=c("mMN","lMN","N
TPA", "TS", "PL")) +
  scale_fill_manual(values =
c("forestgreen")) + # change colours of
bar, see colour chart
  theme_bw() + theme(panel.border =
element_blank(), panel.grid.major =
element_blank(),
                     plot.title =
element_text(size = 12, face = "bold"),
# alter title
                     axis.text =
element_text(colour = "black"), # alter
axis text
                     panel.grid.minor =
element_blank(), axis.line =
element_line(colour = "black"),
                     legend.position =
"none")



aneuro_plot <- ggplot(aneuro_long,
aes(x= Biozone, y = Disparity, fill =
Genus)) +
  geom_boxplot() +
  geom_jitter(shape = 16, position =
position_jitter(0.2)) +
  theme_minimal() + # get rid of grey
background
  scale_y_continuous(limits = c(5,20)) +
# change y axis scale
  ylab("Disparity score") + # label y
axis
  xlab("") +

scale_x_discrete(limits=c("mMN","lMN","N
TPA", "TS", "PL")) +
  scale_fill_manual(values =
c("forestgreen")) + # change colours of
bar, see colour chart
  theme_bw() + theme(panel.border =
element_blank(), panel.grid.major =
element_blank(),
                     plot.title =
element_text(size = 12, face = "bold"),
# alter title
                     axis.text =
element_text(colour = "black"), # alter
axis text
                     panel.grid.minor =
element_blank(), axis.line =
element_line(colour = "black"),
                     legend.position =
"none")



apiculi_plot <- ggplot(apiculi_long,
aes(x= Biozone, y = Disparity, fill =
Genus)) +
```

```
  geom_boxplot() +
  geom_jitter(shape = 16, position =
position_jitter(0.2)) +
  theme_minimal() + # get rid of grey
background
  scale_y_continuous(limits = c(5,20)) +
# change y axis scale
  ylab("Disparity score") + # label y
axis
  xlab("") +

scale_x_discrete(limits=c("mMN","lMN","N
TPA", "TS", "PL")) +
  scale_fill_manual(values =
c("forestgreen")) + # change colours of
bar, see colour chart
  theme_bw() + theme(panel.border =
element_blank(), panel.grid.major =
element_blank(),
                     plot.title =
element_text(size = 12, face = "bold"),
# alter title
                     axis.text =
element_text(colour = "black"), # alter
axis text
                     panel.grid.minor =
element_blank(), axis.line =
element_line(colour = "black"),
                     legend.position =
"none")

apiculi_plot

apiculi_plot

chelinosp_plot <- ggplot(chelinosp_long,
aes(x= Biozone, y = Disparity, fill =
Genus)) +
  geom_boxplot() +
  geom_jitter(shape = 16, position =
position_jitter(0.2)) +
  theme_minimal() + # get rid of grey
background
  scale_y_continuous(limits = c(5,20)) +
# change y axis scale
  ylab("Disparity score") + # label y
axis
  xlab("") +

scale_x_discrete(limits=c("mMN","lMN","N
TPA", "TS", "PL")) +
  scale_fill_manual(values =
c("forestgreen")) + # change colours of
bar, see colour chart
  theme_bw() + theme(panel.border =
element_blank(), panel.grid.major =
element_blank(),
                     plot.title =
element_text(size = 12, face = "bold"),
# alter title
                     axis.text =
element_text(colour = "black"), # alter
axis text
                     panel.grid.minor =
element_blank(), axis.line =
element_line(colour = "black"),
                     legend.position =
"none")

cymbosp_plot <- ggplot(cymbosp_long,
aes(x= Biozone, y = Disparity, fill =
Genus)) +
  geom_boxplot() +
  geom_jitter(shape = 16, position =
position_jitter(0.2)) +
  theme_minimal() + # get rid of grey
background
  scale_y_continuous(limits = c(5,20)) +
# change y axis scale
  ylab("Disparity score") + # label y
axis
  xlab("") +

scale_x_discrete(limits=c("mMN","lMN","N
TPA", "TS", "PL")) +
  scale_fill_manual(values =
c("forestgreen")) + # change colours of
bar, see colour chart
  theme_bw() + theme(panel.border =
element_blank(), panel.grid.major =
element_blank(),
                     plot.title =
element_text(size = 12, face = "bold"),
# alter title
                     axis.text =
element_text(colour = "black"), # alter
axis text
                     panel.grid.minor =
element_blank(), axis.line =
element_line(colour = "black"),
                     legend.position =
"none")

emphani_plot <- ggplot(emphani_long,
aes(x= Biozone, y = Disparity, fill =
Genus)) +
  geom_boxplot() +
```

```
  geom_jitter(shape = 16, position =
position_jitter(0.2)) +
  theme_minimal() + # get rid of grey
background
  scale_y_continuous(limits = c(0, 20))
+ # change y axis scale
  ylab("Disparity score") + # label y
axis
  xlab("") +

scale_x_discrete(limits=c("mMN","lMN","N
TPA", "TS", "PL")) +
  scale_fill_manual(values =
c("forestgreen")) + # change colours of
bar, see colour chart
  theme_bw() + theme(panel.border =
element_blank(), panel.grid.major =
element_blank(),
                     plot.title =
element_text(size = 12, face = "bold"),
# alter title
                     axis.text =
element_text(colour = "black"), # alter
axis text
                     panel.grid.minor =
element_blank(), axis.line =
element_line(colour = "black"),
                     legend.position =
"none")

retuso_plot <- ggplot(retuso_long,
aes(x= Biozone, y = Disparity, fill =
Genus)) +
  geom_boxplot() +
  geom_jitter(shape = 16, position =
position_jitter(0.2)) +
  theme_minimal() + # get rid of grey
background
  scale_y_continuous(limits = c(5,20)) +
# change y axis scale
  ylab("Disparity score") + # label y
axis
  xlab("") +

scale_x_discrete(limits=c("mMN","lMN","N
TPA", "TS", "PL")) +
  scale_fill_manual(values =
c("forestgreen")) + # change colours of
bar, see colour chart
  theme_bw() + theme(panel.border =
element_blank(), panel.grid.major =
element_blank(),
                     plot.title =
element_text(size = 12, face = "bold"),
# alter title
                     axis.text =
element_text(colour = "black"), # alter
axis text
                     panel.grid.minor =
element_blank(), axis.line =
element_line(colour = "black"),
                     legend.position =
"none")

synorisp_plot <- ggplot(synorisp_long,
aes(x= Biozone, y = Disparity, fill =
Genus)) +
  geom_boxplot() +
  geom_jitter(shape = 16, position =
position_jitter(0.2)) +
  theme_minimal() + # get rid of grey
background
  scale_y_continuous(limits = c(5,20)) +
# change y axis scale
  ylab("Disparity score") + # label y
axis
  xlab("") +

scale_x_discrete(limits=c("mMN","lMN","N
TPA", "TS", "PL")) +
  scale_fill_manual(values =
c("forestgreen")) + # change colours of
bar, see colour chart
  theme_bw() + theme(panel.border =
element_blank(), panel.grid.major =
element_blank(),
                     plot.title =
element_text(size = 12, face = "bold"),
# alter title
                     axis.text =
element_text(colour = "black"), # alter
axis text
                     panel.grid.minor =
element_blank(), axis.line =
element_line(colour = "black"),
                     legend.position =
"none")

# now we group the plots up..

plot <- ggarrange(ambiti_plot,
aneuro_plot, apiculi_plot,
                  chelinosp_plot,
cymbosp_plot, emphani_plot, retuso_plot,
synorisp_plot,
```

```
          labels = c("A", "B",  "C",
"D", "E", "F", "G", "H"), # add labels
to final fig
          ncol = 2, nrow = 4, align =
"h")

annotate_fig.(plot, top =
text_grob("Selected miospore genus
disparity scores by biozone",

color = "black", face = "bold", size =
14))

#######################################
```

Jaccards dissimilarity indices between localities

```
# Alexander C Ball. This is a script for
testing Jaccard dissimilarity
# between coeval localities

setwd("C:/Users/AlexB/Documents/AB
PhD/Research/Diversity -
disparity/Turnover/Jaccards/vegan")

# read in data

pa_dat <- read.csv("awb_perc_gr2.csv",
sep = ",", row.names = 1, header = TRUE)

library("vegan")

# sep variables for testing
# PL zone

pl_total <- pa_dat[-c(1:13),]
pl_cry <- pl_total[-c(1:192)]
pl_mio <- pl_total[-c(193:250)]

pl_total_dist <- vegdist(pl_total,
method = "jaccard", binary = TRUE)
pl_cry <- vegdist(pl_cry, method =
"jaccard", binary = TRUE)
pl_mio <- vegdist(pl_mio, method =
"jaccard", binary = TRUE)

# ts zone
ts_total <- pa_dat[-c(1:10),]
ts_total <- ts_total[-c(4:5),]
ts_cry <- ts_total[-c(1:192)]
ts_mio <- ts_total[-c(193:250)]

ts_all <- vegdist(ts_total, method =
"jaccard", binary = TRUE)
ts_cry <- vegdist(ts_cry, method =
"jaccard", binary = TRUE)
ts_mio <- vegdist(ts_mio, method =
"jaccard", binary = TRUE)

# NTPA
ntpa_total <- pa_dat[-c(1:7),]
ntpa_total <- ntpa_total[-c(4:8),]

ntpa_cry <- ntpa_total[-c(1:192)]
ntpa_mio <- ntpa_total[-c(193:250)]

# jaccards dissims
ntpa_all <- vegdist(ntpa_total, method =
"jaccard", binary = TRUE)
ntpa_cry <- vegdist(ntpa_cry, method =
"jaccard", binary = TRUE)
ntpa_mio <- vegdist(ntpa_mio, method =
"jaccard", binary = TRUE)

# lower MN
lmn_total <- pa_dat[-c(1:3),]
lmn_total <- lmn_total[-c(5:12),]

lmn_cry <- lmn_total[-c(1:192)]
lmn_mio <- lmn_total[-c(193:250)]

# jaccards dissims
lmn_all <- vegdist(lmn_total, method =
"jaccard", binary = TRUE)
lmn_cry <- vegdist(lmn_cry, method =
"jaccard", binary = TRUE)
lmn_mio <- vegdist(lmn_mio, method =
"jaccard", binary = TRUE)

# middle MN
mmn_total <- pa_dat[-c(4:15),]
mmn_cry <- mmn_total[-c(1:192)]
mmn_mio <- mmn_total[-c(193:250)]

# jaccards dissims
mmn_all <- vegdist(mmn_total, method =
"jaccard", binary = TRUE)
mmn_cry <- vegdist(mmn_cry, method =
"jaccard", binary = TRUE)
mmn_mio <- vegdist(mmn_mio, method =
"jaccard", binary = TRUE)

#######################################
```

Jaccards dissimilarity indices between biozones

```
# Alexander C Ball. This is a script for
testing Jaccard dissimilarity
# between biozones

setwd("C:/Users/AlexB/Documents/AB
PhD/Research/Diversity -
disparity/Turnover/Jaccards/vegan")

# read in data

pa_dat <-
read.csv("awb_perc_gr2_biozone.csv", sep
= ",", row.names = 1, header = TRUE)

library("vegan")

# mio and cryp by biozone

biozone_cry <- pa_dat[-c(1:192)]
biozone_mio <- pa_dat[-c(193:250)]

# d7 tests

biozone_all <- vegdist(pa_dat, method =
"jaccard", binary = TRUE)
bz_cry_d7 <- vegdist(biozone_cry, method
= "jaccard", binary = TRUE)
bz_mio_d7 <- vegdist(biozone_mio, method
= "jaccard", binary = TRUE)

########################################
```

Statistical analysis

```
setwd("C:/Users/AlexB/Documents/AB
PhD/Research/Diversity -
disparity/Disparity
new/disp.stats.tests")

mn_premn <- read.csv("mn_lmn_disp.csv")

head(mn_premn)

mn_premn <- mn_premn[-1]

library(dplyr)
library(ggplot2)
library("ggpubr")

# mio obs

mio_obs <- mn_premn[-3:-4]
head(mio_obs)

# cry obs

cry_obs <- mn_premn[-2]
cry_obs <- cry_obs[-3]

head(cry_obs)

# all obs

all_obs <- mn_premn[-2:-3]
head(all_obs)


# boxplot

d <- ggplot(mio_obs, aes(x = Biozone, y
= Mio.obs, fill = Biozone)) +
  geom_boxplot() +
  labs(y = "Disparity score")  +
  theme_bw() + theme(legend.position =
"none",
                     panel.border =
element_blank(), panel.grid.major =
element_blank(),
                     axis.text =
element_text(colour = "black"),
                     panel.grid.minor =
element_blank(), axis.line =
element_line(colour = "black"))


e <- ggplot(cry_obs, aes(x = Biozone, y
= Cry.obs, fill = Biozone)) +
  geom_boxplot()+
  labs(y = "Disparity score")  +
  theme_bw() + theme(legend.position =
"none",
                     panel.border =
element_blank(), panel.grid.major =
element_blank(),
                     axis.text =
element_text(colour = "black"),
                     panel.grid.minor =
element_blank(), axis.line =
element_line(colour = "black"))


f <- ggplot(all_obs, aes(x = Biozone, y
= all.obs, fill = Biozone)) +
  geom_boxplot()+
```

```
  labs(y = "Disparity score")  +
  theme_bw() + theme(legend.position =
"none",
                     panel.border =
element_blank(), panel.grid.major =
element_blank(),
                     axis.text =
element_text(colour = "black"),
                     panel.grid.minor =
element_blank(), axis.line =
element_line(colour = "black"))



main <- ggarrange(a, b, c, d, e, f,
                  labels = c("A", "B",
"C", "D", "E", "F"),
                  ncol = 3, nrow = 2)
main

# Shaprio for normal distribution
#mio
with(mio_obs,
shapiro.test(Mio.obs[Biozone == "mMN"]))
with(mio_obs,
shapiro.test(Mio.obs[Biozone == "lMN"]))

with(cry_obs,
shapiro.test(Cry.obs[Biozone == "mMN"]))
with(cry_obs,
shapiro.test(Cry.obs[Biozone == "lMN"]))

with(all_obs,
shapiro.test(all.obs[Biozone == "mMN"]))
with(all_obs,
shapiro.test(all.obs[Biozone == "lMN"]))



# f test for normal variance
res.ftest <- var.test(Mio.obs ~ Biozone,
data = mio_obs)
res.ftest

res.ftest <- var.test(Cry.obs ~ Biozone,
data = cry_obs)
res.ftest

res.ftest <- var.test(all.obs ~ Biozone,
data = all_obs)
res.ftest



# t test

t_test <- t.test(all.obs ~ Biozone, data
= all_obs, var.equal = TRUE)
res

# Welch t test

res <- t.test(Mio.obs ~ Biozone, data =
mio_obs, var.equal = FALSE)
res
```

Thesis appendix 4.8: Statistical test boxplots

Boxplots for species richness and species disparity between the MN and pre-MN biozone samples

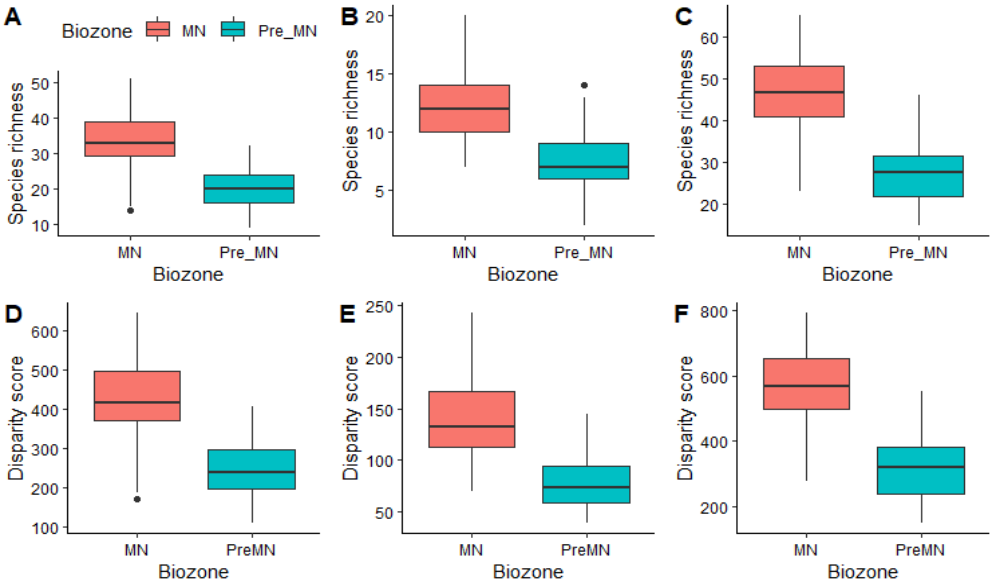

A – C: *MN vs pre-MN species richness;* ***A:*** *Miospore species richness;* ***B:*** *Cryptospore species richness;* ***C:*** *miospore + cryptospore species richness;* ***D – F:*** *MN vs pre-MN disparity scores;* ***D:*** *Miospore disparity scores;* ***E:*** *Cryptospore disparity scores;* ***F:*** *Miospore + Cryptospore disparity. Chart made in R using* `library("ggplot2")`.

Boxplots for species richness and species disparity between lower and middle MN samples

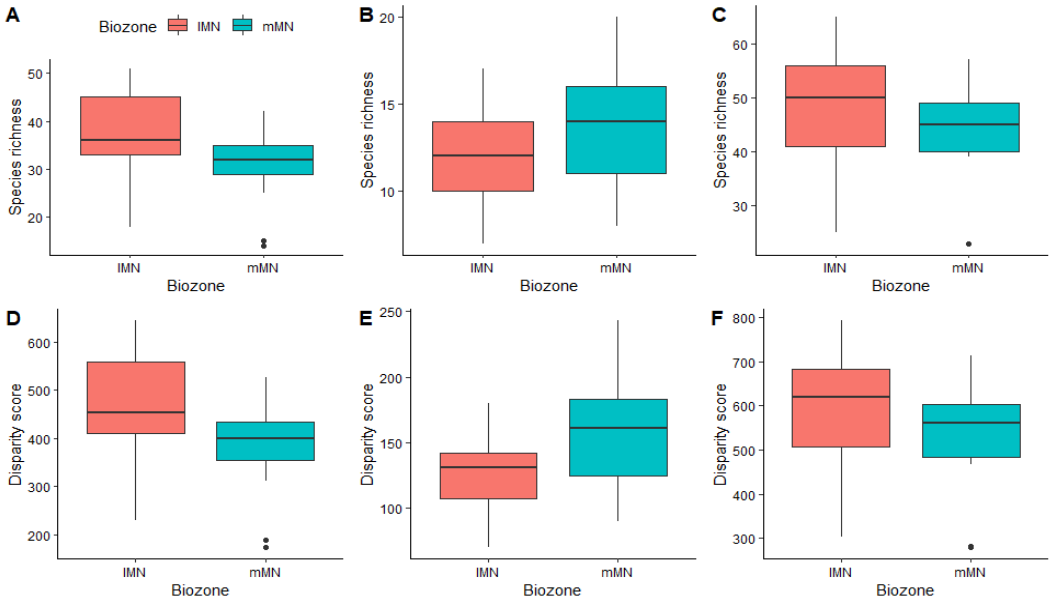

A – C: *lower MN vs middle MN species richness;* ***A:*** *Miospore species richness;* ***B:*** *Cryptospore species richness;* ***C:*** *miospore + cryptospore species richness;* ***D – F:*** ***lower*** *MN vs middle MN disparity scores;* ***D:*** *Miospore disparity scores;* ***E:*** *Cryptospore disparity scores;* ***F:*** *Miospore + Cryptospore disparity. Chart made in R using* `library("ggplot2")`.

Chapter V Early Lochkovian (Early Devonian) mesofossil assemblages from the Anglo-Welsh Basin, UK.

The study was conceived, mesofossil data collected and manuscript written by A.C. Ball. Material was collected by D. Edwards and the BGS. Margaret Collinson, Neil Holloway and Sharon Gibbons processed material for vitrinite reflectance and carried out reflectance data collection.

Abstract

Studies of largely compressed megafossils have revealed a surprising level of diversity amongst the 'lilliputian' rhyniophytic floras of the Early Devonian (Lochkovian), but comparison with the taxonomically richer dispersed spore record highlights the preservational biases present in the former record. Meanwhile, the latter often lacks insights into source-plant morphologies and affinities. The recovery of often exceptionally charcoalified mesofossils containing *in situ* spores from the Přídolí and Lochkovian of the Anglo-Welsh Basin in southern Britain has gone some way towards harmonising the two records. In addition, these mesofossil assemblages have played a prominent role in elucidating other aspects of the late Silurian and Early Devonian terrestrial biota, including plant – animal interactions and cryptogamic crusts, alongside indicating atmospheric composition. Many dispersed spore species are yet to be found *in situ*, and fewer still lack clear affinities to contemporary and modern plants. Here, two mesofossil assemblages recovered from the Early Lochkovian (Early Devonian) lower *micrornatus* – *newportensis* biozone of the Anglo-Welsh Basin, U.K. Vitrinite reflectance confirms that the mesofossils were charred in low temperature fires. The two assemblages, the M50 section and Ammons Hill, both in the Welsh Borderlands, yield very different assemblages. The M50 contains abundant plant remains, including reasonably well-preserved spore masses with *in situ* species of, amongst others, *Emphanisporites* and *Hispanaediscus*, with very rare non-embryophytic 'phytodebris'. Meanwhile, the Ammons Hill section yields abundant nematophytes, other non-embryophytic 'phytodebris' and rare embryophytic debris, with a complete absence of spore masses. The variation is thought to be derived from the hydrodynamic behaviour of charcoal during transportation, rather than a reflection of the respective ecosystems. Amongst the spore masses of the M50 assemblage, contemporary affinities with other spore masses, and with *Paracooksonia*, *Cooksonia* and *Lenticulitheca* are indicated, but without spore wall ultrastructural analyses, confident relationships to contemporary and modern taxa cannot be fielded. The occurrence of the spore masses, combined with the occurrence and abundance of corresponding dispersed spores, may give insights into the palaeoecology of some of these early land plants, and the recovery of plant axes, coprolites and non-embryophytic 'phytodebris' paint a picture of a diverse, terrestrial ecosystem. The occurrence of the charcoalified remains suggests that some of the box models used to indicate atmospheric pO_2 may underestimate atmospheric oxygen concentration in the early Lochkovian.

1. Introduction

The Anglo-Welsh Basin, an extensive, essentially continuous red bed sequence of alluvial sediments (the 'Lower Old Red Sandstone') in southern Britain has played a key role in developing the current understanding of late Silurian – Early Devonian (Přídolí – Lochkovian) land plant morphologies, diversity and affinities. While studies of largely compressed megafossils have revealed a surprising level of diversity

amongst the chiefly 'lilliputian' floras (Edwards and Rogerson, 1979; Fanning et al., 1987, 1992; Morris et al., 2011b; Morris and Edwards, 2014), comparison with the taxonomically richer dispersed spore record (e.g. Richardson and Lister, 1969; Burgess and Richardson, 1995; Wellman et al., 2000; Edwards and Richardson, 2004; Chapter III, IV) highlights the preservational biases present in the former group which often precludes plants lacking resistant biopolymers in their tissues (e.g. Edwards and Richardson, 2004). However, dispersed spores generally lack key insights into source-plant morphologies and their affinities with contemporaneous and modern plants.

Mesofossils are minute (200 – 10,000µm) fossils which, while visible to the naked eye, must be studied via microscopy. Such fossils can be formed from a variety of preservation modes, including compression and charcoalification (e.g. Edwards et al., 1992; Morris et al., 2011a, b). The discovery of such charcoalified mesofossils in the Anglo-Welsh Basin has gone some way towards harmonising the dispersed spore and plant megafossil record, principally through the recovery of *in situ* spores in charcoalified sporangia (e.g. Edwards, 1996; Edwards et al., 1992, 1994, 2014, 2021a, b, 2022; Glasspool et al., 2006; Morris et al., 2011a, b, 2018b). *In situ* spores are typically comparable to species in the dispersed spore record, and in exceptionally preserved specimens allow insights into associated sporangial and axial tissues. In particular, sporangia associated with subtending axes facilitate the investigation of a plant's (and associated *in situ* spores') vascular status (e.g. Edwards et al., 1992, 1994). Much of the study of these charcoalified remains has centred on the mid Lochkovian Brown Clee Hill Konservat Lagerstatte in Shropshire (e.g. Edwards and Richardson, 2004; Glasspool et al., 2006; Morris et al., 2018b) with other work on the Přídolí Ludford Lane assemblage in Shropshire also contributing to understanding of a slightly older suite of land plants (Edwards et al., 1996, 1999; Wellman et al., 1998b), *inter alia* (Jeram et al., 1990). Sporadic reports of charcoalified plant mesofossils from other localities in the Anglo-Welsh Basin also exist (e.g. Edwards et al., 1994; Wellman, 1999), but these promising localities have not yet been investigated in detail. While there is a growing number of dispersed spores now related to parent plants via *in situ* spores (Morris et al., 2011a; Edwards et al., 2014, 2022a, b, c), several prominent dispersed species, particularly patinate forms, remain unaccounted for in the dispersed spore record. Such an absence may be related to taphonomic processes influencing the plant remains prior to burial, and/ or the palaeoecology of the land plants. Such deliberations are enriched by abundance and presence/absence studies of the dispersed spore record between spatially and environmentally distinct, coeval localities across the basin (Edwards and Richardson, 2000; Richardson, 2007; Ball and Taylor, 2022; this chapter).

Study of the assemblages beyond plant remains is informative for revealing further facets of terrestrial life which, together with information from fertile plants remains and the dispersed spore record, paints a picture of the terrestrial landscape of the Anglo-Welsh Basin at a given point in time. Indeed, charcoalified mesofossil horizons yield specimens which shed light on animals and their interactions with plants (Jeram et al., 1990; Edwards et al., 1995c; Brookfield et al., 2022), plant phytodebris such as sterile axes and tissue fragments (e.g. Edwards et al., 2022) and non-embryophytic 'phytodebris' (e.g. Edwards et al.,2013; Honegger et al., 2013; Wellman and Ball, 2021). The latter group represents a diverse suite of organisms, comprising lichens, lichenised fungi and fungi (Edwards and Kenrick, 2015; Wellman and Ball, 2021), which formed an important component of the terrestrial ecosystem (e.g. Strother et al., 2010).

In this chapter, mesofossils from the largely uninvestigated early (not earliest) Lochkovian (lower *micrornatus – newportensis* spore assemblage subzone) Ross – Tewkesbury Spur (M50) motorway (Edwards et al., 1994; Wellman, 1999; Ball and Taylor, 2022) and Ammons Hill (Barclay et al., 1994) sections in the Anglo-Welsh Basin are reported, with their Formation by low temperature wildfires confirmed by vitrinite reflectance. The M50 section in Herefordshire has yielded numerous spore masses containing *in situ* spores comparable to dispersed spore species recovered from the same sample. Several novel species from dispersed genera including *Hispanaediscus* and *Emphanisporites* have been recovered, and new insights are obtained for other well-known *in situ* species such as *Laevolancis*, which have been

previously recorded from the slightly younger (mid Lochkovian) Brown Clee Hill lagerstatte and older (Přídolí) Ludlow Lane assemblage (e.g. Wellman et al., 1998b). In addition, specific groups of vegetation, including the eophytes (Edwards et al., 2022a, b, c) are recognised from fertile and infertile remains for the first time in the lower Lochkovian. However, the sporangial remains yielding *in situ* spores in the M50 assemblage are not exceptionally preserved, with a dearth sporangial tissue associated in nearly all of the specimens. Given the absence of such tissues, it is prudent to refer to the specimens as spore masses, rather than sporangia. The Ammons Hill assemblage provides an interesting contrast to the M50 section, because despite yielding an abundance of nematophyte remains and some highly fragmentary infertile plant remains, no spore masses or sporangia have been recovered from the assemblage. Nonetheless, a diverse suite of nematophytes from this site proffers insights into the non-embryophytic portion of the terrestrial ecosystem, in addition to deliberations around the effects of taphonomy on the components of the studied assemblages. Despite the taphonomically influenced and unexceptional preservation of the horizons, they serve to support Morris' *et al*. (2018b) hypothesis that: "due to the widespread nature of wildfires… more charcoalified assemblages are likely to exist".

2. Geological setting

The Anglo-Welsh Basin is a ± continuous, extra-montane foreland basin which developed from either regressive load induced flexural subsidence of the Avalonian foreland (James, 1987; King, 1994; Friend *et al*., 2000) or basin wide, sinistral mega-shearing (e.g. Dewey and Strachan, 2003; Soper and Woodcock, 2003) associated with the Caledonian Orogeny. The associated shrinkage of the Palaeozoic Marine Welsh Basin led to the Formation of a regressive offlap sequence whereby the basin was gradually infilled with shallow marine and then terrestrial sediments derived from the northern Caledonian Mountains. Deposition in the Přídolí and earliest Devonian (earliest Lochkovian) was dominated by muddy, ephemeral river channels. Intermittent ashfall from distant Plinian eruptions accompanied this fluvial deposition (Allen and Williams, 1981). Early Devonian (early to mid Lochkovian) deposition was dominated by more channelised, sandy perennial rivers (Allen and Tarlo, 1963; Hillier et al., 2008; Morris et al., 2012b) which deposited sediments derived from within the basin, following a shift from flexural subsidence to sinistral transtensional regimes in the earliest Devonian (Crowley et al., 2009). The shift in facies was accompanied by a basin-wide quiescent period in the Early Devonian which was associated with a depositional hiatus and the development of mature calcretes (Allen, 1974). The hiatus resulting from tectonics and/ or an extended period of aridity (Morris et al., 2012b). The Anglo-Welsh Basin lay 17±5° south of the paleoequator (Channel et al., 1992) and is suggested to have exhibited a strongly seasonal semi-arid climate

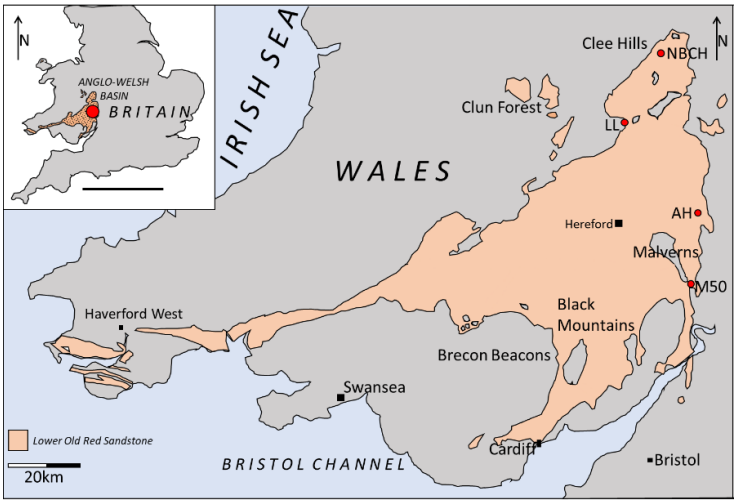

Figure V-1: ***Inset left****: location of the Anglo-Welsh Basin in Southern Britain;* ***Main****: Localities of mesofossil sites in the Anglo-Welsh Basin.* ***NBCH:*** *North Brown Cee Hill (mid Lochkovian, middle MN subzone);* ***LL:*** *Ludlow Lane, Early Přídolí, TS zone;* ***AH:*** *Ammons Hill, Early Lochkovian, lower MN subzone;* ***M50:*** *M50 section, Early Lochkovian, lower MN subzone.*

with well developed wet and dry seasons (Allen, 1974; Marriot and White, 2004). The shift from ephemeral to dominantly perennial river systems between the late Silurian and Early Devonian has been attributed to a shift to a slightly wetter climate (Morris et al., 2012b).

2.1. Ross – Tewkesbury Spur (M50) motorway section, Hereford and Worcester. *SO 664 260*

The fine beige siltstone yielding the mesofossils was collected by Dianne Edwards and John B. Richardson in 1976 from +2 m above the base of the Freshwater West Formation, just south-west of Junction 3 of the northern side of the M50 Motorway (Section F of the generalised succession laid out by Allen and Dineley, 1976; near the 29.5 furlong marker post their fig. 2, Allen and Dineley, 1976). The section comprises steeply dipping beds (45°), and some faults are developed along the section. The locality is no longer easily accessible.

The material is interpreted to have been deposited in a seasonally semi-arid terrestrial-fluvial setting, by variously meandering perennial sandy streams and rivers (e.g. Allen and Tarlo, 1963; Morris *et al*., 2012b). Analysis of dispersed spore assemblages reveals *Streelispora newportensis* and *E.* cf. *micrornatus*, alongside other taxa such as tripapillate *Aneurospora* species suggesting that the horizon belongs to the lower *micrornatus-newportensis* sporomorph assemblage biozone of Richardson and McGregor (1986) **(**Edwards and Richardson, 2004; Chapter III; pers. comm. J.B. Richardson in Wellman, 1999), and as such suggests an early, but not earliest, Lochkovian age (Early Devonian) (Chapter III).

2.2. Ammons Hill section (AH), Shropshire, SO 6850 5290 – 7020 5300

This sample was collected by the British Geological Survey (BGS) during a re-excavation of the section by Barclay et al., (1994), where a 170m trench was dug between SO 6850 5290 – 7020 5300. Palynomorphs were isolated from horizons spanning approximately 47 metres of the 'top' (western end) of the trench. The exposure was covered up following BGS investigation and the area is now heavily overgrown and difficult to access.

The section comprises steeply dipping beds (50°) and is affected throughout by various minor extensional faults. The major Brockhampton fault juxtaposes the Moor Cliffs and Freshwater West formations. Barclay *et al*., (1996) suggested that the Chapel Point Limestone had been faulted out of the sequence by the Brockhampton fault, and as such relative position to this stratigraphic marker is not possible. Based on sedimentology and the fossil assemblages (ostracods, spores and acritarchs), the sediments are interpreted to have been deposited in a largely seasonally semi-arid terrestrial-fluvial setting with limited marine influence giving rise to brackish waters (Barclay et al., 1994). Whilst the stratigraphic positioning of the section relative to the Chapel Point Limestone member is not possible due to faulting, the sporomorph assemblages exhibit key taxa including *Streelispora newportensis* and *E.* cf. *micrornatus*, alongside other taxa such as tripapillate *Aneurospora* species, which are indicative of the lower MN subzone (*sensu* Richardson and McGregor, 1986). This suggests an early (not: earliest) Lochkovian age (Chapter III; Barclay et al., 1994).

3. Materials and methods

Bulk maceration: 100g of sample 19M50-26 (M50 section) and MPA25239 (Ammons Hill section) between 15 and 50mm in size were selected. The samples were not ground or altered prior to acid treatment. 200ml of concentrated hydrochloric acid (HCl) were added to the samples, which were then left for five days, allowing digestion of carbonates. The HCl-sample mixture was then diluted with water seven times, waiting twenty-four hours between individual dilutions to allow settling and minimise sediment loss. 300ml of 40%

concentrated hydrofluoric acid (HF) was added to digest silicates that were adhering to the mesofossils and left for two days to react. The HF solution was then diluted eight times with water, leaving twenty-four hours between each dilution to allow for settling. The diluted solution was then sieved through an 80µm nylon mesh with organic matter >80µm being collected in a large, covered petri-dish for picking and SEM analysis.

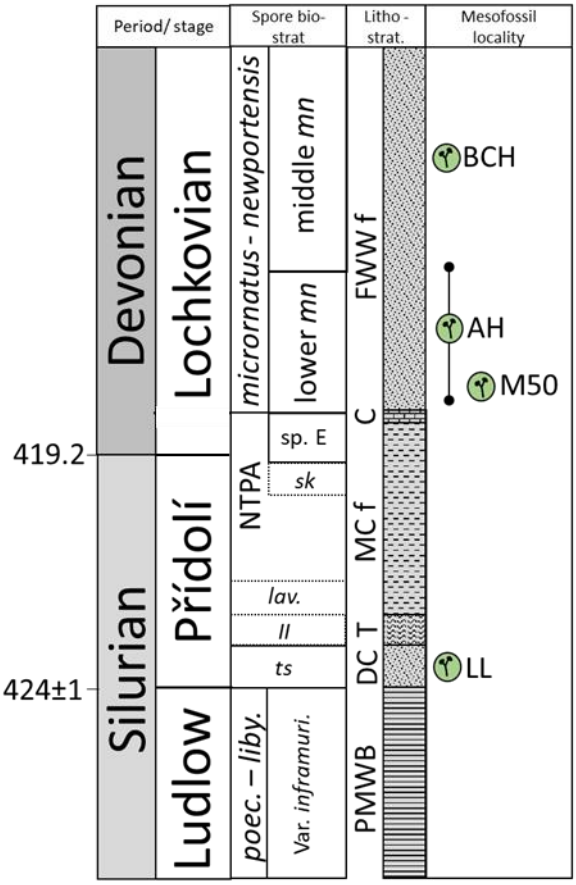

Figure V-2: Lithostratigraphic and biostratigraphic positions of mesofossil horizons in the Anglo-Welsh Basin. ***BCH:*** *Brown Clee Hill****,*** *+64m above the Chapel Point Limestone* ***(C)****;* ***AH:*** *Ammons Hill, position relative to the Chapel Point Limestone uncertain due to faulting, see text for further details;* ***M50,*** *+2m relative to the Chapel Point Limestone;* ***LL:*** *Ludlow Lane. Lithostratigraphy* sensu *Barclay et al. (2015).* ***PMWB:*** *Palaeozoic marine Welsh Basin****;*** ***DC:*** *Downton Castle Sandstone formation (also part of PMWB);* ***T – FWWf:*** *The lower Old Red Sandstone Anglo-Welsh Basin,* ***T:*** *Temeside shales formation****;*** ***MCf:*** *Moor Cliffs formation;* ***C:*** *Chapel Point Limestone member;* ***FWWf:*** *Freshwater West formation. Dates Ma,* ***424±1*** *for the Ludlow Bone Bed sensu Catlos et al., 2021; 419 sensu Cohen et al., (2013). Lochkovian ends at 410Ma.*

Picking and strew mounting: picking was carried out using a single-bristled size 1 paintbrush under a Vickers dissecting microscope. Promising specimens were identified and individually picked. They were initially transferred to a glass slide to allow them to dry. Once dried, specimens were transferred onto an SEM stub with a carbon tab attached using the single-bristled paint brush.

In order to investigate the very fine fraction of the mesofossil assemblage (<400µm), a small amount of fine material was collected with a plastic pipette from the mesofossil suspension and strewed onto an SEM slide with a carbon tab attached and left to dry.

Scanning Electron Microscopy: Following picking, samples were then gold coated for two minutes using an Edwards S105B sputter coater, prior to imaging with a Tescan Vega-3 Scanning Electron Microscope at 15 - 20Kv. Following initial examination and photography, samples were recoated with gold for a further three minutes to reduce any charge and rephotographed where necessary.

Light microscopy (dispersed spores): 20g ± 1g of the samples were ground into <5mm gravel-sized fragments using a pestle and mortar. 50ml of 35% concentrated Hydrochloric acid (HCl) was added to the

samples in order to digest any carbonate present in the rock. The samples were left to fully react for 24 hours. Two dilutions then followed, whereby water was added to the sample and HCl mixture and then poured off. Prior to each dilution, samples were left to settle for 24 hours in order to minimise the potential loss of suspended palynomorphs. Following initial dilutions, a further 10ml of 35% HCl and 12ml of 40% concentrated Hydrofluoric acid (HF) was added to the samples. HF was added in order to digest any silicates that were present in the rock. The samples were then agitated over several days and allowed to fully react before a further eight dilutions per sample were carried out to neutralise the acids, with 24 hours left between each dilution to allow settling of palynomorphs

Sieving of the macerated preparation was carried out using a nylon sieve mesh and plastic sieves in order to remove minute fragmentary, indeterminate organic material and mineral residue that may obscure palynomorphs. Sieve size was selected based on the smallest palynomorph present in the assemblage (smallest spore: 12µm). Samples were sieved using a 10µm mesh. Diluted mixtures were poured onto the mesh and washed through with running water whilst being gently agitated over a suction flask. >10µm fraction was collected. The >10µm residue was then checked under light microscope to assess effectiveness of sieving; samples typically needed two to three sieves to sufficiently remove fine particulates <10µm.

Samples were then transferred to 45ml centrifuge tubes and centrifuged in an Eppendorf centrifuge 5702 for ten minutes at 3000RPM in order to separate excess water, organics and mineral residue. Water was then poured off as far as possible from the tube, and a Zinc Chloride ($ZnCl_2$) and Hydrochloric acid (HCl) mixture was added to the organic and mineral residue. Because of its high density, $ZnCl_2$ + HCl facilitates the separation of the less dense organic material and higher density mineral residue. The samples were then centrifuged at 2000RPM for ten minutes. Following centrifugation, organic material was separated and collected. The mineral residue fraction was then checked for organic material and, if separation was successful, disposed of. Organic material was diluted with water and 10% HCl, then sieved again using a 10µm sieve to remove $ZnCl_2$ + HCl and any remnant material <10µm.

Vitrinite reflectance:

Ammons Hill MPA25242 and M50 section sample DE98 samples were gently sieved using a 1mm brass mesh in order to separate a coarse (>1mm) and fine (<1mm) fraction, before being sent to the Earth Sciences department at Royal Holloway, University of London for vitrinite reflectance preparation and analysis. Blocks for Vitrinite reflectance were prepared by Neil Holloway of the Department of Earth Sciences at Royal Holloway, University of London, and vitrinite reflectance measurements were made by Margaret Collinson and Sharon Gibbons at the Earth Sciences dept. at Royal Holloway, University of London. The samples were embedded in a polyester resin block, cut and then polished. Two blocks each from Ammons Hill coarse and fine fractions and the M50 section coarse and fine fractions were made as replicates for a total of eight blocks.

Mean random reflectance of samples were converted to temperatures using equations 1 and 2 (below). Equation 1 is a composite 3rd order polynomial trend-line from experimental 1 – 24hr duration wood charring data from Scott and Glasspool (2005) following Glasspool and Gastaldo (2022). The methods of the latter were closely followed as the material used there was closely comparable in composition to the material analysed here. Equation 2 uses data derived from Scott and Glasspool (2005) and is a 3rd order polynomial calibration curve derived from experimental charring of *Ganoderma* (bracket) fungus. The latter was used by Glasspool and Gastaldo (2022) to measure charcoalified Silurian Nematophytes as it is possible that *Ganoderma* may better represent the original cell wall chemistry of nematophytes. This method is also used here.

(1) $y = 5.3103*R_0^3 - 50.454*R_0^2 + 206.87*R_0 + 220.17$

(2) $y = 1.5242*R_0^3 - 9.0073*R_0^2 + 116.22*R_0 + 300.66$

Where R_o is reflectance value. Data is given in thesis appendix 5.1.

Curation: ABM50 and DE98 stubs are housed at the Centre for Palynology, The University of Sheffield, Western Bank, Sheffield, S10 2TN. MPA25239 stubs are housed at the British Geological Survey, Keyworth, Nottingham, NG12 5GG. Light microscope slides from the M50 section are housed at the Natural History Museum, Cromwell Road, London, SW7 5BD. NBCH Slides are housed at the University of Sheffield. Slides from Ammons Hill are housed at the British Geological Survey.

4. Results

4.1. Reflectance

4.1.1. M50 reflectance

Cuticular and axial plant fragments dominate the organic residues of the M50 section. Fire-impacted reflectance from 100 samples give a mean random reflectance R_o of 0.53% SD: 0.45% (fig. 3b), with a minimum $R_o\,\%$ = 0.17 and maximum $R_o\,\%$ = 3.12 (indicating medium volatile bituminous, Teichmuller, 1987). The structure of three specimens is quite different from the rest of the M50 sample (particles 1, 69 and 14). Plots indicate that these three specimens have unusually high reflectance and are relative to the rest of the group, considered outliers. Coupled with their considerably different structure, this may suggest these particles are modern contaminants (thesis appendix 5.1 and 5.2). Including these outliers, charred fragments from the M50 indicate that fire temperatures (*T°C*) ranged from *w*254 – *w*535°C and *g*320 – *g*621°C (*w* = calibrated against wood, equation 1; *g* = calibrated against *Ganoderma* bracket fungus, equation 2). Mean *T°C* of 100 phytoclasts is *w*316°C (*g*359°C). Excluding the outliers, M50 *T°C* ranges between *w*254 – *w*416°C and *g*320 – *g*440°C, mean *w*305 (*g*352). Recorded temperature ranges for both M50 data sets (outliers and outliers removed) are closely similar to Ammons Hill (4.1.2.), although mean *T°C* is lower in the M50 than Ammons Hill. Temperature results are positively skewed with sparsely populated outliers.

4.1.2. Ammons Hill reflectance

Nematophyte phytoclasts dominate the assemblage at Ammons Hill. Fire impacted reflectance from 100 samples give a mean random reflectance R_o 1.06% SD: 0.37% (fig. 3a) with a minimum R_o = 0.26 % and maximum R_o = 1.86% (indicating medium volatile bituminous, Teichmuller (1987). No outliers were identified in Ammons Hill. Charred fragments from Ammons Hill indicate *T°C* ranged from *w*271 – *w*465°C and *g*330 – *g*496°C. Mean *T°C* of 100 phytoclasts is *w*389°C (*g*416°C). The distribution of reflectance values at Ammons Hill tends towards bipolar, with a primary peak occurring at *w* 360°C and a secondary peak at *w*450. Because of the largely nematophytic composition of the Ammons Hill assemblage, the *Ganoderma* calibration is preferred here (after Glasspool and Gastaldo, 2022). Fungi, which nematophytes have been related to (Wellman and Ball, 2021), require higher temperatures to achieve the same reflectance as wood (Scott and Glasspool, 2005).

4.2. Scanning Electron Microscopy (SEM): Mesofossils from the Ross – Tewkesbury Spur (M50) motorway section (Hereford and Worcester).

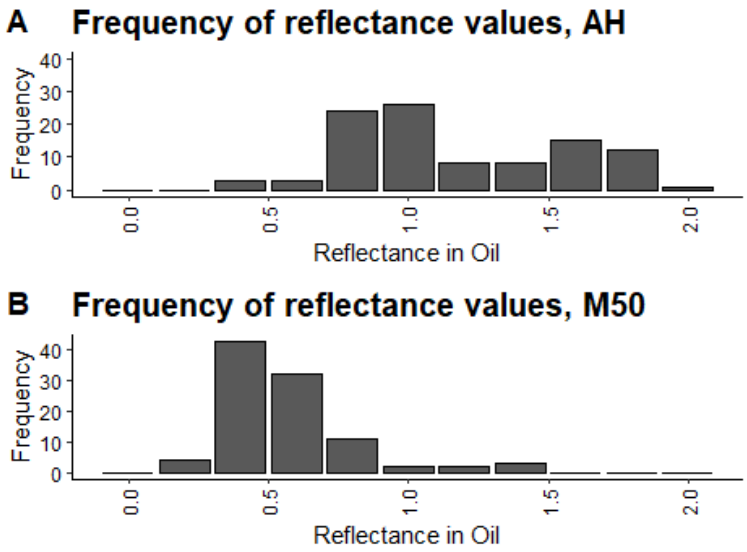

Figure V-3: Reflectance data collected from Ammons Hill and M50 mesofossils. ***A:*** *Ammons Hill section;* ***B:*** *M50 section. 100 measurements for each locality (a), with outliers removed Ammons Hill n = 100, M50 n = 97. Thesis appendix 5.1.*

4.2.1. Cryptospore bearing spore masses

ABM5014-005: *Laevolancis divellomedium-plicata* in a discoidal spore mass

Plate I, figures a – c

Spore mass: approximately circular in plan, being 457 x 404µm. The spore mass is compressed but some topography and structure is retained. Whilst the edges and sides of the spore mass are variously straight, convex or concave, the enveloping layer (below) encompasses the mass, and no internal spores are exhibited around the edges. No sporangial walls or subtending axes are observed. A limiting layer encompasses the specimen nearly entirely, with only a small section broken away. The layer itself is distinctive, with robust, continuous 'ridges', 4.8 – 9.6µm wide, forming a continuous raised reticulum. Between these ridges, polygonal, but often ± square to rectangular, spaces (?lumen) are developed, 4(19)36µm wide. Fine cracks disrupt the layer, and in some areas its appears ragged and pockmarked, as if decayed. A small piece of limiting layer has broken off one end of the mass, revealing a limited number of *in situ* spores.

In situ spores: The *in situ* spores are generally well preserved, but are folded and torn in some cases, and there is some probable internal pyritisation which has a limited effect on the overall structure of the spores. The proximal faces of the spores are generally intact. Very little extraneous material is present on the spores. The *in situ* spore ambs are circular and measure between 25 - 35µm. Proximally, the spores have a wide hilum which is universally concave and laevigate. The outer area is laevigate, except for a narrow band (*c.* 1.5µm wide) of irregularly arranged, round tipped micro-ornament, *c.* 0.1µm high and wide, on the inner edge of the crassitude (Plate I, fig. c arrow). Equatorially and distally the spores are laevigate.

Comparisons: The *in situ* spores here are most similar to spores of the *Laevolancis divellomedium-plicata* complex Burgess and Richardson (1991) (Chapter III, Plate IX, figures b – d). Their laevigate hilum and distal hemisphere are continuous with the descriptions of the complex, with the folded exine perhaps indicating that the spores are more closely related with the *L. plicata* end member than the more robust *L. divellomedium* end member (*sensu* Steemans et al., 2009). The micrornament on the inner edge of the crassitude would likely be missed in light microscope studies, and such a feature has not been reported from dispersed or *in situ Laevolancis* species.

The raised reticulum is a striking feature of this spore mass, with similar features being reported from newly described eophytes (Edwards et al, 2022; plate VII, figures1-2, 4-5). However, the sporangia in those specimens are much smaller (<100μm). The entirely encompassing nature of the layer suggests that the original gross morphology of the sporangium is ± preserved accepting the loss of the external sporangial tissues. If the spore mass is indeed the original size of the sporangium, it is interesting to note the considerably smaller size of the mass relative to the other, nearly complete spore masses (fig. 8).

ABM5014-007: *Laevolancis divellomedium-plicata* in an oval, ?bivalved spore mass

Plate I, figures d - g

Spore mass: Unequally ellipsoid in outline and appears to be mostly uncompressed with a relatively wide, pronounced equatorial ridge of differing texture to the central portion. The sporangium has a total length of 1225μm and is 887μm wide. The spore mass may have been bivalved in life (see below), although one valve is almost entirely lost. The thick equatorial margin is reasonably continuous, although some areas along the edge are damaged. Additionally, some large cracks separate closely associated fragments of the inner area. A portion of sporangium, interpreted as an associated valve, is attached along one edge and is very similar in structure and exhibits the same spore type as the complete valve. No sporangial wall cells or a subtending axis is seen. Little to no limiting material is visible on the inner portion of the sporangium, but the outer edge is composed of a dense, encompassing structure comprising tightly packed spherules which measure between 7 - 20μm. This may represent the sporangial wall but given the spheroidal morphology of the bodies, and their variable sizes, which contrast with typical cellular walls amongst these early land plants, they are tentatively considered to be the reproductive bodies of fossil saprotrophic fungi.

In situ spores: Spores are generally well preserved, but some pitting, damage and folding is present, often accompanied by extraneous material; although this does little to obscure the structure of the spores. The pits are penetrative holes measuring 0.2 - 3μm; they are generally circular but are sometimes polygonal and they are not bevelled. The spores have circular to sub-triangular ambs, measuring 31 (35) 40μm. Spores are hilate, with a proximally and distally laevigate exine. Proximally, the 2 - 3μm wide crassitude delimits the circular to ovoid hilum, the exine of which is typically lightly folded. The distal exine is essentially rigid, with some minor folds.

Comparisons: The most striking feature of this spore mass is the apparently bivalved structure. This feature has not been identified in any other *Laevolancis* spp. yielding spore masses or sporangia, which are chiefly discoidal or rarely elongate (Wellman *et al*., 1998b).

Encrusting layers have been variously reported in mesofossils. In the Anglo-Welsh Basin, the most prominent example is *cf. Horneophyton*, which is coated in a putative microbial or fungal coating comprising tubes and amorphous material (Edwards and Richardson, 2000). That encrusting material differs markedly from the encrusting material observed in specimen ABM5014-007, where no tubes are seen, and the encrusting 'coat' is exclusively comprised of subspherical structures. This putative encrusting material has not been identified in the fossil record before. It may be possible that the encrusting layer is in fact derived from contemporary mineralisation rather than biological activity.

ABM5014-009: *Laevolancis divellomedium-plicata* in a circular spore mass

Plate I figures h – j

Spore mass: Approximately discoidal in plan, likely compressed although with some topography retained across the specimen. The spore mass lacks sporangial cells and a subtending axis and is considered incomplete. Most edges are rounded and appear un-fragmented, aside for one edge which appears more

angular and ragged. No subtending axis is present. The specimen is 619µm x 587µm. Some folded, tightly adherent acellular limiting material is observed in patches across the surface of the spore mass.

In situ spores: The spores are relatively well preserved but are often folded and are often internally pyritised, as indicated by framboidal shapes interrupting the spore structure. Extraneous material is found on most spores, although it does not obscure their structure. The spores have circular ambs, 37 (46) 50µm, with laevigate distal and proximal exines. Proximally, they exhibit a crassitude 3 - 5µm wide which delimits a circular hilum. The proximal face is smooth but may be variously folded; folds may be random or concentric, and sometimes appear to simulate a triradiate mark, although laesurae are not present. Distally, the exine is generally rigid but sometimes shows mild folding.

Comparisons: The spores in this spore mass are comparable to the dispersed spore complex *Laevolancis divellomedium – plicata*. Some spores have a pseudo-triradiate mark (Plate II, fig. j), but the lack of laesurae refutes these spores being triradiate, and upon closer inspection it is clear the fortuitous folds are a product of differential compression and exine folding. Whilst the spore mass is generally incomplete, some semblance of a discoidal structure is retained, making the mass superficially comparable in morphology to larger, more complete specimens such as M50DE98-003. However, the incomplete nature of the mass precludes any confident association.

The high rate of pyritisation amongst the *in situ* spores may suggest that the mass formed part of the litter, and was partially decayed prior to charcoalification. This could go some way towards explaining the lack of sporangial tissue and the erratic occurrence of acellular material across the specimen, but no evidence of saprotrophy, such as interdigitating tubes, is observed

ABM5014-010: *Laevolancis divellomedium-plicata* in a fragmentary spore mass

Plate I, figures k – m

SEM observations: The spore mass forms a roughly sub-triangular shape, 474µm x 525µm wide. No sporangial cell wall is preserved, and no subtending axis is seen. An irregular pitted acellular layer encompasses much of the central region of the spore mass but is lost towards the edges.

In situ spores: in situ spores are exposed along the edges of the spore mass. Some folding occurs, alongside small amounts of tearing and pitting. Many of the spores are partially obscured by the acellular membrane which encompasses much of the spore mass, and nearly all exhibit variously densely packed, approximately spherical to oval bodies irregularly scattered across the proximal and distal exine, measuring 0.9 -1.8µm. The spores have circular to subtriangular ambs, 30 (36) 42µm in diameter. Proximally and distally the spore exhibits a very fine, densely packed isodiametric micrornament, 0.2µm high and wide, rounded in plan and profile. The proximal structure of the spores is not well demonstrated, but they appear to be proximally hilate, although some invaginations of the crassitude may suggest that a trilete mark was present, but these are not exhibited in all of the spores.

Comparisons: These spores are tentatively comparable to spores of the dispersed *Laevolancis divellomedium – plicata* complex, but (1) the lack of a positive identification of the proximal face, and (2) the ubiquitous microrname nt may distance these spores from that complex. Considering the latter, comparable diminutive sculpture was described on 'Group B' *L. divellomedium* spores by Wellman *et al*. (1998b) from the Přídolí Ludford Lane assemblage. It is also interesting to note that those specimens, and also specimens belonging to groups C and E, also exhibited extra-exosporal material (EEM), which may be seen on ABM5014-010. On this specimen, the small globules which are irregularly distributed and often coalesced into dense groups are interpreted as EEM, being consistent in size and habit with descriptions elsewhere (e.g. Edwards *et al*., 1995c; Wellman *et al*., 1998b). The encompassing acellular layer is interpreted here as a probable microbial or fungal layer.

ABM5023-003: *Laevolancis divellomedium-plicata* cf. group A in an oval spore mass

Plate II figures a – e

SEM observations: An oval spore mass, 838μm wide x 1087μm in length. The spore mass is compressed but some apparent topography remains. No sporangial wall cells or structures are seen, and no subtending axis is present. The edges of the spore mass appear to be largely continuous and unbroken, suggesting that shape may be comparable to the gross sporangial shape; however, it is uncertain if this is a plan view or lateral view of the mass. Small sections of cracked acellular material are present across the spore mass, but it is not as widespread as in other specimens. Abundant *in situ* spores are observable.

In situ spores: Spores show good levels of preservation. Although few are intensely folded, most are folded to some degree. Most of the *in situ* spores show small amounts of pitting and some are torn or cracked. The spores themselves have circular to subcircular ambs and are 16 (20) 22μm in diameter. They are proximally and distally laevigate. The hilum is often folded or torn, whilst the distal hemisphere remains more rigid. In some cases, folding simulates a triradiate mark but no laesurae are seen and no evidence of invaginations are present in spores where the proximal face has been lost, which may indicate the presence of a Y-mark.

Comparisons with the dispersed spore record: The *in situ* spores in this specimen are generally comparable to spores of the *L. divellomedium – plicata* complex, except for the holes or pores developed in the exine. Wellman *et al*. (1998b) reported redolent structures from *in situ L. divellomedium* type A from Ludford Lane, also from discoidal sporangia. The spores there were described as bevelled, having an inner, concentric step within the larger, outer hole. Such bevelled pores are exhibited in some cases in this specimen, also. Here, they occur in slightly lower densities (0 – 6 per spore), which is concordant with those of Wellman *et al*. (1998b), where 0 – 13 are observed per spore. The pores in ABM5023-003 are also comparable in size and distribution to the Ludford Lane specimens. Although rare, such spores have also been reported in the dispersed record of the M50, from lower MN assemblages (Chapter III Plate XVI, fig. g), and hence it remains possible that these bevelled pores are a feature of this particular group of *L. divellomedium* rather than a decay feature. The presence of this spore mass and dispersed spores may indicate the continuation of the 'type A' lineage, that is, the persistence of diminutive plants with discoidal, probably terminal, sporangia producing type A *L. divellomedium* spores with distinct, bevelled pores. Whilst this is plausible, TEM analysis on the M50 specimens is necessary to confirm an ultrastructural relationship.

M50DE98-001: *Laevolancis divellomedium-plicata* in a fragmentary spore mass

Plate II figures f – h

SEM observations: The spore mass is roughly cylindrical in shape, being 810μm long x 360μm at the widest point; the mass has some topography but is generally flattened. No cellular remains are found on the mass and no subtending axis is seen. No indication of the original shape of the spore mass remains. A small area of acellular material is exhibited on one end of the mass. Some fine cracks are seen across the spore mass.

In situ spores: in situ spores are exhibited across much of the surface of the spore mass. Many of the spores in the 'interior' of the spore mass show high degrees of cracking and pitting; this may in part be remnants of an acellular layer which is tightly adherent to the spores. Spores along the edges of the mass are better preserved, although most are folded and pitted, and some are torn and/or cracked, especially on proximal surfaces. The spores are hilate, with circular ambs 41 (44) 50μm. They are proximally and distally microgranulate, with granules always <1μm, are irregularly sized and ornamented and tightly spaced. Some EEM may also be present.

Comparisons with the dispersed spore record: The spores here are generally comparable to *L. divellomedium*, although the irregular micrornament and/ or EEM would distance the spores somewhat from that species (but see comparison section of ABM5014-010).

M50DE98-003: *Laevolancis divellomedium-plicata* in a circular spore mass

Plate II figures i – l

SEM observations: Spore mass is approximately circular in shape, being 1256µm long x 1000µm wide. The edges of the spore mass are all ragged and fragmented. No cellular material is preserved, and no subtending axis is seen. Some areas of the spore mass are covered by discontinuous, pitted, torn, acellular layer. In between *in situ* spores (below) is an irregular, amorphous material which interdigitates the *in situ* spores.

In situ spores: Spores are generally well preserved, although are often affected by the interdigitating material. Small spherical bodies are scattered across the spores as well, although in very low proportions. Spores are generally folded with small amounts of pitting. Tearing is present on some of the spores, especially proximally, and some internal pyritisation occurs in some specimens. The spore ambs are circular to subtriangular, between 27 (30) 33µm. They are proximally hilate, with the hilum being concave and often folded. The spores are proximally and distally laevigate and are show folding across the exine.

Comparisons with the dispersed spore record: The approximate shape of the spore mass is reminiscent of ABM50-23 (fig. 8). The *in situ* spores are comparable to the *Laevolancis divellomedium – plicata* complex in terms of size and morphology. They are most comparable to the *L. plicata* end member of that complex, as they exhibit folded proximal and distal exines and narrow crassitudes.

ABM5027-001: *Laevolancis divellomedium – plicata* cf. group A in a fragmented spore mass

Plate II figures m – p

Spore mass: The spore mass is poorly preserved. Although some semblance of an original oval morphology may be discerned along one edge, the other edge is cracked and angular and hence precludes confident assessment of the original morphology. The mass is 746µm long and 517µm at its widest point. Some three-dimensional topography is retained although the specimen is largely compressed. No cellular detail is retained and no subtending axis is observed. Some elements of folded, pitted and loosely adherent acellular material is seen in patches across the spore mass.

In situ spores: Spores are well preserved, although typically folded. The spores have circular ambs, 19 (24) 27µm. Proximally, spores are laevigate. The crassitude enclosing the hilum is *c.* 1µm wide. Equatorial and distal exine is also laevigate. Many, but not all, of the spores exhibit, proximally and distally, unevenly distributed pits, which appear to only penetrate the exine in which they are observed (i.e. distal pits only penetrate the distal exine). The pits are circular to oval (although the latter may be a function of deformation) and are 1 – 1.5µm wide. The pits are bevelled, with an internal 'step' 0.2µm in from the edge of the outer pit.

Comparisons with the dispersed spore record: The entirely laevigate, hilate cryptospores are comparable to the *Laevolancis divellomedium – plicata* complex. Wellman et al. (1998b) described a 'group' of *in situ Laevolancis* spores, group A, with bevelled pits. It is possible that these spores are comparable to that group but see the section 5.2. Nonetheless, these *L. divellomedium – plicata* spores are tentatively referred to as *Laevolancis divellomedium – plicata* cf. group A. These *Laevolancis* spores may therefore also be comparable with ABM5023-003.

ABM5029-001: *Laevolancis ?plicata* in a decayed, fragmentary spore mass

Plate III, figures a – c

Spore mass: The spore mass is pear shaped, 653µm long with a distinctly wide, curved top measuring 646µm at the widest point. This tapers sharply to 154µm at the base. The edges of the spore mass are ragged and in some cases are obviously broken. The narrower portion distinctly tapers away from the spore mass and may represent the upper portion of a subtending axis. On tilting of the specimen under SEM, no axial anatomy or structure was discernible. No sporangial cell walls have been preserved on the spore mass. Across the surface of the spore mass amorphous, irregular, acellular material adheres to the surface. This layer is chaotic, and interdigitating banded and smooth tubes are observed throughout. The tubes are discontinuous, measuring between 17 - 163µm long and 10 - 16µm wide.

In situ spores: Spores are relatively well preserved with minimal folding, tearing or pitting, but are affected by minerals and amorphous material which sometimes cluster on the exine. This is not interpreted as EES. Spore ambs are circular, measuring 24µm. The proximal face is marked by a crassitude 2µm wide; the proximal hilum is concave, lightly folded and laevigate. Equatorially and distally, the exine is laevigate.

Comparisons with the dispersed spore record: The limited selection of observable *in situ* spores precludes confident assignment of the *in situ* spores, but those available specimens allow tentative assignment. The entirely laevigate spore with a circular, smooth proximal hilum suggests a relationship with *Laevolancis*, and the delicate structure of the spores is reminiscent of *L. plicata*.

ABM5032-001: *Cymbohilates allenii* var. *allenii* in a fragmented spore mass

Plate III figures d – f

SEM: Fragmentary spore mass, 620µm long by 540µm wide. The mass is compressed, showing little three-dimensional topography. The edges of the mass are ragged and angular, and no remnants of sporangial wall cells or a subtending axis are observed. In some areas, a continuous, sometimes folded, pitted or torn acellular limiting layer adheres to the spore mass. Numerous *in situ* spores are observed.

In situ spores: Spores are well preserved, sometimes showing folding and some pitting but pyritisation and tearing are minimal. Spores have circular ambs, 19 (20) 21µm. Proximally, the spores are laevigate and concave. The hilum is gently folded and sometimes torn. Distally and equatorially ornamented with equidimensional micrograna and some microconi, which are sometimes biform. Elements have a basal with of 0.4µm and a maximum height of 0.3µm. Elements are very dense, being 0.06 - 0.4µm apart, and irregularly arranged.

Comparisons with the dispersed spore record: The very densely packed distal and equatorial ornament of the *in situ* spores is comparable to *C. allenii* var. *allenii* Richardson (1996) (Chapter III, Plate XI fig. m) in dimension, distribution and morphology. Similarly, the amb diameters of these spores corresponds well to that species variant. As such, these spores are confidently related to dispersed *C. allenii* var. *allenii* spores.

ABM5014-006: *Hispanaediscus* cf. *verrucatus* in a circular spore mass

Plate III figures g - i

Spore mass: The spore mass is sub-circular in plan, with one edge broken away. The sporangium is 683µm long, with a width of 666µm. The mass is concave, but it is not certain if this is a function of folding or an indication of the sporangial structure. The spore mass lacks any subtending axis, sporangial walls or cellular remains and is hence incomplete. In some areas, the spore mass is covered by an acellular layer, which is patchy and often pitted and cracked in places. Much of the spore mass is unobscured, however, revealing numerous *in situ* spores.

In situ spores: Preservation of these *in situ* spores is good. Some minor tearing, cracking and folding has occurred, but this does little to obscure the spore structure or ornament. Furthermore, little extracellular

material is present which might obscure the spore structure. Spores are small, having circular to sub-circular ambs 12 (16) 24µm. Proximally, the spores have a laevigate hilum, which is often lightly folded or slightly torn. Equatorially, the spore is laevigate. Confined to the distal hemisphere are distinct, verrucate elements which may be discrete, subcircular bodies up to 4µm wide, or drawn out into straight or curved ridges up to 10µm long and 4µm wide. Verrucae are often coalesced, and are very closely packed, <1µm apart. All spores are exhibited as individual monads; no dyads are seen.

Comparisons with the dispersed spore record: These hilate cryptospores with verrucate sculpture on the distal hemisphere places these *in situ* spores into the cryptospore genus *Hispanaediscus* Cramer (1966). The distal verrucae, which coalesce to form muri, are similar to the descriptions given for *H. verrucatus* specimens by Burgess and Richardson (1991) (Chapter III, Plate XXI, figures e – f). However, in that species the verrucae do tend to be more discrete. These *in situ* spores are therefore referred to as *H.* cf. *verrucatus*.

4.2.2. *Trilete spore bearing sporangia and spore masses*

ABM5014-004: *Ambitisporites* cf. *avitus – dilutus* in a hemisphaerical spore mass

Plate III figures j - m

Spore mass: Compressed, with approximately oblong, rounded edges and having a wide, rounded edge which gently tapers towards a flatter edge with narrower sides (± hemisphaerical). The sporangium appears to be relatively complete, although the narrower (basal?) half appears to have been damaged, exposing internal *in situ* spores. The narrow end may also be damaged, and no subtending axis is seen. The spore mass measures 983µm long by 565µm wide. A limiting layer appears to be present, variously lying across the surface and obscuring the sporangial contents. The limiting layer lacks structure and is acellular. The layer also appears to be slightly decayed, exhibiting an irregular pattern.

In situ spores: In situ spores numerous where the acellular limiting layer affords a view of them. Spore ambs are roundly sub-triangular to subcircular, measuring 16 (18) 20µm. They are generally well preserved, although some folding, occasional proximal face loss and pitting is present in some. Some limited, chiefly amorphous, but sometimes spherical, extraneous material is sparsely distributed across the surface of many of the *in situ* spores, but it does not seriously obscure them. The spores themselves have a proximally and distally laevigate exine. The triradiate mark is relatively distinct, accompanied by narrow, low lips, which extend very near to the equator. A thin, relatively indistinct equatorial crassitude is seen in most specimens, and is best observed in folded examples.

Comparisons with the dispersed spore record: These crassitate laevigate trilete spores are most comparable to *Ambitisporites* Hoffmeister (1959). These spores may also be comparable to spores of the *Ambitisporites avitus – dilutus* complex (Chapter III, Plate IV, figures d – e) although the amb diameter of those spores do not typically measure below 20µm. *A. avitus – dilutus* spores exhibit a variety of amb shapes and may lack lips, with some dispersed specimens being similar to those found *in situ*. As such, these *in situ* spores are tentatively related to the *A. avitus – dilutus* complex, but due to the differences are referred to as *A.* cf. *avitus – dilutus*.

ABM5020-001: ?*Ambitisporites* cf. sp. A in an elongate spore mass

Plate IV figures a - c

SEM observations: The spore mass is elongate and slightly tapering, being 1730µm long by 500µm wide. The spore mass does not exhibit any sporangial wall remnants or cells, but a highly folded, pitted and

'patchy' acellular membrane encompasses much of the spore mass. The spore mass has been mounted in a diluted PVA mixture which has softened the edges of the spore mass.

In situ spores: This spore mass yields a mixture of partially separated trilete spore tetrads and individual trilete monads. All of the spore tetrads and monads are proximally and distally laevigate. The tetrads generally have convex distal hemispheres with distinct lines of attachment between the spore-units. Occasionally, the distal hemispheres of the spore units are concave, presumably a result of collapse. Spore tetrads measure 36 (37) 38µm, while individual trilete monads measure 25 (26) 28. Where visible, the proximal faces of the *in situ* spores are laevigate, with robust crassitudes up to 2µm wide, and robust lips which accompany the trilete mark, up to 2µm wide. Associated and partially associated trilete spore tetrads dominate the contents of the spore mass.

Comparisons with the dispersed spore record: Individual trilete spores, and those where the proximal face is visible, are comparable to *Ambitisporites* sp. A *sensu* Wellman and Richardson (1996) (Chapter III, Plate IV, fig. j) because of the wide lips accompanying the triradiate mark, which distinguishes the species from other species of *Ambitisporites*. However, the crassitude of the *in situ* spores here are somewhat wider than those typical of *A.* sp. A, and therefore they are referred to as *Ambitisporites* cf. sp. A. These spores are not considered patinate, despite the width of the crassitude, because no concentric fold is observed about the proximal face.

ABM5027-004 *Ambitisporites avitus – dilutus* in an oval spore mass

Plate IV figures d – f

Spore mass: The spore mass is elongate, tapering towards one end and expanding out to form an approximately circular edge across one side. The mass is 832µm long, 608µm at the widest point and 252µm at the narrowest point. The spore mass is compressed, although some three-dimensional structure is retained. Across large areas of the spore mass there is a robust, albeit cracked, acellular layer which appears to be variously adherent. Where this layer is lost, *in situ* spores are exposed.

In situ spores: Spores are reasonably well preserved, with some folding and pitting affecting them. In some cases, the spores have lost the proximal face. They are often at least partially obscured by an interdigitating amorphous material which is prevalent throughout the mass. The spores have circular to sub-triangular ambs, measuring between 22 (24) 27µm. Proximally, the spores exhibit a narrow crassitude <1.5µm wide which delimits the contact area. The triradiate mark is distinct on those spores which have retained the proximal face and is accompanied by lips 1µm wide; these extend to the inner edge of the crassitude. The equatorial and distal exine is laevigate.

Comparisons with the dispersed spore record: These *in situ* spores are most comparable to the dispersed *Ambitisporites avitus – dilutus* complex. These *in situ* spores are probably closest to the *dilutus* end member of that complex, given the weakly defined equatorial crassitude.

M50DE98-004: *Ambitisporites* cf. sp. 1 in an oval spore mass

Plate IV figures g – j

SEM observations: This small spore mass is oval, measuring 354µm wide by 600µm long. The mass is flattened, with limited topography. The edges of the spore mass are broken and irregular, exposing numerous *in situ* spores. There is a semi-continuous, incomplete (possibly decayed) acellular layer covering much of the 'interior' surface of the spore mass, which shows folding, pitting and tearing across its entirety.

In situ spores: The spores show reasonable preservation but are generally mildly pitted, folded and torn in some places, with pyritisation in some specimens and sparse, extraneous material variously coating the spore exines. The gross morphology of the spores remains readily observable, however – although often

the proximal face is damaged or absent. Ambs are circular to rarely roundly subtriangular and are typically 16 (20) 23µm. Proximally, the spores are laevigate with a distinct crassitude up to 4µm wide. The triradiate mark is distinct (although laesurae are not seen), and this extends to the inner edge of the crassitude. In some cases, the triradiate mark is accompanied by lips (<2µm), although in some specimens lips are not observed. Equatorial and distally the spores are laevigate. Extraneous material is sometimes spherical but is more often amorphous or crystalline and may therefore not be biological.

Comparisons with the dispersed spore record: These crassitate trilete spores are comparable to the dispersed spore genus *Ambitisporites*, in that they are proximally and distally laevigate. Based on the amb size and general features, these spores could be comparable to spores of the *A. avitus – dilutus* complex *sensu* Steemans et al. (2009). However, the crassitude is too wide to reasonably assign these spores into that complex. Some other species of *Ambitisporites* found throughout the assemblages exhibit crassitudes of similar width, up to 3.8µm wide, such as *Ambitisporites* sp. (Chapter III). *A.* sp. 1 also exhibits similarly wide lips. However, *A.* sp. 1 is not found in lower MN dispersed assemblages, and furthermore the amb size has not been measured below 20µm in the dispersed record. These spores are not considered to be *Archaeozonotriletes chulus* var. *nanus* (Cramer) Richardson and Lister (1969) (Chapter III, Plate VII, figures h – i), despite the width of the crassitude, because no concentric fold around the proximal face is exhibited. The *in situ* spores are therefore tentatively referred to as *Ambitisporites* cf. sp. 1.

M50DE98-005: *Ambitisporites* cf. *avitus - dilutus* in a circular spore mass

Plate IV figures k - m

Spore mass: The spore mass is approximately oval, being 590µm long and 466µm wide. The mass is compressed, with little three-dimensional structure. No sporangial cell walls are preserved, and no subtending axis is seen. The edges of the spore mass are faintly ragged indicating some breakage and loss of material. A folded, torn and variously adherent acellular layer is observed across much of the spore mass.

In situ spores: Numerous *in situ* spores are preserved. They are generally well preserved but are typically relatively heavily folded. The spores have circular ambs, 12 (15) 18µm and are crassitate. The proximal faces of the spores are difficult to discern and appear to be often lost. In some cases, a triradiate mark can be discerned further qualification was not forthcoming; in specimens where no proximal face is seen, invaginations marking a triradiate mark appear to be present, suggesting that the proximal face has been lost. Representative crassitudes are equally difficult to discern, but they do not appear to exceed 1.5µm. Proximally and distally, the spores are laevigate.

Comparisons with the dispersed spore record. Given the size of the amb diameter and narrow crassitude, these *in situ* spores are comparable to the dispersed species *A. avitus - dilutus*.

ABM5021-001: *Scylaspora* sp. 1 in an elongate spore mass

Plate V figures a – e

SEM observations: The spore mass is narrow and elongate, being 1857µm long and 500µm wide. The spore mass is flattened but retains some topography. The edges of the spore mass are softened due to slight encompassing by the PVA mounting fluid. The spore mass is generally incomplete despite probably retaining its more or less original shape; no sporangial cells are exhibited, and no subtending axis is seen. Across the spore mass, a discontinuous, acellular layer variously covers the surface This layer is ragged and pitted, and is often folded or broken away entirely, revealing *in situ* spores.

In situ spores: The spores are folded, pitted and in some cases show pyritisation. Extraneous material also coats the spores in most cases, obscuring certain details. In some specimens, sculpture appears to have been lost or damaged. The spores have subcircular to subtriangular ambs, 25 (26) 28 Proximally, the spores show

a fine micro-reticulum in the interadial areas which halts at the inner edge of the narrow crassitude. The triradiate mark is distinct, with narrow lips 1μm wide; these diverge at the inner edge of the crassitude and no laesurae are seen. Equatorially and distally the spores are laevigate. Extraneous material is amorphous and ragged, sometimes forming small spheres.

Comparisons with the dispersed spore record: The *in situ* spores and spore mass morphology is similar to *in situ Scylaspora* sp. specimens described by Wellman (1999), in that they have a delicate micro-reticulum on the proximal face and a laevigate distal hemisphere, in addition to similar amb diameters. The elongate morphology of Wellman's (1999) specimens are reflected in ABM5021-001, and while the former are up to 4800μm long, the widths are very similar especially in those with a similar length to ABM5021-001, although Wellman (1999) posited that the sporangia could be up to 850μm wide. The *in situ* spores also compare well with *Scylaspora* sp. 1 (Chapter III, Plate VI, fig. e) in terms of morphology and amb diameter, which are 21(24)30μm. Those spores occur in the lower MN also and may have been produced by similar plants. Confident association between Wellman's (1999) *in situ Scylaspora*, dispersed *Scylaspora* sp. 1 spores and ABM5021-001 requires further ultrastructural examination.

ABM5023-001: *Aneurospora* cf. *trilabiata* in a circular spore mass

Plate V figures f - i

Spore mass: The spore mass is approximately circular in plan, being 682 x 713μm. The spore mass is thin and appears to have been compressed, although some topography and general structure remains. This spore mass was mounted in thinned PVA and this appears to have slightly obscured the edges of the spore mass. No sporangial cell walls remain, and the spore axis is lost. The spore mass is largely encompassed by the remnants of an ?acellular layer which is folded and ragged, revealing *in situ* spores underneath.

In situ spores: Spores are generally well preserved, with some folding and tearing, but with little effect on the overall structure of the spores. In some specimens, the distal hemisphere appears to have collapsed. The ?acellular layer adheres to some of the spores, and other extracellular material coats the spores as well. In some cases, this prevents proper observation of the spore structure, but generally has little effect. The spores are circular to subcircular, 23 (26) 30μm. Proximal faces are laevigate and slightly concave, and are rarely seen. Equatorially and distally the spores are ornamented with dense, blunt or rounded tipped cones, grana, spinae and tuberculae up to 1μm tall and 0.3μm wide at the base.

Comparisons with the dispersed spore record: The mixture of tuberculae, spinae, coni and grana on the equatorial and distal hemisphere of the spore suggest that the *in situ* spores are similar to *Aneurospora trilabiata* Richardson (2011)(Chapter III, Plate V, figures m – n) however given that the proximal face is not observed, they are referred to here, tentatively, as *A.* cf. *trilabiata*.

ABM5031-003: *?Aneurospora* sp. in an oval mass

Plate V figures j - l

Spore mass: The spore mass is large, with a curved top but otherwise broken edges. The mass has a total length of 652μm and at its widest point is 456μm. Little indication of three-dimensional shape is preserved, with the mass appearing highly compressed. No sporangial cell walls are preserved and no subtending axis is observed. A patchy, closely adherent acellular layer is retained on some areas of the spore mass. Some pitting and cracks are exhibited on this layer, but it does not appear to be as chaotically folded as on other specimens described in this work.

In situ spores: These are abundant across the spore mass and are well preserved, although often folded with rare pitting on the exine. The spores are crassitate, with subcircular to subtriangular ambs 17 (18) 19μm in diameter. Proximally and distally the spores appear to be laevigate, however on closer inspection a very

dense arrangement of hemisphaerical globules, 0.15μm wide, are distributed across both the proximal and distal exine. Proximally, the triradiate mark is indistinct, with narrow lips 0.4μm wide accompany the triradiate mark to the crassitude.

Comparisons with the dispersed spore record: The dense microornament is unlikely to be identifiable during routine light microscopy examination of dispersed spores and would likely be attributed to the *Ambitisporites avitus-dilutus* complex. The micro-ornament itself may not be a sculptural feature and may be alternatively interpreted as extra-exosporal material. Because of the presence of the ?micrornament material, this spore cannot be attributed to *A. avitus – dilutus*, and is posited to relate to an uncertain member of the *Aneurospora* genus.

ABM5014-002: *Aneurospora* sp. in a fragmentary spore mass

Plate VI figures a - d

SEM observations: The spore mass is roundly triangular in outline with an uncertain degree of compression. It is 657μm long and 525μm at its widest point. The specimen is clearly incomplete, likely being a large fragment of a sporangium of uncertain geometry. There is a dearth of limiting material on the spore mass leaving numerous *in situ* spores exposed across the surface and edges.

In situ spores: Spores are generally well preserved, with limited folding and pyritisation. There is negligible amounts of extraneous material on several spores, but this is of little consequence. Spores are subcircular to triangular, 15 (19) 22μm Proximally, the contact faces are laevigate except for three distinct interadial papillae, with one in each interadial area. The trilete mark is distinct with high, narrow lips that extend the inner edge of the narrow, equatorial crassitude. The lips show some variation between specimens, with some being more discrete (0.2μm) whilst others are more membranous and distinct (1.1μm). The spores are distally and equatorially ornamented with unevenly distributed, equidimensional coni 0.6 x 0.6μm, 0.6 – 1.7μm apart, with rare tuberculae.

Comparisons with the dispersed spore record: The general characteristics of the *in situ* spores suggests that they are comparable to the dispersed species *Aneurospora isidori* (Cramer and Diez) Richardson et al. (1984) (Chapter III, Plate V, fig. i). The occurrence of tuberculae is somewhat problematic, however, as this sculpture is not reported on dispersed specimens of *A. isidori*. The mixture of cones and tubercules may be suggestive of *A. trilabiata*, except the lips accompanying the triradiate mark differs considerably from that species. As such, the *in situ* spores are tentatively referred to as *A.* cf. *isidori*.

ABM5028.1-001 ?*Aneurospora* sp. in a circular spore mass

Plate VI figures e - h

Spore mass: This compressed, circular spore mass is 1067μm x 933μm and is approximately circular in plan. The edges of the spore mass are fragmented, and no sporangial wall cells are preserved, and no subtending axis is observed. The spore mass is partially coated with a tightly adherent, patchy and folded acellular layer.

In situ spores: The *in situ* spores in this spore mass vary in terms of (1) extra-exosporal material distribution, and (2) sculpture, of which there appears to be two types exhibited by the specimen. All of the spores have circular to subcircular ambs and are between 18 (21) 24μm. They are all crassitate, trilete spores. Proximally, the spores are laevigate with distinct triradiate marks, which are accompanied by robust lips up to 2μm wide. They extend to the inner edge of the crassitude. In one spore, a tentative hint of an interadial papillae is developed, although it is unclear whether this could be fortuitous pyritisation. Distally, some have well defined micrograna 0.7 wide x 0.5μm tall with little EES; in others the distal ornament is obscured by the densely distributed EES, which sometimes clusters into dense groups. The EES is equidimensional

spherical to sub spherical, <0.5μm wide and tall. It is found on both the proximal and distal hemisphere. In other spores, the apiculate distal ornament is not observed, instead an almost foveolate sculpture is developed. These spores lack EES, with 'lumen' and 'muri' <1μm wide. The disparity between the spore sculpture and EES distribution is puzzling. It may be a result of differential decay, or perhaps parts of the mass were exposed to modern contaminant, although the EES appears to be natural. The sculpture differences could be due to the mass being a coprolite, although this is unlikely as the shape of the mass is inconsistent with those found elsewhere in the Anglo-Welsh Basin, and, on comparison with those specimens, one might expect to find more than two types of spore in a coprolite in addition to interdigitating cuticles and tubes. The sculptural variations could also be a result of decay, where in the 'fovealate' spores, the original sculpture has been lost and the exine has become pitted. Alternatively, this small group of spores may have experienced some failure of sporopollenin deposition during ontogeny which resulted in the final apiculate ornament not developing.

Comparisons with the dispersed spore record: These crassitate, distally apiculate trilete spores are comparable to *Aneurospora*, although further comparison is complicated due to a lack of clear proximal and distal features.

ABM5028-005 *Aneurospora* sp. 7 in a circular spore mass

Plate VI figures i - n

Spore mass: the spore mass is spherical and is partially attached to a flattened piece of ?cuticle, which adheres to the underside of the mass. The small spherical component is 315 x 310μm and exposes abundant *in situ* spores. The ?cuticular fragment to which it adheres has straight sides and measures 456μm across. Whilst the spore mass may be fortuitously laid on top of the cuticular fragment, it should be noted that the mass was picked as a single piece and placed on the carbon stub separate to any other fragments. Furthermore, similar cuticular layers are associated with other spore masses from this assemblage. The spherical spore mass is devoid of any limiting layer, exposing numerous *in situ* spores. The cuticular fragment appears bilayered; exhibiting an inner, cracked acellular layer which contacts the spherical spore mass. The outer layer is more complex, showing regularly sized (*c.* 20 x 20μm) polygonal regions, marked by regular, continuous ridges. These ridges appear to map out the remnant cellular structure of the sporangium where the inner periclinal cells walls have been lost. The inner 'laevigate' layer is interpreted as the inner periclinal cell walls; no subtending axis is identified.

In situ spores: The *in situ* spores are very well preserved, showing little folding and no tearing or decay. The spores are small, having subcircular to subtriangular ambs, measuring 12 (14) 18μm. Proximally, the spores are laevigate with distinct triradiate marks which are accompanied by narrow, tapering lips which extend to the crassitude. The lips are 1μm at the inner edge of the crassitude and taper to 0.2μm near the proximal pole. Equatorially and distally, the spores are ornamented with distinctive, densely arranged micrograna and microconi. Elements are typically 0.6μm tall, and between 0.5 - 1μm wide at the base, typically 0.2μm or less between elements.

Comparisons with the dispersed spore record: These spores are most comparable to *Aneurospora* sp. 7 (Chapter III). This is based on the small amb diameter, which is between 18 - 19μm in the dispersed record, and the dense, isodiametric microconi with rounded tips. Proximally, the spores are also similar with indistinct trilete marks and laevigate proximal faces.

ABM5029-002 *?Streelispora newportensis* in a fragmentary spore mass

Plate VII figures a - e

Spore mass: This small, fragmentary spore mass is heavily compressed, measuring 540 x 440µm. The edges are ragged and irregularly shaped. No sporangial wall cells are preserved and no subtending axis is observed. No acellular limiting material is observed.

In situ spores: The spores are often folded and are sometimes partially obscured by EES and amorphous material. Spores have subcircular to triangular ambs, 21 (26) 30µm. Proximally, the spores are laevigate except for interadial papillae in each contact area. The proximal face is disrupted by gentle folds which may betray a bilayered proximal face. The triradiate mark is distinct, and is accompanied by lips <1.5µm wide. The equatorial crassitude is distinct, being 2.2µm wide. Distally and equatorially, the spores are ornamented with distinct, blunt tipped spinae (which may verge on tuberculae in some cases) 0.6 – 0.8µm tall and 0.3µm wide. Elements in some spores appear to be coalesced into small ridges.

Comparisons with the dispersed spore record: Microgranules of small spheres may indicate sporopollenin deposition, that is, spore sculpture in development and hence a level of immaturity. Nonetheless, the proximal features, including tangential folds, and distal ornament of cones and rare tuberculae, facilitate the comparison of this spore into *Streelispora newportensis* (Chaloner and Streel) Richardson and Lister (1969) (Plate VI, figures h - i) with confidence.

M50DE98-002: *Emphanisporites* sp. in an elongate spore mass

Plate VII figures f – k

Spore mass: The spore mass in elongate, being 1,400µm in length and 500µm at the widest end; a slight tapering is observed, narrowing the spore mass to 200µm. The spore mass exhibits a very small amount of acellular layer along one edge. No sporangial cell wall remains, nor is a subtending axis seen. Numerous, well preserved *in situ* spores are exposed.

In situ spores: The spores are well preserved, with minor folding present and sometimes intense pitting and tearing. Pyritisation has affected the exines in some cases, also. Extraneous material is variously present on the spores, generally amorphous or 'raft'-like. The spores have circular to subtriangular ambs, between 18 (21) 25µm. Proximally, the spores show well developed curvaturae perfectae with distinct invaginations at the radial area. The curvaturae are wholly exhibited on the proximal face and do not contact the equator. The triradiate mark is distinct, with lips 1µm wide sometimes exhibited, or folds accompanying the triradiate mark. In other cases, no lips are seen, with regions of typically randomly orientated ?muri forming a fine reticulum which approximately follows the position of the triradiate mark. Interadial muri are distinct. They sometimes taper, never bifurcate and extend from the inner edge of the curvaturae to near the proximal pole, becoming confluent with the approximately tangential? reticulum about the triradiate mark. The proximal face is slightly concave. The spores are equatorially and distally laevigate.

Comparisons with the dispersed spore record: The *in situ* spores are highly distinctive and represent the third species of *Emphanisporites* McGregor (1961) to be found *in situ* in this assemblage, the other two being *E. epicautus/ E.* cf. *epicautus* and *E.* sp. (Ball and Taylor, 2022). Superficially, they may resemble *E. epicautus*, but the apical and Y-ray thickenings are not present here and *E. epicautus* does not exhibit sinuous muri which become chaotic towards the proximal pole. Several specimens of *Emphanisporites* spp. in the lower MN dispersed record of the M50 correspond reasonably well with these *in situ* spores in terms of gross morphology and amb diameter, but in those specimens the curvaturae perfectae extend to the equator, while in these *in situ* specimens, in most cases the curvaturae perfectae are subequatorial, extending up to ¾ of the radius of the spore, however they may extend to the equator. The most striking resemblance between these spores and similar dispersed examples is the sinuous interadial muri which extend to near the proximal pole before becoming chaotic to form a fine mural network. These spores are very rare in the dispersed spore record.

ABM5032-002 *?Emphanisporites* sp. in a circular spore mass

Plate VIII figures l - p

Spore mass: The spore mass is circular. Some topography is retained although the mass appears to be flattened. The mass is 310µm long x 337µm wide. The sometimes angular edges and small size hint that the spore mass was larger in life, and the dearth of sporangial wall cells or a subtending axis indicate that this specimen is incomplete. Much of the spore mass is coated in a patchy, folded and closely adherent acellular layer which obscures much of the internals of the spore mass. Small gaps occur, allowing observation of the *in situ* spores.

In situ spores: Small spores with subcircular to subtriangular ambs, 12 (13)14µm in diameter (four spores measured). Proximally, the spores appear to have a distinct triradiate mark which is accompanied by thick lips, 1µm wide extending to the inner edge of the crassitude. Interadial areas are ornamented by 3 – 4 robust interadial muri, tapering from 1µm at the equator towards the proximal pole. The proximal face is marked by a narrow crassitude and the inception of spinose sculpture. These spines encompass the equator and distal hemisphere of the spore, they are dense and irregularly arranged. They are sometimes biform, with blunt to sharp tips, and are rounded in plan. They are <0.5µm tall and typically <2.5µm wide at the base. Sometimes the spines are coalesced or disrupted by some extra-exosporal material. This appears as spheres or oblong globules, sparsely distributed across the proximal and distal hemispheres of the spores.

Comparisons with the dispersed spore record: In terms of the *in situ* spores, two examples have been found in the dispersed spore record from the Earliest Lochkovian NTPA zone and from the Early Lochkovian lower MN subzone, but are otherwise extremely rare and have not been formally described in this work.

ABM5027-006 *?Stellatispora inframurinatus* cf. var. *inframurinatus* in an elongate ?spore mass

Plate VIII figures a – d

Spore mass: The spore mass is fragmentary, with irregular, angular edges and sites where large portions of the mass have been cleaved off. The mass is elongate, measuring 936µm long and 331µm wide. Some three-dimensional shape is retained although the spore mass is largely compressed. No sporangial cell walls or subtending axis is retained. No acellular limiting layer is exhibited on this spore mass.

In situ spores: Spores are well preserved, showing limited folding and scattered extraneous material, although this is not interpreted as EES. Some pyritisation and pitting is also present, although this is minimal. The spores have subcircular to triangular ambs, 19 (21) 22µm. Proximally, spores are laevigate, with distinctive triradiate marks accompanied by narrow lips 0.1 – 0.5µm wide. The lips extend to the equator. The proximal exine is often disrupted by radial folds which simulate inter-radial muri, but these are not exhibited on all the specimens, and are irregular on specimens on which they are found. Sometimes, the proximal face has sunk, and the distal ornament is impressed onto the proximal face. Distally, the exine sculptured with robust, often elongate, and tightly packed radial verrucae. Verrucae may anastomose and rarely bifurcate, and very few discrete elements exist. Verrucae are typically between 2.1 – 7.9µm long and 0.7 – 1.1µm wide. These verrucae often extend to, and are exhibited on, the equator. In plan, they are rounded and do not exceed 0.5µm tall.

Comparisons with the dispersed spore record: The *in situ* spores compare well in terms of morphology and amb diameter with examples of *Stellatispora inframurinatus* cf. var. *inframurinatus* (Chapter III, Plate IX, fig. c) which measure between 20(26)36µm. These specimens are chiefly present in the NTPA and lower MN subzone of the M50 and differ from older *S. inframurinata* var. *inframurinatus* Burgess and Richardson (1995) (Chapter III, Plate IX, fig. a) Ludlow – earliest Přídolí, Rumney-1 and Usk-1 boreholes) proper as they are smaller with an apparently more robust proximal face.

ABM5031-001: Circular spore mass

Plate VIII figures e - h

Spore mass: The spore mass is circular in plan, and despite compression the mass appears to have a hemispherical three-dimensional structure with an apparently slightly concave region towards the centre. The mass is small, being 336μm x 347μm. The edges are generally smooth although are fragmented and ragged in some areas. No sporangial cell walls are preserved, and no subtending axis is seen. The entire spore mass is covered by a tightly adherent, acellular layer which is entirely cracked and folded. Towards the centre of the spore mass, the layer appears to exhibit radial folds which converge towards the centre of the mass. Because of the extent of this layer, very few *in situ* spores are preserved.

Comparisons with the dispersed record: The absence of clear *in situ* spores precludes assignment of this spore mass. The only observable spore may be fortuitously associated with the spore mass (i.e. not biologically associated). It is of interest that some of the features of the spore mass, including the discoidal shape, acellular cuticular layer and radial folds are redolent of *Paracooksonia* Morris et al. (2011b), although a firm assignment is not made.

4.2.3. M50 Axes, phytodebris and coprolites

ABM5027-007: Stomatate fertile eophyte axis

Plate VIII figures i - l

Description: Fragmentary specimen representing the base of a sporangium attached to a short length of axis. Stomata are clustered around the base of the sporangium. The axis section is 857μm long, 223μm wide. It is somewhat jagged along the edges where some of the axis has likely been broken away from the specimen, and the base of the axis, where the fragment has broken away from the rest of the plant is also fragmented. Along the axis there are some wide pits which are probably a result of decay or transport. In some cases, small fragments of acellular material adhere to the axis, but it is not clear if this is an original feature of the plant. The axis exhibits elongate striations amongst minor folds. These elongate folds and/ or striations are seen on the sporangial base, too. Around the base of the bowl – shaped sporangium are at least five stomata complete with guard cells which are partially open to reveal the stoma; these stomata are 20μm in diameter and are set up to 75μm apart. Observation of the inside of the sporangia did not yield any *in situ* spores.

Comparisons: The morphology of this specimen is very similar to Fertile specimen V 68856 in Edwards *et al*. (2021a) (their Fig. 4, a – c) having the remnants of a bowl-shaped sporangium with stomata clustered about the base, alongside the elongate striations along the axis. The specimens are also similar in size. As such, this specimen is probably an eophyte. Fertile specimen V 68856 was recovered from the mid Lochkovian North Brown Clee Hill section which is interesting as, given the similarities between that specimen and the one shown here from the lower Lochkovian M50, may tentatively suggest some level of morphological stasis in these plants between the lower and mid Lochkovian, although an absence of *in situ* spores precludes direct comparison between the two specimens.

ABM5028-003: ?Sterile eophyte axis

Plate IX figure a

Description: Fragmentary horn-shaped specimen, comprising a short length of axis, 1577μm in length, tapering from 100μm to 422μm wide at the other. The latter end may represent the remnants of a terminal sporangium but this is unclear. Both ends of the axis have been broken away. Much of the axis is enclosed by a tightly adherent acellular layer, which exhibits elongate ridges in the narrower half of the specimen.

Some pits are also exhibited but these are not thought to be anatomical. Towards the wider end of the specimen, the regular ridges are lost and are replaced by largely chaotic folds. No *in situ* spores or axial anatomical information was recovered from this specimen.

Comparisons: The elongate ridges on this specimen are redolent to those seen in the eophytes, and it is probable that the original plant belonged amongst this group. A specimen (Fertile specimen V 68855, fig. 3 f – n) in Edwards *et al*. (2021a) is superficially similar to ABM5028-003 in the 'horn-like' appearance, but the differences in diameter are attributed there to differential compression. It is not clear if the tapering in ABM5028-003 is also due to compression, but certain subtle differences in morphology probably distance this eophyte from ABM5028-003, and a lack of *in situ* spores precludes more direct comparison.

ABM5028-005: Stomatate fertile axis

Plate IX figure b

Description : This specimen comprises a bowl-shaped fragment of a lower sporangium with a subtending axis attached. The axis is *c.* 480µm long, and tapers from 63 - 154µm towards the terminal sporangium. Ridges running parallel to the long axis, to 19µm wide, are clearly observed. These ridges show a small degree of twisting through the axis. The axial – sporangial juncture sees a gradual loss of the elongate ridges, which become more chaotic about the sporangial base before being lost entirely, replaced by chaotic folds. About the base of the sporangium, where the elongate ridges are becoming sinuous, are evenly distributed stomata. These stomata are circular, bearing two hemispherical guard cells and measuring 67µm in diameter. They are only observed about the base of the sporangium. The upper region of the sporangium has been broken away, revealing a hollow internal structure. No *in situ* spores are observed in this specimen.

Comparisons and remarks: This is the second specimen exhibiting stomata arranged about the base of the sporangium (specimen ABM5027-007). However, these specimens differ from one another, notably in terms of the sporangial – axial juncture. In this specimen (ABM5028-005), the juncture is more truncated (*c.* 90°) than in ABM5027-007, where the juncture angle is shallower, *c.* 130°. In addition, elongate cells are visible on the sporangium of the latter, and the axis of ABM5028-005 is narrower. Finally, whilst little remains of the sporangia in both of the specimens, what does remain may suggest that they exhibited different morphologies, although this is equivocal. As such, accepting that taphonomic and possible ontogenetic influence, it is tentatively suggested here that ABM5028-005 and ABM5027-007 were probably derived from at least generically different plants.

Given the parallel, elongate axial ridges and stomata clustered around the sporangial base, it is likely that ABM5028-005 is derived from an eophyte. Indeed, Edwards *et al* (2022) illustrate a specimen from NBCH similar to this (Edwards *et* al. fig. 2, 46) which is placed in Group V.

ABM5028-004: sterile ?valvate axis

Plate IX figure c

Description: This specimen is an elongate, fragmented axial segment with a bifurcation on one end a distinctly tapered middle-section. The fragment is 540µm long and 263µm at the narrowest region, widening to 394µm. At the bifurcating end, the daughter branches are poorly preserved, with only the basal portions preserved. The branches are set 221µm apart, and while the angle at which they branch relative to each other is difficult to gauge, this is *c.* 45° angle to the axis. The base of these branches are 189 - 221µm wide, although some breakage is likely to have occurred.

No internal anatomical structure was accessed in this specimen. The external features are complicated; the entire surface appears to be covered with a tightly adherent, acellular layer which is chaotically folded

across the entire extent of the specimen. In some cases, these 'folds' appear to be developed into elongate ridges (Plate IX fig. c, arrow), but these are far from consistent across the specimen.

Comparisons and remarks: Whist this specimen is poorly preserved, some hints of elongate ridges are present on a portion of the specimen (plate IX fig. c, arrow), and this may tentatively suggest an association with the eophytes but this is far from satisfactory. In addition, several eophytes, including those placed in group III of Edwards *et al*. (2022) exhibit valvate structures on their axes (no. 42, their fig. 2, Edwards et al. 2022), which this specimen could plausibly represent given the upper? bifurcation, tapered middle section and lower bulging region. Nonetheless, a more concrete association for this specimen is not possible.

The branching on this specimen is interesting as if differs from the other branching specimens described below, which have wider branching angles and show little to no tapering in the axial portion. The eophytes exhibit a range of branching angles (Edwards *et al*. 2022), and some exhibit branches separated by a flattened section, in those cases derived from a triangular 'wedge', although that feature is not seen here.

ABM5028-004: ?fertile eophyte axis

Plate IX figures d – h

Description: Fragmentary specimen featuring a short length of slightly curved axis, terminated at one end by a large section of flattened, partially complete material. A biological continuum between the two parts has not been verified. The axis is 817μm in length and 200μm wide. There are small amounts of tightly adherent, acellular material on the axis. Where that material is absent, distinct, elongate continuous ridges are developed, parallel to the axis. These ridges are 10 – 15μm wide and are tightly packed. The nature of the connection between the axis and the flattened material remnants was not fully resolved, but it appears to have been relatively sharp. Upon breaking open and rotation of the axis, some very limited internal anatomical detail can be seen. Much of the anatomy appears to have been compressed and/ or homogenised, but it is clear that discrete, elongate cells populated the axis of the plant. The visible lumen walls do not exhibit any pits, mounds or globules, but this may be a result of homogenisation an subsequent loss of features during burning or fossilisation. The flattened piece is 1264μm wide and 971μm tall, the edges of which are fragmented and broken, sometimes with distinctly angular planes. An interdigitating, smooth tube comparable to those seen under LM and attributed to a *Laevitubulis* sp. is present. On turning over, much of the piece is barren of structure beyond intense folding of the acellular cuticle. However, towards the axis, small, spherical to oval bodies 5 – 10μm wide are set in the cuticle, separated by narrow ridges.

Comparisons and remarks: The elongate ridges on the axis suggest that the plant probably belonged amongst the eophytes, but it is frustrating that little can be gleaned from the internal anatomy of the specimen. As for the flattened material, its associations are less clear. The acellular layering proffers little information towards the affinities, but the small pseudospherical bodies observed upon turning over are somewhat comparable to cortical cells identified in thalli by Edwards *et al*. (2013, their fig. 7). The cortical protrusions there are associated with specimens with similar, tripartite stratified morphologies to *Nematothallus* and *Cosmochlaina*, but with distinctive features of the cortex. Superficially, the cortical protrusions there resemble the pseudospherical bodies found here, but the other features of those thalli are not observed in this specimen. Notably, the palisade layer and weft layer are not present. Furthermore, the lattice network, if present, is not as well defined here.

The most parsimonious explanation is that the flattened region represents a compressed, fragmentary sporangium. No *in situ* spores were identified, but this does not preclude the explanation, as other fertile axes have not yielded *in situ* spores. In this hypothesis, could the spherical bodies be early-stage spore mother cells? This is possible, but bodies similar to this have not been identified in other sporangia as yet.

A less parsimonious hypothesis is that flattened region is the remnants of a gametophytic thallus with the attached basal axis, but further evidence for this interpretation is not forthcoming.

The presence of the ?*Laevitubulis* sp. interdigitating with the fossil suggests that the specimen was partially decayed prior to charcoalification. This points towards a litter of decaying plant matter being present in the environment, which was also subject to burning alongside living plant matter. This has been observed in other mesofossil sites, notably at NBCH in *cf. Horneophyton*, where the sporangium is encased in a crust.

M5026PIN-1: Sterile axis

Plate IX figures j – m

Description: The main length of axis is 776.2µm long and 200µm wide. The base of the axis has been broken away, exposing the internal anatomy. The other end of the axis bifurcates, with secondary axes extending away at a 50˚ angle; this axis is 266µm long and 65µm wide. Opposite this, the remains of the second secondary axis is seen, although this has been broken close to the main axis. The axis comprises numerous elongate ridges and depressed troughs, which are interpreted as elongate cells which have been approximately bisected parallel to the long axis. The cell walls which form the ridges are 2µm in width, whilst the troughs, representing the inside of the cell wall, are 12 – 18µm wide. The cells are approximately square to rectangular in plan. Where the ends of the cells are visible, they exhibit numerous, minute circular to oval holes up to 2.5µm in width. Many of the 'troughs' exhibit numerous circular to elongate-oval pores, also. These features are tightly packed, typically 1µm long. They are not exhibited along the whole length of the cell, nor are they exhibited in every cell. Large 'pores' are visible across the specimen; however these are interpreted to be cells which have been bisected at an angle. Very little evidence for an enclosing layer exists on the specimen, although some smooth, acellular (although heavily cracked) material is visible across the top of the specimen, between the bifurcating secondary axes.

M5026PIN-2: Sterile axis

Plate IX figures n – p

Description: the axis is 2,250µm long and 330µm wide. The main section is straight and dichotomises at one end into unevenly sized axes at an angle of 135˚. The left axis is 190µm wide and 150µm long, whilst the other is 490µm long and 260µm wide. The disparity in axial size is attributed here to preservational effects, rather than being an original feature of the plant. Across the entirety of the specimen are closely spaced elongate ridges which are parallel to the long-axis of the specimen. At the point of axial dichotomy, the elongate ridges bend rather than bifurcate. Upon magnification, the narrower ridges are the prominent cell walls which have been bisected to show the interior walls of cells. The cell walls are *ca.*2µm wide. Internally, the interior lumen wall exhibit ridges which are developed perpendicular to the cell wall, up to 4µm long and <1µm wide. The occur at ± regular intervals at every 2 – 3µm. Also in the cell lumen are hemisphaerical globules distributed randomly, either individually or in small groups. These globules are up to 1µm wide.

Comparisons: The long, bifurcating axis is reminiscent of many of the eophytes reported by Edwards et al . (2022a). In particular, the granules/ globules observed in the lumen of the elongate cells are often observed in the lumen walls of eophytes (Edwards et al 2022a, their table 1 and fig. 3).

DSM501003: Coprolite

Plate X figures a – e

Description: The coprolite is approximately oval in shape and is largely compressed, although retaining some three-dimensional topography. The specimen has a total length of 850µm and a width of 250µm. The

coprolite appears to clinch about the central area, but this may be an artefact of preservation. There is a very small amount of pockmarked and folded acellular material present adhering to the coprolite. The main body of the coprolite comprises numerous spores, which are generally well preserved with at least three types present, *Streelispora newportensis* (Chapter III, Plate VI, figures h - i), *Chelinospora vermiculata* (Chapter III, Plate VIII, figures i – j) and *Aneurospora* spp. The spores are well preserved although some are affected by folding, pitting and minor breakage. Minor amounts of internal pyritisation is observed, also. Small, amorphous to spherical bodies are distributed across the proximal and distal hemispheres of the spores, although they are disparate and only rarely clustered into small groups.

Comparisons and remarks: Coprolites are distinguished from spore masses as they contain more than one spore species or complex, contain interspersed cuticles and sheets, plant debris and tubes. This fossil provides evidence of animal-plant interaction, probably via myriapods (Edwards et al., 1995c). Previous coprolites have been attributed to detritovores (Jeram *et al*., 1990) based on the wide variety of spores incorporated into the coprolite. These were presumably accidentally consumed whilst the animal was feeding on other detritus with more available nutrients (Edwards *et al*. 1995c). The morphology of the coprolites is comparable with other examples.

ABM5014-011: ?Coprolite

Plate X figures f - h

SEM observations: The specimen is elongate, tapering outwards towards one end. At its narrowest, the mass is 100µm, tapering out to 224µm at the widest point. The mass is 624µm long. At the narrower end, the some damage is observable. The edges of the mass are reasonably coherent but still fragmented. No sporangial cells or structure remains; however, an amorphous acellular layer is visible across much of the surface of the sporangium. This layer is largely fragmented but remains tightly adherent. On inspection, there appears to be spores associated with the mass. A variety of sculptures are observed, from densely packed to discrete cones. The proximal faces of the spores are not readily observed, although one small spore may exhibit a triradiate mark. Spores range between 15 (23) 26 µm in diameter, and the mass appears to comprise large fragments of amorphous material. The variation in spores associated with the mass, and association with fragmentary, amorphous material, necessitates caution when interpreting this specimen. It is not considered here to be a spore mass and is instead tentatively referred to as a coprolite.

4.3. Scanning Electron Microscopy (SEM): Mesofossils from Ammons Hill section, Shropshire

MPA25239-4-1: Sporangial cuticle?

Plate XI figures a – b

Description: Semi-circular, flattened, fragment of thin cuticle measuring 1235µm long, 409µm wide and 30µm thick. The specimen exhibits a continuous, circular outer edge and shows some folding, especially towards the inner edge, which is also approximately semi-circular. The surface exhibits a continuous array of ± evenly sized, angular to rounded polygonal structures, 9 – 22µm long, mean 16µm (nineteen measured) and 7 - 13µm wide, mean 9µm (nineteen measured). These are separated by narrow channels, typically 5µm wide and forming a continuous 'reticulum' between the raised polygonal structures. Also across the surface of the specimen are possible perforations, which may rarely extend through the specimen (Plate XI, fig. b, arrows). They do not appear to represent a loss of the polygonal structures, but do not exhibit any associated structures. In general, the cross section is homogenous, but in some cases these structures are hollow, bounded by enclosing walls and extend up to 17µm into the specimen. The cross-sectional wall of

the specimen typically comprises two of these structures stacked on top of one another to give the total thickness of *c.* 30µm.

Comparisons and remarks: It is posited here that the polygonal structures represent cellular structure, given the regularity and consistency across the surface of the specimen. The perforations are more peculiar, especially as in general they do not appear to fully perforate the specimen. It is tempting to suggest that they represent stomata, although no guard cells or additional structures are observed alongside them; nonetheless, they may represent some method of gas exchange. Given the shape of the specimen, it is plausible to suggest that the entire specimen was circular, and hence this specimen might represent a fragment of a basal portion of a terminal sporangium.

MPA25239-4-2: ?Fertile axial fragment

Plate XI fig. c

Description: This small, fragmentary specimen exhibits a slight tapering from a narrow (88µm) axis which exhibits densely packed ridges which are aligned parallel to the long axis of the specimen, into a wider (231µm) portion. The latter section, whilst still exhibiting elongate ridges, also shows wide spaces (20 - 43µm wide) between the ridges, contrasting with the lower, narrower portion of the specimen. The structures appear to widen out of the narrower ridges portion, before converging on one another towards the tip of the specimen. The structures in the wider section are interpreted as elongated, bisected cellular remains. Here, the ridges represent cell walls and the spaces between them represent lumen. Meanwhile, the ridges of the lower section represent the ridged epidermis of the plant (Edwards et al., 2022a, b).

Comparisons and remarks: This sterile axial fragment is peculiar given the contrasting features on the narrow and wide sections of the plant. Here, the difference is interpreted as the transitional juncture between a subtending axis (narrow section) and the basal portion of a fragmented, terminal sporangium. The axial-sporangial junctures of other plants exhibit similar transitions, although typically the ridges become more chaotic into the juncture. The stomatiferous axis ABM5028-005 shows wider cells in the sporangial base relative to the ridges on the axis, but the specimens are otherwise quite different.

The heavily longitudinally ridged axis and diminutive size of the specimen suggests that the plant from which it derives was an eophyte.

MPA25239-1-1: ?Fertile axis

Plate XI figures d – g

Description: This fertile specimen exhibits a short section of twisted axis which tapers outwards into the basal remains of a sporangium. The axial section and lower portion of the sporangium exhibit distinct major and minor longitudinal ridges. The ‘major’ ridges are *c.* 80µm wide, showing some outward tapering towards the sporangial section. These major ridges are separated by equally wide longitudinal furrows, with both appearing to be slightly twisted. This is replicated in the minor ridges. The densely packed minor ridges are 8µm wide and appear in both the major ridges and furrows. On closer inspection, some exhibit rare circular perforations which may represent pores. These ‘pores’ are more regular and differ in shape and regularity to fractures produced by torsion. The upper sporangial section sees the rapid loss of the longitudinal ridges at the putative axial – sporangial junction, where the ridges are replaced by chaotic ridges and folds with numerous perforations. The axial – sporangial junction tapers at a *c.* 50° angle. No stomata are observed about the juncture.

Comparisons and remarks: Similar to fertile group II specimens in Edwards *et al,* (2022), which exhibit axes tapering into distally hollow, funnel-shaped sporangial bases.

The general features of the specimen, particularly the longitudinally arranged minor ridges, suggest a relationship with the eophytes. The major ridges may be a feature peculiar to this plant or could be a result of taphonomy. Likewise, the twisting is probably taphonomic in origin, indicated by the minute torsion-related tears across the specimen. The circular 'pore', if an original feature of the plant, could represent a transfer mechanism to the other axial cells of the plant, although this requires further qualification. Similar putative 'pores' were identified in M50PIN1, although these were generally less circular and were clustered into groups. In this specimen, the circular 'pores' are not a common feature. Similar pits have been observed amongst eophytes (Edwards et al., 2022, plate VI), but again these are typically accompanied by others, often as a continual feature of the inner wall of the cell lumen.

MPA25239-5-3: Sporangial cuticular fragment?

Plate XI figures h – j

Description: This specimen is a fragmentary wedge of cuticle which exhibits interior and exterior features in relation to one another, measuring 638µm from the tip to outer curved edge, and 562µm at the widest point. The exterior features are reminiscent of specimen MPA25239-4-1, in that raised, polygonal to approximately rectangular bodies 9.6 – 25.4µm long, mean 17µm and 3.5 – 5.5µm wide, mean 5.5µm, are separated by channels 2.6µm wide. The raised areas typically exhibit a single or several depressions in the centre of the structure, and these may reflect the shape of the structure or be in repeating patterns of elongate depressions. These external features are generally isolated, separated by the narrow channels, but they are sometimes elongated and may rarely bifurcate and/ or coalesce. The features become more isolated and circular towards the outside edge of the specimen. Turning to the interior features of the specimen, a regular network of approximately polygonal to circular features is observed, comprised of tall, narrow ridges. This reticulum is decayed in places, but it is posited here that it would have been a consistent feature across the interior surface in life. The pronounced ridges are 3 – 5µm wide, mean 4µm and continuous. The lumen the ridges describe are equidimensional to elongate, and measure 17 - 27µm, mean 21µm, in length and 9 - 21µm, mean 17.2µm. Across the internal and external surfaces, semi to fully penetrative pits are observed, but these do not appear to be associated with any specialised structures such as guard cells.

Comparisons and remarks: External – internal feature relationships: it is posited here that the exterior and interior features exhibited on this specimen are both remnants of the cellular construction of the original plant, and that the both interior and exterior features are analogous to one another, but shown in differential relief (i.e., the ridges on the internal surface = the channels on the exterior surface, while the raised cells on the exterior = the lumen on the inner). It is probable that the pits and elongate furrows exhibited on the cells of the exterior represent folding or collapse of the cell wall.

As mentioned, the external cellular structure is comparable to specimen MPA25239-4-1 in terms of gross morphology and dimensions. It has not been ascertained if a similar reticuloid structure is exhibited on the other side of MPA25239-4-1 as it is in this specimen. Furthermore, semi to fully penetrative pits are exhibited on both specimens, and the curved morphology of MPA25239-5-3 is comparable to the curved habit of MPA25239-4-1. Nonetheless, a direct relationship between the two specimens is not made here on the basis of the fragmentary nature of the specimens.

MPA25239-6-1: ?Fertile eophyte axis

Plate XI figures k – l

Description: This fragmentary specimen measures 923µm long, and superficially simulates a single bifurcation, with a small portion of the daughter/ major axis retained (plate XI fig. K, I and II). The striated axis (arrow II) is 340µm wide. The specimen appears to be compressed and flattened, with little three – dimensional structure retained. While charging affects a large portion of the specimen, the portion indicated

by arrow II exhibits longitudinal, tightly packed parallel ridges, and these appear to be lost towards the portion indicated by arrow I, becoming anastomosing and less tightly packed. Indeed, towards the top of the specimen (surface opposite arrow II), the ridges are lost entirely. Around arrow I, then, there is a loss of the tightly packed, longitudinal ridges. From what is preserved, the specimen bends between arrows II and I with a gentle, concave curve at an angle of *c.* 55°. A similar, parallel curve is observed on the other fragmented side of the specimen. This 'widening' and the loss of the longitudinal ridges suggests that the region above the striated axis is the basal remains of a sporangium, with the area indicated by arrow II representing the remains of a subtending axis.

Comparisons and remarks: While the specimen is fragmentary and hence difficult to fully interpret, it is posited here that it represents a fertile eophyte axis, with arrow II representing the subtending axis, and arrow I indicating a broken, basal portion of a terminal sporangium. With the loss of the parallel, elongate ridges towards and around arrow I, the specimen probably does not represent the bifurcating region of a sterile axis, as the ridges would be expected to persist across the specimen. Instead, the ridges are lost towards the base of the putative sporangium (as they are in other eophyte specimens, e.g., plate VIII figuresa – b). The loss of the ridges, in addition to the gentle concave curves which are mirrored on either side of the specimen (most completely demonstrated by the edge between arrows II and I), further support this interpretation. In terms of botanical association, the presence of the parallel, elongate ridges on arrow II, alongside its small width, strongly suggest an association with the eophytes, although further deliberation of affinity is not possible. No stomata are identified about the base of this sporangium. The angular breakage lines suggest that the specimen was damaged post-mortem and post charcoalification.

MPA25239-5-1 & MPA25239-5-3: Pachytheca

Plate XII figures a – b & Plate XII, figure c

Description: Two Pachytheca have been collected from the Ammons Hill section. These measure 2370µm and 1896µm respectively and are typical of Pachytheca specimens. Some damage is present, most notably on MPA25239-5-3, which exhibits radiating minor and major cracks with some internal structure present as a result of these cracks, and as a result of patchy loss of the outer layer. MPA25239-5-1, too, shows some damage, although in this case the damage is restricted to a loss of the outer layers of the specimen, revealing some internal structure. Otherwise, the specimens remain largely intact. Upon closer inspection, MPA25239-5-1 (plate X fig. b) clearly demonstrates a 'honeycomb' structure, which lies just beneath the occasionally lost amorphous outer layer. These internal features comprise raised, continuous ridges, 3µm wide, which together are developed into a continuous reticulum, describing polygonal to sub-rectangular lumen, 8 - 14µm wide, mean 11µm.

Comparisons and remarks: These specimens compare well with descriptions of *Pachytheca* (Hooker, 1853) with their circular shape, size and and smooth surface.

MPA25239-5-2: *?Nematophyte*

Plate XII figure d

Description: This specimen is fragmentary in habit, forming a sharply rectangular shape 2333µm long and 2270µm wide. Some of the sharper corners of the specimen have been rounded, and the surface is generally smooth. Minor to major parallel, perpendicular and anastomosing cracks populate the specimen. The structure is comprised entirely of longitudinally arranged, fine tubes which are of ± equal diameter.

Comparisons and remarks: The affinities of this specimen are uncertain, but the organisation of densely packed tubes may tentatively suggest that it is Nematophytic in origin (*sensu* Lang, 1937). However, because this specimen comprises densely packed, equally sized tubes it is distanced from *Nematosketum*,

and perhaps from *Prototaxites*, also. It may be worth reiterating that the fragment is large and must have been derived from a relatively large organism comprising, at least in part, this dense tubular structure. The specimen may represent a cleaved section of the inner tubes of *Pachytheca*, but the specimen exceeds the dimensions of that fossil *sensu* Hooker (1853).

MPA25239-5-4: *?*Nematophyte

Plate XII figures e – f

Description: This is a sub-rectangular, blocky fragment 1294µm long and 647µm wide. The specimen is populated by rare minor cracks. The specimen comprises elongate, ± evenly sized longitudinally parallel tubes, with a smooth internal wall. Tubes are continuously long (at least 1294µm) and are 8 - 13µm wide, mean 10.7µm. They are straight, and do not anastomose or bifurcate. Widespread, amorphous 'ragged' material adheres to the outer lumen of many of the tubes. While equivocal, an indication that this may be a biological feature rather than a decay or post-depositional feature, is the observation that it is not exhibited on the internal lumen of broken tubes.

Comparisons and remarks: As for MPA25239-5-2, the affinities of this specimen are uncertain, but it may be relatable to the Nematophytes *sensu* Lang (1937).

MPA25239-5-5: *?*Nematophyte

Plate XII figures g – h

Description: This specimen is 1072µm long and 736µm wide and is approximately rectangular, although most of the angular edges have been rounded off. A small section of amorphous, adherent layer remains attached to the surface, which partially obscures the underlying structure on the face of the specimen where it occurs. The underlying structure is visible in several dimensions. In plan view, it comprises abundant, circular perforations up to 21µm apart, and 10.6µm in diameter. In cross section, these pores are clarified as elongate, longitudinally parallel tubes with thick walls and a finely banded internal lumen, which have diameters up to 10.6µm. The tubes are straight and may anastomose, but bifurcation has not been observed.

Comparisons and remarks: As for MPA25239-5-2 and MPA25239-5-4, the affinities of this specimen are uncertain. The tubular structure and smooth outer cuticle may relate the specimen to the Nematophytes *sensu* Lang (1937), or perhaps to *Pachytheca*. The latter is considered less likely given the size.

MPA25239-5-6: *Cosmochlaina*

Plate XII figure i

Description: This wedge-shaped fragment measures 389µm long with a thickness of 150µm and comprises two distinct layers: a thin, outer, cuticular layer and a thicker internal tubular layer. The outer cuticular layer comprises a well-developed reticulum of raised, continuous and often curved ridges, 3 - 4µm wide, which describe polygonal, rounded lumen up to 24µm wide. The ridges comprising the lumen sometimes form pointed 'peaks'. In section, this layer is 8µm thick and exhibits stratified circular to oval voids 3.7 – 6.3µm wide, towards the base of the layer. These voids are separated by amorphous, thick walls. The thicker, inner section contrasts sharply with the thinner upper layer. This comprises elongate, densely packed, longitudinally parallel tubes with a circular, internally and externally smooth walled lumen measuring 4 - 8µm in diameter. These tubes appear to narrow slightly away from the upper cuticular layer, and generally anastomose towards the opposite edge. Bifurcation is not observed in these tubes.

Comparisons and remarks: This specimen compares well with the original descriptions of *Cosmochlaina* Edwards et al. (2013) given the stratified hyphal structure and randomly orientated units bordered by inwardly directed flanges.

MPA25239-4-6: ?cortical *Pachytheca* fragment

Plate XII figure j

Description: This specimen is 1000µm in length and 462µm thick. It shows clear stratification, with a thin, finely perforate layer and thick, inner tubular layer. The former has a maximum thickness of 17µm cross section, and on the surface is hummocky and uneven. In cross section, this surface may show some fine lumen or pores towards the surface, but otherwise the layer appears to be largely homogenous. The surface is populated with minute, ± circular perforations 1 - 2µm in diameter and evenly distributed across the surface, set 3 - 6µm apart. Minor cracks are present across this surface. The thicker layer beneath the porous outer layer is populated by densely packed, longitudinally parallel tubes, with a circular, smooth inner and outer lumen 11 – 12µm in diameter. While the tubes anastomose somewhat away from the outer, perforate, layer, they are not seen to bifurcate.

Comparisons and remarks: This specimen may be related to *Pachytheca* based on the nature of the cuticular fragment and subtending, parallel tubes. The cuticular layer contrasts with that of other *Pachytheca* specimens, but this may be due to damage. The specimen is not thought to compare with *Nematothallus* due to the lack of an inner hyphal layer.

MPA25239-4-6: *Nematothallus – Cosmochlaina complex*

Plate XII figures k – l

Description: This fragmentary specimen measures 752µm in length and is 447µm wide. The specimen is stratified, with an outer layer of chaotically arranged tubes and amorphous material, with which the tubes interdigitate. The tubes in this region are continuous (although their actual length cannot be ascertained given their weaving with one another and the amorphous material) and are 9µm in diameter. Many do not appear to be internally 'hollow' and as such may only superficially resemble tubes (Plate XII, fig k arrow). The thicker, internal layer comprises regularly arranged, longitudinally parallel tubes, which are generally straight but sometimes anastomose and may be twisted. Tubes have internally and externally smooth lumens, with a diameter of 9 - 12µm. As such, they do not differ significantly in diameter to the 'tubes' in the outer layer, although the tubes in this inner layer are typically hollow. They maintain and ± constant diameter throughout the layer.

Comparisons and remarks: Given the stratified hyphal layers this specimen is reminiscent of the *Nematothallus – Cosmochlaina* complex, although without the cuticular layer, the specimen cannot be differentiated further. It is possible that the tubes have been homogenised during burning.

5. Discussion

5.1. Contrasting assemblages and early land plant taphonomy

The most striking difference between the M50 and Ammons Hill mesofossil assemblages is the paucity of sporangia, spore masses or coprolites in the latter (table 1). The absence of these mesofossil types does not indicate a lack of embryophytes in the Ammons Hill area at this time, given that further investigation of the Ammons Hill 'fine fraction' has demonstrated eophyte and ?tracheophyte remains. In addition, the palynology of the site indicates a rich embryophytic flora represented by a suite of 64 species of cryptospores and trilete miospores (Chapter III). Equally, nematophyte cuticles in the dispersed microfossil record of the M50 and elsewhere suggest that these organisms were growing alongside the plants there, too (Chapter III, VII; Wellman and Ball, 2021), but larger mesofossils of this type are excluded from the site.

Locality	*In situ* spores*	Subtending axes**	Sterile axes	Sporangial wall cells	Evidence of saprotrophy	Complete sporangia	Nematophyte mesofossils
M50	✓	×	✓	(✓)	✓	×	✓
NBCH	✓	✓	✓	✓	✓	✓	✓
AH	×	×	✓	×	✓	×	✓

Table V-1: Comparisons in fossil composition between the M50 section (M50), Ammons Hill (AH) and North Brown Clee Hill (NBCH) mesofossil assemblages.

This disparity between Ammons Hill and the M50 is probably largely taphonomic in origin and may have been driven by a number of causes including decay and transport distance, which are briefly reviewed here (fig. 4). A key factor influencing the early land plant fossil record which has been widely discussed is decay (Edwards and Richardson, 2000, 2004; Wellman et al., 2000; Gensel, 2008), with a preservational bias towards plants with recalcitrant tissues; where labile plants lacking resistant tissues are lost to the fossil record. Plants may also be excluded from the fossil record because they did not grow in or near areas suitable for fossilisation.

In some cases, labile plant tissues can be preserved through burning (e.g. Glasspool et al., 2006), with the amount of anatomical detail and structure preserved by a charcoalified plant being partly dependent on the timing of charcoalification. Glasspool et al. (2006) discussed whether the remains recovered from Brown Clee Hill were burned while the plants were still alive, or whether they were burned as part of the plant litter. Given the exceptionally preserved state of many of the mesofossils, exhibiting *inter alia*, undehisced sporangia, vascular strands and intercellular spaces (e.g. Edwards et al., 1992; Edwards, 1996; Glasspool et al., 2006; Morris et al., 2011b, 2012a), in combination with other plant remains exhibiting interdigitating tubes and putative saprotrophic encrustations (e.g. Edwards and Richardson, 2000), these workers suggested that a mixture of living plants and decaying litter had been burned there.

There is a clear difference in the quality of preservation between Brown Clee Hill and the M50 section, and this is considered to be due, in large part, to much of the material being derived from burning of plant litter rather than living plants in the M50. Fig. 5 illustrates putative decay features of the spore masses from the M50 section, with holes and damage to the cuticle (if present) and in *in situ* spores a common feature amongst the plant remains. These features are less clearly derived from decay prior to burning and must therefore be considered with caution as they may have been formed during or after burning, but the total lack of sporangial cell walls points towards the decay of labile tissues. Interdigitating tubes and putative saprotrophic crusts (Plate I, fig. d; VII, fig. e) occur less often (n = 1 for each) but are the firmest indicators of decay prior to burning amongst the plants, suggesting that at least some of the material recovered from the M50 was derived from charring of the litter. There is less evidence for the charring of living plants in the M50. Certainly, the exceptional preservation identified in the Brown Clee Hill assemblages (e.g. Glasspool et al., 2006), is not seen. Indeed, very little anatomical information of the sporangial walls is retained on the spore masses. The absence of the sporangial walls in most of the recovered spore masses is interpreted here to suggest that prior to burning, labile tissues which originally enclosed the spore masses were preferentially lost to decay. Before the spore masses were fully decayed, the remaining material was then charred. While death prior to burning remains equivocal, it is suggested that if the plants were burned in life more of the putative labile sporangial tissues would be preserved, as they are in Brown Clee Hill (e.g. Glasspool et al., 2006). The sporangial tissues of at least one spore mass are retained, however, (ABM5028-005), suggesting that these tissues were either recalcitrant and hence resisted decay, or that the plant was charred in life.

If the spore masses were largely burned after death, then, why do most exhibit fully dissociated spores? Spore dissociation from tetrads/ dyads occurs near maturity and may indicate that the spores were nearly

ready for dispersal (section 5.2). The presence of the undispersed, ± mature spores could be due to (1) plants being burned in life and hence not releasing mature spores, or (2) plants being killed by another mechanism, such as flash flooding, before being able to release spores. As discussed, the absence of sporangial wall tissues in many of the spore masses may largely preclude (1), instead hinting at the latter. Flash flooding was common in the Early Lochkovian of the M50, where ephemeral interfluvial channels were likely to be seasonally activated during wet seasons (e.g. Allen and Williams, 1979; Hillier et al., 2007; Morris et al., 2012b). A variety of sites, including flood plains and deep, pool forming scours in ephemeral channels were likely to have been sites for plant growth (Morris et al., 2012b) and plants growing in these areas were likely subject to destruction and transport via flash flooding.

In addition to spore masses, sterile axial remains are also recovered in the M50 and may have been burned in life, especially where delicate features are retained (e.g., ABM50PIN1, ABM50PIN2), however, while some cuticle is lost, clear evidence for decay, or absence of decay, is not forthcoming. It is possible either way that the axes were less labile than sporangial tissue and were hence more resistant to decay and were burned as part of the litter. Alternatively, they were burned in life and subsequent transport and/ or diagenetic effects resulted in fragmentation of the fossils (below). It is also worth pointing out that the

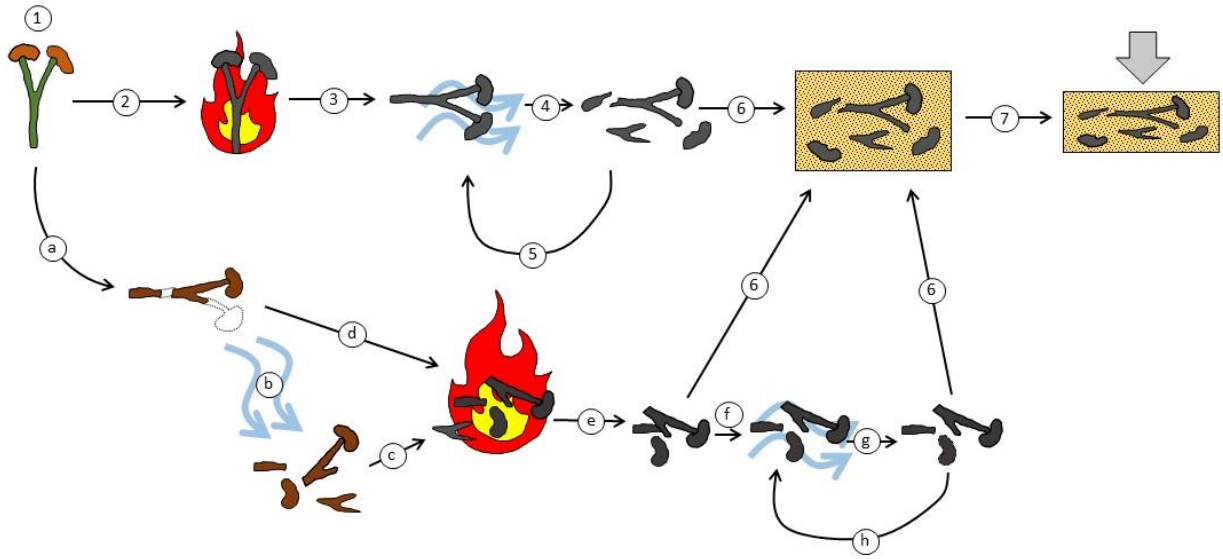

Figure V-4 Some hypothetical pathways by which charcoalified plants are incorporated into the fossil record. ***1:*** *Living plant in growth position;* ***2****: burning in life position, charcoalification;* ***3****: transportation of charcoalified remains by a variety of vectors, e.g. wind and/ or water;* ***4:*** *deposition of remains, e.g. as strandline on sediment surface;* ***5:*** *potential for further transportation of remains;* ***6:*** *final deposition and incorporation into sediments;* ***7:*** *burial, diagenesis and compression. Alternative path:* ***a:*** *death of plant, ± transport, decay, incorporation into plant litter;* ***b:*** *transport and deposition on sediment surface of decayed material as plant litter;* ***c, d:*** *burning of decayed material/ plant litter;* ***e:*** *formation of charcoal;* ***f:*** *transportation of charcoalified remains by a variety of vectors, e.g. wind and/ or water;* ***g:*** *deposition of remains, e.g. as strandline on sediment surface;* ***h:*** *potential for further transportation of remains. See text for details.*

eophytes are thought to be poikilohydric (as are many modern bryophytes). Such a response to water stress is thought to be a plesiomorphic feature of land plants, and as such it is likely that a variety of plants, including eophytes, were burned in a quiescent, desiccated state. When in this state, typically under conditions of water stress, the moisture content of the plants is low and they are likely to have contributed to the fuel load of wildfires.

It is of further interest that no subtending axes associated with complete sporangia, similar to those recovered at Brown Clee Hill, have been recovered. This may be attributable to transport and/ or diagenetic

effects. Whilst axial remains have been recovered from Ammons Hill, neither these, nor the non-embryophyte remains, are forthcoming in evidence for the timing of charring.

Fluvial action by rivers was likely the main mechanism by which charcoalified specimens were transported from the site of Formation in the Anglo-Welsh Basin. Morris et al. (2018b) posited that the Brown Clee Hill assemblage was devoid of larger zosterophyll sporangia due to hydrodynamic sorting of different size fractions prior to deposition. While zosterophylls were not present in the Anglo-Welsh Basin in the lower *micrornatus – newportensis* zone, the same is probably true of the M50 and Ammons Hill assemblages in that larger plant remains were been separated according to their hydrodynamic properties. Such sorting might account for the difference between the M50 and Ammons Hill assemblage, although there is broad overlap in mesofossil size between the two sites, with Ammons Hill exhibiting slightly larger particles. It is stressed here that no systematic measuring of the mesofossils was carried out, however.

The hydrodynamic sorting of unburned plants is different to that of charcoalified remains, with separation of the two occurring because of different hydrodynamic properties. For charcoal, the temperature of Formation, size of particle and type of source plant are understood to partly control the potential transport distance of charcoalified material (e.g. Nichols et al., 2000; Scott, 2010). In modern trees, ferns and woody shrubs, temperature may variously affect the waterlogging rate, and hence depositional timing of charcoal, with higher temperatures resulting in greater fracturing and higher waterlogging rates (Nichols et al., 2000). These differences are compounded by variations between species (Nichols et al., 2000). Such interspecific variations occur due to, *inter alia*, differences in bulk densities of tissues. Because the plants used in experiments by Vaughan and Nichols (1995) and Nichols et al. (2000) are poor analogues for the herbaceous, diminutive early land plants studied in this work, caution must be taken with comparisons and conclusions. Similar experiments to ascertain the behaviour of more appropriate analogues such as bryophytes and fungi following charcoalification is an interesting line of enquiry for future work. Vitrinite reflectance analysis from Ammons Hill and the M50 both suggest that the fires burned at low temperatures for each of the sites. This removes the possibility that differences in temperature of charring may have separated the spore masses and nematophyte remains, resulting in the distinct differences in composition between the M50 and Ammons Hill (table 1). Similarly, because of the overlapping size ranges of the mesofossils in each site, sorting of the fossils is not likely to have been based on size. Because there is a clear difference in mesofossil affinity between the two localities, some influence based on the rate of waterlogging between charred nematophytes and charred spore masses may have been responsible, hence leading to the separation of the two and exclusion from respective assemblages. Nichols' et al. (2000) findings that plant affinity derived differences in tissue density, *inter alia*, can influence transport distance and waterlogging rate (where factors such as temperature were controlled) support this hypothesis, although it is fielded tentatively and it is stressed that further experiments, such as with modern analogues, are required to qualify it.

Mechanical damage of mesofossils during transport is not thought to have contributed to the differences in composition between the M50 and Ammons Hill. Fluvial and aeolian mechanisms transport charcoalified material and lead to fragmentation and alteration of remains, such as the rounding of angular edges (e.g. Nichols et al., 2000; Scott, 2010). Nonetheless, such mechanical damage would not preferentially exclude material derived from a particular organism.

In both cases, the mesofossils are drawn from sections which have been lightly affected by tectonics, resulting in steeply dipping beds. The thermal maturity of the rocks gauged by the palynomorph darkness index (PDI) (Goodhue and Clayton, 2010) and for both localities is estimated to be between 41 – 43%, suggesting low thermal maturity. It is important to note that the reflectance results obtained here may have been influenced by the thermal history of the rocks. Therefore, the lowest reflectance values in these samples may represent a degree of thermal maturity of the sediments and may not relate to wildfire products.

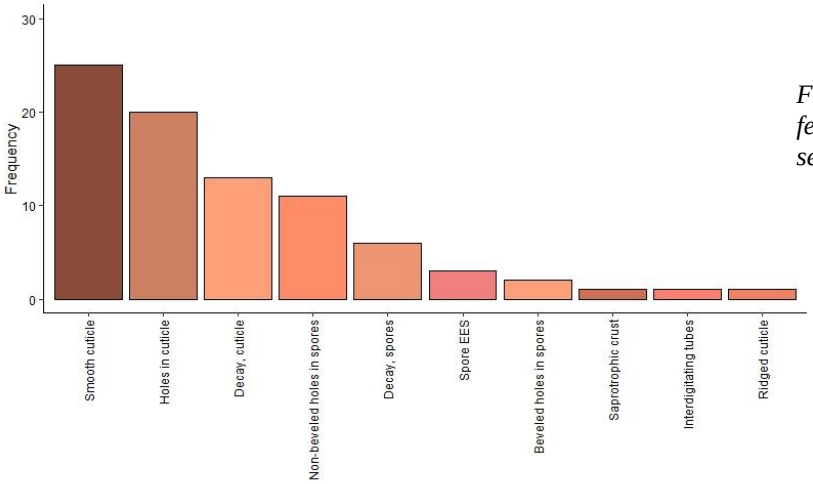

Figure V-5: Frequency of putative decay features on spore masses from the M50 section.

Indeed, the vitrinite reflectance expected from these low thermal maturity rocks is estimated to be <0.4% (Staplin, 1969).

5.2. Comparisons with the dispersed spore record and mesofossil diversity

Maturity of in situ spores

Sporogenesis amongst cryptospores and miospores varies, with differing degrees and timings of meiosis I and II, and cytokinesis in both of the meiotic stages (e.g. Edwards et al., 2012, 2014), and establishing the maturity of the plants is important prior to deliberating possible affinities and palaeoecologies. During the early ontogeny of miospores, sporogenesis occurs amongst immature spores as part of an associated spore tetrad. It is only towards the end of the ontogeny that the tetrad dissociates and separate miospores are observed in the sporangium (*in situ*), ready to be dispersed. Similarly, in cryptospore dyads early ontogeny occurs initially as a tetrad and then dyad, which may then lead onto further separation of the dyad depending on the species. As such, if *in situ* trilete spores are dissociated it is likely that the *in situ* spores are close to maturity. Similarly, in cryptospores typically dispersed as monads (e.g. hilate cryptospores such as *Cymbohilates*), if the hilate monads are all fully dissociated then the plant is verging on mature. Following this, the second method to gauge the maturity of an *in situ* spore is to compare the *in situ* specimen to the dispersed spore record. Assuming that spores in the dispersed record were generally dispersed at maturity, if *in situ* spores are closely comparable to dispersed specimens, then it is likely that they are nearing maturity and dispersal.

Because no *in situ* spores were recovered from Ammons Hill, the following discussion focuses on the M50 section. Fig. 6 a – b illustrates the diversity of *in situ* spores recovered. Overall, twenty-nine spore masses were recovered, with twenty-seven investigated here and a further two in Ball and Taylor (2022). Of those discussed here, fifteen masses yield miospores, while twelve yield cryptospores. Fig. 6b indicates that the most frequent *in situ* genus is comparable to the hilate cryptospore *Laevolancis*. Following these, the laevigate, crassitate miospores related to *Ambitisporites* and distally apiculate, crassitate miospores related to *Aneurospora* (n of each = 5) were the most common. Proximally 'emphanoid' (proximal radial muri) species of *Emphanisporites* followed (n = 4 including those of Ball and Taylor, 2022), with apiculate hilate cryptospores comparable to *Cymbohilates* species also occurring (n=3). Other genera were represented by

a single incidence each. Thus, despite miospores together outnumbering cryptospores, the single most common *in situ* spores are comparable to *Laevolancis*.

The frequency of miospores and cryptospores from the M50 sample from which these mesofossils were recovered is given in fig. 6, c – d. All of the *in situ* spore genera recovered here were recorded in the 250 dispersed spore count of the 19/DE/98 sample, with most identified to species level. Generally, the spores which comprise the greatest proportion of the dispersed palynoflora are represented in the mesofossil record, although a few key absences are observed. The most distinctive miospore absence in the mesofossil record are species of *Archaeozonotriletes*, which comprise 8.9% of the dispersed record. Likewise, species of *Chelinospora* and to a lesser extent, *Cymbosporites*, are also absent. These absences surmount to a total

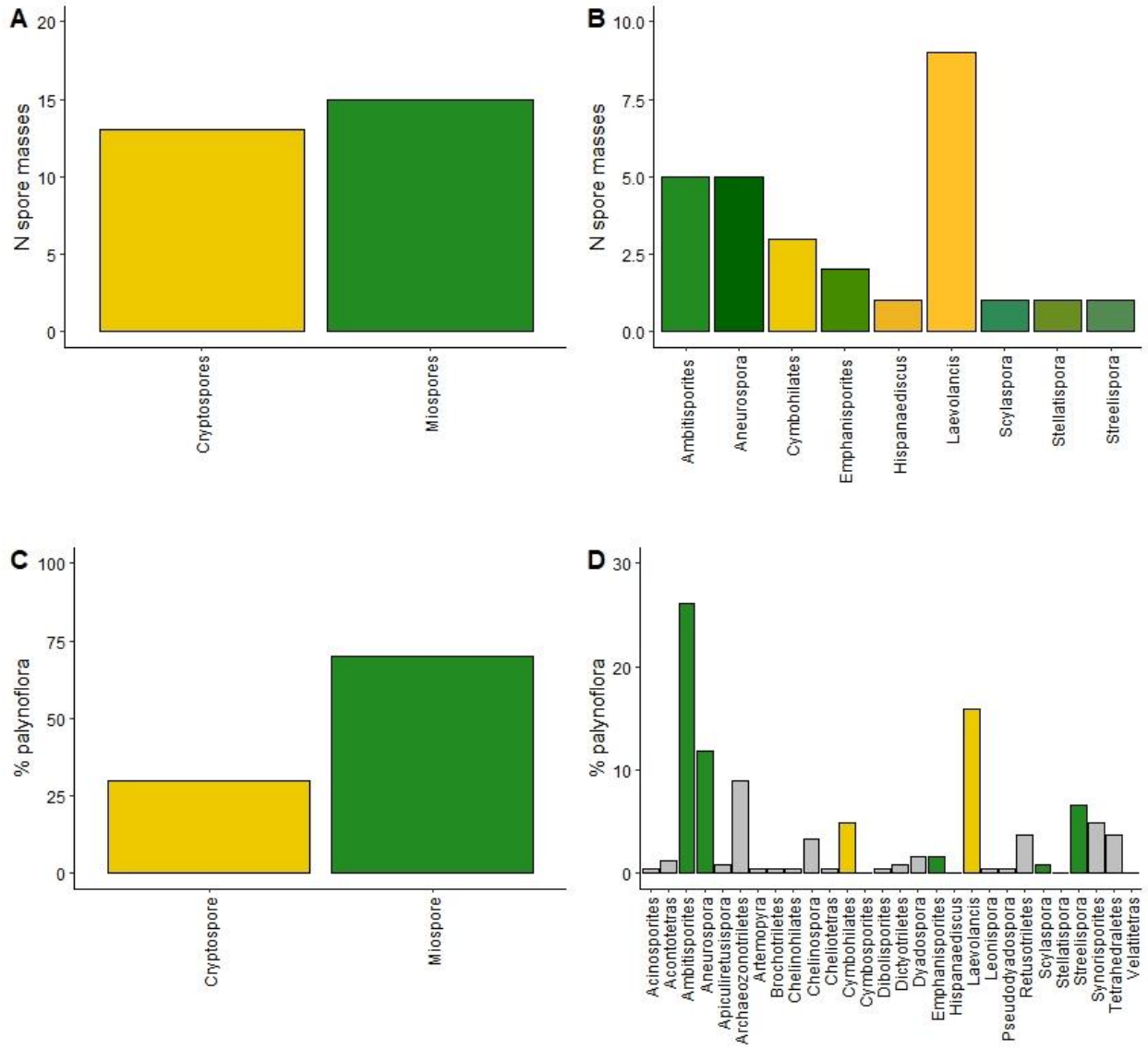

Figure V-6: ***A – B:*** *The diversity of in situ spores,* ***A:*** *frequency of in situ miospores and cryptospores;* ***B****: frequency of genera recovered in situ in spore masses;* ***C – D:*** *Spore mass volumetric calculations,* ***C:*** *proportion of cryptospores and miospores in the dispersed palynoflora from the DE98 sample from which the mesofossils were recovered, from a count of 250 spores in Ball (in prep);* ***D:*** *proportion of dispersed genera included in a 250 spore count from the DE98 sample. Grey = not found in situ. Mesofossil data in thesis appendix 5.3. count data in thesis appendix 3.3.*

absence of patinate trilete spores which have yet to be recovered from any mesofossil horizons in the Anglo-Welsh Basin despite extensive searching (e.g. at Brown Clee Hill) and importance in the dispersed record. There is also an absence of *in situ Retusotriletes*, which is again well documented across the Anglo-Welsh Basin at this time. The M50 has not yet consigned *in situ Synorisporites* species, although these are known from elsewhere (e.g., Fanning et al , 1988). Several key cryptospore genera are also absent from the *in situ* mesofossil record of the M50 section. Most notably, *Tetrahedraletes medinensis* and *Dyadospora murusdensa – murusattenuata*, which are both common in the dispersed record from the area are absent. *In situ* examples of these genera are known from elsewhere in the Anglo-Welsh Basin (Edwards et al., 2014).

Some *in situ* genera have been recovered despite the paucity of comparative species in the dispersed record. One incidence of *in situ Scylaspora* was recovered from the DE/98 sample, and Wellman (1999) reported a further eight variously fragmentary examples of the same *Scylaspora* species in comparable spore masses from the same M50 horizon and these findings were probably derived from the same species of plant (5.2.). This regular occurrence of *in situ Scylaspora* contrasts with the genera's low incidence in the dispersed record (<1%). Species of *Emphanisporites* also appear to be disproportionately represented in the *in situ* record here, especially relative to such species as *Archaeozonotriletes*, with four different species reported *in situ* despite comprising <2% of the dispersed palynoflora. Focusing further on *Emphanisporites*, it is of interest that the most common *Emphanisporites* species, *E. micrornatus* cf. *micrornatus*, has not been observed *in situ*, while others not recorded in the dispersed assemblage, such as *Emphanisporites* sp. in Ball and Taylor (2022), are.

Whilst some key taxa are missing, it is worth comparing the relative proportions of *in situ* and dispersed genera. *Laevolancis* has the greatest frequency of *in situ* spores but is secondary to *Ambitisporites* in the dispersed spore record, comprising 15.9% of the palynoflora whilst *Ambitisporites* comprise 26.1%. Likewise, dispersed *Ambitisporites* comprise a greater proportion of the dispersed record than *Aneurospora*, but they are equally abundant in the mesofossil record. Some species, such as *Hispanaediscus* are recovered *in situ* where more abundant species such as *Synorisporites*, are not. Whilst the proportions of *in situ* spores do not typically reflect the relative contribution of the genus to the dispersed record, many of the rare dispersed species are also excluded from the M50 section. Some of these genera, such as *Artemopyra* and *Velatitetras*, have been recovered from elsewhere in the Anglo- Welsh Basin.

There is a well-documented disparity between the taxonomic diversity amongst dispersed spores relative to macrofossils (e.g. Servais et al., 2019), with the former group appearing to better reflect the taxonomic diversity and distribution of these early land plants. Mesofossils go someway towards harmonising this disparity, including by revealing that similarly shaped sporangia, which if recovered as compression fossils would be categorised as the same megafossil morphospecies, often yield very different spore species and hence have quite different affinities. However, examination of the small sample of mesofossils from the M50, and from the much more extensive analyses of North Brown Clee Hill (e.g. Edwards et al., 2014; Morris and Edwards, 2018) indicate that the mesofossil record still does not match the taxonomic diversity of the dispersed spore record. Regarding the M50 section, only 25% of dispersed spore genera are represented *in situ*. With further investigation of the M50 record, it would be expected that further *in situ* genera would be recovered; but it still stands that some, such as *Archaeozonotriletes*, remain unaccounted for. As such, caution must be observed when considering the diversity of the plants, and subsequent palaeoecological inferences, from the mesofossil record given these absences. Furthermore, (1) specimens were picked for SEM analysis because they had a shape or size suggestive of a sporangium or spore mass and researcher bias consequently influences the results, and (2) the study was not exhaustive of the assemblage and could benefit from a greater sample size.

5.2. Affinities and spore mass morphological diversity (disparity)

In situ spores offer a biological link between a dispersed spore species and its parent plant, (e.g. Edwards and Richardson, 2004). The absence of *in situ Archaeozonotriletes*, for example, precludes any insights into the morphology of the parent plant, and more importantly, the exploration of possible affinities. Such affinities, between coeval plants and modern taxa, can be explored by comparing the sporangial and axial morphology, and the sculpture and structure of *in situ* spores. Ultrastructural analysis provides further morphological characters with which to deliberate the affinities of the plants, although problems exist.

Details of the gross morphologies, and hence morphological characters, of the parent plants are typically precluded from the sporangial masses in the M50. Nonetheless, some morphological features persist amongst the more complete specimens described here and elsewhere (e.g. Wellman et al., 1998; Edwards and Richardson, 2000; Morris et al., 2011b, 2018b) and a range of sporangial morphologies exists between and amongst the parent plants of dispersed morphogenera (e.g. Wellman et al., 1998; Ball and Taylor, 2022). Generally, it is plausible that many of the plants reported in this work lacked much recalcitrant tissues in their sporangia, although in some cases an amorphous sporangial cuticular layer is entirely or partially preserved. All of the plants were presumably homosporous, producing isospores which were free of an enveloping perine or extra-exosporal material, although some of the specimens do exhibit the latter. However, the absence of subtending axes with other distinctive morphological characters, and absence of ultrastructural analyses precludes deliberations of any tracheophytic affinities of the plants (e.g. Edwards et al, 1992, 2014; Wellman, 1999). Nonetheless, generic comparisons can be made between the sporangial morphologies of the more complete specimens recorded here, and cautiously compared to those contemporaneous or closely contemporaneous sporangial morphologies and associated *in situ* spores

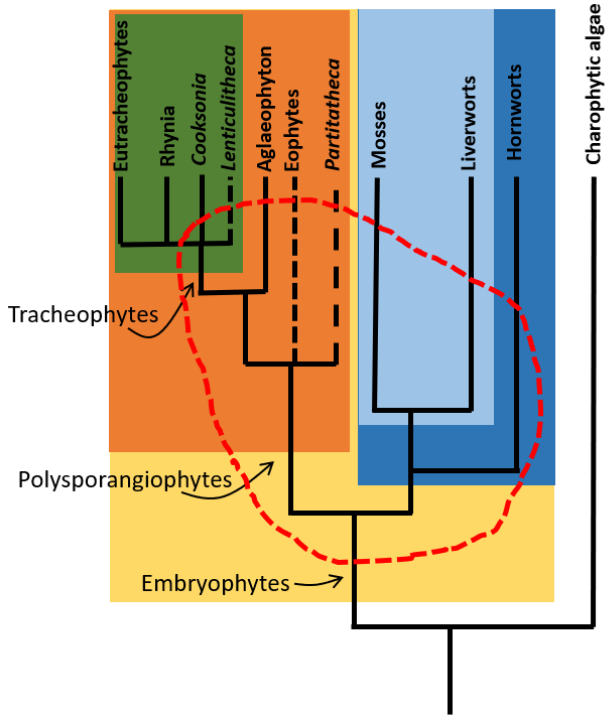

Figure V-7: Possible positions which cryptospore producing plants may occupy (red dashed oval), following Edwards et al. (2014, 2021a) and Puttick et al (2018). Green: tracheophytes; Orange: Polysporangiophytes; pale blue: Setaphytes; dark blue: bryophytes; yellow: embryophytes.

reported elsewhere (e.g. Edwards and Richardson, 2000; Morris et al., 2011b, 2012a; Edwards et al., 2014; Ball and Taylor, 2022).

The palaeobotanical record from the early Lochkovian (~lower *micrornatus* – *newportensis* subzone) of the Anglo-Welsh Basin indicates that the flora was principally comprised of rhyniophytes/ rhyniophytoids *sensu* Edwards (1996), eophytes (Edwards et al., 2022a, c) and cryptospore producing plants. The affinities

of many of these plants remain equivocal, although some rhyniophytes have been related to tracheophytes through vascular tissue (e.g. Edwards et al., 1992). Other plants with rhyniophytic organisation lack demonstratable vascular tissue and are hence referred to as rhyniophytoids *sensu* Edwards (1996). Rhyniophytes and many rhyniophytoids produce trilete spores, which have traditionally been suggested to derive exclusively from tracheophytes (e.g. Gray, 1985). However, work on modern taxa has shown that trilete spores are produced by some extant bryophytes such as *Sphagnidae* (e.g. Kenrick et al., 2012; Salamon et al, 2018). Furthermore, ultrastructural analyses of fossil trilete spores has shown the presence of certain characteristics, such as pseudosutures, which are found in extant hornworts (Taylor et al., 2011) and may suggest a relationship amongst some to that group. As such, it is not possible to posit that a trilete spore was derived from a tracheophyte unless vascular tissue, and other putative tracheophytic features, are demonstrated.

Complicating 'clear cut' bryophyte – tracheophyte affinities further is the recent identification of the eophytes, which exhibit a mixture of bryophytic and tracheophytic features such as a branching sporophyte, stomata and permanent tetrads and dyads (cryptospores) (Edwards et al., 2014, 2022a, b, c). These plants yield exclusively permanent cryptospores such as *Dyadospora*, and exhibit, *inter alia*, "… forking, striated axes with rare stomata terminating in valvate sporangia" (Edwards et al., 2022a, pg. 1440). This combination of features distinguished the eophytes from bryophytes and the tracheophytes. Edwards et al. (2021a) considered the possible phylogenetic position of the eophytes and placed them as probably an early branching group of the polysporangiophytes, which diverged prior to the loss of matrotrophy and gain of water conducting cells. A comprehensive list of published eophytes is provided by Edwards et al. (2022a, table 2). Plants producing non-obligate cryptospore dyads and tetrads are not included amongst the eophytes *sensu* Edwards et al. (2022a). Their affinities are less distinct, but they are probably derived from a pool of early embryophytes from which crown group tracheophytes and bryophytes are derived (e.g. Edwards et al., 2014). Several of these cryptospore producing plants may have had an organisation similar to the rhyniophytoids, that is, diminutive plants with terminal sporangia, although features such as sporophytic branching and stomata have not been reported.

Laevolancis

The most abundant *in situ* spore reported from the M50 thus far is of *Laevolancis* type hilate cryptospores. These are also reported in abundance from other mesofossil producing horizons, including the mid Lochkovian (middle *micrornatus* – newportensis subzone) Brown Clee Hill assemblage and the Přídolí (*tripapillatus* – *spicula* biozone) Ludford Corner assemblage (e.g. Wellman et al., 1998b). Gross comparison between the spore mass morphologies described here, reveals some similarities amongst *Laevolancis* producing spore masses. Typically, more complete specimens exhibit a discoidal, slightly oblate shape (fig. 8; Wellman et al., 1998b), although ABM5014-004 (fig. 8, h, plate I, figures d – g**)** is distinct as it may have been bivalved. No such bivalving has been observed in any other *Laevolancis* parent plants, despite their broadly similar shapes, and the feature may be unique to a particular group (*sensu* Wellman et al. 1998) of *Laevolancis* producing plants. Ultrastructural testing may help to differentiate the spore masses. SEM and TEM analysis of *Laevolancis* producing plants allowed Wellman et al. (1998) to described five discrete groups of *Laevolancis* producing parent-plants from Ludford Corner and Brown Clee Hill, and it is likely that some of the *in situ Laevolancis* spores described here could be included in those groups.

At Ludford Corner, 'Group-B' *Laevolancis* type spores are recovered from elongate and discoidal spore masses and sporangia, whilst at the M50 section and NCBH, only discoidal examples have been recovered, perhaps suggesting a loss of these plants by the lower MN. Four further types of *in situ Laevolancis* spores from discoidal spore masses were recognised by Wellman et al. (1998). Of these, type A is represented in

at least one case, ABM5027-001 (Plate II, figures m – p) where the *in situ* spores exhibit distinctive beveled pits. Furthermore, whilst incomplete the remnant shape of the spore mass may indicate that the sporangia was discoidal, and it has a similar size to the type-A yielding spore masses in Wellman et al. (1998). Whilst ultrastructural analysis is required to confirm a relationship, the recovery of this group-A *Laevolancis* in a putative discoidal spore mass may hint at the continuation of this lineage between at least the Přídolí (*tripapillatus* – *spicula* zone) and Early Lochkovian (lower *micrornatus* – *newportensis* zone). Spore mass ABM5023-003 (Plate II, figures a – e) can be tentatively related to type-A *Laevolancis* spores also, although there are several key differences. Firstly, the pits exhibited by the *in situ* spores in that spore mass are not beveled. Such non-beveled holes occur throughout the *in situ* spores and are probably a decay feature rather than a biological feature. Secondly, the size of the spore mass, whilst not remarkably greater than the maximum diameter given in Wellman et al. (1998b) (900µm) is greater (1087µm). The shape differs somewhat also. This may be due to this spore mass being more complete than those reported by Wellman

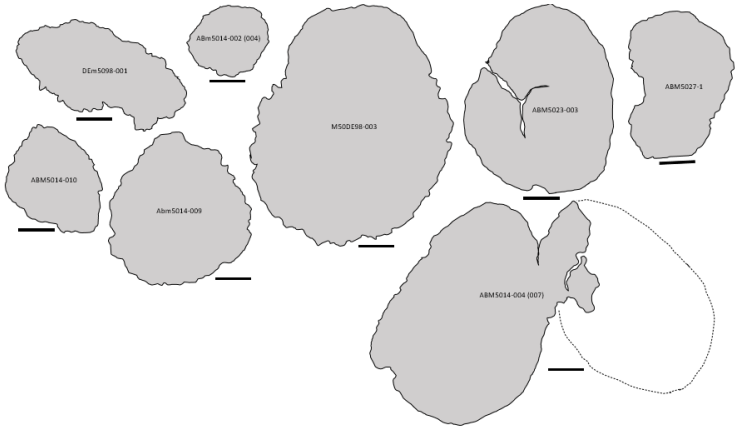

Figure V-8: outlines of Laevolancis yielding spore masses from the M50 section (lower micrornatus – newportensis *zone, early Lochkovian). For details, see plates I and II and* Laevolancis *descriptions. Dashed line in ABM5014-004 infers probable bivalving of spore mass.*

et al. (1998b), however ABM5023-003 is essentially comparable in shape to NMW96.30G.2 (fig. 1g in Wellman et al. 1998b). As such, whilst an affinity with Group-A *Laevolancis* types is not refuted here, it is not a confident association, either. Again, ultrastructural analysis is required for a more confident association.

The other *in situ Laevolancis* type spores are more difficult to place into Wellman's et al. (1998b) groups, as a function of the fragmentary nature of the spore mass and a lack of structural and ultrastructural characters. M50DE98-001 may be comparable to Group-E of Wellman et al. (1998b) based on the EES exhibited on the spore, but the globules are larger in these specimens and the proximal faces differ considerably between Group-E specimens in Wellman et al. (1998b) and M50DE98-001.

The most striking *Laevolancis* bearing spore mass is ABM5014-004, which appears to have been bivalved in life. Whilst the generic morphology of individual valves is comparable to other *Laevolancis* bearing spore masses (fig. 8), the strong indication for bivalving sets the spore mass apart. Bivalved sporangia are known from several Lochkovian plants, such as *Sporathylacium salopense* (Edwards et al., 2001) from NBCH. In that plant, there are distinct anatomical modifications relating to the dehiscence mechanism of the sporangia, including a wedge of cells with thick outer periclinal walls (Edwards et al. 2001). No such mechanism for dehiscence is observed in ABM5014-007, nor indeed are any sporangial cellular layer remains preserved, instead being seemingly replaced or obscured by an encrusting layer of dense ?saprotrophic spherules. As such, the nature of the dehiscence mechanism in this sporangium remains equivocal, but it is not thought to have been similar to *S. salopense*. Further distancing the spore mass from that species is the nature of the *in situ* spores; in *S. salopense*, trilete spores with a verrucate distal hemisphere are observed, whilst ABM5014-007 exhibits laevigate hilate cryptospores. This key feature also distances the specimen from several other bivalved sporangia reported from the Silurian - Devonian,

including those of the Zosterophylls, which yield retusoid trilete spores (e.g. Edwards, 1969b) in addition to being marginally thickened. *Partitatheca* spp. yield *in situ* cryptospores, but these are dyads (Edwards *et al*., 2012a) or tetrads (Edwards *et al*., 2012b). Furthermore, the sporangia of *Partitatheca* spp. are quadrivalvate. Two examples of elongate bivalved cryptospore bearing sporangia have been recorded from Brown Clee Hill also, but none exhibit *in situ Laevolancis* species. One exhibits permanent tetrads most similar to *Cheliotetras*, whilst the other yields enveloped tetrads, most similar to species of *Velatitetras* (Habgood, 2000; Edwards *et al*., 2014). By the mid Lochkovian, then, bivalved sporangia had been adopted by two quite different plants, and the recovery of ABM5014-007 adds a third lineage of cryptospore-bearing plant to utilise the mechanism. It is interesting to note that all three of the spore morphospecies recorded thus far from bivalved sporangia are from long-ranged lineages, which all extend back to the Upper Ordovician. From this, it is tempting to postulate that the development of bivalved sporangia could have been a relatively early innovation for sporangial dehiscence and spore dispersal but given the variation in ultrastructure in many fossil spores, particularly in *Laevolancis divellomedium*, it is not possible to determine the continuity of the spore morphospecies or indeed of sporangial bivalving from the Ordovician without additional plant body-fossil evidence from that time. In extant plants, bivalved sporangia are known principally from Hornworts, but also occur rarely amongst Setaphyta (liverworts + mosses, *sensu* Puttick et al., 2018) and Tracheophytes (Edwards *et al*., 2014).

Most of the *Laevolancis* bearing spore masses have a morphology reminiscent of *Lenticulitheca* (Morris et al., 2011b). However the discoidal spore masses limited by an acellular cuticular layer cannot be attributed to that genus because the *in situ* hilate cryptospores are distally laevigate, rather than apiculate. Furthermore, no ultrastructural information has been gathered for these specimens, and this is especially important for species of *Laevolancis* as there is at least five types of ultrastructure exhibited by these morphologically simple spores (Wellman et al., 1998b). Whilst an ultrastructural analysis would be required to qualify a relationship between these *Laevolancis* producing specimens, there is a possibility, based on their similar sporangial morphologies and features and corresponding *in situ* spores, that several of these specimens are derived from the same, or group of, plants. This is especially true for M50DE98-003, ABM5023-004 and ABM5014-004 with the latter differing most by the unconfirmed nature of the enveloping layer and likely bifurcation.

Hispanaediscus

This is the first reported example of an *in situ Hispanaediscus* sp., of which dispersed examples occur throughout the Anglo-Welsh Lower 'Old Red Sandstone' succession in low proportions. As has been mentioned, discoidal spore masses are a common feature of compressed macrofossils and compressed mesofossils (e.g. Edwards and Richardson, 2004; Morris et al., 2011a, b; Edwards et al., 2014), and thus the spore mass could be attributed to several plant taxa on the basis of morphology alone. The spore mass is likely to have been terminal, with the axis attaching to the opposite side of the specimen to that imaged. A particularly striking feature of this spore mass is its concave organisation with a partially preserved distinctly raised edge. Such an arrangement is a common feature of subspecies of *Cooksonia pertoni* (e.g. Fanning et al., 1988; Edwards et al., 1995), which demonstrate an outer thickened area of sporangial tissue which encloses the *in situ* spores within. The absence of a sporangial cellular wall in this specimen precludes a direct comparison to *Cooksonia*, in addition to the presence of an acellular layer, which is partially lost on the latter and which is not present in *Cooksonia* (Morris et al., 2011b). The raised region could conceivably be derived from shrinkage during burning.

Discoidal spore masses with a partially acellular layer, yielding hilate cryptospore monads, were grouped into to the genus *Lenticulitheca* by Morris et al. (2011b). In essence, this *Hispanaediscus* producer shares most of the broad characteristics of *Lenticulitheca*, including spore mass morphology and features, and *in*

situ spore structure. However, *Lenticulitheca* contains species of apiculate hilate monads of *Cymbohilates*, and as such the *Hispanaediscus* producer described here cannot be grouped into *Lenticulitheca*. It is of interest that the discoidal sporangia belonging to the *Lenticulitheca* complex were attributed to *Paracooksonia* and *Cooksonia* partially based on similarly shaped, discoidal sporangia and similar distally apiculate ornament amongst the *in situ* spores between the sporangia. The bilayered exine was provided as further evidence for the association, and Edwards et al. (2014) posited that this suggested that the *Lenticulitheca* complex was probably closely associated with the tracheophytes. This was despite *Lenticulitheca* not exhibiting the sporangial wall arrangement of *Cooksonia*, instead exhibiting an acellular layer similar to *Paracooksonia* and the *Hispanaediscus* producer. *Cooksonia pertoni* subsp. *synorispora* yields distally verrucate trilete spores of *Synorisporites verrucatus* (Fanning et al., 1988; Edwards et al., 1995), which are comparable in distal structure to the *Hispanaediscus* sp. described here. With the association of *Lenticulitheca* to *Paracooksonia* and *Cooksonia* and from the limited evidence provided from this *Hispanaediscus* specimen, it may be plausible to tentatively posit a similar relationship between this parent plant and *Cooksonia*. Given that no ultrastructural analysis has been performed on these *in situ* spores, further evidence for this relationship is currently lacking.

Cymbohilates

Spore masses yielding *Cymbohilates* were the second most recovered *in situ* cryptospore from this small survey (fig. 6b). Morris *et al*. (2011b) grouped several species of *Cymbohilates* which occurred in discoidal spore masses in the middle *micrornatus – newportensis* Brown Clee Hill horizon into *Lenticulitheca*. These discoidal spore masses were also united in being limited by an acellular cuticular layer, whilst the spores all exhibited distally apiculate sculpture and a bilayered exospore. *C. allenii* var. *allenii* is reported *in situ* here in a fragmented spore mass (ABM5032-001, Plate IV figures a – c) with remnants of an adherent acellular layer. Whilst the nature of the *in situ* spores and presence of an acellular cuticular layer suggests a relationship with *Lenticulitheca allenii*, the inability to diagnose the original morphology of the spore mass and nature of the exospore ultrastructure precludes assigning it fully to *L. allenii*, and it is best referred to as cf. *Lenticulitheca allenii*. *C. allenii* var. *allenii* appears in the dispersed spore record at the onset of the lower *micrornatus - newportensis* zone, with scattered reports from the latest *Apiculiretusispora sceacga* zone in the earliest Lochkovian. It persists throughout the investigated Anglo-Welsh Basin section (to +168m above the Chapel Point Limestone member, middle *micrornatus – newportensis* zone; Chapter III). There is no corroborating ultrastructural data which links the earliest appearing dispersed *C. allenii* var. *allenii* in the lower *micrornatus – newportensis* zone, coeval to the M50 section and cf. *L. allenii* ABM5032-001, to the slightly younger spores in the middle *micrornatus newportensis* zone, coeval to the *L. allenii* circumscribed by Morris et al. (2011b) from North Brown Clee Hill. Nonetheless, it is plausible that the persistence of the morphogenus represents a continual persistence of *L. allenii* from lower to middle *micrornatus newportensis* times, but it is stressed that corroborating spore mass morphology and exospore structural data is required to confirm this.

Aneurospora and *Streelispora*

Species of *Aneurospora* and *Streelispora* have been reported *in situ* from Brown Clee Hill from *Paracooksonia* and *Cooksonia* (e.g. Morris et al., 2011b), in addition to spore masses in the M50 section (Edwards et al., 1995). The examples reported in this paper are recovered from variously fragmentary spore masses, which are generally associated with acellular, and more rarely cellular, cuticular layers. ABM5023-001 derives from a discoidal spore mass which is associated with an acellular cuticular layer. The other spore masses exhibit an acellular layer, and the presence of *Aneurospora* species with spore masses of this nature may relate these specimens with *Paracooksonia* from the middle *micrornatus – newportensis* zone

(Morris et al., 2011b). ABM5023-001 (Plate VI, figures a – d) is considered most similar to *A. trilabiata*, and as such is closest to group 2 of *P. apiculispora* (Morris et al., 2011b). However, a full association with this species is not made here because of the lack of information regarding the proximal faces of the *in situ* spores, in addition to other missing characters included in the circumscription of *Paracooksonia*. Morris et al. (2011b) includes radially arranged folds in the acellular cuticular layer on the proximal surface of the spore masses in her descriptions of *Paracooksonia*. This was not observed in ABM5023-001 and in addition to the lack of proximal details of *in situ* spores and ultrastructural evidence, a confident association with *P. apiculispora* is precluded. It is interesting to note that the uncertain circular spore mass reported here (ABM5031-001) does exhibit such a radial arrangement of folds on one side of the spore mass. In addition, it shares several further features in common *Paracooksonia*, namely the discoidal spore mass of a similar size to those figured in Morris et al. (2011) which is limited by an acellular cuticular layer. However, the lack of insight into the *in situ* spores precludes assignation to *Paracooksonia*.

Specimen ABM5028.1 (Plate VI, figures e – h) could be grouped amongst *Paracooksonia*, also, given the co-occurring features and *in situ* spores. However, the *in situ Aneurospora* are not comparable to *A.* cf. *trilabiata* or *Streelispora newportensis*, and hence cannot be grouped into the *P. apiculispora* complex *sensu* Morris et al. (2011b). In addition, absence of radial folds in the acellular layer and an understanding of the nature of the spore wall ultrastructure precludes a confident assignment to *Paracooksonia*. Specimen ABM5014-002 (Plate VI, figs h – k) is a fragmentary spore mass, although an originally ± discoidal morphology is inferred by the more complete outer edges. The *in situ* spores are grouped into *Aneurospora*, but comparable species have not been reported *in situ* from the dispersed record of the M50. This may be due to the diminutive nature of the ornament, which might not be recognised during normal light microscopy. Returning to the spore mass, an acellular cuticular layer adheres to the external surface of the spore mass, although it is largely lost. Again, the spore mass morphology and *in situ* spores may imply a relationship with *Paracooksonia*. However, as before the absence of, *inter alia*, radial folds in the acellular layer, and lack of ultrastructural information for the *in-situ* spores, precludes a full assignment.

Tripapillate *Aneurospora* species proliferate in the Anglo-Welsh Basin from the lower *micrornatus* – *newportensis* subzone (Chapter III), and so it is surprising that so few tripapillate *Aneurospora* species were identified *in situ* from the sample. Indeed, in the dispersed palynoflora from the sample from which these mesofossils are found, tripapillate *Aneurospora* species comprise some 20% of the assemblage. Specimen ABM5014-002 is a fragmentary specimen yielding a tripapillate *Aneurospora* species, which are considered here as *A.* cf. *isidori*. The fragmentary nature of the spore mass precludes an assessment of the original morphology of the sporangium. No limiting material has been identified on this specimen. The absence may be a function of the fragmentary nature of the specimen, but in other poorly preserved specimens some acellular material is retained and so it may not have been present in life. The dearth of acellular material precludes assignment to *Paracooksonia* species. Several early land plants yield species of *Aneurospora* (e.g. Fanning et al., 1988; Edwards et al., 1994, 1995). While it is not possible to assign this spore mass to any of these parent plants because of its fragmentary nature, it is of interest to posit some possibilities. Species of *Cooksonia* do not exhibit an acellular layer, instead exhibiting a well-developed cellular sporangial wall. The absence of the acellular layer in ABM5014-002 may be suggestive of a further relationship with *Cooksonia*, although the lack of sporangial characters and spore wall ultrastructural information precludes a confident assignment.

Streelispora newportensis is a prolific apiculate crassitate trilete spore genus, which is differentiated from *Aneurospora* by the tangential and small radial folds on the proximal face developed from layering of an outer and inner exospore (Richardson et al. 1982; Edwards et al., 1995). *Streelispora newportensis* has a complex relationship with tripapillate *Aneurospora* species, with both *Paracooksonia apiculispora* and *Cooksonia pertoni* subsp. *apiculispora* yielding spores of the *Streelispora* – *Aneurospora* complex (Fanning et al., 1988; Morris et al. 2011b, 2012a). The fragmentary nature of specimen ABM5029-002

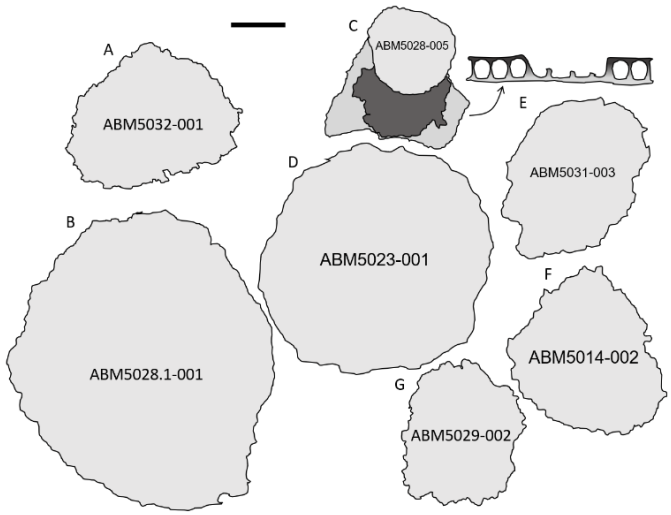

Figure V-9: Cymbohilates, Aneurospora *and* Streelispora *yielding spore masses recovered from the M50 section.* ***A:*** *ABM5032-001* Cymbohilates allenii *var.* allenii *yielding spore mass, cf.* Lenticulitheca allenii*;* ***B – F:*** Aneurospora *yielding spore masses;* ***B:*** *ABM5028.1-001 yielding* Aneurospora *sp.,* ***C:*** *ABM5028-005* Aneurospora *sp., colouration indicates reticulate (light grey) and smooth (dark grey) area. The arrow indicates an interpreted cross section. see text for details;* ***D:*** *ABM5023-001, yielding* Aneurospora *cf.* trilabiata*;* ***E:*** *ABM5031-003, yielding* Aneurospora *sp.;* ***F:*** *ABM5014-002 yielding tripapillate* Aneurospora *sp.;* ***G:*** *ABM5029-002, fragmentary spore mass yielding* Streelispora newportensis. *It is likely that A is related to* Lenticulitheca*, whilst B, D and E may be related to* Paracooksonia*. Meanwhile, C, F and G are less clear, although may be related to* Cooksonia*. Scale bar 200µm.*

which yields *S. newportensis* means that it cannot be assigned to a plant genus, however, as with ABM5014-002, it is interesting to note the dearth of acellular limiting material on this specimen. With reference to this, it is possible that the mass was derived from a *Streelispora* yielding *Cooksonia pertoni* var. *pertoni*, but this is far from secure. The final specimen yielding *in situ Aneurospora* (ABM5028-005) comprises an 'outer' layer with a clear reticulate arrangement, topped by a cracked, fragmented smooth 'inner' layer, which in turn is capped by a spherical, uncompressed mass of spores attributable to *Aneurospora* sp. 7 (Chapter III). The spherical mass of spores is interesting as there is no retention of the acellular layer, which instead adheres to the reticulate cuticle. Whilst appearing bilayered, the associated reticulate + smooth layer is interpreted as a single layered wall of sporangial wall cells. The reticulate layer is developed where portions of the sporangial layer have cleaved off leading to the loss of inner periclinal cell walls. The laevigate layer therefore represents portions of the complete cell walls, where the inner periclinal cell wall is preserved. Where the sporangial cell wall is incomplete, the isodiametric, blocky shape of the cell walls are indicated. Based on the absence of an acellular layer, the spore mass cannot be attributed to *Paracooksonia*, but the single layer of blocky cell walls and *in situ Aneurospora* is suggestive of a relationship with *Cooksonia*. However, the lack of sporangial morphological features precludes assignment, in addition to the lack of information regarding *in situ* spore wall ultrastructure.

Ambitisporites

Ambitisporites is a common spore recovered in the dispersed and *in situ* record (e.g. Fanning et al., 1988; Edwards, 1996; Morris et al., 2012b; Morris and Edwards, 2018; Chapter III). Five spore masses yielding *in situ* spores comparable to the dispersed genus *Ambitisporites* were recovered in this investigation, with at least two different sporangial morphologies being apparent. The least complete specimens, ABM5027-004, M50DE98-004 and M50DE98-005, yield *Ambitisporites avitus – dilutus, Ambitisporites* cf. sp. 1 and *A.* cf. *avitus - dilutus* respectively. While the *in situ* spores differ, the spore masses are united by the presence of an adherent acellular cuticular layer which is variously preserved and retained. More tentatively, the shapes of the spore masses hint at an originally discoidal sporangial shape. This discoidal morphology is best preserved in M50DE98-005 but is noted that in all cases the shape may be fortuitous following abrasion and attrition of the fossils during transport. However, accepting that the discoidal morphology is tenuous, the presence of *in situ Ambitisporites* and the presence of an acellular cuticle point towards a relationship with *Paracooksonia ambitispora* Morris et al. (2011b). This *Paracooksonia* species

is reminiscent of the *Aneurospora* yielding *P. apiculispora* discussed earlier, in that the original diagnosis requires an acellular layer, discoidal spore mass morphology and *in situ* crassitate apiculate or laevigate trilete spores. Several specimens figured in the original descriptions of Morris et al. (2011b) are very similar in morphology to M50DE98-005, and as such the relationship to *P. ambitispora* is somewhat firmer with that specimen than for the other two specimens. In addition, the maximum diameter of the spore masses described here, were they complete, is not thought to have exceeded 1780µm, the maximum size given for *P. ambitispora* by Morris et al. (2011b). Nonetheless, given the tenuous insight into the shape of the spore mass and the absence of ultrastructural information of the *in situ* spores, these specimens cannot be confidently assigned to *P. ambitispora*. Furthermore, the *in situ* spores reported here differ somewhat from the *in situ* spores associated with *P. ambitispora* in Morris's et al. (2011b) original descriptions, which tend to have more robust crassitudes.

Specimen ABM5020-001 is distinguishable by its elongate morphology, which suggests that the sporangium of the parent plant was elongated in life. Whilst the morphology of the plant separates it from the *Ambitisporites* producers above, the specimen does exhibit an adherent, acellular, cuticular layer, in common with the other *Ambitisporites* producers. Along with the similar *in situ* spores, this may suggest a link between these plants. However, in order to more fully qualify a relationship with the *Paracooksonia ambitispora* – esque spore masses discussed above, not only would the *in situ* spore wall ultrastructure need to be investigated for bilayering, but the acellular wall would need to be investigated to test whether it has a lamellar ultrastructure, as it does in *Paracooksonia* (Morris et al., 2011b). The generic difference in the shape of the spore mass necessitates caution, and a relationship with *Paracooksonia* is not inferred here, despite some similar features being shared. Given the diversity of spore wall ultrastructure recorded in various *in situ* and dispersed *Ambitisporites* species, which can be bilayered or homogenous (Edwards et al., 1995; Taylor, 2003), such caution is warranted. The shape and diminutive nature of the spore mass may suggest that the parent plant was a rhyniophyte, but because of a lack of vascular tissue it must be referred to as a rhyniophytoid.

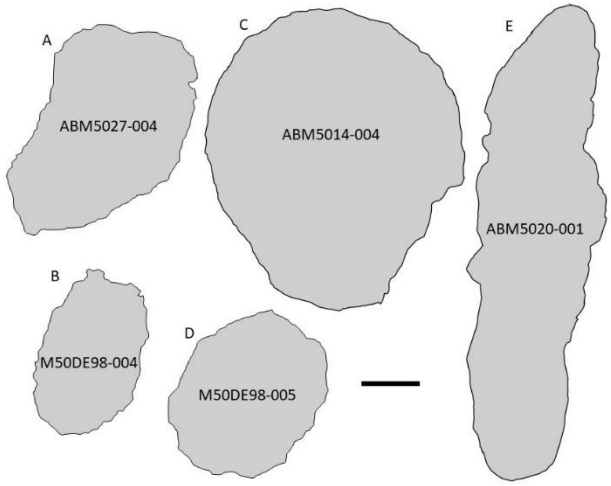

Figure V-10: Ambitisporites *yielding spore masses from the lower MN M50 assemblage circumscribed in this study.* ***A, B and D*** *may be comparable to* Paracooksonia ambitispora. ***C*** *may be comparable to* P. ambitispora *but exhibits a shape reminiscent of* C. hemisphaerica. ***E****: is generically different from A,B,C and D in terms of sporangial morphology, although an acellular layer is retained. Scale Bar 200µm.*

The high number of associated and partially associated *Ambitisporites* tetrads in this spore mass is of note. *Ambitisporites* spores are predominantly dispersed at maturity as individual trilete spores. The maturity of this spore mass is called into question because not all of the trilete tetrads are dissociated, suggesting that ontogeny was not completed prior to death. Whilst maturity is a likely solution for the abundance of associated trilete tetrads in this spore mass, several spore masses have been reported with *in situ* associated tetrads in addition to individual trilete spores (e.g Edwards et al., 1996, 1999). Edwards et al. (1996, 1999) posited that the parent plant of *Synorisporites downtonensis* may have produced a mixture of associated

trilete tetrads and fully dissociated trilete miospores. Lavender and Wellman (2002) suggested that some plants may have been flexible in their ability to produce individual monads and trilete tetrads, the latter during periods of environmental stress. The sacrifice in genetic diversity resulting from the production of associated tetrads (e.g. Gray, 1985) may have been counterbalanced by the higher likelihood of fertilisation of gametes in stressed settings. Laevigate trilete tetrads are found in varying proportions through the Anglo-Welsh sequence (up to 6%), with negligible change through the Přídolí and Lochkovian (Chapter III), suggesting that the dispersal of associated trilete tetrads was part of the normal background spore rain. Where associated trilete tetrads are concentrated, workers (e.g. Visscher et al., 2004; Marshall et al., 2020; but see also Stukins, 2022) have posited that this may be an indication of widespread environmental perturbation. This is not considered the case here, as (1) this is the only spore mass exhibiting *in situ* trilete tetrads, and (2) there is no spike in trilete tetrads in the dispersed record of this sample. Trilete tetrads comprise 1.6% of the dispersed palynoflora in this mesofossil sample, which is below the mean trilete tetrad incidence of 3.5% throughout the sequence (range 0.4 – 20%) (Chapter III).

Specimen ABM5014-004 has a distinctively 'spoon shaped' morphology which, in addition to *in situ Ambitisporites*, is redolent of *Cooksonia hemisphaerica* (Fanning and Edwards, 1991; Edwards, 1996). However, the acellular limiting layer distances the specimen from *C. hemisphaerica*, in addition to the absence of other key features. The acellular layer is reminiscent of the *Paracooksonia* spore masses (Morris et al., 2011b). *Paracooksonia* are discoidal and may be subcircular to elliptical in shape. Given the damage to the spore mass, it is not possible to discern the original morphology of the spore mass, however it is plausible that the mass was elliptical. Nonetheless, without the radial folds exhibited by *Paracooksonia*, or evidence of where the subtending axis was attached, it is difficult to ascertain the affinities. Furthermore, without ultrastructural analysis of the spores, a more confident assessment cannot be made.

Scylaspora

A detailed account of the possible affinities of similar *Scylaspora* producing plants to the one reported in this work (ABM5021-001) were given by Wellman (1999), who surmised that these plants were probably closely related to Rhyniopsida based on their size, morphology and *in situ* spores. These features excluded them from the Zosterophylls, but given the absence of demonstratable vascular tissue, they were referred to as rhyniophytoids. Because of the similarities in spore mass morphology and the structure and sculpture of *in situ* spores, it is posited that the *Scylaspora* specimen described here is derived from the same group of plants as those described earlier by Wellman (1999) (i.e. rhyniophytoid). Further supporting an association with tracheophytes for *Scylaspora* is the bilayering of the wall observed by Wellman (1999), which Edwards et al. (2014) posited might indicate a tracheophytic affinity. In comparison, Wellman (1999) noted that loose dyads of *Dyadospora murusdensa – murusattenuata* complex and hilate cryptospores comparable to *Laevolancis divellomedium* had spore wall ultrastructures comparable to that of *Scylaspora*, that is, an inner laminated layer and an outer homogenous layer. Subtle differences such as extra-exosporal material (Wellman et al., 1998b) and envelopes (Taylor 1995a, 1996, 2000) existed in those spores, distancing them somewhat from the ultrastructure of *Scylaspora*. Other trilete spores have similar spore wall ultrastructures to those found in *Scylaspora*. An *Emphanisporites* sp. recovered by Ball and Taylor (2022) from the same M50 horizon as these fossils, yielded an ultrastructure similar to *Scylaspora*, except the *Emphanisporites* sp. exhibited a separation between the inner laminated and outer homogenous layer, in addition to lacunae, which distanced it from *Scylaspora*.

Emphanisporites

Spore masses yielding *in situ Emphanisporites* neatly demonstrate the disparity that the parent plants of a single dispersed morpho-genus can exhibit. Seven examples of sporangial morphologies amongst

Emphanisporites species have been recovered from the lower and middle *micrornatus – newportensis* subzones of the Lochkovian of the Anglo Welsh Basin (Edwards and Richardson, 2000; Morris et al., 2012b; Ball and Taylor, 2022; this work), and one from the Pragian-Emsian Rhynie Chert (*polygonalis – emsiensis* biozone) (Wellman et al., 2004). The latest recovery of the genus *in situ* are specimens ABM5032-002 and M50DE98-002 (Plate VII), described here from the lower *micrornatus – newportensis* of the M50 section. M50DE98-002 is the fourth 'elongate' spore mass to yield *in situ Emphanisporites* spores, with the others yielding *E. epicautus* and *E.* cf. *epicautus* spores (Ball and Taylor, 2022), *E.* cf. *micrornatus*, and *E.* sp. A *sensu* Richardson and Lister (Edwards and Richardson, 2000). The latter two are bifurcating and '*Salopella*-esque' respectively (Edwards and Richardson, 2000), and it is possible that the *E. epicautus/* cf. *epicautus* producer was bifurcating also, although this is equivocal. *E.* sp. A (Morris et al., 2012a) *E.* sp. (Ball and Taylor, 2022) and *E.* sp. in ABM5032-002 (below) are all derived from discoidal spore masses. Hence, there are at least five sporangial morphologies from which *in situ Emphanisporites* are found, indicating generic difference amongst the parent plants (fig. 11). Coupled with the diversity of the spore wall ultrastructure of *Emphanisporites* spores, of which there are at least seven types based on dispersed (Taylor et al., 2011) and *in situ* (Ball and Taylor, 2022) sectioning, it is apparent that emphanoid structure is a result of evolutionary convergence between at least two lineages (e.g. Taylor et al., 2011), one of which is tracheophytic.

A further source of diversity amongst the parent plants of *Emphanisporites* is the presence of acellular layers on some, and paucity or absence in others. These acellular layers have been interpreted as sporangial cuticle following previous workers (Wellman, 1999; Morris et al., 2011b, 2012a), possibly preventing moisture from permeating the sporangium. While it is not possible to deliberate on the relative resistance of these putative sporangial cuticles between parent plants, it is plausible that those specimens with no evidence of cuticle (e.g. M50DE98-002) lacked such a feature in life, as has been shown with comparisons between *Cooksonia* and *Paracooksonia* (Morris et al., 2011b) although the possible influence of taphonomy must also be considered.

The presence of an acellular cuticular layer on some of the *Emphanisporites* yielding spore masses may suggest a relatively closer relationship between these specimens than with those which do not, especially where the sporangial morphology is similar. However, the diversity of sporangial ultrastructure in *Emphanisporites* producers necessitates caution here, especially where the morphology of the *in situ* spores clearly differ. Acellular cuticles occur on many of the spore masses described in this work, and elsewhere (e.g. Wellman et al., 1998b; Morris et al., 2011b, 2012a). This acellular cuticle may be a homologous feature amongst a certain, as yet undefined group of early land plants, indicating a generic distinction from those plants that do not exhibit the feature.

Few, if any, of the features presented by the gross sporangial morphology of the *Emphanisporites* parent plants described here and elsewhere proffer firm indications of the plant affinities. Detailed discussion regarding the affinities of *Emphanisporites* producers can be found in Taylor et al. (2011) and Ball and Taylor (2022). Edwards and Richardson (2000) related the bifurcating spore mass to the Rhynie Chert plant *Horneophyton lignieri*, based on the shape of the sporangium and similarity of *in situ* spores, with *H. lignieri* yielding *E. decoratus* (Wellman et al., 2004) and cf. *Horneophyton* sp. yielding *E.* cf. *micrornatus*, which are both distally apiculate *Emphanisporites* spores. A tracheophytic affinity has recently been demonstrated for *H. lignieri* (Cascala-minanas et al. 2019), but whether cf. *Horneophyton* sp. was tracheophytic remains equivocal. Indeed, apart from the various sporangial morphologies and nature of *in situ* spores indicating that the parent plants were likely rhyniophytoids, little else can be discussed regarding the various affinities of these plants. Similarly, for those specimens which have been analysed ultrastructurally, little equivocal evidence regarding their affinities can be made, although a mixture of tracheophytes and possibly hornworts is possible (e.g. Taylor et al., 2011; Ball and Taylor, 2022).

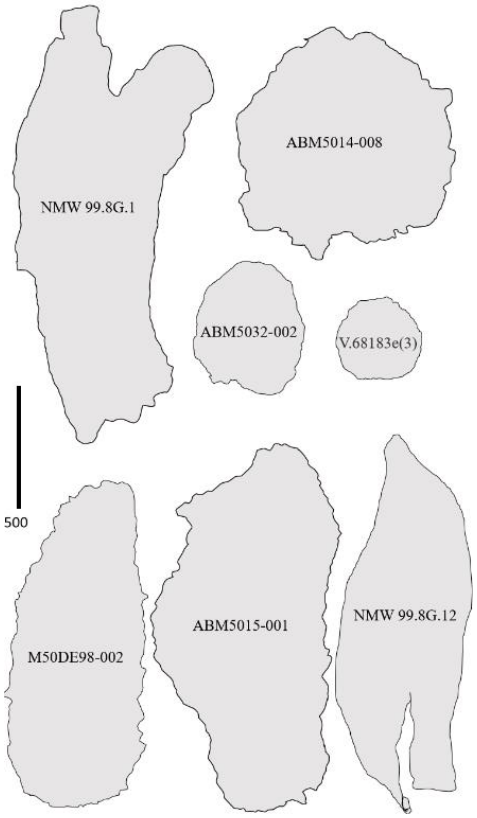

Figure V-11: Outlines of spore masses yielding the trilete spore genus Emphanisporites, *demonstrating the disparity of spore masses exhibited by the parent plants of the genus, which ranges from elongate bifurcating to discoidal.* ***A****: NMW 99.8G.1 cf.* Horneophyton *sp., yielding* E. *cf.* micrornatus. *Middle* micrornatus – newportensis *zone, North Brown Clee Hill, Edwards et al., 2000;* ***B****: ABM5014-008 discoidal spore mass, yielding E. sp., lower* micrornatus – newportensis *zone, M50 section, Ball and Taylor, 2022;* ***C:*** *ABM5032-002, discoidal spore mass yielding E. sp., lower* micrornatus – newportensis *zone, M50 section, this paper;* ***D:*** *V.618183e(3), discoidal sporangia yielding E. sp. A sensu Richardson and Lister, middle* micrornatus – newportensis *zone, North Brown Clee Hill, Morris et al., 2012;* ***E:*** *M50DE98-002, elongate spore mass yielding* E. *sp. 4 sensu Ball (Chapter III), lower micrornatus – newportensis zone, M50 section, this paper;* ***F:*** *ABM5015-001, elongate, ?bifurcating spore mass yielding* E. epicautus/ E. *cf.* epicautus, *lower* micrornatus – newportensis *zone, M50 section, Ball and Taylor 2022;* ***G:*** *NMW 99.8G.12* Salopella*-esque spore mass yielding E. sp. A sensu Richardson and Lister, Middle* micrornatus – newportensis *zone, North Brown Clee Hill, Edwards et al., 2000.* ***Scale bar 500µm****.*

Stellatispora

In the Anglo-Welsh Basin, species of *Stellatispora* are much reduced after the Ludlow (*poecilomorphus – libycus* zone), with a major decrease in *S. inframurinatus* var. *inframurinatus* (Burgess and Richardson, 1995), although the genus persists through the Přídolí and into the Earliest Devonian (Higgs, 2022; Chapter III). *S. inframurinatus* cf. var. *inframurinatus* occurs in the Earliest Lochkovian (*Apiculiretusispora sceacga* subzone) before being lost altogether in the dispersed record by the Early Lochkovian with the onset of the lower *micrornatus – newportensis* subzone. Indeed, the species recovered *in situ* here was not observed in the dispersed spore record from the sample from which these mesofossils were recovered. This suggests that, whilst the palynological record is generally much more representative of the taxonomic diversity of the vegetation, in some cases the diversity may not be fully represented. Turning to the spore mass, it is not possible to ascertain the original morphology of the sporangium given its fragmented nature, however it may have been elongate. No acellular cuticle is retained on the mass, suggesting that it may have been absent in life. As previously discussed, the association with trilete spores may suggest an affinity with the tracheophytes, but this is not certain. Given the size of the spore mass, and the likelihood that it was terminally arranged on the axis, it is probable that the plant was rhyniophytic in organisation. However, given the lack of definitive vascular tissue, the plant must be referred to as a rhyniophytoid.

Problems with assigning affinities

Typically, subtending axes are necessary to determine the nature of the conducting tissues and supply distinctive features for classification (e.g. Edwards, 1996; Edwards et al., 2014; Edwards et al., 2022a). Especially in the case of the M50 specimens, such subtending axes are rare and this immediately poses difficulties. Further problems arise with the decay or loss of features of sporangia due to taphonomy (5.1);

distinctive cellular arrangements may be lost and dehiscence mechanisms obscured, further reducing the possibility of a confident assignment. The shape of a sporangium may enable some discussion as to affinities (e.g. Wellman, 1999), but ultimately with the original morphological homogeneity, and subsequent loss of features associated with decay, transport and, to a lesser degree, burning, often one is left with pronounced difficulties in relating *in situ* taxa to contemporary plants, and to extant modern plants. These problems, and others, were neatly surmised by Edwards et al (1996) as "the palaeobotanical taxonomist's equivalent to clutching at straws" (Edwards et al., 1996 pg. 798). In this astute assessment, Edwards et al. (1996) included ultrastructural work, which while providing a useful means for comparison between coeval plants and lineage assessment, has some major caveats. Chief amongst these is the limited, although growing, database available for the comparison of a specimen's ultrastructure to other fossil taxa and to modern taxa. This problem is further compounded by problems with understanding modern and fossil spore ontogeny, although this has been built on from earlier work (e.g. Brown and Lemmon, 1990) by the work of, amongst others, Wellman (2004) and Brown et al. (2015), but comparisons between fossil and modern spore wall ultrastructures remain problematic (e.g. Taylor et al., 2011; Ball and Taylor, 2022). The database spore wall ultrastructural database has slowly grown since Edwards et al. (1996), with numerous prominent species having now been assessed ultrastructurally (e.g. table 2 in Edwards et al., 2014). Dispersed spores can also be assessed ultrastructurally in attempts to determine the affinities of spore species (e.g. Taylor, 2002; Taylor and Johnson, 2005; Taylor et al., 2011, 2017), although the morphology of the parent plant remains equivocal, and the other challenges discussed above and below are also prevalent irrespective of whether the spores are *in situ* or dispersed. The problems posed by the limited (although growing) ultrastructural database are compounded by an incomplete understanding of the effects of diagenesis (e.g. Edwards et al., 1996; Taylor, 2005; Taylor et al., 2011; Ball and Taylor, 2022). This may result in the obliteration of ultrastructural features such as white line centered lamellae, making the spore wall ultrastructure appear homogenous. Further complicating this is differentiating diagenetic from ontogenetic effects, whereby the successive laying down of sporopollenin may result in an apparently homogenous spore wall ultrastructure (Wellman, 2004).

5.3. Fecundity and ecological considerations

Modern bryophytes are extremely efficient spore dispersers, utilising wind to transport spores which measure between 10 - 20µm considerable distances (Patino and Vanderpoorten, 2018). Adaptation to dispersal by wind in spores is indicated where diameter is less than 25µm in diameter (Morgenson, 1981), with spores predicted to be able to persist suspended in turbulent air according to Stoke's law where the amb diameter is <50µm. As such, it is likely that most of the *in situ* spores recorded here, and dispersed spores recorded from the sequence, were capable of wind dispersal. Following initial dispersal and deposition, spores may then be further transported by fluvial action (e.g. Traverse, 2009).

Such ability for wind and water dispersal means that spores may be transported considerable distancs from the source plant. Nonetheless, spore distribution demonstrates a leptokurtic pattern from the mother sporophyte; that is, there is a high density of spore deposition close to the source plant (e.g. McQueen, 1985; Suderstrom and Johnson, 1989) with a high deposition occurring through to substantial distances (Morgenson, 1981). However, bryophyte spore deposition curves typically show long, fat tails away from the source (Sundberg, 2005; Patino and Vanderpoorten, 2018), deposition of a few spores occurring at considerable distance form the source plant. In combination with these long-tailed curves, investigations have also demonstrated that only a small proportion of spores are deposited immediately adjacent to the source plant, for example, Sundberg (2005, their fig. 2) found that often <20% of *Sphagnum* spores are deposited within 1 m of the source plant, with a sharp increase and then lectotypic cumulative spore

deposition within 3 m of the source plant. Lane et al. (1982) studied spore dispersal in another moss, *Atrichum*, and while recording again a leptokurtic pattern as for that in *Sphagnum*, they found that 97% of the dispersed spores fell within 2 m of the source plant, with 1% of spores recorded at the farthest distance measured (15 m).

Spore dispersal amongst many extant bryophytes is often facilitated and advanced by sporangial mechanisms such as explosive dehiscence or elaters, the former occurring in *Sphagnum.* Others are more passive, such as *Atrichum*, which disperses spores as a 'pepper shaker' (Ingold, 1959), driven by external forces on the sporangium. Evidence for such mechanisms in the late Silurian – Early Devonian land plants is not forthcoming. Some dehiscence mechanisms are recorded in sporangia from these early land plants, such as *Cooksonia*, but these typically appear more passive, with dispersal occurring by disintegration of part of the sporangia or via splitting along predetermined dehiscence lines (e.g. Gonez and Gerrienne, 2010). Such mechanisms may suggest that a greater proportion of spores were deposited adjacent to the source plant than in extant bryophytes as in *Atrichum*, and Steemans et al. (2007) considered that most of the liberated spores of late Silurian – Early Devonian land plants settled rapidly via gravity close to the source plant (>95%). With the diminutive height of the late Silurian – Early Devonian sporophytes, the ability of spores to become entrained in air currents may have been limited, although on the other hand, the lack of air current impediment from tall plants may have allowed incorporation of spores into air currents (Steemans et al., 2007). No cumulative deposition curves have been calculated for spores of this age, but they are likely to be lectotypic also, considering their ability to be transported great distances by wind and/ or water based on similar patterns for modern bryophyte spores of similar dimensions. Given the proportion of spores deposited locally to the source plant, it is probable that the ambient spore rain largely reflects local vegetation.

Wellman et al. (2003) described a spore fragment from the Ordovician of Libya, containing *in situ Tetrahedraletes medinensis*, and estimated that a discoidal spore mass <1mm in diameter containing those spores could contain *c.* 95,000 spore tetrads. The dimensions of the spore mass were selected based on comparisons with extant bryophytes and Silurian land plant spore masses and sporangia (Wellman et al., 2003). Edwards et al. (1996) later posited that the density of spores released by a single sporangium of these dimensions may suggest that the plant would have been well adapted to colonizing stressful environments, possibly as a pioneering plant. It is of some interest to explore the fecundity of the spore masses reported here, setting the results in context with the dispersed spore record and comparing the spore yield to Wellman's et al. (2003) spore mass as a benchmark as a possible ecological signal. Because many of the spore masses are fragmentary, estimates of their fecundity should be treated with some caution, but they do represent a minimum spore content of a spore mass (fig. 12a) Estimates for spore contents in *Paracooksonia*, *Lenticulitheca*, additional *Scylaspora*, *Emphanisporites* and *Tetrahedraletes* are given in fig. 12b (Wellman, 1996; Wellman et al., 2003; Morris et al., 2011b; Ball and Taylor, 2022), and compared/ integrated with some of the more complete M50 specimens described here. Notable caveats with these estimates are: (1) assumption of perfect packing, (2) use of mean amb size, and (3) estimates for partially incomplete spore masses. Highly fragmentary 'pieces' of spore mass, such as sample ABM5029-002 (yielding *S. newportensis*), are not considered here.

Spore masses yielding *Ambitisporites* have one of the highest median values for estimated number of spores in a single spore mass, with the greatest number being derived from the elongate spore mass (ABM5020-001). The 'spoon shaped' spore mass (ABM5014-004) overlaps with the upper quartile of estimates from *Paracooksonia*, which are derived in part from estimates of *P. ambitispora*. The median of *Ambitisporites* spore masses corresponds closely to the estimate for *Tetrahedraletes* sp. (Wellman et al., 2003). However, the 'spoon-shaped' spore mass (ABM5014-004), which is closest in shape and size to the *Tetrahedraletes* spore mass yields considerably fewer spores.

Spore masses yielding *Aneurospora* do not typically match the estimated volume of spores produced by the *Tetrahedraletes* fragment unless they are large. The estimates for *Aneurospora* yielding spore masses correspond closely to estimates for the *Paracooksonia* group, which includes *P. apiculispora*, and also overlap the lower estimates for similarly sized and shaped *Ambitisporites* spore masses. Estimates for *Emphanisporites* show a wide range, although the division is not as clear as discoidal and elongate spore masses. Specimen M50DE98-002, which is elongate, has an estimated spore contents of *c.* 187,900 spores, which is considerably greater than the estimates for the other elongate *Emphanisporites* yielding mass (ABM5015-001), at *c.* 25,000 spores. The latter measurement corresponds more closely with the estimates for the other *Emphanisporites* spore masses. ABM5014-008 (Ball and Taylor, 2022), approaches a similar size to that posited *Tetrahedraletes* spore mass, and contains far fewer spores, *c.* 3180. However, ABM5032-002 is essentially complete and yields a considerably greater number of spores relative to ABM5014-008, despite its diminutive size. The *Hispanaediscus* spore mass yields a comparable spore estimate to the larger *Tetrahedraletes* specimen, yielding an estimated 101,100 spores compared to *c.* 95, 000 (Wellman et al., 2003). Indeed, the *Hispanaediscus* spore mass has a greater estimated yield than most other similarly shaped spore masses yielding other *in situ* spore genera. Furthermore, the spore mass has a similar yield to some elongate spore masses, although such masses are typically less complete. *Laevolancis*

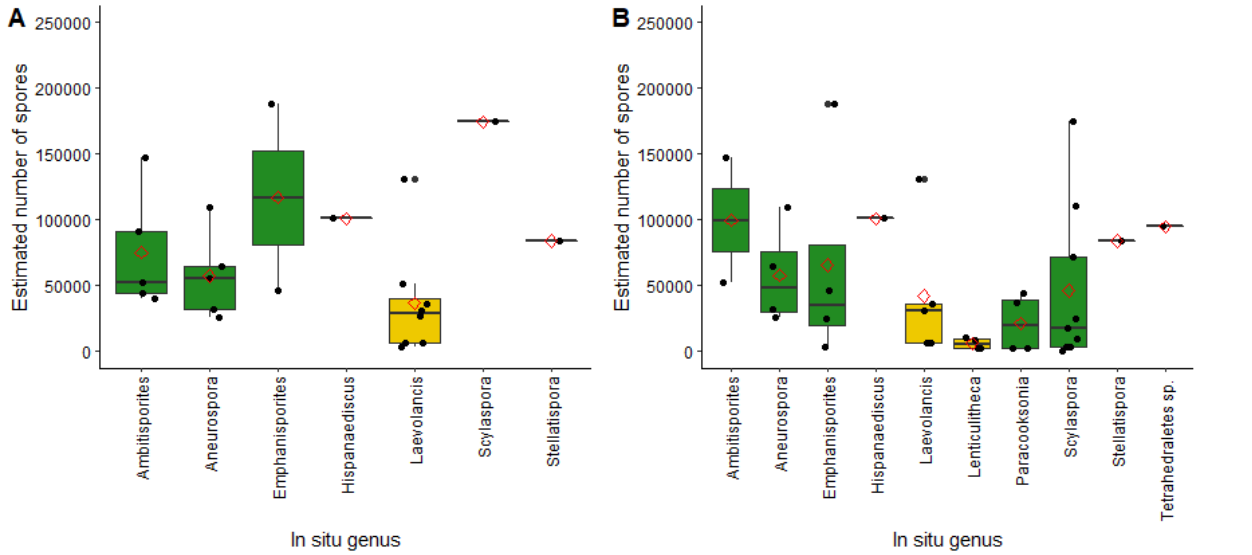

Figure V-12: estimated spore yield for spore masses. ***A:*** *spore masses reported in this paper.* ***B:*** *spore masses in this paper compared and combined with selected spore masses recorded in other research. Emphanisporites estimates integrated with Ball and Taylor (2022). Lenticulitheca and Paracooksonia estimates from Morris et al. (2011). Scylaspora estimates integrated with estimates from Wellman (1996). Tetrahedraletes estimate from an Ordovician plant fragment Wellman et al. (2003), and is used a benchmark for a possible pioneering land plant. Green: trilete spires; Gold: cryptospores; red diamond: mean estimated spore number. Data in thesis appendix 5.3.*

yielding spore masses generally do not yield > *c.* 50, 000 spores, although the estimate for ABM5023-003, at *c.* 131,200 spores is considerably greater. Such a yield in comparison with similar sized and shaped *Laevolancis* spore masses is likely a function of the smaller mean amb size of the spores. In general, *Laevolancis* spore masses do not yield on a similar scale to *Tetrahedraletes*. Spore masses assigned to *Lenticulitheca* (Morris et al., 2011b), have a narrow, low range of estimated spore yield, which overlaps slightly with the lower quartile of *Laevolancis* and *Lenticulitheca* spore masses. *Lenticulitheca* spore masses exhibit the lowest median yield of any of the spore masses examined here. As already mentioned, spore masses assigned to *Paracooksonia* overlap with morphologically similar *Ambitisporites* and *Aneurospora* yielding spore masses, and the bottom estimates for *Paracooksonia* overlap with the estimates

for *Lenticulitheca*. It is interesting that the interquartile range and median for estimated spore yield in *Paracooksonia* is closely similar to estimates for *Laevolancis*. *Scylaspora* spore masses have a wide range, with estimated yields of up to 200,000 spores. Many of the estimates, however, cluster below 50,000 spores. This is a result of many of the *Scylaspora* spore masses being fragmentary. Because of proposed continuity in morphology of these spore masses (i.e., all were likely elongate), these lower values should be treated as bottom estimates. Following this, the elongate *Scylaspora* yielding spore masses had a typically much higher estimated yield than many of the other spore masses, particularly discoidal masses. Finally, *Stellatispora*, derived from another elongate spore mass, shows an estimated yield of *c.* 100,000 spores. This is less than many of the more complete *Scylaspora* yielding spore masses, but the *Stellatispora* mass is somewhat smaller. Some general patterns emerge from this basic analysis. Firstly, elongate spore masses generally yield considerably greater numbers of spores than discoidal spore masses. This is not always the case, however, as some elongate masses yield similar estimates of spores as discoidal spore masses (e.g. *Emphanisporites*), whilst some discoidal spore masses are capable of yielding great numbers of spores (e.g. *Tetrahedraletes* and *Hispanaediscus*).

Such spore numbers in individual sporangia are comparable to extant bryophytes. In *sphagnum*, which often have similarly sized spores and spore capsules to the Early Devonian plants described here, spore content can range between 18,500 – 217,000 (Sundberg and Rydin, 1998); similar to the estimated spore number in the Early Devonian sporangia. Other species, such *Atrichum*, produce up to 450,000 spores (Kreulen, 1972). There does not appear to have been a study investigating whether the number of spores per sporangia is increased in colonizing bryophytes, but Ryoma and Laaka-Lindberg (2005) note that effective colonization potential is vital for such bryophytes, which includes high spore production.

What, if anything, can be drawn from the observations above and in fig. 12 a, b with respect to the ecology of the parent plants, *sensu* Edwards et al. (1996) One major issue is that, with such fragmentary mesofossils alone, it is impossible to ascertain how many terminal sporangia any one plant may have had. Therefore, it is not possible to surmise the fecundity of a plant based on spore yield estimates from one sporangia nor suggest that one plant had a greater spore output than another. In the eophytes, axes typically dichotomise, sometimes several times. Putatively more basal specimens, from what may be the same plant, may exhibit > 10 axes, which presumably will have led to numerous bifurcations (Edwards et al., 2022). *Cooksonia paranensis* another rhyniophyte, has been recovered as a group of five bifurcating sporophytes attached to a putative basal gametophyte (Gerrienne et al., 2006). Other terminal sporangia may have been terminated a simple, unbranched sporophyte, as they do in modern bryophytes. Such modern plants may have several sporophytes per plant, and it is perhaps not such a great leap of the imagination that some early land plants were comparable, although this remains speculative.

While it is not possible to confidently resolve the overall fecundity of a plant, broad ecological interpretations may be possible using the *Tetrahedraletes* sp. described by Wellman et al. (2003) as a benchmark for a putative pioneering plant in combination with the mesofossil and dispersed spore record. The latter follows Edwards and Richardson (2000), who fielded a rationale to gauge taphonomic and palaeoecological effects (table 2) in order to interpret the paucity of dispersed and *in situ Emphanisporites* spores. This rationale can be used to consider the broad ecologies of some of the mesofossils and their *in situ* spores are described here.

Possible cause of under representation	Effect on dispersed spore record
Plants living outside of river catchment areas and hence rarely entrained in deposited sediment.	Dispersed spores would be represented in the spore rain but would be swamped out by local plants.
Plants occupied restricted ecological niches and were hence rare in local vegetation.	Sporadic to no representation of dispersed spores from assemblages in local geographical areas.

The plants lacked recalcitrant biopolymers in their vegetative tissues, prohibiting fossilisation	The plants would be represented in the dispersed spore record dependent on local numbers and proximity to depositional environments.

Table V-2: Rationale of Edwards and Richardson (2000) outlining ecological and taphonomic impacts on the dispersed spore record.

Several spore masses have estimated spore yields which are greater than that of the *Tetrahedraletes* sp., although these spore masses are typically larger and are therefore not comparable. Most similar in dimensions and estimated spore yield is the *Hispanaediscus* cf. *verrucatus* yielding spore mass, which may tentatively suggest a similar ecology for these plants. *H. verrucatus* comprises <1% of the dispersed spore assemblage, suggesting that the plants may have lived outside of river catchment. The spore occurs in low proportions across the basin in other coeval localities and was thus unlikely to be confined to a specialised niche. Nonetheless, the possibility that the plant grew outside of river catchment may suggest habitation in a stressed setting, with stressors perhaps related to drought. The high estimated yield of the *H.* cf. *verrucatus* spore mass may therefore be an adaption to such stressed settings. The occurrence of the spore mass in this depocenter is likely due to transport, perhaps via ephemeral channels draining interfluvial areas (Allen and Williams, 1979).

Perhaps surprising is the low estimated spore yield from *Laevolancis* spore masses. One might expect that such a cosmopolitan and long ranging cryptospore would be well adapted for colonizing a variety of settings, including stressed areas. *Laevolancis divellomedium – plicata* is always well represented in the dispersed spore record, suggesting that the parent plant/ plant complex was (1) abundant in the depositional environment, and (2) growing close the site of deposition, and was therefore suited to colonizing equable settings despite competition from a growing diversity of trilete spore producing plants. It is also of note that those *Laevolancis* spores <25µm will have been readily dispersed by air currents, bu as mentioned, most spores are posited to have been deposited close to the source plant (Steemans et al., 2007). It is possible that these *Laevolancis* producers colonized temporarily stable environments living out rapid lifecycles before seasonal devastation (Wellman et al., 2000). The common occurrence of *Laevolancis* yielding spore masses in the M50 assemblage and elsewhere in the basin may lend some partial support to this interpretation, although transportation and mixing of vegetation from a variety of habitats must also be considered. Spores of the *Ambitisporites avitus – dilutus* complex are also common in the dispersed record and occur across coeval localities, and therefore have a similar broad palaeoecological interpretation to *Laevolancis*.

Other plants may have been growing outside of immediate catchment of rivers and are likely to have been transported in from various habitats. The elongate spore masses of *Scylaspora* yield some of the highest numbers of spores for sporangia included in these calculations. Conversely, the spores produced by these plants (*Scylaspora* sp.) are comparatively rare, with the genus comprising <2% of dispersed spore assemblages. Furthermore, their occurrence is sporadic, principally being confined to the M50 locality (Chapter III). A question is posed, then, that if the plants were capable of producing such vast volumes of spores from a single sporangium, why are dispersed *Scylaspora* so rare in the palynological record? The first point could in large part be attributable to the paleoecology of the plant (table 2), with the rare occurrence of dispersed spores indicating growth away from the main catchment of rivers. If the plant grew outside of river catchment, then, why does the spore mass occur in this mesofossil assemblage? This is almost certainly due to transport. If the hypothesis that the parent plant was growing outside of the catchment areas of rivers is borne out, then the remains of the *Scylaspora* parent plant must have been transported to the depocenter, by one or a combination of transport mechanisms discussed earlier (5.1). in this manner, the parent plant could have been carried a considerable distance from the original growth site (e.g. Scott, 2010). The recovery of several similar sporangial remains containing *in situ Scylaspora* by Wellman (1999) may suggest that there was a repeated influx of *Scylaspora* sporangia to the depocenter

where they were preserved (e.g. via a repeatedly activated ephemeral channel) or there was a single influx of the remains of the same or group of *Scylaspora* producing plants.

The ecology of *Emphanisporites* producers has been discussed elsewhere (Edwards and Richardson, 2000; Ball and Taylor, 2022). The paucity of *Emphanisporites* species in the dispersed spore record and scarce occurrence in the mesofossil record has been used to suggest growth outside of river catchment, with some species being confined to restricted ecological niches (e.g. Edwards and Richardson, 2000). Interestingly, there are some *in situ Emphanisporites* spores that are not known in the dispersed spore record, suggesting that these remains were transported some distance from their growth site, where their dispersed spores no longer make up part of the ambient spore rain. Others, like *Scylaspora*, are likely to have been delivered from areas away from the immediate depositional center, but still within their spore catchment.

Species of *Cymbohilates*, while becoming increasingly common in the dispersed record through the *micrornatus – newportensis* zones, remain relatively rare in the dispersed record. *In situ* species are commonly reported from the middle *micrornatus – newportensis* Brown Clee Hill assemblage (e.g. Morris et al., 2011b, 2012a), but only a single specimen was recovered from the lower *micrornatus – newportensis* M50 section. The paucity of dispersed spores may suggest that *Cymbohilates* parent plants were growing outside of the catchment of rivers around the M50, indeed, they are prevalent in the Brown Clee Hill assemblages, but this may be due to a higher intensity of research in that area. It remains possible that these *Cymbohilates* producers, including *Lenticulitheca* spp., preferentially grew in relatively more upland floodplains, represented by Brown Clee Hill and the upper parts of the M50 section. However, whilst there is a 4 – 8% increase in the proportion of the genus through the lower – middle MN M50 section (lower to middle *micrornatus – newportensis*, Chapter III), the change is not considerable. In addition, there is little change between lower and middle MN *Cymbohilates* proportions in Ammons Hill and Clee Hill assemblages. The increasing proportion of *Cymbohilates* may also be due to a proliferation of the genus towards the middle MN zone, with gradual colonization of settings closer to depocenters.

5.4. Embryophytic and non-embryophytic ‘phytodebris’

Sterile and fertile axes and other fragmentary embryophytic remains occur in Ammons Hill and the M50 section, despite the exclusion of spore masses from the former. Most of the axial remains are posited to be derived from eophytes (*sensu* Edwards et al., 2022a, b), with key features such as longitudinal axial striations, stomata arranged about the base of sporangia (where present) and glaebules on the interior lumen of axial cells. While loose cryptospore dyads have not been recovered *in situ* from any of the remains, the axes are grouped with some confidence, although an unequivocal relationship cannot be made. The presence putative eophytes in both the M50 section and Ammons Hill indicates that this group of plants inhabited these, or nearby, areas alongside the plants evidenced by the spore masses described above. The presence of the axes reinforces the inferences of the dispersed record, where the presence of eophytes is indicated by the presence of dyads, including species of *Dyadospora*.

Interestingly, axes of plants of other affinities, such as tracheophytes, have not been recovered from the M50 at present, although this is likely due to limited targeted collection of sterile axes for this work. However, specimen M50PIN-1 elucidates a further facet of vegetation which, at present, has not been linked with dispersed spores.

The recovery of non-embryophytic organisms represented here by *inter alia*, *Nematothallus* and *Cosmochlaina*, give insights into another facet of the terrestrial biota which existed alongside miospore an cryptospore producing plants. Edwards and Kenrick (2015) discussed the presence of cryptogamic covers in Early Devonian ecosystems and suggested that the covers may have been comparable in gross composition to extant examples, containing fungi, lichens algae and bryophytes, *inter alia*. These cryptogamic covers likely covered large areas (Strother, 2010), and their components probably played an

important role in the carbon cycle. The recovery of *Pachytheca* and *Cosmochlaina* from Ammons Hill points towards the presence of algae and lichens, respectively, although whether the latter were involved with fungi is not certain (Edwards et al., 2013). Other nematophytes from NBCH have been related to fungi and lichenized fungi (Honegger et al., 2013; Wellman and Ball, 2021), although the remains of these organisms are yet to be recovered from the assemblages explored here. The presence of *Prototaxites* in the M50 and Ammons Hill remains equivocal from the mesofossil record, although it has been recorded from elsewhere in the Anglo-Welsh Basin as body fossils and as 'rooting' structures (Hillier et al., 2008; Morris et al., 2012b).

5.5. Implications of wildfire

The interaction between wildfire and late Silurian and Early Devonian vegetation is well-documented (e.g. Wellman et al., 2000; Edwards and Axe, 2004; Edwards and Richardson, 2004; Glasspool et al., 2004, 2006; Glasspool and Gastaldo, 2022), and the results of the reflectance study have implications for the ecology of the plants and for atmosphere. The recovery of a further two charcoalified mesofossil horizons adds to the relatively rare record of Early Devonian wildfire (Scott, 2010). The low temperature fires indicated by the low reflectance values encountered in the M50 and Ammons Hill assemblages indicate that in most cases the fires were smoldering or short lived with insufficient intensity to completely char the plant remains. Low temperature fires, producing semi-fusinite with low reflectance values, are in common with values obtained from the Přídolí Ludlow Lane and mid Lochkovian Brown Clee Hill assemblage (Glasspool et al., 2004, 2006). These short lived or low intensity fires may have been derived from a low level of embryophytic fuel load, with a limited litter layer and high-water content living embryophytes and lichens, *inter alia* (Glasspool and Gastaldo, 2022) and may have been typical of late Silurian – Early Devonian wildfires. Ludlovian nematophytes have also been interpreted to have been derived from low temperature wildfires, although earlier Silurian (Homerian) fires may have burned at up to 800°C (Glasspool and Gastaldo, 2022). The interpretation of the M50 assemblage was that, for the most part, the mesofossils were derived from the litter layer, having already been partially decayed. It is possible that the fires were ignited and fueled in large part by the seasonally dried litter layers, which allowed charring of living hydrophilic vegetation (Glasspool et al., 2004). The bipolar reflectance scores of the Ammons Hill section may implicate two sperate fire events of different temperatures. Meanwhile, the spread of reflectance scores in the M50 may suggest that a low proportion of material burned at a higher temperature, perhaps implicating that the higher reflectance temperature was closer to, or formed the locus of, the fire. Other scenarios remain possible for both assemblages, and a detailed survey of the systematics of the measured particles would be useful to identify whether a common affinity amongst higher reflectance particles exists. Glasspool et al. (2006) found that *Prototaxites* and *Pacytheca* were typically more charred than the rhyniophytic remains, and those authors suggested that *Prototaxites* logs may have formed the nucleus of the fire event. The occurrence of wildfires in terrestrial ecosystems will have contributed phosphorous to terrestrial and marine systems, providing nutrients to a suite of organisms. In marine settings, this input will have contributed to increases in atmospheric oxygen concentration pO_2 through marine algal blooms (Kump, 2014).

The pO_2 of the late Silurian and Early Devonian can be estimated via several models (Glasspool and Gastaldo, 2022), and the presence of charcoal permits the testing of the efficacy of these models in predicting pO_2 at the time of charcoal Formation. Charcoal is an effective proxy for indicating pO_2 at the time of burning (Belcher et al., 2010; Glasspool, 2015), providing a minimum threshold required for sustained burning (Belcher and McElwain, 2008), which is 16% pO_2, or 0.75 of present atmospheric oxygen level (PAL) (Cope and Chaloner, 1980; Chaloner, 1989), and constraining pO_2 in the range of 0.7 – 1.4 PAL (Belcher et al., 2010). The three principal models, GEOCARBSULF model (Berner et al., 2009), the

COPSE-reloaded model (Lenton et al., 2018), and the GEOCARBSULFOR model (Krause et al., 2018), were compared with Glasspool and Gastaldo's (2022) Silurian charcoal deposits, and they found that the estimations of the Berner (2009) model were the most accurate for predicting the Silurian pO_2. GEOCARBSULFOR and GEOCARBSULF both predict pO_2 over the minimum 16% threshold for sustained burning, at 18.5% and 24% respectively. The COPSE-reloaded model predicts PO_2 at 15%. Belcher et al. (2010) developed a scale for predicting burn probability related to pO_2. At the 15% pO_2 predicted by the COPSE-reloaded mode, burn probability *sensu* Belcher et al. (2010) is <3.3%. Meanwhile, the burn probabilities for the GEOCARBSULFOR (pO_2 = 18.5%) and GEOCARBSULF (pO_2 = 24%) models have burn probabilities of *c.* 10 % and >94% respectively. Considering the fuel that these fires would be burning is useful when deliberating the accuracy of these models. Dry fuels require a 16% pO_2 threshold to ignite and sustain burning (Belcher et al., 2010). Where rainfall is low and or the area is seasonally dry, the pO_2 threshold for ignition and burning is *c.* 18% (Belcher et al., 2010). While Belcher et al. (2010) found that moss charred at pO_2 >15%, the high-water content of late Silurian – Early Devonian embryophytes and lichenized fungi, *inter alia*, may have precluded burning until pO_2 >18% (Belcher et al., 2010; Glasspool and Gastaldo, 2022). Even where dead and possibly seasonally dried, or temporarily dried tissues were burned, the latter in poikilohydric eophytes (Edwards et al., 2022a), the latent moisture content may have precluded fires until *c.* 18%. Low temperature fires may be indicative of lower pO_2, or of low availability of poor-quality fuels. Both may have facilitated the low reflectance and low implicated fire temperatures, but the former may be countered by the increasing occurrences of charcoalified horizons from this time, which may suggest pO_2 was relatively high and facilitated more common wildfire events.

6. Conclusions

- Two mesofossil horizons from the lower MN biozone (Early Lochkovian) are presented. Vitrinite reflectance confirms that the fossils from both were formed by low temperature wildfires. The presence of charcoal derived from the hydrophilic vegetation indicates that pO_2 must have exceeded 16% and was likely greater than 18% (Belcher et al., 2010). As such, the GEOCARBSULF (Berner, 2009) box-model predicting pO_2 may most accurately reflect pO_2 in the early Lochkovian.

- The M50 section has yielded 29 spore masses with 16 different *in situ* trilete spore and cryptospore species. *Laevolancis* is the most common *in situ* spore, with *Aneurospora*, *Ambitisporites* and *Emphanisporites* species also having a good recovery rate. Most of the major dispersed species, are recorded, but other prominent species such as *Archaeozonotriletes* persist in their absence from the *in situ* spore record. Many of the *in situ* spores recovered in the M50 are comparable to species that are rare in the dispersed spore record of the same sample, suggesting transportation of the spore masses. In addition to *in situ* spores, terrestrial arthropod coprolites and sterile axes are also recorded from the M50. While nematophytic remains are present in the dispersed record, charcoalified remains of these non-embryophytic phytodebris are not present in the M50. Meanwhile, the Ammons Hill section yields an abundance of charcoalified nematophytes and non-embryophytes, in addition to 'fertile' and sterile plant axes but *in situ* spores or spore masses have been recovered, despite a rich assemblage of dispersed trilete spores and cryptospores.

- The Ammons Hill and M50 assemblages were likely both influenced by taphonomy and transportation. Given the absence of exceptionally preserved mesofossils which exhibit, *inter alia*, sporangial tissues, and the presence of likely (e.g. interdigitating tubes) and putative (e.g. pits in sporangial cuticles) decay indicators in spore masses, it is probable that the plant fossils were burned after death as part of the

litter, following a period of partial decay. The difference in composition between the M50 and Ammons Hill is attributed to taphonomy and transport, which may be a result of the variation in the tissues and their response to burning between embryophytes and non-embryophytes, including nematophytes. The Brown Clee Hill assemblage exhibits both embryophytic and non-embryophytic remains, and this may be due to the proximity to the source of the fire.

- Early Lochkovian vegetation comprised tracheophytes, eophytes and other cryptospore bearing plants, which were diminutive and rhyniophytic. Several of the *in situ Laevolancis* spore masses were comparable to each other and are reminiscent of *Lenticulitheca* spore masses (Morris et al., 2011b) and Wellman's et al. (1998b) groups. A new bivalved arrangement is shown for one *Laevolancis* producer. The *Hispanaediscus* spore mass is reminiscent to those of *Cooksonia* and may form a lineage with species of *Cooksonia* which produce verrucate trilete spores such as *Synorisporites verrucatus*, similar to the relationship suggested by Edwards et al. (2014) for the *Lenticulitheca – Paracooksonia – Cooksonia* complex. Spore masses yielding *Cymbohilates*, *Aneurospora* and *Ambitisporites* may be comparable to *Lenticulitheca* and *Paracooksonia* species with respects to the similar sporangial morphology and co-occurring *in situ* spores. Others may be more comparable to *Cooksonia*. The new *in situ Emphanisporites* specimens further add to the sporangial diversity observed amongst this morphogenus. Finally, while the affinities of *Stellatispora* remain uncertain, it has been shown that the spore was derived from a probably rhyniophytic parent plant with an elongate, terminal sporangium. Ultrastructural analysis would be beneficial to advance discussions on the affinities of these *in situ* spores and their parent plants.

- Wellman et al. (2003) reported an *in situ Tetrahedraletes*, which was suggested by Edwards et al. (1996) to show indications of being adapted as a colonising or founding plant. The spore mass dimensions and spore yield of spore masses recovered in this work, and from other publications (e.g. Morris et al., 2011a; Wellman, 1999) were calculated and compared to Wellman's et al. (2003) *Tetrahedraletes* specimen. Most of the spore masses with a greater estimated number of *in situ* spores are considerably larger than the *Tetrahedraletes* spore mass, but the *Hispanaediscus* yielding spore mass, which was of a similar morphology and dimensions, yielded a similar number of estimated spores. This might indicate some level of adaptation to invading inequable habitats based on the vast number of spores produced by a single spore mass, but such deliberations have a number of caveats. Broader ecological implications may be ascertained by integrating the dispersed spore record and mesofossil record. The paucity and sporadic occurrence of *Scylaspora* sp. 1 and some *Emphanisporites* species, including those investigated here, may suggest restriction to a niche outside of river catchment. Meanwhile, other *Emphanisporites* species, such as *E, epicautus* (Ball and Taylor, 2022) and *Hispanaediscus*, may have existed across less restricted niches, but outside of the general catchment of rivers. The parent plants of *Laevolancis* and *Ambitisporites*, meanwhile, appear to have been widespread in areas within river catchment, but ultrastructural work may produce a more nuanced understanding of the distribution of these species.

Acknowledgments

M50 material was provided Dianne Edwards and Lindsay Axe at Cardiff University. Ammons Hill material was provided by the British Geological Survey. Further materials for dispersed spore analysis were provided by the Micropaleontological Unit at the Natural History Museum, London, The British Geological Survey, Cardiff University and the University of Sheffield collections. Margaret Collinson, Neil Holloway and Sharron Gibbons are thanked for their processing and assistance of the vitrinite reflectance portion of

this work at the Earth Sciences dept. at Royal Holloway, University of London. SEM studies were carried out at the University of Sheffield Electron Microscopy Unit. Charles Wellman, Paul Kenrick, Stephen Stukins and John Richardson are thanked for their useful comments on early drafts of this manuscript.

Bibliography

ALLEN, J.R.L. & DINELEY, D.L. 1976. The succession of the Lower Old Red Sandstone (Siluro-Devonian) along the Ross-Tewkesbury Spur Motorway (M. 50), Hereford and Worcester. *Geological Journal*, **11** (1), 1 – 14.

ALLEN, J.R.L. AND TARLO, L.B., 1963. The Downtonian and Dittonian facies of the Welsh borderland. *Geological Magazine*, *100*(2), pp.129-155.

BALL, A.C. AND TAYLOR, W.A., 2022. Reconstructing the Lower Devonian (Lochkovian) vegetation from the Anglo-Welsh Basin: Two spore masses containing Emphanisporites McGregor spores. *Review of Palaeobotany and Palynology*, *301*, p.104647.

BARCLAY, W.J., RATHBONE, P.A., WHITE, D.E. & RICHARDSON, J.B., 1994. Brackish water faunas from the St Maughans Formation: The Old Red Sandstone section at Ammons Hill, Hereford and Worcester, UK, re-examined. *Geological Journal*, **29** (4), 369 – 379.

BARCLAY, W.J., DAVIES, J.R., HILLIER, R.D. AND WATERS, R.A., 2015. Lithostratigraphy of the Old Red Sandstone successions of the Anglo-Welsh Basin.

BROOKFIELD, M.E., CATLOS, E.J. AND SUAREZ, S.E., 2022. Vertebrate lies? Arthropods were the first land animals! *Geology Today*, *38* (2), pp.65-68.

BROWN, R.C., LEMMON, B.E., 1990. Sporogenesis in bryophytes. In: Blackmore, S., Knox, R.B. (Eds.), Microspores: Evolution and Ontogeny. Academic Press, London, UK, pp. 55–94.

BROWN, R.C., LEMMON, B.E., SHIMAMURA, M., VILLARREAL, J.C. AND RENZAGLIA, K.S., 2015. Spores of relictual bryophytes: diverse adaptations to life on land. *Review of Palaeobotany and Palynology*, *216*, pp.1-17.

BURGESS & RICHARDSON, J.B. 1991. Silurian cryptospores and miospores from the type Wenlock area, Shropshire, England. *Palaeontology*, **34** (3), 601 – 628. Pls.

BURGESS & RICHARDSON, J.B. 1995. Late Wenlock to early Prídolí cryptospores and miospores from south and southwest Wales, Great Britain. *Palaeontographica Abteilung B,* **236**, 1 – 44. Pls.

CASCALES-MIÑANA, B., STEEMANS, P., SERVAIS, T., LEPOT, K., GERRIENNE, P., 2019. An alternative model for the earliest evolution of vascular plants. Lethaia 52 (4), 445–453.

CATLOS, E.J., MARK, D.F., SUAREZ, S., BROOKFIELD, M.E., MILLER, C.G., SCHMITT, A.K., GALLAGHER, V. AND KELLY, A., 2021. Late Silurian zircon U–Pb ages from the Ludlow and Downton bone beds, Welsh Basin, UK. *Journal of the Geological Society*, *178*(1).

CHALONER & STREEL, M. 1968. Lower Devonian spores from South Wales. *Argumenta Palaeobotanica*, **1**, 87 – 101. Pls.

COHEN, K.M., FINNEY, S.C., GIBBARD, P.L. & FAN, J.-X. (2013; updated) The ICS International Chronostratigraphic Chart. Episodes 36: 199-204.

CRAMER, F.H. 1966. Palynology of Silurian and Devonian rocks in northwest Spain. *Boletín del Instituto Geológico y Minero de España*, **77**, 223-286.

CRAMER & DIEZ, M.D.C.R.1975. Earliest Devonian miospores from the Province of Leon, Spain. *Pollen et Spores*, **17**, 331 – 344. Pls.

EDWARDS, D.E. 1996. New insights into early land ecosystems: a glimpse of a Lilliputian world. *Review of Palaeobotany and Palynology*, **90** (3-4),159-174.

EDWARDS, D., AXE, L., 2004. Anatomical evidence in the detection of the earliest wildfires. PALAIOS 19, 113–128.

EDWARDS, D. AND KENRICK, P., 2015. The early evolution of land plants, from fossils to genomics: a commentary on Lang (1937)'On the plant-remains from the Downtonian of England and Wales'. *Philosophical Transactions of the Royal Society B: Biological Sciences*, *370*(1666), p.20140343.

EDWARDS D, ROGERSON ECW. 1979. New records of fertile Rhyniophytina from the late Silurian of Wales. Geological Magazine116: 93–98.

EDWARDS, D.E. & RICHARDSON, J.B. 2000. Progress in reconstructing vegetation on the Old Red Sandstone Continent: two Emphanisporites producers from the Lochkovian sequence of the Welsh Borderland. *Geological Society, London, Special Publications* **180** (1), 355-370.

EDWARDS, D., RICHARDSON, J.B., 2004. Silurian and Lower Devonian plant assemblages from the Anglo-Welsh Basin: a palaeobotanical and palynological synthesis. Geol. J. 39 (3–4), 375–402

EDWARDS D, DAVIES KL, AXE L. 1992. A vascular conducting strand in the early land plant *Cooksonia.* Nature 357: 683–685

EDWARDS, D., FANNING U., & RICHARDSON, J.B. 1994. Lower Devonian coalified sporangia from Shropshire: Salopella Edwards & Richardson and Tortilicaulis Edwards. Botanical Journal of the Linnean Society **116**, 89–*110*.

EDWARDS D, SELDEN PA, RICHARDSON JB, AXE L. 1995C. Coprolites as evidence for plant-animal interaction in Siluro-Devonian terrestrial ecosystems. Nature 377: 329–331.

EDWARDS D, DAVIES KL, RICHARDSON JB, WELLMAN CH, AXE L. 1996. Ultrastructure of Synorisporites downtonensis and Retusotriletes cf. coronadus in spore masses from the Pr̆ı́dolı́of the Welsh Borderland.Palaeontology39: 783–800

EDWARDS D, WELLMAN CH, AXE LP. 1999. Tetrads in sporangia and spore masses from the Upper Silurian and Lower Devonian of the WelshBorderland.Botanical Journal of the Linnean Society130: 111–156.

EDWARDS D, AXE L, MENDEZ E. 2001. A new genus for isolated bivalved sporangia with thickened margins from the Lower Devonian of theWelsh Borderland.Botanical Journal of the Linnean Society137: 297–310.

EDWARDS, D., RICHARDSON, J.B., AXE, L., DAVIES, K.L., 2012A. A new group of Early Devonian plants with valvate sporangia containing sculptured permanent dyads. Bot. J. Linn. Soc. 168 (3), 229–257.

EDWARDS, D., AXE, L. AND HONEGGER, R., 2013. Contributions to the diversity in cryptogamic covers in the mid-Palaeozoic: Nematothallus revisited. *Botanical Journal of the Linnean Society*, *173*(4), pp.505-534.

EDWARDS, D., MORRIS, J.L., RICHARDSON, J.B. & KENRICK, P. 2014. Cryptospores and cryptophytes reveal hidden diversity in early land floras. *New Phytologist* **202** (1), 50-78.

EDWARDS, D., MORRIS, J.L., AXE, L., DUCKETT, J.G., PRESSEL, S. AND KENRICK, P., 2022A. Piecing together the eophytes–a new group of ancient plants containing cryptospores. *New Phytologist*, *233*(3), pp.1440-1455.

EDWARDS, D., MORRIS, J.L., AXE, L., TAYLOR, W.A., DUCKETT, J.G., KENRICK, P. AND PRESSEL, S., 2022B. Earliest record of transfer cells in Lower Devonian plants. *New Phytologist*, *233*(3), pp.1456-1465.

EDWARDS, D., MORRIS, J.L., AXE, L. AND DUCKETT, J.G., 2022C. Picking up the pieces: New charcoalified plant mesofossils (eophytes) from a Lower Devonian Lagerstätte in the Welsh Borderland, UK. *Review of Palaeobotany and Palynology*, *297*, p.104567.

FANNING U. 1987. Late Silurian–Early Devonian plant assemblages in the Welsh Borderland. PhD Thesis, University of Wales (Cardiff).

FANNING U, EDWARDS D, RICHARDSON JB. 1992. A diverse assemblage of early land plants from the Lower Devonian of the Welsh Borderland. Botanical Journal of the Linnean Society109: 161–188.

GENSEL, P.G., 2008. The earliest land plants. *Annual Review of Ecology, Evolution, and Systematics*, pp.459-477.

GLASSPOOL, I.J. AND GASTALDO, R.A., 2022. Silurian wildfire proxies and atmospheric oxygen. *Geology*, *50*(9), pp.1048-1052.

GLASSPOOL, I.J., EDWARDS, D., AXE, L., 2004. Charcoal in the Silurian as evidence for the earliest wildfire. Geology 32, 381–38

GLASSPOOL, I.J., EDWARDS, D. AND AXE, L., 2006. Charcoal in the Early Devonian: a wildfire-derived Konservat–Lagerstätte. *Review of Palaeobotany and Palynology*, *142*(3-4), pp.131-136.

GONEZ, P. AND GERRIENNE, P., 2010. A new definition and a lectotypification of the genus Cooksonia Lang 1937. *International Journal of Plant Sciences*, *171*(2), pp.199-215.

GRAY, J., 1985. The microfossil record of early land plants; advances in understanding of early terrestrialization, 1970–1984. Phil. Trans. R. Soc. Lond. B 309, 167–195

HABGOOD KS. 2000B. Two cryptospore-bearing land plants from the Lower Devonian (Lochkovian) of the Welsh Borderland. Botanical Journalof the Linnean Society133: 203–227.

HIGGS, K.T., 2022. Palynology of the Freshwater East Formation (Upper Silurian, Přídolí), Pembrokeshire, South Wales, UK. *Palynology*, (just-accepted), p.2070785.

HILLIER, R.D. AND WILLIAMS, B.P.J., 2006. The alluvial old red sandstone: fluvial basins.

HOFFMEISTER, W.S., 1959. Lower Silurian plant spores from Libya. *Micropaleontology*, **5** (3), 331-334.

STRICKLAND, H.E. AND HOOKER, J., 1853. On the Distribution and Organic Contents of the "Ludlow Bone Bed" in the Districts of Woolhope and May Hill. With a Note on the Seed-like Bodies found in it. *Quarterly Journal of the Geological Society*, *9*(1-2), pp.8-12.

HONEGGER, R., EDWARDS, D. AND AXE, L., 2013. The earliest records of internally stratified cyanobacterial and algal lichens from the Lower Devonian of the Welsh Borderland. *New Phytologist*, *197*(1), pp.264-275.

JOHNSON, T.R. AND TAYLOR, W.A., 2005. Single grain analysis of the Late Silurian spore Cymbosporites echinatus from the Welsh Borderland. *Review of Palaeobotany and Palynology*, *137*(3-4), pp.163-172.

KENRICK, P., WELLMAN, C.H., SCHNEIDER, H., EDGECOMBE, D., 2012. A timeline for terrestrialization: consequence for the carbon cycle in the Palaeozoic. Philos. Trans. R. Soc. Lond. B 367, 519–536

LANG, W.H., 1937. IV-On the plant-remains from the Downtonian of England and Wales. *Philosophical Transactions of the Royal Society of London. Series B, Biological Sciences*, *227*(544), pp.245-291.

LAVENDER, K. & WELLMAN, C.H. 2002. Lower Devonian spore assemblages from the Arbuthnott Group at Canterland Den in the Midland Valley of Scotland. *Review of Palaeobotany and Palynology*, **118** (1-4), 157 – 180.

MARSHALL, J.E., LAKIN, J., TROTH, I., AND WALLACE-JOHNSON, S.M., 2020, UV-B radiation was the Devonian–Carboniferous boundary terrestrial extinction kill mechanism: Science Advances, v. 6, 0768.

MCGREGOR, D.C., 1961. Spores with proximal radial pattern from the Devonian of Canada. Geol. Surv. Can. Bull. 76, 1–11.

MCQUEEN, C. B. 1985. Spatial pattern and gene flow distances inSphagnum subtile./Bryologist 88: 333/336

MOGENSEN, G.S., 1981. The biological significance of morphological characters in bryophytes: the spore. *Bryologist*, pp.187-207.

MORRIS, J.L. AND EDWARDS, D., 2014. An analysis of vegetational change in the Lower Devonian: new data from the Lochkovian of the Welsh Borderland, UK. *Review of Palaeobotany and Palynology*, *211*, pp.28-54.

MORRIS, J.L., RICHARDSON, J.B., EDWARDS, D., 2011A. Lower Devonian plant and spore assemblages from Lower Old Red Sandstone strata of Tredomen Quarry, South Wales. Rev. Palaeobot. Palynol. 165 (3–4), 183–208.

MORRIS, J.L., EDWARDS, D., RICHARDSON, J.B., AXE, L., DAVIES, K.L., 2011B. New plant taxa from the Lower Devonian (Lochkovian) of the Welsh Borderland, with a hypothesis on the relationship between hilate and trilete spore producers. Rev. Palaeobot. Palynol. 167, 51–81.

MORRIS, J.L., EDWARDS, D., RICHARDSON, J.B., AXE, L. & DAVIES, K.L. 2012. Further insights into trilete spore producers from the Early Devonian (Lochkovian) of the Welsh Borderland, U.K. *Review of Palaeobotany and Palynology* **185**, 35– 63.

MORRIS, J.L., EDWARDS, D. & RICHARDSON, J.B. 2018. The advantages and frustrations of a plant Lagerstätte as illustrated by a new taxon from the Lower Devonian of the Welsh Borderland, U.K. *In* KRINGS, M., HARPER, C.J., RUBÉN CÚNEO, N. AND ROTHWELL, G.W. (Eds). Transformative Paleobotany. Academic Press, 49-67.

MORRIS, J.L. AND EDWARDS, D., 2014. An analysis of vegetational change in the Lower Devonian: new data from the Lochkovian of the Welsh Borderland, UK. *Review of Palaeobotany and Palynology*, *211*, pp.28-54.

NICHOLS, G.J., CRIPPS, J.A., COLLINSON, M.E. AND SCOTT, A.C., 2000. Experiments in waterlogging and sedimentology of charcoal: results and implications. *Palaeogeography, Palaeoclimatology, Palaeoecology*, *164*(1-4), pp.43-56.

PATIÑO, J. AND VANDERPOORTEN, A., 2018. Bryophyte biogeography. *Critical Reviews in Plant Sciences*, *37*(2-3), pp.175-209.

PUTTICK, M.N., MORRIS, J.L., WILLIAMS, T.A., COX, C.J., EDWARDS, D., KENRICK, P., PRESSEL, S., WELLMAN, C.H., SCHNEIDER, H., PISANI, D.,

DONOGHUE, P.C., 2018. The interrelationships of land plants and the nature of the ancestral embryophyte. Curr. Biol. 28 (5), 733–745.

RICHARDSON, J.B. 2007. Cryptospores and miospores, their distribution patterns in the Lower Old Red Sandstone of the Anglo-Welsh Basin, and the habitat of their parent plants. *Bulletin of Geosciences*, **82** (4), 355-364.

RICHARDSON, J.B. & LISTER, T.R. 1969. Upper Silurian and lower Devonian spore assemblages from the Welsh borderland and south Wales. *Palaeontology*, **12** (2), 201-245.

RICHARDSON, J.B. & MCGREGOR, D.K. 1986. Silurian and Devonian spore zones of the Old Red Sandstone Continent and adjacent regions. *Geological Survey of Canada, Bulletin* **364**, 1– 79.

RICHARDSON, J.B., FORD, J.H. & PARKER, F. 1984. Miospores, correlation and age of some Scottish Lower Old Red Sandstone sediments from the Strathmore region (Fife and Angus). *Journal of Micropalaeontology*, **3** (2), 109-124.

RYÖMÄ, R. AND LAAKA-LINDBERG, S., 2005. Bryophyte recolonization on burnt soil and logs. *Scandinavian Journal of Forest Research*, *20*(S6), pp.5-16.

SALAMON, S.A., GERRIENNE, P., STEEMANS, P., GORZELAK, P., FILLIPIAK, P., HÉRISSÉ A, L.E., PARIS, F., CASCALES-MIÑANA, B., BRACHANIEC, T., MISZ-KENNAN, M., NIEDZWIEDZKI, R., 2018. Putative late Ordovician land plants. New Phytol. 218, 1305–1309.

SERVAIS, T., CASCALES-MIÑANA, B., CLEAL, C.J., GERRIENNE, P., HARPER, D.A. AND NEUMANN, M., 2019. Revisiting the Great Ordovician Diversification of land plants: Recent data and perspectives. *Palaeogeography, Palaeoclimatology, Palaeoecology*, *534*, p.109280.

SCOTT, A.C., 2010. Charcoal recognition, taphonomy and uses in palaeoenvironmental analysis. *Palaeogeography, Palaeoclimatology, Palaeoecology*, *291*(1-2), pp.11-39.

SCOTT, A.C. AND GLASSPOOL, I.J., 2005. Charcoal reflectance as a proxy for the emplacement temperature of pyroclastic flow deposits. *Geology*, *33*(7), pp.589-592.

SODERSTROM, L. AND JONSSON, B. G. 1989. Spatial pattern and dispersal in the leafy hepaticPtilidium pulcherrimum./J.Bryol. 15: 793/802

STONEBURNER, A., LANE, D.M. AND ANDERSON, L.E., 1992. Spore dispersal distances in Atrichum angustatum (Polytrichaceae). *Bryologist*, pp.324-328.

STROTHER P.K. 2010. Thalloid carbonaceousincrustations and the asynchronous evolution of embryophyte characters during the Early Paleozoic.Int. J. Coal Geol.83, 154–161. (doi:10.1016/j.coal.2009.10.013)

STUKINS, S., 2022. Is aberrancy a reliable indicator for major paleoclimatic disturbance?. *Palaios*, *37*(5), pp.145-149.

SUNDBERG, S., 2005. Larger capsules enhance short-range spore dispersal in Sphagnum, but what happens further away?. *Oikos*, *108*(1), pp.115-124.

SUNDBERG, S. AND RYDIN, H., 1998. Spore number in Sphagnum and its dependence on spore and capsule size. *Journal of Bryology*, *20*(1), pp.1-16.

TAYLOR, W.A., 2002. Studies in cryptospore ultrastructure: variability in the tetrad genus Tetrahedraletes and type material of the dyad Dyadospora murusattenuata. Rev. Palaeobot. Palynol. 119 (3–4), 325–334.

TAYLOR, W.A., 2003. Ultrastructure of selected Silurian trilete spores and the putative Ordovician trilete spore Virgatasporites. Rev. Palaeobot. Palynol. 126 (3–4), 211–2

TAYLOR, W.A., GENSEL, P.G., WELLMAN, C.H., 2011. Wall ultrastructure in three species of the dispersed spore Emphanisporites from the Early Devonian. Rev. Palaeobot. Palynol. 163 (3–4), 264–280.

TAYLOR, W.A., STROTHER, P.K., VECOLI, M., 2017. Wall ultrastructure of the oldest embryophytic spores: implications for early land plant evolution. Rev. Micropaleontol. 60 (3), 281–288.

TEICHMULLER, M., 1987. Organic material and very low-grade metamorphism. *Low temperature metamorphism*, pp.141-161.

VAUGHAN, A. AND NICHOLS, G., 1995. Controls on the deposition of charcoal; implications for sedimentary accumulations of fusain. *Journal of Sedimentary Research*, *65*(1a), pp.129-135.

VISSCHER, H., LOOY, C.V., COLLINSON, M.E., BRINKHUIS, H., VAN KONIJNENBURG-VAN CITTERT, J.H., KÜRSCHNER, W.M., AND SEPHTON, M.A., 2004, Environmental mutagenesis during the end-Permian ecological crisis: Proceedings of the National Academy of Sciences , v. 101, p. 12952– 12956.

WELLMAN, C.H., 1999. Sporangia containing Scylaspora from the lower Devonian of the Welsh Borderland. *Palaeontology*, *42*(1), pp.67-81.

WELLMAN, C.H., 2004. Origin, function and development of the spore wall in early land plants. In: Hemsley, A.R., Poole, I. (Eds.), The Evolution of Plant Physiology. Royal Botanic Gardens, Kew, pp. 43–63.

WELLMAN, C.H. AND BALL, A.C., 2021. Early land plant phytodebris. *Geological Society, London, Special Publications*, *511*(1), pp.309-320.

WELLMAN, W.H. & RICHARDSON, J.B. 1996. Sporomorph assemblages from the Lower Old Red Sandstone of Lorne, Scotland. *Special Papers in Palaeontology*, **55**, 41-102.

WELLMAN, W.H., EDWARDS, D, & AXE, L. 1998B. Ultrastructure of laevigate hilate spores in sporangia and spore masses from the Upper Silurian and Lower Devonian of the Welsh Borderland. *Philosophical Transactions of the Royal Society London B*, **353**, 1983– 2004.

WELLMAN, W.H., HABGOOD, K., JENKINS, G. & RICHARDSON, J.B. 2000. A new plant assemblage (microfossil and megafossil) from the Lower Old Red Sandstone of the Anglo–Welsh Basin: its implications for the palaeoecology of early terrestrial ecosystems. *Review of Palaeobotany and Palynology*, **109** (3-4), 161 – 196.

WELLMAN, C.H., OSTERLOFF, P.L. AND MOHIUDDIN, U., 2003. Fragments of the earliest land plants. *Nature*, *425*(6955), pp.282-285.

SEM Plates

Plate I, a – c: ABM5014-005: *Laevolancis divellomedium-plicata* in a circular spore mass; **a:** spore mass, showing the enveloping layer, scale bar 100μm; **b:** in situ spore, showing concave hilum, scale bar 10μm; **c:** magnified image of micro-elements on the inner edge of the hilum, scale bar 5μm; **d – g:** ABM5014-007: *Laevolancis divellomedium-plicata* in an oval, ?bivalved spore mass; **d:** spore mass, note bivalved appearance and encrusting layer, scale bar 500μm; **e:** in situ spore, proximal view, scale bar 10μm; **f:** in situ spore, distal hemisphere, scale bar 10μm; **g:** magnified view of encrusting layer, showing tightly packed spherules, scale bar 10μm; **h – j:** ABM5014-009: *Laevolancis divellomedium-plicata* in a circular spore mass; **h:** spore mass, scale bar 200μm; **i:** in situ spore, proximal view, scale bar 10μm; **j:** in situ spore, showing fold imitating a triradiate mark, scale bar 10μm; **k – m:** ABM5014-010: *Laevolancis divellomedium-plicata* in a fragmentary spore mass; **k:** spore mass, scale bar 100μm; **l:** in situ spores, showing the proximal hilum, scale bar 10μm.

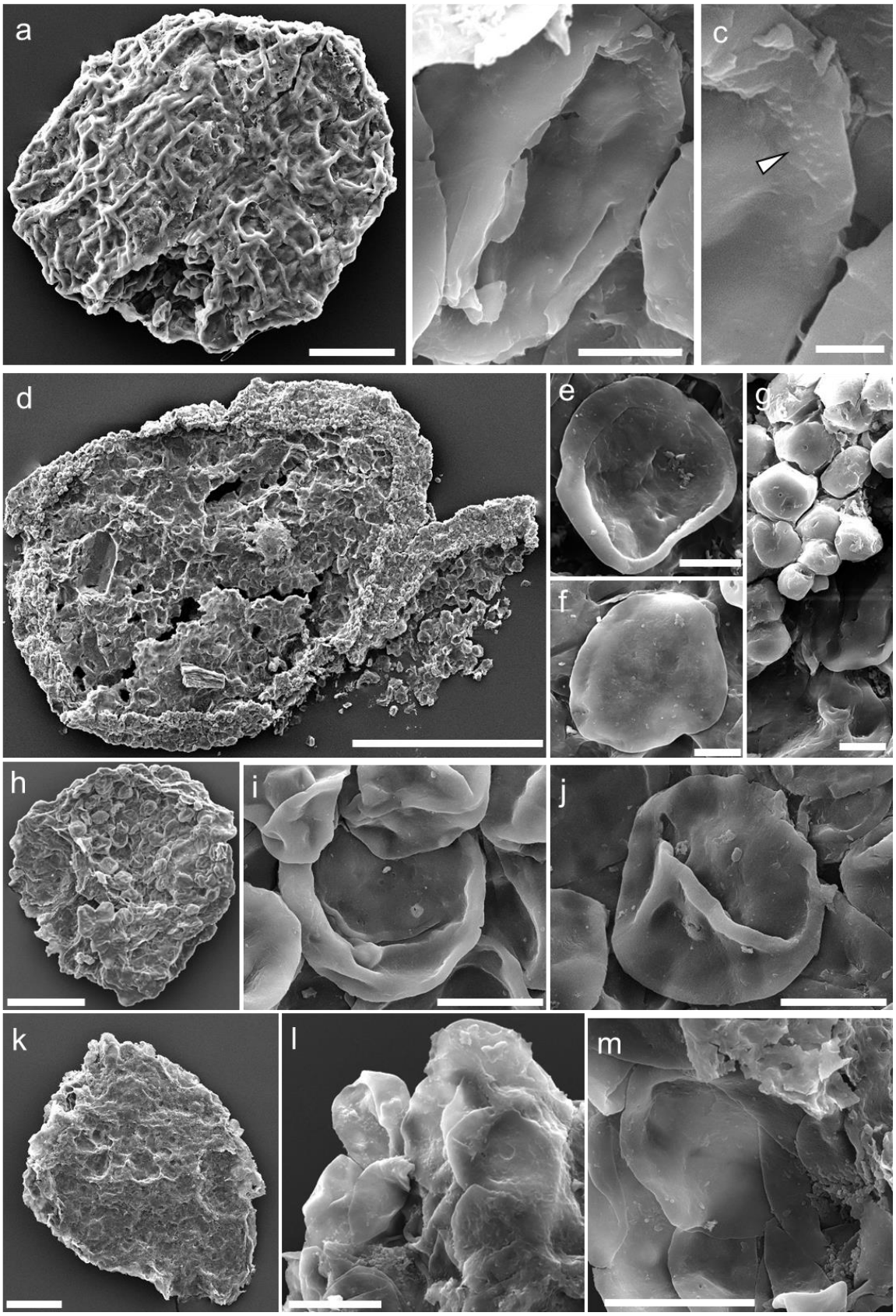
a
c
d
e
f
g
h
i
j
k
l
m

Plate II, a – e: ABM5023-003: *Laevolancis divellomedium-plicata* in an oval spore mass; **a:** spore mass, scale bar 500μm; **b:** in situ spore, ?distal view, scale bar 10μm; **c:** In situ spore, showing folds simulating a triradiate mark, scale bar 10μm; **d:** in situ spore, proximal view, not concave, slightly torn hilum, scale bar 10μm; **e:** in situ spore, magnification of simulated y-ray folds, note lack of suturae; arrows indicate small holes in exine which lack 'steps', scale bar 5μm; **f – h:** M50DE98-001: *Laevolancis divellomedium-plicata* in an elongate spore mass; **f:** spore mass, scale bar 200μm; **g:** in situ spore, proximal view, note the torn exine, scale bar 10μm; **h:** in situ spore, distal hemisphere, note irregular granules, scale bar 10μm; **i – l:** M50DE98-003: *Laevolancis divellomedium-plicata* in a circular spore mass; **i:** small spore mass, scale bar 500μm; **j:** in situ spore, proximal face, note torn hilum and small holes, scale bar 20μm; **k:** in situ spore, proximal face, scale bar 20μm; **l:** in situ spore, note holes in exine, scale bar 20μm; **m – p:** ABM5027-001: *Laevolancis divellomedium – plicata* in a fragmented spore mass; **m:** fragmented spore mass, 200μm; **n:** in situ spore**,** distal exine, note the numerous pores, scale bar 10μm; **o:** in situ spore, folded with numerous pores, scale bar 10μm; **p:** magnified pore, note steps and cf, with ABM5023-003, scale bar 1μm.

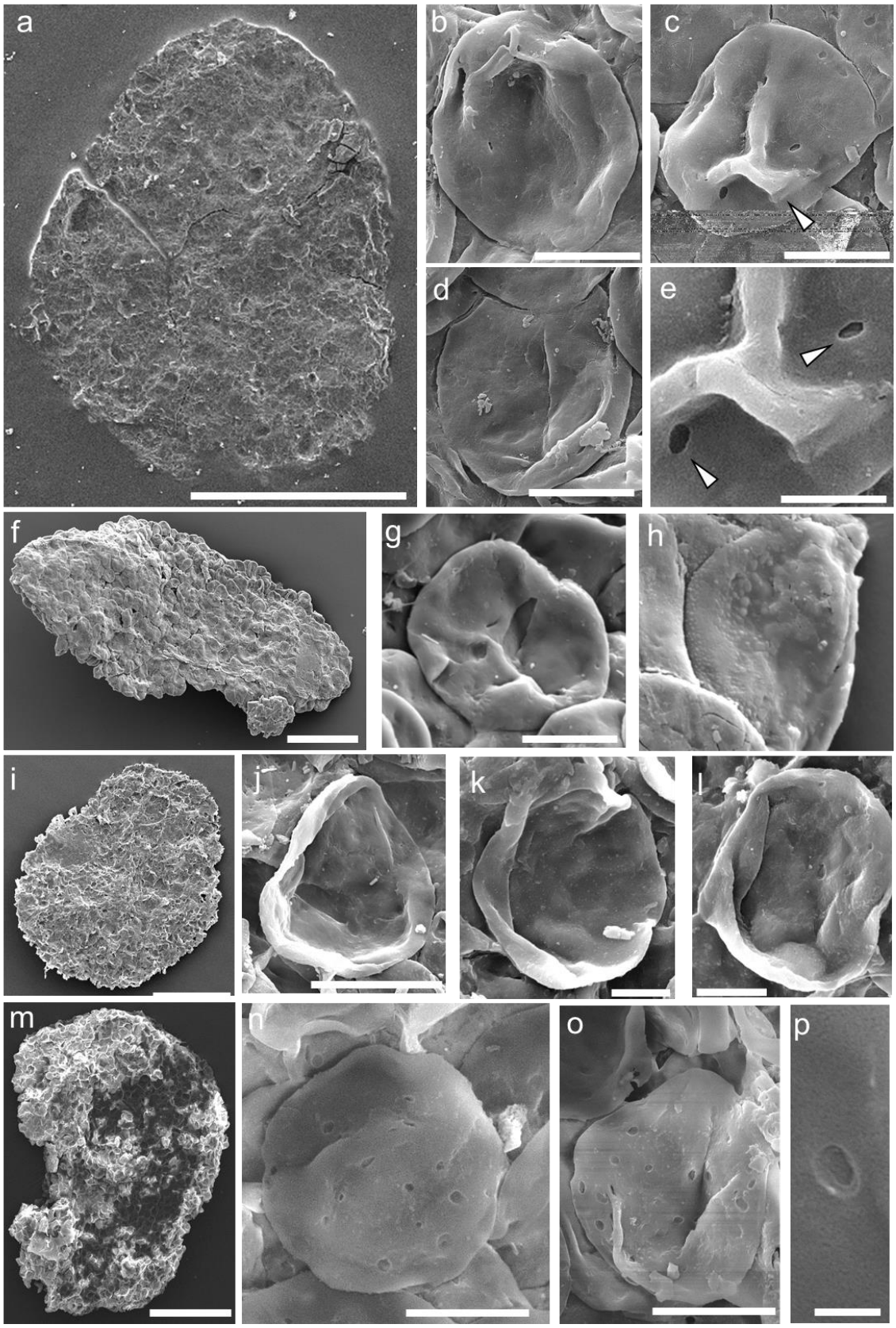
a
b
c
d
e
f
g
h
i
j
k
l
m
n
o
p

Plate III, a – c: ABM5029-001: *Laevolancis divellomedium-plicata* in a decayed, fragmentary spore mass; **a:** decayed spore mass, scale bar 200μm; **b:** in situ spore? Proximal view, scale bar 10μm; **c:** interdigitating banded tube (?*Porcatitubulis annulatus)*, scale bar 50μm; **d - f:** ABM5032-001: *Cymbohilates allenii* var. *allenii* in a fragmented spore mass; **d:** fragmented spore mass, scale bar 200μm; **e:** in situ spore, proximal face, scale bar 10μm; **f:** in situ spore, distal hemisphere showing dense grana, scale bar 10μm; **g - i:** ABM5014-006: *Hispanaediscus* sp. in a circular spore mass; **g:** spore mass, scale bar 200μm; **h:** in situ spore, proximal face, showing collapsed hilum, scale bar 10μm; **i:** in situ spore, distal hemisphere showing verrucae, scale bar 10μm; **j - m:** ABM5014-004: *Ambitisporites* sp. in an oval spore mass; **j:** spoon shaped spore mass, scale bar 200μm; **k:** in situ spore, showing proximal face and triradiate mark, scale bar 10μm; **l:** in situ spore, showing proximal face, scale bar 10μm; **m:** detail of the acellular layer which encompasses much of the spore mass, scale bar 50μm.

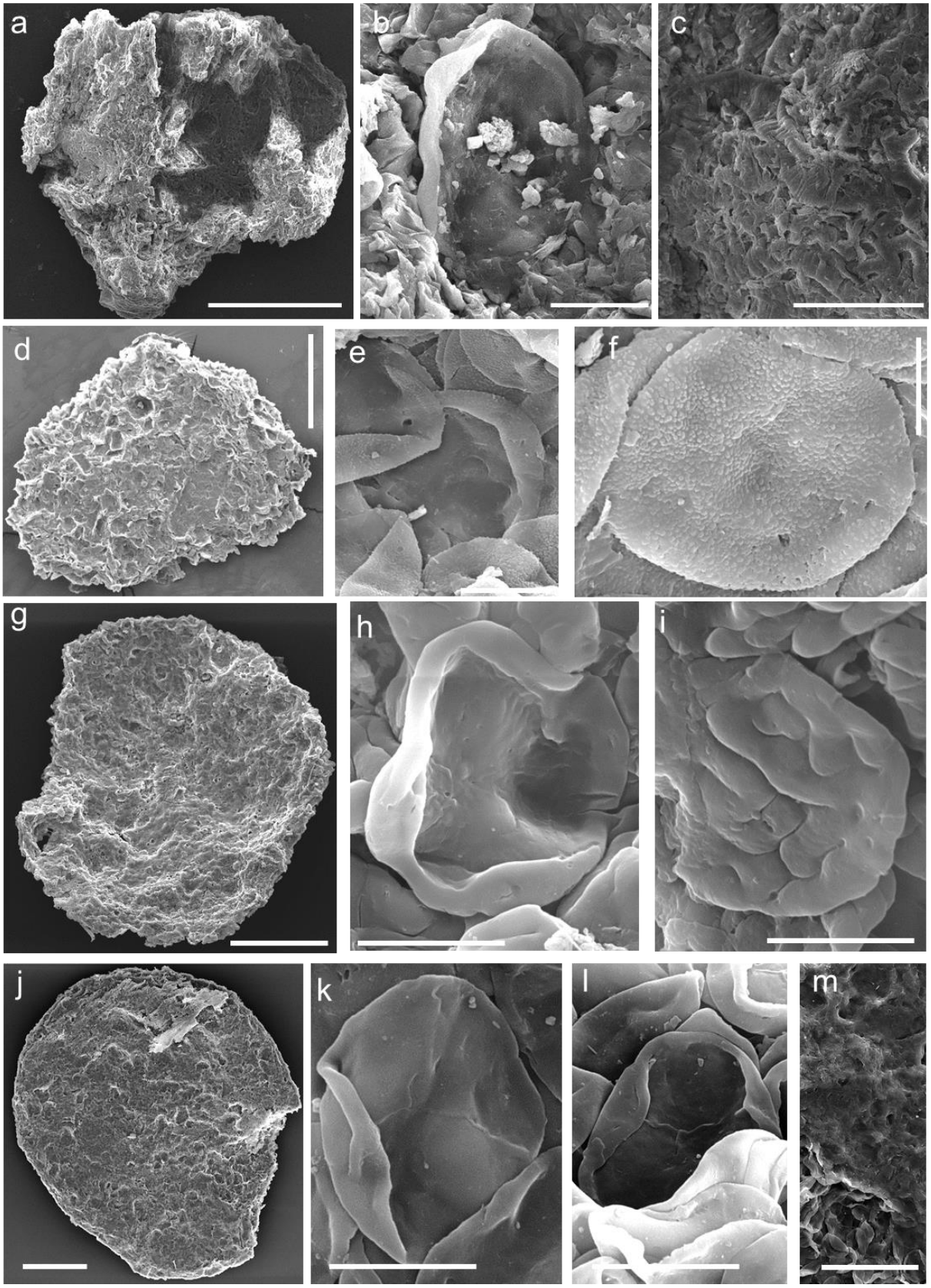
a
b
c
d
e
f
g
h
i
j
k
l
m

Plate IV: a – c: ABM5020-001: ? *Ambitisporites* sp. in an elongate spore mass; **a:** elongate spore mass, scale bar 500μm; **b:** in situ spore, partially dissociated tetrad, scale bar 20μm; **c:** in situ spores, scale bar 5μm; **d - f:** ABM5027-004 *Ambitisporites* sp. in an oval spore mass; **d:** spore mass, scale bar 200μm; **e:** in situ spore, proximal face showing triradiate mark, scale bar 10μm; **f:** in situ spore, proximal view, spore has lost proximal face, scale bar 10μm; **g - j:** M50DE98-004: *Ambitisporites* sp. in an oval spore mass; **g:** spore mass, scale bar 200μm **h:** in situ spore, proximal hemisphere, contact face lost, scale bar 10μm; **i:** in situ spore, proximal face, scale bar 10μm; **j:** in situ spore, proximal hemisphere, fold about the laesurae, scale bar 10μm; **k - m:** M50DE98-005: *Ambitisporites* sp. in a circular spore mass; **k:** spore mass, scale bar 200μm; **l:** in situ spore, proximal face, scale bar 10μm; **m:** in situ spores, scale bar 10μm.

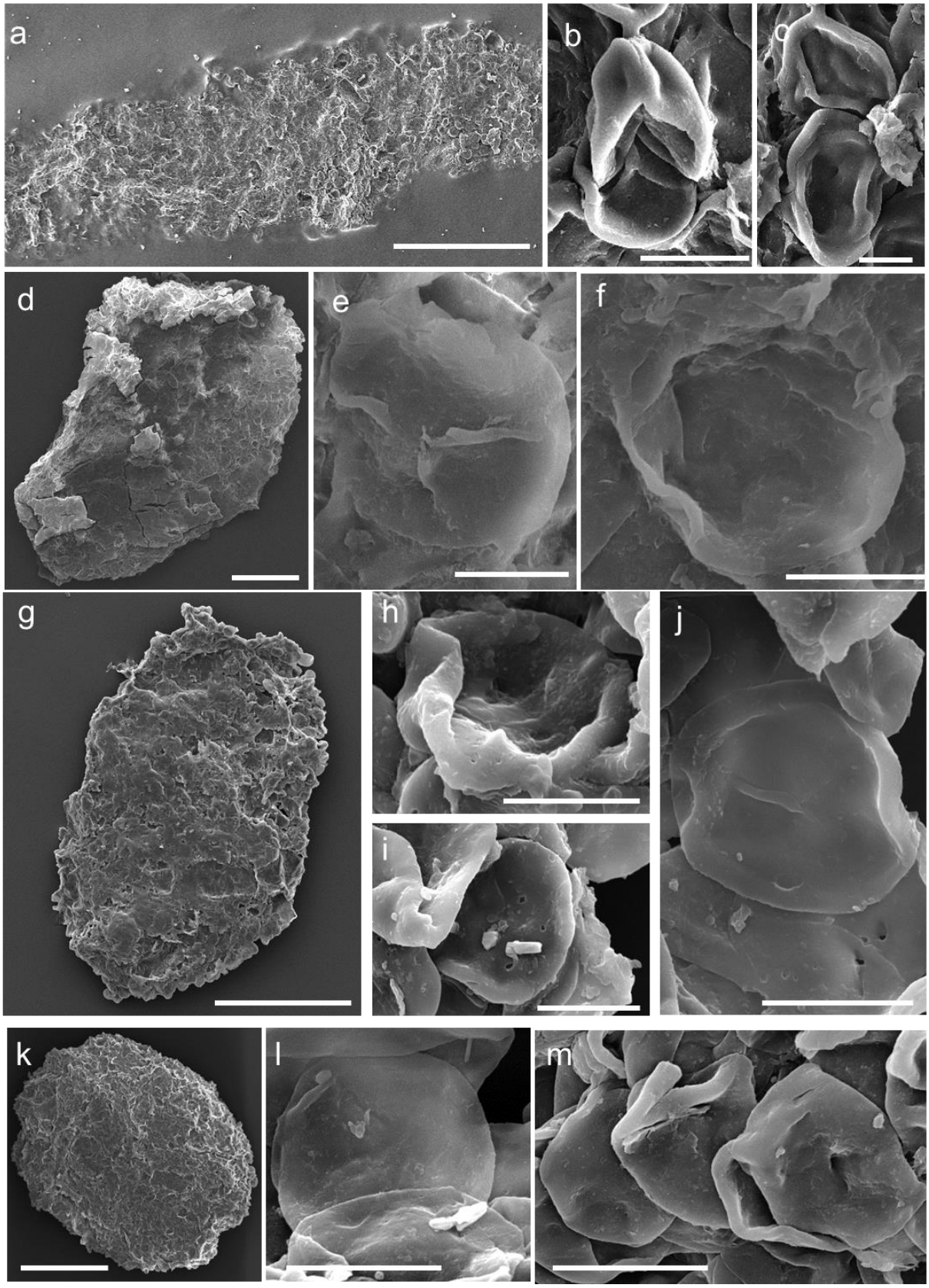
a
b
c
d
e
f
g
h
i
j
k
l
m

Plate V: a - e: ABM5021-001: *Scylaspora* sp. in an elongate spore mass; **a:** spore mass, scale bar 500µm; **b**: in situ spore showing well developed proximal ornament, scale bar 10 µm; **c:** partially associated tetrad, showing distal and proximal hemispheres; note the small pits on the distal hemisphere, scale bar 10µm; **d:** proximal hemisphere, with less distinct sculpture, scale bar 10µm; **e:** magnified view of (c), showing proximal ornament, scale bar 10µm; **f - i:** ABM5023-001: *Aneurospora* sp. in a circular spore mass; **f:** spore mass, scale bar 200µm; **g:** in situ spore, scale bar 5µm; **h:** in situ spores, scale bar 10µm; **i:** in situ spore, scale bar 20µm; **j - l:** ABM5031-003: *?Aneurospora* sp. in an oval mass; **j:** spore mass, scale bar 200µm; **k:** *in situ* spore, showing proximal face, scale bar 10µm; **l:** detail of microrнament, scale bar 5µm;

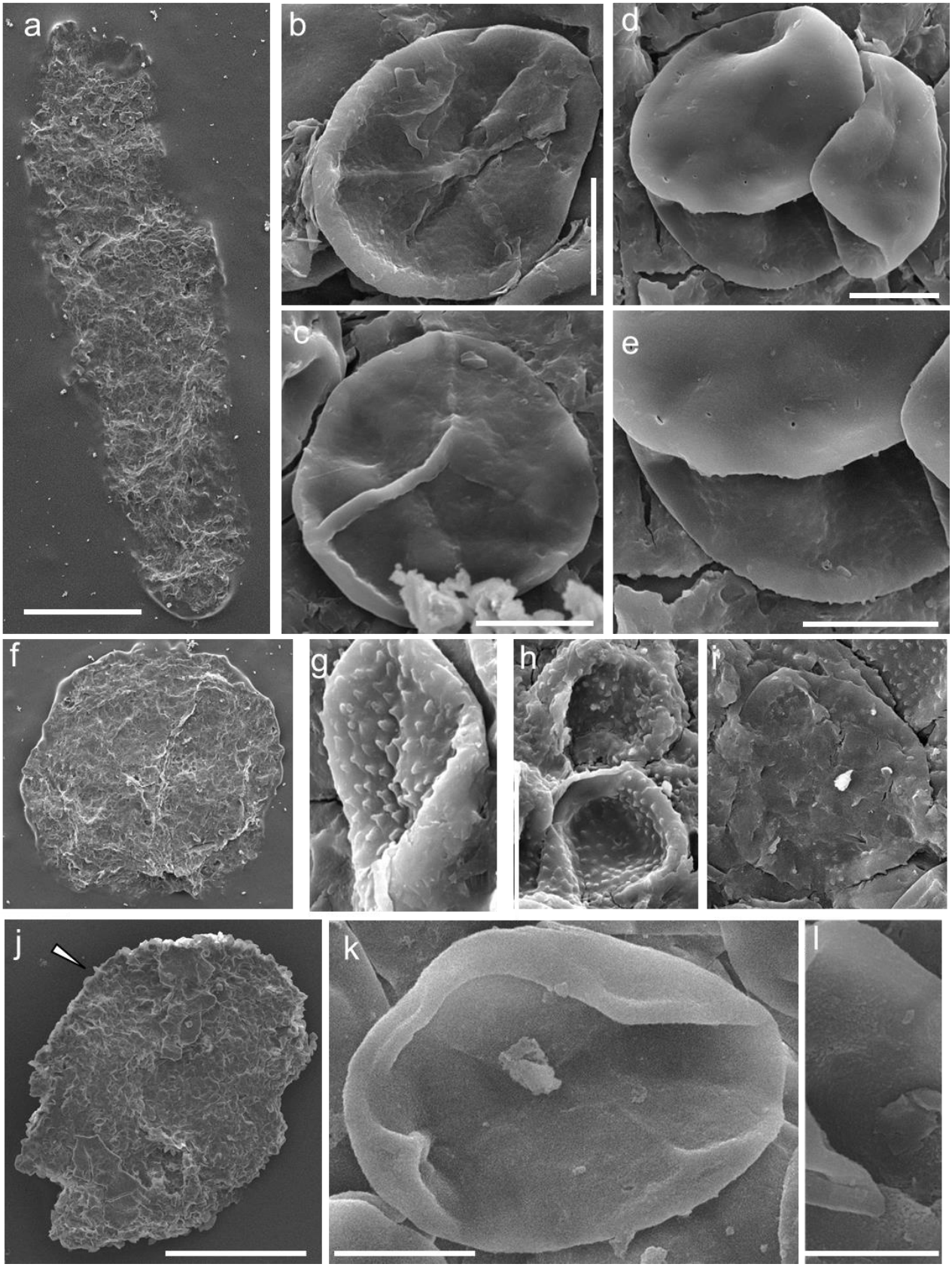
a
b
d
c
e
f
g
h
i
j
k
l

Plate VI: a - d: ABM5014-002: *Aneurospora* sp. in an oval spore mass; **a:** fragmentary spore mass, scale bar 200µm; **b:** in situ spore, showing proximal and distal hemispheres, scale bar 10µm; **c:** in situ spore, distal hemisphere, scale bar 10µm; **d:** magnification of proximal face, showing interadial papillae and latera view of equatorial and distal ornament, scale bar 10µm; **e – h** ABM5028.1-001 *Aneurospora* sp. in a circular spore mass; **e:** spore mass, scale bar 200µm; **f:** in situ spore, scale bar 10µm; **g:** in situ spore, scale bar 10µm; **h:** in situ spores, not different sculpture, scale bar 20µm; **, i - n:** ABM5028-005 *Aneurospora* sp. in a circular spore mass; **i:** spore mass, note the central, spherical body of spores with the ?enveloping cuticle with cellular remnants, scale bar 200µm; **j:** magnification of cuticle, scale bar 50µm; **k:** magnification of spherical spore body, scale bar 50µm; **l:** distal hemisphere of spore, scale bar 5µm; **m:** proximal face, showing y-ray, scale bar 5µm; **n:** detail of distal ornament, scale bar 1µm;

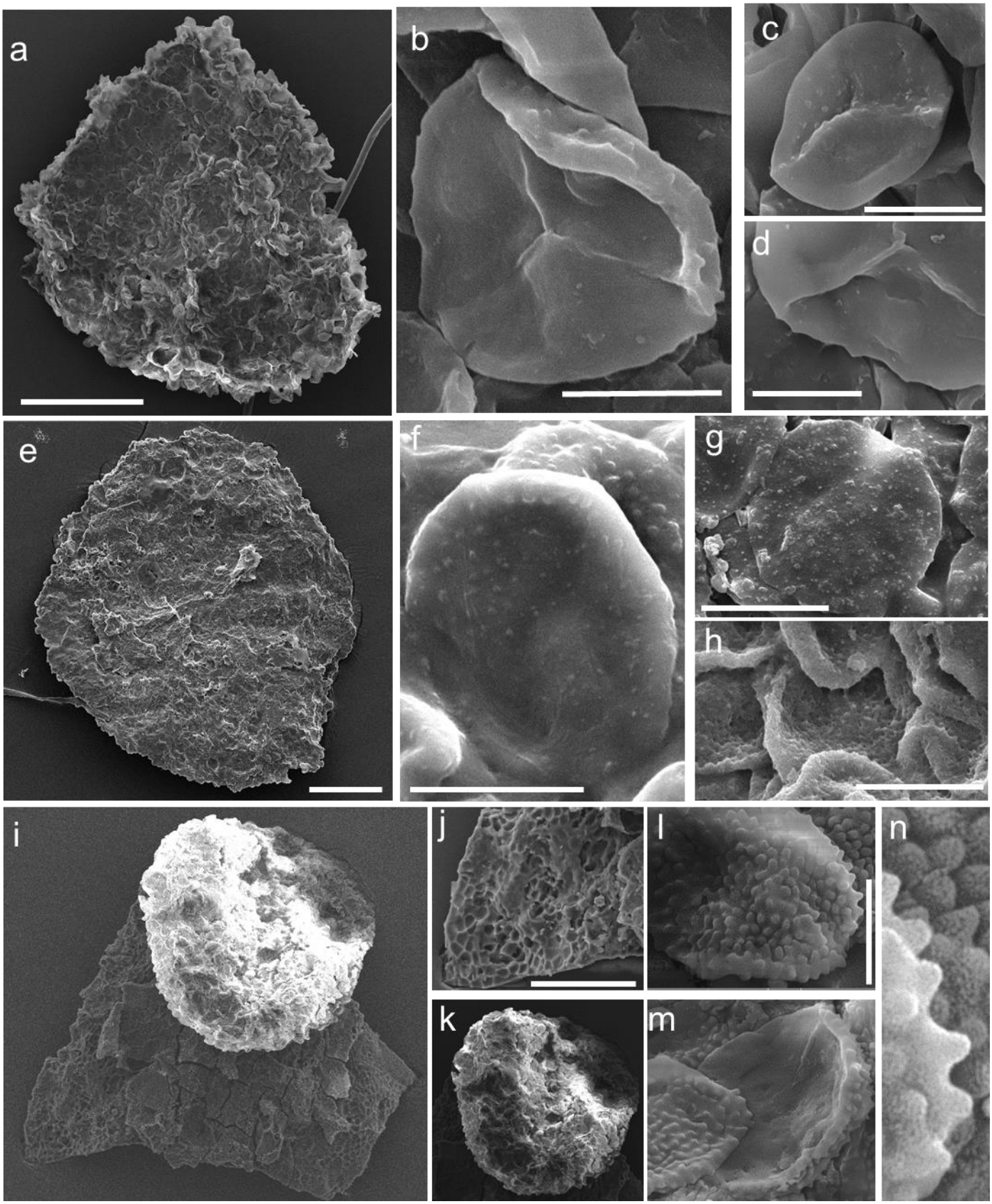
a
b
c
d
e
f
g
h
i
j
l
n
k
m

Plate VII a – e: ABM5029-002 *?Streelispora newportensis*. in a fragmentary spore mass; **a:** spore mass, scale bar 200µm; **b:** proximal face of in situ spore, scale bar 10µm; **c:** ornament detail, not partially coagulated elements on top left of spore, scale bar 10µm; **d:** distal hemisphere, scale bar 10µm; **e:** detail of ornament, scale bar 2µm; **f - k:** M50DE98-002: *Emphanisporites* sp. in an elongate spore mass; **f:** spore mass, scale bar 500µm; **g:** detail of acellular layer fragment on spore mass, scale bar 200µm; **h:** in situ spore, proximal view, scale bar 10µm; **i:** in situ spore, proximal face, scale bar 10µm; **j:** in situ spore, proximal face, scale bar 20µm; **k:** in situ spore, distal hemisphere, scale bar 10µm; **l - p:** ABM5032-002 *?Emphanisporites* sp. in a circular spore mass; **l:** spore mass, 100µm; **m:** in situ spore, distal hemisphere showing ornament, scale bar 5µm; **n:** magnification of acellular layer on spore mass, scale bar 50µm; **o:** in situ spore, proximal hemisphere showing radial muri, scale bar 5µm; **p:** detail of elements, scale bar 2µm.

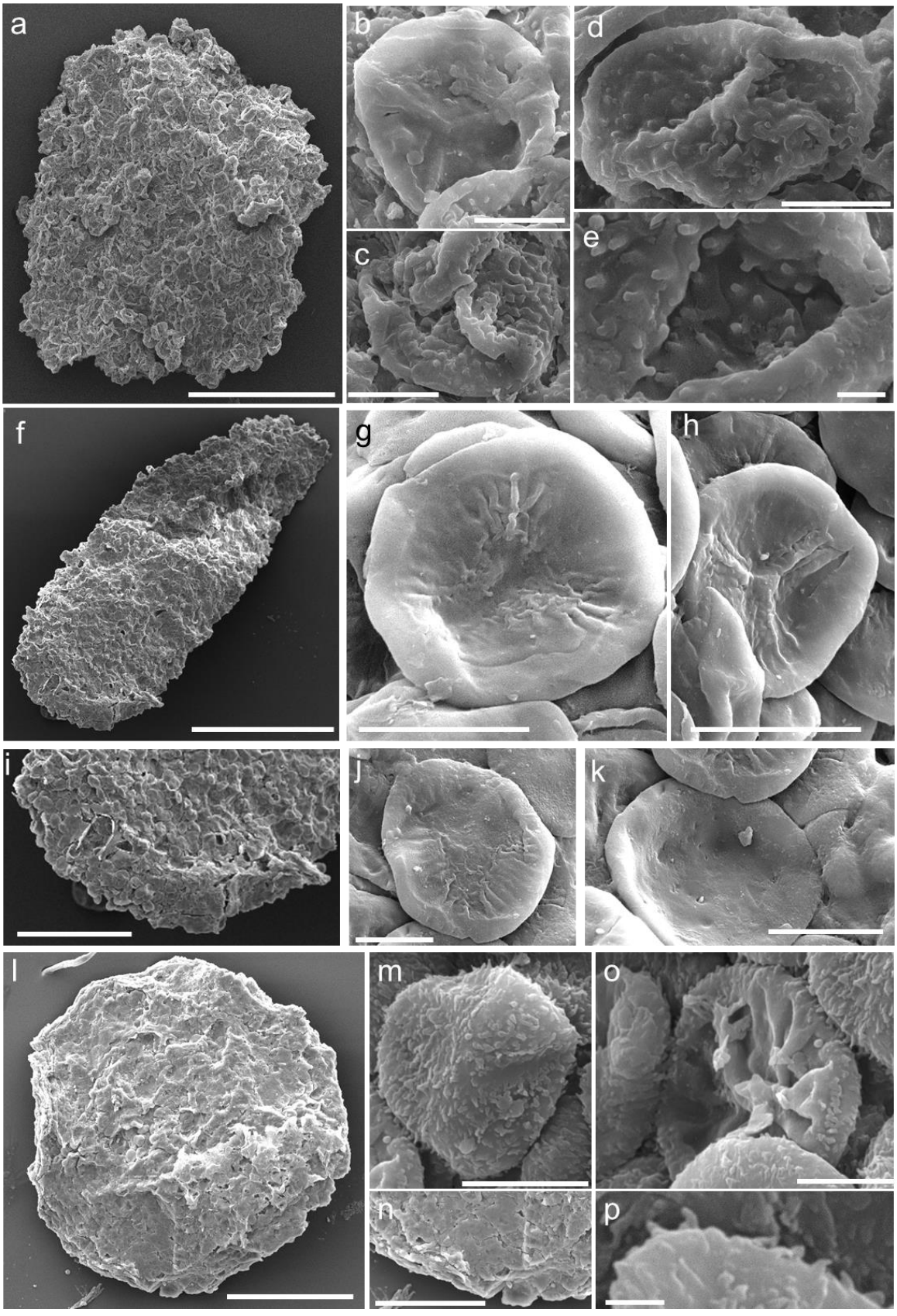
a
b
d
c
e
f
g
h
i
j
k
l
m
o
n
p

Plate VIII,; **a – d:** ABM5027-006 *?Stellatispora inframurinatus* in an elongate spore mass; **a:** spore mass, scale bar 200μm; **b:** in situ spore, distal hemisphere showing radial sculpture, scale bar 5μm; **c:** in situ spore, distal hemisphere, scale bar 10μm; **d:** distal hemisphere with radial sculpture, scale bar 5μm; **e - h:** ABM5031-001: *Cymbohilates?* sp. in a circular spore mass; **e:** spore mass, scale bar 100μm; **f:** spore mass, with radial folds indicated by dashed lines, scale bar 100μm; **g:** possible an accessory spore, scale bar 10μm; **h:** detail of ornament, scale bar 2μm; **i - l:** ABM5027-007 fertile eophyte? axis with stomata; **i:** axis, scale bar 200μm; **j:** stomata with guard cells, scale bar 20μm; **k:** detail of axis, showing elongate cells, scale bar 200μm; **l:** stomata clustered around the sporangial base, indicated by arrows and elongate cells, scale bar 40μm.

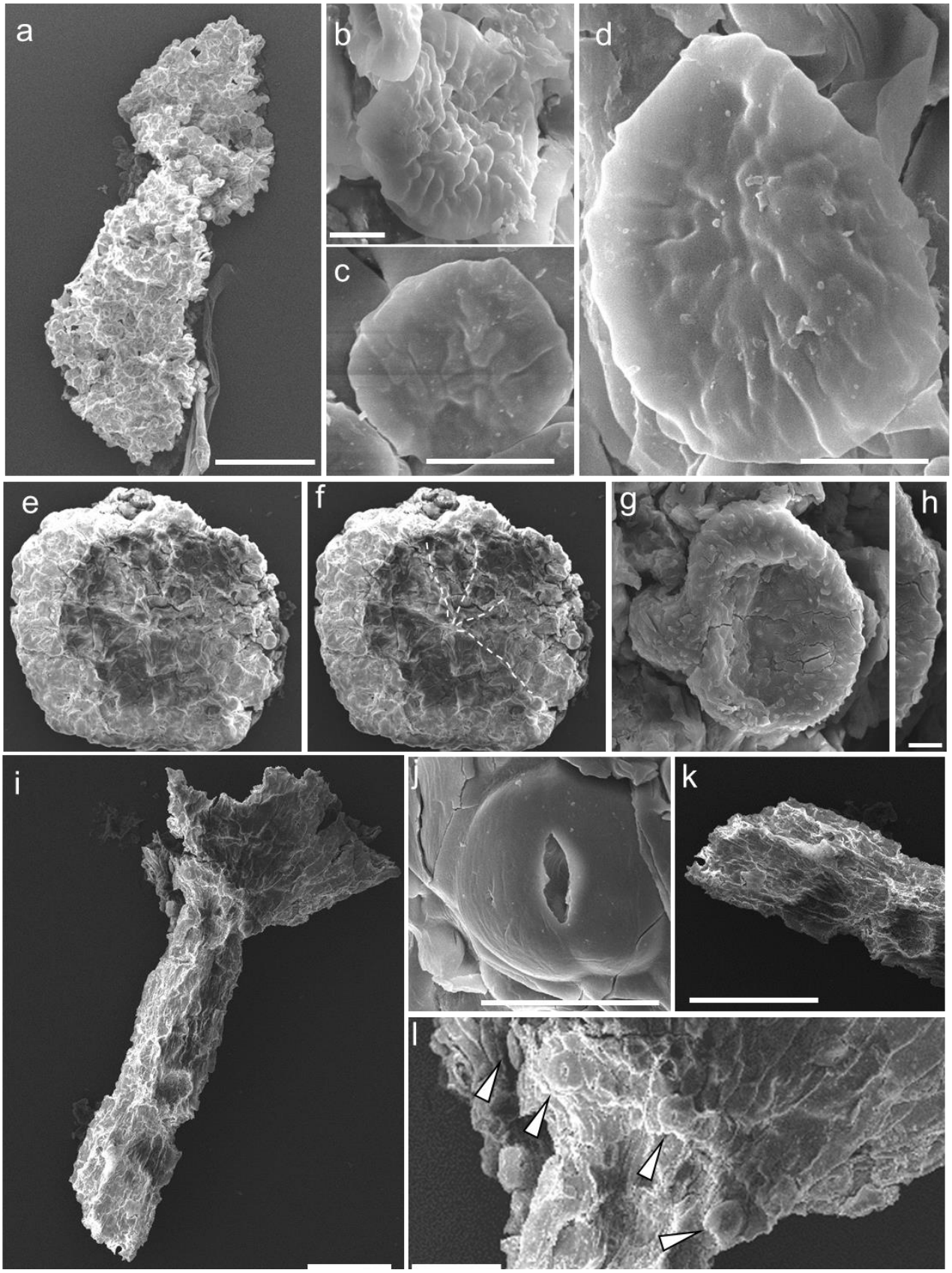
a
b
c
d
e
f
g
h
i
j
k
l

Plate IX, a: ABM5028-003 indeterminate 'trumpet shaped' ?sterile axis, scale bar 500μm; **b:** fertile axis, circles indicate position of possible stomata, scale bar 200μm; **c:** ABM5028-002 partially 'valvate' sterile axis, scale bar 500μm; **d – h:** ABM5028-004 indeterminate fragmented fertile axis; **d:** axis and flattened ?sporangial remains, scale bar 500μm; **e:** smooth tube, suggesting partial decay of this specimen prior to fossilisation, scale bar 50μm; **f – g:** broken axis of ABM5028-004; **f:** axis, plan view showing ?elongate cells;, scale bar 100μm; **g:** bisected axis, compressed but retaining the cross sectional anatomy of the axis, note homogenisation, scale bar 10μm; **h:** overturned fragment of ?sporangial cuticle from near the axis, showing small, spherical bodies, scale bar 10μm; **i:** ?fertile axis, M50. Scale bar 500μm; **j – m:** ABM50PIN1: sterile bifurcating axis; **j:** axis, not wide angled bifurcation of daughter branches and striated surface, scale bar 200μm; **k**: detail of perforated lumen 'end' wall, scale bar 5μm; **l:** detail of bisected transfer cell showing internal and external lumen walls; **m**: detail of interior cell lumen showing perforated region, not presence of cracks also, scale bar 10μm; **o – q:** ABM50PIN2 sterile bifurcating axis; **o**: axis, not wide angled bifurcation of daughter branches and striated axial surface, scale bar 500μm; **p:** straited region showing bisected ?transfer cell, scale bar 20μm; **q:** detail of bisected wall, note hemisphaerical nodules and ridges, scale bar 10μm.

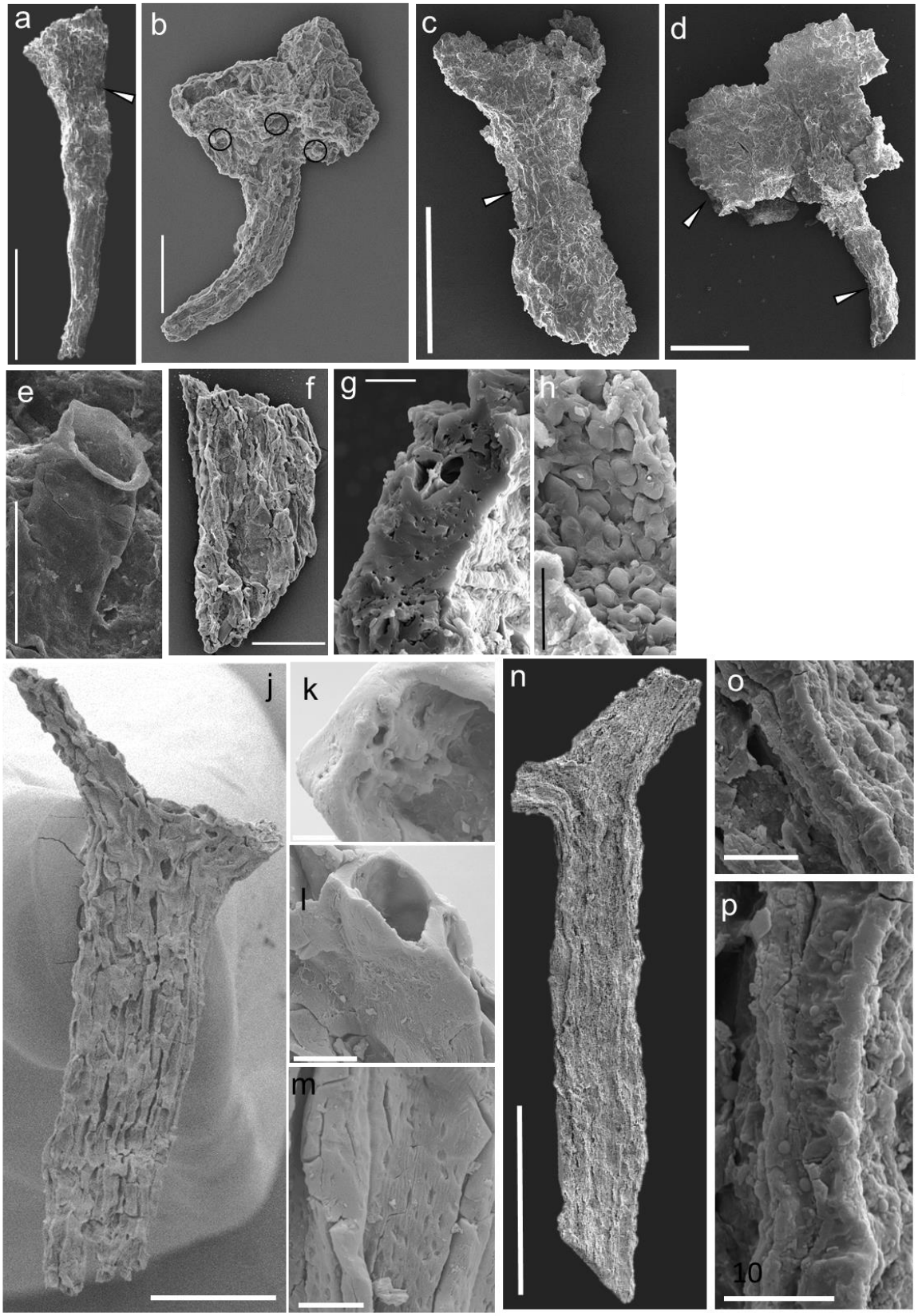
a
b
c
d
e
f
g
h
j
k
l
m
n
o
p
10

Plate X: a - e: coprolite; **a:** coprolite body, scale bar 200µm**; b:** *Chelinospora vermiculata*; distal hemisphere of spore, exhibiting vermiculate ornament, scale bar 10µm; **c:** Distal hemisphere, *?*Aneurospora**; d:** proximal face of an *?Aneurospora* sp., scale bar 10µm; **e?***Streelispora* sp. proximal face, scale bar 10µm; **, f - h:** ABM5014-011: *Cymbohilates?* sp. in an elongate spore mass; **f:** elongate spore mass, note bottle-like shape, scale bar 20µm; **g:** in situ spores, note dense apiculate ornament, scale bar 20µm; **h:** in situ spores, note different ornament to e, scale bar 20µm.

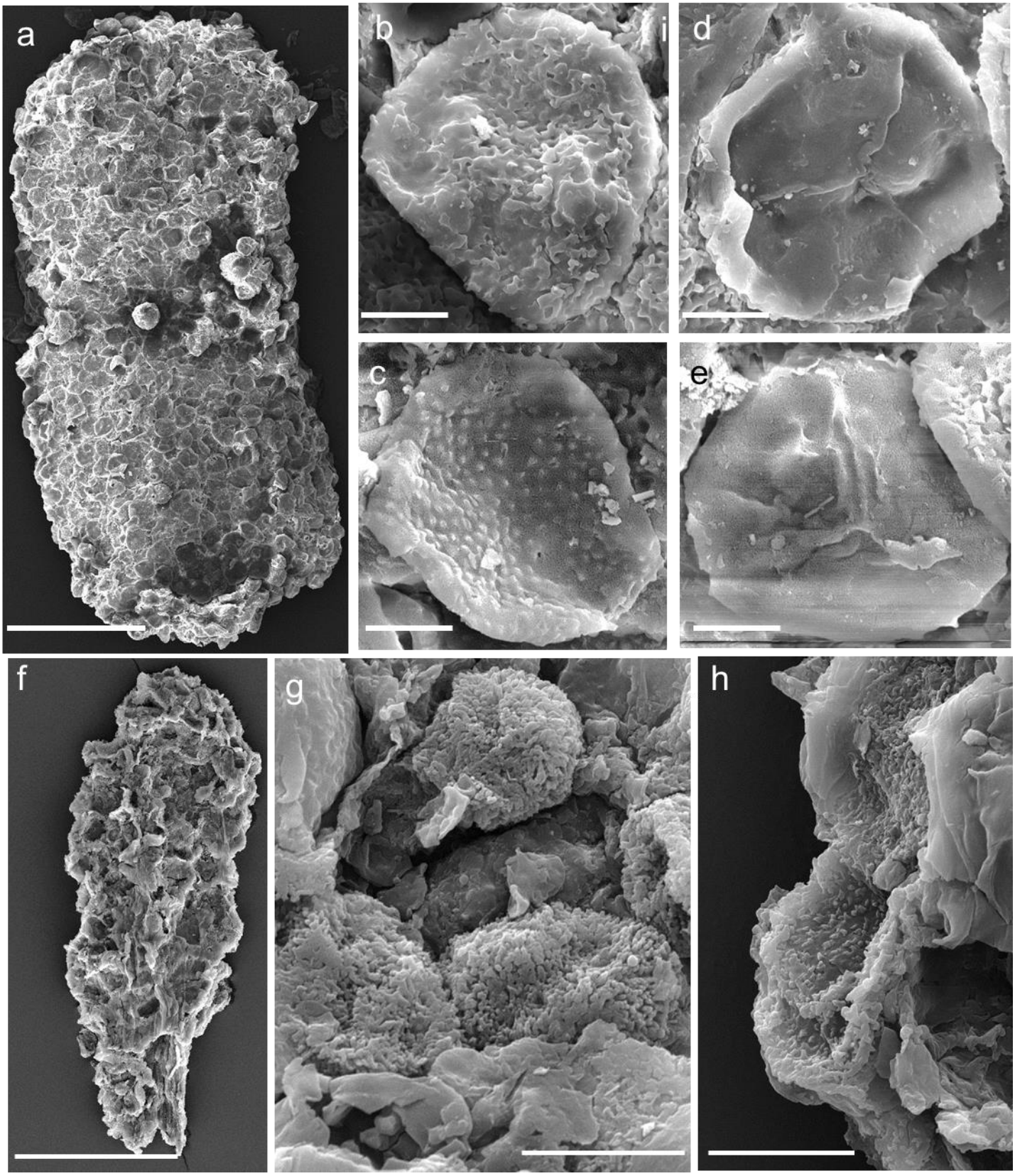
a
b
i
d
c
e
f
g
h

Plate XI: a – b: MPA25239-4-1 sporangial cuticle? a: semi-circular fragmentary specimen, scale bar 500μm; **b**: detail of (a), showing ?cellular detail, scale bar 100μm; c – e: MPA25239-1-1 ?fertile eophyte axis, **c:** axis with cup shaped, fragmentary sporangial base, note twisting and striated surface of axis, scale bar 200 μm; **d**: Axis, showing straited surface, scale bar 200 μm; **e:** detail of straited axial surface, scale bar 100 μm; **f:** detail of straited axial surface, scale bar 20 μm; **g:** detail of inner surface of lumen, note torsion of wall and compare this with the putative 'pore', indicated by arrow, scale bar 5 μm; **h – j:** MPA25239-5-3 ?sporangial cuticular fragment, **h:** fragment, showing outer ?cellular layer and inner cuticular layer, scale bar 200 μm; **i:** detail of cellular layer, scale bar 50 μm; **j:** detail of cuticular layer, scale bar 50 μm; **k – l:** MPA25239-6-1 bifurcating sterile axis, **k:** fragment of axis, note wide angled bifurcation and striated surface, 500 μm; **l:** detail of striations, scale bar 100 μm.

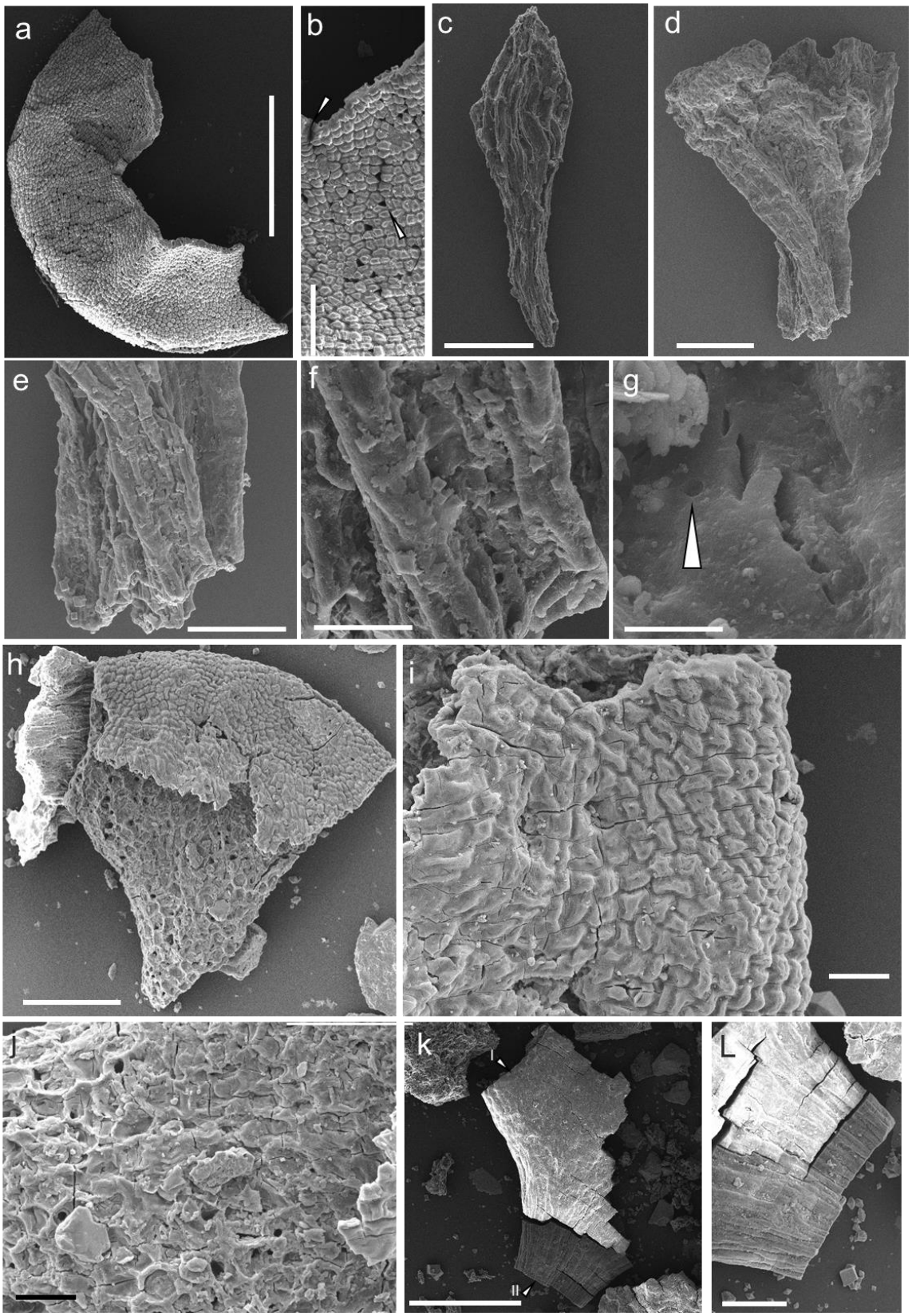
a
b
c
d
e
f
g
h
i
J
k
I
II
L

Plate XII: a – b: MPA25239-1: Pachytheca, **a:** entire specimen, scale bar 500 μm **b**: detail of specimen showing honeycomb structure, beneath smooth surface, scale bar 100 μm; **c:** MPA25239-3: Pachytheca, entire specimen, note fracturing and cracking, scale bar 500 μm; **d:** MPA25239-2, angular specimen of *Nematosketum*, scale bar 1mm; **e – f:** MPA25239-4, *Nematosketum*, **e:** angular fragment, scale bar 500 μm; **f:** detail of tubular structure, scale bar 100 μm; **g – h**: MPA25239-5, nematophyte fragment, **g:** specimen, showing smooth surface and underlying tubular structure, scale bar 500 μm; **h:** lateral detail of tubes, scale bar 20 μm; **i: MPA25239-5-6** *Cosmochlaina*, showing cuticle, palisade section and possible basal hyphal layer, scale bar 100 μm; **j:** MPA25239-4-6: *Nematothallus*, showing palisade layer and upper cuticular layer, scale bar 200 μm; **k – l**: *Nematothallus*? **K:** showing palisade layer and inner hyphal layer, scale bar 200 μm; **l:** detail of palisade layer, scale bar 50 μm.

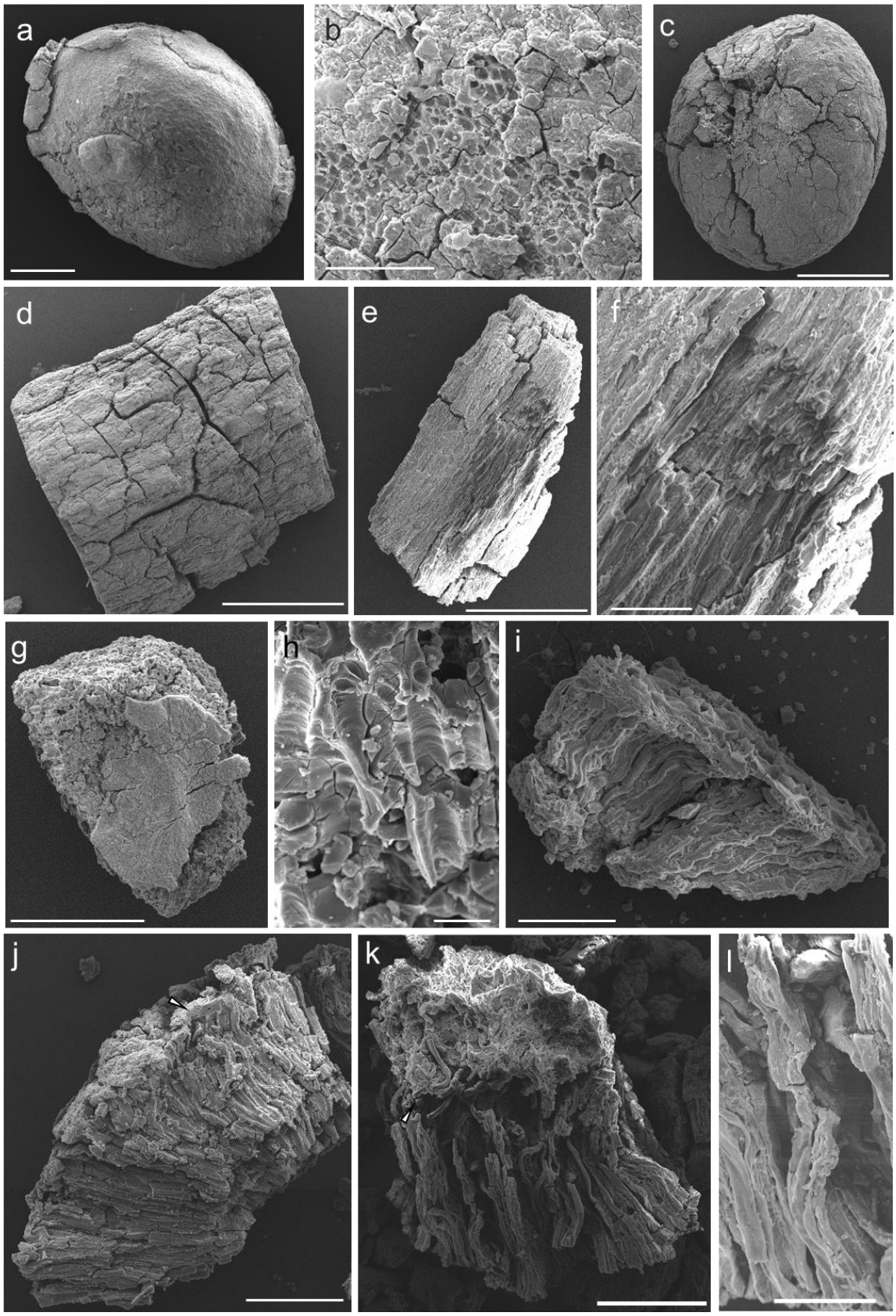
a
b
c
d
e
f
g
h
i
j
k
l

Thesis appendix 5

Thesis appendix 5.1: Vitrinite reflectance results

M50 Section

Lab. Ref.		**Operator**			
Wellname		**wsname**		**Country**	
TopDepth	0	**Bottom Depth**	0	**DepthUnit**	
SampleType		**Prep. Type**		**Rock Fraction**	

Std. Refer.	Spinel [0.393] YAG [0.929] GGG [1.749]
Description	
Exp. Descr.	

Channel	<Chan 02>	**Method**	Point Scan		
Minimum	0.173	**Maximum**	3.1203	**Mean**	0.5284
Standard Dev.	0.4537	**Variance**	0.2058	**Total Meas.**	100

V-Step	Mid-Point	Reflectivity [%]	Number	Volume [%]
0.1	0.32	0.17 to < 0.47	61	61
0.4	0.615	0.47 to < 0.76	28	28
0.7	0.91	0.76 to < 1.06	3	3
1	1.205	1.06 to < 1.35	5	5
1.3	1.499	1.35 to < 1.65	0	0
1.6	1.794	1.65 to < 1.94	0	0
1.9	2.089	1.94 to < 2.24	1	1
2.2	2.383	2.24 to < 2.53	0	0
2.5	2.678	2.53 to < 2.83	0	0
2.8	2.973	2.83 to < 3.12	2	2

	Wood	Fungus
Mean	316.176463	359.78062
Min	254.475967	320.504372
Max	535.75998	621.909075

Ammons Hill

Lab. Ref.		**Operator**			
Wellname		**wsname**		**Country**	
TopDepth	0	**Bottom Depth**	0	**DepthUnit**	
SampleType		**Prep. Type**		**Rock Fraction**	

Std. Refer.	Spinel [0.393] YAG [0.929] GGG [1.749]
Description	

Exp. Descr.

Channel	<Chan 01>	**Method**	Point Scan		
Minimum	0.2642	**Maximum**	1.8677	**Mean**	1.0669
Standard Dev.	0.3762	**Variance**	0.1415	**Total Meas.**	100

V-Step	Mid-Point	Reflectivity [%]	Number	Volume [%]
0.2	0.344	0.26 to < 0.42	3	3
0.4	0.505	0.42 to < 0.58	2	2
0.5	0.665	0.58 to < 0.75	12	12
0.7	0.825	0.75 to < 0.91	27	27
0.9	0.986	0.91 to < 1.07	17	17
1	1.146	1.07 to < 1.23	3	3
1.2	1.306	1.23 to < 1.39	8	8
1.3	1.467	1.39 to < 1.55	13	13
1.5	1.627	1.55 to < 1.71	13	13
1.7	1.788	1.71 to < 1.87	2	2

	Wood	Fungus
Mean	389.898013	416.253357
Min	271.401212	330.764708
Max	465.139402	496.234221

Typical particles: Ammons Hill

Ammons Hill typical particle type, many particles are like this – no distinctive morphology; often cracked and always very scratched (but still measurable when scratches can be avoided). This specimen chosen to include a cluster of tiny pyrite crystals, c. 1 micron across, inferred to be the causes of the scratches that are present throughout specimens in the AH sample. This type of material is present in M50 – but very rare (e.g. one or two particles in an entire transect).

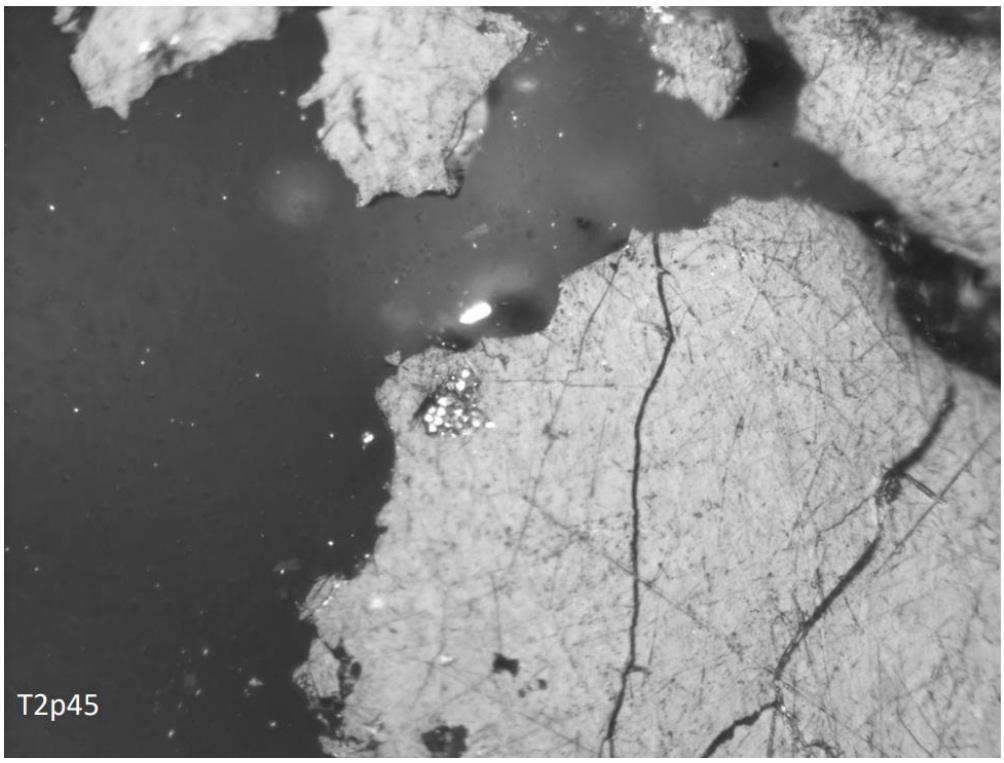

Ammons Hill – examples of typical particle structures encountered in two transects (numbers are continuous from 1 – 100, transects distinguished by T1 and T2)(all photos taken at x50).

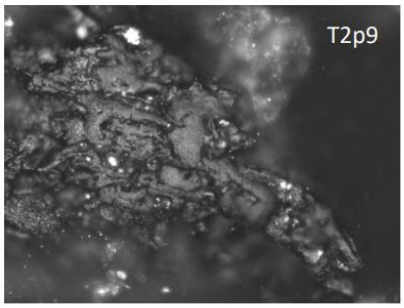

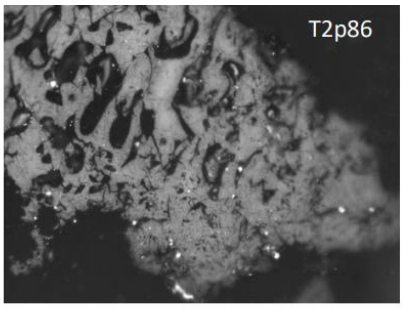

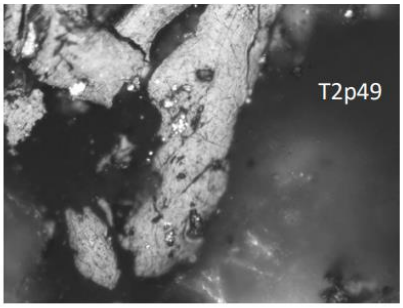

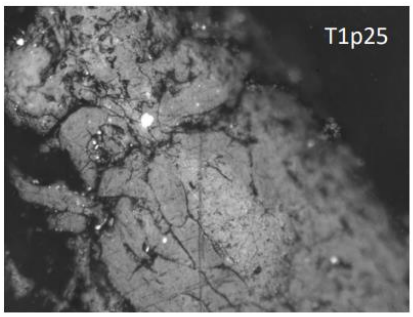

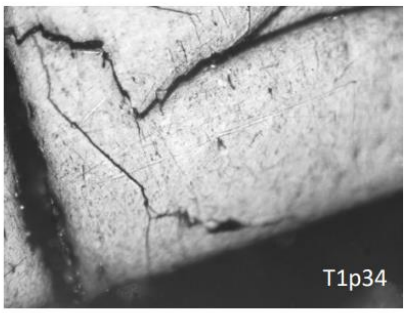

Note seemingly infilled 'scratches' so possibly original not caused by pyrite during polishing

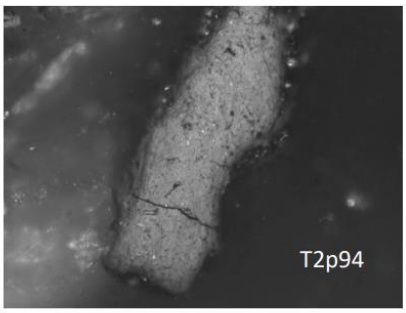

Note possible elongate crystal inclusion just below crack

Bright spots are mineral, most likely pyrite; cluster of small pyrite crystals in T2p49 like that in T2p45

For reflectance values of particles see the data table

Reflectance levels: Ammons Hill coarse fraction (field view 440µm)

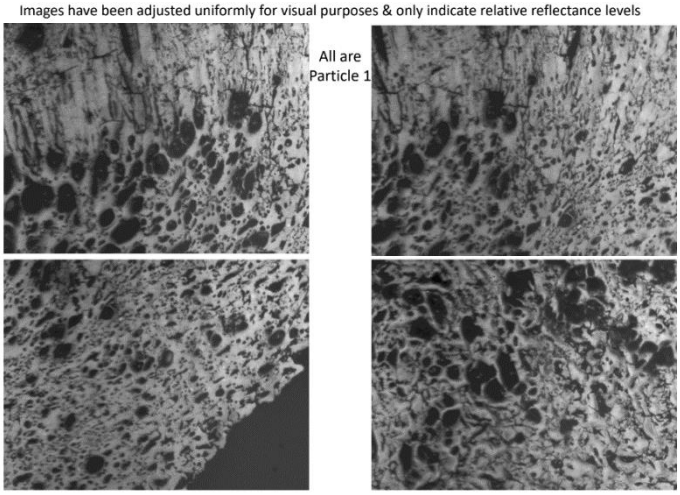

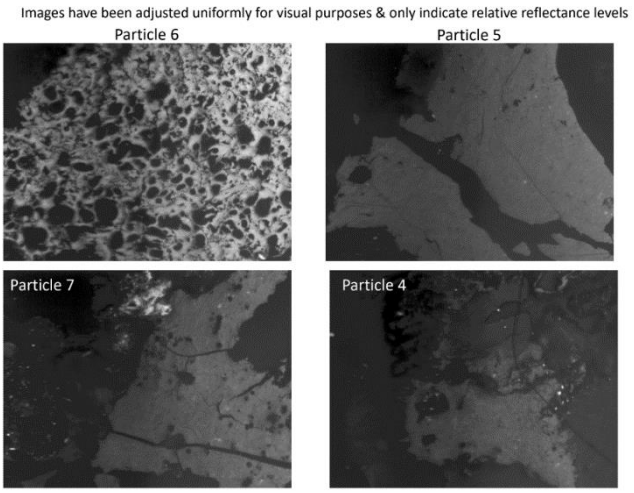

Reflectance levels: Ammons Hill fine fraction (field view 440µm)

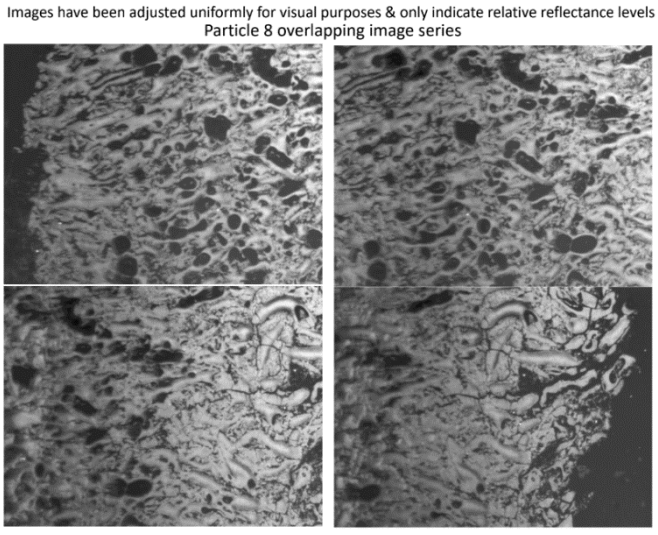

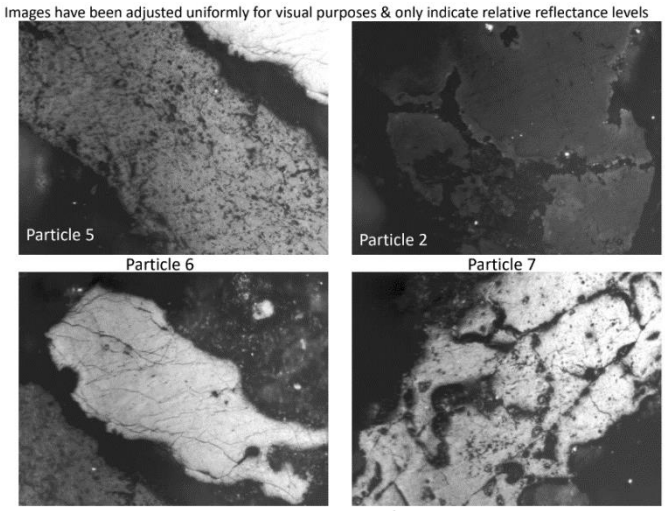

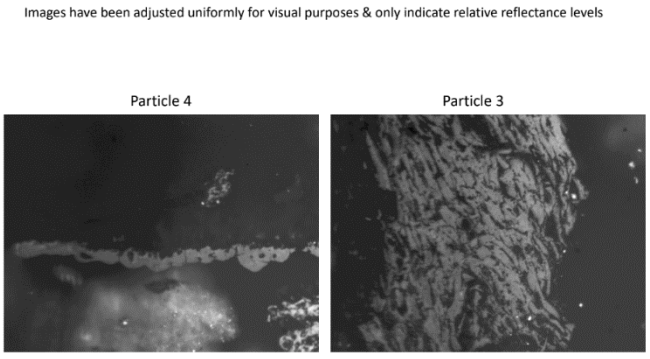

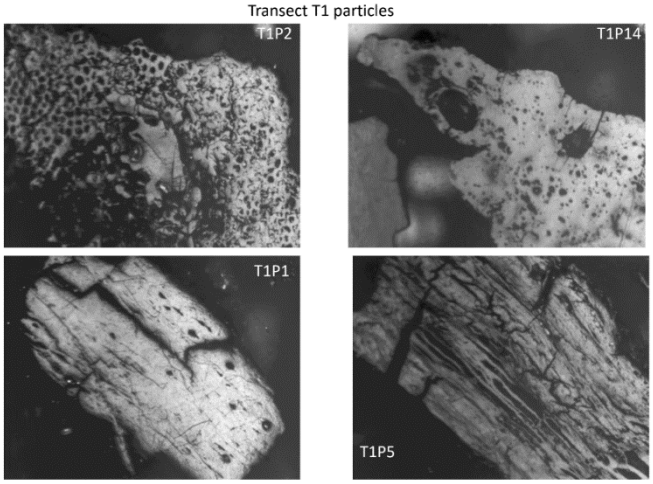

M50

Examples of range of particles encountered in transect (photos taken at x50).

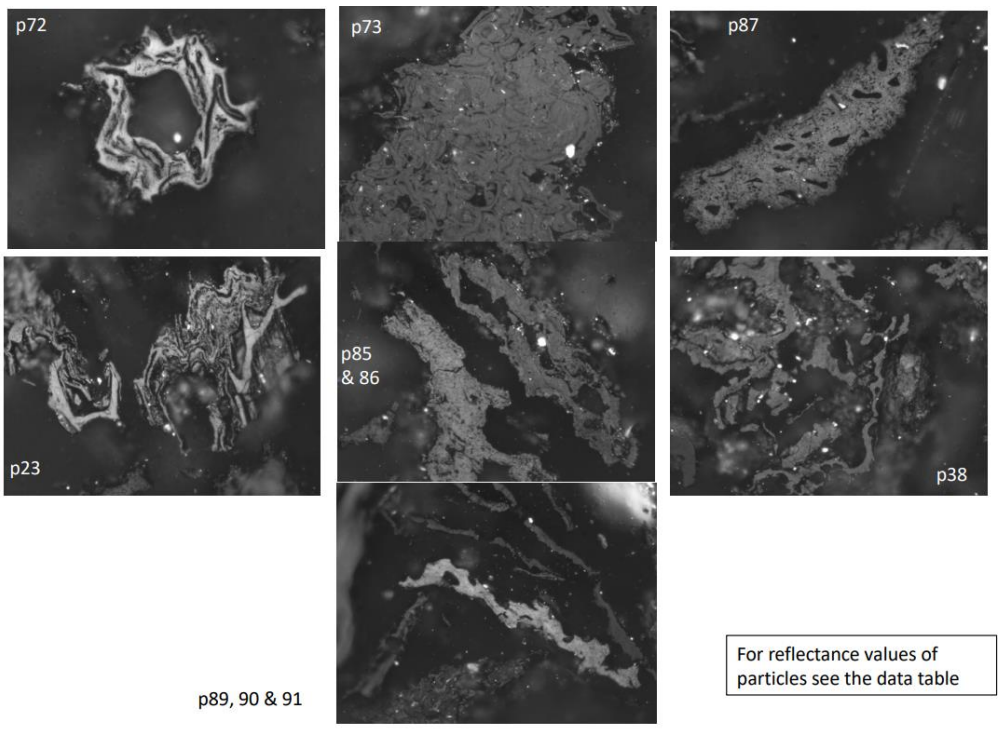

M50: three exceptionally highly reflecting particles and one (p24) at maximum of main distribution. P24 has structure in keeping with the other material in the M50, others do not, and may be modern contamination.

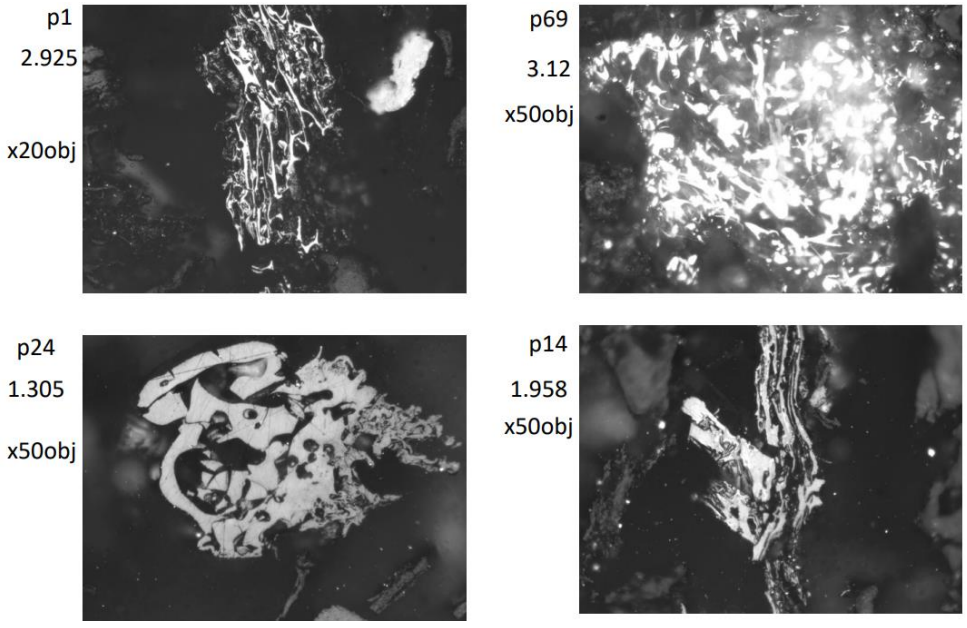

Reflectance levels: M50 coarse fraction (field view 440µm)

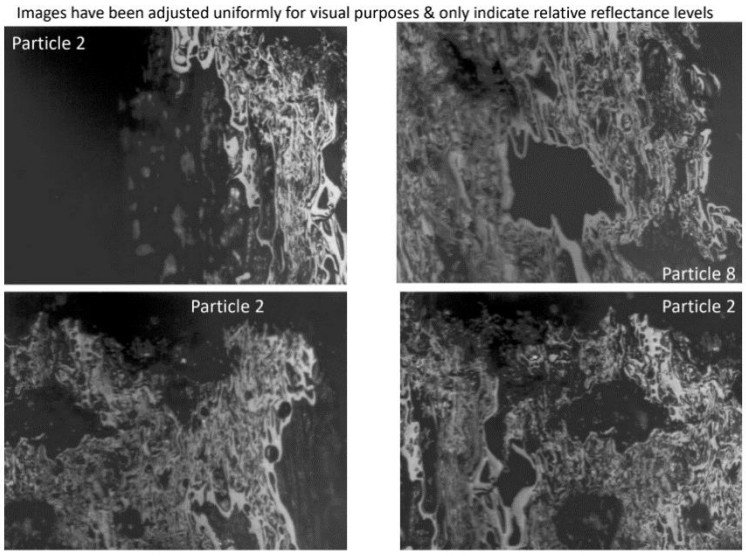

Reflectance levels: M50 fine fraction (field view 440µm)

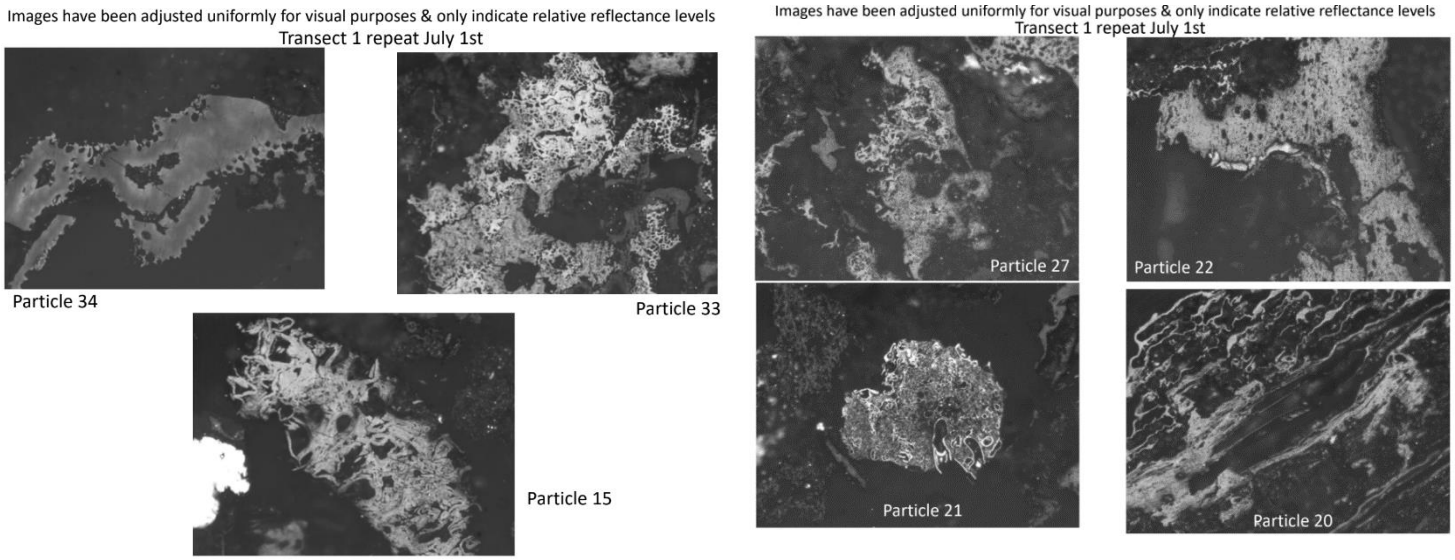

Thesis appendix 5.2: Particle reflectance scores

Ammons Hill reflectance and particle reflectance data:

"C:\Users\AlexB\Documents\AB PhD\Thesis chapters\Appendices\Thesis appendix 5\5.1\ACB22AH_vitrinite_refl_results.xls"

M50 reflectance and particle reflectance data:

"C:\Users\AlexB\Documents\AB PhD\Thesis chapters\Appendices\Thesis appendix 5\5.1\ACBM50_vitrinite_refl_results.xls"

Thesis appendix 5.3: Mesofossil data

Frequency of in situ genera

Genus	*Turma*	*Freq*
Laevolancis	*Cryptospore*	*9*
Cymbohilates	*Cryptospore*	*1*
Hispanaediscus	*Cryptospore*	*1*
Ambitisporites	*Miospore*	*5*
Aneurospora	*Miospore*	*5*
Streelispora	*Miospore*	*1*
Scylaspora	*Miospore*	*1*
Stellatispora	*Miospore*	*1*
Emphanisporites	*Miospore*	*2*

Turma	*n*
Cryptospores	*11*
Miospores	*15*

Specimen code	*in situ* spore genus	Spore mass shape	Spore mass L	Spore mass W	in situ amb diameter range	mean amb diameter
ABM5014-005	*Laevolancis*	discoidal	457	404	25(30)35	30
ABM5014-007	*Laevolancis*	discoidal	1225	887	31(35)40	35
ABM5014-009	*Laevolancis*	discoidal	619	587	37(46)50	46
ABM5014-010	*Laevolancis*	sub-triangular	525	474	30(36)42	36
ABM5023-003	*Laevolancis*	oval	1087	838	16(20)22	20
ABM5027-001	*Laevolancis*	oval	746	517	19(24)27	24
ABM5029-001	*Laevolancis*	pear shaped	643	656	24	24
M50DE98-001	*Laevolancis*	Cylindrical	810	360	41(44)50	44
M50DE98-003	*Laevolancis*	oval	1256	1000	27(30)33	30
ABM5014-011	*Cymbohilates*	elongate	624	224	18(23)26	23
ABM5031-001	*Cymbohilates*	discoidal	347	336	26	26
ABM5032-001	*Cymbohilates*	fragmented	620	540	19(20)21	20
ABM5014-006	*Hispanaediscus*	discoidal	683	666	12(16)24	16
ABM5014-004	*Ambitisporites*	spoon shaped	983	565	16(18)20	18
ABM5027-004	*Ambitisporites*	elongate	832	608	22(24)27	24
M50DE98-004	*Ambitisporites*	oval	600	354	16(20)23	20
M50DE98-005	*Ambitisporites*	oval	590	466	12(15)18	15

ABM5020-001	*Ambitisporites*	elongate	1730	500	36(37)38	37
ABM5031-003	*Aneurospora*	oval	652	456	17(18)19	18
ABM5014-002	*Aneurospora*	triangular	657	525	15(19)22	19
ABM5028.1-001	*Aneurospora*	discoidal	1067	933	18(21)24	21
ABM5028-005	*Aneurospora*	discoidal	315	310	12(14)18	14
ABM5023-001	*Aneurospora*	discoidal	713	682	23(26)30	26
ABM5029-002	*Streelispora*	fragmented	540	440	21(26)30	26
ABM5021-001	*Scylaspora*	elongate	1857	500	25(26)28	26
ABM5027-006	*Stellatispora*	elongate	936	331	19(21)22	21
ABM5032-002	*Emphanisporites*	discoidal	337	310	12(13)14	13
M50DE98-002	*Emphanisporites*	elongate	1400	500	18(21)25	21

Specimen code	*in situ* spore genus	Spore mass shape	Spore mass L	Spore mass W	Spore mass r*	in situ amb diameter range	mean amb diameter	Spore mass volume	Vol of mean spores	est. n spores in mass	Notes
ABM5014-005	*Laevolancis*	discoidal	457	404	200	25(30)35	30	131157172	14130	6868.811556	Representative?
ABM5014-007	*Laevolancis*	discoidal	1225	887	200	31(35)40	35	942392500	22437.91667	31080	Representative?
ABM5014-009	*Laevolancis*	discoidal	619	587	200	37(46)50	46	240625108	50939.17333	3495.592258	Fragment
ABM5014-010	*Laevolancis*	sub-triangular	525	474	200	30(36)42	36	173092500	24416.64	na	Fragment
ABM5023-003	*Laevolancis*	oval	1087	838	200	16(20)22	20	742025332	4186.666667	131154.159	Representative?
ABM5027-001	*Laevolancis*	oval	746	517	200	19(24)27	24	349492048	7234.56	35748.42361	Representative?
ABM5029-001	*Laevolancis*	pear shaped	643	656	200	24	24	259645972	7234.56	26558.3559	Fragment
M50DE98-001	*Laevolancis*	Cylindrical	810	360	200	41(44)50	44	412030800	44579.62667	6839.509767	Representative?
M50DE98-003	*Laevolancis*	oval	1256	1000	200	27(30)33	30	990692608	14130	51883.40622	Fragment
ABM5032-001	*Cymbohilates*	fragmented	620	540	200	19(20)21	20	241403200	4186.666667	na	Fragment
ABM5014-006	*Hispanaediscus*	discoidal	683	666	200	12(16)24	16	292955092	2143.573333	101133.3574	Representative?
ABM5014-004	*Ambitisporites*	spoon shaped	983	565	200	16(18)20	18	606829492	3052.08	147130.4239	Representative?
ABM5027-004	*Ambitisporites*	oval	832	608	200	22(24)27	24	434716672	7234.56	44465.77778	Fragment
M50DE98-004	*Ambitisporites*	oval	600	354	200	16(20)23	20	226080000	4186.666667	39960	Fragment
M50DE98-005	*Ambitisporites*	oval	590	466	200	12(15)18	15	218606800	1766.25	91588.97778	Fragment
ABM5020-001	*Ambitisporites*	elongate	1730	500	200	36(37)38	37	1879541200	26508.40333	52468.66326	Representative?
ABM5031-003	*Aneurospora*	oval	652	456	200	17(18)19	18	266965312	3052.08	64727.76955	Representative?
ABM5014-002	*Aneurospora*	triangular	657	525	200	15(19)22	19	271075572	3589.543333	55883.41041	Fragment
ABM5028.1-001	*Aneurospora*	discoidal	1067	933	200	18(21)24	21	714971092	4846.59	109165.126	Representative?
ABM5028-005	*Aneurospora*	discoidal	315	310	200	12(14)18	14	62313300	1436.026667	32110.71429	Representative?
ABM5023-001	*Aneurospora*	discoidal	713	682	200	23(26)30	26	319255732	9198.106667	25684.55121	Representative?
ABM5029-002	*Streelispora*	fragmented	540	440	200	21(26)30	26	183124800	9198.106667	na	Fragment
ABM5021-001	*Scylaspora*	elongate	1857	500	200	25(26)28	26	2165625972	9198.106667	174227.5098	Representative?
ABM5027-006	*Stellatispora*	elongate	936	331	200	19(21)22	21	550188288	4846.59	84005.31778	Representative?
ABM5032-002	*Emphanisporites*	discoidal	337	310	200	12(13)14	13	71321332	1149.763333	45903.17342	Representative?
M50DE98-002	*Emphanisporites*	elongate	1400	500	200	18(21)25	21	1230880000	4846.59	187936.5079	Representative?

Thesis appendix 5.4: Code scripts

Grouped barplots

```
# grouped barplots for in situ spore details
fig.

# set working directory
setwd("C:/Users/AlexB/Documents/AB
PhD/Research/Mesofossils/Quantification")

library("ggplot2")
library("ggpubr")

#give R data

t_c_dat <- read.csv("t_c.csv") ## mio vs cry
data
t_c_dat <- t_c_dat[-1]  # remove sacrificial
col
head(t_c_dat) # check

gen_dat <- read.csv("genus_in_situ.csv") # in
situ genera
gen_dat <- gen_dat[-1] # tidy
head(gen_dat)

disp_gen <-
read.csv("disp_spore_perc_de98.csv")
disp_gen <- disp_gen[-1]
head(disp_gen)

disp_t_c<-
read.csv("disp_turma_perc_de98.csv")
disp_t_c <- disp_t_c[-1]
head(disp_t_c)



#mio vs crypto n

t_m <- ggplot(t_c_dat, aes(x= Turma, y = n,
fill = Turma)) +
  geom_bar(stat="identity", color="black") +
  theme_minimal() + # get rid of grey
background
  scale_y_continuous(limits = c(0, 20)) + #
change y axis scale
  ylab("N spore masses") + # label y axis
  xlab("") +
  scale_fill_manual(values = c("gold2",
"forestgreen")) + # change colours of bar,
see colour chart
  theme_bw() + theme(panel.border =
element_blank(), panel.grid.major =
element_blank(),
                     plot.title =
element_text(size = 12, face = "bold"), #
alter title
                     axis.text =
element_text(colour = "black"), # alter axis
text
                     panel.grid.minor =
element_blank(), axis.line =
element_line(colour = "black"),
                     legend.position =
"none")

# in situ gen

gen <- ggplot(gen_dat, aes(x=Genus, y = n,
fill = Genus)) +
  geom_bar(stat="identity", color="black",
position=position_dodge())+
  theme_minimal() + # get rid of grey
background
  scale_y_continuous(limits = c(0, 10)) + #
change y axis scale
  ylab("N spore masses") + # label y axis
  xlab("") +
  scale_fill_manual(values = c("forestgreen",
"darkgreen", "gold2", "chartreuse4",
"goldenrod2", "goldenrod1",
                               "seagreen",
"olivedrab", "palegreen4" )) + # change
colours of bar, see colour chart
  theme_bw() + theme(panel.border =
element_blank(), panel.grid.major =
element_blank(),
                     plot.title =
element_text(size = 15, face = "bold"), #
alter title
                     axis.text =
element_text(colour = "black"), # alter axis
text
                     panel.grid.minor =
element_blank(), axis.line =
element_line(colour = "black"),
                     legend.position =
"none", axis.text.x = element_text(angle =
90, vjust = 0.5, hjust=1)) # edit angle of x
axis labels

#de98 dispersed mio vs crypto

t_m_disp <- ggplot(disp_t_c, aes(x= Turma, y
= Proportion, fill = Turma)) +
  geom_bar(stat="identity", color="black") +
  theme_minimal() + # get rid of grey
background
```

```
  scale_y_continuous(limits = c(0, 100)) + #
change y axis scale
  ylab("% palynoflora") + # label y axis
  xlab("") +
  scale_fill_manual(values = c("gold2",
"forestgreen")) + # change colours of bar,
see colour chart
  theme_bw() + theme(panel.border =
element_blank(), panel.grid.major =
element_blank(),
                     plot.title =
element_text(size = 12, face = "bold"), #
alter title
                     axis.text =
element_text(colour = "black"), # alter axis
text
                     panel.grid.minor =
element_blank(), axis.line =
element_line(colour = "black"),
                     legend.position =
"none")


# dispersed genera de98


gen_disp <- ggplot(disp_gen, aes(x=Genus, y =
Percent, fill = Genus)) +
  geom_bar(stat="identity", color="black",
position=position_dodge())+
  theme_minimal() + # get rid of grey
background
  scale_y_continuous(limits = c(0, 30)) + #
change y axis scale
  ylab("% palynoflora") + # label y axis
  xlab("") +
  scale_fill_manual(values =
c("forestgreen","gold2", rep("forestgreen",
times = 4), "gold2", "forestgreen",
                                "gold2",
"forestgreen",rep("gold2", times = 2),
rep("forestgreen", times = 3),
                                "gold2",
"forestgreen", rep("gold2", times = 2),
"forestgreen", "gold2", rep("forestgreen",
times = 5),
                                rep("gold2",
times = 2))) + # change colours of bar, see
colour chart
  theme_bw() + theme(panel.border =
element_blank(), panel.grid.major =
element_blank(),
                     plot.title =
element_text(size = 15, face = "bold"), #
alter title
                     axis.text =
element_text(colour = "black"), # alter axis
text
                     panel.grid.minor =
element_blank(), axis.line =
element_line(colour = "black"),
                     legend.position =
"none", axis.text.x = element_text(angle =
90, vjust = 0.5, hjust=1)) # edit angle of x
axis labels



ggarrange(t_m, gen, t_m_disp, gen_disp,
          labels = c("A", "B", "C", "D"), #
add labels to final fig
          ncol = 2, nrow = 2, align = "h")

##########################################
```

Boxplot for amb diameter distribution

```
# this is a boxplot for the amb diameter
distribution in samples
#composite anglo-welsh basin seqence


setwd("C:/Users/AlexB/Documents/AB
PhD/Research/Spores/Final
counts/measurements")


library("ggplot2")


amb.dat <-
read.csv("composite_measurements.csv")


head(amb.dat)


amb.dat$ï..Sample <-
as.factor(amb.dat$ï..Sample)


comp <-ggplot(amb.dat, aes(x=ï..Sample,
y=Diameter, fill = ï..Sample)) +
  geom_boxplot() +
  geom_smooth(method = "lm", se=FALSE,
color="grey22", aes(group=1)) +
  stat_summary(fun=mean, geom="point",
shape=19,
               size=2, color="red") +
  scale_fill_manual(values =
c("darkslategray4", "darkslategray3",
"darkslategray3",
"darkslategray3","darkslategray3","darkslateg
ray3","darkslategray3",


"darkslategray3","darkslategray4",
"darkslategray4","darkslategray",
"darkslategray","darkslategray","darkslategra
y",


"darkslategray1","darkslategray1","darkslateg
ray2","darkslategray","darkslategray","darksl
ategray","darkslategray",


"darkslategray3","darkslategray3","darkslateg
ray3","darkslategray","darkslategray","darksl
ategray4","darkslategray4","darkslategray4","
darkslategray4",
```

```
"darkslategray1","darkslategray1","darkslateg
ray1","darkslategray2")) +
  labs(title = "Composite amb diameter", x =
"", y = "Amb diameter (µm)") +
  scale_x_discrete(limits=c("21/USK/1",
"RU/21/1", "RU/21/2", "21/USK/2", "RU/21/3",
                           "RU/21/4",
"21/USK/3", "M50/2", "19/M50/85/2B",
       "19/M50/85/2C",
                           "19/M50/85/2D",
       "19/M50/2E",   "19/M50/2F",
       "19/M50/2G",   "19/M50/2H",
                           "M50/3",
       "M50/4",       "19/M50/86/2A",
       "19/DE98",     "19/M50/86/2B",
                           "M50/85/5B",
       "M50/85/5E",   "M50/85/5F",
       "M50/85/5G", "M50/7",  "M50/8",
                           "21/HD/003",
       "21/HD/002",   "21/HD/001",
       "21/HD/005", "M50/10", "M50/11",
       "M50/12",
                           "M50/13")) +
  theme_bw() + theme(axis.text.x =
element_text(angle = 90, vjust = 0.5,
hjust=1, colour = "black"),
                     panel.border =
element_blank(), panel.grid.major =
element_blank(),
                     panel.grid.minor =
element_blank(), axis.line =
element_line(colour = "black"),
                     legend.position =
"none", text=element_text(color="black"))
```

Chapter VI Reconstructing the Lower Devonian (Lochkovian) vegetation from the Anglo-Welsh Basin: Two spore masses containing Emphanisporites McGregor spores.

Alexander C. Ball[1, 2], Wilson A. Taylor[3]

[1]School of Biosciences, The University of Sheffield, Western Bank, Sheffield. S10 2TN, UK
[2]Dept. of Earth Sciences, The Natural History Museum, Cromwell Road, London. SW7 5BD, UK
3Dept. of Biology, University of Wisconsin-Eau Claire, Eau Claire, WI 53706, USA

A.C. Ball conceived the study, collected the mesofossils and wrote the manuscript. W.A. Taylor carried out the ultrastructural analyses. Material collected by D. Edwards.

Abstract

In situ spores have gone some way towards harmonising the prominent disparity between the Early Devonian dispersed spore and megafossil records, greatly advancing but often challenging our understanding of early vegetation. Here, we investigate an elongate and a discoidal spore mass, yielding *Emphanisporites epicautus* Richardson and Lister and *Emphanisporites* sp. respectively from the early (not earliest) Lochkovian (Lower *micrornatus newportensis* spore assemblage biozone) of the Ross-Tewkesbury Spur (M50) motorway section in the Anglo-Welsh Basin, UK. We explore their morphology and spore wall ultrastructure using SEM and TEM. A paucity of useful phylogenetic characters precludes formal identification or description of the parent plants but a relationship to the rhyniophytes is hypothesised. A dearth of vascular tissues, however, necessitates their placement amongst the rhyniophytoids. Both the sporangial morphology and spore wall ultrastructure differ between the specimens, distancing them from each other and from other *Emphanisporites* species. While similarities exist, no unequivocal relationships with contemporaneous or extant taxa, or indeed lineages, can be made using sporangial morphology or spore wall architecture. These differences lend further support to deliberations that the 'emphanoid' condition was a consequence of convergent evolution. Using the dispersed spore record we explore the paleoecology of the plants, which points towards them being minor components of the vegetation, restricted to areas away from river catchment. This interpretation is redolent of the mid Lochkovian cf. *Horneophyton* sp. (*E*. cf. *micrornatus* parent plant) from North Brown Clee Hill, but that plant may have been restricted to a more specialised niche. What characterised the niches of these plants is uncertain, but they may have been ephemerally water stressed, perhaps hinting at a moisture sensing function for the 'emphanoid' spore structure.

Review of Palaeobotany and Palynology 301 (2022) 104647

Contents lists available at ScienceDirect

Review of Palaeobotany and Palynology

journal homepage: www.elsevier.com/locate/revpalbo

Reconstructing the Lower Devonian (Lochkovian) vegetation from the Anglo-Welsh Basin: Two spore masses containing *Emphanisporites* McGregor spores

Alexander C. Ball [a,b,*], Wilson A. Taylor [c]

[a] School of Biosciences, The University of Sheffield, Alfred Denny Building, Western Bank, Sheffield S10 2TN, UK
[b] Dept. of Earth Sciences, The Natural History Museum, Cromwell Road, London SW7 5BD, UK
[c] Dept. of Biology, University of Wisconsin-Eau Claire, Eau Claire, WI 53706, USA

ARTICLE INFO

Article history:
Received 12 August 2021
Accepted 16 March 2022
Available online 23 March 2022

Keywords:
Spores
In situ
Charcoal
Ultrastructure
Palaeoecology
Early land plants

ABSTRACT

In situ spores have gone some way towards harmonising the prominent disparity between the Early Devonian dispersed spore and megafossil records, greatly advancing but often challenging our understanding of early vegetation. Here, we investigate an elongate and a discoidal spore mass, yielding *Emphanisporites epicautus* Richardson and Lister and *Emphanisporites* sp. respectively from the early (not earliest) Lochkovian (Lower *micrornatus-newportensis* spore assemblage biozone) of the Ross-Tewkesbury Spur (M50) motorway section in the Anglo-Welsh Basin, UK. We explore their morphology and spore wall ultrastructure using SEM and TEM. A paucity of useful phylogenetic characters precludes formal identification or description of the parent plants but a relationship to the rhyniophytes is hypothesised. A dearth of vascular tissues, however, necessitates their placement amongst the rhyniophytoids. Both the sporangial morphology and spore wall ultrastructure differs between the specimens, distancing them from each other and from other *Emphanisporites* species. While similarities exist, no unequivocal relationships with contemporaneous or extant taxa, or indeed lineages, can be made using sporangial morphology or spore wall architecture. These differences lend further support to deliberations that the 'emphanoid' condition was a consequence of convergent evolution. Using the dispersed spore record we explore the paleoecology of the plants, which points towards them being minor components of the vegetation, restricted to areas away from river catchment. This interpretation is redolent of the middle Lochkovian cf. *Horneophyton* sp. (*E.* cf. *micrornatus* parent plant) from North Brown Clee Hill, but that plant may have been restricted to a more specialised niche. What characterised the niches of these plants is uncertain, but they may have been ephemerally water stressed, perhaps hinting at a moisture sensing function for the 'emphanoid' spore structure.

1. Introduction

Over the last 80 years a considerable amount of research has shed light on the late Silurian - Lower Devonian vegetation of the Anglo-Welsh Basin (e.g. Richardson and Lister, 1969; Wellman et al., 2000; Edwards and Richardson, 2004; Edwards et al., 2014, 2021a, b; Morris et al., 2011a, b, 2012a, b). Essentially, research points towards a major floral turnover near the Siluro-Devonian boundary, in which primitive cryptospore-bearing plants gave way to apparently rapidly diversifying tracheophytes and their immediate progenitors via an adaptive radiation and later competitive replacement amongst the latter group (Wellman et al., 2000; Edwards and Richardson, 2004; Edwards and Morris, 2014).

Palynomorph assemblages from the basin are particularly well preserved and provide a nearly ubiquitous insight into floral diversity and development through time. The excellent preservation and diversity of dispersed spores mean they have been used to construct regionally and internationally important spore assemblage biozones (e.g. Richardson, 1974; Richardson and McGregor, 1986; Richardson, 1996a), although these remain problematic in the late Silurian and Earliest Devonian of the basin (Edwards and Richardson, 2004). In contrast to the spore record, the plant macrofossil record, whilst informative and diverse (e.g. Morris et al., 2011a), provides less insight in terms of taxonomic richness, mainly due to preservational bias. Caveats also exist in the dispersed spore record, however, principally when attempting to relate dispersed spores to parent plants.

* Corresponding author.
E-mail address: ACBall1@sheffield.ac.uk (A.C. Ball).

https://doi.org/10.1016/j.revpalbo.2022.104647

Minute, charcoalified sporangia and spore masses have been instrumental for reconciling the macrofossil and dispersed spore records. These often provide information for which, individually, neither can offer (e.g. Fanning et al., 1988; Fanning et al., 1990; Fanning et al., 1991a, b; Edwards et al., 1999; Morris et al., 2012b; Edwards et al., 2014), although they are far from a panacea (e.g. Morris et al., 2018). The sporangia and spore masses contain *in situ* spores often comparable to dispersed spore species, and extensive work demonstrates that a given sporangium or spore mass contains a single, or complex of, spore species (e.g. Wellman, 1999; Morris et al., 2012a, b; Edwards et al., 2014). Thus, they are useful for: (1) demonstrating a biological link between the dispersed and macrofossil records, often allowing reconstruction of vegetation using dispersed spores without macrofossils (although complications exist, e.g. Wellman et al., 1998b); (2) understanding aspects of anatomy and physiology of the plants, and; (3) adding morphological characters which aid investigations into the wider phylogenetic affinities of the plant and associated dispersed spore species (Morris et al., 2018).

One prominent trilete spore genus in late Silurian and Early Devonian assemblages is *Emphanisporites* McGregor. This diverse genus, characterised by proximal, 'spoke-like' interadial ('emphancid') muri, reaches peak diversity in the Early Devonian. The genus is used extensively in biostratigraphy but despite being widely reported, is consistently rare in assemblages, typically comprising <6% of palynofloras (Edwards and Richardson, 2000). The phylogenetic affinities of *Emphanisporites* have been explored through ultrastructural analysis of dispersed specimens (Taylor et al., 2011), and other workers have reported a limited number of species *in situ* from the Pragian Rhynie Chert (Wellman et al., 2004) and middle *micrornatus-newportensis* (MN) spore biozone of the Anglo-Welsh Basin (Edwards and Richardson, 2000; Morris et al., 2012b) (Fig. 1). Understanding of affinities and phylogenetic relationships remains clouded, however, with studies pointing to at least two separate lineages producing the *Emphanisporites* genus (Taylor et al., 2011; Morris et al., 2012b), leading workers to posit that the structural, emphanoid features characterising the genus is probably a result of convergent evolution.

Here, we present *in situ Emphanisporites epicautus* Richardson and Lister and *E.* sp. from the lower MN spore biozone (early, but not earliest, Lochkovian) of the Ross-Tewkesbury Spur (M50) motorway section in the Anglo-Welsh Basin. We use SEM and TEM to investigate the morphology and ultrastructure of the specimens and deliberate their affinities and wider phylogenetic relationships. We also explore spore wall development in these *Emphanisporites* species and use the dispersed spore record to deliberate on the palaeoecology of the parent plants.

2. Geological setting

The mesofossils were isolated from a fine beige siltstone, collected by D. Edwards in 1986 from the Freshwater West formation (*sensu* Barclay et al., 2015), 2 m above the Chapel Point Limestone member, just south-west of Junction 3 on the northern side of the Ross–Tewkesbury Spur (M50) motorway (near the 29.5-furlong marker post, fig. 2, Allen and Dineley, 1976) (Fig. 2). The lower Freshwater West formation was deposited in a seasonally semi-arid, terrestrial-fluvial setting by variously meandering perennial and ephemeral sandy streams and rivers (e.g. Allen and Dineley, 1976; Morris et al., 2012c).

Analysis of the dispersed spore assemblage from the sample identified *Streelispora newportensis* Richardson and Lister, *Emphanisporites* cf. *micrornatus* Richardson and Lister and *Chelinospora vermiculata* Chaloner and Streel, alongside an absence of *E. micrornatus* Richardson and Lister. This assemblage is indicative of the lower *micrornatus-newportensis* subzone, with *E. micrornatus* proper not appearing until the middle subzone of the MN biozone. The location of the assemblage in the lower MN subzone indicates an early, but not earliest, Lochkovian age (Early Devonian) for the specimens described herein (Fig. 1).

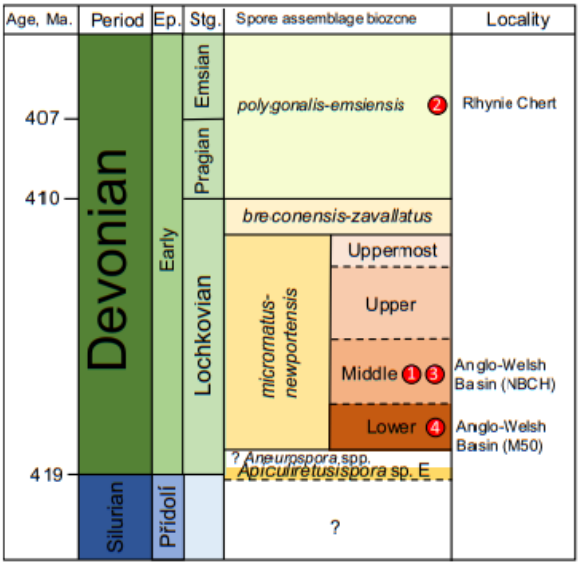

Fig. 1. Stratigraphy and spore assemblage biozones of the upper Silurian and Lower Devonian of Great Britain from which specimens containing *in situ Emphanisporites* spores have been described – numeration is in order of publication. **(1)** cf. *Horneophyton* sp. and numerous fragmentary *Salopella*-esque sporangia in Edwards and Richardson, 2000 **(2)**; *Horneophyton lignieri* in Wellman et al., 2004; **(3)** Discoidal spore mass in Morris et al., 2012b; **(4)** Elongate? and discoidal spore masses, this study. Figure modified from Edwards and Richardson (2000). Age constraints from GSA Geologic timescale v. 5.0 (2018). Constraints on stratigraphic positions of *in situ Emphanisporites*: (1) Edwards and Richardson (2000); (2) Wellman et al., 2004 (approximate); (3) Morris et al. (2012b); (4) Edwards et al. (1994), Allen and Dineley (1976).

In terms of other Anglo-Welsh Basin mesofossil localities, the lower MN subzone placement means that the M50 assemblage predates the North Brown Clee Hill (NBCH) locality (middle MN subzone, Lochkovian) (e.g. Morris et al., 2012a, b; Edwards et al., 2014) (Fig. 1) but is younger than the Ludford Lane locality (*tripapillatus-spicula* biozone, earliest Přídolí) (Jeram et al., 1990; Edwards, 1996).

3. Material and methods

3.1. Bulk maceration

100 g of 15–50 mm sized fragments from sample 19M50-26 were selected for bulk maceration. The samples were not ground down or otherwise processed before bulk acid maceration. 200 ml of concentrated hydrochloric acid (HCl) was added to the samples, which were then left for five days, allowing time for carbonate digestion. The HCl-sample mixture was then diluted with water seven times. The diluted mixture was then poured off as far as possible waiting twenty-four hours between individual dilutions to allow settling. 100 ml of 40% concentrated hydrofluoric acid (HF) was then added to digest silicates that were adhering to the mesofossils and left for two days. The HF solution was then diluted eight times with water, again leaving twenty-four hours between each dilution to allow for settling. The diluted solution was then sieved through an 80 μm nylon mesh. Organic matter >80 μm was collected for picking.

3.2. SEM

Mesofossils were picked from macerated material using a single-bristled paintbrush under a Vickers dissection microscope and individually mounted on SEM stubs with mounted graphite discs. Samples

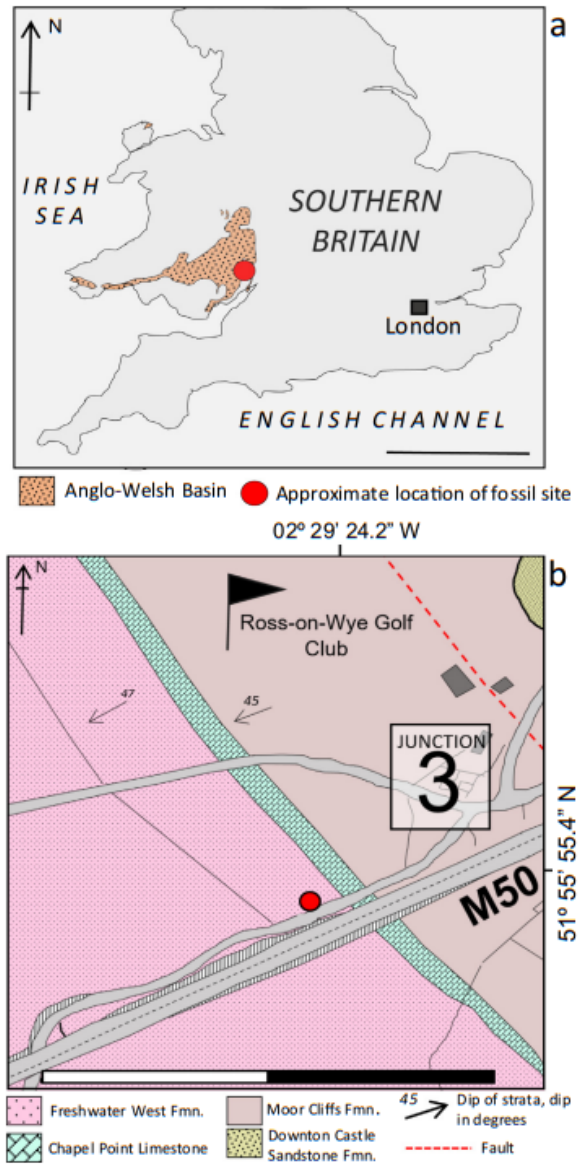

Fig. 2. a: Extent of the Anglo-Welsh Basin in South Wales and the Welsh Borderlands, scale bar 200 km. b: Geological map of the Ross-Tewkesbury Spur M50 motorway. Red circle indicates approximate site of mesofossil horizon. Scale bar: 500 m. Map based on Ordnance Survey and British Geological Survey Data, modified from Digimap ®. British National Grid projection lines. (For interpretation of the references to colour in this figure legend, the reader is referred to the web version of this article.)

were then covered and left to dry. Following drying, samples were gold coated using an Edwards S105B sputter coater for three minutes, prior to imaging with a Tescan Vega-3 Scanning Electron Microscope at 15–20 KV. Following initial examination and photography, samples were recoated with gold for a further three minutes to reduce any charge and rephotographed where necessary.

3.3. TEM

Once examined under SEM, a fragment (approximately half) of each spore mass was prised from the carbon tab using a steel razor blade and placed in a solution of pure ethanol. Samples were then sent to the University of Wisconsin Eau-Claire for TEM analysis by WAT. The spore masses were not oxidised or stained prior to imaging. The specimens were sectioned using a diamond knife before imaging with a JEOL-2010 Transmission Electron Microscope.

3.4. Curation

All SEM stubs and 19M50-26 sample and light microscope slides are housed at the Centre for Palynology at the University of Sheffield, Western Bank, Sheffield, S10 2TN, UK. All other light microscope slides are housed in the Micropalaeontology Unit at the Natural History Museum, London, SW7 5BD, UK. All TEM blocks and sections are curated in the Department of Biology of the University of Wisconsin-Eau Claire, Eau-Claire, WI, 53706, USA.

4. Results

Two specimens bearing *in situ Emphanisporites* spores were recovered (Table 1) alongside abundant spore masses, sterile axes and other 'phytodebris'. Both show varying degrees of completeness and different morphologies (Fig. 3). No sporangial cell walls or subtending axes have been observed in either of the specimens, but some acellular material is preserved. The occurrence of single or closely similar spore types, the absence of interspersed cuticular sheets, plant debris or tubes and the morphology of the specimens indicates that they are not coprolites. Sporangia and spore masses differ as the former exhibit enclosing sporangial wall layers, and while both specimens exhibit some remnants of an acellular wall layer, we refer to them here as spore masses given their largely incomplete nature. Both of the specimens were examined under SEM and then TEM. Light microscopy was attempted, but this was unsuccessful for both specimens. Whilst fragmentary, no saprotrophic encrustations or other evidence of decay, such as tubules, were observed.

4.1. Specimen ABM5015-001: *Emphanisporites epicautus* Richardson and Lister in an elongate spore mass (Plate I, a–d)

4.1.1. SEM observations

4.1.1.1. Spore mass. A large, incomplete spore mass appearing to be elongated, possibly originally being cylindrical (Plate I). A distinctive 'lump' is developed on one edge and the specimen appears to bend slightly to one side, away from the 'lump' (Plate I, fig. a, arrow). No subtending axis or sporangial wall cells are preserved. The mass is compressed and flattened with little three-dimensional shape retained. The spore mass has a total length of 1540 μm and is 725 μm at its widest point. A small amount of acellular material adheres to the specimen, but no sporangial wall cells are preserved which leaves numerous *in situ* spores readily observable. A small amount of amorphous material adheres to some of the spore mass and *in situ* spores and appears to form an intersporal matrix.

4.1.1.2. In situ spores. The spores are relatively well preserved with limited damage, despite the fragmentary and compressed nature of the spore mass. Some pitting, folding and pyrite growth is present, alongside common extraneous material which is present across most of the spores – this material does not obscure spore structure, however. This extraneous material is angular to approximately spherical in habit, up to 1 μm wide. Spores have circular ambs, 26 μm to 38 μm (10 measured), mean size 33 μm. Proximally, the spores exhibit an emphanoid ornament of 8–12 very fine interadial muri, typically 0.7 μm wide, in each interadial area. The trilete mark has lips but is relatively indistinct and there is an apical thickening. The triradiate mark extends approximately 2/3rds of the spore radius before diverging into fine curvaturae perfectae which are not greatly invaginated at the radial points. Distally

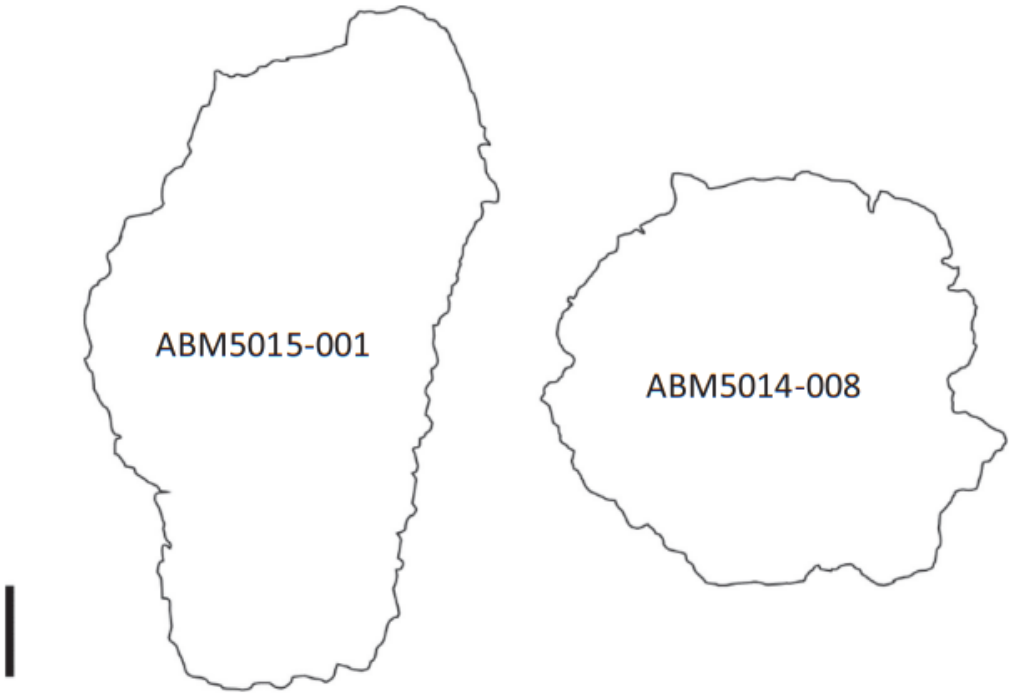

Fig. 3. Outlines of the spore masses described in this paper (Table 1). Scale bar 200 μm.

and equatorially the spores are laevigate. *In situ* spores show some variation in the apical thickening and interadial muri.

4.1.1.3. Comparisons with the megafossil and dispersed spore record. The incomplete nature of this spore mass makes it difficult to relate it to a megafossil genus, given the absence of complete morphology and key anatomical features. The gross shape may suggest the sporangium was elongate, perhaps cylindrical, in life, rather than discoidal or reniform, but the shape may result from fortuitous breakage. Elongate sporangia are common in compressed megafossils, variously seen in *Salopella*, *Tortilicaulis* (Edwards et al., 1994) and other unnamed compressed mesofossils (e.g. Morris et al., 2011a). The spore mass does not appear to have been bivalved, there is no indication of tapering and the presence of *Emphanisporites* species rather than *Apiculiretusispora* species precludes assignment to *Salopella*. Similarly, *inter alia*, the rounded tips and tapering apices of *Tortilicaulis* are not observed, precluding assignment to that genus. The lump on one side of the spore mass may suggest that the sporangium was bifurcating in life, perhaps reminiscent of *Horneophyton lignieri* (Kidston and Lang) Barghoorn and Darrah sporangia, or cf. *Horneophyton* sp., although this is tenuous; perhaps less speculatively it is a result of breakage. Ultimately, the lack of specimens and morphological characters exhibited on the spore mass precludes us from making a formal description or placement of the spore mass.

The size range and mean size of spores, character and number of interadial muri, excellent curvaturae perfectae and probable apical thickening on most of the in situ spores corresponds well with the description of *E. epicautus* Richardson and Lister. Those that differ (Plate I, fig. d) are reminiscent of *E.* cf. *epicautus sensu* Richardson and Lister, having the apical 'bald' region where interadial muri fail to reach the proximal pole, and a similar extent, number and robustness of the interadial muri and distinct curvaturae perfectae.

4.1.2. TEM observations

The specimen is heavily compressed and brittle, offering suboptimal preservation but examination of the ultrastructure remains possible. 'Chattering' occurs across the spore wall (vertical lines across entirety of specimen), which is a methodological artefact derived from the specimen being brittle (described in Taylor, 2002). Fig. 4a illustrates the wall ultrastructure of an *E. epicautus* spore, as sectioned through the equator, Fig. 4b is a schematic diagram of the ultrastructure. The internal wall ultrastructure is entirely homogenous with no lamellae or differentiation of the exine. Because of the angle of sectioning of the spore, it is difficult to ascertain which is the proximal and distal hemisphere; regardless, both are similar in thickness of *c.* 1 μm. Compression makes the lumen unclear across much of the specimen, but a part is visible near the centre of the spore (Fig. 4b, arrow 2).

Table 1
Specimens described in this paper. Dimensions describe the widest and longest portions of the spore masses. * ten in situ spores measured: smallest (mean) largest; † estimated number of spores in each spore mass (nearest 100), calculated by (0.74 x Volume of spore mass($\pi r^2 h$)/Volume of mean spores ($4\pi r^3/3$), assuming (1) spores are perfect spheres giving rhombohedral packing to give a porosity of 26%, and (2) that sporangia are cylindrical, following Wellman (1999).

Specimen	Description	In situ spore	Dimensions	Spore size*	*c.* Number of spores†
ABM5015-001	Elongate spore mass	*E. epicautus*	1540 × 725 μm	26 (33) 38	*c.* 6200
ABM5014-008	Discoidal spore mass	*E.* sp.	909 × 969 μm	28(32) 40	*c.* 5500

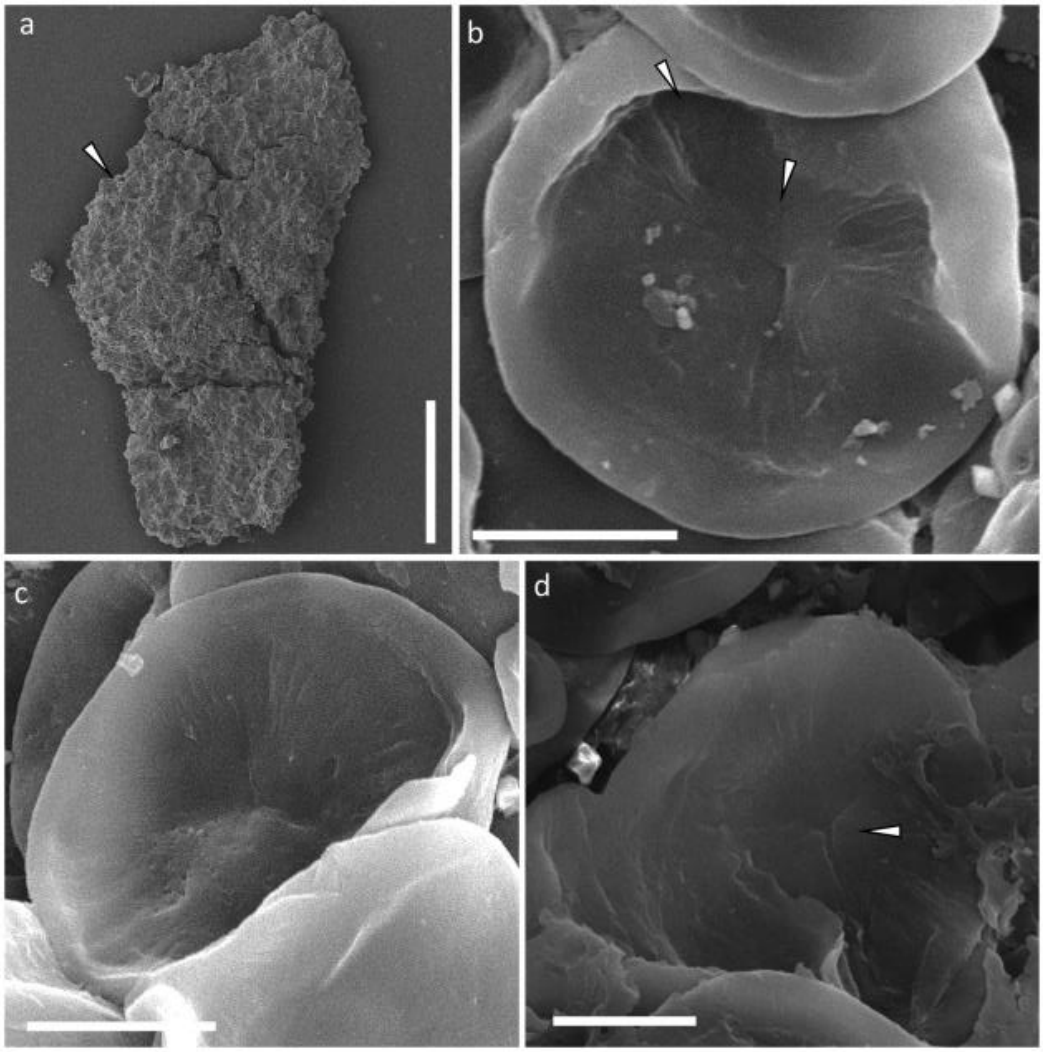

Plate I. SEM micrographs of spore mass yielding *in situ Emphanisporites epicautus*, ABM5015-001. **A**: Spore mass. Note apparently elongate slightly bent structure with distinctive 'lump' about the middle-upper margin (arrow), scale bar: 500 μm. **b:** *In situ E. epicautus*, note the apical thickening and thickened Y ray terminations (arrows). Consider also the well-defined curvaturae perfectae, fine inter-radial muri and concave proximal face. This specimen also shows the rare cubic to spherical excess mineralisation; **c:** Subcircular *E. epicautus*, note again the thickening at the proximal pole and fine interadial muri; **d:** an *in situ* spore redolent of *E.* cf. *epicautus*, exhibiting the much larger apical thickening (apical 'bald patch', arrow) on the proximal face and slightly coarser interadial muri relative to *E. epicautus* proper; this specimen also shows the amorphous material found across the spore mass adhering to the spore. Scale bars 10 μm.

4.2. Specimen ABM5014-008: Emphanisporites sp. in a discoidal spore mass (Plate II, a–g)

4.2.1. SEM observations

4.2.1.1. Spore mass. Approximately discoidal in plan, it is compressed but retains some three-dimensional shape. The spore mass has a length of *c.* 909 μm and a width of *c.*969 μm. The gross morphology of the spore mass is visible, although some cracking is observed and portions have been cleaved off. The edges of the mass are damaged, and no subtending axis is present. Limiting material is present across some areas of the spore mass but is largely lost. This material is acellular, variously adherent and largely unstructured aside from small, randomly orientated folds. Areas without limiting material expose numerous in situ spores. No evidence of saprotrophy is observed.

4.2.1.2. In situ spores. The spores are reasonably well preserved although folding, pitting and proximal face loss affect them. Apparent extraneous material is present and variously coats the spores, although never significantly so. Spores have a subtriangular to circular amb, 27–38 μm, mean 32 μm (nine measured). The proximal face is distinctly concave, and interadial areas are ornamented by 8–10 robust, straight, tapering interadial muri which are 2 μm at their widest point at the inner crassitude. Muri become more distinct towards the equator and show some tapering towards the proximal pole, petering out before they reach it. A thickening is present, extending approximately ¼ of the length of the triradiate mark at the proximal apex. The triradiate mark is distinct, accompanied by well developed, tall lips up to 2 μm wide which rise above the interadial muri. Rays extend ⅔ to ¾ of the radius of the spore before reaching the inner crassitude. The robust equatorial region is 3–4 μm wide and is sometimes laevigate but chiefly exhibits small

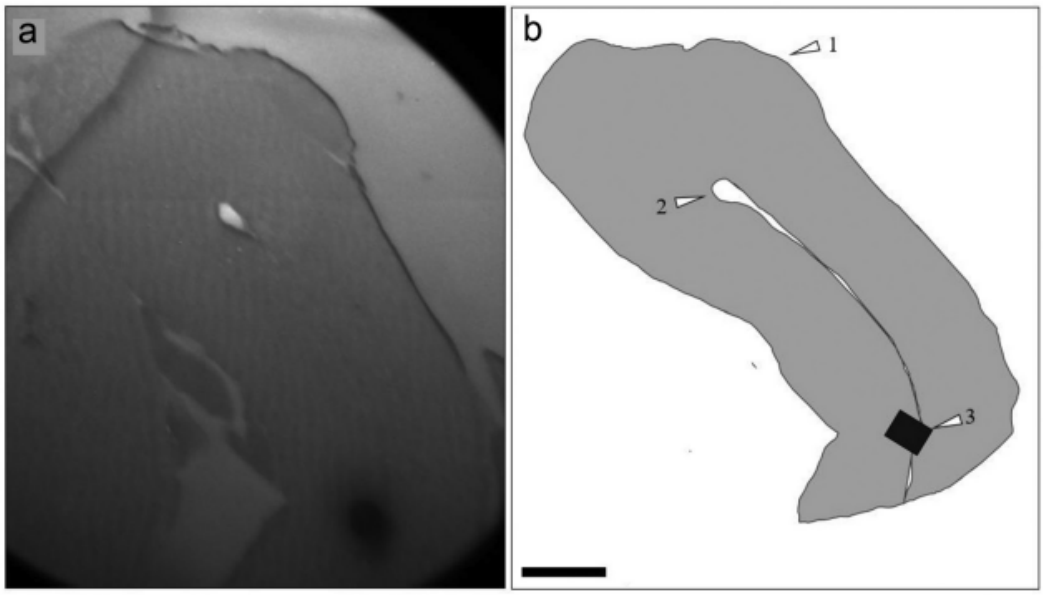

Fig. 4. TEM micrograph showing the ultrastructure of in situ *Emphanisporites epicautus*. Note the 'chattering' occurring as vertical lines across the specimen. The black line along the 'top' margin of the specimen is remnant gold coating from SEM analysis. **b**: schematic of *E. epicautus* ultrastructure. Note homogenous wall. **1:**?Equator; **2:** spore lumen; **3**: Pyrite grain. (For interpretation of the references to colour in this figure legend, the reader is referred to the web version of this article.)

folds and 'hummocks'. The distal exine is robust with an irregular 'hummocky' sculpture (Plate II, d–f). Given the irregularity and failure to identify comparative features in the dispersed record, this may be a result of decay rather than sculpture, but this is not certain.

4.2.1.3. Comparisons with the megafossil and dispersed record. Spheroidal sporangia and spore masses are common in the compressed record and the latter have already yielded *in situ Emphanisporites* spores (Morris et al., 2011b). The discoidal spore mass may be comparable to various *Cooksonia*, *Paracooksonia* or *Lenticulitheca* species (e.g. Edwards, 1979; Edwards et al., 2014; Morris et al., 2011b); however, in all instances *in situ* spores from these plants (where known) differ from the *E.* sp. described here, with the former two yielding crassitate, apiculate trilete spores of the *Aneurospora-Streelispora* complex (e.g. Morris et al., 2011b) and the latter yielding cryptospore species belonging to *Cymbohilates* (Morris et al., 2011b). The difference between *in situ* spores and the unclear nature of the subtending axis and overall anatomy distances this specimen from those genera mentioned above. The *in situ Emphanisporites* spores in the discoidal sporangium described in Morris et al. (2012b) differ from this specimen, with the former being comparable to *E.* sp. A *sensu* Richardson and Lister. In terms of gross morphology the two spore masses are quite similar, being discoidal with a roughly circular outline although ABM5014-008 is slightly more oblate. Both exhibit an acellular, cracked surface which may represent remnants of the sporangial wall or a cuticular layer (Morris et al., 2012b). If the morphology reflects the sporangial shape, it is plausible that, if these spore masses were found as megafossils, they would be classified as the same morphospecies. Because of a lack of specimens and morphological characters, we do not formally describe this *Emphanisporites* yielding spore mass.

The *Emphanisporites* species from ABM5014-008 does not appear to have a direct published counterpart in the palynological record, and *in situ* and dispersed spore size comparisons are complicated by shrinkage of the former during burning. Of similar dispersed species, the *in situ* spores have some similarities with *Emphanisporites rotatus* McGregor and *Emphanisporites neglectus* Vigran, although significantly differs from both in terms robustness of the spore and the nature of the distal hemisphere. Neither *E. neglectus* nor *E. rotatus*, or indeed any other published *Emphanisporites* species, fully satisfies the features exhibited by this *Emphanisporites* species. Given the robust nature of the equatorial and distal exine this spore might be considered patinate. TEM analysis, however, (below) indicates that the spore wall is not considerably thicker than other *Emphanisporites* spores (Taylor et al., 2011) and is distinctly thinner than other sectioned patinate spores (*Cymbosporites echinautus* in Johnson and Taylor, 2005).

Analysis of the dispersed spore assemblage from 19M50-26 did not yield comparable spores and attempts to extract *in situ* spores from the spore mass to observe under light microscope failed. A single example of a reasonably comparable *Emphanisporites* sp. spore was identified from the dispersed record of the M50 (Plate II, g). This spore exhibits a roundly subtriangular amb (29 μm), robust equator, distinct triradiate mark accompanied by narrow lips extending to the inner edge of the equator and interadial areas populated by *c.* 10 robust, tapering interadial muri which do not reach the proximal apex; although an apical thickening may be present it is not certain. Equatorially and distally, the spore is sculptured with angular micro-?verrucae. This differs from the distal hemisphere on *in situ E.* sp., which appears more chaotic. Interestingly, this spore was identified from the pre-MN?Earliest Lochkovian *Apiculiretusispora* sp. E spore biozone (−35.3 m relative to the Chapel Point limestone).

4.2.2. TEM observations

A partial montage exhibiting *c.* 60% of the spore and schematic are illustrated in Fig. 5. The specimen has been heavily compressed and folded but ultrastructural architecture remains. Part of the distal and possibly proximal wall is partially obscured by a fold in the plastic (black region along the lower right of the spore, Fig. 5). Proximally, the spore wall thickness is *c.* 0.7 μm. The proximal face is folded, but the aperture may be exhibited (Fig. 5, arrow Ⅳ); no variation in spore wall architecture is observed about this region. The distal spore wall is up to 1.5 μm thick. It appears to be divisible into two parts: (1) an inner, possibly faintly lamellate layer up to 0.5 μm thick, with a (2) wider, faintly spongy surface layer comprised of a series of knobs, which are variously connected to the laminate layer, up to 1 μm thick.

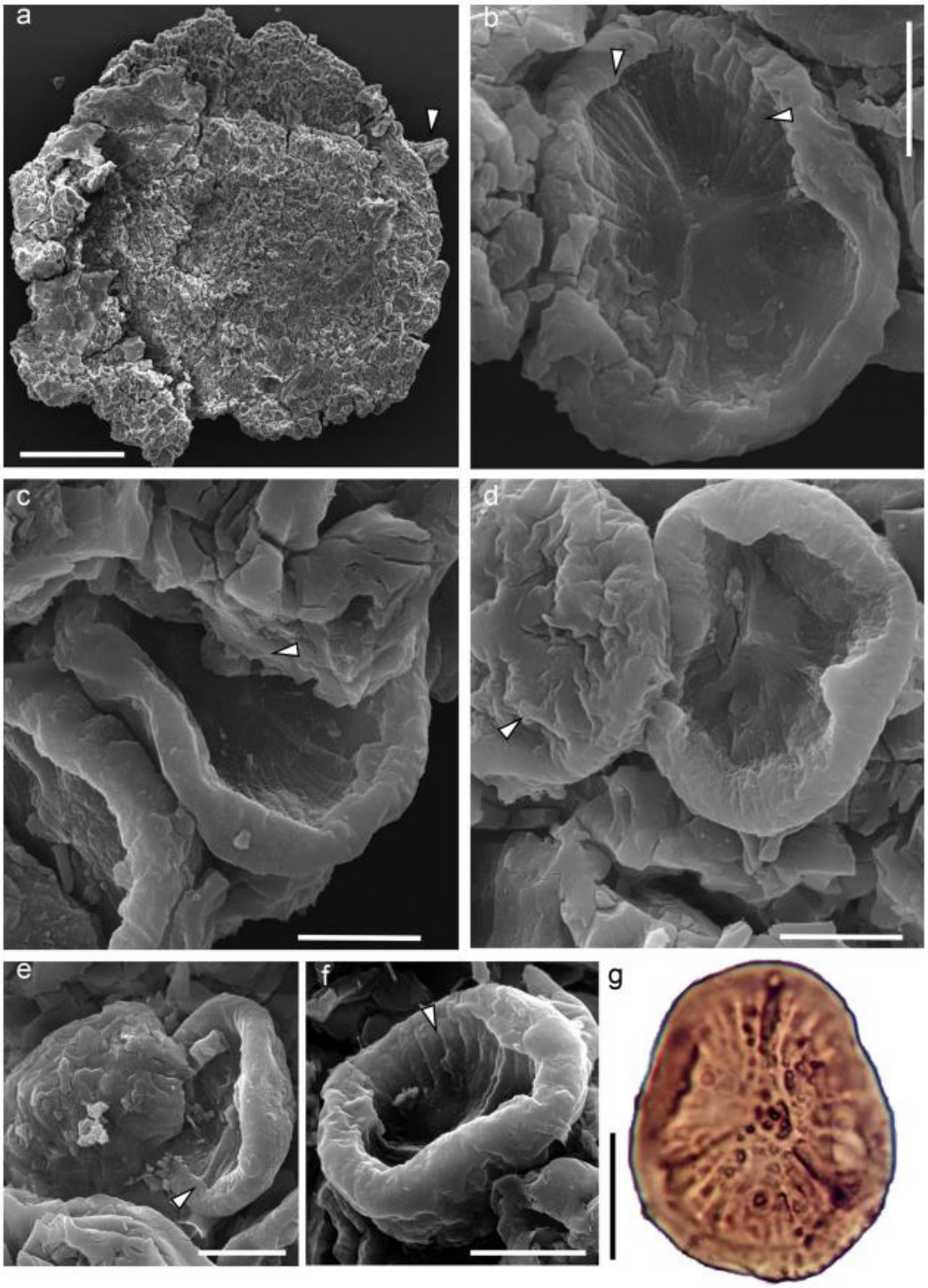

Plate II. SEM micrographs of the discoidalspore mass yielding *in situ Emphanisporites* sp., ABM5014-008. A: Spore mass. Note discoidal morphology with fractured outer edge: arrow indicates a section of the sporangium which has been fortuitously preserved; this is not a subtending axis, scale bar: 200 μm. b: *in situ* spore, proximal face. Arrows indicate robust inter-radial muri and distinctive lips. Note the robust equator and the distinctive apical thickening. c: Proximal face, note the concave habit and apical thickening (arrow) d: Proximal and distal hemispheres: note the chaotic, hummocky nature of the distal hemisphere. This may be compounded by shrinkage of the spore. Note also the highly robust equator of the specimen on the right. e: Proximal and distal view, note again the irregular nature of the distal hemisphere. f: Tipped spore, note how the distal 'sculpture' continues to a lesser extent onto the equator; b – f scale bars 10 μm. g: Light micrograph of the most comparable *Emphanisporites* sp. identified in the dispersed spore record, from the *Apiculiretusispora* sp. E biozone, Moor Cliffs formation. Note the robust tapering muri which are lost towards the proximal apex, the robust equator, and distal?sculpture. Ross-Tewkesbury Spur (M50) motorway section, slide M50-85-2C-1, E.F. no. U11. Scale bar 10 μm.

These are populated by occasional lacunae, which sometimes mark the separation between the layers. The distal sculpture is exhibited in cross section, having the same architecture as the homogenous outer layer, suggesting that this is a sculptural, rather than a decay, feature. No interadial muri are identified in the section.

4.3. Dispersed Emphanisporites species in sample 19M5026

A major analysis of the Siluro - Devonian dispersed spore record from the Lower 'Old Red Sandstone' of the basin building on Richardson and colleagues' work (e.g. Richardson, 1996, 2007; Wellman et al., 2000; Morris et al., 2011a; Richardson and Lister, 1969) is being carried out by ACB. The dispersed spores recovered from this sample are extremely well preserved with low thermal maturity. Some mild pyritisation and/or decay occurs in some specimens, but this is minimal. In quantitative counts of 250 spores the diverse assemblage briefly comprises species of *Aneurospora* (12%), *Ambitisporites* (26%) and *Laevolancis* (16%), with accessory ornamented hilate cryptospores including *Cymbohilates* (5%), cryptospore tetrads such as *Tetrahedraletes medinensis* (4%) and laevigate, apiculate and muromate crassitate and patinate trilete spore species of *Streelispora* (6%) and *Archaeozonotriletes* (9%), amongst others. Five species of *Emphanisporites* were identified in these samples with the spores comprising 2% of the overall assemblage or 114 *Emphanisporites* spores per gram of rock processed. Individual species of *Emphanisporites* all occur in low relative abundances and most are 'rare', that is, are identified during logging outside of spore counts.

5. Discussion

5.1. Spore mass maturity

The morphology of the ABM5015-001 *in situ* spores is comparable to the dispersed species *E. epicautus* and *E.* cf. *epicautus* which, on the assumption that spores are dispersed as individual monads at maturity suggests that the *in situ* spores must be close to maturity. The maturity

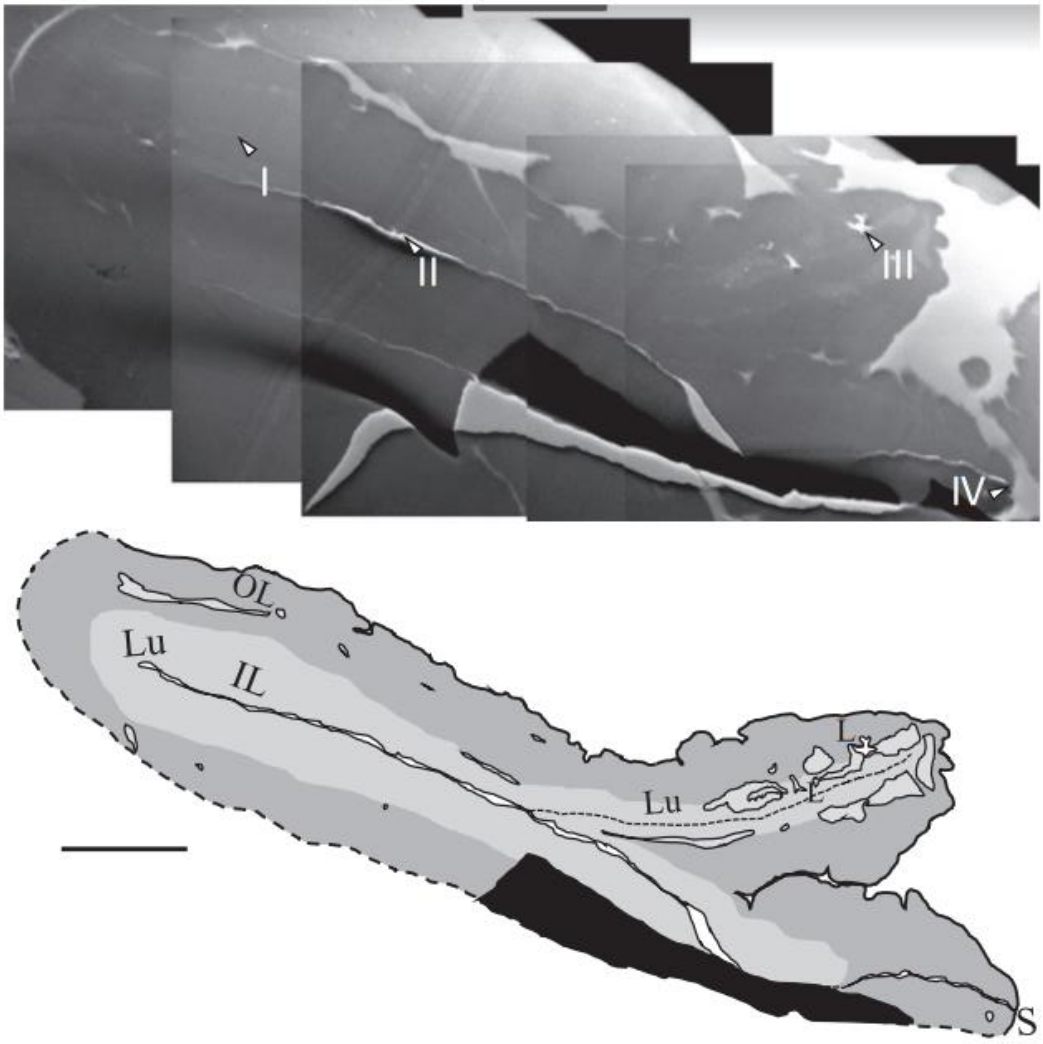

Fig. 5. (Top) TEM montage micrograph showing the ultrastructure of in situ *Emphanisporites* sp., with the spore outlined by black dashed lines. Arrow I:?inner lamellate layer; arrow II indicates part of the lumen. Note that due to folding, the lumen probably folds into the upper right extension of the wall but is not visible due to compression/ fusion; Arrow III: rare lacunae; Arrow IV indicates the suture. The black region along the bottom right of the spore is a fold in the plastic and is a preparative artefact. Scale bar 1 μm. Bottom: Schematic diagram showing the bilayered exine of *E.* sp. The dark layer is the homogenous outer layer, whilst the paler layer is the inner homogenous layer. OL: Outer layer, IL: inner layer, Lu: lumen, L: lacunae, S:suture. Scale bars 1 μm.

of the spores of *E.* sp. is less certain, as no unequivocal comparative dispersed species have been identified. Whilst this may be a function of the rarity of this *Emphanisporites* species, it may also suggest that the *in situ* spores had some morphological additions/ reductions to come in the latter stages of ontogeny. However, as with *E. epicautus*, no associated tetrads were found in the spore mass, indicating that the spores were mature or nearly so.

5.2. Comments on spore wall development

Detailed commentary of the spore wall development of *E. epicautus* is problematic given the homogenous architecture of the exine which obscures the original method of sporopollenin deposition. Most embryophytes utilise white line centred laminations (WLCL) to accumulate sporopollenin during sporogenesis (Wellman, 2004), so the lack of lamellations in the mature spore wall does not exclude their presence in initial stages of sporopollenin deposition; they may have been heavily compressed and subsequently obliterated or obscured by later deposition of sporopollenin. The apparent occurrence of *E. epicautus* and *E.* cf. *epicautus* in the same sporangium is evidence that they are both derived from the same plant, rather than a complex of similar plants as has been previously suggested (e.g. Edwards and Richardson, 2000). They could represent different developmental stages (with *E.* cf. *epicautus* perhaps representing some ontogenetic failure), or indicate some failure or disruption in sporopollenin deposition as the interadial muri were forming, or may be a result of some genetic disruption leading to malformation. The common occurrence of *E. epicautus* and *E.* cf. *epicautus* together in the dispersed record (see 5.4) may suggest that, if they are indeed derived from the same plant, that this malformation was either common or the production of spores with slightly different morphologies was a deliberate strategy of the plant. It is important to note that these dispersed species are not always contemporaneous, however (Higgs, 2004; Morris et al., 2011a).

The bilayered architecture of *E.* sp. spores suggest a different mode of development. The partially separated bilayered wall structure suggests that the lamellate and homogenous layer formed by different mechanisms, although the timing of formation is not certain. Given the faint laminations, the inner layer probably formed by WLCL, as lamellae were laid down on the spore plasma membrane, followed by sporopollenin accumulation on either side. Sporopollenin deposition may have been quite significant, largely obscuring the initially formed lamellae. Formation of the outer layer is less clear. A possible mechanism for the formation of the outer layer might be found in the extant moss *Andreaea*, where the spongy exospore develops via the accumulation of discrete globules of sporopollenin (Brown and Lemmon, 1984) secreted onto the sporocyte, an ontogenetic pathway peculiar to these plants. In this case, the lamellar layer would develop underneath the previously deposited layer, i.e. centripetally (Blackmore et al., 2000). Alternatively, it may have formed by the secretion of sporopollenin from a tapetum, such as in *Rhabdosporites langii* (Wellman, 2009), onto the lamellar layer, i.e. centrifugally. We cannot rule out either of these mechanisms, or other mechanisms of formation, but note that no evidence of a tapetum is observed in this specimen. The entire wall may have developed by WLCL, with lamellations in the 'outer' layer being obscured later on in ontogeny. Alternativley, given the highly folded nature of the spore wall, it may also be possible that intense folding lead to partial delamination of layers along weak horizons.

5.3. Affinities and phylogenetic considerations

5.3.1. Broad affinities

The wider coeval mega-, mesofossil and dispersed spore record indicates that in life these plants shared their environment with herbaceous, diminutive rhyniophytes, rhyniophytoids, primitive cryptospore-bearing plants and eophytes alongside larger zosterophylls, this being a plant community typical of the Early Lochkovian of the Anglo-Welsh Basin (e.g. Wellman et al., 2000; Edwards and Richardson, 2004; Morris et al., 2011a; Edwards et al., 2021a).

Of these, their production of trilete spores excludes them from the cryptospore producing eophytes and other primitive cryptospore-bearing plants. Likewise, a zosterophyll affinity can be excluded based on the shape of the spore mass and the fact that *Emphanisporites* species have not been identified *in situ* from zosterophyll sporangia (e.g. Edwards, 1969; Allen, 1980). We conclude that these *Emphanisporites* producers probably belong amongst the rhyniophytes. However, given the absence of vascular tissue we must refer to them as rhyniophytoids. It is possible that these plants closely resembled the rhyniophytic body plan, being diminutive with terminal sporangia - but features such as sporophytic branching or stomata are unknown. The rhyniophytoids comprise a particularly diverse complex of plants from a variety of lineages (Steemans et al., 2012), and thus it is interesting to explore how closely related to one another *E. epicautus* and *E.* sp. are. Due to a lack of morphological characters, this is largely unclear from SEM studies. The apparently different morphologies of the spore masses (and indeed, the *in situ* spores) indicate that the parent plants were at least generically distinct, but ultrastructural features of the *in situ* spores provide the firmest evidence that they were in fact derived from quite different taxa.

5.3.2. Comparisons with other Emphanisporites spp.

This is the first TEM study of *in situ Emphanisporites* spores, but comparisons can be made with three dispersed species from Gaspé Bay in Canada (*E. rotatus*, *E. schultzii* and *E. annulatus*: Taylor et al., 2011). Broadly, Taylor et al. (2011) found that *Emphanisporites* generally exhibit (1) a single layered exospore ranging from laminated to spongy in structure, and (2) proximal radial ribs that were compositionally confluent with the outer part of the exospore. Both *in situ Emphanisporites* spores described here differ significantly (Table 2).

It is possible that the ultrastructure of the spore walls was obliterated or altered during diagenesis, especially in the case of *E. epicautus*. However, the ultrastructure of *E.* sp. appears to be well preserved and, considering the two masses were recovered from within at most a few centimetres of each other, they are unlikely to have had different diagenetic histories. Similarly, both of the spore masses were exposed to the same treatment; HF + HCl maceration and were not oxidised or stained. There is a possibility that more subtle structures such as fine lamellations have not been identified because the spore masses were not stained. Whilst this remains possible even very subtle structures would be hinted at under the TEM (as they are in *E.* sp.). We conclude that the ultrastructure exhibited by these *in situ* spores is natural.

The most striking difference between *E. epicautus* and other *Emphanisporites* spore wall ultrastructures is the lack of lamellations in the exospore, a common feature amongst all but one *Emphanisporites* specimen (*E. rotatus* II) in Taylor et al. (2011).Those workers found that lamellations range from very subtle to distinctive across the examined *Emphanisporites* spores, leading them to suggest that the homogeneity of *E. rotatus* II may be derived from diagenetic or preparative influence, but note that all of the specimens again have similar diagenetic and preparative histories. Furthermore, the sectioning of the *E. epicautus* spore mass was not comprehensive across several specimens; it could be that this specimen simply exhibits no lamellations, whilst others of the same species do, or that they were largely obliterated during ontogeny and only remain in isolated sections of the spore, which were not seen under TEM (as hypothesised for *Chelinospora vermiculata*, Johnson and Taylor, 2005). Similarly at odds with the findings of Taylor et al. (2011) is the dearth of a spongy layer or larger lacunae in the exospore. Finally, the thickness of the spore wall is slightly less than in other *Emphanisporites* species. While differentiating the proximal and distal hemispheres is problematic, the areas towards the poles are no thicker than 0.7 μm, thickening to 1 μm at the equator. Ultimately, if the homogenous spore wall in *E. epicautus* is indeed natural, then (1) the ultrastructure distances it

from other species of *Emphanisporites*, including *E.* sp. and (2) there may be some relationship with *E. rotatus* II (Taylor et al., 2011) in terms of the mature wall ultrastructure, ontogenetic developmental pathways aside (discussed in 5.3.3).

Morris et al. (2012b) described a discoidal spore masses yielding *in situ Emphanisporites* sp. A *sensu* Richardson and Lister from the middle MN spore biozone NBCH site. While no TEM imaging of the spore wall of *E.* sp. A was carried out, it is of interest that they noted that the fractured surfaces of the spore walls were homogenous to faintly granular, hinting at a similarity between *E.* sp. A and *E. epicautus*.

Considering *E.* sp., initial congruence with most of the other *Emphanisporites* species is found with regard to the inner lamellate layer, setting the ultrastructure of *E.* sp. at odds with *E. epicautus*. The thickness of the spore wall is also comparable to other *Emphanisporites* specimens. On the other hand, a distinctive feature which sets *E.* sp. apart from the other *Emphanisporites* ultrastructures is the bilayered exine. The outer, semi-detachable surface layer appears to be peculiar to *E* sp. and is not seen in other species of *Emphanisporites*. It is worth noting, however, that some *Emphanisporites* species do exhibit some differentiation in the single layered exospore, such as *E. rotatus* I, but it is difficult to gauge how far this feature differs from the bilayering seen in *E. sp.*

5.3.3. Comparisons with contemporaneous fossil taxa

Many fossil spores exhibit some element of a homogenous wall in their ultrastructure but this is normally associated with other features such as lamellae (e.g. in *Scylaspora* sp., Wellman, 1999) or a combination of features (e.g. in *Cymbohilates horridus* var. *splendidus*, Edwards et al., 2012a). Mature spore walls that are fully homogeneous are less common and are mainly found in the spore walls of cryptospores such as *Tetrahedraletes medinensis* (variant #1; Taylor, 2002) but also in some trilete spores. Alongside the dispersed *E. rotatus* II spore, Pre-Silurian (lower Wenlock to lower Ludlow) *Ambitisporites* spores have homogenous walls (Taylor, 2003), but this could be diagenetic. Most interestingly, two spore masses from NBCH yielded emphanoid spores probably belonging to *Ibereospora* which exhibited entirely homogenous spore wall architecture (Morris et al., 2012b).

Given the similarities between the mature spore walls of *E. epicautus* and the above taxa, perhaps the homogenous spore wall is a homologous feature between them? The amount, composition and timing of sporopollenin deposition during ontogeny of the spore wall is probably under genetic control (Wellman, 2004) and an entirely homogenous wall is considered to be a derived condition, with the primitive condition being lamellate walls (Taylor et al., 2017):could the loss and/ or obliteration of lamellae during ontogeny have occurred in a common ancestor between these homogenously walled taxa? Cryptospore tetrads such as *T. medinensis* persist, and are contemporaneous, with *E. epicautus*, but they are probably representatives of more ancient (and cryptically diverse) lineages, some of which are possibly ancestral to more derived trilete spores. However, ultrastructural analysis on older and contemporaneous material is required to trace such lineages.

The question of a close relationship between these taxa not only depends on the nature of the mature spore wall, however, but the ontogenetic pathway by which the spore wall develops. Wellman (2004) notes that because of the variety of methods by which any given spore wall type can form, it is desirable to study the ontogenetic pathway. There is certainly more than one ontogenetic pathway that can lead to the formation of homogenous spore walls, including the obliteration of lamellations formed in the early stages of ontogeny by latterly deposited sporopollenin. Furthermore, given the nature of the wall it is particularly difficult to unpack the mode of formation, which is not necessarily comparable to extant processes. A focused study of fossil spores inside sporangia at different developmental stages could shed light on spore wall ontogeny, but this would be extremely difficult.

Considering the ultrastructure of *E.* sp., bilayered spore walls are common in late Silurian–Early Devonian spores (e.g. Edwards et al., 1995a, b; Wellman, 1999; Johnson and Taylor, 2005). *Ambitisporites–Synorisporites–Streelispora/Aneurospora* and *Scylaspora* all exhibit a bilayered exine. Some cryptospores, too, exhibit bilayered ultrastructure (e.g. *Lævolancis divellomedium* type 2 Wellman et al., 1998b). Interestingly, the combination of a bilayered exine and discoidal spore mass could ally *E.* sp. with the *Lenticulitheca–Paracooksonia–Cooksonia* complex (Morris et al., 2011b; Edwards et al., 2014). However, the presence of the separating outer layer in the ultrastructure of *E.* sp. sets it at odds with the spore wall architecture from the *in situ* spores in those plants, and the lack of key morphological characters exhibited by the *E.* sp. spore mass precludes assignment to any of the constituents of that complex, not to mention the differences in spore morphology. An inner lamellate layer with an outer homogenous layer has been identified in *in situ Scylaspora* (Wellman, 1999). However, *E.* sp. differs considerably due to the separation of the outer layer, and additionally, no lacunae are exhibited in *Scylaspora* spore walls. Indeed, few spore ultrastructures exhibit such a separation of layers. One example, however, is *Dyadospora murusattenuata* type I from the Ordovician (Taylor, 1997), which has varying degrees of separation between an inner lamellate

Table 2
Current data for *Emphanisporites* ultrastructure.

Species	Gross wall ultrastructure	Laminations?	Wall thickness (μm)	Reference
E. rotatus I*	• Inner: laminated • Outer: spongy with lacunae	Yes	4 P. & D.	Taylor et al., 2011
E. rotatus II*	• Homogenous	No	2 D. 1.5 P.	Taylor et al., 2011
E. rotatus III*	• Faint laminations • Inner wall has large lacunae	Yes	3 D. 2.5 P.	Taylor et al., 2011
E. rotatus IV*	• Faintly laminar	Yes	2.5 D. 1.5 P.	Taylor et al., 2011
E. rotatus V*	• Faintly laminar • ?Pseudosture • Thick laminar surface layer	Yes	1.5 P. & D.	Taylor et al., 2011
E. schultzii I*	• Distal wall laminated throughout • Spongy innermost exospore	Yes	5 D. 2 P.	Taylor et al., 2011
E. schultzii II*	• Distal wall laminated • Lacunae in proximal wall • Pseudosuture	Yes	3–4 P. & D.	Taylor et al., 2011
*E. annulatus**	• Inner laminations • Outer coarse sponginess	Yes	1–2.5 P. & D.	Taylor et al., 2011
E. epicautus† *E.* sp. †	• Homogenous • Inner laminations • Outer homogenous, partially detachable surface layer	No Yes	0.7 1.5	This paper This paper

layer and outer homogenous layer, but the spore wall ultrastructures are otherwise quite different. Considering this, a contemporaneous spore wall architecture to *E.* sp. is yet to be identified.

5.3.4. Affinities to extant taxa

A possible relationship between some *Emphanisporites* spores and hornworts was posited by Taylor et al. (2011), based on (1) ultrastructural features reminiscent of some characteristic features of extant hornworts, (2) the phylogeny of Qiu et al. (2006) which posited that hornworts were the sister group to tracheophytes, and (3) the occurrence of a columella, a characteristic feature of extant hornworts, in *H. lignieri*, the parent plant of *E. decoratus* (Wellman et al., 2004). Recent land-plant phylogenies by Puttick et al. (2018) and the recent placement of *Horneophyton lignieri* into the tracheophytes (Cascales-Miñana et al., 2019) cast some doubt on the hornwort – *Emphanisporites* association. Whilst hornwort placement remains equivocal in Puttick et al. (2018), the most significantly supported result was for hornworts as a sister group to the 'setaphyta' (mosses + liverworts) and being the most basal of the Bryophyta, distancing them from the tracheophytes. Puttick et al. (2018) suggest that the simplistic nature of the putative plesiomorphic liverwort body plan was in fact derived from a loss of ancestral characters, such as stomata, rather than simply an absence of derived embryophytic characters. Instead, the basal embryophyte may have had body plan more congruent with stem-tracheophytes than previously thought. The results of Puttick et al. (2018) may go some way towards explaining the hornwort associations of some of the *Emphanisporites* spores found by Taylor et al. (2011). Tentatively, the presence of characteristic features of extant hornworts in the ultrastructure of certain dispersed *Emphanisporites* spores (pseudosuture +/− external laminar layer) and some tracheophytic *Emphanisporites* producers (the columella in *H. lignieri*) are not indicative of hornwort association *per se* in these fossil plants and spores, but instead perhaps the retention of primitive features from some enigmatic, possibly relatively complex, basal embryophyte (Puttick et al., 2018) or may be a further example of evolutionary convergence amongst these plants.

Regarding the affinities of *E. epicautus*, the homogenous ultrastructure may indicate an association to Anthocerotopsida, where the mature trilete spores exhibit homogenous spore wall architectures (Brown and Lemmon, 1990). However, these plants also exhibit a number of key features including pseudoelaters, columellae and sequential spore maturation. Whilst the incomplete nature of the spore mass means we cannot rule these features out, their presence remains equivocal. In other hornworts, although little studied, the ultrastructure is highly diverse (Taylor, 2003) and, *inter alia*, some may exhibit a 'pseudosuture' and external laminar layers (e.g. Renzaglia et al., 2008) alongside often subdivided walls with two or more wall layers and an inner granular layer about the suture and sometimes beyond, as seen in the specimens in Taylor et al. (2011). The spore wall ultrastructure of *E. epicautus* exhibits none of these features (with granular features about the suture equivocal), undermining any strong associations with other members of the hornworts. Whilst some taxa outside of the hornworts do exhibit a homogenous ultrastructure, other features distance them from *E. epicautus*. Members of bryopsida often exhibit homogenous spore walls but are generally not trilete and also have an additional perine. In the case of leptosporangiate ferns which exhibit a homogenous exospore at maturity, an outer perispore is also observed which is not seen in *E. epicautus*. As such, there is little indication of a direct extant counterpart to *E. epicautus*. Additionally, the problem of comparative ontogenetic pathways persists.

In terms of *Emphanisporites* sp., several extant taxa have significant involvement of lamellae in some or all of their spore wall ultrastructure, including hepatics (Brown and Lemmon, 1990), Sphagnidae mosses, ferns and lycophytes. Liverworts typically exhibit lamellations in at least some part of the spore wall (Blackmore and Barnes, 1987), but spores derived from these plants lack trilete sutures and typically lack a homogenous outer layer or bilayering. In Sphagnidae mosses, an inner lamellate layer is overlain by a homogeneous outer layer, as in *E.* sp., but the former wall is highly derived, comprising five layers (Wellman, 2004). Lycopsids exhibit a laminar layer and an outer homogenous layer in the spore wall but they also exhibit a granular region (e.g. Lugardon, 1990) beneath the spore aperture, a feature not exhibited in *E.* sp., which is further distinguished from Lycopsids by the detachable surface layer. Extant, homosporous Filicopsida also exhibit an inner lamellate layer and an outer homogeneous layer (e.g. Tryon and Lugardon, 1991), but always exhibit a perine and the layers do not partially separate. Thus, no extant direct comparisons are yet known. Taylor et al. (2011) found that the ultrastructure of some *Emphanisporites* species exhibited lamellae and spongy areas reminiscent of extant lycophyte spores - offering tentative support for a basal-tracheophytic affinity of some species of *Emphanisporites*. Furthermore, the bilayered construction of the spore walls from taxa in the *Lenticulitheca-Paracooksonia-Cooksonia* complex was used to tentatively suggest the association of the complex to the stem-tracheophytes (Edwards et al., 2014), although as discussed, *E.* sp. is different to those spores. *E.* sp. does exhibit lamellae, but the outer spongy areas are not seen. Whilst the combination of an inner lamellate and outer homogenous layer might hint at a tracheophytic affinity, the strongest link to lineage is the triradiate mark which has long been attributed to vascular plants (e.g. Gray, 1985). However, authors (Kenrick et al., 2012; Edwards et al., 2014; Salamon et al., 2018) have noted that trilete marks are not peculiar to tracheophyte-derived spores, as they occur in several living bryophytes, also. Some extant hornworts even produce triradiate spores with a superficial resemblance to *Emphanisporites* (e.g. Boros and Jarai-Komlodi, 1975; Tryon and Lugardon, 1991; but see Taylor et al., 2011), although this may not have been true of fossil hornworts also. With extant trilete spores occupying a broader grouping outside of tracheophytes, it is probable that the same is true of fossil trilete spores (e.g. Edwards et al., 2014), and this complicates their relationships to any lineage which is compounded a lack of key morphological characters such as associated vascular tissue.

It is difficult to explore the phylogenetic relationships of *Emphanisporites* producers with such fragmentary fossils and limited data, but it may be that some of the producers lie outside of the tracheophytes proper, despite having a fully formed and functioning triradiate mark. What does seem clear is that the varied, although still largely enigmatic, lineages of *Emphanisporites* parent plants, evidenced by *H. lignieri*, dispersed *Emphanisporites* and the specimens described here, strongly support previous hypotheses that the emphanoid condition is an example of convergent evolution (e.g. Taylor et al., 2011; Morris et al., 2012b). Emphanoid muri are not peculiar to *Emphanisporites*, being identified in other trilete spore taxa (Morris et al., 2012b) and some hilate cryptospores such as *Artemopyra* (Burgess and Richardson) Richardson and some species of *Cymbohilates* Richardson. The reason for this convergence remains uncertain, but as previously hypothesised (e.g. Taylor et al., 2011) it is possible that, with so many taxa selecting for the emphanoid muri, it conferred some advantage to a reasonably common environmental or ecological pressure.

5.4. Broad palaeoecology – Inferences from the dispersed record

The parent plants of *Emphanisporites* remain poorly represented in the mesofossil record. They are largely outnumbered in charcoalified mesofossil assemblages by sporangia and spore masses yielding laevigate hilate cryptospores such as *Laevolancis* or crassitate trilete spores such as *Ambitisporites* and *Aneurospora*/ *Streelispora* (e.g. Morris et al., 2012b). This is reflected in the dispersed spore record. When considering the dearth of cf. *Horneophyton* sp. and other *Emphanisporites* producers in the megafossil record, Edwards and Richardson (2000) assessed the implications of taphonomy and palaeoecology on the likelihood of the plants being fossilised (Table 3).

Table 3
Palaeoecological and taphonomic effects on the dispersed spore record, after Edwards and Richardson (2000).

Possible cause of under representation	Effect on dispersed spore record
Plants living outside of river catchment areas and hence rarely entrained in deposited sediment.	Dispersed spores would be represented in the spore rain but would be swamped out by local plants.
Plants occupied restricted ecological niches and were hence rare in local vegetation.	Sporadic to no representation of dispersed spores from assemblages in local geographical areas.
The plants lacked recalcitrant biopolymers in their vegetative tissues, prohibiting fossilisation.	The plants would be represented in the dispersed spore record dependent on local numbers and proximity to depositional environments.

Here, we apply the rationale of Edwards and Richardson (2000) to the two *Emphanisporites* plants to assess the impact of taphonomy on their presence in the fossil record and explore their broad palaeoecologies.

Examination of the sample from which the specimens were isolated did not yield any dispersed spores directly comparable to *E.* sp. Extensive logging of material from the latest Silurian/earliest Lochkovian to the middle Lochkovian of the M50, Ammons Hill and NBCH found few comparatives, with only one relatively convincing specimen (Plate II, g) identified from the earliest Lochkovian of the M50 (−34.3 m below Chapel Point Limestone; *Apiculiretusispora* sp. E spore biozone, Fig. 1). The absence of the spore in the horizon from which the spore mass was uncovered suggests that the plant was either extremely rare or not growing in the M50 at that time, but the possible occurrence in the Moor Cliffs formation may indicate that it was growing near the area in the earliest Lochkovian – although the single occurrence necessitates caution. The lack of published records of *E.* sp. and paucity across the Anglo-Welsh assemblages suggests that the plant was not a common constituent of this Lochkovian vegetation, perhaps growing far from the present-day sample sites, with spores very rarely being incorporated into these assemblages. In this scenario the spore mass may have been transported a considerable distance, which is a plausible hypothesis for charcoalified remains.

Deciphering the exact relationship between all dispersed *E. epicautus* and *E.* cf. *epicautus* spores is not possible from the single occurrence recorded here and requires further ultrastructural study to confirm a consistent relationship, especially in dispersed specimens. As such, we will consider dispersed *E. epicautus* and *E.* cf. *epicautus* separately. Logging by ACB and previous work (Richardson and Lister, 1969; Edwards and Richardson, 2000; Higgs, 2004; Morris et al., 2011a) indicates that *E. epicautus* and *E.* cf. epicautus are widespread but rare constituents of the Anglo-Welsh basin palynoflora (Fig. 6). In the *Apiculiretusispora* sp. E zone (earliest Lochkovian) both *E. epicautus* and *E.* cf. *epicautus* are 'rare' in the M50 assemblage (cf. Edwards and Richardson, 2000), with *E.* cf. epicautus sometimes comprising up to 0.4% of the 250 spore count. A similar pattern is seen at Ammons Hill and NBCH (*E. epicautus* being rare and *E.* cf. *epicautus* comprising up to 0.4%). In the Lower MN zone of the M50, *E. epicautus* is sometimes rare, but more frequently comprises between 0.4 - 1.6% of the assemblage. *E.* cf. *epicautus* is found in lower proportions, at around 0.4%. Both are rare constituents in Ammons Hill, while only *E.* cf. *epicautus* is present, but rare, at NBCH. At Gardeners Bank (lower MN only), both comprise up to 0.4% of the assemblage. Finally, in the middle MN of the M50, *E. epicautus* is sometimes rare, but generally comprises between 0.4 – 0.8% of counts, while *E.* cf. *epicautus* comprises up to 0.4%. At Ammons Hill, *E. epicautus* comprises up to 0.4% of the assemblage, whilst *E.* cf. *epicautus* comprises up to 0.8%. At NBCH, *E. epicautus* is rare, whilst *E.* cf. *epicautus* is rare, or comprises up to 0.4%.

It is interesting to note here that *E.* cf. *epicautus* is ubiquitous, in varying proportions, across the investigated sites and biozones. Meanwhile, *E. epicautus* is observed in all of the sites and across all of the biozones except NBCH in the lower MN biozone, where only *E.* cf. *epicautus* is observed. If ABM5015-001 is representative of all *E. epicautus* and *E.* cf. *epicautus* parent plants (that is, that both spores are derived from the same plant) then the absence of the former in the lower MN of NBCH could be a result of taphonomy. Alternatively, it may suggest that the plant was not present in NBCH, and the observation of *E.* cf. *epicautus* in the assemblage results from fortuitous transport of that spore from some distance away. This is supported as only a single *E.* cf. *epicautus* specimen was found throughout extensive logging of these lower MN NBCH samples. Whether or not the plant was present in NBCH at this time, the plant was probably not restricted to a specialised niche given how widespread and consistent its occurrence is in the rest of the basin through time. However, the plants probably comprised a small proportion of the flora and seem to have been restricted to areas outside

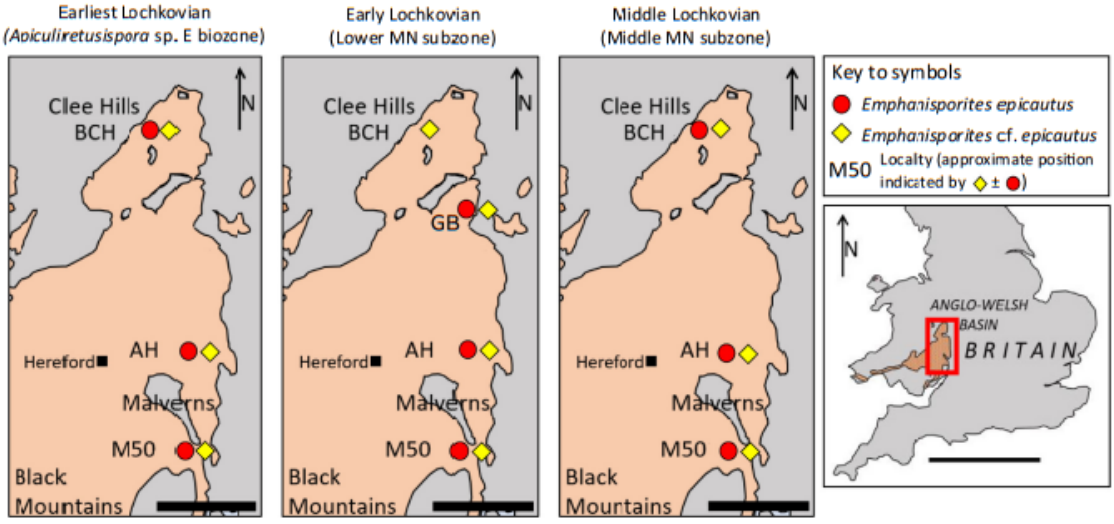

Fig. 6. Spatial and temporal distribution of E. epicautus and E. cf. epicautus across sites in the Welsh Borderlands. **BCH** = Brown Clee Hills area (including NBCH); **GB** = Gardeners bank (only present in the lower MN; **AH** = Ammons Hill; **M50** = M50 motorway. Locations approximate. Scale bar 20km. Bottom right, map: Outcrop of Anglo-Welsh Basin in South Wales and the Welsh Borderlands, red box

of river catchment. Because a single source plant for these spores cannot be confidently ascertained at present, an alternative hypothesis could be that the *E. epicautus* parent plant was not growing in NBCH during the lower MN, while the parent plant of *E.* cf. *epicautus* was, but both remained otherwise widespread in low proportions. As such, regardless of whether ABM5015-001 is representative of the *E. epicautus* and *E.* cf. *epicautus* producers, it is probable that the plant or plants, whilst not restricted to a specialised niche, were restricted to areas outside of river catchment and comprised a small proportion of the flora. As such, the spore mass found here was likely transported some distance to the depocenter, but was more local than the *E.* sp. mass.

Whilst the occurrence of *E. epicautus* and *E.* cf. *epicautus* spores across the basin supports a widespread, somewhat restricted niche, the possibility remains that this was located proximally rather than distally to rivers, with the *Emphanisporites* source plants simply being rare amongst the riparian vegetation or being lost to preservational biases. The chief support for the plants growing outside of the catchment area of rivers is the paucity of their spores in the dispersed record in these riparian deposits. Had they grown near depositional settings such as rivers, it seems plausible that despite their rarity a higher incidence might be expected. Sorting of spores is a possible explanation, however the size range of dispersed spores in the assemblages ranges between 16 and 52 μm, with a mean size of 27 μm. Dispersed and *in situ E. epicautus* and *E.* cf. *epicautus* from the Lochkovian measure between 26 and 38 μm, and *in situ* E. sp. measure between 28 and 40 μm, suggesting that these spores were unlikely to have been removed from the assemblage due to sorting, supporting the hypothesis that these plants inhabited niches outside of river catchment, but does not discount a taphonomic explanation altogether.

If the largely palaeoecological hypothesis holds, then, the paleoecology of the *E. epicautus* and *E.* cf. *epicautus* parent plant (or plants) is somewhat similar to that posited for cf. *Horneophyton* sp. by Edwards and Richardson (2000), except that the latter seems to have been more restricted and absent in marine influenced settings at Ammons Hill during lower MN times.Both appear to have been growing away from the catchment areas of rivers, but cf. *Horneophyton* may have inhabited more specialised niches, only occurring sporadically. Growth in presumably less equable settings away from moist depocenters would have necessitated adaptations to cope with physiologically stressful conditions. It follows that fine moisture sensing capabilities of dispersed spores would be particularly important for such plants, perhaps suggesting a function for the 'emphanoid' condition.

6. Conclusions

We present the oldest-yet published examples of *in situ Emphanisporites* and add to the growing diversity of sporangial morphologies found amongst rare *Emphanisporites* producers. *E. epicautus* and *E.* sp. are most comparable to the rhyniophytes, although a lack of unequivocal vascular tissue necessitates their grouping amongst the rhyniophytoids. We have uncovered enough morphological and ultrastructural information to confidently ascertain that they belonged to quite different, although equivocal, lineages. They differ significantly from other *Emphanisporites* species, especially *E. epicautus*, and do not have any directly comparable contemporaneous fossil or extant taxa. While the homogenous exospore of *E. epicautus* makes comparisons difficult, the bilayered exine comprising an inner lamellate layer and outer homogenous layer of *E.* sp. may relate it to some modern tracheophytes, but this remains problematic. Investigation of sporocyte development for *E. epicautus* is difficult given the homogenous architecture of the spore wall, but *E.* sp. on the other hand may have formed by a variety of means. Whilst the Andreaea mode of formation for the outer homogenous layer is plausible in the absence of evidence for a tapetum and rare lacunae, the overall spore wall development remains clouded. Given the paucity of *E.* sp. in the dispersed record, we cannot currently explore the palaeoecology of this plant. The dispersed spore record of *E. epicautus* and *E.* cf. *epicautus* indicates that the parent plant/ plants inhabited widespread ecological niches away from the catchment areas of rivers, but these do not appear to have been as restrcted as the niche of cf. *Horneophyton* sp. It is possible that the emphanoid muri conferred some advantage to propagation in water stressed environments, as the diversity of *Emphanisporites* producers, and other emphanoid muri bearing taxa, strongly indicates that the emphanoid condition is convergent (Edwards and Richardson, 2000; Taylor et al., 2011; Morris et al., 2012b) and may have offered some selective advantage due to some environmental and/ or evolutionary pressure.

Author contributions

ACB conceived the study, performed SEM and light microscopy work and wrote the manuscript. WAT performed TEM sectioning and photography and reviewed the manuscript.

Declaration of Competing Interest

The authors declare that there are no conflicts of interest.

Acknowledgments

This work has been carried out as part of A.C.B.'s pursuit of a Ph.D. qualification and is supported by a NERC funded ACCE (Adapting to Challenges of a Changing Environment) Doctoral Training Partnership Ph.D. studentship [grant number NE/L002450/1] that is a CASE partnership with the Natural History Museum, London. ACB would like to thank Dianne Edwards and Lindsay Axe for the material and his Ph.D. supervisors Paul Kenrick, John Richardson, Stephen Stukins and Charles Wellman for reviewing early copies of the manuscript and their helpful input, in addition to Dave Bodman and the University of Sheffield Electron Microscopy Unit.

References

Allen, K.C., 1980. A review of in situ Late Silurian and Devonian spores. Rev. Palaeobot. Palynol. 29, 253–269.

Allen, J.R.L., Dineley, D.L., 1976. The succession of the Lower Old Red Sandstone (Siluro-Devonian) along the Ross-Tewkesbury Spur Motorway (M50), Hereford and Worcester. Geol. J. 11, 1–14.

Barclay, W.J., Davies, J.R., Hillier, R.D., Waters, R.A., 2015. Lithostratigraphy of the Old Red Sandstone successions of the Anglo-Welsh Basin. British Geological Survey Research Report, RR/14/02, p. 96.

Barghoorn, E.S., Darrah, W.C., 1938. *Horneophyton*, a necessary change of name for *Hornea*. Harvard University Botanical Museum Leaflet 6, 142–144.

Blackmore, S., Barnes, S.H., 1987. Pollen wall morphogenesis in *Tragopogon porrifolius* L. (Compositae: Lactuceae) and its taxonomic significance. Rev. Palaeobot. Palynol. 52 (2–3), 233–246.

Blackmore, S., Takahashi, M., Uehara, K., 2000. A preliminary phylogenetic analysis of sporogenesis in pteridophytes. In: Harley, M.M., Morton, C.M., Blackmore, S. (Eds.), Pollen and Spores: Morphology and Biology. London, Kew, Royal Botanic Gardens, pp. 109–124.

Boros, A., Jarai-Komlodi, M., 1975. An Atlas of Recent European Moss Spores. *Akademiai Kiado*. Publishing House of the Hungarian Academy of Sciences, Budapest.

Brown, R.C., Lemmon, B.E., 1984. Spore wall development in Andreaea (Musci: Andreaeopsida). Am. J. Bot. 71 (3), 412–420.

Brown, R.C., Lemmon, B.E., 1990. Sporogenesis in bryophytes. In: Blackmore, S., Knox, R.B. (Eds.), Microspores: Evolution and Ontogeny. Academic Press, London, UK, pp. 55–94.

Burgess, N.D., Richardson, J.B., 1991. Silurian cryptospores and miospores from the type Wenlock area, Shropshire, England. Palaeontology 34, 601–628.

Cascales-Miñana, B., Steemans, P., Servais, T., Lepot, K., Gerrienne, P., 2019. An alternative model for the earliest evolution of vascular plants. Lethaia 52 (4), 445–453.

Chaloner, W.G., Streel, M., 1968. Lower Devonian spores from South Wales. Argum. Palaeobot. 1, 87–101.

Edwards, D., 1969. Zosterophyllum from the Lower Old Red Sandstone of South Wales. New Phytol. 68 (4), 923–931.

Edwards, D., 1979. A late Silurian flora from the Lower Old Red Sandstone of south-west Dyfed. Palaeontology 22, 23–52.

Edwards, D., 1996. New insights into early land ecosystems: a glimpse of a Lilliputian world. Rev. Palaeobot. Palynol. 90 (3–4), 159–174.

Edwards, D., Richardson, J.B., 2000. Progress in reconstructing vegetation on the Old Red Sandstone Continent: two *Emphanisporites* producers from the Lochkovian sequence of the Welsh Borderland. Geol. Soc. Lond., Spec. Publ. 180 (1), 355–370.

Edwards, D., Richardson, J.B., 2004. Silurian and Lower Devonian plant assemblages from the Anglo-Welsh Basin: a palaeobotanical and palynological synthesis. Geol. J. 39 (3–4), 375–402.

Edwards, D., Fanning, U., Richardson, J.B., 1994. Lower Devonian coalified sporangia from Shropshire: *Salopella* Edwards & Richardson and *Tortilicaulis* Edwards. Bot. J. Linn. Soc. 116, 89–110.

Edwards, D., Davies, K.L., Richardson, J.B., Axe, L., 1995a. The ultrastructure of spores of *Cooksonia pertoni*. Palaeontology 38, 153–168.

Edwards, D., Duckett, J.G., Richardson, J.B., 1995b. Hepatic characters in the earliest land plants. Nature 374, 635–636.

Edwards, D., Richardson, J.B., Axe, L., Davies, K.L., 2012a. A new group of Early Devonian plants with valvate sporangia containing sculptured permanent dyads. Bot. J. Linn. Soc. 168 (3), 229–257.

Edwards, D., Wellman, C.H., Axe, L., 1999. Tetrads in sporangia and spore masses from the Upper Silurian and Lower Devonian of the Welsh Borderland. Bot. J. Linn. Soc. 130, 111–156.

Edwards, D., Morris, J.L., 2014. An analysis of vegetational change in the Lower Devonian: New data from the Lochkovian of the Welsh Borderland, U.K. Review of Palaeobotany and Palynology 211, 28–54. https://doi.org/10.1016/j.revpalbo.2014.09.006.

Edwards, D., Morris, J.L., Axe, L., Taylor, W., Duckett, J.G., Kenrick, P., Pressel, S., et al., 2021a. Piecing together the eophytes – a new group of ancient plants containing cryptospores. New Phytologist 233 (3), 1440–1455. https://doi.org/10.1111/nph.17703.

Edwards, D, Morris, J.L., Axe, L., Taylor, W.A., Duckett, J.G., Kenrick, P., Pressel, S., 2021b. Earliest record of transfer cells in Lower Devonian plants. New Phytologist 233 (3), 1456–1465. https://doi.org/10.1111/nph.17704.

Edwards, D., Morris, J.L., Richardson, J.B., Kenrick, P., 2014. Cryptospores and cryptophytes reveal hidden diversity in early land floras. New Phytol. 202 (1), 50–78.

Fanning, U., Richardson, J.B., Edwards, D., 1988. Cryptic evolution in an early land plant. Evol. Trends Plants (ETP) 2 (1), 13–24.

Fanning, U., Edwards, D., Richardson, J.B., 1990. Further evidence for diversity in late Silurian land vegetation. J. Geol. Soc. 147 (4), 725–728.

Fanning, U., Edwards, D., Richardson, J.B., 1991a. A new rhyniophytoid from the late Silurian of the Welsh Borderland. Neues Jahrb. Geol. Palaontol. Abh. 183, 37–47.

Fanning, U., Richardson, J.B., Edwards, D., 1991b. A review of in situ spores in Silurian land plants. In: Blackmore, S., Barnes, S.H. (Eds.), Systematics Association Special Volume. Pollen and Sporesvol. 44, pp. 25–47.

Gray, J., 1985. The microfossil record of early land plants; advances in understanding of early terrestrialization, 1970–1984. Phil. Trans. R. Soc. Lond. B 309, 167–195.

Higgs, K.T., 2004. An Early Devonian (Lochkovian) microflora fromthe Freshwater West Formation, Lower Old Red Sandstone,southwest Wales. Geological Journal 39, 359–374. https://doi.org/10.1002/gj.994.

Jeram, A.J., Selden, P.A., Edwards, D., 1990. Land animals in the Silurian: arachnids and myriapods from Shropshire, England. Science 250 (4981), 658–661.

Johnson, T.R., Taylor, W.A., 2005. Single grain analysis of the late Silurian spore Cymbosporites echinatus from the Welsh Borderland. Rev. Palaeobot. Palynol. 137 (3–4), 163–172.

Kenrick, P., Wellman, C.H., Schneider, H., Edgecombe, D., 2012. A timeline for terrestrialization: consequence for the carbon cycle in the Palaeozoic. Philos. Trans. R. Soc. Lond. B 367, 519–536.

Kidston, R., Lang, W.H., 1920. On Old Red Sandstone plants showing structure, from the Rhynie Chert Bed, Aberdeenshire. Part II. Additional notes on *Rhynia gwynne-vaughani*, Kidston and Lang: with descriptions of *Rhynia major*, n. sp., and *Hornea lignieri*, n. g. n. sp. Trans. R. Soc. Edinb. 52, 603–627.

Lugardon, B., 1990. Pteridophyte sporogenesis: a survey of spore wall ontogeny and fine structure in a polyphyletic plant group. In: Blackmore, S., Knox, R.B. (Eds.), Microspores: Evolution and Ontogeny. London Academic Press, pp. 95–120.

McGregor, D.C., 1961. Spores with proximal radial pattern from the Devonian of Canada. Geol. Surv. Can. Bull. 76, 1–11.

Morris, J.L., Richardson, J.B., Edwards, D., 2011a. Lower Devonian plant and spore assemblages from Lower Old Red Sandstone strata of Tredomen Quarry, South Wales. Rev. Palaeobot. Palynol. 165 (3–4), 183–208.

Morris, J.L., Edwards, D., Richardson, J.B., Axe, L., Davies, K.L., 2011b. New plant taxa from the Lower Devonian (Lochkovian) of the Welsh Borderland, with a hypothesis on the relationship between hilate and trilete spore producers. Rev. Palaeobot. Palynol. 167, 51–81.

Morris, J.L., Edwards, D., Richardson, J.B., Axe, L., 2012a. New dyad-producing plants from the Lower Devonian (Lochkovian) of the Welsh Borderland. Bot. J. Linn. Soc. 169, 569–595.

Morris, J.L., Edwards, D., Richardson, J.B., Axe, L., Davies, K.L., 2012b. Further insights into trilete spore producers from the Early Devonian (Lochkovian) of the Welsh Borderland, U.K. Rev. Palaeobot. Palynol. 185, 35–63.

Morris, J.L., Wright, V.P., Edwards, D., 2012c. Siluro-Devonian landscapes of southern Britain: the stability and nature of early vascular plant habitats. J. Geol. Soc. Lond. 169, 173–190.

Morris, J.L., Edwards, D., Richardson, J.B., 2018. The advantages and frustrations of a plant Lagerstätte as illustrated by a new taxon from the Lower Devonian of the Welsh Borderland, UK. In: Krings, M., Harper, C.J., Rubén Cúneo, N., Rothwell, G.W. (Eds.), Transformative Paleobotany. Academic Press, pp. 49–67.

Puttick, M.N., Morris, J.L., Williams, T.A., Cox, C.J., Edwards, D., Kenrick, P., Pressel, S., Wellman, C.H., Schneider, H., Pisani, D., Donoghue, P.C., 2018. The interrelationships of land plants and the nature of the ancestral embryophyte. Curr. Biol. 28 (5), 733–745.

Qiu, Y.-L., Li, L., Bin, W., Chen, Z., Knoop, V., Growth-Malonek, M., Dombrovska, O., Lee, J., Kent, L., Rest, J., Estabrook, G.F., Hendry, T.A., Taylor, D.W., Testa, C.M., Ambros, M., Crandall-Stotler, B., Duff, R.J., Stech, M., Frey, W., Quandt, D., Davis, C.C., 2006. The deepest divergences in land plants inferred from phylogenomic evidence. Proc. Natl. Acad. Sci. 103, 15511–15516.

Renzaglia, K.S., Villarreal, J.C., Duff, R.J., 2008. New insights into morphology, anatomy, and systematics of hornworts. In: Goffinet, B., Shaw, A.J. (Eds.), Bryophyte Biology, 2nd edition Cambridge University Press, Cambridge, UK, pp. 139–172.

Richardson, J.B., 1974. The stratigraphic utilization of some Silurian and Devonian miospore species in the northern hemisphere: an attempt at a synthesis. Int. Symp. Belg. Micropaleontol. Limits, Publ. No. 9, pp. 1–13.

Richardson, J.B., 1996. Taxonomy and classification of some new Early Devonian cryptospores from England. Spec. Pap. Palaeontol. 55, 7–40.

Richardson, J.B., 2007. Cryptospores and miospores, their distribution patterns in the Lower Old Red Sandstone of the Anglo-Welsh Basin, and the habitat of their parent plants. Bull. Geosci. 82 (4), 355–364.

Richardson, J.B., Lister, T.R., 1969. Upper Silurian and Lower Devonian spore assemblages from the Welsh Borderland and South Wales. Palaeontology 12, 37–43.

Richardson, J.B., McGregor, D.K., 1986. Silurian and Devonian spore zones of the Old Red Sandstone Continent and adjacent regions. Geol. Surv. Can. Bull. 364, 1–79.

Salamon, S.A., Gerrienne, P., Steemans, P., Gorzelak, P., Fillipiak, P., Hérissé A, L.E., Paris, F., Cascales-Miñana, B., Brachaniec, T., Misz-Kennan, M., Niedzwiedzki, R., 2018. Putative late Ordovician land plants. New Phytol. 218, 1305–1309.

Steemans, P., Petus, E., Breuer, P., Mauller-Mendlowicz, P., Gerrienne, P., 2012. Palaeozoic innovations in the micro-and megafossil plant record: from the earliest plant spores to the earliest seeds. In: TALENT, J.A. (Ed.), Earth and Life, International Year of Planet Earth. Springer, Dordrecht, pp. 437–477.

Taylor, W.A., 1997. Ultrastructure of lower Paleozoic dyads from southern Ohio II: *Dyadospora murusattenuata*, functional and evolutionary considerations. Rev. Palaeobot. Palynol. 97, 1–8.

Taylor, W.A., 2002. Studies in cryptospore ultrastructure: variability in the tetrad genus Tetrahedraletes and type material of the dyad *Dyadospora murusattenuata*. Rev. Palaeobot. Palynol. 119 (3–4), 325–334.

Taylor, W.A., 2003. Ultrastructure of selected Silurian trilete spores and the putative Ordovician trilete spore Virgatasporites. Rev. Palaeobot. Palynol. 126 (3–4), 211–223.

Taylor, W.A., Gensel, P.G., Wellman, C.H., 2011. Wall ultrastructure in three species of the dispersed spore Emphanisporites from the Early Devonian. Rev. Palaeobot. Palynol. 163 (3–4), 264–280.

Taylor, W.A., Strother, P.K., Vecoli, M., 2017. Wall ultrastructure of the oldest embryophytic spores: implications for early land plant evolution. Rev. Micropaleontol. 60 (3), 281–288.

Tryon, A.F., Lugardon, B., 1991. Spores of the Pteridophyta. Surface, wall structure and diversity based on electron microscope studies. Springer, New York, NY, pp. 523–540.

Vigran, J.O., 1964. Spores from Devonian deposits, Mimerdalen, Spitsbergen. Skrifter Norsk Polarinstitutt 132, 1–30.

Wellman, C.H., 1999. Sporangia containing Scylaspora from the lower Devonian of the Welsh Borderland. Palaeontology 42 (1), 67–81.

Wellman, C.H., 2004. Origin, function and development of the spore wall in early land plants. In: Hemsley, A.R., Poole, I. (Eds.), The Evolution of Plant Physiology. Royal Botanic Gardens, Kew, pp. 43–63.

Wellman, C.H., 2009. Ultrastructure of dispersed and in situ specimens of the Devonian spore *Rhabdosporites langii*: evidence for the evolutionary relationships of progymnosperms. Palaeontology 52 (1), 139–167.

Wellman, C.H., Edwards, D., Axe, L., 1998b. Ultrastructure of laevigate hilate spores in sporangia and spore masses from the Upper Silurian and Lower Devonian of the Welsh Borderland. Phil. Trans. R. Soc. Lond. B 353, 1983–2004.

Wellman, C.H., Habgood, K., Jenkins, G., Richardson, J.B., 2000. A new plant assemblage (microfossil and megafossil) from the Lower Old Red Sandstone of the Anglo–Welsh Basin: its implications for the palaeoecology of early terrestrial ecosystems. Rev. Palaeobot. Palynol. 109 (3–4), 161–196.

Wellman, C.H., Kerp, H., Hass, H., 2004. Spores of the Rhynie chert plants *Horneophyton lignieri* (Kidston & Lang) Barghoorn & Darrah, 1938. Trans. R. Soc. Edinb. Earth Sci. 95, 429–443.

Chapter VII Early land plant phytodebris

Charles H. Wellman[1] & Alexander C. Ball[1, 2]

[1]*School of Biosciences, The University of Sheffield, Western Bank, Sheffield. S10 2TN, UK*
[2]*Dept. of Earth Sciences, The Natural History Museum, Cromwell Road, London. SW7 5BD, UK*

Abstract

Historically, phytodebris (often considered a type of non-pollen palynomorph – NPP) has played a prominent role in research into the fossil record of early land plants. This phytodebris consists of cuticles and cuticle-like sheets, various tubular structures (including tracheids and tracheid-like tubes) and sundry other enigmatic fragments. Initial research focused on elucidating their morphology, attempts to identify them *in situ* in plant megafossils and comparisons with potentially homologous structures in extant plants. The fragmentary nature of these remains, and associated difficulties in positively identifying their presence in fossil/extant plants, resulted in vigorous debate regarding what many of these microfossils actually represented and their relevance to early land plant studies. More recently a wider array of analytical techniques has been applied (e.g. ultrastructural analysis, geochemistry and taphonomic experiments). However, positive identification of the affinities of at least some of these enigmatic fossils remained elusive. Ongoing investigations based on exceptionally preserved material from Lagerstätten (charcoalified and silicified) seem to have finally demonstrated that the more enigmatic of these remains derive from nematophytes that probably represent fungi and possibly also lichenized fungi.

Early land plant phytodebris

Charles H. Wellman[1]* and Alexander C. Ball[1,2]

[1]Department of Animal & Plant Sciences, University of Sheffield, Alfred Denny Building, Western Bank, Sheffield S10 2TN, UK

[2]Department of Earth Sciences, Natural History Museum (London), South Kensington, London SW7 5BD, UK

CHW, 0000-0001-7511-0464; ACB, 0000-0002-2687-553X

*Correspondence: c.wellman@sheffield.ac.uk

Abstract: Historically, phytodebris (often considered a type of non-pollen palynomorph – NPP) has played a prominent role in research into the fossil record of early land plants. This phytodebris consists of cuticles and cuticle-like sheets, various tubular structures (including tracheids and tracheid-like tubes) and sundry other enigmatic fragments. Initial research focused on elucidating their morphology, attempts to identify them *in situ* in plant megafossils and comparisons with potentially homologous structures in extant plants. The fragmentary nature of these remains, and associated difficulties in positively identifying their presence in fossil/extant plants, resulted in vigorous debate regarding what many of these microfossils actually represented and their relevance to early land plant studies. More recently a wider array of analytical techniques has been applied (e.g. ultrastructural analysis, geochemistry and taphonomic experiments). However, positive identification of the affinities of at least some of these enigmatic fossils remained elusive. Ongoing investigations based on exceptionally preserved material from Lagerstätten (charcoalified and silicified) seem to have finally demonstrated that the more enigmatic of these remains derive from nematophytes that probably represent fungi and possibly also lichenized fungi.

Land plants (embryophytes) produce potentially fossilizable parts both throughout their lives and upon their death. During life, they naturally shed (including abscission) organs such as roots, branches and leaves, and propagules such as seeds and spores/pollen. Upon death they begin to disintegrate, whereupon all of their structures become potential fossils. Many plant parts have a high fossilization potential because they are composed of, or at least contain, highly resistant organic macromolecules (for example, the lignin of woody tissues, the cutan of cuticles and the sporopollenin of spore and pollen walls).

Palaeobotanists generally study fossils of relatively large plant organs (that may or may not be preserved in organic connection with other plant organs). Typically, these have been little transported and rapidly buried, except in the cases of leaves and seeds that can undergo considerable transportation before being incorporated into sediment relatively intact. Plant megafossils are most commonly preserved as standard coalified compressions or sediment casts. Less often they may be better preserved by permineralization or even charcoalification following natural burning. General reviews of the taphonomy of fossil plants are provided by Cleal and Thomas (2009) and Taylor *et al.* (2009).

The palynologist, on the other hand, chiefly studies dispersed plant microfossils, liberated from the host sediment by palynological acid-maceration techniques. These fossils may have experienced vast transportation distances, usually by wind and water, prior to deposition. These either represent essentially complete organs (spores, megaspores, pollen or seeds) or disarticulated fragments (including cuticle fragments and bundles of tracheids). These palynomorphs and disarticulated fragments are essentially preserved as coalified compressions, although they can be charcoalified. General reviews of the taphonomy of fossil palynomorphs are provided in Jansonius and McGregor (1996) and Traverse (2007).

The terminology used to describe dispersed fragments of land plants is somewhat confused. Here we use the term phytodebris (*sensu* Gensel *et al.* 1991). But other terms have been utilized, such as palynodebris (particularly in palynofacies classifications) and nematoclasts (when referring specifically to fragments derived from an enigmatic group of 'plants' called nematophytes). However, when excluding dispersed spores and pollen and considering only dispersed fragments, we are dealing with what is often considered to be a discrete group of non-pollen palynomorphs (NPP). This paper is concerned solely with phytodebris and is confined to that produced by the earliest land plants. Consequently, it is stratigraphically circumscribed between the Middle Ordovician and Early Devonian (Fig. 1).

From: Marret, F., O'Keefe, J., Osterloff, P., Pound, M. and Shumilovskikh, L. (eds) *Applications of Non-Pollen Palynomorphs: from Palaeoenvironmental Reconstructions to Biostratigraphy*.
Geological Society, London, Special Publications, **511**,
https://doi.org/10.1144/SP511-2020-36

d3ws3

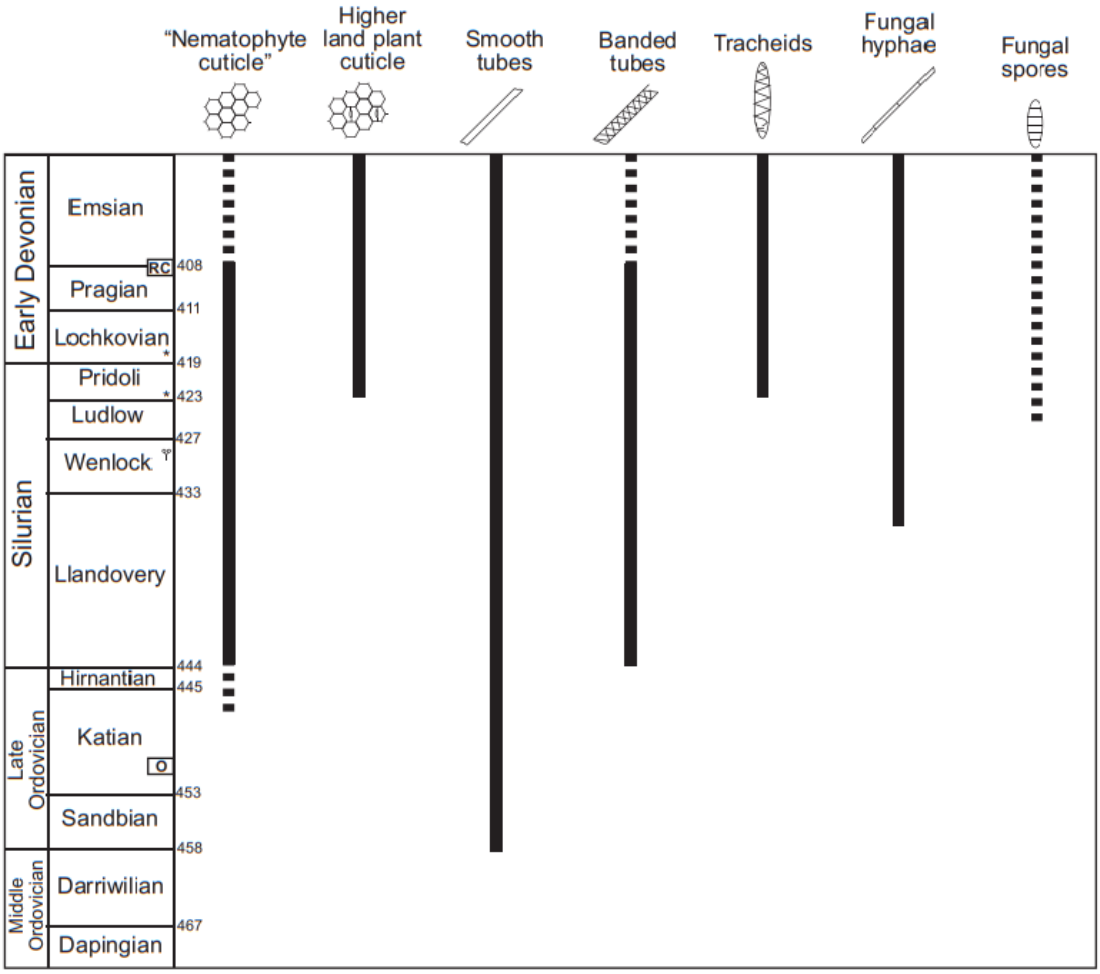

Fig. 1. Stratigraphical distribution of phytodebris. The stratigraphical column is based on *A Geologic Timescale* v. 5 (Walker *et al.* 2018). Dashed lines represent uncertain distribution. The small fossil rhyniophytoid plant illustrated in the Wenlock represents the earliest generally accepted land plant megafossils. The asterisks in the Pridoli and Lochkovian represent the Ludford Lane and Hudwick Dingle charcoalified plant assemblages, respectively. RC in the Pragian–?earliest Emsian represents the Rhynie chert. O in the Katian represents the earliest evidence for cryptosporophyte sporangia from Oman (Wellman *et al.* 2003).

Examples of early land plant phytodebris are illustrated in Figures 2 & 3.

The origin and early evolution of land plants

The origin of land plants was one of the most important events in the history of life on Earth. From a biological perspective land plants (embryophytes) represent one of the main kingdoms of multicellular life. Ecologically, their colonization of the land opened up the continents and subaerial world for the aquatic animals that followed the plants on to the land, be that from the saline oceans or freshwater bodies such as lakes, rivers and marshes (Shear and Selden 2001). Furthermore, they had enormous effects on the actual environment of planet Earth due to their actions involving: (i) weathering and soil formation; and (ii) photosynthetic carbon-capture, resulting in biomass accumulation and carbon burial. This not only created soils and affected sedimentation patterns in many other ways, but also changed atmospheric composition leading to, *inter alia*, climate change.

As a consequence of the above, much research activity has been dedicated to exploring the origin and early evolution of land plants. Whilst numerous lines of scientific enquiry have been explored, the fossil record of early land plants has, of course, always featured prominently. Initially this concentrated on early land plant megafossils recovered from late Silurian–Early Devonian deposits (e.g.

Fig. 2. Phytodebris recovered from Late Silurian–Early Devonian 'Lower Old Red Sandstone' sediments from the Ross-Spur M50 motorway succession of the Anglo-Welsh Basin (for details see Edwards 1986). Scale bar (top right-hand corner) is 75 µm. (**a**) Banded tube. Freshwater West Formation, Sample 19M5001.1, Specimen (M22). (**b**) Banded tube. Moor Cliffs Formation, Sample 19M5009.1, Specimen (U30/2). (**c**) *Constrictitubulus*. Freshwater West Formation, Sample 19M5001.3, Specimen (G36/2). (**d**) Banded tube. Freshwater West Formation, Sample

Lang 1937). The advent of palynological techniques through the 1950s–60s saw new evidence become available in the form of dispersed palynomorphs and phytodebris. Indeed, it is clear that dispersed land plant microfossils began to play an increasingly prominent role in research into the earliest land plants from this time. Early reviews of the palynological evidence include those of Chaloner (1960, 1970) and, more recently, reviews of both the microfossil and megafossil evidence include those of Wellman and Gray (2000), Edwards and Wellman (2001), Gensel (2008), Kenrick *et al.* (2012), Wellman *et al.* (2013) and Meyer-Berthaud *et al.* (2016*a*, *b*).

By the 1970s Jane Gray and colleagues (Gray and Boucot 1971; Gray *et al.* 1974) had proposed a critical role for early land plant phytodebris, revealing an early hidden history of land plant evolution not represented in the megafossil record. Fierce debate ensued as to the authenticity and relevance of this dispersed microfossil record (Banks 1975*a*, *b*; Gray and Boucot 1977). By the 1980s many of these debates had essentially been resolved. It became widely accepted that by the Middle Ordovician a rather cryptic period of early land plant evolution was represented by dispersed microfossils (including phytodebris) (Pratt *et al.* 1978; Strother and Traverse 1979; Gray 1985; Johnson 1985) which existed prior to, and later complemented, the late Silurian appearance of plant megafossils (Edwards *et al.* 1979; Libertín *et al.* 2018; Morris *et al.* 2018).

Early land plant spores

Initial research on land plant dispersed microfossils concentrated on their dispersed spores/pollen and, over the succeeding decades, a vast literature emerged on the subject (reviewed in Jansonius and McGregor 1996; Traverse 2007). It was soon realized that the land plant (embryophyte) megafossil record is rather poor compared to the rich dispersed spore record. This is because the latter are produced in vast numbers, readily transported long distances by wind and water and have high fossilization potential. Research into early land plants also relied heavily on the dispersed spore record, particularly as megafossils are so rare. To date less than 25 megafossil localities are known worldwide from the entire Silurian and these are almost exclusively of allochthonous plant remains transported into marine environments (Edwards and Wellman 2001; Wellman *et al.* 2013). Furthermore, the dispersed spore record appears to extend back further in time than the plant megafossil record. This almost certainly reflects the facts that: (i) dispersed spores have higher preservation potential than plant megafossils; and (ii) the earliest land plants may have been very small and lacking in preservable resistant tissues and consequently lost to the fossil record.

Early land plant phytodebris

Somewhat lagging behind the study of land plant dispersed spores/pollen was the study of the phytodebris they produce. However, due to the paucity of early land plant megafossils, studies of phytodebris became increasingly important for research into these earliest plants (e.g. Gray and Boucot 1977). These other 'bits-and-pieces' (rather endearingly termed 'Hooker's "Waifs and strays"' by Gensel *et al.* 1991) began to feature prominently because it was considered that they may represent disarticulated fragments of the earliest land plants that lacked a megafossil record. However, interpretation of early land plant dispersed phytodebris (Figs 1 & 2) was often problematic, owing to: (i) multiple organisms producing similar, morphologically simple structures, of which the original biological affinities are difficult to trace; and (ii) difficulties in reconciling these fragmentary structures with equivalent material produced by extant land plants.

Dispersed cuticles and 'cuticle-like sheets'

Some bryophytes (non-vascular plants) and the vast majority of tracheophytes (vascular plants) produce a cuticular covering composed primarily of cutan

Fig. 2. *Continued*. 19M5001.1, Specimen (E44/3). (**e**) Banded tube. Freshwater West Formation, Sample 19M5001.1, Specimen (O34). (**f**) Banded tube. Freshwater West Formation, Sample 19M5001.3, Specimen (P50/4). (**g**) Laevigate tube. Freshwater West Formation, Sample 19M5001.3, Specimen (O42/1). (**h**) Banded tube. Freshwater West Formation, Sample 19M5002.3, Specimen (W44/1). (**i**) Banded tube. Freshwater West Formation, Sample 19M5002.1, Specimen (K43). (**j**) *Constrictitubulus*. Freshwater West Formation, Sample 19M5001.1, Specimen (O51/3). (**k**) Banded tube. Freshwater West Formation, Sample 19M5001.1, Specimen (N24). (**l**) Banded tube. Freshwater West Formation, Sample 19M5002.3, Specimen (M44). (**m**) Laevigate tube. Freshwater West Formation, Sample 19M5001.1, Specimen (M50/4). (**n**) Sporangial cuticle of ?cryptosporophytic origin. Freshwater West Formation, Sample 19M50026.3, Specimen (N45). (**o**) Embryophyte cuticle. Freshwater West Formation, Sample 19M5001.3, Specimen (E35/1). (**p**) Nematophyte cuticle. Freshwater West Formation, Sample 19M5001.3, Specimen (S30/3). (**q**) Nematophyte cuticle. Freshwater West Formation, Sample 19M5001.3, Specimen (N31). (**r**) Nematophyte cuticle. Freshwater West Formation, Sample 19M5001.1, Specimen (N42/3). (**s**) Nematophyte cuticle. Freshwater West Formation, Sample 19M5001.3, Specimen (E35/1).

Early land plant phytodebris

and waxes. As leaves, axes and other cuticle-covered structures decompose, the cuticle can be shed and fragment. The organic macromolecule cutan is highly resistant and readily fossilized. Thus, fragments of cuticle can undergo extensive transportation before finally being deposited and incorporated into sediment and, as such, these cuticle fragments frequently occur in palynological preparations. Cuticles preserve the patterning of the epidermal cells underlying the cuticle and often indicate from which part of the plant the cuticle is derived. For example, axial cuticles often have elongate cells whereas those from leaves may be more equidimensional (e.g. Edwards *et al.* 1981, 1996; Guo and Wang 2015). Cuticles are often also of taxonomic value, particularly when considered alongside characters of stomata that are preserved in the dispersed cuticles of stomatiferous plants (Edwards *et al.* 1998*b*). The distribution of these stomata can also be used to calculate the stomatal density/index, which can be used as proxies for past atmospheric CO_2 levels (e.g. McElwain and Chaloner 1995). The earliest unequivocal stomata reported from plant megafossils are from rhyniophytoid plants from the upper Silurian (Pridoli) of Ludford Lane in the Anglo-Welsh Basin (Jeram *et al.* 1990). The earliest dispersed cuticles with stomata have been reported from the Lower Devonian (Lochkovian) of the same basin (Edwards and Axe 1992; Edwards *et al.* 1996).

Early research highlighted the presence of 'cuticle-like sheets' that were very similar to the cuticles of land plants, although they differed from many in that they lacked stomata. Gray and Boucot (1977) argued that these were most likely cuticles of early land plants, and called them 'cuticle-like remains', although other workers urged caution (e.g. Banks 1975*a*, *b*). Detailed taxonomic studies were undertaken (Edwards 1982, 1986; Edwards and Rose 1984), and these authors interpreted many of the cuticles as representing the covering of nematophytes (see below), with Edwards (1986) including formal systematic naming of some of the cuticles.

Enigmatic megafossils that co-occurred with early land plants in Silurian–Devonian non-marine strata were called nematophytes by Lang (1937). These strange, so-called 'plants', had an anatomy based on various different forms and combinations of tubular structure with some, Lang believed, possessing a cuticular covering. The unfamiliar anatomy appeared to have no counterpart among the living world and Lang suggested that nematophytes may represent a new phylum that had experimented with life on land before going extinct. Subsequently much attention was paid to these enigmatic remains and other workers suggested affinities with algae, fungi, lichens and other groups represented in the living biota. As noted above, Dianne Edwards was firmly of the opinion that at least some of the dispersed cuticle-like sheets represented fragments of nematophyte coverings (Edwards 1982, 1986; Edwards and Rose 1984).

One line of enquiry that has been pursued regarding the affinities of the cuticles is their geochemistry. Various techniques have been utilized, such as flash pyrolysis–gas chromatography–mass spectrometry (Ewbank *et al.* 1996), Fourier transform IR (FTIR; e.g. Abbott *et al.* 1998) and ^{13}C solid-state nuclear magnetic resonance (NMR; e.g. Edwards *et al.* 1997), on both dispersed cuticles, fragments of vascular land plant and nematophyte megafossils. These authors reported the presence of cutan in some early vascular land plants, which presumably derived from their cuticle covering (reviewed in Edwards *et al.* 1996, 1998*a*). Furthermore, it was shown that cuticles of *Nematothallus* had a distinctly different geochemical profile than those from vascular plants (Edwards *et al.* 1998*a*). As geochemical techniques improve and new technique emerge this line of enquiry has the potential to be explored further. However, limitations due to taphonomic effects, including thermal maturity, need to be fully appreciated.

In the 1990s Linda Graham and co-workers began reporting on a series of taphonomic experiments relevant to the debate regarding the affinities

Fig. 3. Phytodebris recovered from sediments hosting the Early Devonian (late Pragian–?earliest Emsian) Rhynie cherts from Scotland (for details of palynological investigation see Wellman 2006). Scale bar (top right-hand corner) is 60 μm (a–j), 125 μm (k–m), 80 μm (n–o) and 140 μm (**p**). (**a**) Tracheid. Sample 97/2 (39.0)/4. (**b**) Tracheid. Sample 97/2 (39.0)/4. (**c**) Tracheid. Sample 97/2 (39.0)/4. (**d**) Two attached tracheids. Sample 97/2 (39.0)/4. (**e**) Banded tube associated with a cluster of narrow laevigate tubes. Sample 97/2 (32.5)/2, Specimen (N39.1). (**f**) Wide laevigate tube in association with narrow laevigate tubes (?*Prototaxites* spp.). Sample 97/9 (24.0)/2, Specimen (W44.4). (**g**) Two ?attached banded tubes. Sample 97/2 (34.8)/2, Specimen (G38). (**h**) Fungal hypha. Sample 97/2 (94.0)/2, Specimen (V29.2). (**i**) H-shaped branching in a laevigate tube. Sample 97/8 (14.5)/2, Specimen (W28.4). (**j**) Fungal hypha. Sample 97/2 (39.0)/4, Specimen (H29). (**k**) Cuticle-like sheet (*Nematothallus*). Sample 97/2 (36.2)/3, Specimen (S41). (**l**) Cuticle of a stomatous plant (note the hole where a stoma was situated). Sample 97/9 (24.0)/2, Specimen (Q44.2). (**m**) Cuticle of a stomatous plant (note the stoma with the guard cells in place). Sample 97/2 (36.2)/3, Specimen (F35.2). (**n**) Fragment of arthropod cuticle. Sample 97/2 (89.0)/6, Specimen (O29). (**o**) Fragment of arthropod cuticle. Sample 97/2 (94.0)/2, Specimen (E35). (**p**) Spiny ?tube of unknown affinity. Sample 97/2 (34.8)/2, Specimen (Q43).

of early land plant phytodebris. They selected representatives of living plants considered to be basal (phylogenetically early diverging) and acetolysed them. The process of acetolysis mimics the results of natural rotting, stripping out labile components and leaving only those composed of or containing resistant parts (i.e. those parts that are most likely to survive in the fossil record). When acetolysing various bryophytes they recovered fragments reminiscent of Middle Ordovician–Early Devonian cuticle-like sheets and suggested that some may derive from ancient bryophytes (Kroken *et al.* 1996; Cook and Graham 1998; Graham *et al.* 2004). However, it has been suggested that some of these resemblances are only superficial with such basic morphological structures produced by a variety of organisms (e.g. Edwards *et al.* 1998*a*).

The debate around the origin of the cuticle-like sheets seemingly found a solution in the exquisitely preserved charcoalified plants from the late Silurian–Early Devonian of the Anglo-Welsh Basin (Edwards 1996). These contained spectacularly preserved nematophytes described in detail by Edwards *et al.* (2013, 2018). Some of these have a clear 'cuticular' covering associated with their internal tubular anatomy. The superior preservation of the charcoalified forms, compared to those preserved as coalified compressions, revealed structures that Edwards and co-workers interpreted as of fungal and lichen affinities (Edwards and Axe 2012; Edwards *et al.* 2013, 2018; Honegger *et al.* 2013, 2017).

Dispersed 'tubular structures'

Co-occurring with the 'cuticle-like sheets' in palynological preparations are usually a variety of tubular structures existing either as individual tubes of varying morphology, or as associations of tubes, either of one or a mixture of morphologies. The conducting tissues of tracheophytes comprise xylem (tracheids and their equivalents) and phloem. Tracheids themselves are lignified and, as such, have a high preservation potential. When a plant disintegrates after death, individual tracheids (or more usually bundles of tracheids) may be extensively transported prior to deposition as phytodebris. The earliest reported *in situ* tracheids in plant megafossils are found in rhyniophytoid plants from the upper Silurian (Ludlow) (Edwards and Davis 1976) and Lower Devonian (Lochkovian) (Edwards *et al.* 1992) of the Anglo-Welsh Basin. Meanwhile, dispersed tracheids are first reported from the Lower Devonian (Pragian) (e.g. Gensel *et al.* 1991).

Gray and Boucot (1977) postulated that many of the tubes that could not be positively identified as tracheids of vascular plants were derived from early land plants. Although these were clearly not genuine tracheids they argued that they represented conducting tissues and called them 'tracheid-like tubes' noting that those with internal annular and spiral thickenings bore a resemblance to the tracheids of vascular plants. Banks and others again urged caution (e.g. Banks 1975*a*, *b*; Schopf 1978). Clearly, many of the tubular structures resembled those known *in situ* from nematophytes (Lang 1937; Høeg 1942; Lyon 1962) and both parties agreed that at least some of these tubular structures may derive from the nematophytes (Gray and Boucot 1977; Gray 1985). Subsequently, Burgess and Edwards (1991) erected a formal taxonomic system for naming and classifying the dispersed tubular structures (see also Wellman 1995).

The taphonomic acetolysis experiments undertaken by Graham and co-workers (see above) also produced various structures that they related to the dispersed tubular structures. For example, Kodner and Graham (2001) reported on tubes produced by acetolysis of bryophytes. However, it has been suggested that these resemblances are also in this case only superficial (e.g. Edwards *et al.* 1998*a*).

Again, the exquisitely preserved charcoalified megafossils from the upper Silurian–Lower Devonian of the Anglo-Welsh Basin appear to have provided a partial solution to this problem. It is clear that the types of tubular structure forming the anatomy of the different nematophytes are very similar to dispersed forms that occur in palynological preparations from the same, and other coeval, deposits (see discussion below). Thus, it seems that many of the tubular structures are of nematophyte (i.e. probable fungal and possibly also lichen) origin.

It is highly likely, however, that not all of the tubes derive from nematophytes and some probably have entirely different sources. Strother (2010) noted that where we have plant megafossil remains in continental deposits of Middle Ordovician–Early Devonian age thalloid forms often dominate over axial forms. These thalloid forms are difficult to interpret due to a paucity of recognizable characters, but it is plausible that many may represent the remains of nematophytes. On the other hand, it has been suggested that others may represent cyanobacterial mats (Tomescu and Rothwell 2006; Tomescu *et al.* 2006, 2008, 2009). These authors showed that cyanobacterial mats did indeed form a component of these embryonic terrestrial biotas, as they are preserved in early Silurian (Llandovery) non-marine deposits such as the Massanutten Sandstone of Virginia, USA. These mat remains occur as flattened coalified thalloid structures on bedding planes and are run through with simple tubular structures that probably represent the sheaths of cyanobacteria. At least some of the simple laevigate tubes that occur dispersed in non-marine deposits of this age are thus likely derived from disintegrated cyanobacterial

mats. These are equivalent to the simple tubes common in Precambrian palynological preparations that represent the sheaths of cyanobacteria, such as those described from one-billion-year-old non-marine deposits from the Torridonian of Scotland (Strother *et al.* 2011). Tomescu *et al.* (2010) reported on taphonomic simulation experiments on various modern taxa, including cyanobacteria that demonstrated that similar structures might survive in the fossil record.

Ultrastructural and geochemical analysis of dispersed tubular structures has also been undertaken with a view to better understanding them. Taylor and Wellman (2009) reported on a transmission electron microscope (TEM) ultrastructural analysis of both banded tubes and early land plant dispersed tracheids. They noted marked differences between the two in terms of gross structure, concluding that the banded tubes most likely derived from nematophytes.

The geochemistry of various types of tubular structure and fragments of vascular plant and nematophyte megafossils has also been analysed. Edwards *et al.* (1997) reported the presence of a signal for degraded lignin from the xylem of early vascular land plants, but unequivocal evidence for lignin was not forthcoming (Edwards *et al.* 1998*a*). Boyce *et al.* (2003) analysed conducting tissues in silicified plants preserved in the Rhynie chert Lagerstätte; following this, they suggested that some Rhynie chert plants lacked lignin in their vascular thickenings. Associations of tracheid-like tubes were analysed by Niklas and Pratt (1980) who interpreted their results as indicating the presence of lignin-like constituents. Regarding nematophyte megafossils, Niklas (1976) reported cutin and suberin derivatives from *Prototaxites*. However, following their geochemical analyses, Abbott *et al.* (1998, p. 1416) concluded that *Prototaxites* might contain 'an extinct polyphenolic structural biomacromolecule that was a failed experiment during terrestrialisation'. Overall the various geochemical investigations that have been undertaken, utilizing various techniques, have provided rather ambiguous and inconclusive results thus far. This is probably a consequence of taphonomy, with many of the coalified and permineralized remains being of rather high thermal maturity and the charcoalified remains certainly being of very high thermal maturity. Again, as geochemical techniques improve and new techniques are developed, this may prove a fruitful line of enquiry in the future.

The nematophyte story

We have previously encountered the nematophytes, an enigmatic group of so-called 'plants'. Lang (1937) proposed the group Nematophytales based on his analysis of *Nematothallus* and *Prototaxites* recovered from the upper Silurian–Lower Devonian of the Anglo-Welsh Basin. Lang's concept of *Nematothallus* was of a thalloid organism with tubular anatomy covered by a cuticle and with spores produced among the tubes. Subsequently Strother (1988) described further specimens from North America and reported on a re-examination of Lang's material (Strother 1993). Also included in the nematophytes by Lang was *Prototaxites* that had long been known from Silurian–Devonian localities worldwide. *Prototaxites* occurred as 'trunks', and fragments thereof, composed of associations of tubes (Hueber 2001). Subsequently further nematophyte taxa were established by Lyon (1962) describing *Nematoplexus* and Burgess and Edwards (1988) later erecting a new genus, very similar to *Prototaxites*, called *Nematosketum*.

The nematophytes have a most peculiar anatomy, making comparisons with extant organisms difficult and, as such, a large literature debating their affinities has accumulated. When initially establishing the Nematophytales, Lang (1937, p. 287) noted that '[w]hat is required, however, is not discussion, but an increase in our knowledge of these plants, which appear to have had a very general distribution in Siluro-Devonian times'. Fortunately, new information on the anatomy of these plants became available following the discovery of material in three Lagerstätten: the Rhynie chert and the charcoalified plant assemblages from Ludford Lane and Hudwick Dingle. The charcoalified plant remains from the upper Silurian–Lower Devonian of the Welsh Borderland yielded nematophyte specimens with exquisitely preserved anatomical detail. Following anatomical examination of the specimens, Edwards and Axe (2012) concluded that *Nematosketum* was of fungal affinity. Edwards *et al.* (2013, 2018) reported that the anatomy of *Nematothallus* was indicative of lichenized fungi. Silicified specimens of *Prototaxites* from the Early Devonian Rhynie chert, alongside charcoalified specimens from the upper Silurian–Lower Devonian of the Anglo-Welsh Basin, demonstrated an anatomy indicative of fungal affinities. Subsequently, Honegger *et al.* (2013) also described cyanobacterial and algal lichens among the assemblages of charcoalified fossil plants.

Whilst some of the phytodebris recovered from Middle Ordovician–Lower Devonian terrestrial deposits may be derived from land plants, it seems likely that many of the tubular structures and cuticle-like sheets derive from nematophytes. The current picture that might be drawn of these embryonic terrestrial environments appears to be that the earliest land plants shared the terrestrial surface with fungi/?lichens belonging to the Nematophytales, the latter of which may have formed a significant component of the biota.

The fungal story

The remit of this review is early land plant phytodebris. However, it seems prudent to discuss fungal phytodebris because it has historically played a significant role in discussions of early land plant phytodebris and because the nematophytes, as discussed, have now been shown to be of probable fungal/lichen affinity. Often co-occurring with early land plant phytodebris in palynological preparations are fungal remains in the form of dispersed spores and fragments of hyphae. The spores and hyphae of most extant fungi are constructed of the resistant macromolecule chitin, and Graham *et al.* (2017) recently reported on taphonomic acetolysis experiments on extant fungi, confirming that some fungal structures are indeed resistant and likely to survive in the fossil record. The earliest reported dispersed fungal spores are from the upper Silurian (Ludlow) (Sherwood-Pike and Gray 1985), with fragmented hyphae being reported from the same deposits. However, older hyphae have been reported, for example, from the lower Silurian (Llandovery) (Pratt *et al.* 1978; Johnson 1985) and possibly uppermost Ordovician (e.g. Thusu *et al.* 2013). Some of these early fossil fungi are from unequivocal non-marine deposits (e.g. Pratt *et al.* 1978; Wellman 1995). These remains are generally accepted as fungal in origin, although more precise taxonomic assignments are problematic due to a lack of morphological characters (e.g. Auxier *et al.* 2016; Smith 2016). We know from phylogenetic analyses and molecular clock studies that fungi originated early in the Mesoproterozoic (e.g. Parfrey *et al.* 2011), but it is entirely unclear when they first appeared on the land and if this was before, during or after the invasion of the land by plants. However, it seems highly likely that symbiotic relationships between multicellular green algae and fungi were intimately related to the origin of land plants and their invasion of the land. An excellent review of our current understanding of the earliest terrestrial fungi is provided by Taylor *et al.* (2015).

Early terrestrial animals

The colonization of the land by plants paved the way for aquatic animals to invade subaerial habitats (reviewed by Shear and Selden 2001; Kenrick *et al.* 2012). Phylogenetic analysis reveals that many different animal groups invaded the land on many different occasions. In some cases, this may have been directly from marine environments and, in others, it may have been via 'half-way houses' such as estuaries or continental freshwater rivers, lakes and waterlogged land. Non-marine animal-derived palynodebris from the Middle Ordovician–Lower Devonian consists predominantly of fish scales (the organic component survives palynological preparation techniques) and fragments of the chitinous exoskeleton of arthropods (Shear and Selden 2001). Whilst the fish remains are clearly aquatic, it is difficult to know if the arthropod cuticle derives from aquatic or truly terrestrial forms, unless positive taxonomic assignments can be made. The earliest fragments of arthropod that are known to be of non-marine origin (because they derive from terrestrial deposits) are from the early Silurian (Llandovery) deposits of the Tuscarora Formation in North America (Gray and Boucot 1993) and the late Silurian (early Wenlock) deposits of the Silurian inliers of the Midland Valley of Scotland (Wellman and Richardson 1993; Wellman 1995). However, it is unclear if these represent animals that inhabited aquatic freshwater environments or the land.

Conclusions

It is clear that non-pollen palynomorphs (phytodebris) continue to play an important role in research into the earliest land plants and their co-inhabitants of the land. Whilst recent years have witnessed a dramatic increase in knowledge regarding the affinities and nature of many of their producers, particularly regarding the nematophytes, there is still much to learn concerning this 'smorgasbord' of fossil remains.

Acknowledgement ACB would like to thank his PhD supervisors Paul Kenrick, John Richardson, Stephen Stukins and Charles Wellman.

Author contributions **CHW**: writing – original draft (equal); **ACB**: writing – original draft (equal).

Funding This research was supported by a NERC grant NE/R001324/1 to CHW and a NERC-funded ACCE (Adapting to Challenges of a Changing Environment) Doctoral Training Partnership PhD studentship NE/L002450/1, which is a CASE partnership with the Natural History Museum, London, to ACB.

Data availability All materials and datasets generated during the current study are housed in and available from the Centre for Palynology of the University of Sheffield repository.

References

Abbott, G.D., Ewbank, G., Edwards, D. and Wang, G.-Y. 1998. Molecular characterisation of some enigmatic Lower Devonian fossils. *Geochemica et Cosmochimica*

Acta, **62**, 1407–1418, https://doi.org/10.1016/S0016-7037(98)00078-7

Auxier, B., Bazzicalupo, A. *et al*. 2016. No place among the living: phylogenetic considerations place the Palaeozoic fossil *T. protuberans* in Fungi but not in Dikarya. A comment on M. Smith (2016). *Botanical Journal of the Linnean Society*, **182**, 723–728, https://doi.org/10.1111/boj.12479

Banks, H.P. 1975*a*. Early vascular land plants: proof and conjecture. *BioScience*, **25**, 730–737, https://doi.org/10.2307/1297453

Banks, H.P. 1975*b*. The oldest vascular land plants: a note of caution. *Review of Palaeobotany and Palynology*, **20**, 13–25, https://doi.org/10.1016/0034-6667(75)90004-4

Boyce, K.C., Cody, G.D., Fogel, M.L., Hazen, R.M., Alexander, C.M.O'D. and Knoll, A.H. 2003. Chemical evidence for cell wall lignification and the evolution of tracheids in Early Devonian plants. *International Journal of Plant Sciences*, **164**, 691–702, https://doi.org/10.1086/377113

Burgess, N.D. and Edwards, D. 1988. A new Palaeozoic plant closely allied to *Prototaxites* Dawson. *Botanical Journal of the Linnean Society*, **97**, 189–203, https://doi.org/10.1111/j.1095-8339.1988.tb02461.x

Burgess, N.D. and Edwards, D. 1991. Classification of uppermost Ordovician to Lower Devonian tubular and filamentous macerals from the Anglo-Welsh Basin. *Botanical Journal of the Linnean Society*, **106**, 41–66, https://doi.org/10.1111/j.1095-8339.1991.tb02282.x

Chaloner, W.G. 1960. The origin of vascular plants. *Science Progress*, **191**, 524–534.

Chaloner, W.G. 1970. The rise of the first land plants. *Biological Reviews*, **45**, 353–377, https://doi.org/10.1111/j.1469-185X.1970.tb01645.x

Cleal, C.J. and Thomas, B.A. 2009. *An Introduction to Fossil Plants*. Cambridge University Press, Cambridge.

Cook, M.E. and Graham, L.E. 1998. Structural similarities between surface layers of selected Charophycean algae and bryophytes and the cuticles of vascular plants. *International Journal of Plant Sciences*, **159**, 780–787, https://doi.org/10.1086/297597

Edwards, D. 1982. Fragmentary non-vascular plant microfossils from the Late Silurian of Wales. *Botanical Journal of the Linnean Society*, **84**, 223–256, https://doi.org/10.1111/j.1095-8339.1982.tb00536.x

Edwards, D. 1986. Dispersed cuticles of putative non-vascular plants from the Lower Devonian of Britain. *Botanical Journal of the Linnean Society*, **93**, 259–275, https://doi.org/10.1111/j.1095-8339.1982.tb01025.x

Edwards, D. 1996. New insights into early land ecosystems: a glimpse of a Lilliputian world. *Review of Palaeobotany and Palynology*, **90**, 159–174, https://doi.org/10.1016/0034-6667(95)00081-X

Edwards, D. and Axe, L. 1992. Stomata and mechanics of stomatal functioning in some early land plants. *Courier Forshungsinstitut Senckenberg*, **147**, 59–73.

Edwards, D. and Axe, L. 2012. Evidence for a fungal affinity for *Nematosketum*, a close ally of *Prototaxites*. *Botanical Journal of the Linnean Society*, **168**, 1–18, https://doi.org/10.1111/j.1095-8339.2011.01195.x

Edwards, D. and Davis, E.C.W. 1976. Oldest recorded *in situ* tracheids. *Nature*, **263**, 494–495, https://doi.org/10.1038/263494a0

Edwards, D. and Rose, V. 1984. Cuticles of *Nematothallus*: a further enigma. *Botanical Journal of the Linnean Society*, **88**, 35–54, https://doi.org/10.1111/j.1095-8339.1984.tb01563.x

Edwards, D. and Wellman, C.H. 2001. Embryophytes on land: the Ordovician to Lochkovian (Lower Devonian) Record. *In*: Gensel, P.G. and Edwards, D. (eds) *Plants Invade the Land*. Columbia University Press, New York, 3–28.

Edwards, D., Bassett, M.G. and Rogerson, C.W. 1979. The earliest vascular land plants: continuing the search for proof. *Lethaia*, **12**, 313–324, https://doi.org/10.1111/j.1502-3931.1979.tb01017.x

Edwards, D., Edwards, D.S. and Rayner, R. 1981. The cuticle of early vascular plants and its evolutionary significance. *Linnean Society Symposium Series*, **10**, 341–361.

Edwards, D., Davies, K.L. and Axe, L. 1992. A vascular conducting strand in the early land plant *Cooksonia*. *Nature*, **357**, 683–685, https://doi.org/10.1038/357683a0

Edwards, D., Abbott, G.D. and Raven, J.A. 1996. Cuticles of early land plants: a palaeoecophysiological evaluation. *In*: Kerstiens, G. (ed.) *Plant Cuticles*. BIOS Scientific, Oxford, 1–31.

Edwards, D., Ewbank, G. and Abbott, G.D. 1997. Flash pyrolysis of the outer cortical tissues in Lower Devonian *Psilophyton dawsonii*. *Botanical Journal of the Linnean Society*, **124**, 345–360.

Edwards, D., Wellman, C.H. and Axe, L. 1998*a*. The fossil record of early land plants and interrelationships between primitive embryophytes: too little too late? *In*: Bates, J.W., Ashton, N.W. and Duckett, J.G. (eds) *Bryology for the Twenty-First Century*. British Bryological Society, 15–43.

Edwards, D., Kerp, H. and Hass, H. 1998*b*. Stomata in early land plants: an anatomical and ecophysiological approach. *Journal of Experimental Botany*, **49**, 255–278, https://doi.org/10.1093/jxb/49.Special_Issue.255

Edwards, D., Axe, L. and Honegger, R. 2013. Contributions to the diversity of in cryptogamic covers in the mid-Palaeozoic; *Nematothallus* revisited. *Botanical Journal of the Linnean Society*, **173**, 505–534, https://doi.org/10.1111/boj.12119

Edwards, D., Honegger, R., Axe, L. and Morris, J.L. 2018. Anatomically preserved Silurian 'nematophytes' from the Welsh Borderland (UK). *Botanical Journal of the Linnean Society*, **187**, 272–291, https://doi.org/10.1093/botlinnean/boy022

Ewbank, G., Edwards, D. and Abbot, D. 1996. Chemical characterization of Lower Devonian vascular plants. *Organic Geochemistry*, **25**, 461–473, https://doi.org/10.1016/S0146-6380(96)00140-4

Gensel, P.G. 2008. The earliest land plants. *The Annual Review of Ecology, Evolution, and Systematics*, **39**, 459–477, https://doi.org/10.1146/annurev.ecolsys.39.110707.173526

Gensel, P.G., Johnson, N.G. and Strother, P.K. 1991. Early land plant debris (Hooker's 'Waifs and strays'?). *Palaios*, **5**, 520–547, https://doi.org/10.2307/3514860

Graham, L.E., Wilcox, L.W., Cook, M.E. and Gensel, P.G. 2004. Resistant tissues of modern marchantioid liverworts resemble enigmatic Early Palaeozoic

microfossils. *Proceedings of the National Academy of Sciences*, **101**, 11025–11029, https://doi.org/10.1073/pnas.0400484101

Graham, L.E., Trest, M.T. and Cook, M.E. 2017. Acetolysis resistance of modern Fungi: testing attributions of enigmatic Proterozoic and early Paleozoic fossils. *International Journal of Plant Sciences*, **178**, 330–339, https://doi.org/10.1086/690280

Gray, J. 1985. The microfossil record of early land plants: advanced in understanding of early terrestrialisation, 1970–1984. *Philosophical Transactions of the Royal Society London B*, **309**, 167–195.

Gray, J. and Boucot, A.J. 1971. Early Silurian spore tetrads from New York: earliest New World evidence for vascular plants? *Science*, **973**, 198–221.

Gray, J. and Boucot, A.J. 1977. Early vascular land plants: proof and conjecture. *Lethaia*, **10**, 145–174, https://doi.org/10.1111/j.1502-3931.1977.tb00604.x

Gray, J. and Boucot, A.J. 1993. Early Silurian nonmarine animal remains and the nature of the early continental ecosystem. *Acta Palaeontologica Polonica*, **38**, 303–328.

Gray, J., Laufield, S. and Boucot, A.J. 1974. Silurian trilete spores and spore tetrads from Gotland: their implications for land plant evolution. *Science*, **185**, 260–263, https://doi.org/10.1126/science.185.4147.260

Guo, Y. and Wang, D. 2015. Studies on plant cuticles from the Lower–Middle Devonian of China. *Review of Palaeobotany and Palynology*, **227**, 42–51, https://doi.org/10.1016/j.revpalbo.2015.11.007

Høeg, O.A. 1942. The Downtonian and Devonian flora of Spitsbergen. *Skrifter Norges Svalbard- – og Ishavs-Undersøkelser*, **83**, 1–228.

Honegger, R., Axe, L. and Edwards, D. 2013. Bacterial epibionts and endolichenic actinobacteria and fungi in the Lower Devonian lichen *Chlorolichenomycites salopensis*. *Fungal Biology*, **117**, 512–518, https://doi.org/10.1016/j.funbio.2013.05.003

Honegger, R., Edwards, D., Axe, L. and Strullu-Derrien, C. 2017. Fertile *Prototaxites taiti*: a basal ascomycete with inoperculate, polysporous asci lacking croziers. *Philosophical Transactions of the Royal Society B*, **373**, 1–14, https://doi.org/10.1098/rstb.2017.0146

Hueber, F.M. 2001. Rotted wood-alga-fungus: the history and life of *Prototaxites* Dawson 1859. *Review of Palaeobotany and Palynology*, **116**, 123–158, https://doi.org/10.1016/S0034-6667(01)00058-6

Jansonius, J. and McGregor, D.C. 1996. Palynology: principles and applications. *American Association of Stratigraphic Palynologists Foundation*, **1**.

Jeram, A.J., Selden, P.A. and Edwards, D. 1990. Land animals in the Silurian: Arachnids and Myriapods from Shropshire, England. *Science*, **250**, 658–661, https://doi.org/10.1126/science.250.4981.658

Johnson, N.G. 1985. Early Silurian palynomorphs from the Tuscarora Formation in central Pennsylvanian and their palaeobotanical and geological significance. *Review of Palaeobotany and Palynology*, **45**, 307–360, https://doi.org/10.1016/0034-6667(85)90006-5

Kenrick, P., Wellman, C.H., Schneider, H. and Edgecombe, G.D. 2012. A timeline for terrestrialisation: consequences for the carbon cycle in the Palaeozoic. *Philosophical Transactions of the Royal Society of London Series B Biological Sciences*, **367**, 519–536, https://doi.org/10.1098/rstb.2011.0271

Kodner, R.B. and Graham, L.E. 2001. High-temperature, acid hydrolysed remains of *Polytrichium* (Musci, Polytrichaceae) resemble enigmatic Silurian–Devonian tubular microfossils. *American Journal of Botany*, **88**, 462–466, https://doi.org/10.2307/2657111

Kroken, S.B., Graham, L.E. and Cook, M.E. 1996. Occurrence and evolutionary significance of resistant cell walls in charophytes and bryophytes. *American Journal of Botany*, **83**, 1241–1254, https://doi.org/10.1002/j.1537-2197.1996.tb13908.x

Lang, W.H. 1937. On the plant-remains from the Downtonian of England and Wales. *Proceedings of the Royal Society of London. Series B Biological Sciences*, **227**, 245–291.

Libertín, M., Kvaček, J., Bek, J., Žárský, V. and Štorch, P. 2018. Sporophytes of polysporangiate land plants from the early Silurian period may have been photosynthetically auronomous. *Nature Plants*, **4**, 269–271, https://doi.org/10.1038/s41477-018-0140-y

Lyon, A.G. 1962. On the fragmentary remains of an organism referable to the Nematophytales, from the Rhynie Chert, *Nematoplexus rhyniensis* gen. et sp. nov. *Transactions of the Royal Society of Edinburgh*, **65**, 79–87, https://doi.org/10.1017/S0080456800012382

McElwain, J.C. and Chaloner, W.G. 1995. Stomatal density and index of fossil plants track atmospheric carbon dioxide in the Palaeozoic. *Annals of Botany*, **76**, 389–395, https://doi.org/10.1006/anbo.1995.1112

Meyer-Berthaud, B., Servais, T., Vecoli, M. and Gerrienne, P. 2016*a*. The terrestrialization process: a palaeobotanical and palynological perspective – Volume 1. *Review of Palaeobotany and Palynology*, **224**, 1–108.

Meyer-Berthaud, B., Servais, T., Vecoli, M. and Gerrienne, P. 2016*b*. The terrestrialization process: a palaeobotanical and palynological perspective – Volume 2. *Review of Palaeobotany and Palynology*, **227**, 1–110.

Morris, J.L., Puttick, M.N. *et al.* 2018. The timescale of early land plant evolution. *PNAS*, **115**, 1719588115, https://doi.org/10.1073/pnas.1719588115

Niklas, K.J. 1976. Chemotaxonomy of *Prototaxites* and evidence for possible terrestrial adaptation. *Review of Palaeobotany and Palynology*, **22**, 1–17, https://doi.org/10.1016/0034-6667(76)90008-7

Niklas, K.J. and Pratt, L.M. 1980. Evidence for lignin-like constituents in Early Silurian (Llandoverian) plant fossils. *Science*, **209**, 396–397, https://doi.org/10.1126/science.209.4454.396

Parfrey, L.W., Lahr, D.J.G., Knoll, A.H. and Katz, L.A. 2011. Estimating the timing of early eukaryotic diversification with multigene molecular clocks. *Proceedings of the National Academy of Sciences*, **108**, 13624–13629, https://doi.org/10.1073/pnas.1110633108

Pratt, L.M., Phillips, T.L. and Dennison, J.M. 1978. Evidence of non-vascular land plants from the early Silurian (Llandoverian) of Virginia, U.S.A. *Review of Palaeobotany and Palynology*, **25**, 121–149, https://doi.org/10.1016/0034-6667(78)90034-9

Schopf, J.M. 1978. *Foerstia* and the recent interpretations of early vascular land plants. *Lethaia*, **11**, 139–143, https://doi.org/10.1111/j.1502-3931.1978.tb01298.x

Shear, W.A. and Selden, P.A. 2001. Rustling in the undergrowth: animals in early terrestrial ecosystems.

In: Gensel, P.G. and Edwards, D. (eds) *Plants Invade the Land*. Columbia University Press, New York, 29–51.

Sherwood-Pike, M.A. and Gray, J. 1985. Silurian fungal remains: probable records of the class Ascomycetes. *Lethaia*, **18**, 1–20, https://doi.org/10.1111/j.1502-3931.1985.tb00680.x

Smith, M.R. 2016. Cord-forming Palaeozoic fungi in terrestrial assemblages. *Botanical Journal of the Linnean Society*, **180**, 452–460, https://doi.org/10.1111/boj.12389

Strother, P.K. 1988. New species of *Nematothallus* from the Silurian Bloomsburg formation of Pennsylvania. *Journal of Palaeontology*, **62**, 967–982, https://doi.org/10.1017/S0022336000030237

Strother, P.K. 1993. Clarification of the genus *Nematothallus* Lang. *Journal of Palaeontology*, **67**, 1090–1094, https://doi.org/10.1017/S0022336000025476

Strother, P.K. 2010. Thalloid carbonaceous incrustations and the asynchronous evolution of the embryophyte characters during the Early Palaeozoic. *International Journal of Coal Geology*, **83**, 154–161, https://doi.org/10.1016/j.coal.2009.10.013

Strother, P.K. and Traverse, A. 1979. Plant microfossils from Llandoverian and Wenlockian rocks of Pennsylvania. *Palynology*, **3**, 1–21, https://doi.org/10.1080/01916122.1979.9989181

Strother, P.K., Battison, L., Brasier, M.D. and Wellman, C.H. 2011. Earth's earliest non-marine eukaryotes. *Nature*, **473**, 505–509, https://doi.org/10.1038/nature09943

Taylor, E.L., Taylor, T.N. and Krings, M. 2009. *Paleobotany: the Biology and Evolution of Fossil Plants*. Academic Press.

Taylor, T.N., Krings, M. and Taylor, E. 2015. Fungal diversity in the fossil record. *In*: McLaughlin, D.J. and Spatafora, J.W. (eds) *The Mycota VII Part B, Systematics and Evolution*, 2nd edn. Springer-Verlag.

Taylor, W.A. and Wellman, C.H. 2009. Ultrastructure of enigmatic phytoclasts (banded tubes) from the Silurian–Lower Devonian: evidence for affinities and role in early terrestrial ecosystems. *Palaios*, **24**, 167–180, https://doi.org/10.2110/palo.2008.p08-046r

Thusu, B., Rasul, S., Paris, F., Meinhold, G., Howard, J.P., Abutarruma, Y. and Whitham, A.G. 2013. Latest Ordovician–earliest Silurian acritarchs and chitinozoans from subsurface samples in Jebel Asba, Kufra Basin, SE Libya. *Review of Palaeobotany and Palynology*, **197**, 90–118, https://doi.org/10.1016/j.revpalbo.2013.05.006

Tomescu, A.M.F. and Rothwell, G.W. 2006. Wetlands before tracheophytes: Thalloid terrestrial communities of the Early Silurian Passage Creek biota. *Geological Society of America, Special Paper*, **399**, 41–56, https://doi.org/10.1130/2006.2399(02)

Tomescu, A.M.F., Rothwell, G.W. and Honegger, R. 2006. Cyanobacterial macrophytes in an Early Silurian (Llandovery) continental biota: Passage Creek, lower Massanutten Sandstone, Virginia, USA. *Lethaia*, **39**, 329–338, https://doi.org/10.1080/00241160600876719

Tomescu, A.M.F., Honegger, R. and Rothwell, G.W. 2008. Earliest fossil record of bacterial–cyanobacterial mat consortia: the Early Silurian Passage Creek biota (440 Ma, Virginia, USA). *Geobiology*, **6**, 120–124, https://doi.org/10.1111/j.1472-4669.2007.00143.x

Tomescu, A.M.F., Rothwell, G.W. and Honegger, R. 2009. A new genus and species of filamentous microfossil of cyanobacterial affinity from Early Silurian fluvial environments (lower Nassanutten Sandstone, Virginia, USA). *Botanical Journal of the Linnean Society*, **160**, 284–289, https://doi.org/10.1111/j.1095-8339.2009.00980.x

Tomescu, A.M.F., Tate, R.W., Mack, N.G. and Calder, V.J. 2010. Simulating fossilization to resolve the taxonomic affinities of thalloid fossils in Early Silurian (ca. 425 Ma) terrestrial assemblages. *In*: Nash, III, T.H. (ed.) *Biology of Lichens – Symbiosis, Ecology, Environmental Monitoring, Systematics, Cyber Applications*. Bibliotheca Lichenologica, **105**, 183–190.

Walker, J.D., Geissman, J.W. and Bowring, S.A. 2018. *Geologic Time Scale v. 5.0* (Babcock, L.E. compiler). Geological Society of America, https://doi.org/10.1130/2018.CTS005R3C

Traverse, A. 2007. *Paleopalynology*. Springer, Dordrecht.

Wellman, C.H. 1995. 'Phytodebris' from Scottish Silurian and Lower Devonian continental deposits. *Review of Palaeobotany and Palynology*, **84**, 255–279, https://doi.org/10.1016/0034-6667(94)00115-Z

Wellman, C.H. 2006. Spore assemblages from the Lower Devonian 'Lower Old Red Sandstone' deposits of the Rhynie outlier, Scotland. *Transactions of the Royal Society of Edinburgh: Earth Sciences*, **97**, 167–206, https://doi.org/10.1017/S0263593300001449

Wellman, C.H. and Gray, J. 2000. The microfossil record of early land plants. *Philosophical Transactions of the Royal Society London B*, **355**, 717–732, https://doi.org/10.1098/rstb.2000.0612

Wellman, C.H. and Richardson, J.B. 1993. Terrestrial plant microfossils from Silurian inliers of the Midland Valley of Scotland. *Palaeontology*, **36**, 155–193.

Wellman, C.H., Osterloff, P.L. and Mohiuddin, U. 2003. Fragments of the earliest land plants. *Nature*, **425**, 282–284, https://doi.org/10.1038/nature01884

Wellman, C.H., Steemans, P. and Vecoli, M. 2013. Palaeophytogeography of Ordovician–Silurian land plants. *Geological Society, London, Memoirs*, **38**, 461–476, https://doi.org/10.1144/M38.29

Chapter VIII Conclusions

Chapter III: Taxonomy and biostratigraphy of late Silurian – Early Devonian cryptospores and trilete spores from the Lower 'Old Red Sandstone' of the Anglo-Welsh Basin, U.K.

- Over 100 species of cryptospores and trilete spores in over 30 genera have been recovered from the late Silurian – Early Devonian (Ludlow – Lochkovian) Anglo-Welsh Basin sequence. Counts demonstrate that a considerable increase in species richness and morphological diversity occurs, principally amongst trilete spores but also amongst cryptospores at the onset of the Lochkovian. Trilete spores show the greatest increase in species and morphological diversity, but there are considerable changes amongst certain cryptospore genera. A gradual loss of marine palynomorphs occurs with the assemblages being entirely terrestrial by the late Přídolí, although sporadic brackish water incursions result in rare acritarchs in the Ammons Hill assemblage.

- Study of the spore assemblages around the Silurian – Devonian boundary (the *Apiculiretusispora* sp. E (Edwards and Richardson, 2004) zone) demonstrated a distinct assemblage of non-tripapillate *Aneurospora* and *Apiculiretusispora* species, which occurs before the lower *micrornatus – newportensis* subzone (Edwards and Richardson, 2004). *Aneurospora sheafensis* sp. nov., *Aneurospora kensingtonii* sp. nov., *Emphanisporites corralinus* sp. nov. and *Apiculiretusispora sceacga* sp. nov. define the non-tripapillate *Aneurospora* spp. assemblage biozone, which straddles the Silurian – Devonian boundary and terminates at the lower *micrornatus – newportensis* biozone. The inception of this zone is unclear because of the middle – late Přídolí sampling gap, but it is sufficiently different in species composition from the gap-preceding *lavidensis* biozone (mid Přídolí) (Higgs, 2022) to warrant distinction. The non-tripapillate *Aneurospora* spp. zone can be subdivided into the preliminary *Aneurospora sheafensis* assemblage subzone and the *Apiculiretusispora sceacga* assemblage subzone. The latter initiates with the FAD of *Ap. Sceacga*, which closely corresponds to the FAD of *Turina pagei*.

- Regional and global correlation is facilitated by the established and preliminary biostratigraphy of the basin (Richardson et al., 1981, 1985; Richardson and McGregor, 1986; Richardson and Edwards, 1989; Burgess and Richardson, 1995). Regional biostratigraphy is generally very good, although some problems are presented by the diachroneity of the Chapel Point Limestone (Morris et al., 2011a). International biostratigraphic correlation is hindered by palynological provincialization and the vast geographical distances, in addition to an occasional lack of independent dating of sequences.

Chapter IV: Floral diversity, disparity and community turnover at the Silurian - Devonian boundary: palynological evidence from the Anglo-Welsh Basin, UK.

- A quantitative assessment of spatial and temporal species and morphological change in the Anglo-Welsh Basin sequence shows a significant increase in species richness amongst trilete spores and cryptospores between the pre-MN and MN biozones (Ludlow – earliest Lochkovian and early – mid Lochkovian). A considerable turnover at this time amongst the cryptospore and trilete spore species

occurs, with cryptospores having a lower degree of unique species and a lower species diversity between biozones and coeval localities than the trilete spores.

- A considerable increase in morphological diversity (disparity) is observed between the pre-MN and MN biozones. Miospores show the highest degree of disparity increase, with sharp changes between the pre-MN and MN spore assemblages. Similarly, a less pronounced but sustained disparity increase is observed amongst the cryptospores.

- Several underlying causes may have driven the radiation in species diversity and disparity between the Ludlow and Lochkovian of the Anglo-Welsh Basin. Previous workers attributed the change to evolution amongst the source plants, but facies change may also have contributed to the change, with a switch from ephemeral to perennial river systems. The shift towards a wetter climate which drove this facies change may have facilitated the invasion and establishment of a diverse suite of rhyniophytes, and later zosterophylls. Sorting and taphonomic influences are not considered to have considerably contributed to the changes observed in the spore assemblages though the Anglo-Welsh Basin.

- With the increasing diversity of vegetation, there is evidence for floral heterogeneity in the Anglo-Welsh Basin. Whilst such spatial differentiation is hinted at in the Ludlow, there is a clear development of 'pockets' of putatively specialised vegetation in the landscape by the lower MN (early Lochkovian). This is most clearly demonstrated in the lower MN Gardeners Bank locality, which is peculiarly dominated by the otherwise rare *Acinosporites salopiensis*. Subtler changes may also be observed in the abundance and distribution of other species, such as *Emphanisporites*, some of which appear to have been restricted to specialised, sporadically occurring ecological niches away from river catchment while others may have been more widespread.

Chapter V: Early Lochkovian (Early Devonian) mesofossil assemblages from the Anglo-Welsh Basin, UK.

- Two mesofossil horizons from the lower MN biozone (Early Lochkovian) are presented. Vitrinite reflectance confirms that the fossils from both were formed by low temperature wildfires. The presence of charcoal derived from the hydrophilic vegetation indicates that pO_2 must have exceeded 16% and was likely greater than 18% (Belcher et al., 2010). As such, the GEOCARBSULF (Berner, 2009) box-model predicting pO_2 may most accurately reflect pO_2 in the early Lochkovian.

- The M50 section has yielded 29 spore masses with 16 different *in situ* trilete spore and cryptospore species. *Laevolancis* is the most common *in situ* spore, with *Aneurospora*, *Ambitisporites* and *Emphanisporites* species also having a good recovery rate. Most of the major dispersed species, are recorded, but other prominent species such as *Archaeozonotriletes* persist in their absence from the *in situ* spore record. Many of the *in situ* spores recovered in the M50 are comparable to species that are rare in the dispersed spore record of the same sample, suggesting transportation of the spore masses. In addition to *in situ* spores, terrestrial arthropod coprolites and sterile axes are also recorded from the M50. While nematophytic remains are present in the dispersed record, charcoalified remains of these non-embryophytic phytodebris are not present in the M50. Meanwhile, the Ammons Hill section yields an abundance of charcoalified nematophytes and non-embryophytes, in addition to 'fertile' and sterile

plant axes but *in situ* spores or spore masses have been recovered, despite a rich assemblage of dispersed trilete spores and cryptospores.

- The Ammons Hill and M50 assemblages were likely both influenced by taphonomy and transportation. Given the absence of exceptionally preserved mesofossils which exhibit, *inter alia*, sporangial tissues, and the presence of likely (e.g. interdigitating tubes) and putative (e.g. pits in sporangial cuticles) decay indicators in spore masses, it is probable that the plant fossils were burned after death as part of the litter, following a period of partial decay. The difference in composition between the M50 and Ammons Hill is attributed to taphonomy and transport, which may be a result of the variation in the tissues and their response to burning between embryophytes and non-embryophytes, including nematophytes. The Brown Clee Hill assemblage exhibits both embryophytic and non-embryophytic remains, and this may be due to the proximity to the source of the fire.

- Early Lochkovian vegetation comprised tracheophytes, eophytes and other cryptospore bearing plants, which were diminutive and rhyniophytic. Several of the *in situ Laevolancis* spore masses were comparable to each other and are reminiscent of *Lenticulitheca* spore masses (Morris et al., 2011b) and Wellman's et al. (1998b) groups. A new bivalved arrangement is shown for one *Laevolancis* producer. The *Hispanaediscus* spore mass is reminiscent to those of *Cooksonia* and may form a lineage with species of *Cooksonia* which produce verrucate trilete spores such as *Synorisporites verrucatus*, similar to the relationship suggested by Edwards et al. (2014) for the *Lenticulitheca* – *Paracooksonia* – *Cooksonia* complex. Spore masses yielding *Cymbohilates*, *Aneurospora* and *Ambitisporites* may be comparable to *Lenticulitheca* and *Paracooksonia* species with respects to the similar sporangial morphology and co-occurring *in situ* spores. Others may be more comparable to *Cooksonia*. The new *in situ Emphanisporites* specimens further add to the sporangial diversity observed amongst this morphogenus. Finally, while the affinities of *Stellatispora* remain uncertain, it has been shown that the spore was derived from a probably rhyniophytic parent plant with an elongate, terminal sporangium. Ultrastructural analysis would be beneficial to advance discussions on the affinities of these *in situ* spores and their parent plants.

- Wellman et al. (2003) reported an *in situ Tetrahedraletes*, which was suggested by Edwards et al. (1996) to show indications of being adapted as a colonising or founding plant. The spore mass dimensions and spore yield of spore masses recovered in this work, and from other publications (e.g. Morris et al., 2011a; Wellman, 1999) were calculated and compared to Wellman's et al. (2003) *Tetrahedraletes* specimen. Most of the spore masses with a greater estimated number of *in situ* spores are considerably larger than the *Tetrahedraletes* spore mass, but the *Hispanaediscus* yielding spore mass, which was of a similar morphology and dimensions, yielded a similar number of estimated spores. This might indicate some level of adaptation to invading inequable habitats based on the vast number of spores produced by a single spore mass, but such deliberations have a number of caveats. Broader ecological implications may be ascertained by integrating the dispersed spore record and mesofossil record. The paucity and sporadic occurrence of *Scylaspora* sp. 1 and some *Emphanisporites* species, including those investigated here, may suggest restriction to a niche outside of river catchment. Meanwhile, other *Emphanisporites* species, such as *E. epicautus* (Ball and Taylor, 2022) and *Hispanaediscus*, may have existed across less restricted niches, but outside of the general catchment of rivers. The parent plants of *Laevolancis* and *Ambitisporites*, meanwhile, appear to have been widespread in areas within river catchment, but ultrastructural work may produce a more nuanced understanding of the distribution of these species.

Chapter VI: Reconstructing the Lower Devonian (Lochkovian) vegetation from the Anglo-Welsh Basin: Two spore masses containing Emphanisporites McGregor spores.

- The oldest-yet published examples of *in situ Emphanisporites* add to the growing diversity of sporangial morphologies found amongst these rare *Emphanisporites* producers. *E. epicautus* and *E.* sp. are most comparable to the rhyniophytes, although a lack of unequivocal vascular tissue necessitates their grouping amongst the rhyniophytoids.

- Morphological and ultrastructural information demonstrate that these source plants and their associated *in situ* spores belonged to quite different, although equivocal, lineages. The ultrastructures differ significantly from other *Emphanisporites* species, especially for *E. epicautus,* and neither are directly comparable to contemporaneous fossil or extant taxa. While the homogenous exospore of *E. epicautus* makes comparisons difficult, the bilayered exine comprising an inner lamellate layer and outer homogenous layer of *E.* sp. may relate it to some modern tracheophytes, but this remains problematic. Investigation of sporocyte development for *E. epicautus* is difficult given the homogenous architecture of the spore wall, but *E.* sp. may have formed by a variety of means. Whilst the *Andreaea* mode of Formation for the outer homogenous layer is plausible in the absence of evidence for a tapetum and rare lacunae, the overall spore wall development remains clouded.

- Given the paucity of *E.* sp. in the dispersed record, we cannot currently explore the palaeoecology of this plant. The dispersed spore record of *E. epicautus* and *E.* cf. *epicautus* indicates that the parent plant/ plants inhabited widespread ecological niches away from the catchment areas of rivers, but these do not appear to have been as restricted as the niche of cf. *Horneophyton* sp. (Edwards and Richardson, 2004). It is possible that the emphanoid muri conferred some advantage to propagation in water stressed environments, as the diversity of *Emphanisporites* producers, and other emphanoid muri bearing taxa, strongly indicates that the emphanoid condition is convergent (Edwards and Richardson, 2000; Taylor et al., 2011; Morris et al., 2012b) and the spore record appears to suggest that all emphanoid taxa grew outside of the catchment of rivers. Such areas may have been water stressed, and as such the emphanoid may have offered some selective advantage due to some environmental and/ or evolutionary pressure.

Chapter VII: Early land plant phytodebris

- Phytodebris are dispersed fragments derived from a variety of embryophytic (land plant) and non-embryophytic (including fungi) sources. These phytodebris appear to have been produced by the components of the earliest terrestrial ecosystems, and have featured in palynological research since the 1950s. However, their affinities have remained uncertain.

- Some of the cuticular fragments, particularly those with preserved patterning of elongate cells, were postulated to derive from early land plants (e.g. Edwards et al., 1998b). Further detailed taxonomic studies indicated that many of these cuticle-like sheets were derived from the nematophytes, an enigmatic group of non-embryophytic organisms. Geochemical and taphonomic decay studies suggested that there may have been an embryophytic link to these phytodebris, but the recovery of

exceptionally preserved nematophytes from the mid Lochkovian (Edwards et al., 2013, 2018) provided strong evidence that these cuticles were linked to organisms with fungal and lichen affinities.

- Tubes occur alongside cuticles described above, and these have again been attributed to a variety of embryophytic and non-embryophytic sources. The exceptionally preserved nematophytes from the mid Lochkovian of the Anglo-Welsh Basin again consigned nematophyte fossils which exhibited tubes comparable to the dispersed specimens as a part of their anatomy (Edwards et al., 2013). Whilst these findings indicate a fungal or lichenised fungal affinity for some, it remains likely that some tubes at least were derived from other sources, such as cyanobacterial mats.

- It is clear that non-pollen palynomorphs (phytodebris) continue to play an important role in research into the earliest land plants and their co-inhabitants of the land. Whilst recent years have witnessed a dramatic increase in knowledge regarding the affinities and nature of many of their producers, particularly regarding the nematophytes, there is still much to be understood about these enigmatic plant remains.